

BOXGROVE

*A Middle Pleistocene hominid site
at Eartham Quarry, Boxgrove,
West Sussex*

M B Roberts and S A Parfitt



ENGLISH HERITAGE

BOXGROVE

*A Middle Pleistocene hominid site
at Eartham Quarry, Boxgrove,
West Sussex*

This work is dedicated to two friends, Bob Welch and John Roffey:
anglers, shots, gentlemen, and *bons viveurs*

— MBR, 1999

BOXGROVE

*A Middle Pleistocene hominid site
at Eartham Quarry, Boxgrove,
West Sussex*

M B Roberts and S A Parfitt
Institute of Archaeology, University College London

with contributions by

L A Austin, M R Bates, C A Bergman, D Q Bowen,
D R Bridgland, J A Catt, C R Cartwright, S N Collcutt,
A David, G Gard, P Goldberg, R Grün, R Harland,
C J O Harrison, J A Holman, B G Irving, S G Lewis,
P Linford, R I Macphail, D A Parks, R C Preece,
A M Rae, H M Rendell, E J Rhodes,
C L Roberts, J R Stewart, C B Stringer,
G A Sykes, E Trinkaus, F F Wenban-Smith,
J E Whittaker, and K H Wilhelmsen



ENGLISH HERITAGE

1999

ARCHAEOLOGICAL REPORT 17

Contents

Contributors	vi	4 Mammalia by <i>S A Parfitt</i>	
Figures	vii	4.1 Introduction	197
Tables	xiv	4.2 Systematic palaeontology	197
Preface	xvii	4.3 Summary: taphonomy and palaeoecology	274
Acknowledgements	xviii	5 Methods of age estimation	
Summary	xix	5.1 Introduction	291
Résumé	xx	5.2 Uranium series dating by <i>A M Rae</i>	291
Zusammenfassung	xxi	5.3 Luminescence dating of brickearth by <i>D A Parks and H M Rendell</i>	292
Glossary compiled by <i>D M Jones</i>	xxii	5.4 Optically stimulated luminescence by <i>E J Rhodes</i>	293
1 Introduction		5.5 Electron spin resonance: coupled ESR-U series dating by <i>R Grün</i>	294
1.1 Background	1	5.6 Amino acid geochronology by <i>D Q Bowen</i> and <i>G A Sykes</i>	295
1.2 Lower Palaeolithic archaeology in the context of Middle Pleistocene chronostratigraphy by <i>M B Roberts</i>	5	5.7 Palaeomagnetic measurements by <i>A David and P Linford</i>	297
1.3 A history of research in the Boxgrove area by <i>M B Roberts</i>	8	5.8 Calcareous nannoplanktons by <i>G Gard</i>	300
1.4 Project methodology by <i>M B Roberts</i>	15	5.9 Biostratigraphy and summary by <i>M B Roberts and S A Parfitt</i>	303
2 Geology and sedimentology		6 Archaeology	
2.1 Geological framework by <i>M B Roberts</i>	21	6.1 Introduction by <i>M B Roberts</i>	309
2.2 Location of the buried cliff-line using resistivity methods by <i>S G Lewis and C L Roberts</i>	37	6.2 Archaeology of excavated areas by <i>L A Austin</i> , <i>C A Bergman, M B Roberts and</i> <i>K H Wilhelmsen</i>	312
2.3 Structural sedimentology at Boxgrove by <i>S N Collcutt</i>	42	6.3 Flintwork from other contexts by <i>M B Roberts</i>	378
2.4 Analysis of the raised beach gravel deposits at Boxgrove and related sites by <i>D R Bridgland</i>	100	6.4 Knapping technology by <i>F F Wenban-Smith</i>	384
2.5 Particle size distribution and mineralogy of the deposits by <i>J A Catt</i>	111	6.5 Human modification of faunal remains by <i>S A Parfitt and M B Roberts</i>	395
2.6 Sediment micromorphology by <i>R I Macphail (with contribution by</i> <i>P Goldberg)</i>	118	6.6 The Middle Pleistocene hominid record by <i>C B Stringer</i>	415
2.7 Geological summary by <i>M B Roberts</i>	149	6.7 The human tibia from Boxgrove by <i>C B Stringer and E Trinkaus</i>	420
3 Palaeontology		6.8 Concluding remarks and discussion by <i>M B Roberts</i>	422
3.1 Introduction by <i>S A Parfitt</i>	157	Appendices	
3.2 Foraminifera and Ostracoda by <i>J E Whittaker</i>	163	1 Charcoal by <i>C R Cartwright</i>	427
3.3 Mollusca by <i>R C Preece and M R Bates</i>	170	2 Dinoflagellate cyst analysis by <i>R Harland</i>	427
3.4 Ichthyofauna by <i>S A Parfitt</i> and <i>B G Irving</i>	175	3 The Slindon Formation by <i>M B Roberts</i>	428
3.5 Herpetofauna by <i>J A Holman</i>	181	Bibliography	429
3.6 Avifauna by <i>C J O Harrison</i> and <i>J R Stewart</i>	187	Index	447

Contributors

- L Austin *Cambria Archaeology, The Shire Hall, Carmarthen, Llandeib, Carmarthenshire, SA19 6AF*
- M R Bates *Department of Archaeology, University of Wales, Lampeter, Ceredigion SA48 7ED*
- C A Bergman *Northern Kentucky University and 3D Environmental Services Inc, 781 Neeb Road, Suite 5, Cincinnati, Ohio 45233, USA*
- D Q Bowen *Earth Studies, University of Wales, Cardiff, CF1 3YE*
- D R Bridgland *Department of Geography, University of Durham, Durham DH1 3LE*
- J A Catt *Soil Science Department, AFRC Institute of Arable Crops Research, Rothamsted Experimental Station, Harpenden, Hertfordshire, AL5 2JQ*
- C R Cartwright *Department of Scientific Research, British Museum, Great Russell Street, London WC1B 3DG*
- S N Colcutt *Oxford Archaeological Associates, Lawrence House, 2 Polstead Road, Oxford, OX2 6TN*
- A David *Ancient Monuments Laboratory, English Heritage, 23 Savile Row, London, W1X 2HE*
- G Gard *Department of Geology and Geochemistry, University of Stockholm, Sweden*
- P Goldberg *Department of Archaeology, Boston University, 675 Commonwealth Avenue, Boston, Mass 02215, USA*
- R Grün *Research School of Earth Sciences, Australian National University, Canberra, ACT 0200, Australia*
- R Harland *DinoData Services, 50 Long Acre, Bingham, Nottingham, NG13 8AH*
- C O Harrison *19 Kennington Road, Kennington, Oxford OX1 5NZ*
- J A Holman *Michigan State University Museum, East Lansing, Michigan, 48824-1045, USA.*
- B G Irving *Soltway Rural Initiative, Resource Centre, King Street, Aspatria, Cumbria CA5 3ET*
- S G Lewis *School of Environment, Cheltenham and Gloucester College of Higher Education, Francis Close Hall, Cheltenham, GL50 4AZ*
- P Linford *Ancient Monuments Laboratory, English Heritage, 23 Savile Row, London W1X 2H.*
- R I Macphail *Institute of Archaeology, University College London, 31-34 Gordon Square, London WC1H 0PY*
- S A Parfitt *Institute of Archaeology, University College London, 31-34 Gordon Square, London WC1H 0PY*
- D A Parks *Redland Technology Ltd, PO Box 6, Graylands, Langhurstwood Road, Horsham, West Sussex, RH12 4QG.*
- R C Preece *Department of Zoology, University of Cambridge, Downing Street, Cambridge, CB2 3EJ*
- A M Rae *Research Laboratory for Archaeology and History of Art, 6 Keble Road, Oxford OX1 5QJ*
- H M Rendell *Geography Laboratory, University of Sussex, Falmer, Brighton, East Sussex, BN1 9QN*
- E J Rhodes *Research Laboratory for Archaeology and History of Art, 6 Keble Road, Oxford OX1 5QJ*
- C L Roberts *School of Applied Sciences, University of Wolverhampton, Wulfruna Street, Wolverhampton, WV1 1SB*
- M B Roberts *Institute of Archaeology, University College London, 31-34 Gordon Square, London WC1H 0PY*
- J R Stewart *The McDonald Institute for Archaeology and Research, Downing Street, Cambridge CB2 3ER*
- C B Stringer *Human Origins Group, Department of Palaeontology, Natural History Museum, London, SW7 5BD*
- G A Sykes *Earth Studies, University of Wales, Cardiff, CF1 3YE.*
- E Trinkaus *Department of Anthropology, Washington University, Campus Box 1114, Saint Louis, MO 63130-4899, USA, and
UA 376 du CNRS, Laboratoire d'Anthropologie, Université de Bordeaux I, 33405 Talence, France*
- F F Wenban-Smith *Institute of Archaeology, University College London, 31-34 Gordon Square, London WC1H 0PY*
- J E Whittaker *Department of Palaeontology, Natural History Museum, London SW7 5BD*
- K H Wilhelmsen *Department of Anthropology, DH-05, University of Washington, Seattle, Washington 98195, USA*

Figures

Fig 1a	Location of Boxgrove (AEP)	xxiv	Fig 28	The cliff and beach buried under angular chalk cliff collapse and colluvium.....	38
Fig 1b	Principal European Early and Middle Pleistocene sites mentioned in the text	1	Fig 29	Map of the Boxgrove quarries showing the probable position of the cliff line and the position of the resistivity soundings along the three north-south traverses	39
Fig 2	Location of towns and rivers mentioned in the text.....	2	Fig 30	Apparent Resistivity (SLM) plotted against depth (m).....	39
Fig 3	Raised beaches in the Boxgrove area superimposed on the solid geology.....	2	Fig 31	Results of resistivity modelling processes, showing changes in apparent resistivity with depth (left-hand side), together with the lithological interpretation of the resistivity model (right-hand side).....	40
Fig 4	Eartham Quarry, Boxgrove 1995	3	Fig 32	North-south cross-sections along traverses A-B, C-D, and E-F, showing configuration of chalk surface and thickness of Quaternary deposits	41
Fig 5	Aerial view of the quarries looking east, Q1 in foreground.....	4	Fig 33	West-east transect through the geology at Boxgrove.....	43
Fig 6	Quarry 2, looking north past Q2/A towards GTP 25 and the South Downs.....	4	Fig 34	North-south section through Q2 based upon boreholes, test pits, and quarry exposures	44
Fig 7	Quarry 1, looking west.....	7	Fig 35	North-south section through Q1 based upon boreholes, test pits, and quarry exposures	45
Fig 8	Location of sites and raised beaches between Brighton and Portsmouth, inset shows location of Fig 9.....	10	Fig 36	Trace fossils in the marine sands at GTP 13.....	45
Fig 9	Location of quarries and raised beaches in the Boxgrove area.....	11	Fig 37	Trace fossil burrows in the marine sands at Sand Extraction Pit 3.....	45
Fig 10	Isometric model of the Downland block and upper coastal plain between Chichester and Tortington	14	Fig 38	Detailed sedimentary log through the sediments at Q2 SEP 3	47
Fig 11	Quarrying at Boxgrove.....	15	Fig 39a	The section at GTP 35 in Q2 SEP 3 (location of section shown on Fig 4).....	48
Fig 12	Q1 GTP 26: Gravels overlying marine deposits of the Slindon Formation	16	Fig 39b	Section through GTP 35 in Q2 SEP 3 (location of section shown on Fig 4).....	48
Fig 13	Plan of the quarry complex in 1987; compare with Fig 4.....	17	Fig 40	Plan and schematic section of GTP 25, the beach section, showing section locations	50
Fig 14	Sampling sediments at Boxgrove	18	Fig 41	GTP 25, the beach section in Quarry 2, looking north towards the cliff.....	51
Fig 15	Geological map of the Boxgrove area showing the solid geology.....	24	Fig 42a	Section through the Boxgrove beach at GTP 25 (location of sections shown on Fig 40)	52
Fig 16	Solid geology outcrops beneath the drift.....	25	Fig 42b	Detailed sedimentary log of combined section logs 1, 2 and 3 at GTP 25	54-5
Fig 17	Schematic sections through the Pleistocene deposits and solid geology of the coastal plain	25	Fig 42c-l	Detailed sedimentary logs through the sediments at GTP 25... between pages 54-5	
Fig 18	The soliflucted Tertiary regolith overlying chalky gravels at Boxgrove	26	Fig 43	The thickness of the raised beach at GTP 25, showing the steeply rising platform near the cliff.....	53
Fig 19	The base of the chalk cliff at Boxgrove	26	Fig 44	Composite log through the lower part of the sequence in Q2 GTP 13, showing the relationship between Marine Cycles, unit numbers, and members	54
Fig 20	The Boxgrove type section, Q2 GTP 13.....	26			
Fig 21	Isometric view of the Downland block and coastal plain in the Boxgrove area	27			
Fig 22	Composite section through the geology in Quarry 2.....	28			
Fig 23	Palaeogeography of the South Coast before and after the Anglian Glaciation.....	31			
Fig 24a	Soliflucted head gravel unconformably overlying the Marine Slindon Sands	34			
Fig 24b	Preservation of the Slindon Silts and Brick-earth Beds in a solution feature.....	35			
Fig 25	Unit 4c overlain by sediments of the Eartham Lower Gravel Member	35			
Fig 26	Fan gravels of the Eartham Upper Gravel Member overlying sediments of the Slindon Silt Member	36			
Fig 27	The chalk cliffs at Seaford Head.....	37			

Fig 45a	Detailed sedimentary logs through the sediments at GTP 13 between pages 54–5	Fig 68	Fe–Mn bands in the chalky gravel above Unit 5a and the Slindon Silts 89
Fig 45b	Detailed sedimentary log through the sediments at GTP 13 4 55	Fig 69	Mud cracks on the surface of Unit 5a at Q2 GTP 20 89
Fig 46	GTP 13, showing boulders at the base of the section 56	Fig 70	Post-depositional faulting of Unit 5a at Q2/A 89
Fig 47	<i>Pholas</i> bored chalk at the base of GTP 13 56	Fig 71	Unit 5b visible between the Fe–Mn layer of Unit 5a and the Brickearth Beds, Unit 6. 90
Fig 48	Detailed sedimentary log through Q1 GTP 26 between pages 56–7	Fig 72	Q2 GTP 5, Units 4b–6; note surviving residue of Unit 5b to left of section 91
Fig 49a	Q2 GTP 10; note the partial decalcification of the sediments 57	Fig 73	Soft sediment deformation features at the contact between the Slindon Silts and the chalky muds and gravels at GTP 25 92
Fig 49b	Detailed sedimentary log through the sediments at Q2 GTP 10 ... between pages 56–7	Fig 74	Thick deposits of the Brickearth Beds west of GTP 5 93
Fig 50	Section through the sediments at GTP 10 57	Fig 75	Chalky pellet gravels in Quarry 2 95
Fig 51	Detailed section through the sediments at GTP 10 (location of section shown on Fig 50) 58	Fig 76	Q1/A: deformation feature running through the main excavation 96
Fig 52	Deeper water fine-grained sediments overlying the beach at Q2 GTP 13 58	Fig 77	Calcareous Head Gravel, with solution hollow containing the overlying decalcified head gravel 97
Fig 53	Chalk rubble overlying the beach near to the cliff at GTP 25 61	Fig 78	Lower Head Gravel unconformably overlying the Slindon Silts; note frost wedge to right of scale 98
Fig 54	Marine Cycles 1 and 2 at GTP 13 62	Fig 79	Upper Silt Bed between the Upper Middle and Upper Head Gravels (contains the uppermost archaeological horizon) 99
Fig 55	Detail of sediments at the top of Marine Cycle 1 (a) and the base of Marine Cycle 2 (b) 63	Fig 80	Histograms of angularity/roundness data from Table 13 106–7
Fig 56	Prepared logging section at the southern end of GTP 13; note the flint flake in sediments of Marine Cycle 2 67	Fig 81	The Pleistocene sediments of the coastal plain and their relationship to the raised beaches of the Isle of Wight 108
Fig 57	Fine-grained sediments of Marine Cycle 3 above the chalk raft in GTP 13; note the handaxe thinning flake (arrow) on top of the raft 72	Fig 82	Redeposited Slindon Sand in the Head Gravel of Unit 11 116
Fig 58	Q2 GTP 25; the Slindon Sands and Silts between the raised beach gravels and the chalk rubble flows, showing chalk inclusions 73	Fig 83a	Quarry 1/A: sample 36; flint flake (artefact) within the calcareous silty clays of Unit 4b. Crossed polarised light (XPL), frame length 5.5mm 121
Fig 59	Detailed sedimentary log through the sediments at Q2 GTP 5 75	Fig 83b	GTP 3: typical iron-poor, decalcified and homogenised zone of terrestrial soil horizon of Unit 4c. XPL, frame length 5.5mm .. 121
Fig 60a	Section through the sediments at Q2 GTP 5 76	Fig 83c	GTP 10: sample 5; ironpan zone within terrestrial soil Unit 4. XPL, frame length 5.5mm 121
Fig 60b	Detailed section through the deposits at Q2 GTP 5 (location of section is shown on Fig 60a) 77	Fig 83d	Quarry 1/B, Trench 4: sample 34; detail of finely laminated peaty silts towards top of Unit 4d, Plane polarised light (PPL), frame length 5.5mm 121
Fig 60c	Q2 GTP 5, looking south 78	Fig 83e	Quarry 2, Pit C: sample 39. PPL, frame length 3.5mm 121
Fig 61	Detailed sedimentary log through the sediments at Q2/A 79	Fig 83f	GTP 3: sample 3; iron and manganese pan material of Unit 5a. PPL, frame length 5.5mm 121
Fig 62	The Slindon Silts at GTP 10 80	Fig 83g	GTP 25: sample 27; projected microfiche reader view of Units 4c, 5a, and 5b, microfiche frame length 0.11mm 122
Fig 63	Contact between the sands and silts at GTP 13 82	Fig 83h	Detail of mink scat (see book cover) set in Unit 5b marl. UV light, frame length 0.33mm 122
Fig 64	Possible seaweed-rafted pebble cluster from Unit 4 in Q2/A 83		
Fig 65	Slindon Sands and Silts 'wedging out' over the raised beach at GTP 25 83		
Fig 66	Unit 4c: note contrast between modified soil horizon and underlying Unit 4b 87		
Fig 67	Bear (<i>Ursus deningeri</i>) mandible from Unit 4c 87		

Fig 83i	GTP 17; sample 19; projected microfiche reader view of a flint artefact within the layered fine sands and organic matter of Unit 5c. Frame length 0.11mm.....	122	Fig 95	Absolute frequencies of shells per kg for selected samples.....	170
Fig 83j	Quarry 2, Pit C: sample 40; massive silty brickearth of Unit 6. PPL _s frame length 5.5mm.....	122	Fig 96	Percentage of slug plates for selected samples.....	172
Fig 83k	GTP 10; sample 5; Unit 6 showing possible incipient argillic brown earth formation in the brickearth. PPL _s frame length 3.5mm.....	122	Fig 97	<i>Vitrinobrachium breve</i>	172
Fig 83l	Quarry 1, GTP 31; sample 30; soliflual deposited chalk clasts, chalk soil, flint and silt to sand-size quartz of Unit 8. PPL _s frame length 5.5mm.....	122	Fig 98	<i>Neptunea contraria</i>	173
Fig 83m	GTP 25; sample 23; flint artefact within chalky pellet gravel of Unit 8. XPL _s frame length 5.5mm.....	123	Fig 99	<i>Nucella lapillus</i>	174
Fig 83n	GTP 25; sample 23; probable mammilated earthworm excrements. XPL _s frame length 5.5mm.....	123	Fig 100	a <i>Littorina saxatilis</i> b <i>Littorina littorea</i>	174
Fig 83o	Sample 53: Unit 11; wood charcoal fragment within compact dusty soil containing textural features. PPL _s frame length 0.33mm.....	123	Fig 101	Chalk bored by bivalve mollusc (?pholas) from the base of the marine deposits at Q2 GTP 13.....	174
Fig 83p	Sample 54: Unit 11; coarse and fine granular soil was affected by multiphase mechanical silt and clay inwash. XPL _s frame length 3.35mm.....	123	Fig 102	<i>Modiolus modiolus</i>	174
Fig 84	Example of SEM/EDXRA of Unit 4b at GTP 13, showing general calcareous nature of deposit.....	127	Fig 103	Fish from Amey's Eartham Pit, Boxgrove.....	176
Fig 85	Example of SEM/EDXRA of general calcareous Unit 4b at GTP 17.....	128	Fig 104	Number of fish bone fragments per kg recovered from sequential bulk samples of the Slindon Silt Member (Units 4b and 4c) from GTP 10.....	179
Fig 86	Example of SEM/EDXRA of some dark fine lenses in Unit 4b with apparently less Ca than the surrounding matrix (cf Fig 85) at GTP 17.....	128	Fig 105	Concentration of fish bones from Slindon Sands and Silt Members.....	180
Fig 87	Boxgrove during the deposition of the Slindon Sands.....	151	Fig 106	a Vertebra of <i>Triturus vulgaris</i> ; b left ilium of <i>Pelobates fuscus</i> ; c right ilium of <i>Pelobates fuscus</i> ; d left ilium of <i>Bufo bufo</i> ; e left ilium of <i>Rana arvalis</i> ; f right ilium of <i>Rana temporaria</i> ; g left ilium of <i>Bufo calamita</i>	182
Fig 88	Boxgrove during the deposition of the Slindon Silts.....	151	Fig 107	a-f Osteoscutes of <i>Anguis fragilis</i> ; g vertebra of <i>Anguis fragilis</i>	184
Fig 89	Boxgrove during the grassland stage of Unit 4c and the marsh of Unit 5a.....	152	Fig 108	Rearticulated wing bones of a mallard (<i>Anas platyrhynchos</i>).....	188
Fig 90	Boxgrove during the deposition of the upper part of Unit 6, through to Unit 9.....	154	Fig 109	Proximal right humerus of a great auk (<i>Pinguinus impennis</i>).....	191
Fig 91	Boxgrove during the deposition of Units 10 and 11, in the Anglian Glaciation.....	154	Fig 110	Associated pectoral girdle and left wingbones of a mallard (<i>Anas platyrhynchos</i>).....	196
Fig 92	Number of identifiable bone fragments per kg of unprocessed sediment, by unit.....	160	Fig 111	<i>Erinaceus</i> sp: right mandible with M ₁₋₃ (Q2 GTP 17 BS86-76 Unit 5a).....	198
Fig 93	Quarry 2, GTP 13: stratigraphy, location of samples, and foraminiferal and ostracod species diversity.....	165	Fig 112	<i>Erinaceus</i> sp: right M ¹ (Q2 GTP 17 BS86-76 Unit 5a).....	198
Fig 94	Some significant foraminifera (a-f) and ostracods (g-i) from the Slindon Sand Member, Quarry 2, Section GTP 13, Boxgrove.....	168	Fig 113	<i>Erinaceus</i> spp and <i>Aethechinus algirus</i> : log ratio diagram showing relative proportions in the a) upper dentition and b) lower dentition.....	198
			Fig 114	<i>Erinaceus</i> spp and <i>Aethechinus algirus</i> : bivariate plots of length against width of upper and lower teeth.....	200-2
			Fig 115	Measurements taken on soricid a) mandibular ramus and b) mandibular condyle.....	203
			Fig 116	<i>Neomys</i> sp: mandibles and incisors (Q2 GTP 3).....	203
			Fig 117	<i>Neomys</i> spp: Coronoid height in fossil and recent specimens.....	204
			Fig 118	<i>Sorex minutus</i> : mandible and incisors (Q2 GTP 3).....	205
			Fig 119	<i>Sorex minutus</i> : coronoid height in fossil and recent specimens.....	205
			Fig 120	<i>Sorex runtonensis</i> : mandible and incisors (Q2).....	205

Fig 121	<i>Sorex</i> spp: length of the lower facet of condyle plotted against condyle height for fossil and recent specimens 206-7	fourth cervical vertebra of Recent and fossil spotted hyaena 225	
Fig 122	<i>Sorex (D) savini</i> : mandible and incisors (Q2 GTP3) 208	Fig 149	<i>Felis silvestris</i> : bivariate plot of astragalus greatest length against trochlea width for Recent Scottish male and female wild cat compared with <i>F. cf silvestris</i> from Boxgrove 225
Fig 123	<i>Talpa</i> spp: distal epiphysis width (DW) in relation to shaft width (SD) of humeri 209-11	Fig 150	<i>Felis silvestris</i> : histograms of the minimum antero-posterior height of the ulnar semilunar notch for Scottish male and female wild cat 225
Fig 124	<i>Plecotus auritus</i> : right upper canine (Q1/B BS88-955 Unit 4c) 211	Fig 151	<i>Equus ferus</i> : left M _{1,2} (Q2 GTP 25) 227
Fig 125	<i>Plecotus auritus</i> : right lower canine (Q2 GTP 17 BS86-18 Unit 5a) 212	Fig 152	<i>Equus ferus</i> : associated P ₃ fragment and M _{1,2} (Q2 GTP 17 Unit 4b) 228
Fig 126	<i>Plecotus auritus</i> : left lower canine fragment (Q2 GTP 17 BS86-62 Unit 5a) 212	Fig 153	<i>Equus</i> spp: measurement comparisons of early Middle Pleistocene <i>E. altidens</i> with early Middle to Late Pleistocene <i>E. ferus</i> 228
Fig 127	<i>Plecotus auritus</i> : left P ₂ (Q2 GTP3 BS87-251 Unit 4c) 212	Fig 154	<i>Stephanorhinus hundsheimensis</i> : left P ⁴ (Q2 SEP 2 F10 Unit 4c) 229
Fig 128	<i>Plecotus auritus</i> : right M ³ (Q2 GTP 3 BS87-251 Unit 4c) 212	Fig 155	<i>Stephanorhinus hundsheimensis</i> : mandible fragment with right P ₃ (EQP Q1 TP1 B) 230
Fig 129	<i>Myotis mystacinus</i> : left upper canine (Q1 GTP 16 BS86-24 Unit 4c) 212	Fig 156	<i>Stephanorhinus hundsheimensis</i> : left M ₃ (EQP Q1 TP1 C) 230
Fig 130	<i>Myotis mystacinus</i> : right upper canine (Q2 GTP 3 BS87-273 Unit 4c) 213	Fig 157	<i>Stephanorhinus hundsheimensis</i> : right humerus (Q2 GTP 17 F64 Unit 4c) 230
Fig 131	<i>Myotis bechsteini</i> : left upper incisor (Q2 GTP 3 BS86-36 Unit 4c) 213	Fig 158	<i>Stephanorhinus hundsheimensis</i> : right ulna (Q1/B F412 Unit 4) 231
Fig 132	<i>Myotis bechsteini</i> : left lower canine (Q1/B BS87-247 Unit 4c) 213	Fig 159	<i>Stephanorhinus hundsheimensis</i> : right astragalus (EQP Q2 TP4 B3 Unit 5a) 231
Fig 133	<i>Canis lupus</i> : skull (Q1/A F3445 Unit 4b) 214	Fig 160	<i>Cervus elaphus</i> : rearticulated lower hind limb bones (Q2 TP4 and TP6) 233
Fig 134	<i>Canis lupus</i> : left mandible (Q2 TP4 F2 Unit 4c) 214	Fig 161	<i>Dama dama</i> : left P ⁴ (Q1/B F8 Unit 4c) 234
Fig 135	<i>Canis lupus</i> : measurement comparisons of British Pleistocene with recent European wolf 216	Fig 162	<i>Dama dama</i> : left M ¹ (Q1/B F12 Unit 4c) 235
Fig 136	<i>Ursus deningeri</i> : right mandible (Q2/B F50 Unit 4c) 217	Fig 163	<i>Dama dama</i> : left M ² (Q1/B F4 Unit 4c) 235
Fig 137	<i>Ursus deningeri</i> : left humerus (Q1 TP220-80 Unit 4c) 218	Fig 164	<i>Dama dama</i> : right mandible with P ₃ -M ₃ (Q1/B F264 Unit 5a) 235
Fig 138	<i>Ursus deningeri</i> : rearticulated tarsals and metatarsals (Q1/B Unit 4c) 218	Fig 165	<i>Capreolus capreolus</i> : right antler (Q2 SEP 2 F15 Unit 4c) 236
Fig 139	<i>Ursus</i> spp: bivariate plot of length against width of P ₁ 219	Fig 166	<i>Capreolus capreolus</i> : right mandible with P ₃ -M ₃ (Q2 GTP 3 F19 Unit 4c) 236
Fig 140	<i>Ursus</i> spp: histograms of length of M ₁ 219	Fig 167	<i>Capreolus capreolus</i> : comparison of Boxgrove scapula fragment (Q2 GTP 17 F46 Unit 4c) with that of a Recent roe deer from West Sussex 238
Fig 141	<i>Ursus</i> spp: histograms of length of M ₂ 219	Fig 168	<i>Capreolus capreolus</i> : comparison of Boxgrove calcaneus (Q2 GTP 3 F18 Unit 4c) with that of a Recent roe deer from West Sussex 238
Fig 142	<i>Mustela erminea</i> : right mandible (Q2 GTP 3 BS87-136 Unit 4c) with P ₃ -M ₃ buccal view 220	Fig 169	<i>Capreolus capreolus</i> : measurement comparisons of British Pleistocene and early Holocene with Star Carr roe deer (early Holocene) 238
Fig 143	<i>Mustela</i> spp: histograms and ranges of M ₁ length of early Middle Pleistocene and Recent small mustelids 221	Fig 170	<i>Megaloceros cf verticornis</i> : left P ² and P ³ (Q1/A F3357 and F3325 Unit 4b) 239
Fig 144	<i>Mustela lutreola</i> : left mandible with I ₃ , C ₁ -M ₂ (Q1 GTP 8 Unit 4c) 222		
Fig 145	<i>Meles</i> sp: left mandible with M ₁ (Q1/A F227 Unit 4c) 222		
Fig 146	<i>Meles</i> sp: left M ³ (Q1/A F1740 Unit 4c) 224		
Fig 147	<i>Crocota crocota</i> : fourth cervical vertebra fragment (Q2 GTP 3 F12 Unit 4c) 224		
Fig 148	<i>Crocota crocota</i> : bivariate plot of greatest length against greatest breadth across the cranial articular process of the		

Fig 171	<i>Megaloceros</i> cf <i>verticornis</i> : right M ¹ -M ³ (Q1/A F3325, F3355, F3356).....	239	Fig 200	<i>Sicista</i> spp: distribution of living northern birch mouse (<i>S. betulina</i>) and southern birch mouse (<i>S. subtilis</i>) compared with the Pleistocene distribution of <i>Sicista</i> spp.....	265
Fig 172	<i>Megaloceros</i> spp: length-width scatter-plots of upper premolars and molars of giant deer from Boxgrove, West Runton (<i>Megaloceros</i> sp 'A' and 'B', Cromerian <i>sensu stricto</i>), Kent's Cavern (<i>M. giganteus</i> , Devensian), and Ireland (<i>M. giganteus</i> , Devensian Lateglacial).....	240	Fig 201	<i>Sicista</i> spp: ratio diagram for measurements of recent and fossil birch mouse on log difference scale.....	266
Fig 173	<i>Megaloceros</i> spp: log ratio diagram showing the relative proportions in the upper dentition of giant deer.....	241	Fig 202	<i>Apodemus</i> spp: bivariate plot of length against width of <i>Apodemus sylvaticus</i> and <i>A. maastrichtiensis</i> molars from Boxgrove.....	268-9
Fig 174	<i>Bison</i> sp: left M ¹ or M ² (EQP Q1 TP1 F22).....	242	Fig 203	<i>Apodemus</i> spp.....	271
Fig 175	<i>Bison</i> sp: left metacarpal (Q2 GTP 17 F137 Unit 4c).....	242	Fig 204	<i>Lepus timidus</i> : right lower incisor (Q2 GTP 3 BS86-35 Unit 5a), cross-section.....	271
Fig 176	<i>Bison</i> sp: rearticulated forelimb bones (Q2 GTP 17 Unit 4c).....	243	Fig 205	<i>Lepus</i> spp and <i>Oryctolagus cuniculus</i> : bivariate plot of bucco-lingual width against mesio-distal length of lower incisor.....	272
Fig 177	<i>Sciurus</i> sp: left M ₃ (Q2 GTP 3 BS87-308).....	245	Fig 206	<i>Lepus timidus</i> : right P ₃ (Q2 GTP 17 Unit 5a).....	273
Fig 178	<i>Sciurus</i> spp: bivariate plot of M ₃ length against width in Pleistocene and Recent squirrel species.....	245	Fig 207	<i>Lepus timidus</i> : right P ³ fragment (Q1/A BS87-92 Unit 4b).....	273
Fig 179	<i>Myopus schisticolor</i> and <i>Lemmus lemmus</i>	245	Fig 208	<i>Lepus timidus</i> : right M ² (Q1/A F255 Unit 5a/6).....	273
Fig 180	<i>Myopus schisticolor</i> and <i>Lemmus lemmus</i> : discriminant function plotted against molar length as a percentage of Recent <i>Lemmus lemmus</i>	246	Fig 209	<i>Oryctolagus</i> cf <i>O. cuniculus</i> : right upper incisor (Q2 SEP 2 Unit 5a), cross-section.....	273
Fig 181	<i>Lemmus lemmus</i>	247	Fig 210	Taxonomic Habitat Index distributions of faunas from Boxgrove arranged in stratigraphic order.....	275
Fig 182	<i>Clethrionomys glareolus</i>	247	Fig 211	Summary of the Taxonomic Habitat Index for the main fossiliferous deposits at Boxgrove plotted as a cumulative percentage frequency graph.....	276
Fig 183	<i>Clethrionomys rufocanus</i>	248	Fig 212	Taxonomic Habitat Index spectra for Recent European habitats.....	277
Fig 184	<i>Plionomys episcopalus</i>	249	Fig 213	Percentage frequency histograms of small mammal taxa.....	278
Fig 185	<i>Arvicola terrestris cantiana</i>	249	Fig 214	Percentage frequency histograms of major vertebrate groups in the Boxgrove sequence.....	279
Fig 186	<i>Microtus (Terricola) cf subterraneus</i>	250	Fig 215	Histograms showing the relative abundance of fish, amphibians, reptiles, birds, insectivores, and rodents.....	280
Fig 187	<i>Microtus agrestis/arvalis</i> : bivariate plot of LT4/LT5 index plotted against M ₁ length for <i>Microtus agrestis</i> and <i>Microtus arvalis</i> from Boxgrove.....	250	Fig 216	Area of sympatry for the Unit 4c small mammals and herpetofauna.....	280
Fig 188	<i>Microtus gregalis: gregaloides</i> and <i>gregalis</i> morphotype.....	251	Fig 217	Taxonomic Habitat Index spectra of two British peak interglacial small mammal assemblages compared with the Taxonomic Habitat spectrum of Unit 4c from Boxgrove.....	281
Fig 189	<i>Microtus oeconomus</i>	252	Fig 218	NRM values of declination, inclination, and intensity plotted in relation to the stratigraphy at the sampling site.....	298
Fig 190	<i>Castor fiber</i> : right mandible.....	253	Fig 219	Changes in direction and intensity of remanent magnetism.....	299
Fig 191	<i>Castor fiber</i> : right P ₁ -M ₃	254	Fig 220	Abundance of calcareous nannofossils in a) GTP 13; b) GTP 35.....	300
Fig 192	<i>Castor fiber</i> : right P ₁ -M ₂	254			
Fig 193	<i>Muscardinus avellanarius</i>	255			
Fig 194	<i>Muscardinus avellanarius</i> : bivariate plot of length against width of M ₁	257			
Fig 195	<i>Muscardinus avellanarius</i> : log ratio diagram for tooth dimensions of recent and fossil hazel dormouse.....	258			
Fig 196	<i>Eliomys quercinus</i> : bivariate plot of length against width of deciduous P ⁴ in recent and fossil garden dormouse.....	259			
Fig 197	<i>Eliomys quercinus</i>	260			
Fig 198	<i>Sicista</i> cf <i>S. betulina</i>	261			
Fig 199	<i>Sicista</i> spp: bivariate plots of length against width in recent and fossil birch mouse.....	262-4			

Fig 221	Location of DSDP Hole 552A, V28-56, Boxgrove, and present day surface current patterns	302	Fig 251	Plan of flints comprising refitting groups D-H from Unit 4c at Q1/B	353
Fig 222	Relative abundances of <i>Gephyrocapsa</i> morphogroups in DSDP Hole 552A in Oxygen Isotope Stages 5 through 13	302	Fig 252	Q2/A excavation in 1983, Brickearth Beds removed down to the surface of Unit 5a	354
Fig 223	Relative abundance of <i>Gephyrocapsa</i> morphogroups in Boxgrove GTP 13, 2.95m through 3.65m in height	302	Fig 253	Q2/A, looking east	354
Fig 224	Relative abundance of <i>Gephyrocapsa</i> morphogroups in V28-56	303	Fig 254	Flintwork scatter in Q2/A east extension	355
Fig 225	Three-dimensional plan of section locations of Quarry 1/A	312	Fig 255	Flint scatter affected by faulting in Q2/A	355
Fig 226	Geology of the sections of Quarry 1/A (location of sections shown on Fig 225)	between pages 312-13	Fig 256	Refitted broken flakes from Q2/A	356
Fig 227	The excavation area of Quarry 1/A	313	Fig 257	Horizontal distribution of refitted broken flakes from Q2/A	357
Fig 228	Isometric plot of the Quarry 1/A Unit 4c surface	314	Fig 258	Main refitting scatter in Q2/A	358
Fig 229	Quarry 1/A: sediments removed down to the surface of Unit 5a, viewed from the east	314	Fig 259	Detail of scatter from Fig 258	358
Fig 230	Quarry 1/A: excavation of Unit 4c, viewed from the east	315	Fig 260	Horizontal distribution of flakes refitted by ventral/dorsal contact from Q2/A	359
Fig 231	Frequency diagram of flintwork distribution in Unit 4c	317	Fig 261	Refitted nodule from Q2/A	360
Fig 232	Plan of flintwork larger than 20mm in Unit 4c	317	Fig 262	Variability in handaxe shape from Q2/A	360
Fig 233	Refitting flintwork from Unit 4c	319	Fig 263	Refitted tranchet flakes on handaxe 9070 from Q2/A	361
Fig 234	Graph showing distance in metres between refitting pieces	320	Fig 264	Surface topography of the Organic Bed, Unit 5a	363
Fig 235	Rose diagram showing orientation of refits	321	Fig 265	Distribution of macroartefacts	363
Fig 236	Handaxes from Units 4c and 4b at Q1/A	323-6	Fig 266	Distribution of microfaulting across the Organic Bed (Unit 5a) and underlying deposits	363
Fig 237	Scatter in Unit 4b prior to excavation; inset shows flint density	327	Fig 267	Plots of macroartefact frequency, depth, size, and weight (n=573)	365
Fig 238	Spall distribution of scatter in Unit 4b	328	Fig 268	Log (% SSE) plots indicating characteristics of a hypothetical distribution	366
Fig 239	Unit 4b scatter after first cleaning	329	Fig 269	Log (% SSE) plot of macroartefacts (n=573)	367
Fig 240	Sequential excavation of the Unit 4b scatter 330-4		Fig 270	Log (% SSE) plots of individual macroartefact classes	367
Fig 241	Main refitting groups from Unit 4b scatter	336-38	Fig 271	Plots of optimal cluster solutions	368
Fig 242	Refitting group B from Unit 4b scatter	339	Fig 272	Density of macroartefacts in 0.5 x 0.5m excavation units	369
Fig 243	Flake densities for Trenches 1 and 2 (Unit 4c) at Q1/B; inset shows plan of Q1/B trenches	340	Fig 273	Density of microartefacts in 0.5 x 0.5m excavation units	370
Fig 244	Flint and fauna distributions at Q1/B Trench 1	341	Fig 274	Composite distribution of lithic macroartefacts and faunal remains	371
Fig 245	Flint and fauna distributions at Q1/B Trench 2	342	Fig 275	Plan of excavated areas at Quarry 2 GTP 17	372
Fig 246	Flint and fauna distributions at Q1/B Trench 3	343	Fig 276	GTP 17, looking east	373
Fig 247	Flint and fauna distributions at Q1/B Trench 4	344	Fig 277	Excavated trench in Q2 GTP 17	373
Fig 248	Hammerstone and flake tools from Unit 4c	345	Fig 278	Handaxes from Unit 4c at GTP 17	374
Fig 249	Handaxes from Unit 4c at Q1/B	346-7	Fig 279	Plan of flintwork and faunal remains from Unit 4b at GTP 17	between pages 374-5
Fig 250	Refitting groups A-H from Trench 2, Unit 4c at Q1/B	352	Fig 280	Plan of faunal remains from Unit 4b at GTP 17	between pages 374-5
			Fig 281	Flintwork scatter from horse butchery at GTP 17	375
			Fig 282	Detail of Fig 281	375
			Fig 283	Artefact plan of scatter in Fig 281	375
			Fig 284	Ventral/dorsal and break refits from scatter in Fig 281	376

Fig 285	Dense distribution of primary knapping debris at the horse butchery site.....	377	Fig 309	Opposing impact scars, produced during marrow bone breakage.....	398
Fig 286	Handaxe reduction scatter from the horse butchery site.....	377	Fig 310	Cut marks on the zygomatic arch of bear.....	398
Fig 287	Recording the archaeology at GTP 17.....	377	Fig 311	Outline of horse skeleton showing the anatomical location of bone fragments recovered from Q2 GTP 17 Unit 4b.....	399
Fig 288	Excavation at GTP 17.....	378	Fig 312	Location of cut marks on a) skull and b-c) mandible of horse from Q2 GTP 17.....	400
Fig 289	Part of the horse scapula exhibiting semicircular wound, probably from a projectile impact.....	378	Fig 313	Location of cut marks on horse vertebrae and rib from Q2 GTP 17.....	401
Fig 290	Handaxe thinning flake in basal sediments of Marine Cycle 3 at GTP 13.....	378	Fig 314	Position of cut marks on horse scapula from Q2 GTP 17.....	402
Fig 291	Cleaned section through the beach deposits and overlying Chalk Pelletl Beds at GTP 25.....	379	Fig 315	Cut marks on the pelvis of horse from Q2 GTP 17.....	402
Fig 292	Relationship of the flint scatter to the chalky gravels.....	379	Fig 316	Location of cut marks on horse humerus (a-c) and radius (d-g) from Q2 GTP 17.....	403
Fig 293	Vertical view of the refitting flint scatter.....	379	Fig 317	Location of marrow bone impact damage on horse limb bones from Q2 GTP 17.....	403
Fig 294	Detail of Fig 293; note the sharpness of the flakes.....	380	Fig 318	Cut marks on horse femur from Q2 GTP 17.....	403
Fig 295	a) 'Rough-out' from the gravels of the Eartham Formation, b) Handaxe from the head gravel deposits of the Eartham Formation (see Fig 298).....	381	Fig 319	Horse humerus from Q1/B showing the location of filleting, disarticulation, and impact scars.....	404-5
Fig 296	The head gravel deposits containing refitting flintwork in the western edge of Quarry 2.....	383	Fig 320	Rhinoceros left lower third molar with cut marks on enamel.....	406
Fig 297	Refitting flintwork from the mass movement head gravels.....	383	Fig 321	Rhinoceros mandible fragment from Q1/B showing location of fragment and position of disarticulation marks on the condyle.....	406
Fig 298	Handaxe from the mass movement head gravels.....	383	Fig 322	Rhinoceros scapula showing the location of filleting and disarticulation cut marks.....	406
Fig 299	Different percussors used in the knapping experiments.....	386-7	Fig 323	Rhinoceros pelvis showing the portions of the pelvis present and the location of disarticulation and filleting marks.....	407-8
Fig 300	Flake attributes potentially significant in identifying percussor.....	388	Fig 324	Rhinoceros right calcaneus showing the location of disarticulation cut marks and carnivore, possibly hyaena, gnawing which occurred after the butchery of the animal.....	408
Fig 301	Diagram of flake showing measured attributes.....	389	Fig 325	Scanning electron micrograph showing the truncation of a cut mark (a) by carnivore gnawing (b) on the rhinoceros calcaneus illustrated in Fig 324.....	408
Fig 302	Plot of positions of experimental units along first two components of CVA 2.....	391	Fig 326	Skull fragments of red deer from GTP 17 showing the location of the pieces and cut marks close to the base of the antler produced during skinning.....	409
Fig 303	Plot of positions of experimental units and controls along first two components of CVA 3.....	392	Fig 327	Skull fragments of a female red deer with cut marks.....	410
Fig 304	Plot of positions of experimental units and archaeological samples along first two components of CVA 3.....	394	Fig 328	Red deer left upper second molar with cut marks on buccal face.....	410
Fig 305	Scanning electron micrograph of a cut mark on a fragment of red deer skull from Q1/B (magnification x75).....	396			
Fig 306	Sediment scratches on vertebra fragment from Q2 GTP 17 (magnification x75).....	396			
Fig 307	Scrape marks, probably produced during periosteum removal, on the shaft of a horse humerus from Q1/B.....	397			
Fig 308	Impact damage produced during marrow bone breakage on the shaft of a horse humerus from Q1/B.....	397			

Fig 329	Cervid rib fragment (proximal end) showing location of cut marks	410	Fig 334	Scanning electron micrograph of flint chip (arrowed) embedded within a cut mark	414
Fig 330	Red deer proximal radius fragment showing disarticulation cuts and impact mark	411	Fig 335	Red deer metacarpal showing the location of the fragment and position of opposing impact damage	415
Fig 331	Red deer femur showing anatomical location of the conjoining fragments and position of scrape and cut marks	411	Fig 336	Red deer metatarsal showing location of fragments and impact damage and cut marks	416
Fig 332	Red deer tibia shaft fragment with cut marks produced during filleting and marrow bone impact mark	412–13	Fig 337	Red deer sized cervid first phalanx showing location of cut marks	416
Fig 333	Cervid tibia showing location of the fragment and position of cut marks	414	Fig 338	Giant deer teeth with cut marks on buccal and lingual part of the crown	417
			Fig 339	The hominid tibia from Q1/B	420–1

Tables

1	Characteristics of atmospheric-based climatic forcing during the Pleistocene	5	17	Mineralogical comparison of coarse silt (16–63µm) fractions from selected Boxgrove samples, with loesses of three different ages	118
2	Penck and Bruckner's 1909 northern alpine subdivision of glacials and interglacials	6	18	Thin section sample list	119
3	Stratigraphic table of the British Quaternary	6	19	Percentage of organic carbon and calcium carbonate, and layer designation at Boxgrove	120
4	Isotope stratigraphy, magnetostratigraphy, and geochronology for the last 1.2myr of the Quaternary period	7	20	Boxgrove grain size data	124
5	Revised geochronological correlation for part of the Middle and Late Pleistocene	8	21	Summary of the stratigraphy at Boxgrove	125
6	Chronostratigraphy and lithostratigraphy for British Geological Survey Sheet 317/332: Chichester and Bognor	22	22	Stratigraphy at GTP 10 (thin section 5) according to soil micromorphology	133
7	The Sussex Chalk biostratigraphy and lithostratigraphy	23	23	Stratigraphy in upper part of GTP 13 (thin sections 8, 9, 10, and 11), according to soil micromorphology	133
8	Chronostratigraphy and lithostratigraphy of the Middle Pleistocene and Upper Cretaceous deposits of the West Sussex Coastal Plain, in the Boxgrove area	30	24	Soil micromorphology and interpretation	136
9a	Correlation between lithostratigraphy, unit numbers, and sediment description/interpretation	32	25	Unit 11: brief field description and location of thin section samples	147
9b	Detailed subdivision of sediments in Quarry 2 around GTP 25	33	26	The vertebrate fauna from Boxgrove	158–9
10	Summary of resistivity data	40	27	Distribution of ostracods in the Slindon Sand and Slindon Silt Members at GTP 13	166
11	Clast lithological analysis data from gravels in the Boxgrove area	102	28	Distribution of foraminifera in the Slindon Sand and Slindon Silt Members at GTP 13	167
12	Angular/roundness categories	103	29	Non-marine mollusca from Eartham Quarry, Boxgrove	171
13a	Angular/roundness of flint from the Boxgrove raised beach and other Sussex beaches	104	30	Marine mollusca from Eartham Quarry, Boxgrove	173
13b	Angular/roundness of flint, using the same samples as Table 13a but shown as % total broken flint	105	31	Stratigraphic distribution and abundance of fish from Boxgrove	177
14	Boxgrove sediment samples, particle size distribution, and chemical composition	113	32	Seriation of fish taxa	180
15	Boxgrove sediment samples, composition of fine sand (63–250µm) fractions	114	33	List of Boxgrove herpetofauna by unit	186
16	Boxgrove sediment samples, composition of coarse silt (16–63µm) fractions	115	34	Skeletal element representation of dabbling ducks (<i>Anas</i> sp) at Boxgrove (all units)	194
			35	Skeletal element representation of house sparrow sized passerines at Boxgrove (all units)	194
			36	Numbers of skeletal elements of birds per taxa or size category for the different sedimentary units in Quarry 1	195
			37	Numbers of skeletal elements of birds per taxa or size category for the different sedimentary units in Quarry 2	195

38	<i>Erinaceus</i> sp: measurements of teeth	202	65	<i>Capreolus capreolus</i> : measurements of postcrania and teeth	237
39	Comparative measurements (mm) of the coronoid process height and condyle in Recent and fossil <i>Neomys</i> spp	204	66	<i>Megaloceros</i> cf <i>verticornis</i> : measurements of teeth	240
40	Dimensions of Boxgrove <i>Sorex minutus</i> mandibles compared with British and European fossil material and a Recent sample from Poland	205	67	<i>Bison</i> sp: measurements of postcrania	243
41	Measurements (mm) of <i>Sorex runtonensis</i> mandibles from Boxgrove	205	68	Comparisons of postcranial measurements (mm) in British early Middle Pleistocene <i>Bison</i>	243
42	Comparisons of coronoid height measurements in Pleistocene <i>Sorex runtonensis</i> , <i>Sorex</i> sp from Barnham (Hoxnian) and Recent <i>S. araneus</i>	206	69	Comparative measurements of <i>Sciurus</i> sp M_1	244
43	Mandible measurements (mm) of <i>Sorex (D.) savini</i> from Boxgrove	208	70	Comparative femur measurements of <i>Sciurus</i> sp	244
44	Comparative measurements (mm) of the coronoid process height in early Middle Pleistocene <i>Sorex (Drepanosorex)</i> spp	208	71	Comparative lower incisor measurements of <i>Sciurus</i> sp	244
45	<i>Talpa</i> spp: measurements (mm) of Pleistocene and Recent mole humeri	209	72	Stratigraphic occurrence of <i>Lemmus</i> and <i>Myopus</i> at Boxgrove	246
46	Comparative measurements of Recent and fossil <i>Plecotus</i> spp	210	73	Comparative measurements of M_1 (mm) of <i>Clethrionomys glareolus</i> from Boxgrove and Poland (Recent)	248
47	Comparative measurements of the upper canines of <i>Myotis mystacinus</i> from Boxgrove and Recent specimens from England	213	74	Dental characters of the European red backed voles (<i>Clethrionomys</i> spp)	248
48	Comparative measurements of <i>Myotis bechsteini</i> from Boxgrove and Recent specimens from England	213	75	Comparative measurements of M_1 in <i>Phiomys episcopalis</i>	249
49	<i>Canis lupus</i> : measurements of postcrania, mandibles, and teeth	215	76	Comparative measurements of M_1 in <i>Microtus (T.) subterraneus</i>	250
50	Comparative measurements of the lower carnassial in British Pleistocene and Recent <i>Canis lupus</i>	217	77	Comparison of M_1 length of <i>Microtus agrestis</i> from Boxgrove and from Poland (Recent)	251
51	<i>Ursus deningeri</i> : measurements of postcrania and teeth	218	78	Comparison of M_1 length of <i>Microtus arvalis</i> from Boxgrove and from Poland (Recent)	251
52	<i>Mustela erminea</i> : measurements of teeth	220	79	Comparative measurements of M_1 in <i>Microtus gregalis</i> and <i>M. gregalis</i> (' <i>gregaloides</i> ' morphotype)	252
53	<i>Mustela lutreola</i> : measurements of teeth	221	80	Comparative measurements (mm) of M_1 in <i>Microtus oeconomus</i>	252
54	<i>Meles</i> sp: measurements of mandible and astragalus from Boxgrove	223	81	Measurements of upper and lower dentitions of <i>Castor fiber</i> from Boxgrove	253
55	Comparative measurements of dentition in Recent and fossil <i>Meles</i> spp	223	82	Comparison of morphotypes in P^1 , M^1 , and M^2 of <i>Muscardinus avellanarius</i> from Boxgrove and four Recent populations	255
56	<i>Meles</i> spp: comparative measurements of lower carnassial in Recent and fossil sample	224	83	Measurements of lower cheek teeth of <i>M. avellanarius</i> from Boxgrove and Recent comparative specimens	256
57	Measurements of fourth cervical vertebra from Pleistocene and Recent <i>C. crocuta</i>	225	84	Measurements of upper cheek teeth of <i>M. avellanarius</i> from Boxgrove and Recent comparative material	256
58	<i>Panthera leo</i> : comparative measurements of midshaft diameters (mm) in fossil and Recent lion	226	85	<i>Eliomys quercinus</i> : measurements of dP^1 in Recent comparative specimens from Spain and France compared with Boxgrove	260
59	<i>Equus ferus</i> : measurements of teeth	227	86	Measurements of <i>Sicista</i> cf <i>betulina</i> cheek teeth from Boxgrove	267
60	Measurements of <i>S. hundsheimensis</i>	229	87	Measurements (mm) of <i>Apodemus maastrichtensis</i> molars from Boxgrove	267
61	<i>Cervus elaphus</i> : measurements of postcrania and teeth	232	88	Dental characters of <i>Apodemus maastrichtensis</i> and European <i>Apodemus</i> spp	267
62	Comparison of M_3 length of <i>Cervus elaphus</i> from Swanscombe, Hoxne, Star Carr, and Boxgrove	233	89	Occurrence of British Pleistocene <i>Apodemus</i> : a summary of species and localities	270
63	<i>Dama dama</i> : measurements of teeth	234			
64	Comparison of M_3 length (mm) in Recent and fossil <i>Dama dama</i>	235			

90	Measurements (mm) of <i>Apodemus sylvaticus</i> from Boxgrove.....	271	115	Distance between the refits of the different handaxe reduction groups from Q1/A Unit 4c.....	320
91	Comparative measurements of the lower incisor in Recent <i>Oryctolagus cuniculus</i> and in Recent and fossil <i>Lepus timidus</i>	272	116	Handaxes from Q1/A Unit 4b.....	322
92	Measurements (mm) of upper incisors in Recent and fossil <i>Oryctolagus</i> and <i>Lepus</i> spp.	272	117	Number and percentage of individual fragments of flakes from the Unit 4b scatter.....	329
93	Faunal list for the stratigraphic units at Boxgrove.....	283–5	118	Technological attributes of complete flakes from Q1/A Unit 4b scatter.....	329
94	Summary of numbers of identifiable fragments (NISP) and minimum number of individuals (MNI) of small mammals.....	286–7	119	Refitted breaks from Unit 4b scatter.....	335
95a	Summary of the number of identifiable fragments and of concentration (NISP/kg) for the major vertebrate groups from the Boxgrove sequence.....	288	120	Ventral/dorsal refits from Unit 4b scatter. .	335
95b	Summary of the taphonomy of the Boxgrove mammal faunas.....	289	121	Comparison of frequency of complete flakes between Q1/A and Q1/B, Unit 4c.....	340
96	Activity ratios from Boxgrove bone samples.....	291	122	Assemblage composition from Q1/A and Q1/B Unit 4c.....	340
97	Luminescence age estimates for Boxgrove silt samples.....	293	123	Handaxes from Q1/B Unit 4c.....	348
98	Dose rate data and ED (from un-normalised total integral equal weights data, sample 290) used to calculate age estimate.....	294	124	Refitted broken flakes from Q1/B Unit 4c....	348
99	U-series analyses of sample 519.....	294	125	Ventral/dorsal refits from Q1/B Unit 4c.....	349
100	ESR analysis of samples 519 and 520.....	294	126	Number and percentage of individual fragments of flakes from Q1/B Unit 4c.....	351
101	ESR age estimate of samples 519 and 520.....	295	127	Technological attributes of complete flakes from Q1/B Unit 4c.....	351
102	Amino acid D/L ratios on nucellids from Boxgrove and Waterbeach.....	296	128	Number and percentage of individual flake fragments and complete flakes from Q2/A Unit 4c.....	356
103	Amino acid D/L ratios on littorinids from Boxgrove.....	296	129	Categories of complete flakes from Q2/A Unit 4c by number and percent.....	356
104	Amino acid D/L ratios on miscellaneous species from Boxgrove and Waterbeach.....	296	130	Refitted broken flakes from Q2/A Unit 4c..	361
105	Mean NRM values of declination, inclination, and intensity.....	297	131	Ventral/dorsal refits from Q2/A Unit 4c.....	361
106	Samples collected for studies of calcareous nannofossils.....	300	132	Attributes recorded for experimentally produced flakes.....	389
107	Reworked Cretaceous and Tertiary nannofossils.....	301	133	Groups of flakes produced by different percussors.....	389
108	Biostratigraphically significant mammalian taxa from Boxgrove.....	305	134	Flake attribute means for all of the experimental reduction groups.....	391
109	Number and percentage of individual fragments of flakes from Q1/A Unit 4c.....	316	135	Results of canonical variates analysis 2.....	391
110	Technological attributes of complete flakes from Q1/A Unit 4c.....	318	136	Results of canonical variates analysis 3.....	392
111	Technological attributes of all pieces with edge damage/wear from Q1/A Unit 4c.....	318	137	Flake attribute means for archaeological samples.....	394
112	Handaxes from Q1/A Unit 4c.....	319	138	Summary of hominid modification of large mammal bones.....	396
113	Refitted broken flakes from Q1/A Unit 4c.....	320	139	List of percussion-marked bone fragments.....	397
114	Ventral/dorsal refits from Q1/A Unit 4c.....	320	140	Distribution of humanly modified large mammal bones from the main faunal horizons at Boxgrove.....	399
			141	European Middle and Late Pleistocene hominid sites and lineages.....	417
			142	Boxgrove and comparative tibia dimensions.....	422
			143	Samples for dinoflagellate analysis from GTP 13.....	427

Preface

Sussex, as stated in the summary of the history of research at Boxgrove in this volume, is not especially rich in Lower Palaeolithic sites. There were no early discoveries and Sir John Evans in his first edition of *Ancient stone implements* in 1872 could not record any. Even in his second edition in 1897, apart from one handaxe from the Brighton 'Elephant Bed', there were only a few surface finds noted around East Dean. However, for nearly a century raised beaches had been recognised. So, when Curwen found some handaxes in 1912 at Slindon Bottom there was little to suggest that their discovery would lead eventually to excavation of the Boxgrove site, revealing the largest areas of any undisturbed Lower Palaeolithic land surfaces uncovered in Britain. Also, that such a rare occurrence would be within a stratigraphy that tells a sequence of events that, in itself, is a major contribution to Quaternary studies.

Meticulous excavation, which would have warmed the heart of Wheeler, coupled with modern technology, has culminated in this outstanding volume. Every conceivable aspect is recorded, from sedimentary ripples in the Slindon beds, to nanofossils, reptiles, birds, mammals, the soils, and, of course, the human tibia. These studies are complemented by the archaeology, dating methods, and general conclusions. Irrespective of the ten long years of annual seasons of excavation, it all represents a prodigious labour of scientific endeavour in what is somewhat cursorily described as post-excavation.

Although this is a report for specialists, by specialists, it conveys results which concern any thinking person who would dwell upon the behaviour of their antecedents. I heard a well-known Professor of Archaeology comment that this site has told us more about how people lived half a million or so years ago than any other in Britain, or elsewhere for that matter. It is not that it has produced much that is unusual, but it has adequately demonstrated many things that, when archaeologists are honest, hitherto were matters of intelligent speculation. The ifs, buts, probabilities, and possibilities of conclusions on most of the rare primary context sites of this period, however well excavated, can in many cases now be verified by the evidence so ably recorded, studied, researched, and published in this volume.

The people *were* hunters of large mammals; they *did* hunt with spears; they *did* retain useful objects for future use (curating in archaeological parlance). We knew that they had craftsmen among them with a concept of symmetry, if not beauty. They performed tasks that involved a division of labour and there is much to imply a social order of groups larger than usually imagined working together. The report concludes that their ability to survive and thrive places them closer to modern humans than previously thought.

There is much to suggest that there was little change in the mode of life during the time of Boxgrove until some 40,000 years ago in Europe or, to put it more

accurately, there is little to show that it did change. This implies success rather than stagnation. Thus, it is reasonable to assume that people were behaving in a similar way during that great span of time, depending on the environments they were exploiting. So, the Boxgrove evidence can be safely applied to other Lower Palaeolithic sites, where little is left but discarded flint tools and debitage in derived contexts.

It is a strange coincidence that two sites which have attracted great public attention by discoveries of fossil bones of alleged and genuine antiquity should both be in Sussex: ie Pittdown and Boxgrove. This has prompted an intriguing paper in a recent volume of the county archaeological journal, in which the author (Somerville 1996) notes that the society gave little attention to anything of a palaeolithic nature until Grinsell's paper on the Lower and Middle Palaeolithic periods in Sussex in 1929. Even Pittdown was ignored. It was almost as if such lowly beings who existed during that time were no subject for decent archaeologists. Putting it more realistically, she emphasised that such early prehistory was only seen as the concern of anthropologists and geologists. This was not an attitude restricted to Sussex, but prevalent in most county proceedings and even national ones. It was mainly through the growth of the Prehistoric Society of East Anglia that this dichotomy gradually began to break down. However, its legacy is still with us, but nearly gone.

The first-mentioned Professor of Archaeology has been determined to see it gone forever. His campaign has been to 'demystify the Palaeolithic'. The study of Boxgrove has done much to help to do this. Such is the nature of the evidence that the period is being much more widely seen by non-archaeologists, and even some archaeologists, as something more than gravel sections and flint artefacts.

It is, of course, part of the unbroken line of evolution from the type of life so well exemplified at Boxgrove to whatever surrounds the reader at the moment. The manner in which palaeoarchaeologists conduct their research is epitomised in this report. A glance at the table of contents shows how archaeologists are outnumbered off the actual digging area by scientists engaged in other disciplines. It is this multidisciplinary approach used at Boxgrove, and at other sites in Britain such as High Lodge, Hoxne, Clacton, and Pontnewydd, that is so successful. Coupled with the surge of progress in Quaternary studies during the last few decades, blood is being squeezed out of the archaeological stone. The organisation, effort, and expense of such a large-scale project as Boxgrove is immense and the Institute of Archaeology of University College London, and the state archaeological service, has made this possible.

Such results and a volume such as this can only inspire and guide future research into what is the most important subject confronting us: ourselves.

J J Wymer

Acknowledgements

We would like to thank the landowners, ALIH Farms Ltd, for permission to excavate and for donating the finds to the Natural History Museum and the British Museum. We also thank ARC, the quarry operators, for their constant support and patience during our time at Boxgrove; special reference must be made to the late John Horrocks, Frank Fagan, Siân Holmes, and David Miles. We are beholden to the tenant farmers, Michael and Mark Langmead for the use of Ounces Barn and adjoining facilities. Thanks are also due to the villagers of Boxgrove and Halnaker and to the other inhabitants of the Chichester area for all the help they have given the project, especially Nicholas Brooks, Nicholas Dalton, and Chris Houseman.

The excavation team that worked on the Boxgrove Project included over five hundred students and volunteers from around the globe and we offer our heartfelt thanks for all their efforts. The excavation staff worked tirelessly and thanks are due to the following: Duncan Lees, Louise Austin, Sarah-Jane Wilcock, Liz Dyson, Virginia Neal, Greg Priestly-Bell, Anthony Tynan, Francis Wenban-Smith, Jules Tipper, Sharon Gerber, Indira Mann, Jamie MacKenzie, Alain Chéene, Darren Norris, and Roger Pedersen.

This monograph is the result of a vast collective effort and we would like to acknowledge on behalf of the other contributors, everyone involved in the production of their contributions. We have been ably supported by the staff at the Natural History Museum, namely Barbara West, Chris Stringer, Peter Andrews, Andrew Currant, Fred Greenaway and the other staff of the photographic department, and at the British Museum by Nick Ashton and Jill Cook, and by many members of staff at the Institute of Archaeology, not least Mark Newcomer, Peter Drewett, Barbara Brown, and David Harris and personnel of the Field Archaeology Unit; and to Julian Cross and Perry Hardacre for drawing the flintwork. Members of the Quaternary Research Association have been especially helpful and kind and we are indebted to them for spending the time to both teach us and guide us through the many disciplines that constitute Quaternary research. Don Aldiss, Peter Hopson, and Roy Shephard-Thorn, Ian Wilkinson, and Mark Woods of the British Geological Survey provided immense help on the geology of the Boxgrove area and many hours of stimulating debate.

Assistance has been given to the specialist contributors as follows: Lewis and Roberts would like to thank R Barker for comments on the paper and K Sharp for the drawings. A research grant from Cheltenham and Gloucester College is acknowledged. Simon Colclutt thanks Rupert Cook and Simon Parfitt for drawing the graphic logs. Macphail acknowledges A McConnell and J Brigham for the bulk analysis, and J Brigham and S Bond for SEM and EDXRA work. The Institut

National Agronomique and Stirling University provided thin section manufacture. M-A Courty, N Federoff, P Goldberg, R Kemp, and A McConnell are thanked for assistance with the microfabric interpretations, and J Catt for comments on the text. Whittaker thanks J R Haynes, University of Wales, Aberystwyth, and J E Robinson, University College, London, for their time and opinions, and C A Whittaker for sorting the samples. C G Miller and H Taylor produced the figures. Preece and Bates thank R Shepard-Thorn, British Geological Survey, Keyworth, T Meijer, Rijks Geologische Dienst, Haarlem, and D Reid, Natural History Museum, for useful discussions. Holman acknowledges the National Geographic Society for Grant 415089 to support study of the Boxgrove herpetofauna, and T Petersen for drawing the figures. Harrison and Stewart thank J Bailey, Natural History Museum facility at Tring, for access to the comparative collection. C A Walker, Natural History Museum, and J Bailey gave assistance with the identifications. Parks and Rendell thank S G E Bowman, who kindly arranged for a loan of the British Museum Research Laboratory portable gamma spectrometer. The work was completed during the term of a NERC research training award to D Parks. In David and Lindford's report the sampling was done by the authors, while the labour of subsequent laboratory measurements was undertaken by Dan Shiel and Andy Payne to whom we are most thankful. Mark Noël and the late Tony Clark gave comments on an initial draft of this report, for which we are most grateful. Neither of them are responsible for any errors that remain. Wenban-Smith thanks J McNabb for help with the knapping and recording. J McArdle helped with transformation of raw data and C Orton with the statistical methods. K Lockyear and S Laidlaw took the photographs.

The authors acknowledge with gratitude the funding of the project by English Heritage for excavation, post-excavation, and publicity, together with support and encouragement provided by Geoffrey Wainwright, Roger Thomas, Amanda Chadburn, George Smith, Jon Humble, and Clare de Rouffignac. Individuals who merit recognition for inspiring academic stimulus towards this research include Clive Gamble, David Bridgland, Richard Preece, Philip Gibbard, David Bowen, Wil Roebroeks, Thijs van Kolfschoten, and Alain Tuffreau.

Mark Roberts would like to make a special mention of the following gentlemen from the disciplines of archaeology and Quaternary research. Con Ainsworth, Roy Shephard-Thorn, Antony Sutcliffe, Richard West, and John Wymer; these individuals have been instrumental in introducing me to the subject and nurturing my interest in it. I hope that I may pass on to the next generation, with equal humility, the same knowledge and enthusiasm that they gave to me.

Summary

Between 1983 and 1992 rescue excavations were carried out in Quarries 1 and 2 at Boxgrove in advance of gravel and sand extraction. The results from the excavations that took place between 1983 and 1989 and the ensuing research and analysis are presented in this monograph.

The quarry site at Boxgrove is located 12km north of the current shoreline of the English Channel, in the county of West Sussex in southern England. The Pleistocene sediments at the site sit upon and are contained within a marine platform and chalk cliff cut into the Cretaceous Upper Chalk of the South Downs. These features were formed during a Middle Pleistocene high sea-level event that entailed a marine transgression moving northwards over the deposits of the Lower Coastal Plain and cutting into the south-facing dip slope of the Downs. The marine beach complex associated with this high sea-level attains a maximum elevation of 43.5m OD at the junction of the cliff and the wave-cut platform; this high altitude is likely to be a result of subsequent tectonic activity in the area. Associated with the high sea-level are a marine sand unit, the Slindon Sands, which grades up into a lagoonal regression unit, the Slindon Silts. The known west to east extent of these deposits is in excess of 30km. The Slindon Silts were formed by a combination of marine regression and the partial blocking of the direct path of the sea into a large embayment, formed by the Downs. Although the exact barring mechanism is not yet known, a large salt water, tidally fed lagoon/intertidal flat area was created. At the end of the lagoonal phase a soil developed on the surface of the silts, which represents the most extensive Pleistocene landsurface at the site. Subsequent sedimentation derives from the north of the site, firstly when the soil was flooded with fresh water to create an alder/fen carr and then, secondly, as the soils covering the relict chalk cliff and the downland block to the north of the site were stripped off, as vegetation cover declined under an increasingly severe climatic regime. Finally, under periglacial conditions large amounts of gravel from the chalk cliff and the Tertiary regolith covering the Downs moved downslope as periglacial mass movement deposits. Archaeological material has been found in all of the sedimentary units at the site.

An extensive vertebrate fauna was recovered from the site; analysis of this fauna in conjunction with other environmental evidence supports the framework built up by sedimentological analysis, and points to an open area in front of the cliff that developed from open shore-face through intertidal flats, to grassland, and finally freshwater marsh. The Downland block above the cliff was covered by mixed forest vegetation, which is thought to have become dominated by coniferous woodland by the interglacial/glacial transition.

The site is dated by mammalian biostratigraphy to the last temperate stage of the 'Cromerian Complex'. Precise correlation between terrestrial and deep ocean stratigraphy remains to be attained. However, the best fit for the sediments of the Boxgrove sequence, based upon research in the UK and mainland Europe, is with Oxygen Isotope Stage 13 for the temperate deposits and 12 for the cold. This correlation gives a broad date range of between 524 and 420kyr bp.

The stone tool assemblage, all of which is made from local flint, is dominated by the production of handaxes. There are fewer than 20 flake tools, although categories such as end scrapers, side scrapers, transverse scrapers, and notch scrapers are all represented. The handaxes, which are predominantly ovates, were used to butcher large carcasses such as giant deer, red deer, bison, and rhinoceros. There are no traces of cut marks on any of the bones from smaller animals such as roe and fallow deer, suggesting that the larger animals were deliberately targeted. It is also clear that the hominids at Boxgrove had access to complete carcasses; cut marks from stone tools always underlie secondary carnivore gnawing, and cut marks around the head show that the soft perishable parts inside the skull were still intact when the carcass was procured. Whether the animals were all hunted or partially confrontationally scavenged is as yet unclear but as more evidence is uncovered and research undertaken, then the first option seems more likely. A hominid tibia, discovered in 1993, is described and assigned to the species *Homo cf heidelbergensis*. The find is included in this monograph to complement the other areas of research.

Résumé

Entre 1983 et 1992 des fouilles de sauvegarde ont été entreprises dans les carrières 1 et 2 à Boxgrove avant qu'on ne commence à en extraire du sable et du gravier. Les résultats de ces fouilles, effectuées entre 1983 et 1990, ainsi que les études et analyses qui en ont découlé sont présentés dans ce monographe.

Le site de la carrière de Boxgrove se trouve à 12 kilomètres au nord de l'actuel littoral de la Manche, dans le comté de West Sussex, dans le sud de l'Angleterre. Les sédiments du pléistocène du site reposent sur une plateforme marine, et sont limités par une falaise calcaire taillée dans la craie supérieure du crétacé des South Downs, collines du sud de l'Angleterre. Ces particularités apparurent au cours d'une période de haut niveau marin du milieu du pléistocène qui avait entraîné une transgression marine se déplaçant vers le nord en recouvrant les dépôts de la plaine côtière inférieure et taillant dans le versant sud des Downs. Cet ensemble comprenant la plage marine associée à ce haut niveau marin atteint une hauteur maximale de 43,5m au-dessus du niveau de la mer à l'endroit où se rejoignent la falaise et la plateforme taillée par les vagues; cette altitude élevée semble être une conséquence d'une activité tectonique ultérieure dans cette région. Associée au haut niveau marin on trouve une étendue de sable marin appelée les sables de Slindon, qui devient une lagune de régression, les limons de Slindon. L'aire connue de ces dépôts dépasse les trente kilomètres d'ouest en est. Les limons de Slindon sont le résultat de la régression marine associée à l'obstruction partielle de la route directe à la mer par la formation d'une large baie causée par les Downs. Bien que le mécanisme exact d'obstruction ne soit pas encore connu, il entraîna la formation d'une vaste lagune alimentée par la marée/aire plate entre les marées d'eau salée. A la fin de la phase de lagunage, une couche s'est formée sur la surface des limons qui représente la plus importante étendue du pléistocène du site. La sédimentation qui a suivi provient du nord du site, dans un premier temps quand le sol fut inondé par de l'eau douce pour créer une tourbe d'aulnaie, puis, dans un deuxième temps, quand les sols couvrant ce qu'il restait de la falaise calcaire et le bloc au nord du site furent décapés car la couverture de végétation diminuait sous des conditions climatiques de plus en plus rigoureuses. Finalement, dans des conditions quasi glaciaires de vastes quantités de gravier provenant de la falaise calcaire et le régolithe tertiaire couvrant les Downs ont dévalé la pente en un mouvement de masse de dépôts périglaciaires. On a trouvé du matériel archéologique dans tous les niveaux sédimentaires du site.

On a découvert sur le site une importante faune vertébrée. L'étude de cette faune, en conjonction avec d'autres témoignages relatifs au milieu naturel, confirme la théorie établie à partir des analyses sédimentologiques et révèle une région ouverte devant la falaise qui a évolué passant par les stades suivants: littoral ouvert, plaine entre marées, herbage et finalement marais d'eau douce. La plaine en haut de la falaise était recouverte de forêt mixte qui, à notre avis, semble avoir été dominée par des bois de conifères au moment de la transition interglaciaire/glaciaire.

Grâce à la biostratigraphie mammifère on a pu faire remonter le site à la dernière période tempérée du 'complexe cromérien'. Il nous reste à parvenir à une corrélation précise entre la stratigraphie terrestre et celle des fonds marins. Cependant, le meilleur parallèle en ce qui concerne les sédiments de la séquence de Boxgrove, établi à partir de recherches au Royaume Uni ainsi qu'en Europe occidentale, est avec des isotopes d'oxygène niveau 13 pour les dépôts tempérés et niveau 12 pour la période froide. Cette corrélation nous donne une datation approximative s'étalant entre 524 et 420 milliers d'années bp.

La collection d'outils en pierre, tous fabriqués à partir de silex de la région, consiste surtout en production de coups de poing/bifaces. Il y a moins de 20 outils façonnés sur éclats, bien que des catégories telles que racloirs de bout, de côté, transversal et à encoche soient toutes représentées. Les coups de poing, qui étaient principalement de forme ovale, avaient été utilisés pour découper de grosses carcasses telles que cerfs géants, cerfs communs, bisons et rhinocéros. Il n'y a pas de traces de coupures sur aucun des os provenant d'animaux plus petits tels que daims ou chevreuils, ce qui donne à penser qu'on s'attaquait délibérément aux plus gros animaux. Il est également évident que les hominidés à Boxgrove avaient accès à des carcasses entières car les entailles faites par les outils en pierre se trouvent toujours en-dessous des traces de rongement carnivore secondaire, et les entailles autour de la tête montrent que les parties tendres et périssables à l'intérieur du crâne étaient encore intactes quand ils obtenaient la carcasse. On n'a pas encore éclairci si tous les animaux étaient chassés ou si certains provenaient de confrontation et pillage, mais, au fur et à mesure que nous avançons dans nos découvertes et nos recherches, la première option semble la plus probable.

Un tibia d'hominidé, découvert en 1993, est décrit et attribué à l'espèce *Homo cf heidelbergensis*. Cette trouvaille est incluse dans le monographe afin de compléter les autres domaines de recherches.

Traduction: Annie Pritchard

Zusammenfassung

Von 1983 bis 1992 wurden in den offenen Gruben 1 und 2 von Boxgrove vor dem Kies- und Sandabbau Notgrabungen durchgeführt. In dieser Monographie werden die Ergebnisse der Ausgrabungen von 1983 bis 1989 sowie der folgenden Auswertung und Analyse vorgestellt.

Die offenen Gruben von Boxgrove befinden sich in der Grafschaft von West Sussex in Südengland, 12 km nördlich der heutigen Küstenlinie des Ärmelkanals. Die pleistozänen Sedimente sitzen an dieser Stelle auf und sind enthalten in einer Meeresterrasse und einem Kalkkliff, das in den kreidezeitlichen Oberen Kalkstein der South Downs eingeschnitten ist. Diese Strukturen bildeten sich während eines einmaligen hohen Meeresspiegels im mittleren Pleistozän, mit dem eine marine Transgression verbunden war, die sich nach Norden über die Ablagerungen der unteren Küstenebene bewegte und in den nach Süden ausgerichteten Abhang der Downs einschneidet. Der Meeresstrandkomplex, der mit diesem hohen Meeresspiegel verbunden war, erreicht eine Maximalhöhe von 43,5 m üNN, wo sich das Kliff und die wellenförmig geschnittene Ebene treffen; diese hohe Höhe ist vermutlich das Ergebnis späterer tektonischer Aktivität in dem Gebiet. Mit dem hohen Meeresspiegel ist eine marine Sandeinheit, die Slindon Sande (Slindon Sands), verbunden, die schrittweise in eine rückläufige Laguneneinheit übergeht, die Slindon Schwemmsande (Slindon Silts). Die bekannte West-Ost-Ausdehnung dieser Ablagerungen beträgt mehr als 30 km. Die Slindon Schwemmsande wurden gebildet durch eine Kombination von Meeresrückgang und teilweiser Umlenkung des Meeres in eine große Einbuchtung, die von den Downs gebildet wurde. Was genau den direkten Weg des Meeres blockierte, ist noch nicht bekannt, doch steht fest, daß eine große Salzwasserlagune, die von der Flut mit Wasser versorgt wurde, bzw. ein zwischenezeitliches, flaches Gebiet entstand. Am Ende der Lagunenphase entwickelte sich auf der Oberfläche der Schwemmsande ein Boden, der die am weitesten ausgedehnte pleistozäne Landoberfläche darstellt. Spätere Sedimentierungen kommen von nördlich der Stelle. Die erste ereignete sich, als der Boden mit Süßwasser überflutet war, so daß sich ein Erlensumpfland bildete; die zweite, als die Vegetationsdecke durch ein zunehmend härteres klimatisches Regime zurückgegangen war und die Böden, die das frühere Kalkkliff und den Unterlandblock nördlich der Stelle bedeckten, abgeweht wurden. Unter periglazialen Bedingungen bewegten sich schließlich große Mengen von Kies von dem Kalkkliff und dem tertiären Verwitterungsboden, der die Downs bedeckte, als periglaziale Massenbewegungsablagerungen

hangabwärts. In allen Sedimenteinheiten der Stelle wurde archäologisches Material gefunden.

Außerdem wurde eine ausgedehnte Wirbeltierfauna freigelegt; eine Analyse dieser Fauna, in Verbindung mit anderen umweltgeschichtlichen Anhaltspunkten, unterstützt das auf sedimentologischer Analyse beruhende Grundmodell, und weist auf ein offenes Gebiet vor dem Kliff hin, das sich von einem offenen Uferstrand über ein zwischenezeitliches Watt zum Grasland und schließlich zur Süßwassermarsch entwickelte. Der Unterlandblock oberhalb des Kliffs war mit gemischter Waldvegetation bedeckt, von der angenommen wird, daß sie zur Zeit des Übergangs von der Zwischeneiszeit zur Eiszeit mit Nadelwald bedeckt war.

Die Fundstelle ist durch Säugetierbiostratigraphie in die letzte gemäßigte Phase des Cromerischen Komplexes ("Cromerian Complex") datiert. Eine präzise Korrelation von terrestrischer und Tiefseestratigraphie steht noch aus. Doch auf der Basis von Forschungen in Großbritannien und dem europäischen Festland besteht die beste Übereinstimmung der Sedimente der Boxgroveabfolge mit Sauerstoffisotop Stufe 13 für die gemäßigten Ablagerungen und Stufe 12 für die kalten. Diese Übereinstimmung ergibt einen groben Datierungsbereich von 524 bis 420 tausend Jahren vor heute.

Die Kollektion der Steinwerkzeuge, die alle aus lokalem Feuerstein hergestellt sind, wird beherrscht von der Faustkeilproduktion. Es wurden weniger als 20 Abschlagsgeräte gefunden; darunter sind Endschaber, Seitenschaber, Querschaber und Nasenschaber. Die Faustkeile sind vorwiegend eiförmig und wurden zum Schlachten großer Kadaver, wie z.B. Riesenhirsch, Rotwild, Bison und Nashorn, benutzt. An Knochen kleinerer Tiere, wie z.B. Rehe und Damwild, wurden keinerlei Schnittpuren entdeckt—was darauf hinweist, daß mit Bedacht größere Tiere ausgewählt wurden. Außerdem ist klar, daß die Hominiden von Boxgrove Zugang zu vollständigen Kadavern hatten; Schnittpuren von Steinwerkzeugen liegen stets tiefer als sekundäre Nagespuren von Raubtieren, und Schnittpuren im Kopfbereich zeigen, daß die weichen und leicht verderblichen Teile innerhalb des Schädels noch intakt waren, als die Hominiden sich den Kadaver beschafften. Ob alle Tiere gejagt oder manche in Konkurrenz mit anderen Fleischfressern als Aas ausgeschlachtet wurden, ist noch unklar, doch eine zunehmende Anzahl von Indizien und Studien scheinen die erste Möglichkeit wahrscheinlicher zu machen. Die Tibia (Schienbein) eines Hominiden, die 1993 entdeckt wurde, wird beschrieben und der Spezies *Homo cf. heidelbergensis* zugeordnet. Um die übrigen Forschungsgebiete zu ergänzen, ist dieser Fund in die Monographie miteingeschlossen worden.

Übersetzung: Cornelius Holtorf

Glossary

compiled by D M Jones

allochthonous Not indigenous. A term applied to material (eg sediment, plant remains, nutrients, energy) that did not originate in the place in which it has been found. The opposite term is autochthonous.

arcuate Curved or arched, as in a geological formation or in a morphological feature. An arcuate delta is one in which microtidal wave action is sufficiently strong to redistribute sediment into an arcuate bar along the accumulating delta margin.

bathymetry (also bathometry) The oceanographic equivalent of land topography, that is, the measurement of the depth contours of the seabed or ocean floor from sea-level.

biocoenosis The biotic or living component (the biome) of a biogeocoenosis (or ecosystem: living organisms and their physical and chemical environment). The biocoenosis comprises the phyto-coenosis (primary producers), the zoo-coenosis (secondary producers and/or consumers), and the microbiocoenosis (decomposer organisms, including detritivores). In geological use it refers to the 'life assemblage', ie the fossil remains that represent the former biome, used to interpret the nature of the ancient environment, but normally representing only part of the former biological community.

birefringence The property of isotropic minerals (ie the majority of rock-forming minerals that crystallise in non-cubic systems) that causes their optical and/or other physical properties to vary with the direction from which they are viewed. Birefringence refers specifically to an anisotropic mineral's ability to split plane-polarised light into two rays as it passes through it.

bioturbation The localised disturbance of sediments by living organisms, usually burrowing animals. Its intensity ranges from the complete disruption of the sediment, destroying the sedimentary sequence, to clearly recognisable animal or plant traces (eg burrows, trails, root disturbance). Intense bioturbation normally indicates a well-oxygenated environment with slow rates of deposition.

boudinage structures 'Sausage'-shaped stratigraphic structures. Boudins are formed when competent strata are stretched by geological forces into thick and thin forms ('pinch-and-swell structures'), sometimes to the point of breaking up into lines of lozenge or sausage shapes.

cyclothem (cyclothemic) A unit or set of deposits that has accumulated as the result of cyclic or rhythmic sedimentation. A cyclothem is the entire succession of cyclic deposits; a rhythmic sequence is the repeated set of deposits within the cyclothem.

doggers A large spherical or oblately spherical calcareous concretion as opposed to smaller nodules.

endichnial (forms) or enichnia A form of trace fossil (ichnoform or ichnofossil) comprising the tubes or animal burrows formed within the casting medium; exichnia are **bioturbation** formed outside the main casting medium.

endobiont community A group of organisms living within a substratum or within another living organism (eg within the gut). *Also* endobiotic.

epibiont community A group of organisms living on the surface (eg skin, shell, feathers) of another living organism, or on a surface, as of the sea bottom. *Also* epibiotic.

Enchytraeid(ae) A family of tiny annelid worms of the order Prosothea (class Oligochaeta, phylum Annelida). Most species are land and fresh water animals, but a few are marine; first appeared in the Tertiary Period, beginning *c* 65myr.

euryhaline A term describing an organism that can tolerate a wide range or fluctuation of external salinity. The opposite of **stenohaline**.

exoedaenodonty 'Bulbous' cheek teeth (eg *Drepanosorex* antemolars are distinguished from those of other shrews because they are exoedaenodont).

flaser (bedding) Rock bedding comprising closely interbedded deposits of sand and mud generated by an environment in which current flows vary widely through time or in cycles. Flaser beds (as opposed to wavy and lenticular beds) are characterised by cross-laminated sand and thin mud, clay, or silt drapes over the sand ripples; it is typical of mid tidal flats, where the mud is deposited around high tide when current speed is reduced and clay and silt in suspension is able to settle out.

foraminifera Single-celled marine organisms that secrete a skeleton (test) of varying composition, often calcareous. Measurements of the relative abundances of 'light' and 'heavy' oxygen isotopes can be used to estimate water temperature and the volume of global seawater held in the ice caps at the time they were living. Various types are important zone fossils and several planktonic types are used for regional and global stratigraphic correlations.

foresets The inclined laminations within a cross set, produced by the forward movement of the slip-face in cross-stratification (sedimentary structures formed by the migration of the slip-faces of rippled beds or bars; cf **linguoid**). The inclined laminations are bounded by planar or trough-shaped surfaces and dip at the same angle of repose as the sediments on the ripple slip-face.

gastroliths Rounded, polished stones that are swallowed by some species of reptiles and birds and which aid in digestion by breaking up the food before chemical digestion.

homotaxis A term used to refer to strata from different areas or regions that include similar rock and/or fossil successions but which are *not necessarily* of the same age.

linguoid The term used to describe asymmetrical, tongue-shaped water- or wind-formed ripples characterised by sinuous crests and prominent three-dimensional forms. The migration of linguoid ripples generates trough-shaped cross-stratification (cf **foresets**).

linsen Lenticular bedding, in which the ripples or lenses are discontinuous and isolated both in vertical and in horizontal directions.

meniscate (fills) In geology, these are meniscus-shaped fills, that is, fills in which the normally flat surface of the liquid (eg molten) rock is distorted upwards by surface tension where the liquid has met a solid barrier.

papules Fragments of eroded soil, commonly of a former clay coating or textural feature.

paraconformities A type of unconformity in which strata are parallel, there is little apparent erosion, and the unconformity surface resembles a simple bedding plane. Also known as a nondepositional unconformity.

pedogenesis Soil formation by natural processes, including humification, weathering, leaching, and calcification and other chemical processes.

phytolith A stoney or mineral structure, generally microscopic, secreted by a living plant; often composed of calcium oxalate or opaline silica.

pleochoirism Differential absorption of polarised light by a mineral in different orientations. When viewed in thin section through a microscope in plane-polarised light the mineral's colour changes as the microscope stage is rotated.

polychaete Composed of segments of repeated tissues and organs at intervals along the length of the body, including movable paired appendages (parapodia) on each segment. The Polychaeta are a class of annelid worms, bristleworms, with distinct bristly parapodia. Most are marine, although fresh water and land species also occur. Polychaete worms are most often represented in the fossil record by their burrows, tubes, and paired pharyngeal jaw assemblages; first appeared in the Cambrian Period, beginning c 545myr.

pseudobeds False bedding.

pseudomorphs A secondary or random aggregate mineral formation that has replaced an earlier mineral or organic remain (by coating it) and retained the first mineral's or organic remain's shape.

refractive index A measurement of the refractive property of minerals. As light enters a mineral, its velocity is reduced and its path is refracted. The refractive index n is determined by $\sin I/\sin r$

(where I is the angle of incidence of light from the air into the mineral and r is the angle of refraction within the mineral), or by V/v (where V is the speed of light in the air and v is the speed of light in the mineral).

regolith Unconsolidated, non-cemented, weathered rock material comprising large fragments, mineral grains, and other superficial deposits on solid bedrock.

rhythmites Thin, interlayered bedding, such as tidal bedding or varves indicative of rhythmic deposition/sedimentation.

spreites (from spreiten, German, 'to spread out') Sedimentary laminae caused by animal behaviour (eg feeding, burrowing, or travelling) preserved as trace fossils. Characteristic forms are U-shaped, sinuous traces, blade-like tracks, or spiral trails, left by organisms such as *Diplocraterion*, *Rhizocorallium*, or *Daedalus*.

stenohaline A term describing an organism that can tolerate only a narrow range or fluctuation of external salinity (eg most marine organisms). The opposite of **euryhaline**.

stoss In bedding formed by flowing water the stoss slope is the shallower, up-stream face of the asymmetric bed and the lee slope is the steeper, depositional, down-stream face. In glaciated topography the stoss slope is the smoothly abraded up-glacier face, and the lee slope is the rough, ice-plucked, down-glacier face.

stromatolites A structure in calcareous rocks comprising concentrically laminated masses of calcium carbonate or calcium-magnesium carbonate, which are believed to be of calcareous algal origin; the structures are irregular to columnar and hemispherical in shape and range from one millimetre to several metres in thickness. Stromatolites form in shallow and intertidal sediments and in cross-section appear as thin laminations or 'pancake-like' stacks.

swash/swash zone The swift, turbulent rush of water up the beach when a wave breaks; the swash-zone is the band of beach covered by the breaking waves and their rush of water.

thalweg The line linking the lowest points in a succession of cross-sections along a river channel or its valley.

vughs (or vug) A cavity within rock or sediment, often with a lining of crystalline minerals.

younging seawards A phrase used to describe the direction in which a stratigraphic succession becomes progressively younger (ie deposited more recently), in this case towards the sea. In other words, when the beds were deposited horizontally, those layers now nearest the sea were the latest deposited.

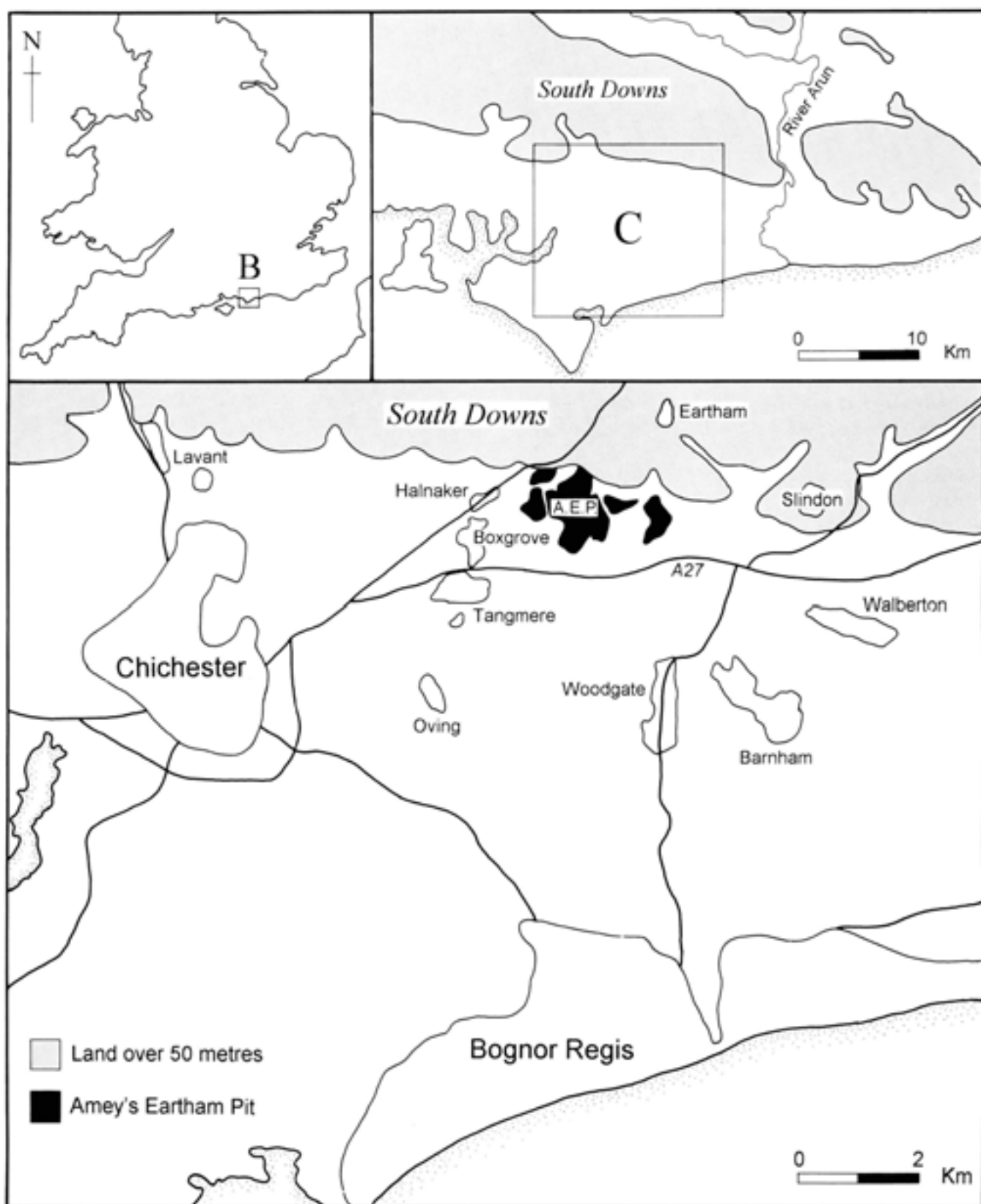


Fig 1a Location of Boxgrove (AEP = Amey's Eartham Pit, Boxgrove) in the United Kingdom, in West Sussex, and in its local setting

1 Introduction

This monograph sets out to provide a framework within which the archaeology at Boxgrove can be accurately studied, by establishing firm lithostratigraphic, chronostratigraphic, and palaeoenvironmental contexts for the material culture of the hominids who lived in the area. The foundations of this framework are the geological and sedimentological analyses, which range from a study of the geology of the area as a whole to the critical examination of important beds within the Boxgrove sequence. The environmental analyses are mainly provided by the study of the vertebrate fauna, which is one of the most extensive from any open air site in Europe. The archaeology recorded here represents the areas and sediments excavated by the project in its early stages (between 1983 and 1992), from Quarries 1 and 2, in advance of gravel and sand extraction. During this phase of the Boxgrove Project an area of 2426m² was excavated for archaeological, geological and environmental purposes. The main excavations and test pits opened up for purely archaeological work have a combined area of 1221m². The volume of sediment removed is far harder to gauge due to the different depths reached at the various excavations. However, the section drawings included throughout the monograph provide a means of measuring the volumes of the major excavations and geological test pits. A larger and more detailed description of the lithics and our interpretation of human behaviour in the Middle Pleistocene will be published in the

future (Roberts et al in prep). The decision to include a chapter on the tibia, which was not found until 1993, was made to provide the reader with an idea of the type of hominid who made tools in and roamed the many changing environments of Boxgrove around half a million years ago.

1.1 Background

The oldest Middle Pleistocene sediments and preserved landsurfaces of the West Sussex Coastal Plain are and have been exposed by quarrying along the southern margin of the dip-slope of the South Downs (Figs 1–3), between the River Lavant (SU 857 088) and the River Arun (TQ 020 070).

The most extensive exposures, and the only place where the complete conformable sequences may be seen, are in the ARC Earham Quarry (SU 918 087/SU 924 085). These workings, which cover an area of some 250 hectares, are located 12km from the present day coastline of the English Channel and 7km east of Chichester, the county town of West Sussex (Fig 1a). The quarry complex straddles the parish boundaries of Boxgrove to the west and Earham to the east but the conformable geological sequences, within which the Palaeolithic archaeology is preserved, are found only in the Parish of Boxgrove after which the site is named (Fig 4).

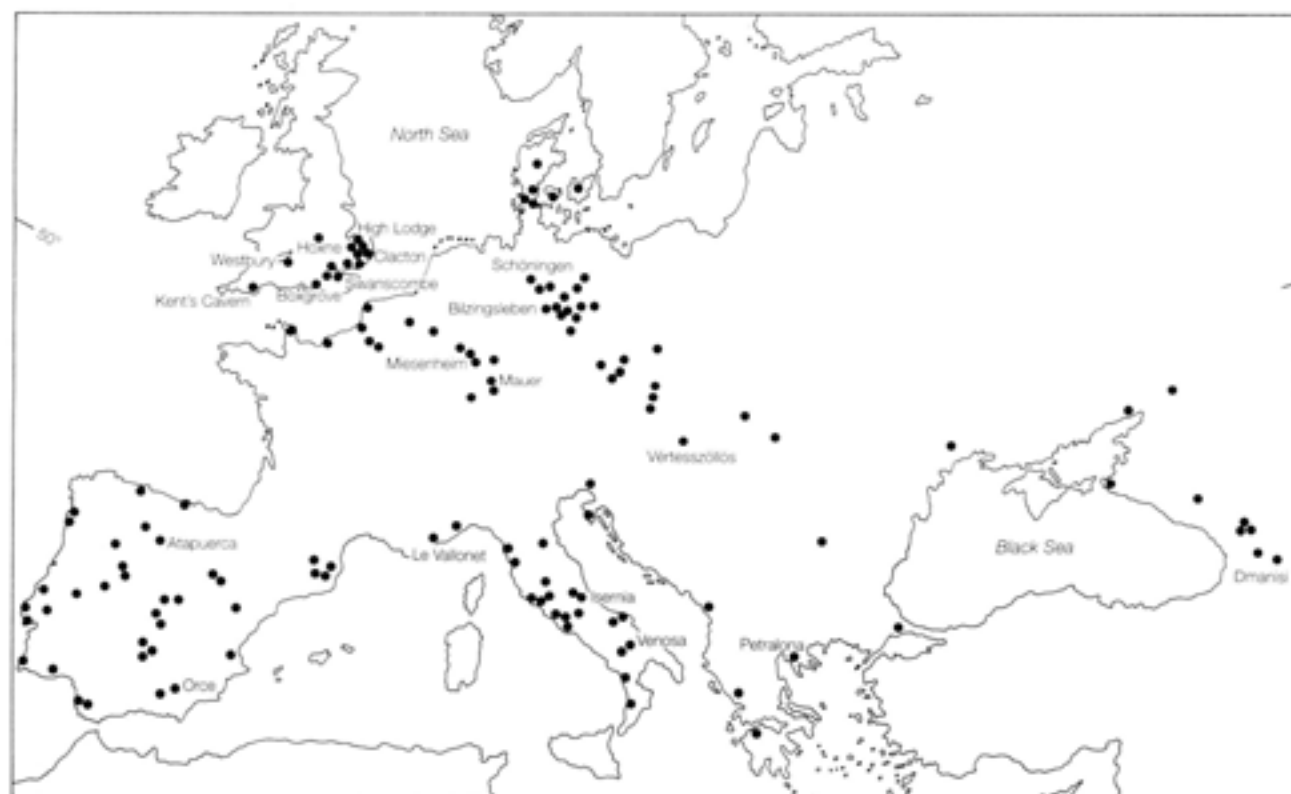


Fig 1b Principal European Early and Middle Pleistocene sites mentioned in the text; other sites from this time period are marked with a dot (after Roebroeks and van Kolfschoten 1995a); the shaded area represents glacial ice cover during the Anglian/Elsterian Stage



Fig 2 Location of towns and rivers mentioned in the text

The interest in the raised beach deposits and their associated Palaeolithic archaeology began in the last century. The area has been a source of gravel working

since medieval times and nearly all of the farms and estates had their own small pits to procure gravel for house building and road metalling. A study of the flint-built houses of the area shows that northwards of a line that approximately follows the Aldingbourne Raised Beach (Fig 3), in the vicinity of Boxgrove, the houses are predominantly built of flint dug either from the solifluction gravels or 'hoggin', as it is locally known, or from the chalk. The choice of stone from these two sources is largely an economic one, with the more important dwellings being constructed from chalk flint which could be properly dressed, allowing for elaborate and ornate facings, whereas the farm buildings and labourers' houses are normally built from undressed flint blocks dug from the gravels. South of the A27 (Fig 1a) most of the houses are built of beach cobbles from the present shoreline or dug from small, local, pits in the raised beaches. In the nineteenth century, programmes of public works resulted in an increasing number of commercial gravel companies opening up larger workings in the area; these in conjunction with the plethora of smaller pits enabled the early researchers to record and map the stratigraphic succession. The process of gravel extraction prior to mechanisation was particularly advantageous to the antiquarians who were interested in the flint tools that workmen were finding as the gravel was both dug and screened. After an interest was registered with the workmen and financial remuneration agreed, artefacts were kept and their locations recorded until such time as the material was

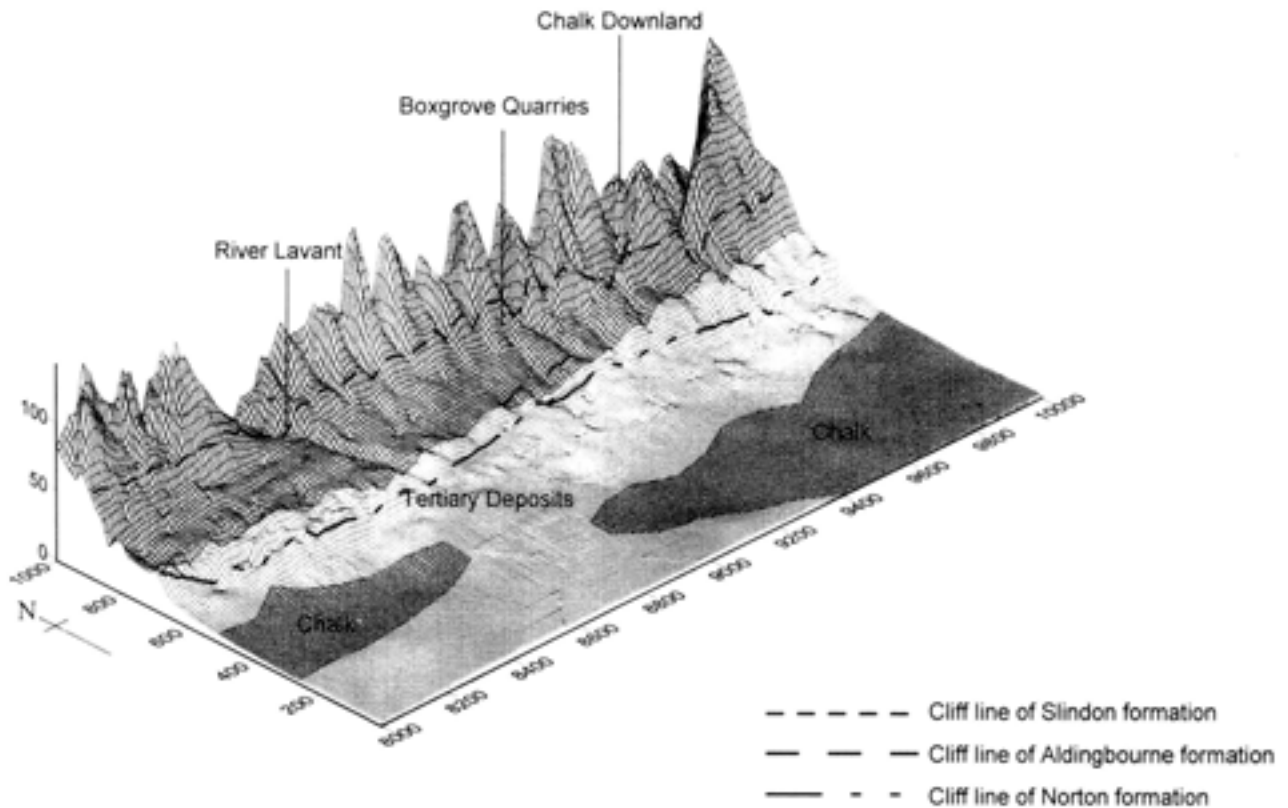


Fig 3 Raised beaches in the Boxgrove area superimposed on the solid geology. The numbers on the x and y axes are Ordnance Survey grid co-ordinates and the y axis gives the height (m) above sea level (OD)

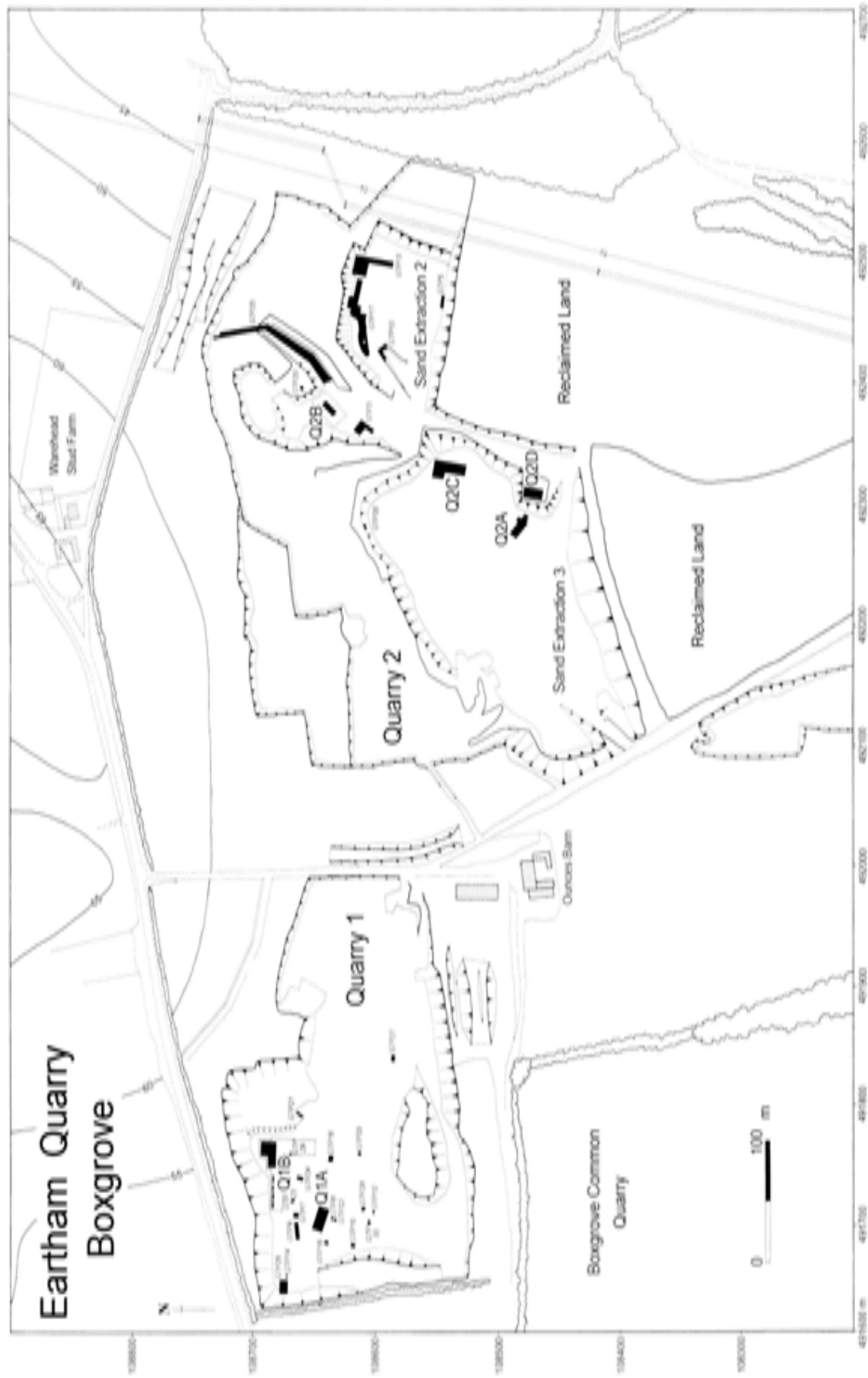


Fig 4 Earsham Quarry, Boxgrove 1995, showing the location of the principal excavation areas (in black)

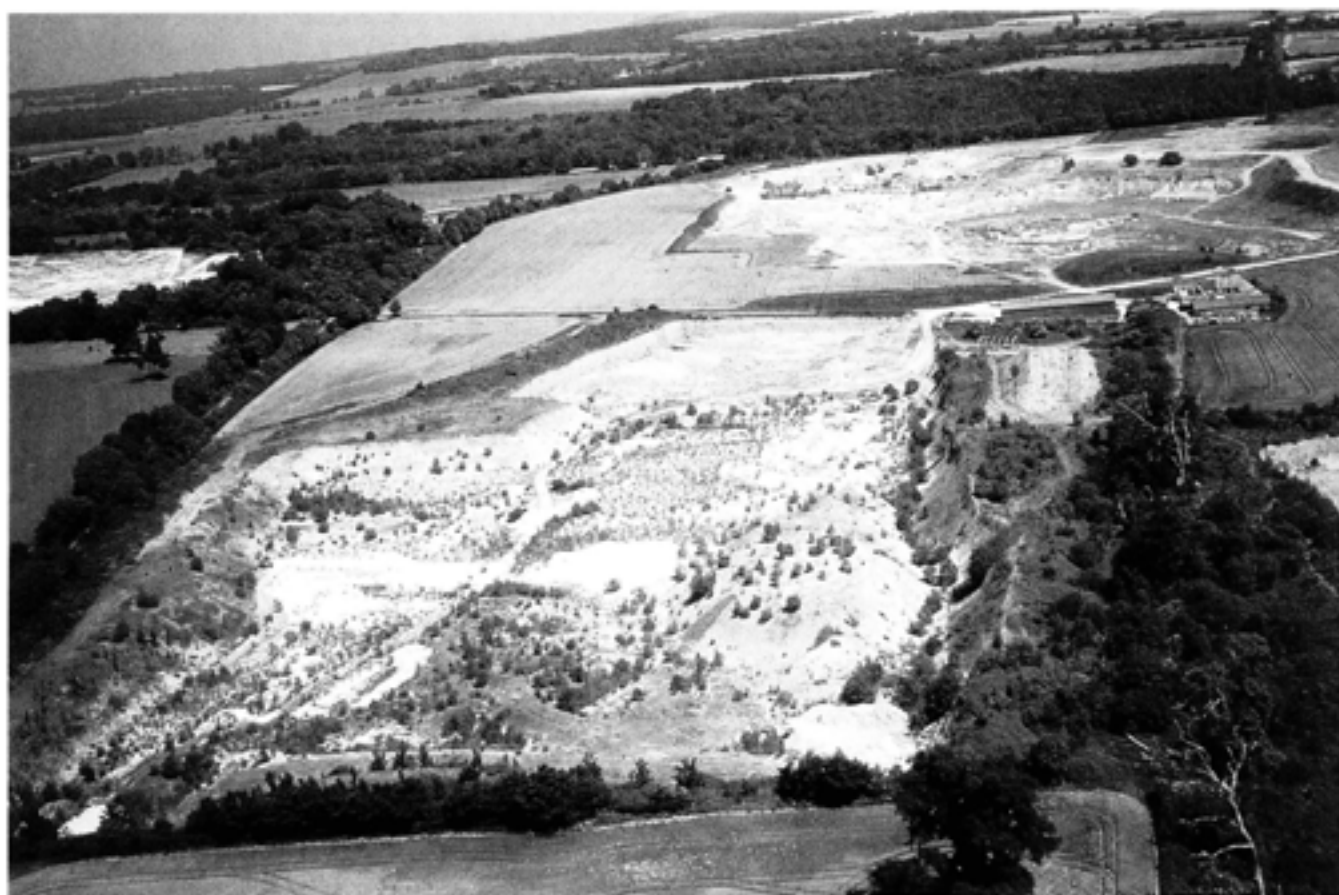


Fig 5 Aerial view of the quarries looking east, Quarry 1 (Q1) in foreground

collected (Wymer personal communication; Calkin 1934). This resulted in the early collections being greatly skewed in favour of tools rather than debitage, a phenomenon visible in many museums' Palaeolithic archives at the present day.

The archaeological and associated environmental material at Boxgrove is found at various levels within deposits of Middle Pleistocene age, and in archaeological terms may be said to be of Lower Palaeolithic date; the lithic industry is typologically known as an 'Acheulean' industry. The sediments at the site are dated biostratigraphically to around 500kyr bp. It should be noted that the word 'site' carries with it certain connotations which are not readily applicable to the contexts at Boxgrove, which may be better described as a series of Pleistocene landsurfaces situated at different levels within the sedimentary sequence. The activities of early man may be seen at many locations across these landsurfaces but these are not thought to represent settled areas with defined activities occurring within them; rather they are seen as random exploitation of the landscape. Therefore in this research the word 'site' will refer to the Quarry complex as a whole and to areas excavated or selected for excavation rather than an area of hominid activity.

Both quarries (Fig 4) contain the complete geological sequence, with the exception of the calcareous spring deposits (Unit 4d) which are only found in

Quarry 1 (Chapter 2.1) (Fig 5). The conformable boundary of the deposits runs east-west through Quarry 2 at a distance of approximately 375m south of Warehead Stud Farm (Fig 4) (Roberts 1986). The main differences between the quarries are that Quarry 2 contains a longer section through the sequence and extends right up to the cliff at its northern end (Fig 6). Quarry 1 (Fig 7) has a much thicker blanket of calcareous cover, which is thought to relate to its position in front of the Downland block. The east-west trending unconformity seen in Quarry 2 has not been located



Fig 6 Quarry 2, looking north past Quarry 2/A (Q2/A) towards GTP 25 and the South Downs



Fig 7 Quarry 1, looking west. Q1/A (covered by the shelter) is in the middle of the quarry

within Quarry 1, but this area does have a large north-south running unconformity at its eastern margin. This feature is probably the result of greater water drainage directly from the cliff in this location. These points are discussed in greater detail in Chapter 2 and will also be covered in a future Boxgrove monograph (Roberts *et al* in prep).

1.2 Lower Palaeolithic archaeology in the context of Middle Pleistocene chronostratigraphy

M B Roberts

The multitude of schemes by which Pleistocene time is and has been divided through the efforts of workers in all the contributory disciplines is often a source of great confusion, especially to archaeologists. Problems arise because the very nature of the research is multidisciplinary and thus reflect the biases of each particular discipline. Other problems that are often encountered involve the use of local terminology and erroneous allocation of stage names and stratigraphic boundaries (Gibbard and Turner 1988; Rose 1988; 1992)

In Europe the presence of hominids coincides with the period of the Quaternary known as the Middle Pleistocene (Roebroeks and van Kolfschoten 1995b), the climatic characteristics of which are described in Table 1.

To study meaningfully the evidence from the multidisciplinary site at Boxgrove we must consider the climatic and geological events of the last 800kyr of time. This figure represents the greater part of the duration of the Middle Pleistocene, *c* 0.79myr–0.12myr bp. The climatic, evolutionary and archaeological events of this period are all pertinent to the resolution of the age and significance of the Boxgrove sediments and their associated hominid activity regimes.

As Quaternary research has developed as a discipline, there has been a corresponding increase in the complexity of the chronostratigraphic record of the Pleistocene period, which, as will become increasingly apparent from this work, is far from resolved. As many

Table 1 Characteristics of atmospheric-based climatic forcing during the Pleistocene (after Whiteman and Rose 1992)

<i>age</i>	<i>characteristics</i>
<i>c</i> 2.2myr–1.7myr bp	Early Pleistocene characterised by low amplitude, non-glacial climatic oscillations
<i>c</i> 1.7myr–0.8myr bp	Early–early Middle Pleistocene characterised by moderate amplitude, mountain glaciations in temperate latitudes
<i>c</i> 0.8myr–present	Middle–Late Pleistocene characterised by high amplitude, low frequency, climatic oscillations with sufficient range and duration to build up ice over mid-latitude lowland regions

of the texts referred to in the following chapters use a differing set of time scales and names for the stages and substages of Pleistocene time, a synopsis is presented in Table 4. The most comprehensive recent work on cross-correlation is contained in the report on the findings of the *International Geological Correlation Programme Project 24, Quaternary Glaciations in the Northern Hemisphere* (Šibrava *et al* 1986). The tasks of linking the Palaeolithic archaeological sequences to the Pleistocene chronostratigraphic time scale are discussed below and by Roberts (Chapter 6.1).

The Swiss zoologist Agassiz (1840a; 1840b) first promulgated the theory of ice ages and suggested that deposits hitherto ascribed to the biblical flood, Diluvium, were more likely to be the results of past glaciations. By the mid-nineteenth century, at least two major glacial advances were recognised in Europe. It then became a logical next step to describe the sediments between the glacial deposits as interglacial. Biological evidence, mainly from fossil mammals and molluscs, suggested that these were warm phases and thus the concept of oscillating temperate and cold periods began to develop.

The most famous and still widely used scheme to describe and categorise the events was devised by Penck and Bruckner (1909), who related the river terrace sequences and glacial moraines in the Northern Alps to four separate glacial episodes (Table 2). The Alpine model was utilised by Quaternary researchers throughout Europe, including Britain, and is still prevalent in the French archaeological literature today. In Britain during the early twentieth century, archaeologists often used the names of French type sites as stage definitions, hence terms like Chelles period and the Le Moustier period (Dewey 1919). This predilection for using archaeological typological nomenclature was applied to the archaeology from the raised beaches in the Sussex area (Roberts Chapter 1.3) and led to problems reconciling the geological succession of the various transgressive marine events. Other descriptions that were used as age equivalent were combinations of

Table 2 Penck and Bruckner's 1909 northern alpine subdivision of glacial and interglacials

age	stage	climate	sub series
youngest	Postglacial	interglacial	Holocene
	Würm	cold/glacial	Upper Pleistocene
	Riss-Würm	interglacial	
	Riss	glacial	Middle Pleistocene
	Mindel-Riss	interglacial	
	Mindel	glacial	
oldest	Günz-Mindel	interglacial	

geomorphological features and altitudes, for example the Thames 100 foot Terrace/Boyn Hill Sea (Zeuner 1945) and the 100 foot Goodwood-Slindon Raised Beach (Reid 1892). River terraces and sea level events became crucial to Pleistocene correlation and dating throughout the twentieth century. They are still today vital research areas in the Quaternary, though the evidence from the studies of these topics is applied differently (cf the work of Gibbard 1985, Whiteman 1992, and Bridgland 1994, on the Thames Valley). Arguably the most comprehensive synopsis of the Pleistocene Period was compiled by Zeuner (1945) in his book *The Pleistocene Period*. On the basis of information available at the time, this book was one of the finest and most useful works on the chronology of the period and was a significant benchmark in multidisciplinary studies.

The first formal definition of the British Quaternary, based largely on the succession in East Anglia, was defined, primarily on palaeobotanical observations, by West (1963). This was developed by the Geological Society of London to form the stratigraphical table of the British Quaternary (Mitchell *et al* 1973, and see Table 3).

The British stratigraphic table (Table 3) has, over the past 20 years, been tested on two main fronts. Firstly the continuous Oxygen Isotope Record (OIS) from the deep sea oceans (Table 4) shows that there were many more major warm and cold climatic fluctuations than had previously been recognised from the continental record. Fourteen stages are recognised during the period of the Middle Pleistocene alone. Secondly, parts of Europe where the continental record was better preserved, for example the Netherlands (Zagwijn *et al* 1971; Zagwijn 1985; 1992) showed that some of the stages of the time scale were in fact complexes that occupied greater periods than single climatic cycles and could thus be further subdivided into actual stages. The 'Cromerian Complex', for example, comprised three cold stages and four temperate stages and the 'Saalian Complex' two cold stages and two temperate stages (Table 5). Inevitably the record of the deep sea stages, which reflects most accurately Pleistocene climatic oscillations, has been applied to the continental record, notably by Šibrava *et al* 1986; Bowen and Sykes 1988; Bowen 1989; 1991; Whiteman and Rose 1992; Rousseau and Puisségur 1990; Rousseau *et al* 1992; Bridgland 1994, to name but a few.

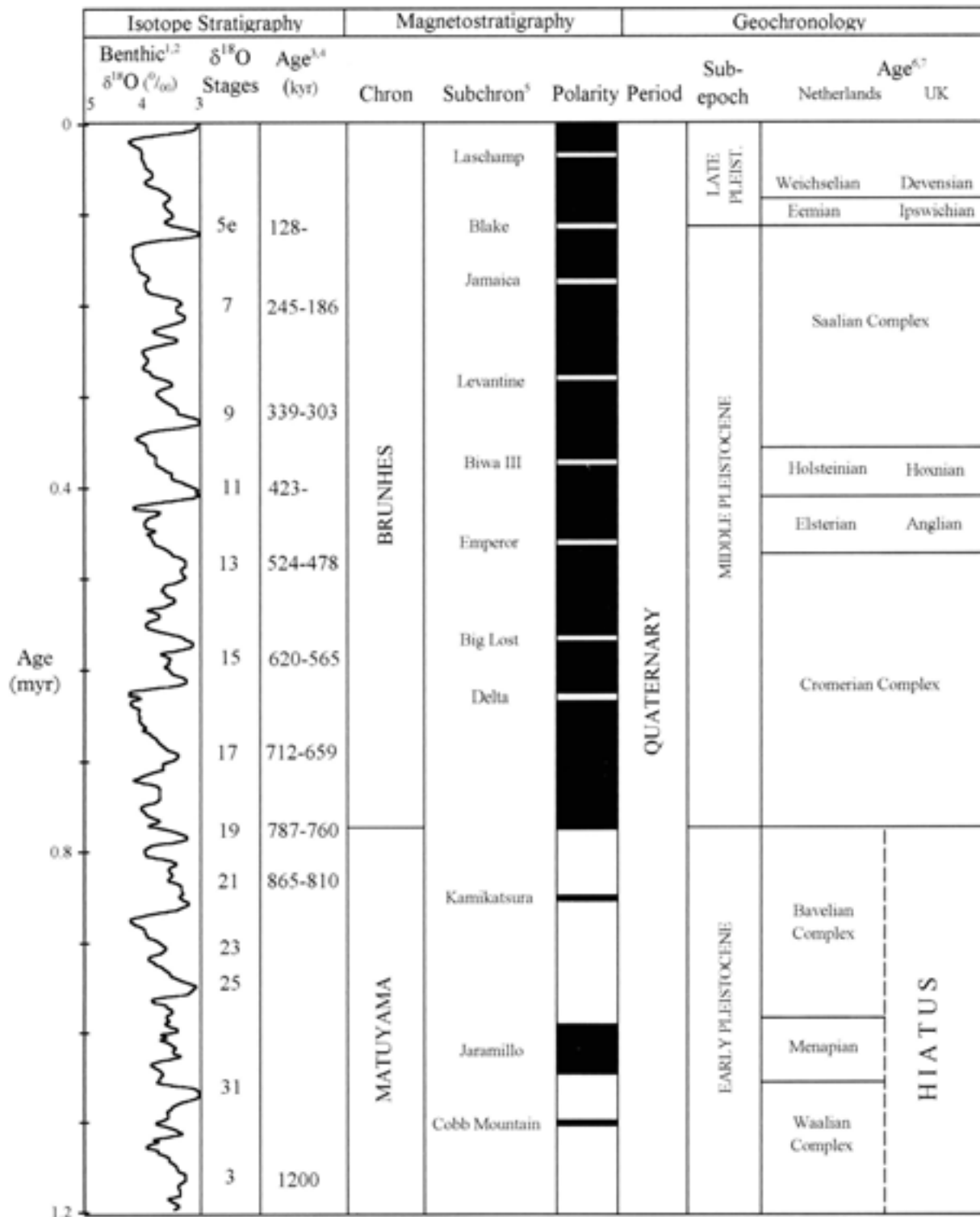
Table 3 Stratigraphical table of the British Quaternary. T=temperate, C=cold

After Mitchell *et al* 1973 and Bowen 1978; for a revised correlation of the lower part of the sequence see Gibbard *et al* 1991 and Tables 4 and 5

stage	European mainland equivalent
T Flandrian	Flandrian
C Devensian	Weichselian
T Ipswichian	Eemian
C Wolstonian	Saalian
T Hoxnian	Holsteinian
C Anglian	Elsterian
T Cromerian	'Cromerian Complex'
C Beestonian	
T Pastonian	

The deep sea cores not only provided a more detailed record than the terrestrial sequences, but also gave evidence for an increased number of cold and warm stages. Thus continental researchers who, as mentioned earlier, were finding evidence of greater stratigraphical complexity in their own work were able to break free from the confines of the sequences established on land. Using the deep sea record for correlation in the Middle and Upper Pleistocene is not without problems; firstly, there are only two fixed points that are recognised both on land and in the oceans. These are the Matuyama/Brunhes magnetic boundary, which is also the boundary between the Lower and Middle Pleistocene (Table 4) (Richmond 1996), and Oxygen Isotope Stage 5e. In the oceanic records this transition was originally thought to have occurred during OIS 19, at around 730kyr bp. However, the boundary dates have been recalibrated to around 790kyr bp (Johnson 1982), leading to a better fit with the continental record. In Europe this magnetic reversal is located in sediments associated with a cold stage (Zagwijn *et al* 1971; Koči *et al* 1973; Koči and Šibrava 1976), and probably represents the cold stage prior to the first interglacial of the 'Cromerian Complex' in OIS 20. The correlation is supported by the position of the boundary in Moselle fluvial gravels of the Kärlich gravel pit unit Bb, in Germany (Brunnacker *et al* 1976; Bosinski *et al* 1980; van den Bogaard *et al* 1989).

The later concordant point between the oceanic and continental records occurs around 125kyr bp, where Oxygen Isotope Stage 5e is correlated with the Eemian temperate stage (Mangerud *et al* 1979; Shackleton 1977). Between the fixed points of the Matuyama/Brunhes boundary and Stage 5e, cold and temperate events have been ranked in stratigraphic succession and correlated to the oceanic Oxygen Isotope Stages (Table 4). Simple pigeon-holing however, is likely to lead to many problems in formulating the Middle Pleistocene record, as the continental record is obviously incomplete, with many stages missing due to non-depositional sequences through time and later erosion, especially

Table 4 Isotope stratigraphy, magnetostratigraphy, and geochronology for the last 1.2myr of the Quaternary periodSources: 1 Imbrie *et al* 1993; 2 Shackleton *et al* 1990; 3 Imbrie *et al* 1984; 4 Bassinot *et al* 1994; 5 Champion *et al* 1988; 6 Zagwijn 1992; 7 Gibbard *et al* 1991

in areas affected by glaciation. A greater measure of control is available from sites with long sequences such as Schöningen in Germany (Thieme *et al* 1993; Thieme and Maier 1995), and regional studies of landscape development like the pre-diversion Thames sequence (Bridgland 1994). Additionally, the degree of climatic complexity, as determined by analysis, for Middle

Pleistocene stages is less than that of the later post-5e stages, where the oceanic and continental geological and palaeoenvironmental records are more complete (Greenland Ice-Core Project, GRIP Members 1993). Thus, the proviso must be that geological events that reflect climatic forcing regimes may represent only part of an isotope stage and that caution must be invoked in

Table 5 Revised geochronological correlation for part of the Middle and Late Pleistocene(Sources: 1 Mitchell *et al* 1973; 2 Roberts *et al* 1995; 3 adapted from Zagwijn 1992; 4 Shackleton 1987)

<i>conventional British stages¹</i>	<i>modified scheme²</i>	<i>interglacial sites</i>	<i>Dutch/European sequence³</i>	<i>OIS⁴</i>
OIS do not apply to this column				
Devensian	Devensian		Weichselian	5d-2
Ipswichian	Ipswichian	Bobbitshole, Trafalgar Square	Eemian	5c
these stages not recognised	cold stage		'Saalian Complex'	6
	temperate/interglacial stage	Marsworth, Stanton Harcourt		7
	cold stage			8
	temperate/interglacial stage	Little Thurrock, Globe Pit, Purfleet		9
Wolstonian	cold stage			10
Hoxnian	Hoxnian <i>sensu</i> Swanscombe	Swanscombe, Barnham, Beeches Pit, Clacton, Hoxne	Holsteinian	11
Anglian	Anglian		Elsterian	12
Cromerian	temperate/interglacial stage	Boxgrove, High Lodge, Wivenhoe, Westbury-sub-Mendip, Kent's Cavern, Warren Hill, Waverley Wood	Cromerian IV	13
Beestonian	cold stage		Glacial C	14

interpretation and correlation. Otherwise the inevitable result will be that there are too many geological events to fit into the stage system, rather than the reverse scenario that prevailed when using strictly lithostratigraphic and biostratigraphic modelling.

The geochronology of the Pleistocene obviously has direct relevance for archaeologists working in the period. The implications of time for interpreting matters such as hominid evolution, the colonisation of Europe, and technological variability and change, are immense. Correlation of sites, and thus evidence, across a large geographic area is largely dependent on knowing that comparison of like with like is being made, in terms of a chronological framework. It is therefore incumbent upon archaeologists working within this period to provide a cogent contribution to the development of geochronology and chronostratigraphy, as many of the hypotheses constructed when data are removed from the intra-site context to the inter-site context require a chronological correlation to remain workable.

1.3 A history of research in the Boxgrove area

M B Roberts

The development of Quaternary research in the area around Boxgrove, which includes the coastal plain of western Sussex and eastern Hampshire and the southern flanks of the South Downs, is not widely known. The contribution of studies in the area to the discipline is both important and ongoing, as attested by this research and the recent Southern Rivers Project

(Wessex Archaeology 1994). Accordingly, this chapter sets out to redress the situation by studying the development of theories pertaining to the formation of the Pleistocene geological units, and their associated archaeological remains, through time.

Many of the hypotheses of past workers were shaped by the ideologies that were extant at the time they were writing, and also by the general structure or framework of the many disciplines that constitute Quaternary research at any given time in history. Broad examples of these trends may be seen, for example, in the literal belief in the Biblical Flood, the early concept of the Ice Age as a single cold event, and the use of archaeological tool types as marker fossils to date Quaternary deposits and events. Present day Quaternary researchers have a far broader knowledge base than was available to earlier workers. Perhaps the most striking example of this is a realisation of the duration of the Pleistocene and the complexity of climatic events that characterise this period of geological time. It is therefore appropriate to acknowledge the efforts of the workers described below, and to consider their labours within the context of the scientific knowledge available to them. Indeed, it may be demonstrated that many workers showed remarkable prescience in their conclusions and have provided an invaluable base upon which this current research is built.

The earliest mention of the raised beach deposits in the Sussex area was recorded by Mantell (1822; 1833) and concerned the buried raised beach section at Black Rock, Brighton (Fig 8). The raised beach deposit was described as being buried by Diluvium, a catch-all phrase that was applied to all the superficial sediments

of the area. In the area of the Brighton Raised Beach the Diluvium was named the 'Elephant Bed' by Mantell due to the large number of mammoth remains found therein. The Elephant Bed was acknowledged as being a waterlain deposit that was not part of the original solid rock stratigraphy, and thus at this early date was already perceived as a composite deposit formed by the erosion of the surrounding geology 'at some distant period' (Mantell 1833, 41). Palaeontological remains were known from Diluvial sediments from various parts of England but Mantell believed them to be quite scarce in Sussex, although he does record horse, ox, deer, and elephant. Two of the discoveries of elephant/mammoth are associated with the River Arun at Burton Park and at Peppering. Although the exact location of these sites is unknown, the finds would appear to have come from fluvial terrace deposits of the western Rother, which is a right bank tributary of the River Arun, and the Arun itself (Fig 2).

The Brighton Raised Beach (interpreted here as an easterly continuation of the Norton Formation, Bates *et al* in press; Roberts Chapter 2.1) is readily visible in the current coastline at Brighton and so provided stimulus to geologists interested in the Drift or Diluvial Period (Lyell 1841). It was the work of Dixon (1850), however, that began to expand the Pleistocene succession inland and westwards. Dixon recorded raised beach deposits from Portslade, Shoreham, and Lancing, including the recently re-investigated site at the Sussex Pad (Bowen *et al* 1989; Parks and Rendell 1992). Moving further west, raised beach deposits were recorded at Broadwater, and for the first time a division of the littoral deposits was made, as Dixon believed this beach to be older than that traced between Worthing and Brighton. He mentioned no other deposits further westwards, until those of the Selsey Peninsula. This led to the erroneous view that that no deposits of the Brighton beach existed west of the Arun — a view that prevailed until the next century (Martin 1938).

At Bracklesham, Dixon was intrigued by the large erratic boulders on the foreshore that are still the subject of debate and speculation (Kellaway *et al* 1975; Bridgland Chapter 2.4). Dixon concluded with a statement that would be verified by later work: 'The remains of still more recent strata or beaches in the neighbourhood of Worthing, extending along the coast to Selsey, confirm the opinion that many comparatively modern changes must have taken place in the south-west part of Sussex between the sea-shore and the Downs.'

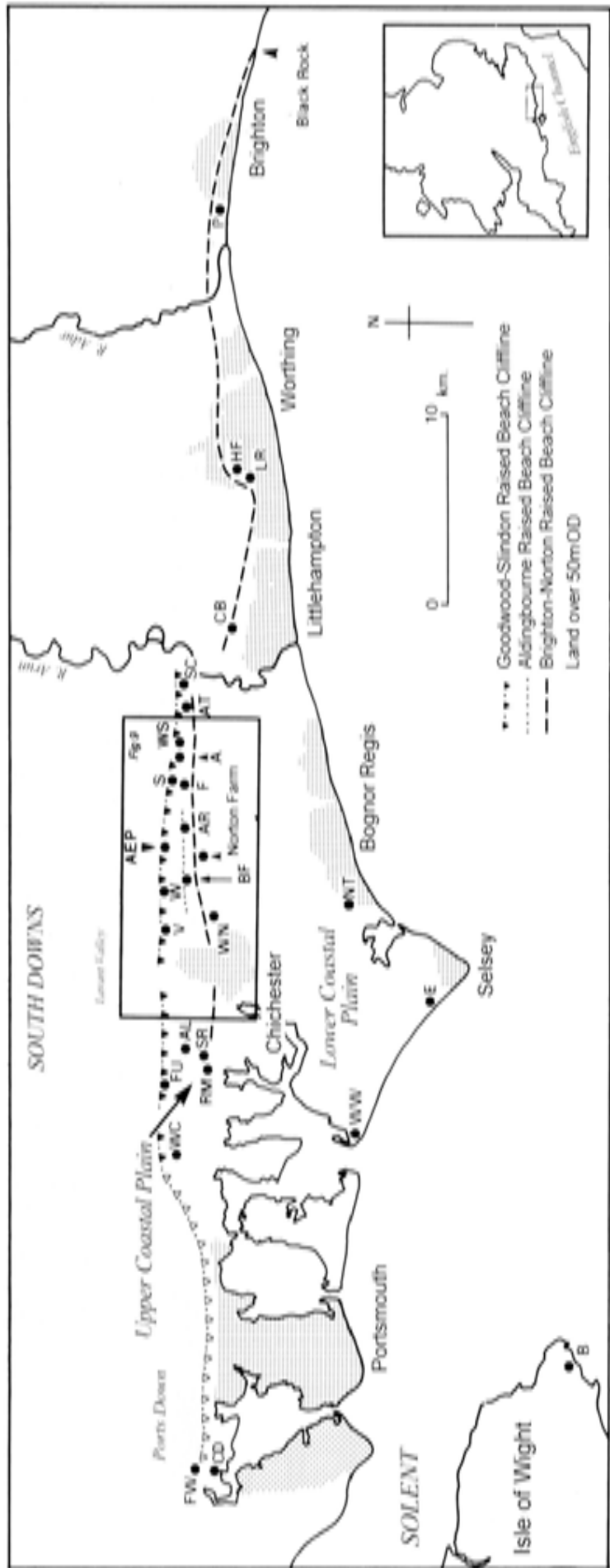
At around the time that lively interest was being shown in the raised beach deposits, research also commenced on the large spreads of drift deposits that mantled the coastal plain, and the remnants of this drift found on the high ground of the South Downs. Murchison's (1851) explanation of the origin of the drift was certainly more cataclysmic than any proposed since: he invoked earthquake movements in the Weald which, like so many of these early hypotheses, is not as far-fetched as it first seems. The process that formed

the Wealden Anticline, and hence was the causative factor behind the modern geomorphology of the area, was the Alpine Orogenic event. Subsequent erosion of the anticline provided much of the source material for the drift deposits of the area. Murchison's study was complemented and expanded by Martin (1856); these papers were the first in a long series, by various authors, published in the Quarterly Journal of the Geological Society. Between 1851 and 1892, over 15 papers were published on the Pleistocene of Sussex and its immediate area.

In 1857 the study of the erratics around the Selsey Peninsula was expanded by Godwin-Austin (1857) (Figs 2, 8). He described a bed containing many far travelled rocks, overlying a marine mud, in a yellow sandy clay matrix with crushed chalk. This unit was overlain by another marine deposit containing molluscs of a distinctive southern provenance and finally by the raised beach deposit. Godwin-Austin believed these rocks, which included granites, syrenites, hornblende greenstones, and gneisses, came from a source westwards across the channel around the Cotentin Peninsula in Normandy (Bridgland Chapter 2.4). Also in this paper, Godwin-Austin stated that he believed the red gravels or rubble drift pre-dated the white gravels of the lower coastal plain, a fact that was later demonstrated to be correct (Roberts Chapter 2.1). Thus, Godwin-Austin (1857, 69) raised questions about the chronological and lithological simplicity of the Diluvial Period and with remarkable insight makes the following prediction: 'The amount of change..., when fully worked out in all of its details, may perhaps enable us to arrive at a cosmical law for the course of such changes on the earth's surface.'

This statement, which no doubt grew out of the recognition of a succession of lithological units representing deposition under markedly different climatic regimes, could be seen as the beginning of a hypothesis which came to fruition in the Milankovitch Theory (Milankovitch 1941) and subsequently with the work of Hays *et al* (1976) and Imbrie *et al* (1984).

The higher raised beach deposits of the coastal plain, which include those at Boxgrove (Roberts Chapter 2.1) were first recognised by Joseph Prestwich (1859) in his attempt to trace the Brighton beach westwards. Like Dixon, he was unable to find deposits between Broadwater and the River Arun but located marine sediments three kilometres west of Arundel, just north of the present A27 (Fig 9) or the Chichester High Road as it was known then. At Avisford Bridge (973 067, Fig 9) Prestwich located angular flint gravel overlying beach shingle, which in turn overlay eight feet (2.5m) of marine sand. The wave-cut platform was cut into the Tertiary Reading Beds at this location (Table 6). Further north at Avisford Dell (SU 974 073, Fig 9) the sequence was repeated, the height at the top of the sands being around 30m OD. Prestwich also found further traces of marine deposits westwards at Eartham, Boxgrove, and most importantly at the Waterbeach Pit,



- | | | | | | |
|-----|---------------------------|----|--------------------|----|-----------------------|
| AR | Aldingbourne | E | Earmley | S | Slindon |
| AEP | Ameys Earham Pt, Boxgrove | F | Fortwell | SR | Sparrows Rough |
| AT | Anoldi Tree Nursery | FW | Fort Wallington | SC | Stewards Copse |
| AL | Ashling Lodge | FU | Furlingdon | W | Waterbeach |
| A | Avisford Dell | HF | Ham Farm | WC | Westbourne Common |
| B | Bembridge | LR | Littlehampton Road | WN | Westhamnett |
| BF | Brook's Field, Boxgrove | NT | Nyetimber | WS | West Stubbs Copse Pit |
| CD | Cains Down | P | Portslade | WW | West Wittering |
| CB | Crosbush | RM | Ratham Mill | V | Valdoe Pit |

Fig 8 Location of sites and raised beaches between Brighton and Portsmouth; inset shows location of Fig 9

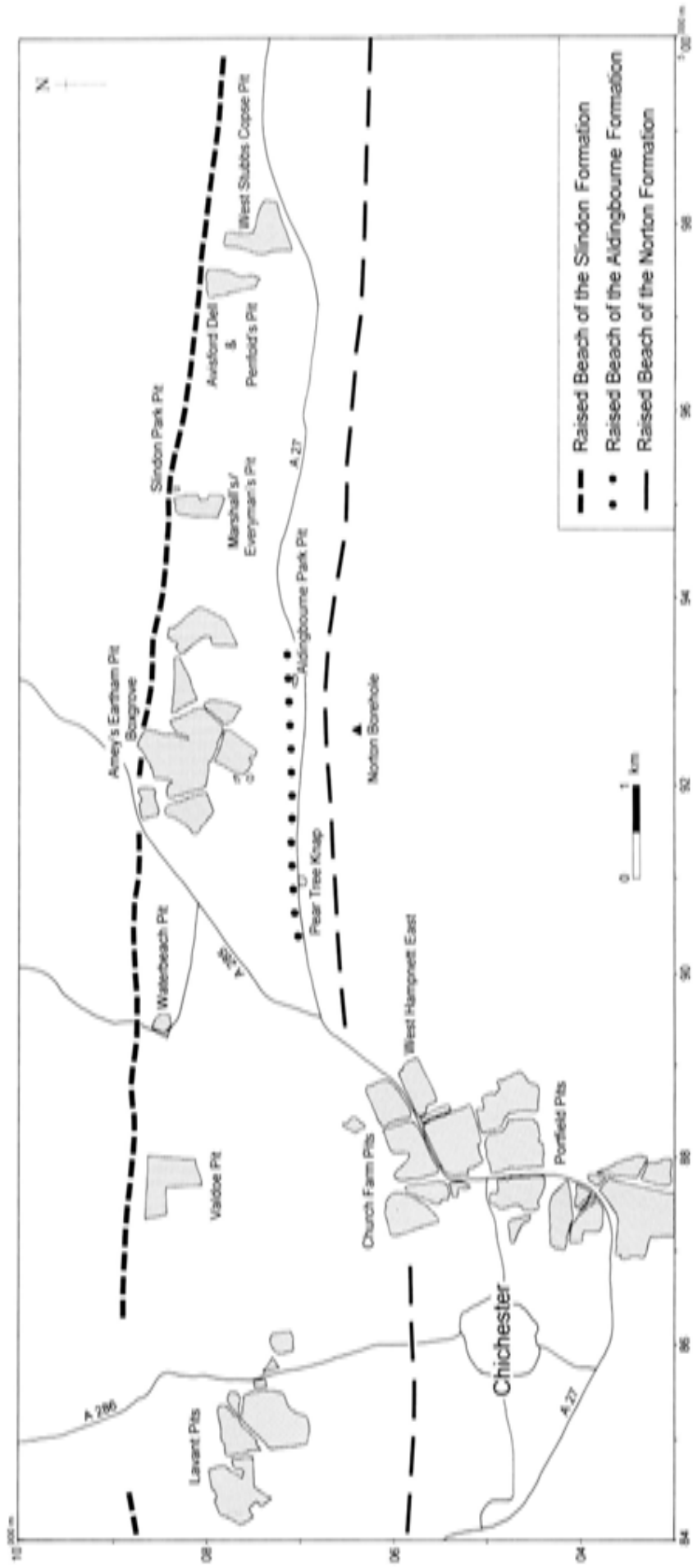


Fig 9 Location of quarries and raised beaches in the Bognor area

Goodwood (SU 894 085). At Waterbeach, which is a westward extension of the deposits at Eartham Quarry, Prestwich recorded ferruginous gravels which were piped into the underlying chalky gravel. The gravel deposits overlay 3–4 feet (c 1–1.2m) of laminated and slightly argillaceous clay which probably represents the Slindon Silts (Roberts Chapter 2.1); this unit passed down into the Slindon Sands proper (Shephard-Thorn and Kellaway 1978). Progress to the chalk platform was inhibited by the fact that Prestwich's workmen could not dig through the carbonate sedimented slabs of Slindon Sand that occur at the base of this unit (Collcutt Chapter 2.3). In an attempt to interpret the environment of deposition, Prestwich also collected marine molluscs and foraminifera from the sands (Bowen and Sykes Chapter 5.6, Table 102; Preece and Bates Chapter 3.3; Whittaker Chapter 3.2). Although the deposits from Avisford to Waterbeach attained a much higher elevation than those known east of the Arun (Fig 8), Prestwich believed them to be of the same age and deposited by the same inundation: a view that was to persist for over 50 years.

After Codrington's paper (1870) which ascribed the Pagham elephants to *Palaeoloxodon antiquus* (ie associated with warm stages) and not *Mammuthus trogontherii* (which was associated with cold stages) as earlier workers had thought, there followed a spate of papers concentrating on the drift or head deposits of the area. Of particular interest was the origin and mode of deposition of these sediments. Tylor (1869) believed they were the result of intense pluvial activity, whereas Wood (1882) suggested snow melt as the likely agent of deposition. The most lucid description of their probable origin came from Clement Reid (1887), who invoked permafrost to great depths as being the catalyst for the mode of deposition. He postulated that a frozen surface would affect drainage patterns and that rain and snow melt would remove the upper partially thawed layers of chalk and rubble and move them downslope as a fan gravel. The chalk particles were not washed out or dissolved because they were still partly frozen. This theory has not been greatly improved upon at the time of writing. In the same year, Elsdon (1887) described the drift on the north side of the South Downs; the importance of this paper was to become apparent with the later discovery of Lower Palaeolithic handaxes and flakes in the Rother and Arun Valleys (summary in Woodcock 1981) (Fig 2). However, the paper is probably best remembered for Osbourne-White's descriptive quote (1924) in which he regards Elsdon's in-depth analysis of these deposits as possibly unmerited: 'for a less prepossessing set of deposits it would be difficult to find', a view echoed by many later researchers into the head/drift deposits. Whilst the debate continued on the drift deposits, Prestwich had discovered and written up another high level raised beach on Portsdown Hill (Fig 8) near Portsmouth (Prestwich 1872) and, despite ill health, at the end of the century produced a paper on raised beaches and head or rubble drift that was read to

the Geological Society in 1892. Included in the paper is the first mention of archaeology from the Brighton Raised Beach deposits at Birling Gap (Prestwich 1892). Prestwich then followed the established format by looking at occurrences of the raised beach further westwards, starting with a section at Portslade, near the railway station (Fig 8). Prestwich regarded all the drift/head deposits in the area as being the same age and explained differences in lithological composition as a factor of distance travelled from the cliff-line and downland. At Selsey (Figs 2, 8), Prestwich was drawn back again to the problem of the large number of erratic blocks and hypothesised for the first time that their origin may have been through the Straits of Dover rather than from the west. The blocks were, he believed, rafted onto the coast by icebergs at the time of the Waterbeach (Goodwood-Slindon) high sea-level event. Importantly, in this 1892 paper Prestwich pointed out that the relationship between the drift and the raised beaches was coincidental, the drift merely filling in the gap created by the cutting of sea cliffs and the underlying marine deposits. The character of the head/drift reflected the superficial cover on the high ground behind the cliffs, a fact which is now known to be correct (Bates and Roberts, in Roberts 1986). Further to this, Prestwich remarked on the similarity of the red ferruginous head deposits to the Clay-with-flints pockets surviving on the Downs and concluded, correctly, that the former is a downslope equivalent of the latter. However, when it came to the origin of the head deposits Prestwich agreed with Murchison (1851) in the belief that they formed sub-aquatically, thus rejecting Reid's (1887) theory of sheetwash and ice melt. Throughout his work Prestwich was hampered by the belief that the Coastal Plain deposits were all deposited by the same high sea-level event, as were Reid and, later, Palmer and Cooke (1923), and therefore had to invoke a complex sequence of land submergence to fit the theory together.

The raised beaches were further discussed by Clement Reid (1892). Most of this work concentrated on the Selsey Pleistocene deposits, especially the erratic suites. Reid dismissed Godwin-Austin's section drawing (1857) and placed the erratics and cold deposits immediately overlying the Tertiary Bracklesham Beds (Table 6, Fig 15), earlier than the marine sediments and the raised beach. An important factor in Reid's research was the discovery that many of the Selsey erratics were of local origin, such as Bembridge Limestone, Bognor Rock, greywether sandstone, chalk flint, and Upper Greensand from the Isle of Wight. This fact would only make sense if the ice containing the exotic erratics came from the south-west. One of the large blocks of Bognor Rock weighing over two tons was glacially striated, although Reid stressed that this was not necessarily indicative of glaciation in this area.

The study of the raised beach deposits in the east of Sussex was further enhanced at the end of the nineteenth century (Hazzledine-Warren 1897; Chapman 1900)

with accurate logs through the sediments being produced, but despite an OD differential of 40m, correlation with both Selsey and Waterbeach continued to be made. The state of knowledge west of the Arun was summarised by Reid (1903), who for the first time correlated the Clay-with-flints with the Eocene deposits of the area. This important step meant that ferruginous red gravels were no longer to be simply interpreted as a decalcified coombe or head deposit.

The beginning of the twentieth century saw an input of archaeological papers relating to the Pleistocene deposits of the area. Garraway-Rice (1905) found the first handaxes west of the Arun in terrace deposits of the River Rother (Fig 2); the singularity of this discovery was remarked upon by a Mr Dale who noticed that, compared with other areas, Sussex was particularly unproductive for palaeoliths. Further discoveries of a similar type from this area were reported by Garraway-Rice (1911; 1920), but no connection with the coastal artefact-bearing horizons were made. Other archaeological discoveries from the raised beaches were reported by Heron-Allen (1912) at Selsey and Smith (1915) at Black Rock, Brighton. Although there is no disputing the piece from the latter site, the material from Selsey is now largely considered to be all natural, but at the time cololiths and rostrocarinates were accepted from many parts of the country as real tools.

The discovery of supposed artefacts, some of which were described as Acheulean, from Selsey caused problems for Palmer (1922) and Palmer and Cooke (1923) who had artefacts of a similar cultural type from the high level gravels (Curwen's (1925) handaxe from Slindon) and the lowest marine deposits. Palmer and Cooke recognised three levels of beach at 100', 50' and 15'. There was, as mentioned above, Acheulean material from the highest and lowest beaches, and what were interpreted as Mousterian implements from the 50' beach. Therefore like Prestwich (1872) and Reid (1892), Palmer and Cooke had to introduce a convoluted sequence of events to produce all three beaches in a single transgressional phase; this again involved raising and lowering the land mass to cut the beaches and deposit the littoral sediments. Interestingly, within this scheme the authors correlated the 50' beach with that at Brighton, a hypothesis not considered again until recently (Bates *et al* in press). In correlating the archaeology with the marine and head deposits of the coastal plain, Palmer and Cooke (1923) recognised three brickearth or fine gravel seams in the Upper Head Deposits. This stratigraphical observation has recently been partly confirmed at Boxgrove (Chapter 2), although no Aurignacian archaeological material has been found within these brickearth seams, as previously reported (*ibid*, 261).

The hypothesis that the raised beaches were all of the same age or part of the same event, was finally questioned by Osbourne-White (1924) who believed that the 100' and 15' levels were the product of separate transgressions. He also believed the Goodwood event did not

exist east of the Arun, as it had been destroyed by the transgression associated with the Brighton Raised Beach.

In the 1920s the first Palaeolithic implements and handaxes were recovered from the higher raised beach deposits at Slindon Park Pit (Figs 8, 9), also known as Slindon Bottom (SU 951 084), (Curwen 1925; Fowler 1929). At this exposure a dry valley runs north-south through the Pleistocene deposits, which has led to problems interpreting the geology, even for later workers such as Calkin (1934) and Woodcock (1981). The archaeological material comes from the west side of the dry valley either from the surface of the raised beach or in the coombe rock or head just above it. The handaxes and flakes are identical to those from similar contexts at Boxgrove. The Lower and Middle Palaeolithic periods in Sussex were eventually summarised by Grinsell (1929) who again remarked upon the paucity of Palaeolithic flintwork from Sussex. At that time he considered there to be less than three to four hundred implements or flakes, and most of these are from the river valleys such as the Cuckmere and Arun/Rother. Grinsell's work was followed by what is considered to be the seminal early study on the raised beach deposits by the Reverend Joseph Fowler (1932). Fowler also believed it was impossible for the 15' and 100' beaches to be of the same age, as he had identified marine deposits between the 70' and the 135' contour between Arundel and Chichester and asked the rhetorical question (*ibid*, 88) whether the Boxgrove (70' deposits near the village) and the Slindon deposits represent two separate shore levels. (These two sets of deposits are now assigned to the Aldingbourne and Slindon Formations respectively, see Table 8 and Bates *et al* 1997.) This enigma mirrored that faced by Palmer and Cooke (1930) when they attempted to compare the drift deposits overlying the beaches at Lavant and Waterbeach. Fowler examined twenty-one locations in both the Slindon Beach and the Aldingbourne Beach but was unable to differentiate between the two; nonetheless his work is still invaluable to researchers in the field today.

Archaeological discoveries in the study area were first presented in a modern report form, linking the finds accurately to the geology, by Bernard Calkin (1934). Calkin, taking a lead from Fowler, separated the 80'-90' (Aldingbourne Stage) beach from the 100'-135' (Slindon Stage) but interpreted the former as the older of the two. The assumption that the 80'-90' beach was older was based on archaeological typology, since the finds from this beach consisted of flakes and cores which were interpreted as Clactonian, whereas the upper beach contained handaxes. Therefore the geological evidence, which pointed to the contrary, had to be ignored. At Slindon Park, Calkin was able to link the marine lug sands (Slindon Sands) to the raised beach deposits. The section he produced (*ibid*, 347) is very similar to that at Eartham Pit, Boxgrove, especially in the lower units. However, it is clear that a large amount of the overlying gravel/head, the north end of

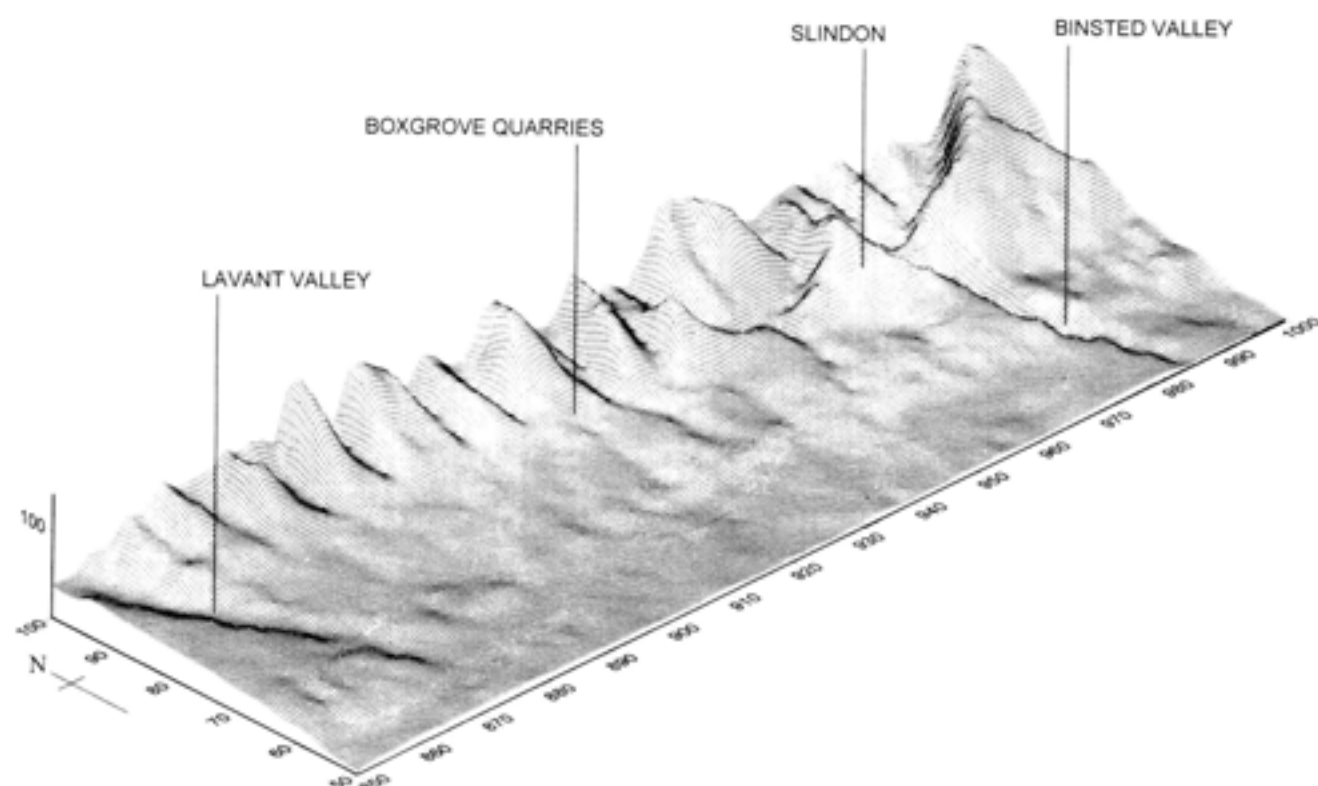


Fig 10 Isometric model of the Downland block and upper coastal plain between Chichester and Tortington; note the dry valley configuration to the west of Slindon. The numbers on the x and y axes are Ordnance Survey grid coordinates and the y axis gives the height (m) above sea level (OD)

the beach, and the relict cliff-line have been lost. As mentioned earlier, this is due to the fact that the deposits at Slindon Bottom are only 55m wide, running eastwards from Everyman's Pit (Figs 9, 21). The erosion is a consequence of a dry valley that cuts north-south through the deposits. This valley is fed at the north-east and north-west corners by two further valleys descending from the chalk high ground behind the site (Fig 10), and it is postulated that this configuration channelled downland snow melt southwards out through this valley. A more extreme example of this process can be seen in the Binsted Valley between Penfold's Pit and West Stubbs Copse Pit (Figs 9-10). Despite the lack of exposures, Calkin identified two levels of archaeology at the site, one within the beach producing rolled artefacts and one on the surface of the beach; also mentioned are over 50 burnt flints in two concentrations on the surface of the beach, but unfortunately these were either not kept or have subsequently been lost.

Oakley and Curwen (1937) accepted Calkin's hypothesis that there were two beaches above 80' OD and further concurred that the lower beach was the older. They also clarified the various earlier hypotheses concerning the original source and Pleistocene mode of deposition of the so called red or ferruginous gravel, that overlay the Slindon Sands and beach deposits. These were described as solifluction deposits by Oakley and Curwen, who surmised that their non-calcareous character largely reflected the original deposit from

which they derived, thus corroborating Reid's earlier hypotheses (1903). During further work at Marshall's Pit (SU 950 082), Oakley and Curwen also noticed interbedding of the coombe rock and the sands and interpreted this as evidence of a high sea level reworking the head deposits. Unlike their earlier theories, this one was somewhat wide of the mark, as it has been demonstrated (Roberts 1986) that the reverse was in fact true and the head deposit, and the outwash associated with it, were reworking the marine sands.

As more published work on the highest beach of the coastal plain became accessible, it became more puzzling to many researchers that no trace of this beach had been found east of the River Arun (Osbourne-White 1924). One explanation, proposed by Martin (1938), was that the chalk inlier known as the Littlehampton Anticline (Fig 16, Chapter 2) was intact between Arundel and Worthing; that is the Upper Chalk succeeded the existing Middle Chalk to form a ridge that blocked the path of the high sea level further inland. If this theory, which has yet to be disproved, is correct then approximately 150m of chalk must have been removed by subsequent Pleistocene marine transgressions.

Another consequence of the amount of work being published on the raised beaches was that correlation with Pleistocene deposits both in Britain and further afield was inevitable. Green (1943) correlated the highest raised beach with the Boyn Hill Sea and therefore was able to link the archaeology with that at Swanscombe, also part of the Boyn Hill Terrace of the

River Thames. Zeuner (1945; 1958) correlated the high beach with his 100' Tyrrhenian level and had to explain away the height of the sediments at Waterbeach (135'–140') as an exception; no account being taken at the time of local neotectonics. Zeuner (1945) did though make the 80'–90' younger than the >100' beach but calls it a regressional phase of the same event, a theory that was extant until quite recently (Woodcock 1981; Shephard-Thorn *et al* 1982). However, by 1958 the 80' beach had been correlated with the main Monasterian event and was thus regarded as a separate transgression episode in its own right.

While the debate about the beaches was reaching a wider audience Curwen (1946), Pyddoke (1950) and Jeffrey (1957) were all finding more handaxes, the latter two at Slindon and the former at Chichester. Pyddoke's handaxe deserves further attention because it was found on the surface of the sands immediately below the coombe rock/head at Penfold's Pit (SU 974 074) and thus it had either eroded out of the sands or been deposited on the eroded surface of the sands during the onset of the succeeding cold stage. This handaxe was therefore the first *in situ* piece recovered from the sediments of the Slindon Formation.

Penfold's Pit (Fig 9) was also the site of one of the first scientific analyses of the head deposits (Dalrymple 1957). During this research, Dalrymple confirmed earlier views that the red head gravels were partly composed of weathered Tertiary material with a Rotlehm soil fabric similar to the Clay-with-flints. Within the head gravel, bands of fine material were interpreted as a weathered soil horizon forming on the solifluction gravel and higher up the profile as reworked loess soils with *braunerde* fabrics and *sol lessivé* features. These units were interpreted as forming during fully temperate stages later in the Pleistocene (for an alternative hypothesis see Roberts Chapter 2.1 and Macphail Chapter 2.6).

During the 1960s and early 1970s research in this area lessened in comparison with previous decades, although two important papers were published. The first was by Jeffrey (1960) and showed two beaches at Avisford Dell Pit, and the second was by Hodgson (1964), who mapped all the low-lying deposits of the lower coastal plain and described a section through the raised beach of the Norton Formation at *c* 12m OD near Westhampnett (SU 881 060).

Perhaps the most radical hypothesis since work began in this area was proposed by Kellaway *et al* (1975) for the origin of the coastal plain Pleistocene deposits. The hypothesis stated that the Slindon sediments were of a fluvio-glacial origin, being the outwash of an English Channel glaciation from the west. The authors believed that the unusual bathymetry of the channel floor, especially the deeps and fosses, taken with the evidence of far travelled and more localised erratics from Pleistocene deposits around the present shore-face were proof of a channel ice-sheet. It might be that the channel ice hypothesis of Kellaway *et al* will

be substantiated in the future; however, it is clear that the Slindon deposits are fully marine and temperate, a point which was later acknowledged by the authors (Shephard-Thorn and Kellaway 1977; 1978).

A proposed western end of the Goodwood-Slindon raised beach was rediscovered in 1972 in Hampshire (ApSimon *et al* 1977) on the western limb of the Portsdown Anticline (Fig 8), and slightly to the south a lower beach at 16m OD was discovered that may correlate with either the Aldingbourne or Norton Stages. In a similar fashion to the higher raised beach exposures to the east, Palaeolithic archaeology has been found in association with the Portsdown beach (Gamble and ApSimon 1986) at Red Barns, where bifaces and flaking debitage have been moved down the slope of the beach in a calcareous debris flow. Later work in the west of the area on the Isle of Wight (Preece *et al* 1990) attempted correlation between the higher Bembridge deposits (SZ 642 865) and the Goodwood-Slindon raised beach deposits exposed at Eartham Quarry; the results of this work are discussed in detail below (Chapter 2).

A major contribution to the Palaeolithic archaeology of the area was made by Woodcock (1981) who, following the lead of Roe (1968), compiled a gazetteer of Lower and Middle Palaeolithic sites in Sussex. This volume also contains the results of two trial excavations undertaken at Eartham, in one of the brickearth horizons in the mass-movement/head gravel, and at Slindon, where Woodcock reopened the site of Calkin's excavations.

In 1983 the present Boxgrove Project began, the results of which are presented in this monograph. Earlier published work (Bergman and Roberts 1988; Bergman *et al* 1990; Roberts 1986; Roberts 1990) has been integrated into the current monograph structure and is discussed below.

1.4 Project methodology

M B Roberts

The Boxgrove Project adopted a flexible methodology early in its developmental process. At the outset this was largely determined by the fact that the site was located in a working quarry (Fig 11) and therefore



Fig 11 Quarrying at Boxgrove



Fig 12 Q1 GTP 26: Gravels overlying marine deposits of the Slindon Formation; scale unit 0.5m

excavation methodology had to be tailored to work with and around the extraction and backfilling processes. The archaeological landsurfaces are located between the two most commercially important sediments, the flint-rich solifluction gravels and the Slindon Sands (Fig 12). Fortunately, there was normally a hiatus between the removal of the overlying gravel deposits and the extraction of the underlying sand. During this hiatus the intervening brickearth and Slindon Silts were removed, normally by box-scaper, to form embankments for the silt ponds. This method of quarrying allowed for time to sample areas in a logical and progressive manner, as the intended scale and direction of quarrying were known well in advance. It became obvious early on, if not at the moment of the project's inception, that the key to success in project management lay in being able to anticipate and respond to different extraction policies executed by the quarry company.

This system of working the quarry continued until changes in the economic climate in the late 1980s and early 1990s forced the extraction company to rethink its strategy so that the mineral resource remained economically viable (Fig 13). The resulting change in extraction methods was directed in the main at

Quarries 1 and 2 (Fig 4) where the conformable sequences are found, and resulted in removing the solifluction gravels *en masse* as make up or ground fill for road programmes or other construction projects. The policy of bulk removal extended to the deposits underlying the gravels as well, thus removing the hiatus time which was essential for adequate sampling and excavation to take place. Additionally, the work was now to be carried out by sub-contractors working to strict timetables. The implications of this change of events were that the strategy developed between the excavation team and the quarrying company, ARC, would no longer be as effective in formulating extraction and excavation policies once third parties were involved. At the same time it was decided that Quarry 1 (Fig 4) should be flooded with silt, the fine residue from gravel washing, without removing the underlying Slindon Sands. Although this meant that the archaeological horizons would not be physically removed, it was felt by the Project Director that the deformation of the sediments and the destruction of the biological remains contained within them brought about by large amounts of water moving through the fine-grained deposits would produce an equally unacceptable scenario. Accordingly, dialogue began between the interested parties, the results of which were to remove the western end of Quarry 1 and the northern end (Fig 4) of Quarry 2 from any further threat and to preserve them for posterity. Both of these areas were adjudged to contain the best geological exposures and archaeological material of the highest integrity. Both of the preserved areas have a calcareous capping above the Pleistocene landsurfaces that ensures the preservation of faunal and other palaeoenvironmental evidence essential for palaeoecological reconstruction (see Collcutt and Macphail Chapter 2). Another consequence of ongoing negotiations, in response to the change in quarrying methods, was that English Heritage commissioned Boxgrove Project B (Roberts *et al* 1997) and the Eartham Quarry Project (Roberts *et al* in prep). These projects extensively sampled the archaeological areas under threat and the latter is on-going at the time of writing with regard to post-excavation, and will be published as part of the next Boxgrove monograph.

The Boxgrove Project was originally conceived by the author as a research project aimed at studying the geology of the quarry deposits at a very general level and determining whether any landsurfaces, the *in situ* spatial and sometime temporal equivalent of the archaeology in the overlying implementiferous fan and mass movement gravels, existed. Having established the fact that flintwork was present *in situ* in the fine-grained sediments of the Slindon Formation as well as in the gravels (Woodcock 1981) and that major excavation was required in advance of quarrying, a research methodology was formulated.

This methodology involved digging and cutting geological sections from the northern end of the site at GTP 25 (Fig 4), where the cliff-line had been revealed,

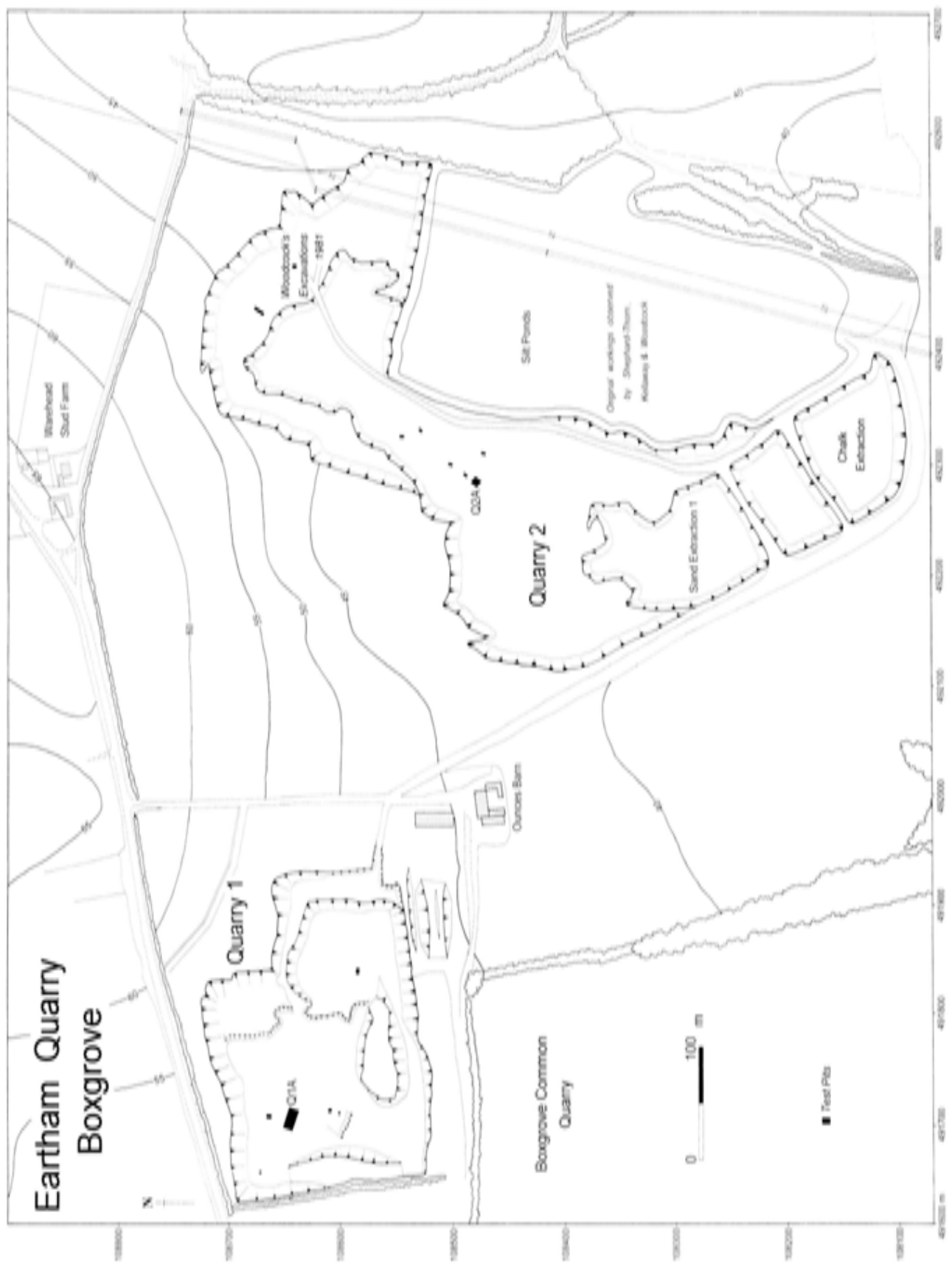


Fig 13 Plan of the quarry complex in 1987; compare with Fig 4



Fig 14 Sampling sediments at Boxgrove; scale unit 0.5m

to the most southerly of the quarry workings (Fig 13). Lateral variation in the sedimentary sequence was tested by expanding the series of pits to the west, to include Quarry 1, and to the east. The sides of the quarries were also cleaned to aid interpretation and to provide composite sections. Samples were collected from the sections and test pits, both by the excavation team and the project specialists, and finally the sections were drawn, described and photographed (Fig 14). Archaeological areas were sited in response to threats from mineral extraction; Quarry 2/A, Quarry 2 GTP 17 (Quarry 2 C/D, Roberts *et al* 1997), or as the result of test pit sampling Q1/A and Q1/B (Fig 4). At all stages of the project, specialists from the various contributing disciplines were kept in touch with each other's research and the work in the field.

Multidisciplinary Quaternary and Palaeolithic projects had begun to blossom in the 1970s, and the trend has continued through into the 1990s. Examples include the following sites: Biache-Saint-Vaast (Tuffreau and Sommé 1988), Bilzingsleben (Mania *et al* 1980; Mania and Weber 1986), Caddington (Sampson 1978), La Cotte de St Brelade (Callow and Cornford 1986), Hoxne (Singer *et al* 1993), High Lodge (Ashton *et al* 1992a), Maastricht-Belvédère (van Kolfschoten and Roebroeks 1985; Roebroeks 1988), Olduvai (Leakey 1971), Olorgesailie (Isaac 1977), Pontnewydd (Green 1984) and Swanscombe (Conway *et al* 1996). These works have been complemented by non-archaeologically driven, site-based Quaternary research projects. The tradition of this type of work is very strong in Britain and is exemplified in the reports on sites such as Selsey (West and Sparks 1960), Earnley (West *et al* 1984), Bembridge (Preece *et al* 1990), Waverley Wood (Shotton *et al* 1993) and wider geographical areas like the Thames (Bridgland 1994) and the southern North Sea Basin (Gibbard *et al* 1991). The Boxgrove Project methodology and this monograph have followed this trend.

Perhaps the single most difficult problem facing the palaeolithic archaeologist, whether at Boxgrove or elsewhere, is determining the context of the material which has to be firstly excavated and subsequently studied.

Palaeolithic find spots tend to be uncovered primarily by chance, especially in quarries or in deep cuttings and often by non-archaeologists. The contexts that contain the archaeological remains are often daunting in a variety of ways; this is normally most evident when trying to reconstruct the palaeogeography of the site area. Given the long periods of time that have elapsed subsequent to burial of the finds, topographical features which are now prominent in the landscape may simply not have existed at the site occupation stage. Conversely, major features of the physical landscape such as areas of relief, drainage systems, and coastlines, may for a variety of reasons have disappeared. The integrity of archaeological finds and assemblages is obviously determined by the processes that have operated on them, or their parent sedimentary medium, since burial. In a geological context such as solifluction gravels the archaeology may no longer be in association with its primary or secondary sedimentary context, due to successive re-working of the sediments through time. The solution to these and other contextual problems is to understand fully the stratigraphic succession of the site and the area within which it is located; from this base other lines of multi-disciplinary research may be utilised. Palaeolithic archaeological remains have often been studied in isolation from the sedimentological, climatological and environmental data. However, the academic returns from such work are likely to be self-justifying, as the ground rules are formulated in an *a priori* fashion. The corollary of investigation or categorisations of the archaeology is likely to be as much the result of the language framing the research principles, than a true reflection of the behavioural signatures behind the material culture that forms the Palaeolithic fossil record (Dunnell 1978; Gamble 1986).

Whereas methods such as the metrical analyses of bifaces have been shown to be flawed if used to provide a chronological perspective through typological comparison (Wymer 1988; Roberts *et al* 1995), fields of study pertaining to lithic analyses such as refitting, technological innovation and development, and use-wear traces have an intrinsic value. However, unless the stone tools themselves can be placed in a chronological context and their post-depositional history known, meaningful comparisons with similar material from other sites, except on a purely technological level, is impossible. Thus the primary requirement, at any site, is to understand the modes and environments of deposition of the sediments that encapsulate the archaeological horizons and cultural remains. This system of analysis is progressive and logical and enables research to move outwards spatially and temporally from local to regional to continental frameworks, or whatever geographical or timescale divisions are deemed appropriate to the level of study being undertaken. Additionally, extra criteria can be added to the progressively expanding framework model to incorporate other relevant factors operating upon and possibly affecting the fossil record.

These may occur at either the macro or micro scale, such as latitude, climate, and subdivisions of these, for example chorology and sea level fluctuations.

To conclude, the broad methodology of the Boxgrove Project, notwithstanding the rescue context of the site, has been to place the archaeological material excavated into a secure lithostratigraphical and chronostratigraphical framework. Upon satisfying this condition, the framework is further fleshed out by reconstructing the palaeoclimate regimes,

palaeoenvironments and palaeoecologies extant during the time period covered by the sediments. These objectives were achieved by using a multidisciplinary approach to analysis of the site. The archaeology has been interpreted firstly against this database and secondly against the state of knowledge in the subject generally, at the time of writing.

The methodology utilised by each of the disciplines involved in the project are outlined in the individual chapters.

2 Geology and sedimentology

2.1 Geological framework

M B Roberts

Pre-Pleistocene deposits

The oldest component of the solid geology in the area of the downland dip slope and upper coastal plain is the chalk of the Upper Cretaceous. In the study area this lithology is restricted to the Upper Chalk (Fig 15), except for an outcrop of Middle Chalk to the south-east of Arundel in the Littlehampton Anticline (Fig 16). The Upper Chalk of the downland dip slope, cut into by the Boxgrove marine transgression, is located entirely within the Campanian Stage, the highest stage of the chalk represented in this area (Tables 6, 7). Older lithologies belonging to the Lower Cretaceous Series are found to the north of the South Downs in the Weald, to the south in outcrops on the Isle of Wight and westwards up the mainland coast. Their relevance to this report is as exotics rafted into the sediments of the Slindon Formation (Bridgland Chapter 2.4). A knowledge of the solid geology of the Boxgrove area is also vital for ongoing research, using stable isotopes, into the diet and habitat range of mammals found at Boxgrove (Horn *et al* 1994; Roberts *et al* in prep).

The chalk is unconformably overlain to the south by sediments of the Reading Beds and the London Clay Formations (Table 6). These formations were deposited during the Palaeocene and early Eocene, and they are cut into by deposits of the Aldingbourne Formation to the east and throughout by the Norton Formation (Table 8) (Fig 17). Sediments of the Reading Beds Formation also unconformably overlay the Chalk of the pre-uplifted Weald. After late Oligocene/early Miocene uplift and erosion of the central Wealden area, followed by further tectonic deformation and subaerial weathering during the Miocene/Pliocene, these sediments survived as a regolith on the downland block to the north of Boxgrove (Fig 18). Where the regolith remains on the chalk uplands it is accorded many different names, the most common of which is the Clay-with-flints (Roberts Chapter 1.3); other terms used are Plateau Gravel and the generic term, Drift (Avery *et al* 1959; Catt and Hodgson 1976; Catt and Hagen 1978; Hodgson *et al* 1967; 1974; Loveday 1962). The origin of all these groups is considered to be the result of weathering of the chalk, primarily by solution, under the Tertiary mantle.

At the southern margin of the coastal plain, in the region of the Selsey Peninsula (Fig 17), outcrop the youngest pre-Pleistocene deposits of the Bracklesham Group. These mainly marine sediments were deposited in the Lutetian Stage of the Middle Eocene (Table 6). They are cut into by a number Pleistocene channels, of varying ages, between Selsey and the Witterings

(Fig 8) (Stinton 1985; West and Sparks 1960; West *et al* 1984; Whittaker Chapter 3.2).

The disposition of the pre-Pleistocene geology in the eastern part of the Hampshire Basin (Melville and Freshney 1982) is the result of sharp east-west folding, resulting from Oligocene and later Miocene/Pliocene tectonic activity, associated with the Alpine orogenic event. Two anticlines, the Portsdown Anticline in the west and the Littlehampton Anticline in the east, have resulted in extended inliers of Upper Chalk within the Tertiary outcrop (Fig 16). Further details of the geological structure of the area can be found in Shephard-Thorn *et al* (1982). The geology beneath the drift has an effect on the basal contours of the marine Pleistocene deposits of the coastal plain. Borehole records (Lovell and Nancarrow 1983) and limited exposures show that there has been a lowering of the chalk wave-cut platform, probably due to post-depositional solution (Hodgson 1964), relative to the height of the platform on the Tertiary deposits. This phenomenon is largely restricted to the post-Boxgrove beaches of the Aldingbourne and Norton Formations (Bates *et al* 1997; in press) (Fig 17, Table 8). Although not proven, it is thought that the deposits of the Slindon Formation lie partly on the Tertiary deposits in the east in the area around Arundel (Fig 16).

The Boxgrove Pleistocene sediments were deposited on a marine beach cut into the Upper Chalk (Fig 16). Foraminiferal analysis (Wilkinson 1994) of the chalk at the base of the cliff below a horizon of tabular flint (Fig 19) in GTP 25 (Fig 4), indicate a position at the top of the *Offaster pilula* Zone. Samples taken 0.15m and 1.5m above the flint band are indicative of the early part of the *Goniatethis quadrata* Zone; both these biostratigraphic zones fall in the early Campanian (Table 7). At GTP 13, samples (Fig 20) were taken from a chalk raft or debris flow approximately 30–40m south of the cliff (Lewis and C Roberts Chapter 2.2), which has been interpreted by Collicutt (Chapter 2.3) as a cliff collapse episode. One of the samples included a species which ranges from the latest *G. quadrata* Zone to the *Belemnitella mucronata* Zone. The presence of this fossil suggests that the cliff exposed a minimum sequence from just below the top of the Newhaven Chalk up to the base of the Portsdown Chalk. There may therefore have been four lithostratigraphic members of the Chalk exposed in the cliff at Boxgrove; the Newhaven, Tarrant, Spetisbury, and Portsdown (Table 7). This interval corresponds to what Mortimore (1986) refers to as the Culver Chalk, which he reports to be between 60–100m thick in

Table 6 Chronostratigraphy and lithostratigraphy for British Geological Survey Sheet 317/332: Chichester and Bognor. Empty boxes indicate no agreed lithostratigraphic designation available at present (after BGS 1996 and D T Aldiss, P M Hopson, and E R Shephard-Thorn personal communication) (not to scale)

<i>system</i>	<i>series</i>	<i>stage</i>	<i>group</i>	<i>formation</i>	<i>member</i>
Palaeogene	Eocene	Lutetian	Bracklesham Group	Selsey Sand	
				Marsh Farm	
				Earnley Sand	
				Wittering	
	Ypresian	Thames Group	London Clay	Barn Rock Bognor Sand (Pebble Bed)	
Palaeocene	Thanetian	Lambeth Group	Reading		
Unconformity					
Cretaceous	Upper Cretaceous	Campanian	Chalk Group	Upper Chalk	Portsdown Chalk
		Santonian			Spetisbury Chalk
					Tarrant Chalk
		Coniacian			Newhaven Chalk
		Turonian			Seaford Chalk
					Lewes Chalk
	Cenomanian	Lower Chalk	New Pit Chalk		
			Holywell Chalk		
			Zig Zag Chalk		
	Lower Cretaceous	Albian		Upper Greensand	
				Gault	
		Aptian	Lower Greensand Group	Folkestone	
				Sandgate	Marehill Clay
					Pulborough Sandrock
					Rogate Selham Ironshot Sands Fittleworth
Hythe				Easebourne	
Atherfield Clay					
Barremian-Hauterivian		Wealden Group	Weald Clay		

Table 7 The Sussex Chalk biostratigraphy and lithostratigraphy (after BGS 1996; Young and Lake 1988; Mortimore 1986; and D T Aldiss, P M Hopson, and E R Shephard-Thorn personal communication) (not to scale)

<i>formation</i>	<i>stage</i>	<i>biostratigraphic zone</i>	<i>lithostratigraphy members</i>	<i>lithostratigraphy beds</i>
Top of Upper Chalk absent in this area				
UPPER CHALK	CAMPANIAN	<i>Belemnitella mucronata</i>	Portsdown Chalk	Redoubt
		<i>Goniatoceras quadrata</i>	Spetisbury Chalk	Whitecliff
			Tarrant Chalk	Sompting
				Castle Hill
	<i>Offaster pilula</i>	Newhaven Chalk	Bastion Steps	
			Meeching	
			Peacehaven	
	Old Nore			
	SANTONIAN	<i>Marsupites testudinarius</i>		Splash Point
		<i>Urtacrinus socialis</i>		
	CONIACIAN	<i>Micraster coranguinum</i>	Seaford Chalk	Haven Brow
				Cuckmere
		Belle Tout		
	TURONIAN	<i>Micraster cortestudinarium</i>	Lewes Chalk	Beachy Head
Light point				
Beeding				
Hope Gap				
Cliffe				
Navigation				
South Street				
<i>Sternotaxis plana</i>	Kingston			
	Ringmer			
<i>Terebratulina lata</i>	Caburn			
	Glynde			
MIDDLE CHALK	<i>Mytiloides spp</i>	New Pit Chalk	New Pit	
		Holywell Chalk	Holywell	
LOWER CHALK	CENOMANIAN	<i>Neocardioceras juddii</i>	Zigzag Chalk	Melbourn Rock
		<i>Metoicoceras gestlinianum</i>		Plenus Marls
		<i>Calycoceras guerangeri</i>		
		<i>Acanthoceras jukesbrovnei</i>		
		<i>Acanthoceras rhotomagensis</i>	West Melbury Chalk	Under review Bristow <i>et al</i> in press
<i>Mantelliceras dizoni</i>				

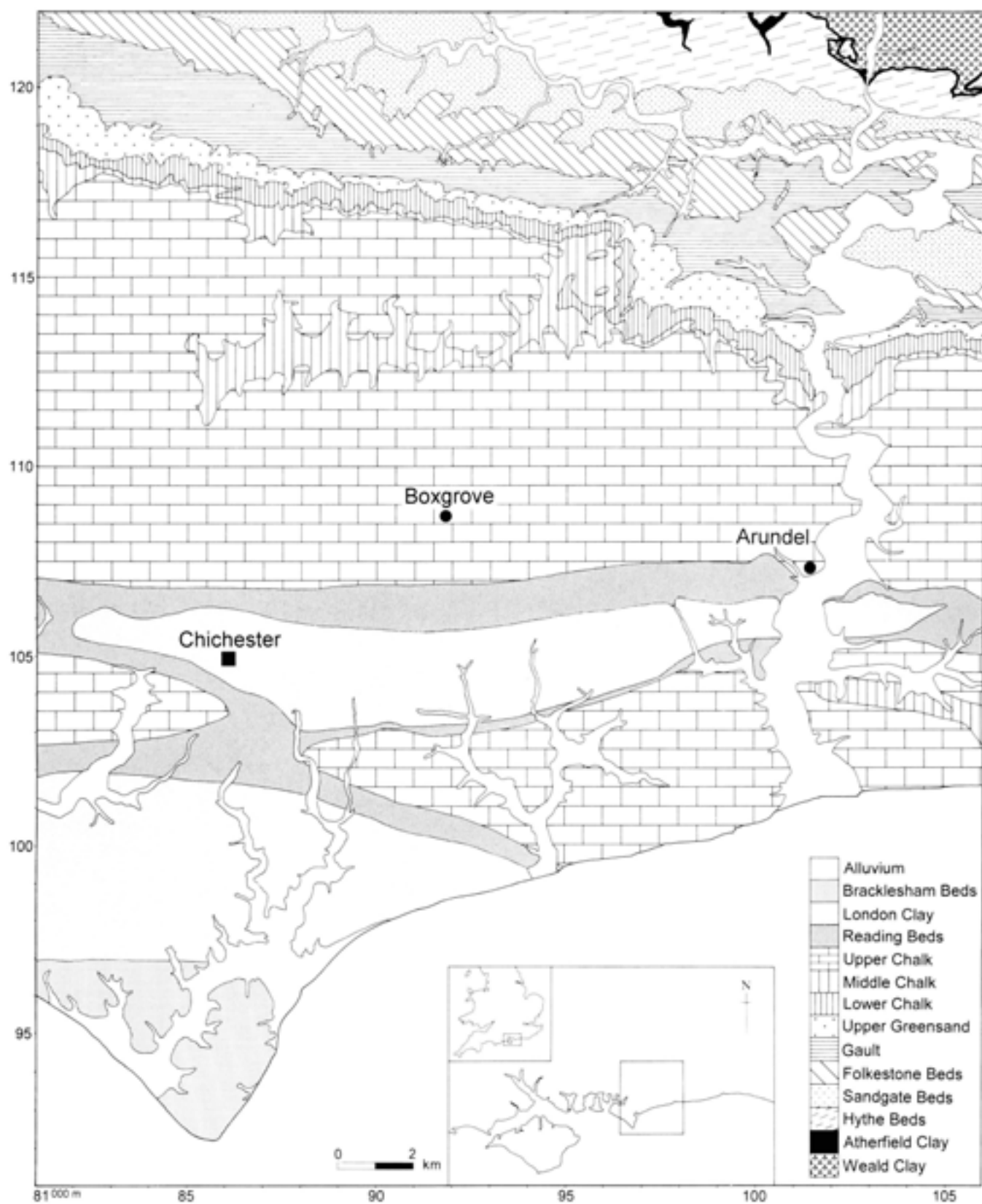


Fig 15 Geological map of the Boxgrove area showing the solid geology

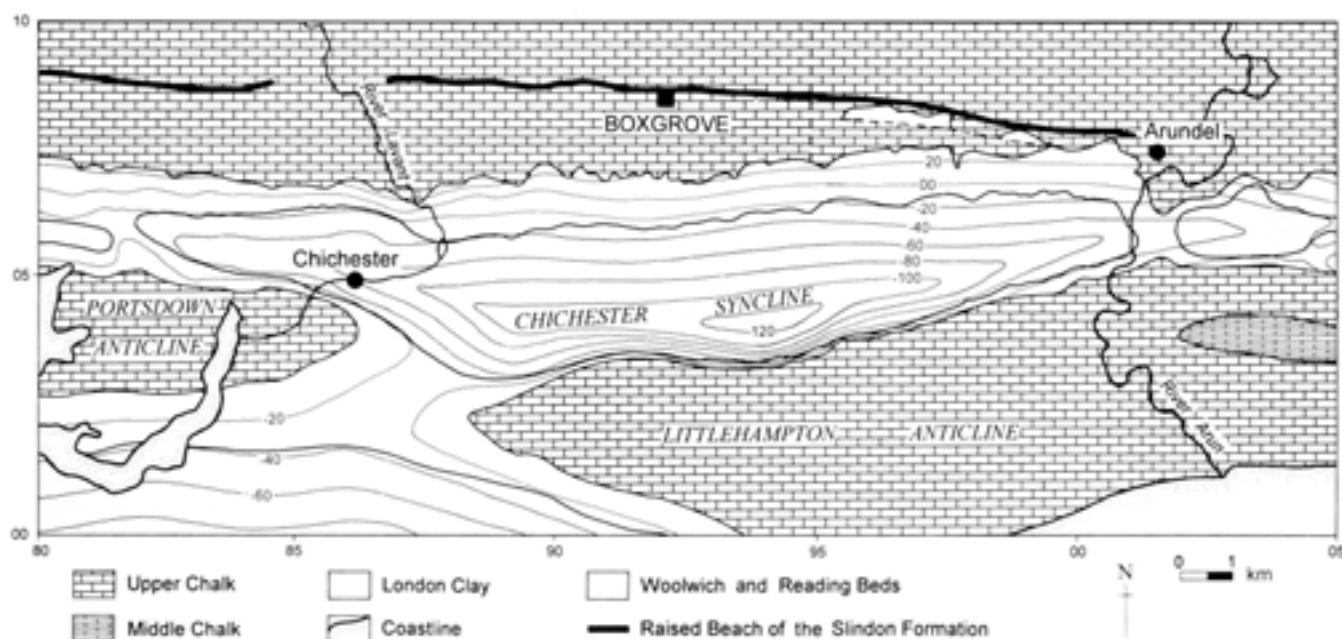


Fig 16 Solid geology outcrops beneath the drift. The structural contours are the base of the Tertiary Formations (after Shephard-Thorn et al 1982)

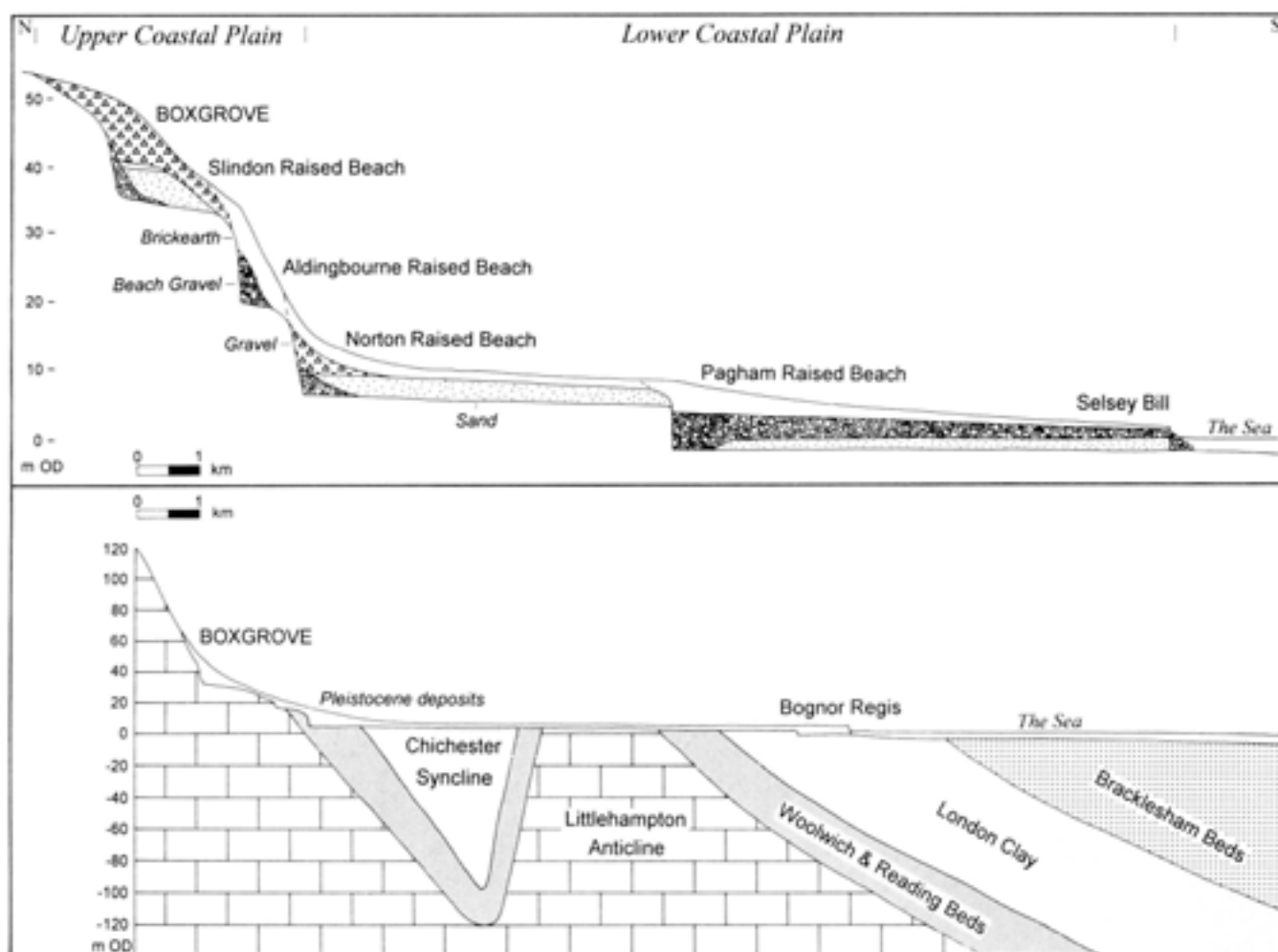


Fig 17 Schematic sections through the Pleistocene deposits (top) and solid geology (bottom) of the coastal plain

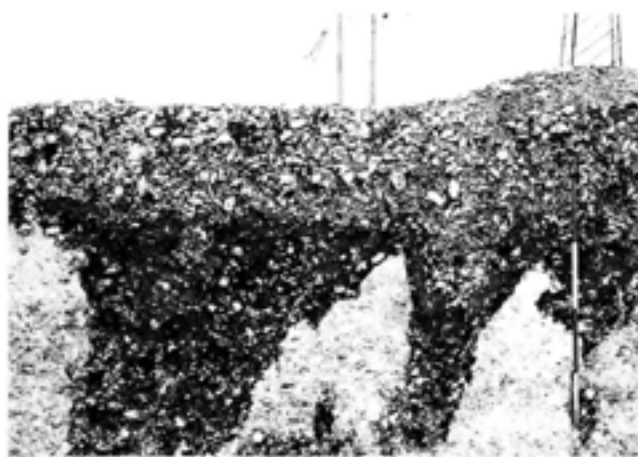


Fig 18 The soliflucted Tertiary regolith overlying chalky gravels at Boxgrove; scale unit 0.5m



Fig 19 The base of the chalk cliff at Boxgrove: note the line of tabular flint; scale unit 0.5m

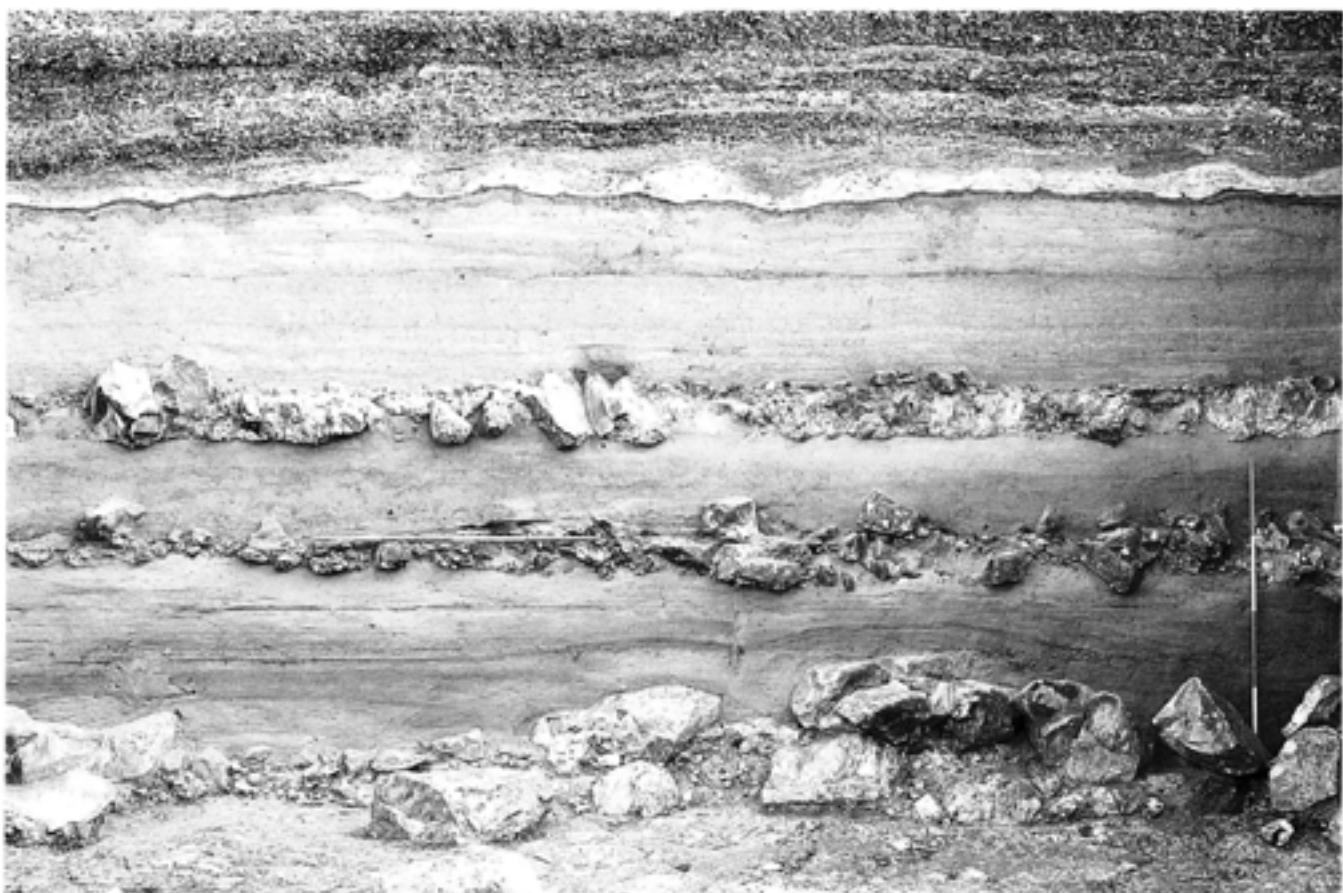


Fig 20 The Boxgrove type section, Q2 GTP 13: the upper coarse band in the Slindon Sands is the debris flow; scale unit 0.5m

Sussex and southern Hampshire. Thus, 60m represents a minimum height for the cliff at Boxgrove during the occupation of the area in the Middle Pleistocene. Analysis of the pre-Pleistocene nannofossils in the Slindon Sands by Gard (Chapter 5.8) indicates that all the stages of the chalk are represented by the assemblage, including the late Campanian. The assemblage probably represents fossils discharged into the marine environment by nearby fluvial systems and

erosion of what are now off-shore lithologies.

The dominant members of the exposed chalk in the Boxgrove cliff were the Tarrant and Spetisbury Chalk. These members contain abundant bands of both nodular and tabular flint, as opposed to Newhaven chalk exposed at the base of the cliff. Investigation of the Pleistocene cliff collapse talus from these higher members shows large amounts of flint that would have been accessible to hominids for tool making.

The West Sussex Coastal Plain

The West Sussex Coastal Plain extends from the Hampshire border in the west to the River Adur in the east (Fig 8). The palaeogeography of the coastal plain was shaped by marine action, which took the form of a series of transgressions and regressions, beginning at least 500kyr before present and continuing up to the present day (Fig 17). The northern boundary comprises the Cretaceous chalk downland, while to the south the plain runs gently into the English Channel. The plain is at its widest between Emsworth and the River Arun and achieves a maximum width of 17km between Mid Lavant and Selsey Bill, although the average width is in the region of 9km. Within this western area, the deposits are divided into group status (Table 8). The Upper Coastal Plain Group includes the Slindon (Appendix 3), Eartham, and Aldingbourne Formations; the Lower Coastal Plain Group includes the Norton Formation and all other younger, as yet undefined, sediments of the coastal plain.

The upper coastal plain runs roughly between the 65m and the 20m contour which represents a strip about 2km wide; it can be seen therefore that the lower zone covers the greater part of the plain and is an area of low relief (Fig 17). The soils of the upper coastal

plain are developed on solifluction or head deposits. These are remnants of the Tertiary regolith, which once covered the Downs in this region, mixed up with and/or interbedded with calcareous coombe rock (Hodgson 1967). On the lower coastal plain the soils are mainly developed on loessic deposits, which are wind blown silt-sized particles derived from glacial melt-out debris.

The deposits of the Slindon Formation are cut into and overlie the chalk in all exposures seen to date. The marine component of the Aldingbourne Formation is cut into the chalk in the type area (SU 931 071) (Fig 21) but into Palaeogene sediments further to the east in the Binsted/Arundel area. The sediments of the Lower Coastal Plain Group overlie both the Palaeogene sediments and the Cretaceous Chalk of the Littlehampton and Portsdown Anticlines.

The oldest Pleistocene marine deposits recorded thus far on the coastal plain (Shephard-Thorn *et al* 1982) are those that directly abut the chalk dip slope (Fig 22); these deposits are known in the literature as the '100 Foot Goodwood-Slindon Raised Beach' and have been exposed at Waterbeach, Slindon, and most recently during the excavations at Eartham Quarry, Boxgrove (Fig 4). Geological investigation shows that the beach deposits, as opposed to the marine facies as

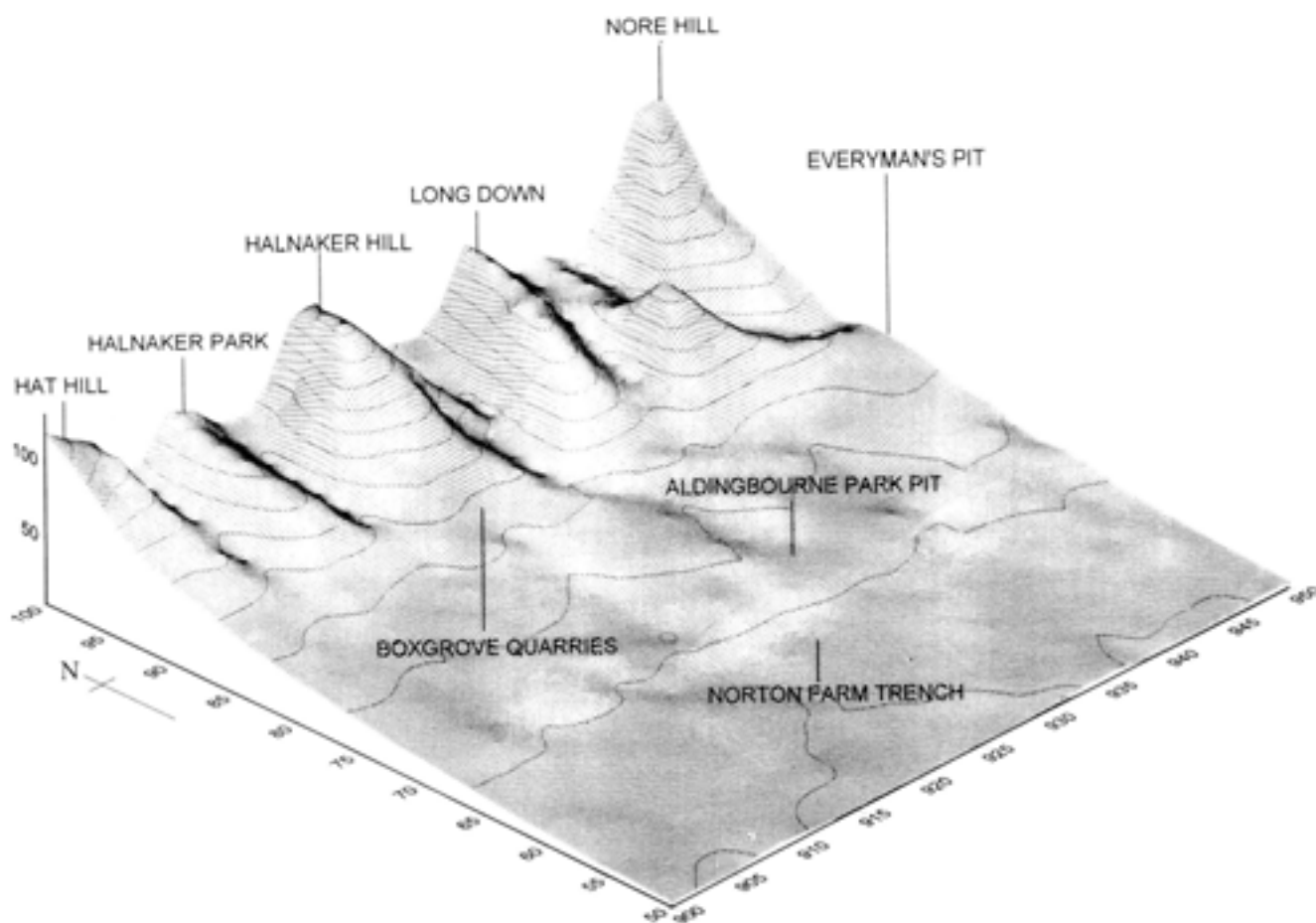


Fig 21 Isometric view of the Downland block and coastal plain in the Boxgrove area; the type sites of the raised beaches are indicated. The numbers shown on the x and y axes are Ordnance Survey grid coordinates and the y axis gives the height (m) above sea level (OD)

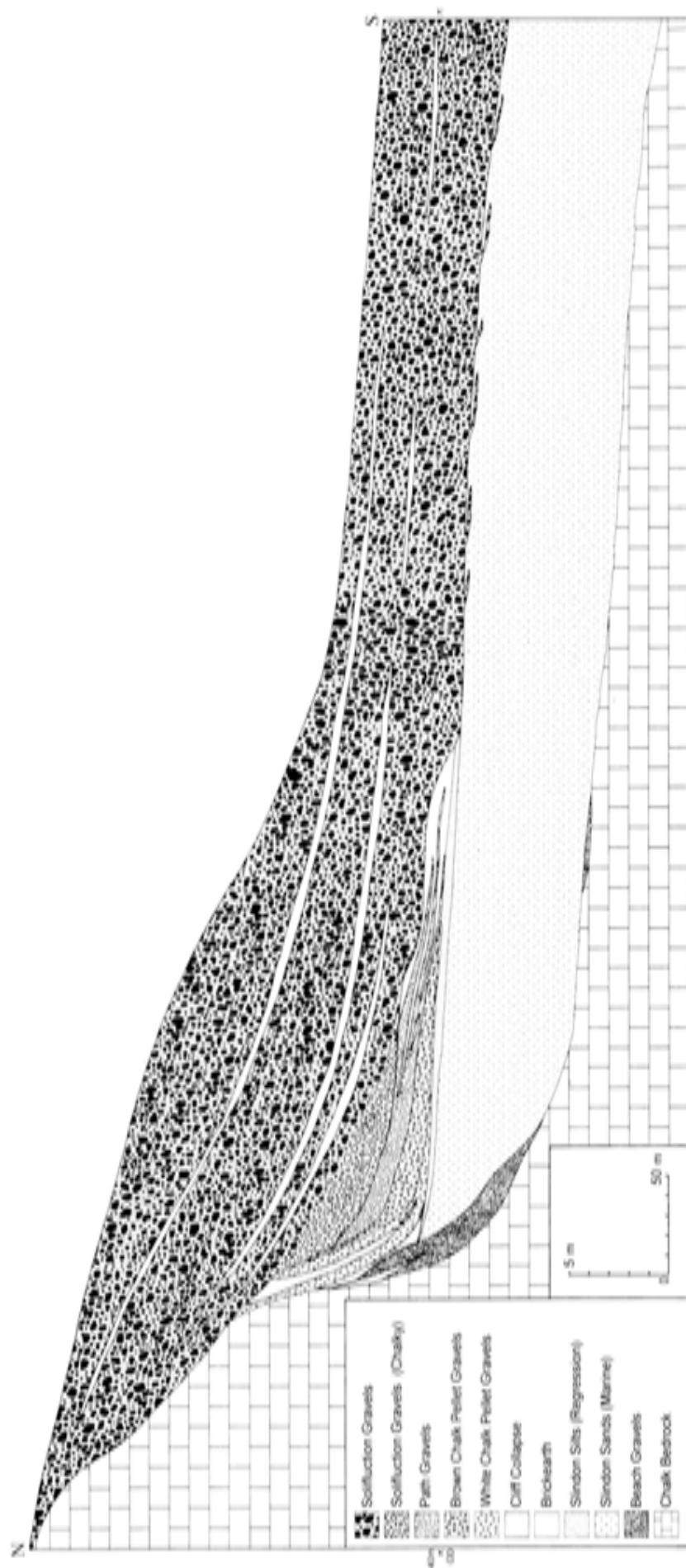


Fig 22 Composite section through the geology in Quarry 2. The path gravels are the Fox Gourd Beds, and the brown and white chalk pellet gravels correspond with the Upper and Lower Chalk Pellet Beds respectively

a whole, attain an elevation of 43m OD at Eartham (Fig 22); the surface of the Slindon Silts drops from 41m OD in the beach section to 39m OD at the southern end of the conformable sequence. Current research across the coastal plain indicates that the 'Goodwood' Raised Beach has a far wider west to east distribution than previously thought: namely that it extends from Portsdown in the west to the River Arun in the east, a length in excess of 40km.

The altitude of the Goodwood-Slindon Raised Beach, hereafter referred to as the 40m beach, is something of an enigma as there are no Middle Pleistocene littoral deposits with a similar elevation known from the coastline of Britain, with the exception of the Bembridge higher marine deposits on the Isle of Wight (Preece *et al* 1990) which are thought to be contemporary with the 40m beach deposits in West Sussex (Bridgland Chapter 2.4, Fig 81). It is considered unlikely that sea level was significantly higher than its present level during any of the Middle Pleistocene temperate stages (Shackleton 1987), certainly not in excess of 10m. This statement implies that this area of southern England is almost certainly tectonically active and that the higher raised beach deposits and the coastal plain bedrock have been elevated subsequent to their deposition.

It is extremely difficult to assess the uplift rate (U), as it may have been punctuated with tectonic pulses rather than a constant. Other variables that affect the equation are time elapsed since the deposition of the sediments (t), and the presumed height of sea level during the marine transgression (h). A constant is provided by the current height of the sediments above OD (h_1). There may also be a positive effect from isostatic rebound subsequent to the end of the last glaciation but the effects of this are considered to be minimal. The palaeotidal range at Boxgrove during the Middle Pleistocene is discounted as being too small a variable to concern this study (Collcutt Chapter 2.3), but it is potentially countered by setting h_1 at 40m.

The rate of uplift in mm per year is calculated as follows:

$$U = \frac{h_1 - h}{t}$$

t is taken as a mid point in the Specmap ages given by Imbrie *et al* (1984).

h_1 is taken as 40m OD, the mean marine surface sediment height at Boxgrove.

h in these models is calculated at (1) 0m OD, (2) 5m OD, and (3) 10m OD.

The following calculations include different permutations of the main variables discussed earlier.

1. A sea level at 0m OD equals tectonic uplift of 40m, over 500kyr (OIS 13).

This model gives a constant uplift rate of 0.08mm per year, 0.08m per thousand years, and 8m per one hundred thousand years.

The same model over 400kyr (OIS 11) gives a constant uplift rate of 0.1mm per year, 0.1m per thousand years, and 10m per hundred thousand years.

2. A sea level at 5m OD equals tectonic uplift of 35m, over 500kyr (OIS 13).

This model gives a constant uplift rate of 0.07mm per year, 0.07m per thousand years, and 7m per hundred thousand years.

The same model over 400kyr (OIS 11) gives a constant uplift rate of 0.088mm per year, 0.088m per thousand years, and 8.8m per hundred thousand years.

3. A sea level rise of 10m OD equals tectonic uplift of 30m, over 500kyr (OIS 13).

This model gives a constant uplift rate of 0.06mm per year or 0.06m per thousand years, and 6m per hundred thousand years.

The same model over 400kyr (OIS 11) gives a constant uplift rate of 0.075mm per year, 0.075m per thousand years, and 7.5m per hundred thousand years.

The Pleistocene tectonic uplift in this part of southern England is largely responsible for the preservation of a staircase of raised beach deposits on the coastal plain, although other factors such as the opening of the Straits of Dover and absolute sea level rise in each temperate stage would also have been contributory factors. Successive episodes of tectonism have lifted the beaches of earlier stages out of the reach of the sea during ensuing episodes of high sea level. It is, however, unlikely that this mechanism has perfectly preserved all the temperate stage marine deposits of the Middle and Upper Pleistocene and caution is advised in treating the staircase as a complete record. This is especially true of the sediments of the Aldingbourne Formation, which contain no evidence of age apart from their position between the Slindon/Eartham Formations and the Norton Formation (Table 8).

The Slindon Formation has been traced in the Eartham/Boxgrove area southwards to a line running between Aldingbourne Park Pit (SU 931 071) and the Boxgrove roundabout (SU 908 070) (Figs 8, 21). Along this line, which is roughly parallel to the present A27, the heavily weathered wave-cut platform of the Slindon Formation is cut through by the cliff-line and deposits of a later marine transgression (Table 8), referred to here as the Aldingbourne event (Fig 3). This formation has a north-south width of no more than 500m before it too is truncated by the sediments of another marine transgression, the Norton event (Figs 8, 21). Unlike the two earlier marine events, the basal sediments of the Norton Formation overlie the Tertiary London Clay rather than the chalk (Fig 17). The Aldingbourne deposits are essentially wholly marine, trending from beach gravels at the cliff to intertidal sand deposits in the south. Preliminary excavation at Aldingbourne Park Pit (Bates *et al* 1997), of this formation, indicates that in the present study area fossil preservation is quite poor, probably because there is a lack of terrestrial sediments covering the marine units. This contrasts with the sediments of the Norton Formation which have been revealed at Norton Farm (9256 0638) (Fig 21) (Bates *et al* in press). Here the deposits attain a depth of up to 8m and are remarkably similar in their

Table 8 Chronostratigraphy and lithostratigraphy of the Middle Pleistocene and Upper Cretaceous deposits of the West Sussex Coastal Plain, in the Boxgrove area (not to scale)

<i>stage</i>	<i>group</i>	<i>formation</i>	<i>member</i>	<i>beds (informal, except Cretaceous)</i>	
Saalian Complex	Lower Coastal Plain Group	Norton	Norton Gravels and Brickearth Member	Beds not yet defined	
			Norton Silts		
			Norton Sands		
			Norton Beach		
Possible Unconformity					
Hoxnian/ Holsteinian?		Aldingbourne	Aldingbourne U. Gravel	Beds not yet defined	
			Aldingbourne Sands		
			Aldingbourne L. Gravel		
Possible Unconformity					
Anglian/ Elsterian	Upper Coastal Plain Group	Eartham	Eartham Upper Gravel Member	Upper Head Gravel	
				Upper Silt Bed	
				U. Middle Head Gravel	
				Middle Silt Bed	
				L. Middle Head Gravel	
				Lower Silt Bed	
			Lower Head Gravel		
			Calcareous Head Gravel		
			Fan Gravel Beds		
			U. Chalk Pellet Beds		
			Brickearth Beds		
Cromerian IV			Eartham Lower Gravel Member	L. Chalk Pellet Beds	
				Calcareous silty clays	
				Angular Chalk Beds	
			Slindon Silt Member	Organic Bed	
				Slindon Soil Bed	
				Lagoonal/Intertidal Beds	
		Slindon	Slindon Sand Member	Beds of:	
					Marine Cycle 3
					Marine Cycle 2
				Marine Cycle 1	
			Slindon Gravel Member	Beach Gravel Beds	
Major Unconformity					
Campanian	Chalk Group	Upper Chalk	Portsdown	Redoubt	
			Spetisbury	Whitecliff	
			Tarrant	Sompting	
				Castle Hill	

environments of deposition to the sediments of the Slindon Formation. The southern extent of the Norton deposits is not known but the coastal plain itself extends gently southwards for another 7.5km. Over this distance the plain is very flat, with minimal relief south of the 10m contour, which is fairly linear in its east-west distribution in this area. Little is known about the distribution of marine deposits under this part of the plain; indeed it is not until the present coast is reached that Pleistocene marine deposits are accessible again (Fig 17).

The most well known of these low level marine deposits is the Selsey Raised Beach (SU 855 921) (West and Sparks 1960). Other Pleistocene deposits occur in channels incised into the Tertiary bedrock, below the present ordnance datum, at Earnley and the Witterings (Stinton 1985; West *et al* 1984). The exact age or climate cycle assignation for these channels is unknown but current opinion supports the view that they all post-date the Boxgrove interglacial (Roberts Chapter 1.3). At Earnley this opinion is supported by the very different foraminifera and ostracod faunas to that from the Slindon

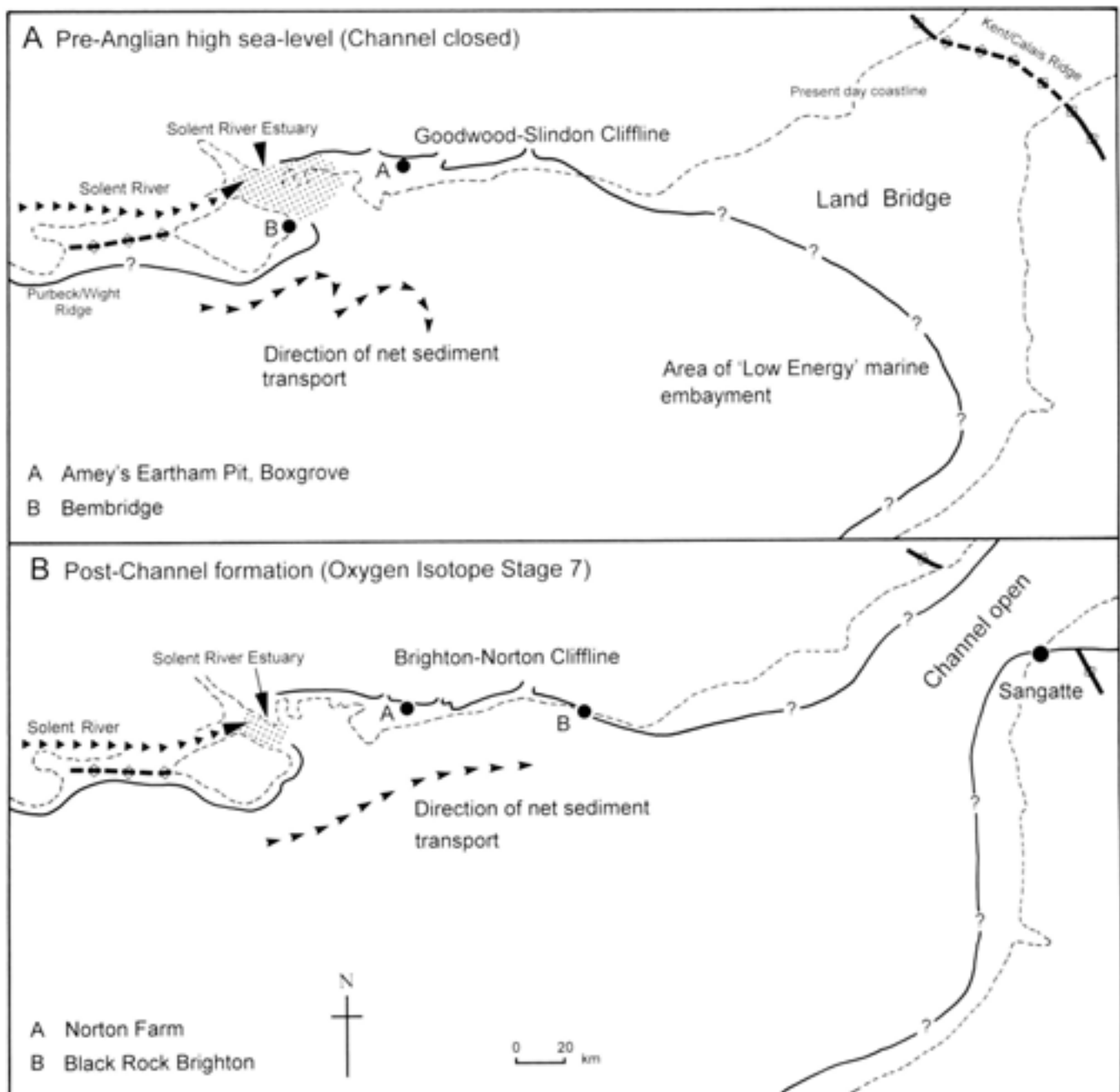


Fig 23 Palaeogeography of the south coast before (A) and after the Anglian Glaciation (B)

Sands and Silts (Whittaker Chapter 3.2), which imply much warmer conditions, normally associated with the post-Anglian temperate stage (Shackleton 1987).

The Pleistocene deposits of the coastal plain to the east of the River Arun have undergone less examination than their western counterparts. The main reason for this is that the deposits of the Upper Coastal Plain Group (Table 8) have never been located east of the Arun. It is considered most likely that later transgressions have successively reworked the older material, both marine and terrestrial. If this is the case, it would suggest that tectonic uplift decreases to the east of the area, although this remains unproven. There also exists the possibility that the geography of the coastline to the

east was significantly different during the early part of the Middle Pleistocene, in that the coast swept south-eastwards from Arundel, implying that the Littlehampton Anticline was still extant as a feature of relief at this time (Martin 1938). The marine deposits on this margin may then have been subsequently removed by a combination of later higher sea levels and the erosive effects of the opening of the channel after the Anglian Glaciation. The extent of the chalk landbridge linking Britain to mainland Europe is still unresolved, but estimated erosion rates for the chalk (Smith 1985) allow for it to have come as far west as the Arundel/Worthing area (Fig 23). Resolution of these hypotheses has been made difficult by the limited mineral

Table 9a Correlation between lithostratigraphy, unit numbers (Roberts 1986; 1990; 1994; Roberts et al 1997), and sediment description/interpretation. The most complete part of the sequence is recorded over the length of Q2 GTP 25 (Figs 40, 42a). The column showing the area between GTP 5 and Q2/A illustrates reduced sediment diversity to the south, away from the Downland block and the cliff (not to scale)

Formation	member (applies to GTP 25 column only)	beds (informal) at GTP25	unit numbers	description/interpretation	beds (informal) between GTP 5 and Q2/A	
Earthenham	Earthenham Upper Gravel Member	Upper Head Gravel UHG	Unit 11	Soliflucted Tertiary regolith with finer bands of essentially stone free silts, showing traces of cold climate soil development.	SURFACE	
		Upper Silt Bed USB			Upper Head Gravel UHG	
		U. Middle Head Gravel UMHG			Upper Silt Bed USB	
		Middle Silt Bed MSB			U. Middle Head Gravel UMHG	
		L. Middle Head Gravel LMHG			Middle Silt Bed MSB	
		Lower Silt Bed LSB			L. Middle Head Gravel LMHG	
		Lower Head Gravel LHG			Lower Head Gravel LHG	
		Calcareous Head Gravel CHG			Calcareous Head Gravel CHG	
		Fan Gravel Beds FGBs			Unit 10 MB: See Table 9b Unit 9 (Path Gravels)	Similar to Unit 7 but represents main weathering and lowering of the cliff, soliflucted southwards across site
		UCLPBs			Unit 8 U. Chalk, Peffer Beds 67: See Table 9b Unit 6 Brickearth Beds Be	See sorted flint gravel sometimes clay supported, water-lain, intercalated seams of brickearth
Earthenham Lower Gravel Member	Chalk Peffer Beds LCLPBs	67	Unit 8 U. Chalk, Peffer Beds 67: See Table 9b Unit 6 Brickearth Beds Be	Weathered cliff collapse/slope moved downslope by water and creep. Noticeable brown staining. Cold conditions		
		63	Unit 6 Brickearth Beds Be	Redeposited soils from Downland Regolith and calcareous soils from stee slopes and exposed chalk		
		5b	Units 5b, 5c at GTP 17	Calcareous washes and redeposited soils from stee slopes		
			Unit 8 L. Chalk Peffer Beds	Weathered cliff collapse/slope. Colluvium formed under temperate and cool/temperate conditions		
			Unit 7 ACKBs Angular Chalk Beds	Massive cliff collapse, induritates with L. Chalk Peffer Beds. Temperate conditions. Truncated by Lower Head Gravel at north end of GTP 25		
			1129 see Table 9b	Calcareous silty clays derived from cliff collapse deposits		
			Organic Bed	Mineralised organic material deposited in fenbiller cut		
			Slendon Soil Bed	Soil horizon (4c) and calcareous spring deposit (4d)		
			Lagooonal/Intertidal Beds	Unit 4b Unit 4a	Marine silts with clay laminations, gentle deposition in shallow water	
		Slendon	Slendon Sand Member	Beds of Marine Cycles 1-3	Unit 3	Nearshore and intertidal fine grained marine sands, divided into 3 marine cycles. Contain coarse components near the cliff
Beach Gravel Beds	Units 1 & 2			Marine flint shingle beaches	Beach Gravel bed (Lag)	

Table 9b Detailed subdivision of sediments in Quarry 2 around GTP 25, based upon sediment mapping and sampling for vertebrate fauna (together with two test pits from Quarry 1) (Parfitt Chapter 4.3, Tables 93–95a)

area	bed/unit (Table 9a)	SAP designation	description	vertebrate fauna	climate
Q1 GTP 21	Unit 10	MB	Calcareous silty clay in Calcareous Head Gravel	No fauna recovered (Table 95a)	Cold
Q2 GTP 3	Unit 8	SG	Chalky pellet gravel	<i>P. episcopalis</i> , <i>A. terrestris cantiana</i> , <i>M. agrestis</i>	Cold
Q2 GTP 20	Unit 8	BCG	Compacted chalk pellet gravel with broken flint	No fauna recovered (Table 95a)	Cold
Q2 GTP 3	Probable soil horizon developed on the surface of 6'3	6'3 Fe	Dark brown ferric stained horizon on top of 6'3	<i>A. fragilis</i> , <i>E. rubecula</i> , <i>Neomys</i> sp., <i>S. ransonensis</i> , <i>S. savini</i> , <i>Talpa</i> sp., <i>Lemus/Myopus</i> , <i>C. glareolus</i> , <i>P. episcopalis</i> , <i>A. terrestris cantiana</i> , <i>Microtus</i> spp., <i>M. arcellumarius</i> , <i>A. sylvaticus</i>	Temperate
Q2 GTP 3	Bed unassigned to a unit	6'3	Highly calcareous silty clay, c 40mm thick at GTP 3. Silty mud derived from brown chalky pellet gravels, Unit 8 (Fig 42a)	<i>S. ransonensis</i> , <i>S. savini</i> , <i>Talpa</i> sp., <i>M. arcellum</i> , <i>Lemus/Myopus</i> , <i>C. glareolus</i> , <i>P. episcopalis</i> , <i>A. terrestris cantiana</i> , <i>Microtus</i> spp. including <i>M. grogali</i> , <i>A. sylvaticus</i>	Cool/Temperate
Q2 B	Bed unassigned to a unit. Between 200mm and 20mm thick. A silty mud derived from weathering of the chalk cliff collapse, Unit 7 and the lower part of Unit 8, the white chalky pellet gravels (Fig 42a)	LGC	White/grey light brown silty clay with chalk pellets stratified between Units 5a and 8. Same bed as 1129, 6'20 and GCF	<i>S. savini</i> , <i>S. ransonensis</i> , <i>S. savini</i> , <i>Talpa</i> spp., <i>M. schreineri</i> , <i>Lemus/Myopus</i> , <i>C. glareolus</i> , <i>P. episcopalis</i> , <i>A. terrestris cantiana</i> , <i>Microtus</i> spp. <i>M. arcellumarius</i> , <i>E. quercinus</i> , <i>A. sylvaticus</i>	Temperate
Q2 GTP 20		GCF	Grey silty clay with flint. Same bed as 1129, 6'20 and LGC	<i>S. savini</i> , <i>Talpa</i> sp., <i>C. glareolus</i> , <i>P. episcopalis</i> , <i>A. terrestris cantiana</i> , <i>Microtus</i> spp., <i>M. arcellumarius</i> , <i>S. cf. benedina</i> , <i>A. sylvaticus</i>	Temperate
Q2 GTP 20		6'20	Light brown silty clay with chalk pellets and occasional flints. Same bed as 1129, GCF and LGC	<i>S. ransonensis</i> , <i>S. savini</i> , <i>Talpa</i> spp., <i>Lemus/Myopus</i> , <i>C. glareolus</i> , <i>P. episcopalis</i> , <i>A. terrestris cantiana</i> , <i>Microtus</i> spp., <i>S. cf. benedina</i> , <i>A. mazzucchinensis</i> , <i>A. sylvaticus</i>	Temperate
Q2 GTP 25		1129	Light grey silty clay with chalk pellets, above beach gravels (Fig 42a). Same as 6'20, GCF and LGC Q2	<i>Neomys</i> sp., <i>S. ransonensis</i> , <i>Talpa</i> spp., <i>C. glareolus</i> , <i>A. terrestris cantiana</i> , <i>Microtus</i> spp.	Temperate
Q2 GTP 20	Unit 5a	LS>5a	White/light grey very fine sand, filling desiccation cracks in Unit 5a	<i>A. terrestris cantiana</i> , <i>Microtus</i> spp., <i>M. arcellumarius</i>	Temperate
Q1 GTP 15	Unit 5a	LS	White/light brown very fine sand, below Unit 5a	<i>A. terrestris cantiana</i> , <i>Microtus</i> sp.	Temperate
Q2 GTP 3	Unit 4c	GC	Grey silty clay	<i>G. aculeatus</i> , <i>P. fuscus</i> , <i>S. savinus</i> , <i>Talpa</i> spp., <i>C. glareolus</i> , <i>P. episcopalis</i> , <i>A. terrestris cantiana</i> , <i>Microtus</i> sp., <i>M. arcellumarius</i> , <i>A. sylvaticus</i>	Temperate
Q2 GTP3	Unit 4c	GB4	Grey/dark grey clayey silt with Fe/Mn mottling	<i>G. aculeatus</i> , <i>A. fragilis</i> , <i>S. ransonensis</i> , <i>Talpa</i> spp., <i>C. glareolus</i> , <i>P. episcopalis</i> , <i>A. terrestris cantiana</i> , <i>Microtus</i> spp., <i>M. arcellumarius</i> , <i>A. sylvaticus</i>	Temperate
Q2 GTP20	Unit 4b	4'20	Compact green/grey clayey silt containing occasional chalk pellets. Below Unit 4c	<i>Talpa</i> sp., <i>A. terrestris cantiana</i> , <i>Microtus</i> spp., <i>S. cf. benedina</i> , <i>A. sylvaticus</i>	Temperate

extraction in the eastern area, because of the paucity of solifluction gravels and marine sands which constitute the main commercial quarry product west of the Arun. The northern part of the coastal plain region east of the River Arun along to the town of Worthing is occupied by large country estates developed for agricultural and sporting interests; this fact has kept quarrying to a minimal, local level. Additionally, the whole of the coastal plain in this area has seen greater urban development than the rest of the study area and this has meant that long term exposures are rarer.

The age of the various marine transgressions across the coastal plain is still a matter for debate. However, a bracket may be put on the sequence as the age of the oldest and youngest marine events, Cromerian IV and the Eemian/Ipswichian respectively, are known (Table 4).

Sediments of the Slindon and Eartham Formations

The sediments of these formations are formally named down to member status in this volume (Table 8; Appendix 3). Beds within the members are informally named and, to a large extent, correspond with the unit numbering system that is used in this and previous publications on the Boxgrove Project. These correlations are described in Table 9a, which illustrates considerably greater sediment diversity at the northern

end of the quarry, in the area of the chalk cliff (Fig 22). The Boxgrove sequence, as originally described (Roberts 1986; 1990), was based upon exposures further to the south between GTP 5 and Q2/A (Fig 4).

The 40m raised beach deposits are formally named as the Slindon Formation, after the type site at Slindon. The members of this formation are disposed as a packet of sediments that have been mapped between the Valdoe Quarry (SU 876 085) and West Stubbs Copse Pit (SU 978 078) (Fig 9), a distance from west to east of 10km. This formation includes three members (Fig 20, Tables 8, 9): the Slindon Gravel Member (Raised Beach), the Slindon Sand Member, which includes both near shore marine and littoral sediments, and the Slindon Silt Member, which post-dates the sands and represents regressional tidal flat sedimentation, possibly in a lagoon. The complete Slindon sequence is preserved southwards from the cliff up to a distance of 250m, forming a corridor of sediments that run almost parallel to the cliff. Southwards of this line the upper sediments of the Slindon Formation have been eroded away by surface drainage water and hence the sands are unconformably overlain by the solifluction gravels (Fig 24a-b).

The uppermost beds/units of the Slindon Formation are the palaeosol Unit 4c and the organic bed Unit 5a (Fig 25). Unit 4c developed upon the surface of and within the Slindon Silts to a depth of *c* 150mm.

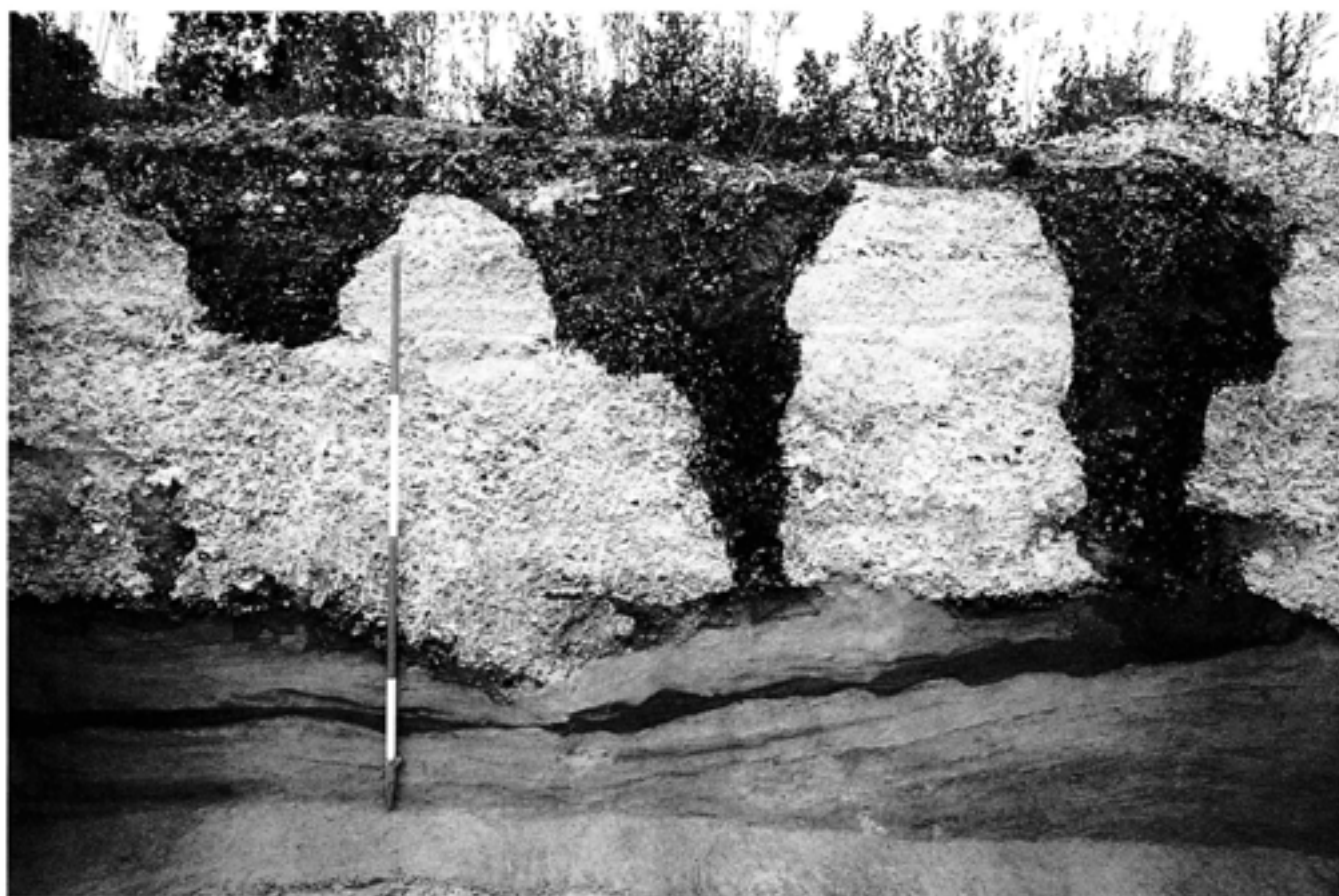


Fig 24a Soliflucted head gravel unconformably overlying the Marine Slindon Sands at the southernmost end of Quarry 2; scale unit 0.5m

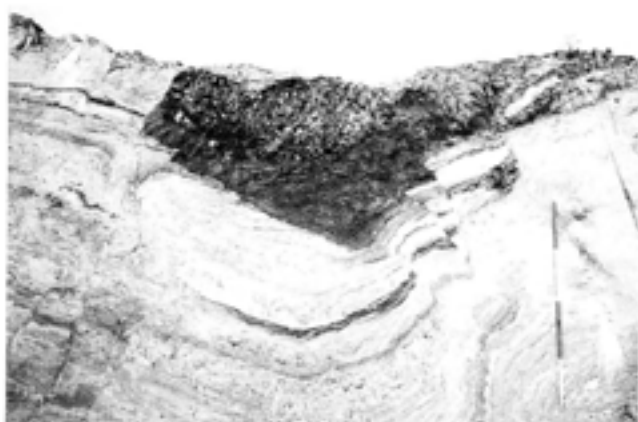


Fig 24b Preservation of the Slindon Silts and Brickearth Beds in a solution feature, south of the main east–west running unconformity in Quarry 2; scale unit 0.5m

Although this unit is not a bed *per se* and was not laid down under marine conditions, it is an integral part of the Slindon Silt Member because the background sedimentary constituents and fauna/flora are marine. Unit 5a formed as a result of flooding the Unit 4c palaeoland surface with freshwater, leading to the development of a fen/alder carr (Macphail Chapter 2.6, Table 24). The thickness of the constituent members and beds of the Slindon and Eartham Formations varies considerably across the site; precise measurements at various

locations can be found in Figures 33–5 and the detailed sedimentary logs in Chapter 2.3.

The overlying sediments of the Eartham Formation all have a terrestrial source, namely the chalk cliff and screes together with the sediments of the Downland Block and dipslope; they are also formally defined here (Tables 8, 9a). (See Catt Chapter 2.5 for a discussion on the contribution of sediments of the Slindon Formation to the mineralogical composition of the sediments of the Eartham Formation.) The members have the same lateral extent as that observed for the Slindon Formation but, given the nature of their deposition, exhibit greater variability. Deposits similar to the head gravels are found right across the upper coastal plain but it has not been possible, outside the study area, to determine whether they overlie sediments which represent a continuation of the Slindon Formation. The sediments of the Eartham Lower Gravel Member were laid down during the same temperate stage as the Slindon Formation (Table 8). Erosion of the cliff was an ongoing process by marine and various sub-aerial mechanisms throughout this stage, and resulted in the formation of the Angular Chalk Beds (Table 9a). These sediments exhibit a time transgressive relationship with all the members of the Slindon Formation and other beds of the Eartham Lower Gravel Member.

Detailed sediment mapping and sampling for vertebrate fauna has revealed localised sedimentary

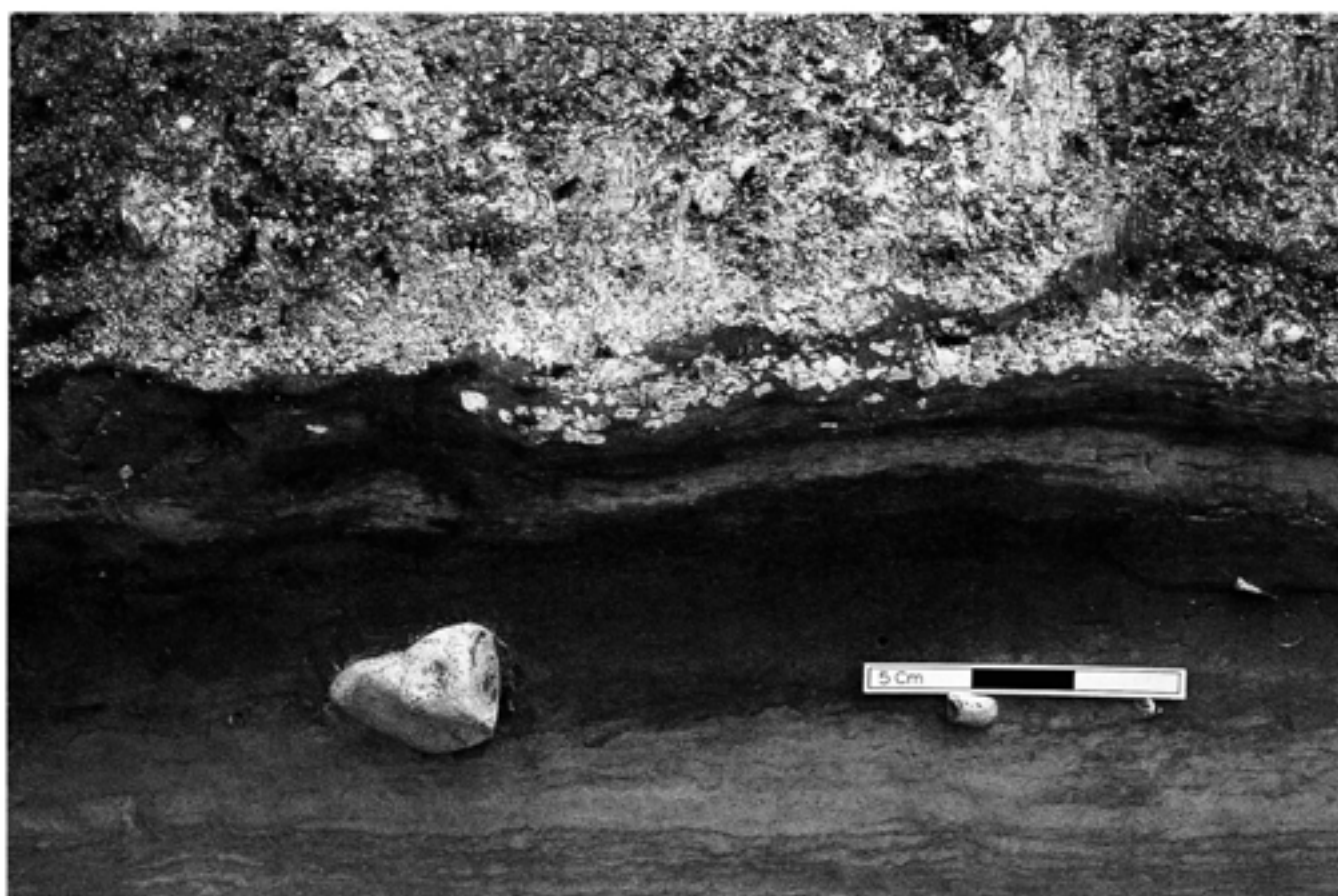


Fig 25 Unit 4c overlain by sediments of the Eartham Lower Gravel Member: note the boundary between Unit 4c and the underlying sediments of Unit 4b; scale unit 50mm

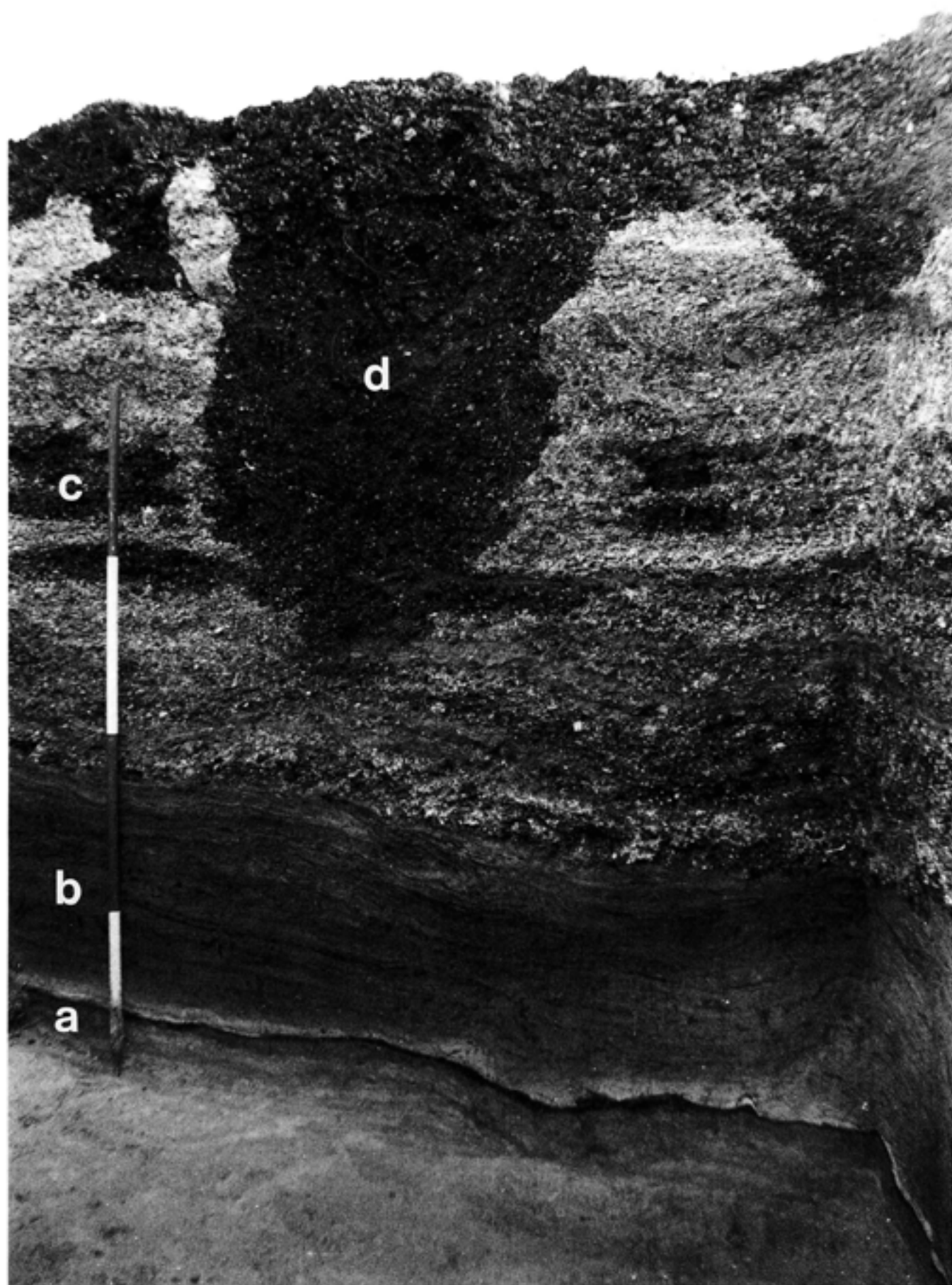


Fig 26 Fan gravels of the Eartham Upper Gravel Member overlying sediments of the Slindon Silt Member. Section shows a) palaeosol (Unit 4c), b) laminated Brickearth Beds, c) Fan Gravels Beds, and d) solution feature; scale unit 0.5m

subunits in both the Slindon and Eartham Formations (Table 9b). In the latter formation the most important of these sub-units are found in the vicinity of the cliff-line at GTP 3, 20, 25, and Q2/B (Fig 4). It has been determined through linking sedimentary logs that sub-units 1129, 6'20, GCF and LGC comprise a single bed of variable thickness. The bed derives from weathering of the chalk cliff collapse and the basal Lower Chalk Pellet Gravels and contains an abundant, temperate, small mammal fauna. In the Eartham Upper Gravel Member, evidence of a brief return to warmer conditions is found in sub-unit 6'3Fe; this sediment and the underlying 6'3 (Tables 9a, 9b) are almost certainly southerly lateral equivalents of a similar horizon containing artefacts, examined in the Upper Chalk Pellet Beds at GTP 25 by Macphail (Chapter 2.6, Tables 18, 24, Figs 83m-n; Roberts Chapter 6.3, Figs 291-4).

The sediments of the Eartham Upper Gravel Member were deposited under cold conditions, either as fans of sediment washed from the Downland and cliff slope (Fig 26), as a result of the decline in vegetation cover and hence slope stability, or as mass movement deposits under periglacial conditions (Table 9a). Detailed analysis of the geology and sedimentology are described in the following chapters of this section.

2.2 Location of the buried cliff-line using resistivity methods

S G Lewis and C L Roberts

Introduction

The assemblage of Lower Palaeolithic artefacts from Eartham Pit, Boxgrove, is associated with a sequence of marine sediments overlying a chalk platform some 35–40m above sea level, adjacent to a chalk cliff now 12km inland from the present coast. The cliff morphology (Fig 27) has subsequently been altered by weathering and erosion under periglacial conditions, reducing the angle of the cliff in its upper part and burying the chalk and overlying marine deposits



Fig 27 The chalk cliffs at Seaford Head. The cliff at Boxgrove would have been similar

beneath a thick accumulation of calcareous and non-calcareous gravels of the Eartham Formation (Fig 28). The relationship of the marine deposits to the chalk platform and cliff has been demonstrated in Quarry 2 in the beach section GTP 25 (Fig 4), where the cliff is between 3–4m in height (Fig 19).

The cliff-line is not present in Quarry 1, where the marine Slindon Sands and Slindon Silts overlie the chalk platform, neither is there any trace of the chalk boulder layers within the Slindon Sands like those observed in Quarry 2 GTP 13 (Fig 20), proximal to the cliff. It may be assumed that the cliff is located in a position some distance to the north of Quarry 1 (Fig 29). As the cliff has no geomorphological expression in the modern landscape, tracing the line of the buried cliff may best be achieved using sub-surface investigations. To this end, a resistivity survey was undertaken in the summer/autumn of 1993 to attempt to locate the cliff-line by establishing the configuration of the chalk surface and the depth of the overlying Pleistocene deposits.

Methods

Resistivity has been successfully employed over many years as a tool for examining sub-surface features in both archaeological and geological research (Merkel 1972; Barker and Worthington 1972; Aspinall and Walker 1975; Barker and Harker 1984; Raines and Chadsfield 1991; Noel 1992). Vertical electrical sounding (VES) is used to study horizontal or near-horizontal interfaces below sub-horizontal ground surfaces (Kearey and Brooks 1984). The term 'sounding' refers to a set of measurements used to determine apparent resistivities at progressively deeper levels below the surface.

This VES survey used the Offset Wenner system of measurement (Barker 1981) with a maximum multi-core cable length of 256m and an ABEM Terrameter SA300 as suitable digital instrumentation. Soundings were carried out using the Wenner configuration, a collinear array of four equally spaced electrodes; the spacing is increased about a fixed central point, with electrode spacing set at 0.5, 1, 2, 4, 8, 16, 32, 64 and 128m. A current is passed through the outer two electrodes, and the resulting potential difference or voltage is measured across a further pair of electrodes. A five channel switch-box facilitated rapid measurement of the entire array and also provided monitoring of correct instrument operation.

For each separation layout, four readings were taken to obtain a reproducible sample of apparent resistivity data. Calculation in the field of the switch-box variables allowed constant monitoring of spurious readings, which could be immediately re-measured if errors exceeded an arbitrary level of 2%.

Apparent resistivity data were analysed using 'Resix', a highly interactive 2-D modelling software package. In this the user inputs apparent resistivity values for each electrode spacing, and chooses a model



Fig 28 The cliff and beach buried under angular chalk cliff collapse and colluvium; scale unit 0.5m

with a number of depth layers of variable resistivity. The computer then compares the theoretical response to this model with the observed data and adjusts the resistivity and thickness values of the layers in the model until a best-fit curve has been obtained. The user then has the option of changing or fixing all values and/or the number of layers, with the object of producing the lowest possible fitting error in conjunction with a geologically feasible model. A homogeneous single layer produces a straight, horizontal plot, whereas variations in the sub-surface lithology might be expected to produce a curved plot. As long as the models are feasible geologically and there are exposures or adequate borehole control to constrain the models, VES can provide a good indication of the sub-surface lithological variations with a reasonable degree of accuracy.

Survey area

The locations of the 16 resistivity soundings (Fig 29) were selected to form three north-south traverses roughly perpendicular to the projected position of the cliff-line, and to provide some degree of control on the field data from known stratigraphic sequences. The locations were constrained by the need to develop the electrode arrays in an approximately east-west direction, thus avoiding steep, south-dipping slopes and to allow sufficient lateral space to accommodate a total electrode spread of 512m.

Traverse A-B was aligned over a distinct colour change in the ploughsoil visible on the 1986 aerial photograph of the area, running in a west-east direction, which may mark the point at which chalk outcrops at the surface. Traverse C-D extends north from Quarry 1 to a point adjacent to an exposure of chalk at the ground surface north of the road. Traverse E-F extends north from Quarry 2 to a point close to an exposure of chalk created by a fallen tree. North of the road at this point is a disused chalk pit (Fig 29).

Results

Field data

The field data (Fig 30) indicate apparent resistivity values in the range 26–198m. Although this range is small with respect to the possible theoretical range of values, the changes in slope of the plotted data evident in many of the apparent resistivity curves (Fig 30) indicate that a contrast in resistivity can be detected in this area. Four readings were taken for each electrode spacing at all stations and averaged to give one value for apparent resistivity. A set of values with a mean standard deviation of up to 2% was taken to indicate a reliable sample. If readings showed significant variability during each cycle of measurement, repeat readings were taken until a regular pattern was established. Such variability is thought to be caused by either poor electrode contact or polarisation, and was rectified by improving the electrode contact with the soil.

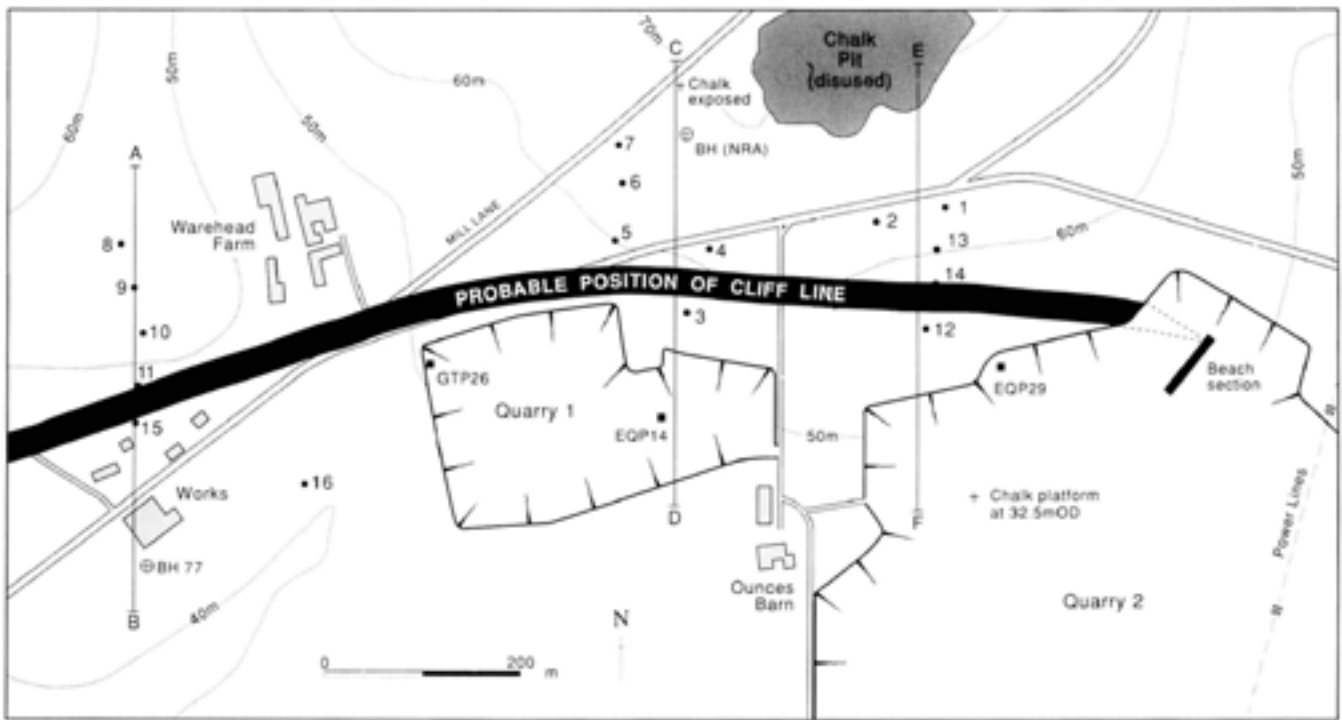


Fig 29 Map of the Boxgrove quarries showing the probable position of the cliff-line and the position of the resistivity soundings along the three north-south traverses

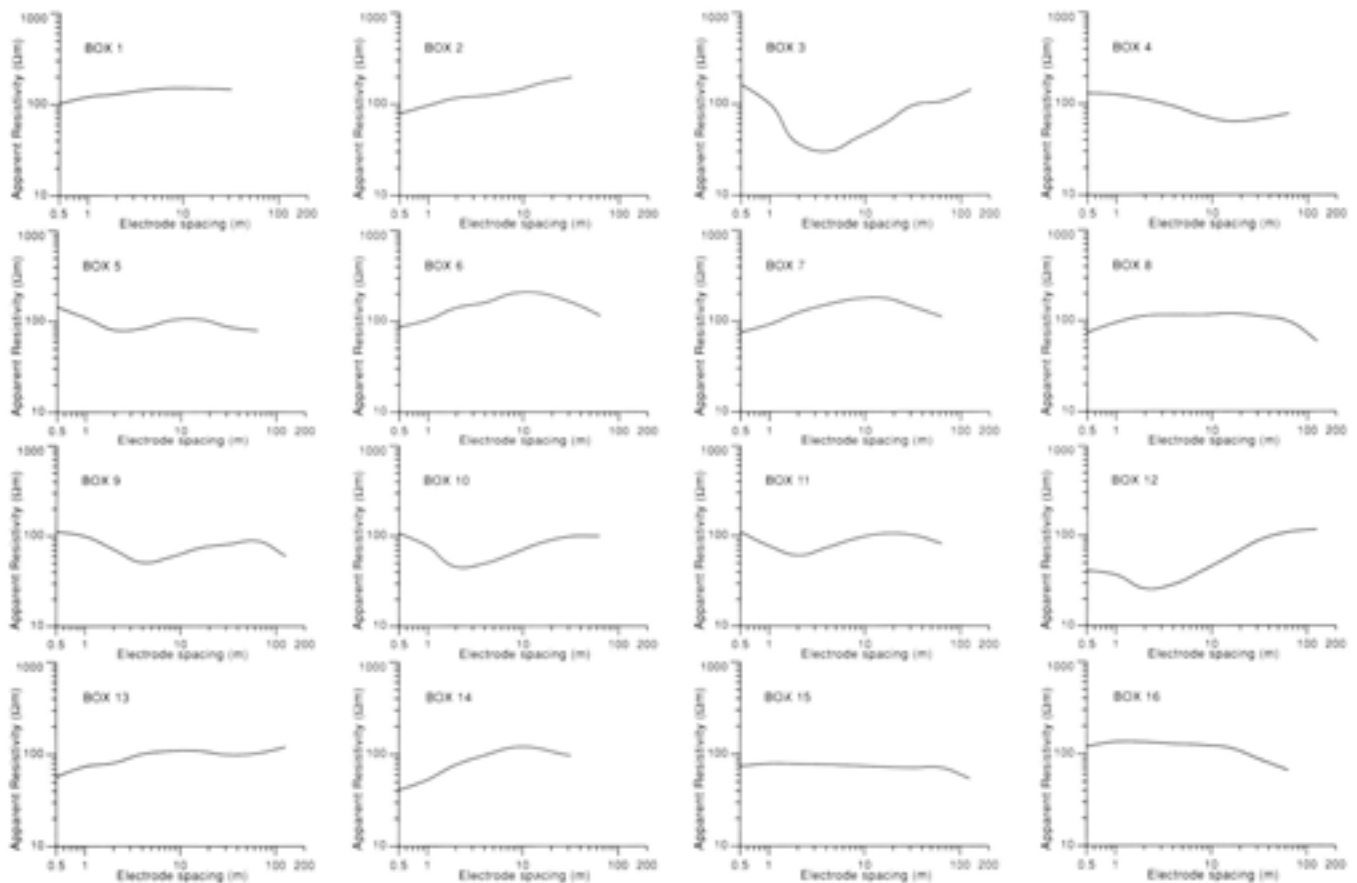


Fig 30 Apparent Resistivity (SLM) plotted against depth (m), for Box 1-16 both axes have log scales

Computer modelling

The best-fit computer response to the field data have been generated for each sounding (Fig 30). Fitting errors between the observed and computed resistivity curves for locations 1–2, 4–8, 10–12 and 14–16 were $1.3 \pm 0.6\%$, and $4.9 \pm 0.4\%$ for locations 3, 9 and 13. Model layers were initially set at three with additional layers being used to reduce fitting errors. A maximum of six layers was considered feasible for modelling purposes. Table 10 gives computed resistivity values for the lithological units present at the site. These are also compared with data from additional published sources to assess the compatibility of these results with previous research.

Lithological interpretation

Most rock-forming minerals are very poor conductors, and so electrical currents are transferred through the sub-surface strata by the movement of ions in waters held in pores and fissures. Resistivity thus generally decreases as porosity increases. In addition to porosity, the resistivity is also affected by the water content of the material (saturated or unsaturated), the resistivity of the groundwater and the grain size characteristics (Griffiths and King 1985). Therefore a highly porous lithology, such as a gravel unit, may have a high resistivity in the

Table 10 Summary of resistivity data, showing mean, standard deviation, and range of values for each recognised layer in the resistivity models

lithology	apparent resistivity (Ωm)				n
	mean	SD	max	min	
soil	109.4	72.6	288	25	14
mass-movement					
gravels	72.9	43.4	159	50	16
beach gravels	655.0	–	–	–	1
chalk	112.5	43.6	200	36	29

absence of water, and a lower value when saturated. As a consequence, it is not possible to identify different lithological types purely on the basis of resistivity data, as a wide range of values may be obtained for similar lithologies, with order of magnitude variations possible (Milsom 1989). However, reasonable estimates can be inferred, with the aid of additional stratigraphic information to provide a control on the geophysical data.

The computed resistivity models for each sounding together with the lithological interpretation (Fig 31) indicate the magnitude of apparent resistivity variations calculated from the best-fit curves. Four different lithological types are recognised (Table 10) on the basis of interpretation of the resistivity data in conjunction with control from exposures and boreholes (Fig 29). There is some overlap in the ranges of

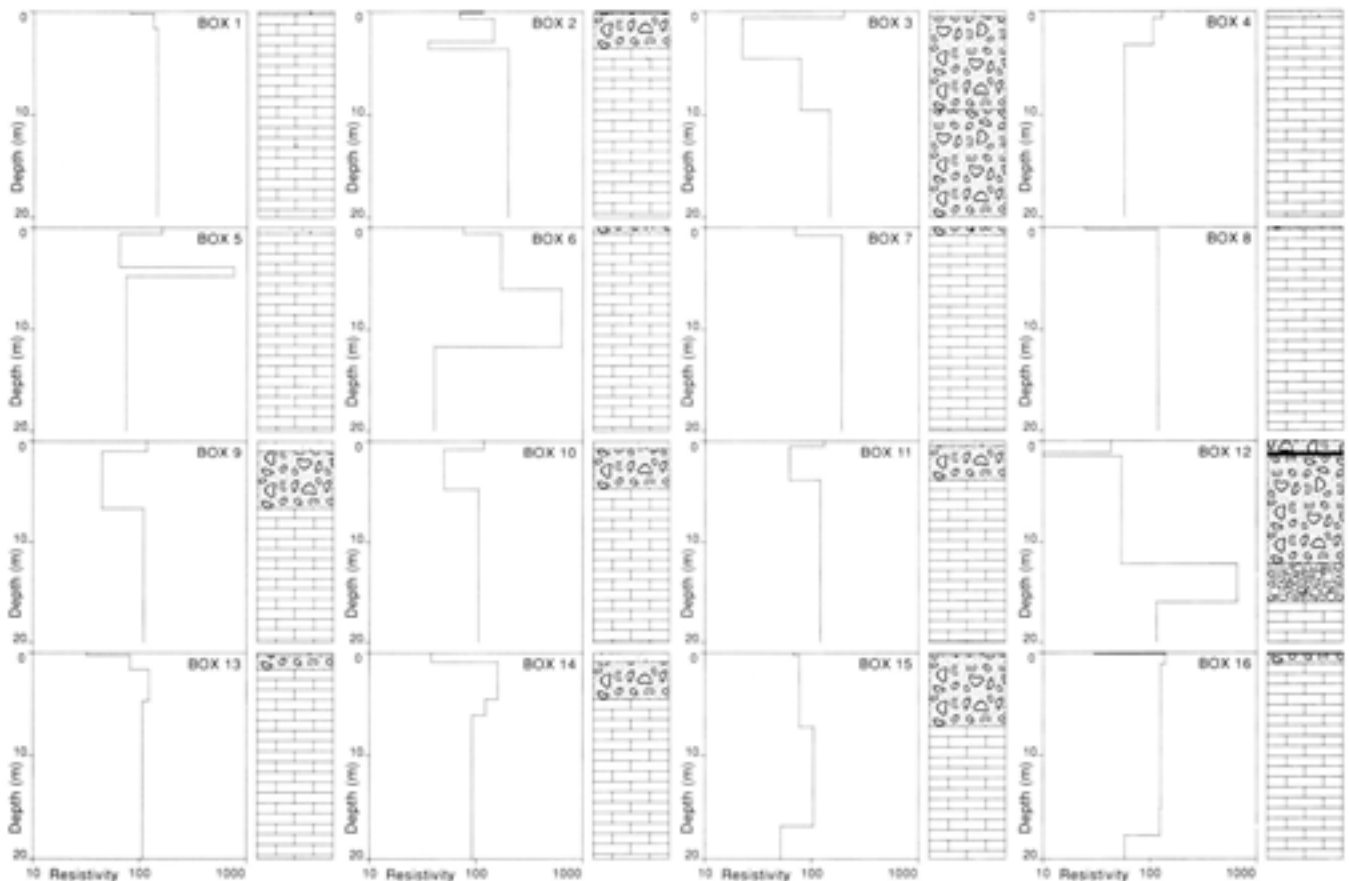


Fig 31 Results of resistivity modelling processes, showing changes in apparent resistivity with depth (left-hand side), together with the lithological interpretation of the resistivity model (right-hand side)

resistivity values for chalk, mass-movement gravels and soil, with a high degree of variability in values for the soil layer, possibly reflecting differing water content and compaction of the soil. Two anomalously high values obtained for chalk are excluded from the data in Table 10; these high values may reflect voids in the chalk or variations in the chalk at depth.

The range of values for the mass-movement gravels falls into two groups; a lower range, around 50–80 Ω m and a higher group of 140–159 Ω m. This may reflect differences in the matrix composition, with lower values associated with a finer grained matrix with a higher clay content. In the absence of borehole data to support this, the mass-movement gravels are undifferentiated. The interpretation of the high resistivity layer in location 12 (Figs 29 and 31) as beach gravels is based upon, firstly, the probability that an unsaturated open-framework gravel layer would display a high resistivity, secondly its position above a layer with a typical chalk resistivity value, and finally the proximity to the known sequence in the EQP (Eartham Quarry Project, Roberts *et al* in prep), Test Pit 29 (Quarry 2).

Location of the buried cliff-line

The geophysical data described above provide some evidence to constrain the position of the chalk cliff, now buried beneath Quaternary sediments. This interpretation of the resistivity data is supplemented with borehole records and data from the quarry exposures.

The position of the cliff and its altitude is known from the exposure in the beach section (GTP 25) in Quarry 2. The line of the cliff must run approximately north-west from this point. The data from traverse E-F suggest that the cliff lies between locations 12 and 14 (Fig 32) where the chalk surface rises from *c* 40m OD to above 46m OD.

The position of the cliff-line in traverse C-D (Fig 32) appears to be between locations 3 and 4 where the chalk surface rises from somewhere below 45m OD at location 3 (the chalk is probably around 34–35m on the basis of exposures in GTP 26), to *c* 58m OD at location 4. Exposures at the northern end of traverse C-D and a borehole record in the field to the north of the road confirms the presence of chalk close to the ground surface.

To the west of Quarry 1, in traverse A-B (Fig 32) the position of the cliff is most likely to be between locations 15 and 11. At location 11 the cover of Pleistocene deposits is thin, with chalk at 45m OD. At location 15 the chalk surface is at *c* 41m OD. South of location 15, a borehole record indicates chalk at 36m OD (Fig 32), which is again consistent with the height of the chalk platform in the quarry exposures.

The data from this geophysical survey therefore suggest that the cliff follows a curved line from the eastern end of Quarry 2, where it has been revealed in GTP 25, westwards 50–100m north of Quarry 1, and then from a position to the north of Quarry 1, in a direction slightly south of west. The nature of the survey methods and

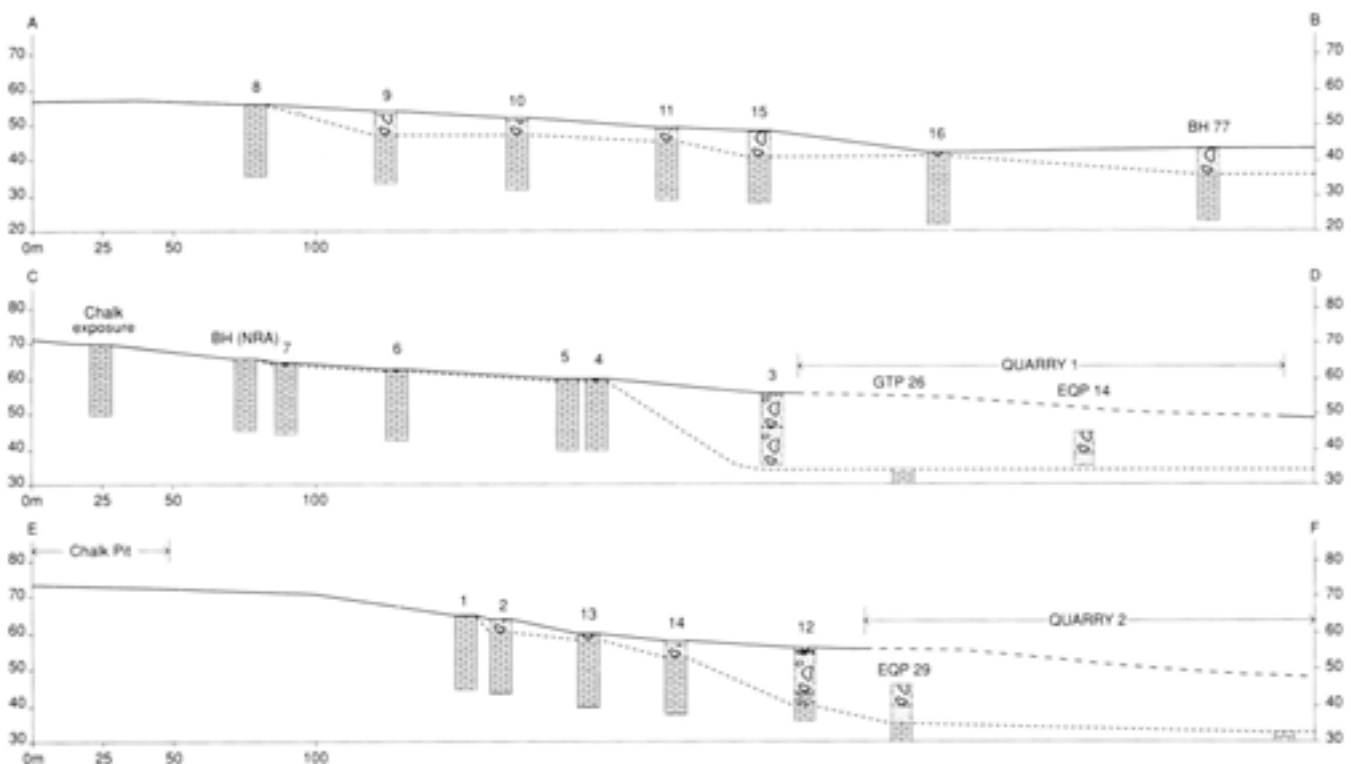


Fig 32 North-south cross-sections along traverses A-B, C-D, and E-F, showing configuration of chalk surface and thickness of Quaternary deposits

the position of the three traverses precludes a detailed investigation of smaller scale features which may characterise this 'palaeocoastline'. However, the results provide a coarse resolution view of the configuration of the cliff-line. The use of resistivity methods to determine the nature of the sub-surface geology and the geometry of the chalk surface, provide additional data on the geomorphological context of the archaeological assemblage. The position of the cliff-line may be of some significance in the interpretation of the marine and terrestrial depositional sequences in which evidence for human occupation is found at Boxgrove, in terms of proximity to raw material sources and local palaeoenvironments.

2.3 Structural sedimentology at Boxgrove

S N Colcutt

Introduction

The Boxgrove sediments were observed during two main field seasons in 1987 and 1988, as well as during a number of other, shorter, visits. The aim was to describe and interpret the structural sedimentology, concentrating upon the deposits of the Slindon Formation and the Eartham Lower Gravel Member (Tables 8, 9). Sediments of the Eartham Upper Gravel Member will be described in greater detail in the next monograph (Lewis in Roberts *et al* in prep).

The approach used was totally field-based but also drew on the geological data collected by Roberts and Parfitt during the course of the project. Their logs (Figs 33–5) form the geological framework within which the detailed structural sedimentology fits (Roberts Chapter 2.1). Various sections from the geological test pits (GTPs), formal archaeological/palaeontological excavation areas, and the quarry sides, were cleaned and described, unit by unit, to produce detailed sedimentary logs. Preparation was normally carried out using a fine blade but, in some cases, etching with dilute acid or by means of air-blasting was used to bring out particularly subtle features. Observations were made by eye, assisted by lenses up to a power of 20x. Angles were recorded using compass and inclinometer capable of half a degree resolution. Floating height sequences were established for each exposure and later tied into absolute altitude by total station survey. The interpretation of such complex deposits as are found at Boxgrove depends, critically, upon exact recognition of structures grouped into vertical and lateral sequences of change — an approach usually referred to as 'facies analysis' (Reineck and Singh 1980).

The observations made are reported below, after first lithocorrelation (where possible) and then genetic correlation, with section headings representing a broad sediment-based chronostratigraphy. As well as general section drawings and photographs compiled by Roberts

and Parfitt, some of the original sedimentary logs are shown graphically. The conventions used are those commonly applied in sedimentology (cf Gardiner and Dackombe 1983; Lindholm, 1987; Tucker 1982). From the left side of each log are shown (see Fig 38):

- Distance up-log in metres (the whole log being tied into ordnance datum).
- General texture.
- Structure (with bedding structures and nature of contacts, together with coarse-tail texture).
- Mineral enrichment and banding (iron, manganese and carbonates).
- Palaeocurrents and trends (with true north vertically upwards).
- Finer chalk debris (CHK) (larger bodies of chalk being shown with 'brickwork' ornamentation within the structural column).
- Obvious palaeontological body parts ('articulated' bivalves [lamellibranchs], single bivalve valves, marine gastropods, marine molluscan debris [marked 'x' to 'xxx' depending upon abundance], immature [pelagic] bivalves, barnacles, ostracods, terrestrial/freshwater molluscs, mammalian microfauna, mammalian megafauna).
- Degree of bioturbation (marked 'S' to 'SSS' depending upon degree of estimated loss of original depositional structures).
- The more distinct ichnofossils (see below) and root casts/pseudomorphs.
- Human artefacts (flints) actually observed in section (marked as a boxed-A)

When the text refers to these graphic logs, the sediment interval under discussion is identified by distance up-log set, in metres, within square brackets.

The importance of ichnofossils in the interpretation of the Boxgrove sediments

It is possible that many sedimentologists might find the description of ichnofossils unfamiliar, so a brief introduction will be given here (a general section will be found in Reineck and Singh 1980; cf also Bromley 1990 and the bibliography therein). An ichnofossil is the trace left in sediment from the activity of an animal; a footprint in the sand, for instance. Ichnofossils may be classified according to the supposed behaviour which produced them, the main categories being:

- Fugichnia (escape traces produced when animals have to dig upwards rapidly when buried in sediment).
- Cubichnia (resting traces or the traces left by a carnivore waiting in ambush).
- Repichnia (crawling traces, including footprints).
- Pascichnia (surface grazing traces).
- Fodichnia (substrate feeding traces).
- Domichnia (substrate dwelling and suspension feeder traces).

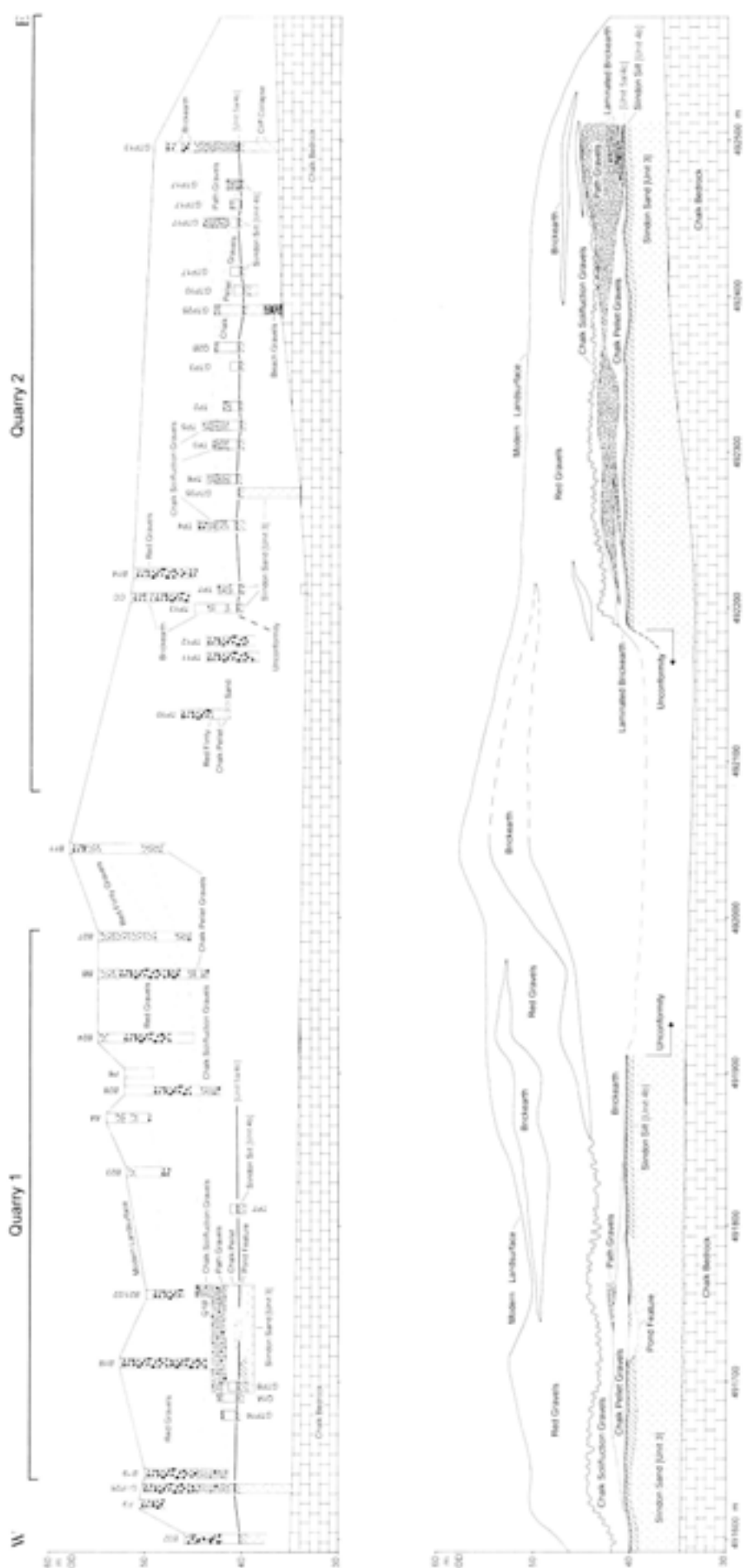


Fig 33 West-east transect through the geology at Boxgrove, showing ground surface, platform surface and sediment contacts, based on boreholes and test pit exposures. Note the following correlations: Laminated Brickearth = Brickearth Beds, Chalk Solifluction Gravels = Calcareous Head Gravels, Red Gravels = Head Gravels of Unit 11, Brickearth in Red Gravels = Silt Beds (Table 9a). These correlations are also applicable to Figs 34 and 35

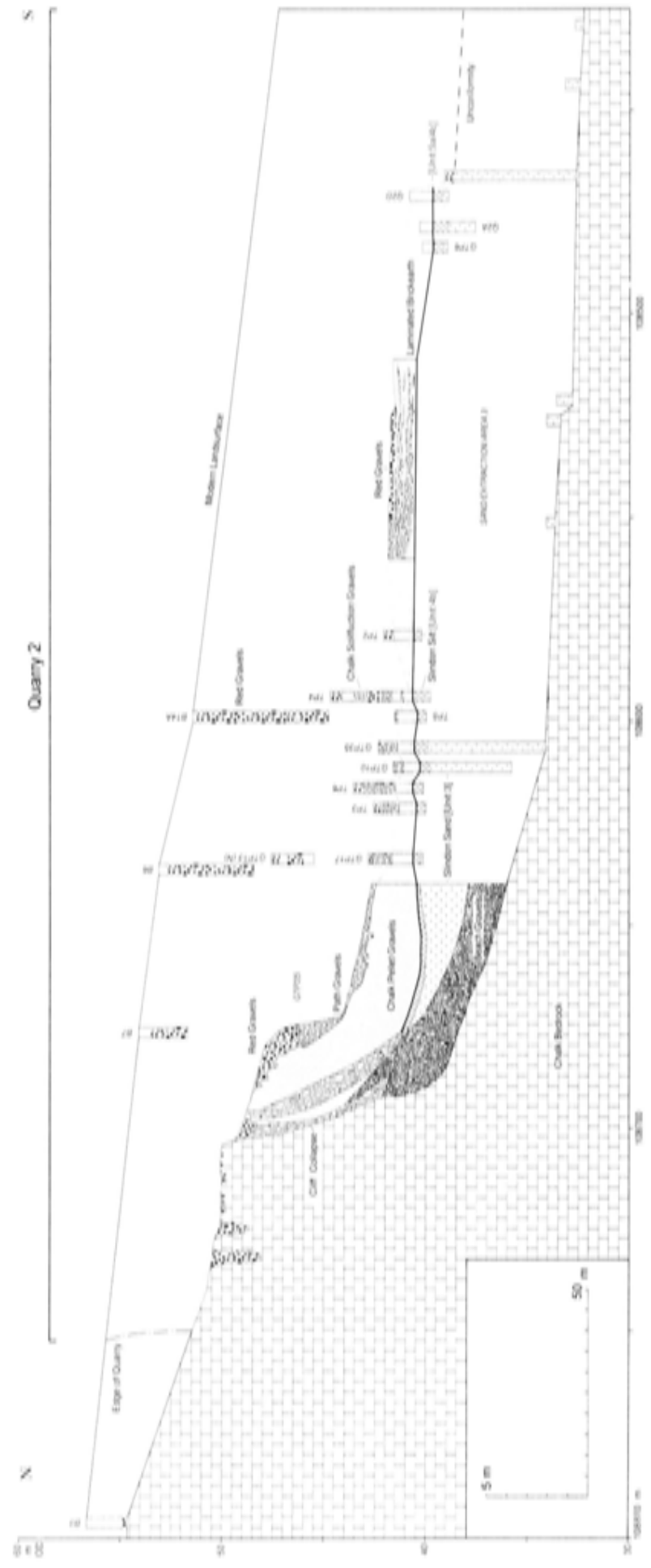


Fig. 34 North-south section through Q2 based upon boreholes, test pits, and quarry exposures

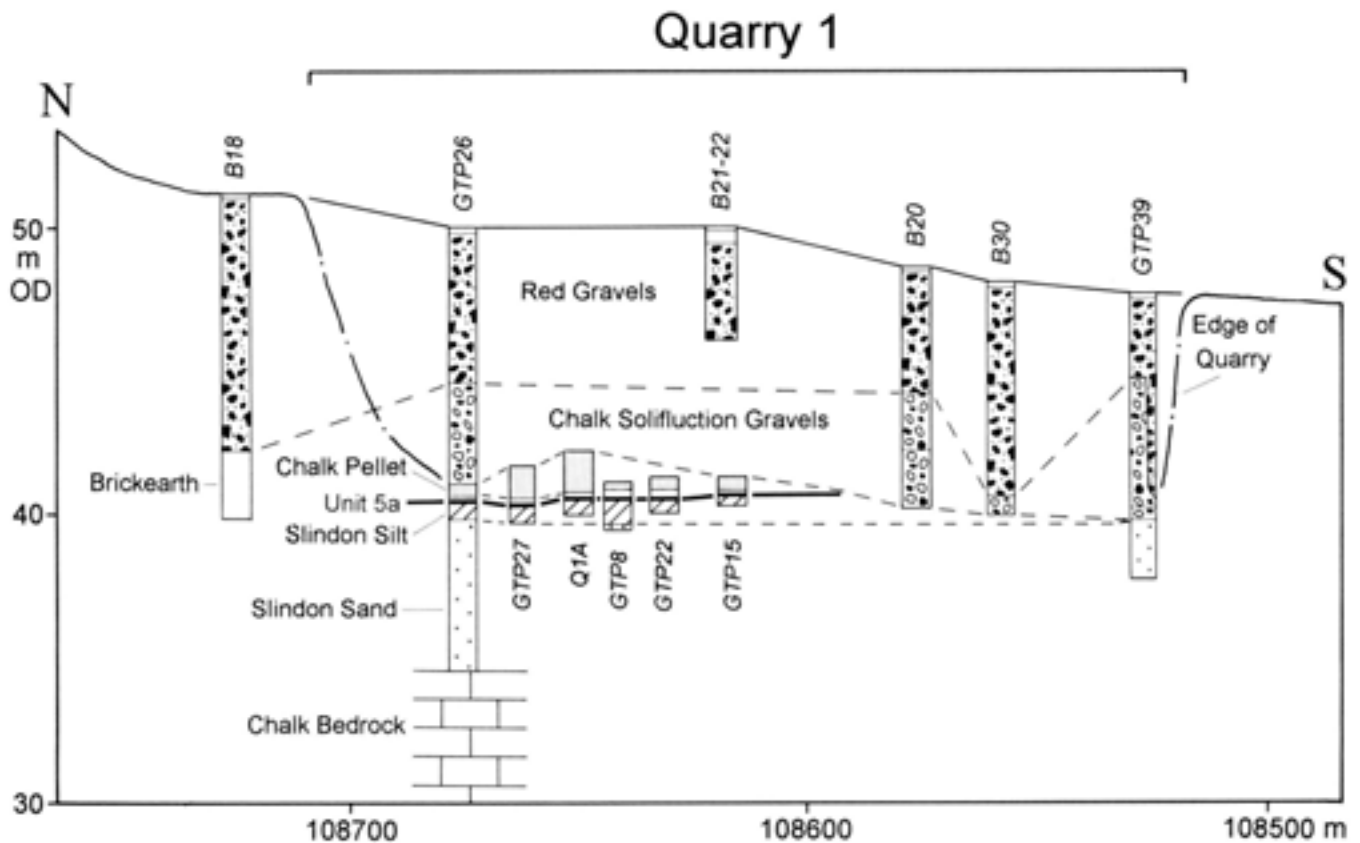


Fig 35 North-south section through Q1 based upon boreholes, test pits, and quarry exposures

Much can be learnt from the observation of modern animals as they interact with sediments but it should never be forgotten that (a) a given species may make many different types of trace depending upon the activity involved, (b) identical traces may be made by different species, possibly even engaged in slightly different activities, and that (c) modern analogues have not yet been found for many common fossil traces. As a partial solution to these difficulties, ichnofossils are treated as if they themselves were discrete organisms, and are given taxonomic status according to (approximately) normal Linnaean rules.

The Boxgrove marine sediments contain excellent ichnofossils (Fig 36). Unfortunately, the present

author has been able to give these traces only superficial attention. In many cases, only gross morphological designations can be given (eg U-tubes, J-tubes, etc), whilst more detailed informal descriptions are sometimes given for more complex traces. On a few occasions, the identity of a trace seemed likely enough for a suggestion (indicated by the use of 'cf') of an actual ichnogenus to be given (eg cf *Arenicolites*, a simple U- or V-shaped domicnial tube often made by such creatures as lugworms) (Fig 37). Care was taken to try to discover the three-dimensional morphology of traces but, given the starting point from vertical sections,



Fig 36 Trace fossils in the marine sands at GTP 13



Fig 37 Trace fossil burrows in the marine sands at Sand Extraction Pit 3; scale unit 10mm

there will be a strong bias in the reported descriptions towards traces which penetrate greater vertical intervals; traces developed predominantly on bedding surfaces (especially repichnia and pascichnia) will be markedly underrepresented.

The study of the Boxgrove ichnofossils has been mainly used to relate the broad assemblages of forms present to their sedimentary environment. For instance, burrowing creatures are very sensitive to the balance between erosion and deposition. On a seafloor subject to rapid erosion and deposition, the safest style will be a vertical burrow, whilst on a more stable seafloor a burrower can risk the effort of branching out laterally. As a general trend, increasing horizontal development of burrows will indicate deeper, calmer water. Another response to instability, especially when a creature wants to construct tunnels in very soft, plastic sediment, is to 'plaster' the walls with mucus-bound mud; rare complex lined burrows at Boxgrove have been referred to *Ophiomorpha*, although most lined forms are simple vertical/oblique tubes or J-tubes. Deliberate displacement of a burrow laterally can result in a series of parallel traces, called 'spreites', marking former positions of the burrow. Some creatures use this method to 'mine' organic material from the sediment substrate whilst, at other times, the method is used to maintain the creature at a given depth within the sediment when erosion/deposition causes the surface to fluctuate (a U-tube with spreites both above and below is given the apt ichnospecific name *Diplocraterion yoyo*). One particular class of forms, which is very common at Boxgrove and indicated by the designation cf *Monocraterion*, is problematical. A variety of relatively large cone shapes (or simple V-shapes in section alone) are involved, opening upwards to an erosion plane. Such forms can be true ichnofossils, resulting from relatively 'strong' creatures (often molluscs or larger crustaceans) escaping upwards when sediment has been rapidly dumped upon them, or they can be abiotic deformation structures resulting from water escaping in the same way; except when other details are also present (such as 'stalks' at the base of cones representing an original burrow) it can often be impossible to differentiate between the two causes. In practice, this is not particularly important since both mechanisms indicate rapid sedimentation, often associated with storms. A characteristic assemblage of ichnofossils, known as an 'ichnofacies' and often named after a typical ichnogenus, may be associated with a particular sedimentary environment; thus, the *Glossifungites* ichnofacies is typical of sandy shoals.

Finally, most contemporary assemblages of traces (as observed in modern contexts) exhibit a phenomenon known as 'tiering', with different types of trace developed from the same upper surface but reaching different depths within the sediment. Probable tiering can be recognised at some points within the Boxgrove sediments but much more detailed study would be

necessary to interpret the phenomena correctly. Misunderstanding of tiering can lead to stratigraphic errors, with deep tiers (that may extend downwards by several metres) wrongly referred to the much older sediments into which they are cut; for this reason, time (as much as a day in a few instances) was taken during the project to try to trace examples of a given environmentally diagnostic ichnofossil type upwards to their origin (or at least truncation point) at a bedding plane before making use of the environmental inference.

The stratigraphic sequence

The Slindon Sands and Gravels

Basal beds beneath Marine Cycle 1









The simplest model of marine transgression in a region such as this, with comparatively soft but nevertheless relatively competent bedrock, would involve the development of a landward migrating notch (cliff), leaving a sloping unconformity between the chalk and the subsequent marine beds. There would be a strong discontinuity in both lithology and geomorphology. The corresponding facies model would involve a coarse lag, followed by relatively high energy beach and shore face sediments, fining upwards as water depth increased.

At the lowest altitude so far observed (31m OD), cut into the chalk wave-cut platform at the base of the main commercial sand extraction pit (SEP) 3 in Quarry 2, 50m to the west of Q2/A (Fig 4), a small exposure was observed which does not fit this simple model of transgression. A similar sequence has also been logged and drawn by Roberts at GTP 35 (Figs 4, 38, 39a-b).

The chalk planation surface, with small scale irregularities due to both mechanical and chemical erosion, is covered by a rather chaotic bed of partially clast supported flint gravel in a medium to coarse sand matrix. The gravel shows a wide range of forms, from well rounded pebbles to angular clasts with only slight edge-rounding; all of these forms are also present in subsequently fractured states, consistent with a high energy environment. To this point [0-0.012] (Fig 38), the observations follow the expected pattern: the coarse lag is the 'tool' with which the rising sea is cutting laterally into the chalk.

However, the next set of deposits is highly anomalous. Clays, with isolated fine sand grains, are draped over the basal lag, passing rapidly to a sequence of composite bedding, showing a bulk upward-coarsening trend [0.12-0.22]. Clays, with obscure zones of silt and fine sand, are followed sequentially by good fine sand linsen bedding, flaser bedding, mud-draped fine sand lenses and finally by very well organised small-scale shore-perpendicular trough (festoon) shallow-climbing ripple cross-bedding with occasional mud partings. The next beds [0.22-0.28] comprise massive medium sand with rare coarser elements, passing upwards into a planar cross-bedded interval, dipping gently (by 2°-3° only) to the north-north-east and with

Key for this and subsequent graphic logs

CHK	Chalk
	Minor unconformity
	Terrestrial root traces
OSTRAC	Ostracods
	Barnacles
	Bivalve mollusc
	Articulated bivalve
	Gastropod mollusc
IM	Immature bivalves
x x	Molluscan shell fragments
 Micro F	Microvertebrates
 Mega F	Megavertebrates

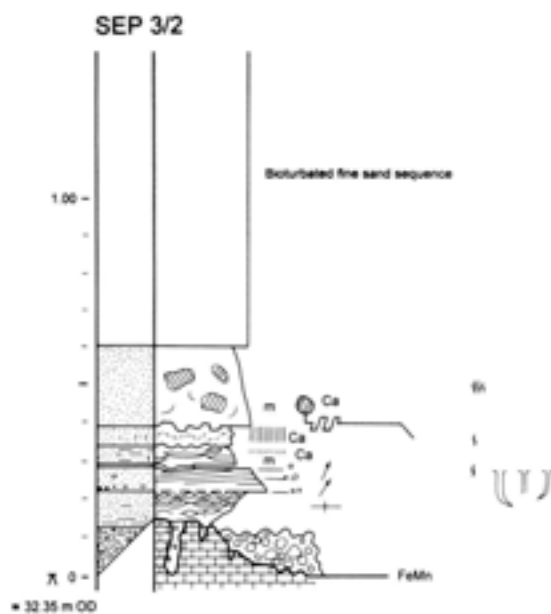


Fig 38 Detailed sedimentary log through the sediments at Q2 SEP 3, c 50m west of Q2/A

isolated coarser elements on some bedding planes; there is a minor bioturbation zone (mostly diffuse forms but with some distinct J-tubes) at the top of this interval. There follows a series of beds [0.28–0.39] with few depositional structures: discontinuous clay, often ripped-up and associated with isolated gravel particles; fining-upwards silty clayey fine sand, showing some small-scale lenticular bedding with penecontemporaneous microfaulting; and disturbed silty sand. These upper deposits are often strongly cemented and the uppermost interval may be composed of massive lenticular doggers (several metres across and up to 150mm thick) with obvious crystalline cement. Subsequently, the tops of doggers have in places been redissolved and attacked by bioturbation from above; in other places, the doggers have been mechanically eroded and rounded pebbles of derived calcarenite appear in the uncemented overlying bed [0.39–0.60].

In broad terms, this thin transgressive sequence represents intertidal mud flats, passing upwards to mixed flats, then relatively high velocity shallow-water wave and current conditions in a sediment-rich environment, followed by the invasion of a sand bar, and finally alternations between intertidal and minor storm beds. The cementation is not strongly diagenetic, since calcarenite clasts occur in the overlying bed; there may have been some carbonate input from molluscan debris (none of which now visibly survives) but a generally hypersaline environment (or one with strongly fluctuating salinity) would appear to be indicated, also suggested by the very weak and localised traces of bioturbation.

The problem here is produced by the misfit between the planation surface and lag, and the relatively low (but upwards-increasing) energy deposits above. On the one hand, it is assumed that a rising sea is cutting laterally into chalk, removing many metres of bedrock at a cliff-face and leaving a relatively steeply shelving surface to seaward. On the other hand, the next sedimentary sequence would have required a very significant horizontal zone in which to develop, undisturbed by the erosion front of a primary energetic transgression.

There are two possible solutions to this problem. The first possibility is that the coarse lag may represent a quasi-non-sequence, developed during a long interval of scour with zero net sedimentation and during which the chalk cliffs retreated a considerable distance northwards; after a minor marine regression (with no surviving sedimentary trace), renewed gentle transgression caused the deposition of the intertidal flats sequence, there now being enough space to accommodate the latter. The second possibility is that the assumption that great thicknesses of chalk needed to be removed in this immediate area is incorrect and that the sea was indeed eroding a little (coarse lag) but that the dominant process was the invasion of an existing valley-form in the chalk. Although the sediments have been described as those of intertidal flats, there are in

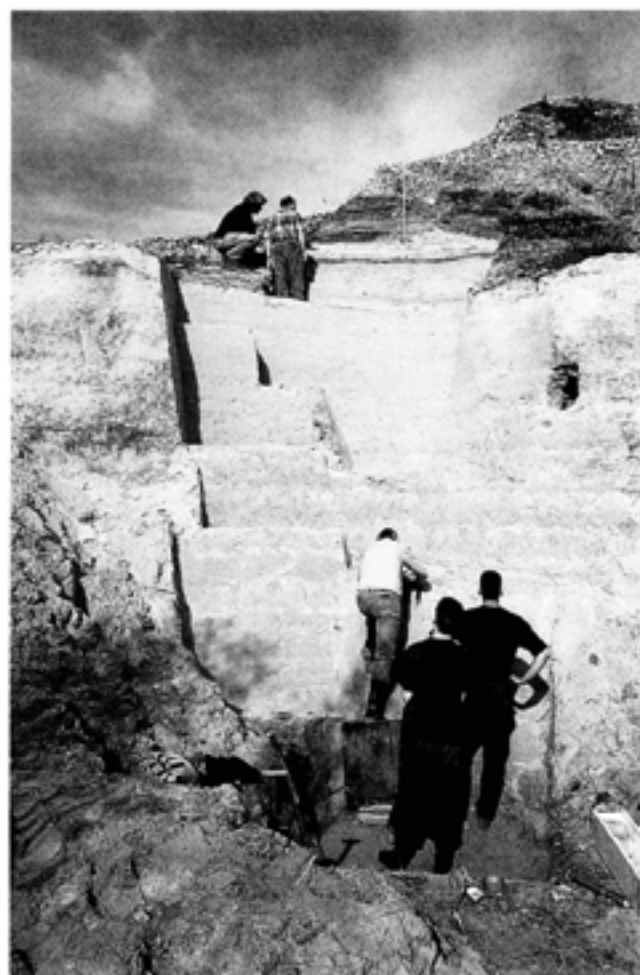
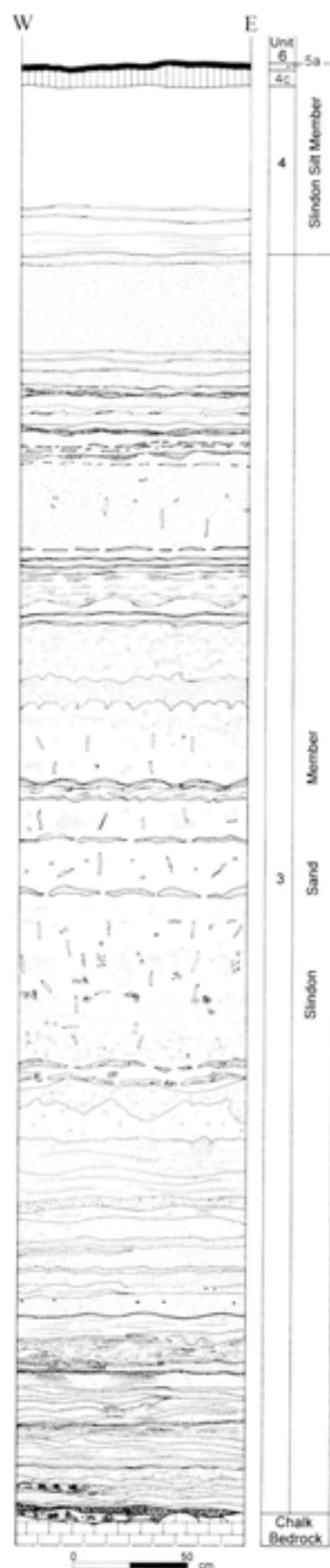


Fig 39a The section at GTP 35 in Q2 SEP 3 (location of section shown on Fig 4)

fact strong similarities with the seaward facies of estuarine deposits; fluvial and organic marsh facies are absent and one would have to assume that the exposure is not on the thalweg of the hypothetical drowned valley-form (ria). The first possible solution is unsatisfactory, since it requires a complicated series of events for which there is no physical evidence. The second solution requires only the initial condition of a valley-form cutting too close to this altitude (similarly unsupported by available data), the sedimentary sequence then being internally consistent. However, it is stressed that only one small exposure of these sediments has yet been observed and it would be premature to accept any given hypothesis. The exposure is therefore referred to as sub-marine Cycle 1, there being no clear evidence whether a discrete minor marine transgressive/regressive phase is represented (as a non-sequence) or whether this is merely a conformable, but local, topographically controlled variant.

Whatever the relationship between the planation surface and the overlying deposits, the intertidal sediments of this phase are transgressive. Because of the

Fig 39b Section through GTP 35 in Q2 SEP 3 (location of section shown on Fig 4)



massive cementation of the top of this sequence before erosion of the cemented beds, there must be a non-sequence of some sort; there is therefore a possibility that these sediments belong to a significantly different chronozone from that represented by the rest of the Boxgrove deposits. No major oblique unconformity has been recognised and it is most unlikely that this sequence post-dates the main Boxgrove sequence. Similarly, there is no trace of the prograding coarse terrestrial deposits which should occur if these units represent a separate earlier interglacial. There is therefore no reason at present to suggest that the sediments represent anything but an early stage in the Boxgrove interglacial itself; without evidence of an intervening regression, the deposits may therefore be part of Cycle 1.

Marine Cycle 1

Transgression

Available exposures other than at Q2 SEP 3 show sequences broadly compatible with the 'simple' model of transgression noted above. It is convenient to begin the discussion with the most northerly exposures, corresponding to the maximum transgression, and then to move southwards (and slightly back in time).

The main beach

The ancient cliff-line itself is deeply buried at Boxgrove and it had not been possible to expose it at the time of the observations reported here, although it has been exhumed since (Figs 19, 28, 40). Nevertheless, the major trench represented by GTP 25 in 1988 (Fig 41) must have fallen short of the stubs of the last cliffs (probably originally several tens of metres in height, confirmed by Roberts Chapter 2.1) by only a matter of a few metres; the maximum inland (altitudinal) penetration of marine deposits is certainly shown.

Except in the case of local bedrock solution features (cf GTP 25 C, Fig 42f), the unconformity in the chalk approaches the cliffs in a series of upward-sloping planation surfaces, increasingly interrupted northwards by small steps to slightly higher levels. Each surface between steps is slightly steeper northwards, starting seawards with a slope of $c 4.5^\circ$ and increasing to 7.5° on the highest observed surface. The long-orientations of the steps are consistent and suggest that the cliff-lines trended along a bearing of $c 108^\circ$ in this immediate vicinity (Lewis and Roberts Chapter 2.2).

In this single trench (Figs 42a-1), it is not absolutely clear which of the planation surfaces can be referred to which transgressive cycle. The sea would have been at its most aggressive near the cliff-line, so that coarse regressive beaches would tend to remove immediately underlying finer sediments, giving an overall geometrically concordant sequence of beds, with obscure paraconformities (Fig 43). Ideal vertical sequences just seaward of the cliff-line(s), with clear tongues of finer marine sediment pointing north and tongues of coarse

beach material pointing south, are therefore absent. Again, the tongues of terrestrial material that would normally be present on the landward side of a 'soft' coastline to represent regression had no space to develop at Boxgrove; even sand dunes are absent. The only major oscillations in sediment type visible here are between true storm beaches and chalky cliff collapse material; together, these types form a major seaward-thinning wedge lying upon the chalk and (leaving aside for the moment a few useful clues to stratigraphic continuity at certain points within the sequence) the dipping upper surface of the wedge produces a lithological discontinuity with the generally overlapping (onlapping) finer marine deposits (Fig 44). The actual moment at which significant volumes are spalled from a cliff is dependent upon many local factors, both physical and historical. However, there is a slightly greater chance for beds of collapse material to survive after the main rise in sea level in any transgression. By referring basal storm beach material to main transgressive phases and intervals dominated by chalky collapse (Fig 43) to post-main transgression, no major stratigraphic inconsistencies appear at Boxgrove and this will therefore be the approach used here. It should nevertheless be remembered that only when a number of exposures at different points along the shoreline have proved consistent will this approach be validated.

The planation surfaces associated with Cycle 1 certainly reach 40m OD, although (in keeping with the caveats noted above) it is possible that this transgression (rather than that of Cycle 2) reached 43m OD.

Very near the cliffs (GTP 25 1-3, Fig 42b), the sedimentary sequence begins with a pebble bed [0-0.23] (mostly flint but with some rounded chalk elements) in a medium to fine sand matrix, with traces of barnacles and bivalves, followed by an interval of flint shingle and coarse sand in roughly planar sets. The next flint pebble bed [0.23-0.27] which penetrates a little further shorewards on a minor bedrock step, has a matrix dominated by fine chalk debris with interspersed marine sand. This sequence represents storm beach deposits. There follows a thick bed [0.27-0.73] comprising large chalk blocks and boulders, set in chalk debris, with only occasional flint pebbles. The rounding of some large chalk elements shows that the sea occasionally disturbed this deposit, although smaller cobbles and pebbles could have been thrown to these positions during storms (Fig 43). There is then a thin lens of flint and chalk pebbles [0.73-0.88], abutting a bedrock step riser without additional landward erosion. The sequence is capped by a massive deposit of chalk rubble [0.88-1.23] (Figs 28, 42a), with some large blocks and almost completely lacking in marine-derived elements. There is no trace of weathering or other landward-derived deposition at the top of the sequence and it is assumed that any such phenomena were eroded by the next transgression.

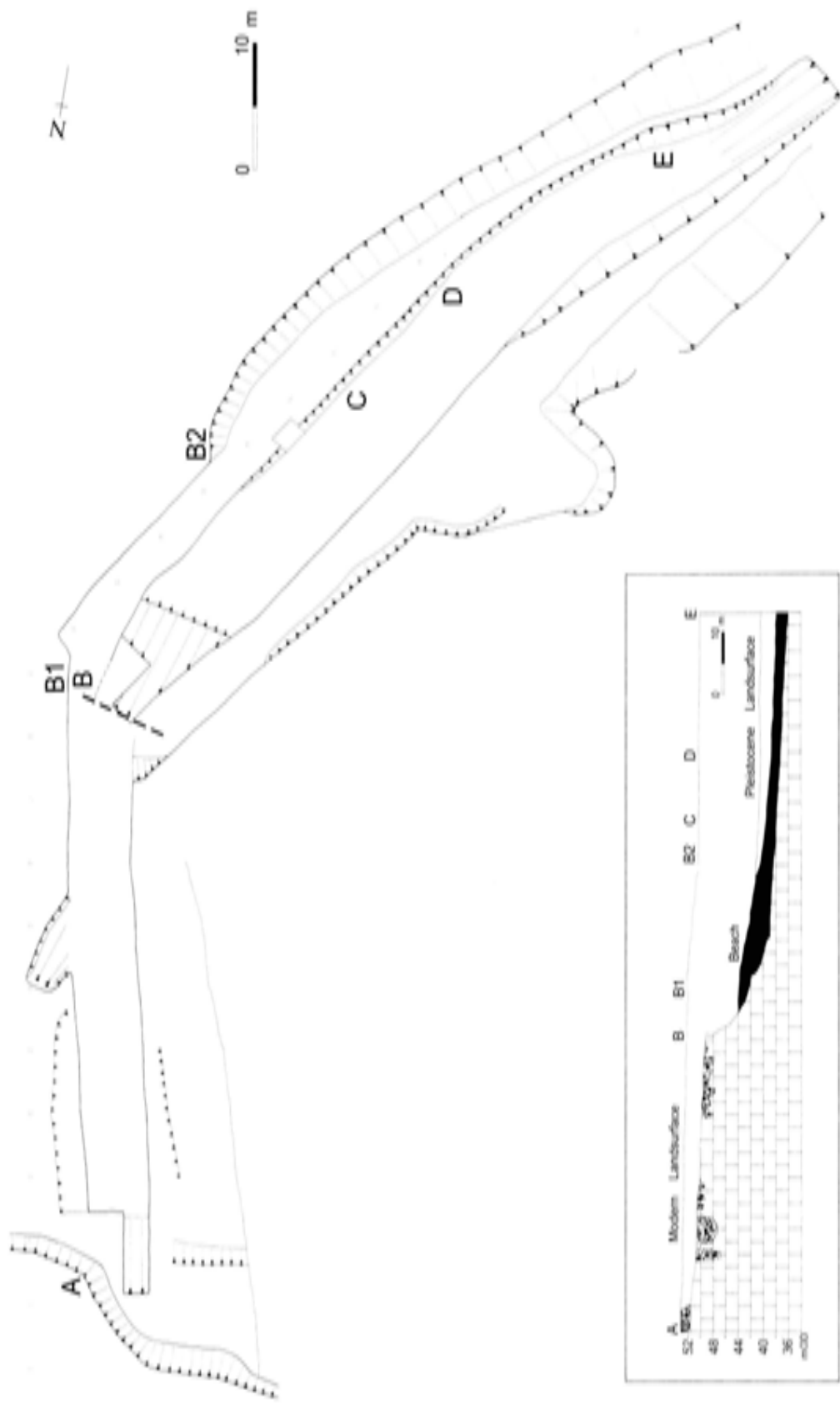


Fig 40 Plan and schematic section of GTP 25, the beach section, showing section locations



Fig 41 GTP 25, the beach section in Quarry 2, looking north towards the cliff; scale unit 0.5m

Moving slightly seawards (GTP 25 5, Fig 42c), the beach sequence [0–0.67], with generally tabular beds, comprises: flint pebbles with lenses of well sorted medium to medium coarse sand; oblate chalk cobbles; sand to pebbly sand upwards; chalk cobbles and pebbles; and flint and chalk pebbles, shingle and a few small edge-rounded chalk blocks. In the chalk-dominated interval above [0.67–1.37], the distinction is maintained between the lower deposit with some rounded elements and a little marine-derived material and the upper deposit comprising only collapse material (with some large chalk blocks); the intervening flinty lens has disappeared.

Further seaward still (GTP 25 E, Fig 42d), the sequence begins with a thick bed [0–0.65], with clast-supported flint pebbles in a clean sand matrix in the central zone, but also with chalk boulders, pebbles and finer debris at the base and top of the deposit. This is followed by a bed of very slightly muddy sand with small-scale bidirectional rhomboid ripple cross-bedding [0.65–0.72]. There is then a bed [0.72–1.14] of finest coarse to coarse medium (set-wise upward-fining) sand, with sets, bounded by reactivation surfaces, of planar bedding mostly dipping gently seawards but with some scours with steeper cross-laminations; there are also a few landward-dipping ripple sets, more common and with some chalk elements nearer the base. A single vertical burrow with internal spreites was noted in these otherwise unbioturbated sands. This transgressive

sequence is interpreted as: initial storm beach; upper beach-face showing high velocity wave/swash-dominated shallow water forms; and swash zone beach- or bar-face in slightly deeper tide (with no sign of longshore runnels). The chalk-dominated interval above [1.14–1.65] is still vaguely divided into a lower part with a little shingle and rare pebbles (some of chalk) between larger chalk blocks and debris, and an upper part with metre-scale blocks set in a pure chalky 'magma'. For the first time, reddish terrigenous clays (weathering residues of the chalk) appear in the lower, slightly washed sediments (Macphail Chapter 2.6). The marine sequence a few metres seawards (GTP 25 D [0–0.92], Fig 42e) is similar, save that there are some shingle and fine pebble beds within the swash zone sands, representing beach ridges. The chalk-dominated interval [0.92–1.37] shows much greater marine influence and reworking throughout. Above this interval (as in all sections to seawards in GTP 25), there is another set of marine deposits [1.37–1.55], starting with coarser storm beach and passing quickly to beach-face sands. It seems best to treat this material as a progradational element of Cycle 1, responding to the need to re-establish shoreline equilibrium after dumping of large volumes of debris from the cliffs, rather than a discrete transgressive phase.

The basal sequence is very heavily disturbed in GTP 25 C (Fig 42f), due to gradual collapse into an underlying solution feature, but a discrete bed of flint

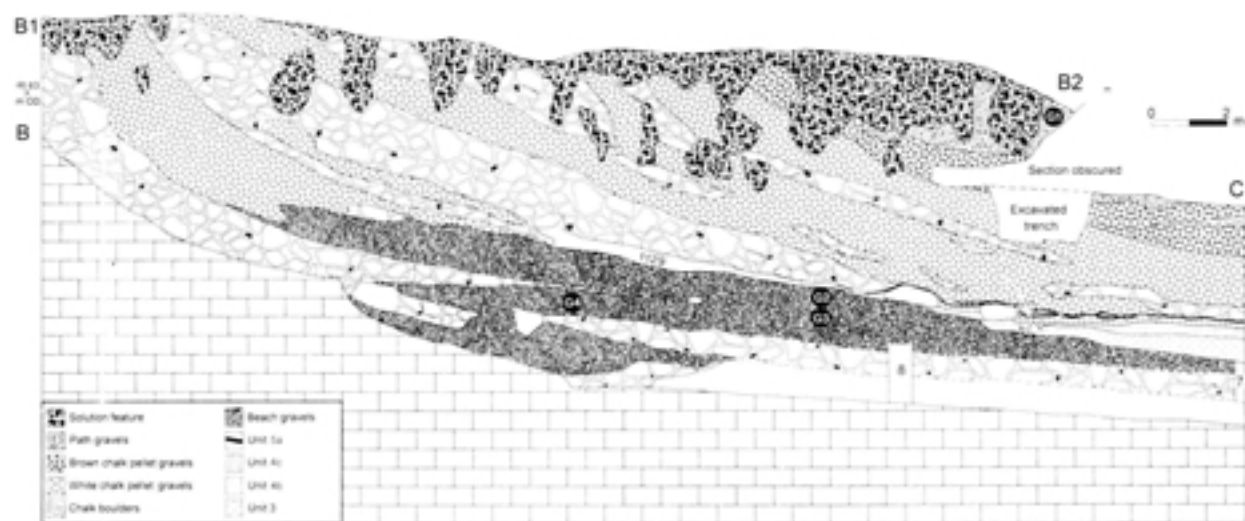
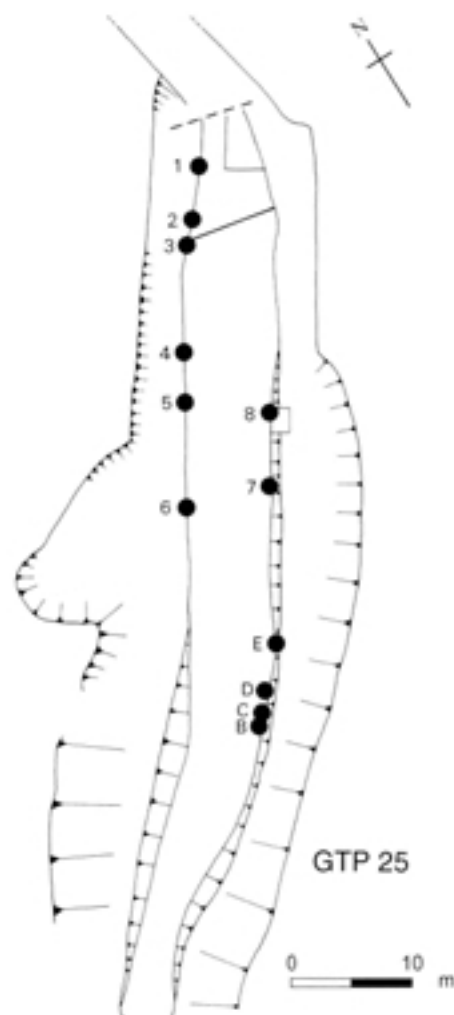


Fig 42a (above and facing) Section through the Boxgrove beach at GTP 25, showing the location of Collcutt's sections (B, C, D, E, 7, 8; Chapter 2.3), Bridgland's gravel samples (G1–G4; Chapter 2.4) and the flint scatter ('excavated trench') at the junction of the Lower Chalk Pellet Beds (white chalk pellet gravels) and Upper Chalk Pellet Beds (brown chalk pellet gravels). (Location of main sections are shown on Fig 40.) The inset (below) shows the position of all the GTP 25 section logs



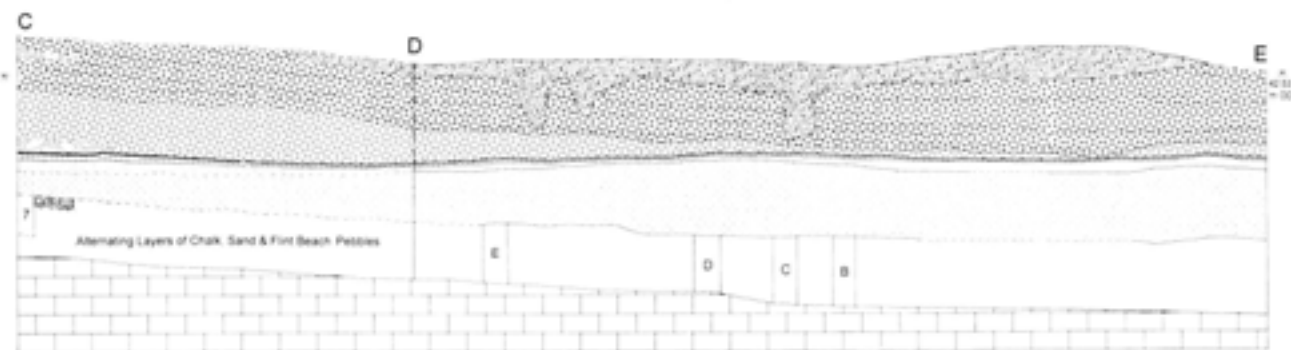
pebbles and less rounded elements, set in a poorly sorted sandy shingle, is present [0–0.15] below the chalk blocks and debris [0.15–0.80] in GTP 25 B (Fig 42g). In GTP 25 C there is an upper sequence of deposits interpreted as progradational, with chalk

boulders/cobbles/pebbles, flint pebbles and shingle, passing upwards into beach-face and ridge/bar sands with occasional fine gravel stringers and chalky input from landward [1.98–2.45]. Bedding forms are not well developed, consisting mostly of seaward-dipping planar sets with reactivation surfaces, with only rare landward current cross-bedding and a single case of bidirectional, slightly asymmetrical wave ripple cross-lamination. Patchy light cementation is probably a post-depositional effect due to reorganisation of finest chalk debris.

In summary, the main beach sequence in GTP 25 is generally very immature, since it is continually interrupted by more or less massive input from the chalk cliffs to landward. Many beds contain chalk, sometimes rounded, but few beds are pure silicate, so that little time could have elapsed for the mechanical/chemical removal of chalky debris. Bioturbation is absent or low and there is very little shell debris, underlining the dominance of land-derivation of sediment, high energy and high sedimentation rates. Beach-face deposits are present, including probable ridge/bar sediments, but the sequence is too immature for stable longshore back-bar runnels to have developed. It seems likely that the sequence is very incomplete (many hidden non-sequences at erosive contacts).

Seaward exposures

A much more coherent transgressive sequence is present in GTP 13 (Figs 20, 44, 45a–b, 46). At GTP 13 1 clayey gravel and chalk debris [0–0.17] (Fig 45a), with very localised planar sand sets and a little bivalve and gastropod debris, fill minor solution/scour hollows in the planation surface lying at 36m OD. The bedrock is littered with boulders and large cobbles of chalk (Fig 46), often showing scalloping but with only rare and



very superficial traces of boring (and none of incrustation) by marine organisms (Fig 47). The first persistent beds [0.17–0.22] are of medium sands, with large-scale parallel planar sets separated by reactivation surfaces, the laminae dipping gently, to relatively steeply, seawards. A unit of varied bedding then follows [0.22–0.32], with (a) tabular sets between reactivation surfaces dipping gently seawards but dominant foreset dips to landward (although there are minor dip reversals), with increasingly climbing ripple cross-lamination upwards, mostly in-phase but with some shoreward translation, representing sinuous-crest ripples

(ripple index 5–6 and symmetry 1.1–2.0), (b) small-scale trough ripple cross-bedding, with trough bases dipping seawards and a steeply seawards foreset dip (with rare reversals), and (c) almost horizontal planar bedding. Types (a) and (b) tend to dominate, and to have mud-draped foresets, especially in the lower part of the interval, whilst type (c) tends to occur higher and usually to cap the sequence; bioturbation is minimal. The next group of deposits [0.32–0.46] begins with a finest flint and chalk lag (coarsening seawards), passing upwards into medium sand, with finest flint and chalk debris, in weakly bedded sets with symmetrical



Fig 43 The thickness of the raised beach at GTP 25 showing the steeply rising platform near the cliff; scale unit 0.5m

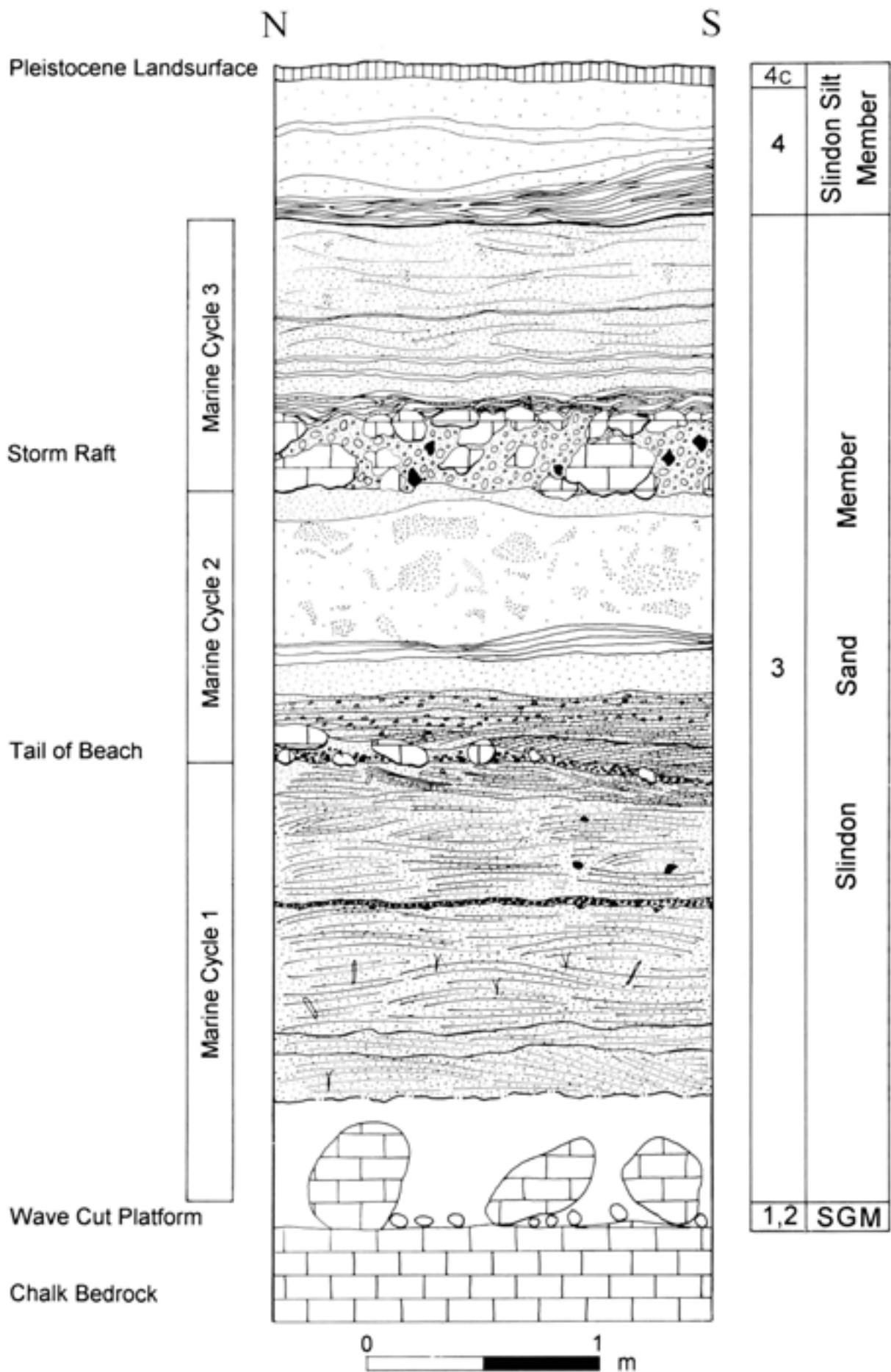


Fig 44 Composite log through the lower part of the sequence in Q2 GTP 13 showing the relationship between Marine Cycles, unit numbers, and members

ripple-form contacts switching to planar contacts dipping gently seawards towards the top; the sands are unbioturbated but there is a little molluscan debris. Towards the centre of the group, there is a fining-upwards horizontal lens (coarse lag, medium then fine sand) with cross-laminae dipping gently landwards. An almost identical interval to that occupying the lower part (again starting with a lag coarsening seawards) completes this group. At various points within the group, and becoming more prominent slightly landwards, there are longshore troughs with cross-laminae dipping generally eastwards or westwards. After a more persistent lag of flint pebbles and a little, more angular flint debris [0.46–0.47], there is a medium sand unit [0.47–0.54], with symmetrical seaward-dipping ripple cross-bedding, often climbing, and common reactivation surfaces, sometimes capped by sets of planar laminae dipping gently seawards; the unit shows weak bioturbation. Finally [0.54–0.72], after an impersistent minor lag, there are bundles of planar laminated medium sand (possibly representing large-scale trough bedding), dipping variably seawards; there is only very minor and localised bioturbation.

This GTP 13 1 sequence is interpreted as follows. After the rather chaotic lag deposits in solution/scour hollows, low to medium high angle beach-face deposits develop, helping to form the rounded chalk boulders and cobbles around which they are being deposited. These large chalk elements may have moved a little down the slope under tidal action but it is assumed that they represent the remains of blocks left behind during initial cliff-retreat. Then the unit with sinuous shoreward climbing sets (type a), seaward-dipping troughs (type b) and landward-dipping planar sets (type c) represents higher energy, lower beach-face to upper shore-face deposits. Tidal current (rather than wave) influence is clear, especially in the lower part where clay drapes have been deposited at slack water. The next group represents a shore-face (ie mostly subtidal) longshore bar, with minor bidirectional back-bar runnels; the form was probably generated near a breaker zone, since there is no sign of the influence of strong longshore drift/currents. The unit with climbing wave

ripple sets, capped by planar sets, and with weak bioturbation, is a middle to lower shore-face facies, possibly indicating a rip-channel. More generalised shoreface deposits are represented by the final bundled sand sets. All these deposits were developed under relatively high energy regimes (reactivation surfaces, coarser textures, general lack of bioturbation) with abundant sediment (climbing forms).

The transgressive sequence at the base of Q1 GTP 26 is significantly different (Figs 4, 12, 35). The scalloped chalk surface at 34m OD is overlain by pebbles and edge-rounded flint in a medium to coarse sand matrix [0–0.14] (Fig 48). Obscure sets of finer coarse sand follow [0.14–0.24], lower intervals showing some fine chalk debris. There is then a finest coarse to medium sand unit [0.24–0.55], lacking bioturbation and with common reactivation surfaces, showing a variety of bedding types: (a) slightly muddy sand, with sinuous bifurcating ripple cross-lamination dipping eastwards; (b) large-scale planar laminations dipping eastwards; (c) large-scale sets with diffuse bedding apparently dipping eastwards; and (d) large-scale planar cross-bedding dipping seawards (developed nearer the top of the unit). The next unit [0.55–0.91] is developed in medium sands, with many reactivation surfaces in dominantly low angle planar sets, giving the following sequence: (a) at the base, irregular sinuous small-scale trough cross-lamination dipping south-eastwards; (b) large-scale planar sets with laminae dipping seawards; (c) large-scale sinuous cross-lamination dipping south-eastwards; (d) large scale planar sets with cross-laminae dipping eastwards; (e) large-scale planar sets with laminae dipping seawards; and (f) capping the unit, small-scale ripple cross-lamination dipping seawards in a generally muddier sand with a muddy ripple train at the top. The uppermost muddier interval shows very weak bioturbation but the unit is otherwise undisturbed. There is then a unit [0.91–1.14] of sand with muddy laminae, followed by a slightly muddy medium sand, with seaward- and landward-dipping asymmetrical ripple cross-lamination with off-shoots; only very weak bioturbation is apparent, except at the top, where there are some mud-lined pouches and J-tubes. Two very thin beds cap the sequence [1.14–1.16], first a laminated calcareous sand, partially cemented, and then a muddy sand, with wave ripple cross-bedding with off-shoots dipping seaward.

This GTP 26 sequence is not strongly diagnostic but can nevertheless be interpreted as follows. After the initial lag, the relatively formless lower deposits are probably high energy (lower) beach-face facies. The rest of the deposits are probably upper (and possibly middle) shore-face facies; the first multi-set unit may represent an oblique-wave-built longshore bar sequence (easterly migration), the middle unit still shows a longshore tendency under dominantly current influence but with tidal influence near the top, and the third unit shows wave influence. The lack of well developed upper beach-face deposits, the co-occurrence of muds and relatively coarse sands, and the absence of coarse chalk

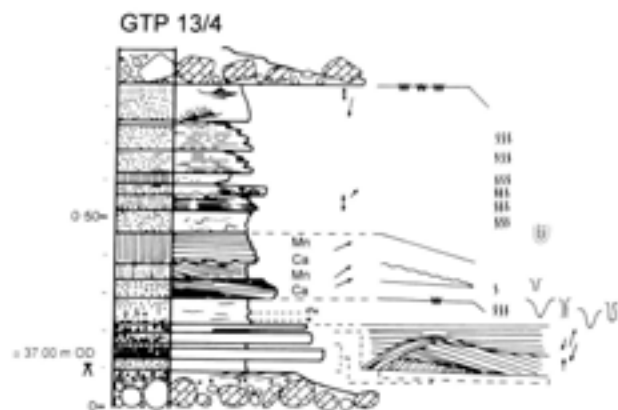


Fig 45b Detailed sedimentary log through the sediments at GTP 13 4



Fig 46 GTP 13, showing boulders at the base of the section; a) Slindon Sands (Marine Cycle 1), b) tail of beach, c) Marine Cycle 2, d) debris flow, e) Marine Cycle 3, f) Slindon Silts (Unit 4b), g) path gravels; note top of the section truncated by quarrying. Scale unit 0.5mm

debris (perhaps suggesting slightly more competent bedrock in this vicinity), imply rapidly increasing water depth in a more steeply shelving environment than, say, in the area of GTP 13. This implication is supported by the nature and geometry of overlying beds, together with the present best estimate of the cliff-line which would seem to be relatively close to the north (Lewis and Roberts Chapter 2.2). Wave ripples are nevertheless still present in the unit capping this sequence.

The lowest deposits in Q2 GTP 10 (Figs 4, 34) may be mentioned here (Figs 49a–51), although the chalk planation surface was not quite reached. The



Fig 47 Pholias bored chalk at the base of GTP 13; scale unit 10mm

sequence [0–0.62] (Fig 49b) comprises sets of medium sand, with very obscure bedding features, but with slight bioturbation and a minor mud component appearing upwards. The highest deposit of relevance here [0.62–0.7] consists of thick mud sets (laminated and with sand partings), separated by thin medium sand beds; the lowest mud set shows reversing cross-lamination with discordant ripple-form tops and medium to high bioturbation, apparently indicating combined current/wave ripple bedding, probably with tidal influence. The whole sequence would seem to consist of lower shore-face facies.

The matter of cementation should be mentioned here. It was noted above that cementation in outer deposits of GTP 25 is probably post-depositional. No cemented beds appear in the GTP 13 sequence. However, very strongly cemented beds occur in both GTP 26 and GTP 10 (Fig 50), often with the obliteration of internal bedding features; cement may strengthen (either upwards or downwards) from contacts, may turn a bed into a concordant dogger, or may appear as nodular forms. Traces of fine chalk debris and tiny molluscan fragments hint at a source for the cement. However, rip-up clasts appear to be absent and there is no proof of penecontemporaneous cementation. Therefore, although there are superficial resemblances between better cemented beds in GTP 26 and GTP 10 on the one hand, and the doggers of SEP 3 on

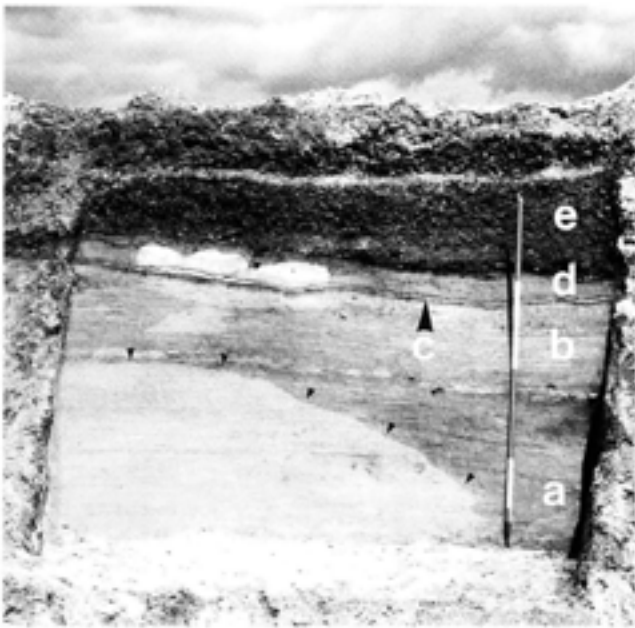


Fig 49a Q2 GTP 10; note the partial decalcification of the sediments (decalcification front marked by small arrows.) a) Slindon Sands (Unit 3), b) Slindon Silts (Unit 4), c) palaeosol (Unit 4c) and Unit 5a, d) Brickearth Beds (Unit 6), e) Fan Gravel Beds (Unit 9); scale unit 0.5m

the other, there is as yet no reason to link these occurrences stratigraphically, although they were probably both formed as the result of decalcification in overlying deposits, and the subsequent redeposition of CaCO_3 lower down in the sedimentary profile.

Deeper water conditions

In-shore sequences

The outer exposures in GTP 25 show very few signs of deeper water before the onset of regression, which is not surprising this close to the cliff-line. At GTP 25 B SW (Fig 42h), there is a unit [(0.8+0.46)–(0.8+0.54)] of medium to coarse sand, with finest chalk and flint granules; bedding structures are obscure and there is slight, formless bioturbation throughout. A pair of relatively thick reddish clay laminae [(0.8+0.54)–(0.8+0.59)] cap the sands, and the whole is disturbed by cf *Monocraterion* forms. The next unit [(0.8+0.59)–(0.8+0.84)] consists of fine coarse to coarse medium sands (fining upwards) with some chalk pellets and Fe–Mn-staining; bedding structures are obscure but there are some shoreward-dipping laminae. This unit shows moderate formless bioturbation but also a few

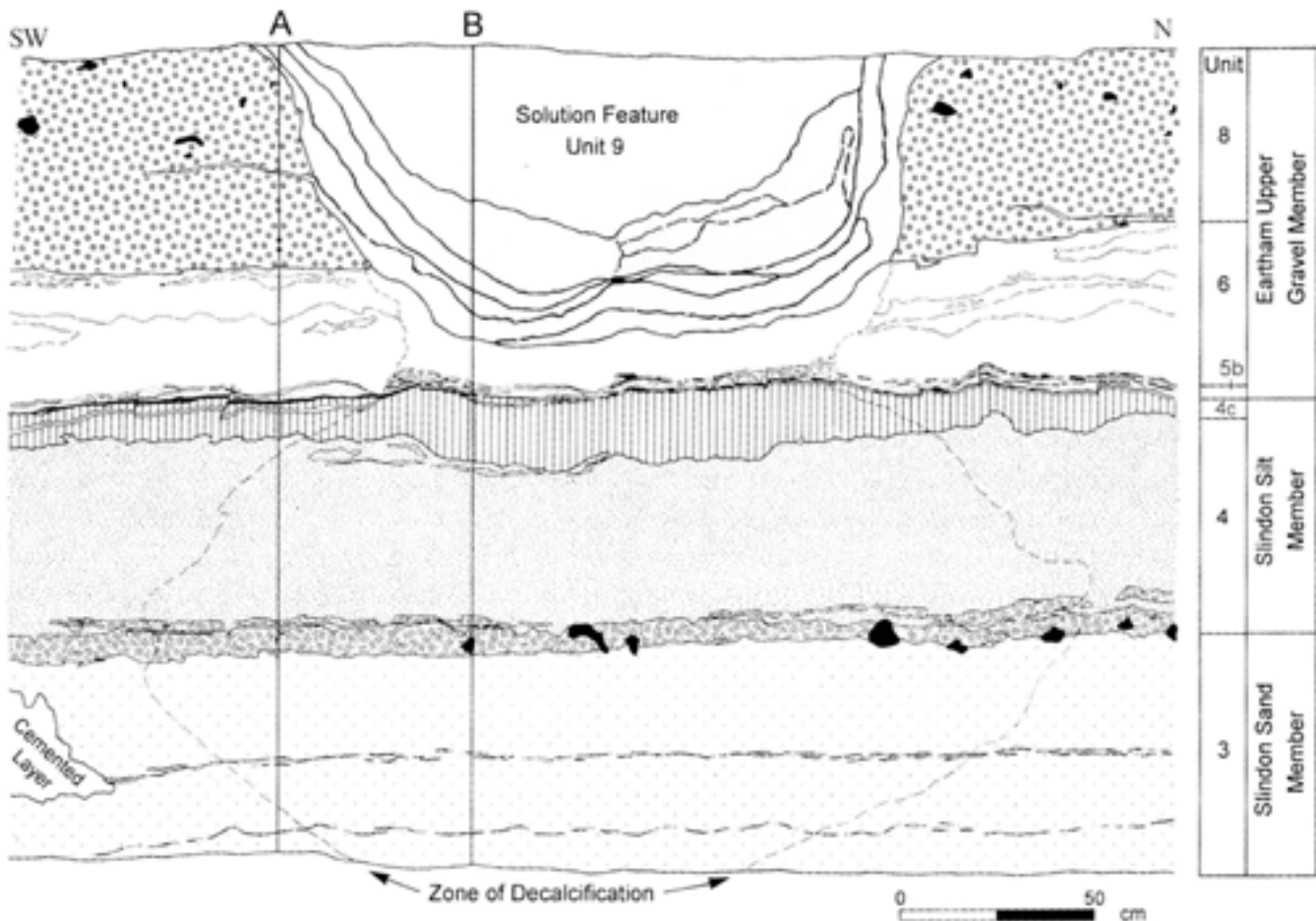


Fig 50 Section through the sediments at GTP 10

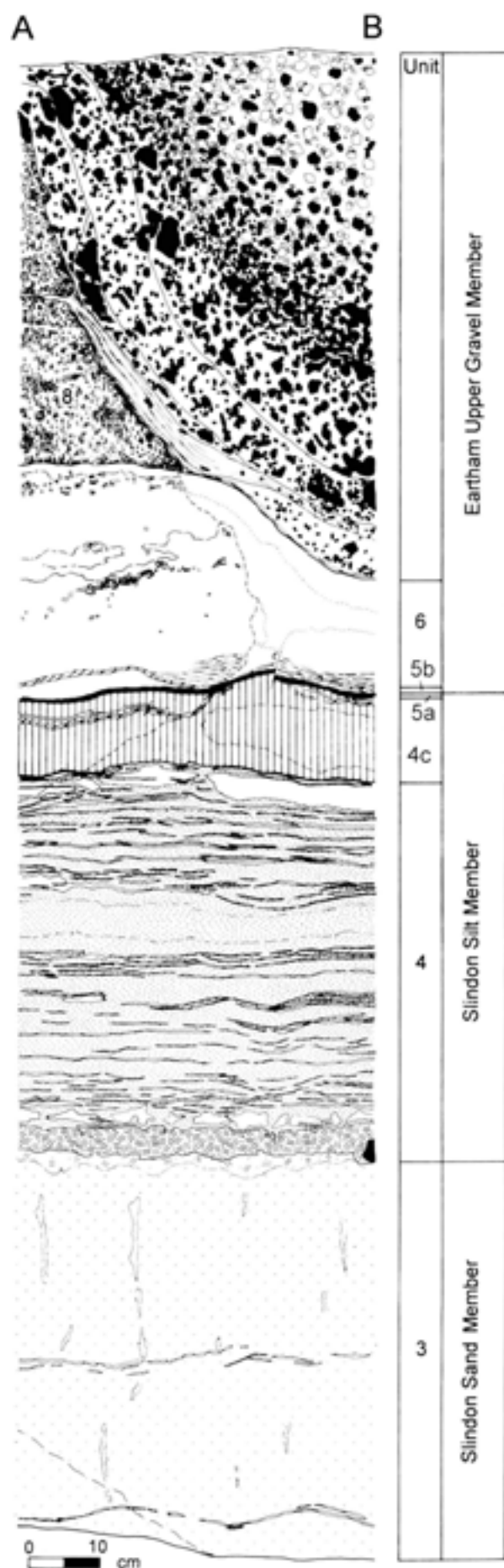


Fig 52 Deeper water fine-grained sediments overlying the beach at Q2 GTP 13; scale unit 0.5m

oblique, clay-lined tubes. The highest deeper water unit consists of a pair of bioturbated sandy mud laminae sets [(0.8+0.84)–(0.8+0.86)], rather wavy in form and multiplying rapidly seawards (Fig 52). This very condensed/incomplete sequence in GTP 25 B shows oscillations between calmer conditions, during which organisms can establish themselves, and more energetic intervals (probably storms), with the rapid dumping of coarser sediment and the washing of clays from the shoreline, later to be deposited as mud laminae once calmer conditions resume. Nevertheless, the main motifs of the deeper water sequences further offshore are already apparent here.

Off-shore sequences

The sequence in GTP 13 (Fig 45a) shows a continuation of the dominance of planar laminated sands. First, there is a planar bed [0.72–0.79] of moderately to strongly calcareous, parallel laminated finer medium sand, with some coarser laminae with finest chalk pellets, dipping gently seawards, with minor and discontinuous lenses of siltier/clayier sand and a zone of

Fig 51 (left) Detailed section through the sediments at GTP 10 (location of section is shown on Fig 50)

isolated ripple-forms with foresets dipping shorewards. The main change from the lower (transgressive) deposits is that bioturbation now becomes moderate, with broadly tube-shaped burrows developed from the top of the ripple-forms and from other clayier lenses. The tubes normally have strongly deflected bases towards the southerly quadrant. Small *cf Monocraterion* forms are developed within the unit. Ostracods are present (Whittaker Chapter 3.2), especially in slightly coarser calcareous matrices. The next unit [0.79–0.89] is a weakly calcareous medium sand, retaining only traces of parallel laminations in places; there are some cut-and-fill structures at the base, with mud-draped foresets dipping shorewards. Heavy bioturbation obscures the bedding, unit-internal burrows including pouch-forms with some southerly deflection of bases; there is a continuous zone of intrusive *cf Monocraterion* forms developed from the top. The next deposit [0.89–1.0] is badly sorted, with both flint pebbles and more angular flint debris in sand. Strong bioturbation has removed any traces of primary bedding (if any such existed), mostly by penetration by contorted but laterally continuous, large *cf Monocraterion* forms, with coarser particles concentrated at margins and slightly muddier traces splaying out upwards. The last deposit [1.0–1.25] in this mid-Cycle 1 sequence is a relatively thick unit of coarser medium sand, probably containing several cycles of deposition but quite heavily disturbed by bioturbation. The lower portion is homogenised, with a fine pebble lag at the base. In the upper portion, there are large sets of planar parallel laminations, moderately rich in carbonates and with some coarser laminae with finest chalk and molluscan debris. Sets dip gently both landwards and seawards but with no regular alternation. Near the top of the unit, there are small, rare lenses of cross-bedded sand with mud-draped foresets dipping shorewards. There are zones at several levels of *cf Monocraterion* forms, becoming irregularly smaller upwards, with many elongate mud clasts in their fills. Other ichnofossils visible in the upper portion of the unit include curved pouch forms, common vertical mud-lined pouch forms with a spur at the base and muddy escape traces above, horizontal mud-lined chambers and signs of more complex three-dimensional branching structure, near the top, a crustacean hunting trace (indentations from body and feet as the animal lies hidden in the superficial sediment), and a convergent *cf Diplocraterion* with retrusive spreites; and vertical (mostly but not entirely epichnial) tubes, commonly of 5mm diameter.

The surviving bedding forms in the GTP 13 sequence seem to suggest a lower shoreface environment, with some muddier zones perhaps indicating the boundary with the transition zone off-shore. Both scours and ripple-trains, with landward foreset dips, indicate on-shore currents (and possibly wave action), still with a tidal influence where mud-drapes are present. However, there are also clear signs of storm conditions, which have brought coarser elements into this deeper

water and have probably produced intervals of rapid sand deposition. Clear graded beds (coarse elements, then sand, capped by muds) have not survived, probably due to subsequent bioturbation (see below), but it may be deduced that a few such beds were once present. This tension, between calmer deeper water conditions and energetic storm conditions, is also seen in the trace fossils. Forms with deflected, and even horizontal or three-dimensional, elements would indicate the relative rarity of major erosive events. There are a variety of pouched, chambered and mud-lined forms (some of them probably referable to *Ophiomorpha*). The crustacean cubichnial trace and the *Diplocraterion* indicate a biologically active zone, although the latter has had to adjust to input of sediment. The vertical tubes of *Skolithos* (both internal to these sediments and originating from higher deposits now lost to erosion) also indicate significant biological activity. In stark contrast, the variety of disruptive *cf Monocraterion* forms (whether true fugichnia or merely water-escape structures) show the influence of storm events with rapid sediment dumping. The resulting sedimentary sequence therefore shows alternations between laminated and 'scrambled' (bioturbated) intervals, often abbreviated to 'lam-scam'.

Further off-shore in GTP 10 (Fig 49b) there is a similar 'lam-scam' sequence, with primary sedimentary structure often extremely disturbed or even totally missing. The first unit [0.7–0.81] can still be seen to be a laminated finer medium sand, with some mud-drapes. There is very strong bioturbation, with many generally funnel-shaped forms and, near the base, some large *cf Monocraterion*, with crinkled internal conical laminations; there is also a small *cf Diplocraterion yoyo* with retrusive and protrusive spreites. There follows a pair of thick mud laminae with high clay content [0.81–0.82], probably originally horizontal but now deformed. The next unit [0.82–0.85] is a muddy medium sand, with very strong bioturbation, including small pouched forms with horizontally deflected bases and various large simple *cf Monocraterion* forms near the base. The next unit [0.85–0.94] comprises laminated medium to fine sand, with slight carbonate cementation and moderate bioturbation, including some deflected pouched forms. There follow two slightly fining-upwards cycles of laminated muddy medium to fine sand [0.94–1.10]; there is very strong bioturbation, including pouched forms with horizontally deflected bases, curved tubes, bifurcating tubes (*cf Chondrites*) and broad pouches with asymmetrically structured laminar fills. The normally bioturbated sequence is briefly interrupted [1.10–1.20] by bundles of laminated medium sand, with many reactivation surfaces, but always with seaward dip; there are patches of carbonate cementation. The more typical style returns at the top of this sequence [1.20–1.50] with bioturbated mud and coarser medium sand, passing gradually upwards into muddy coarser fine sand, laminated with minor

mud-drapes in places. Ichnofossils include pouched forms with horizontally deflected bases; there are funnel-shaped forms (rather more rounded in profile than the average cf *Monocraterion*), especially towards the base of the unit where they are also more laterally continuous, some with concentrations of coarse material, including molluscan debris and tiny immature bivalves (Mytilidae).

This sequence is broadly similar to that in GTP 13 1 (Fig 45a), although here bioturbation is more extreme and overall mud content is higher, consistent with the position slightly further off-shore (transition zone). Scours and ripple-trains no longer appear, although there is one unbioturbated interval, representing a higher energy episode; it is noteworthy that the tiny translucent shells of immature bivalves (pelagic phase) appear here, as they do in most calmer, deeper, water contexts at Boxgrove.

The off-shore sequence in GTP 26 (Fig 48) begins with a unit [1.16–1.56] of at least seven cycles of rare shingle and fine chalky pellets, passing upwards to slightly muddy medium sand, weakly cemented in places, with increasing platy mud clasts; there are still traces of ripple cross-bedding and sets seem to cross-cut each other with both landward- and seaward-dipping surfaces but the geometry is very disturbed at all scales. Medium to small cf *Monocraterion* forms are common, turbating the whole unit and obscuring the bedding; many of these forms have basal tubes and are thus almost certainly fugichnia. There are also isolated mud-lined vertical tubes. There follows a slightly muddy fine sand [1.56–1.60], highly turbated, especially by small cf *Monocraterion* forms. The next unit [1.60–2.26] contains at least eight coarsening-upwards cycles, consisting of cross-laminated slightly muddy sands, first medium sand and then coarse medium to fine coarse chalk-rich sand, relatively well sorted and with only a few small flint pebbles; each cycle is capped by heavily disturbed mud, probably originally deposited as continuous drapes. Each cycle is then turbated, with J-tubes and medium to small cf *Monocraterion*. A large scour form, cored by a chalk cobble and a few pebbles, shows north-westerly dipping cross-laminae a third of the way up the unit. At the top of the unit, there is an interval with regularly alternating landward and seaward wave ripple cross-lamination with off-shoots, each set never thicker than a centimetre; there are also traces of similar bedding near the base of the unit. The last unit in the sequence [2.26–2.30] consists of slightly muddy finer medium sand, with wave ripple cross-lamination with off-shoots, in alternating landward- and seaward-dipping sets and showing a slight tendency to climb in places; the unit is not bioturbated and there are no mud-drapes.

The GTP 26 sequence contains two main cyclothem units, each of which comprises beds starting with laminated sands and capped by muds. The lower cyclothem has beds with normally graded tops, before disturbance by bioturbation. The upper

cyclothem has beds that are laminated throughout, and which coarsen upwards, before the mud capping and bioturbation. These cyclothem units are governed by recurrent storm events. The generally coarse texture, the presence of chalk debris and the tendency for ripple-forms to climb combine to reinforce the impression of a relatively exposed and steeply shelving shore in GTP 26 already suggested by the initial transgressive deposits. The ichnofacies is dominated by cf *Monocraterion* forms, with only minor development of J-tubes and mud-lined oblique/horizontal tubes, presumably because, although scour is not dominant, rapid deposition produces a rather hostile benthonic environment. Water depth is difficult to judge but a generally subtidal (shore-face) environment is indicated.

Regression

The shoreward deposits of a marine regression are inherently vulnerable to erosion during the subsequent transgression. We can hope to identify the lowest beach deposits, representing the maximum regression, but the high energy of the beach zone will still cause some loss of older, deeper water, deposits. Seawards, the shallowing tendency will be more smoothly reversed during the subsequent transgression, probably resulting in difficulty identifying an exact boundary between cycles.

In GTP 25 B SW (Fig 42h), close to the coastline, there is a bed [(0.8+0.86)–(0.8+0.93)] of coarse medium sand with no visible bedding structure; bioturbation is still moderate but there are traces of simple divergent U-tubes (cf *Arenicolites*). The final unit in Cycle 1 [(0.8+0.93)–(0.8+0.96)] consists of fine coarse sand, with traces of planar cross-lamination dipping seawards; there are many small cf *Monocraterion* forms. In the main GTP 25 B sequence (Fig 42g), a bed [1.61–1.66] of finest gravel and small pebbles, in a coarse sand matrix, represents the succeeding transgression. Only the drop in mud content in coarser sands and the appearance of *Arenicolites* forms hint at shallowing water before the next beach phase, and it is evident that erosion has removed a significant interval.

In GTP 13 1 (Fig 45a), there is a bed [1.25–1.33] of coarser medium sand, with roughly trough-bedded ripple cross-lamination. Near the base, ripples are small and often show silt-drapes on foresets. Ripple length increases markedly upwards, with some landward and some shoreward foreset dips but no regular alternation; larger ripples are perfectly symmetrical. There are some irregularly spaced and relatively small cut-and-fill structures with landward-dipping foresets. There is very little bioturbation and the bed is weakly to moderately calcareous. The highest bed [1.33–1.46], before the coarse beach of the succeeding transgression, consists of alternations of clean coarser medium sand and finer coarse sand, with sets of planar parallel laminae dipping gently seawards but becoming horizontal nearer the top. There are a few minor wedge-sets, with foresets dipping generally eastwards or westwards.

Coarser laminae in this bed contain chalk pellets, Cretaceous sponge spicules, and small flint flakes. There are some small *Monocraterion* forms traversing the unit but, otherwise, the bed is unbioturbated; the bed is moderately calcareous, becoming only weakly so upwards. The lower unit in this final interval of Cycle 1 in the GTP 13 sequence shows tidal influence, gradually superseded by increasing energy wave influence; this ripple-form bed would indicate a high shore-face environment. The upper unit shows the planar laminations (high energy plane bed), with minor longshore events and lags of well sorted (with respect to both size and shape) finest coarse debris, typical of lower beach-face (intertidal) facies.

In more off-shore locations, there are no clear traces of regression. At the [1.5] level in GTP 10 (Fig 49b), a 'bulk' colour change in sandier zones (from generally pinker below, to generally 'rusty' tones above) is the main sign of the Cycle 1/2 boundary, along with a change in bedding style. In SEP 3 (Fig 38), the whole of Cycle 1 is represented by obscure fine sand beds (not logged in detail) with very strong formless bioturbation; nevertheless, the colour and bedding style changes mark the Cycle 1/2 boundary at the [2.57] level. The situation in GTP 26 (Fig 48) is particularly obscure, it being possible to suggest the most plausible boundary between Cycles 1 and 2 only after the information from this exposure itself has been considered in the light of the morphology and altimetry

of the Boxgrove deposits as a whole. The unbioturbated wave ripple cross-lamination, with alternating bedding and lacking in mud-drapes, seen in the minor [2.27–2.29] interval (described above with the main GTP 26 sequence) might indicate a degree of shallowing but would not be sufficient on its own to prove regression. Given the overall steep palaeoslope of both the basal Chalk surface and the overlying unconformity with Cycle 2 deposits, it seems likely that there are significant non-sequences in Cycle 1 deposits in the off-shore locations.

Marine Cycle 2

Transgression

The main beach GTP 25

The difficulties in relating coarse storm beach material to the corresponding finer intertidal deposits was noted above during the discussion of the Cycle 1 transgression.

The chalk planation surface at the cliff, 43m OD, probably relates to the Cycle 2 transgression (Figs 41, 42a, 43). This surface is overlain, in GTP 25 1 (Fig 42b), by an intermittent band of spherical and slightly chatter-marked flint pebbles, rarely more than one or two pebbles thick. In the [1.0–1.8] interval in GTP 25 2 (Fig 42b), the basal bed is represented by large flint cobbles; there are then fining-upwards cycles of flint



Fig 53 Chalk rubble overlying the beach near to the cliff at GTP 25; scale unit 0.5m

pebbles in a badly sorted matrix with much fine chalk debris. The same deposits continue southwards down the exposure (GTP 25 3, Fig 42b). Above this storm beach material, there is a wedge of edge-rounded chalk rubble (with some blocks larger than a metre in diameter) set in a degraded chalky matrix (Fig 53). This rubble shows high-angle (30° – 35°) diffuse internal bedding and the whole has a cone morphology (as seen in the two sides and the end of the GTP 25 trench); the edge-rounding, maximum angle of rest and diffuse bedding show that this is a true talus (relatively gradual accretion) rather than a chaotic collapse body. The source of the material (presumably a weaker zone or even a gully in the chalk cliffs) is clearly to the north; a maximum thickness of 2.40m is reached in the peaked (cross-cone) end-trench exposure but the cone [1.8–1.82] has almost wedged out 2.5m south of the cliff (GTP 25 3, Fig 42b) and is represented only by isolated small chalk blocks in more seaward exposures.

Further to the south in GTP 25 4 (Fig 42i) there is again a bed [0.12–0.37] of flint pebbles and cobbles, above the chalk debris of Cycle 1. There are then two or more fining-upward cycles [0.37–0.6], from 50mm pebbles to shingle or coarse sand, a deposit which is certainly representative of the normal highest swash zone. A tabular chalk fragment is an outlier of the landward talus cone. In GTP 25 5 (Fig 42c), the

[1.37–2.02] interval again starts with flint cobbles and is followed by pebbles, shingle and coarse sand, although no clear fining cycles are present; there are still small chalk fragments at the very top of the interval. Further seaward still, in GTP 25 7 (Fig 42j), a layer [0.73–1.04] of flint pebbles and small chalk blocks, in a chalky silt matrix lies between the chalk debris of Cycle 1 and the tidal deposits of Cycle 3. In GTP 25 E (Fig 42d), a bed [1.65–1.69] of well rounded flint and chalk pebbles, in chalky magma with medium to coarse sand, lies below finer sediments apparently representing a much later phase in Cycle 2.

Only in the outermost exposures of GTP 25 is the base of Cycle 2 present above truly marine deposits of Cycle 1. In GTP 25 D (Fig 42e), there is first a bed [1.55–1.57] of pebbles and shingle. There follows a bed [1.57–1.72] of medium, fining to silty fine sand with constant cross-lamination dipping regularly to the north-east; this is a bar-like deposit and, although lacking in bioturbation, probably already represents conditions relatively close to mean low water mark. In GTP 26 (Fig 48), the sequence begins with a bed [2.72–2.80] of flint pebbles in medium sand, but deeper water sediments follow immediately above. In GTP 25 B (Fig 42g), a bed [1.61–1.66] of finest gravel and small pebbles in a coarse sand matrix begins the sequence, but apparently deeper water conditions again follow

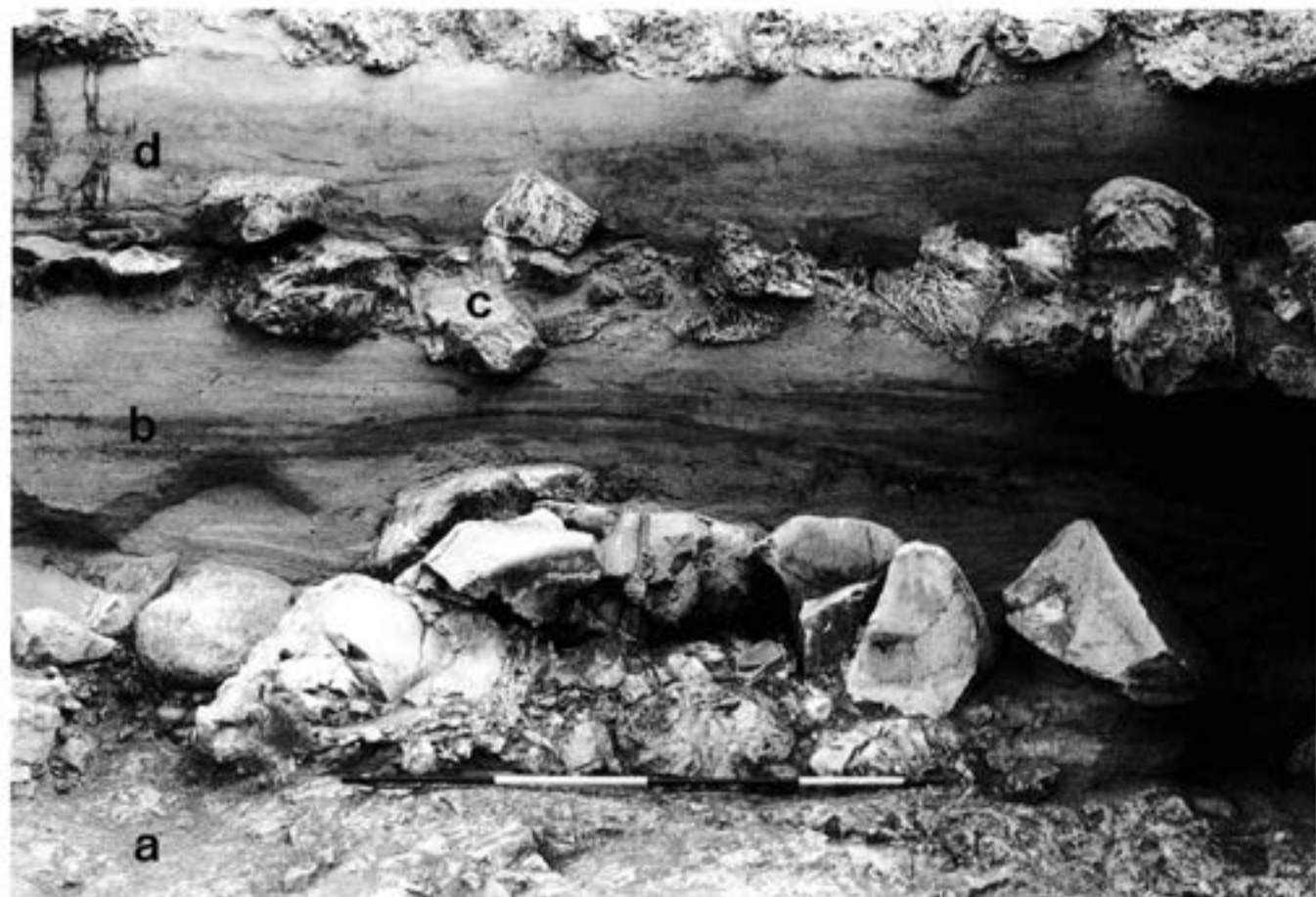


Fig 54 Marine Cycles 1 and 2 at GTP 13; a) chalk bedrock, b) Slindon Sands (Marine Cycle 1), c) tail of beach, d) Marine Cycle 2; scale unit 0.5m

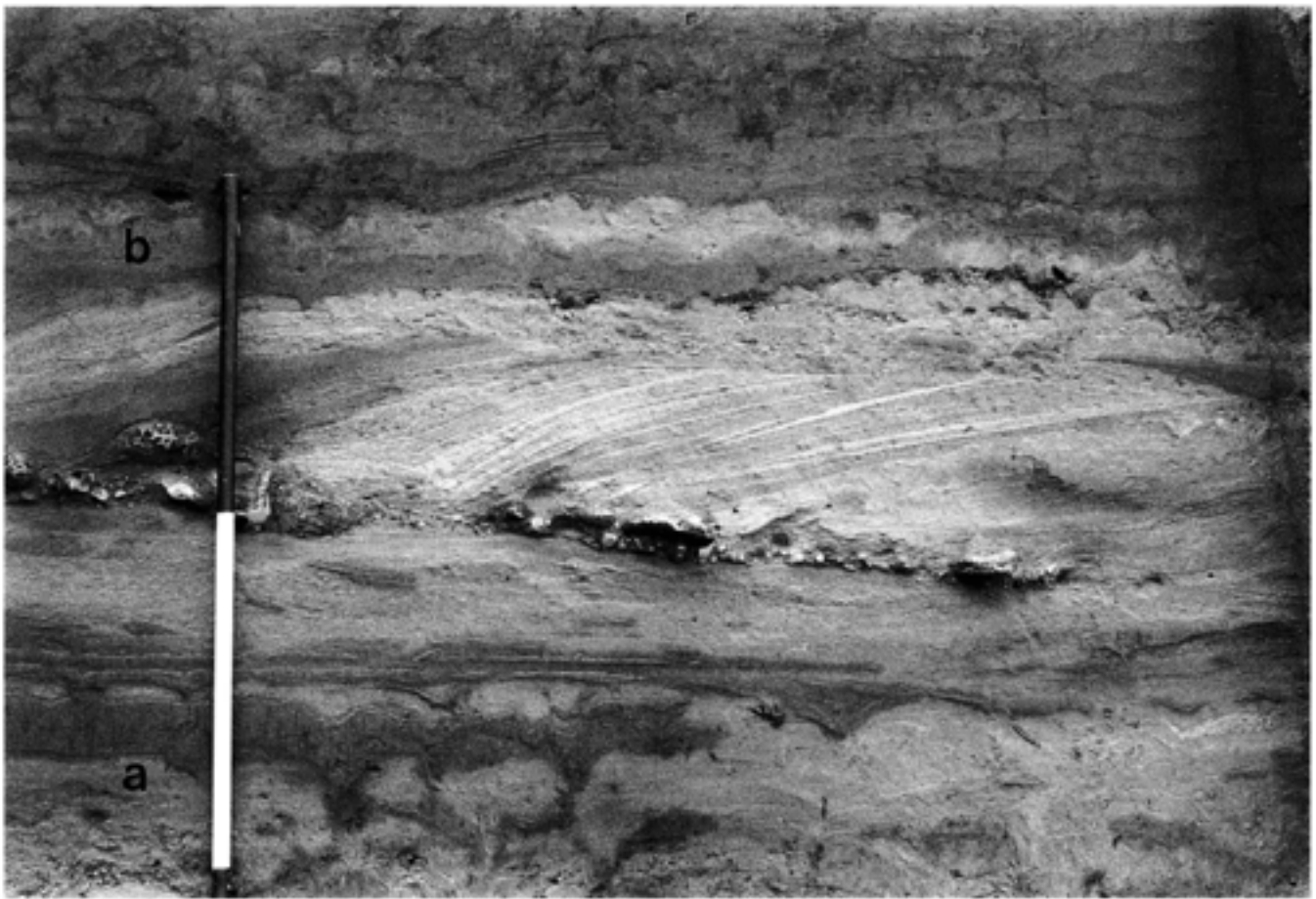


Fig 55 Detail of sediments at the top of Marine Cycle 1 (a) and the base of Marine Cycle 2 (b); scale unit 0.5m

immediately (but with a later return to coarser input — see below); there is, however, a coarse medium sand [(0.8+0.96)–(0.8+1.0)] just seaward in GTP 25 B SW (Fig 42h) before the deposits above the [1.66] level in GTP 25 B.

Seaward exposures

In GTP 13 1 (Fig 45a), the first bed of this sequence [1.46–1.59] is a true beach deposit (Figs 20, 54). The main component is well rounded chalk pebbles and cobbles, becoming rapidly larger (up to c 0.7m diameter) shorewards. These chalk elements are either spherical or markedly oblate; the dip of oblate pebbles is rather irregular but with a shoreward tendency, and their long-axes are most commonly shore-perpendicular but sometimes shore-parallel. Flint pebbles and cobbles become increasingly common landwards, usually grading upwards into badly sorted silty coarse sand with chalk pellets and angular flint debris, showing medium scale cross-laminae with irregular landward dip. There is also a large cut-and-fill structure, with medium to coarse sand cross-lamination dipping due north. The next bed [1.59–1.68] comprises very well sorted alternations between moderately to strongly calcareous medium and coarse sand, in planar sets of laminations, either horizontal or gently landward-dipping. There are also some thin concordant lenses (lags) with chalk

pellets and flint flakes, and small flint pebbles and molluscan debris become common in all subunits landwards. Bioturbation is restricted to forms penetrating from above. The next unit [1.68–1.71], present as a lens cut out quickly seawards and landwards by subsequent erosion, already contains much finer sediment; it is a moderately calcareous badly sorted fine to medium sand with appreciable silt/clay content and traces of mud-draped cross-laminations. Bioturbation is strong but originates from above. The final unit in this sequence [1.71–1.76] is a relatively localised lens of laminated, moderately to strongly calcareous coarse sand and finest chalk debris, with increasingly marked landward cross-lamination dips towards the shore and a discordant asymmetrical ripple-form upper surface (stoss landwards). Bioturbation forms (penetrating into underlying material) are clear; the most common are small cf *Monocraterion* forms and simple strongly divergent U-tubes (*Arenicolites*) with the arms aligned along a shore-perpendicular trend.

The GTP 13 1 sequence lies very close to the point of maximum regression and the true beach is lost quickly seawards; the exposure in GTP 13 1 thus represents a very early stage in the Cycle 2 transgression (close to the regression/transgression cusp, Fig 55). The slightly imbricated structure of the pebble bed is typical of a swash zone beach; it is interesting that the chalk and flint zones are beginning to differentiate, the

anomalous seaward concentration of chalk (instead of the more normal landward concentration of less competent lithologies on most beaches) is presumably due to both significantly lower density (specific gravity) and abundant input. The laminated beds above represent rapid encroachment of transgressive sands, so rapid that silty chalk debris has not usually been totally removed. The broad and gentle palaeoslope thus developed seems to have allowed finer sedimentation, under tidal influence, to have developed, with no signs of a wave-ripple interval. However, before the onset of deeper water conditions, a bar of better sorted coarse sands sweeps rapidly across the area, probably producing slight shoaling; the *Arenicolites* would indicate relatively shallow water, perhaps totally within the intertidal range. This sequence is basically immature, with a clear overlap (onlap) geometry in the deposits overlying the beach.

The northernmost, east-west running, section of GTP 13 4 (Fig 45b), provides useful additional detail for this general area. The storm beach is represented by flint and chalk pebbles with a few cobbles. There is then a set of units [0.1–0.2] which, together, form a low bar, with the crest parallel to shore; the first bed (itself dipping slightly seawards) is a silty fine sand, with weak planar laminations dipping shorewards; the next bed is a chalky/flinty fine gravel, with planar bedding dipping seawards concordantly with the bed-form; the next bed is silty fine sand, with planar laminations dipping seawards concordantly with the bed-form, and thickening locally seawards; the last bed is composed of chalky/flinty very fine gravel and coarse sand, with planar bedding dipping shorewards concordantly with the bed-form (and thus truncating the lower beds in this unit). These beds are not stratigraphically continuous with units 6m to the south in GTP 13 1. There is no significant bioturbation. The final unit in this sequence [0.2–0.22] comprises a mud-drape over the underlying bar-form, and then finest gravel and fine sand, with horizontal laminations and a roughly horizontal upper boundary (having completely 'drowned' the underlying bar-form); again, there is no significant bioturbation.

This short GTP 13 4 northern sequence represents a beach ridge and subsequent dominantly coarse unit, deposited in a beach-face environment with significant drops in energy (silts and clay drapes). As in GTP 13 1, rapid sediment-rich transgression over a gently shelving base has produced an immature sequence; despite the ridge, no longshore runnels are apparent.

In GTP 10 (Fig 49b), as noted above, the point of maximum regression is marked most obviously by a colour change; it seems most unlikely that the sea ever retreated completely from this location. The first bed [1.50–1.63] consists of isolated patches of finer medium sand, with formless bioturbation throughout. The next bed [1.63–1.80], often starting with a highly erosive pebble lag, is composed of medium sand with very thin and discontinuous mud laminae and rare flint

pebbles, together with a coarse sand and finest shingle component at the top. The base of the bed has patchy carbonate cementation and there is common fine molluscan debris including immature bivalves (*Mytilidae*). The swing from regression to transgression is therefore very subtle in this exposure, expressed more as a transitory 'disturbance' of the deeper water environment than as a true facies shift. In SEP 3, the boundary between Cycles 1 and 2 is even more subtle (cf colour change), with no obvious signs of shallower water. The obscure situation in GTP 26 has been noted above; the earliest sediments thought to be referable to Cycle 2 are described below with the rest of the deeper water deposits at this exposure.

Deeper water conditions

In-shore sequences

In GTP 25 E (Fig 42d), the sequence begins with a clayey chalk magma impregnating the coarse deposit below; this clayey material is stratigraphically continuous with the [2.13–2.20] interval in GTP 25 D (see below). The next unit [1.69–1.76] consists of fine sand and coarse silt ripple-forms with obscure internal structure, together with medium sand in a few discordant wave ripple-form trains with off-shoots. The next unit [1.76–1.87] comprises ripple-form alternations between clay and sand laminae, the latter becoming finer-grained and thicker seawards and the former thickening landwards; this interval has strong formless bioturbation. There follows a unit [1.87–1.94] of muddy sand, coarser near the base (and generally shorewards), with mud-drapes, showing both seaward and shoreward cross-lamination; there is moderate bioturbation and a suggestion of penecontemporaneous warping. After a persistent erosive (lower-bed-discordant) ripple-form contact, the final unit [1.94–2.01] consists of at least two sets of mud laminae, with intermediate disturbed sand, quite coarse in places; there is strong formless bioturbation.

In GTP 25 D (Fig 42e), the sequence begins with a variable unit [1.72–2.13] comprising muddy/silty fine sand, medium sand and thin clay drapes. There are also at least two persistent pebble 'lines' with fine chalk debris; these coarse elements are always present as isolated particles. There is generally low angle cross-lamination, with cleaner sand beds normally dipping seawards (south-westwards) and siltier material mostly dipping landwards (north-eastwards); however, in the lowest interval there are regular seaward-landward alternations of asymmetrical wave ripple cross-lamination in small scale erosive troughs, irrespective of texture. The next unit [2.13–2.20] comprises two strong clay ripple-form sets, increasingly separated by a sand interval landwards; the unit is stratigraphically continuous with the [3.35–3.39] interval in GTP 25 C (see below). The top of the intermediate sand has a complex ripple form with strike 110° and stoss dip bearing

30° overprinted obliquely by minor ripples; this would seem to represent a temporal shift in flow direction (late minor longshore flow) rather than a true rhomboid system. The next unit [2.20–2.36], which has an erosive base that tends to truncate the ripple-forms below, is composed of a series of clean fine sand current ripple-forms, with thin but continuous mud-drapes. The lowest sets are an almost lingoid form dipping north-eastwards, then come regular cusped forms dipping more closely to landwards; higher sets are more or less strongly undulatory and dip in the general landward direction. There is then a unit [2.36–2.43] of fine to medium sand ripple-forms with clay drapes; the bedding is obscured by bioturbation from above. The final unit in the sequence [2.43–2.53] comprises fine sand with strong mud-drapes/laminae and one diffuse interval of medium sand. Formless bioturbation is strong in this unit, obscuring the primary bedding structures.

In GTP 25 C (Fig 42f), the sequence begins with a thick unit [2.75–3.35] comprising three obscure intervals. The first half of the unit is composed of rather grey silty units, with moderate bioturbation, including small vertical tubes and pouched forms. There follow fining-upward sets, from finer medium sand, to fine sand/coarse silt, to impersistent mud-drapes. These two subunits are composed of planar laminations, dipping mostly seawards but with minor reversals. The top subunit has ripple cross-lamination with landward-dipping foresets. The next unit [3.35–3.39] is a major set of ripple-form mud laminae, with occasional sand linsen, and a planar, discordant upper surface; this unit is stratigraphically continuous with the [2.4–2.54] interval in GTP 25 B (see below). There is much formless or obscure bioturbation but also a few deflected pouched forms. The next unit [3.39–3.55] consists of fine sand with muddy partings, in low angle planar sets and ripple-form sets, either horizontal or with dips generally to the south-west; bioturbation is weak to moderate. The last unit in this sequence [3.55–3.74] consists of fine sand, with coarse sand lenses and mud-drapes and laminations, the mud being stronger lower in the unit; the bedding is strongly disturbed by bioturbation, apparently originating from the bed above.

In GTP 25 B (Fig 42g), the sequence begins with a unit [1.66–1.73] of grey silty fine sand, laminated and traces of ripple-forms; the unit is very heavily bioturbated, especially by traces originating from the overlying bed. That bed [1.73–1.90] consists of medium sand with common fine flint gravel, occasional flint pebbles and rare chalk cobbles; no bedding structure survives the very strong bioturbation. The next unit [1.90–2.07] is a grey silty sand, containing some finer medium sand ripple-forms with ripple strike of 293°, the unit is quite strongly bioturbated, especially by vertical tubes below funnels reaching the top of ripple-forms. The unit above this [2.07–2.49] consists of a series of minor fining-upwards subunits, from slightly muddy fine medium sand, to muddy fine sand, to

clay drapes. The sediment was originally laminated, with very low angle more or less planar bedding and mostly shoreward (between north-westward and north-eastward) dips. There are also some isolated ripple-forms and cut-and-fill structures of coarser sand with foresets dipping mostly shorewards. At a few points in the lower part of the unit, there is better developed cross-lamination, with a variety of current bedding: larger scale ripple-forms with dips to the south-west; strongly undulatory (slightly discontinuous crest) ripple train with dips to the north-east; lunate (regular discontinuous crest) sets with dips to the east-north-east; and lingoid sets with dips to the east-north-east. Bioturbation is often strong, with significant zones of mottling where bedding has been lost; long simple vertical tubes originate from some clay drapes. The next set [2.49–2.54] comprises mud and clay laminae with intercalated quite persistent sand linsen; the unit has a planar, discordant upper surface. Small scale bioturbation structures are common (including many J-tubes and some *cf Diplocraterion* and *cf Arenicolites*), originating from the upper surface and from internal bedding planes. As has been noted above, this unit is stratigraphically continuous across the GTP 25 D to B exposures, and beyond to seaward (Fig 42a). The final unit in this sequence [2.54–2.83] shows fine sand, often capped by laminae of coarse sand, with flaser bedding. In the lower half, relatively thick sets of laminae, on a lateral scale of up to a metre, show low angle foreset dips to seaward (south to south-west), with a few smaller (100mm scale and much thinner) sets dipping landward (north-east to east-north-east); moderate bioturbation is mostly represented by small pouched forms. Towards the middle of the unit, there is a thin but more continuous clay lamina, with carbonate cementation sometimes including the top of the underlying sands. The upper half of the unit shows irregular reversal of metre-scale sets, with generally landward and seaward sets of equal importance; there is only rare, small scale bioturbation.

The above sequences in GTP 25 (E to B) (Fig 42a), although represented at exposures that are relatively close together, show extreme variation and therefore correlation between exposures is difficult. Furthermore, facies shifts are not present in any one exposure that are easily interpretable in terms of smooth trends in water depth; for this reason, the entire sequence in each exposure (up to the base of the overlying Cycle 3 sediments) has been described here. Several general points may be made, before attempting an interpretation of these deposits. The palaeoslope at the base of these deposits (represented by the coarser material of the transgressive beach) is steep, so that successive fine deposits have accreted in an overlapping (onlapping) manner. Water depth and depositional slope in any particular zone through time would have been a complex function of sea level, deposition and erosion, a function which no doubt explains why it is so difficult to correlate and interpret these sequences.

Individual clay laminae nearly always thicken landwards, and clay/mud sets tend to split, with sand wedges pushing in from seawards; this, together with the pure pinkish red colour of unmixed clays, would strongly suggest a terrestrial source (Macphail Chapter 2.6), probably the weathering residue of the chalk and chalk debris along the base of the cliffs. All beds with coarser material (whether flint, chalk or coarser sand) similarly thicken landwards, and represent material dragged off the upper beach-face. The texture of all the sediments at all levels in these exposures is strongly bimodal, the two main stocks being clays and fine to medium sands; apart from representing the two obvious transport directions (from landward and seaward, respectively), the co-occurrence indicates strongly fluctuating energies, with normal calmer intervals interspersed with tidal currents and storms, the two types of higher energy event not always being easy to distinguish.

A synthetic interpretation of these GTP 25 exposures can only be given in very tentative and general terms. At the base of the series, wave action is only identifiable at the in-shore end, the end where finer coarse elements dragged from the land are most common. However, a lower coarse interval is present in GTP 25B, which probably represents a storm event earlier in that (later) part of the transgression represented here. Generally calmer conditions are then represented by bioturbated silty sand intervals with mud-drapes (exposures C and B). A reasonably normal wedge of planar laminated sands, dipping mostly seawards, still with mud-drapes, then builds up (exposures D and C, and a trace in B at about the [2.10] point; Fig 42g), representing shore-face conditions; energy pulses (either tidal or storm) are shown by the seaward development of normal grading, the mud-drapes and by the minor sets of steeper but silty, landward-dipping ripple cross-laminae. In exposure B (and as a trace in C at about the [3.34] point; Fig 42f), there is then an interval including sets of various higher energy current ripple cross-lamination types (undulatory, lunate and lingoid, a suite perhaps indicating intermittently increasing energy and/or decreasing water depth) dipping shorewards. All these forms are still set in a general context of more planar laminations with mud-drapes and bioturbation (probably deeper water tidal conditions close to the transition zone), although the generally northerly dips even in planar beds would indicate on-shore encroachment of deposits, only occasionally reworked by seaward currents. The generally landward-dipping planar beds then become dominant in exposure B, although the increasingly divergent dip bearing might suggest a degree of longshore drift. Calm conditions must still be common in order to explain the mud-drapes and strong bioturbation. The only unit which is demonstrably continuous across all exposures then follows: two strong clay/mud laminae (internally ripple-formed), separated by sand (quite coarse at the shoreward end). This unit possibly represents storm

events, perhaps coinciding with spring tides, during which large volumes of chalk-derived residues have been mobilised; a typical *Skolithos* trace fossil facies then overprints the succeeding calm water fine laminae. In shoreward exposures, the intercalated sand (and even some sand intervals lower in the series) show a degree of longshore current deflection, but probably no more than is necessary in the circulatory cells developed to evacuate water piling up near the shore. A planar unconformity cuts the persistent clay/mud unit. In the following sediments, wave influence is again seen only at the shoreward end (exposure E) (Fig 42d). There is another strong current ripple interval (lingoid, cusped, undulatory, apparently indicating waning energy) in exposure D above the unconformity (Fig 42e). Laminated sands with mud-drapes, first with horizontal or seaward dips (exposure C) (Fig 42f) and then with only dominantly seaward dips (exposure B) (Fig 42g), are developed seawards, with increasing bioturbation. The top of the series is represented landwards (exposures E and D) by increasing inputs of mud/clay and coarser sand, with a tendency towards alternating sets of cross-lamination dips, and quite high bioturbation. Seawards (exposures C and B), the mud content declines a little but alternating sets of quite large scale low-angle trough bedding appear, with a tendency towards coarsening upwards, before mud-drapes and flasers cap each set; these are typical moderate energy tidal current sediments. In summary, this GTP 25 series seems to represent strongly fluctuating shore-face conditions, under tidal (and storm) influence, with frequent switches between calm water, abundant sedimentation and erosive ripple or plane bed migration. At no point is there a typical beach-face (intertidal) deposit. Since the cliffs and coarse storm beach nevertheless lay very close to the north, it seems likely that all these deposits post-date any active transgression (the period of cliff and ancient storm beach retreat due to direct marine erosion).

Off-shore sequences

In GTP 13 1 (Figs 45a, 56), the sequence begins with a unit [1.76–1.94] of weakly calcareous, irregular coarsening-upwards sets, from muddy fine sand, to slightly muddy fine to medium sand, to thin intervals of cleaner coarser medium sand, capped by mud laminae and drapes; there are isolated fine flint particles throughout. The bedding is obscure but seems to be dominated by low angle planar laminations, with rare traces of shoreward-climbing ripples and some small cut-and-fill structures. Formless bioturbation is very strong; clearer internal forms include simple shallow burrows and very thin upward-branching forms (probably made by Polychaeta) which are 'rooted' in underlying beds, whilst large *cf Monocraterion* (with internal cone-in-cone structure) penetrate right through the unit (and below) from its irregular top surface. The next unit [1.94–2.01] is a strongly calcareous muddy



Fig 56 Prepared logging section at the southern end of GTP 13; note the flint flake in sediments of Marine Cycle 2; scale unit 10mm

silt with isolated fine flint particles, capped by erosive but contorted, weakly calcareous finer medium sand lenses (perhaps originally ripple-forms); there are rare traces of mud-draped planar bedding in places and the whole unit seems to be wedging out seawards. Bioturbation is very strong and mostly formless, although there are some small cf *Monocraterion* forms with sandier cores. The next unit [2.01–2.07] is similar, with a muddy base, then probably originally laminated, strongly calcareous silts, passing upwards into fine sand with increasing mud-drapes. Bioturbation is very strong, with clear gastropod escape structures and oblique tubes capped by broad 'escape' funnels. The next two obscure units [2.07–2.25] comprise very muddy silts with clay-rich zones, becoming strongly calcareous towards the top; formless bioturbation is very strong but there are a few short tubes with bases deflected landwards. The next unit [2.25–2.32] starts with a little dispersed coarse sand and isolated flint pebbles (strengthening seawards), and then continues as perhaps the finest interval in this sequence, with

strongly calcareous silt and finest sand, interstratified with mud-drapes, and a discontinuous muddy zone at the top with rip-up clasts. There are sets of planar laminations, showing slight fining-upward trends, with reactivation surfaces (sometimes ripple-forms cutting underlying parallel bedding). Bioturbation is less extreme than in underlying beds but still dominantly formless; nevertheless, there are a few strongly deflected short tubes with random orientation originating from the top surface. The next unit [2.32–2.47] consists of strongly calcareous muddy fine sand passing upwards into laminated coarse silt and fine sand, with increasing mud-drapes and laminae upwards, capped by slightly gritty material with much mud, sometimes as clasts; in the seaward direction, the upper interval begins to include strong clayey ripple-forms. Bioturbation is again very strong, with tubes markedly deflected seawards and traces of coarse lining; a few of these tubes are capped by large and wide funnels. Ostracods are present in this deposit. The last unit in this sequence [2.47–2.55] consists of strongly calcareous fine sand and silt, with a tendency to fine upwards; the unit was probably originally laminated. Heavy bioturbation includes a few pouched forms and more vertical tubes, sometimes capped by small funnels. Ostracods are again present.

The sequence 6m north in GTP 13 4 (Fig 45b), provides useful additional detail on the Cycle 2 deposits (Fig 53). The first unit [0.22–0.29] is a silty sand with some very fine gravel; bioturbation is strong, with small, internal and epichnial cf *Monocraterion* forms and also large vertical tubes and rarer pouched forms developed from the top surface. The next unit [0.29–0.46] comprises beds which, together, form a shore-parallel bar. After a markedly erosive base, the first bed contains medium to fine sand with some mud, set in very broad troughs with planar cross-laminae dipping to the east-north-east. The next bed, which wedges out quickly seawards with a discordant ripple-form upper boundary, contains badly sorted and strongly calcareous finer sands and silts; planar laminae dip gently to the east-north-east discordantly with the bed-form. The uppermost, seaward-dipping bed consists of moderately to strongly calcareous silt with a little fine sand; planar laminations dip gently to the east-north-east discordantly with the bed-form. Bioturbation is almost absent in the three beds of this bar-form unit, save for a few vertical tubes originating in the lowest interval. The next unit [0.46–0.52] is a grey silty sand; strong formless bioturbation is present throughout, with a small cf *Diplocraterion* form with retrusive spreites near the base. The overlying unit [0.52–0.56] consists of silt and fine sand with mud-drapes, becoming muddier upwards; sets are defined by planar almost horizontal reactivation surfaces, and contain low angle cross-laminae showing shoreward-landward reversals in dip between sets. Bioturbation is strong and homogenises the deposit (destroying the bedding) in places. The next unit [0.56–0.59] is a fine

sand symmetrical ripple-form, with cross-laminae dipping to the north-east; the ripple-form is capped by mud laminae, the troughs are then filled with more fine sand, and the whole is capped by a horizontal set of mud laminae. Formless bioturbation is strong, obscuring all internal stratification in the upper sandy trough fills. The unit above this [0.59–0.62] is a heavily bioturbated muddy silt, which is strongly persistent seawards (although the exposure is not available to trace the unit southwards into GTP 13 1. The final two units in this sequence [0.62–0.76] are sets of silty fine sand with mud-drapes increasing upwards, the upper unit being capped by a discontinuous but persistent true clay lamination; the units are laminated, with possible reactivation surface, although it is not clear whether or not dip reversal is present. These units show strong formless bioturbation.

Bioturbation is generally so strong in the deposits of these two GTP 13 sequences, that bedding structures (and even trace fossils themselves) are obscure. The thicker units in GTP 13 1 seem to show more common escape structures, in addition to the mottled appearance (presumably due to sediment-feeders), than those seen in in GTP 13 4. The exception is the bar-form near the base of the GTP 13 4 sequence (cf the ridge in this same location early in the Cycle 2 transgression, described above), which is unbioturbated, allowing the survival of the signs of persistent longshore drift and in-shore migration. Towards the centre of the northern sequence, there is an interval of planar reversing lamination, followed by at least one ripple train of symmetrical wave cross-lamination. Nevertheless, laminar sets seem to be the norm, with only rare discordant ripple-form contacts and even rarer ripple cross-lamination. Overall, these GTP 13 sediments would seem to represent a sequence to lowest shoreface and even transition zone conditions, with oscillations between relatively calm conditions with strong bioturbation, and storm conditions with strong sedimentation, including the input of clays and flint grit from the land.

In GTP 10 (Figs 49b–51), the sequence begins with a bed [1.80–2.10] consisting of slightly muddy medium sand with disrupted clayey mud laminae throughout, passing upwards into an increasingly muddy interval; there are obscure cross-bedding features in the lower part. Bioturbation is strong and often formless, although clearer types originate from higher in the bed; these include large mud-lined pouched forms, some large traces with meniscate fills and a few long vertical and sinuous tubes. There is common fine molluscan debris, including immature bivalves (Mytilidae). The next bed [2.10–2.36] consists of medium sand, passing upwards to fine sand and then muddy sediment with isolated flint granules; traces of planar bedding are clear lower in the bed but become increasingly obscure upwards. Bioturbation is strong, with many cone and cone-above-tube forms (some possibly cf *Monocraterion*), a generally vertical development, and some more rounded burrows in the

upper interval. There is common fine molluscan debris, including immature bivalves (Mytilidae), fragments often being concentrated within the trace fossils. The next unit [2.36–2.47] is a well bedded fine and medium sand, approximately horizontally laminated but this disturbed and obscured cross-bedding near the base. Very strong bioturbation takes the form of cf *Monocraterion* horizons (concentrating coarsest sand and very small fragments of mollusca in the cone bases) and some short deflected or sinuous pouches/tubes, but otherwise dominantly vertical development. The final bed in this sequence [2.47–2.65] consists of fine sand and lenses of medium sand, with a slightly muddy top. Strong bioturbation comprises cone forms at all levels but especially at the top, some of them clearly escape structures, together with some tubes/pouches tending towards vertical development.

This GTP 10 sequence again shows alternations between rapid sedimentation and calmer intervals with strong bioturbation, in a broadly (lower) shore-face environment. These deposits are not quite so muddy and retain slightly coarser sands than in exposures nearer the shore, probably reflecting the dual effects of landward derivation of clays and more continuous current action off-shore.

In GTP 26 (Fig 48), the sequence begins with a unit [2.28–3.06] composed of at least nine obscure cycles, with laminated slightly muddy medium sand, coarsening upwards to poorly sorted sand with a minor coarse sand element, shingle (including chalk debris and relatively large mud clasts) and a few flint pebbles, each cycle being capped by mud clasts and smears; the coarse intervals themselves coarsen upwards in series. Each cycle is heavily disturbed by cf *Monocraterion* forms, becoming larger upwards; a few examples lower in the unit have basal tubes, whilst larger forms near the top often have layered conical internal structure. Within the laminated lower interval of each cycle, there are also mud-lined tubes, often oblique and sometimes horizontal. Towards the base of the unit, there is a set of irregular ripple-forms, with seaward-dipping cross-laminations tending to climb. A little higher, there is an interval with obscure zones of landward-dipping climbing (c 17°) sinuous ripple cross-lamination, followed just above by a very small zone of landward-dipping laminae with finest chalk debris. Then, half way up the unit, there is a major cut-and-fill structure, with foresets dipping to the south-west. The next bed [3.06–3.18] consists of slightly muddy calcareous fine sand. The sediment shows planar laminations, picked out by ferrous oxides, with a very slight seaward dip. As in all succeeding units in this sequence, there are occasional low angle reactivation surfaces and sets are disposed in wedges and lenses, the scale being too large to allow estimation in this exposure of the overall geometry. Bioturbation is low. The next bed [3.18–3.20] is a heavily disrupted clay lamina set, with fine flint debris. There are small open cone forms, with upward-divergent clay streaks, suggesting escape structures.

The next bed [3.20–3.33] consists of coarser medium sand, passing upwards to finer sand. Relatively low angle cross-lamination is apparent throughout most of the bed, with dips to both landward and shoreward, without regular alternation; at the very top, there is an interval of wave ripple cross-lamination with shoreward-dipping foresets and off-shoots tending to climb. Bioturbation is very low. The final bed in this sequence [3.33–3.63] is a slightly muddy fine to medium sand, with a few discontinuous mud ripple forms; the sands show low angle laminations. Cleaner sand wedges, with seaward-dipping cross-bedding and muddy bases with some shingle, tongue in from a shoreward direction. Bioturbation is very low.

The difficulty in placing the boundary between Cycles 1 and 2 in this exposure has already been noted. The earliest deposits apparently referable to Cycle 2 show similarities with the cyclothem units earlier in the GTP 26 sequence. The later (Cycle 2) cyclothem has beds each with an apparently coarse-tail, reverse graded upper portion, becoming very coarse towards the top; the cf *Monocraterion* forms in these beds are probably a mixture of true fugichnia and water-escape structures. The theme of recurrent storm events is therefore continued but conditions here are extreme and close to those in turbidity currents. It is impossible to determine whether the climbing ripple intervals (indicative of rapid but more 'structured' sedimentation) pre-date or post-date a more chaotic 'dumping' event, but they are nevertheless probably associated closely in time with a waxing or waning storm. The traces of laminated zones represent the calmer episodes between storms; it is noteworthy that there is considerable horizontal development of ichnofossils, indicating relatively deep water, probably on the lower shoreface. Above the [3.06] level (Fig 48), the influence of storm events decreases and the sequence is mostly composed of planar sets interrupted by low angle reactivation surfaces. In at least one instance, wave ripples appear, associated with signs of relatively rapid sedimentation. Both clay and coarser elements intrude into the sequence from the landward direction in places, probably corresponding to less energetic storm events. What little bioturbation there is seems to be associated with the sediment of these storm events, taking place in each subsequent calmer phase.

SEP 3 (which has not been recorded in detail) is the exposure furthest from the land (Fig 38). The sequence seems to be largely unbioturbated, laminated fine sands and silts, although there are individual small-scale, dominantly vertical traces. It is not immediately obvious why these deeper water (uppermost transition zone) deposits should have so few signs of biological activity (a trend already seen in GTP 26), although the cause must lie in some combination of water chemistry, current conditions and sedimentation/erosion balance which will not become clear until more detailed study is undertaken. However, one may speculate that nutrient availability for bottom and sediment

feeders was low, since most landward-derived clays/muds seem to have deposited out (probably by flocculation in strongly saline conditions) before reaching this location.

Regression

The full sequence of in-shore Cycle 2 deposits in GTP 25 has already been described above. There are no surviving traces of obvious regression.

In the south of GTP 13 1 (Fig 45a), there is a unit [2.55–2.65] of strongly calcareous coarse silt, showing a series of bed-forms. The lowest interval is generally bioturbated but there are many small cut-and-fill structures with mud-draped foresets dipping mostly seawards. The middle of the unit shows both continuous and discontinuous trains of form-discordant, slightly asymmetrical ripple sets, the asymmetry alternating irregularly between landwards and seawards in successively stacked sets where present. There are also non-sinusoidal ripples, due to irregular erosion/deposition interaction (possibly longitudinal combined current/wave conditions), with internal bundles of strongly mud-draped laminae dipping irregularly both landwards and seawards, and some foreset off-shoots and mud laminae which pass continuously across ripple troughs. The ripple index is only 2–3 in better expressed forms in this middle interval. There is usually a rather structureless zone at the top of the unit. Clear bioturbation forms are mostly developed from the upper surface, and include vertical tubes and large, markedly divergent simple U-tubes (cf *Arenicolites*).

In GTP 13 4 (Fig 45b), there is a unit [0.76–0.86] of coarse silt, with isolated or grouped ripple cross-bedding features increasing upwards. There are dominantly seaward-dipping mud-draped foresets with strong off-shoots, the ripple crests often being truncated. There are also trains of strongly form-discordant symmetrical ripple-forms, with reversing seaward-landward internal lamina sets and mud-drapes thickening into intervening troughs; ripple crests are shore-parallel.

The exposures of final Cycle 2 sediments in GTP 13 show very strong wave and current influence and intrusive bioturbation forms probably developed under slightly later, even more energetic conditions. Greyer colours might suggest greater input of organic matter. These sediments represent conditions very close to (probably just above) mean low water mark (Whittaker Chapter 3.2).

In GTP 10 (Fig 49b), there is a unit [2.65–2.92] of fine sand, mud and a little coarse sand with fine pebbles; the fine sand seems to represent the 'normal' sediment, with intrusive coarser intervals capped by mud. Bioturbation is very strong, including pouched forms with markedly deflected bases (dominantly seawards), small cf *Monocraterion* developed through muddier intervals, and irregular tubes and chambers with carbonate-cemented walls. There is an iron oxide build-up

associated with most trace fossils. This unit is not certainly regressive, although the much stronger input of coarser elements might suggest the closer approach of the beach-line (or a series of major storms); the trace fossils seem to represent a compromise between energetic and calmer conditions. After a persistent erosive ripple-form contact, there is a thin bed [2.92–2.95] of fine sand with mud-drapes, once possibly cross-laminated but now rather contorted. The significance of this bed is unclear.

In GTP 26 (Fig 48), there is a bed [3.63–3.66] of coarse fine to fine medium sand. Cross-bedding is clear and undisturbed but rather variable in orientation, giving a generally 'bundled' appearance, landward dips being dominant, with secondary seaward dips and one instance of a dip to the east-north-east. The next bed [3.66–3.69] is composed of muddy fine to medium sand; the low angle bedding dips variously towards the north to almost the east, suggesting onshore and longshore encroachment. This bed thickens rapidly shorewards, possibly representing the beginning of a bar. The last bed in the Cycle 2 sediments [3.69–3.82] is a calcareous coarse fine to fine medium sand, becoming slightly muddy towards the top. The bed starts with sets of 'bundled' bedding which appear to represent sinuous trough-forms, dominant landward dip shifting upwards to dominant seaward dip through the sequence; there are some zones with carbonate nodules, continuous cementation appearing seaward of the main exposure. There is then a mud ripple-form, with shingle (including very small chalk pellets), small edge-rounded flint particles and rare true pebbles appearing landwards, followed by a cut-and-fill structure with seaward-dipping cross-laminae. The upper interval is composed of large scale concave-up planar bedding sets, dipping mostly seawards. There are moderately strong, mostly formless bioturbation traces throughout the bed but especially in the muddier top interval. This last bed seems to be composed dominantly of current megaripple cross-bedding, developed close to the shore-face/beach-face transition.

The very top of the Cycle 2 sequence in SEP 3 (Fig 38) shows a thin interval in which small cf *Monocraterion* forms appear in lateral sets, indicating more rapid sedimentation perhaps induced by the penetration of storm influence.

Marine Cycle 3

Transgression

The main beach GTP 25

At the most landward exposure of GTP 25 1 (Figs 42a–b), the talus cone morphology, noted above, in the Cycle 2 chalk debris is continued in the Cycle 3 deposits. Up to 2.5m of poorly sorted, very chalky material is disposed in well bedded alternations

between angular flint stone-lines and stony, 'earthy' material dominated by fine chalk debris; Cretaceous fossils and small particles of banded, fissile iron-rich rock (possibly weathered chert) are common. The same crest line is maintained as in the earlier talus, with bedding dipping at even higher angles; this bedding is almost planar, as compared with the slightly concave-up form in the earlier talus. This material is a totally terrestrial deposit, derived from essentially local stocks.

Lower on the slopes of the talus cone, chatter-marked flint pebbles and cobbles begin to appear in the stone lines, first as individual particles and, lower still, as the dominant element. Concomitantly, the finer chalky matrix becomes less abundant. There is therefore a smooth and complete facies shift from terrestrial talus to storm beach. The highest observed beach pebbles lie at an altitude of 44.5m OD, stratigraphically at the base of the unit. In later beds, the interstratified boundary between talus and beach migrates slightly seawards and downwards (broadly a 'regressive' morphology, the beach offlapping and the talus prograding).

The beach material continues seawards (GTP 25 2–4, Fig 42a) as rather diffuse sets of fining-upwards pebbles. In GTP 25 4 (Fig 42i), the [0.6–0.94] interval comprises three or more fining-upward cycles, from 50mm pebbles to shingle or coarse sand, a deposit which is certainly representative of the normal highest swash zone. After a clear angular unconformity dipping seawards, a more massive bed follows [0.94–1.22], with clast-supported flint pebbles and a largely intrusive fine matrix (see below, Unit 4b). This disposition continues in GTP 25 5, with the unconformity cutting downwards (Fig 42c), so that the [2.02–2.27] interval (pebbles with intrusive matrix) lies immediately above the outliers of chalk from the regressive part of Cycle 2 (corresponding to the tail of the chalk talus). Traces of the top of the pebbles with intrusive matrix appear at the base [0–0.23] of the sequence in GTP 25 8 (Fig 42k). In GTP 25 6 an irregularly bedded muddy unit [0.13–0.33], with isolated pebbles, coarse to medium sand and small molluscan fragments nearer the base, overlies an irregular unconformity developed in the Cycle 2 storm beach. In GTP 25 7, there is a similar deposit [1.04–1.24], with lenses of fine and coarse sand with chalk pellets, passing up into contorted laminae of mud and medium to coarse sand.

In GTP 25 E to B (seawards) (Fig 42a), the erosive (unconformable) base of the Cycle 3 sequence cuts into the underlying fine sediments of Cycle 2, with only individual floating coarse sand particles and granules (if that) to mark the transgression.

The transgression in GTP 25 is therefore constantly indicated by an unconformity, dipping quite strongly seawards, above which lie the tidal deposits of Cycle 3 (dipping much less markedly seawards) in an overlapping (onlapping) sequence.

Seaward exposures

In GTP 13 1 (Fig 45a), the first unit in Cycle 3 [2.65–2.74] overlies a planar unconformity, dipping seawards and quickly resulting in the loss of the highest Cycle 2 sediments. This unit is composed of relatively angular 0.1–0.4m blocks of chalk, with only those blocks protruding upwards into overlying units showing signs of significant rounding (Figs 20, 44, 45a, 54, 57). Other coarse elements include totally unworn flint nodules (fresh from the chalk) and rare chattermarked pebbles. The strongly calcareous matrix, which provides at least partial support, consists of chalk pellets in muddy fine sand with a little coarse flint sand and rare lenses of angular flint granules. There are often complete barnacles, rare terrestrial microvertebrates and rare flint artefacts. The top of this unit has been reworked, with trails of relatively well sorted sandy material dragged off seawards into overlying deposits. Localised lenses of fine sediment sometimes occupy the troughs between higher chalk blocks, first laminated fine to medium sand with mud partings thickening upwards to laminae, and then a muddy zone with small, isolated and sharply differentiated undulating fine sand linsen. The next more persistent bed [2.74–2.78] comprises strongly calcareous, contorted but laminated fine sand and mud-drapes, with patches of muddy chalk pellets and flint coarse sand/fine gravel derived from the unit below; tiny lenses of better sorted sand sometimes overlie more chalky material. There are traces of ostracods. The next bed [2.78–2.85] comprises strongly calcareous, clayey sediment, apparently originally deposited as thin coarser fine sand linsen set between undulating clay laminae. Bioturbation, mostly originating from the top of this bed, is strong, with many sand-cored tubes and pouched forms, some of the latter slightly oblique to the bedding. The next unit [2.85–2.90] is a cross-laminated climbing ripple interval, showing frequent alternation between landward and seaward dip of foresets; ripple-forms are symmetrical but quite low (ripple index 6.0–6.5). Textures are quite varied, with a typical microsequence consisting of a clean fine sand set at the base, medium sand lenses, an irregular muddy to clayey lamina-set, a major fine sand set, and discontinuous muddy sets with strong off-shoots; strong mud-drapes usually mark each dip reversal, with weakening drapes on succeeding foresets. Cleaner sand intervals contain rare molluscan fragments. Bioturbation is almost absent, there being only a few very small deflected pouched forms developed from mud-drapes. The next unit [2.9–2.94] comprises very strongly calcareous, thick undulating clay lenses and laminae, with an only partially concordant lower boundary with the ripple-forms in the unit below. Isolated fine sand ripple-forms occur within the clay, showing landward/ seaward alternation between dominant foreset dips in successive (separated) ripple-form trains; within any single ripple-form, dip also reverses

in the top few foresets. Bioturbation is moderate and formless. The next unit [2.94–2.98] consists of strongly calcareous fine sand sets, with slightly coarser sand and flint debris at the base of each set and rare mud-drapes at the top. Erosive sets consist of relatively low angle concave-up laminae (shallow trough cross-bedding), although there are more complex cross-laminated ripple-forms near the top, with alternating foreset dips and ripple widths of no more than 20mm. Weak bioturbation is restricted to a few small pouched forms. The next unit [2.98–3.01] consists of very strongly calcareous muddy fine sand, with clay flasers, conformable to the underlying unit; bioturbation is strong and formless. The next unit [3.01–3.04] consists of very strongly calcareous fine sand. After a slightly erosive lower boundary, there are irregular intervals of almost symmetrical relatively low, wave ripple cross-lamination with very strong off-shoots and even over-shoots; there is reversal of dips in each set, and foresets and especially reversal surfaces show strong mud-drapes. Bioturbation is weak. The next unit [3.04–3.06] consists of very strongly calcareous mud/clay laminae and thin fine sand linsen, the latter becoming more isolated upwards; there is generally wavy bedding, concordant with the unit below, the sand set in ripple-forms with the mud thinning over crests and thickening in troughs. Bioturbation is weak. The final unit in this sequence [3.06–3.12] consists of very calcareous finest sand, with rare and discontinuous mud partings and slightly muddier intervals near the base and top; the lower boundary is erosive. The bedding shows weak linsen development at the base and very low angle erosive lamina-sets in the main interval; laminae dip mostly seawards but there are also minor intervals with high angle foreset dips to landward. Bioturbation is slightly stronger than below, with small elongate pouched forms. There are rare tiny molluscan fragments and extremely fragile ostracods. High-angle bidirectional microfaulting (the two superimposed sets dipping symmetrically landwards and seawards) appears to be a post-depositional response to vertical compaction coupled with extension down-slope.

The lowest unit in this sequence, GTP 13 1, is an unusual coarse deposit which is certainly not a beach; the main points of interest are (a) an erosive base, (b) relatively unweathered terrestrial debris (Fig 57), intimately mixed with rarer marine elements, and (c) massive structure and very poor sorting with at least partial matrix support. These characteristics suggest a fast-moving subaqueous debris flow, triggered when a talus deposit at the base of the coastal cliffs was destabilised. Although this could well have happened either as hydraulic (and possibly fine sediment) support was withdrawn from the talus or as rising waves reached the talus again (in either case, possibly during a storm event), this unit does not itself prove a cusp between regression and transgression (it is the evidence of shallowing water in the unit immediately below which

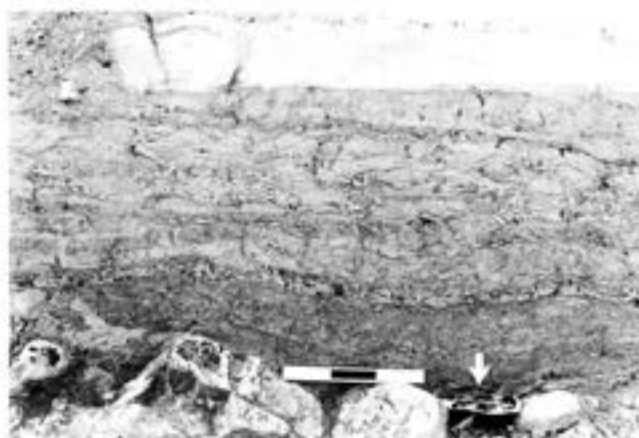


Fig 57 Fine-grained sediments of Marine Cycle 3 above the chalk raft in GTP 13; note the handaxe thinning flake (arrow) on top of the raft; scale unit 50mm

allows this inference). The thin and discontinuous beds immediately above the chalky flow represent the resorting necessary to re-establish a normal, smooth bed-form over what would originally have been a 'lumpy' surface. The remainder of this sequence is very complex, with many bedding styles crammed into an interval of only 260mm; these deposits appear to show much shallower water than could be accounted for simply by the progradation of the underlying debris flow, especially since the latter probably resulted in a net removal of sediment (from underlying beds) rather than a build-up. The main themes common in these deposits are (a) alternating wave and/or tidal current bedding, (b) composite bedding (fine sand and mud/clay bimodality), (c) common signs of both rapid sedimentation and reworking (both planar and ripple-form), and (d) usually weak bioturbation. Although no true beach-face sediments survive, these deposits would seem to represent a rapidly transgressive and sediment-rich lower intertidal facies, entailing a general immaturity of sequence development and an overlapping (onlapping) geometry above the debris flow (or even a minor overstep, since the restricted lenses above the main debris flow may show a disposition younging seawards — i.e. the direction in which the sediments become younger, showing their sequence of original deposition). Although bioturbation is usually weak in this sequence, there are also simple iron-stained, very long vertical tube segments (with diameters from 'hairline' to c 5mm), which, in most cases, are probably the deepest part of a tiered system developed from overlying beds.

Some 14m to the west-south-west of the main GTP 13 sequence, there was an additional exposure of Cycle 2 and 3 deposits. The debris flow at the base of Cycle 3 was present, but the chalk elements have almost totally disappeared, leaving clayey 'ghosts' rich in iron and manganese oxides, with the occasional tiny unsound chalk core to originally larger blocks. However, 0.2–0.25m lower into the Cycle 2 sequence, there is another interval with large chalk blocks (up to 0.7m diameter), 0.1–0.15m diameter round flint

pebbles and, exceptionally, a cobble of 0.25m diameter (one of the largest flint cobbles yet observed in the marine deposits at Boxgrove), together with a very small amount of fine gravel and coarse sand, all distributed in a very patchy and discontinuous manner. Such coarse material could only reach this area by debris flow and it is assumed that its original fine matrix was washed away, leaving only the coarse lag. This event possibly correlates with the pebbles (at point [2.25]) or the rip-up mud clasts (at point [2.32]) in the GTP 13 1 Cycle 2 sequence (see above) (Fig 45a). In any case, 'catastrophic' input of coarse debris from the cliffs and talus along the coast clearly began before the event at the base of Cycle 3, perhaps favouring the 'regressive' trigger alternative, noted above, and inviting a comparison with the chalky talus in GTP 25 which post-dates the Cycle 2 storm beach.

In GTP 10 (Fig 49b), there is a bed [2.95–2.99] of relatively clean fine sand; the sand has planar laminations and the base shows a very slight angular unconformity with respect to underlying deposits (the erosion plane apparently sloping very gently seawards). There is then a set [2.99–3.02] of strong but disrupted clay laminae, containing immature bivalves (Mytilidae). These sediments are not particularly diagnostic but would appear to represent a general shore-face environment; the magnitude of any non-sequence at the base is unclear.

In GTP 26 (Fig 48), there is a bed [3.82–3.91] of calcareous fine to medium sand, interrupted by a few discordant muddy ripple-forms; the sand is set in gently seaward-dipping laminations, whilst the ripple-forms seem to have translated shorewards. Ostracods, immature bivalves (Mytilidae) and small shell fragments are present. Again, this sediment is not itself obviously transgressive but, rather, marks the beginning of a sedimentary style to be continued in the overlying sequence.

The beginning of Cycle 3 in SEP 3 (at 38.8m OD) is marked, first by a shift from cf *Monocraterion* ichnofossils to more typical *Skolithos* facies, and then (some 0.14m higher) by the first ripple-form clay laminae.

Deeper water conditions

In-shore sequences

In GTP 25 6 (Fig 42i), the first bed in this sequence [0.33–0.4] consists of fine sand laminae with increasing muddy laminae upwards; there are small molluscan fragments. The next bed [0.4–0.53] comprises wavy sets of mud and clay laminae with minor fine sand and silt lenses; molluscan fragments are present. The last unit in the sequence [0.53–0.71] consists of sets of laminated fine sand and silt, with wavy and even contorted clay laminae becoming weaker upwards; molluscan fragments are still present. In GTP 25 7 (Fig 42j), there is a lower unit [1.24–1.44] of very muddy, wavy laminated sediment with rare chalk fragments (Fig 58).



Fig 58 Q2 GTP 25; the Slindon Sands and Silts between the raised beach gravels and the chalk rubble flows, showing chalk inclusions

There is then a bed [1.44–1.55] comprising a fine sand with wavy clay lamina-sets; there is a gross dip in any given lamination of $c 3^\circ$ to the south-west.

In GTP 25 E (Fig 42d), only a single unit [2.01–2.41] is relevant (the higher units surviving to landward having been eroded here). The unit consists of muddy fine sand and silt, with isolated coarse sand particles and traces of a wavy finest coarse sand lamina near the base, and traces of a ripple-form mud lamina nearer the top. Formless bioturbation is extremely strong, giving mottling in both colour and texture throughout the unit. Imprinted onto this background are relatively common long, simple, tubes (both vertical and horizontal elements but with no junctions observed) highlighted by iron oxides; some of these forms may be endichnial but the majority probably represent the lowest facies of a deep tiered system developed from overlying beds. In GTP 25 D (Fig 42e), there is a unit [2.53–2.97] of muddy silt and fine sand, very heavy formless bioturbation leaving only diffuse traces of ripple-form structure in a few places. The overprinted simple tubes are again present. In the GTP 25 C exposure (Fig 42c), there is a similar unit [3.74–4.22] of muddy silt and fine sand, with heavily disturbed ripple-form clay laminae near the base. In GTP 25 B (Fig 42g), one may differentiate an early bed [2.83–2.89] of muddy silt to fine sand, with thick mud-drapes and strong symmetrical ripple-forms with

shore-parallel strike; bioturbation is moderately strong but has not totally obscured the bedding style. Above this is a thick bed [2.89–3.36] of the same muddy silt/fine sand texture, with disturbed traces of minor mud-drapes; formless background bioturbation is very strong and there is again overprinting by simple long tubes, their sandier fills often encouraging slight cementation of the walls by iron oxides.

These GTP 25 exposures are not amenable to a full explanation. On the one hand, the ripple-forms and textural bimodality (silts and fine sands with clays and muds) would suggest an intertidal sand flat environment (lower foreshore). On the other hand, even setting aside the strongly dipping erosional contact at the base of Cycle 3, there is still a persistent and significant seaward (south-westerly) dip in the contacts between units. It is stressed that the deposits show at least local overlap (onlap) and an interpretation as longitudinal (epsilon) cross-bedding, due to seaward migration of tidal creeks, would not seem to be readily available in this in-shore material.

Off-shore sequences

In GTP 13 1 (Fig 45a) the lower of two relevant sequences begins with a unit [3.12–3.15] of very strongly calcareous, interbedded clay and (thinner) fine sand laminae, with tiny chalk pellets (coarse sand grade) and isolated flint sand grains set in the clay

laminae, and rare small shell fragments in the sands; the original wavy bedding has been strongly disrupted by formless bioturbation. The next unit [3.15–3.19] is a relatively clean, very strongly calcareous fine sand; the sand is laminated but the bedding is obscure due to increasing high-angle bidirectional microfaulting and bioturbation. Bioturbation forms include relatively long mud-lined tubes/pouches with increasingly horizontal deflection of bases. There are also simple iron-stained, very long vertical tube segments (with diameters from 'hairline' to c 5mm), with no clear point of origin (and therefore possibly, at least in part, penetrating from above in a tiered system); some of these forms may be of plant, rather than animal, origin. The next very strongly calcareous unit [3.19–3.22] shows a tripartite muddy silt–sand–muddy silt division; microfaulting and bioturbation are very strong. Bioturbation forms include horizontally deflected pouches with basal lateral and sometimes also underlying spreites; this description probably only refers to restricted planes cut through complex three-dimensional forms, possibly either *Rhizocorallium* or *Thalassinoides*. The next very strongly calcareous interval [3.22–3.26] consists of coarse silt to fine sand, capped by a very thin mud unit; all levels were probably originally laminated but the interval has been disrupted by extreme bioturbation and microfaulting. Trace fossils do not usually have thick mud linings and include cf *Rhizocorallium/Thalassinoides* (as in the preceding unit), classic *Thalassinoides* and twisted U-tubes with protrusive spreites (cf '*Glossifungites*'); iron-stained tubes are common and seem to originate from above, sometimes cutting through the native ichnofacies. Ostracods, small Mytilidae and small fragments of Pectinidae are present. The next unit [3.26–3.31] is a very strongly calcareous, dominantly coarse silt bed, again capped by muddy laminae, and similar in all respects to the underlying interval; the same suite of native trace fossils are present but penetration from above by long iron-stained tubes is now extreme. Ostracods, small Mytilidae, small fragments of Pectinidae and possible Myidae fragments are present. The next unit [3.31–3.33] consists of thin (c 8mm) low-angle sets of cross-laminated, very strongly calcareous silt, possibly showing reversing foreset dips between sets; microfaulting is present and bioturbation from above is moderately strong. The final very strongly calcareous unit in this lower sequence [3.33–3.35] comprises persistent brown (purer) clay laminae interstratified with coarse silt; the silts may originally have been set in ripple-forms, although this is no longer clear due to strong bioturbation from above.

The colours of the GTP 13 1 Cycle 3 sediments are of interest. The dominant colours in the interval [2.78–3.35] (thus, including the transgressive sequence described earlier), seen in less bioturbated and slightly coarser (mud-free) units, are a variety of relatively strong yellows (1–2.5Y 7/7–4 in Munsell notation); slightly redder colours occur near clay laminae, and

iron-staining of sandier trace fills gives ginger streaks. Purer clays give pink or pale brown colours on fresh cuts, whilst more mixed muds give greyer browns. Strong background bioturbation tends to produce mottled or speckled reds, yellows and grey/browns. This colour suite begins to change in the uppermost [3.31–3.35] interval, the chroma fading through pale yellow to light grey (2.5Y 7/2–3). The [2.78–3.35] interval may be referred to informally as the 'Yellow Interval'. The succeeding [3.35–3.67] interval (to be described below) has a more consistently light grey (2.5Y 7/2) base colour, with cherry red trace fills; this upper sequence may be referred to informally as the 'Grey Interval'. This colour shift probably has environmental significance, with oxidising conditions below, and more reducing conditions (probably due to increased input of organic matter) above.

The upper sequence (Grey Interval) in GTP 13 1 begins with a bed [3.35–3.52] of very strongly calcareous and even patchily cemented silt, with fine horizontal lamination; high-angle bidirectional microfaulting is weaker than in the underlying interval. Bioturbation is very strong but mostly composed of recognisable structural forms. The most common ichnofossils are long, vertical but sinuous tubes, with a clean fine sand core strongly stained with iron oxides, varying in diameter along their lengths from 0.5mm to 2.0mm; some instances appear to branch upwards in their higher levels and downwards in their lower levels, some tubes appear 'anchored' to small flint pebbles, some vertical sections appear to be linked by hair-line horizontal sections, and top or bottoms of a tube may end in c 4–5mm diameter spherical 'pods'. It seems likely that these tubes are the burrows of Polychaeta. Other forms include extremely fine undulating horizontal tubes, and pouched and U-tube forms with spreites (cf *Rhizocorallium/Thalassinoides* and *Diplocraterion*), normally lacking mud linings and not markedly stained by mineral salts; there are also some thin unbranched tubes which may be of plant origin. Ostracods and small molluscan fragments are present. The next bed [3.52–3.54] is a short interval with stronger mud laminae between silt laminae, but otherwise similar to the rest of this sequence. The last bed in the sequence [3.54–3.67] is almost identical to the first bed, with a zone of exceedingly strongly calcareous silt at the top. Many of the long vertical tubes, which may continue downwards as far as the [3.20] point or even further, seem to originate from the upper surface of this bed.

In GTP 13, relatively wide (lateral) exposures are available, including the main trench and a secondary trench set at right angles (Fig 4). Consequently, rather more can be deduced concerning the large-scale geometry of these earlier Cycle 3 units than is the case in older material. The Yellow Interval thickens appreciably to seaward, with a dropping base (above the chalky debris flow). Each sandier subunit starts with coarser medium sand landwards and passes into fine sand by c -10m seawards; ripple-form clay laminae begin as the

finest films within sand units, and develop and split one from another seawards. There is thus both a true onlap of main subunits and an expansion (thickening and subdivision) seawards. Although the distinction between the Yellow and Grey Intervals is maintained, the top of the Yellow Interval itself takes on greyer colours seawards, whilst microfaulting decreases. Within the Yellow Interval in GTP 13, the large-scale dip of main bedding planes is $c. 2.5^\circ$ along bearing 131° ; this is almost exactly coast-parallel and at right angles to the almost perfectly seaward dips in GTP 25. It should also be noted that, even with these relatively wide exposures, no instances of curving (concave-up) fault planes are present. As in the in-shore exposures, longitudinal (epsilon) cross-bedding, due to seaward migration of tidal creeks, is not a valid explanation.

In GTP 10 (Figs 49b–51), the first bed in the sequence [3.02–3.21] is a very slightly muddy fine sand. Bioturbation is strong, with considerable horizontal development of trace fossils, including randomly deflected pouches; there are also muddy divergent U-tubes (*Arenicolites*). Immature mollusca (*Mytilidae*) are common. The next bed [3.21–3.22] is a disrupted ripple-form mud lamina-set, with fine sand lenses containing immature *Mytilidae*. The bed above this [3.22–3.28] is very similar to the first unit in the sequence, with both vertical and horizontal development of traces, mostly originating from the upper surface. The next bed [3.28–3.35] is a clean medium sand, with some mud-draped foresets and reactivation surfaces often with more continuous mud laminae; sand set boundaries dip gently to the south-east, while internal cross-lamination dips in the opposing direction, possibly representing climbing ripples in drift. Bioturbation is very weak. The overlying bed [3.35–3.38] comprises highly disturbed and contorted mud and clay laminae, with immature *Mytilidae*. The next bed [3.38–3.45] is a slightly muddy fine sand; bioturbation is strong but patches of cross-lamination survive, mostly reversing ripple-form sets with offshoots from mud-draped foresets. Immature *Mytilidae* are present. Above this [3.45–3.5] is a fine sand, with stacked bundles of cross-bedding, showing reversing dip, each erosional boundary being followed by weak ripple-form mud laminae. A similar bed follows [3.5–3.53], with strong ripple-form mud laminae above erosional planes, ripple troughs usually being subsequently filled by muddy sand before the next cross-laminated sand set. After a continuous planar discontinuity, the next bed [3.53–3.63] comprises a structureless fine sand with ripple-form mud laminae towards the top. Bioturbation is relatively strong, with vertical and deflected short tubes. Immature *Mytilidae* are present. The next bed [3.63–3.75] is similar but cross-laminae, with mostly seaward foreset dips, are still visible. Bioturbation is very strong and includes quite thick (up to 4mm) tubes, together with simple tubes which may be of plant origin. The next bed [3.75–3.79] is a calcareous muddy fine sand, with a

ripple-form top surface; immature *Mytilidae* are present. The succeeding bed [3.79–3.87] is a clean fine sand, becoming muddier upwards and capped by 2–4 ripple-form mud laminae. Formless bioturbation is very strong. The last bed in this sequence [3.87–4.0] comprises laminated fine sand with a minor wavy mud lamina near the base. Formless bioturbation continues to be very strong. Throughout the [3.02–4.0] interval, muddier and clayier units may be locally cemented by carbonates, cementation increasing in thickness below or above muddy zones as one moves seaward; no instances of mechanically eroded upper surfaces of cemented zones have been observed. Tiny manganese-rich flecks are common in this sequence (unlike the overlying deposits), probably due to replacement of shell debris. Colours are similar to those of the Yellow Interval described in GTP 13.

The uppermost bed of the deeper water Cycle 3 deposits is exposed [0–0.9] in GTP 5 (Figs 4, 59–60c) as clean fine sand, with rare and very thin wavy mud laminae, which thicken and multiply shorewards. There is patchy cementation around or

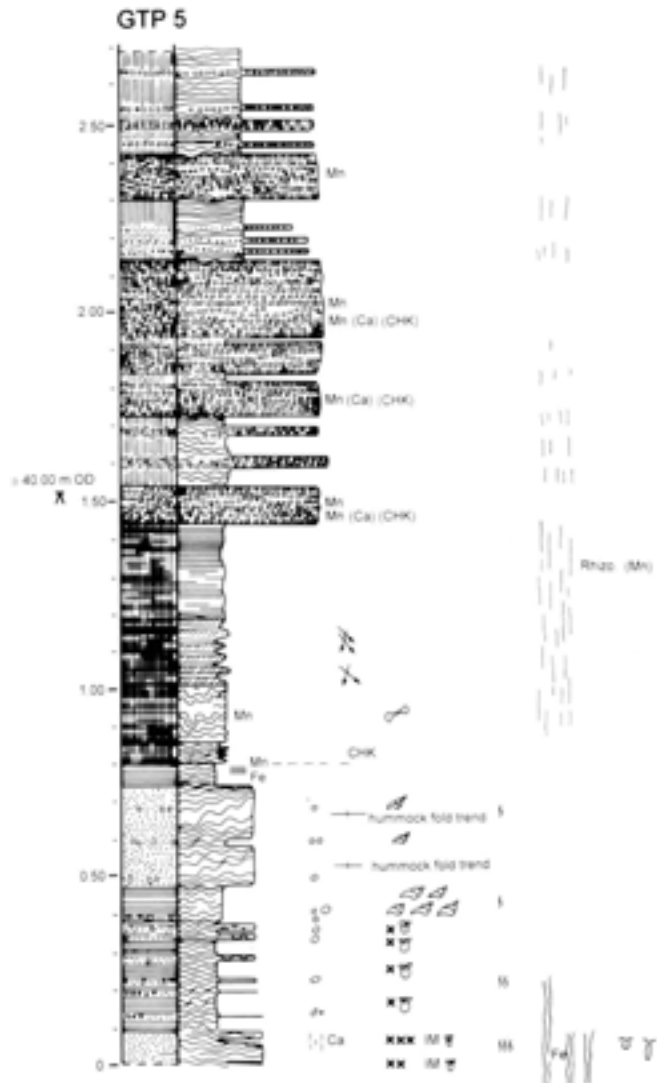


Fig 59 Detailed sedimentary log through the sediments at Q2 GTP 5

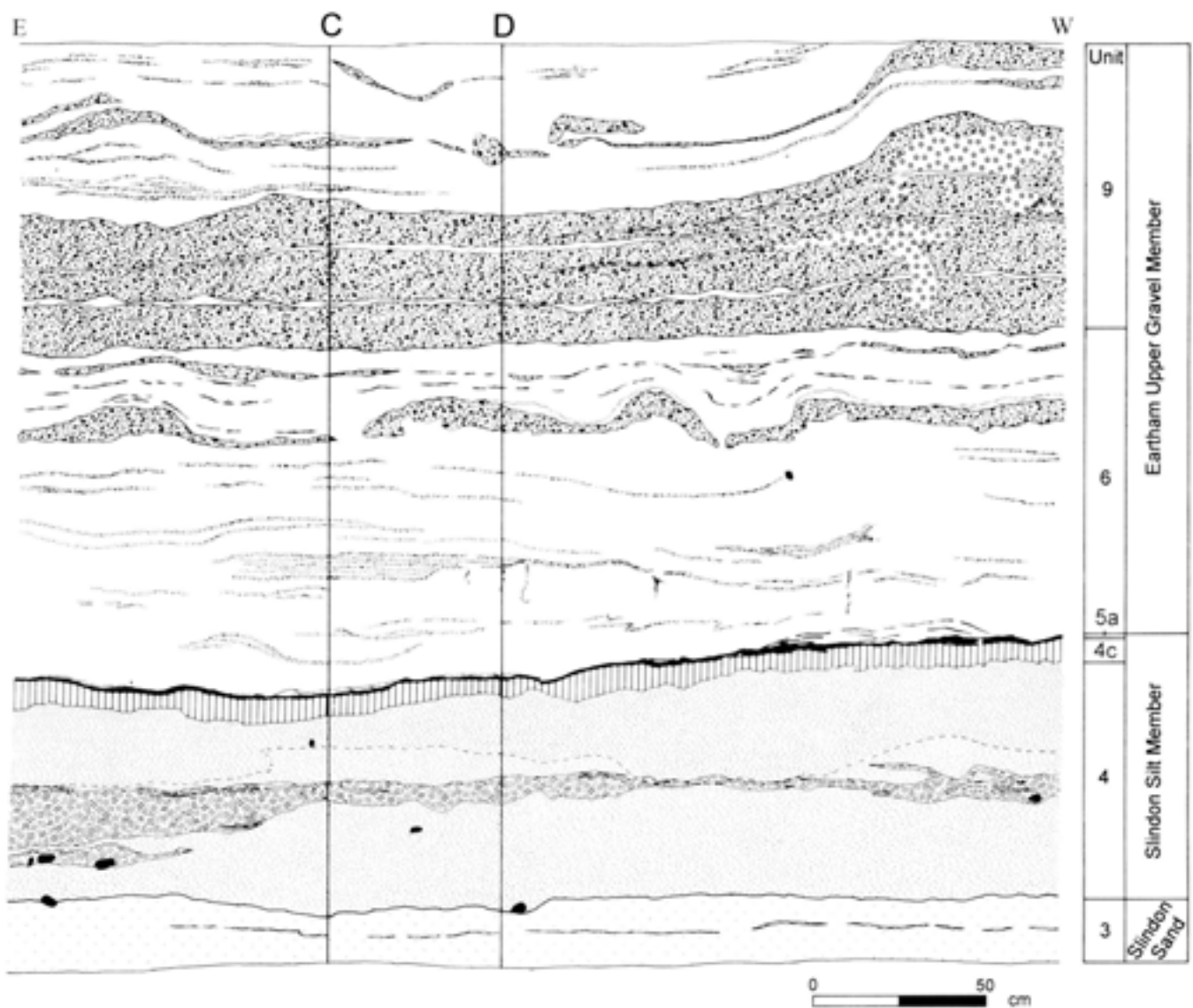


Fig 60a Section through the sediments at Q2 GTP 5

between mud laminae. Bioturbation is strong, with long vertical tubes stained by iron oxides and many smaller unstained forms. Very small bivalve fragments and immature Mytilidae are common. Colours are grey to greyish yellow.

In Q2/A (Figs 4, 61), the exposure starts with a bed [0–0.18] of clean coarse silt and fine sand, with traces of horizontal fine lamination nearer the top. Formless bioturbation decreases upwards. The last bed in this sequence [0.18–0.43] comprises, after a basal muddy zone, a coarse silt and fine sand, becoming muddier and more clearly laminated upwards. Bioturbation is strong, mostly formless but with some stained vertical tubes. Small shell fragments are seen in all states as far as complete manganese replacement. Colours in this Q2/A sequence are mostly pale yellow/brown.

In GTP 26 (Fig 48), the sequence begins with a bed [3.91–3.94] of mud with a few sand lenses and small flint fragments; the original bedding seems to have comprised ripple-form lamina-sets. Bioturbation is strong, with many short and thick pouched/tube forms.

After a disturbed boundary, the next bed [3.94–4.04] consists of fine to finest medium sand; bedding is mostly planar sets, with extremely low angle dip seawards. Bioturbation is moderate to moderately strong. The next bed [4.04–4.15] comprises clay laminae with thin sand units, mostly heavily bioturbated. Small curved tubes and pouches, mostly 2–4mm in diameter but rarely up to 10mm, are present and there is generally a significant amount of horizontal development. The next bed [4.15–4.17] is a ripple train, continuous over the several metres width of the exposure. The bed includes a basal laminated mud, a sand core (with mud-draped foresets upwards) and a top clay drape or lamination. The sand core comprises tiny sets of shoreward-translating climbing ripples (in troughs in the basal mud surface), followed by seaward-dipping sand cross-laminae, followed by minor sets of discordant shoreward- or seaward-dipping laminae. The ripple-form shows continuous, sinuous crests, with low asymmetry. The main bedding form is therefore dominantly composed of bidirectional, incomplete ripples.



The next bed [4.17–4.37] comprises fine sand with patches of fine medium sand, showing only obscure, low angle (possibly reversing) bedding traces near the top. Bioturbation is quite strong, especially in a muddier zone near the base which has small V-shaped and U-shaped (cf *Arenicolites*) traces. The succeeding bed [4.37–4.38] is a thick pair of bioturbated clayier mud ripple-form laminae. The bed above this [4.38–4.47] consists of laminated fine sand, a little coarser at the base; planar sets are obscure but seem to show dominantly seaward dips. Tubes and pouches penetrate the bed from its top surface and from just above. The next bed [4.47–4.50] consists of disturbed mud ripple-forms with intervening sand, showing broadly shore-parallel strike. The overlying bed [4.50–4.57] consists of two fining-upward cycles, from finest medium and coarsest fine sand to fine sand; structures are rather deformed but zones with both landward and seaward ripple cross-lamination are present, together with zones with larger scale planar bedding sets dipping seaward. There are cemented patches and bioturbation is weaker than in most underlying beds, consisting mostly of small tubes and pouches originating in the overlying bed.

This [3.91–4.57] interval in GTP 26 (and, indeed, even the first bed in the Cycle 3 deposits in this area) shows a persistent 'ideal' pattern of sedimentation, even though bioturbation may obscure most bedding over wide zones. The first event in an ideal cycle is the deposition of sand in planar sets, the bounding surfaces dipping gently seaward (south-westwards); within each set, very low concave-up bundles of climbing ripple cross-lamination translate rapidly shorewards. More rarely, thin zones of more clearly shoreward-dipping, higher angle cross-lamination develop. These sands are then eroded to give a ripple-form discordant to the main sand set; a few concordant shoreward-dipping foresets may be draped over the erosion form (incomplete ripples). The ripple-form shows very little asymmetry and a ripple index in the range 5–6; crest lines are sinuous in-phase. More rarely, the 'ripple-form' is irregular (stepped sides), showing the influence of some longitudinal erosion. Mud-drapes or more continuous mud laminae are then added, usually thicker in the troughs. Where mud is present only as fine partings, ripples may be more than an erosive form, with form-discordant internal structure composed of tiny sets of reversing cross-lamination. A phase of bioturbation follows, burrows often showing thin mud linings. The next ideal cycle starts with deposition of muddy sand in remaining troughs to re-establish a planar surface. This interval is very calcareous throughout, with many tiny shell fragments, immature Mytilidae and ostracods, the latter accounting for most of the coarser texture seen in some beds. Weak carbonate cementation may occur above some muddier zones.

Fig 60b (left) Detailed section through the deposits at Q2 GTP 5 (location of section is shown on Fig 60a)



Fig 60c Q2 GTP 5, looking south; a) Slindon Sands (Unit 3), b) Slindon Silts (Unit 4b), c) palaeosol (Unit 4c) and Unit 5a, d) laminated Brickearth Beds, e) Fan Gravel Beds; scale unit 0.5m

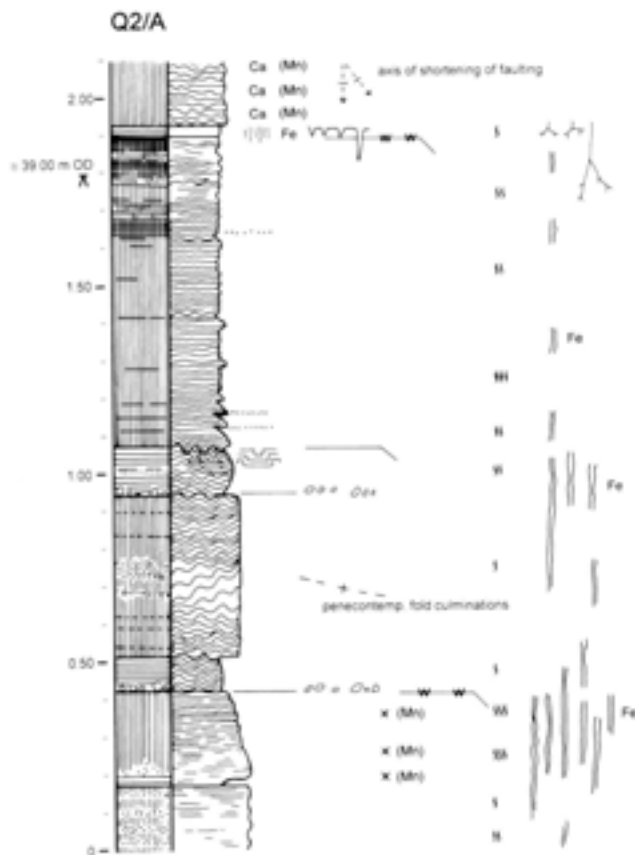


Fig 61 Detailed sedimentary log through the sediments at Q2 A

The GTP 26 sequence continues with a bed [4.57–4.58] comprising ripple-form mud laminae with sand partings. The next bed [4.58–4.72] consists of alternations between mud and finest sand; shell fragments and whole valves of Mytilidae are present. Recognisable bioturbation forms consist mostly of long iron-stained tubes originating from much higher in the sequence. The next bed [4.72–4.77] consists of silty mud laminae in ripple-form sets, separating in places to accommodate fine sand lenses. The succeeding bed [4.77–5.05] comprises a clean finest sand becoming slightly muddy towards the top; bioturbation obscures the bedding but wavy lamination seems to be present, sometimes picked out by discontinuous mud-drapes/partings, thickening in troughs. Bioturbation is mostly formless but there are common iron-stained tubes, with hairline horizontal extensions, originating from higher in the sequence. The next bed [5.05–5.12] is almost identical to the [4.58–4.72] unit; very small V-shaped traces are present. The final bed in this sequence [5.12–5.28] is a calcareous coarse silt/fine sand; structure is obscure, save for a few wavy mud-drapes nearer the base. Formless bioturbation seems to be strong, with mottling appearing near the top; recognisable forms consist of iron-stained tubes originating from higher deposits. There is discontinuous carbonate cementation in this bed, tending to form roughly columnal nodules.

Although there are the usual pale yellows and greys, the Cycle 3 deposits in GTP 26 do not show clear sequential colour differentiation but the overall 'styles' of the lower [3.90–4.57] and upper [4.57–5.28] intervals are very similar to those of the Yellow and Grey Intervals, respectively, in GTP 13.

The sequence in Q1/A (Fig 4) was not studied in any detail by the present author. Nevertheless, it may be noted that two or more thin (<50mm) persistent carbonate concretions occur in the uppermost surviving Unit 3 deposits in this area (Austin and Roberts Chapter 6.2, Fig 226; Roberts *et al* in prep).

In SEP 3 (Fig 38), the early Cycle 3 deposits (truncated by much later terrestrial deposits at a major unconformity, cf Units 10–11 below) show a similar fine sand and (very thin) ripple-form mud facies to shoreward exposures. Considerable horizontal development in trace fossils is first apparent (including classic *Thalassinoides*), with later vertical tube/pouch development, including some instances with clear 'spaghetti' castings at the base of burrows (Polychaeta).

The Cycle 3 deposits described in this section of the text constitute the uppermost series of the Slindon Sand Member at Boxgrove (Tables 8, 9a). Because of the often obscure bedding, coupled with relatively strong bioturbation, an interpretation has not been attempted for each exposure. Even combining the observations from all exposures, an interpretation is not simple. In full exposures, there is a general subdivision into a lower interval (the Yellow Interval in GTP 13, the [3.02–3.53] interval in GTP 10, the [3.90–4.57] interval in GTP 26) with clearer differentiation between sand/silt and muds/clays, and an upper interval (typified by the Grey Interval in GTP 13) with poorly sorted sediment showing fewer (surviving) mud/clay units. It should be stressed, however, that this facies shift is almost certainly time-transgressive.

The lower interval combines certain recurrent motifs. The bulk of sedimentation appears to have occurred in units of lamina-cosets, each coset dipping gently seawards; properly, therefore, these 'laminae' are pseudobeds. Each coset usually shows internal climbing ripple cross-lamination in strong shoreward drift (partial stoss-side preservation but very low angle of climb), with low asymmetry and rather peaked crests. In in-shore exposures, there is clear onlap, both of lamina-cosets and larger scale bedding units. Major bed boundaries (the more continuous erosion surfaces) also dip seawards, at a gentle but nevertheless significant angle (2°–3°). Both erosive ripple-forms and more complete ripples or ripple cross-bedding, showing between the main sand/silt units, are due to wave action; there is a range of energy conditions represented, from erosive ripple-forms (and a few possible longitudinal forms), to incomplete ripples, to ripples with reversing internal structure and off-shoots, usually in sets with continuous, slightly sinuous in-phase crests. Nowhere in these sequences are there significant occurrences of typical, strongly asymmetrical current ripples.

Although sands/silts are always dominant, muds/clays continually interrupt the sequences. In addition, there is a weak trend in each exposure for the lowermost units only to contain a little gritty material, and then for textures to fine irregularly up-sequence (usually fine sands to coarse silts). All beds are strongly calcareous and sometimes patchily cemented. Shell debris is common, almost always as fragments, very rarely as almost complete valves and never as undisturbed death assemblages. Ostracods are common and immature Mytilidae represent the pelagic phase. Formless bioturbation is common. More obvious ichnofossils usually show an increasing trend towards horizontal deflection/development and more continuous mud linings, even in simple tubes and pouched forms; in more complex forms, cf *Arenicolites* and cf *Diplocraterion* may give way to cf *Rhizocorallium*/ *Thalassinoides*, *Thalassinoides* and cf 'Glossifungites' towards the middle of the interval.

These characteristics almost certainly indicate a subtidal environment; intertidal sands (and even subtidal sands in an area of high tidal range) would show more horizontal bedding, stronger current forms, channel migration, intraformational deformation (stronger than the simple compaction faulting actually observed) and much lower bioturbation. Neither strong longshore currents nor concentrated linear currents (lack of scours, lags, high angle cross-bedding) are present. Sediment movement is on-shore and accretive, with minor erosional events usually being associated with wave action. The ratio between suspension load and bedload must be relatively high to allow climbing ripples to start to form. Although the co-occurrence of silts/sands and muds/clays must indicate energy fluctuation (probably of tidal origin), over the longer term the sequences are not interrupted by either very strong energy events or by long periods of calm. The bioturbation forms indicate reasonable stability but with frequent superficial erosion events, and their abundance would indicate an ample food supply. Again, fine shell debris is very common, and with the greatest taxonomic (family level) variation of any deposits observed by the present author at Boxgrove, but true shell beds (either concentrated lags or death assemblages) do not appear to be present (Whittaker Chapter 3.2, Bates and Preece Chapter 3.3). The overall impression is of the inexorable on-shore encroachment of a large scale, fine-sand body, with moderate energy conditions never truly interrupted by either slack water or turbulence. It is very tempting to suggest some form of off-shore bar (south of all observed exposures) which might have protected the deposits shorewards from storm events. It is also noteworthy that the main unit boundary dip direction is to the south-west on the western side of the site (GTP 26 in Quarry 1) but to the south-east on the eastern side (GTP 13 and GTP 10 in Quarry 2) (Fig 33). It may also be suggested that the sediments share certain characteristics with the most seaward facies of some deltas and estuaries.

There can certainly be no strong fluvial input, since seaward-oriented structures would be much more common, but it is not impossible that a minor embayment lies to the north (approximately between Quarries 1 and 2), perhaps with a small bayhead stream (Roberts Chapter 2.7).

The upper interval in these deposits is not greatly dissimilar, but discrete mud/clay wavy laminae are rarer and the sediments more muddy overall. Major bedding planes are closer to the horizontal. Carbonate cementation is stronger, with nodular forms appearing towards the top of the sequence, and even persistent tabular concretions in Q1/A. A more typical *Skolithos* ichnofacies is present, with polychaete burrows being the dominant form; there is a possibility that the rooting structures of simple (aquatic) plants are also present at times. The more reducing conditions seen in the Grey Interval of GTP 13 are not obvious everywhere but some other exposures do show a slight tendency in this direction. These characteristics perhaps suggest a shallowing, even more protected, water body. There is even a possibility that some surfaces may have been covered by vegetation and/or algae.

The Slindon Silts (Unit 4)

All the marine deposits so far described (Cycles 1 to 3) are referred to the formal lithostratigraphic unit, the Slindon Sand Member of the Slindon Formation. The next formal lithostratigraphic unit, the Slindon Silt Member (Fig 62), is referable to the last part of Marine Cycle 3 (an interpreted genetic designation). At Boxgrove, the Slindon Silts are represented by the deposits designated as Unit 4, itself divided into four main subunits (a-d) (Table 9a). Unit 4 is a roughly tabular (horizontal) body of sediment; despite the fact that there is a subtle and complex lateral facies distribution, the unit lacks strong (global) lateral facies shifts related primarily to distance from the land. Accordingly, each Unit 4 subunit will be described in turn below, although not all subunits are clearly differentiated in all exposures; the question of lateral facies will then be raised at the end of each subunit description.

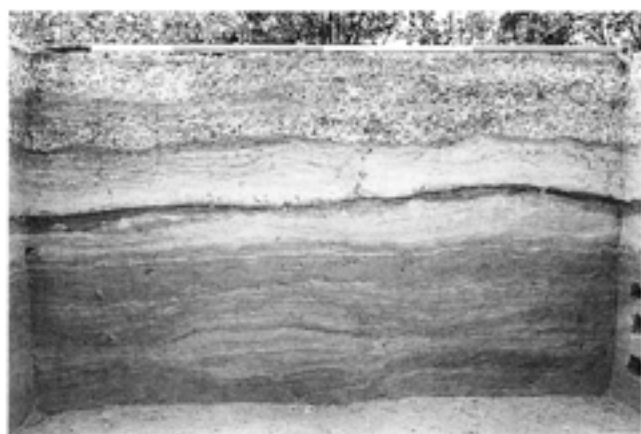


Fig 62 The Slindon Silts at GTP 10; scale unit 0.5m

Unit 4a

In GTP 25 8 (Fig 42k), the Slindon Silts begin with a thick mud band [0.23–0.25] draped over the underlying beach deposits. The next interval [0.25–0.43] consists of contorted laminated grey silts with frequent thin mud laminae. In GTP 25 6 (Fig 42l), Unit 4a again begins with a thick continuous clay band [0.71–0.72], which may well have been wavy but is now slightly contorted. Above this lies a bed [0.72–0.82] of very finely laminated grey fine sand/silt, with extremely thin mud partings and one more prominent mud band near the middle of the bed. In the basal 20mm, there are small molluscan fragments, and a tiny flint trimming flake (artefact) was also noted, but otherwise there are no coarse elements, not even coarser sand. Strong bioturbation is present throughout, rather formless but with a degree of surviving vertical development. In GTP 25 7 (Fig 42j), there is a bed [1.55–1.62] of grey silty fine sand, originally laminated and with an apparent dip of 3° along bearing 220°; this bed is heavily bioturbated.

In GTP 25 E (Fig 42d), there is a bed [2.41–2.49] of grey, muddy or clayey sediment, very heavily bioturbated, with quite strong Fe-staining on textural discontinuities; there are no coarse elements. The next interval [2.49–2.66] consists of relatively clean finest sand or coarse silt, with some major mud bands; there is common shell debris and bioturbation is strong, with lighter galleries over an Fe-stained ground. In GTP 25 D (Fig 42e), there is a strong bed [2.97–3.28] containing several subdivisions. First, there is muddy grey silt with quantities of shell and rather angular isolated flint debris (together forming a continuous band at the base), followed by purer silts with thicker ripple-form mud laminae, and then another particularly muddy band with floating coarse elements. From [3.08] upwards, the bed consists of more uniform grey silt with thin mud laminae. Bioturbation is quite strong at most levels, with Fe-stained tubes showing dominant vertical development, but with some horizontal examples. In GTP 25 C (Fig 42f), there is a similar strong bed [4.22–4.57], consisting of laminated silts and muds, with shell debris in the lower half becoming very common, with the addition of small chalk and flint fragments at the base. Colours are greyish nearer the top, increasingly ginger downwards, but with grey haloes around and within ichnofossils, some of which have Fe-stained boundaries; indeed, the varied colours would allow the establishment of a temporal sequence in individual ichnofossils. Bioturbation is relatively strong, with a particularly heavy interval towards the middle of the bed, where the ground mass is totally mottled. Recognisable forms in the bed as a whole are mostly vertical tubes. The last feature in the central interval (superimposed on the mottled ground) is a very complex three-dimensional gallery system, often with hair-line Fe-stained tubes running through galleries suggesting a dominant polychaete influence (but

note that such complex forms may be due to co-habitation by several species of animal); the upper boundary of the system is planar and thus erosional. In GTP 25 B (Fig 42g), there is again a strong bed [3.36–3.69] originally composed of finely laminated silt and mud. The lower half is muddier, with discrete shell bands (*Mytilus*, *Neptunea contraria*), especially strong at the base where there are also some small flint pebbles and more angular fragments. Colours are again increasingly ginger downwards, with various grey zones associated with ichnofossils. Mostly formless bioturbation increases downwards, eventually with almost complete loss of depositional structures.

In GTP 13 1, there are two beds which, strictly, are inter-formational but, since they have been observed so far only at this locality, they will be subsumed within Unit 4a (Catt Chapter 2.5, Macphail Chapter 2.6). The first of these [3.67–3.69] comprises an irregular but reasonably continuous string of lenses and pockets of chalk pellets, with rare even larger chalk fragments, set in a gritty calcareous mud; this bed thickens irregularly but rapidly shorewards. The second bed [3.69–3.70] is dominated by clean structureless, strongly calcareous finer medium sand (Fig 63). There is a double symmetrical coarse-tailed grading across the width of the unit, with the central zone including silty mud lithorelics, small chalk fragments and isolated flint of coarse sand grade; there are clear signs of post-depositional fluidisation in places. This sandy bed is always erosive at the base, probably originally so.

These two units are clearly true depositional beds, in the stratigraphic order described. However, at various points within the GTP 13 exposures, chalky debris, sand or a mixture of both is involved in a persistent suite of post-depositional deformation structures (fragmentation and dispersal of mud/silt clasts as lithorelics, grading and other fluidisation forms, dish-and-pillar structures, clastic sills and dikes, fault and thrust planes) extending in places almost to the base of Cycle 3 and also often involving disruption of sediments as high as the top of Unit 4b (see below) by upward injection. All thrust forms (usually associated with sills) involve over-thrust in a seaward direction, whilst high angle curving faults (usually associated with dikes) are normal and organised in coast-parallel (c 302°–122°) belts; movement is therefore consistently off-shore. It can be demonstrated that this movement was occurring before the end of Unit 4 times and had nothing whatsoever to do with the pressures developed much later when thick terrestrial deposits overran this area; although no true intertidal channels have yet been identified at Boxgrove, the deformation structures described above strongly imply instability due to the development of a free sub-vertical erosion face seawards of GTP 13 at one or more points within the Unit 4 chronozone.

Returning to the GTP 13 1 (Fig 45a) sedimentary sequence, the next deposits are more typical of Unit 4a. The first bed [3.70–3.74] is a muddy silt, passing upwards to thin silt lenses between wavy mud laminae,



Fig 63 Contact between the sands and silts at GTP 13; scale unit 10mm

and then returning to muddy silt. Colours are typical of the entire interval, with muds showing as light olive grey (5Y 6/2) and silts as light grey (2.5Y 7/2-3); again like the whole of this interval, this bed is very strongly calcareous. The next bed [3.74-3.77] consists of inter-stratified wavy laminae of muddy silt and purer silt, with the latter strengthening upwards; shell fragments are common, with both individual valves and 'articulated' pairs of *Mytilus*. The succeeding bed [3.77-3.79] shows mud dominant over silt. The next bed [3.79-3.80] is a continuous set of wavy silt laminae, the set-form being composed of a line of discordant 'pinched' lenses, with shell fragments. The bed above this [3.80-3.83] comprises wavy mud laminae with silt linsen; shell fragments are present and often associated with stacked arcuate concave-up traces (molluscan escape structures) originating mostly from the two beds below. The last bed in this sequence [3.83-3.84] consists of wavy silt laminae; in places, the very low ripple-forms show bidirectional, shore-perpendicular foresets. Shell fragments and escape structures are still present. It is noteworthy that bioturbation is relatively weak throughout this interval, with molluscan escape structures being the only clear form, apart from rare thin vertical tubes.

In GTP 10 (Figs 49a-51, 62), there is a bed [4.0-4.15] composed of strongly calcareous, grey muddy material, with an erosive base associated with flint pebbles and shell debris. There is moderate

bioturbation, including arcuate concave-up stacked traces (molluscan escape structures). Near the top of the bed, there is a zone with adult *Mytilus* in death position. In GTP 5 (Fig 59), there is a bed [0.09-0.33] comprising wavy grey mud laminae, with some thin fine sand laminae and isolated small flint pebbles; fragile adult *Mytilus* are present, becoming common shorewards. The last bed in this sequence [0.33-0.38] is similar in all respects, save that fine sand has become dominant over mud. In Q2/A (Fig 61), there is a unit [0.43-0.52] with gentle wavy bedding, comprising alternations between dominant laminated muddy sediment and thinner, coarse silt/fine sand linsen or laminae. There are diffuse concentrations of flint pebbles, up to 70mm in diameter, at the base (Fig 64). Bioturbation is weak, consisting entirely of thin vertical tubes. Only slight post-depositional deformation can be seen at this level (see Unit 4b in Q2/A, described below). In GTP 26, there is a thin bed [5.28-5.32] of silty mud laminae, with shell debris and rip-up clasts of the underlying cemented sediments; large disturbed valves of *Mytilus* and flint pebbles often stand vertically. Bioturbation is weak, consisting of vertical tubes, most originating from higher levels but a few from the top surface of this bed. In Q1/A, there is possibly an unconformity at the base of the Unit 4a deposits where the concretions in the underlying Unit 3, noted above, served to limit downward erosion.



Fig 64 Possible seaweed-rafted pebble cluster from Unit 4 in Q2/A; scale unit 50mm

Seen together, the muddy Unit 4a occurrences have much in common. There are nearly always signs of strong basal erosion, with coarse elements (shell, flint pebbles, more angular flint particles, and rarer chalk fragments) included as a lag. This would suggest lateral scour or even channel migration, although longitudinal (epsilon) cross-bedding has still not been observed and all larger scale current structures are very rare. Where not disturbed, thinly laminated horizontal wavy composite (mud/silt) bedding is the norm. Whenever it is a case of such alternating, linsen or flaser bedding, the designation of formal 'beds' unavoidably becomes very subjective; the observations reported here reflect the degree of textural differentiation and the abundance of erosional planes, so that exposures with more defined 'beds' in Unit 4a probably represent more hydrodynamically active locations. Fine sand appears only close to the shoreline and well off shore. In the few cases where foresets appear, bi-directional tidal bedding is indicated. Penecontemporaneous deformation is present but only extreme in a few locations. Bioturbation is generally low enough not to obscure primary bedding, except near the shore, where polychaetes appear to be abundant. Further off shore, mollusca are the dominant biota. Even on this dangerously soft substrate, there are mussel beds; when sediment is dumped, the mussels (and

their predators) are either entombed (death assemblages) or manage to escape upwards (stacked cusped traces). Simple aquatic plants may have rooted in some zones, although it is difficult to be sure that such traces do not originate from higher levels. The generally grey base colours, together with the later mobility of iron salts, would suggest that organic matter was readily available; very small scale variation in carbonate content (ie localised decalcification and perhaps weak recementation), together with colour differences showing overlaid 'generations' of post-depositional structures, suggest a relatively active biochemical system. The environment indicated by these deposits is an intertidal mudflat, in a generally estuarine/lagoonal setting.

The two inter-formational beds at the base of the GTP 13 sequence deserve further mention. The chalky debris is obviously a land-derived deposit, although subsequent deformation makes it impossible to tell whether a subaqueous debris flow was again involved. The lack of original depositional structure in the medium sand bed is even more unfortunate, since emplacement could have been in the form of a weak beach, a sand bank/shoal or even a subaerial dune.

Unit 4b

In GTP 25 5 (Fig 42c), Unit 4b begins with an interval [2.27-2.4] of horizontally laminated coarse silt and fine sand with rare mud-drapes. The next interval [2.4-2.55] consists of laminated silt and mud, with stringers of small chalk fragments and a few fine flint fragments; the whole is slightly contorted in places. These sediments show an offlap relationship and both intervals thicken seawards but wedge out within 1.5m shoreward of this exposure (Fig 65). As discussed earlier, the matrix of the clast-supported beach deposits below the silts consists of intrusive grey or 'olive' silt; the transition from dominantly land-derived matrix to an intrusive matrix of marine grey silt is seen in Figure 52. These intrusive matrices mark the maximum observed transgression of Unit 4, in both lateral and altitudinal terms.



Fig 65 Slindon Sands and Silts 'wedging out' over the raised beach at GTP 25; scale unit 0.5m

In GTP 25 7 (Fig 42j), there is an interval [1.62–1.89] of laminated silt, fine sand and mud, with scattered very fine chalk pellets and with an apparent dip of 3° along bearing 220° (as in the underlying unit); shells of *Nucella lapillus* occur mid-way up this interval. In GTP 25 6 (Fig 42i), Unit 4b begins with an interval [0.82–1.02] containing four cycles, each starting with muddy silt laminae and passing gradually upwards into cleaner, finely laminated silt. The next interval [1.02–1.12] consists of grey mud laminae, up to 10mm thick, with thin fine sand laminae, the whole being muddier in the upper half; there are small chalk fragments and some isolated small flint pebbles.

In GTP 25 E (Fig 42d), Unit 4b begins with an interval [2.66–2.80] consisting of wavy bedding, with mud dominant and some chalk pellets; bioturbation is generally moderate, with common Fe-stained tubes. The next interval [2.80–2.84] comprises a slightly muddy fine sand, homogeneous in structure probably due to bioturbation. The succeeding interval [2.84–2.87] shows wavy bedding, with equal amounts of mud and silt or fine sand. The final interval in this sequence [2.87–2.97] is a mud with contorted silt/fine sand linsen. In GTP 25 D (Fig 42c), the first interval [3.28–3.35] consists of quite heavily laminated mud and silt laminae. The next interval [3.35–3.42] shows more silt, with thinner mud-drapes and laminae. The last interval [3.42–3.56] is disrupted but still shows some fine sand and silt structure in a generally muddy ground. In GTP 25 C (Fig 42f), the first interval [4.57–4.58] is a continuous mud band with relatively strong Fe–Mn build-up. The next interval [4.58–4.69] consists of laminated silts set in mud-defined lenses. The succeeding interval [4.69–4.76] consists of wavy bedding, with mud slightly dominant over silt. The final interval [4.76–4.86] is a mud with some contorted silt laminae; weak bioturbation is represented by tubes, and these and mud partings are stained by Fe–Mn. In GTP 25 B (Fig 42g), the sequence again starts with a continuous silty mud [3.69–3.70]. The next interval [3.70–3.91] consists of slightly muddy silts with mud laminae, divided into sets by stronger mud bands; bedding is generally wavy but is overprinted by 'micro-crinkling' (see below). Bioturbation structures include pouches, tubes of various diameters and stacked cusped escape marks, usually Fe-stained against the buff (silt) and dark grey (mud) background. The final interval [3.91–4.0] is a laminated mud, with muddy coarse silt lenses and lamination, and rare flint pebbles at the base; the bedding is generally wavy although sometimes 'incomplete', with mud-drapes bifurcating laterally but failing to enclose silt lenses (incomplete flasers). Major mud partings and bioturbation structures (fine tubes) are stained with Fe–Mn. Vertical tubes show zigzag distortion, suggesting significant post-depositional compaction probably by loss of bulk volume in the matrix (removal of original carbonates and possibly of organic matter).

In GTP 13 1 (Fig 45a), Unit 4b starts with an interval [3.84–3.88] showing wavy bedding dominated

by 2–7mm thick mud lamina-sets; clusters of arcuate escape structures occur near the top. The next bed [3.88–3.98] consists of wavy silt lamina-sets with fine mud flasers and laminae, there being a slightly muddier interval near the middle. In the lower siltier zone thus defined, there are common shell fragments as well as 30–50mm paired valves of *Mytilus* in death position; the upper siltier zone also has shell fragments, together with rare *Nucella lapillus* lying aperture downwards. The next bed [3.98–4.02] is a muddy unit, with increasing very thin silt laminae and dumpy (deformed) linsen upwards; small shell fragments are present. The succeeding bed [4.02–4.06] consists of dominant wavy mud laminae with only very thin silt linsen. The next bed [4.06–4.09] comprises mud-capped wavy silt laminae, with isolated edge-rounded flint particles up to 50mm in diameter; *Mytilus* are again found in death position and shell debris includes fragmentary *Neptunea contraria*. The overlying bed [4.09–4.11] is a muddy unit with wavy bedding. The last unit in this sequence [4.11–4.18] consists of a series of wavy fining upwards lamina-sets, from silt to silty mud, with some bidirectional shore-perpendicular cross-lamination; shell fragments are associated with siltier zones. The upper surface of a mud cap, just below the top of this bed, shows clear raindrop impact craters. Throughout this interval, the only bioturbation is due to very fine and sinuous vertical traces (non-bifurcating but tapering downwards), suggesting simple subaqueous plant rooting, in part originating from higher levels, creating little overall disturbance.

In GTP 10 (Fig 49b), there is a light grey interval [4.15–4.29] of moderately strongly calcareous, well laminated fine sand/silt and mud, with parallel slightly wavy bedding; bioturbation is moderate, consisting dominantly of vertical tubes originating from above, and there are fragile *Neptunea contraria* and fragments of other mollusca. Some 4m seawards of this exposure, Unit 4b shows an additional interval of wavy mud laminations at the base. The highest interval in the main sequence [4.29–4.45] consists of an olive grey, strongly calcareous muddy material, with small flint pebble stringers; the many Fe-stained tubes, which pass down into lower deposits, originate at or near the top of this interval.

In GTP 5 (Fig 59), Unit 4b begins with an interval [0.38–0.47] of laminated grey mud, with rare ironstone fragments; there are regular large clumps or 'nests' of flint pebbles (20–50mm diameter) and very fragile shells of *Neptunea contraria* (some as large as 100mm in diameter), together with shells of other small gastropods (with normal coiling). The next interval [0.47–0.74] consists of laminated fine sand 'hummocks' (see below) in two main sets, separated by a muddier zone; the long axes (culminations) of the 'hummocks' are oriented almost exactly east-west. Rare isolated flint pebbles and shells of *Neptunea contraria* occur at various levels, usually in troughs between 'hummocks'.

In Q2/A (Fig 61), Unit 4b begins with an interval [0.52–0.95] of dominant silt laminae, with muddy partings and rarer mud laminae, set in wavy bedding with some linsen and flasers; edge-rounded flint gravel particles lie horizontally, with no preferred orientation of long axes and no associated scour marks. Bioturbation structures, mostly originating from higher in the sequence and consisting of Fe-stained tubes averaging 5mm in diameter, give only 8–13% interruption of primary depositional structures.

The fine structure typical of much of Unit 4b has been studied in most detail in this interval in Q2/A (Wilhelmsen Chapter 6.2). There is a striking pattern of silt 'hummocks', best described initially as a non-cylindrical fold system of gentle dome and basin form. Each dome is asymmetrical in plan, with a slightly sinuous main culmination hinge line oriented roughly along the trend 100°–280°; the pattern is not exact but the frequency of dome culminations is *c.* 2.0–2.5m along this axis. In vertical section along the long axes, silt laminae thin towards the intervening basins and may disappear completely; alternatively, silt may survive in the basins as minor boudinage structures set in mud. Folding is tighter along the short axes of domes, with culmination frequencies varying between 0.5 and 0.75m. In vertical section along the short axes, mud laminae thin near the crest of domes but thicken and show high frequency disharmonic microfolding ('crinkling') in the core of the fold near the base. It is reiterated that the pattern is not exact but there appears to be a tendency for domes to be set in a rhombic rather than an orthogonal plan pattern. Maximum amplitude of domes is 0.25–0.30m.

The description of folding given above might apply to a single generation post-dating deposition. However, a series of small scale internal structures shows that the history of deformation was more complex. First, although the basic (original) bedding pattern was one of parallel wavy lamination, the silts near the crests and flanks of some domes show reactivation surfaces, above which the laminae are folded to a different (usually lesser) degree. No cross-stratification (ie laminations meeting a lower boundary at an angle) has been observed. Second, some mud laminae, especially nearer crests, have minor high frequency folds when seen in vertical section across the short axes of domes; these minor folds display strong vergence towards the dome crests. Indeed, in some areas, the main dome pattern is of lower amplitude than usual (ie domes are composed of only the lower laminations in the whole interval) and basins are filled with another series of silt laminations, downwarped on these occasions but with minor folding of internal mud laminae displaying marked vergence towards the troughs. These features clearly indicate that at least some of the folding must have been syndepositional or penecontemporaneous; in addition, the vergence patterns show that folding often affected the currently superficial levels before deeper levels were deformed. The gravel

concentrations at or near the base of the overlying bed occur within the basins in the 'hummocky' interval; it seems most unlikely that folding could have segregated this gravel and it is therefore deduced that the folding did have some contemporary surface expression. The vertical tubes developed through this interval are not radically deformed, showing that they post-date much of the folding.

Relatively wide areas have been excavated in Q2/A (Bergman and Roberts; Wilhelmsen Chapter 6.2), so that larger scale characteristics of the 'hummocky' interval can be reported. First, although this interval is often seen to be sandwiched between two muddier units (described formally in Q2/A as the [0.43–0.52] and [0.95–1.08] intervals, respectively), observation of individual laminae over lateral distances of as little as 10m shows that they may pass up or down between the three intervals and may disappear at upper or lower boundaries of this set of deposits. The recognition of time planes within this material will be impossible except on very small lateral scales. It follows that the lithostratigraphic distinction between Unit 4a and Unit 4b deposits at Boxgrove may not always (if ever) translate to chronostratigraphy: these sedimentary facies are time-transgressive, certainly in an irregular manner with respect to the subunits of Unit 4 and possibly in a more ordered geographical manner with respect to Unit 4 in bulk (ie there may be gross younging seawards or at least a seaward younging of maximum sedimentation rate). Other characteristics are seen over the wider area in Q2/A. Some 'hummock' sequences may show gross fining upwards, whilst others do not. Boundaries between individual sedimentary cycles may vary from diffuse to very sharp. In a few places (cf also GTP 5), there are two clear generations of 'hummocks', without significant overprinting. There is one clear geographical trend within Q2/A: moving towards the north-west, deformation decreases markedly with a corresponding decrease in overall unit thickness (this is also true of the muddier intervals above and below the 'hummocky' interval), culminations are more angular, microfaulting and vergence are more rare, the displacement (up, down or none) of individual laminae varies more markedly between immediate stratigraphic neighbours, and the top of the 'hummocks' may show zones with mud clasts dispersed in homogenised silt, suggesting water-escape structures. Thus, despite the fact that the dome and basin structure is maintained right across the excavated area in Q2/A with the same basic directional properties, response to deformation becomes increasingly less plastic towards the north-west.

The [0.95–1.08] interval in Q2/A may also be referred to Unit 4b (Fig 61). This is a muddy deposit with slightly thicker silt laminae in the central portion. The oval concentrations of gravel near the base, set in the troughs in the underlying 'hummocky' interval, have already been mentioned. Bioturbation, in the form of 50–100mm long vertical tubes originating from the top of the unit, shows 25–30% interruption of

the primary bedding. Wavy bedding is the main style but, higher in the interval, there may be c 30mm thick zones of strongly convoluted lamination ('box folds'), which may pass into very minor silt 'hummocks', similar to those in the underlying interval, towards the northern side of the Q2/A exposure.

In GTP 26 (Fig 48), there is a 'hummocky' interval [5.32–5.59], with the same central dominance of silt laminae as seen elsewhere. Mud laminae are pinker than in most other exposures, suggesting a more oxidised derivation or maturation history. Fine flint gravel and small shells of *Mytilus* occur in muddier zones, with 'articulated' examples of the latter nearer the top of the interval. Bioturbation is stronger than in most other exposures of Unit 4b, with some longer Fe-stained tubes but also quite common short tubes and pouches. Further deposits with wavy bedding are referable to Unit 4b: the [5.59–5.65] interval is dominated by silt, the [5.70–5.80] interval by mud and the [5.66–5.76] has equal proportions of mud and silt. The last interval [5.80–5.87] is still laminated but very strongly disturbed; pockets of this material may reach downwards and may there be accompanied by edge-rounded flint and even the break-up of the underlying sediment to give mud clasts. Although this phenomenon might be associated with escaping water, it seems more likely that it is a result of major (terrestrial) root penetration from above, seen more clearly in overlying deposits.

The environment indicated by the Unit 4b deposits is still very much a tidal flat, in a generally estuarine/lagoonal setting. The common silt to fine sand textures show a tendency towards more mixed flats than in Unit 4a. Coarser elements (both gravel and larger derived shells) are not hydrodynamically consistent with either the matrix textures or the lack of obvious creek facies (higher angle cross-bedding or epsilon cross-bedding) and are therefore probably referable to rafting on drift seaweed (Bridgland Chapter 2.4). Bioturbation is comparatively low and of reduced morphological diversity, with some instances of simple traces probably due to rooting of aquatic plants; this pattern is not common on flats open to the sea and would suggest a comparatively sheltered but biologically hostile situation, probably with decreased, and possibly fluctuating, salinity and oxygen availability (Macphail Chapter 2.6). There can be no doubt that these deposits, with their composite wavy bedding, are broadly intertidal but absolute proof is provided in one instance by raindrop impact craters (emergence features with an extremely low probability of survival in the sedimentary record) and also by the presence of primary flint artefact scatters (cf the lowest material in Q1/A, which occurs within finely laminated silts and muds, showing no desiccation or significant bioturbation features (Austin and Roberts Chapter 6.2)). Occasional bone fragments from terrestrial mammals also occur in the upper levels of this sequence. The most interesting feature of these sediments is the

'hummocky' style developed in most exposures not too close to the shore. It has been shown that this style is at least partly penecontemporaneous with deposition. It is possible to see this style as representing a 'harmonic' between the sediments and the swell of the sea, oscillating pressure from low waves causing the soft bottom sediments to deform, thus creating the gentle dome and basin morphology, which itself perpetuated oscillating pressures in water moving across it. The particular scale of the rhombic form developed no doubt represents the equilibrium between modal wave characteristics, deposition rates, sediment competence and tidal energy. Actual deposition in 'hummocks' ('hummocky cross-stratification') is usually a feature of sandy shoreface facies but even the Boxgrove 'hummocks', with their clear contribution from deformation, suggest that exposure by dropping tide was a gentle and not greatly prolonged process, those features developed under a body of water, rather than during subaerial channelled flow. The occasional intervals of convolute bedding are another typical feature of (inter-) tidal flats and result when saturated, incompetent, sediments receive a shock (normally from a breaking wave) and momentarily fluidise. Although small scale erosion features (especially low angle reactivation surfaces) are ubiquitous, there are very few larger scale current forms and, as has already been noted, no sign of creeks. Creek development is usually proportional to tidal range, since this is the only way that sediments can drain when sea level drops rapidly; the absence of such features here suggests low tidal range. The lack of erosion benches and of more continuous coarse lags with mudballs, together with the relative rarity of convolute bedding, suggest that storm effects did not often penetrate what must have been a reasonably sheltered body of water. Although bioturbation (endobiont activity) is weak, it is possible that some superficial coherence may have been produced by algal mats (with an impoverished epibiontic invertebrate fauna of grazers, suspension feeders and predators as the dominant biofacies); other surfaces may have been buffered by a basal suspension of flocculated fine sediment (a common occurrence where waters of differing salinity mix).

Unit 4c

This unit (Fig 66) is defined from the point of view of its lithology as a macroscopically massive mud. However, there are traces of original depositional structures in places, and it is clear that the present condition of this sediment is the result of a complex series of modifications by penecontemporaneous and post-depositional deformation, both animal and plant bioturbation, and chemical alteration, during a period of rather low sedimentation rate. There are two important consequences of this developmental history. First, the lower boundary of the unit will be somewhat arbitrary and time-transgressive, depending upon the

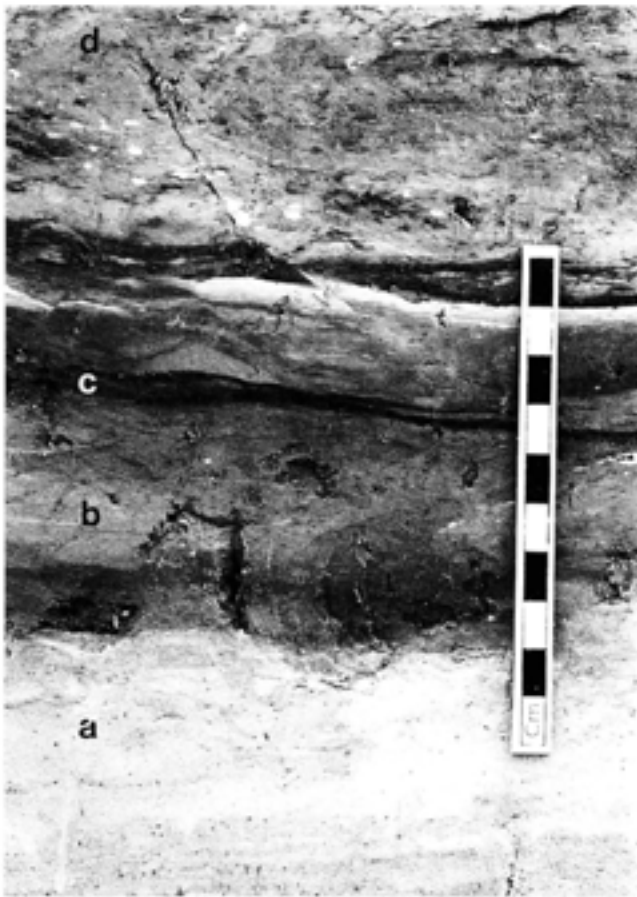


Fig 66 Unit 4c; note contrast between modified soil horizon (b) and underlying Unit 4b (a). a) Slindon Silts (Unit 4b), b) palaeosol (Unit 4c), c) Organic Bed (Unit 5a), d) Brickearth Beds (Unit 6); scale unit 10mm

degree (in terms of both depth and severity) of penetration by modificatory processes in any given area; it is quite possible that more clearly laminated sediments in one area may be referred to the very top of Unit 4b, whilst contemporary and originally similar sediments in another area will have been more profoundly modified and thus referred to Unit 4c. This observation applies only to the finer detail and the broad stratigraphic sequence is perfectly legitimate. Second, macroscopic observation of this unit provides only very basic and incomplete information. Much more precise and useful information is provided by micromorphological study (Macphail Chapter 2.6), which is capable of showing the complex overprinting resulting from major environmental shifts.

Sediments clearly referable to Unit 4c do not appear on the shoreward side until the exposure in GTP 25 E (Fig 42d), where the [2.97–3.0] interval is a massive grey-green mud. Similar sediment is present in the [3.56–3.6] interval in GTP 25 D (Fig 42e), in the [4.86–4.91] interval in GTP 25 C (Fig 42f) (with macroscopic traces of lamination still surviving in small patches) and in the [4.0–4.04] interval in GTP 25 B (again with patches of possibly original laminated structure) (Fig 42g).



Fig 67 Bear (*Ursus deningeri*) mandible from Unit 4c; scale unit 50mm

In GTP 13 1 (Fig 45a), the [4.18–4.31] interval consists of a massive mud with silty mottles, showing some fissility in the horizontal plane; the sediment is strongly calcareous at the base but the carbonate content fades quickly upwards and is lost completely in the upper half of the deposit. In GTP 10 (Fig 49b), the [4.45–4.50] interval might be referable to Unit 4c or to a higher unit (see below). In GTP 5 (Fig 59), the [0.74–0.80] interval consists of a laminated grey clayey mud. In Q2/A, there is a particularly thick interval [1.08–1.90] which contains deposits referable to Unit 4b as well as to Unit 4c. There are very fine alternations of fine silt and mud, fining upwards into laminated mud with floating coarser (silt to fine sand) grains, and thin fine sand lenses near the top; bioturbation is mostly represented by amorphous 'mottles' but some simple vertical tubes are also present. Laterally, adjacent to the main Q2/A exposure, a massive zone may develop obliquely and slightly irregularly across the top of this otherwise laminated interval. In GTP 26 (Fig 48), the [5.87–5.91] interval is a homogeneous grey-green mud; there is some disturbance in this area, probably due to penetration by tree/shrub roots.

All that can be said from the macroscopic information is that Unit 4c represents the completion of the transition from marine to (often wet or damp) terrestrial conditions. In places, bone fragments may be quite an obvious component of the sediment (Fig 67), as, more locally, may flint artefacts.

Unit 4d

This main occurrence of this unit consists of pond marls in Quarry 1 (Q1/B), probably associated with a spring (Roberts *et al* 1994); these sediments were not observed by the present author (cf Macphail Chapter 2.6 and Austin and Roberts Chapter 6.2).

Unit 5a, the Organic Bed, Fe–Mn mobility and continuing minor clastic deposition

The problems for macroscopic observation, due mostly to post-depositional effects noted above in the discussion of Unit 4c, continue into the Unit 5 deposits. Indeed, in places it is difficult to decide upon the proper boundary between 4c and 5a. There is also quite marked lateral variation, and the occurrence of restricted lenses of material, set in only a thin sedimentary interval, often makes it impossible to specify the detailed stratigraphic relationships. Again, a much more coherent picture is provided by the micromorphological study; in deference to the microstratigraphy demonstrated by Macphail (Chapter 2.6), these sequences will here be referred to as 'condensed'.

The true mineralogy of the iron and manganese enrichment noted in this section is no doubt complex and varied. As a simple shorthand, material which is red to ginger in colour is referred to as 'Fe' and material which is chocolate brown to almost black as 'Mn' (note that the latter material was repeatedly subjected to flame tests on site which would have allowed the recognition of (hydro-) Carbon content in excess of c 5% but no such organic survivals were observed). A strong 'pan', usually associating both Fe and Mn (sometimes more or less segregated as horizontal bands), is referred to as 'Unit 5a', although 5a also appears to contain small clastic lenses in places.

In GTP 25 5 (Fig 42c), the [2.55–2.57] interval contains an irregular Fe-band which is totally discordant with the structure in the underlying laminated silts and which may even wander down and overprint the laminations in an irregular manner. The [2.57–2.60] interval is composed of a structureless, Mn-impregnated, clayey silt. The [2.60–2.62] interval comprises a strong Mn-accumulation with a minor Fe-band directly below. This uppermost interval may be referred to Unit 5a but the exact stratigraphic position of the two lower intervals is unclear. The overlying interval [>2.62 , 0.66+] consists of recemented fine chalk debris with very large chalk blocks; multiple Mn-bands, with a few weak Fe-bands, are common at the base of this material, but may wander upwards over chalk blocks to heights exceeding 1m above the base of this interval. It is not even clear which (if any) is the main occurrence of Unit 5a in this exposure. In GTP 25 6 (Fig 42l), the [1.12–1.14] interval contains a minor channel-like feature, with dark brown mud and fine sand. The bedding is obscure, due to later distortion (including injection of small packets of mud from below), but the sediment was apparently laminated. The trend of elongation is 165°–345° (palaeoslope-parallel and broadly shore-perpendicular). The deposits directly below this feature are downwarped and overprinted with fine Fe-bands 'concentric' with the cross-section of the channel-like feature itself. The [1.14–1.15] interval is an Mn-band, apparently referable to Unit 5a. In GTP 25 7 (Fig 42j), the

[1.89–1.99] interval is a muddy clay with small chalk pellets, showing highly convoluted and very abrupt upper and lower boundaries; the deposit is overprinted with fine bands, dominantly Fe in the lower part and Mn in the upper. Since there are no clear occurrences of typical Unit 4c sediments in these exposures, the detailed stratigraphic relationships are unclear. Note that Fe–Mn banding occurs both below and above more typical 'pan-like' occurrences of Unit 5a.

In GTP 25 E (Fig 42d), the [3.0–3.02] interval is a foliated Mn-band, with an internal fine sand lens of irregular outline; desiccation cracks (giving a polygonal net in plan) pass right through the Mn–sand–Mn sequence and show zigzag distortion compatible with at least 25% post-formational compaction in the vertical axis. In GTP 25 D (Fig 42e), the [3.6–3.61] interval is an Mn-band, whilst the [3.61–3.62] interval is a greyish chalky silt with minor Fe-partings. In GTP 25 C (Fig 42j), the [4.91–4.92] interval is a foliated Mn-band, containing a small clean fine sand lens, which swells upwards to thicknesses of up to 25mm, leaving the uppermost Mn similarly up-domed (a diagenetic morphology, due to chemical stability of the sand as compared with solubility of much of the original material surrounding it); although warped, the sand shows small-scale ripple cross-lamination, apparently dipping along the elongation of the lens on an unexpected bearing of 8°. The [4.92–4.94] interval is a grey/mauve mud with flattened (compacted) chalk pellets and multiple, very thin Fe-bands, referable to subunit 1129 (Table 9b). In GTP 25 B (Fig 42g), the [4.0–4.04] interval has already been referred to Unit 4c but there is a 2–4mm Mn-band near the top, followed upwards by very thin Fe-bands developed in irregular patches of mauve grey mud; fine Fe-bands also wander below the Mn-band, crossing structural features downwards by as much as 120mm.

It has already been noted how Fe–Mn bands may occur within chalky deposits referable to units higher than Unit 5a (Fig 68). In fact this is a relatively common occurrence along the whole GTP 25 exposure and elsewhere in the chalky pellet gravels. Multiple Fe–Mn bands climb shorewards into the chalky debris, sometimes as apparently diagenetic features, but often at true surfaces, sometimes with tiny mud or silt laminae between the Fe–Mn and the underlying chalk; these tiny sequences may even show mud cracking. When the Fe–Mn (and/or mud) is peeled from the chalk, a gently undulating 'annealed' surface is exposed, lacking in recognisable root marks. Some 8m south-west of the cliff-line, there is however a 0.7m wide and 0.4m deep depression which could be a shallow treefall effect. Again, along the whole GTP 25 exposures, the main Fe–Mn 'pan' (Unit 5a) very commonly contains finest sand or silt laminae and lenses.

The deposits in GTP 20 (Fig 4) have not been studied in detail by the present author, but there is a short sequence of relevance here. Above reasonably

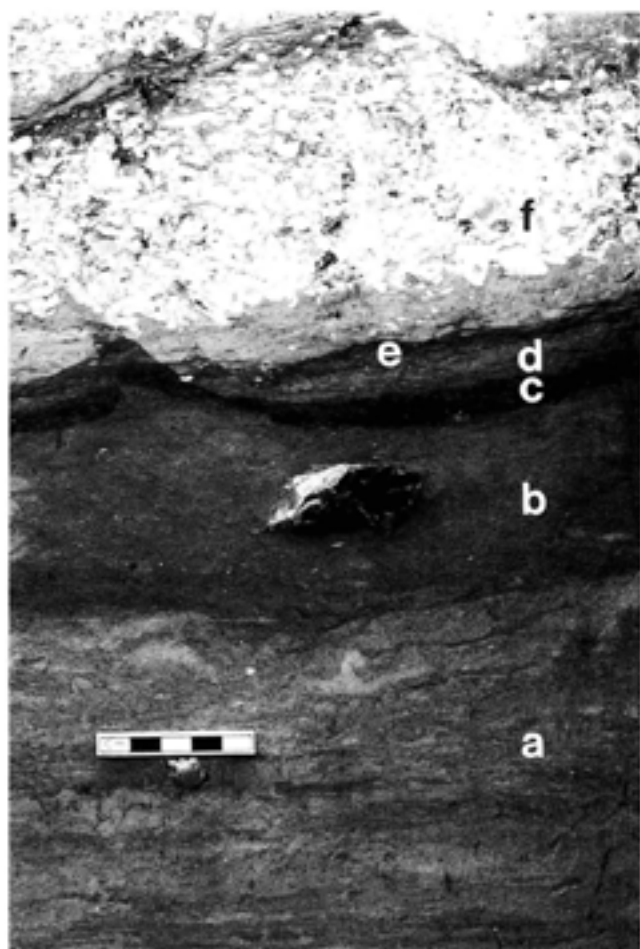


Fig 68 Fe-Mn bands in the chalky gravel above Unit 5a and the Slindon Silts; a) Slindon Silts (Unit 4), b) palaeosol (Unit 4c), note handaxe, c) Organic Bed (Unit 5a), d) Unit 6'3, e) Unit 6'3'Fe, f) Upper Chalk Pellet Beds with Fe-Mn band; scale unit 10mm

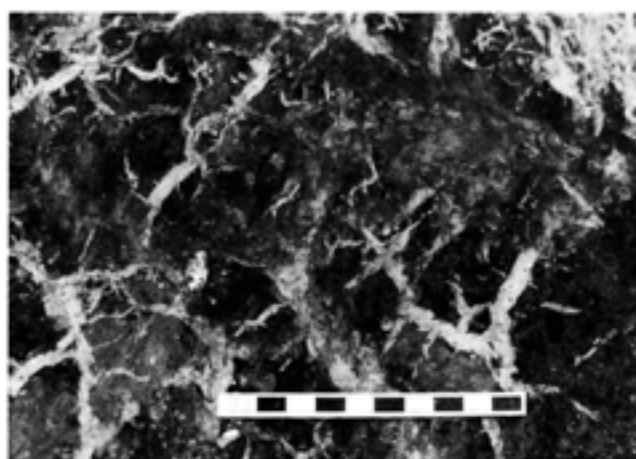


Fig 69 Mud cracks on the surface of Unit 5a at Q2 GTP 20; scale unit 10mm



Fig 70 Post-depositional faulting of Unit 5a at Q2/A; scale unit 50mm

typical Unit 4b silts, there is a thin interval of clean fine sand (Table 9b); above this there is a thin mud lamina and then a strong Mn-band (Unit 5a). Mud cracks (showing a polygonal net in plan) have developed from the top of the Mn-band (Fig 69) and through the mud; there has been a minor degree of fluidisation of the underlying sand which has been injected upwards to fill the cracks. In GTP 13 1 (Fig 45a), the [4.18-4.31] interval has been referred to Unit 4c. However, there is an Fe-band in the body of this interval and an Mn-band at the top, both of which have a foliated structure in the central portion. Small zones of mud cracks are developed from the top surface downwards, and there are both simple/undulating and complex/dendritic root casts which also appear to originate from this level. In GTP 10 (Fig 49b), the [4.45-4.50] interval has again been referred to Unit 4c, but the mud contains a strong foliated Mn-band sandwiched between two thinner Fe-bands. In GTP 5 (Fig 59), the [0.74-0.80] interval, referred to Unit 4c, has thin multiple Fe and Mn bands. In Q2/A (Fig 61), the [1.9-1.93] interval contains a strong Fe-band referable to Unit 5a; there is

some mud cracking and dendritic root penetration from the top surface. It is noteworthy that the underlying laminated Unit 4c sediments (below the [1.7] point) show gentle warping (lower amplitude than, and out-of-phase with, the 'hummocks' in Unit 4b) and that most of the longer, simpler root pseudomorphs in the 4c sediments are developed at right angles to the warped laminations, showing that the deformation occurred after the root penetration (Fig 70). The base of the strong Fe-band (taking into account yet later generations of warping) was more or less horizontal and therefore represents an erosion surface which has planed off the previous undulations. In GTP 26, the [5.91-5.92] interval is a foliated Mn-band, which may thicken up to c 40mm and which may contain grey-green mud laminae and cream-coloured chalky mud lenses. The lenses are distorted but seem to be elongated along a trend 24°-204°; the chalky mud is internally laminated and there are even a few extremely thin grey mud partings. Further occurrences of Unit 5a were observed in the westernmost angle of Quarry 1.

A number of main themes may be retained from the above descriptions. Both iron and manganese banding can occur either as structure-discordant (overprinted) post-depositional features or as replacement of the substance (presumably dominantly organic but also possibly calcareous in some minor occurrences) of true stratigraphic units. Overprinting seems to be most common on Unit 4c substrates. The replacement bands often contain minor elongated clastic bodies (from mud to fine sand), with signs of current flow where not too strongly distorted; these are clearly small drainage rills and channels. Mud cracking seems to be quite common from the top of the main Fe-Mn band (ie Unit 5a), perhaps suggesting a slightly drier phase. However, the formation of mineral bands over clastic laminae continued sporadically into the next phase, when chalky debris was starting to be mobilised, especially nearer the cliffs. Macphail (Chapter 2.6) has been able to reconstruct a much more precise history from micromorphological data from the top of Unit 4c and from Unit 5a, involving dropping of the water-table, soil ripening and bioturbation by terrestrial faunas and floras, followed by increasing wetness, springline activity (Unit 4d) and localised deposition of organic detritus, followed by true peat deposition under intermittent gentle fluvial

and mire conditions, followed perhaps by a short period of drying-out of the marsh. The macroscopic observations, although much coarser, are wholly consistent with Macphail's reconstruction.

Unit 5b

Typically, Unit 5b is composed of a chalky marl. The unit may easily be recognised where it lies stratigraphically between Unit 5a and Unit 6 (Brickearth Bed, see below) (Fig 71). However, Unit 6 is not present in much of Quarry 1, nor near the old cliffs in Quarry 2, whilst later deposits are themselves very chalky, sometimes making it difficult to differentiate Unit 5b (if, indeed, it exists at all locations). Even when Unit 6 is present, it may not be clear whether to refer a basal chalky laminated interval to Unit 6 itself or to Unit 5b (cf the westernmost angle of Quarry 1, below) (Catt Chapter 2.5, Macphail Chapter 2.6).

The more typical occurrences of Unit 5b will be described first. In GTP 13 (Fig 45a), the [4.31-4.36] interval is an often finely laminated, very strongly calcareous clay, with small chalk pellets, especially near the base. In the north-eastern exposure in GTP 13, small V- and U-shaped forms with pellets penetrate

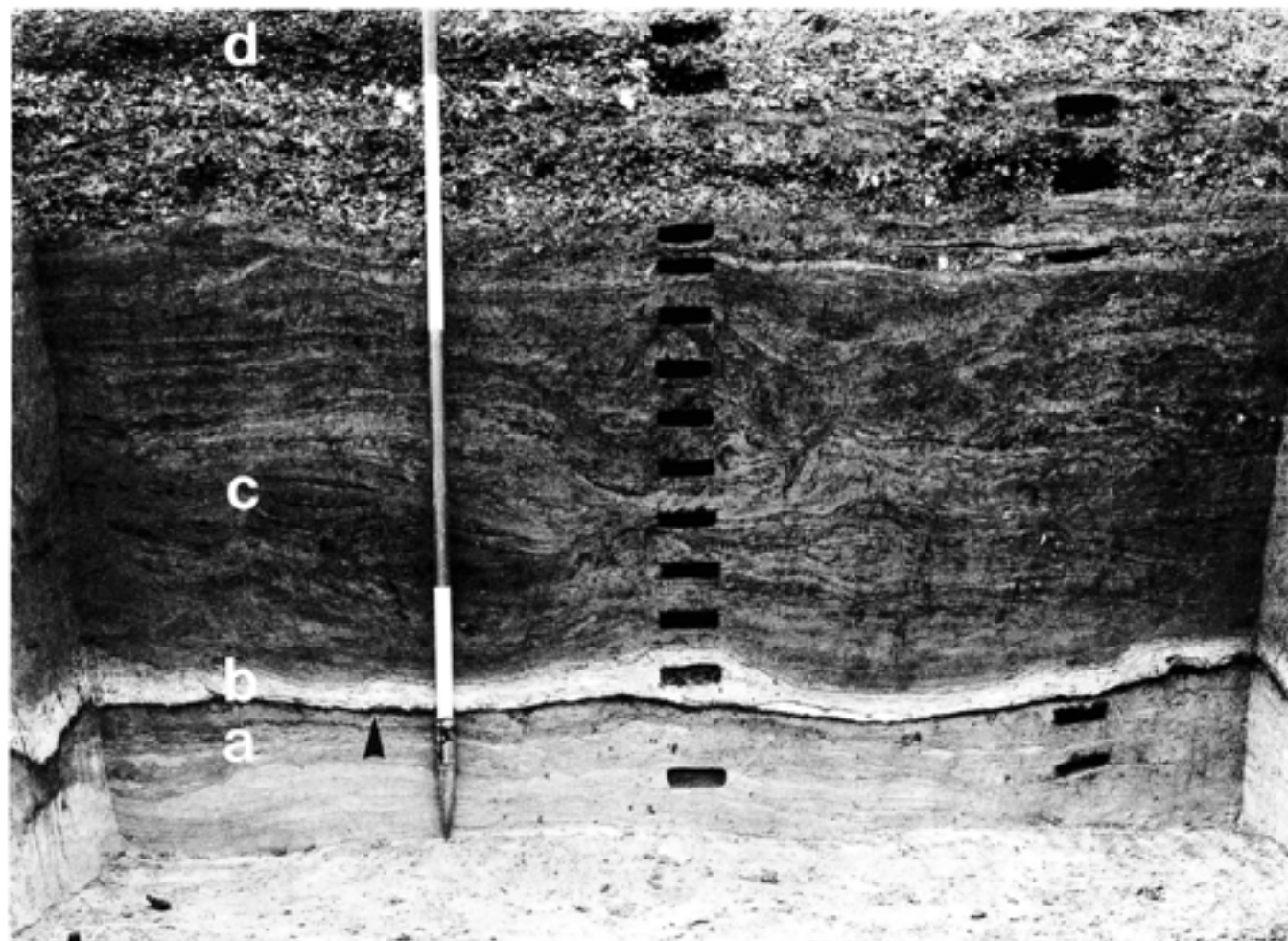


Fig 71 Unit 5b visible between the Fe-Mn layer of Unit 5a (black arrow) and the Brickearth Beds, Unit 6; a) Slindon Silts (Unit 4), b) Unit 5b, c) Brickearth Beds, d) Fan Gravel Beds; scale unit 0.5m

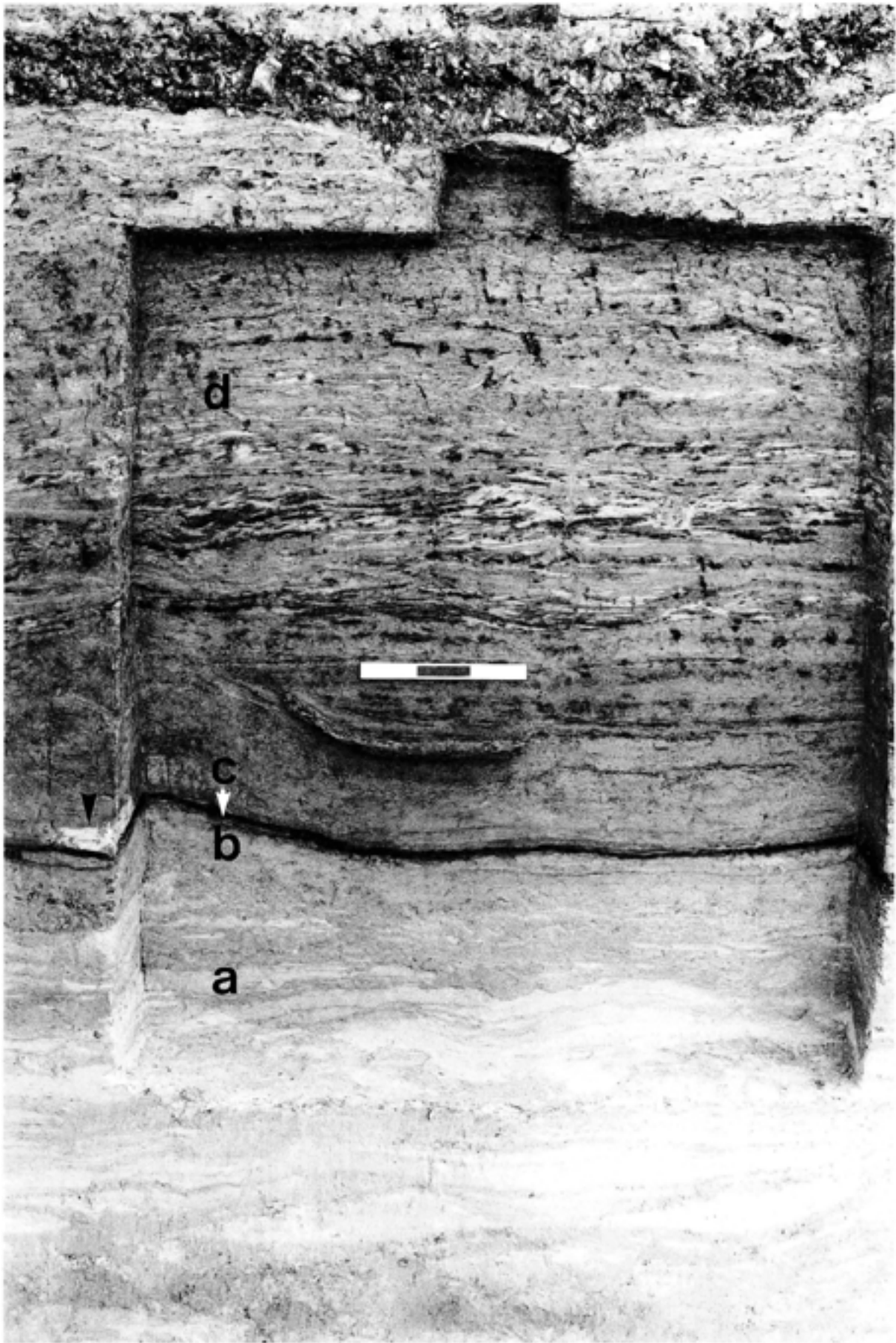


Fig 72 Q2 GTP 5 Units 4b–6; note surviving residue of Unit 5b (black arrow) to left of section; a) Slindon Silts (Unit 4), b) palaeosol (Unit 4c), c) Organic Bed (Unit 5a), d) Brickearth Beds (Unit 6); scale unit 50mm

downwards from the base of Unit 5b for no more than 80mm. In GTP 10 (Fig 49b), the [4.5–4.55] interval consists of recemented chalk mud with increasing chalk pellets upwards. The deposit has been heavily eroded by the emplacement of the overlying sediments; in places it is absent, in others there seem to be disturbed blocks, and in yet others it is up to 150mm thick and shows two reverse graded intervals, from mud to pellets. In GTP 5 (Fig 59), at the [0.8] level there are discontinuous eroded remnants of chalky mud, never more than 50mm thick and more usually just a 'smear' (Fig 72). No true Unit 5b muds survive in Q2/A. In GTP 26, the [5.91–5.92] interval, Unit 5a, already contains lenses of chalky mud. The [5.92–6.00] interval consists of a chalky mud, almost white at its base and finely laminated throughout. There are common Mn-replaced root pseudomorphs, of a simple bifurcating 'sedge-like' type, some of which can be demonstrated to hang from internal bedding planes (ie they are contemporary with the mud); the pseudomorphs have been significantly compressed, even when horizontal (30–40% compression to give oval cross-sections). The lowest 20mm of the interval have 'hairline' Fe-bands, thinning upwards, with traces of cracking into fine polygonal nets when seen in plan; cracks penetrate no more than *c* 1mm downwards). The [6.00–6.07] interval is very similar, save that the base colour is a little more orange and the laminations have been contorted slightly by pressure from above. This 5.92–6.07 interval almost certainly belongs to the Brickearth Bed (Unit 6), except for the basal 10–15mm which are attributed to Unit 5b. Overlying deposits are chalk pellet gravels referable to higher units.

Chalk pellets are ubiquitous in all the GTP 25 exposures, although, on simple theoretical grounds, one would expect a coarser facies this close to the cliffs. The [0.50–0.66] interval in GTP 25 8 (Fig 42k) has already been described and correlated with sub-unit 1129 (Tables 9a, 9b). There may be a link between the V- and U-shaped features at the base of Unit 5b in the north-western corner of GTP 13 and much larger, but generally similar, features derived from the pelley material in GTP 25 8. There are five wedge-shaped features within a 2m exposure at GTP 25 8 (Fig 73). The wedges have a maximum height of 0.7–0.8m and a maximum width of 0.28m. In cross-section, they are conical in the main lower part, often with a 'mushrooming' towards the top. At right-angles to the conical section, the wedges continue laterally (it was only possible to follow them for 1m into this high section), with a strike of 100°–280° (ie broadly cross-palaeoslope). The tapering bases penetrate vertically well down into laminated intertidal deposits, the laminations in the host being locally deflected downwards along the margins of the wedges; however, there is absolutely no gross vertical displacement of laminae on either side of a wedge (ie the wedges are not developed along obvious fault planes). There is a weak tendency for vertical or side-parallel orientation of elongated

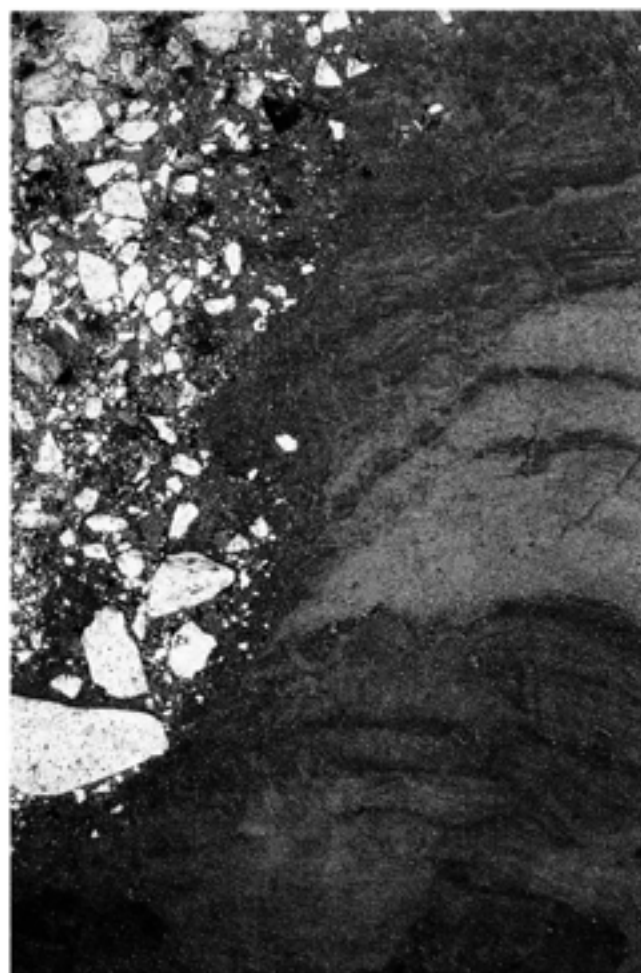


Fig 73 Soft sediment deformation features at the contact between the Slindon Silts and the chalky muds and gravels at GTP 25

chalk particles in the wedge fills. The 'mushroom' tops penetrate well up into the main chalky deposits (above the [0.66] level) and there are signs of fluidisation, with larger particles (including a few flint pebbles) sinking and silt injected upwards. The present author has not yet come across a satisfactory explanation of this phenomenon. Although superficially resembling small ice-wedge casts, the geometry and micro-fabric of the fills are not those of cryogenic features. Although it is difficult to see why fault displacement did not occur, it may be that some cross-slope weakness (fissures) was exploited during the emplacement of one or more bodies of chalk slurry; if the top surfaces 'set' first, confined subsurface erosion might have occurred along the lines of weakness, deepening the wedges until the whole chalky body had drained. The much smaller occurrences in GTP 13 would be consistent with the thinner sediment body and lower slope in this area.

The Unit 5b marls were clearly derived from the weathered chalk cliffs and their unstable talus cones, probably at a time of increasing humidity and possibly cooler temperatures. Proximal facies have common pellets, mesial facies often show some pulses of coarser material, whilst distal facies are composed mostly of

laminated muds. Terrestrial molluscan fragments are present in places, probably including freshwater types. As suggested by Macphail (Chapter 2.6), the laminated occurrences may represent wide, shallow pools.

Unit 5c

These sediments have not been observed by the present author. Macphail describes a short sequence, broadly contemporary with the other Unit 5 deposits, consisting of a shallow fan of sandier material in GTP 17, probably eroded from sediments upslope towards the cliffs.

The Brickearth Bed (Unit 6)

This unit is not present close to the cliffs in Quarry 2 in the GTP 25 exposures. In the north-eastern exposure in GTP 13 1 (Fig 45a), the [4.36–4.43] interval consists of a clayey silt, coarsening upwards to planar (but non-parallel) silt laminations, with tiny cut-and-fill structures; the sediment is moderately calcareous, especially at the base, and matrix colours range from strong brown to reddish-yellow upwards. There is a discontinuous Fe-band at the base and, at or near the top, there is an Mn-band sometimes superimposed upon and sometimes just above a second Fe-band. The next interval [4.43–4.53] consists of silt and fine sand laminations. Minor convolution and microfaulting are common, but where less disturbed, the bedding in the basal portion consists of *c* 7mm thick sets of climbing ripple cross-lamination in-drift (leeside only), with foresets dipping along a bearing of 252°. Higher in this

interval, there are larger scale cross-laminations but the geometry is obscure due to post-depositional effects. Individual laminae in this interval may be weakly calcareous (sometimes with small chalk fragments) or non-calcareous, and may be variably stained on bedding planes with Fe or Mn; matrix colours range from pink to reddish-yellow. There follows another laminated interval [4.53–4.58] which is very similar to the [4.36–4.43] interval; there may be one or more Mn-bands and the whole is moderately calcareous. Yet another cross-bedded interval, similar to the [4.43–4.53] interval, survives later erosion in places just east of GTP 13. Dendritic (terrestrial) root pseudomorphs and bone fragments are present at various levels within the Unit 6 sediments in the GTP 13 area.

In GTP 10 (Fig 49b), the [4.55–4.64] interval consists of strong brown, weakly laminated clayey silts, with isolated small flint particles; the bedding has been strongly distorted/compacted at a later date.

In GTP 5 (Figs 59, 74), the [0.80–0.86] interval consists of reddish-brown laminated clays and silts; the chalky smears at the base have already been noted in the discussion of Unit 5b. The next interval [0.86–1.01] is a reddish brown clayey silt; the deposit was probably originally laminated but was later very strongly distorted into chaotic 'swirls'. There are Mn-stained patches and fragments of bone. The next interval [1.01–1.19] consists of reddish brown silty clays and silts. Despite later deformation and microfaulting, weak current bedding is apparent in most places, with very variable sets of cross-bedding dipping along bearings between 135° and 195°, dip and bearing differing markedly in vertically and horizontally adjacent sets. The next



Fig 74 Thick deposits of the Brickearth Beds west of GTP 5; scale unit 0.5m

interval [1.18–1.44] consists of reddish brown clayey silts, with distorted and obscure (basically laminar) bedding. The whole sequence contains short Mn-stained root pseudomorphs of a very simple (usually non-bifurcating) type, probably referable to herbaceous plants.

The sequence in Q2/A has unfortunately been truncated by quarrying (Fig 61). The surviving interval [1.93–2.20+] comprises strong brown to reddish-brown, contorted muddy silt laminations, with alternations of more or less calcareous material and Mn-flecks. However, at one point to the north-west of the main Q2/A exposure, there are relatively undisturbed zones of very well differentiated and internally well sorted silt/clay rhythmities, set in what appear to be shallow but very broad lenses.

The deformation structures within the area around Q2/A are of interest. On a fine scale, the Unit 6 sediments show internal deformation and even some convolution of the laminae, some of which appears to be syndepositional. However, some of the small scale deformation, together with large scale warping of the unit as a whole, appear to be totally post-depositional (Fig 70). The 5a/6 boundary shows a broad dome and basin morphology (totally discordant with and superimposed upon the 'hummocks' described from Unit 4b and the warping of Unit 4c), with frequencies in the order of 8m, amplitudes of c 0.8m, and no dominant geographical axis (ie the domes are roughly circular); the large-scale pattern of domes could not be observed, although there is a certain regularity. The domes are associated with generally concentric high angle reverse faults, originating within the brickearth but passing downwards to die out before the base of the Unit 4 deposits. It may therefore be said that, within the Q2/A area, there was a long history (from Unit 4b to Unit 6) of lateral shortening and thickening of deposits. However, within Unit 6 there are a number of smaller scale deformational features, associated with the dome margins, with strong horizontal directional properties, including (as seen in the vertical plane): upward drag folds on and quite far beyond the footwalls of only those reverse faults which face south to south-east; southerly to south-easterly-oriented low angle thrusts, with overturned bedding above, or even rootless intrafolial folds; and southerly to south-easterly reverse fault sets with curving, increasingly overturned fault planes and progressive rotation (pseudo-dip increasing to the south or south-east) of the bedding in the sediment interval sandwiched between fault pairs. These features indicate that the last main deformational events in this area involved extreme pressures from above, with a strong southerly to south-easterly drag; such features could not be simply diagenetic (ie due to the settling and compaction of the sediments through time) and must be associated with the actual emplacement of later deposits (see below).

Laminated reddish-brown silt clays, referable to Unit 6, were also observed in places within the westernmost angle of Quarry 1. This sediment is up to 150mm thick and overlies c 120mm of laminated chalky mud (either Unit 6 of 5b), which in turn overlies a typical occurrence of Unit 5a.

Although Macphail (Chapter 2.6) has recognised a degree of pedogenesis affecting Unit 5b in places and although Unit 5b has been partially or fully eroded in other places, from a purely sedimentological point of view the 5b to 6 sequence appears broadly conformable. Three general sub-facies of Unit 6 have been recognised. First, there were episodes of relatively weak, rather irregular and mostly unchannelled flow, producing wide bodies of planar, non-parallel laminated sediment; the current energies were nevertheless a little stronger and more persistent than during Unit 5b times. Second, there were episodes of true fluvial activity, producing cross-bedded units and capable of transporting some sand-sized material; the climbing ripple intervals are typical of rapid deposition dominantly from suspension load, so that streams would then have been pulsing with very turbid water. Streams seem to have been flowing generally westwards in the vicinity of GTP 13 and southwards to south-eastwards in the vicinity of GTP 5. The third facies, observed only in the vicinity of Q2/A consists of rhythmities, probably laid down in shallow pools of still water; given the signs of relatively rapid sedimentation in many exposures of Unit 6 as a whole, it seems likely that the cycles involved were short term, possibly deriving from individual rain storms. Macphail has recognised some pedogenic activity in places during Unit 6 times, so that a generally undulating plain is indicated (not markedly different in purely topographic terms from the Unit 5b landscape), with some zones periodically above water (and perhaps carrying more stable vegetation) and lower zones occupied by meandering and shifting streams, shallow pools and sheets of flood loam (occasionally occupied by low pioneer vegetation).

Before leaving the discussion of Unit 6, it is of interest that Catt (Chapter 2.5) has suggested that the coarse silt mineralogy of all the units from 5 to 11 contains an element that probably derived from the Slindon Sands and Silts (Units 3–4); wind transport onto the Downs is the most likely mechanism, eventually followed by a return southwards due to the various surface processes responsible for the emplacement of Units 5–11. Moreover, in the case of Unit 6, Catt has suggested that a phase of significant weathering, probably under full interglacial conditions, occurred prior to any movement of the regolith off the Downs. Catt has used a simple model of marine transgression/regression, so that an apparent difficulty arises: if Units 3–4 only become available for wind erosion when the regression is well advanced, one would need to postulate a separate, later, interglacial (before the emplacement of Unit 6) to account for the weathering. That there are no bodies of sediment that can be unequivocally

the mass movement events, accompanied by water-escape structures and even transient surface drainage forms in distal exposures. The suite of structures observed would be most likely under a relatively cold climatic regime.

The Fan Gravel Beds (Unit 9)

The Unit 9 Path Gravels (Table 9a) were reported by Roberts (1986) as occurring towards the northern side of the Boxgrove quarries (thickening towards the cliffs), overlying and interstratified with Units 6 and 8. These sediments comprised relatively well sorted, sub-rounded flint fine gravel, with strong cortical alteration; towards the base, seams of matrix-free material occurred, stained almost black with manganese, whilst higher levels had a strong brown silty matrix, with some surviving chalk fragments in places (Fig 26).

In the exposure on the northern side of GTP 13 1 (Fig 45a), the [4.58–4.85] interval comprises chalk pellets and fine flint gravel, coarsening upwards to 30–40mm angular flint gravel, with a very poorly sorted matrix and little internal structure; colours are strongly variegated (Fe–Mn) and the whole is strongly calcareous. The interval contains a few contorted laminated silt lenses. The base of the interval is highly erosive, cutting across both depositional and some post-depositional structures in the underlying Unit 6 sediments. The next interval [4.85–4.96] comprises a tripartite unit of yellowish-red clayey silts, light reddish-brown cross-laminated silts and again clayey silts, the upper and lower divisions being moderately calcareous but the middle division being almost completely carbonate-free. The internal structure is strongly deformed and the geometry of the cross-bedding is obscure. The [4.96–5.30] interval is very similar to the first gravel unit, including a chalky base, and the [5.30–5.35] interval is another clayey silt, with traces of laminations. The local sequence continues upwards in this fashion, the gravel units becoming thicker and the silty units thinner and less continuous. Large decalcification pockets reach down as far as the [5.30] point in some places. Some 6m to the south-east of the deposits just described there is another small exposure of interest. The sequence starts with a discontinuous and very thin, apparently cross-laminated, silt unit followed by a minor gravel lens. Above this is a major channel-fill, with clayier material at top and bottom and well stratified silty material between. These central silts are trough-bedded (individual troughs being 0.1m wide and 0.6–0.7m long) with internal foresets dipping along a bearing of 235°; the lowest point of the channel-form cuts to a level equivalent to the [4.53] point in the main GTP 13 1 sequence. It may also be noted that, in the general vicinity of GTP 13, rare normal microfaults, which cut down through Units 6 and 5 and even into the top of Unit 4, have slip bearings in the range 210°–245°. This observation may be compared with the deformation in Unit 6 deposits in Q2/A, noted above, where drag towards the south-east was dominant (Fig 70).

In GTP 5 (Fig 59), the sequence [1.44–2.69] consists of alternations between dominantly fine angular gravel with silt seams and dominantly clayey silts with gravel/granule stringers. Coarser beds still contain a little chalk, but usually with thick manganiferous crusts. All beds are warped with no obvious directional control. All finer beds contain Mn-replaced root pseudomorphs of a simple, unbranching type, probably referable to herbaceous vegetation. The combined observations in GTP 13 and GTP 5 suggest sedimentation in the form of fan gravels, fining distally, with coarser deposits emplaced by torrential or even debris flow, interspersed with finer material of a basically alluvial type.

The rounding characteristics of this gravel are of interest, since there would appear to have been little opportunity for sound flint to have been so modified during transport within the relatively short catchment available. It seems likely that old gravels, which had already been altered during the Boxgrove interglacial (or earlier), were stripped off the chalk north of the cliffs, their softer weathering crusts permitting rapid rounding during movement over even quite short distances.

Head Gravels and Silt Beds (Units 10 and 11)

Roberts (1986) reported deposits of Unit 10, Calcareous Head Gravel (Fig 77), again thickest towards the north. Chalk fragments of various sizes

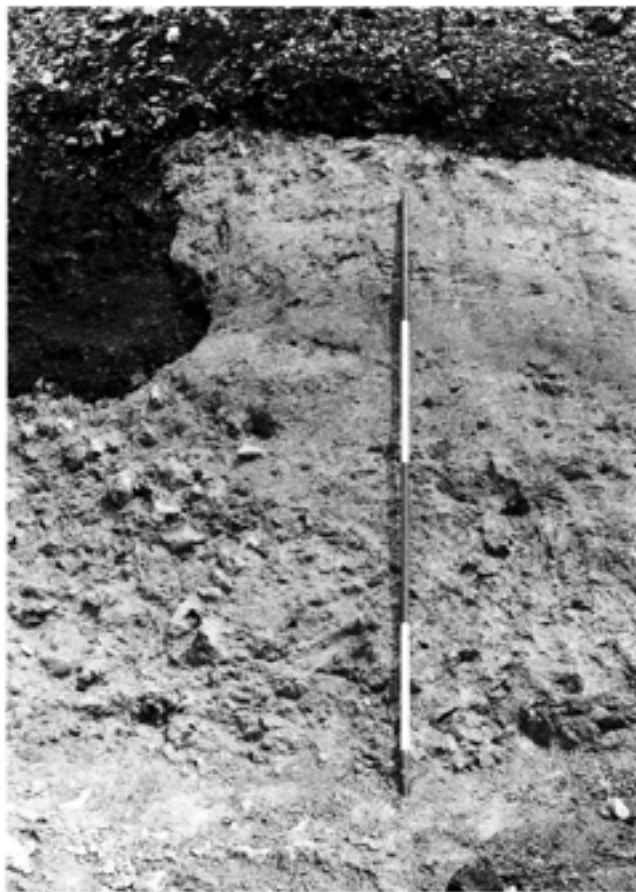


Fig 77 Calcareous Head Gravel, with solution hollow containing the overlying decalcified head gravel; scale unit 0.5m



Fig 76 Q1/A: deformation feature running through the main excavation; scale unit 0.5m

The bedding angles, undulating but otherwise regular bedding planes, and general structure (including weak imbrication in places) imply mass movement, probably in a relatively wet state at times. The emplacement of this deposit seems to have been by increment, since there appear to be surviving traces of true surfaces (annealed and slightly stained i.e. sub-unit 6'3 Fe, Table 9b) (Macphail Chapter 2.6, Roberts Chapter 6.3), in one observed case with minor root pseudomorphs.

In GTP 26 (Fig 48), the intervals [5.92–6.07] have been referred to Unit 5b/6, due to their consistently laminated structure. However, some weakly laminated zones persist a little higher and it would require micro-morphological study to place the 6/8 boundary accurately. The [6.07–6.55] interval is nevertheless marked by an extremely contorted lower boundary, which might well indicate a cryogenic effect. The body of the interval consists of rounded to very well rounded chalk pellets (*c* 10–30mm), with good size sorting at any given level, set in a very pale chalky mud. There is also a noticeable proportion of sub-rounded granules which appear to be reworked lithorelics (a porous clayey chalk mud), together with fragmented calcareous root casts. The sediment is usually matrix-supported but there are some globular zones of clast-support with a few minor fluid injection structures ('flames') near

their upper boundaries. Mass movement may have been quite rapid at times, with some sedimentation as a true slurry.

Within the main Q1/A excavated area, a body of Unit 8 chalk pellets has filled a large trough-shaped feature along a bearing of *c* 190° (Austin and Roberts Chapter 6.2). The surrounding Unit 4 sediments, whilst retaining their original laminations, have suffered massive plastic deformation, with contorted loops of material thrust out laterally, at right-angles to the long axis of the trough. This implies the very rapid emplacement of the chalk pellets over saturated Unit 4 sediments, probably most likely during a period of thawing but when drainage was still impaired by frozen conditions at depth (Fig 76).

During brief observations in the westernmost angle of Quarry 1, a body of chalk pellets was noted which contained, 0.15m up from its base, a heavily contorted but apparently channel-form body (0.2–0.30m wide) of pale chalky silt (not unlike more calcareous facies of the Unit 6 brickearth); the trend was roughly 60°. The feather-edge of another such silt lens was observed within the chalk pellets in an exposure just west of Q1/A.

There is therefore a global trend towards finer and more rounded chalk fragments away from the cliffs in Unit 8, accompanied by signs of increasing fluidity of

the mass movement events, accompanied by water-escape structures and even transient surface drainage forms in distal exposures. The suite of structures observed would be most likely under a relatively cold climatic regime.

The Fan Gravel Beds (Unit 9)

The Unit 9 Path Gravels (Table 9a) were reported by Roberts (1986) as occurring towards the northern side of the Boxgrove quarries (thickening towards the cliffs), overlying and interstratified with Units 6 and 8. These sediments comprised relatively well sorted, sub-rounded flint fine gravel, with strong cortical alteration; towards the base, seams of matrix-free material occurred, stained almost black with manganese, whilst higher levels had a strong brown silty matrix, with some surviving chalk fragments in places (Fig 26).

In the exposure on the northern side of GTP 13 1 (Fig 45a), the [4.58–4.85] interval comprises chalk pellets and fine flint gravel, coarsening upwards to 30–40mm angular flint gravel, with a very poorly sorted matrix and little internal structure; colours are strongly variegated (Fe–Mn) and the whole is strongly calcareous. The interval contains a few contorted laminated silt lenses. The base of the interval is highly erosive, cutting across both depositional and some post-depositional structures in the underlying Unit 6 sediments. The next interval [4.85–4.96] comprises a tripartite unit of yellowish-red clayey silts, light reddish-brown cross-laminated silts and again clayey silts, the upper and lower divisions being moderately calcareous but the middle division being almost completely carbonate-free. The internal structure is strongly deformed and the geometry of the cross-bedding is obscure. The [4.96–5.30] interval is very similar to the first gravel unit, including a chalky base, and the [5.30–5.35] interval is another clayey silt, with traces of laminations. The local sequence continues upwards in this fashion, the gravel units becoming thicker and the silty units thinner and less continuous. Large decalcification pockets reach down as far as the [5.30] point in some places. Some 6m to the south-east of the deposits just described there is another small exposure of interest. The sequence starts with a discontinuous and very thin, apparently cross-laminated, silt unit followed by a minor gravel lens. Above this is a major channel-fill, with clayier material at top and bottom and well stratified silty material between. These central silts are trough-bedded (individual troughs being 0.1m wide and 0.6–0.7m long) with internal foresets dipping along a bearing of 235°; the lowest point of the channel-form cuts to a level equivalent to the [4.53] point in the main GTP 13 1 sequence. It may also be noted that, in the general vicinity of GTP 13, rare normal microfaults, which cut down through Units 6 and 5 and even into the top of Unit 4, have slip bearings in the range 210°–245°. This observation may be compared with the deformation in Unit 6 deposits in Q2/A, noted above, where drag towards the south-east was dominant (Fig 70).

In GTP 5 (Fig 59), the sequence [1.44–2.69] consists of alternations between dominantly fine angular gravel with silt seams and dominantly clayey silts with gravel/granule stringers. Coarser beds still contain a little chalk, but usually with thick manganiferous crusts. All beds are warped with no obvious directional control. All finer beds contain Mn-replaced root pseudomorphs of a simple, unbranching type, probably referable to herbaceous vegetation. The combined observations in GTP 13 and GTP 5 suggest sedimentation in the form of fan gravels, fining distally, with coarser deposits emplaced by torrential or even debris flow, interspersed with finer material of a basically alluvial type.

The rounding characteristics of this gravel are of interest, since there would appear to have been little opportunity for sound flint to have been so modified during transport within the relatively short catchment available. It seems likely that old gravels, which had already been altered during the Boxgrove interglacial (or earlier), were stripped off the chalk north of the cliffs, their softer weathering crusts permitting rapid rounding during movement over even quite short distances.

Head Gravels and Silt Beds (Units 10 and 11)

Roberts (1986) reported deposits of Unit 10, Calcareous Head Gravel (Fig 77), again thickest towards the north. Chalk fragments of various sizes

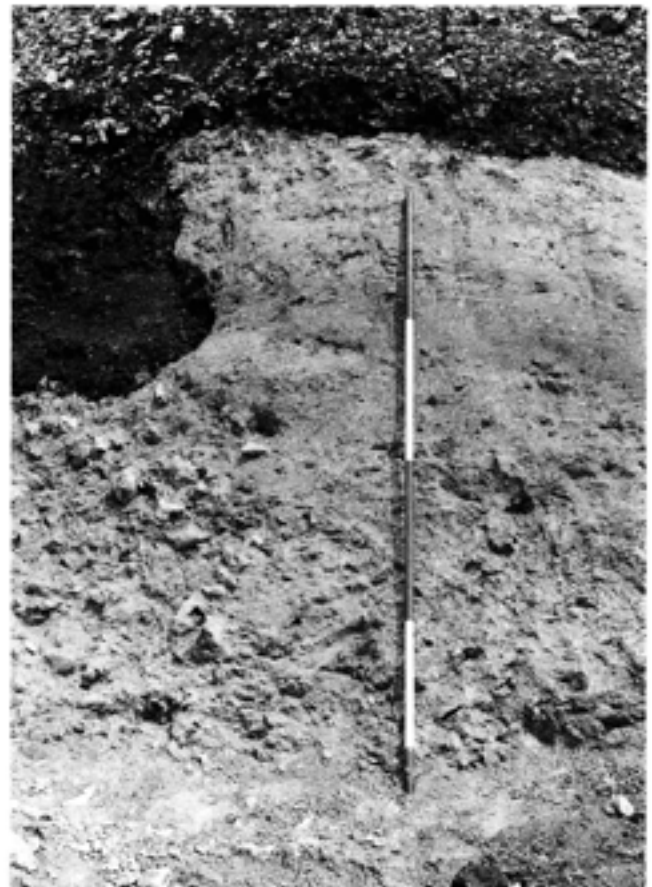


Fig 77 Calcareous Head Gravel, with solution hollow containing the overlying decalcified head gravel; scale unit 0.5m



Fig 78 Lower Head Gravel unconformably overlying the Slindon Silts; note frost wedge to right of scale; scale unit 0.5m

were included, and a degree of decalcification was observed to have occurred after each phase of deposition. The Unit 11 Decalcified Head Gravels (Fig 78) were reported as crudely stratified angular flint, sometimes very coarse, set in a reddish-brown silty clay matrix. Within these gravels, seams of brickearth-like material were observed; three major occurrences, to thicknesses of up to 2m, being termed the Lower, Middle, and Upper Silt Beds (Fig 79; Table 9a). The emplacement of the Unit 11 gravels, and probably that of the Unit 10 gravels too, was both a protective and erosive event. In Quarry 2 a major unconformity developed towards the south, cutting well down into the Slindon Silts and Sands, sometimes at points as little as 250m from the cliff-line (Roberts Chapters 2.1 and 2.7). Conversely, to the north of this unconformity the fine-grained sediments were protected by the deposition of the mass movement gravels.

The present author has observed these gravel deposits only at a small number of locations, mostly in the southern part of the site.

In 1987, a temporary mineral working face was observed in the western part of Quarry 2, some 80m north and north-west of SEP 3 (Fig 4). At a point estimated to be 5–6m above the expected level of Unit 5a (this marker not being present in the actual face but nevertheless being observed within 15m laterally of the base of the exposure of interest), there is a slightly contorted but persistent unit of clayey silt, up to 0.2m thick, interbedded with the gravels (Lower Silt Bed).

In the reddish gravels immediately above the silt, strong patterned ground has developed. In this the only available section, the pattern takes the form of contiguous stone nests, 1.0–1.75m deep and 1.5–2.25m wide. Flint gravel particles lie tangentially to the roughly semi-circular form of each nest, so that their major planes lie horizontally at the base but rotate progressively towards the vertical as one passes upwards around the sides of a nest. Nests sometimes show particle size sorting, with considerably finer material concentrated in the core. Because this exposure is roughly perpendicular to the probable palaeoslope, the plan pattern of these features cannot be observed; either stone polygons or stone stripes are involved, depending upon the slope. The patterned ground, an obviously cryogenic feature normally observed only in areas of permafrost, persists laterally along at least 100m of gravel exposure, presumed to represent part of Unit 11.

On the northern side of Quarry 1, from the middle to the eastern end, major silty clay seams were briefly observed high in the gravel sequence; these are silt beds of the Eartham Upper Gravel Member (Table 9a). These deposits are poorly stratified pellet muds; the pellets are now highly compressed but would have ranged in size from sand to granules and occasionally even larger forms. Such fabric suggests mass erosion in an unstable landscape (probably including the cutting of ravine-like features at the source), with transport by rapid sheet flooding or even debris flow. Most of the

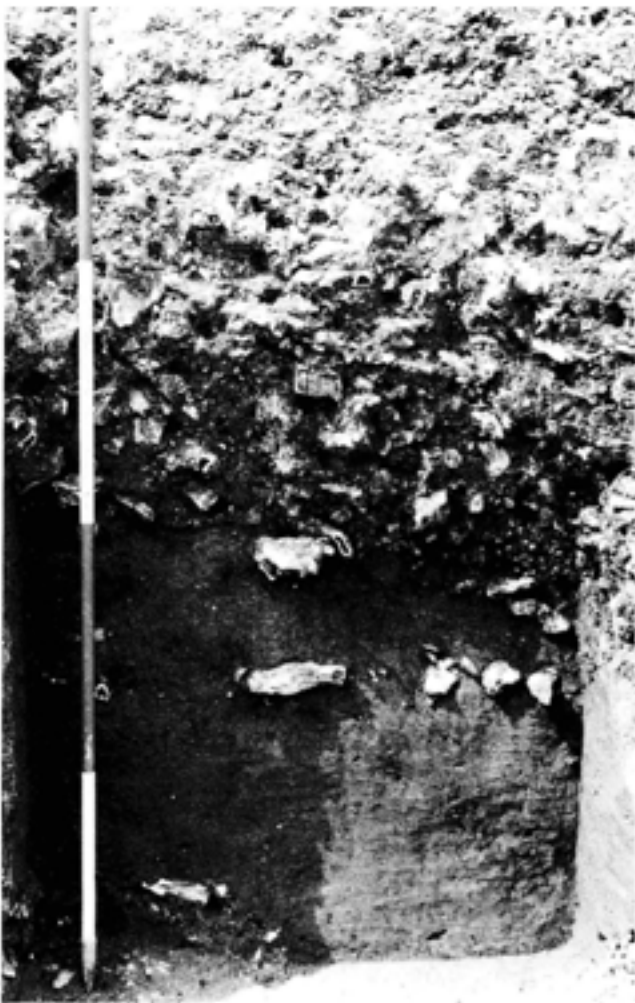


Fig 79 Upper Silt Bed between the Upper Middle and Upper Head Gravels. This unit contains the uppermost archaeological horizon at the site; scale unit 0.5m

pellets are too large to be accounted for by aeolian processes. There are nevertheless common root pseudomorphs in these beds (Catt Chapter 2.5, Macphail Chapter 2.6).

The beds of the Eartham Upper Gravel Member deserve much more detailed study (Lewis in Roberts *et al* in prep), but on present evidence an overall description as mass movement gravels would appear suitable. A variety of energy levels (solifluction, creep, wash, sheet flow, temporary channelled flow and debris flow) are indicated but there are no signs of persistent fluvial activity. Catt (Chapter 2.5) has reported a dominantly local mineralogy and there is therefore no reason to suspect that a wider catchment than the Chalk Downland generally north of Boxgrove was involved. Future study may identify more temperate episodes within the Chalk Pellet Bed sequence (Macphail Chapter 2.6, Parfitt Chapter 4.3), although micro-morphological work tends to discount this (Chapter 2.6), for the upper units of the member. The emplacement of the bulk of this material would have been a cold climate phenomenon.

Conclusion

In passing, a brief reference may be made to the hypothesis, voiced at various times (Kellaway *et al* 1975) in the past concerning Boxgrove and other South Coast sites, that cold climate (glacial period) waters may have been responsible for some at least of the deposits. First, the Slindon Sands at Boxgrove are unequivocally a marine phenomenon. Second, there is no trace whatsoever of drift-ice action (eg drop stones, coarse lenses or 'seed beds' lacking in current structures, erratics, berg ploughing or pitting, etc), pressure effects from littoral ice (eg compressional beach ridges, mud injection structures, mud 'beaches', etc), or patterned ground or other cryogenic structures on exposed beaches. Third, the palaeontology, both marine and terrestrial, could not accommodate such a hypothesis, especially given the patent lack of regional-scale unconformities in the Boxgrove marine sequence. Fourth, there is no evidence, either at Boxgrove or anywhere else in Sussex, for the enormous degree of uplift, followed or preceded by a similar degree of downthrow, which would be required to bring glacio-marine and full interglacial deposits into such close altitudinal proximity.

The colour shift from Cycle 1 to Cycle 2 is consistent over all exposures at Boxgrove and deserves some comment in its own right. The 'bulk' shift is quite subtle and easier to see in undisturbed field exposures than in small hand samples. The Cycle 1 sediments, especially when they consist of cleaner sand, usually have a formal base colour of pink (10YR 7/4) but there is often a bluer/greyer, almost 'bruised' or 'dusky' tinge to them. The Cycle 2 sediments, again especially when sandy, are more variable in the pale to medium brown range (7.5-10YR 5-7/3-4), individual grains and the material seen in bulk often having a stronger, slightly 'rusty' tinge. It seems unlikely that there is a true lithological (involving different source rocks) reason for this shift (Catt Chapter 2.5), although mineralogical studies would be needed to test this suggestion. It seems more plausible that the Cycle 1 sediments are mineralogically immature (closer to simple rock debris), whilst the Cycle 2 sediments have been subjected to more advanced 'weathering', partially during marine recycling and partially during pedological modification on land. Cycle 2 almost certainly has a different balance of secondary iron minerals, which perhaps indicates the increased influence of stable plant and endobiont communities (both marine and terrestrial) in the immediate catchment, no longer subject to such violent marine erosion/encroachment of the initial transgression. A differential in the concentration and state of manganese oxides may also play a part in this colour shift, with finely divided manganese (perhaps mostly as a replacement mineral for chalk particles) perhaps being slightly more common in Cycle 1.

2.4 Analysis of the raised beach gravel deposits at Boxgrove and related sites

D R Bridgland

Introduction

The raised beach and other gravel deposits exposed at Boxgrove, and indeed the gravels of lower raised beaches in this part of southern England, appear, at first impression, to be decidedly dull. It is immediately apparent that they contain little else but flint, which has been derived in huge quantities from the chalk that forms the local bedrock. This first impression would be wrong, however. There is much to be learned from studies of the make up of these gravels. Rare non-flint clasts may have important implications for the Quaternary history of southern Britain and, at the very least, tell us something about the palaeogeography of the Channel region during the Middle and Late Pleistocene. At a more mundane level, examination of the shape, or more particularly the angularity/roundness, of the flints can help to determine the environment of deposition and provide information on transport history, current energies and other palaeoenvironmental factors.

It has long been recognised that many, if not all, of these gravels contain rare clasts of exotic rocks, and such rocks have also been found on the modern foreshore. The term exotic is used here to describe these lithologies, which are foreign to this part of southern England, instead of the often-used term 'erratic', which has, to many Quaternary specialists, connotations of glacial derivation. Many earlier workers have indeed considered glacial transport in one form or another to have been responsible for the introduction of these rocks into the region, but this remains to be demonstrated without equivocation. The best discussion of the evidence is probably that by Reid (1892, 353), who favoured the agencies of 'shore-ice and frost alone'. This was despite his having found a striated block at Medmerry, near Selsey (Fig 2). The fact that this was identified as 'Bognor Rock', a hard calcareous lithology from the local Palaeogene (Tertiary), may have influenced Reid's interpretation. The main advocates of a fully-fledged English Channel glaciation to explain phenomena such as these were Kellaway *et al* (1975).

Truly exotic clasts are too rare at Boxgrove to be encountered in samples taken for gravel analysis, but they have been recovered by scrutinising exposures and spoil heaps, and have even been encountered in trowelling surfaces within the sedimentary sequences during the course of archaeological excavation. In the latter case such material occurs as isolated clasts within generally non-gravelly sediments; it clearly constitutes a much higher proportion of the (admittedly small) gravel component in such beds than of the flint-rich beach gravels. Any explanation of its origin must seek to explain this phenomenon.

Determining the provenance of these exotic rocks is not straightforward by any means. They are often in advanced states of decay, the result of weathering since deposition, and in many cases they are extremely small. Both of these factors make identification difficult, as any distinctive features of the source rock may not be apparent in the clast. In any case, many rocks are insufficiently distinctive for their provenance to be determined with precision. Even when a good match seems to exist between an exotic clast and a potential source outcrop, it is necessary to demonstrate that an indistinguishable lithology cannot be located elsewhere. It is worth quoting from Wells (in Wells *et al* 1947, 211), in his review of the types of exotic pebbles found in the Lower Cretaceous, and of their likely provenances:

'In the course of this work the writer has come to appreciate the serious limitations of attempting correlation on the evidence of mere petrographic similarity. The value of such evidence is directly proportional to the rarity of the rock-type concerned. It may be laid down as axiomatic that with such common and widely distributed rock-types as quartzites, sandstones and cherts, it is not sufficient to demonstrate that a certain pebble resembles, however closely, a known source-rock, but that it is dissimilar from all others of the same type. In the writer's opinion this calls for a far greater detailed knowledge of the variation of such rocks than anyone can reasonably be expected to possess.'

Although agreeing with Wells's sentiments, the present author has attempted to show that certain distinctive types of chert can be separated one from another and can, as a result, be of great value in providing evidence for the provenance of many Quaternary gravels in southern and eastern England (Bridgland 1986a; 1990a). It is quite possible that certain igneous and metamorphic rocks are sufficiently distinctive to provide detailed provenance information, but the varieties of such rocks are considerably more numerous than with cherts, and Wells's point about whether anyone can be expected to possess the necessary knowledge again comes to the fore.

Analyses of gravel samples: clast lithology

History of research of this type

Systematic analysis of gravel deposits has a rather short history in Britain; although some Victorian geologists quoted proportions of the various components present in certain gravels (eg Prestwich 1890; Shrubsole 1898), they gave few details of how they arrived at these figures. Many of these early workers collected any rare exotic clasts that came to their attention and provided lists of these. For example, John Brown of

Stanway, discoverer of the Clacton Channel Deposits, published a very early list of foreign rocks encountered in the drift of Essex (Brown 1837). British geologists became very interested in this type of study in the middle years of the present century, when papers were published on exotic rocks found in various Cretaceous formations, including the Hastings Beds (Allen 1960; 1961), the Lower and Upper Greensand (Hawkes 1943; Wells *et al* 1947) and the Chalk (Hawkes 1951). The suggested explanations for the derivation of some of these, given that there can have been no glaciation during the Cretaceous, may be of relevance to the explanation of the occurrences in the Sussex raised beaches (see below).

Systematic studies of Quaternary gravel composition began with analyses of fluvial deposits, which generally have a more varied composition and therefore promise more obviously meaningful results. S H Warren, who, coincidentally, followed up John Brown's discovery by devoting much of his life's work to studying the Clacton Channel Deposits, clearly carried out somewhat crude 'stone counts', publishing a table of such results (Warren 1957). His segregation of different types of flint was influential in persuading the present author to proceed along similar lines. In the Quaternary of southern Britain, the first application of the technique of identifying and counting stones, or clast-lithological analysis, in the form in which it continues to be used, was by Hey (1965). Hey was the first to divide his samples into size-ranges, using gravel sieves, and the range he adopted for most of his work (Hey 1965; 1967; 1976; 1980; 1986), 16–32mm, is still employed today. In order to obtain larger numbers of rare exotic clasts, Hey (1976) also studied smaller clasts, in the 10–16mm size-range. This is close to the 11.2–16mm range utilised by a number of more recent workers (Green and McGregor 1978; 1983; Maddy *et al* 1991). These two size-ranges, 16–32mm and 11.2–16mm, are based on whole or half phi (ϕ) divisions (the ϕ scale of particle size is based on the halving, for $+\phi$, or doubling, for $-\phi$, in successive whole ϕ units of size from 1mm, which is the arbitrary zero point of the scale, 0ϕ). They were both recommended for future studies of this type in the Quaternary Research Association's technical guide on the application of clast-lithological analysis (Bridgland 1986b).

Method of application to samples from the Boxgrove beach and related deposits

Procedures for sampling and processing samples for clast-lithological analysis followed the recommendations of the above-mentioned technical guide (Bridgland 1986b). Sampling locations are recorded elsewhere in this volume (Figs 4 and 42a). The recommended minimum sample size of 250–300 clasts has been obtained where possible, and generally exceeded (Table 11). The larger of the two size-ranges recommended by the guide, 16–32mm (see above; Bridgland 1986b), has

been adopted. This was selected because the limited existing data from the region (Bridgland 1990b), with which comparison was clearly desirable, used this size-range. The author had also compiled a substantial database of angularity/roundness analyses of flint, a technique that had clear potential for studies of the flint-rich Sussex gravels. One of several known drawbacks of this size-range, in comparison with the smaller 11.2–16mm material, is that exotic material is often, but not always, present in larger quantities at smaller sizes. In addition to the advantages of comparison with previous work, already explained, it was considered that exotic material was so infrequent in the gravels to be studied that the use of the smaller size fraction was likely to be of little benefit in this respect. Assessment of material collected from wider examination of the deposits, rather than from discrete samples, would clearly be necessary, so it was decided to rely on this to provide a picture of the exotic component and to collect 16–32mm samples for systematic analysis, mainly of the flint component. In retrospect, the fact that very occasional non-flints were encountered in the samples suggests that the analysis of the 11.2–16mm component might have provided further information on these, such as an impression of their true frequency. Very large samples would have been required, however, involving considerable work sifting through huge numbers of the ubiquitous flint clasts, for a relatively small return of new information.

Samples for clast analysis were duly collected from the beach gravels (Fig 42a) exposed in the 'cliff section' at Earham Pit, Boxgrove (a total of five samples), and from test pits in the lower-level Aldingbourne beach (Bates *et al* 1997), at Aldingbourne Park Pit and at Brooks' Field (Figs 8, 21) (SU 908 071, SU 908 068). A sample of the Fan Gravel Bed (Path Gravels) (GTP 25 1) was also analysed, by way of comparison (Tables 9a, 11; Fig 42a).

Results

As explained above, two types of clast analysis were carried out in tandem; a straightforward lithological analysis, to determine the nature, identity and likely provenance of the gravel material, and an angularity/roundness analysis of the flint component (Table 12), designed to assess the degree to which clasts have been subjected to attrition and abrasion in a littoral environment. The results of all these various analyses are set out in Tables 11 and 13, which also include details of additional samples, from other sites, that are of value for the purpose of comparison.

The lithological analyses of the Boxgrove and Aldingbourne beach gravels confirmed the visual impression that these deposits are both composed almost entirely of flint. In only one sample, from the Boxgrove beach Boxgrove 2, did flint constitute 100% of the total gravel material, however. The other samples from the Boxgrove beach gravel each contained

Table 11 Clast lithological analysis data from gravels in the Boxgrove area (the Bembridge raised beach and Priory Bay gravel, both from the eastern end of the Isle of Wight, are included for comparison)

¹ Beach pebbles, of Pleistocene or Tertiary origin, that can be separately recognised as reworked; * Cannot be separately recognised; + Not separately recorded

locality/sample	nodules	flint %			total	chert %			other %				total (n)
		beach ¹	broken			greensand	Jurassic	Rhaxella	qtz/qrtzite	igneous	chalk	other	
Boxgrove 1	18.3	*	+	99.8		0.2							619
Boxgrove 2	47.3	*	6.7	100.0									357
Boxgrove GTP 25 1	26.5	0.0	1.0	80.2						19.8			298
Boxgrove GTP 25 2	27.9	*	5.4	99.0						1.0			294
Boxgrove GTP 25 3	24.4	*	6.8	99.6	0.2					0.2			619
Boxgrove GTP 25 4	38.7	*	7.3	99.6						0.4			274
Brooks' Field 1	12.9	*	+	99.3	0.5	0.1		0.1					781
Brooks' Field 2	16.3	*	4.8	99.6		0.4							547
Aldingbourne Park 1	26.8	*	3.5	99.1	0.6	0.3							339
Priory Bay 1	12.5	7.3	+	90.9	5.7	1.8	0.3	1.3					384
Priory Bay 2	7.6	11.3	+	86.0	12.5	0.8					1.6		513
Bembridge 1	3.8	*	+	91.5	3.8	2.0	0.4	1.2	0.7		0.4		557
Bembridge 2	7.1	*	+	84.0	7.5	3.2	0.1	2.0	0.6		2.6		693

between one and three non-flint clasts (Table 11). These were as follows: Boxgrove 1 contained a single pebble that was identified as chert, probably Jurassic; Sample GTP 25 2 included three pebbles of rather soft chalk, clearly of local derivation; Sample GTP 25 3 also contained chalk, this time a single hard clast, as well as a sub-rounded pebble of Greensand chert. Sample GTP 25 4 again contained a single locally-derived chalk clast. No chalk was found in the samples from the Aldingbourne beach, but cherts were again encountered, including examples of both Jurassic and Greensand type (Table 11).

The single Fan Gravel Bed sample GTP 25 1 was found to contain 19.8% chalk. This material was soft and fragmentary, showing little evidence of shaping during transport over even a short distance (the shape of soft clasts is rapidly modified during transport). It was difficult to process the sample without damaging these soft chalk clasts, so rendering them smaller than the 16mm sieve mesh size. The recorded chalk count is thus likely to be an underestimate.

Analyses of gravel samples: angularity/roundness

Method of application

The angularity/roundness analysis of flint clasts within these various samples was carried out according to procedures described by Bridgland (1983; Fisher and Bridgland 1986). This method is a modification of that proposed by Powers (1953) for sand grains, but is adapted for flint clasts of 16–32mm size. The same six categories recognised by Powers were used, but these were redefined for the application to flint pebbles (Fisher and Bridgland 1986; Table 12). A type collection

was assembled to provide a visual standard with which to compare borderline clasts (Bridgland 1983). In this way it was hoped to minimise variance between results of analyses carried out at different times.

The interpretation of these results is hampered by an almost complete absence of comparable published data. The author, however, has compiled a database of similar analyses over the past 15 years, including data from known fluvial and glaciofluvial gravels, known marine gravels and deposits of less certain origin. It is hoped that the results of this work will be published separately, but it is appropriate for a summary to appear here.

Problems with the technique

Subjectivity

Although Table 12 outlines the method for classifying clasts into the six categories, it will be noted that certain of the boundaries are defined more easily than others. Unfortunately it is the boundaries that require more subjective judgements that are the most meaningful in terms of the aqueous transport history of the clasts (see below).

Another area in which the problem of subjectivity arises is in deciding whether small-scale 'damage' to a clast should be considered in the analysis. Thus there is a continuum between 'chatter marks' on rounded clasts, which are not considered, and small angular cavities arising from both abrasion/attrition during transport and frost-pitting; the edges of these can be assessed as very angular to sub-rounded. Since the analysis is intended to assess the most recent transport history of gravel deposits, such small-scale damage is considered to be pertinent and it has therefore been taken into account when categorising clasts.

Table 12 Angularity/roundness categories, based upon verbal descriptions by Schneiderhöhn (1954, in Pryor 1971) of the categories devised by Powers (1953). Simplified from Fisher and Bridgland (1986)

<i>angularity/roundness</i>	<i>description</i>
well rounded	no flat faces, corners or re-entrants discernible; a uniform convex clast outline
rounded	few remnant traces, with corners all gently rounded
sub-rounded	poorly to moderately developed flat faces with corners well rounded
sub-angular	strongly developed flat faces with incipient rounding of corners
angular	strongly developed faces with sharp corners
very angular	as angular but corners and edges very sharp, with no discernible blunting

To a large extent the problems of subjectivity can be minimised by the use of a type collection of standard and extreme examples of each category. This is especially recommended if more than one operator's results are to be combined, although the author is solely responsible for the data presented here.

Differences in hardness

The restriction of the analyses to flint clasts is intended to ensure that the differences in the proportions of different rocks do not bias the results. Flint is the most useful rock type to study in southern and eastern England because of its ubiquity in gravelly deposits; it is also useful in that there is a clear limit to how much rounding of fresh flint has proceeded in the fluvial environment (see below). However, it has been observed that weathered flints are often more rounded than fresher clasts, suggesting that the proportion of weathered flint in a sample may be a source of bias (this is the case only when the flint has been weathered prior to incorporation in the deposit). The proportion of weathered flint recorded in the lithological analysis of the sample (where available) provides an approximate guide, but this category includes all flints that have surfaces sufficiently weathered as to preclude their identification as pebble, nodular or broken surfaces. Clasts having such surfaces may have other fresher faces and, as it is the most recent 'damage' that is assessed in the angularity/roundness analysis, the latter might not be affected by the weathering.

Reworking

Clasts that are reworked from earlier deposits without modification may bias the results of angularity/roundness analyses. This is only likely to be a problem when the reworked clasts cannot be recognised as such. For example, fluvial gravels in the London Basin often

contain significant quantities of flint pebbles reworked from the marine Palaeogene. These pebbles are easily recognised, as they are predominantly highly rounded and they have crescentic percussion scars ('chatter marks'), classic features of beach pebbles. They contrast with the other flint in the gravels (nodular and broken flint), although weathering may obscure the distinction. The angularity/roundness of broken Palaeogene pebbles can be assessed along with the flint from other sources, but unbroken pebbles should be assessed separately, the results pertaining to the environment of deposition in the Palaeogene rather than in the Pleistocene. A separation of this type is employed in Table 13b, which should be compared with Table 13a, particularly in respect of data from the non-marine gravels of the Thames basin. Data from the Thames basin should also be compared with that from the Ingham Gravel of Suffolk, laid down by a pre-Anglian river flowing from the Midlands and therefore carrying no reworked flint in the form of marine pebbles.

It was impossible to identify separately a reworked Palaeogene element in the Boxgrove and Aldingbourne beaches, although it is strongly suspected that a small one exists, particularly in the latter. A number of the most rounded clasts in the samples had notable weathered 'crusts', with a characteristic faded grey coloration typical of the reworked Palaeogene pebbles encountered in Thames gravels. The distribution of angularity/roundness classes in these counts is normal, with the minor exception of the well-rounded category in Brooks' Field 1 (Fig 8), which exceeds the rounded category in this particular count (Table 13; Fig 80a). This latter detail, and the high incidence of rounded and well-rounded pebbles in the otherwise poorly rounded Aldingbourne beach (see below), would seem to confirm the presence of a small reworked Palaeogene component.

Post-depositional damage

Post-depositional damage to clasts may have occurred as a result of freezing and thawing during periods of permafrost (frost damage) and during sampling (the latter is largely avoidable if care is taken, except with borehole samples; breakage is often along lines of incipient frost damage). The results of both types of damage will be to create clasts belonging to the 'very angular' category. The proportion of very angular clasts is found to vary considerably between samples, factors such as proximity to the land surface having an important effect (more frost-damaged flint is found nearer the surface). If the main aim of the analysis is to assess the role of aqueous transport in modifying clast angularity, a good policy is to exclude the flints classified as very angular from the interpretation (Table 13b).

The various problems encountered in interpreting these results have led to a decision not to attempt the calculation of any of the numerical indices or coefficients of angularity/roundness advocated by some

Table 13a Angularity/roundness of flint from the Boxgrove raised beach and other Sussex beaches. Data from the Fan Gravel Beds (Unit 9) (Boxgrove GTP 25 1, Fig 42a) and gravel samples from various sources are included for comparison. All flints as % total flint (excluding unmodified nodules). Sources: Bridgland 1983; 1988; 1994; Bridgland and D'Olier 1995; Bridgland *et al* 1995a; 1995b

Key to table: wr=well rounded, r=rounded, sr= sub-rounded, sa=sub-angular, a=angular, va=very angular

site	wr%	r %	sr %	sa %	a %	va %	total	location
Boxgrove project								
Boxgrove 1	1.9	5.8	23.4	29.9	21.0	18.0	618	(Raised beach)
Boxgrove 2	1.4	7.4	38.5	28.8	19.1	4.8	351	(Raised beach)
Boxgrove GTP 25 1		0.4	4.6	16.4	44.5	34.0	238	(Fan Gravels)
Boxgrove GTP 25 2	2.1	8.9	34.0	34.0	13.1	7.9	291	(Raised beach)
Boxgrove GTP 25 3	0.2	2.1	18.2	43.1	25.1	10.9	619	(Raised beach)
Boxgrove GTP 25 4		4.4	19.2	35.4	32.1	8.9	274	(Raised beach)
Brooks' Field 1	2.6	2.5	8.1	37.6	23.6	25.6	774	(Raised beach)
Brooks' Field 2	1.7	5.9	18.7	45.3	21.9	6.6	547	(Raised beach)
Aldingbourne Park 1	2.4	6.0	14.0	45.4	19.1	13.1	335	(Raised beach)
Samples from other Pleistocene beach gravels (including supposed beach gravels)								
Bembridge 1	9.6	21.0	30.5	24.6	11.4	2.9	509	(Raised beach)
Bembridge 2	4.6	11.7	30.0	35.9	13.6	4.3	582	(Raised beach)
Priory Bay 1	2.3	3.2	4.6	51.0	28.4	10.6	349	(?Raised beach)
Priory Bay 2	3.7	3.0	5.1	36.8	32.9	18.6	435	(?Raised beach)
Eye Gravel Pit			0.9	14.2	65.8	19.1	225	(March Gravels)
Southwold 1	37.7	27.1	16.9	10.7	3.2	4.4	591	(Westleton Beds)
Samples from other Pleistocene gravels								
Barling 1	6.1	2.5	1.2	38.4	26.1	25.7	245	(Late Middle Pleistocene)
Barling 2A	11.4	5.1	1.8	17.2	13.6	50.9	273	(Thames-Medway)
Barling 2B	10.7	6.5	2.1	31.2	22.5	27.0	666	
Barling 3	13.4	5.7	1.7	27.0	21.7	30.4	470	
Dammer Wick 1	12.7	5.2	0.4	24.0	15.3	42.4	229	
Barvills Farm 1	24.8	7.2	3.1	24.1	21.2	19.6	638	(Lower Thames)
Shakespeare Pit 2A	24.1	6.9	1.3	18.5	22.3	26.8	622	(River Medway)
Holland Haven 1A	4.1	2.5	0.9	25.6	26.2	40.8	321	(Kesgrave Group)
Holland Haven 1B	9.7	1.4	1.4	33.8	16.7	37.0	216	(Early Middle Pleistocene)
Holland Haven 2	3.9	1.8	0.7	22.4	26.5	44.7	434	
Cooks Green 1A	3.1	1.5	1.9	44.7	29.6	19.2	521	(Pleistocene Thames)
Cooks Green 1B	4.8	3.2	1.7	41.9	29.8	18.6	413	(Thames-Medway)
Cooks Green 2	11.6	3.1	1.2	41.3	28.4	14.4	327	
Rampart Field 4				18.3	54.5	27.2	226	(Ingham River)
Knettishall 2			1.5	14.1	52.0	32.3	474	(Glacial outwash)
Samples from Palaeogene marine gravels								
Aveley A13 2.1	58.2	22.1	4.1		1.0	14.6	294	(Woolwich Beds)
Aveley A13 5.2	50.0	35.1	5.6		0.4	9.0	268	
Aveley A13 7.3	65.4	18.7	3.7	0.9		11.2	107	

authors (for review, see Fisher and Bridgland 1986). Instead, an assessment from the raw data or from histogram plots of this data is preferred.

The results from the five counts from the Boxgrove beach, taken in combination, would seem to point to the sub-angular category as the modal class; this is the mode in four of the five samples, although in one of these (GTP 25 2) modal status is shared with the sub-rounded class (Table 13). The remaining count, Boxgrove 2, has its mode in the sub-rounded class.

The three samples from the Aldingbourne Raised Beach reveal a greater degree of angularity, on average,

than the Boxgrove beach, although there is an overlap between the two data sets; the most angular Boxgrove sample, GTP 25 3 was slightly more angular than the most rounded sample from the Aldingbourne beach, Brooks' Field 2 (Table 13).

The sample from the Fan Gravel Bed (Path Gravels, GTP 25 1) comprised nearly 80% angular or very angular flint, with only 5% rounded or sub-rounded (none well rounded). Much of the rounded and sub-rounded flint was highly weathered and might have been more readily rounded as a result.

Table 13b Angularity/roundness of flint, using the same samples as Table 13a but shown as % total broken flint, including broken reworked pebbles (ie without whole reworked beach pebbles and nodules), with the va category excluded. Reworked unbroken beach pebbles, where separable, are shown together with whole nodules in the right hand part of the table, as % of total broken flint

Key to table: wr=well rounded, r=rounded, sr=sub-rounded, sa=sub-angular, a=angular, nods=unmodified nodules. NB The entries for Boxgrove 1 and 2 and Priory Bay 2 are corrections of those published previously (see references in Table 13a)

site	wr	fresh and broken reworked				a	wr	unbroken reworked			nods
		r	sr	sa	r			sr	sa		
Boxgrove project											
Boxgrove 1	2.3	7.1	28.2	36.6	25.8					0.3	
Boxgrove 2	1.5	7.8	40.4	30.3	20.1					1.7	
Boxgrove GTP 25 1		0.6	7.0	24.8	67.5					0.6	
Boxgrove GTP 25 2	2.2	9.7	36.9	36.9	14.2						
Boxgrove GTP 25 3	0.2	2.4	20.5	48.6	28.3					0.5	
Boxgrove GTP 25 4		4.9	21.1	38.9	35.2					0.4	
Brooks' Field 1	3.9	3.7	12.3	56.8	35.7					0.2	
Brooks' Field 2	2.1	7.5	23.9	57.6	28.1					0.2	
Aldingbourne Park 1	3.3	8.1	19.2	62.0	26.1					0.4	
Samples from other Pleistocene beach gravels (including supposed beach gravels)											
Bembridge 1	9.9	21.6	31.4	25.5	11.8					0.2	
Bembridge 2	4.8	12.2	31.3	37.5	14.2						
Priory Bay 1		2.0	4.7	59.9	33.3	2.7	1.7	0.7			
Priory Bay 2	1.2	2.4	4.5	48.5	43.3	2.9	0.7	1.7		0.7	
Southwold 1	39.5	28.3	17.7	11.2	3.4						
Samples from other Pleistocene gravels											
Barling 1			1.3	58.8	40.0	9.4	3.8	0.6			
Barling 2A			2.3	54.7	43.0	36.1	16.3	3.5		1.2	
Barling 2B		0.3	2.7	56.4	40.7	19.2	11.4	1.1		1.1	
Barling 3			2.1	54.3	43.6	26.9	11.5	1.3			
Dammer Wick 1			1.1	60.4	38.5	14.3	13.2				
Barvills Farm 1			4.3	51.0	44.7	52.3	15.2	23.0		1.3	
Shakespeare Pit 2A			1.2	44.8	54.1	58.4	16.7	2.0		2.0	
Holland Haven 1A			0.6	49.1	50.3	7.8	4.8	1.2			
Holland Haven 1B			1.8	65.8	32.4	18.9	2.7	0.9			
Holland Haven 2				45.8	54.3	8.0	3.8	1.4		1.9	
Cooks Green 1A			1.5	59.3	39.2	4.1	2.0	1.0		0.3	
Cooks Green 1B		0.3	2.0	57.1	40.6	6.6	4.0	0.3		0.3	
Cooks Green 2			0.9	58.5	40.6	16.6	4.4	0.9		0.4	
Rampart Field 4				22.4	66.7					1.1	
Knettishall 2			2.2	20.9	76.9			0.3		2.2	
Samples from Palaeogene marine gravels											
Aveley A13 2.1	68.1	25.9	4.8		1.2						
Aveley A13 5.2	54.9	38.5	6.1		0.4						
Aveley A13 7.3	73.7	21.1	4.2	1.1							

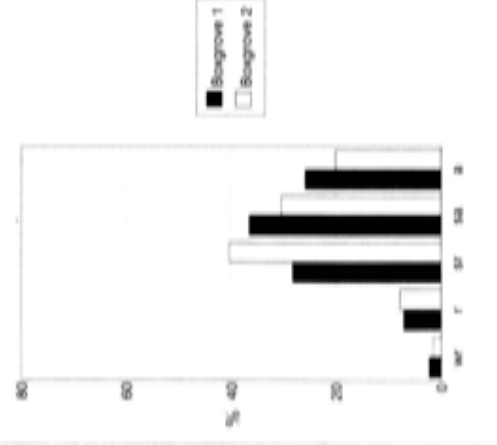
Comparison with pre-existing angularity/roundness information

Angularity/roundness analyses of flints have shown distinctive differences between fluvial gravels and classic beach and marine gravels, such as the Palaeogene gravels already mentioned (sampled from temporary exposures at Aveley, in SW Essex), and the Lower Pleistocene Westleton Beds of East Anglia (Table 13; Fig 80b). These examples clearly represent flints that have been subjected to considerable rolling in a high energy environment, so that a significant proportion have reached the ultimate 'well rounded' state. Few Pleistocene or modern beaches show this degree of rounding of flint, however. This is perhaps because of the lack of long-term

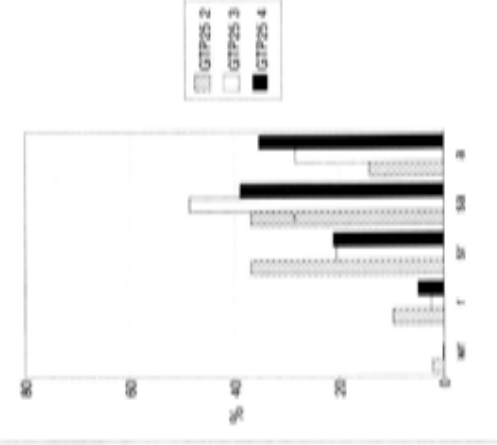
stability of sea-level since the Early Pleistocene, which has meant that beach deposits have been reworked less frequently before being isolated from the coastal environment. In the case of south coast and some east coast beaches, the lack of fetch (ie the length of water surface over which wind blows in making the wave) as a limitation on wave power is also likely to be a factor.

Nevertheless, it is generally possible to recognise the influence of the beach environment on flint angularity/roundness in analyses of beach deposits. The flint from the Bembridge Raised Beach, for example, has attained a degree of roundness unknown in river gravels, although the largest category is sub-rounded and much of the flint remains sub-angular or even angular (Bridgland 1990b; Table 13, Fig 80a).

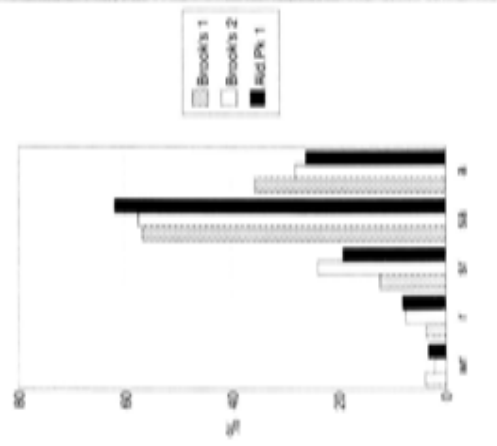
A Boxgrove beach gravel
(Slindon Gravel Member)



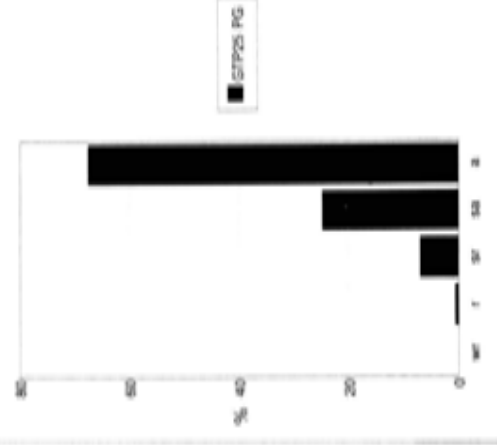
B Boxgrove beach gravel
(Slindon Gravel Member)



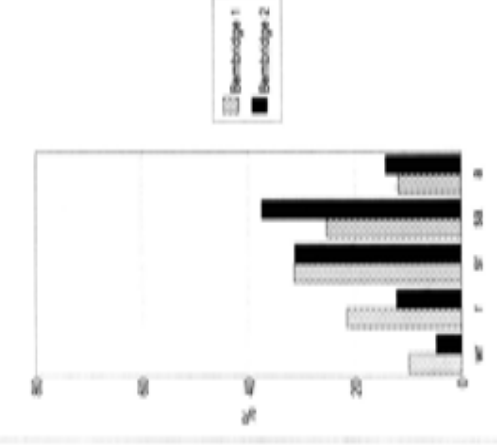
C Aldingbourne beach gravel
(Aldingbourne Lower Gravel Member)



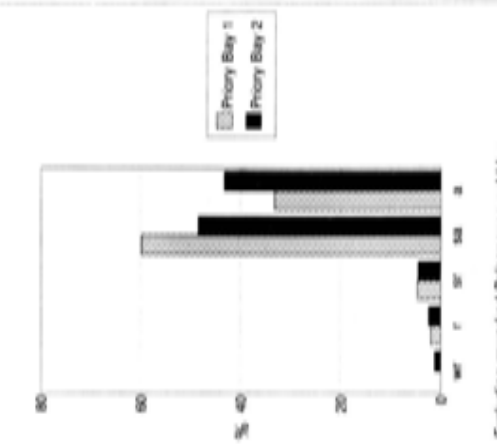
D Earham Path Gravel



E Bembridge Raised Beach
flint clasts 15-30mm



F Priory Bay Gravel
flint clasts 16-30mm



Excluding reworked Palaeogene pebbles

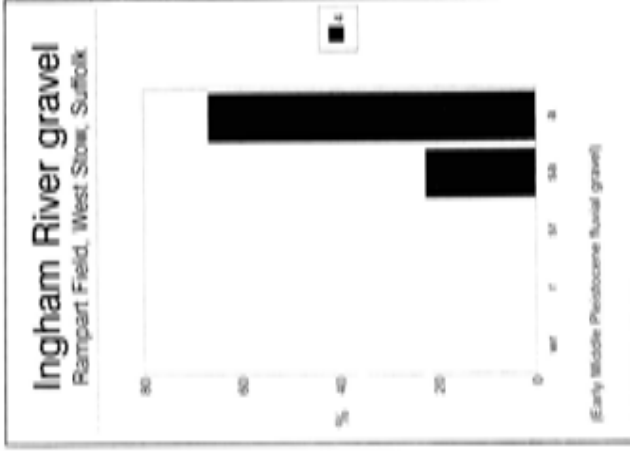
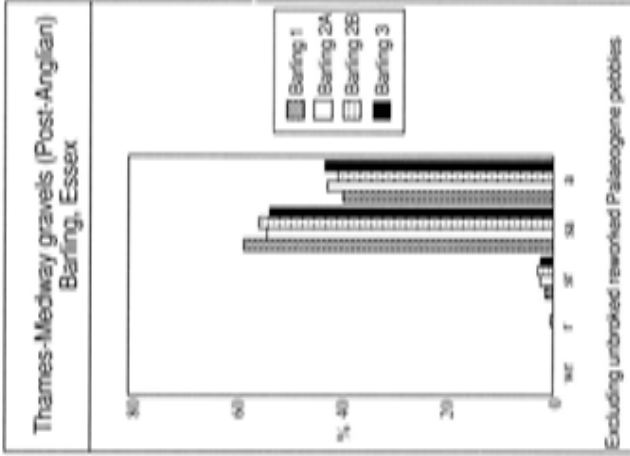
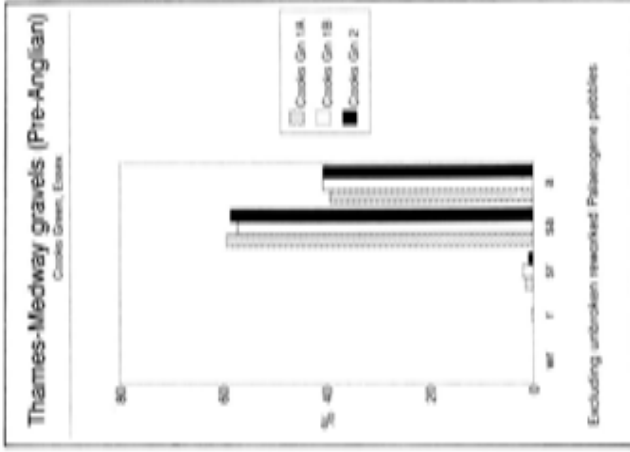
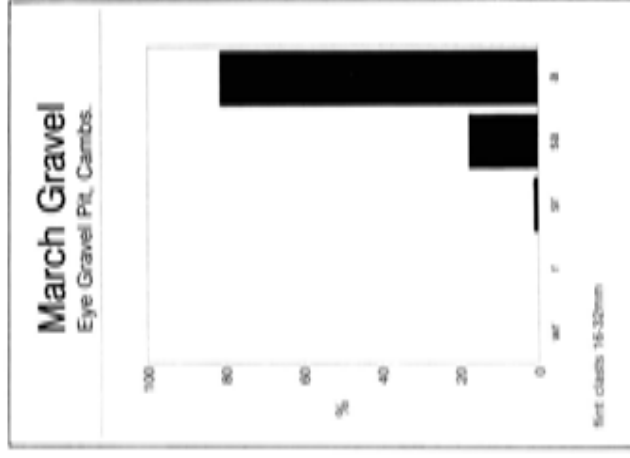
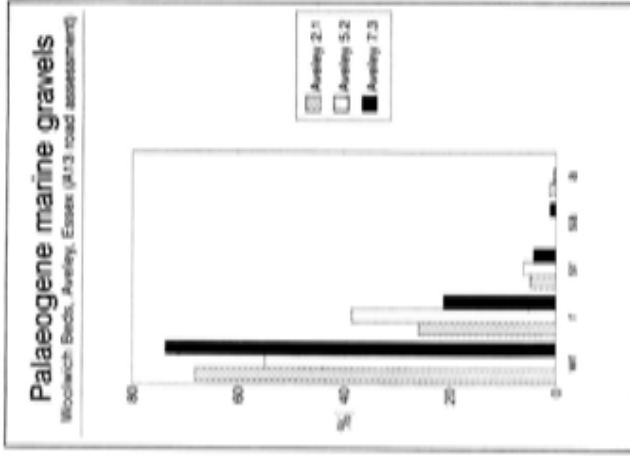
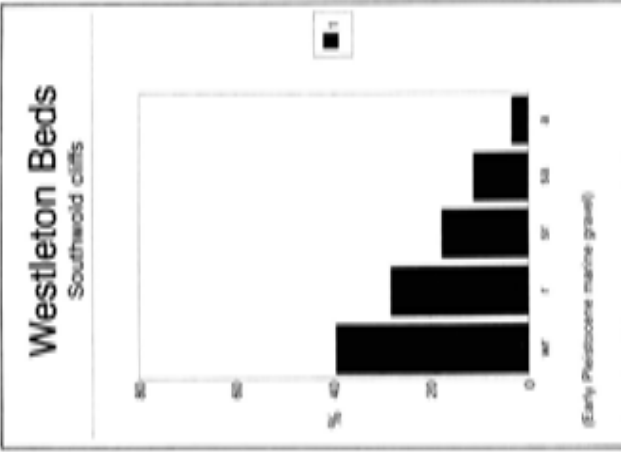


Fig 80a-b Histograms of angularity/roundness data from Table 13

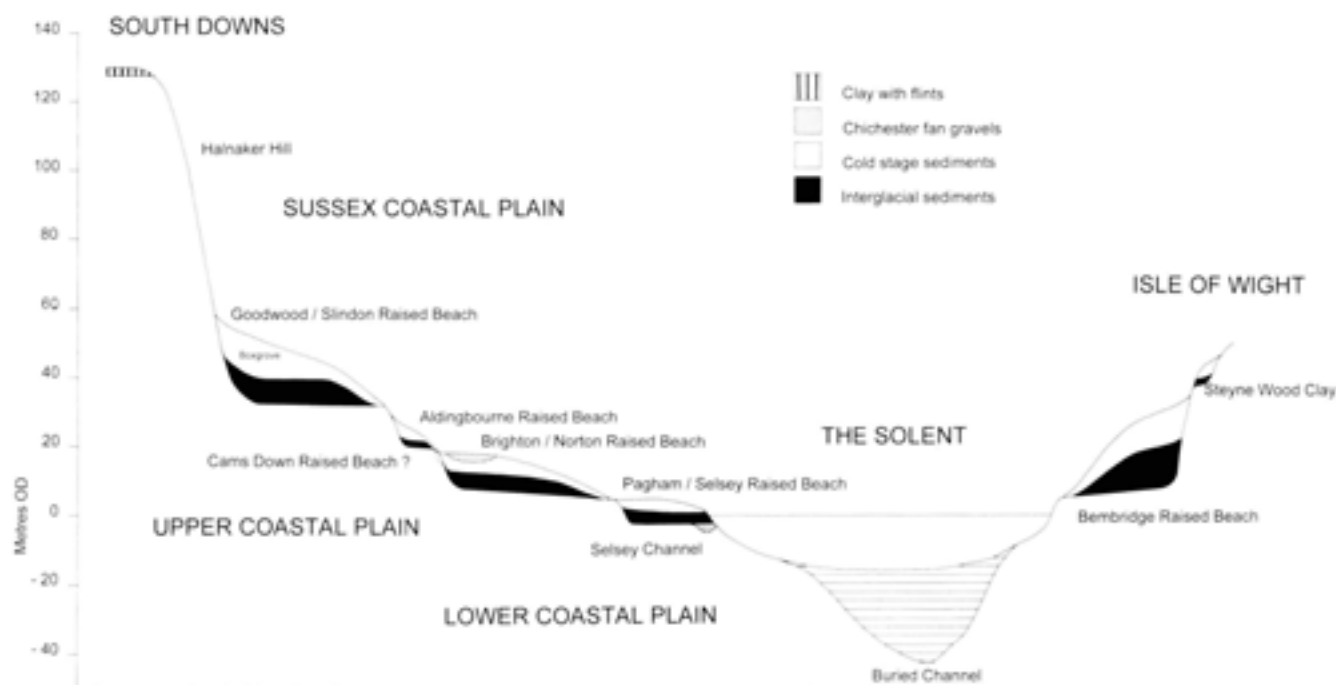


Fig 81 The Pleistocene sediments of the Coastal plain and their altitudinal relationship to the raised beaches of the Isle of Wight

With the increasingly large data set now available, it is becoming possible to utilise the results of angularity/roundness analyses to interpret the environment of deposition of gravels whose origin has been a source of controversy. An example is the deposit exposed in cliffs at Priory Bay, on the Isle of Wight (Preece *et al* 1990), the richest source of palaeoliths on the Island (Fig 81). Two samples of this gravel were analysed and were found to be predominantly sub-angular in character (Bridgland 1990b; Table 13). Although less rounded even than the Aldingbourne beach, the Priory Bay gravel contains a higher proportion of pebbles in the rounded categories than any of the Thames gravels, if the reworked Palaeogene material in the latter is discounted. The distribution of data from the second of the Priory Bay samples, in which well-rounded pebbles exceed rounded ones, hints at the occurrence there of a small reworked element, similar to that in the Aldingbourne beach. This is probably insufficient to account for the distinction between the Priory Bay clasts and those in fluvial deposits, the balance of evidence favouring interpretation as a raised beach gravel. This would explain the considerable battering displayed by some of the artefacts found *in situ* in the deposit, although care must be taken, as most of the collections from Priory Bay are from the modern beach, which is fed by gravel from the cliff. A rounded clast of granite that apparently fell from a newly cut exposure in the gravel (Preece and Scourse 1987) would also seem to point to a marine origin, as such material is found in south coast beaches (see below) but not in fluvial gravels. The low degree of rounding and the scarcity of non-flint material, in comparison to the nearby Bembridge beach (Tables 11 and

13), can probably both be explained by the more sheltered position of Priory Bay, within the eastern mouth of the Solent.

In contrast to Priory Bay, another supposed raised beach gravel that has been analysed, the March Gravel at Eye, near Peterborough (Keen *et al* 1990; Bridgland *et al* 1991) has been found to be of extremely angular character, raising doubts about its marine origin. Flint accounted for nearly 60% of the 16–32 mm material counted in the sample from Eye. There was no reworked Palaeogene element, this area being well to the north of the Tertiary sedimentary basins. The analysis showed a strong peak in the angular category, exceeded by few fluvial gravels (see below), and none of those illustrated in Table 13. The Eye deposit has been interpreted as a fluvially-fed fan deposited in a shallow marine bay, with minimal reworking of the gravel by wave action, on the strength of palaeontological evidence, particularly from ostracods (Keen *et al* 1990; Bridgland *et al* 1991). Recently, it has been suggested that the fossils in the gravel at Eye are reworked (West *et al* 1994), the implication being that the gravel is a cold-climate fluvial deposit. Although this suggestion appears to contradict taphonomic evidence from the distribution of ostracod instars (Keen *et al* 1990), it is very much in keeping with the angularity/roundness characteristics of the gravel.

When results are compared from various fluvial gravels it is clear that very little flint attains even the sub-rounded category in the river environment (Table 13). Indeed, only the gravels of major rivers such as the Early Pleistocene Thames-Medway (sampled from NE Essex), in which at least some of the flint component has probably travelled a considerable distance, show a

preponderance of sub-angular over angular material. The Rampart Field sample from the Ingham Gravel was found to contain predominantly angular flint, despite the apparent large size of the erstwhile Ingham River (Rose 1989; Bridgland and Lewis 1991). This probably reflects the fact that nearly all the flint in the Ingham Gravel has been picked up in Norfolk and Suffolk, and so has not travelled particularly far.

Glaciofluvial outwash deposits are perhaps likely to represent the highest-energy sedimentary environments in which flowing water is the transportation and depositional agent. Examples of such gravels in East Anglia are known to include flint clasts with considerable evidence of battering, including percussion scars or 'chatter marks' similar to those found on beach pebbles. Such scars are normally found predominantly on the corners of sub-angular nodular flints in these gravels. However, these glaciofluvial deposits include the 'Cannonshot Gravel' of north Norfolk, in which numerous highly rounded, almost spherical flints, occur, some (and only some) of which carry percussion scars. Although no analyses are as yet available from these deposits, the author has observed that near spherical unaltered flint nodules occur in them, so these could explain the occurrence of highly rounded clasts, rather than reworking from Pleistocene beach deposits, as has sometimes been suggested. Data from a sample of glaciofluvial gravel, in which battered flints have been observed, are included in Table 13. This shows that the general characteristics of the deposits, namely the preponderance of angular clasts, are fully in keeping with rapid deposition in a fluvial environment, with a short transport history.

The ratio between the angular and sub-angular categories has been found to be useful in the interpretation of analyses of fluvial gravels. In particular, it has been demonstrated, using this ratio, that flints within a single fluvial system generally become progressively less angular downstream (Fisher and Bridgland 1986). The examples provided above reveal that angularity/roundness analysis is a technique that is potentially sensitive to different depositional environments amongst water-lain deposits. Thus the results of such analyses are of value in assessing the environments in which the gravels of the Slindon and Aldingbourne Formations were laid down.

Angularity/roundness: discussion

The analyses of the various samples has shown that neither the Boxgrove nor the Aldingbourne beach contains highly rounded flint. In all but one sample the largest counts were in the sub-angular category. Boxgrove beach sample 2 peaked in the sub-rounded category and other samples from the Boxgrove beach also contained large sub-rounded components (Table 13, Fig 80a). The samples from the Aldingbourne beach contained less sub-rounded flint, but at between 8 and 20% of the total (excluding very angular clasts), this is still

significantly more than the most rounded fluvial gravels thus far analysed, those from Lower Pleistocene (Kesgrave Group) Thames deposits. The limited degree of rounding of the flints in these two beach gravels may be indicative of a restricted fetch or a sheltered palaeogeographical position on the Pleistocene coastline, as well as suggesting that relatively brief periods with sea level at the appropriate height are represented. Casual observation of several modern south coast beaches suggests that they are not dissimilar.

Rare gravel components

As explained above, non-flint clasts were encountered very rarely in samples of the Boxgrove and Aldingbourne raised beach sediments collected for clast analyses. Non-flint material was, however, encountered at Boxgrove in residues of bulk sampling for biostratigraphic purposes and in trowelling of archaeological surfaces as part of the excavation procedure. Comparable material has been recovered during trial pit excavation in the Aldingbourne beach and in the Norton Farm beach (Bates *et al* in press). All this material has been examined to determine the range of rocks that have contributed to the deposits, albeit only in trace quantities. From Boxgrove this material comes from the fine-grained silts (Unit 4b) and from the palaeosol formed above this unit (4c) (Table 9a). There was little opportunity to collect from the beach gravels, as these were neither sampled for fossils nor manually excavated. Sampling for clast analyses produced a minimal haul of non-flint clasts, providing an indication of the rarity of exotic material in this gravel. Potential non-flint material passed to the author from the silt and palaeosol included occasional small weathered flints. Otherwise, the following is a list of rocks encountered, in approximate order of the proximity to the Chichester area of likely source outcrops:

Rocks available from sources in south-central England

- Chalk, mainly from hard bands, some with borings by marine bivalves
- Weakly cemented sand (sandstone), possibly indurated Quaternary sand
- Greensand chert (presumably from the Upper Greensand of the Isle of Wight or Wessex)
- Sandstones of probable Greensand origin (source as for chert), some containing conspicuous spicules
- Sandy limestone/calcareous sandstone from the Greensand (source as for chert), with conspicuous glauconite
- Glauconitic marl (transitional Greensand-Chalk lithology)
- Various ironstones, some clearly concretionary, of unknown provenance
- Various non-distinctive calcareous sandstones and/or detrital limestones, of unknown provenance, probably Palaeogene (may include 'Bognor Rock')

- Non-distinctive calcareous mudstone/marl, of unknown provenance
- Jurassic chert, superficially similar to flint and probably undercollected as a result. Recognised where distinctively fossiliferous
- Vein quartz. A thoroughly exotic material if only primary sources are considered, but present in the area as pre-formed pebbles, particularly in the gravels of the Solent river system
- Orthoquartzite. As with vein quartz. Conglomeratic examples are common

Rocks that are exotic to south-central England

- Granite. Found consistently in both the sand and the palaeosol, granitic rocks vary from rare fine-grained (?microgranite) examples to typical coarser-grained granite. Some may be quartz porphyries rather than granites. Many of these granitic clasts are of large pebble size, up to 70mm. They are often weathered, sometimes to the extent of fragmentation, with quartz crystals being liberated from between the crumbling weathered feldspars. One example was found in association with a flint scatter, BE 21-GTP 17. Another seems to incorporate some large subhedral crystals of possible interest [might be non-quartz, and worth further examination — GTP 17 2048–1020]
- Schistose metamorphic rocks, often conspicuously micaceous, sometimes with an obvious quartz component, ranging towards schistose metaquartzite. Includes specimens with slaty, rather than strictly schistose, characteristics. Many of these apparent metamorphic rocks are weathered. One specimen, marked 'top of beach' is either a highly micaceous sandstone or a quartz-mica schist
- Slate. This is clearly represented as a lithology separate from the above, mainly amongst the smaller-sized material
- Sedimentary rocks of possible greywacke affinity, generally sandstones of 'immature' type, ie containing much non-quartzose, non-durable material, which could not have withstood a lengthy transport history and would therefore be expected only in rapidly deposited sediments such as greywackes. Examples were mainly (but not all) of fine-sand grade and frequently appeared to come from ripple-laminated beds, the clasts having formed by breakage along ripple bedding structures
- Arkosic sandstone [one specimen, Q1 GTP 30]
- Flagstone (sandstone with prominent horizontal bedding, along which it readily breaks, forming clasts of platy shape)

The Aldingbourne Raised Beach gravel has yielded a wide range of non-flint rocks from a relatively superficial examination in trial-holes at Brooks' Field and from cleaning of exposures at the Aldingbourne Park Pit. Clast-lithological analysis samples from here included Jurassic and Greensand cherts (Table 11; see above).

Five conspicuous large cobbles of exotic rocks were collected from the exposures in the Aldingbourne pit. Identifications of these by the author have been verified by Dr G Chinnor (Department of Earth Sciences, University of Cambridge). They comprised the following: dolerite; medium-grained granite; two specimens of arkosic sandstone; ?granodiorite. Also, a large rounded cobble of quartzitic sandstone was encountered in the excavation of Trial Hole 1 at Brooks' Field. In addition to these records from Boxgrove and the Aldingbourne beach, preliminary examination of the Norton Farm (5–7m) raised beach yielded a few non-flint clasts, although no gravels have been encountered in the examination of this beach thus far, and so no systematic analyses have been possible. The non-flints are as follows: Greensand chert [mammal sample 5, no 10]; ironstone [ditto]; a flat pebble of flaggy sandstone, possibly of greywacke type [mammal sample 7, no 11].

Rare gravel components: discussion

The range of exotic material encountered in the various raised beach gravels in the Chichester area broadly confirms earlier records, in which rocks such as granite, porphyry, Palaeozoic sandstone, Greensand and Bembridge Limestone were reported (Reid 1892; Palmer and Cooke 1923; Stinton 1985).

Exotic rocks have been recorded from Quaternary marine/estuarine deposits at numerous localities along the south coast of England, including Selsey (Reid 1892), Stone Point (Palmer and Cooke 1923), Earnley (West *et al* 1984) and in the 'Brighton Raised Beach' at points from Lancing to Brighton and Seaford (Kellaway *et al* 1975 — these authors provide a useful review). The present author (Bridgland 1990b) encountered such rocks in samples from the Bembridge raised beach, at the eastern end of the Isle of Wight (Table 11). Two samples from this beach gravel contained a range of Jurassic and Greensand cherts, quartz pebbles, various igneous rocks (the latter amounting to just under 1% of the total, in each case) and a single specimen of tourmalinised rock (appears under the heading 'other' in Table 11). This gravel is clearly endowed with a significantly larger non-flint component, at up to 16%, than the raised beaches of the Chichester area. The same is true of the truly exotic component, comprising only material foreign to south-central England, which accounted for around 1% of the Bembridge counts (quartz is excluded since it could be reworked from local Mesozoic sources) but which was never encountered in clast-lithological analyses of samples collected from the West Sussex raised beaches, although it is known to occur in them as a result of chance finds (see above). Preece *et al* (1990, 440) noted that the suite of rocks from the Bembridge beach was suggestive of 'a provenance from the west along the south coast of England'.

Although Preece *et al* (1990) did not discuss potential modes of transportation that might have brought these various rocks from western sources to the eastern extremity of the Isle of Wight, the occurrence of so-called erratic material in south coast raised beaches has often given cause for comment and has led to the suggestion that glaciation of the English Channel occurred at some time during the Pleistocene (Kellaway *et al* 1975). Others have preferred to explain such material as introduced to the channel coast by floating ice (Collcutt Chapter 2.3), implying that it was dropped from melting icebergs to the sea floor and subsequently washed up on to interglacial beaches. Even assuming the difficulties inherent in envisaging icebergs penetrating the English Channel in sufficient quantities to provide these rocks, given the fact that such bergs do not approach these areas during the present interglacial and can have come nowhere near the modern coast during glacials, when sea-level would have been very much lower, this theory patently fails to explain the western provenance, as opposed to a northern one, that appears to be indicated by the range of lithologies encountered. Other, less drastic explanations should also be explored. One possibility is that the material has been transported eastwards by longshore drift (however, see Collcutt Chapter 2.3). Relatively little is known of the capabilities of longshore drift in long-distance transportation of pebbles, but it has been suggested as a mechanism for transporting Rhaxella chert southwards from Yorkshire to be incorporated in the Westleton beds of Norfolk and Suffolk (Sinclair 1990; 1993). Notwithstanding the fact that alternative explanations are favoured by other workers (Green and McGregor 1990), in this particular case the lithology concerned is a highly durable one, clearly capable of withstanding long-distance transport in an aqueous environment. In contrast, many of the exotic rocks in the south coast beaches that have the most distant provenances are the least durable, notably the granites. Thus while the movement of Greensand and Jurassic cherts by longshore drift eastwards from the Dorset coast is fairly readily envisaged, these being highly durable rocks, it is hard to accept that granites and other relatively silica-poor rocks could have survived this means of transportation from much further west.

A possible alternative explanation for the transportation of these semi-durable rocks from the extreme south-west does exist, however. This is one that has been used to explain the sporadic occurrence of pebbles in marine rocks of Mesozoic age, such as the Chalk (Hawkes 1951) and the Cambridge Greensand (Hawkes 1943), namely the floating of pebbles on rafts of vegetable material. This might include pebbles carried between the roots of trees that have fallen from cliffs and been carried out to sea, to be washed up on a beach many kilometres away, as well as clumps of floating seaweed that might have incorporated pebbles from their position of growth. Clearly neither glaciation nor icebergs can have been responsible for transporting the

Cretaceous pebbles, since it is believed that the earth was essentially ice-free at that time, so an alternative mechanism for transporting such material across areas covered by sea water must exist. Various non-glacial methods of transporting drop-stone 'erratics' have recently been explored by Bennett *et al* (1994), in connection with Neogene marine deposits in south-east Spain. After considering various mechanisms for transporting pebbles into an area of generally fine-grained marine deposition, including, in addition to most of those discussed above, the role of animals carrying such material as gastroliths, these authors concluded that rafting by sea-weed was the most likely explanation (Fig 64). Clasts rafted by kelp have been reported from the coast of southern Africa (Woodborne *et al* 1989).

A potential obstacle to the transport by longshore drift of even durable material eastwards to West Sussex, from the source areas of the Jurassic cherts and the Wessex Upper Greensand (the former is from Dorset, whereas the latter is present on the Isle of Wight and the Dorset coast), is presented by the estuaries of several important south-coast rivers. Most of the present rivers have terrace systems that point to the existence of Pleistocene forebears, while at the time the Boxgrove beach was active it seems likely that there was a substantial Solent River estuary between the Sussex-Hampshire coast and the Isle of Wight, which may have been a peninsula joined to Purbeck at that time (Bridgland 1996). It is known, however, that sediment can be transported across the mouths of estuaries and embayments, particularly by offshore currents rather than wave action (Robinson 1964). Research on the mobility of offshore sediments, however, suggests that gravel-sized material remains essentially immobile once it is outside the wave zone, tidal currents being rarely capable of transporting material of greater than sand size (Anon 1984). The role of marine currents in the derivation of exotic material in south coast beaches by flotation is worthy of further consideration; the mapping of near surface currents in the English Channel (MAFF 1981) suggests that transportation of floating material from Brittany to the south coast of England would be perfectly feasible, raising the possibility of an Armorican source for some of the exotic rocks described earlier. However, it remains unknown whether this mechanism would have operated in a closed channel (Fig 23).

2.5 Particle size distribution and mineralogy of the deposits

J A Catt

Introduction

Seventeen samples were taken from locations in Quarries 1 and 2 (Table 14) for particle size analyses, mineralogical studies of fine sand (4–2 ϕ , 63–250 μ m) and coarse silt (6–4 ϕ , 16–63 μ m) fractions, and carbonate

analyses, to determine the provenance of the finer sediments, clarify certain stratigraphic correlations across the site, and investigate depositional processes. It was also the intention to date some of the silty, loess-like deposits by mineralogical comparison with English loesses of known ages, a technique used by Avery *et al* (1982) to reconstruct a Quaternary history of depositional, weathering and erosional events associated with chalkland dolines on the Chilterns. In addition, organic carbon, pH, dithionite-extractable iron and manganese, and clay minerals were determined in four of the samples (from Unit 4 at GTP 13), to investigate a possible buried soil profile at this level.

Analytical methods

The samples were air-dried for several days at room temperature, and then gently ground to pass a 2mm sieve; stones >2mm (entirely flint fragments) were present in three of the samples only. The particle size distribution of <2mm fractions was determined at ϕ intervals ($\phi = -\log_2$ mm) by sieving and the pipette sampling technique after treatment with acetic acid to remove calcium carbonate, followed by dispersion by overnight shaking in a dilute solution of sodium hexametaphosphate made weakly alkaline by the addition of sodium carbonate.

Fine sand and coarse silt fractions, separated by sieving and repeated settling under gravity in aqueous suspension respectively, were divided into light and heavy fractions by flotation in bromoform (specific gravity 2.9). Each light and heavy fraction was then analysed mineralogically by identifying >500 grains with a petrological microscope, and expressing the proportion of each mineral type as a percentage of the total number of grains counted. Minerals were identified by habit and optical properties such as colour, pleochroism, refractive indices, birefringence, optic sign and optical orientation.

Calcium carbonate content was determined from the volume of carbon dioxide released by treatment with hydrochloric acid, using a calcimeter of the type developed by Bascomb (1961). Organic carbon was determined by wet oxidation using the Tinsley III method of Kalembsa and Jenkinson (1973). pH was measured in 1:2.5 suspensions of soil and deionised water, and soil and 0.01M calcium chloride solution, using a meter with combined glass electrode and calomel half cells (Schachtschabel 1971).

Clay (<2 μ m) fractions were separated from dispersed samples by repeated settling in aqueous suspension, and then analysed mineralogically by the semi-quantitative X-ray diffraction methods given by Bullock and Loveland (1982). Diffraction traces were obtained from oriented clay films which were (a) air dried, (b) treated with ethylene glycol vapour at 800°C for 4 hours, (c) heated at 335°C for 4 hours, and (d) heated at 550°C for 4 hours.

Results

Particle size distribution (Table 14)

Apart from the marine Slindon Sands (Unit 3) and certain layers in the overlying Slindon Silts (Unit 4) (Table 9a), which are composed mainly of fine sand (4–2 ϕ), all the deposits analysed contained mainly clay (>9 ϕ) and coarse silt (6–4 ϕ). Plotted on the triangular textural diagram of Hodgson (1976), 12 of the 15 samples from Units 4–11 fall into the clay particle size class (>35% >9 ϕ), though all 15 contain >24% coarse silt (6–4 ϕ). The most clay-rich horizons are 5a and 5b at site GTP 13 and the Upper Silt Bed in the solifluction gravels (Unit 11) in Quarry 2. Coarse and medium sand (2 to –1 ϕ) are minor constituents (<1.2% together) of all the samples, except those from Units 8 (chalky pellet gravel) and 11 (solifluction gravels), in which these fractions are the fine tail of the flint gravel component.

Calcium carbonate content (Table 14)

All but 5 of the 17 samples contained some calcium carbonate, though amounts ranged from 0.3% in Unit 5a to 73.0% in Unit 8. The non-calcareous samples were from Unit 4c (the uppermost Slindon Silts) at GTP 13, Unit 6 (the Brickearth Beds) at Q2/D, and Unit 11 (Fig 4). Extremely calcareous Quaternary sediments, such as Units 8, 6, and 5b, are often associated with periglacial episodes in chalkland areas; these deposits were therefore derived principally from the Downs to the north.

Organic carbon (Table 14)

Amounts of organic carbon in the four samples from Units 4b and 4c at site GTP 13 ranged from 0.2 to 0.4%. From Unit 4b the amount increased upwards to the iron-rich layer in 4c as calcium carbonate decreased from 25.7% to zero; these changes resemble those in a soil profile such as a brown earth.

pH (Table 14)

The changes in pH through Units 4b and 4c at GTP 13 also resembled those in a brown earth profile, with an upward decrease from 8.3 (7.7 in calcium chloride) in the unaltered calcareous Slindon Silts to 7.3 (6.9 in calcium chloride) in Unit 4c.

Dithionite-extractable iron and manganese (Table 14)

The upward increase in extractable iron through the 4b–4c sequence also resembled that in a brown earth soil profile subject to weathering of iron-containing minerals. However, the large amount of extractable iron in the strongly ferruginous layer of Unit 4c is uncharacteristic of such a soil, and may result from

Table 14 Boxgrove sediment samples, particle size distribution, and chemical composition

	Unit 3 1.4m below Fe/Mn GTP 10	Unit 3 coarse sand GTP 13	Unit 4a GTP 10	Unit 4b GTP 13	Unit 4b below archaeology Q1/A	Unit 4b above archaeology Q1/A	Unit 4c basal GTP 13	Unit 4c perched Fe pan GTP 13	Unit 4c upper GTP 13	Unit 5a GTP 13	Unit 5b GTP 13	Unit 5b GTP 10	Unit 6 GTP 10	Unit 6 Q2/D about	Unit 8 Q2/B	Unit 11 Upper Silt Bed Q2	Unit 11 Middle Silt Bed Q1
Particle size distribution																	
<i>Sand</i>																	
1000–2000µm	0.0	0.1	0.1	0.0	0.0	0.0	0.0	0.0	0.0	0.1	0.1	0.1	0.1	0.0	1.0	3.6	0.9
500–1000µm	0.7	0.1	0.1	0.1	0.2	0.1	0.1	0.1	0.1	0.1	0.1	0.1	0.1	0.1	0.9	2.7	0.7
250–500µm	0.5	1.1	0.3	0.1	0.5	0.1	0.1	0.1	0.1	0.1	0.2	0.1	0.1	0.3	1.5	1.6	0.7
125–250µm	7.9	14.2	0.2	0.2	1.2	0.3	0.2	0.8	0.2	0.3	1.1	0.1	0.7	1.3	2.0	1.1	1.1
63–125µm	59.8	50.6	10.4	6.8	45.2	9.8	5.0	5.5	5.5	9.8	2.9	1.5	3.0	6.2	5.3	1.9	2.0
<i>Silt</i>																	
31–63µm	17.0	22.7	39.9	25.6	39.1	28.5	22.6	22.5	20.9	16.0	11.9	16.4	13.0	22.4	13.9	14.6	14.0
16–31µm	0.8	1.2	7.3	10.2	4.7	11.2	12.1	10.7	11.5	10.1	13.2	19.5	17.3	17.7	10.8	12.8	20.1
8–16µm	0.4	0.3	5.6	7.0	1.8	6.5	9.0	8.1	8.0	7.1	8.4	10.9	7.2	9.5	6.3	8.0	9.5
4–8µm	1.9	0.4	3.7	4.3	0.2	3.6	6.0	5.1	5.9	9.1	3.7	7.4	5.8	2.8	5.0	3.9	8.4
2–4µm	1.0	2.0	2.6	4.4	0.8	3.4	5.1	2.2	6.7	4.5	4.1	4.3	4.0	2.7	3.7	3.8	5.2
<i>Clay</i>																	
< 2µm	4.3	3.4	26.3	39.2	7.7	31.2	40.0	42.6	41.2	48.7	46.9	38.8	44.4	35.9	39.9	46.0	37.4
% CaCO ₃	16.8	13.0	23.1	25.7	19.9	23.0	1.7	0.0	0.0	0.3	56.3	38.1	51.9	0.0	73.0	0.0	0.0
% Organic C				0.2			0.3	0.4	0.2								
pH (water)				8.3			7.9	7.3	7.3								
pH (0.01M CaCl ₂)				7.7			7.5	6.9	6.9								
% dithionite Fe				0.37			0.45	4.6	0.66								
% dithionite Mn				0.02			0.15	0.03	0.01								

precipitation of iron at this level from groundwater after the horizon had been buried beneath the overlying deposits (Macphail Chapter 2.6). Dithionite-extractable manganese increases upwards from Unit 4b to the basal layer of 4c, but then decreases into the upper layers of 4c.

Clay mineralogy

The X-ray diffraction traces of clay (>9φ) fractions from four samples from Units 4b and 4c at GTP 13 indicated approximately similar mineral assemblages. All four contained mainly smectite with subsidiary amounts of illite and kaolinite. In addition, small amounts (5–10%) of quartz were identified in all the samples, and goethite in the iron-rich layer of Unit 4c. The relative proportions of smectite, illite and quartz are similar to those in the acetic acid insoluble residues of the Upper Chalk in Sussex (Weir and Catt 1965), but the Sussex Chalk contains no kaolinite. The amounts of quartz increased upwards from 4b into the iron-rich layer of 4c, but the uppermost layer of 4c contained a similar (ie intermediate) quantity to the basal Unit of 4c. The iron-rich layer of 4c probably contained some non-crystalline iron oxide as well as

goethite, because its goethite pattern was less intense than would be expected from the amount of dithionite-extractable iron in the whole sample.

Fine sand mineralogy (Table 15)

The light minerals present in the fine sand (4–2φ) fractions of all the samples studied were mainly quartz with subsidiary alkali feldspar and flint fragments and traces of glauconite. Traces of muscovite were found in approximately half of the samples; this mineral was most abundant in the white clay layer (Unit 5b) at GTP 10 and in Unit 11 (Figs 49 and 79). Feldspar and glauconite were both more abundant in lower parts of the succession (Units 3, 4, and 5a) than in upper parts (Units 5b, 6, 8, and 11). In contrast, flint fragments were more abundant in Units 5b–11 than in lower Units (3–5a).

The heavy minerals of the fine sand fractions were dominantly opaque types (limonite, haematite, magnetite, ilmenite and leucoxene), which together formed over 60% of the heavy fraction in all samples except the Chalk Pellet Beds (Unit 8). Aggregates of the iron oxides limonite (probably mainly goethite) and haematite were especially abundant in the iron-rich horizon of Unit 4c at GTP 13, Unit 5a at GTP 13, the

Table 15 Boxgrove samples, composition of fine sand (63–250µm) fractions

	Unit 3 1.4m below Unit 5a GTP 10	Unit 3 coarse sand. GTP 13	Unit 4a GTP 10	Unit 4b GTP 13	Unit 4b below archaeology Q1/A	Unit 4b above archaeology Q1/A	Unit 4c basal GTP 13	Unit 4c perched Fe pan GTP 13	Unit 4c upper GTP 13	Unit 5a GTP 13	Unit 5b GTP 13	Unit 5c GTP 10	Unit 6 GTP 10	Unit 6 Q2/D discol	Unit 8 Q2/B	Unit 11 Upper Silt Bed Q2	Unit 11 Middle Silt Bed Q1
Light fractions %																	
Quartz	88.6	87.2	86.5	85.7	88.2	87.8	85.5	89.0	87.6	89.3	89.2	88.6	90.2	85.4	92.3	74.4	89.6
Flint	5.4	5.2	4.8	6.7	5.2	5.5	6.3	4.7	7.6	6.4	9.0	8.4	8.4	12.7	7.4	22.0	7.6
Alkali feldspar	5.2	5.7	7.5	5.6	5.4	4.7	7.0	5.2	3.6	4.1	1.7	2.2	1.3	1.8	0.2	2.7	2.4
Muscovite	0.0	0.0	0.1	0.0	0.1	0.2	0.2	0.3	0.2	0.0	0.0	0.7	0.0	0.0	0.0	0.6	0.3
Glauconite	0.8	1.9	1.1	2.0	1.1	1.8	1.0	0.8	1.0	0.2	0.1	0.1	0.1	0.1	0.3	0.1	0.1
Heavy fractions %																	
Limonite/hematite	40.6	19.0	9.6	12.8	10.3	15.7	18.4	78.1	19.4	87.6	29.4	37.4	60.3	69.8	27.7	89.3	78.8
Magnetite/ilmenite	12.3	25.2	10.4	7.5	44.0	6.8	7.8	2.4	8.6	2.3	16.2	10.4	4.5	10.0	1.8	1.8	5.5
Leucoxene	20.8	24.9	43.8	40.2	19.6	44.7	34.8	10.8	36.6	6.2	16.2	22.6	7.6	12.0	7.3	4.6	9.0
Pyrite	0.0	0.0	0.4	0.0	0.0	0.0	0.7	0.0	0.0	0.0	0.0	0.0	0.0	0.0	0.0	0.0	0.0
Zircon	1.8	4.8	1.0	0.6	11.5	2.4	0.0	0.4	3.2	0.6	1.9	6.1	0.8	2.3	1.4	1.9	2.1
Tourmaline	5.1	5.6	5.8	7.5	3.5	5.3	2.8	1.3	9.7	0.4	3.8	0.9	1.9	3.4	1.3	1.1	2.6
Yellow rutile	0.2	1.1	0.0	0.0	0.4	0.3	0.0	0.0	0.0	0.0	0.0	1.7	0.4	0.3	0.0	0.2	0.4
Brown rutile	1.3	1.4	0.6	0.0	0.6	0.3	0.0	0.2	0.0	0.0	1.9	1.7	0.4	0.4	0.3	0.0	0.3
Red rutile	0.0	0.2	0.0	0.0	0.0	0.0	0.0	0.0	0.0	0.0	0.0	0.0	0.0	0.0	0.0	0.0	0.0
Anatase	0.3	1.0	0.0	0.0	0.8	0.0	0.8	0.0	0.5	0.0	0.0	0.9	0.2	0.1	0.0	0.0	0.2
Brookite	0.0	0.0	0.0	0.0	0.3	0.0	0.0	0.0	0.0	0.0	0.0	0.0	0.0	0.0	0.0	0.0	0.0
Staurolite	0.3	0.4	1.0	0.0	0.3	0.9	1.4	0.2	0.0	0.0	1.0	0.0	0.3	0.6	0.1	0.8	0.6
Kyanite	0.7	0.6	0.4	1.7	0.4	1.5	1.4	0.1	0.5	0.4	1.0	0.0	0.3	0.1	0.1	0.3	0.2
Andalusite	0.1	0.0	0.6	0.0	0.0	0.0	0.0	0.0	0.0	0.0	0.0	0.0	0.0	0.1	0.0	0.0	0.1
Sillimanite	0.1	0.0	0.0	0.0	0.0	0.0	0.0	0.0	0.0	0.0	0.0	0.0	0.0	0.0	0.0	0.0	0.0
Epidote	7.4	6.6	5.4	9.2	4.7	4.5	5.7	1.9	5.9	1.3	1.9	0.0	0.0	0.6	0.1	0.0	0.0
Garnet	2.0	3.1	0.4	0.0	1.3	0.6	0.0	0.5	1.0	0.0	0.0	0.0	0.1	0.0	0.1	0.0	0.0
Green hornblende	1.2	1.2	2.5	2.3	0.9	0.6	4.3	0.6	3.5	0.0	0.0	0.0	0.1	0.1	0.0	0.0	0.0
Brown hornblende	0.0	0.3	0.0	0.0	0.0	0.0	0.0	0.0	0.0	0.0	0.0	0.0	0.0	0.0	0.0	0.0	0.0
Tremolite	0.4	0.2	0.8	0.0	0.0	0.0	0.0	0.0	0.3	0.0	0.0	0.0	0.0	0.0	0.0	0.0	0.0
Chlorite	1.8	0.5	2.3	4.6	0.1	1.5	7.8	0.4	3.8	0.0	0.0	0.0	0.1	0.0	0.0	0.0	0.0
Biotite	1.6	0.1	1.7	0.6	0.1	1.8	2.8	0.0	0.0	0.0	0.0	0.9	0.0	0.0	0.0	0.0	0.1
Apatite	0.4	0.4	0.6	0.0	0.1	0.0	0.7	0.0	0.0	0.2	0.0	0.0	0.0	0.0	0.0	0.0	0.0
Collophane	1.6	3.2	11.8	13.0	1.0	13.1	10.6	3.1	7.0	1.0	26.7	17.4	23.1	0.1	59.8	0.0	0.1
Sphene	0.0	0.2	0.0	0.0	0.1	0.0	0.0	0.0	0.0	0.0	0.0	0.0	0.0	0.0	0.0	0.0	0.0

Brickearth Beds (Unit 6), and the Head Gravels (Unit 11). On the basis of the non-opaque heavy minerals, it is possible to divide the deposits into two groups. Units 3 and 4 contained a wide range of non-opaque minerals, mainly zircon, tourmaline, rutile, staurolite, kyanite, epidote, garnet, green hornblende, chlorite, biotite and collophane, with small amounts of anatase, brookite, andalusite, sillimanite, brown hornblende, apatite and sphene in some samples. Units 5–11 contained a more restricted suite, mainly zircon, tourmaline, rutile, staurolite, kyanite and collophane, and only sporadic grains of anatase, andalusite, epidote, garnet, green hornblende, chlorite, biotite and apatite.

Coarse silt mineralogy (Table 16)

The light and heavy fractions of the coarse silts contain the same minerals as those present in the fine sands, though the opaque minerals in the heavy fractions of the silt were not counted because it was difficult to reflect light from their surfaces using the high power (short working distance) objective necessary for observation of silt particles. However, many of the mineralogical changes through the succession observed in the fine sands were not repeated in the coarse silts. Instead, the mineral assemblage typical of Units 3 and 4 persists almost throughout the succession. The only

Table 16 Boxgrove samples, composition of coarse silt (16–63µm) fractions

	Unit 3 1.4m below Unit 5a GTP 10	Unit 3 coarse sand GTP 13	Unit 4a GTP 10	Unit 4b GTP 13	Unit 4b below archaeology Q1A	Unit 4b above archaeology Q1A	Unit 4c basal GTP 13	Unit 4c perched Fe pan GTP 13	Unit 4c upper GTP 13	Unit 5a GTP 13	Unit 5b GTP 13	Unit 5b GTP 10	Unit 6 GTP 10	Unit 6 Q2/D decal	Unit 8 Q2/B	Unit 11 Upper Silt Bed Q2	Unit 11 Middle Silt Bed Q1
Light fractions %																	
Quartz	86.5	90.0	86.3	86.0	89.9	87.2	86.6	90.1	86.1	89.2	92.5	90.9	92.8	89.6	92.5	87.2	90.1
Flint	5.1	2.2	5.9	4.8	3.9	4.9	5.2	3.5	5.8	4.7	4.1	3.9	3.7	5.7	3.9	3.0	2.9
Alkali feldspar	6.5	6.0	6.4	7.9	4.8	5.6	6.0	5.5	6.9	5.6	3.1	5.1	3.2	4.5	3.3	6.8	6.2
Muscovite	0.0	0.2	0.6	0.5	0.4	0.7	1.1	0.6	1.0	0.4	0.3	0.1	0.3	0.2	0.3	1.8	0.8
Glauconite	1.9	1.6	0.8	0.8	1.0	1.6	1.1	0.3	0.2	0.1	0.0	0.0	0.0	0.0	0.0	1.2	0.0
Heavy fractions %																	
Zircon	40.0	24.8	37.3	33.2	30.7	23.3	32.9	34.8	32.8	25.6	36.9	39.3	36.7	46.7	47.8	44.3	32.5
Tourmaline	11.9	15.7	9.7	9.8	12.5	16.2	9.7	10.5	10.7	16.2	12.2	7.2	12.9	10.0	12.5	15.5	15.9
Yellow rutile	9.6	7.1	11.3	9.3	10.0	7.4	6.1	9.5	10.5	9.2	15.8	19.3	16.4	14.4	16.0	16.0	15.9
Brown rutile	3.4	4.2	4.3	6.7	3.8	4.3	5.4	3.2	4.5	6.8	5.5	8.6	9.8	5.8	4.0	4.9	4.7
Anatase	1.9	4.6	6.4	5.3	6.2	5.8	9.1	8.8	7.8	6.6	11.8	11.2	9.6	8.4	5.3	9.8	6.1
Brookite	0.4	0.4	0.3	1.4	0.9	1.1	0.4	0.6	0.8	0.4	0.4	1.1	0.0	0.5	0.0	0.0	0.3
Staurolite	3.2	1.0	2.3	0.4	0.2	0.4	0.1	0.2	0.0	0.4	0.4	0.6	0.7	0.5	9.8	6.3	1.6
Kyanite	0.9	0.2	0.3	0.8	0.2	0.7	0.5	0.2	0.6	0.2	0.6	1.3	0.5	0.9	0.5	1.9	0.6
Andalusite	0.0	0.0	0.0	0.0	0.0	0.2	0.1	0.0	0.2	0.6	0.0	0.0	0.0	0.0	0.0	0.5	0.0
Sillimanite	0.0	0.2	0.0	0.0	0.0	0.0	0.1	0.0	0.0	0.2	0.0	0.0	0.0	0.0	0.0	0.0	0.0
Epidote	18.3	24.6	17.9	19.8	20.2	27.5	19.9	20.4	19.8	17.0	13.0	8.6	10.5	11.4	0.0	0.0	16.2
Garnet	3.6	7.1	3.1	5.3	5.6	4.5	3.4	3.4	3.3	5.5	0.6	0.4	0.2	0.0	0.3	0.0	0.6
Green hornblende	1.7	5.2	2.3	1.2	2.4	1.1	2.3	1.3	1.2	1.8	0.4	0.2	0.0	0.0	0.0	0.0	0.3
Brown hornblende	0.0	0.2	0.0	0.0	0.0	0.0	0.0	0.0	0.0	0.0	0.0	0.0	0.0	0.0	0.0	0.0	0.0
Tremolite	0.9	0.8	1.2	1.0	1.6	1.3	1.1	1.1	1.7	1.0	0.2	0.2	0.0	0.2	0.3	0.5	0.5
Chlorite	1.7	2.3	1.0	3.0	3.1	3.6	3.6	2.7	4.1	4.3	0.8	0.8	1.0	0.7	0.0	0.0	3.2
Biotite	0.6	0.6	0.7	2.0	0.4	1.3	1.3	0.8	0.6	1.2	0.2	0.2	0.0	0.0	0.0	0.0	0.5
Apatite	0.2	0.4	0.5	0.2	0.7	0.2	1.1	0.4	0.2	1.8	0.4	0.2	0.0	0.0	0.0	0.0	0.0
Collophane	1.3	0.0	0.7	0.0	0.2	0.4	1.6	0.4	0.2	0.0	0.2	0.4	1.2	0.5	3.2	0.3	0.3
Sphene	0.4	0.6	0.7	0.6	1.3	0.7	1.3	1.7	1.0	1.2	0.6	0.4	0.5	0.2	0.3	0.0	0.8

changes resembling those in the fine sands are in the following heavy minerals:

1. Tremolite is slightly less abundant in Units 5–11 than in Units 3 and 4.
2. Apatite is present in Units 3–5, but absent from Units 6–11.
3. Biotite is present in Units 3–5, but absent from all samples of Units 6–11 except the Upper Silt Bed in Unit 11 in Q1.
4. Epidote is present in Units 3–6 and the Upper Silt Bed in Unit 11 in Q1, but is absent from the remainder of Unit 11 and from Unit 8.
5. Green hornblende is present in Units 3–5 and the Upper Silt Bed in Unit 11 in Q1, but is absent from the remainder of Unit 11 and Units 6 and 8.
6. Apart from the Upper Silt Bed in Unit 11 in Q1, all the samples from Units 5b upwards contain little (<1.0%) or no chlorite, whereas those from Units 3 and 4 contain >1.0%.

This means that only two of the samples from upper parts of the sequence have similar heavy mineral assemblages in the fine sand and coarse silt fractions. These are the Chalk Pellet Beds (Unit 8) and the Upper Silt Bed in the solifluction gravels (Unit 11) in Quarry 2. Even these two samples contain dissimilar light mineral assemblages in the fine sand and coarse silt fractions, because their coarse silt fractions have light mineral suites resembling those of samples from lower parts of the succession (Units 3 and 4).

The following conclusions may be drawn from this comparison of the fine sand and coarse silt mineral assemblages:

1. Units 3 and 4 are fairly uniform in composition, with approximately similar sand and silt mineral assemblages, both containing a fairly wide range of minerals; this indicates a single, well-mixed and homogeneous sediment.
2. Units 5–11 contain a slightly different assemblage of sand minerals, with less alkali feldspar and glauconite

and a more restricted suite of heavy minerals; apart from two horizons (Unit 8 and the silt bed in the solifluction gravels of Unit 11 in Quarry 2), which have silt mineral assemblages akin to this sand mineral assemblage, the silt fractions from Units 5–11 are mineralogically different from the sand fractions, indicating mixing of sand from one source with silt from a second.

3. In the two horizons containing silt mineral assemblages similar to the sand mineral assemblages characteristic of Units 5–11, there is little or no silt from the second source.
4. In terms of its fine sand mineral assemblage, the lowest part of Unit 5 (bed 5a) is transitional from the lower group of deposits (Units 3 and 4) to the upper group (5–11), probably because it contains some sand eroded from Units 3 and 4 beneath.

Discussion

Provenance of the deposits

The fairly uniform assemblage of fine sand and coarse silt minerals in Units 3 and 4 is probably derived from several sources. The flint fragments and colophane could be derived partly or wholly from the Upper Chalk, in which the cliff and wave-cut platform were incised; fine sand and coarse silt fractions of acetic acid-insoluble residues from most zones of the Upper Chalk in Sussex are dominated by these two minerals (Weir and Catt 1965). However, other sand and silt minerals in the chalk (including quartz) are present in such small quantities that they cannot entirely account for the composition of these fractions in Units 3 and 4. Similarly, the proportions of smectite, illite and quartz suggest that much of the clay in Units 4b and 4c is derived from the chalk, but the presence of kaolinite shows that at least some of the clay is from another source (Table 6).

The Reading Beds could be a source of much of the quartz and some of the opaque heavy minerals in the sand and silt fractions, but they contain a more restricted suite of non-opaque heavy minerals and less alkali feldspar and glauconite than the Slindon Sands and Silts (Hodgson *et al* 1967). Their non-opaque heavy sand and silt fractions consist almost exclusively of zircon, tourmaline, rutile, staurolite, and kyanite; other non-opaque heavy minerals which are consistently important constituents of the Slindon Sands and Silts, such as epidote, garnet, green hornblende, chlorite, biotite, and apatite, are rare or absent from the local Reading Beds. Two of these minerals (epidote, garnet) were reported from the London Clay of the Isle of Wight (Walder 1964) and Havant Thicket, West Sussex (Hodgson *et al* 1967); like the Reading Beds, this formation crops out to the south of the interglacial cliff, and therefore is likely to have contributed sand and silt to Units 3 and 4 (Table 6, Figs 15–17).



Fig 82 Redeposited Slindon Sand in the Head Gravel of Unit 11; scale unit 0.5m

In north-east Kent, the London Clay also contains chlorite, biotite, hornblende, alkali feldspar, muscovite and glauconite (Weir and Catt 1969), and these could account for the remaining constituents of the Slindon Sands and Silts, though they have not yet been reported in any abundance from the London Clay in Sussex. However, many other pre-Quaternary rocks occurring on or near the Channel coast could have contributed some or even all the sand and silt minerals in Units 3 and 4; all the minerals are fairly common and widespread, and the grains in the Slindon Sands and Silts do not show any features characteristic of any specific source (Table 6).

The restricted fine sand mineral suite present in Units 5–11 (quartz and flint, with small amounts of alkali feldspar and glauconite in the light fractions, and a non-opaque heavy mineral containing little other than zircon, tourmaline, rutile, staurolite, kyanite and colophane) is characteristic of the Clay-with-flints on the South Downs, which is a thin weathered veneer of basal Reading Beds mixed with insoluble residue of the underlying chalk (Hodgson *et al* 1967). This suggests that Units 5–11 are derived partly by mass movement (eg solifluction or slopewash) of soil material from the land surface of the Downs north of the cliff (Roberts

Chapter 2.1). The similar assemblage of coarse silt materials in Unit 8 (Chalk Pellet Beds) and the fine silt bed within the solifluction gravels (Unit 11) in Quarry 2 serves to confirm this origin for the bulk of these two deposits (Table 9a). The large amounts of carbonate in Units 5b, 6, and 8 indicate that chalk was also periodically removed from the Downs by the mass wastage (Fig 77).

However, other samples from Units 5–11 contain coarse silt fractions which are mineralogically more like the silt or fine sand of Units 3 and 4 than the fine sand of Units 5–11. The simplest interpretation of this evidence for mixing of mineralogically different sand and silt fractions is that, following the interglacial in which the Slindon Sands and Silts were deposited, the sea level fell eustatically, exposing Units 3 and 4 to wind erosion, which carried silt northwards onto the Downs, from where it was subsequently moved southwards downslope, along with the solifluction chalk and Clay-with-flints (see Roberts Chapter 2.1). This is a preferred origin even for the loess-like Brickearth Beds (Unit 6), and Upper Silt Bed in Unit 11 in Q1, because they contain more clay than any purely aeolian loess, and their fine sand fractions are mineralogically like that of Clay-with-flints, which originated on the Downs. If fairly large amounts of silt from Units 3 and 4 were blown as loess up on to the chalk dip slope before mass movement started (Fig 82), then the earliest solifluction or slopewash deposits would consist mainly of this silt, thus producing the extensive but fairly thin Brickearth Bed (Unit 6).

Comparison of the silt mineralogy of the Brickearth Beds with that of other English loess deposits

As explained above, all the coarse silt minerals present in Units 5–11, including the Brickearth Beds (Unit 6), could have been derived from the Slindon Sands and Silts (Units 3 and 4). However, there are some differences, so it is perhaps possible that the windblown silt component was derived from other sources, the most likely of which would be glacial outwash deposits of various ages, aeolian reworking of which produced at least three widespread loess deposits with slightly different silt mineralogical compositions in southern England (Avery *et al* 1982).

Table 17 shows the mean compositions of coarse silt fractions from these three loesses, the Slindon Sands and Silts and the Brickearth Beds (Unit 6). The table includes 27 different minerals, 18 of which are present in Unit 6, and the amounts of 13 of these are more like the amounts in the Slindon Sands and Silts than in any of the loesses. A further four minerals (brookite, staurolite, kyanite, and collophane) occur in very small amounts in all the deposits, and thus indicate approximately equal similarity of the Brickearth Beds both to the Slindon Sands and Silts and to the loesses. The remaining mineral present in the Brickearth Beds (garnet) is much less abundant than in either the Slindon Sands and Silts or in any of the

loesses and thus indicates similarity to neither. The similarity of the brickearth to the Slindon Sands and Silts is further strengthened by the absence of six minerals in the brickearth, which are either absent in the Slindon Sands and Silts but present in the loesses, or occur in much smaller amounts in the Slindon Sands and Silts than in the loesses.

Some of the mineralogical differences between the Brickearth Beds and the Slindon Sands and Silts could result from weathering. In particular, the absence of glauconite, green hornblende, and apatite, and the smaller quantities of alkali feldspar, muscovite, and garnet may be explained in this way. This weathering would probably have occurred in soils on the Downs, and implies an episode of fairly prolonged (probably interglacial) warm, humid, conditions between aeolian deflation of the Slindon Sands and Silts and mass movement of soil material southwards over the cliff edge. However, there is no other evidence for this interglacial in the sequence at Boxgrove.

The mineralogical evidence therefore accords with ultimate derivation of the Brickearth Beds from the weathered Tertiary regolith and the Slindon Sands and Silts, rather than from any of the known loess sheets of southern England. Consequently, mineralogical comparisons with loesses of known ages cannot be used to date the Brickearth Beds.

Evidence for weathering of Unit 4b

The chemical similarities of the two lower horizons of Unit 4c at GTP 13 to a soil profile developed on the intertidal Slindon Silts (Unit 4b) at Q1/A and GTP 17 (Fig 4; Chapter 6.2), as noted earlier, is supported by mineralogical differences between these horizons. In the fine sand fractions, there are upward decreases in amounts of several weatherable minerals, such as glauconite, epidote, green hornblende, chlorite, biotite, apatite, and collophane, from Unit 4b into the iron-rich layer of Unit 4c. Also some weatherable sand minerals occurring in most of the other Slindon Sand and Silt samples are rare or absent from all three horizons; these include brown hornblende, tremolite, and garnet. In the coarse silt fractions, there are upward decreases in some weatherable minerals (glauconite, biotite, apatite, and collophane) and brown hornblende is absent, but the overall effect of weathering is less clear than in the fine sands. This is possibly because silt grains lost by weathering have been partly replaced by others produced by weathering and decrease in size of fine sand grains. This suggests that the weathering episode was fairly weak and short-lived (Austin and Roberts, Roberts Chapter 6.2). The thin horizons and absence of evidence for weathering of clay fractions (apart from the small upward increase in quartz) also indicate that this interval of weathering and soil formation was quite brief. In the intertidal depositional environment indicated by the sedimentary nature of Unit 4, this type of pedogenetic episode probably resulted

Table 17 Mineralogical comparison of course silt (16–63µm) fractions from selected Boxgrove samples, with loesses of three different ages

	<i>mean of 7 Anglian loesses</i>	<i>mean of 6 Wilstonian loesses</i>	<i>mean of 32 Devensian loesses</i>	<i>mean of 9 Slindon Sands and Silts</i>	<i>mean of 2 Brichearth Bed samples</i>	<i>mean of 2 Silt Bed samples from Unit 11</i>
Light fractions %						
Quartz	85.1	83.7	82.0	87.6	91.1	88.7
Flint	1.3	1.2	0.9	4.6	4.7	3.0
Alkali feldspar	9.2	11.4	15.0	6.2	3.9	6.5
Muscovite	3.6	2.9	1.4	0.6	0.3	1.3
Glauconite	0.8	0.8	0.7	1.0	0.0	0.6
Heavy fractions %						
Zircon	18.4	21.0	12.7	32.2	41.7	38.4
Tourmaline	5.0	6.5	3.2	11.9	11.5	15.7
Yellow rutile	7.9	4.4	3.3	9.0	15.4	16.0
Brown rutile	1.1	1.5	1.2	4.4	7.8	4.8
Red rutile	0.1	0.1	0.3	0.0	0.0	0.0
Anatase	4.4	2.3	1.8	6.2	9.0	8.0
Brookite	0.6	0.3	0.3	0.7	0.3	0.2
Staurolite	0.3	0.9	0.6	0.9	0.6	4.0
Kyanite	0.2	1.0	0.4	0.5	0.7	1.3
Andalusite	0.1	0.1	0.0	0.1	0.0	0.3
Epidote	36.0	33.2	40.7	20.9	10.9	8.2
Garnet	5.0	6.4	4.5	4.4	0.1	0.3
Green hornblende	3.6	7.6	11.0	2.1	0.0	0.2
Brown hornblende	0.1	0.2	0.7	0.0	0.0	0.0
Tremolite	2.2	1.8	2.8	1.2	0.1	0.5
Chlorite	11.3	11.0	14.1	2.8	0.8	1.6
Biotite	1.7	1.1	1.8	0.9	0.0	0.3
Apatite	1.1	0.1	0.3	0.4	0.0	0.0
Collophane	0.7	0.3	0.2	0.5	0.8	0.3
Sphene	0.1	0.0	0.0	0.9	0.3	0.4
Spinel	0.1	0.1	0.0	0.0	0.0	0.0
Augite	0.0	0.1	0.1	0.0	0.0	0.0

from a short (<100 years) emergent period when the sea-level was only a few metres lower than during deposition of Unit 4.

2.6 Sediment micromorphology

*R I Macphail (with a contribution by
P Goldberg)*

Introduction

The great age of this site and the taphonomic results of pedogenesis and burial, have produced important post-depositional (diagenetic) effects on the sediments and these are considered in detail in this investigation. Soil micromorphology was applied routinely to units and unit sequences, especially those containing *in situ* artefacts and fauna. The study was carried out to understand better the details of the depositional environment experienced by animals and hominids, as well as to allow fully for post-depositional processes and their effects on the stratigraphic sequence.

Methods and samples

Fifty-seven undisturbed samples from some twenty-two locations across the site, were taken for soil micromorphological study (Table 18; Fig 4). These were either air dried before impregnation by crystic resin under vacuum, or soil water was removed by acetone replacement (Murphy 1986). Impregnated blocks were sliced and manufactured into thin sections according to Guilloché (1985) at the Institut National Agronomique, Paris-Grignon or made at the University of Stirling. The resulting fifty-seven thin sections, some of which spanned up to five archaeological units (Tables 9, 18, 21), were systematically described according to Bullock *et al* (1985). Preliminary interpretations were made following the guidelines of Courty *et al* (1989), with particular regard to sedimentary, pedological and palaeosolic features (Romans and Robertson 1974; Bullock and Murphy 1979; Reineck and Singh 1980; Bal 1982; Van Vliet-Lanoë 1982; Kemp 1985a; 1985b; 1986; Rose *et al* 1985; Catt 1986, 1990; Fedoroff *et al* 1990).

Table 18 Thin section sample list: SMA=small mammal accumulation. Q2 Tps C and Q were excavated during Boxgrove Project B (Roberts *et al* 1997)

<i>no</i>	<i>area</i>	<i>unit</i>	<i>year/letter designation</i>	<i>bulk sample</i>
1	Q2: GTP 1	4c-5a/5b	84/87 A	
2	Q2: GTP 1	4c/5a/5b	84/87 B	
3	Q2: GTP 3	4b/4c/5a/5b	84/87 C	a, b, c, d
4	Q2: GTP 10	4c/5a/5b	88 H	
5	Q2: GTP 10	4c/5a/6	84/87 D	
6	Q2: GTP 10	4b (fish bone accumulation)	89 F	
7	Q2: GTP 10	3/4a	90 L	
8	Q2: GTP 13	6	84/87 K	f
9	Q2: GTP 13	6	84/87 J	g
10	Q2: GTP 13	5b/6	84/87 I	h
11	Q2: GTP 13	4c/5a/5b/6	84/87 H	i, j, k
12	Q2: GTP 13	4b	84/87 G	l
13	Q2: GTP 13	4a	84/87 F	m
14	Q2: GTP 13	3/4a	84/87 N	n
15	Q2: GTP 13	3 (Marine Cycle 3)	84/87 E	o, p
16	Q2: GTP 13	3 (Marine Cycle 3)	84/87 M	
17	Q2: GTP 13	3 (Marine Cycle 2)	84/87 L	
18	Q2: GTP 17	5a/5b/5c/8 (artefact horizon)	90 O	
19	Q2: GTP 17	4c/5a/5b/5c (artefact horizon)	90 P	q
20	Q2: GTP 17	4b/4c	90 Q	
21	Q2: GTP 17	4b (artefact horizon)	90 N	
22	Q2: GTP 17	4b (artefact horizon)	90 M	
23	Q2: GTP 25	8 (artefact horizon)	91 A	
24	Q2: GTP 25	chalk mud/4c/5a/5b	91 B	
25	Q2: GTP 25	4b/4c/5a	88 D	
26	Q2: GTP 25	4b/4c/5a	88 E	
27	Q2: GTP 25	4b/4c/5a	88 F	
28	Q2: GTP 25	terrestrial clay/Marine Cycle 3	88 G	r
29	Q1: GTP 30	4d/5a/5b/8	89 G	
30	Q1: GTP 31	4d/8	89 H	
31	Q1: GTP 32	4c/5a/5b/8	89 J	
32	Q1/B:Trench 5	4d ('tufa')	89 I	
33	Q1/B: Trench 4/1	4d/8	88 A	s
34	Q1/B: Trench 4	4d/5a/5b	88 B	
35	Q1/B: Trench 2	4b/4d/5a	88 C	
36	Q1/A	4b (artefact horizon W-E section)	84/87 O	
37	Q2/A	4c (artefact horizon)	84/87 P	
38	Q2/A	4c (artefact horizon)	84/87 Q	
39	Q2 Tp C	4c (artefact horizon)/5a/6	89 A	
40	Q2 Tp C	5a/6	89 B	
41	Q2 Tp Q	5b/6?/8	89 D	
42	Q2 Tp Q	4c (artefact horizon)/5a/5b	89 C	
43	Q2 Tp Q	4c/5a/5b/6?-8?	89 E	
44	Q2/B	4c/5b/8	90 K	
45	Q1/B	6 (SMA)(F196)	-	
46	Q1/B	4c (SMA) (F146)	-	
47	Q1/B	4c (SMA) (F148)	-	
48	Q1/B	4c (SMA) (F218)	-	
49	Q1/B	4c (SMA) (F196)	-	
50	Q2 north of GTP 25	11	93 A	
51	Q2 north of GTP 25	11	93 B	
52	Q2 north of GTP 25	11	93 C	
53	Q2 north of GTP 25	11	93 D	
54	Q2 north of GTP 13	11	93 E	
55	Q1 north face	11	93 F	
56	Q1 north face	11	93G	
57	Q1 north face	11	93 I	

Thin sections (designated in bold 1–57) were observed by eye (x1), using a hand lens (x5), microfiche reader (x20) and polarising microscope (x20–x400). In the last, plane polarised light (PPL), crossed polarised light (XPL), oblique incident light (OIL) and ultra violet light (UV), were employed (Fig 83a–p). Generous advice on most microfibrils was obtained from Drs N Fedoroff (Institut National Agronomique, Grignon, France), M A Courty (CNRS, Université de Paris, France), P Goldberg (University of Texas, Austin, USA) and Dr R Kemp (RHBNC, London). The scientific basis of the application of soil micromorphology to ancient soils and sediments is further elucidated below.

Complementary analyses Nineteen bulk samples (samples a–s) were taken from individual units, mainly those exposed at GTP 3 and GTP 13 (Tables 19 and 20). The study of these bulk samples was carried out to complement soil micromorphological analyses and the mineralogical investigation by Catt (Chapter 2.5). Samples were analysed for grain size, organic carbon and calcium carbonate, employing the standard techniques of Avery and Bascomb (1974). The ferruginous character of Unit 5a was scrutinised under Scanning Electron Microscopy (SEM), with semi-quantitative elemental analyses being carried out by Energy Dispersive X-ray Analysis (EDXRA). In addition, some calcareous features from Unit 4b, interpreted under the polarising microscope, were checked by SEM/EDXRA on the appropriate impregnated blocks (Figs 84–6).

Sample representation In igneous and metamorphic geology, normally only small (30 x 25mm) thin sections are commonly used to characterise a rock, and sedimentary sequences may be studied from a series of thin sections. At Boxgrove, large format thin sections, typically 65 x 65mm, 70 x 80mm or 130 x 6.5mm in size were used. This permitted up to four stratigraphic units to be studied in one thin section at some locations, although most thin sections sampled only one to three units. Sampling attempted both to examine vertical sequences and monitor lateral variations. The 57 thin sections are regarded as a reasonably sufficient number to study the 12 units under scrutiny (Table 18). At Boxgrove, thin sections from the available exposures normally only permitted the sediments to be studied in two dimensions and Collcutt (Chapter 2.3) had to excavate in three dimensions to be fully satisfied with the identification of some sedimentary structures and features resulting from biota. Samples for thin sections were only taken once a clear comprehension of unit variation was gained, through the guidance of Roberts and other workers who had been active at Boxgrove for long periods. Samples were taken systematically over the nine-year excavation period. Collcutt admits that field logging alone was inadequate for a full study of Units 4c, 5a, and 5b, for example, because of the thinness of these layers, and hence the need for microstratigraphic studies.

Table 19 Percentage of organic carbon and calcium carbonate, and layer designation at Boxgrove

bulk sample	locality/unit	% organic carbon	% calcium carbonate	thin section
Quarry 2: GTP 3				
a	6 (brickearth)	0.1	7.2	–
b	5b (chalk marl)	0.1	55.6	3
c	5a (iron and manganese pan)	0.9	–	3
d	4c (upper unit Slindon Silts)	0.1	2.5	3
e	4b (middle unit Slindon Silts)	0.1	23.6	–
Quarry 2: GTP 13				
f	6 (brickearth)	<0.1	3.6	8
g	6 (brickearth)	<0.1	1.5	9, 10
h	5b/6 (marl/brickearth)	<0.1	42.6	10
i	5b (marl)	<0.1	63.9	10, 11
j	5a (iron and manganese pan)	0.8	1.6	11
k	4c (upper unit Slindon Silts – terrestrial)	0.2	11.5	11
l	4b (middle unit Slindon Silts)	0.2	29.0	12
m	4a (lower unit Slindon Silts)	<0.1	29.9	13
n	3 (Slindon Sands)	<0.1	22.9	14
o	3 (Slindon Sands)	<0.1	20.3	15
p	3 (Slindon Sands – burrow infill)	<0.1	21.2	15
Quarry 2: GTP 17				
q	5c (narrow clay loam layer)	0.3	5.3	19
Quarry 2: GTP 25				
r	3 (terrestrial clay laminae near cliff at GTP 25)	0.2	14.3	28
Quarry 1B 4/1				
s	4d (pond deposits)	<0.1	60.0	33

Sampling strategy aimed to characterise all the archaeological/sedimentological units as exposed at GTP 13 (Fig 4) where a full sequence of samples from the second marine cycle (Unit 3) to the Brickearth Beds (Unit 6) was taken (Table 18; Figs 20, 44, 45). This was carried out at this section to complement sampling for fauna, mineralogy and Collcutt's sedimentary log. Variations in stratigraphy that were noted in the field were also sampled from excavations and test pits across the site in an attempt to achieve full representation of the sedimentary sequence. Units 1 to 3, studied in great detail by Collcutt (Chapter 2.3), were little sampled. In contrast, locations particularly rich in human artefacts were of particular interest. These included the lowest *in situ* material in Unit 4b, the main occupation layers in Unit 4c, and the more rare refitting flintwork in Units 8 (GTP 25) and 11 (Table 21). The relationship between sediments and faunal material, including molluscs, amphibia, birds, fish and mammals, and including the probable scat of a European mink, were also fully investigated. It is therefore considered that for Units 4b to 6 sufficient samples were taken to cover the geographical and temporal variations represented by these deposits reasonably, as exposed by the excavation process. Two facies types of Unit 8 were investigated, including a flint scatter site

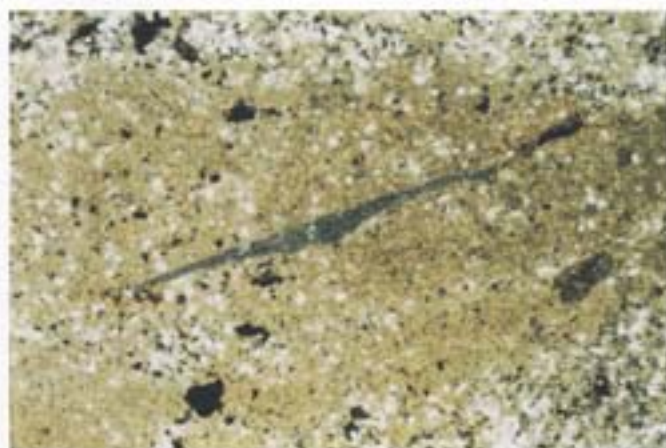


Fig 83a Quarry 1/A: sample 36; *finn* flake (artefact) within the calcareous silty clays of Unit 4b; the presence of coarse and fine laminae in this artefact-bearing layer are clear evidence that tidally influenced fine sedimentation on the lagoonal mudflat was not biologically disturbed, hence the perfectly undisturbed character of the artefact scatter. Crossed polarised light (XPL), frame length 5.5mm

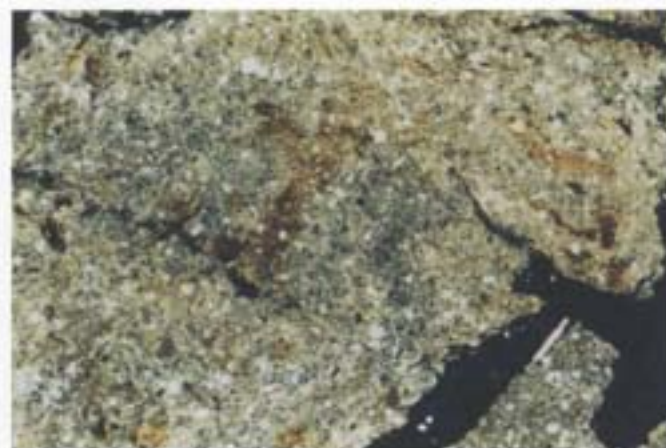


Fig 83b GTP 3: typical iron-poor, decalcified and homogenised zone of terrestrial soil horizon of Unit 4c; original laminated lagoonal/mudflat calcareous silts and clays were totally homogenised and decalcified by biological activity and subaerial weathering. Later inundation of the site (Unit 5a) has led to iron depletion, soil slaking and loss of structure and a typical grano-striated birefringent fabric has formed. XPL, frame length 5.5mm

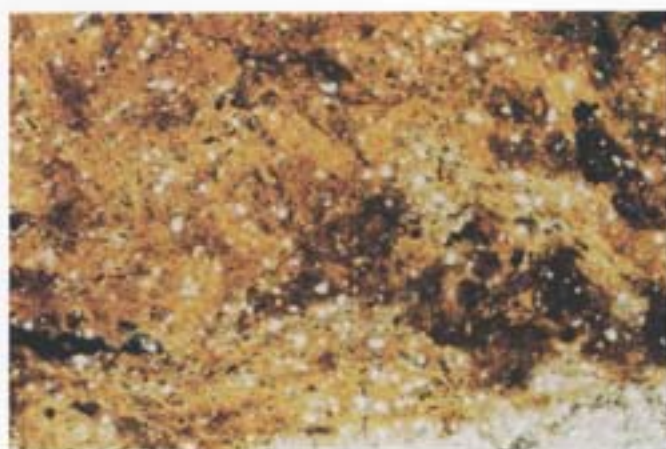


Fig 83c GTP 10: sample 5; 'ironpan' zone within terrestrial soil Unit 4c; impregnation of iron, perhaps first initiated during seasonal water table fluctuations before full site inundation (Unit 5a), led to some preservation of soil structures and evidence of biological activity; some birefringent clay coatings around voids may relate to soil slaking and translocation during inundation. XPL; frame length 5.5mm



Fig 83d Quarry 1B, Trench 4: sample 34; detail of finely laminated 'poaty' silts towards top of Unit 4d; the normally highly calcareous pond deposits become increasingly less calcareous at this level of organic silts. These contain fragments of bone (centre of photo). Many fish, aquatic bird, and amphibian bones were recovered from this unit. PPL, frame length 5.5mm

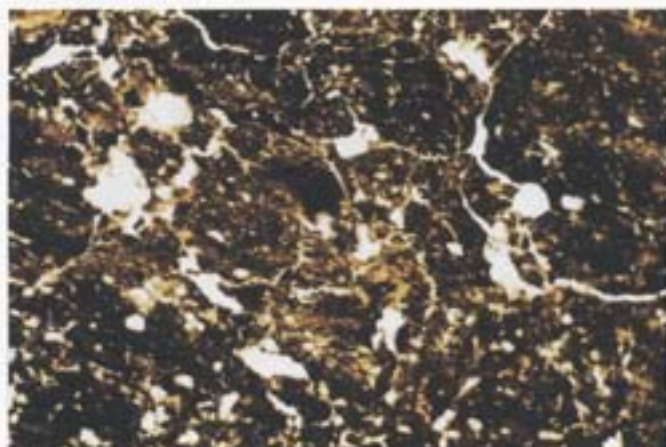


Fig 83e Quarry 2, Pit C: sample 39; here in Unit 5a, amorphous poaty deposits are the thickest at Bognor. They also show some drying-out and biological activity has affected the peat, developing a biological fine rough and channel porosity pattern and a weak fine subangular blocky structure. The once laminated peats and silts have become partially homogenised. PPL, frame length 3.5mm

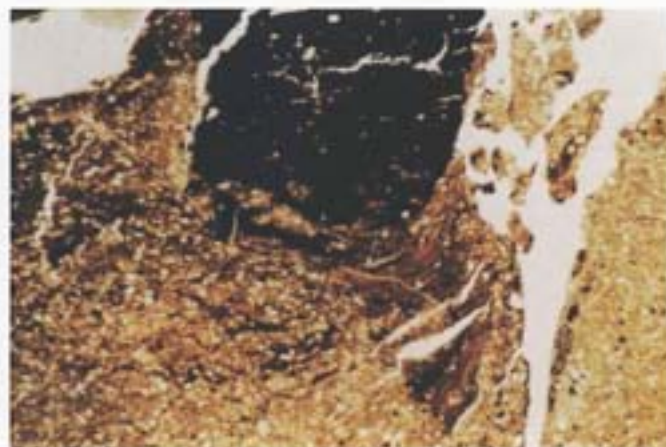


Fig 83f GTP 3: sample 3; iron and manganese pan material of Unit 5a has been microfaulted into the top of Unit 4c. This occurred prior to Unit 5b deposition and suggests both contemporary ferruginisation and drying out of the peat prior to Unit 5b (Marl) deposition. PPL, frame length 5.5mm



Fig 83g GTP 25: sample 27; projected microfiche reader view of Units 4c, 5a, and 5b. Bottom; mainly massive Unit 4c becoming weakly laminated at the top. Centre; dark brown Unit 5a with a basal laminated organic layer succeeded by a more mineralogenic layer containing organic fragments. Top; massive grey Unit 5b marl containing crushed and flattened mollusc fragments (upper centre right of photo). Frame length 0.11mm



Fig 83i GTP 17: sample 19; projected microfiche reader view of a flint artefact within the layered fine sands and organic matter of Unit 5c; thin silty clay crusts occur along these laminae; note small mammal tooth just below flint artefact (centre of photo). Frame length 0.11mm

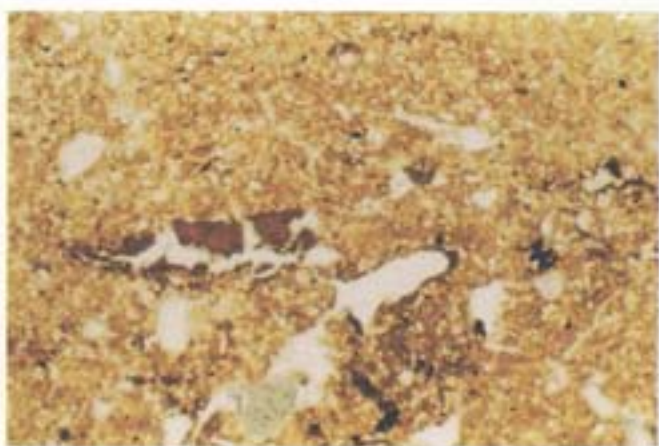


Fig 83k GTP 10: sample 5; Unit 6 showing possible incipient argillic brown earth formation in the brickearth, as indicated by sediment homogenisation, pore formation and the coating of these by moderately 'limpid' clay. The coatings and infills are not ferruginised and it is difficult to identify their original character. Their cracked nature (centre left of photo) may possibly be a result of cold climate, the overall soil resembling a fragipan. PPL, frame length 3.5mm

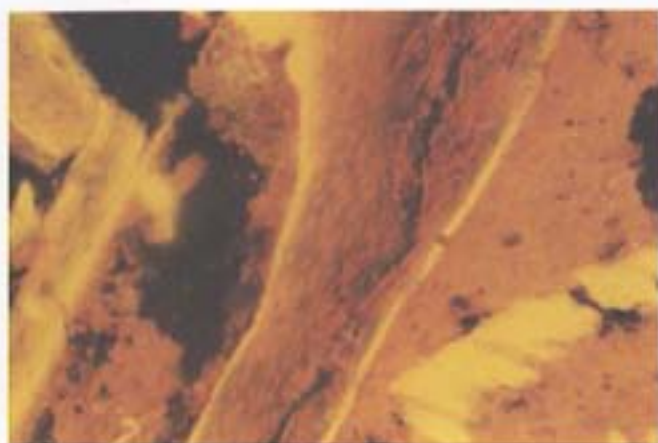


Fig 83h Detail of mink scat (see book cover) set in Unit 5b marl; various bone fragments and parts of the bone fluoresce differently under ultra violet light illumination, with perhaps apatite-rich areas being the most fluorescent. Patches of reddish staining are amorphous coprolitic material impregnating the calcareous marl which here appears as an orange coloured matrix. Frame length 0.33mm



Fig 83j Quarry 2, Pit C: sample 40; massive silty brickearth of Unit 6 deposited by generally low energy fluvial activity. This landscape became vegetated at times, hence these mineralised root traces. PPL, frame length 5.5mm

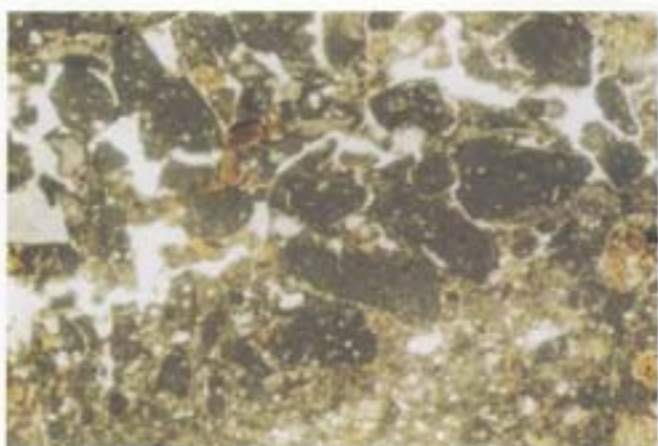


Fig 83l Quarry 1, GTP 31: sample 30; soliflual deposited chalk clasts, chalk soil, flint and silt to sand-size quartz of Unit 8 which seals Unit 4d sediments here in the absence of Units 5a and 5b. The poorly sorted deposit subsequently became cemented by secondary micritic calcite. Similar materials locally preserved the hominid bone found nearby. PPL, frame length 5.5mm

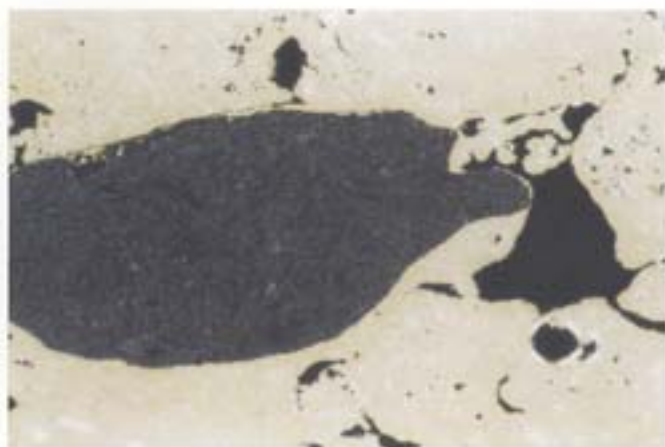


Fig 83m GTP 25: sample 23; flint artefact within chalky pellet gravel of Unit 8 The refitting in situ flint scatter is set in a pedological microfabric composing chalk and micritic chalk soil. A later phase of freezing and thawing activity has induced post-depositional intowash of colloidal chalk, coating some pores (centre right). XPL, frame length 5.5mm

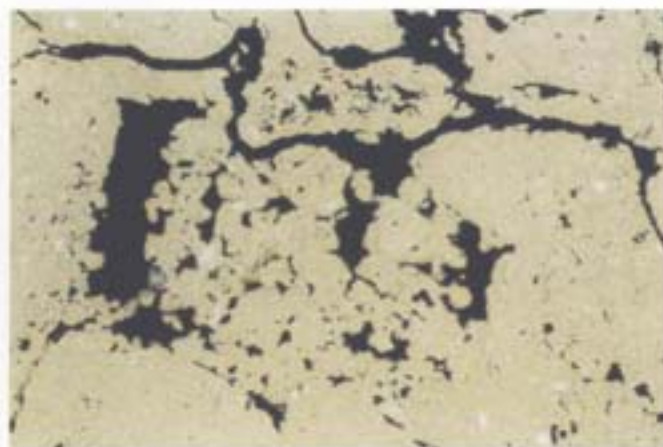


Fig 83n GTP 25: sample 23; probable mammilated earthworm excrements illustrating biological activity contemporary with human occupation at this location. This microfabric probably marks an interstadial during the formation of the generally cold climate Upper Chalk Pellet Beds. XPL, frame length 5.5mm

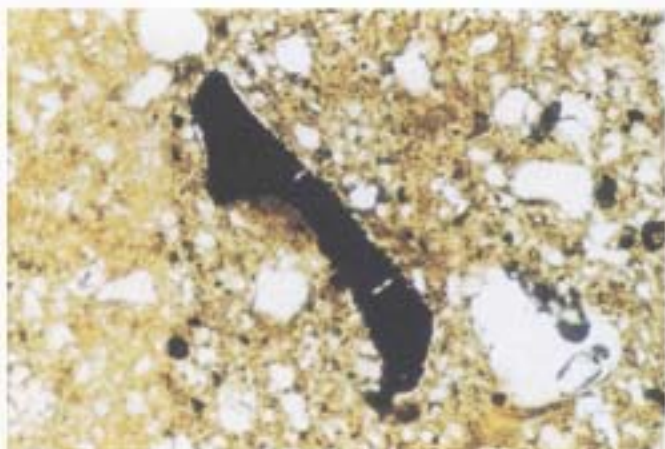


Fig 83o Sample 53: Unit 11, Upper Silt Bed; wood charcoal fragment within compact dusty soil containing textural features. These textural features were caused by mechanical clay translocation under humid arctic conditions. Charcoal suggests presence of woodland and fires, the latter resulting from lightning strikes or human activity. PPL, frame length 0.33mm

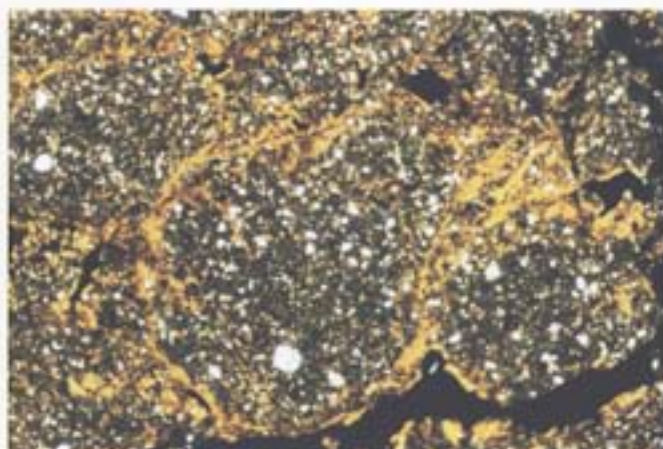


Fig 83p Sample 54: Unit 11, Middle Silt Bed; coarse and fine granular soil was affected by multiphase mechanical silt and clay intowash; the large amounts of textural features in this layer may be contributing to the yellowish red field colours of this soil, rather than any 'palaeoargillic' process, such as the rubification of the clays. Granular soil formation and mechanical translocation of fine soil are humid cold climate effects. XPL, frame length 3.35mm

(Roberts Chapter 6.3), and Unit 11 was sampled from three locations (Table 25). The resulting data are considered sufficient to characterise these particular units in the context of the present project.

The main research question for the soil micromorphological investigation was to establish the sedimentary/pedological conditions of the landscape occupied by humans, in relation to inferences based upon the archaeology and other environmental data. At Boxgrove this necessitated a specific approach for the micromorphologist, as outlined below.

Approach

There are no exact analogues for Boxgrove. As Boxgrove is dominated by sedimentary processes, Reineck and Singh (1980) has become a major text

used by the field geomorphologists at Boxgrove and for aiding microfabric interpretations. In addition, reference has been made to thin sections from sediments and soils of drowned landscapes (Essex coast: Macphail 1990a; 1994) and sites of increasing wetness (Uxbridge: Lewis *et al* 1992). Boxgrove has also benefited from published studies of ripening sediments (Bal 1982; Schoute 1987) and the mass of literature on palaeosols and cold soil features (Romans and Robertson 1974; Bullock and Murphy 1979; Van Vliet-Lanoë 1982; Kemp 1985; 1986; Rose *et al* 1985; Catt 1986; Fedoroff *et al* 1990). Studies of microfibrils of past soils and sediments, have to consider taphonomic post-burial processes and their effects (Mücher *et al* 1981; Fedoroff and Goldberg 1982; Coutard and Mücher 1985). There are useful experimental data on

Table 20 Boxgrove grain size data. NB: except for sample s, which was pre-treated by decalcification, all other samples were not pretreated by decalcification (see Catt Chapter 2.5 for decalcified sample grain sizes)

ZCL — silty clay loam, CL — clay loam, SL — sandy loam, ZC — silty clay, FZ — fine silt, MZ — medium silt, CZ — coarse silt, VFS — very fine sand, FS — fine sand, MS — medium sand, CS — coarse sand, VCS — very coarse sand

sample/unit	clay <2 µm	FZ <6 µm	MZ <20 µm	CZ <50 µm	silt	VFS <100 µm	FS <200 µm	MS <500 µm	CS <1 mm	VCS <2 mm	sand	texture	thin section
Quarry 2 GTP 3													
a/6	30	17	21	22	60	9	+	+	+	+	10	ZCL	-
b/5b	40	30	20	7	57	2	+	+	+	-	3	Marl	3
d/4c	47	8	18	20	46	6	2	1	-	-	9	ZC	15
e/4b	23	15	24	26	65	11	1	+	+	-	12	ZCL	15
Quarry 2 GTP 13													
f/6	22	8	29	29	66	11	1	+	+	+	12	ZCL	8
g/6	25	6	29	25	60	14	1	+	+	+	15	ZCL	9, 10
i/5b	24	36	25	10	71	4	1	+	+	+	5	Marl	10, 11
k/4c	38	12	18	18	48	13	1	+	+	-	14	ZC	11
l/4b	21	8	15	24	47	31	1	+	+	-	32	CL	12
m/4a	34	9	15	16	40	25	1	+	+	-	26	CL	13
n/3	14	3	7	25	35	50	1	+	-	-	51	fine SL	13
o/3	9	3	6	23	32	58	1	+	-	-	59	fine SL	15
p/3	17	4	9	20	33	41	5	2	1	1	50	fine SL	15
Quarry 2 GTP 17													
q/5c	35	14	13	3	30	30	3	3	+	-	36	CL	19
Quarry 2 GTP 25													
r/3'	35	3	11	8	22	12	23	8	-	-	43	CL	28
Quarry 1/B 4/1													
s/4d	15	21	19	13	53	22	9	1	1	+	33	fine CL	33

the short-term effects of burial that can help with interpretation of long buried soils (Bell *et al* 1996). Geochemical transformations, movement of iron and compression of stratigraphy are only some of the phenomena that have been considered. Lastly, the multi-disciplinary nature of the investigations at Boxgrove allows independent checks on interpretations made from soil microfabrics, permitting a degree of confidence that may not be possible in investigations based purely upon micromorphology.

Results

Chemical and grain size data are presented in Tables 19 and 20 respectively. In Table 24, field, soil micromorphological, and other data are combined to characterise each sedimentary unit and its variants. A summarised interpretation of environmental conditions is also suggested for each unit and variant. Heights above the chalk platform are measured from GTP 13. The generalised sedimentary sequence at Boxgrove above the chalk platform is outlined in Table 21.

Soil micromorphology

Each unit or part of a unit is first described according to its field, soil micromorphological (sedimentological, diagenetic and pedological), grain size and chemical character under the heading 'Data'. The unit is then interpreted according to this information.

Unit 3. The marine sequence of the Slindon Formation

In this section the heights above the wave-cut platform were taken at the southern end of GTP 13. Therefore the heights are somewhat less than those illustrated on Figs 44 and 45a-b.

Field analyses by Collcutt (Chapter 2.3) indicate that there were three marine cycles recorded above the chalk platform. Each one produced a boulder strewn beach, as seen in the deep excavations at GTP 13 (Fig 46) and GTP 25 (Fig 41). A longitudinal section of the raised beaches that coincides with the relict cliff-line, is visible in trench GTP 25 (Collcutt Chapter 6.3; Fig 42a). These marine cycles are believed to relate to three sea level fluctuations. The last is followed by a regression and the deposition of terrestrial deposits.

Unit 3, 2nd marine cycle

Data

Located just above the littoral horizon (Figs 44, 54), thin section 17 (GTP 13) sampled the foraminifera-rich (Adams *et al* 1984, 107-11) calcareous and massive-bedded fine and medium sand. This layer contains a few narrow (20mm) micritic clay bands that feature occasional mineralised root traces (Table 24). In the more coarse textured layers, fragments of well sorted and rounded micritic (<10µm size calcite; Folk 1959) clay are present.

Table 21 Summary of the stratigraphy at Boxgrove and the interpretation of depositional environment and climate (see also Tables 9a and 9b)

<i>unit</i>	<i>general environment</i>	<i>climate</i>	<i>data source</i>
11 Head Gravels	terrestrial	cold	field <i>in situ</i> artefacts
10 Calcareous Head Gravel	terrestrial	cold	field
9 Fan Gravel Beds	terrestrial	cold-cool	field
8 Chalk Pellet Beds	terrestrial	temperate-cool	field <i>in situ</i> artefacts
7 Angular Chalk Beds	terrestrial	temperate	field
6 Brickearth Beds	terrestrial	cool-cold	field
Calcareous silty clays (Table 9b)	terrestrial	temperate and cool	field
5c Clay loam layer	terrestrial	cool/temperate	field/fauna <i>in situ</i> artefacts
5b Marl	terrestrial	cool	field/fauna
5a Iron and manganese pan/ Organic Bed	terrestrial	temperate	field/fauna/pollen
4d Alkaline (pond) marl	terrestrial	temperate	field/fauna
4c Slindon Silts (decalcified upper layer)	terrestrial transformation of Unit 4b	temperate	field/fauna main artefact layer
4b Slindon Silts (calcareous and laminated deposit)	lagoonal/intertidal	temperate	field/fauna artefact layer
4a Slindon Silts (homogenised calcareous sediment)	lagoonal/intertidal	temperate	field/fauna
3 Slindon Sand	Marine Cycles 1, 2, 3	temperate	field/fauna
2 Raised beaches	Marine Cycles 1, 2, 3	temperate	field/fauna
1 Chalk platform and cliff	Marine Cycles 1, 2, 3	temperate	field/fauna

Interpretation

Thin section 17, from just above the beach, seems to represent moderate to low energy near-shore calcareous sedimentation. The obvious source of the fine calcareous sediment is the local chalk coastline, although very few chalk clasts were noted in this thin section. The evidence from the beds that were sampled may indicate that phases of low energy deposition, when plants were able to root in micritic clay bands, were succeeded by higher energy deposition. The last produced deposits containing poorly sorted, fine to coarse sand-size quartz, chalk, flint and reworked micritic clay. These perhaps result from local wave erosion during storms of beach and clay bands (Reineck and Singh 1980).

Unit 3, 3rd marine cycle

Data

At 2.75m above the chalk platform (Figs 44, 57), thin section 16 (GTP 13) shows coarsely bedded fine sands with micritic clay bands composed of highly birefringent detrital chalk. Catt (Chapter 2.5) only recovered 3–4% clay in his decalcified samples from this unit as a whole. Chalk fossils and chalk fragments also occur. Coarse (2–3mm to 20–30mm) burrows by Polychaete worms and molluscs (Reineck and Singh 1980) and micro-faulting/slippage (cracks) affected the bedding. Plants mainly rooted in the fine layers, whereas their mineral replacement and the iron staining of cracks seem to have been a later process.

Higher up in Unit 3, at approximately 3m above the chalk platform, thin section 15 represents an almost totally biologically worked calcareous fine sandy loam (Tables 19 and 20, samples o and p). Originally it

probably featured finely bedded fine sand and calcareous clay. The sediment here was later affected by very coarse faunal burrowing and some rooting, the last becoming subsequently mineralised. The bioturbation mixed in coarser, less well sorted material (Table 20, samples o and p).

Thin section 14 from approximately 3.70m above the chalk platform at GTP 13 and thin section 7 from GTP 10 (Figs 49a–51), sample the top of Unit 3 and the base of Unit 4a. The character of this topmost part of Unit 3 appears to be exactly the same as found lower down (sample 15; Table 18). It is again a strongly biologically worked calcareous fine sandy loam that seems originally to have been finely bedded (Tables 19, 20, sample n).

Included within Marine Cycle 3 are calcareous, slightly organic greyish brown laminated clays and silts (thin section 28; bulk as clay loam; Tables 19, 20, sample r). At GTP 25 these occur over beach sands and chalk rubble, and under marine sands. They contain non-calcareous clay mixed with calcitic silts and fine sands of probable marine origin. Also present are medium sand-size papules (fragments) of brickearth (see Unit 6), weathered glauconite and chalk fragments. Micrite impregnates the clay and silts around chalk clasts and most pores.

The junction of Unit 3 and Unit 4a

In places (thin sections 7, 14), the uppermost part of Unit 3 exhibits a sharp boundary between the faunally mixed fine sands and clays, and a 12–15mm thick sand lens, informally called Unit 3b (Collcutt Chapter 2.3, Catt Chapter 2.5, Tables 14–16). This sandy material

is coarser and less well sorted than the sediments beneath, and comprises very fine to fine sand-size quartz and clasts of detrital chalky clay. The chalky clay is presumably eroded from the finer underlying sediments. The top of this sandy deposit also contains faunal burrows containing Unit 4a material (Fig 63).

Interpretation

During Marine Cycle 3 (or earlier), but before the maximum transgression, ground water may have been flushing through the chalk rubble of the beach at GTP 25. This water seems to have carried fine chalk debris and silts, clays, and weathered material from decalcified superficial deposits on the chalk Downland. Sorting under presumed phreatic conditions within fissures in the chalk rubble and beach sand produced layered clays and silts. These fine deposits are of a facies type more commonly found in karstic caves (Courty personal communication; cf Westbury-sub-Mendip, Somerset, Goldberg and Macphail 1990) but at Boxgrove they are interbedded with calcareous marine sands. Possible exposure (Collcutt Chapter 2.3) of these terrestrial silts and clays led to minor cracking and rooting and these features are now mainly iron stained. Later, as the full marine (3rd) transgression took place these deposits were increasingly affected by calcification as they became buried by calcareous marine sands (see below).

In this marine cycle, just above the third beach, this calcareous marine deposit comprises mainly fine sands interbedded with probable detrital chalky clay. Possible fossils from the chalk and fine chalk fragments also occur, and the mineralogy points to the chalk as a major sediment source (Catt Chapter 2.5). The possible increase in the deposition of detrital chalky clays in Marine Cycle 3 may indicate changes in the configuration of the local sea and sources of sediment. At this low level in Unit 3 (sample 16) the chalk cliff may have been undergoing erosion. The general upward fining of the sands from Marine Cycle 2, may also indicate the decreasing influence of storm-affected open water in this part of the Unit at GTP 13. The finely bedded sediments that relate to cyclical phases of moderate and low energy deposition are strongly reworked, for example by molluscs and polychaetes. Slippage and microfaulting also occur at this level, perhaps by settling under thixotropic (water-saturated) conditions that pre-dated later staining mainly by iron (Hatch and Rastall 1965, 160).

Upwards (thin sections 7, 14, 15), Unit 3 continues as a finely bedded sediment, almost totally worked by fauna, possibly encouraged by the less vigorous conditions of Marine Cycle 3 (Collcutt Chapter 2.3). The major source of this chalky sediment may be alluvial, rather than just wash from cliff talus. The mineralogy also suggests sediment sources other than the chalk were involved, for example the local Reading Beds, although it must be noted again that the decalcified clay content of this deposit is still very low (3–4%, Catt Chapter 2.5).

The clay bands in Unit 3 are commonly perforated by the mineralised remains of plant roots, and mineralised plant fragments also occur. It seems therefore that the sea was shallow at times and plants grew during periods of low energy deposition. At the same time detrital organic matter became deposited. Some slight ripening (Avery 1990, 301), such as cracking, pore and structure formation, possible glauconite weathering, iron staining of pore margins (hypocoatings), and iron and manganese impregnation of plant material, has also occurred. These conditions are reflected in the foraminifera, which are mainly estuarine and marshy types, with an admixture of shallow marine allochthonous species (Whatley and Haynes in Roberts 1986; but see Whittaker Chapter 3.2 for a different interpretation).

The boundary between the fine sediments of Unit 3 and the uppermost (discontinuous) sand lens of this unit is particularly sharp. Elsewhere, later faunal activity from Unit 4a has blurred the junction of Unit 3 and Unit 4a. The sharp boundary at the top of the faunally worked (thin section 14), once finely bedded Unit 3 deposits, suggest that these were truncated before the deposition of the coarser sand lens. A high energy event, such as a storm, may have led to their erosion. It may also have been responsible for the moderately high energy deposition of a sand lens containing clasts of detrital chalky clay presumed derived from Unit 3. The discontinuous sand lens, which is found at a number of locations across the site, may in fact be relic of more substantial sandy deposits (?beach), that were themselves eroded by tidal or even aeolian activity. There may have been therefore, a hiatus in sedimentation between the end of marine conditions and the ensuing estuarine/lagoonal deposition of Unit 4a.

Unit 4. Regressional/lagoonal sediments of the Slindon Formation

Unit 4a

Data

The sediments mainly consist of massive calcareous clay loams (Tables 19, 20 sample m), that contain a few examples of the originally finely bedded silt-size quartz and clay (thin sections 7, 13, 14). The sediments are finer; Catt records a seven-fold increase in the non-calcareous clay content compared with Unit 3. In thin section, the calcitic clays are perhaps more dusty than those found in the marine deposits beneath, and because of this increased non-calcareous clay content could be considered more muddy in character. Porosity features, iron staining especially along root channels and cracks, also seem better developed. In places, sand laminae containing mollusc fragments, chalky clay clasts and stone-size chalk fragments occur. A wavy boundary marks the junction between Units 4a and 4b (thin section 12) and is in part a result of a 4–5mm deep and 20mm wide fine silt-filled rill.

Interpretation

Although no less calcareous than the fully marine sediments, these estuarine/lagoonal deposits (Whatley and Haynes in Roberts 1986; Whittaker Chapter 3.2) are much more fine grained and perhaps slightly more organic. Once more, the source of sediment is probably marine erosion, although there may be an alluvial component from the Solent River (Fig 23). A great deal of clay-sized material and minerals such as weathered glauconite, derived from the Chalk, Reading Beds and London Clay is present (Catt Chapter 2.5). Bates and Roberts (in Roberts 1986) have suggested that Unit 4a represents a tidal regime affecting a lagoonal rather than an estuarine body of water. The fine laminar deposition of silts and clay possibly reflects this, because reworking by water appears to be of such a low energy. Within Unit 4a, the rare occurrence (thin section 13) of stone-size chalk fragments associated with a sand layer containing weakly iron-stained chalky clay clasts and foraminifera fragments, is of interest. Obviously, the chalk could have been rafted in on seaweed, but the other material could be of Unit 3 origin. In one scenario this layer could relate to the erosion and redeposition of an exposed (subaerially weathered) deposit of Unit 3, possibly a relic beach or even a sand bar.

Many of the sediments are turbated and, although much of this could result from bioturbation, tidal flow can also rework sediments and could additionally have been active (Reineck and Singh 1980, 432). The sediments show many features of estuarine/lagoonal deposits (Kooistra 1978; Macphail 1990a), having pore development in addition to plant roots, iron staining and iron and possibly manganese replacement of plant material. Such features may result from short-lived sediment ripening.

At GTP 13 (thin section 12) the top of Unit 4a appears to have been affected by subaerial drainage, which formed a shallow rill. This feature, preserved by Unit 4b sedimentation, is evidence of surface drainage.

Unit 4b

Data

These deposits are calcareous clay loams (Tables 19, 20, sample 1), with 30–40% non-calcareous clay that gives them a finely speckled and very cloudy dirty brown grey colour. They may have slightly more sand compared with Unit 4a (Table 20), although the mineral sources seem to be the same (Catt Chapter 2.5). It is remarkable that the coarse and fine bedding of silt-size quartz and brown, speckled detrital chalky clay, has been so little bioturbated. In fact there is very little evidence of animal burrowing, and only the finest laminae show evidence of homogenisation. Some faunal fragments do occur but molluscs, for example, are poorly represented here compared with Units 3 and 4a (Bates and Preece Chapter 3.3; Roberts personal communication). Rooting by plants seem no more than in Unit 4a, although detrital organic matter may have

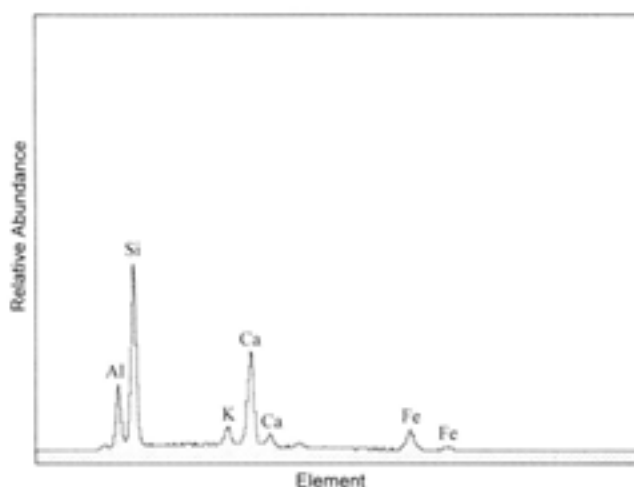


Fig 84 Example of SEM/EDXRA of Unit 4b at GTP 13, showing general calcareous nature of deposit

slightly increased, as measured by organic carbon (Table 19, sample 1). Unit 4b was examined from six locations.

At GTP 10 (thin section 6), some 0.5m beneath the ironpan (Unit 5a) (Figs 49a–51), some clay layers within the very well bedded silts and clays are cracked and these have been preferentially affected by iron staining and rooting. These beds contain a concentrated death assemblage of fish bones (Parfitt and Irving Chapter 3.4). Higher in Unit 4b, regular fine bedding is present at GTP 13 all the way up to its junction with Unit 4c. A series of SEM/EDXRA analyses (Fig 84) indicated that Unit 4b is uniformly calcareous below Unit 4c at GTP 13 (Table 19, sample 1). Some variations in Unit 4b were noted at locations where there is evidence of human activity such as flint knapping or butchery, within the unit. These flint working levels were examined at Quarry 1/A (Fig 83a) and at GTP 17 (thin sections 21, 22) where there is an associated butchery of a single horse (Roberts Chapter 6.2). Again, bedding is very well developed and preserved (Fig 83a), but in places the strata are often strongly affected by sediment deformation as a whole. Iron staining and iron and manganese impregnation of roots, sometimes pseudomorphically, occur throughout.

Unit 4b is particularly heterogeneous at GTP 17 compared with Unit 4b, for example, at GTP 10 and GTP 13 (Fig 4). Within the generally calcareous sediment, there are instances of finely bedded calcareous clay sedimentation that is darker in colour than the general calcareous clay in this unit. According to SEM/EDXRA of the polished block, this sediment appears to be significantly (x2) less calcareous than the surrounding fine sediment (Figs 85, 86). In addition, sand-size ferruginised sediment fragments occur in places within this darker sediment. Another example of unusual heterogeneity within this Unit 4b at GTP 17 is the inclusion of a coarse (5mm) fragment of laminated calcareous clay, apparently rich in fine organic matter particles.

Near the top of Unit 4b, as studied in the field and in the thin sections (eg 3), sedimentary laminae become finer. Both tongues of 'decalcification' from the overlying Unit 4c and presumably related secondary calcite formation can be recognised.

Interpretation

Unit 4b has a similar but more clay-rich sedimentary component as compared with Unit 4a. More detrital organic matter may be present and fish data show the potential influence of a freshwater input, presumably draining the chalk and hinterland, although there are almost no freshwater ostracods from this unit. The interbedded silt and detrital chalky clays seem to represent the low and very low energy deposition of suspended material in a body of water that was affected by diurnal/tidal rising and falling water levels. Perhaps this occurred in a delta or delta-influenced system (Donaldson *et al* 1970). No alluvial channelling was noted in Unit 4b. Thus, as marine regression continued, and freshwater influences became more dominant, this body of water may have been partially enclosed and protected from strong marine influences. On the other hand, as during Unit 4a deposition, sedimentation of Unit 4b was on mudflats that had water depths apparently still controlled by tidal influences. Water flow was insufficient to rework the coarse bedding, but possibly enough water movement was present from sheet flow to rework the finest laminae mechanically (Reineck and Singh 1980, 432). Activity by animals such as molluscs and polychaetes, which so turbated Unit 4a deposits, is rare in Unit 4b. Roberts (personal communication) suggests that animal and floral levels may be low here because of the amount of sediment carried in suspension. The mudflats were affected by saline (estuarine) surges as well as by a freshwater component; as a result no fauna or flora could have a stable environmental niche.

Periodic flooding and drying out of the mudflats may have produced muddy pools, possibly in the 'lowest' areas of the mudflats, that held trapped fish. These localised environments produced a rich death assemblage of fish and probable mud-cracked clays. Additionally, where deposits are associated with human activity, Unit 4b apparently is more heterogeneous and has some layers distorted. Calcium carbonate can strongly mask non-calcareous materials in thin sections (Wilding and Drees 1990). This phenomenon makes it difficult to recognise the higher amounts of non-calcareous material in the chalky clay in Unit 4b compared with Unit 4a, although the calcareous clay in Unit 4b may appear a little darker. At GTP 17 some clay laminae of a darker colour still apparently contain less calcium carbonate than the fine laminae present generally here (Tables 19, 20). Some of these relatively less calcareous lenses contain inclusions of sand-size ferruginised sediment. The evidence at GTP 17 therefore suggests the possibility that local environmental conditions at times led to the deposition of less

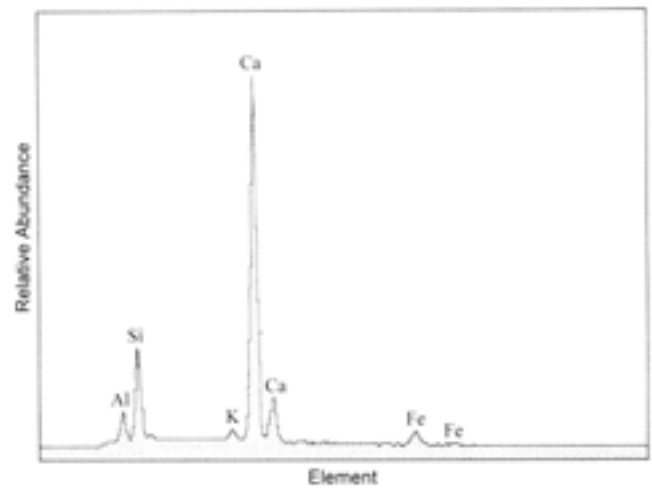


Fig 85 Example of SEM/EDXRA of general calcareous Unit 4b at GTP 17

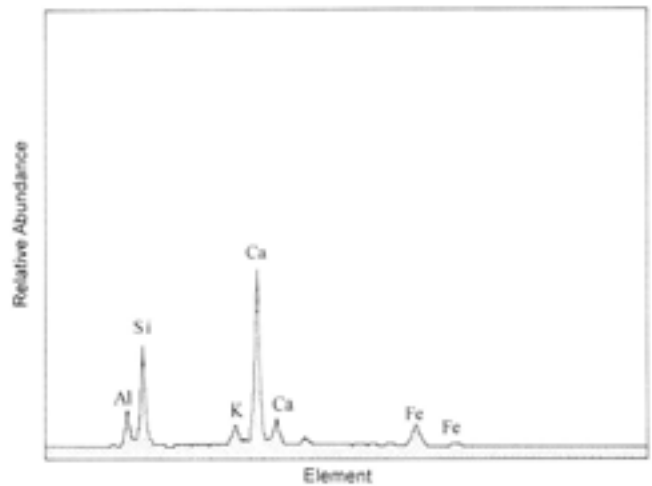


Fig 86 Example of SEM/EDXRA of some dark fine lenses in Unit 4b with apparently less Ca than the surrounding matrix (cf Fig 85) at GTP 17

calcareous and more 'impure' sediment than 'normal' for Unit 4b (Figs 84-6). The presence of a coarse fragment of calcareous clay, which may have originated in a subaerial puddle for example, is also enigmatic. As the fragment is not rounded and does not appear to have been washed into the sediment, its origin could possibly be associated with the focus of hominid activity at this part of the site.

The evidence from GTP 10 indicates drying out of Unit 4b occasionally. The features described above, along with short-lived ripening features such as iron and manganese replacement of root material, may seem to suggest occasional lengthier periods of exposure than may be influenced by just daily tidal regimes. This was a possible trend that became fully developed during the formation of Unit 4c (below). Areas of occupation may have been intermittently 'higher' and relatively 'drier' ground that was favoured by humans, with water levels perhaps influenced by seasonally varying river discharge and by monthly and seasonally

low tidal influences. Nevertheless, the environment continued to be dominantly a depositional one, hence the continued perfect preservation of artefact scatters. It is also worth noting that the sediments containing evidence of human activity were affected by sediment deformation features. In contrast, these features appeared to be absent from the lower sediments that contained concentrated fish remains at GTP 10 for example, or at GTP 13. The deformation features may thus reflect de-watering of these possibly higher areas of Unit 4b as seen at GTP 17. On the other hand, although features of intensive trampling *sensu stricto* (Gé *et al* 1993) are absent, the strongly distorted microstratigraphy seen in the sample (36) of a flint working surface could possibly relate to an impact by a foot or knee. However, other types of deformation processes, including those due to overloading by later deposits, also have to be considered (Reineck and Singh 1980, 79).

Unit 4c

Data

This unit was studied from 21 thin sections at 12 localities (Table 18). Although rich in remains of large animals (Fig 67), it is the small animal remains that clearly indicate the terrestrial nature of the unit (Parfitt Chapter 4.2). This conjecture is similarly supported by the mineralogy and the archaeology. The uppermost part of Unit 4c is complex and reflects post-depositional transformations (Goldberg and Macphail 1990) induced by the ensuing sedimentary environments of Units 5a and 5c (see below). Unit 4c can also be considered to be broadly coeval with Unit 4d (see below) in Quarry 1 (Table 9).

Unit 4c comprises a mainly non- or poorly calcareous silty clay (Tables 19, 20, samples d and k). In comparison with Unit 4b (Fig 66), Unit 4c has similar amounts of organic matter (0.1–0.2%), but contains far less calcium carbonate. Close inspection of the sediments in the field and the thin sections, shows that Unit 4c has up to three zones (Tables 22–24).

Zone 1 The uppermost zone is related more to Unit 5a conditions (Tables 23, 24) than the environment that formed Unit 4c. Briefly, it comprises some 5mm of non-calcareous fine laminae of mineralised organic particles and dusty clay void infills and related features. At Quarry 2, Pit Q (42, 43) (Roberts *et al* 1997), the uppermost part of Unit 4c features mineralised peat-like amorphous organic matter (see 46). It is completely unlike the calcareous and laminated Unit 4b.

Zone 2 Below organic zone 1 is a non-calcareous and homogenised layer. It occurs generally between the depths of 20–40mm (GTP 25 and GTP 3, Fig 83b) and 40–60mm (GTP 13 and 17), although at Quarry 2/A Unit 4c is homogenised down to 80–90mm (37, 38).

Zone 3 Here, Unit 4c is non-calcareous, but not fully homogenised. This non-calcareous zone seems to retain Unit 4b sedimentary laminae to shallow depths

that vary across the site. It can be noted that the areas with the deepest homogenisation exhibit deepest areas of non-calcareous material (GTP 25, 30–40mm; GTP 3, 70mm; GTP 13, 60–90mm), with non-calcareous deposits down to some 120mm at Quarry 2/A.

Soil features Apart from specific areas of secondary ironpans, which are discussed below, Unit 4c is a unit depleted in iron and clay, so that in Zone 2 it is generally massive/structureless (Fig 83b). At GTP 17, some possible prismatic structures are apparent in the field, but these are unique to this part of the site. Elsewhere structures are mainly only present in the depleted part of Unit 4c. Throughout Unit 4c there are numerous roots that are mainly replaced by iron. These rooting features generally appear to be unrelated to the relic structures described above.

In the secondary ironpans (Tables 23, 24), however, fine porosity (vughs and channels), pedological structures, possible relic rooting and possible earth-worm-like burrow infills (5) can be present (Fig 83c). At GTP 17, other evidence of biological activity comprises mineralised root remains with associated material resembling Enchytraeid-like excrements. Many of the voids preserved within the ironpans are coated with dusty clay, whereas ferruginous hypocoatings and impregnations that make up the ironpans (several at GTP 10) may represent some surfaces or pedological structures. At GTP 25, the ironpan also marks the base of Unit 4c. Elsewhere towards the base of Unit 4c, some patches of calcitic fabric are present, and some rare voids may have secondary calcium carbonate infills. Lastly, towards the top of Unit 4c at GTP 17 there is evidence of structural collapse and the infilling of pores by elutriated (washed) silt.

Faunal remains Mollusc fragments of varying degrees of decalcification also occur in this lower Zone 3. Within Unit 4c as a whole, a few fine flint fragments may occur and occasionally bone and teeth can also be present. At specific locations, Unit 4c can contain small (48, 1 x 2mm; 49, 2 x 3mm; 47, 5 x 4mm) concentrations of pale, poorly birefringent bone fragments that are strongly autofluorescent (UV), and have a dotted ferruginous staining. Fragments of teeth (eg enamel coated incisors) are also often associated, and surrounding Unit 4c material can contain a scatter of finer bone fragments. Such bone concentrations can occur at the base of the homogenised zone, or as deep as the partially calcareous laminated Zone 3. One example (46) also seems to occur at the very top of Unit 4c.

Interpretation

Unit 4c appears to be the weathered (Roberts Chapter 2.1, Catt Chapter 2.5) and partially homogenised upper part of the Slindon Silts (Unit 4b). There is little evidence to suggest that Unit 4c derives from a non-calcareous sedimentary source different from Unit 4b. Rather, a number of features clearly indicate that it is the decalcified upper part of Unit 4b. These are the

presence of partially decalcified mollusc fragments, the strong variation in thickness of non-calcareous Unit 4c, the occurrence of patchy calcareous fabric, and the presence of some secondary calcium carbonate at the base of the unit. Some occasional indications of sediment ripening in Unit 4b from the exposure of the deposit have been discussed. Here at Unit 4c, exposure to sediment ripening (Duchauffour 1982, 186–7; Bonneau and Souchier 1982, 363; Avery 1990, 301) must have been much more prolonged and without any obvious sedimentary activity, in order to produce this strongly weathered and decalcified unit.

Soil thickness By decalcification, Unit 4c would also have lost some 20–30% of its total weight (Table 19), and thus could be thinner as a decalcified unit than it was as a calcareous one. A reduction in thickness for this unit would also result from loss of organic matter, structure and porosity (Catt 1990; Bell *et al* 1995). At Overton Down, Wiltshire, short-term (32 years) burial of a biologically active mineral Ah horizon led to some 40–50% loss of thickness, and the buried organic Ah horizon at Silbury Hill, Wiltshire, may have suffered compression by x_6 – x_9 caused by some 30+ metres of overburden (Crowther *et al* 1996).

Pedogenesis Across the site, Unit 4c displays a homogenised zone (Table 24). The presence of relict features of rooting, pedological structure formation and biological homogenisation of sedimentary layering — including the possible activities of earthworms and Enchytraeids (Fig 83c) — suggest that pedogenesis occurred when the sediment was exposed through a lowering of the water table. Information from artefact refitting (Roberts 1986; Bergman and Roberts 1988; Bergman and Roberts Chapter 6.2) indicates mixing of material throughout Unit 4c, supporting the micropedological evidence of biological reworking. Data from small mammal analysis also suggest the possible presence of moles and voles. These fauna suggest a woodland environment, and although some animal material appears to be of definite predatory bird pellet origin (Parfitt Chapter 4.3), the birds themselves may have needed perches for their regurgitation activity. The microfabric character of bone concentrations both on the surface of and within Unit 4c suggest that they are coprolitic, sometimes being biologically worked into the soil. They may be scat from mink (Parfitt personal communication), one of the major predators present.

Ripening and occupation timescales Work by Bal (1982) who monitored the zoological ripening of the drained fresh water polder at IJsselmer in Holland, shows how rapidly sediments can ripen and lose their depositional layering through biological activity. In addition, a terrestrial ecosystem soon developed, and the invasion of pioneer plants led to a closed shrub woodland canopy in some 10 to 20 years. Here planting took place, but at Boxgrove the wooded downland beyond the cliff would have readily supplied seed and animals. At Boxgrove the ripening lagoonal sediments

would have been transformed into something like a Raw Gley Soil (Avery 1980), calcaric-alluvial soil (Avery 1990), or Aquic Udifluent (Soil Survey Staff 1975). On draining the IJsselmer polder, sediments were rapidly ripened and biologically reworked to a depth of about 0.4m during the 14 years or so it took to develop a full terrestrial ecosystem. At Boxgrove, soil homogenisation appears to be shallow, although loss of bulk by decalcification and post-burial effects and compression needs to be taken into consideration. This immediately indicates that the period of soil ripening, and main human occupation could have been of short duration if we are employing depth of ripening as directly reflecting time. Hydromorphic features (Bouma *et al* 1990), such as the ferruginisation of various 'surfaces' or pedological structures and roots and excrements, however, indicate water table fluctuations (Macphail 1990b; Lewis *et al* 1992). There is therefore the likelihood that Unit 4c, although terrestrial, may have been seasonally wet, in the same way as Unit 4b seems to have been affected by seasonal water table fluctuations. As they are likely to be all part of the same lagoonal system, this is not unexpected. There is also evidence from across the site of areas where biological homogenisation and decalcification were deeper, suggesting that there were drier and better drained locations. These areas also have marked concentrations of human activity, for example, around Q2/A (see Unit 5a). At GTP 17, a chosen occupation site, dryness during the formation of Unit 4b and Unit 4c is indicated by the well-preserved soil structural features; at this time this was the driest area studied at Boxgrove. At present, however, it is not possible to state whether these areas were actually higher than the surrounding landscape at the time. The depth of artefact reworking and the character of Unit 4c as a whole implies that it represents only a short period of soil ripening and human occupation, perhaps as little as 10–20 years. This interpretation is based purely on simple comparisons with the IJsselmer Polder soil (11–14 years, Bal 1982) and the long (*c* 1000 years) pedological sequence at Uxbridge, Middlesex (Lewis *et al* 1992). On the other hand, uncertainties relating to the probable fluctuating nature of local water tables and the effects of weathering and post-depositional compression on Unit 4c could argue for a longer timescale being involved. Catt (Chapter 2.5) suggested a timescale of around 100 years for the weathering effects in Unit 4b.

Site inundation The susceptibility of the area to water table fluctuations and periods of increasing wetness is first suggested by possible peaty soil formation at Pit Q (excavated during Boxgrove Project B, just north-west of Q2/C, Fig 4; Roberts *et al* 1997), and the presence of scat in peat either at the very top of Unit 4c or at the base of Unit 5a (46). The main effects of increasing site wetness at the end of the soil ripening phase were to slake the soil and waterlog it. This led to hydromorphic iron depletion of Unit 4c (Fig 83b), a general structural collapse of soil peds, and periodic

downwash of dusty clay released by this slaking event. Only rare parts of Unit 4c survived as a result of iron-pan development and sometimes these have dusty clay void infills that may relate to the slaking event(s). At GTP 17, which was perhaps a drier area, coarse pedological structures survived better, and site wetness caused these to be infilled with iron and clay depleted silt (elutriated silt). Thus the site seems to have undergone fluctuating rises in water table, until it became totally waterlogged. Relic organic laminae that characterise the top of Unit 4c are probably not sedimentary features as such. Instead, they may relate to fine organic matter filtering into the water-saturated and slaked topsoil of Unit 4c that developed during the deposition of Unit 5a (see below) forming thin micropans. Comparable hydromorphic and slaking effects have been recorded in the estuary of the River Blackwater, Essex, where Neolithic landsurfaces were buried by estuarine silts and peat and slaked topsoils under peats developed these organic micropans (Wilkinson and Murphy 1986; Macphail 1990a; 1994). Similar micropans were noted at Uxbridge, Middlesex, where early Holocene alluvial soils were affected by increased wetness and mire formation (Macphail 1990b; Lewis *et al* 1992). The Quaternary site of Swanscombe, Kent, also records decalcification of calcareous alluvium through pedogenesis, and later hydromorphic effects of an ensuing base level rise (Kemp 1985).

Unit 4d, alkaline 'pond' marl

Data

Unit 4d occurs only in a single small area in Quarry 1 Area B (Austin and Roberts Chapter 6.2), and is probably some 50–60m in lateral east–west extent (Table 9a). Where it occurs, Unit 4c is rarely present, and Unit 4d rests directly on Unit 4b. Unit 4d is an alkaline (pH 8.9; see Catt Chapter 2.5 for pH of other units) marl (60% calcium carbonate; Table 19, sample s), with a non-calcareous fine sandy loam mineral component (Table 20, sample s). Examination of its junction with Unit 4b (35) shows that Unit 4b is here homogenised, although elsewhere Unit 4b has always been found to be laminated (Austin and Roberts Chapter 6.2). The edge and basal part of Unit 4d examined here contains numerous iron replaced organic matter laminae (Fig 83d), and it appears that some organic matter has diffused into the top of Unit 4b.

Unit 4d, although appearing uniform in the field, is microscopically heterogeneous. It is generally composed of thin silt laminae in a micritic fabric, and sometimes these appear to have a small organic matter component. Commonly, however, some parts of the unit show that this sedimentary layering has been mixed by scouring and possible biological activity forming a channel and vuggy porosity. These voids have been mainly infilled by transformed/inwashed micritic material causing recementation and indurated nodular areas to form. As no stromatolite or algal

pseudomorphs (Courty *et al* 1989) are present, these features are not tufa *sensu stricto*. Towards the top of Unit 4d fine layering is replaced by coarse layers that include high percentages of silt-size quartz, sand-size flint, rounded chalk and reworked fragments of marl. Also commonly present in some mixed chalky 'soil' inclusions, that are rich in calcite, fossils, etc, are very pale yellow and very poorly to non-birefringent clay clasts. These yellow clay clasts, which also contain silt-size quartz, have been tentatively identified as palygorskite (Kerr 1959, 414). They require further study by clay mineralogical techniques, but as palygorskite does not occur in clay soils formed on the brickearth or on the chalk itself at Boxgrove, they may be Cretaceous relics (Courty and Fedoroff, personal communication).

The very top of the unit, just below Unit 5a or Unit 5b, is composed of a 5mm thick layer of numerous silt and iron replaced organic matter laminae. Here, bird and probable amphibia bone occurs (Fig 83d). Where Unit 4d is directly overlain by Unit 8 material, the sediment can be strongly broken up. Turbated Unit 4d also occurs as part of a soft sediment deformation feature and nearby has a platy microstructure imposed upon it.

Interpretation

Unit 4d has been difficult to interpret fully. It seems that when base level fell during the formation of Unit 4c, an area in Quarry 1 was similarly affected, but Unit 4b, although homogenised by sediment ripening activity, did not decalcify. This may have been because it was also influenced by calcareous water from a spring. This preservation of a homogenised Unit 4b seems to have occurred at the margins of the unit. Towards the centre of this unit, however, the suggested phreatic activity seems to have partially eroded Unit 4b, forming a hollow or pond-like feature (Roberts *et al* in prep). The presence of bones from aquatic bird and amphibia (Chapters 3.5, 3.6) support this interpretation.

Calcareous material and silts could have been reworked from Unit 4b, and then deposited as fine micritic laminae according to the state of water level within the pond. The coarser mineral component of Unit 4d, however, indicate that sediment originated from sources other than Unit 4b (see below). It is probable that base level fluctuations affecting the area allowed periods of biological activity to rework the sediment at times when water levels were low. As water levels rose, perhaps through seasonal spring activity (see below), biological voids and possible scour features were infilled by a calcitic slurry. Later cementation occurred through the growth of secondary micrite and microsparite. Samples from near the top of Unit 4d contained layers of coarse inclusions (Table 24), which suggest high energy erosion and reworking of the pond sediments. The chalk and other possible relics of Cretaceous sediments (palygorskite) may have increased the pH of this unit, so it seems spring or fluvial

activity occurred in the area of the chalk to the north. Erosion of calcareous soils is also indicated by the presence of calcite root pseudomorph fragments. Sometimes the coarse layering is interdigitated with fine layering, which may suggest a possible seasonal water flow. As the deposit contains no molluscs, it may indicate that alkalinity was too high for molluscan activity (K Thomas personal communication).

The top of the unit is composed of organic layers separated by silt bands, which, together with the bird bone evidence, suggest that a thin peat-covered marsh may have formed when the pond was unaffected by low energy fluvial activity.

Unit 5a, iron and manganese pan

Data

Unit 5a varies in thickness across the site, from a few mm above the chalk mud at GTP 25, to some 20mm at Pit Q. On average, however, it is 10mm thick. It can be regarded as non-calcareous, apart from post-burial inwash from Unit 5b. It is an organic deposit, with nearly 1% organic carbon still remaining (Table 19, samples c and j) even after very strong organic matter mineralisation (Table 24) (Catt 1990, 67). Generally, but not at GTP 17 and Pit C (Fig 83e), Unit 5a merges gradually with Unit 4c. This boundary is characterised by increasing amounts of layered, highly humified, detrital organic matter (Tables 22–24) that is replaced by manganese and iron (see Catt Chapter 2.5) ('manganese pan', Fig 83f). It is composed of clay and silt and can have abundant very dusty clay intercalations (Table 24, sediment type (a)). This layer may contain very large fragmented pieces of organic matter up to several hundred microns in length, with one possible lignified fragment at GTP 25 being around 800µm long.

At GTP 10 (Table 22), this sediment type (a) is the only component of Unit 5a. Elsewhere (eg GTP 3, GTP 13) (Table 23), however, the manganese stained horizon can be succeeded by multiple layered silts and fine sand with included layered/lenticular or rounded fragments of ferruginised amorphous organic matter (sediment type (c), Table 24). Commonly a central layer (sediment type b) is present and this has only fine silt laminated with dominant amounts of ferruginised amorphous organic matter. Again, these often occur as lenticular or rounded fragments. Occasionally, apparent *in situ* organic matter may occur, and this can contain ferruginised 'woody root-like' pseudomorphs. Other less clear, but probable organic, pseudomorphs are common. Clay is also included in this fine textured layer, giving Unit 5a a bulked clay texture (Catt Chapter 2.5). Within this layer some 50–100 or more laminae can be discerned. At GTP 3, GTP 13, and elsewhere, sediment type (b) is succeeded by more sediment type (c) material. Sometimes this upper layer may cut into underlying laminae, and at GTP 1 forms a silt infilled rill 20mm long and 5mm deep.

Occasionally, the main part of Unit 5a is dominated by massive, seemingly *in situ* amorphous organic matter. At Pit Q this forms a 10mm thick layer that contains possible mineralised woody remains (Hather personal communication). It also has common iron infills of an unusual character, resembling concentric layered booklets. Catt (Chapter 2.5) found Unit 5a to contain goethite and non-crystalline iron. At Pit C, the mineralised amorphous organic matter has relic features of probable biological channelling and mixing, thus pedological structure and porosity are preserved here (Fig 83e). Bone fragments occur at GTP 25 and, as at Q1/B, such bone concentrations could have a scat origin. Rare phytoliths and pollen/spore grains (Scaife 1986) could be discerned throughout Unit 5a by observation in ultra-violet light. The probable acid nature of Unit 5a may be inferred from occasional decalcification at the base of Unit 5b marl (Pit Q).

Interpretation (Unit 5a; intermittent gentle fluvial and mire conditions)

Depositional environment and timescales The interpretation of the uppermost part of Unit 4c (zone 1) suggests that Boxgrove became increasingly wet, until the site itself became generally inundated with water. Low energy muds containing large amounts of detrital organic matter were deposited (Tables 22, 23). This could have occurred under a shallow lake environment that developed into a marsh. It was probably under these waterlogged conditions that Unit 4c was generally depleted of iron and clay. It also became penetrated by the roots of marsh plants, the iron- and manganese-replaced roots being the last features impressed upon Unit 4c. Above the manganese pan, the ironpan of Unit 5a is commonly made up of iron replaced amorphous organic matter with varying amounts of iron impregnated clay, in addition to silt laminae. Recognisable organic matter pseudomorphs indicate (M A Courty, N Fedoroff, and R Kemp personal communication) that the mineralised amorphous organic matter is relic of peaty material. The large amounts of clay that can be included are similar to early Holocene valley mires formed for instance under marsh conditions (Lewis *et al* 1992; Macphail 1990b). These are classed as moderately organic clays.

The various types of layers recorded in Unit 5a (Table 24) have been located across the site (Figs 69, 70). At GTP 3 and 13, for example, there is a succession of sediments after the accumulation of detrital organic muds;

- i) laminated silts (and fine sands) with few to many amorphous organic matter fragments,
- ii) laminated silts dominated by fragments of amorphous organic matter, locally *in situ*, and
- iii) the same as i, but sometimes eroding into underlying laminae.

At Pit Q, the amorphous organic matter layer appears to be almost totally *in situ*.

Table 22 Stratigraphy at GTP 10 (thin section 5), according to soil micromorphology

<i>depth</i>	<i>stratigraphy</i>	<i>unit</i>
0	Erosive and decalcified path gravels	Unit 9
140mm	Massive, totally slaked, collapsed and compacted possible incipient argillic brown earth, now forming a fragipan-like soil	Unit 6 (Brickearth)
	Partially slaked, collapsed and compacted incipient argillic brown earth, with relict biological structures, porosity and occasional void clay coatings (now cracked), forming a fragipan-like soil that subsequently became strongly ferruginised at its base	Unit 6 (Brickearth)
150mm	Massive, totally decalcified fine silt ('Marl'), with rare limpid clay void coatings	Unit 5b (Marl)
155mm	Finely laminated, weakly iron and manganese impregnated ('manganese pan') silty clays with abundant detrital organic matter	Unit 5a
160mm	Massive, totally iron-depleted ripened soil (now without structures)	Unit 4c
165mm	Massive iron impregnated ripened soil, with relict (partially collapsed) soil structures (iron ironpan)	Unit 4c
169mm	Massive, moderately iron-depleted ripened soil (now without structures)	Unit 4c
200mm	Bottom of thin section.	

Table 23 Stratigraphy in the upper part of GTP 13 (thin sections 8, 9, 10, and 11) according to soil micromorphology

<i>depth</i>	<i>stratigraphy</i>	<i>unit</i>
	Path gravels	Unit 9
0mm	Strongly laminated coarse silts, with coarse bands of sand-size quartz, flint and abundant dusty clay papules/clasts of slaked 'brickearth soil' (see Table 22, GTP 10) and frequent limpid clay papules (eroded from mature argillic brown earths developed on the Downs and/or from fine brickearth sediments) and clay curls	Unit 6 (Brickearth)
30mm	Laminated coarse silts with cut and fill features, and iron and manganese replaced roots and organic inclusions	Unit 6
110mm	Curved non-parallel laminated coarse silts with cut and fill features and occasional clay bands	Unit 6
125mm	Coarsely laminated fine silts with clay clasts, few sand-size flint and <i>in situ</i> calcite root pseudomorphs	Unit 6
135mm	Partially fragmented and 'brown' stained micritic marl	Unit 5b (Marl)
140mm	Laminated fine silts and micritic marl	Unit 5b
170mm	Massive micritic marl with gravel-size rounded chalk clasts	Unit 5b
210mm	Iron cemented laminated coarse silts and commonly fragmented iron-replaced peat (ironpan)	Unit 5a (iron and manganese pan)
220mm	Iron and manganese stained silty clay with very abundant detrital organic matter (manganese pan)	Unit 5a
225mm	Massive iron-depleted ripened soil (without relict structures).	Unit 4c
260mm	Iron-cemented ripened soil with collapsed relict structures (thin ironpan)	Unit 4c
275mm	Massive iron-depleted ripened soil (without relict structures) with few sedimentary laminae relict of Unit 4b (calcareous) sediment	Unit 4c
290 mm	Bottom of thin section.	

These layers broadly indicate a sequence of silts and fine sands deposited in an environment of moderate energy. They also include peat and peaty clay that was often locally eroded (hence 'lenticular fragments') or perhaps accumulated only in patches. Periods of intermittent sedimentation of very low energy silt and peat and peaty clay also took place, accompanied by local erosion and deposition. At some sites (Pit Q), an undisturbed period of peat formation apparently occurred. At Pit C, in contrast, the organic accumulation seems to have been affected by sub-aerial biological activity, as noted for example in Mor horizons

(Babel 1975; Macphail 1988; 1992a) and peats undergoing drying out (Schoute 1987) (Fig 69). At GTP 17, typical Unit 5a deposits are absent in one area.

These variations in the type of sediment and sediment sequence of the ironpan indicate variations in the depositional environment after the initial inundation of the site. Some areas were influenced by intermittent, low to moderate energy fluvial/colluvial activity punctuated by mire formation. Other areas had steady peat growth, whereas some locations (Pit C) seemed to have been less wet at times allowing periods of biological turbation and mixing (Fig 83e). Here also, drying out

and the Downland itself. The soil cover may have been mature argillic brown earths on the Downland, whereas on the brickearth-covered low ground there may have been only enough time for incipient argillic brown earths to form. Full devegetation and resulting increased downland runoff affected the site. Possible incipient argillic brown earths became water saturated and slaked, making them unstable (see Units 4c/5a: Macphail 1990; 1992b) and runoff eroded them, depositing slaked soil clasts at GTP 13 (Table 24), for example. At GTP 10 only partially transformed and truncated soils were produced, whereas elsewhere soils were completely lost. In addition, possible cryogenic activity with devegetation may have accelerated erosion, fracturing soils into poorly rounded fragments and clay coatings into papules (Van Vliet-Lanoë 1982; 1985; Kemp 1986). Possibly, cryoclastic fracturing was followed by meltwater flow that deposited these coarse soil clasts (cf Westbury-sub-Mendip: Goldberg and Macphail 1990; Macphail and Goldberg 1995). In either case, the uppermost deposits of Unit 6 at GTP 13, are in reality contemporaneous with the conditions that produced the slaked soil at GTP 10.

At the beginning of this section, Unit 5a deposition was compared to sedimentation during Unit 6 formation. The much larger amounts of sediment being deposited during Unit 6, may simply imply greater rates of erosion of the Downland block which, with Unit 9, emphasise the probable effects of a rapidly deteriorating climate.

Chalk mud/calcareous silty clays

Data

These deposits have no formal unit number or bed designations, and were only identified in this study at GTP 25 (Figs 58, 73). They are fully described in Table 9b (Roberts Chapter 2.1). They comprise gravel-size (<10mm) rounded chalk set in a micritic cement, and contain very abundant *in situ* calcite root pseudomorphs. These increase in number upwards in the biologically disturbed top, where organic matter and bone fragments are evident. The chalk mud is buried by some 5mm of Unit 4b/4c, which appears to infill biological pores formed in the top of the mud, but does not affect the obvious root holes. Unit 4c was sealed initially by 1mm of (now ferruginised) organic clays, and by 1mm of silty sediment containing detrital organic matter. Above, Unit 5b marl and more chalk mud deposition ensue. Firstly, organic micritic laminae carry bone fragments up to 4mm in length and these occur within a 5mm thick layer representing primary marl deposition. Upwards, coarse chalk marl/chalk mud deposits occur and these contain both *in situ* calcite root pseudomorphs and their reworked fragmentary remains. Biogenic calcite, similar to earthworm granules, is commonly present. The chalk mud merges upwards into Unit 8.

Interpretation

The chalk mud appears to have been deposited as a slurry from the chalky cliff talus slope, and short-lived weathering and plant growth followed. Probably, extant plants stopped Unit 4b material from washing into some biopores, although biological activity did mix quartz silts of Unit 4b into the top of the chalk mud. Soon after, peat formation ensued and this was followed by fluvial deposition of silts and detrital organic matter. As elsewhere, gentle flooding that was an initial feature of Unit 5b, also carried bone fragments. Ponding was intermittent with inwash of organic matter. The whole was buried by a further chalk mud slurry that resembles facies present in both Unit 5b and Unit 8. Biogenic granules and calcite root pseudomorphs testify to the biological activity on the sloping chalk talus at this time.

Unit 8, Chalk Pellet Beds

Data

Unit 8 was examined from two parts of the site. The basal deposits were observed from a number of locations, for example over Unit 4d, in Quarry 1. Material from within the deposit that contained an *in situ* flint scatter (Roberts Chapter 6.3, Fig 291) was studied at GTP 25. At the latter site the chalky pellet gravel, that overlies cliff talus material upslope, buried the beach deposits (Figs 42a, 53, 75). Roberts (Table 9a) has divided the Chalk Pellet Beds into Lower and Upper parts. The Lower Chalk Pellet Beds were laid down under temperate conditions immediately in front of the cliff (Fig 42a). The Upper Chalk Pellet Beds were deposited under cold conditions and spread out southwards from the cliff time-transgressively, covering a number of older units.

At Quarry 1, Unit 8 Upper Chalk Pellet Beds can overlie undisturbed earlier deposits, or cryoturbated deposits. It can also be wedged up against overthickened Unit 5a material through similar mass-movement activity (Fig 83l). The basal deposits are generally fine laminated calcareous silts, fine sands and micritic marl material, that could include fragments of brown soils, papules and relic chalk material, probably palygorskite (see Unit 4d). The marl parts also contain molluscs and feature fine organic laminae. Thus, in many ways, this element of Unit 8 appears not dissimilar to parts of Unit 5b. Above, for example in the top of thin section 30, these bedded Unit 8 sediments are characterised by a massive deposit of coarse gravel to small stone-size, rounded to subrounded, chalk and chalky soil clasts (Fig 83l). Sometimes this deposit occurs directly over Unit 5a and 4d. Common coarse soil inclusions, as noted below, occur. Some of the chalk and chalky soil inclusions also appear to be weathered. In addition, many fragments of calcite root pseudomorphs are present alongside occasional biogenic calcite (earthworm) granules. Within these layers and below in

(near the cliff) Unit 5b commenced as an erosive, high energy slurry, carrying rounded chalk clasts, soil and brickearth material, and relic soil from the chalk (Table 24). As biogenic calcite (earthworm) granules also occur, it seems that a slurry had been eroded from the contemporary soil and sediment sequence of the chalk Downland block (see Units 4d and 6). Low energy pond marl sedimentation took place, either as here, after this initial rapid slurry deposition, or as elsewhere from the outset of Unit 5a conditions. Locally, as at GTP 13, these pond sediments were again buried under another coarse micro-chaotically bedded deposit, and sometimes even the banded silt and marl layers apparently occur as 10° sloping units. These may be features of small-scale gravity slide and slump deposition (Reineck and Singh 1980, 485–6). The thin sections, however, indicate that the norm for Unit 5b was massive pond marl formation.

The sedimentary sequence could suggest that as the climate cooled (Table 9b), erosion of the chalk cliff was triggered. Perhaps near the cliff or associated with a water-course, an erosive slurry or micro-gravity slide deposit covered Unit 5a deposits, and occasional fluvial activity fed water into the ponded areas that dominated the landscape. During Unit 5b flooding, initial deposition seems also to have buried or incorporated mammalian bone debris that may have been resting on the surface of Unit 5a. This again indicates that Unit 5a may have become dry. Initial flooding, which had only been able to carry coarse mineral material short distances could, however, pick up these lighter bone fragments. Coarse mineral layers within the marl at GTP 13, for example, may suggest some reactivation of erosion and possible micro-gravity slide activity. Generally, the compact marl deposit shows few signs of weathering apart from some rooting effects. On the other hand, the top of the marl became transformed and iron-stained apparently during the initial stages of Unit 6 deposition.

Unit 5c, narrow clay loam layer at GTP 17

Data

Unit 5c has only been found at GTP 17 (Fig 4). It is important not only because it is rich in mammalian remains, but because it holds artefact material at the highest level in the main interglacial sequence (see Units 8 and 11). It comprises a narrow, approximately 1m wide, mottled dark brownish (7.5YR4/6, 7.5YR6/2, 7.5YR6/8, 5YR5/8) unit, some 70–80mm thick. Like Unit 5a in some places, it has a merging boundary with Unit 4c, which lies directly beneath it. Unit 5c seems to merge laterally at its base with Unit 5a. Halfway up, patches of a thin Unit 5b also seem to occur. In the field, sedimentary layering can be observed, but this is overprinted by a weakly developed fine prismatic structure that can be followed into Unit 4c. Mottling, typical of hydromorphic soils, and probable manganese replaced rooting and biological mixing, are

all apparent. Horizontally lying flint artefacts have sediments (Fig 83i) which exhibit root impressions beneath them. Bulk analyses (Tables 19, 20, sample q) show Unit 5c to be moderately organic, weakly calcareous and to have a clay loam texture. It has a large amount of sand-size material but only small quantities of silt were observed compared with Units 4c, 5b and 6, for example. In thin section, Unit 5c appears to have a complicated sedimentary/soil history (Table 24). The lowest part (equivalent to Unit 5a) comprises laminated very fine sands interdigitated with large amounts of long organic matter fragments and fine silty clays. There are also some indications of crust formation. Penecontemporaneous minor rooting and biological activity seem to have occurred before the formation of a narrow (1.5mm) peat-like soil at the surface. Fine roots penetrated this soil. This organic surface soil also developed wide cracks, some as deep as 12mm, that penetrated into the laminated very fine sands beneath. Fragments of this thin organic peat also occur in the overlying weakly calcareous silt (patchy Unit 5b?) that infills these cracks, and occurs over exposed fine sands (ie areas where the peat has been lost). Above this layer, sedimentation of stratified very fine organic sands recommenced, but dusty clay layers and horizontal intercalations suggest crust formation (Fig 83i). Some layers contain secondary dusty clay void infills. Artefacts, teeth and bone fragments lie along these layers. Roots are present alongside the possible excrements of Enchytraeids. Above, Unit 5c is coarsely mixed with large clasts of probable weathered Unit 5b/8 material (Table 24).

Interpretation (Unit 5c, narrow clay loam layer at GTP 17)

The lower part of Unit 5c (Table 24) resembles some facies types of Unit 5a except that the mineral layers are coarser. Moreover, the fine layers are more akin to pedogenetic intercalations (Bullock *et al* 1985) than sedimentary features. This may suggest intermittent dry conditions after colluvial episodes depositing sand and detrital organic matter. Structure formation and biological activity also suggest this. As sometimes occurs in Unit 5a, cessation of mineral sedimentation permitted a thin peaty soil to form at the surface of Unit 5c, which may be approximately classified as a fluvent (Soil Survey Staff 1975). Drying out seems to have produced desiccation cracks (Kemp personal communication) from the peat surface into the underlying mineral soil. Such drying out of Unit 5a, has already been mooted. Inwash of Unit 5b (marl) material seems to have eroded the cracked peaty crust, and weakly calcareous marl material infilled the desiccation cracks. As the marl contains fine fragments of molluscs and calcite, it may not have formed *in situ*. Instead, this layer possibly represents reworked material washed in from Unit 5b. As Unit 5b has been disrupted and pinched out in places by periglacial deposition of overlying material (Unit 8), the exact original extent of Unit 5c itself and the origins of the marl layer are difficult to establish fully.

Table 24 Soil micromorphology and interpretation

<i>unit/sample no</i>	<i>sediment</i>	<i>pedofeatures</i>	<i>interpretation</i>
XI Unit 11 Silt Beds Samples 50–57	Massive (and interbedded with gravels), with variable layers with a granular, laminar or channel and vuggy microfabrics; dominant silt and very fine sand-size quartz; common sand to gravel-size angular flint in some layers; very few to frequent sand to gravel size rounded to subrounded compound and concentric ferro-manganese nodules; very dominant, very dusty and finely speckled darkish brown, poorly birefringent fine fabric to yellowish brown and moderately birefringent; rare wood charcoal present; possible mineralised organic material.	Complex textural features; bands of dusty clay infill laminar voids in places, vughs and channels can be coated by very abundant microlaminated dusty clay, possible dark mineralised humus in textural features, occasional elutriated silt infills occur in places; abundant fine to medium papules; intercalations and embedded grains present in places; occasional iron and manganese nodular impregnation; fabric mixing of clay-poor and clay-rich soil/sediments, occasional faunal coarse burrowing, imbrication of flints in places.	Humid arctic conditions led to mass-movement of frost-shattered gravels and meltwater deposition of brick-earth. Cycles of frost lensing and melting and occasional frost working of soil into granules and vertically orienting flints. Occasional periods of rooting and biological activity worked earlier deposits. Some translocation of possible humus-rich clay possibly occurred under temporary conifer woodland. Charcoal indicates fires were present. Probably humans (artefact concentrations) were active during interstadial periods with marked biological activity and slower rates of sedimentation.
X Unit 8 Samples 23, 29, 30, 31, and 35	Within deposit (artefact layer; sample 23): massive, lamina-like fabric with weak subangular blocky; 20–30% packing pores, open vughs and fine to medium fissures; grey moderately high birefringent micritic matrix around dominant chalk soil and chalk clasts; few flints; frequent calcite root pseudomorphs – some <i>in situ</i> ; many faint humic stains; common fine channels within margin of clasts. Basal deposit: massive, sometimes finely bedded calcareous (micritic) marl, with silt-size quartz, coarse sand-size to gravel-size rounded chalk and chalk soil; possible inclusions of palygorskite clay soil, brown argillic soil fragments (papules) – some showing fractures; biogenic calcite including earthworm granules and calcite root pseudomorphs; mollusc-rich and organic laminae present in marl; 15–20% packing pores and vughs in gravels; deposits lie over disturbed Units 5a, 5b, and 4d or wedge up against them.	Abundant faint yellowish brown (humic) weak staining of matrix and transformation (very fine porosity) of chalk clast margins and some chalk soil clasts (cryodesiccation features). ‘Melting’ of calcitic matrix around flint artefacts. Abundant biological homogenisation. Many to abundant mammilated excrements. Laminar fabrics present in places; very coarse mixing in gravel size material, below which can be abundant calcareous textural features.	Cool conditions cause increased inwash of calcareous fine material over ‘pond’ area of Quarry 1. Soils present on the chalk cliff and talus slope become devegetated, fragmented, and eroded. Cryogenic activity (ice lensing and mass movement) aided erosion and deposition across the site by a ?soliflual slurry which commonly buries the earlier formed marl. Chalk soils are affected by mass-movement (‘melted ground-mass’) forming the chalky pellet gravel. Chalk may also have become affected by weathering under dry, cold conditions, interspersed by interstadials featuring earthworm activity, rooting, and <i>in situ</i> hominid occupation. Temperate conditions, chalky colluvium derived from chalk scree at cliff base. Water and gravity flow move deposit southwards downslope.
IX Unit 6 (40.64m OD at GTP 13) Samples 5, 8, 9, 10, 39, and 40	Generally curved non-parallel bedding, with micro-cut and fills; rarely massive (GTP 10); dominant very finely bedded (0.25mm) fine silts in fine bedded (0.5mm) fine silts, and very coarse bedded (8mm) coarse silt, with fine sand-size quartz, flint and papules. Few medium bedded (1–2mm) medium sand, with clay-curls and soil fragments; coarse bedded (3–4mm) medium to coarse sand and soil fragments, including very abundant ‘argillic’ subsoil and occasional humic and calcareous soil material;	Very abundant iron-staining (iron-panning), ferruginous and iron and manganese impregnation of organic matter and possible humic soil fragments; rare calcite root pseudomorphs, and rare microfaulting and sediment mixing (at base of Unit 6 at GTP 13). Occasional to many dusty clay coatings and infills below some coarse laminae, and rare coarse void dusty clay infills. At GTP 10 very abundant dusty clay void coatings and intercalations, sometimes embedding	Increased water run off from the Downs deposited over a metre of brickearth in places. Conditions varied from probable still water to erosive, and ephemeral surfaces were vegetated. Sediments included both fine reworked brickearth and soil from the Downland. In places possible incipient argillic brown earths formed in the brickearth. Climatic deterioration, however, seems to have caused devegetation, and soils suffered erosion as runoff increased. Soils were flooded and slaked, making them unstable (possibly alongside

Table 24 continued

unit/sample no	sediment	pedofeatures	interpretation
VIII Unit 5c (GTP 17 only) Samples 17, 18, and 19	occasional to many relict <i>in situ</i> roots; rare horizontally laid 2–3mm long relict plant fragments; low porosity with few vughs and coarse root channels; rare (GTP 10) weakly spongy, with cracks, channels and interconnecting fine to medium polygonal vughs and possible vesicles; Unit 6 occasionally infills cuts into Units 5b, 5a, 4c, and 4b. Finely layered, with fine to medium prisms; moderately porous, with dominant fine channels and few coarse vertical fissures/channels. The soil/sediment sequence is: a) lowest 20mm is a layered very fine sand with dark brownish, dusty poorly birefringent organic fine silty clay; b) thin (1–2mm) <i>in situ</i> mineralised peat crust that has deep (up to 12mm) wide-mouth cracks; c) above is a 10mm thick, non-ferruginous, massive pale dusty grey, high birefringent calcareous silt, containing mineralised peat soil fragments up to 7mm in length, and frequent aragonite and calcite fragments; d) an overlying 40mm thick layered organic silty clay resembles (a), and interdigitates with a laminated calcareous silt loam; e) Unit 5c possibly merges vertically and laterally with Unit 5b/8, by including 5–10mm size clasts of 'coarse' Unit 5b-like (quartz sand, brickearth clay, and chalk fragments in a micritic matrix) marl (see Unit 8). Many mammalian teeth and bone throughout; occasional flint including horizontally lying artefact in layered (d) material. Most channels contain mineralised root traces as in (b). Abundant mineralised organic matter in layers a, b, d and e. Root traces in marl clasts (e).	coarse grains, producing a granostriated b-fabric in upper part of slide 5. Lower down, where relict biological porosity remains, rare limpid (now ferruginised) clay coatings occur. Weak fracturing of clay coatings and coarse mixing of soil (GTP 10) and sediment (GTP 13) at base of unit; silt and clay laminar separations and possible capping features. General iron depletion in silts and possibly (c). (a–e are defined in column 2.) Material from (c) infills fissures in peat crust (b) and underlying silts (a). Very abundant silty clay intercalations and infills associated with layering (possible crust). Partial decalcification of (c) and (e). Very abundant ferruginisation of peat, and iron and manganese impregnation of organic matter and roots. Many rooting and decalcification traces on intrusive Unit 5b/8 (e). Fine organo-mineral excrements (Enchytraeid) in (d).	cryoclastic fracturing). High energy water flow eroded and carried possible fragments of the earlier extant argillic brown Downland soil cover, the more recently formed local soils (possible incipient argillic brown earths) and their slaked counterparts. (Later and higher energy run-off led to the (erosive) deposition of path gravels (Unit 9).) Cryogenic activity probably affected the base of the Unit in places (GTP 10). A narrow organic clay loam soil/sediment formed under terrestrial conditions. It contains detrital organic matter, and also included sands that possibly originated from exposed beach material upslope. Possible rill erosion of the palaeo-beach slope led to colluvial fan development onto a 'dry' area of the mire at GTP 17. Pedological and biological features indicate that the deposit was often dry, whereas the concentrated presence of mammalian remains and human artefacts, on short-lived surfaces, may suggest that it was a zone favoured by humans and animals. One possible explanation could be that Unit 5c developed because a game trail breached the vegetation cover, although climatic effects may also have to be considered. If Unit 5c was a trail, this may account for the possible evidence of trampling/puddling crusts. There is also the possibility that rill erosion was also active during the later period of calcareous ponds, although subsequent disruptive Unit 8 deposition has confused the stratigraphy here. The extent of Unit 5c is also uncertain.
VII Unit 5b (40.54m OD at GTP 13) Samples 1, 3, 4, 5, 9, 11, 18, 19, 31, 34, 42, 43, 44, and 45	Massive and compact, with sometimes few to frequent fine vughs and channels; grey, cloudy, very birefringent marl. Generally dominant silt-size quartz. Occasionally contains small stone-size chalk, fine soil and brickearth (Unit 6) fragments (GTP 3, 13); and can be chaotically layered with this coarse material (including biogenic calcite granules and probable relict Cretaceous clay; samples 9 and 10)	Almost total (post-depositional) decalcification at GTP 10 and also rare limpid clay inwash into voids (see Unit 6). Decalcification of basal 6–7mm at Pit Q over thick Unit 5a. Weak transformation of marl associated with pores. Strong iron staining at top of marl and junction with Unit 6 at GTP 13. Very abundant iron and manganese impregnation of organic matter. Occasional microsparite	A change in base level leading to phreatic water movement through the chalk caused flooding of the site by calcareous water. This sometimes commenced with a near-cliff(?) gravity slide/slurry/fluvial deposit carrying coarse mineral material from eroded chalk cliff talus. Other material, such as bone resting on the 'surface' of Unit 5a was also picked up and redeposited at the base of the marl. A generally stable freshwater ponded landscape

Table 24 continued

unit/sample no	sediment	pedofeatures	interpretation
	at the base of, and within the fine marl. Marl layering (250–1000µm) at an apparent 10° slope at GTP 13. Fine marl only at top of sequences at GTP 3 and 13, and at GTP 1, 10, 25, 32, and Pit Q. Marl can be rich in freshwater and pond molluscs. Mammal bone/scat (sample 45) can be present. Rare to many mineralised organic fragments (rare roots). Boundary with Unit 5a generally horizontal, but can be wavy and apparently erosive, sometimes containing fragments of Unit 5a at base (sample 3).	infills. Sometimes Unit 5b intrudes into Unit 5a and can also be turbated within it.	characterised by molluscan activity, was formed. Possible micro-gravity slides occurred infrequently. Little contemporary weathering took place, except for some rooting. Acid conditions of Unit 5a, perhaps generated by post-burial development of CO ₂ from weathering organic matter, occasionally caused the basal marl to decalcify. Deposition of Unit 6 induced both iron staining and erosion of the marl at some locations. (Later, the deposition of Unit 8 caused erosion, convolution and turbation, mixing Units 5a, 5b, and 5c in places.)
VI Unit 5a (40.53m OD at GTP 13) Samples 1, 2, 3, 4, 5, 11, 18, 19, 24, 25, 26, 27, 29, 31, 34, 35, 39, 40, 42, 43, and 48	Very variable; massive, commonly layered; rare shallow (5mm) rills (samples 1 and 31). Sediment types are: a) 'manganese pan' – pale to dark brown, speckled low to moderate birefringent clays containing detrital organic matter (10–200/300µm in size; one fragment at GTP 25 is 800µm in length). These occur as laminae merging with the mineral upper part of Unit 4c (samples 3, 11, 25, 26, and 27); b) 'ironpan' – red brown, speckled, low to non-birefringent series of laminated fine silts with rare fine sand (100µm thick) and mineralised amorphous organic clay, usually in lenticular and rounded fragments; c) upper 'ironpan' – common laminae of silts and very fine sand with mineralised amorphous organic fragments. This full layered sequence of parts (a), (b), and (c) occur in samples 3 and 11, whereas only layer (a) occurs in samples 1, 4, and 5. Other facies types are: d) occasional massive mineralised organic matter ironpans (samples 34, 35, and 42); e) rare mineralised amorphous organic matter with channels, vughs, cracks and turbated laminae (samples 39 and 40). Within Unit 5a are rare pollen/spores phytoliths and 'woody roots' and other woody remains (eg sample 42); scat in Q1/B and GTP 25; rare flints (see Unit 5c).	Common muddy intercalations in (a). Occasional dusty clay void coatings in (c). Rare calcitic infills and crack coatings in 3 (from Unit 5b). Iron depletion especially in samples 4 and 5; 'leaching' of ?bone. Common cracking, micro-faulting of deposit (sample 3). Rare rooting and biological porosity formation and mixing (samples 19, 39, and 40). Very abundant iron and manganese impregnation of detrital organic matter (a). Very abundant ferruginous impregnation of amorphous organic matter and clay (facies b, c, d, and e).	As the site was affected by increasing wetness, the ripened soil of Unit 4c lost its structure and was leached under hydromorphic conditions. Large areas were then flooded and possible lacustrine muds carrying organic detritus were deposited. Marshland developed with vegetation rooting into Unit 4c. Except for rare areas, the marsh developed into a mire. Peat deposits formed that were often regularly (seasonal) influenced by silty deposition perhaps as the result of gently flowing braided (in part ?colluvial) streams migrating across the area. Freshwater fish, amphibia and riverine mammals were present. A (?seasonally) fluctuating water table may also have allowed some drying out permitting stream-flow to erode and carry fragmented peaty material, depositing it alongside silts and very fine sand. Sometimes fluvial activity could be more strongly erosive. Occasional areas remained permanently wet and unaffected by fluvial activity. Some peats contain possible woody remains. In contrast, an area previously favoured by humans, seems to have developed a peat, which because of ensuing less wet conditions became reworked by biological activity. It also developed cracks, that were infilled when this part of the site was affected by the above mentioned migrating streams. Unit 5a could thus represent a mire intermittently influenced by a seasonal ('winterbourne') braided stream over a period from one to several hundreds of years. Possibly during this time, iron-rich groundwater may have induced organic matter mineralisation, transforming it into a weak type of bog iron.

Table 24 continued

<i>unit/sample no</i>	<i>sediment</i>	<i>pedofeatures</i>	<i>interpretation</i>
V Unit 4d (Quarry 1B) Samples 29, 30, 32, 33, and 34	Alkaline, massive, grey, highly birefringent marl, with areas of coarse laminae, dense micro-aggregate or (infilled) channel microstructure; sometimes nodular (sample 32 ?'tufa'); common silt-size quartz, calcite/marl fragments, sand-size flint and patches (sample 30 and 31) of rounded chalk, fragments of calcite root pseudomorphs, possible relict palygorskite in coarse laminae. Upper part of unit has dominant mineralised organic laminae, with occasional bird and ?amphibian bone. Few mineralised organic matter; sometimes (sample 35) mineralised organic matter at base of the unit 'seals' and diffuses into homogenised Unit 4b.	Heterogeneous, with very abundant micritic growth, and occasional micro-sparite infills, cementing common fine (150µm) and coarse (500µm) areas of disrupted and fragmented laminae. Coarse marl fragments and silt and sand-size mineral lamina and void inwash. Common biological channeling and scour; some major associated calcitic transformation and inwash of micrite, and recementation (sample 32). Iron replacement of basal and uppermost organic laminae; iron and manganese impregnation of organic fragments and probable root traces. Major fabric disruption and open fissure infilling; laminar structure formation (sample 30) associated with ice wedge and Unit 8 sedimentation.	During a period of base level fluctuations, when Unit 4c was forming elsewhere across the site, a spring formed a hollow/pond-like feature. No Unit 4c was formed here, but the local Unit 4b was homogenised by biological activity, and remained calcareous. Material from Unit 4b and the chalk were reworked to form a layered silt and calcareous marl. Successions of biological activity (?low water level) were interspersed with periods of scour, calcareous inwash and later calcitic neof ormation (?wet periods). The last led to strong cementation in places. Periodic high energy water flow also reworked the marl in places and deposited coarse material from the chalk. Some relict Cretaceous materials perhaps raised the alkalinity above what molluscs could tolerate. The pond was last affected by alternating gentle fluvial and marsh conditions, and was inhabited by aquatic birds. Later, this unit was (?preferentially) influenced by cold climate and pore release phenomena.
IV Unit 4c (40.43m OD at GTP 13) Samples 1, 2, 3, 4, 5, 11, 19, 20, 25, 26, 27, 31, 37, 38, 39, 42, 43, 44, 46, 47, 48, and 49	<p>Zone 1: 0–5mm; in places (samples 3, 11, 37, and 38) fine mineralised organic laminae (150µm thick) in massive, non-calcareous grey silty clay (as zone 2). Rare to many bone (small mammal teeth); occasional mineralised amorphous organic matter laminae (?peat) (samples 42, 43). Rare possible tangential rooting (samples 19 and 20).</p> <p>Zone 2: 5–30–40mm (mean) (90mm) (max). Massive/structureless non-calcareous grey silty clay; speckled and moderately birefringent. Rare (GTP 17) coarse prisms. Rare, within ironpans, are areas of occasional fine to medium channel and vughy porosity in fine to medium blocky structure. Occasional mineralised roots. Rare to many bone/teeth (eg scat concentrations). Rare partially decalcified mollusc shell. Occasional flint fragments. Many mineralised roots.</p> <p>Zone 3: 30–40–40–90mm (mean) (120mm max): Patchy to coarse to fine residual laminae (see Unit 4b); mainly non-calcareous greyish brown cloudy/speckled, moderately high birefringent silty clay. Crystallitic weakly calcareous patches. (Inclusions, as Zone 2.)</p>	<p>Iron, clay and calcium carbonate depleted soil with few to abundant dusty clay void infills. Silt infills at GTP 17. Iron and manganese impregnation of organic laminae. Homogeneous, and depleted of iron, clay and calcium carbonate. Secondary ferruginisation forming pans has preserved: – rare ?earthworm burrow (1–1.5mm wide), biologically homogenised ?soil and many dusty clay void infills. Ferruginised organic (?Enchytraeid) excrements at GTP 17. Occasional ferruginised roots in ironpans and at GTP 17. Occasional ferruginous hypocoatings of pores, faces and structures that are subhorizontal at GTP 10. Abundant iron and manganese replaced roots, that are little associated with relict porosity.</p> <p>Generally calcium carbonate depleted; poorly homogenised; rare to occasional secondary void infills; abundant iron and manganese replaced roots.</p>	<p>Possibly a short (minimum 10–20 years, maximum 100 years) period of water table fall led to full sediment ripening. Calcareous and laminated nature of original Unit 4b sediments was lost. Invasion by terrestrial plants, including woodland and animals from the Downland, induced shallow soil formation. Woodland small mammal remains within the soil can be <i>in situ</i>, from predatory bird pellets, or buried at the surface as concentrated scat. Some 'dry' or 'higher' areas, where pedogenesis was deepest, were possibly preferentially chosen for human activities. The resulting artefacts were biologically worked throughout the soil. Possible seasonal water table fluctuations caused hydromorphic (Fe and Mn) cementation of the soil fabric in places, perhaps as the site was affected by increased wetness (see Unit 5a). Some soils may have developed a peaty topsoil in 'low ground'. Increasing wetness and later flooding caused waterlogging and destruction of most of the soil structure. Resulting structureless upper soils were affected by slaked soil inwash and inwash of organic matter from the marsh and mire conditions forming Unit 5a. Human occupation seems to have generally ceased except for areas like GTP 17 (see Unit 5c).</p>

Table 24 continued

<i>unit/sample no</i>	<i>sediment</i>	<i>pedofeatures</i>	<i>interpretation</i>
III Unit 4b (40.23m at GTP 13) Samples 3, 6, 12, 21, 22, 25, 26, 27, and 39	Coarse (10mm) and fine (0.5mm) bedded, and finely (150–300µm) laminated calcareous clay loam of silt and dirty pale grey brown, finely speckled, moderately high birefringent clay. Occasional less calcitic brown chalky clay bands and inclusions of ferrugised sediment and fragments of laminated humic clay in samples 21 and 22. Very few mollusc fragments. Mainly packing porosity, with few vughs, cracks and channels. Rare to occasional mineralised root and plant remains. Upwards, sediments become generally only finely bedded.	Only finest laminations appear to be reworked, whereas bedding generally is very well preserved, and only rare faunal burrows are observed. Rooting may be slightly less than in Unit 4a. Iron staining, rooting and iron and manganese impregnation of plant matter. Sediment deformation features in places (samples 21, 22, and 36). Common possible mud cracks associated with fish death assemblage (sample 6). Near top of unit, occasional tongues of decalcification and secondary calcite (microsparite) formation, and calcareous pans in places (Q1/A).	Sediment source seems to be the same as for Unit 4a, but the near absence of faunal burrowing has allowed coarse bedding to be preserved. Disturbance may only be by rooting in places. Paucity of faunal activity may reflect major freshwater input into a lagoon. Coarse and fine bedding may reflect diurnal/tidal water flow, clays depositing out of suspension load. 'Tidal' flow is very gentle and only able to work the finest laminations. Highly concentrated fish bone death assemblage, which occurs in possible mud-cracked layer, may represent the episodic drying out of pools, trapping fish. Some minor ripening of mudflats is evidenced by porosity formation, minor glauconite weathering, iron release and rooting. Further deposition of poorly calcareous clay layers and presence of micro-laminated humic clay may suggest occasional sediment exposure, perhaps associated with similarly located human activity (GTP 17). Marked sediment deformation could relate to sediment slumping and later dewatering processes. It can be noted that human activity is associated with these areas of sediment deformation (samples 21, 22, and 36). It is possible that it was the ephemerally 'higher', 'drier' areas favoured by humans during periods of low water level, that became most deformed later. There is also a possibility that sediment deformation in sample 36 where an undisturbed flint-working surface was located, is a human imprint.
II Unit 4a (40.00m OD at GTP 13) Samples 7, 12, 13, and 14	Massive to finely bedded (according to degree of biological working), calcareous clay loam, with mainly silt-size quartz and brown, finely dusty, moderately birefringent clay. Occasional stones of chalk; rare to occasional roots and organic remains. Many channels, cracks and chambers. Occasional sand laminations containing foraminifera and weakly iron-stained chalky clay clasts.	Abundant burrowing and mixing of originally laminated deposit. Many iron and possible iron and manganese staining of fabric and mineralisation of organic matter.	These estuarine/lagoonal deposits are more fine (muddy) generally than the underlying marine sediments. Again the sediment source is probably alluvial from rivers draining the chalk. The presence of sand lenses and stone-size chalk, with chalky clay clasts may indicate possible erosion of Unit 3 material – perhaps from an exposed beach (?sand bar). Fine laminations of silt and chalky clay are of probable tidal origin, with abundant faunal working, or even reworking by tidal flow. Plant rooting and occasional exposure have produced ripening effects of porosity formation, glauconitic weathering and iron and manganese staining.

Table 24 continued

<i>unit/sample no</i>	<i>sediment</i>	<i>pedofeatures</i>	<i>interpretation</i>
II Junction of Units 3/4a at 40.00m OD at GTP 13 Samples 7 and 14	12–15mm thick, discontinuous, massive, well sorted very fine and fine sand lens, containing many clasts of poorly birefringent chalky clay. Rare organic matter. Single grain structure with packing voids. Sharp boundary over finer Unit 3 sediments below.	Homogeneous sand; top few mm are mixed with overlying Unit 4a material in faunal burrows.	Sharp upper boundary between fine Unit 3 sediments and discontinuous sand lens may suggest truncation by a moderately high energy event, such as a storm. The last may have eroded Unit 3 material, and deposited less well sorted and coarse sand-size material, including clasts of chalky clay. This event seems to have marked the end of fully marine conditions at GTP 13, with the deposition of a sand (?beach). This lens could be relict of a sandy deposit, perhaps eroded by tidal (or wind) activity, marking a hiatus before estuarine/lagoonal sedimentation and associated animal activity.
Ibiii Unit 3 (40.00m OD at GTP 13) Samples 7 and 14	Massive very fine sand and cloudy, dirty grey, moderately birefringent detrital chalky clay. Traces of fine bedding. Complex packing voids and vughs. Few mollusc and mineralised plant remains	Almost total faunal mixing. Iron and manganese replacement of plant remains and iron impregnation of rooting features.	Finely bedded shallow water marine sediments of low to very low energy include detrital chalk mud (?alluvial source). Intense contemporary faunal activity totally worked sediment layers. Later faunal burrowing and plant rooting, with possible weathering of glauconite and iron staining are evidence of weak sediment ripening.
Ibii Unit 3 3rd Marine Cycle (39.33m OD at GTP 13) Sample 15	Massive very fine sand and cloudy dirty grey, moderately birefringent detrital chalky clay. Traces of fine bedding. Complex packing voids and vughs. Few mollusc and mineralised plant remains.	Almost total biological (faunal) mixing, followed by very coarse burrowing. Probable iron and manganese replacement of organic remains.	Finely bedded shallow water marine sediments of low to very low energy include detrital chalk mud (?alluvial source). Intense contemporary animal activity totally worked sediment layers. Later animal burrowing and plant rooting, with possible weathering of glauconite and iron staining are evidence of weak sediment ripening.
Ibi Unit 3 3rd Marine Cycle (39.08m OD at GTP 13) Sample 16	Coarse bedded fine sands and pale cloudy yellowish grey, highly birefringent detrital chalky clay; rounded chalky clay clasts in sand layers; very dominant quartz, with flint, glauconite, shell, fossils and chalk fragments; common cracks and channels; many mineralised root and plant remains.	Much iron staining of mixed coarse and fine features (burrow mixing) and many iron and possibly manganese replacement of plant remains; abundant micro-faulting/slippage; many to abundant coarse faunal burrowing, mixing originally bedded coarse and fine material.	Calcareous clay is composed of detrital chalk. Fossils and chalk fragments also occur indicating Marine Cycle 3 sedimentation is influenced by the erosion of the chalk. Shallow water moderately low energy deposition is interspersed by very low energy chalky mud deposition. Biological activity, including rooting and strong faunal burrowing have occurred, whereas later micro-faulting suggests wet sediment settling. Later rooting, iron staining and possible iron and manganese impregnation indicate some weak ripening effects.
'Terrestrial clays' GTP 25 only Sample 28	Coarsely laminated greyish brown, speckled and moderately birefringent, weakly calcareous clays (3–8mm thick) and silts (2–6mm thick); very dominant well sorted silt-size quartz, with few chalk and brickearth 'papules' and weathered glauconite; mainly packing and crack porosity, with few channels; occasional mineralised roots and organic fragments.	'Root' channels; weak calcite hypocoatings and abundant micritic impregnation of silts; many iron and possible manganese impregnation of organic matter.	Phreatic activity in the relict chalk rubble beach, as water drained from the cliff, led to the deposition of chalk and decalcified material (originating from the Downland) as silt and clay laminae. At times these became subaerially exposed and minor rooting took place. During the 3rd Marine Cycle transgression, the deposition of calcareous sand caused minor calcification of these 'terrestrial' deposits which became interbedded with marine sands.

Table 24 continued

<i>unit/sample no</i>	<i>sediment</i>	<i>pedofeatures</i>	<i>interpretation</i>
Ia Unit 3 2nd Marine Cycle (38.03m OD) Sample 17	Massive, calcareous coarse bedded medium sand, fine sand and micritic clay; dominant micritic clay; dominant well sorted and poorly sorted fine, medium and coarse sand-size quartz, with frequent flint, few glauconite, shell and rounded micritic clay fragments; 20mm thick very pale brownish grey, highly birefringent micritic clay band; packing porosity, with few fine channels in clay band; occasional mineralised roots in clay band; common foraminifera.	Occasional to many iron and possible manganese impregnation of organic matter and channel margins (hypocoatings); occasional rooting 'passage' features.	Variable moderate to low energy deposition in a near-shore (just above beach layer) calcareous environment. Clays represent very low energy deposition of calcareous clays and these were affected by plant growth. Some higher energy sedimentation (sands) eroded micritic clay fragments, rounding and sorting them, perhaps reflecting local wave action after storms. These higher energy events, and rapid sedimentation, probably allowed little biological working of the deposits.

The upper part of Unit 5c is similar to the lowest fine sandy layer. Intercalations may be evidence of crust formation. In addition, some contain fragments of dusty clay textural features, indicating the disturbance and mixing of these possible crusts. Artefacts and mammalian material are scattered within soil/sediment that exhibits many traits of biological activity. Sedimentary activity was therefore often occurring alongside sub-aerial drying out of the sediment, and the possible formation of puddling surface crusts.

In some ways the organic sands of Unit 5c appear to be like the sediments of a 'micro-braided stream' (Courty personal communication), as described for Unit 5a. The mineral content is coarser, however, and Unit 5c appears to form a narrow area of 'high' ground. It also shows much evidence of being a sub-aerial deposit affected by pedogenesis. Fine mineral material has been reorganised into textural features during 'sedimentary' episodes, and structure formation and biological activity have occurred. Unit 5c is interpreted as a colluvial tongue deposit or rill accumulation tongue (Reineck and Singh 1980, 70) that has brought down mineral and organic matter from upslope. As the deposit could not be followed upslope this hypothesis must remain conjectural.

It may seem logical to assume that local devegetation and resulting soil instability and colluvial activity could have been caused purely by climatic change, for example a cold climate also inducing desiccation. The abundance of plant fragments in Unit 5c nevertheless indicate that surfaces were not totally devegetated. These Unit 5c deposits are, additionally, unique to GTP 17. This suggests that the deposition of material eroded by rill action from upslope was concentrated at this one location, as far as can be discerned from the present investigations at Boxgrove. The presence of large amounts of sands could suggest that beach sands (Unit 3) were being eroded. It may also imply that the vegetation cover on the palaeo-beach slope leading down to the marsh (Unit 5a) was breached only along a narrow corridor, otherwise Unit 5c would have been

more widespread. GTP 17 has already been identified as a possible 'dry' area favoured by humans. Unit 5c is unique and occurs together with concentrated evidence of human (Fig 83i) and animal activity at this high level in the stratigraphy (Unit 4c through to Unit 5c). This could support the hypothesis that Unit 5c is not simply an accident of geological conditions; it is worth considering the possibility that Unit 5c may have formed as the result of a narrow game trail. Animals or humans may have triggered erosion when they used the trail to access a 'dry' area of the marsh from the downland, via a vegetated raised beach. Some of the crusting could possibly relate to trampling (Beckman and Smith 1974), which would also accelerate sediment movement downslope. Artefact recovery also shows that humans were active during the formation of this unit. There is the additional possibility that if the 'marl deposit' in Unit 5c is *in situ* and not a phenomenon of cryogenic intrusion, then the colluvial fan/trail could also have been active during the period when calcareous ponds dominated the landscape.

Obviously, these possible interpretations are highly conjectural, but it must be recognised that animals and humans may well have had an impact on unstable surfaces, the very places where artefactual evidence and faunal recovery show them to have been particularly active.

Unit 6, the Brickearth Beds

Data

Sometimes Unit 6 overlies a decalcified part of Unit 5b (Table 22), and it can be difficult to distinguish these two deposits. Fortunately, Unit 5b has a dominant fine silt component, whereas Unit 6 is more often a coarse silty deposit (Table 20, samples a, f, g). The brickearth may also be present over brownish iron-stained marl or, as at Pit C, rest directly upon Unit 5a. In places, Unit 6 may also occur in fills cutting down as deeply as Unit 4b.

Unit 6 is a generally non-calcareous, poorly humic silty clay loam (Tables 19, 20; Fig 74). In the field and in thin section it may be seen in places to contain many

mainly iron-replaced root traces (Fig. 83j). Rare mineralised humic soil clasts also occur along with ferruginised plant fragments that may lie parallel to the bedding. Near the junction with Unit 5b at GTP 13 occasional *in situ* calcitic root pseudomorphs were noted. Some rare calcareous soil fragments are also present higher up in this unit at this location.

The brickearth has generally curved non-parallel bedding (Reineck and Singh 1980), varying from very fine to coarse (Tables 22–24), with many micro-cut and -fill features. Unusually, at GTP 10 (Table 22, thin section 5), Unit 6 is generally massive and compacted, especially upwards (upper 10mm). A little farther down (15–20mm) a polygonal vughy (void type; Bullock *et al* 1985) structure was found. This is partially superimposed on an underlying, probably biological, open vughy and channelled microfabric. The compact fabric is a speckled dark yellowish brown, with a close porphyric, speckled and granostriated b-fabric groundmass. Throughout the brickearth here, typical inclusions (see below), such as flint and papules, still occur. The brickearth is, however, unusually homogenised in its upper 30mm, with possible relict laminae being noticeable only in the lowermost 50mm. Clay coatings and void infills (Fig 83k) are contemporary with the relict vughy and channel porosity. These textural features are patchy, but locally frequent, and some which were probably limpid are now ferruginised. Post-dating these are abundant, very dusty, clay and matrix textures, such as intercalations and infills (Table 24, IX Unit 6). These more coarse features are apparently contemporary with the compact 'uppermost' and closed vughy ('central') microfabrics seen in thin section 5. An ironpan has developed at the base of the unit here where there are occasional vesicular-like voids and possible laminar separation of silts and clays with associated cappings. These features are difficult to discern clearly, because of post-depositional compaction and differential ferruginisation.

Elsewhere, at GTP 13 for example (Table 23), in the bedded brickearth, very fine (10 μ m) iron-replaced clay laminae may occur within the silts. Under coarse laminae that include medium to coarse sand and soil fragments, dusty clay infills affect the underlying 1mm or so of the sediment. The coarse layers that are rich in flint, fragments of clay curls and 'argillic' subsoil material, as well occasional calcareous and humic soil, occur just beneath the Fan Gravel Beds (Unit 9) at GTP 13. The brown soil fragments are medium to coarse sand-size, sub-rounded and are speckled dark yellowish brown. They also feature very dusty clay void coatings and infills. Even a fragment of humic (Ah horizon?) soil was seen to be characterised by a dusty matrix, as well as having laminated dusty clay void infills. In the poorly sorted coarse layer at GTP 13, both papules of dusty clay and limpid to finely dusty clay occur, although the very dusty material is more abundant. The soil fragments themselves commonly

have a groundmass that is close porphyric, with a speckled and granostriated and sometimes weakly reticulate b-fabric. At the base of Unit 6 at GTP 13, there seems to have been coarse mixing and faulting of the coarse sediment at this level. Similar coarse inter-leavings of sediment and/or laminar silt and clay separations were also noticed at GTP 10, at the base of Unit 6.

Interpretation (Unit 6; brickearth deposition, pedogenesis, and erosion)

Deposition: Unit 6 can be interpreted as a generally low energy (freshwater ostracods of stagnant or slow moving water; Whatley and Haynes in Roberts 1986) fluvial deposit of non-calcareous fine material. The possible ultimate origins of this fine deposit are discussed by Catt (Chapter 2.5). He suggests at least some part of the silt may derive from Units 3 and 4, whereas clay may have originated from downland soil weathered from the Reading Beds regolith.

The gentle fluvial and still water (pond) conditions extant during the deposition of Unit 5b, were probably still extant at the beginning of Unit 6. Primary deposition of the brickearth appears to have been of moderately high energy at GTP 13, whereas fine sedimentation is recorded at GTP 10 and Pit C. At the last location, however, Unit 5b was either eroded or was never laid down. The generally curved non-parallel bedding, and cut and fill features (Table 24) are typical of fluvial activity. Experimental and site analogues studied on loess from Belgium and Holland (Mücher and De Ploey 1977; Mücher *et al* 1981; Mücher and Vreeken 1981; Vreeken and Mücher 1981) do not appear to be applicable to the situation at Boxgrove. Firstly, as stated by Catt, the brickearth contains more clay than normally found in loess, and secondly, the sedimentary features at Boxgrove are more related to fluvial activity (Reineck and Singh 1980) than to colluviation. In addition, the brickearth shows that it was vegetated at times, plant roots (Fig 83j) possibly extending into the underlying marl, creating calcite root pseudomorphs. Plant material was also occasionally deposited. At GTP 10, there is also some possible evidence of soil formation in the brickearth (see below), although later events at this location (see below) markedly transformed this soil.

In some ways fluvial activity during brickearth deposition resembled that during the formation of Unit 5a. It differed, however, by apparently being a little more energetic and erosive at times, with a much greater amount of sedimentation. This caused deposits often up to a metre thick to form. Some very fine silty layers, however, may even have been deposited by fluvial activity in standing bodies of water, although such deposits are often cut by later curved beds of coarse silts. Fine papules, as found in coarse parts of the underlying marl, may also occur in the brickearth generally. Only upwards in the sequence, however, are coarse (medium to coarse sand-size) sediments present

as narrow (1–2mm to 3–4mm) laminae (just below Unit 9). As shown below, such coarse bands seem more strongly related to the depositional environment of Unit 9 than Unit 6. In addition to flint, clay curls, papules (Bullock and Murphy 1979) of limpid and dusty clay material, subrounded argillic-like subsoil fragments of brown soils occur alongside occasional humic (Ah) horizon material (Table 24).

Generally within the brickearth, and included within the pedologically homogenised deposit at GTP 10 (Table 22), inclusions of flint and papules suggest general erosion of the downland soil and non-calcareous superficial cover. Clay curl fragments imply some erosion of previously deposited brickearth, as also indicated by cut and fill features. At the top of Unit 6, just beneath the path gravels (Unit 9) at GTP 13, coarse laminae occur that include soil fragments. That these soils were eroded and concentrated into laminae implies that they may be representative of (?immature) contemporaneous soils and are not relics of earlier interglacials. This is especially noteworthy, as no palaeoargillic material was present, whereas it has been 'reported' from overlying soliflucted material (Dalrymple 1957) (see Unit 11) and is common to Middle Pleistocene palaeosols (cf Valley Farm Soil: Kemp 1985; 1986). If these limpid and laminated papules are contemporaneous, they may reflect some typical argillic brown earth pedogenesis on the wooded downland. The main soil type(s) represented by fragments, however, has a granostriated b-fabric groundmass that suggests physical disturbance, for example, slaking and mass-movement. Further, although soil fragments occur with textural features, these are not typical of argillic brown earth Bt horizons, because infills and coatings are very dusty (Fedoroff and Goldberg 1982; Fedoroff *et al* 1990). The great majority of the papules are also composed of very dusty clay, as found within these soil fragments. Even a humic (Ah) horizon soil fragment is dominated by dusty clay infills and intercalations, and one void has been infilled by laminated dusty clay material.

Pedogenesis: Some time during the period represented by Unit 6, vegetated stable landscapes developed in places, such as preserved at GTP 10. Here, an argillic brown earth may have been forming in the weathering non-calcareous material of Unit 6. The pedological evidence recorded in thin section 5 is of a possible Eb/B(t)-like horizon, where there was a combination of biopore formation and possible minor limpid clay illuviation (Table 24). Clay was also possibly translocated into the underlying marl. This possible incipient argillic brown earth formation could represent a period of stability. Because the clay coatings are either strongly ferruginised (Unit 6) or partially iron depleted (Unit 5b), it is not possible to suggest a northern climate/vegetation for the soil, based on colour (Fedoroff and Goldberg 1982; Fedoroff *et al* 1990). There is the suggestion, however, that conifers dominated the landscape earlier during Unit 5a formation

(Scaife in Roberts 1986), but this is not necessarily supported by the faunal evidence (Parfitt Chapter 4). As the profile has been truncated here (0.2m remaining) the soils have not been recognised elsewhere. Nevertheless, the inference from GTP 13, where a variety of soil fragments occur, is that more soils may have once existed. As the soils at GTP 10 were compacted and differentially affected by iron depletion and ferruginisation, the above suggestions concerning pedogenic clay illuviation versus the effects of soil slaking (see below), are tentative.

At a time after major brickearth deposition, but before Unit 9 sedimentation began, water, that later carried the fan gravels of Unit 9, flooded across the soil at GTP 10. This water truncated the possible incipient argillic brown earth soil that had formed in the brickearth. Its subsoil became slaked, collapsing its soil structure and porosity. In its upper, most-slaked part, a compact granostriated b-fabric was produced alongside abundant, very dusty and matrix textural features (Table 24). Lower down, some porosity and clay coatings of the possible incipient argillic brown earth remained, but a general polygonal vughy structure (Courty *et al* 1989) was imposed, and coarse channels developed infillings of matrix material. A similar sequence of textural feature hierarchies, namely, limpid clay followed by very dusty matrix material infills, was described from Late Pleistocene palaeosols in the Paris Basin (Fedoroff and Goldberg 1982). These authors used this microfabric to imply that argillic soil formation had been followed by slaking and truncation.

At GTP 10, later probable cold climate effects were minor fracturing of limpid clay coatings (Fig 83k), compaction, laminar silt and clay separation, vesicular void and possible capping formation at the base of the unit (Van Vliet-Lanoë 1982; 1985; Kemp 1985). These are all features of fragipan formation (Avery 1990, 106). Microfaulting was also noted at the base of Unit 6 at GTP 13. Possible 'squeezing' (*boudinage*) of the deposit may relate to post-depositional compression of a water-saturated deposit (Catt 1990, 66).

Erosion: The abundant soil fragments in laminae at the top of Unit 6, just below Unit 9 at GTP 13, firstly suggest the erosion of argillic brown earth soils (limpid and finely dusty and laminated papules) (Bullock and Murphy 1979; Kemp 1986) and the reworking of fine depositional laminae within the brickearth. The erosion of slaked 'argillic' brown earths, as found at GTP 10 is indicated by the presence of very dusty papule material, and fragments of granostriated b-fabric soil that contain very dusty clay infills. Thus, it appears that the possible incipient argillic brickearth soil cover was being both slaked and eroded by downland runoff. Later in the site's history, similar, but higher energy runoff deposited masses of gravel as Unit 9. Colder climate conditions probably developed rapidly, totally devegetating the brickearth soils formed on the low ground, the talus/cliff slope

and the Downland itself. The soil cover may have been mature argillic brown earths on the Downland, whereas on the brickearth-covered low ground there may have been only enough time for incipient argillic brown earths to form. Full devegetation and resulting increased downland runoff affected the site. Possible incipient argillic brown earths became water saturated and slaked, making them unstable (see Units 4c/5a: Macphail 1990; 1992b) and runoff eroded them, depositing slaked soil clasts at GTP 13 (Table 24), for example. At GTP 10 only partially transformed and truncated soils were produced, whereas elsewhere soils were completely lost. In addition, possible cryogenic activity with devegetation may have accelerated erosion, fracturing soils into poorly rounded fragments and clay coatings into papules (Van Vliet-Lanoë 1982; 1985; Kemp 1986). Possibly, cryoclastic fracturing was followed by meltwater flow that deposited these coarse soil clasts (cf Westbury-sub-Mendip: Goldberg and Macphail 1990; Macphail and Goldberg 1995). In either case, the uppermost deposits of Unit 6 at GTP 13, are in reality contemporaneous with the conditions that produced the slaked soil at GTP 10.

At the beginning of this section, Unit 5a deposition was compared to sedimentation during Unit 6 formation. The much larger amounts of sediment being deposited during Unit 6, may simply imply greater rates of erosion of the Downland block which, with Unit 9, emphasise the probable effects of a rapidly deteriorating climate.

Chalk mud/calcareous silty clays

Data

These deposits have no formal unit number or bed designations, and were only identified in this study at GTP 25 (Figs 58, 73). They are fully described in Table 9b (Roberts Chapter 2.1). They comprise gravel-size (<10mm) rounded chalk set in a micritic cement, and contain very abundant *in situ* calcite root pseudomorphs. These increase in number upwards in the biologically disturbed top, where organic matter and bone fragments are evident. The chalk mud is buried by some 5mm of Unit 4b/4c, which appears to infill biological pores formed in the top of the mud, but does not affect the obvious root holes. Unit 4c was sealed initially by 1mm of (now ferruginised) organic clays, and by 1mm of silty sediment containing detrital organic matter. Above, Unit 5b marl and more chalk mud deposition ensue. Firstly, organic micritic laminae carry bone fragments up to 4mm in length and these occur within a 5mm thick layer representing primary marl deposition. Upwards, coarse chalk marl/chalk mud deposits occur and these contain both *in situ* calcite root pseudomorphs and their reworked fragmentary remains. Biogenic calcite, similar to earthworm granules, is commonly present. The chalk mud merges upwards into Unit 8.

Interpretation

The chalk mud appears to have been deposited as a slurry from the chalky cliff talus slope, and short-lived weathering and plant growth followed. Probably, extant plants stopped Unit 4b material from washing into some biopores, although biological activity did mix quartz silts of Unit 4b into the top of the chalk mud. Soon after, peat formation ensued and this was followed by fluvial deposition of silts and detrital organic matter. As elsewhere, gentle flooding that was an initial feature of Unit 5b, also carried bone fragments. Ponding was intermittent with inwash of organic matter. The whole was buried by a further chalk mud slurry that resembles facies present in both Unit 5b and Unit 8. Biogenic granules and calcite root pseudomorphs testify to the biological activity on the sloping chalk talus at this time.

Unit 8, Chalk Pellet Beds

Data

Unit 8 was examined from two parts of the site. The basal deposits were observed from a number of locations, for example over Unit 4d, in Quarry 1. Material from within the deposit that contained an *in situ* flint scatter (Roberts Chapter 6.3, Fig 291) was studied at GTP 25. At the latter site the chalky pellet gravel, that overlies cliff talus material upslope, buried the beach deposits (Figs 42a, 53, 75). Roberts (Table 9a) has divided the Chalk Pellet Beds into Lower and Upper parts. The Lower Chalk Pellet Beds were laid down under temperate conditions immediately in front of the cliff (Fig 42a). The Upper Chalk Pellet Beds were deposited under cold conditions and spread out southwards from the cliff time-transgressively, covering a number of older units.

At Quarry 1, Unit 8 Upper Chalk Pellet Beds can overlie undisturbed earlier deposits, or cryoturbated deposits. It can also be wedged up against overthickened Unit 5a material through similar mass-movement activity (Fig 83l). The basal deposits are generally fine laminated calcareous silts, fine sands and micritic marl material, that could include fragments of brown soils, papules and relic chalk material, probably palygorskite (see Unit 4d). The marl parts also contain molluscs and feature fine organic laminae. Thus, in many ways, this element of Unit 8 appears not dissimilar to parts of Unit 5b. Above, for example in the top of thin section 30, these bedded Unit 8 sediments are characterised by a massive deposit of coarse gravel to small stone-size, rounded to subrounded, chalk and chalky soil clasts (Fig 83l). Sometimes this deposit occurs directly over Unit 5a and 4d. Common coarse soil inclusions, as noted below, occur. Some of the chalk and chalky soil inclusions also appear to be weathered. In addition, many fragments of calcite root pseudomorphs are present alongside occasional biogenic calcite (earthworm) granules. Within these layers and below in

some of the few pores that are present in the underlying finer sediments of Unit 8, abundant coatings of micrite and weakly yellowish clay occur. Some of these materials wash into disrupted Units 5a and 4d (29).

At GTP 25, a sample was taken across a flint scatter some 3m up from the base of Unit 8 (Figs 291, 292). The massive small stone and gravel-size chalky material seems to have a lamina-like coarse fabric, but there is also evidence of a weakly fine subangular blocky soil structure. A few flints (Fig 83m), some of which make up part of the scatter, are present. Biogenic calcite is common, as crystals perhaps formed by earthworms, as *in situ* cross and transverse sections of root pseudomorphs, or as locally reworked root pseudomorphs. These calcite pseudomorphs comprise both rounded and more angular fragments, whereas others may be *in situ*. Additionally, some root cells seem to have been transformed into the same type of micritic soil that forms the micritic matrix in this deposit. Many of the rounded chalk clasts have an extremely fine porosity within and along their margins. This porosity is not thought to be of a biological origin. Instead, as ongoing oxygen isotope studies of cold climate calcitic features are indicating, this porosity is more likely to be a response to cryo-desiccation processes (Marlin *et al* 1993; Courty *et al* 1994; Courty personal communication). The micritic fine soil matrix around the clasts is often very slightly yellowish stained, possibly indicating some yellowish (humic?) clay could have originated in the same way. A packing porosity characterised the general nature of the unit here, but there are also common open vughs and channels. Some of the void space between coarse clasts was partially infilled by mammillated earthworm excrements composed of micritic soil (Fig 83n). Moreover, the upper part of the thin section shows what seems to resemble a combination of massive structure and total biological fabric.

Interpretation (Unit 8; solifluction chalky gravel deposition and soil formation)

At Quarry 1, many of the lacustrine and fluvial influences affecting Units 4d and 5a were active during the deposition of Unit 8, and Unit 5b-like deposits were formed. Colder conditions probably caused the cryogenic effects that produced laminar fabrics (van Vliet-Lanoë 1985) in disturbed Unit 4d deposits, and the wedging-up of Unit 5a material. Pore-water release phenomena, however, are also reported here (Roberts *et al* in prep). Coarse deposition of chalk gravel and stones and soil material ensued, probably from extant chalky soils developed on the cliff/talus slope. Possible soliflual activity produced a variety of deposits, including coarse matrix-poor material (Fig 83l) and caused slaked decalcified clays and micritic clay to wash down into the underlying sediments.

Upwards in the unit, the solifluction/gelifluction (Catt 1986, 42–3) of chalk soils is recorded. Clasts were also rounded (Van Vliet-Lanoë 1985) and possibly

affected by cryo-desiccation. Both at GTP 25 and at Quarry 1, large amounts of biogenic calcite and calcite-replaced roots occur, indicating the cryogenic fracturing of earlier and possibly extant chalky soils (rendzinas, Avery 1990) and their solifluction downslope. At GTP 25, where an artefact scatter was noted, *in situ* rendzina formation took place and included biological activity such as rooting and earthworm working (Fig 83n). During the general cool climate formation of upper Unit 8, there probably were a number of periods during which the bare chalky landscape became revegetated, hence the frequency of calcite root pseudomorph fragments. In pedological terms the soil is poorly humic, and resembles the subsoil A/C horizon of a grey rendzina (Avery 1990), probably representing interstadial soil formation and human occupation (Catt 1986, 194–6). The uppermost organic top could easily have been lost through erosion and mass-movement (eg frost creep) (Catt 1986, 39) down the $c 20^\circ$ slope, to form colluvial rendzinas such as characterise Allerød deposits of southern England (cf Holborough, Kent: Cornwall's thin section, reported in Macphail and Scaife 1987, fig. 2.4; or Brook, Kent: Kerney *et al* 1964; Preece 1992).

The taphonomy of the refitting artefacts can be possibly explained, through the combination of burial by surface soil creep, which is not unexpected in this fragile mass-movement deposit, combined with earthworm working. It may be considered therefore, that human activity continued on a vegetated and biologically worked surface, that was present on an active slope deposit.

Unit 11, Head Gravels and Silt Beds

Data

Samples were taken from three sections (Tables 18, 24–25), two in Quarry 2 and one in Quarry 1 (Fig 4). At section 1, north of GTP 25 (Fig 79), sample 53 has a well formed compact laminar fabric in which a fine piece of wood charcoal was found (Fig 83o). Sample 52 has a laminar fabric associated with a possible later period of strong granular microstructure formation. The last is sometimes associated with deposition of clay-depleted silt. After major structural organisation, soils were affected by large amounts of microlaminated dusty clay deposition. Sample 51 is similar to 52, but more compact. In sample 50 angular flints were coated by impure clay during deposition and then probably rotated by a phase of granular structure formation. In thin section 52 it was noted that faunal burrowing occurred after granule formation and major clay deposition. The sediment continued to be influenced by particle translocation.

At section 2, north of GTP 13 (Tables 18 and 25), sample 54 is generally a finer material, containing less coarse silt and fine sand compared with samples 50–53. It is composed of two major soil materials, a generally clay-poor one, and a more clay-rich argillic type.

Table 25 Unit 11: brief field description and location of thin section samples from the Silt Beds in the Head Gravels

sample no	depth (m) below modern surface/datum	deposit
Section 1; Unit 11 north of GTP 25		
50	0.97–1.04	0–1.27m: very abundant very coarse flints in red (2.5YR4/8) and yellowish red clay loam matrix; abundant manganese staining.
51	1.25–1.33	1.27–1.53m: yellowish red (5YR4/6) and strong brown (7.5YR5/6–5/8) clay loam with abundant manganese staining.
52	1.49–1.57	At approximately 1.53m a line of a few large flints.
53	1.64–1.73	1.53–1.87m: yellowish red to strong brown clay loam with abundant manganese staining. Below, another solifluction gravel erodes the top of the chalk cliff.
Section 2; Unit 11 north of EQTP 13		
54	–	Yellowish red clay loam with common coarse flints.
Section 3: Unit 11 north face of Quarry 1 (Approximate datum at 2.5m below modern ground surface)		
	2.5	0–0.25m: very abundant coarse flints in yellowish red (5YR5/6) and strong brown (7.5YR5/6) clay loam matrix.
55	0.29–0.37	0.24–0.40m: strong brown (5YR/6) clay loam with few small flints.
56	0.68–0.75	0.40–0.86m strong brown (5YR5/6–5/8) clay loam with many small flints; very abundant manganese root stains.
57	1.10–1.17	0.86–1.43m: massive yellowish red (5YR5/8) clay loam, with few flints and few manganese stains.

The origin of the last was probably similar to that of various materials described from the Brickearth Beds (Unit 6). Granular soil formation took place, in part mixing the two soil types and even some of the clay-poor granules now contain dusty clay void coatings. The very abundant microlaminated clay coatings and infills also became fragmented, as at the same time pores within the granules and post-granular porosity became infilled by more translocated clay (Fig 83p). Many of these clay textural pedofeatures were broken up by biological mixing and rooting, which formed a channel and vuggy porosity. Lastly, very dusty clay was washed into some of these pores.

At section 3 in the north face of Quarry 1 (Tables 18 and 25), the basal samples 57 and 56 have compact laminar and granular microfabrics. The clay coatings that infilled laminar cracks in sample 56 became finely fragmented into papules all along these crack features, suggesting very little vertical movement. A possible coarse burrow some 3mm in diameter occurs, but is infilled by loose soil and dusty clay, some being darkly stained. In 55, coarse flints occur in a fine soil, where all the textural features related to earlier phases of cracking have been totally fragmented into fine papules. There has also been some minor working by biological activity.

Interpretation

Unit 11, deposited by mass-movement in periglacial conditions, makes up the solifluction deposits that bury much of the site (Roberts 1986). These coarse, flinty gravel deposits are typified by frost-shattered flints, further suggesting a cold climate (Bates in Roberts 1986). The soils can be described in broad terms on their field

characteristics as palaeoargillic or chromoluvic brown soils (Avery 1990) because of their strong brown to yellowish-red colours (Table 25), but as their micro-morphology shows, they are neither polycyclic *sensu stricto* (Catt 1986) nor temperate in character.

The microfabrics present (laminar fabrics; granular fabrics; embedded grains; capping features; vertical orientation of previously horizontally capped flints; microlaminated and very dusty clay coatings and infills and the fragmented versions of these (papules); and impure soil and washed silt infills), all suggest that Unit 11 has been affected by cool climate processes (Bullock and Murphy 1979; Fedoroff *et al* 1981; 1990; Kemp 1985; 1986; Romans and Robertson 1974; Rose *et al* 1985; Van Vliet-Lanoë 1982; 1985; Catt 1986). It is also clear that the different textures, silts and fine sands, and silty clay loams, have been affected slightly differently (van Vliet-Lanoë 1982). The finer soils have become rather compact granular soils, whereas the coarser ones were more strongly affected by laminar fractures (ice segregation), coarse open granular formation and elutriated silt inwash. It is clear from the field extent of these solifluction gravels and the micromorphological features, that this depositional phase may well have occurred under wet arctic conditions (Fedoroff *et al* 1990, table 18). This is in contrast, for example, to the dry arctic conditions that produced sand filled desiccation cracks in the Barham Arctic soil associated with the Anglian glacial period (Kemp 1986; Rose *et al* 1985).

At section 1 (Table 18), basal (53) deposition of a silt and fine sand slurry was followed by frost segregation forming a compact soil with a laminar fabric. This may have resulted from localised freezing of the water

saturated sediment. Later (in the year?) meltwater washed dusty clay into the newly formed planar voids. The overlying deposit (52) formed in a similar way but frost segregation developed into gelifluction, forming granules (Van Vliet-Lanoë 1982) and reworked earlier textural features (Fig 83o). Faunal burrowing also took place. Farther up (51) a compact soil was formed by these processes, and some clay infills were notably dark stained. Fedoroff *et al* (1990) have suggested that such dark stained translocated material may occur through melting snow passing through humic soil layers under a vegetation cover dominated by conifers (Fedoroff and Goldberg 1982; Fedoroff personal communication). The dark textural features are formed by snowmelt carrying impure soil mixed with fulvic acid. It can also be noted that thin section 53 contains a coarse fragment of unidentifiable wood charcoal (Fig 83o). Its presence in cold climate soils (Catt 1990, 79) is indicative either of lightning strikes or human activity. The vertically oriented flints in sample 50 are probably related to post-depositional stone movement due to frost action (Van Vliet-Lanoë 1985).

At section 2, finer sediment was deposited, and the microfabric indications are that a fine brickearth 'argillic soil', as at GTP 13, was formed, alongside less clay-rich material. The latter may have originated in the same way as the clay-poor laminar soils in section 1. On the other hand, some clay-poor granules may be relic of clay-depleted Eb (A2) horizons (Bullock and Murphy 1979) as a few of these contain pores indicative of pedogenesis rather than pure mechanical formation through sediment elutriation. There is therefore some evidence to suggest that some clay-depleted soil with the characteristics of an Eb (A2) horizon may have formed rapidly, although typical Bt horizon soil appears to be absent. Rather, the clay-rich 'argillic' soils have dusty intercalated textural features more commonly associated with slaking as described from Unit 6. The poorly argillic material may also have its main origins in the deposition of a moderately clay-poor brickearth deposit. Still, a possibly layered sediment and/or one in which a clay depleted Eb horizon had developed in places, became cryoturbated and mixed. A rather densely packed granular fabric was formed with voids infilled with microlaminated and dusty clay (Fig 83p). Granular soil formation continued and increasingly caused dusty clay to be deposited. This produced a fabric rich in textural features resulting from mechanical translocation. The enhanced clay content from continued soil slaking and mixing of the mechanically active cold soil is in part responsible for the reddish colours of this and other 'soil horizons'. This is because large amounts of iron-stained clay have become concentrated in the packing porosity around the granules. A major phase of rooting and channel and vugh formation succeeded this phase of cold soil formation. This biological activity gently broke up many of the earlier thick microlaminated void infills and coatings, but was not long or intense enough to

homogenise the soil strongly. Lastly, these channels and vughs were affected by very dusty soil inwash, presumably as a result of further mass movement burying this horizon. Certainly here there is the possibility of a short-lived period of 'temperate' interstadial soil formation, especially as the original deposit may have been laid down first through colluviation rather than by solifluction/gelifluction.

At section 3 in Quarry 1 (Table 18), sediment deposition and continued cold soil formation occurred in a very similar way to the deposition at section 1. Again wet, cold, conditions probably continued, with dark (humic?) stained dusty clay coatings perhaps relating to snow melt passing through surface organic horizons possibly formed under a temporary coniferous woodland (Fedoroff *et al* 1990). Faunal burrowing also suggests periodic biological activity affecting these mainly 'active soils', perhaps via tree roots. The amount of soliflucted/geliflucted material again may testify to cold, wet, arctic conditions much of the time (Vandenbergh *et al* 1985).

Unit 11 was studied from three widely separated locations that revealed a consistent history of deposition and soil formation under dominantly wet arctic conditions. Still, episodes of a less harsh environment are indicated and refitting artefact scatters testify to *in situ* and contemporary hominid occupation (Roberts Chapters 6.3, 6.8).

Discussion and conclusions

Twelve units at Boxgrove were analysed through the study of fifty-seven thin sections. Sampling was focused upon layers that were rich in artefacts, so as to understand better the soil and sedimentary environments contemporary with hominid occupation, especially the nature of landsurfaces used as chipping floors. As the site is 500,000 years old and deeply buried, one essential element of the study was to investigate taphonomic problems, so that soil and sedimentary processes active during the occupation could be reliably differentiated from post-depositional events. Both vertical and lateral sequences were sampled to aid this aspect of the investigation. The soil micromorphological study had to be carried out without the benefit of any direct analogues, therefore some of the scientific ground is new. On the other hand, there is a rich literature on sedimentary petrology and the micromorphology of, for example, soft sediment ripening, palaeosols and soils affected by cold climates. The soil micromorphological investigation was carried out within this context and with the independent support of mineralogical, field sedimentary, animal bone and artefactual data, to name just a few of the other disciplines involved.

Soil micromorphology, with other data, indicates that the 2nd marine cycle deposits (Unit 3) were fully marine. During the 3rd marine cycle (Unit 3), shallowing water and a small increase in terrestrial sediment

input seem to have occurred. A possible local delta system developed and sediments began to contain higher amounts of non-calcareous clay. Unit 4a sedimentation probably became lagoonal, perhaps mainly influenced by diurnal tidal flow. Much biological activity is recorded. During the formation of Unit 4b, conditions were still saline, but there was also an important freshwater component in this delta lagoon system, and perhaps because of this only a few biota could find a niche. Large animals and hominids occasionally visited the mudflats, the latter possibly choosing the driest areas to make tools and butcher carcasses. Artefact and bone evidence of these events are almost totally *in situ* because biological activity was so low and continuing low energy sedimentation quickly buried the remains.

As regional sea levels fell, water tables related to local freshwater systems fell also. Mudflats were exposed to full subaerial weathering and biological activity, at least seasonally, such as experienced by a water meadow. A thin fully ripened soil formed, and humans occupied dry areas of it at times. The sediment ripening process affecting Unit 4c, as water tables rose and fell, may have exceeded, in temporal terms, mull soil formation which probably lasted only a few decades. It is impossible to be more exact about these timescales. Although influenced by fluctuating water tables, plants, invertebrates and small mammals have partially vertically reworked human artefacts throughout Unit 4c (Wilhelmsen Chapter 6.2). At the same time, a spring-flush draining the chalk seems to have produced a highly alkaline pond (Unit 4d). Later, a local rise in water table caused the site to flood, and form a shallow lake or marsh. The marsh developed into a mire (Unit 5a) in most areas, and this was affected seasonally by drying-out and by a low energy braided streamflow or colluviation. A woodland vegetation may still have been extant in places. At one location, a coluvial fan (Unit 5c) formed, possibly running from the palaeo-beach slope across onto the mire. This 'high' ground was apparently favoured by animals and humans. Mire deposits (Unit 5a), which may have been forming over a few hundred years, were affected by ferruginous groundwater, and peat was transformed into a form of bog-iron. The site then seems to have dried out, and then, perhaps as an effect of climate cooling which led to more effective precipitation and higher groundwater levels, the site was again inundated. This time, however, it was flooded by calcareous water from the chalk talus cliff-line. A fluviually active ponded landscape (Unit 5b) developed that was occasionally influenced by mass movement deposits.

The wooded argillic brown earth soils parent material cover (Roberts Chapters 2.1, 2.7) on the Downland, and the chalk cliff became increasingly unstable as the cooling climate adversely affected the vegetation. Increased runoff from the Downs allowed possibly seasonally active streams to deposit thick brickearth deposits (Unit 6) across the site, which once more may have become intermittently marshy. It also

seems likely that there was a period of stability, perhaps in the order of a few hundred years. This possibly allowed the development of an incipient argillic brown earth across the site. Unfortunately, the microfabric evidence for this episode comes from only one location and is equivocal. Renewed and more vigorous cooling of the climate then led to full devegetation of the Downs and increased runoff. This runoff first slaked and then eroded the now unstable soils that had formed on the brickearth. Perhaps only a little later, cool conditions led to the rapid erosion of the chalk cliff (Unit 7) and talus slope, producing the Upper Chalk Pellet Bed (Unit 8). Frost fracturing of the probably open vegetated rendzina-covered chalk talus led to frost creep deposits (Unit 8). Surprisingly, this soil landscape was biologically active and occupied by hominids at times. Hominid activity and short-lived soil formation are further evidence of climatic fluctuations during deposition of the solifluction gravels (Units 10 and 11) which succeed the path gravels (Unit 9). Of these deposits, the latter represent high energy runoff from meltwater and the former massive solifluction. The soils within the silt beds of the head gravels developed under humid arctic conditions.

2.7 Geological summary

M B Roberts

The temperate Pleistocene sediments at Boxgrove were deposited during a major warm climatic episode, or interglacial. These sediments overlie and abut the solid chalk. At the northern end of the quarry, the chalk wave-cut platform rises up into a cliff (Lewis and Roberts Chapter 2.2) that during the temperate episode would have been a major feature in the landscape. The temperate sediments of the Slindon Formation are overlain by sediments laid down during the final part of the temperate stage and the ensuing cold stage or glaciation. These deposits, the Eartham Formation (Table 9a), overlie both the temperate Pleistocene deposits and, further up slope, to the north, the chalk (Fig 22).

Within the quarry complex (Fig 4) there is a major unconformity present in Quarry 2. The conformable sequence is present up to an east-west trending line that is approximately 250m south of the cliff-line, just to the south of Q2/A (Figs 4, 22, 29). South of this line the mass movement gravels of the Eartham Upper Gravel Member overlie the Slindon Sands (Fig 24a). The Brickearth Beds and Slindon Silts have been removed and the upper part of the sands have been reworked by relatively high energy water flow. Analysis of bedding structures in the reworked sand indicate a flow direction from the north; this point is strengthened by the presence of bands of angular flint gravel derived from the sediments of the Eartham Formation. The deposition of the missing units is attested by their rare preservation in solution features (Roberts 1986). Solution of the underlying chalk by groundwater, that

post-dates the brickearth deposition, has led to slumping of overlying deposits (Fig 24b). Within these structures the original conformable sequence can be seen.

The unconformity was formed during the mass movement of gravels from the Downland block. The initial flow of gravels must have been relatively fast and reached a point 250m south of the cliff. There then followed a hiatus in gravel deposition during which time water, presumably from snow melt, flowed southwards over the surface of the slumped regolith and produced the unconformity by removing the non-protected fine sediments. It has not been possible to trace this unconformity across into Quarry 1 due to a lack of southerly exposures but it is present at Everyman's Pit, 5km to the east at Slindon (Figs 8, 9).

Another major unconformity was revealed during rescue work in 1992, at the eastern end of Quarry 1 and the western end of Quarry 2 (Fig 33). The results of this work are outside the remit of this publication but a brief synthesis may be added here. Unlike the major unconformity, this discontinuity is north-south trending, and the edges can be mapped in Quarry 1. The cause of the unconformity is freshwater run-off from the Downland block, dating from the end of Marine Cycle 3 (Collcutt Chapter 2.3). It is of course highly probable that seasonal drainage of this nature occurred during the height of the marine transgression but its effects were dissipated as the water ran into the sea.

Quarry 1 appears to have been on the route of the major drainage pattern from Halnaker Hill (Fig 21), whereas Quarry 2 appears to have been more protected (Fig 33). The main palaeodrainage in the quarry complex trended from the north-east to the south-west. Modelling of the palaeodrainage beyond these observations is hampered by the fact that the Middle Pleistocene surface of the Downs was completely changed by the removal of the Tertiary regolith during the subsequent Anglian Glaciation.

Units 2-5a, the Slindon Formation

The Slindon Sands were laid down during a high sea level event at the end of the Cromerian Complex (Tables 5, 8). They exhibit the features of a classic nearshore, subtidal, and intertidal sand deposits. The sediment source for this unit and the overlying silts was the Tertiary deposits of the Lower Coastal Plain (Table 6) and the Cretaceous Chalk (Tables 6 and 7) (Catt Chapter 2.5). Earlier work by Kellaway *et al* (1975) had suggested that the Slindon Sands were deposited by fluvio-glacial outwash (Roberts Chapter 1.3), from an English Channel glaciation (Bridgland Chapter 2.4). The results presented here support later work by the original authors of the paper in rebutting this hypothesis (Shephard-Thorn and Kellaway 1977; 1978). Collcutt (Chapter 2.3) reports that there is little evidence of longshore drift in the structures of the sand. This phenomenon may be due to the protected nature of the coastline, a trend that becomes more

apparent in the silts, or it may result from the fact that the English Channel was probably closed at its eastern end at this time (Preece 1995). The breaching of the Channel landbridge is thought to have occurred at the end of the Anglian Glaciation (Gibbard 1988) as the result of a build up of water in a large ice-dammed lake in what is now the southern North Sea (Smith 1985). The location of the landbridge to the east of Boxgrove remains unknown, although chalk erosion rates suggest it need not have been a considerable distance from Boxgrove half a million years ago. It has been suggested (Martin 1938; Bates *et al* 1997) that the connection was close to Boxgrove, ie just to the east of the River Arun, as this would explain the lack of the 40m beach in this area (Roberts Chapter 2.1). However, the deposition of the lower beaches east of the Arun would require that the coastline changed greatly after the channel opened, and mainly in an easterly direction. Another explanation for the absence of the Boxgrove beach to the east of the Arun is that tectonic uplift decreases to the east and thus the older beaches are eroded and reworked by younger beaches. Using the uplift model outlined in Chapter 2.1 it can be shown that the marine deposits at Boxgrove could have been elevated by between 5 and 7m by the time of the Stage 11 marine transgression. It is clear that further research is required to ascertain the absolute heights of the Pleistocene sea levels relative to the present day.

The open coastline period at Boxgrove, which is indicated by the Slindon Sands (Fig 87), can be seen to be coming to an end in the upper 1-1.5m of this unit (Macphail Chapter 2.6). There is an increase in the deposition of finer arenaceous material and a gradual transition to silt-size particle deposition. The transition of the Slindon Sands to the Slindon Silts is most noticeable as a colour change from a predominantly yellow unit to a grey green (Fig 49a). This colour change is less a reflection of different source sediments (Catt Chapter 2.5) but a result of the change in grain size and calcium carbonate content. The silts were laid down essentially as intertidal mudflats although there is evidence that they were deposited in a protected environment like a lagoon rather than an open shoreface (Fig 88). A lack of channels, limited bioturbation, especially from rooting, restricted mollusc and fish faunas, and undisturbed archaeology, support this view. Both Collcutt and Macphail emphasise that the sands and silts exhibit characteristics that are normally associated with the seaward end of estuarine systems. Therefore the possibility exists that the Solent River (Allen and Gibbard 1993; Bridgland Chapter 2.4) may have had a role in supplying sediment into the system and may also have been instrumental in providing material that barred off this part of the coast to produce a lagoon. If a salt water lagoon did exist, its extent would have stretched at least 30km west to east. Such a large feature would have been reliant on the sediment discharge from a source like from the Solent to create and maintain it. Unfortunately the southern margins

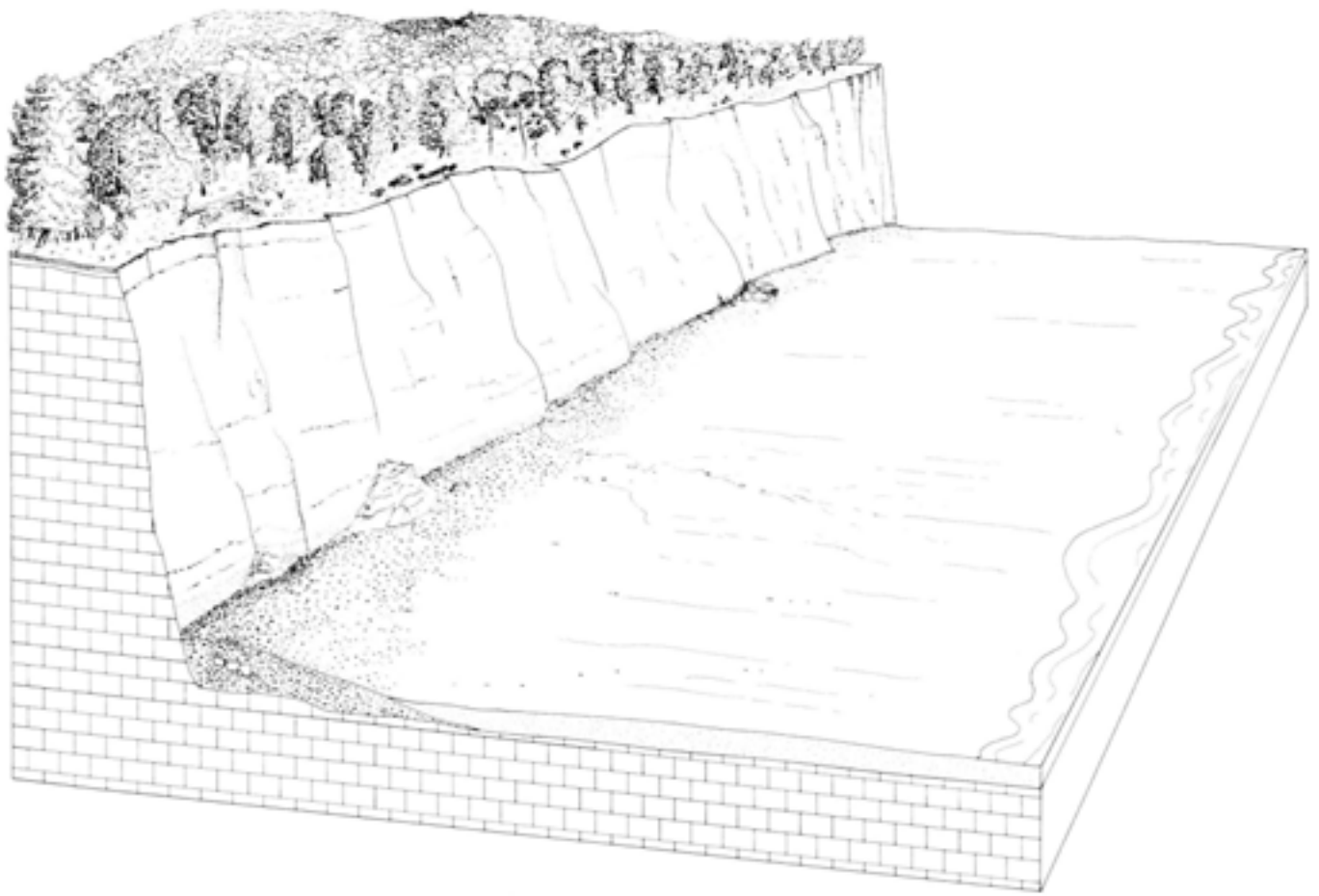


Fig 87 Boxgrove during the deposition of the Slindon Sands

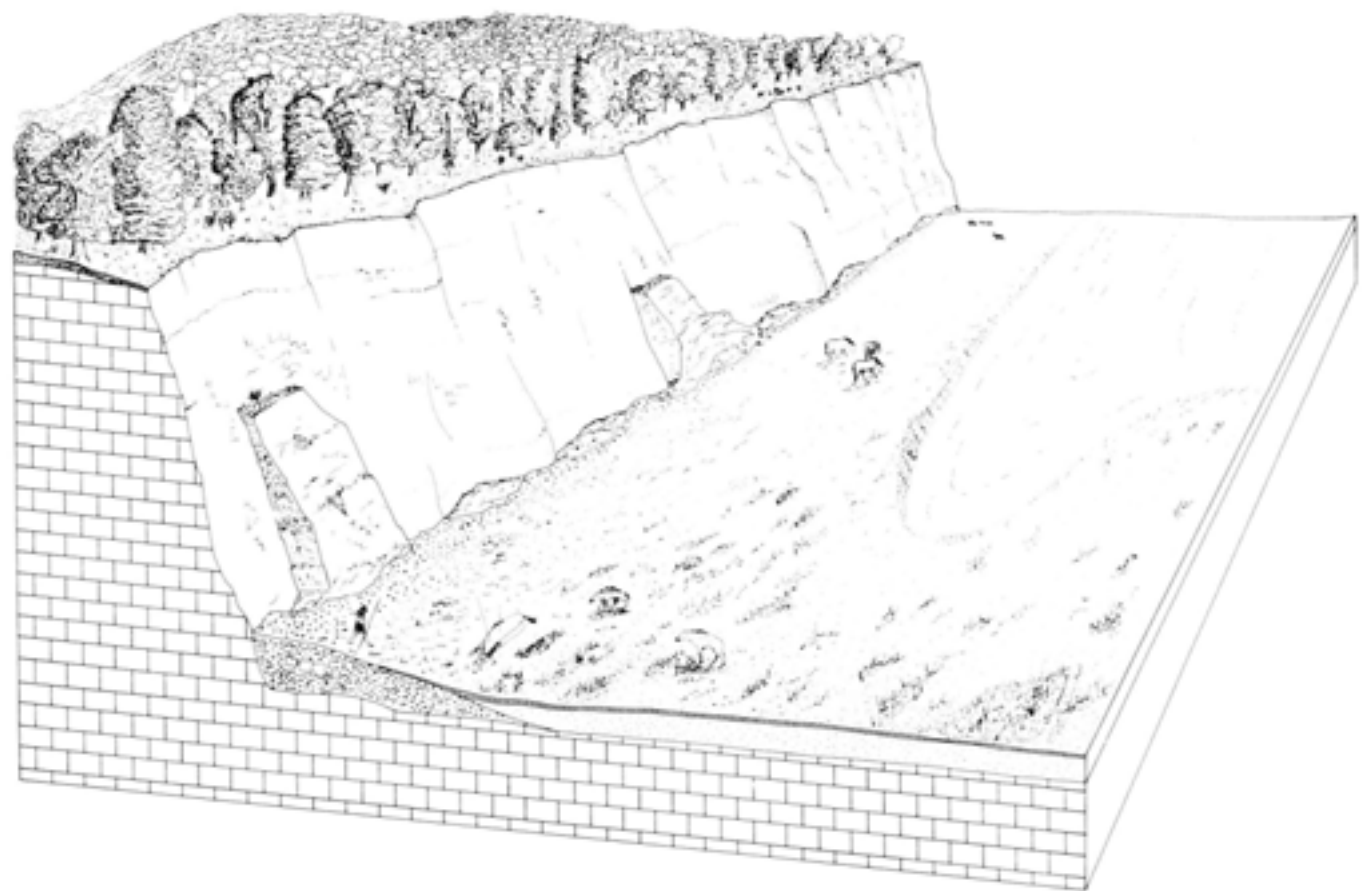


Fig 88 Boxgrove during the deposition of the Slindon Silts

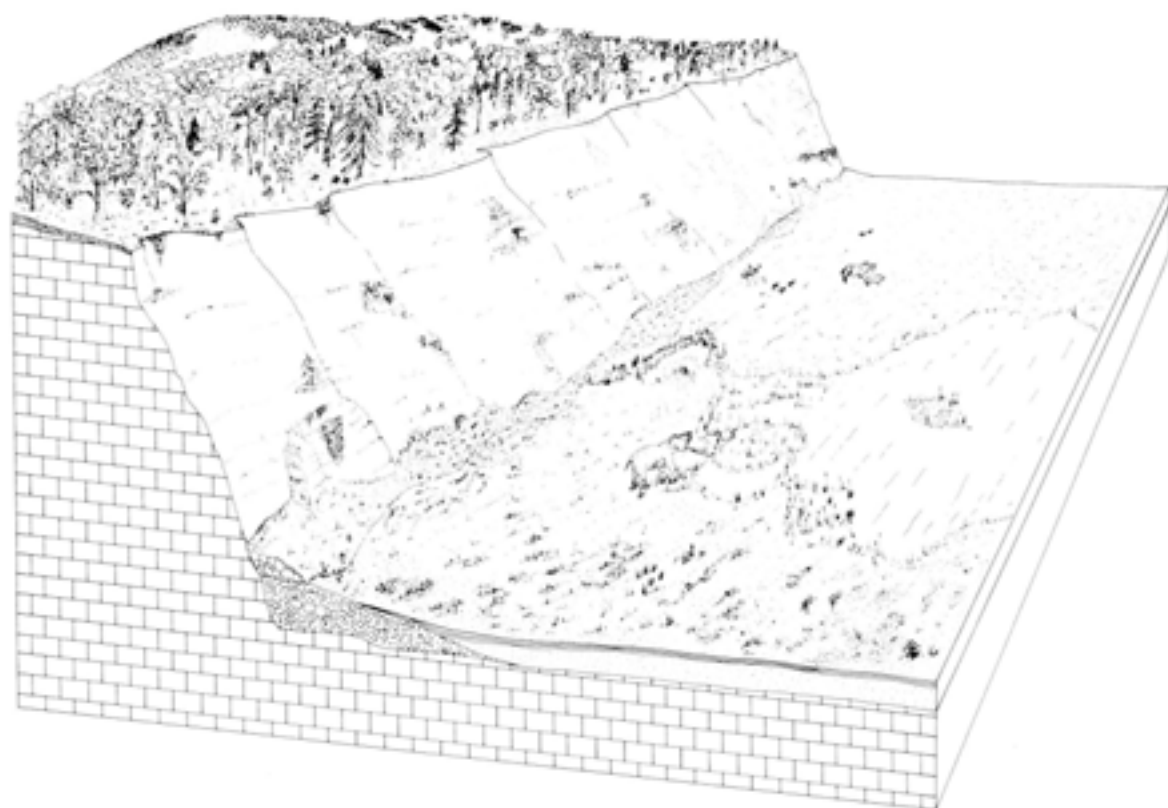


Fig 89 Boxgrove during the grassland stage of Unit 4c and the marsh of Unit 5a

of the silts have been eroded away, and further work is required to trace them westwards into the lagoon. The archaeology contained in the silts and sands is in primary context and attests to the gentle nature of the sedimentary regime. However, whereas the archaeology in the sands is very rare, it becomes more common in the silts at a depth of between 0.3–0.4m below the unit surface. As well as sporadic debris being dropped at low tide, there is at least one major landsurface which developed as the result of exposure of a silt surface out of the tidal reach. The very limited weathering of this surface indicates that it was only open for a short time but its distribution right across the east–west extent of the quarry complex precludes it being a local phenomenon. The landsurface in the silts appears to be confined to an area up to 100m in front of the cliff (Fig 34), with archaeology indicating its presence in areas Q1/A, Q1/B and GTP 17 (Fig 4). This occurrence may reflect a slight lowering in sea level prior to re-inundation and further deposition.

The end of the marine influence at Boxgrove occurs at the surface of the Slindon Silts. After the sea regressed a soil quickly developed on the upper horizon of the silts and a major land surface was formed. The soil horizon, explained in detail by Macphail (Chapter 2.6), was probably open for between a minimum of 20 and a maximum of around 100 years, as indicated by its developmental features. During this period a large grassy plain developed on the flat marine plain to the south of the cliff (Fig 89). There is a surprising lack of

bioturbation features in the soil horizon, especially from root activity of larger shrubs and trees. One possible explanation for this absence is addressed by Macphail, namely that the increasing wetness of this unit through time has destroyed the soil structure in most locations, giving rise to a structureless and homogeneous deposit. Accordingly, many *in situ* bioturbation structures were lost. It is also likely that post-burial compression and decalcification has reduced the thickness of the unit, but it is still to be expected that roots would have penetrated down into the underlying Units 4b and 4a. It therefore seems that a more likely explanation for the lack of rootlet bioturbation was an absence of trees and shrubs from the soil horizon. As conditions of the sedimentary regime and climate seem unlikely to be causative agents, the answer probably lies in herds of grazing ungulates that were moving and feeding across the landscape at this time (Parfitt Chapter 4). Occasional large trees may have survived grazing but the limited cover of the excavations and test pits over this surface are likely to have missed them. The archaeology and faunal remains associated with this deposit are not strictly *in situ* but have been moved by large mammal scuffing, small mammal burrowing and earthworm activity. The increasing wetness eventually led to flooding of the soil surface and the formation of the marsh/mire deposit of Unit 5a (Fig 89). The marsh sediments are present right across the conformable sequence at Boxgrove and are again encountered to the east at Everyman's Pit

(Fig 8), indicating a large scale depositional regime. Unit 5a, the Organic Bed, is a transitional sediment between deposits of the Slindon and Eartham Formations and it shares mineralogical suite characters with both (Catt Chapter 2.5). However, as micromorphological analysis indicates interbedding with the upper part of Unit 4c, and in general these units merge with no evidence of erosive contacts or unconformity; Unit 5a is included in the Slindon Formation (Macphail Chapter 2.6).

Units 5b–11, the Eartham Formation

The sediments of the Eartham Formation had a predominantly different sedimentary source from the underlying sediments of the Slindon Formation (Catt Chapter 2.5). The source for Units 5b–11 is largely from the north, and includes the calcareous deposits of the chalk cliff and its associated screes, the soils of the downland block, and finally the underlying gravels of the Tertiary regolith. However, all the units of the Eartham Formation exhibit a coarse silt mineralogy which appears to be largely derived from wind blown sediments of the Slindon Formation. Only the Chalk Pellet Beds and the Upper Silt Bed in Quarry 2 have coarse silt components more like the fine sand fraction, indicating an origin from the regolith, although the coarse silt light minerals from these units are still similar to those of the Slindon Formation. This phenomenon is probably the result of sediment availability, dictated by the exposure or otherwise of sediments of the Slindon Formation to the south.

The fall in sea level evinced by the end of marine sedimentation at the top of the Slindon Silt Member, may not have been simply a eustatic response to global climate change. The vertebrate faunas from the Slindon Soil Bed (Unit 4c), the Organic Bed (Unit 5a), the calcareous silty clays (Tables 8, 9b) and the Lower Chalk Pellet Beds (Unit 8, Table 9a), attest to a continuation of temperate conditions. An explanation for the fall in sea level is probably linked to a local decline in the marine sediment budget brought about by the inability of the sea to continue to penetrate as far inland. This restriction may have been the result of the lagoon silting up, further off-shore barring of the coast, or localised tectonic uplift (Roberts Chapter 2.1). Alternatively, there may have been a lag response between polar ice build up and continental climate change at this particular interglacial/glacial boundary. The climatic transition/sea level fall at Boxgrove contrasts starkly with that seen at Norton Farm (Roberts Chapter 2.1; Table 8, Figs 8, 9, 21; Bates *et al* in press), where the fall in sea level can be directly linked to the onset of much colder conditions.

The sediments of the Eartham Lower Gravel Member were deposited under temperate conditions at the end of the interglacial (Table 9a). The Angular Chalk Beds (Unit 7) were laid down both syn-depositionally

with and post-depositionally to the sediments of the Slindon Formation, and are the result of erosion of the chalk cliff-line (Lewis and Roberts Chapter 2.2). These beds share a cyclical pattern of deposition with the Lower Chalk Pellet Beds (Unit 8) and calcareous silty clays (sub-Units 1129, 6'20, GCF and LGC; Table 9b), which derived from the screes of the Angular Chalk Beds (Figs 41, 42a). The deposits of the Eartham Lower Gravel Member are found only at the northern end of the site. As noted earlier (Roberts Chapter 2.1), the original unit numbering system was based on earlier exposures further to the south (Table 9a) and thus the numbers do not reflect true chronological ordering in terms of stratigraphic superimposition. In the vicinity of the cliff-line, sediments of this member overlie the marsh/mire deposits of the Organic Bed (Unit 5a). However, further to the south this bed is overlain by a silty deposit, historically called the Brickearth (Dines *et al* 1940; 1954; Shephard-Thorn and Kellaway 1977; 1978), and in places by another calcareous silt Unit 5b (Collcutt Chapter 2.3, Catt Chapter 2.5, and Macphail Chapter 2.6). These beds belong to the Eartham Upper Gravel Member.

The sediments of the Eartham Upper Gravel Member (Tables 8, 9a) were laid down under conditions of increasing cold; this is reflected in their vertebrate faunas, modes of deposition and post-depositional alteration. The Brickearth Beds nearer the cliff are calcareous and are probably derived from the cold climate Upper Chalk Pellet Beds (Unit 8) but become differentially and then totally decalcified to the south. The thick deposits of brickearth around Q2/A and GTP 5 (Fig 4) may never have been a calcareous deposit and were probably derived directly from the soil cover of the Tertiary regolith. At a distance of up to 150m from the cliff the Brickearth Beds interdigitate with Upper Chalk Pellet Beds and the moderately well-sorted angular Fan Gravel Beds (Unit 9) (Bridgland Chapter 2.4). The deposition of the main body of brickearth is probably linked to a decrease in vegetation cover on the cliff screes and the Downs (Fig 90) which, when combined with an increased precipitation rate and/or annual snow melt, led to the stripping of the higher ground fine-grained deposits. Catt (Chapter 2.5) suggests that the Slindon Formation may have provided a partial source for the Brickearth Beds, in the form of locally wind blown silt; which combined with calcareous and non calcareous silts derived from soil formation on the chalk scree slopes and soil formation on the regolith, respectively. This hypothesis is supported by Macphail's work on the micromorphology which identifies soil remnants in the brickearth. The upper part of the Brickearth Beds at their contact with the overlying gravels exhibits cryogenic features, but ice wedges and structural deformation are absent lower down in the unit, probably indicating the increasing severity of the cold climate regime. The lithological evidence from Boxgrove indicates that the transition

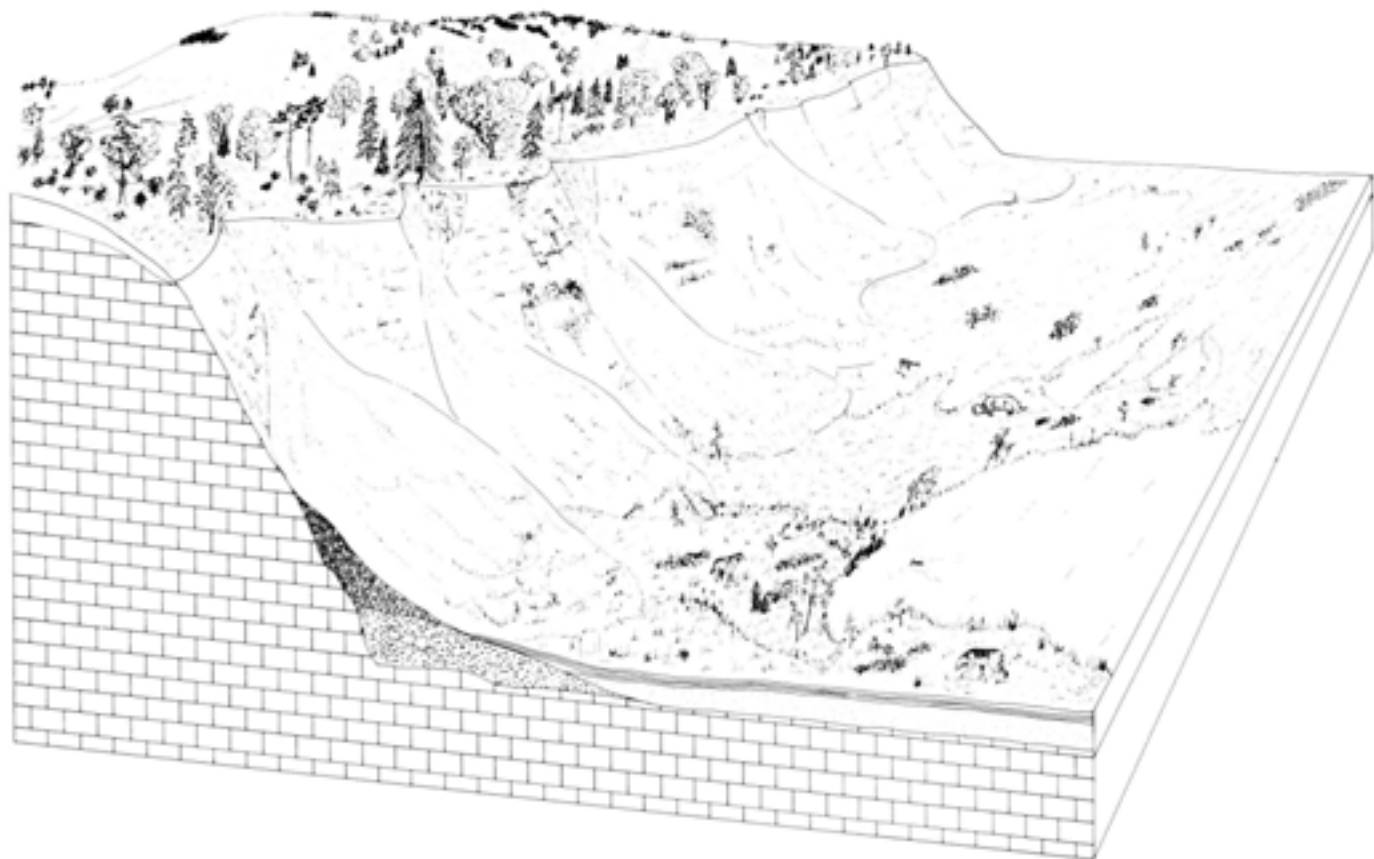


Fig 90 Boxgrove during the deposition of the upper part of Unit 6, through to Unit 9

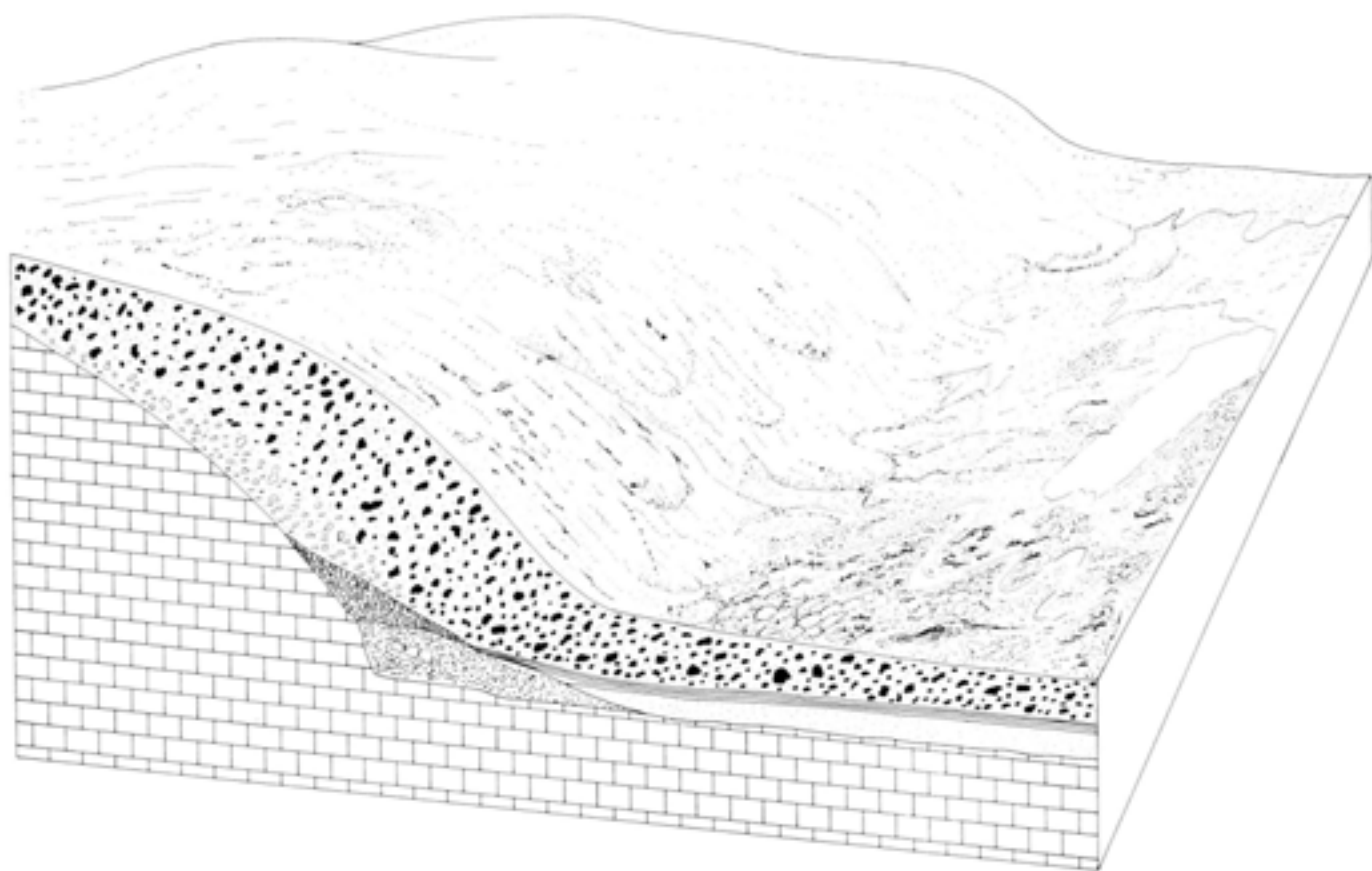


Fig 91 Boxgrove during the deposition of Units 10 and 11, in the Anglian Glaciation

to a cold climate occurred rapidly. There is an obvious unconformity between Unit 5a and the Brickearth Beds, especially to the south of the cliff where the decalcified brickearth overlies the Organic Bed in the area of Q2/A. However, the Organic Bed is never completely truncated or eroded by sub-aerial processes (Macphail Chapter 2.6).

The Brickearth Beds interdigitate with and are covered by the various different gravels present at Boxgrove (Table 8; Fig 90), these contacts are time transgressive, becoming progressively younger to the south, where the Head Gravels (Unit 11) are in direct contact with the brickearth (Figs 22, 34). The Upper Chalk Pellet Bed and the Fan Gravel Beds (Units 8 and 9) are largely fan gravels deposited by moving water and as a melt-out slurry. The Fan Gravel Bed has been extensively decalcified by groundwater running through the unit. The increase in flint in this unit probably relates to the coeval stripping of the Downland soil cover to form the Brickearth Beds, thus revealing the underlying flint-rich regolith. Within the Upper Chalk Pellet Beds are surfaces

containing archaeology that represent short time intervals of climatic amelioration and soil formation. Elsewhere in this unit and the overlying Fan Gravels and Head Gravels, residual archaeological lithic material, in various states of preservation, is found (Roberts Chapter 6.3).

The Head Gravel suites (Units 10 and 11) of the Eartham Upper Gravel Member are thought to have been deposited within a single cold stage, the Anglian Glaciation (Fig 91). There is no evidence for a major warm stage in the form of temperate soil development anywhere in the sediments. Once the Downland block vegetation cover was removed, gravitational movement of material off-slope began. The slope angle had been increased by the formation of the cliff, giving added gravitational impetus to the mass movement flow. The remnants of the regolith remain as outcrops of Clay-with-flints on the Downs, the bulk of the deposits having moved southwards; there they sealed into a unique sedimentary trap the temperate sediments of the Slindon and Eartham Formations and their wealth of environmental and archaeological evidence.

3 Palaeontology

3.1 Introduction

S A Parfitt

The lithostratigraphical framework and the modes and environments of deposition have been set out in Chapter 2. The ensuing data on non-vertebrate and vertebrates also have a significant role to play in palaeoenvironmental and palaeoecological reconstruction, as well as providing information on taphonomy and biostratigraphy.

Samples were collected for charcoal (Appendix 1), dinoflagellates (Appendix 2), diatoms, pollen, calcareous nannoplanktons (Chapter 5.8), foraminifera and ostracods (Chapter 3.2), and molluscs (Chapter 3.3). The sedimentary regime and post-depositional alteration of the deposits was not conducive to the preservation of diatoms, Pleistocene dinoflagellates and pollen. The calcareous fossils were generally restricted to calcified units in the sequence; these units are found in the northern part of Quarry 2 and throughout the conformable sequence in Quarry 1 (Figs 34, 35).

The vegetational history of the deposits is largely inferred from the habitat preferences of the molluscan and vertebrate faunas. Despite extensive sampling of the deposits at many different levels, the vegetational information provided by the surviving pollen has not changed from that reported by Scaife in the preliminary report (Scaife in Roberts 1986). Micromorphological analysis of the sediments (Macphail Chapter 2.6) has provided additional information on the vegetation in the form of mineralised plant remains and root traces. Observation of the Slindon Silts in many area excavations and test pits has shown that the sediments are not subject to any large-scale vegetational bioturbation (Collcutt Chapter 2.3; Macphail Chapter 2.6). Additionally, rootlet scars on mammal bones, together with the lack of extensive vertical displacement of the lithic assemblages, suggest that in fine-grained deposits in front of the cliff, vegetational development was restricted to grasses and herbaceous vegetation.

The presence of woodland on the Downland block is attested by the mineralised detrital vegetation that forms the marsh deposit (Unit 5a), elements of the molluscan fauna, and certain of the mammal species (Parfitt Chapter 4).

The non-vertebrate faunas were collected from various locations at the site (Fig 4), using existing GTPs, excavations, and type sections where possible. The methodology of collection and analyses are given in the individual chapters.

The vertebrates

The early Middle Pleistocene deposits at Amey's Eartham Pit have produced one of the most diverse vertebrate faunas from a Lower Palaeolithic site in

western Europe. Extensive collecting at the site between 1985 and 1991 has recovered a vertebrate assemblage representing a minimum of 88 species consisting of at least 11 species of fish, 9 species of amphibian and reptile, 19 species of bird and 50 species of mammal. A complete list of the vertebrate taxa currently identified from the Slindon and Eartham Formations at Amey's Eartham Pit, Boxgrove (AEP) is given in Table 26. Since the inception of the Boxgrove Project, one of the primary aims of the excavation and post-excavation programme has been the recovery and analysis of vertebrate faunal remains. The vertebrate remains were recovered during archaeological excavations which sampled an extensive area of Pleistocene landsurface parallel to the buried cliff-line. In addition to the vertebrate remains recovered from the excavated areas, over 65 tonnes of sediment have been sieved to recover faunal and artefactual remains.

Quarrying at AEP has exposed a complete stratigraphic column through the Slindon and Eartham Formations (Roberts Chapter 2.1, Collcutt Chapter 2.3), which provided a unique opportunity to recover the vertebrate fauna through a complex stratigraphic sequence, covering a number of climatic oscillations of varying magnitude. The main faunal horizons at the site occur at the transition from intertidal to terrestrial deposits, and continue into a sequence which samples the transition from temperate climatic conditions through a period of major climatic deterioration. The vertebrate fauna from these horizons give an unusually complete picture of the palaeoenvironment and palaeoecology of southern England during a phase of rapid environmental change.

In addition to sampling the vertebrate fauna through a stratigraphic sequence, the extensive nature of many of the deposits comprising the Slindon Formation and basal Eartham Formation has made it possible to investigate differences in faunal composition across the site which are possibly related to microhabitat differences across the palaeolandscape. The recognition of microhabitat variation has important implications for analysis of the distribution of the artefact assemblages and consequently of hominid behaviour at the site.

Early reports on the Goodwood-Slindon Raised Beach deposits have proposed a Hoxnian age for the deposits, based on correlations of the sequence with the Thames terraces (Woodcock 1981). Recent fieldwork and analysis of the vertebrate fauna strongly indicate that the marine and basal terrestrial deposits are pre-Anglian in age, and that the mammal assemblage

Table 26 The vertebrate fauna from Boxgrove

(A: Marine Slindon Sands, B: Lagoonal Slindon Silts, C: Palaeosol and associated deposits, D: Cold stage 'brickearths' and chalky gravels. Hominids are also represented by artefacts in A-D)

		A	B	C	D
PISCES					
<i>Raja clavata</i>	Thornback ray	-	+	+	-
<i>Anguilla anguilla</i>	Eel	-	-	+	-
<i>Conger conger</i>	Conger eel	+	-	-	-
<i>Muraena helena/Conger conger</i>	Moray/Conger	-	+	-	-
Clupeidae	Herring family	+	-	-	-
<i>Salmo trutta</i>	Brown trout	-	-	+	-
Salmonidae	Salmon/trout	-	+	+	-
Gadidae	Cod family	-	+	-	-
<i>Gadus morhua</i>	Cod	-	+	-	-
<i>Gasterosteus aculeatus</i>	Three-spined stickleback	-	+	+	-
Triglidae	Gurnard family	-	-	+	-
Labridae	Wrasse family	-	+	+	-
<i>Thunnus thynnus</i>	Blue fin tunny	-	+	-	-
<i>Platichthys flesus</i>	Flounder	-	+	+	-
Pleuronectidae	Flatfish	+	+	+	-
AMPHIBIA					
<i>Triturus vulgaris</i>	Smooth newt	-	+	-	-
<i>Triturus helveticus/vulgaris</i>	Palmate/Smooth newt	-	-	+	-
<i>Pelobates fuscus</i>	Common spadefoot	-	-	+	-
<i>Bufo bufo</i>	Common toad	-	-	+	-
<i>Bufo</i> sp	Toad	-	+	+	-
<i>Bufo calamita</i>	Natterjack toad	-	-	+	-
<i>Rana arvalis</i>	Moor frog	-	-	+	-
<i>Rana temporaria</i>	Common frog	-	+	+	-
<i>Rana</i> sp	Frog	-	+	+	-
REPTILIA					
<i>Anguis fragilis</i>	Slow worm	-	+	+	-
<i>Lacerta</i> cf <i>L. vivipara</i>	Viviparous lizard	-	-	+	-
<i>Natrix natrix</i>	Grass snake	-	-	+	-
<i>Natrix</i> sp	Snake	-	-	+	-
AVES					
<i>Cygnus</i> cf <i>C. cygnus</i>	Whooper swan	-	-	+	-
<i>Anser anser</i>	Greylag goose	-	-	+	-
<i>Anser</i> sp	Goose	-	-	+	-
<i>Anas platyrhynchos</i>	Mallard	+	+	+	+
<i>Anas penelope</i>	Wigeon	-	+	+	-
<i>Anas</i> cf <i>A. querquedula</i>	Garganey	-	-	+	-
<i>Anas crecca</i>	Teal	-	+	+	-
<i>Anas</i> sp	Dabbling duck	-	-	+	+
<i>Aythya fuligula</i>	Tufted duck	-	-	+	-
<i>Bucephala clangula</i>	Goldeneye	-	-	+	-
<i>Perdix perdix</i>	Partridge	-	-	+	-
<i>Gallinula chloropus</i>	Moorhen	-	-	-	+
Scolopacidae or Charadriidae	Snipe/plover	-	-	+	-
<i>Larus ridibundus</i>	Black-headed gull	-	-	+	-
<i>Rissa</i> cf <i>R. tridactyla</i>	Kittiwake	-	-	+	-
<i>Pinguinus impennis</i>	Great auk	-	-	+	-
<i>Strix aluco</i>	Tawny owl	-	-	-	+
<i>Apus apus</i>	Swift	-	-	+	-
<i>Erithacus rubecula</i>	Robin	-	-	+	-
<i>Prunella</i> cf <i>P. modularis</i>	Dunnock	-	-	+	-
<i>Sturnus vulgaris</i>	Starling	-	-	+	-
MAMMALIA					
Insectivora					
<i>Erinaceus</i> sp	Hedgehog	-	+	+	-
<i>Neomys</i> sp	Water shrew	-	-	+	+
<i>Sorex minutus</i>	Pygmy shrew	-	-	+	-

Table 26 continued

		A	B	C	D
Insectivora continued					
<i>Sorex runtonensis</i>	Extinct shrew	-	+	+	+
<i>Sorex (Drepanosorex) savini</i>	Extinct shrew	-	+	+	+
<i>Talpa europaea</i>	Common mole	-	-	+	+
<i>Talpa minor</i>	Extinct mole	-	+	+	+
Chiroptera					
<i>Plecotus auritus</i>	Common long-eared bat	-	-	+	-
<i>Myotis mystacinus</i>	Whiskered bat	-	-	+	-
<i>Myotis bechsteini</i>	Bechstein's bat	-	-	+	-
Primates					
<i>Homo cf heidelbergensis</i>	Hominid	*	*	+	*
Carnivora					
<i>Canis lupus mosbachensis</i>	Wolf	-	+	+	+
<i>Ursus deningeri</i>	Extinct bear	-	-	+	+
<i>Mustela erminea</i>	Stoat	-	+	+	+
<i>Mustela lutreola</i>	European mink	-	+	+	-
<i>Mustela nivalis</i>	Weasel	-	-	+	-
<i>Meles sp</i>	Badger	-	-	+	-
<i>Crocuta crocuta</i>	Spotted hyaena	-	-	+	-
<i>Felis cf F silvestris</i>	Wild cat	-	+	+	-
<i>Panthera leo</i>	Lion	-	-	+	-
Proboscidea					
Elephantidae gen et sp indet	Elephant	-	+	+	-
Perissodactyla					
<i>Equus ferus</i>	Horse	-	+	-	+
<i>Stephanorhinus hundsheimensis</i>	Extinct rhinoceros	-	+	+	+
Artiodactyla					
<i>Cervus elaphus</i>	Red deer	+	+	+	+
<i>Dama dama</i>	Fallow deer	-	-	+	-
<i>Capreolus capreolus</i>	Roe deer	-	+	+	-
<i>Megaloceros datonkinsi</i>	Extinct giant deer	-	+	-	-
<i>Megaloceros cf verticornis</i>	Extinct giant deer	-	+	+	-
<i>Bison priscus</i>	Bison	-	-	+	+
Caprinae	Ovicaprid	-	-	-	+
Rodentia					
<i>Sciurus sp</i>	Squirrel	-	-	+	-
<i>Myopus schisticolor</i>	Wood lemming	-	-	+	-
<i>Lemmus lemmus</i>	Norway lemming	-	-	-	+
<i>Clethrionomys glareolus</i>	Bank vole	-	+	+	+
<i>Clethrionomys rufocanus</i>	Grey-sided vole	-	-	-	+
<i>Pliomys episcopalis</i>	Extinct vole	-	+	+	+
<i>Arvicola terrestris cantiana</i>	Water vole	-	+	+	+
<i>Microtus (Terricola)</i>					
<i>cf M. (T) subterraneus</i>	Pine vole	+	+	+	+
<i>Microtus agrestis</i>	Field vole	-	+	+	+
<i>Microtus arvalis</i>	Common vole	-	-	+	+
<i>Microtus gregalis</i>					
(<i>gregaloides</i> morph)		-	-	-	+
<i>Microtus oeconomus</i>	Northern vole	-	-	+	+
<i>Castor fiber</i>	Beaver	-	-	+	+
<i>Muscardinus avellanarius</i>	Hazel dormouse	-	-	+	-
<i>Eliomys quercinus</i>	Garden dormouse	-	-	+	-
<i>Sicista cf S. betulina</i>	Birch mouse	-	-	+	+
<i>Apodemus maastrichtensis</i>	Extinct mouse	+	+	+	+
<i>Apodemus sylvaticus</i>	Wood mouse	-	+	+	+
Lagomorpha					
<i>Lepus timidus</i>	Mountain hare	-	+	+	-
<i>Oryctolagus cf O. cuniculus</i>	Rabbit	-	-	+	-

(*Homo cf heidelbergensis* * inferred from cultural remains)

is strikingly similar to faunas of late 'Cromerian Complex' age from Westbury-sub-Mendip and Ostend (Currant 1989). Biostratigraphically important species recovered from the Slindon Formation include the extinct rhinoceros (*Stephanorhinus hundsheimensis*), an extinct cave bear (*Ursus deningeri*), and a number of extinct small mammals, including two species of shrew (*Sorex savini* and *Sorex runtonensis*) and an extinct vole (*Pliomys episcopalis*), which are all known to have become extinct before the Hoxnian Interglacial (Roberts and Parfitt Chapter 5.9)

The Pleistocene sequence at AEP is particularly significant as it is one of a few Middle Pleistocene deposits where a series of distinct faunal assemblages representing a relatively short temporal range have been recovered. The deposition and subsequent burial of the vertebrate remains under low energy sedimentary conditions have occasionally preserved associated faunal remains, including small vertebrate accumulations deposited by predators and associated skeletal remains of large mammals.

The description of the vertebrate remains has been divided into a number of sections which deal with various aspects of the faunal analysis. The taxonomic description of the vertebrate remains is divided into the different taxonomic groups. This is followed by a section on the taphonomy and palaeoecology of the vertebrate assemblages and a discussion of the biostratigraphic implications of the vertebrates.

Previous work

The first Pleistocene vertebrate remains from AEP were collected by Shephard-Thorn and co-workers in 1975 (Shephard-Thorn and Kellaway 1978). This assemblage was studied by Bishop (1976) whose unpublished report was subsequently incorporated by Woodcock (1981) into his description of the AEP deposits. The material came from three horizons which can be related to the current stratigraphic sequence. Small mammal remains were recovered from the basal brickearth (bed b) equivalent to Unit 6, a transitional ferruginous layer (bed b/c) equivalent to Unit 5a, and the top 100mm of a 'fine white silty sand' which is probably equivalent to the palaeosol horizon, Unit 4c. The transitional ferruginous layer produced the most abundant remains which were identified by Bishop as water vole (*Arvicola cantiana*) and a small vole identified as possibly the common vole (*Microtus cf arvalis*). In addition, a complete right and left inominate and an associated vertebra of a bovid were excavated from bed c. Bishop concluded that the fauna indicated 'an age between the Hoxnian and Ipswichian, and reflects a surrounding habitat of open vegetation, possibly a river floodplain' (Bishop 1976, 3). This collection is now housed with the palaeontology collection of the British Geological Survey, Keyworth (accession numbers Z.t.1688-1703) where it was re-examined by the author.

Stratigraphic provenance

Before discussing the collecting methods employed during the recent excavations, it is necessary to establish the stratigraphic provenance of the vertebrate remains. The deposits at AEP represent a complex depositional sequence spanning a series of climatic oscillations. Faunal remains were recovered from a number of lithostratigraphic units within the sequence, although they are only abundant at the base of the terrestrial sequence. The remaining undecalcified deposits, which include the marine sequence, chalky gravels, and brickearths, are poorly fossiliferous.

The variation in the concentration of vertebrate remains from the undecalcified deposits can be illustrated by comparing the number of identifiable bone fragments recovered by screen washing samples of the various fossiliferous horizons. Figure 92 shows the numbers of identifiable bone fragments per kilogram of unprocessed sediment. The diagram shows the relative abundance of faunal remains within the basal terrestrial deposits, in contrast to the paucity of vertebrates in the marine deposits and chalky gravels.

Preservation of the faunal remains across the site is determined by the extent of post-depositional decalcification of the deposits. Undecalcified deposits are preserved in a region immediately to the south of the palaeo-cliff-line, where the archaeological deposits are covered to a considerable depth by chalky gravels which were deposited in a series of lobes along the base of the Downs. As these deposits shallow from the cliff, the underlying deposits become increasingly decalcified as the solution pipes coalesce to form extensive decalcified areas. Bones and other calcareous fossils are rarely recovered from the decalcified deposits, although the remnants of bones were recorded as stains during the excavation of the decalcified areas of the quarry (Chapter 6.2).

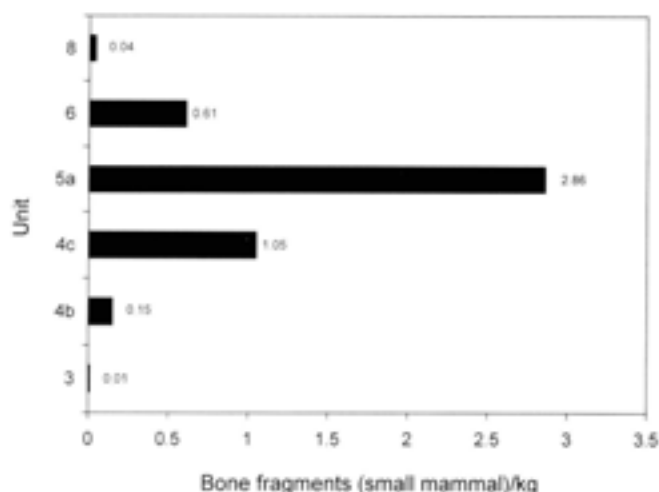


Fig 92 Number of identifiable bone fragments per kg of unprocessed sediment, by unit

The extent of the conformable stratigraphic sequence is shown in Fig 22. The combination of sediment decalcification and reworking of the deposits has confined the fossiliferous deposits to a narrow band approximately 200–250m wide along the base of the buried cliff-line.

Summary of the fossiliferous deposits

(cf Tables 9a, 9b)

The vertebrate fauna from the marine sequence, the Slindon Formation, is composed overwhelmingly of marine fish. Terrestrial vertebrates occur very rarely and the few identifiable mammal fragments have been recovered from chalky beach gravels and cliff collapse deposits within the Slindon Sands. The scarcity of vertebrate remains in the marine deposits does not appear to be an artefact of selective collecting as these deposits were extensively exposed and screened during the excavations.

Towards the top of the marine sequence the sands are replaced by laminated silts and clays which accumulated in a facies of a quiet coastal lagoon (Chapter 2). These tidally flooded mudflat deposits underwent episodes of drying out and sediment ripening. As with the marine deposits, the fauna from these deposits is dominated by fish, although there is an increasing terrestrial component including amphibians, reptiles (Holman Chapter 3.5), and a number of mammal species (Table 26). The majority of the large mammal remains from this part of the sequence were recovered from two artefact and bone concentrations from Quarry 1/A and Quarry 2 GTP 17. These represent single episodes of knapping and butchery respectively, which were buried under low energy sedimentary conditions which characterise these deposits.

These laminated intertidal deposits are capped by a palaeosol horizon which is the main fossil and artefact bearing deposit at AEP. A feature of the vertebrate fauna from this horizon is the diversity of species represented (Table 26) which indicate a range of habitats including woodland, woodland edge and open grassland conditions. The presence of aquatic vertebrates in the palaeosol horizon can be explained by periodic inundations of the land surface; alternatively they may have been transported from a nearby body of water by predators. A comparison of the faunas from Quarry 1 and Quarry 2 shows that semi-aquatic species such as mink and beaver and a range of water-birds are present in Quarry 1 but absent or poorly represented in the fauna from Quarry 2. This disjunct distribution of some of the vertebrate taxa appears to reflect differences in local microhabitat between the two areas (Roberts Chapter 2.7). The presence of a localised spring-fed pond with a series of temporary drainage channels in Quarry 1 may account for the presence of semi-aquatic species in this area. Micromorphological analysis of Unit 4c indicates that the palaeosol developed over a number of decades, which indicates that

the fauna represents an associated group that accumulated over a relatively short period of time within the interglacial represented by the Slindon Formation.

Although areas of primary context and *in situ* knapping debris have been excavated from the palaeosol horizon, there are no concentrated accumulations of butchered bone such as those recorded from the intertidal sequence. This is hardly surprising as any butchered carcass would have been rapidly scavenged and dispersed by carnivores. The taphonomy of the vertebrate remains from the palaeosol is complex and is discussed in more detail in Chapter 4.3.

Immediately overlying the palaeosol horizon and extending across most of the quarry is a thin iron/manganese pan, Unit 5a, which is interpreted as floodplain accretion which developed into a shallow lake or marsh. Large mammals are less abundant in this deposit compared with the underlying palaeosol, although smaller vertebrates are often abundant. This faunal assemblage, together with the more diverse palaeosol fauna, indicate interglacial conditions. One problem encountered in collecting vertebrate remains from this deposit was the difficulty in recognising the stratigraphic provenance of fossils in the ironpan from those in the top of the underlying palaeosol. This was usually resolved by careful excavation and recording of the faunal remains at this stratigraphic interface.

Despite the extensive exposures of undecalcified brickearth and gravels which were searched for vertebrate remains, these predominantly cold stage deposits have produced a sparse vertebrate fauna (Table 26). The upper part of the gravel sequence is decalcified and vertebrate remains are not preserved. The majority of the vertebrate remains which can be attributed to the chalky gravels were collected from quarry spoil dumps and only a small sample (mainly from the beach section GTP 25) were recovered *in situ* and can be related to the complex stratigraphy of this set of deposits (Table 9b).

Collecting methods

The collecting methods and site recording methods employed during the excavations at AEP were initially developed during the excavation of Q1/A in 1985. This was the first large-scale excavation of a fossiliferous area of the site and it produced a substantial quantity of faunal remains associated with flint debitage. During subsequent seasons, vertebrate remains were recovered by a combination of controlled excavation, surface collection and bulk sieving specifically developed to recover microvertebrate remains.

Recovery of vertebrate material from the site posed a number of problems mainly due to the fragile nature of the bones. Large mammal bones were often extremely fragile when first uncovered and the majority of the faunal remains suffered from some degree of crushing and distortion caused by sediment compaction

and microfaulting. The removal of these crushed bones from the sediment and subsequent preparation was often a difficult and time consuming process.

Due to the fragile nature and poor preservation of most of the faunal remains, special care was taken during their excavation and preparation. The majority of the bone fragments were lifted in blocks of sediment which provided a support for the bone fragments. Larger bones were lifted with plaster of paris or expanded polyurethane foam jackets to provide additional support (Carreck and Adams 1969). The unconsolidated nature of the deposits made this method particularly successful in recovering large vertebrate bones intact with minimal excavator damage. The bones were subsequently removed from the sediment blocks and cleaned by careful excavation using wooden tools and fine brushes to minimise damage to the bone surface. Heavily fractured specimens were strengthened with a polyvinyl acetate consolidant (Alvar 1570) dissolved in industrial methylated spirit and injected through a fine hypodermic needle into cracks penetrating the bone surface. Applying the consolidant directly to the surface of the bone was avoided as the consolidant formed a thin film which often obscured surface alterations such as cutmarks. Before the consolidant solution was applied, areas of surface alteration were replicated using a low viscosity dental casting rubber (polyorganosiloxane) which produced high precision replicas of the alteration for microscopic examination.

The majority of the large vertebrate bones were recovered by controlled excavation of archaeological areas. The faunal remains from these areas were numbered sequentially and the position of each find within the trench was recorded from the site grid. For the main excavation areas (eg Q1/A, GTP 17) the absolute height of each bone fragment above Ordnance Datum was also recorded and this has enabled a series of three-dimensional plots of bone distribution to be produced. Other attributes recorded during the excavation were the stratigraphic location, long axis orientation, and a description of the condition of the fragment. This information was entered on to a standard faunal record sheet by the excavator.

Additional material was also recovered during systematic prospecting of the quarry and through the examination of sections cut during sand and gravel extraction. The locations of these specimens were recorded on a series of large-scale plans of the quarry. Unstratified faunal remains recovered from quarry spoil dumps and the talus slopes of eroded sections were also routinely kept. Although the stratigraphic provenance of these finds was often uncertain, it was generally possible to allocate them to an approximate stratigraphic horizon based on bone preservation type or remnants of sediment adhering to the bone.

The numbers of large vertebrate bones recovered from excavated areas and surface collecting are listed in Table 26.

Although manual excavation was used to collect the larger vertebrate remains, microvertebrates were generally poorly represented in the excavated assemblage. Microvertebrates generally occurred as isolated fossils within the sediment, although clusters of small bones were occasionally recognised during excavation. These accumulations were lifted in blocks of sediment for microexcavation in the laboratory. The small vertebrate assemblage was largely collected through bulk sieving of sediment samples using equipment and procedures developed by Ward (1981; 1984) for processing clays and silts. During the 1985 excavation of Q1/A, an attempt was made to record and recover small vertebrates bones which were exposed during manual excavation; however this process caused considerable damage to the fragile bones and teeth (Currant 1986, 229). From 1986, bulk sieving was employed as the main method for recovering isolated small mammal and other small vertebrate remains.

The primary aim of the bulk sieving programme was to sample the vertebrate faunas from the complete fossiliferous sequence at the site and to examine changes in faunal composition through this sequence. After the initial set of samples was processed, it became obvious that although most of the undecalcified deposits contained vertebrate remains they were generally present at extremely low concentrations. It was therefore necessary to collect and wet sieve a large quantity of sediment to provide sufficient samples to allow comparisons between the faunal groups.

One of the advantages of excavating in a working quarry is the potential to examine and sample the stratigraphy in temporary exposures as the quarry face is worked back. At AEP, it was possible to trace individual lithostratigraphic horizons across both quarries and collect a series of samples to examine variations in the spatial distribution of microvertebrates and other biological remains. The bulk samples were largely collected from sections or areas where a sequence of deposits was exposed. The main sample localities are shown in Figure 4.

Bulk samples were collected by stratigraphic unit; in the case of deposits over 0.1m thick, the unit was divided into 0.1m spits and samples were taken following natural bedding planes within the deposit. In addition to the samples collected specifically to recover microvertebrates, samples were routinely collected from excavated sites to monitor the recovery of flint debitage and faunal remains.

The size of individual samples varied from a few kilograms to over 500kg for samples of the Slindon Sand which contained sparse vertebrate remains. After the matrix was collected, each bag of sediment was labelled with the relevant information, including sample location and stratigraphic horizon. The sample was then allocated a bulk sample number and transported to covered tarpaulin sheets where the sediment was allowed to dry. The matrix was sieved in a semi-automatic clay sieving machine which was specifically

developed to sieve the type of cohesive clays found at Boxgrove (Ward 1981). The sieving machine consists of a large polythene tank containing two large stacked sieves and a lid assembly containing a rotary and two oscillating water sprinklers. The matrix, which is loaded on to the top sieve, is gently disaggregated by jets of water from the sprinkler system which travel across the sieves washing the sand and clay fractions through the sieve meshes.

An important consideration during the early stage of the bulk sieving programme was the choice of the optimum mesh diameter for the fine sieve. Ideally, the smallest mesh diameter used should be determined by the minimum size of the majority of the identifiable bone fragments in the sediment. If too large a mesh is employed identifiable bones will be lost and this will bias the species composition of the fauna; alternatively if too fine a mesh is employed then sorting the samples may be prohibitively time consuming. The effect of mesh diameter on the recovery of microvertebrates was examined by sieving a 'bone rich' residue through a stack of sieves with meshes ranging from 10mm to 500µm in diameter. The number of identifiable bone fragments and teeth were then counted for each size fraction.

The results of this experiment show that a substantial proportion of identifiable microvertebrate remains passed through the 1mm sieve mesh, including over 92% of the fish bones and 97% of the soricid and murid teeth. A fine mesh size of 500µm was therefore selected.

The rate at which sediment was disaggregated and washed through the sieve mesh depended to a large extent on the amount of clay in the deposit; usually it was possible to process two buckets of sediment (30 litres) in thirty minutes. The methods employed at Boxgrove were probably more time consuming than some other sieving techniques but had a number of advantages over other such techniques employed on archaeological sites. The main advantage of this system is that it does not rely on manual agitation to disaggregate the sediment, a process which invariably damages fragile remains. This was a particularly important consideration bearing in mind the exceptionally fragile nature of most of the faunal material at Boxgrove. Breakage was further reduced as the coarse components were trapped by the top (10mm) mesh, while the fragile microvertebrate remains were washed into the lowermost sieve. As the system is semi-automatic, the sieving operator was able to process the residues from previous samples while further batches were being sieved. In this way, one or two people were able to run the sampling and sieving programme.

Initial processing of the samples was also undertaken at the site. The residue from the 10mm sieve mesh was sorted for artefacts, erratics and faunal remains at this stage and the natural clasts were discarded. The fine residue from the 500µm sieve was transferred from the clay sieving machine into a tray and allowed to dry.

Later, the dry residue was graded through a nest of sieves and each size fraction was bagged separately and labelled with the relevant sample information.

As the majority of the deposits sampled from the marine and base of the terrestrial sequence lacked a significant coarse component, the sieve residues were relatively easy to sort. These sediments produced a few grams of fine residue which was graded through a stack of sieves, the fraction under 1mm being sorted under a low power binocular microscope. A particular problem was encountered in sorting the fine residues from the Chalk Pellet Beds (Unit 8) and the Brickearth Beds (Unit 6), as the fine residue from these samples consisted of a quantity of chalk debris and a very low proportion of vertebrate remains.

After the vertebrate remains had been extracted from the sieve residues, they were divided into fish, amphibians, reptiles, birds, large and small mammals, and then passed to the relevant specialist for detailed analysis.

Because of the quantity of bulk samples processed, the choice of samples sorted to 500µm was selective. A sub-sample of the bulk samples was totally sorted to recover the complete microfaunal assemblage; this set of samples was used in the taphonomic analysis and studies of faunal composition of the small vertebrate assemblage. The remaining residues were partially sorted to 2mm to recover biological remains, erratics and flint debitage. The notation used to describe a bulk sample or the finds from a sample follow a standard format: for example, BS86-100 Q1/B U4c refers to a sorted bulk sample processed in 1986 from Quarry 1, Area B, Unit 4c.

The bone fragments from site excavations and from the bulk samples were recorded on a standard bone recording form which was specifically designed to allow input of data into a computerised database. A detailed description of the recording method used during the analysis of the bone assemblage and a discussion of the criteria used to identify the vertebrate remains are outlined in the systematic descriptions of the fauna. Additional details of the bone recording system (Parfitt 1986) are kept with the faunal archive which is housed with the vertebrate faunal assemblage in the palaeontology collections of the Natural History Museum (London).

3.2 Foraminifera and Ostracoda

J E Whittaker

Introduction

Foraminifera and ostracods were examined from 53 samples collected in Quarry 2, Boxgrove (Fig 4), covering the entire exposed section GTP 13 of the Slindon Sand and Slindon Silt Members (Figs 20, 44, 45a-b, 46). Initially, 42 samples were collected, for the most part at 100mm intervals (numbered from 0-100mm at

the top down to 4400–4500mm, then the base of the exposed section). Subsequently, a further 11 samples were collected to fill the gaps of the 'Storm Raft' sequence (samples 27–29) and the sediments immediately above the wave cut platform (19–26). The position of these samples within section GTP 13 is shown in Figure 93.

Methods

For each sample, approximately 200–300g of sediment was washed in hot water through a 75µm sieve (using a deflocculent where necessary). The dried residue was then picked for foraminifera and ostracods. Each sample was picked for about 1–2 hours in order to obtain a representative population, rather than the first 200/300 specimens at random, as statistical studies were not to be attempted. However, some notes were kept on the approximate abundance of individual species for future reference. About 29 species of ostracods and over 30 species of foraminifera were identified from this Boxgrove section. Their distribution is given in Tables 27 and 28.

We are now fortunate that the taxonomy and distribution of Recent British ostracods and foraminifera are well known thanks to the work of Athersuch *et al* (1989), and Haynes (1973) and Murray (1979; 1991), respectively. It is therefore possible to compare with some authority the Boxgrove assemblages with the present day faunas of the south coast and elsewhere.

A brief comparison is also made between two adjacent Quaternary deposits whose microfaunas have been described in detail: the high level Steyne Wood Clay, Bembridge (Fig 81) correlated by Preece *et al* (1990) with the Slindon Sands because of identical elevation and similarities in the coccolith floras, and the channel infillings on the foreshore at Earnley, West Sussex (Fig 8), directly to the south of Boxgrove, described by West *et al* (1984).

Slindon Sand Member

The Slindon Sand Member forms the majority of section GTP 13 (Fig 93). The sands are known to have been deposited in the vicinity of a high chalk cliff (Collcutt Chapter 2.3; Lewis and Roberts Chapter 2.2) and indeed the large amount of reworked Cretaceous foraminifera and ostracods in all samples is ample evidence of active erosion throughout the deposition of the sequence. Three marine cycles are recognised (Fig 93). The basal beds directly on top of the wave-cut platform and the early part of Marine Cycle 1 show a low diversity marine foraminiferal fauna, with, apart from a single valve, a complete absence of Ostracoda. These appear to be high energy deposits and it would be natural that flat and generally more fragile ostracod valves would be more selectively destroyed by winnowing than the globular, more robust, foraminiferal tests. There follows a general

increase in diversity in both groups, apart from a short fall-off particularly of ostracods in the 'Storm Raft' sequence (cliff collapse), with a maximum of approximately 20 species each per sample attained in Marine Cycle 2. This seems to represent generally quieter (but entirely marine) conditions as also evidenced by the large numbers of fragile and often very small microfossils preserved. Furthermore, the ostracods contain both adults and a full range of instars (with some complete carapaces) which is usually indicative of a more protected environment and limited sediment transport. The end of Marine Cycle 3 sees a marked reduction in diversity and total disappearance of ostracods; this may partly be due to ecological changes as well as to an increase in winnowing.

The ostracods of the Slindon Sand Member (Table 27) are made up of marine littoral phytal species (dominated by *Hemicythere villosa* and *Hemicytherura clathrata*) and inner shelf/sublittoral benthic species (many of which favour sandy substrates), such as *Cytheropteron nodosum*, *C. latissimum*, *Urocythereis britannica* and *Robertsonites tuberculatus*. Other less common species are listed in Table 27 with their distribution. Leptocytherids are generally rare. True brackish species (eg *Cyprideis torosa*), although present in many samples, occur as a few, often broken, valves. Freshwater ostracods (*Candona* and *Ilyocypris*) are present only as a single valve each in five samples.

The foraminifera (Table 28) are mainly dominated by marine phytal species which cling to seaweeds in the littoral/sublittoral zone. The most abundant are *Ammonia batavus*, *A. falsobeccarii*, *E. clavatum/selseyense* (referred to in Table 28 as *E. excavatum* gr), *Elphidium crispum*, *Nonion depressulus* and *Gibicides lobatulus*. All are members of the Rotaliida, neither a single miliolid nor an agglutinating foraminifer was ever found. Moreover, no exclusively brackish/salt marsh species was present in the Slindon Sands, though several have wide salinity tolerances when found in large estuaries and lagoons at the present day.

Both assemblages are virtually identical to Recent English south coast shallow marine faunas. However, there are some significant differences. For example, amongst the ostracods, species such as *Loxocoelha rhomboidea*, *Heterocythereis albomaculata*, *Aurila* spp, the genus *Xestoleberis* and the Paradoxostomatidae, virtually ubiquitous in all Recent phytal collections, are entirely absent. Therefore, some selective destruction of a component of the biocoenosis may have occurred, even in the sediments of Marine Cycle 2.

Of the species present in the Slindon Sands several, however, are not found in the Recent of British waters, or warrant further comment. Perhaps the most abundant foraminifer throughout the sequence is a species (Fig 94d) transitional between *Elphidium clavatum* (typified by simple sutures and a single umbilical boss surrounded by an opaque band), today found only in arctic climes and considered, when found in interglacials, to represent cold conditions (Haynes personal

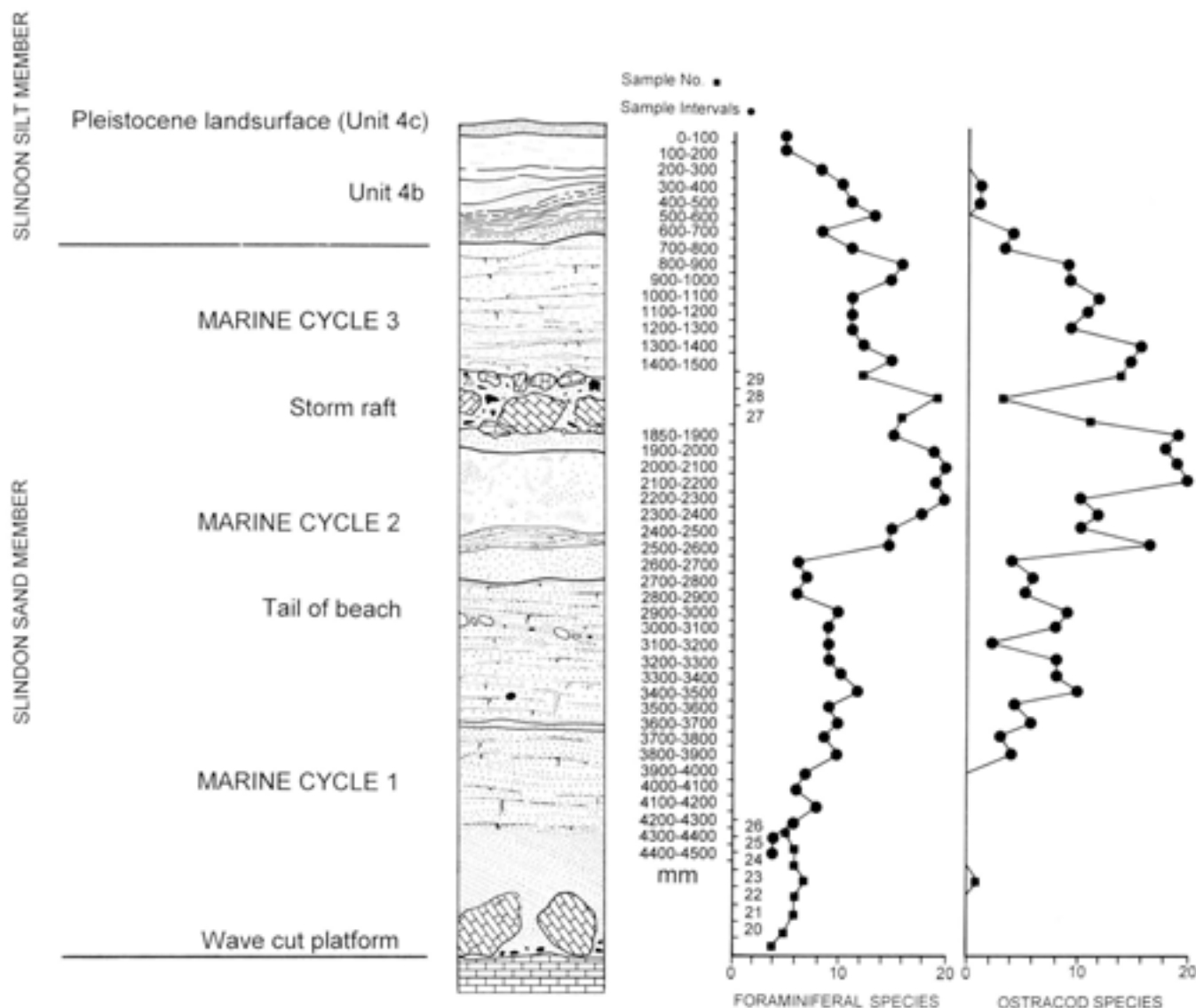


Fig 93 Quarry 2 GTP 13: stratigraphy, location of samples, and foraminiferal and ostracod species diversity

communication) and *E. selseyense* (typified by irregular fissures on sutures and a wide umbilicus, both filled with granules), the member of the *E. excavatum* group common today in southern England. This could signify either conditions slightly colder than today, or be an indication of the antiquity of the Boxgrove deposit, from a time in the Quaternary when these 'species' were evolving. The occurrence of two other foraminifera, *Ammonia falsobeccarii* and '*Rosalina parisiensis*' merits attention. The former is ubiquitous in Section GTP 13 and is a Lusitanian species first described from the Bay of Biscay (Rouvilleis 1974) and at its northernmost limit at the present day in the Western Approaches and off south-west Ireland; I have never seen it in Recent collections from the south coast. It is shown in Figure 94a, b, in comparison with *Ammonia batavus* (Fig 94c) from the same sample. *A. falsobeccarii* occurs extensively in interglacials and, because of its southern aspect, is considered to be an indicator of slightly warmer conditions (Haynes personal communication). '*R. parisiensis*' (Fig 94f),

though rarer, is found from Late Pliocene (St Erth) to Ipswichian times, but is now believed to be extinct. It needs a new name and, with related species, forms the subject of an ongoing revision (Haynes and Whittaker in prep); it is also considered to represent warmer conditions and, significantly, was found by Funnell (in West *et al* 1984) in the Earnley interglacial. Of the others, Murray (1979, 48) in his book on British nearshore foraminifera, states that *Elphidium crispum* (Fig 94e) is '... of southern origin and living close to its northern limit of distribution'.

The publication of Horne *et al* (1990) is significant in that it was the first attempt to review and redescribe those Quaternary ostracods that appear to have potential as indicators of climatic conditions warmer than those existing in north-west Europe at present. Species (mainly leptocytherids) were described from Earnley (see below), Selsey, the Burtle Beds, the Nar Valley Clays, and certain North Sea boreholes. Unfortunately, only one (*Callistocythere curryi*, Horne *et al* 1990) and only a single valve at that (Table 27),

Table 27 Distribution of ostracods in the Slindon Sand and Slindon Silt members at GTP 13. Species are arranged alphabetically; samples are arranged from bottom (19) to top (0-100mm), left to right

	SLINDON SAND MEMBER						SLINDON SILT MEMBER	
	MARINE CYCLE 1		MARINE CYCLE 2		MARINE CYCLE 3			
	19	20	21	22	23	24	25	26
<i>Beudanticythere loweri</i> Huxel								
<i>Callistocythere canyi</i> Hume et al								
<i>Callistocythere lateralis</i> (G.W. Müller)								
<i>Cardinea</i> sp								
<i>Cypridopsis torosa</i> (Jones)								
<i>Cythere lutea</i> (O.F. Müller)								
<i>Cythereopora lativittata</i> (Norman)								
<i>Cythereopora ovalis</i> Brady								
<i>Elphidium pacifica</i> (Brady)								
<i>Encythere argus</i> (Sars)								
<i>Hemicythere rubida</i> (Brady)								
<i>Hemicythere villosa</i> (Sars)								
<i>Hemicytherea cellulosa</i> (Norman)								
<i>Hemicytherea elatiora</i> (Sars)								
<i>Hirsutipecten viridis</i> (O.F. Müller)								
<i>Isoocypris</i> sp								
<i>Leptocythere pellicula</i> (Baird)								
<i>Leptocythere psammophila</i> Goullaine								
<i>Neocythereis subulata</i> (Brady)								
<i>Paracytherea cancyforans</i> (Brady)								
<i>Paracythere elongata</i> (Brady)								
<i>Robertsostrea tuberculata</i> (Sars)								
<i>Semicytherea nigrescens</i> (Baird)								
<i>Semicytherea undata</i> (Sars)								
<i>Semicytherea</i> sp								
<i>Semicytherea</i> sp. nov. (cf. <i>cella</i> (Sars))								
<i>Uvocythereis britannica</i> Ashcroft								

Table 28 Distribution of foraminifera in the Slindon Sand and Slindon Silt members at GTP 13. Species are arranged alphabetically; samples are arranged from bottom (19) to top (0-100mm), left to right

SLINDON SAND MEMBER		SLINDON SILT MEMBER		
		MARINE CYCLE 1	MARINE CYCLE 2	MARINE CYCLE 3
	19			
	20			
	21			
	22			
	23			
	24			
	25			
	26			
	27			
	28			
	29			
	30			
	31			
	32			
	33			
	34			
	35			
	36			
	37			
	38			
	39			
	40			
	41			
	42			
	43			
	44			
	45			
	46			
	47			
	48			
	49			
	50			
	51			
	52			
	53			
	54			
	55			
	56			
	57			
	58			
	59			
	60			
	61			
	62			
	63			
	64			
	65			
	66			
	67			
	68			
	69			
	70			
	71			
	72			
	73			
	74			
	75			
	76			
	77			
	78			
	79			
	80			
	81			
	82			
	83			
	84			
	85			
	86			
	87			
	88			
	89			
	90			
	91			
	92			
	93			
	94			
	95			
	96			
	97			
	98			
	99			
	100			

- Ammonia batavica* (Heller)
- Ammonia fabaeformis* (Roosillius)
- Ammonia perforata* (Heron-Allea & Earland)
- Buccella baccata* sp
- Buccella frigida* (Cushman)
- Cassidulin* sp
- Chicoides lobatus* (Walker & Jacob)
- Ephedusa crispus* (Linne)
- Ephedusa excavatum* (Toupin)
- Ephedusa parvula* van Voorthuyzen
- Ephedusa incertae* (Williamson)
- Ephedusa maculata* (Fichtl & Mull)
- Ephedusa marginicostata* (Cushman)
- Ephedusa williamsoni* Hayes
- Gardineria praeformis* (Heron-Allea & Earland)
- Globobulimina mellei* (Wright)
- Lagena* sp
- Nonion aperticostatum* (Walker & Jacob)
- Orbulina* sp
- Paralaminella constricta* Williamson
- Polysarculina*
- Roosillius parvicostatus* d'Ombeys
- Trochammina angulata* (Williamson)

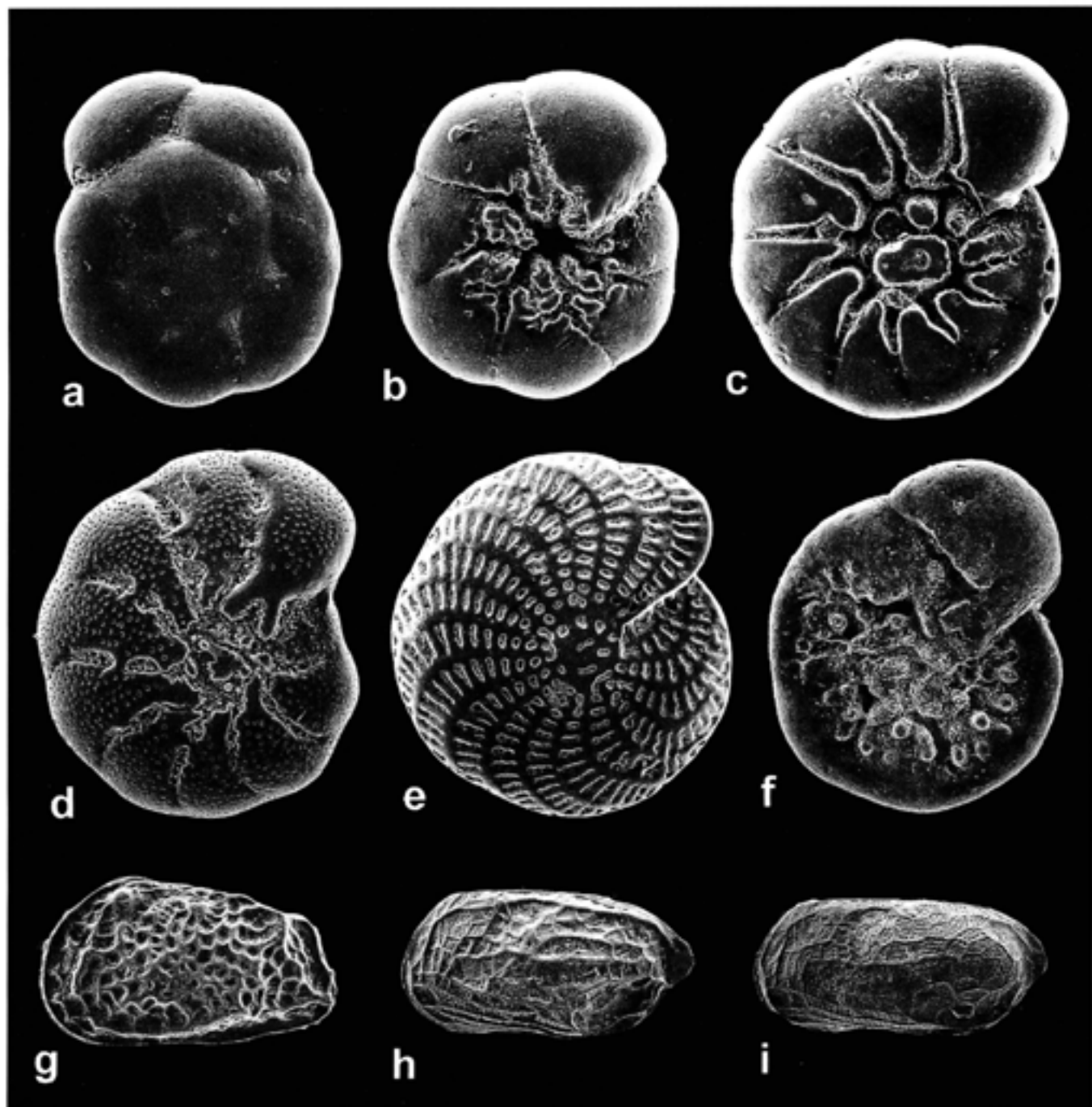


Fig 94 Some significant foraminifera (a-f) and ostracods (g-i) from the Slindon Sand Member, Quarry 2, Section GTP 13, Boxgrove (see discussion in text). a-b) *Ammonia falsobeccarii* (Rouvilleis), spiral and umbilical views, sample 2600-2700mm, $\times 155$; c) *Ammonia batavus* (Hofker), umbilical view, sample 2600-2700 mm, $\times 115$; d) *Elphidium excavatum* gr (transitional specimen between *E. clavatum* Cushman and *E. selseyense* (Heron-Allen and Earland)), side view, sample 2400-2500mm, $\times 165$; e) *Elphidium crispum* (Linné), side view, sample 3000-3100mm, $\times 65$; f) '*Rosalina parisiensis*' d'Orbigny, umbilical view, sample 29, $\times 145$; g) *Baffinicythere howei* Hazel, female left valve, sample 2000-2100mm, $\times 50$; h-i) *Semicytherura* sp nov (cf *S. sella* (Sars)), female and male left valves, samples 2200-2300mm and 2000-2100mm, respectively, both $\times 115$

was found at Boxgrove. The Leptocytheridae are rare throughout the sequence and otherwise identical to Recent shallow marine species found along the Sussex coast. A new species of *Semicytherura*, with affinities to *S. sella* (and to some extent the Lusitanian species *S. arcachonensis*; see Horne *et al* 1990) is illustrated in Figure 94h, i. As far as I am aware, it has not been

reported elsewhere and if it is indeed a precursor of *S. sella* could be a potential indicator of the antiquity of the Boxgrove deposit.

If, so far, the above discourse suggests that the Boxgrove marine cycles may indicate slightly warmer climatic conditions than those prevailing today, the occurrence of *Hemicytherura clathrata* and *Baffinicythere*

howei soon confounds this. The former is probably the most common phytal ostracod in the Slindon Sand Member, but in spite of its occurrence in many Holocene (?sub-Recent) sediments, it was not found live during an extensive survey of British marine ostracods (Athersuch *et al* 1989). Its Recent distribution is therefore unclear but it is certainly common in northern waters as far south as (at least) southern Norway. The occurrence of *Baffinicythere howei* is even more striking. According to Horne and Whittaker (1983), it is a 'characteristic sublittoral marine Arctic species... extending south to about 59°N (Norwegian Province) with an approximate depth range of 20–200m'. In the fossil record, they continue, it is found in the '...Pleistocene [of the] British Isles, including the Bridlington Crag (Hoxnian) of Yorkshire (Brady, Crosskey, and Robertson 1874), and the Red Crag (pre-Ludhamian) of East Anglia. Where abundant, it may be taken to indicate cold temperate to frigid climatic conditions'. Clearly this is a conundrum, but further discussion is beyond the scope of this report. Suffice to say, in the Middle Pleistocene, the geographical range of certain species of foraminifera and ostracods may have been more widespread than today. Far more work needs to be done on this subject.

In spite of the conflicting evidence, I would conclude that the Slindon Sand Member was deposited in a temperate interglacial when climatic conditions were not unlike those prevailing today.

Slindon Silt Member

The silts have a significantly different foraminiferal fauna to the Slindon Sand Member and are totally dominated by *Elphidium williamsoni*. Apart from two single valves, ostracods are absent. Species diversity is low and it would appear that the unit represents intertidal conditions in a regressive sea, though there is still no evidence to suggest the environment was in any way estuarine or brackish. The lack of ostracods is again problematic.

A comparison of Boxgrove with Steyne Wood and Earnley

The Steyne Wood Clay (Figs 8, 81) (resting on Early Oligocene Bembridge Marls, near Bembridge, Isle of Wight) was said by Preece *et al* (1990), on the evidence of its identical elevation to Boxgrove (c 40m OD) and similarities in the coccolith floras (identified by S D Houghton) to be coeval with the Slindon Sands. Further confirmation of this correlation from the ostracods and foraminifera is, unfortunately, illusory because the facies are so different. The Steyne Wood Clay was deposited in a *brackish* (probably estuarine) intertidal flat, as evidenced by the indigenous ostracod fauna (identified by D N Penney) of *Leptocythere* spp (over 90% of the total fauna in some samples), which has virtually nothing in common with the

Boxgrove sequence. The foraminifera (identified by K L Knudsen), likewise support this interpretation, with only the large populations of *Elphidium williamsoni* in the Slindon Silt Member being remotely comparable. No further evidence to support the correlation of the two deposits can therefore be provided from ostracod and foraminiferal assemblages; neither, however, can this correlation be denied.

The interglacial deposits preserved in channels cut in the Eocene Bracklesham Beds in the foreshore, at or below OD at Earnley, Sussex (Figs 2, 8), were said by West *et al* (1984) at the time to be '...older than Ipswichian and may be late Hoxnian or late Cromerian in age'. As they occur on the same coastal plain (though some 40m lower) due south of Boxgrove, and their ostracod/foraminifera faunas have been described in some detail, it is felt some discussion is warranted. Once again, however, environmental considerations preclude a direct comparison. Earnley represents a large, high energy intertidal channel or creek, giving way to intertidal mudflats near the top of the sequence. Thanks to the collaboration of J E Robinson, I have been able to examine the Earnley ostracod faunas in detail. In all the samples examined by him (save the topmost), they are dominated by the brackish creek-living *Cyprideis torosa* (17–40% of the population). This species is rarely found at Boxgrove and usually as broken valves. What is significant about Earnley is the fact that approximately 20% of the ostracod fauna is said to be southern (often Mediterranean) species which are not found today in the Channel Coast. Unfortunately, none of these is found at Boxgrove. On the evidence of these, coupled with the complete absence of the 'cold' Boxgrove species (*Baffinicythere howei* and *Hemicytherura clathrata*), Earnley probably represents a significantly warmer interglacial period, though no direct evidence of relative age can yet be provided.

Conclusions

The foraminiferal and ostracod faunas have provided important information for reconstructing the palaeoenvironments of the Slindon Sand and Slindon Silt Members. They have been less useful in providing evidence for the age of the deposits.

The foraminifera and ostracod faunas of the Slindon Sand Member are *wholly* marine: a mixture of littoral and sublittoral/inner shelf species, many of them phytal in habitat. Marine Cycle 1 appears to have been deposited in a high energy environment. Marine Cycles 2 and 3, even allowing for the 'Storm Raft' deposit (major cliff collapse), were laid down in generally quieter conditions. The Slindon Silt Member represents very shallow intertidal deposits, though still fully marine (*contra* Macphail Chapter 2.6), at the margin of a regressive sea.

The vast majority of the microfauna are found living today along the south coast of England. The exceptions present a conflict of evidence, warmer

Lusitanian species being present in the same samples as cold northern forms. It is concluded, nonetheless, that the Boxgrove sequence was deposited in a temperate interglacial, rather similar to the present day.

Unfortunately, there are very few species that give any clue as to the antiquity of the Boxgrove sediments. Recent work on Quaternary freshwater ostracods (J E Robinson personal communication) certainly suggests the potential of this group, but the biostratigraphic value of marine ostracods and foraminifera is still unproven in the Middle and Late Pleistocene.

It has not been possible to corroborate (or refute) the correlation of the Steyne Wood Clay, Bembridge, with the Slindon Sands made by Preece *et al* (1990) because of major facies differences. Similarly, a re-examination of the ostracod fauna of the interglacial sequence at Earnley, due south of Boxgrove on the same coastal plain, have failed to provide any new direct evidence of the relative age of the two deposits. It has, however, reinforced the notion that the Earnley sequence was deposited in a different interglacial, when climatic conditions were rather warmer than those prevailing at Boxgrove.

3.3 Mollusca

R C Preece and M R Bates

Recent work at Boxgrove has concentrated on gaining a better knowledge of the molluscan fauna listed in the initial report (Bates 1986). This has entailed further sampling from the stratigraphical horizons listed below (Table 9a). The malacological importance of the Boxgrove fauna lies in the fact that it represents the only truly terrestrial assemblage known from the British early Middle Pleistocene. Knowledge of other British faunas of this age come exclusively from fluvial contexts and the terrestrial elements are strongly biased in favour of species that inhabit marshes or similar riverside environments (Meijer and Preece 1996).

Units sampled

Unit 8; chalk pellet gravels of variable thickness that interdigitate with and overlie the brickearth. They thin out from the foot of the fossil cliff.

Unit 6; the brickearth overlying the main interglacial deposits.

Unit 5b; the grey/white clay usually only 30–50mm thick, which occurs in discrete patches at the base of the brickearth.

Sub-unit LGC; a calcareous silty clay, c 20mm thick at Q2/B (Table 9b)

Unit 4d; a white silt (up to 200mm thick), laterally equivalent to Unit 4c, that is thought to reflect the presence of a spring at the base of the cliff.

Unit 4c; this is the palaeosol horizon containing abundant archaeology and faunal remains. Generally only the upper 20–30mm of Unit 4c is shelly and samples

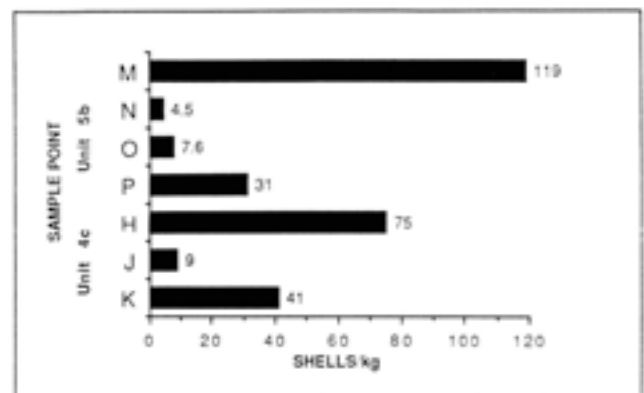


Fig 95 Absolute frequencies of shells per kg for selected samples

L, C, D, and F were taken specifically from this upper horizon (see Table 29). The majority of samples were not stratigraphically subdivided, since the whole unit is only 50–100mm thick.

Non-marine species

Sampling was undertaken at various locations across the site, from test pits as well as from the main areas of excavation (Table 29, Fig 95). The preservation of shells was usually very bad and many had suffered severe decalcification and were represented only as fragments. The number of identifiable shells recovered per 1kg sample was also very low (Table 29). Consequently, much larger samples were taken than is usual for molluscan analysis. These were air dried, broken down in water and wet sieved through a 500µm sieve. The residue was allowed to dry naturally and the samples analysed in the usual way. Neither oven drying nor hydrogen peroxide was used in the process because selected species were intended for use in amino acid analysis (Bowen and Sykes Chapter 5.6). In addition to these samples taken specifically for molluscan analysis, the residues of even larger bulk samples, screened for small vertebrates, were also examined (Samples A, N, and O plus four others; Table 29). Because of the sheer volume of sediment used, rather more vigorous hosing was required to effect disaggregation and this may have caused some damage or loss of the more delicate elements. Those samples marked with an asterisk (*) were picked by a non-specialist during the extraction of small vertebrates and the analyses are therefore not as thorough as the others. Direct comparison of these sets of samples should, therefore, be made with extreme caution. All samples prefixed BG 1988 were taken during excavations in summer 1988 and those prefixed BG were taken the previous summer. The samples from GTP 10 were taken in the summer of 1986. All the mollusc samples (except those asterisked) were collected by MRB in close association with the sampling undertaken by other specialists. Quantitative analyses were undertaken in the laboratory by RCP.

Table 29 Non-marine Mollusca from Eartham Quarry, Boxgrove

sample no	QTP 3 A(263)	QTP 10 B(440)	Q2:B C(38)	GTP 3 D(13)	Q2:B E(26)	GTP 3 F(14)	GTP 3 G(19)	Q2:B H(22)	GTP 3 J(260)	Q2:B K(39)	Q2:B L(33)	Q1:B* 89-1005	Q1:B* 4J	Q1:B* 4I	GTP 17* M(11)	GTP 17 N(68)	Q2:B LGC	GTP 13 O(101)	GTP 10 P(SMD)	Q1:B* 87-118
unit	4c	4c	4c	4c	4c	4c	4c	4c	4c	4c	4c	4c	4c	4c	5c	5c	5b	5b	5b	6
Species																				
<i>Arisia lanceolata</i> (Millet)	-	-	-	-	-	1	-	-	-	1	-	-	-	-	-	-	-	-	-	-
<i>Caryofium</i> sp	-	-	1	-	-	2	1	8	-	8	-	-	1	-	-	-	-	-	-	-
<i>Lymnaea truncatula</i> (Müller)	-	-	-	1	-	-	1	2	-	2	-	-	1	-	-	4	-	-	-	7
<i>Lymnaea peregra</i> (Müller)	-	-	-	1	-	-	-	1	-	1	-	-	-	-	16	-	-	8	-	-
<i>Succinea oblonga</i> Draparnaud	-	2	-	-	-	3	-	-	-	-	-	-	-	-	-	5	1	5	12	-
<i>Succinea/Oryzina</i>	-	-	1	1	2	6	1	5	11	4	1	-	-	-	6	6	3	1	10	-
<i>Cochlicopa</i> sp	9	-	2	2	6	17	2	5	14	5	2	-	-	-	12	11	12	5	18	1
<i>Lirigo pusilla</i> (Müller)	-	-	1	-	-	-	-	1	-	3	-	-	-	-	-	1	1	-	-	-
<i>Lirigo substriata</i> (Jeffreys)	-	-	-	-	1	1	-	-	-	5	-	-	-	-	-	4	2	-	-	-
<i>Lirigo pygmaea</i> (Draparnaud)	-	-	-	-	-	-	-	-	-	-	-	-	-	-	-	1	-	-	-	-
<i>Lirigo</i> spp	-	-	1	-	-	9	1	5	10	6	-	-	-	-	43	1	-	19	-	-
<i>Papilla muscorum</i> (L)	-	-	-	-	-	-	1	-	-	-	-	-	-	-	1	1	2	-	1	-
<i>Valvata costata</i> (Müller)	-	-	-	-	-	1	-	1	-	2	-	-	-	-	6	7	11	1	6	-
<i>Valvata excrucians</i> (Sævið)	-	-	-	-	-	-	-	-	-	-	-	-	-	-	-	-	1	-	-	-
<i>Valvata pulchella/excrucians</i>	-	-	-	-	-	5	-	3	-	2	-	-	-	-	2	2	3	-	-	-
<i>Acanthinula aculeata</i> (Müller)	-	-	-	-	-	-	-	-	-	-	-	-	-	-	7	5	2	4	-	-
<i>Spermodon lamellata</i> (Jeffreys)	-	17	-	-	-	27	-	14	-	32	4	-	-	-	16	12	41	-	3	-
<i>Panormus pygmaeus</i> (Draparnaud)	-	-	-	-	-	3	1	2	-	2	-	-	-	-	3	1	7	-	16	-
<i>Vitrinobacchium breve</i> (Férussac)	-	-	1	-	-	9	-	12	3	-	-	-	-	-	5	-	112	55	-	-
<i>Vitrea cf. crystallina</i> (Müller)	-	-	1	-	-	2	-	2	-	3	-	-	-	-	1	1	-	-	-	-
<i>Nesostrea hammonis</i> (Ström)	-	-	2	-	1	5	-	2	-	1	-	-	-	-	4	10	4	3	33	-
<i>Aegypsinella pura</i> (Alder)	-	-	1	-	-	6	-	24	-	3	-	-	-	-	13	24	9	-	15	2
<i>Aegypsinella viridula</i> (Draparnaud)	1	-	-	-	1	4	-	3	1	7	-	-	-	-	4	11	9	-	1	2
<i>Orychilus</i> sp	-	-	-	-	-	1	-	-	-	-	-	-	-	-	-	-	7	-	-	-
indeterminate Zornitidae	-	4	-	-	-	-	-	-	-	-	1	1	-	-	-	-	-	-	-	-
<i>Drepanoxys</i> / <i>Limax</i>	74	3	8	14	50	38	13	16	505	17	8	7	3	-	21	5	21	16	-	-
<i>Eucosmia fulvus</i> egg	1	-	6	-	1	4	-	11	3	10	-	-	15	6	87	11	1	83	-	-
Clausiliidae ¹	-	2	11	19	16	26	5	23	31	20	10	1	32	62	242	174	7	95	2	-
<i>Trichia hispida</i> (L)	12	+	22	+	9	82	2	85	34	25	6	-	3	15	116	24	144	57	1	-
<i>Arisia arbustorum</i> (L)	-	+	-	+	-	+	-	+	+	+	-	-	-	-	+	+	-	+	-	-
<i>Habigona lapicida</i> (L)	-	-	-	-	-	-	-	-	-	-	-	-	-	-	-	-	-	-	-	-
<i>Cepaea</i> / <i>Arisia</i>	2	-	-	-	3	10	-	7	9	3	2	-	2	15	11	10	-	3	-	-
indeterminate Helicidae	-	-	-	-	-	-	-	1	-	-	-	-	-	-	-	-	-	-	-	-
<i>Pisidium</i> spp	+	+	+	+	+	+	+	+	+	+	+	+	+	+	+	+	+	+	+	+
total	99	7	79	38	91	262	25	226	624	162	34	9	106	179	655	344	308	466	8	-
weight (kg) before sieving	87.0	10.0	3.0	2.0	10.0	4.5	3.5	3	71	4	3.5	287.5	112	137.5	5.5	77	40.5	15	41	-
nos individuals per kg	1.1	0.7	26.3	19	9.0	58.2	7.1	75.3	8.8	40.5	9.7	0.03	0.95	1.3	119.1	4.5	7.6	31.1	0.2	-

¹ At least two species including of *Cochlicopa lamellata*

+ Fragments (counts not included in total)

* Picked by non-specialist during extraction of small vertebrates

A minimum total of 30 taxa has now been recognised (Table 29). There are no significant biostratigraphical differences between the units studied, although Units 4c, 5b, and 5a were far richer than the other levels. The assemblages from the different units will therefore be discussed together. The fauna overall is fully temperate throughout, including the few shells recovered from Unit 6, although these may have been derived from earlier sediments. The fauna from the main units (4c, 5b, and 5a) suggests a moist, well-shaded land surface with the occasional pool, supporting a limited aquatic community (*Anisus leucostoma*, *Lymnaea peregra*, and *Pisidium* spp). A very worn shell of the fluvial bivalve *Pisidium moitessierianum* was recovered from the intertidal laminated clay silts of Unit 4b, 0.3m below Unit 4c, which presumably reflects an input from some local stream. Bare muddy surfaces would have been occupied by *Lymnaea truncatula* and *Succinea oblonga* and some open-country elements (*Vallonia* spp and *Pupilla muscorum*) probably lived on drier ground nearby. A denser vegetation cover is implied by most of the remaining taxa, especially by the frequency of *Aegopinella* and members of the Clausiliidae. It is hard to characterise the precise nature of this cover but dense mossy hollows with thick leaf-mould is implied by the frequency of *Spermodea lamellata* and *Acanthinula aculeata* in certain samples. These are two of the most shade-demanding snails in Britain.

There are marked differences in the proportions of various taxa in different samples. Some of this variation might result from differential preservation and the huge differences in the number of shells recovered (Fig 95), varying from <1 to 119 per kilogram, suggest that this is likely to have occurred. The ecological composition is also somewhat unusual in that *Carychium tridentatum*, which would normally be the dominant species in shaded environments, occurs as odd shells in only a few samples. It would seem that the shells of this small species have been lost during the partial decalcification. Slug plates (*Deroceras/Limax*), on the other hand, are made of calcite and are the most durable elements in terrestrial faunas, where most of the taxa possess shells composed of aragonite. Their abundance in certain samples (eg A, J, D, G, and E) would certainly suggest that differential preservation has occurred (Fig 96). While this clearly hampers interpretation, it cannot explain all the differences between samples, some of which still contain extremely delicate shells such as *Vitrinobrachium* (Fig 97). It seems likely that some of this variation is reflecting the original heterogeneity of the environment. Land snails are particularly good indicators of local environments and are especially valuable in low-energy contexts such as those represented here.

Not surprisingly, several of the taxa recovered constitute the earliest known British records. These include *Vertigo pusilla*, *V. substriata*, *Acanthinula aculeata*, and *Spermodea lamellata*. Although there are much earlier continental records for the first three species,

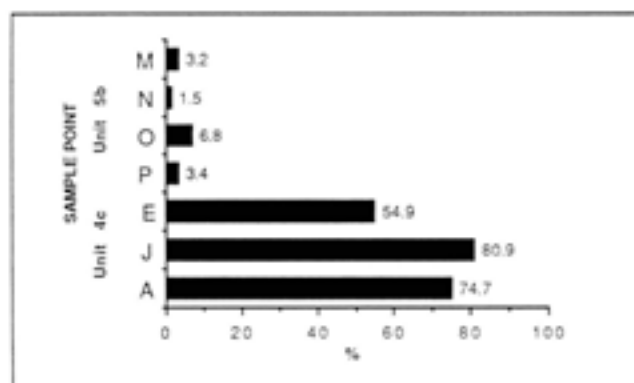


Fig 96 Percentage of slug plates for selected samples

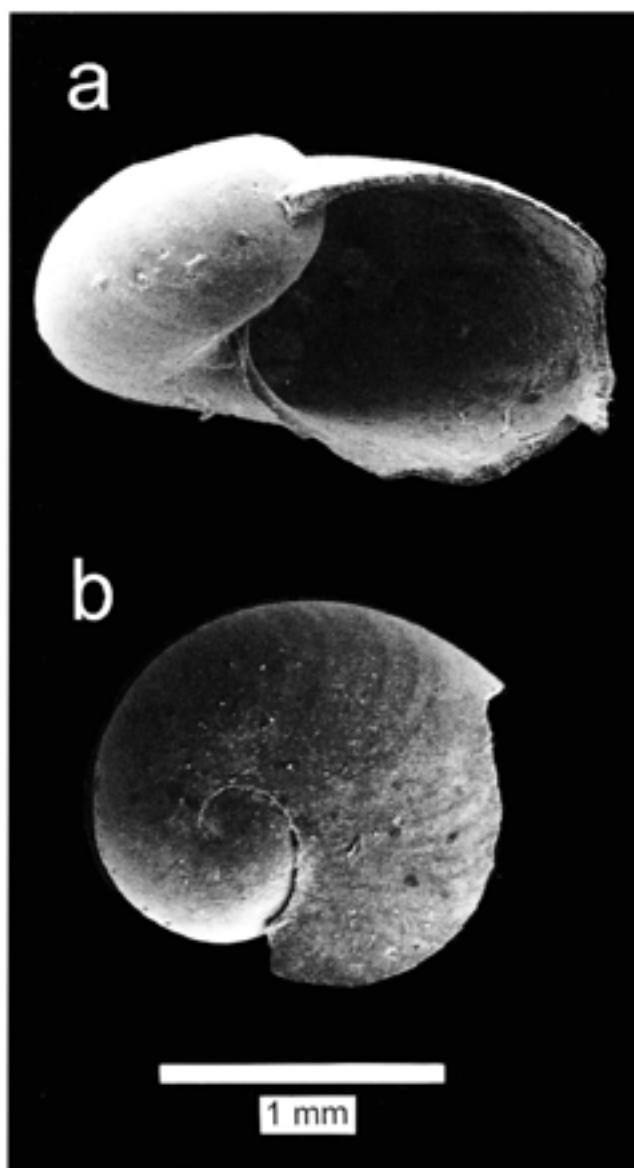


Fig 97a-b *Vitrinobrachium breve*; a) side view, b) apical view

the record of *S. lamellata* appears to constitute its earliest known occurrence, as it is otherwise unknown in a securely pre-Anglian context. The land snails give no clue as to the precise age of the deposits, although the occurrence of *Vitrinobrachium breve* (Fig 97), which

appears to have been quite frequent in the Middle Pleistocene (Holyoak and Preece 1986), suggests that the deposits are of this general age. Indeed no other British site has produced *V. brevis* in such abundance, but this results from the uniqueness of the facies sampled.

Three species, *Azeca goodalli*, *Columella edentula*, and *Truncatellina cylindrica*, listed in the initial report (Bates 1986) have proved to be misidentified and should be deleted from the Boxgrove fauna.

Marine species

Marine molluscs have been sampled from various locations throughout the quarry. The shells occur predominantly as scattered specimens throughout the sequence but occasional concentrations have also been found. In order to obtain adequate data it has been necessary not only to examine sediment deliberately collected for marine molluscs, but also material from the bulk sieving for small vertebrates, as well as individual spot finds. Due to the large sample sizes required and the diverse nature of the samples, it is not possible to give absolute abundances for each species but approximate frequency estimates are possible (Table 30).

In most cases samples were air dried and then broken down in water prior to sieving to 500µm. Residues were then sorted. Larger specimens, such as the *Neptunea contraria*, were carefully excavated when encountered during routine archaeological excavation (Fig 98).

Marine molluscs were recovered from Units 3, 4a, and were particularly frequent in Unit 4b. The range of species is rather small (Table 30) and comprises two distinct groups. The first, associated primarily with the upper chalk raft and basal beach deposits of Unit 3, are typical species of rocky shores (*Nucella lapillus*, *Littorina* spp; Figs 99–100). In addition several chalk boulders and even the surface of the chalk itself, have

Table 30 Marine Mollusca from Eartham Quarry, Boxgrove

species	Unit 3	Unit 3 Upper	Unit 4a	Unit 4b
	Basal Bed	Chalk Raft		
<i>Littorina littorea</i> (L.)	+			
<i>Littorina saxatilis</i> agg*	++			
<i>Nucella lapillus</i> (L.)	+	+	+	+
<i>Neptunea contraria</i> (L.)				+++
<i>Mytilus edulis</i> (L.)				+++
<i>Modiolus modiolus</i> (L.)				+
boring molluscs†	+	+		

+++ >100 observations

++ 10–99 observations

+ <10 observations

* *L. saxatilis* cannot be distinguished from *L. arcana* on shell characters. These fossils must therefore be listed as aggregate records

† Inferred from the presence of bored holes in the surface of chalk boulders

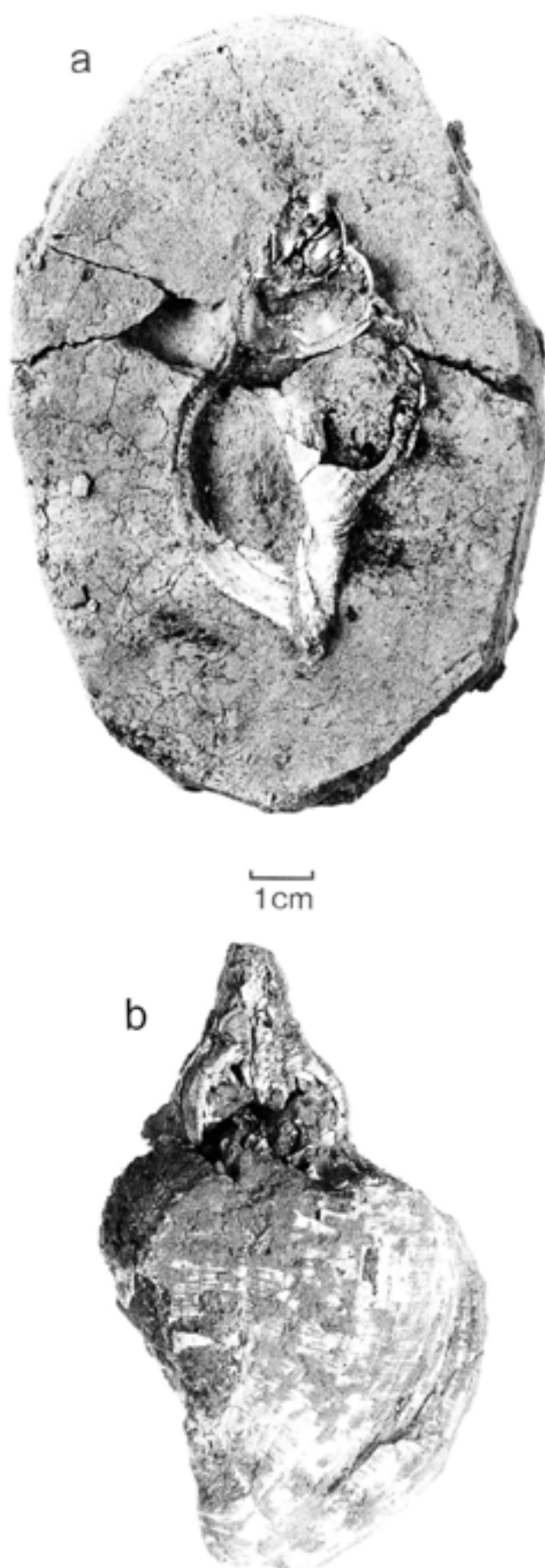


Fig 98a–b *Neptunea contraria* from Unit 4b



Fig 99 *Nucella lapillus* from Unit 3



Fig 101 Chalk bored by bivalve mollusc (?piddock) from the base of the marine deposits at Q2 GTP 13

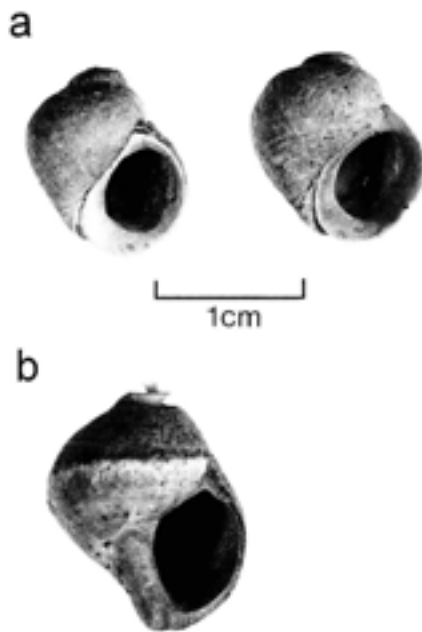


Fig 100 a *Littorina saxatilis* b *Littorina littorea* from Unit 3



Fig 102 *Modiolus modiolus* from Unit 4b

been bored by bivalves, probably *Hiatella arctica* or pid-docks (Fig 101). Several chalk boulders were also covered with barnacles, mostly *Balanus crenatus*, a calcareous-based low littoral to sublittoral species. The second group, from Unit 4b, is composed essentially of mytilid bivalves (*Mytilus edulis* and *Modiolus modiolus*) (Fig 102). Within Unit 4b shells of *M. edulis* are frequent

and in many cases the valves remain articulated, and it seems likely that mussel-beds existed nearby. Earlier work (Shephard-Thorn and Kellaway 1977) also reported the occurrence of *M. edulis* together with cockle shells ('*Cardium*' = *Cerastoderma*), but no trace of the latter were detected in the recent excavations. These records were based on a few poorly preserved

specimens and casts in the sands (E R Shephard-Thorn personal communication). In addition to these shells, the sands contain an interesting suite of trace fossils which suggest an intertidal or sub-tidal environment (Colclutt Chapter 2.3).

The most interesting marine mollusc at Boxgrove is a large sinistral whelk belonging to the genus *Neptunea* and thought to be conspecific with Linnaeus's *N. contraria* (Fig 98). Nelson and Pain (1986) have shown that the single specimen of this taxon in the Linnean Collection is based on a modern shell from Vigo Bay, Spain. This species' now extends from the southern Biscay coast of France to Morocco, so its occurrence at Boxgrove is of considerable interest. This taxon is apparently distinct from the Red Crag fossils, usually known by this name, which according to Nelson and Pain (1986) should be called *N. angulata* (S V Wood).

The occurrence of *Littorina saxatilis* agg is also of particular interest as it appears to represent its earliest known occurrence in Britain. The records from the East Anglian Craggs have all proved to be erroneous (Reid 1996). The only other reliable fossil records of *L. saxatilis* agg in the eastern Atlantic of comparable age were found in sediments between the Maarifian and Anfatian Stages near Casablanca, Morocco (Lecointre 1952). These sediments have been dated to about 0.5myr (Biberson 1977).

The taphonomy of some of the marine species at Boxgrove poses something of a problem, particularly with regard to some of these large *Neptunea*. Within Unit 4b a large number of these whelks (and *Nucella lapillus*) were associated with discrete clusters of well rounded flints (<60mm in diameter) (Fig 64). The origin of these clusters and associated shells is difficult to determine (Bridgland Chapter 2.4) but four possibilities exist: 1) they represent material deposited as a result of sea-weed rafting; 2) they represent the decayed remnants of armoured mud-balls; 3) they represent the remnants of a previously more extensive sheet of pebbles and shells that has undergone differential erosion to leave a patchy distribution, and 4) they represent material intentionally collected and emplaced by man. Since there is no evidence for extensive erosion at this level it is unlikely that they represent the remnants of more extensive deposits (3 above) but we are unable to choose between the other possibilities.

The marine molluscs, like the land snails, cannot throw much light on the precise age of the deposits, as most are common species that have long stratigraphical ranges. The occurrence of *N. contraria* is noteworthy but of uncertain biostratigraphical value. Shephard-Thorn and Kellaway (1977) did report the occurrence of a specimen of '*Macoma obliqua*' in a calcareous dogger from the Slindon Sand, about 0.3m above the surface of the chalk. If correctly identified, this species might have had some biostratigraphical significance, as it is frequent in Lower and early Middle Pleistocene deposits in north-west Europe and was not thought to have occurred later. However, it has recently been

found, very unexpectedly, in Eemian deposits in the southern North Sea basin (Meijer 1993), so that its biostratigraphical value has been weakened. Attempts to trace the Boxgrove specimen have been unsuccessful.

3.4 Ichthyofauna

S A Parfitt and B G Irving

Introduction

The importance of the Boxgrove ichthyofauna assemblage lies in the fact that it represents the first large assemblage of its type from the British early Middle Pleistocene. Remains of fish from other locations during this period have only rarely been reported. Where they are known, these important assemblages, including those from West Runton, Norfolk (Stuart 1992), and Little Oakley, Essex (McGlade in Lister *et al* 1990), consist almost entirely of freshwater species. This predominance of freshwater species, and a lack of contemporary marine deposits which have produced fish remains, has resulted in little being known about the early Middle Pleistocene marine fish fauna. At Boxgrove the fauna, whilst not being particularly diverse, has been collected from a stratified sequence that samples a series of environments ranging from fully marine nearshore and intertidal habitats to shallow saltwater lagoon and freshwater marshes, ponds, and streams. It is these changing environments which are reflected in the fish fauna recovered from the site (listed in Tables 26, 31-2).

Methods

The fish remains were extracted, in the main, by wet sieving bulk samples through a 500µm mesh. A small number of excavated finds were lifted in sediment blocks which were subsequently prepared from their matrix in the laboratory. In comparison with other vertebrate groups from the site, the fish bone material is generally in poor condition. This is probably a result of their relatively fragile nature which has led to a greater degree of post-depositional deformation and fragmentation.

Identifications are based on comparison with recent material in the Natural History Museum and the authors' personal collections. Most of the specimens were examined with a low-power binocular microscope to observe bone modification such as breakage, erosion, weathering, digestive corrosion, etc.

Systematic remarks

Raja clavata, Thornback Ray

Teeth of the thornback ray, *Raja clavata*, were recovered from Units 4b and 4c (Fig 103a). The teeth of rays are very distinctive and identification of this species is based on the shape of the tooth base.

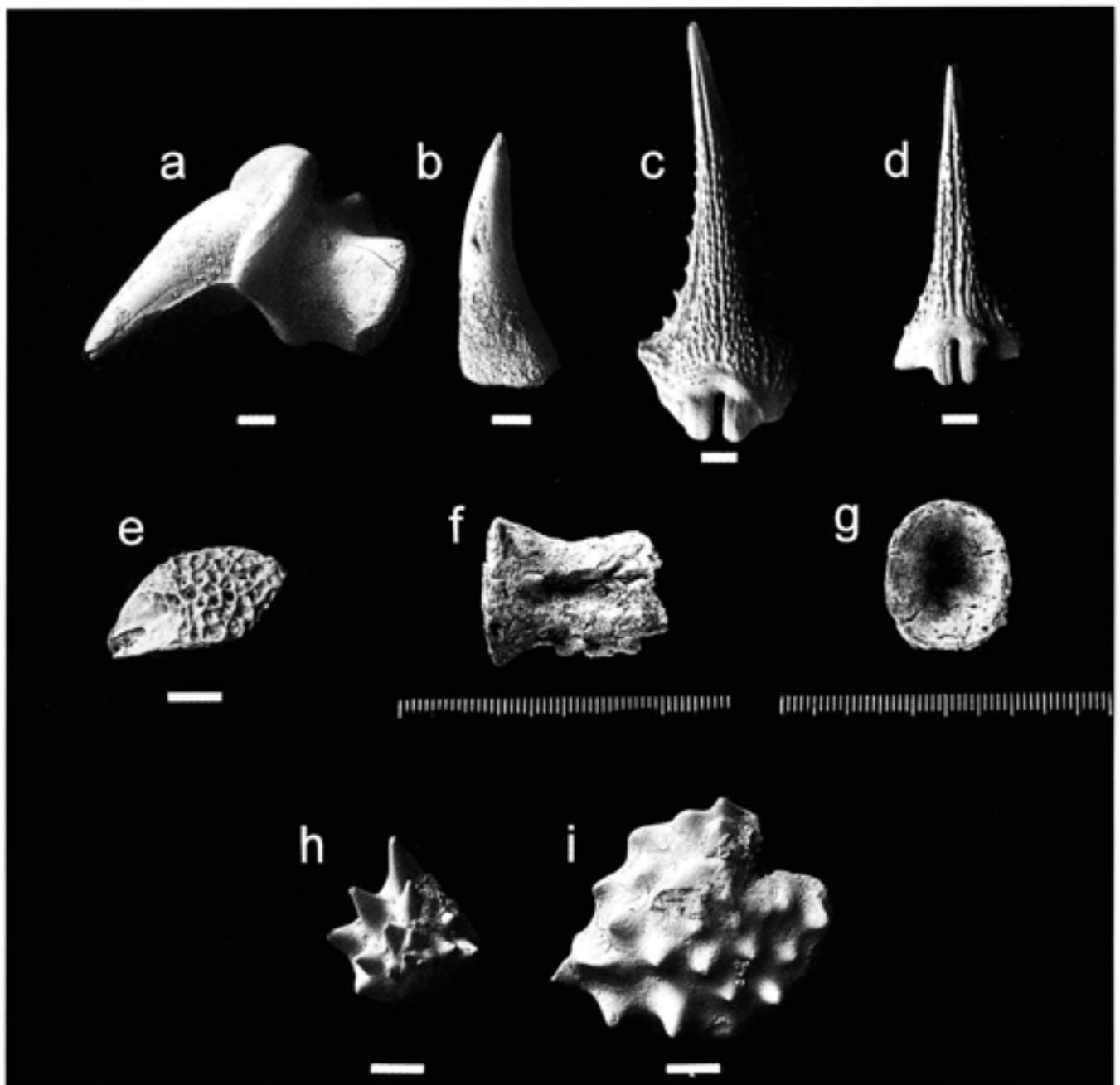


Fig 103 Fish from Amey's Eartham Pit, Boxgrove: a) *Raja clavata* tooth (Q2 GTP 3 4c BS87-125); b) Salmonid (cf *Salmo trutta*) vomerine tooth (Q2 Unit 4b); c) *Gasterosteus aculeatus* spine (Q1/B 4c BS89-898); d) *Gasterosteus aculeatus* spine (Q2 GTP 13 4c BS86-2); e) Triglid scute (Q2 GTP 3 4c BS86-36); f-g) *Thunnus thynnus* vertebra (Q1/A 4b, f) lateral view, g) cranio-caudal view, scale divisions in mm); h) *Platicthys flesus* dermal denticle (Q2 GTP 3 4c BS86-36); i) *Platicthys flesus* eroded dermal denticle (Q2 GTP 17 4c BS86-29). a-e and h-i scanning electron micrographs, scale bars 0.5mm

Anguilla anguilla, Eel

The eel, *Anguilla anguilla*, has been identified from a single adult vertebra from Unit 4d. Vertebrae of *A. anguilla* are distinctive in that they are laterally flattened (Stuart 1982).

Conger conger, Conger eel

This species has been identified from two pre-caudal vertebrae from the Slindon Sands. The vertebrae of the

Conger eel are characteristic in that they are very narrow in lateral view and the centrum has a rounded hexagonal shape when seen in cranio-caudal view.

Clupeidae, Herring family

Two vertebral centra were assigned to Clupeidae based on surface sculpturing and the sub-rounded shape of the centrum when seen in cranio-caudal view. The size and morphology of the vertebrae suggest that they are probably from sardine or pilchard.

Table 31 Stratigraphic distribution and abundance of fish from Boxgrove

number of specimens: +++ (>100), ++ (10–99), + (1–9)

		3	4b	4b/4c	4c	4d	5a
<i>Raja clavata</i>	Thornback ray	–	+	–	+	–	–
<i>Anguilla anguilla</i>	Eel	–	–	–	–	+	–
<i>Conger conger</i>	Conger eel	+	–	–	–	–	–
<i>Muraena helena/Conger conger</i>	Moray/conger eel	–	+	–	–	–	–
Clupeidae	Herring family	+	–	–	–	–	–
<i>Salmo trutta</i>	Brown/sea trout	–	–	–	+	–	–
Salmonidae	Salmon/trout	–	+	–	++	+	+
Gadidae	Cod family	–	++	–	–	–	–
<i>Gadus morhua</i>	Cod	–	+	–	–	–	–
<i>Gasterosteus aculeatus</i>	Three-spined stickleback	–	++	++	+++	+++	++
Triglidae	Gurnard family	–	–	–	+	–	–
Labridae	Wrasse family	–	+	–	+	–	–
<i>Thunnus thynnus</i>	Blue-fin tunny	–	+	–	–	–	–
<i>Platichthys flesus</i>	Flounder	–	+	–	+	+	+
Pleuronectidae	Flatfish	+	+	–	+	–	–

Salmo trutta and Salmonidae, Brown/sea trout and salmon family

Brown trout, *Salmo trutta*, has been identified from a small number of vomerine teeth (Fig 103b), which were identified to this species on the basis of the curvature of the apex of the tooth. In addition, vertebrae of salmonids (either salmon or trout) were recovered from Units 4b, 4c, 4d, and 5a.

Gadus morhua and Gadidae, Cod and cod family

A partial cleithrum (Q1/A Unit 4b) is identical to the modern cod *Gadus morhua*. Gadidae vertebrae are relatively common in the lagoonal silts (Unit 4b); however the identification of this material is problematic as most of the vertebrae are either poorly preserved or from very small individuals.

Gasterosteus aculeatus, Three-spined stickleback

The dominant species of fish in Units 4b, 4c, 4d, and 5a is the three-spined stickleback *Gasterosteus aculeatus*. This species is mainly represented by the highly characteristic dorsal and pelvic spines (Fig 103c, d); other elements include vertebrae, lateral plates, pre-operculars and bones of the skull.

Triglidae, Gurnard family

A single dermal scute (Fig 103e) from Unit 4c is probably derived from a species of Gurnard (Triglidae).

Labridae, Wrasse family

A single vertebra of a wrasse was identified on the gross morphology of the centrum which, although slightly eroded, retains the characteristic mid-lateral ridge.

Thunnus thynnus, Blue-fin tunny.

Quarry 1/A produced a single caudal vertebra of blue-fin tunny, *Thunnus thynnus*, from the lagoonal silts (Unit 4b). This is only the second record of blue-fin

tunny from the British Pleistocene, the other specimen being from the Cromer Forest Bed Formation (Cromerian) of East Anglia (Newton 1882). The Boxgrove specimen, illustrated in Figure 103f–g, shows the typical ovoid centrum (cranio-caudal view) and characteristic scombrid vertebral body. Based on comparisons with specimens of known weight and age at death, the vertebra derives from an individual of around 25kg and a body length of approximately 1.35m. X-ray analysis of the growth annuli on the centrum show that the vertebra derived from a five-year-old individual that probably died during the summer months.

Platichthys flesus Flounder

The flounder, *Platichthys flesus* (Fig 103h–i), has been identified from the distinctive dermal denticles (modified scales), which are found along the lateral line, fin bases, and gill covers in the live fish.

Taphonomy and palaeoecology of the fish assemblage

The stratigraphic distribution of the fish from Boxgrove is summarised in Table 31; data on the relative abundance of the fish remains through the fossiliferous part of the stratigraphic succession are illustrated in Figures 104 and 105.

Beach gravels and Slindon Sands

The beach gravels (Unit 2) and Slindon Sands (Unit 3) were extensively wet screened for fish remains. The lower part of the marine sequence (beach gravels exposed in GTP 25 and 13) produced no fish remains. This is not surprising as the deposition of material occurred within a high energy environment which is not conducive to the preservation of relatively fragile fish bones.

With the exception of a small assemblage recovered from the upper part of the 'chalk raft' at the base of Marine Cycle 3 (Collcutt Chapter 2.3), the three marine cycles within the Slindon Sands at GTP 13 were also devoid of fish remains. From the bones which survived, identifiable material was sparse. This may, again, be due to the nature of the depositional environment. Exposure to marine action has no doubt transported the bones over short distances leading to abrasion and rounding of the bones and breakage of the neural and haemal arches of the vertebrae. As a result only eight vertebral centra could be identified to family (Pleuronectidae, Clupeidae) and two to species (*Conger conger*). Clupeidae (probably sardine or pilchard) was represented by two vertebral centra; Pleuronectidae ('flatfish') by a vertebra and *C. conger* (conger eel) by two pre-caudal vertebrae.

Environmental information provided by this assemblage is limited due to the small size of the fauna; nevertheless some observations can be made. The Clupeidae (herring family) are mainly inshore pelagic shoaling fish and most species of this family inhabit shallow marine environments. Other species, such as shad, can tolerate brackish conditions, spawning in freshwater and occasionally forming non-migratory stocks in rivers and lakes. The conger eel, which today occurs in coastal waters as far north as Iceland and Norway and as far south as the Mediterranean and Morocco, has a very restricted habitat preference for rocky shores where it feeds on bottom-living fishes, octopuses and crustaceans.

Slindon Silts

The Slindon Silts (Unit 4) can be sub-divided into three main subunits (4a/b, 4c, and 4d; see Roberts Chapter 2.1) which correspond to variations in depositional environments, based on both sedimentology (Collcutt Chapter 2.3) and micromorphology (Macphail Chapter 2.6).

Unit 4a/b

The lower unit (Unit 4a/b), consists of rhythmic alternations of muds and silts containing a microfauna that suggests deposition within a saltwater lagoon. Serial samples through Unit 4a/b at GTP 10 (Figs 4, 49a–51) show an increase in fish remains down profile, with the highest frequency being from the clay layer ('*Mytilus* bed') at the base of the Slindon Silt Member (Fig 104). In comparison with the other fossiliferous units, fish remains are sparse (Fig 104); nevertheless, this unit has produced a relatively diverse fish fauna which includes *Raja clavata*, *Muraena helena* or *C. conger*, Salmonidae, Gadidae, *Gadus morhua*, *Gasterosteus aculeatus*, Labridae, *Thunnus thynnus*, *Platichthys flesus* and Pleuronectidae. All of the species, with the exception of cod and blue-fin tunny, can be found in shallow inshore waters and saltwater lagoons. The three-spined

stickleback, the most abundant species in the assemblage, although typically found in freshwaters is tolerant of a wide range of salinities, and in the northern part of its range it is found in estuaries, saltwater lagoons, coastal rockpools, and the open ocean.

Juvenile cod also live in these shallow inshore waters, typically from just below low tide mark to depths of 20m. Most of the gadid material represents small juvenile individuals as would be expected in a shallow nearshore/lagoonal environment. It is the presence of a large adult cod (represented by a fragmentary cleithrum) and a blue-fin tunny which is surprising in this context. The adult cod live in deep waters, and the blue-fin tunny is an offshore species which rarely come in-shore (Wheeler 1969). It is probable that the remains of both the blue-fin tunny and cod represent parts of carcasses washed into the lagoon.

Unit 4c

A large quantity of fish remains were recovered from the palaeosol horizon as a direct consequence of the sampling strategy which concentrated on this horizon. A total of 516 fragments were identified representing the following species: *G. aculeatus*, *Salmo trutta*, a salmonid, a labrid, a triglid, *P. flesus* and a pleuronectid.

The presence of this relatively diverse assemblage, which comprises marine as well as diadromous fishes (Table 32), in the palaeosol horizon is unexpected. Fish remains may have accumulated in the soil layer in four possible ways; as a background natural death assemblage that accumulated prior to soil formation, reworking from underlying deposits, predator accumulation, or as natural death assemblages due to periodic flooding of the landsurface transporting either bones or carcasses after death or allowing fish to colonise temporary pools. This last scenario is supported by the micromorphological evidence (Macphail Chapter 2.6) which indicates periodic (perhaps seasonal) flooding affected the soil horizon, particularly during the later stages of its formation. The relatively well preserved and unabraded fossils (eg Fig 103c) may be derived from material which accumulated as a natural death assemblage in these temporary water-bodies. In addition to the well preserved specimens, a significant proportion of the fish remains from Unit 4c exhibit breakage, rounding, pitting, and often extensive surface corrosion (eg Fig 103i) which can be closely matched with damage produced by the activities of predators. A number of mammalian predators including bear, otter, mink and wild cat, as well as some predatory birds, feed on fish and are known to produce accumulations of fish bones at latrines, nest sites and roosts. Several piscivorous species have been identified in the Boxgrove assemblage; these consist of three species of mammal (bear, European mink, wild cat) and three birds (black-headed gull, kittiwake, great auk). These predators may have been partially responsible for accumulating the

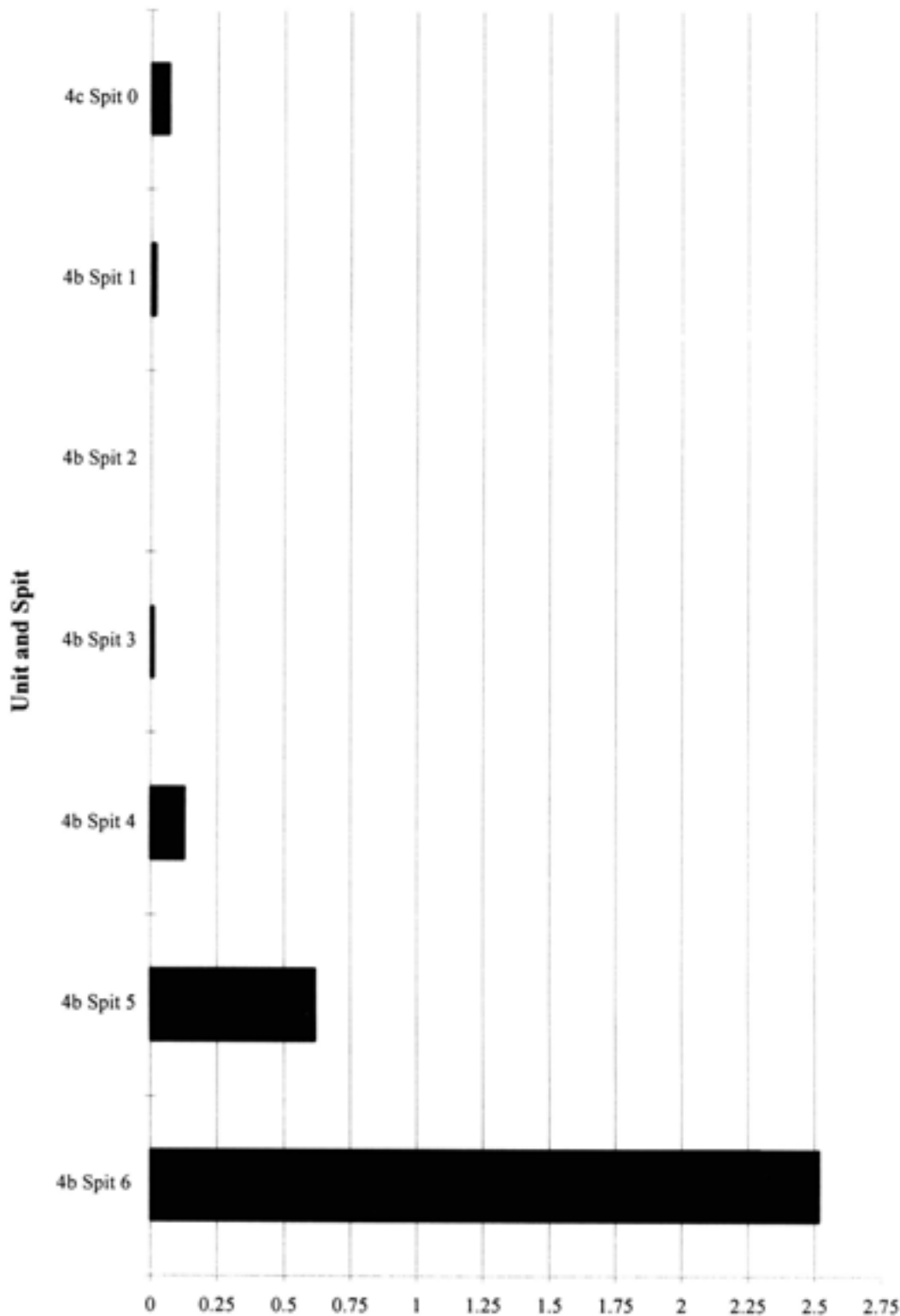


Fig 104 Number of fish bone fragments per kg recovered from sequential bulk samples of the Slindon Silt Member (Units 4b and 4c) from GTP 10

fish assemblage along with other piscivores not represented in the fossil assemblage. The composition and size of the fish remains in the soil horizon is also consistent with the range of fish eaten by these mammalian and avian predators which feed mainly on small to

medium sized fish caught in shallow freshwater, marshland, estuaries and near-shore marine habitats.

Additional evidence for the accumulation of part of the fish assemblage by predator action is supplied by the occurrence of discrete pockets of microvertebrate

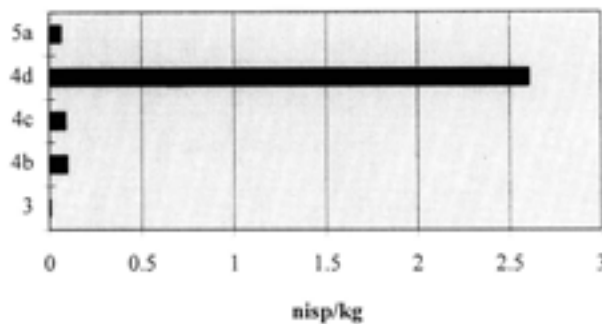


Fig 105 Concentration of fish bones (number of identifiable specimens per kg) from Slindon Sand and Silt Members

fossils from Quarry 1 Area B. These accumulations, which consist of the digested remains of a wide variety of small mammals, amphibians, reptiles, birds and fish, are consistent with the diet of the European mink (a semi-aquatic generalised predator), which is represented in the fossil assemblage.

It is therefore very probable that much of the fish material from Unit 4c derived from prey assemblages transported to the site from an unknown distance. Natural deaths and perhaps also reworking from the underlying lagoonal silts may have contributed to the accumulation of this assemblage.

Until further work is undertaken on the taphonomy of fish bone and the accumulation of fish remains in comparable modern situations, it is difficult to interpret the taphonomic history of the assemblage, or to make inferences on the prevailing environmental conditions, other than observing the mixed origin of the fauna.

Unit 4d

On the basis of its micromorphology (Macphail Chapter 2.6), Unit 4d has been interpreted as a freshwater deposit laid down in gently flowing or still waters

Table 32 Seriation of fish taxa

(MS=Marine stenohaline species, D=Diadromous species that regularly migrate between fresh and saltwater at definite stages of their lifecycle)

		3	4b	4c	4d	5a
MS	<i>Conger conger</i>	+	-	-	-	-
MS	Clupeidae	+	-	-	-	-
MS/D	Pleuronectidae	+	+	+	-	-
MS	<i>Thunnus thynnus</i>	-	+	-	-	-
MS	<i>Gadus morhua</i>	-	+	-	-	-
MS	Gadidae	-	+	-	-	-
MS	<i>Muraena helena</i> /Conger conger	-	+	-	-	-
MS	Labridae	-	+	+	-	-
MS	<i>Raja clavata</i>	-	+	+	-	-
D	<i>Platichthys flesus</i>	-	+	+	+	+
D	<i>Gasterosteus aculeatus</i>	-	+	+	+	+
D	Salmonidae	-	+	+	+	+
MS	Triglidae	-	-	+	-	-
D	<i>Salmo trutta</i>	-	-	+	-	-
D	<i>Anguilla anguilla</i>	-	-	-	+	-

emanating from a spring at the base of the cliff. Restricted to the northern part of Quarry 1, this unit was sampled extensively in Q1/B (Fig 4) and produced the richest ichthyofauna from the site (Fig 105). In total over 900 identifiable fish bones were recovered, of which 19% could be identified to species and family. *Gasterosteus aculeatus* dominates the assemblage with the other species (*Platichthys flesus*, *Anguilla anguilla* and a salmonid) being represented by less than ten fragments. All of the remains, in contrast to those from the soil layer, are well preserved, and few exhibit corrosion or erosion observed in the material from Unit 4c. This assemblage is thought to be an autochthonous accumulation derived from fishes living in the freshwater pools.

Unit 5a

The Organic Bed (Unit 5a) was sampled at a number of locations in Quarries 1 and 2. It produced a restricted fish fauna consisting of *G. aculeatus*, some salmonid material and a dermal denticle of *P. flesus*; the condition of this last specimen suggests that it was reworked from an underlying deposit. Unit 5a is interpreted as a marshland deposit which formed in shallow standing and slow flowing water. The limited fish assemblage is entirely consistent with this interpretation.

Discussion and conclusions

The fossiliferous deposits which have produced fish remains span the transition from marine to freshwater depositional environments during the regression phase of the Boxgrove interglacial. As such the assemblage provides important information on the changing nature of the aquatic environments at the site. Although the species change through the sequence is subtle, seriation of the fish data (Table 32) shows a trend in the composition of the fish assemblage through the sequence. The seriation matrix of the fish

data illustrates the transition from a marine stenohaline fauna in the Slindon Sand Member to one dominated by migratory (diadromous) species in Units 4c, 4d, and 5a. Although none of the species identified from the freshwater deposits are purely freshwater inhabitants, the faunal progression reflects a decrease in marine influence and a change from marine to freshwater conditions during the deposition of the Slindon Sand and Slindon Silt Members. The lack of any purely freshwater species in the assemblage may indicate that freshwater stenohaline fishes were unable to colonise the region as the ponds and streams which formed on the landsurface were not connected to larger bodies of water with a freshwater fish fauna (see Wheeler 1977). In this respect, the assemblages from Units 4d and 5a (freshwater pond and marsh) are particularly interesting as they are dominated by two euryhaline species (*G. aculeatus* and salmonids) which can exercise full life cycles in freshwater. It would seem that the marine link was severed at this stage, leaving these two species isolated within land-locked pools.

The fish assemblage from the palaeosol horizon (Unit 4c) contains both marine stenohaline and diadromous species. The preservation of the material indicates that the assemblage is of mixed origin, perhaps partly reworked from the underlying lagoonal silts, but predominantly accumulated by mammalian or avian predators and natural deaths. The presence of marine species in the assemblage may indicate that the depositional site, although at some distance from the coast, was within the range of the predator(s). A similar inference can be drawn from the presence of great auk (Harrison and Stewart Chapter 3.6), which was probably brought to the site from the coast by a predator.

The fish fauna from the marine sequence (Slindon Sands and Silt Members) is dominated by marine stenohaline species typical of a littoral ichthyofauna and includes some inshore pelagic species. The assemblage is characteristic of that of the coastal waters of the British Isles at the present time.

3.5 Herpetofauna

J A Holman

Introduction

The Boxgrove site has produced one of the largest Middle Pleistocene herpetofaunas in Britain and is equally as important as the Middle Pleistocene Westbury-sub-Mendip and West Runton Freshwater Bed sites in this respect. At least nine species of amphibians and reptiles (probably more) are represented by the fossils. Two of these species are exotic to the fauna of Britain today.

The herpetological remains were largely recovered from the terrestrial sequence, especially from Unit 4c. The bones were collected using the standard bulk sieving techniques discussed elsewhere in this report. The

amphibian and reptile fossils were recorded by date, sample number, area, stratigraphic unit, and subunit. They were initially prepared and sorted into groups by Simon Parfitt and his co-workers.

The bones were preliminarily studied on site and then re-examined at the Vertebrate Paleontology Laboratory at the Michigan State University Museum. Here, the bones were compared with modern skeletons of European and British amphibians and reptiles, and final identifications were made.

Systematic palaeontology

In the following account, specimen references such as 'BS88-701 4b' refer to the date (1988) that the specimen was collected, the specific bulk sieving sample number (701) and the stratigraphic unit represented (4b). The more detailed information recorded with each bulk sieving sample number is on file at the Natural History Museum (London).

Amphibian scientific nomenclature follows Frost (1985). Lizard scientific nomenclature follows Estes (1981) and snake scientific nomenclature follows Rage (1984).

Class Amphibia
Order Caudata
Family Salamandridae
Genus *Triturus* Rafinesque 1815
Newts

This genus presently occurs in England, continental Europe, Asia Minor around the Black Sea and, to the west, portions of the Caspian Sea, thence eastward to the Ural Mountains (Frost 1985). Fossils of this genus occur from the Upper Oligocene to the Holocene, mainly in western Europe, with one occurrence recorded in the former USSR (Estes 1981).

Most fossil *Triturus* have been identified on the basis of individual vertebrae. Estes (1981) has discussed how the vertebrae of *Triturus* may be distinguished from those of other genera of Salamandridae on the basis of several characters.

Triturus vulgaris (Linnaeus 1758)
Smooth Newt

Material:

Unit 4b: Q1 GTP 22 Sp 10 BS88-701 one vertebra, Fig 106a

The vertebrae of both *Triturus helveticus* and *T. vulgaris* are easily distinguished from those of *T. cristatus* on the basis of being smaller and in having a much higher, more elaborate neural spine. The vertebrae of *Triturus vulgaris* may be distinguished from those of *T. helveticus* on the basis that the postzygapophyseal notch is narrower and more deeply indented (see Holman and Stuart 1991, fig 1, and Fig 106a).

Triturus vulgaris presently occurs throughout nearly all of Europe and the western part of Asia south to Asia Minor (Frost 1985). It is widespread to common in

southern England today (Cooke and Scorgie 1983). This species has previously been reported as a British fossil from the Middle Pleistocene Cromerian and Hoxnian Interglacial Stages, from the Late Pleistocene Ipswichian Interglacial Stage, and from the Early Flandrian (Holman 1993).

Triturus helveticus (Razoumowsky 1979)
or *Triturus vulgaris* (Linnaeus 1758)
Palmate Newt or Smooth Newt

Material:

Unit 4c: Q2 GTP 3 BS87-251 seven vertebrae

These *Triturus* vertebrae may be distinguished as being either *Triturus helveticus* or *T. vulgaris* on the basis of the structure of their neural spines, but they are too fragmentary for the shape and extent of the post-zygapophyseal notching to be detected.

Today, *Triturus helveticus* occurs in Britain, continental western Europe from northern Germany to southern France and northern Iberia, and thence east to Poland and Czechoslovakia (Frost 1985). The modern range of *Triturus vulgaris* has been given in the previous species account. *Triturus helveticus* has been reported as a British fossil only from the early Flandrian and another poorly dated Flandrian site (Holman 1993).

Triturus sp. indet

Material:

Unit 4b/c: Q1/B BS87-216 one vertebra

Unit 4c: Q1 GTP 15 BS86-16 one vertebra; Q2/B BS86-100 two vertebrae; Q2 GTP 3 BS86-36 one vertebra, BS87-124 four vertebrae, BS87-136 one vertebra, BS87-184 one vertebra, BS87-263 one vertebra, BS88-463 one vertebra; Q2 GTP 17 BS86-20 one vertebra, BS86-52 one vertebra, BS86-119 two vertebrae, BS86-97 one vertebra

Unit 5a: Q1/B BS88-502 one vertebra

Unit 6'3' Fe: Q2 GTP 3 BS87-252 two vertebrae

These are too fragmentary for specific identification.

Order Anura
Family Pelobatidae
Genus *Pelobates* Wagler 1830
Spadefoots

This genus presently occurs in Europe, western Asia, and north-western Africa (Frost 1985). It occurs as a fossil from the Pliocene to the Holocene of Europe (Carroll 1988).

Pelobates fuscus (Laurenti 1768)
Common Spadefoot

Material:

Unit 4c: Q1/B BS88-910 left ilium; Q2 GTP 3 BS88-461 right ilium, Fig 106c; Q2 GTP 13 BS86-8 left ilium, Fig 106b; Q2 GTP 17 BS86-75 left ilium

The ilia of *Bombina variegata* of the Discoglossidae, the Pelobatidae, and the Pelodytidae are distinguished from all other anuran groups in Britain and Europe in that they either lack or have a very tiny dorsal ilial prominence (Fig 106b, c; Bohme 1977, figs on pp 294-5). *Pelobates* may be distinguished from *Bombina*

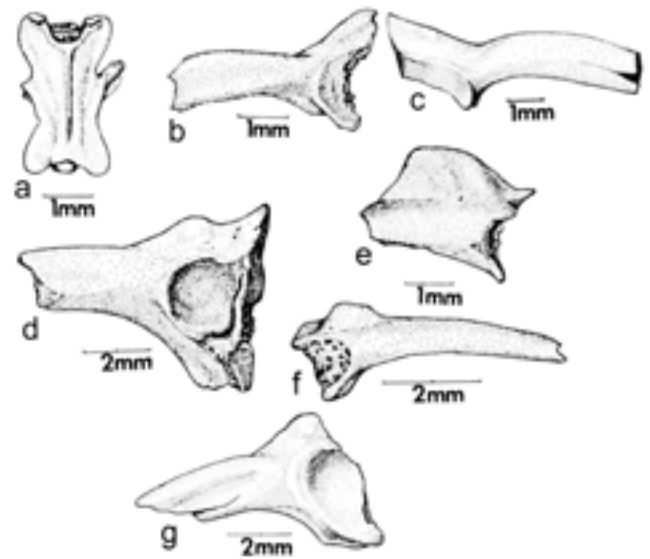


Fig 106 a) Vertebra of *Triturus vulgaris*; b) left ilium of *Pelobates fuscus*; c) right ilium of *Pelobates fuscus*; d) left ilium of *Bufo bufo*; e) left ilium of *Rana arvalis*; f) right ilium of *Rana temporaria*; g) left ilium of *Bufo calamita*

variegata in having a well-developed ventral acetabular expansion (pars descendens ilii of Bohme 1977), a structure that is lacking in *B. variegata*. *Pelobates* may be distinguished from Pelodytidae in having the dorsal border of the dorsal acetabular expansion (pars ascendens ilii of Bohme 1977) sloping in a more upward direction (Fig 106b, c; Rage 1974, fig 7) and in having a more swollen ilial shaft (ala of Bohme 1977).

Pelobates fuscus differs from *P. syriacus* in having the angle between the ventral acetabular expansion and the ilial shaft much greater than in *P. syriacus*. Material of the other European species *P. cultripres* was not available, but this species is confined to Iberia and the southern coast of France today.

This is the first fossil record of this family, genus, and species from Britain. The common spadefoot occurs today in France, Belgium, Netherlands, Denmark, southern Sweden, and northern Italy, east to southern Siberia, western Kazakhstan, and northern Caucasus in the former USSR (Frost 1985) and is not native to Britain.

Family Bufonidae
Genus *Bufo* Laurenti 1768
Toads

This huge genus has a nearly cosmopolitan distribution except for the arctic regions, Madagascar, Australia, and New Guinea (Frost 1985). Fossils of this genus have been reported from the Palaeocene to the Pleistocene of South America, Miocene to Pleistocene of North America, and the Pliocene to Recent of Asia and Europe (Carroll 1988).

There are three species of *Bufo* in modern Europe: *Bufo bufo* (Linnaeus), *B. calamita* Laurenti, and *B. viridis* Laurenti. Sanchez (1977) and Holman (1985) have commented on ilial differences between the three species.

Moreover, Holman (1985) discussed the identification of individual humeri of the genus and Hallock *et al* (1990) discussed the identification of the scapula of the genus *Bufo*.

Bufo bufo (Linnaeus 1758)
Common Toad

Material:

Unit 4c: Q2/B BS87-100 right ilium and humerus; Q2 GTP 3 BS87-36 left ilium Fig 106d; BS88-522 left ilium, scapula, and humerus, BS87-251 right and left ilium; Q2 GTP 17 BS87-97 left ilium, BS87-114 right ilium; Q2 GTP17 BS87-181 right ilium

Bufo bufo has a low, rounded or roughened ilial prominence, whereas *B. calamita* has a relatively high, triangular one (compare Figs 106d and 106g). An unusual morph occurs in an occasional fossil and modern *Bufo bufo* ilium in which the dorsal prominence arises as a low, irregular, sharpened crest (Holman 1985).

Another character may be as reliable as that of the dorsal prominence shape in separating the ilia of *Bufo bufo* and *B. calamita*, namely an elongate ventral ridge on the posterior part of the ilial shaft. In *B. calamita*, it is separated from the upper part of the shaft by an indented area but this structure is absent or only weakly developed in *B. bufo* skeletons that I have observed.

Both *Bufo bufo* and *B. calamita* may be separated from the third European species of *Bufo*, *B. viridis*, on the basis that *B. viridis* has a deep fossa that occurs just anterior to the acetabulum, and a dorsal prominence that tends to be double-lobed (Sanchiz 1977). These characters are lacking in *Bufo bufo* and *B. calamita*.

Presently, *Bufo bufo* occurs in Europe (other than Ireland and some Mediterranean islands), east to Lake Baikal and southern Siberia, northern Asia Minor and northern Iran, as well as north-western Africa (Frost 1985). It is relatively common in West Sussex at the present day (Frazer 1983).

Bufo bufo has been reported as a British fossil from the Middle Pleistocene Cromerian and Hoxnian Interglacial Stages, from the Late Pleistocene Ipswichian Interglacial Stage, and from the Flandrian (Holman 1993).

Bufo calamita Laurenti 1798
Natterjack Toad

Material:

Unit 5a: Q2 GTP 20 BS88-72 left ilium, Fig 106g

The specimen (Fig 106g) has the triangular ilial prominence and the ridge on the ilial shaft that are diagnostic for this species.

Today, *Bufo calamita* occurs in western and central Europe, east to Russia, as well as in Britain and in south-western Ireland (Arnold and Burton 1978). The endangered natterjack has become extinct in West Sussex, but a few modern records exist for Hampshire (Frazer 1983). This is the earliest fossil record of this species in Britain, which has previously been recorded only from the Ipswichian of West Sussex and several Flandrian localities (Holman 1993).

Bufo sp indet

Material:

Unit 4b: Q2 GTP 22 Sp 10 BS88-638 humerus
Unit 4c: Q2 GTP 3 BS87-184 scapula; Q2 GTP 13 BS86-8 left ilium; Q2 GTP 17 BS87-96 sacrum, BS87-119 sacrum

These elements are too fragmentary to identify to the specific level.

Family Ranidae

Genus *Rana* Linnaeus 1758
Typical Frogs

The huge genus *Rana* is cosmopolitan except for southern South America and most of Australia (Frost 1985). The genus is known from the Middle Eocene to the Recent of Europe, from the Miocene to the Recent of North America, and from the Pliocene to the Recent of Asia (Carroll 1988).

Rana may be easily separated from other European anurans on the basis of ilial and sacral characters. The ilium of European *Rana* has a well-developed dorsal ilial blade (vexillum) that is lacking in other European anuran genera. The sacrum of *Rana* has the diplasio-coelous condition in which the sacral vertebra has one anteriorly directed and two posteriorly directed condyles. This condition is not found in other European anurans. Hallock *et al* (1990) have shown that the scapula of *Rana* has a distinctive ridge on the dorso-medial side of the bone that easily distinguishes it from *Bufo*. These authors also point out that the humerus of *Rana* may be separated from that of *Bufo* in that the lateral epicondyle is rounded distally rather than flattened as in *Bufo*.

Rana arvalis Nilsson 1842
Moor Frog

Material:

Unit 4c: Q2 GTP 3 BS87-251 left ilium, Fig 106e

The ilium of *Rana arvalis* has been identified from several British Pleistocene sites mainly on the basis of the following characters from Holman *et al* (1990) and Bohme (1977). They may be separated from those of *R. graeca* and *R. temporaria* in having a much better vexillum or ilial blade, and from *R. 'esculenta'*, *R. lessonae*, and *R. ridibunda* in having a more slender junctura ilioischiadica.

Moreover, *R. arvalis* has a more prominent tuber superior than does *R. ridibunda*, and a much more gentle slope of the tuber superior into the pars ascendens ilii than in *R. lessonae*. *R. arvalis* may be distinguished from *R. dalmatina* and *R. latastei* in having the dorsal border of the vexillum or ilial blade sloping downward rather than upward from the tuber superior (compare Fig 106e, f, with Bohme 1977, fig 9 h, i).

At present, *Rana arvalis* occurs in north-eastern France, in Belgium, the Netherlands, Germany, Denmark, Sweden, and Finland, south to the Alps, northern Yugoslavia, northern Romania, and east to

Siberia as far as Yakutia (Frost 1985). The species does not occur naturally in Britain today (Arnold and Burton 1978).

Rana arvalis has been found as a British fossil from the Middle Pleistocene Cromerian and Hoxnian Interglacial Stages, and from the Late Pleistocene Ipswichian Interglacial Stage. This species has thus far not been recorded from the Flandrian (Holman 1993).

Rana temporaria Linnaeus 1758
Common Frog

Material:

Unit 4a: Q2 GTP 13 BS86-9 one right ilium
Unit 4c: Q2/B BS87-100 one right ilium; Q2 GTP 3 BS87-273 one right ilium, Fig 106f; Q2 GTP 13 BS86-8 two left and two right ilia and one right humerus; Q2 GTP 17 BS87-97 one right ilium and one right humerus, BS87-? one right ilium
Unit 5a: Q2 GTP 17 BS86-18 one right ilium
Unit GCF: Q2 GTP 20 BS86-71 one right ilium

The ilium of *Rana temporaria* is quite distinct among other European species of Anura as it has an ilial blade (vexillum) that is very poorly developed and mainly confined to the area around the tuber superior. As far as I can determine this is a character that does not occur in any other European or North American species.

Today, *Rana temporaria* occurs throughout Europe east to the Urals, but excluding most of Iberia, much of Italy, and the southern Balkans (Frost 1985). This species has been reported in the modern fauna of West Sussex (Frazer 1983).

Rana temporaria has been reported as a British fossil from the Middle Pleistocene Cromerian and Hoxnian Interglacial Stages, from the Late Pleistocene Ipswichian Interglacial and Devensian Glacial Stages, and from the Flandrian (Holman 1993).

Rana sp indet

Material:

Unit 4b: Q1/B BS87-288 left ilium
Unit 4b/c: Q1/B BS87-216 left fragmentary ilium
Unit 4c: Q1/B BS87-155 right ilium; Q2 GTP 17 BS87-96 left humerus, BS87-98 right humerus, BS87-75 left ilium; Q2 GTP 3 BS87-124 right scapula, BS87-136 two left and right fragmentary ilia, BS87-149 right humerus, BS87-156 left fragmentary ilium, BS87-242 left fragmentary ilium, BS87-251 left scapula and right and left humerus
Unit 5a: Fragmentary ilium with no locality or sample number
Unit 6'3Fe: Q2 GTP 3 BS87-252 left humerus and right ilium

This assemblage of *Rana* bones is too fragmentary for specific identification.

Class Reptilia
Order Sauria
Family Anguillidae
Genus *Anguis* Gray 1825
Slow Worms

This monotypic genus occurs in almost all of Europe with the exception of southern Iberia, Ireland, or in the extreme north (Arnold and Burton 1978). The genus occurs as a fossil from the Lower Oligocene to the Recent of Europe (Estes 1981).

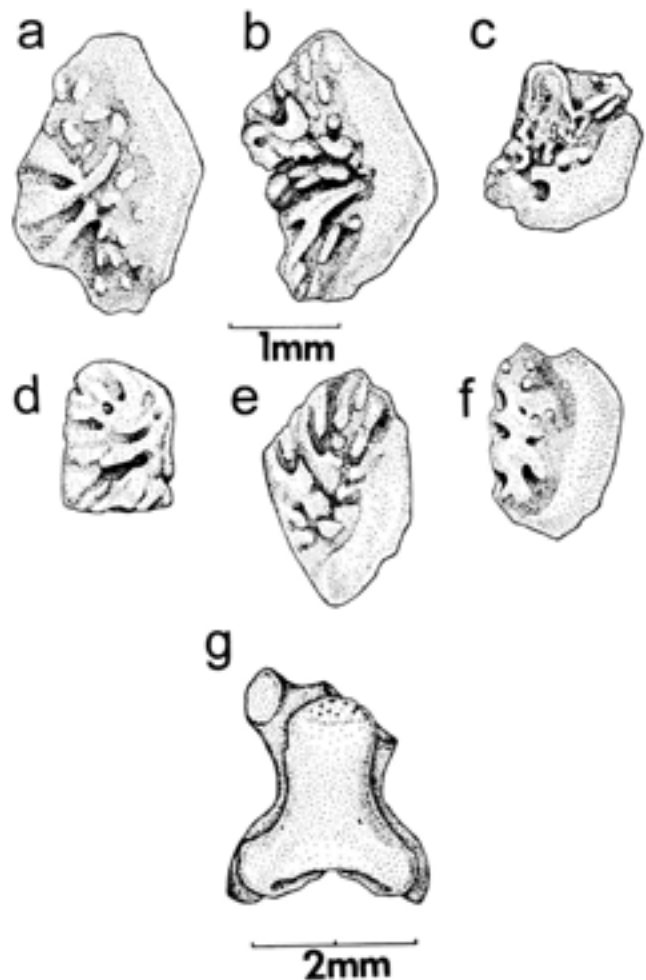


Fig 107a-f Osteoscutes of *Anguis fragilis*; g) vertebra of *Anguis fragilis*

Anguis fragilis
Slow Worm

Material:

Unit 4a/b: Q2 SEP 2 BS86-4 one vertebra
Unit 4c: Q2 GTP 3 BS86-36 one vertebra, BS87-124 four osteoscutes, BS87-136 three vertebrae and one osteoscuta, BS87-184 four vertebrae and two osteoscutes, BS87-251 nine vertebrae, three osteoscutes, and one fragmentary dentary, BS88-463 one osteoscuta; Q2 GTP 17 BS86-26 10 osteoscutes (Fig 107a-f) and one vertebra, BS86-27 three vertebrae and one osteoscuta; BS87-96 one osteoscuta, BS87-97 one vertebra
Unit LGC: Q2/B BS87-116 one vertebra
Unit 6'3Fe: Q2 GTP 3 BS87-252 three vertebrae (Fig 107g)

The vertebrae and osteoscutes of *Anguis fragilis* are quite diagnostic, and the identification of this species on the basis of isolated skeletal parts was discussed in Holman (1985). The vertebrae differ from those of all other lizards from central and northern western Europe in lacking zygosphenes-zygantral articular processes, in having the bottom of the centrum smooth and unkeeled, and in lacking a ventral constriction of the centrum.

The modern distribution of *Anguis fragilis* is the same as given above for the monotypic genus *Anguis*. The slow worm occurs in the modern fauna of West Sussex (Frazer 1983). *Anguis fragilis* fossils have been

reported from the Middle Pleistocene Cromerian and Hoxnian Interglacial Stages and from the Flandrian (Holman 1993).

Family Lacertidae
Genus *Lacerta* Linnaeus 1758
Lacertas

The genus presently occurs widely across Eurasia, Africa, and south-east Asia. Fossils of this genus occur from the Miocene to the Recent of Europe and the Middle Pliocene of East India (Carroll 1988).

Lacerta cf *Lacerta vivipara* Jaquin 1787
Common Lizard

Material:

Unit 4c: Q2 GTP 3 BS87-156 one vertebra

This tiny vertebra appears to be indistinguishable from that of modern *Lacerta vivipara* and is tentatively referred to that species. Vertebrae of *Lacerta* may be at once distinguished from those of *Anguis* on the basis that the ventral surface of the vertebra is keeled rather than smooth.

Today, the common lizard occurs throughout most of Europe, aside from the Mediterranean districts, and across Asia to the Sea of Japan (Frazer 1983). It has been reported from the modern fauna of West Sussex (Frazer 1983).

This species has been reported as a British fossil from the Late Pleistocene Ipswichian Interglacial and the Devensian Glacial Stages (Holman 1993). A record of *Lacerta* sp indet from the Middle Pleistocene Hoxnian Interglacial Stage (Holman *et al* 1990) is likely that of *Lacerta vivipara*.

Order Serpentes
Family Colubridae
Genus *Natrix* Laurenti 1768
European Water Snakes

Natrix is widespread in Europe and into western Asia, except for very cold regions (Matz and Weber 1983). The genus is known as a fossil from the Miocene to the Recent of Europe (Carroll 1988).

Natrix natrix Linnaeus 1758
Grass Snake

Material:

Unit 4c: Q2 GTP 13 BS82-2 the ventral portion of a vertebra

This specimen has a complete hypapophysis that is rounded terminally as in *Natrix natrix*. The other two species of European *Natrix*, *N. maura* and *N. tessellata*, have a more pointed terminal hypapophysis (Szyndlar 1984).

Today *Natrix natrix* occurs throughout Europe, northern Africa, and western Asia. It occurs in the modern fauna of West Sussex (Frazer 1983). *Natrix natrix* has been reported as a British fossil from the Middle Pleistocene Cromerian and Hoxnian Interglacial Stages, from the Late Pleistocene Ipswichian Interglacial and Devensian Glacial Stages, and from the Flandrian (Holman 1993).

Natrix sp indet

Material:

Unit 4c: Q2 GTP 3 BS86-36 fragmentary trunk vertebra, BS87-251 fragmentary vertebra and tiny jaw fragment
Unit 5a: Fragmentary vertebra

Discussion

This discussion deals with the Boxgrove herpetofauna in the light of stratigraphic occurrence, habitat, and palaeoclimate.

Stratigraphic occurrence (Table 33)

Most of the herpetofauna come from the terrestrial sequence, specifically the artefact zone, Unit 4c. Unit 4c yielded herpetological specimens from 55 of 74 sieve samples (74.32%) that had herpetological content. The herpetofauna of Unit 4c includes:

<i>Triturus helveticus</i> or	<i>Rana temporaria</i>
<i>T. vulgaris</i>	<i>Rana</i> sp
<i>Triturus</i> sp	<i>Anguis fragilis</i>
<i>Pelobates fuscus</i>	<i>Lacerta</i> cf <i>L. vivipara</i>
<i>Bufo bufo</i>	<i>Natrix natrix</i>
<i>Bufo</i> sp	<i>Natrix</i> sp
<i>Rana arvalis</i>	

Other units of the terrestrial sequence (5a and 6'3'Fe) yielded herpetological specimens from 8 of 74 sieve samples (10.81%) that had herpetological content. Unit 5a represents a mineralised organic deposit, formed in an alder fen/carr, whereas Unit 6'3'Fe represents the erosion of the cliff-line scree and subsequently soils developed on the hills immediately to the north, thus a more xeric sedimentary environment is indicated than for Unit 4c. The herpetofauna of Units 5a and 6'3'Fe includes:

<i>Triturus</i> sp	5a, 6'3'Fe
<i>Bufo calamita</i>	5a
<i>Rana temporaria</i>	5a
<i>Rana</i> sp	5a, 6'3'Fe
<i>Anguis fragilis</i>	6'3'Fe
<i>Natrix</i> sp	5a

A unit representing the transition between the terrestrial sequence and the marine regression sequence (4b/c) yielded identifiable herpetological remains from 1 of 74 sieve samples (1.35%) that had herpetological content. The only herpetological taxa from Unit 4b/c are:

Triturus sp
Rana sp

Units representing the marine regression sequence/lagoonal silts (4a and 4b) yielded herpetological specimens from 5 of 74 sieve samples (6.76%) that had herpetological content. These units are interpreted as representing low energy, brackish deposition with

Table 33 List of Boxgrove herpetofauna by unit (first number represents the number of identifiable specimens NISP, second number represents minimum number of individuals MNI)

	4a	4a/4b	4b	4b/4c	4c	4d	5a	LGC	63Fe	5b
<i>Triturus vulgaris</i>	-	-	1/1	-	-	-	-	-	-	-
<i>T. helveticus/vulgaris</i>	-	-	-	-	7/1	-	-	-	-	-
<i>Triturus</i> sp indet	-	-	-	1/-	23/-	-	1/-	-	2/-	-
<i>Pelobates fuscus</i>	-	-	-	-	4/4	-	-	-	-	-
<i>Bufo bufo</i>	-	-	-	-	11/5	-	-	-	-	-
<i>Bufo calamita</i>	-	-	-	-	-	-	1/1	-	-	-
<i>Bufo</i> sp indet	-	-	1/-	-	4/-	-	1/-	-	-	-
<i>Rana arvalis</i>	-	-	-	-	1/1	-	-	-	-	-
<i>Rana temporaria</i>	1/1	-	-	-	11/7	-	2/1	-	-	-
<i>Rana</i> sp indet	-	-	1/-	3/-	17/-	1/-	9/-	1/-	2/-	-
<i>Anguis fragilis</i>	-	1/1	-	-	54/2	-	1/1	1/1	3/1	1/1
<i>Lacerta</i> cf <i>L. vivipara</i>	-	-	-	-	1/1	-	-	-	-	-
<i>Natrix natrix</i>	-	-	-	-	1/1	-	3/1	-	-	-
<i>Natrix</i> sp indet	-	-	-	-	3/1	-	-	1/1	-	-

deposition of chalky, silty sediment (Macphail Chapter 2.6). The herpetofauna of Units 4a, 4a/b, and 4b includes:

<i>Triturus vulgaris</i>	4b
<i>Bufo</i> sp	4b
<i>Rana temporaria</i>	4a
<i>Rana</i> sp	4b
<i>Anguis fragilis</i>	4a/b

It is interesting to note that several amphibians (newt, toad, frog) and a lizard occur in the lagoonal silt units. Normally, amphibians cannot survive in saline environments because of the physiological properties of their body fluids and the absorbency of their skins. Nevertheless, at least two of the above taxa occur near the sea today in Britain. I have observed *Rana temporaria* in ponds very near the sea in East Anglia and *Anguis fragilis* is said to be particularly abundant in coastal districts in the south and west of England where it lives near the sea in areas that are covered with salt spray during storms (Smith 1964).

Habitat and palaeoclimate

The herpetofauna of the terrestrial sequence consists of newt (either *Triturus helveticus* or *T. vulgaris*), spadefoot (*Pelobates fuscus*), common toad (*Bufo bufo*), natterjack toad (*B. calamita*), moor frog (*Rana arvalis*), common frog (*R. temporaria*), slow worm (*Anguis fragilis*), viviparous (common) lizard (*Lacerta* cf *L. vivipara*), and grass snake (*Natrix natrix*). This is a substantial herpetofauna of at least nine species, and it would be very unusual to find nine herpetological species in any one locality in Britain today.

The faunal list from the terrestrial sequence (Table 26) includes all of the herpetological taxa known from the Boxgrove locality with the exception of a single vertebra of *Triturus vulgaris* from Unit 4b.

The modern habitats of the terrestrial sequence taxa are as follows. The palmate newt and smooth newts (*Triturus helveticus* and *T. vulgaris*) are fairly

terrestrial species, with the latter said to be more terrestrial than the former. Both breed in a variety of quiet aquatic situations, but the palmate newt is said to prefer rather clear, sometimes rather acidic, water and the smooth newt more enriched, less acidic, water (Arnold and Burton 1978). Spadefoots (*Pelobates fuscus*) are usually confined to areas of sandy soil where they hide during the day in burrows dug by the spades on their hind feet. They often breed in quite deep pools (Arnold and Burton 1978). The common toad (*Bufo bufo*) is a very ubiquitous species that is often found in relatively dry habitats (Arnold and Burton 1978). It breeds in a large variety of shallow, quiet aquatic situations, often temporary ones. Today, the natterjack toad (*Bufo calamita*) is typically found in sandy areas in Britain and may be found in dunes near the sea (Arnold and Burton 1978). On the continent it occupies a wider variety of habitats. It frequently burrows in loose soil. It breeds in quiet pools, sometimes in brackish water.

The moor frog (*Rana arvalis*) occurs in damp fields, meadows, and sphagnum bogs, often in the same area as the common frog, *Rana temporaria* (Arnold and Burton 1978). However, the moor frog is said to prefer wetter habitats than the common frog which is mainly terrestrial. Both species breed in quiet shallow water, and the common frog occurs in ponds near the sea. The slow worm (*Anguis fragilis*) prefers habitats with ground cover and is often found in damp situations (Arnold and Burton 1978). It may be found in pastures, glades, woods, lush scrubland and heaths. The viviparous or common lizard (*Lacerta* cf *L. vivipara*) is found in open woods, field-edges, heaths, bogs, grassland, sand dunes, sea-cliffs, and embankments. It is said to require a rather humid environment in these situations (Arnold and Burton 1978). The grass snake (*Natrix natrix*) is usually found in damp places where it hunts in water at times (Arnold and Burton 1978). It occasionally may be found in rather dry woods.

Putting together the herpetofauna of the terrestrial sequence, one might conceive of pools where the newts, spadefoots, toads, and frogs would be able to breed.

The moor frog might dwell along the edges of these pools and the grass snake might search for food in it from time to time. Surrounding such pools would be a rather humid area with vegetation and ground cover that would support the newts, common toad, common frog, slow worm and viviparous lizard. Outwards of the basin that sustained the pools and surrounding vegetated area would be a sandy area, possibly dunes, that would support the spadefoot, natterjack toad, and occasionally the common toad. The herpetofauna indicates a palaeoclimate at least as warm as the present one. Two exotic forms, the common spadefoot (*Pelobates fuscus*) and the moor frog (*Rana arvalis*), do not occur in the native fauna of Britain today, but occur on the European continent (see discussion of ranges in the taxonomic section of this report). This might indicate that the summers were somewhat warmer than they are in Britain today.

The nearest place on the map where all of the herpetological species of the Boxgrove terrestrial sequence could be found living together today would be the Calais area of France (Arnold and Burton 1978). This nearest 'area of sympatry' might lead one to suggest that the climate at the Boxgrove site at the time of the deposition of the terrestrial sequence was similar to that of the Calais area of France, with slightly warmer summers than occur in West Sussex at present. However, the zone of sympatry for the herpetological species extends from the French coast through central Europe, a broad geographical area which is climatologically varied. The herpetofauna from Unit 4c does not contradict the evidence provided by the small mammal fauna which may indicate a more continental climate than that of the British Isles at the present day.

3.6 Avifauna

C J O Harrison and J R Stewart

Introduction

The avifauna from Boxgrove is the largest open air fauna from the Middle Pleistocene in Britain and is only the second to be recovered from the time span represented by the site. The other site is that of Westbury-sub-Mendip in Somerset which remains unpublished. Therefore, it is of comparable importance to those from Pin Hole Cave in Derbyshire (Bramwell 1984) and Tornewton Cave in Devon (Harrison 1980a) both of which have produced large faunas. The primary reason for the richness of the Boxgrove fauna is the recovery method, as 500µm meshed sieves were extensively used.

The bird remains from Boxgrove are fragmentary and fragile, often consisting of single incomplete bones. Because of this, identification of a species cannot always be wholly certain, especially if there is only a single specimen for that bird. Such species have been indicated by the abbreviation 'cf'. A large volume of

material has been excluded as indeterminate, although it has been classified by size. Amongst these are a great many passerine birds which have not been identified due to their condition and the inherent difficulties of identifying such material. The identifications were achieved by means of comparisons with modern skeletons at the Natural History Museum in Tring, Hertfordshire, and the initials next to 'Material' indicate who identified each species. Find numbers are in italics, and the abbreviations 'Sp' for spit and 'Sq' for square have been used in this and subsequent chapters.

Boxgrove has yielded an overall bird fauna of 19 taxa. These taxa included many types of bird including waterfowl, seabirds, songbirds, a gamebird, a wader, an owl and a swift. All of them, with the exception of the great auk, are living species, in contrast to the mammals at Boxgrove and other Pleistocene sites where a greater proportion of extinct species occur.

This means that there is little evidence of change and species can be identified by direct comparison with recent material. It also means that the presence of a bird gives some indication of the conditions in which it is most likely to have occurred. However, the mobility of birds means that this may involve a broad general distribution of a species through several climatic zones. With single occurrences there is also the possibility that the individual may have met its end while passing through, rather than as a resident enjoying ideal conditions. It is therefore preferable to draw broad inferences from the avian fauna rather than place any great weight on particular instances. In doing so it should be remembered that the fragility of bird bones and the difficulties in their identification make it likely that only part of the range of species originally present has been recovered and identified.

Systematic description

Order Anseriformes

Family Anatidae

cf *Cygnus cygnus* (Linnaeus 1758)

Whooper swan

Material: (CJOH)

Unit 4: Q1 TP5 proximal radius

The specimen is weathered and pitted with little original bone surface remaining. The small round hole on its surface is probably due to weathering and the linear damage, or scratches, are probably the result of trampling.

The whooper swan is not uncommon as a fossil in the British Pleistocene, being present at Gough's Cave, Somerset (Late Devensian: Harrison 1987); possibly at Grays, Essex (Post-Hoxnian/Pre-Ipswichian Interglacial: Harrison and Walker 1977; 1985); Soldier's Hole, Somerset (Devensian or Holocene: Harrison 1987) in addition to Holocene sites. Today, it is a northern breeding species nesting south to Iceland and

southern Sweden in diverse habitats. These habitats include large shallow, reed-fringed lakes in the steppe region, swampy wetlands in low or upland grassland, heath or surrounded by forests. It enjoys coastal lagoons and larger pools, preferably in more open habitats. The species also requires deep water when resting and water less than 1m for grazing, with a rich bottom vegetation with little emergent plant growth. They will also graze on land (Cramp and Simmons 1977).

Anser anser (Linnaeus 1758)
Greylag goose

Material: (CJOH)

Unit 4d: Q1/B Sq D68 shaft fragment of a right scapula (F270) and cranial extremity of a left scapula (F268)

The two specimens, which were found in association (F270 and F268), were fragmentary and required repair.

The greylag goose is present at Soldier's Hole, Somerset (Devensian and Holocene: Harrison 1987); Kirkdale Cave, Yorkshire (Ipswichian or Devensian: Harrison 1980b); Ravenscliffe, Derbyshire (Pleistocene or Holocene: Harrison 1980b), Pin Hole Cave, Derbyshire (Devensian or Holocene: Bramwell 1984); Langwith Basset, Derbyshire (Devensian: Bramwell 1978); Walthamstow, Essex (Devensian: Harrison and Walker 1977; 1985); Ilford, Essex (Post-Hoxnian/Pre-Ipswichian Interglacial: Harrison and Walker 1977; 1985) and Grays, Essex (Post-Hoxnian/Pre-Ipswichian Interglacial: Harrison and Walker 1977; 1985) as well as numerous Holocene sites where it is present as wild and domestic forms.

Found today in boreal and temperate habitats, the greylag goose depends on a combination of secure aquatic and open grassland habitats. It breeds in dense vegetation by open freshwater with access to grasslands or wetlands and forages in grassland, swamps and shallow, saline or fresh water. The species is a migrant in the British Isles (Cramp and Simmons 1977).

Anser sp

Material: (JRS)

Unit 4d: Q1/B Sq D68 F259 left ulna; F286 fragmentary radius; Sq F68 F282 fragment of clavicle

The ulna is crushed, though mostly complete. A facet of the distal end is particularly well preserved (measurements: GL - 156mm, Did - 11.7mm). The radius includes both proximal and distal articulations, although the specimen is not complete ie part of the diaphysis is missing. (Measurements: Bp - 7.68mm, Dp - 9.06mm, Bd - 10.8mm). The clavicle consists of the left hand scapula clavicular

Morphologically and metrically the radius and ulna compare favourably with that of an *Anser* goose, although in terms of size it falls within the range of all the present Palaearctic species (Bacher 1967). The clavicle is referred to this genus due to its relative

close association with the radius and ulna. The scapulae referred to *Anser anser* by CJOH probably belong to the same individual given their close proximity.

Anas platyrhynchos (Linnaeus 1758)
Mallard

Material: (CJOH)

- Unit 3: Q1 TP1 (top of Slindon Sand) right carpometacarpus
Unit 4b: Q1/A TP14 Sq B2 left coracoid
Unit 4a: Q1 Machine trench south of TP4 right distal humerus; Q1 TP1 (10mm above the marine sand) left coracoid.
Gully fill: Q1/A F305 distal ulna fragment, F317 furcula, F2229 Sp 9 proximal scapula; Q1 TP1 Sq 2002/1001 coracoid
Unit 4c: Q1/A F1710 Sp 7 right humerus, F2222 Sp 9 proximal right scapula and tarsometatarsus, F2605 Sp 10 proximal right ulna, F3146 Sp 14 proximal left scapula, F3144 Sp 14 phalange 1 of the digit major, F3039 Sp 12 right coracoid, F2739 Sp 11 left coracoid; Q1/B Sq C59 Sp 2 proximal radius; Q1 TP5 F81 Sq B3 os carpi ulnare
Unit 5a: Q1/B F231 left coracoid, Sq C59 F135 left coracoid
Unit 5a/6: Q1/A F212 left coracoid.
Unit 6: Q1/A F127 right ulna, F300 proximal radius, F314 furcula symphysis, F316 right coracoid, F62 left coracoid, F47 Sp 2 left distal ulna
Misc: Q1 TP4 (redeposited sand) B3 F60 left carpometacarpus, left distal radius, left coracoid, fragmentary left humerus, three fragments of sternum, furcula fragment; left proximal ulna, left proximal radius, phalanges 1 and 2 of the digit major and a fragment of vertebra (Fig 108)

The material is very variable in preservation quality, some specimens being badly crushed (eg humerus F57), while others (ulna F217) are almost perfectly preserved.

The species is found in the Forest Bed Series, Norfolk (Pastonian and Cromerian: Harrison 1985); Walthamstow, Essex (Devensian: Harrison 1985); Ilford, Essex (Post-Hoxnian/Pre-Ipswichian Interglacial: Harrison 1985); Soldier's Hole, Somerset (Devensian: Harrison 1987); Torbryan caves, south Devon (Devensian or Holocene: Harrison 1987); Merlin's Cave, Hereford and Worcester (Devensian or Holocene: Harrison 1987); Neal's Cave, south Devon (Devensian or Holocene: Harrison 1987); Chudleigh, south Devon (Devensian or Holocene: Harrison 1987); Langwith Cave, Derbyshire (Devensian: Bramwell 1978);



Fig 108 Rearticulated wing bones of a mallard (*Anas platyrhynchos*); scale unit 10mm

Pin Hole Cave and Robin Hood's Cave, Derbyshire (Holocene or Devensian: Bramwell 1984) as well as many Holocene sites as wild and/or domestic forms.

Its present day range encompasses the Arctic tundra to the sub-tropical zone, on standing or flowing water, brackish estuaries, lagoons or in shallow saline water. It is a shallow water bird, requiring water less than 1m for foraging with ample plant growth, although it can be found in most water bodies. It avoids deep, exposed, fast flowing, oligotrophic waters. Mallards are partial migrants (Cramp and Simmons 1977).

Anas penelope (Linnaeus 1758)
Wigeon

Material: (CJOH)

Unit 4b: Q1 TP14 Sq B2 os carpi ulnare

Unit 4c: Q1/B F234 right coracoid and other as yet undetermined bones with which the coracoid appears to be articulated or semi-articulated (possibly a humerus shaft and a furcula and/or scapula) in a block of sediment; Q1/B Sq F60 BS88-689 os carpi ulnare

Unit 4d: Q1/B BS88-942 os carpi ulnare

The coracoid is incomplete, lacking both the shoulder and sternal extremities.

Previously found in the Forest Bed Series, Norfolk (Cromerian: Harrison 1985); Tornewton Cave, south Devon (Ipswichian?: Harrison 1987); Soldier's Hole, Somerset (Devensian: Harrison 1987); Robin Hood's cave, Derbyshire (Devensian or Holocene: Bramwell 1984).

The wigeon breeds mainly in boreal and sub-arctic zones but will range into temperate areas. It has a preference for shallow, open, broad freshwater, neither strongly eutropic or oligotrophic with ample vegetation both submerged or floating, but without dense emergent plants. Fast flowing water is avoided, but it tolerates saline wetlands. The species are chiefly migrant (Cramp and Simmons 1977).

cf Anas querquedula (Linnaeus 1758)
Garganey

Material: (CJOH)

Unit 5a: Q1/B Sq D59 BS88-516 fragment of a right coracoid

The specimen consists of the cotyla scapularis and its immediate surroundings.

The species is poorly represented in the Pleistocene to date, only having been found at Pin Hole Cave, Derbyshire (Devensian or Holocene: Bramwell 1984).

The species is fully migratory and breeds in the Mediterranean, steppe, and temperate zones. It is not found in arctic or oceanic conditions, in upland areas or in dense forest and rarely uses marine or tidal habitats, but favours narrow or small water bodies which are sheltered and shallow with proximity to grasslands or wetlands, and winters in similar habitats (Cramp and Simmons 1977).

Anas crecca (Linnaeus 1758)

Teal

Material: (CJOH)

Unit 4b: Q1 TP14 Sq A2 left carpometacarpus

Unit 4c: Q1/B F245 Sq C60 Sp 3 proximal scapula

The specimen is broken into two portions, the proximal and distal extremities with the os metacarpale majus present. The os metacarpale minus is missing.

The species has been found in the Forest Bed Series, Norfolk (Cromerian: Harrison 1985); Tornewton Cave, south Devon (Devensian: Harrison 1987); Soldier's Hole, Somerset (Devensian: Harrison 1987); Pin Hole Cave and Robin Hood's Cave, Derbyshire (Devensian or Holocene: Bramwell 1984).

Teal breeds throughout middle latitudes of west Palaearctic including cold coastal tundra, through steppe forest and steppe to desert fringes, where it is mostly associated with small water bodies. Eutropic waters are favoured with dense plant growth on its borders, while it tends to avoid deep, turbulent or lifeless water. It can be found in tidal water such as estuaries, salt marshes and lagoons, being brackish or saline, where it feeds mainly on seeds and animals in fine mud in very shallow water. Teal nests regularly far from water in heath or scrub. Teal are partial migrants (Cramp and Simmons 1977).

Anas sp and *cf Anas* sp

Material: (CJOH and JRS)

Unit 4c: Q2 SEP 3 distal carpometacarpus

Unit 6: Q1/A F57 Sp 3 right humerus

The carpometacarpus consists of the distal end with the beginning of both the os metacarpale majus and minus (Measurement: Did - 6.72mm). The humerus is crushed, lying with the cranial surface up on a sediment block.

Due to the specimens not being identified to species level and the number of species in the genus *Anas*, little of use can be said about its ecological implications. The carpometacarpus has been identified as an *Anas* duck due to the proportions of the synostosis metacarpalis distalis. In terms of size the specimen falls within the range of *A. platyrhynchos*, *A. acuta*, *A. strepera*, and *A. penelope* (Woelfle 1967)

Aythya fuligula (Linnaeus 1758)

Tufted duck

Material: (CJOH)

Unit 4d: Q1/B distal left humerus

The shaft portion of the specimen was in five fragments, requiring repair.

The tufted duck has previously been recorded from a number of British Pleistocene localities including the Forest Bed Series, Norfolk (Cromerian: Harrison 1985); Walthamstow, Essex (Devensian: Harrison 1985) and Pin Hole Cave, Derbyshire (Devensian or Holocene: Bramwell 1984). Today, it is mostly found

in upper middle latitudes, avoiding both hot and cold areas, and is a partial migrant to the British Isles (Cramp and Simmons 1977). It is a lowland species found on lakes up to 15m in depth where it dives to feed between 3–14m. The tufted duck has a preference for eutropic waters and will use rivers and land-locked seas; as activity on land is minimal, it favours small islands for breeding and nesting.

Bucephala clangula (Linnaeus 1758)
Goldeneye

Material: (CJOH)

Unit 4c: Q1 GTP 16 BS86-24 os carpi ulnare

The specimen is complete and unworn.

There are two other British Pleistocene records of goldeneye from the Forest-bed Series, Norfolk (Cromerian: Harrison 1985) and Robin Hood's Cave, Derbyshire (Devensian: Bramwell 1984).

Goldeneye breed in tall forests with hollow trees near to productive, medium depth, cold water bodies with little vegetation. Its present day range is limited to upper middle latitudes and it occurs in greatest numbers in the coniferous forest zone. The goldeneye is particularly important palaeoecologically as its distribution is restricted by specific arboreal-aquatic requirements. When migrating it will use most water body types, although with a bias for estuaries and marine bays (Cramp and Simmons 1977).

Order Galliformes
Family Phasianidae
Perdix perdix (Linnaeus 1758)
Grey partridge

Material: (CJOH)

Unit 5a: Q2/B distal radius

The grey partridge is relatively common as a fossil in the British Pleistocene, occurring at Soldier's Hole, Somerset (Devensian: Harrison 1987); Ravenscliffe Cave, Derbyshire (Pleistocene or Holocene: Harrison 1980b); Langwith Cave, Derbyshire (Devensian: Bramwell 1978); Aveline's Hole, Burrington (Devensian or Holocene: Newton 1923); Dowel Cave, East Sterndale (Devensian or Holocene: Bramwell 1978); Bridged Pot Cave, Somerset (Devensian: Harrison 1987); Chudleigh Fissure, south Devon (Devensian or Holocene: Harrison 1987); Pin Hole Cave and Robin Hood's Cave, Derbyshire (Devensian or Holocene: Bramwell 1984).

Today it frequents cool mid-latitude lowlands, continental and oceanic, in the temperate and steppe zones. Grey partridge are sedentary, strictly grassland species which avoid forests, coastlines, lake margins, rocky terrains and marshes. It likes neither too wet nor too dry habitats, especially during breeding when it prefers tall dense vegetation to nest among (Cramp and Simmons 1980).

Order Gruiformes
Family Rallidae
Gallinula chloropus (Linnaeus 1758)
Moorhen

Material: (CJOH)

Unit 6: Q1/A F23 Sp 1 left distal humerus

Part of shaft is crushed, as is caudal surface of distal articulation.

The moorhen is known from only two other British Pleistocene localities; the Forest Bed Series, Norfolk (Cromerian: Harrison 1985) and St Brelade's Bay, Jersey (Devensian: Bate 1916). At the present day, it inhabits middle latitudes between the Arctic Circle and the Sahara, and has a wide tolerance to rainfall, humidity, temperature and wind but is vulnerable to freezing conditions. It prefers waters that are sheltered by woodlands or tall emergent vegetation. Its aquatic habitats include flowing or standing water, especially smaller bodies, but it avoids oligotrophic or saline situations (Cramp and Simmons 1980).

Order Charadriiformes
Family Scolopacidae or Charadriidae

Material: (JRS)

Unit 4c: Q2 GTP 17 F516 Sq 2040/1022 proximal right carpo-metacarpus

The articulation is damaged. Part of os metacarpale majus is present, while os metacarpale minus is missing.

The specimen is insufficiently well preserved for further taxonomic diagnosis; however, it resembles *Phievialis* and *Philomachus* in shape and size. These waders and many others are regularly associated with open areas, including grasslands and mudflats.

Family Laridae
Larus ridibundus (Linnaeus 1758)
Black-headed gull

Material: (CJOH)

Gully fill: Q1 TP5 Sq 2001/1000 F82 diaphysis of right humerus

The humerus shaft preserves most of the fossa m brachialis at the distal end, while the beginning of the crista pectoralis is visible at the proximal end.

There are no other Pleistocene records of black-headed gull in Britain. Today, it breeds in middle latitudes from the steppe and Mediterranean zones to the boreal zone and the fringes of the subarctic region. It is closely associated with water bodies whether fresh, brackish or saline, and forages along coasts, grassland and over water. Outside breeding season the black-headed gull frequents mostly inshore water bodies such as estuaries, avoiding exposed coasts (Cramp and Simmons 1983).

cf Rissa tridactyla (Linnaeus 1758)
Kittiwake

Material: (CJOH)

Unit 4c: Q1/A F1729 Sp 7 diaphysis of a right humerus

Distal part of crista pectoralis is present.

The only other British Pleistocene record is from Soldier's Hole, Somerset (Devensian: Harrison 1987).

Kittiwakes breed on cliffs bordering the low and high arctic coast. Along the Atlantic it extends into the temperate zone where suitable nesting sites are available. When not breeding they live out at sea (Cramp and Simmons 1983).

Family Alcidae

Pinguinus impennis (Linnaeus 1758)

Great auk

Material: (JRS and CROH)

Unit 4c: Q2/C Sq 2094/8021 F6 proximal right humerus (Fig 109)

The ventral-most part of bone is missing at the articulation. As a result the pneumatic fossa is missing, as well as the incisura capitis and the tuberculum ventrale. The specimen is also damaged at the dorsal part of the proximal end, ie the proximal part of the crista pectoralis is missing. The specimen was repaired as it was originally in two fragments. The break is across the impressio musculi latissimus dorsi at the proximal end of the shaft.

The only other Pleistocene record of the great auk in Britain is at La Cotte de Saint Brelade in Jersey (Andrews 1920). The La Cotte specimen is Devensian in age and therefore considerably younger than the Boxgrove specimen. In fact the oldest great auk

remains in Europe to date are those records from the Weischelian (or Devensian), such as Grotta Romanelli in Italy (Blanc 1928), Gruta da Figueira in Portugal (Mourer-Chauviré and Antunes 1991), as well as at Devil's Tower, Gibraltar (Bate 1928), and Gorham's Cave, Gibraltar (Eastham 1967). It is also thought that no earlier remains exist in North America, which formed part of the species' recent range. This would mean that the Boxgrove specimen may represent the oldest known record for the species. The importance of this specimen also lies in the fact that the fossil history of North Atlantic auks is not known for the Middle Pleistocene while the record for the Pliocene and Early Pleistocene is much better (Olson 1985; Walker personal communication). This specimen thus forms an important part of an emerging pattern. A diverse Pliocene auk fauna, including species as large and larger than the Recent great auk, had existed in both what are now Florida and Belgium. This fauna became extinct and therefore any information indicating when our modern fauna may have emerged is important. A particular species with which the Boxgrove specimen should be compared is *Pinguinis (sic) alfrednewtoni* (Olson 1977) which has been named as the ancestor of the Recent species. As already mentioned, after the Middle Pleistocene the records for great auk increase and are not uncommon, particularly from the Mesolithic and later archaeological sites of Scotland and Scandinavia (Serjeantson 1988; Hufthammer 1982). The species then, as is well documented (eg Bengtson 1984), became extinct due to persecution by man. The last specimen was killed in Iceland by collectors in 1844.

The great auk was a species of cold-temperate parts of the North Atlantic. It was flightless although it was an expert swimmer and diver, doing so to catch a variety of fish. It is thought to have been confined to isolated islands and skerries when breeding (Bengtson 1984).

Order Strigiformes

Family Strigidae

Strix aluco (Linnaeus 1758)

Tawny owl

Material: (CJOH)

Unit 6: Q1/A Sp 4 F107 proximal radius

The edge of the articulation is abraded.

British Pleistocene records of the tawny owl are uncommon and are only known from Happaway Cave, south Devon (Devensian or Holocene: Harrison 1987) and Robin Hood's Cave, Derbyshire (Devensian or Holocene: Bramwell 1984).

The present day range of the tawny owl is extensive, stretching from the fringes of the boreal zone through temperate and steppe regions, to the Mediterranean. It avoids extreme cold, wet, and dry climates, wetlands and rocky terrain. In Britain it is typically found in deciduous or mixed woodlands. Tawny owls nest in hollow trees and abandoned nests of other species. They are mainly sedentary (Cramp 1985).

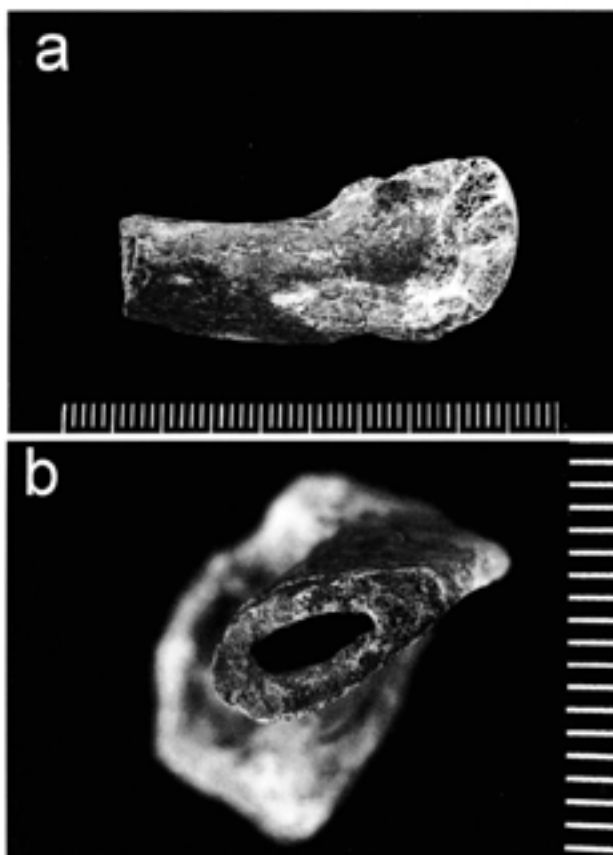


Fig 109a-b Proximal right humerus of a great auk (*Pinguinus impennis*); a) caudal surface, b) cross-section of shaft; scale unit 1mm

Order Apodiformes
 Family Apodidae
Apus apus (Linnaeus 1758)
 Swift

Material: (CJOH and JRS)

Unit 4c: Q2 GTP3 BS86-36 right coracoid, BS87-127 left coracoid

Both the coracoids are represented by the processus procoracoideus regions.

It is the presence of the foramen in the processus procoracoideus which is characteristic of the genus *Apus* which allowed the determination of these elements. The two specimens are likely to belong to the same individual. There are no other records in the British Pleistocene, although *Apus melba*, the alpine swift, is recorded from Pin Hole Cave, Derbyshire (Bramwell 1984).

This species breeds from lower and upper middle latitudes to above the Arctic Circle and nests in crags and sea-cliffs. The nature of the underlying terrain is only important with respect to its relationship to insect abundance. Swifts are migrants (Cramp 1985).

Order Passeriformes
 Family Turdidae
cf Erithacus rubecula
 Robin

Material: (CJOH)

Unit 6³Fe: Q2 GTP3 Sq 43 BS87-252 distal left tibiotarsus

British Pleistocene occurrences of the robin include the Torbryan Caves, south Devon (Holocene or Devensian: Harrison 1987); Aveline's Hole, Burrington (Devensian or Holocene: Newton 1923); Chudleigh Fissure, south Devon (Devensian or Holocene: Harrison 1987); Langwith Cave, Derbyshire (Devensian: Bramwell 1978); Longcliffe, Derbyshire (Devensian: Arnold-Bemrose and Newton 1905) and Pin Hole Cave, Derbyshire (Devensian or Holocene: Bramwell 1984).

The robin breeds in boreal to warm temperate zones and requires ground cover, especially woodlands, both broadleaf and coniferous, and is partially migrant (Harrison 1982).

Family Prunellidae
cf Prunella modularis
 Dunnock (Hedge sparrow)

Material: (CJOH)

Unit 4c: Q2 GTP 3 BS86-36 distal left humerus

The dunnock is recorded from Soldier's Hole, Somerset (Devensian: Harrison 1987); Langwith Cave, Derbyshire (Devensian: Bramwell 1978); Aveline's Hole, Burrington (Devensian or Holocene: Newton 1923) and Pin Hole Cave, Derbyshire (Devensian or Holocene: Bramwell 1984).

Dunnock occupy habitats with low bushy cover, feeding on the ground under trees and shrubs or in nearby open spaces. It is found in deciduous, mixed or

coniferous woodland and is a resident and migrant which breeds in the boreal to temperate zones, wintering in temperate zones (Harrison 1982).

Family Sturnida
Sturnus vulgaris
 Starling

Material: (CJOH)

Unit 4c: Q2 GTP 3 BS86-36 right coracoid, BS87-251 two right coracoids; Q2 GTP 17 BS86-26 right coracoid

The coracoids are all represented by the sternal extremities in each instance.

Found previously in the Forest Bed Series (Cromerian: Harrison 1985); Bacon Hole, south Wales (Ipswichian: Harrison 1987); Minchin Hole, south Wales (Ipswichian: Harrison 1987); Tornewton Cave, south Devon (Ipswichian or Devensian: Harrison 1987); Torbryan, south Devon, (Devensian or Holocene: Harrison 1987); Merlin's Cave, Hereford and Worcester (Devensian or Holocene: Harrison 1987); Chudleigh Fissure, south Devon (Devensian or Holocene: Harrison 1987) and Pin Hole Cave, Derbyshire (Devensian or Holocene: Bramwell 1984).

In the Western Palaearctic, starlings breed within the c 10–30°C July isotherms, encompassing the Arctic fringe though to the Mediterranean climatic zones. They nest in holes or crevices in rocks or trees and will travel considerable distances to feed in open grasslands and floodlands. After fledging, starlings frequent open country such as the upper parts of salt marshes, heaths and rocky shorelines. Low dense vegetation and dense forests, especially conifers and extensive wetlands, are avoided, although trees or reed-beds are required for roosting. Starlings are partial migrants (Cramp and Perrins 1994).

Taphonomy and palaeoecology of the birds (JRS)

Much has been published on the taphonomic significance of bird remains from prehistoric and later archaeological sites in recent years, particularly with reference to human exploitation versus 'natural' accumulation (Mourer-Chauviré 1983; Ericson 1987; Livingston 1989; Baales 1992). It was therefore necessary to consider the means by which the bird fossils of Boxgrove accumulated. It was also noticed that the two quarries at the site contained different proportions of large and small birds, thus further necessitating an investigation.

Because the site is both large in area and open air, it would appear that the avian remains are likely to consist in the main of 'natural' deaths rather than predation by man. Mortality in birds is usually the result of predation (by animals other than man), starvation or cold. However, due to the presence of evidence of hominid modification, such as cut marks, among the larger mammalian remains, a human agent must be considered.

Therefore, all bird bones were examined for cut marks, with negative results throughout. The presence of cut marks is the best method to infer human predation with regard to fossil vertebrate remains. Bird bones, however, rarely show such evidence in prehistory, a notable exception being those from the Upper Palaeolithic at Gough's Cave in Somerset (Harrison 1986).

Because of the general absence of evidence for butchery amongst bird remains, certain authors have sought other methods for inferring human involvement in the accumulation of bird assemblages from archaeological sites. These methods are based on a quantitative assessment of the different ratios of bird limb bones at particular sites (Mourer-Chauviré 1983; Ericson 1987; Baales 1992). Mourer-Chauviré and Baales used the assumption that distal extremity (tarsometatarsus and carpometacarpus) over-representation in medium-sized galliformes indicates bird of prey accumulation, while proximal extremities (humerus and femur) are indicative of human predation. Ericson, on the other hand, considered that 'natural' accumulations are characterised by greater occurrences of anterior (wing) bones compared with posterior (leg) bones which, when more numerous, indicate human activity. In none of these papers, however, are all the criteria satisfied which may allow assemblages to be adequately compared, namely:

- 1 Recovery methods for the assemblages should be identical. As demonstrated by Payne (1975) sample bias will occur if adequate methods of bone recovery are not used. This becomes particularly pertinent when comparisons between assemblages are to be made.
- 2 Sediment matrix from which the assemblages derive should as far as possible be the same.
- 3 Preservation quality of the assemblages should be similar.
- 4 Comparison should not be attempted across taxonomic boundaries, although, it is probably legitimate to use broad taxonomic definitions such as dabbling ducks and possibly house sparrow-sized passerines.

If these criteria are not satisfied it will be impossible to discern which variables were most influential in producing the different assemblages. However, even if the criteria are adhered to, an assemblage may have been affected by poor preservation to an extent that differences are obliterated. Indeed Livingston (1989) stressed the importance of such influences as bone density on survivorship which may consequently skew a skeletal element ratio. This ratio might then be wrongly taken to be indicative of human activity. This appears to negate Ericson's claims (Ericson 1987) for an assemblage dominated by posterior limb bones as indicating human exploitation. Livingston also suggested, due to the similarities in element survivorship between her assemblage and the Tertiary one studied by Rich (1980), that the fluvial transport highlighted

by Rich as a dominant influence on element ratios could not be very important. Livingston did not unfortunately deal with the patterns found by Mourer-Chauviré (1983) and subsequently by Baales (1992). It is possible that in these cases human versus animal predator ratios have been established, although this is difficult to judge from the two papers as no note is made of the criteria above which allow proper comparisons to be made.

Other relevant papers on the taphonomy of birds involve experimentation and observation and include such subjects as the comparison of the mechanical properties of house sparrow (*Passer domesticus*) skeletal elements (Bjordal 1988), observations on the movement and disarticulation of rock dove (*Columba livia*) and gull (*Larus* sp) carcasses (Bickart 1984), the patterns of fragmentation of bird bones in tawny owl (*S. aluco*) and eagle owl (*Bubo bubo*) pellets (Bochenski *et al* 1993) and the sequence of disarticulation of ice-trapped coot carcasses (Oliver and Graham 1994).

An important aspect of the Boxgrove fauna is the method by which it was recovered, and in particular the extensive use of 500µm meshed sieves. This has meant that a more representative sample of the remains in the ground have been retrieved. This in turn greatly facilitates the interpretation of the fauna. However, it also has the effect of multiplying the numbers of indeterminate skeletal remains. In order to investigate the taphonomic history of the birds at Boxgrove, a recording system was first designed with the aim of maximising the information which could be subsequently used. This meant that all material attributable to avian skeletal elements was given a size category. This size category arose either from the full specific or generic identifications or simply by comparison of the elements with a series of size-graded species. The size categories were as follows (becoming progressively larger):

- 1 *Passer domesticus* (House sparrow). Weight 22–32g
- 2 *Turdus merula* (Blackbird). Weight 80–110g
- 3 *Garrulus glandarius* (Jay). Weight 140–190g
- 4 *Anas crecca* (Teal). Weight 250–440g
- 5 *Anas platyrhynchos* (Mallard). Weight 500–700g

The taxa were arbitrarily chosen as a series of progressively differently sized bird species. In addition to the specimens being ascribed size categories they were also sided (left/right) and the anatomical regions of the bones present noted, such as recommended for large mammals (Dobney and Rielly 1988). The system of recording such regions is to be published in detail elsewhere (Stewart in prep).

The first and most apparent pattern in the Boxgrove bird assemblage is the great variation in the preservation quality among the specimens. There is also evidence to suggest that, although variable, on the whole the preservation is relatively poor, with bone being friable and prone to damage. This pattern is undoubtedly the overriding influence seen in the skeletal

Table 34 Skeletal element representation of dabbling ducks (*Anas* sp) at Boxgrove (all units). MNE=minimum number of elements

skeletal element	no	MNE	%
humerus	5	5	14.3
ulna	6	6	17.1
radius	4	3	8.6
carpometacarpus	4	4	11.4
coracoid	12	12	34.3
scapula	4	4	11.4
femur	0	0	0
tibiotarsus	0	0	0
tarsometatarsus	1	1	2.9
total		35	

element ratios calculated for all the Anatidae (Table 34). Here the bones thought to be the most mechanically robust are those which survive best. In this instance it is the coracoid, forming a third of the total major elements recorded. Other well represented bones are the humerus and ulna, while elements such as the femur and tibiotarsus are totally absent. The interpretation of this pattern should be treated with caution because of the relatively small sample size (total 35). It is also relevant to note that of the best represented element, the coracoid, the cotyla scapularis region of the bone is often the only part present. This is the same pattern observed in a collection of sub-fossil duck bones collected on a beach in Cadzand in Holland (Stewart pers obs). The latter were subjected to many mechanical trials including that of being dredged up from the North Sea for beach defence work. The element ratio appears therefore to agree with Livingston (1989), whose emphasis was very much on the mechanical properties of the individual bones in determining their survivability. However, the agreement with Livingston is dependent on whether her explanation for posterior versus anterior limb bone ratios is accepted. This is because the ratio of *Anas* species anterior limb bones far outweigh that of the posterior limb, which would be taken as indicating a natural accumulation by Ericson (1987). Livingston's explanation would be that dabbling ducks have more robust anterior limbs due to their greater use of their wings, thus rendering these elements more prone to survival.

The relative proportions of skeletal elements of house sparrow-sized bones were examined due to the apparent over representation of robust bones in dabbling ducks. Here, as seen in Table 35, the most abundant element is yet again the coracoid, while the humerus and ulna are next best represented. This does not, however, follow the prediction which would be made using the Bjordal (1988) experiment results. There are many differences which may account for the discrepancy between Bjordal's experiment results and the pattern seen at Boxgrove. These include the fact that the bones in the experiment had not undergone diagenetic alteration, the bones at Boxgrove were not

Table 35 Skeletal element representation of house sparrow-sized passerines at Boxgrove (all units)

skeletal element	no	%
humerus	8	18.6
ulna	5	11.6
radius	3	6.9
carpometacarpus	2	4.7
coracoid	19	44.2
scapula	0	0
femur	0	0
tibiotarsus	1	2.3
tarsometatarsus	5	11.6
total	43	

subjected to having a weighted blunt edge placed on them until a break occurred and that the bones at Boxgrove represent different taxa, none of which are likely to have been house sparrows.

The different proportions of large to small birds noticed for the two quarries is well illustrated by means of both Tables 36 and 37. Quarry 1 is dominated by large, generally aquatic species, while Quarry 2 is dominated by small passerine-sized birds.

A problem with the interpretation of this data is the lack of taxonomic definition available for the smaller passerine-sized birds. This discussion is centred on the birds from Unit 4c where the greatest abundance of bird remains in Quarry 2 were found. In Quarry 1, the distribution of birds is more even, although the small birds present are concentrated in Units 4c and 5a. However, it would appear that many of the remains represent passerines rather than small waders etc. The problems with the identification of the passerines are two-fold: firstly, the fragmentary nature of the bones, and secondly, the number of possible species that could be involved. Of the taxonomic identifications which have been made, both the robin (*E. rubecula*) and the dunnock (*P. modularis*) require dense shrub-sized vegetation often in woodlands, while three of the other birds in Quarry 2, the starling (*S. vulgaris*), the grey partridge (*P. perdix*) and the wader, often frequent more open habitats. The swift (*A. apus*) is of little use in this respect, while the great auk (*P. impennis*) is a complete anomaly and will be discussed below. The undetermined passerines in both quarries are of no help in that passerines can be found in most habitats. Quarry 1 is clearly dominated by waterfowl, in particular ducks, and has very few passerine-sized birds. Other work at Boxgrove, such as the sedimentology and soil micromorphology (see Collcutt and Macphail Chapters 2.3, 2.6), have shown that many of the sediments excavated in Quarry 1, particularly Unit 4d (which is probably syndepositional with Unit 4c), represent water bodies such as ponds. This would accord with the dominance of waterfowl in Quarry 1. However, it does not easily explain the relative lack of passerines in that quarry. It is possible that there was

Table 36 Numbers of skeletal elements of birds per taxa or size category for the different sedimentary units in Quarry 1. N=number of specimens, MNI=minimum number of individuals

quarry 1 taxa	3		4b		4b/4c		(4)		4c		4d		Q1/A gully fill		5a		6		5a/6	
	N	MNI	N	MNI	N	MNI	N	MNI	N	MNI	N	MNI	N	MNI	N	MNI	N	MNI	N	MNI
cf <i>C. cygnus</i>							1	1												
<i>Anser</i> sp											3	3								
<i>A. anser</i>											2	1								
<i>A. platyrhynchos</i>	1	1	1	1			13	1	10	3			5	2	2	2	7	1	1	1
<i>A. crecca</i>			1	1					1	1										
cf <i>A. querquedula</i>															1	1				
<i>A. penelope</i>			1	1					4	1	1	1								
cf <i>Anas</i> sp																	1	1		
<i>A. fuligula</i>											1	1								
<i>B. clangula</i>									1	1										
<i>G. chloropus</i>																	1	1		
<i>L. ridibundus</i>													1	1						
cf <i>R. tridactyla</i>									1	1										
<i>S. aluco</i>																	1	1		
mallard size			1						3		6		1		4		1			
teal size									2		1		1		4		1			
teal/jay size									1											
jay size																				
blackbird size			1						3						1					
blackbird/house sparrow size					1				1											
house sparrow size									6						1					

Table 37 Numbers of skeletal elements of birds per taxa or size category for the different sedimentary units in Quarry 2. N=number of specimens, MNI=minimum number of individuals

quarry 2 taxa	3		4b		(4)		4c		4d		Q1/A gully fill		5a		5b		5c		6		5a/6		63Fe		BCG	
	N	MNI	N	MNI	N	MNI	N	MNI	N	MNI	N	MNI	N	MNI	N	MNI	N	MNI	N	MNI	N	MNI	N	MNI	N	MNI
<i>Anas</i> sp							1	1																		
<i>P. perdix</i>											1	1														
Scolopacid or Charadriid							1	1																		
<i>P. impennis</i>							1	1																		
<i>A. apus</i>							2	1																		
<i>S. vulgaris</i>							4	4																		
cf <i>E. rebecula</i>																							1	1		
cf <i>P. modularis</i>							1	1																		
mallard size							4																			
mallard/teal size																										
teal size							4				1															
teal/jay size							1																			
jay size							4																			
jay/blackbird size																										
blackbird size							42				3		1	1												
blackbird/house sparrow size							11				1															
house sparrow size			3				32				2	2					1						2			

Note regarding Tables 36 and 37: not included in the tables were specimens which could not be attributed to bird skeletal elements, some of which may belong to other vertebrate classes. If two or more fragments clearly belonged to the same element they were counted as one fragment. The specimens only attributable to size categories were only expressed as gross numbers and not MNIs



Fig 110 Associated pectoral girdle and left wing bones of a mallard (*Anas platyrhynchos*); scale unit 1mm

little emergent vegetation, allowing for perching, associated with the water bodies in Quarry 1. There must presumably have been grassland in Quarry 2 to attract the grey partridge, the starling and the wader, as well as more dense vegetation as required by the robin and dunnock. Therefore, the vegetation may have been more variable in Quarry 2. The comparatively greater number of passerines may be due to their exclusion from Quarry 1 rather than a true over-representation in Quarry 2. Alternatively, the actions of a predator could explain the comparative abundance in Quarry 2. The pattern could therefore indicate the presence of an avian predator roost producing more passerine remains. This highlights a problem in attempting to explain the occurrence of species and size classes in the two quarries. A working assumption is that the birds died in their preferred habitats and that there is no movement of birds *post mortem*, such as by a predator. The difference in composition between the two quarries is not, however, the product of differential use of fine meshed sieves as similar weights of sediment were sieved from each quarry.

The anomalous occurrence of the great auk humerus should be considered. This is particularly unusual as the species was a flightless marine bird and it was found in a deposit which formed at some distance from the sea at the time. The best explanation would appear to be that a predator had brought it there. The sediments negate the possibility that it was reworked from the marine deposits stratigraphically below. Unfortunately, surface features on the bone indicative of predator activity such as tooth puncture marks, gnaw marks or cut marks, are not present to confirm this hypothesis.

The occurrence of associated bones such as that of most of the elements of a mallard pectoral girdle with the left wing present in the redeposited sand from

Quarry 1, EQP Area TP4, Square B3 (Fig 110) is interesting. This paradoxically demonstrates that the quality of spatial information is high even if in other instances certain elements and parts of elements may not be preserved. It is also interesting as both personal observation and Oliver and Graham (1994) suggest that the pectoral girdle and wing are a commonly occurring suite of bones when a partial carcass is found.

The climatic tolerances of the species identified are on the whole fairly wide and complicated by the presence of a number of migrants. If season at death could be ascertained for the migrants they would be of considerably greater use. This was not, however, possible. The great auk could be thought to be indicative of a colder than present climate, although as pointed out by Dorothea Bate (1928), there is evidence that its Recent range may have extended to the Bay of Biscay and the coast of Spain, making it a more wide-ranging species than generally thought.

Conclusion

The avian fauna at Boxgrove is important because of the mode of recovery, which makes the assemblage more representative of the remains present at a site than at previously published Palaeolithic excavations in Britain. This is demonstrated by the large number of small bird remains recovered, both in terms of taxa such as passerines and elements such as phalanges. A precedent has been set here and sites should not be investigated without similar methods of recovery in the future if optimal samples are to be analysed.

The species present agree with other sources of information in distinguishing between Quarries 1 and 2, particularly with respect to horizon 4c-4d. Quarry 1 is wetter, as shown by the dominance of water fowl. Quarry 2 is dominated by smaller birds, mostly representing passerines, which may be the result of an avian predator. The occurrence of the great auk is anomalous and yet of importance given its age, being the oldest record for this enigmatic flightless seabird.

The preservation of the fauna and the robusticity of the different elements has been shown to influence the skeletal elements present of dabbling ducks, while the pattern seen in the house sparrow-sized birds is at present unexplained. Despite the poor physical preservation of bones, the occurrence of many instances of associated elements of single individuals points to rapid burial. This situation is unusual for the British Pleistocene avian fossil record.

There are, therefore, a number of characteristics of the fauna which are unique principally as a result of the sedimentological environment as well as the excavation techniques used. These have enabled certain of the analyses conducted to be carried out which would not have been possible under other circumstances.

4 Mammalia

S A Parfitt

4.1 Introduction

This chapter provides a systematic description of the mammalian remains from the early Middle Pleistocene deposits at Boxgrove and discusses the implications of these remains for the dating and palaeoenvironmental reconstruction of the Boxgrove sequence.

The deposits at the site comprise five members. The Slindon Gravel, Slindon Sand and Slindon Silt Members were deposited in a nearshore marine and intertidal environment and these deposits are extensively exposed in Quarry 2. However, with the exception of the upper part of the marine clays and silts (Unit 4b), they are poorly fossiliferous. The majority of the faunal remains were recovered from the terrestrial Slindon Silt Member (Units 4c, 5a) and the base of the Eartham Lower Gravel Member (Tables 9a, 9b), which consist of a palaeosol and an overlying sequence of cliff collapse deposits, colluvial calcareous silty clays and Lower Chalk Pellet Beds. A limited cold stage fauna was recovered from the Brickearth Beds and Upper Chalk Pellet Beds of the Eartham Upper Gravel Member.

The mammalian fauna from the lower part of the terrestrial sequence spans the end of a major temperate episode and the start of the ensuing cold stage. Changes in the composition of the mammalian assemblage from this sequence shows that this interval consists of a series of climatic fluctuations which preceded the onset of full periglacial conditions represented by the emplacement of the head gravels.

The mammalian assemblage recovered during the excavations at Amey's Eartham Pit, Boxgrove, is one of the most diverse from a British Pleistocene site, consisting of 50 species, 11 of which are extinct, and includes a number of species which represent either the first or the earliest records from the British Pleistocene. The correlation of the deposits, based on the presence of a number of biostratigraphically important species, is consistent with a 'Cromerian' *sensu lato* date for the marine, intertidal, and the lower part of the terrestrial sequence. The composition of the fauna suggests that the sequence is equivalent to the Dutch Cromerian Interglacial IV (Zagwijn 1992) and broadly contemporaneous with the Calcareous Member at Westbury-sub-Mendip (Andrews 1990) and the channel deposits at Ostend (Stuart 1980).

4.2 Systematic palaeontology

Methods

The faunal remains and the site data archive relating to the collection are housed in the Natural History Museum (London), along with measurements and

detailed descriptions of the remains made during the faunal analysis. Measurements of the larger bones were taken with dial callipers to the nearest 0.1mm, and the measurements of the small mammal bones and teeth were taken with a binocular microscope with a calibrated graticule to the nearest 0.01mm. Unless otherwise indicated, the measurements and abbreviations follow von den Driesch (1976). When measurements have been estimated because of damage or abrasion, the measurement is followed by 'est'. The specimens are numbered using the field numbering system which allocated a sequential set of numbers to the specimens recovered from each excavation area or collecting locality (Parfitt Chapter 3.1)

Order Insectivora
Family Erinaceidae
Genus *Erinaceus*
Erinaceus sp
Hedgehog

Unit 4b: Q2 GTP 3 BS90-1365 left $M_{1,2}$ frag

Unit 4c: Q2 GTP 3 BS87-251 left P^2 , lacks roots, slight wear; Q2 GTP 17 BS87-97 left P^1 , slight wear on tip

Unit 5a: Q2 GTP 17 BS86-76 right mandible with M_1 , M_2 frag, M_3 (alveoli of I_1 - P_4), left mandible frag with alveolus of M_1 + I_1 - M_2 , right P^1 , right P^2 frags, left M^1 , left P^2 frag, left and right M^2 frags, left P^1 frag, two left M_1 frag, incisor frags, right C_1 frag, right P^1 , BS86-25 $M_{1,2}$ frag, unworn, left decid P^2 , slight wear, BS86-63 M^1 frag, unworn, BS86-64 left P^2 frag, left P^4 frag, left M^1 frag, BS86-61 left C^1 , lacks roots, worn, right P^2 , BS86-74 left C^1 frag, right C^1 , right P^2 , left P^2 , left P^3 , left P^3 frag, left P^4 frag, left M^1 frag, left M^2 frag, right M^2 frags, left C_1 frag, right I_2 frags, right P_4 frags, left M_2 frag

The hedgehog (*Erinaceus* sp) is represented by six individuals. Although the material is fragmentary, a number of associated upper and lower teeth were identified as well as a portion of mandible with M_{1-3} (Figs 111a-b, 112). Measurements of the Boxgrove specimens are given in Table 38 and comparisons with Recent European hedgehogs and fossil material are given in Figures 113 and 114. Although the Boxgrove sample is comparatively large, the identification of these remains is hampered by their fragmentary nature and the lack of comparative Pleistocene material.

The hedgehog is uncommon in the Pleistocene of Europe, and where this species occurs in fossil assemblages it is never abundant and generally represented by fragmentary remains. Of the four species described from the Plio-Pleistocene of Europe, *E. samsonowiczi* Sulimski, *E. praeglacialis* Brunner, and *E. lechei* Kormos are all smaller than living *E. europaeus*, while the late Middle Pleistocene species *E. davidi* from La Fage (Jammot 1973) is larger. Biometric data plotted

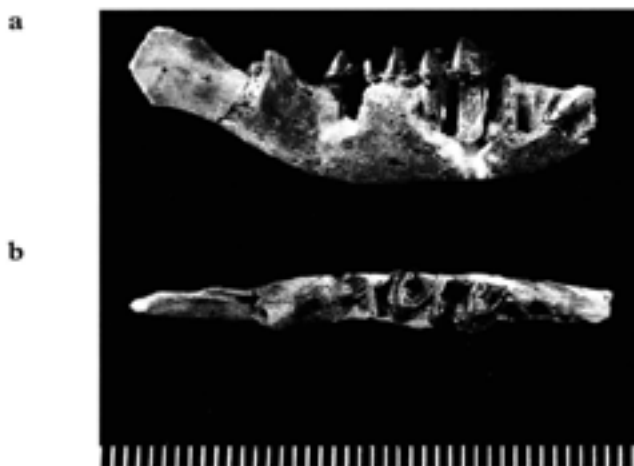


Fig 111 *Erinaceus* sp: right mandible with M_{1-3} (Q2 GTP 17 BS86-76 Unit 5a) a) buccal view, b) occlusal view; scale unit 1mm

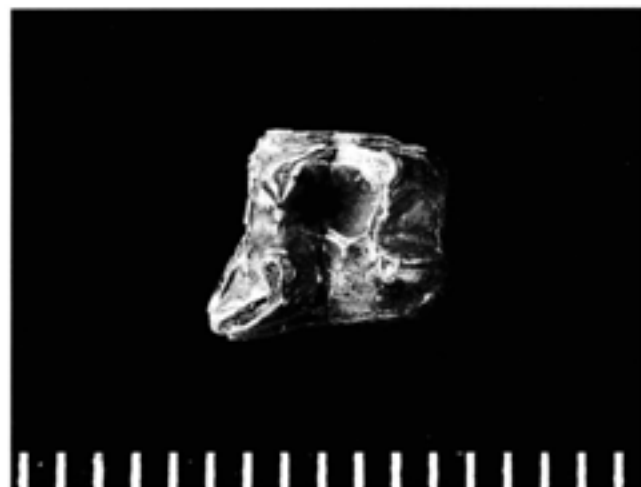


Fig 112 *Erinaceus* sp: right M^1 (Q2 GTP 17 BS86-76 Unit 5a), occlusal view; scale unit 1mm

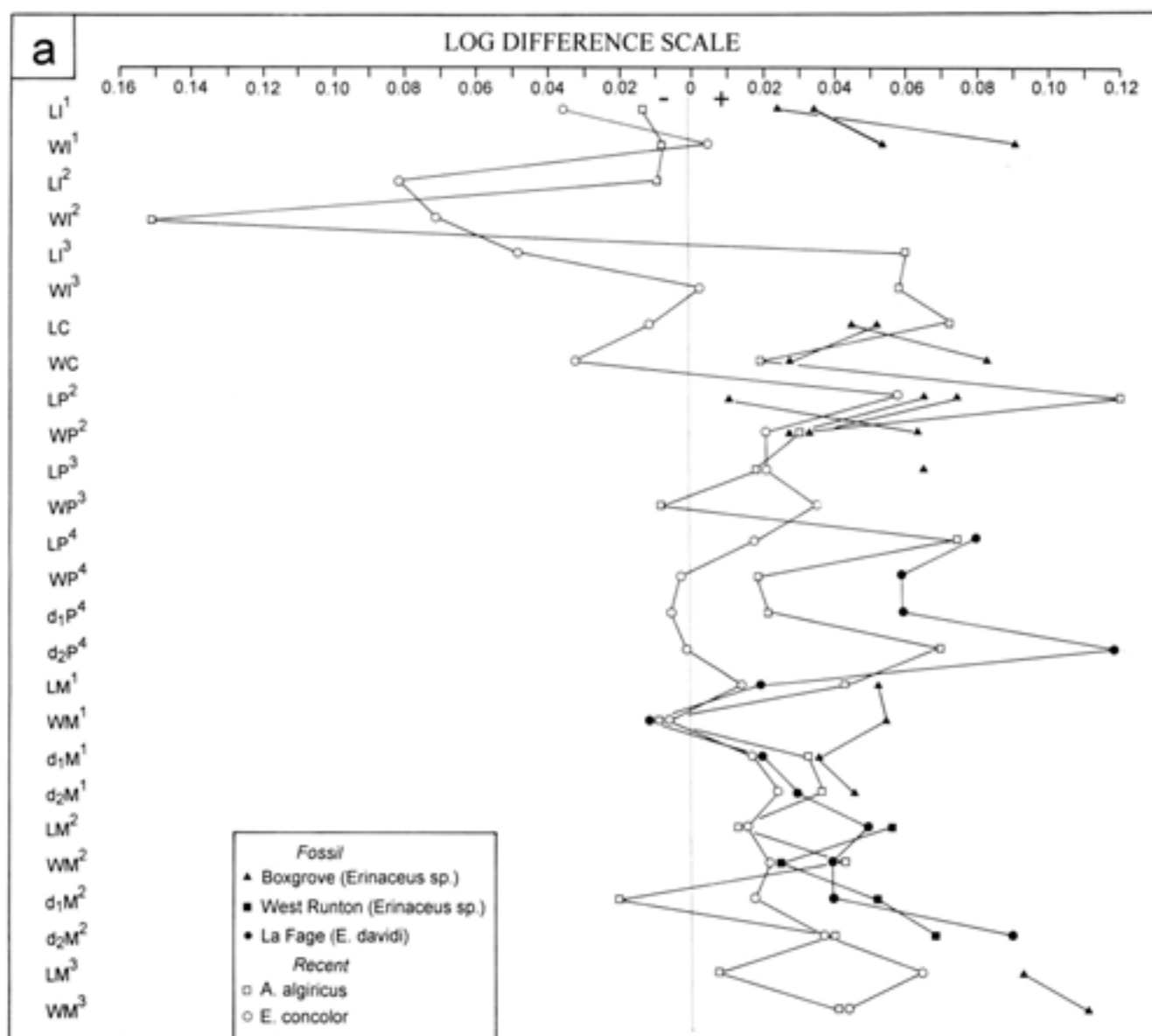
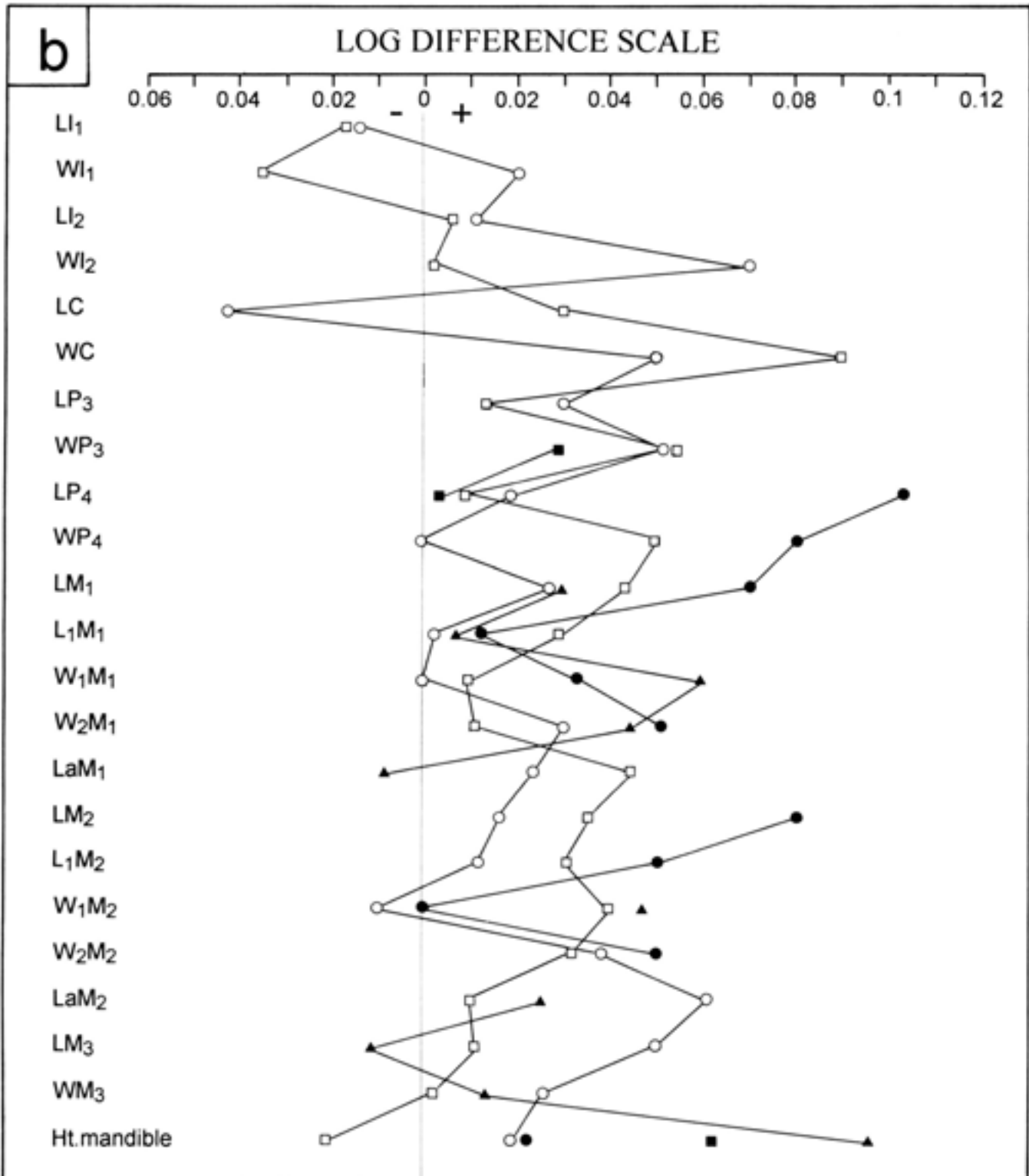


Fig 113 *Erinaceus* spp and *Aethechinus algericus*: log ratio diagram showing relative proportions in a) the upper dentition (above) and b) lower dentition (facing). Standard (vertical line) *E. europaeus* (Recent, England); *E. concolor* (Recent, Europe); *Aethechinus algericus* (Recent, North Africa); *E. davidi* (La Fage, Middle Pleistocene, Jammot 1973); *Erinaceus* sp (West Runton, Cromerian); *Erinaceus* sp (Boxgrove)

in Figures 113 and 114 shows that the Boxgrove specimens are larger than the Recent sample of the western hedgehog (*E. europaeus*) and larger than, or within the upper range of size variation, found in the eastern hedgehog (*E. concolor*). The log ratio diagram (Fig 113) shows that the dental proportions of the Boxgrove specimens are distinct from any of the species with which they are compared although the closest comparisons are with *E. davidi*. Until more complete material is recovered and the taxonomy of the early Middle

Pleistocene hedgehogs is better understood, the Boxgrove material is not identified beyond generic level.

The northern limit of the European hedgehog is determined by climate, particularly the length of the winter which determines the abundance of its invertebrate prey (Macdonald and Barrett 1993). It is found throughout much of Europe with the exception of northern and central Scandinavia. It is a characteristic inhabitant of deciduous woodland, scrub and grassland, and is uncommon in coniferous forests and marshes.



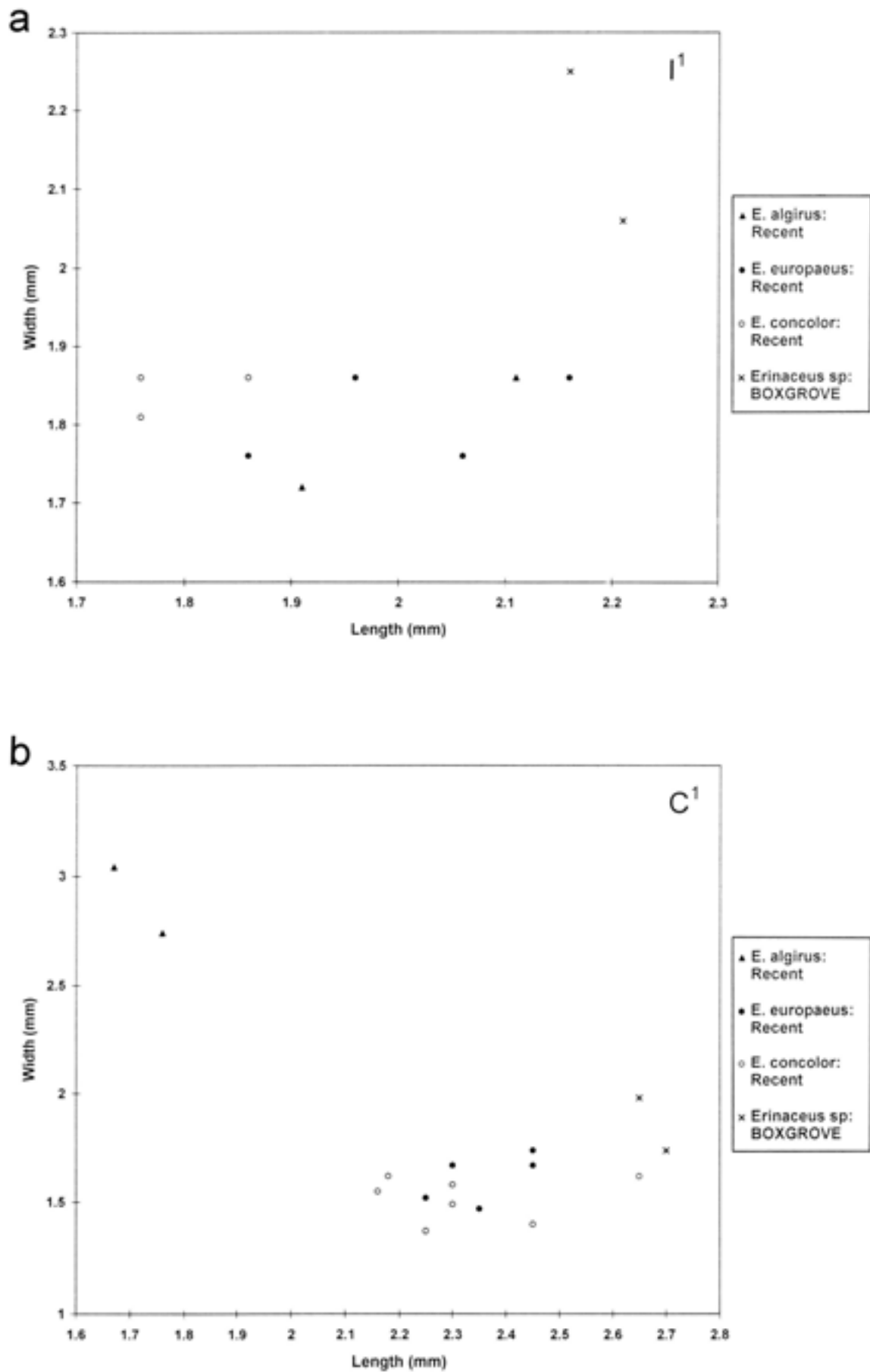
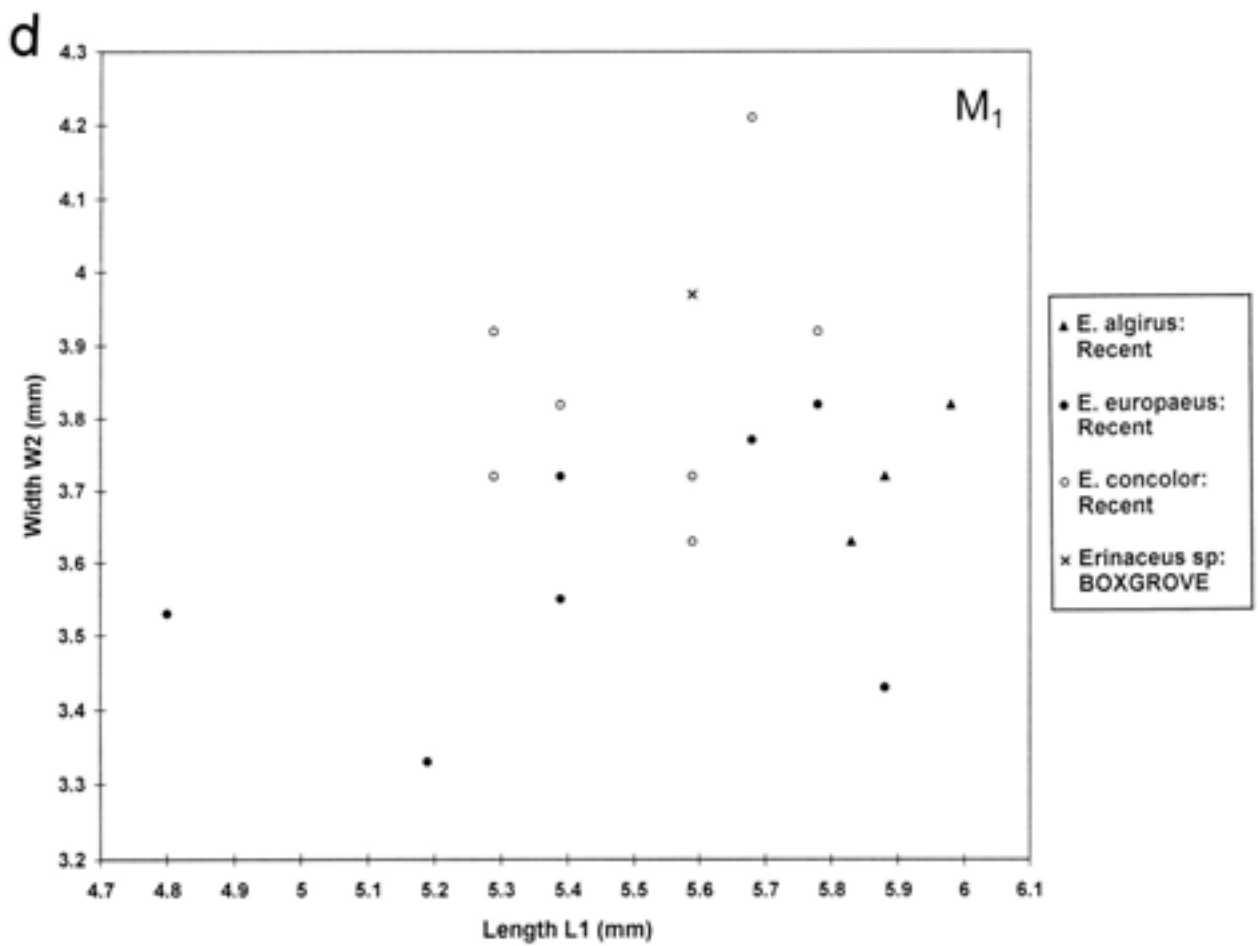
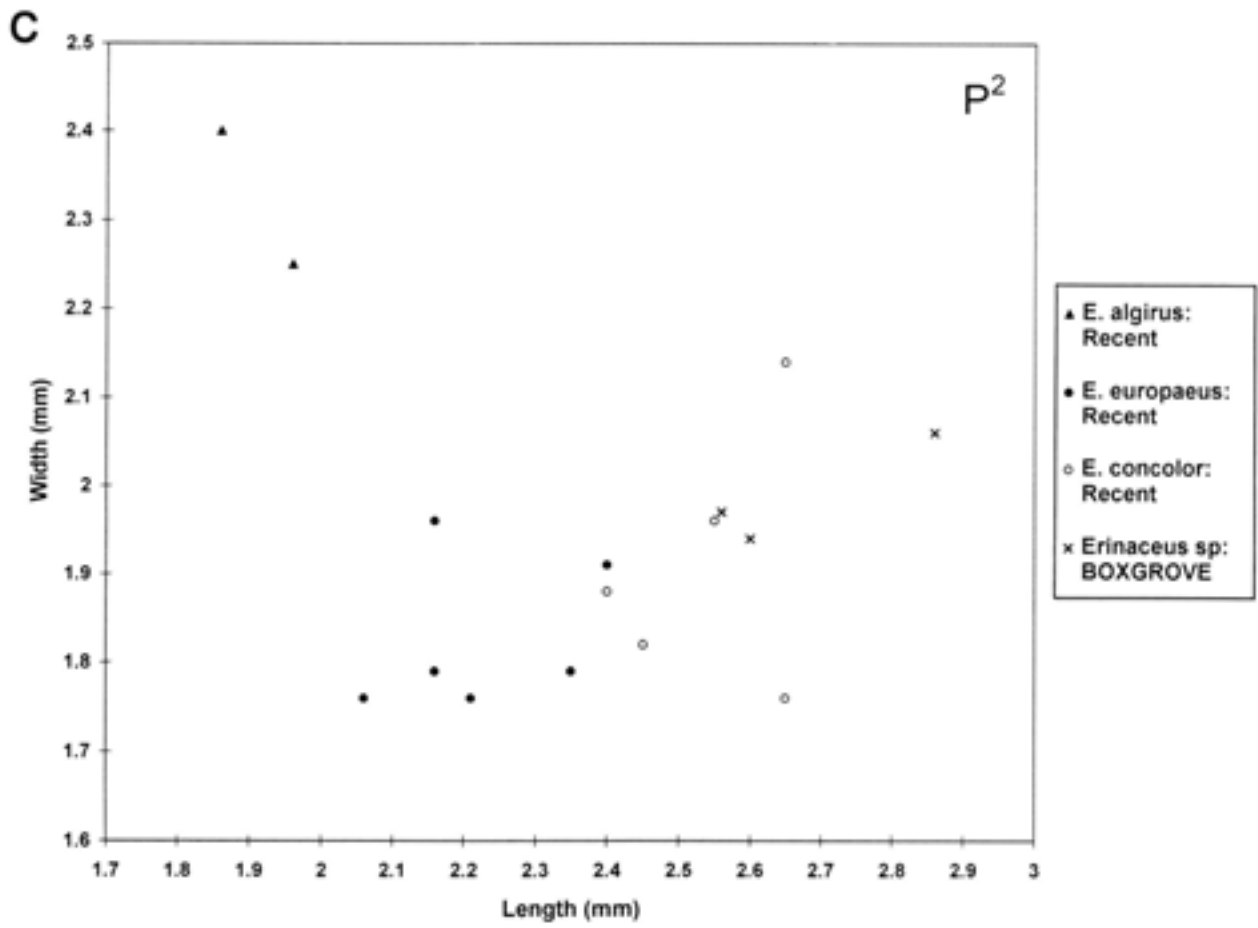


Fig 114a–e *Erinaceus* spp and *Aethechinus algirus*: bivariate plots of length against width of (a–c) upper and (d–e) lower teeth of *Erinaceus* sp from Boxgrove and Recent *E. europæus*, *E. concolor*, and *Aethechinus algirus*



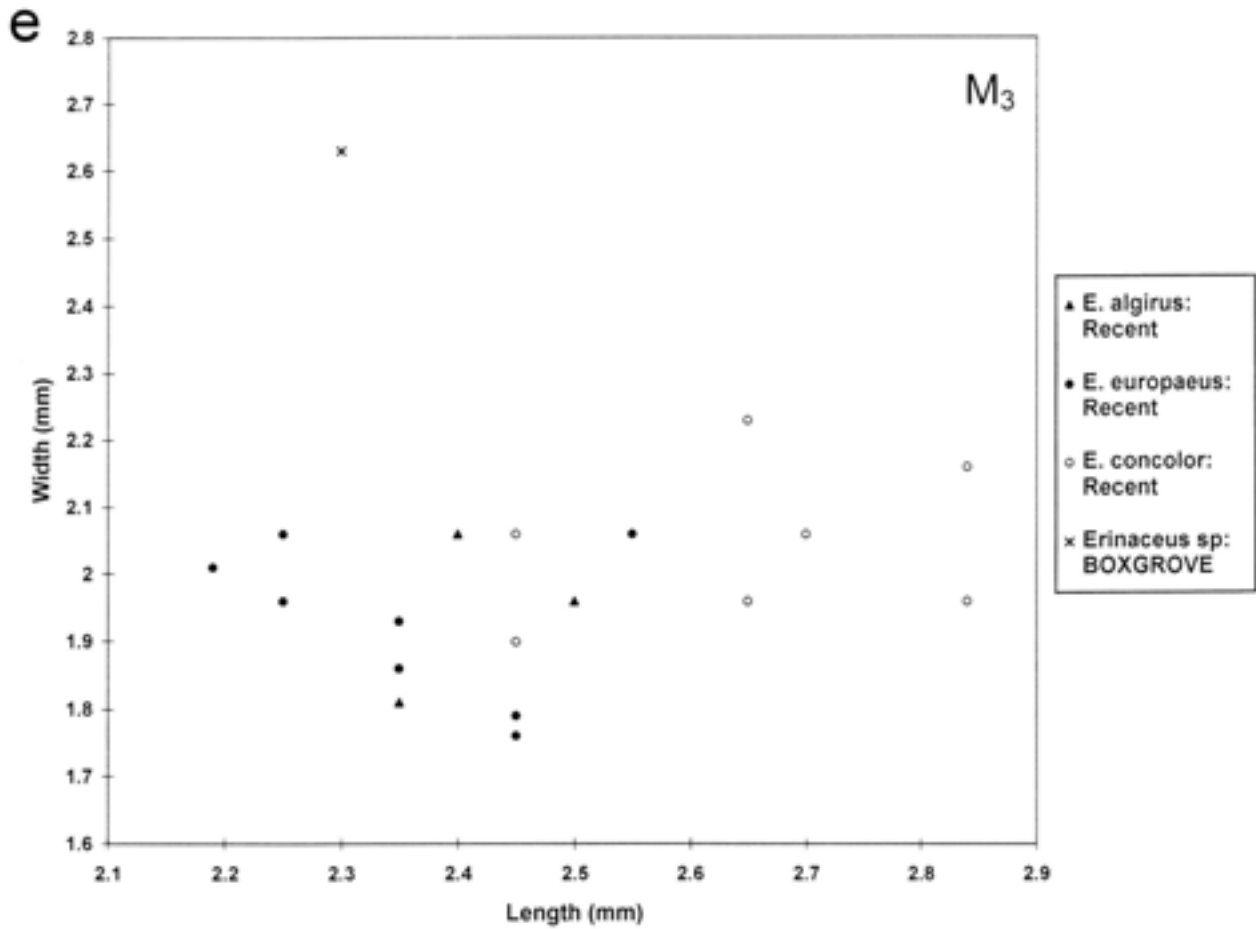


Fig 114e

Table 38 *Erinaceus* sp: measurements (mm) of teeth (q = quarry in this and subsequent tables)

upper dentition

q	area	unit	fauna no	dp ¹		I ¹		C ¹		P ¹		P ²		M ¹					
				L	W	L	W	L	W	L	W	L	W	d1	d2	L	W		
2	GTP 3	4c	BS87-251	-	-	-	-	-	-	2.86	2.06	-	-	-	-	-	-	-	-
2	GTP 17	4c	BS86-97	-	-	2.21	2.06	-	-	-	-	-	-	-	-	-	-	-	-
2	GTP 17	5a	BS86-61	-	-	-	-	2.7	1.74	2.56	1.97	-	-	-	-	-	-	-	-
2	GTP 17	5a	BS86-25	2.47	1.77	-	-	-	-	-	-	-	-	-	-	-	-	-	-
2	GTP 17	5a	BS86-76	-	-	2.16	2.25	2.65	1.98	2.6	1.94	2.63	-	5.68	6.62	6.58	7.64	3.92	2.06

lower dentition

q	area	unit	fauna no	M ₁					M ₂		M ₃		Height of mandible below P ₄
				L	L1	LA	W1	W2	L	W	L	W	
2	GTP17	5a	BS86-76, 74, 64	5.66	5.59	2.06	3.92	3.97 (est)	1.76	3.72	2.3	2.63	7.84

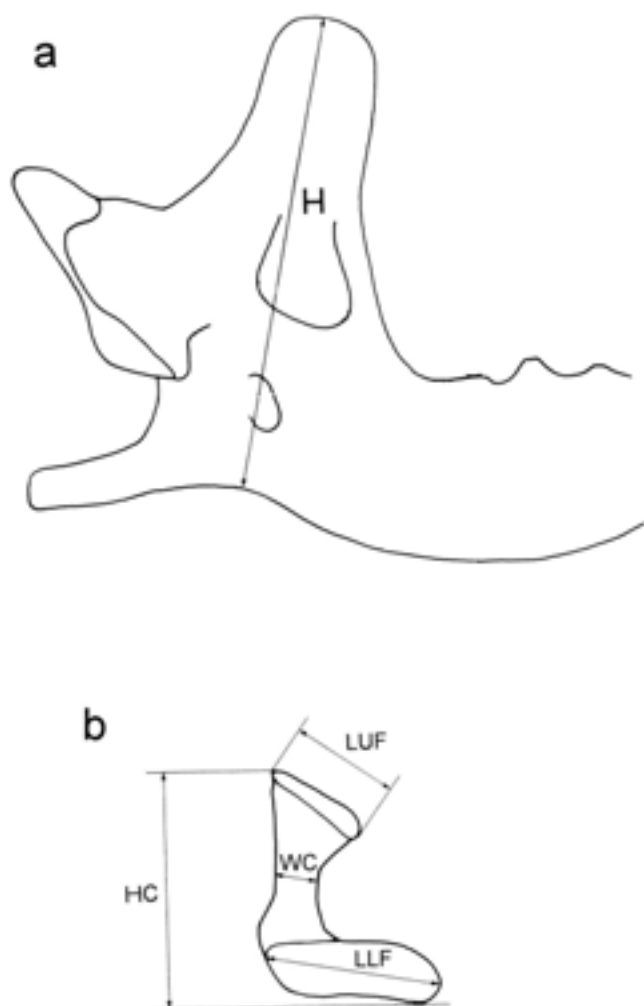


Fig 115 Measurements taken on soricid a) mandibular ramus and b) mandibular condyle; a) height of coronoid process (H), b) height of condyle (HC); lengths of the condylar upper face (LUF) and of the lower face (LLF); and width of the interarticular area (WC)

Family Soricidae

Shrews are common in the Boxgrove fauna and are represented by four species distinguished by morphology and size. The species represented are water shrew (*Neomys* sp), pygmy shrew (*Sorex minutus*), and two extinct shrews, *S. runtonensis* and *S. (Drepanosorex) savini*. The identification of the fossil soricidae is largely based on mandibles and incisors, the presence or absence of pigmentation of the teeth being a useful taxonomic character in Recent Soricidae. In the specimens from Boxgrove, however, pigmentation is rarely preserved. Nomenclature and measurements follow Reumer (1984), and measurements taken on the mandible are shown in Figure 115a-b.

Genus *Neomys*
Neomys sp
 Water shrew

Material summarised in Table 94

The presence of the water shrew (*Neomys* sp) is indicated by mandibles with articular facets separated by a narrow interarticular bridge which is strongly curved inwards, a narrow coronoid process which meets the horizontal ramus at an obtuse angle and an internal temporal fossa which is relatively small and triangular (Fig 116a-b). The lower incisor is unicuspluate (Fig 116e-f) and the upper incisor is bifid with a relatively large talon and a pointed apex (Fig 116c-d). Measurements of the coronoid height of the Boxgrove sample are given in Figure 117 and Table 39 along with a number of Pleistocene and Recent samples of *Neomys* sp.

Two species of *Neomys* have been described by Hinton (1911) from the British Middle Pleistocene: *N. newtoni* from the Upper Freshwater Bed of West Runton, and *N. browni* described on very scanty material from Grays (Thames Middle terrace). According to Hinton (1911), these two species are distinguished on the basis of their small size and on characters of the mandibular condyle. In *N. newtoni*, the interarticular area of the condyle is distinctly narrow and the lower facet is much narrower and longer than *N. browni*; in addition, *N. newtoni* is slightly smaller than *N. browni*.

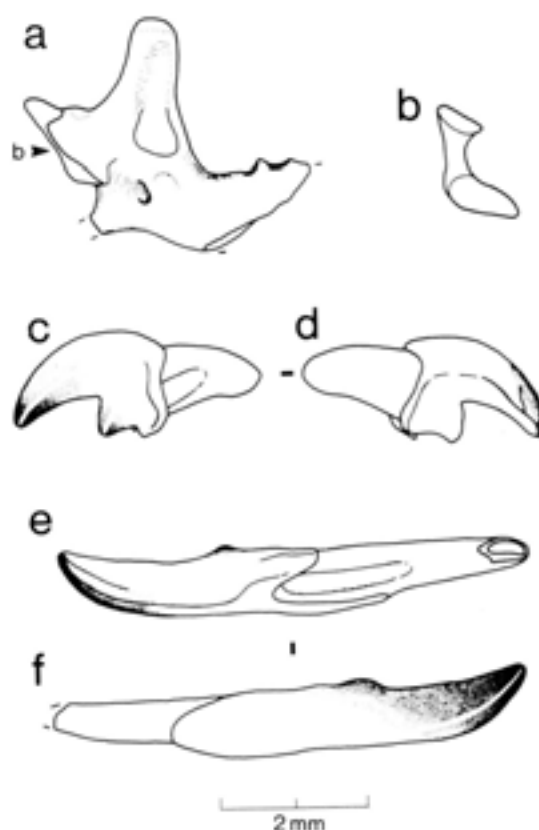


Fig 116 *Neomys* sp: left mandible (Q2 GTP 3 BS86-35 Unit 5a No 42), a) lingual view, b) caudal view of condyle; (c-d) left upper incisor (Q2 GTP 3 BS87-252 Unit 6'3'Fe), c) buccal view, d) medial view; (e-f) left lower incisor (image reversed) (Q2 GTP 3 BS87-252 Unit 6'3'Fe), e) symphyseal view, f) buccal view

Table 39 Comparative measurements (mm) of the coronoid process height and condyle in Recent and fossil *Neomys* spp. The parameters measured on the mandible are: H, height of coronoid process; LUF, length of upper condylar facet; WC, width of interarticular area; LLF, length of lower condylar facet, and HC, height of condyle. Minimum, mean, and maximum values are given for larger samples

	H min- \bar{x} -max	LUF min- \bar{x} -max	WC min- \bar{x} -max	LLF min- \bar{x} -max	HC min- \bar{x} -max
Boxgrove	(4.15, 4.20, 4.21, 4.30)	0.70-0.88-1.00 (n=7)	0.25-0.33-0.40 (n=8)	1.20-1.40-1.70 (n=9)	2.10-2.28-2.45 (n=7)
<i>N. browni</i> , Grays (NHM colln)	(4.15, 4.46)	(0.78, 0.78)	(0.25, 0.39)	(1.37, 1.57)	(2.06, 2.16)
<i>Neomys</i> sp, Beeches Pit		(0.92)	(0.4)	(1.59)	(2.41)
<i>Neomys</i> sp, Barnham	4.41-4.51-4.70 (n=5)	0.85-0.95-1.05 (n=7)	(0.32, 0.33, 0.41)	1.41-1.54-1.63 (n=7)	2.23-2.39-2.68 (n=7)
<i>N. cf newtoni</i> , Westbury (Bishop 1982)	(4.1(est), 4.2, 4.3)	(0.78, 0.88)	(0.29, 0.34)	(1.57, 1.57)	(2.16, 2.25)
<i>N. newtoni</i> , W Runton (NHM colln)	3.82-4.03-4.26 (n=19)	0.88-0.94-0.98 (n=5)	0.25-0.33-0.39 (n=5)	1.47-1.57-1.67 (n=5)	1.96-2.21-2.45 (n=5)
<i>N. fodians</i> , Recent, England (NHM colln)	4.51-4.71-5 (n=10)	1.03-1.16-1.27 (n=10)	0.34-0.49-0.59 (n=10)	1.57-1.81-2.06 (n=10)	2.25-2.48-2.65 (n=10)
<i>N. anomalus</i> , Recent, Spain (NHM colln)	4.21-4.47-4.61 (n=10)	0.88-1.11-1.27 (n=10)	0.49-0.52-0.69 (n=10)	1.47-1.61-1.67 (n=10)	2.06-2.43-2.55 (n=10)

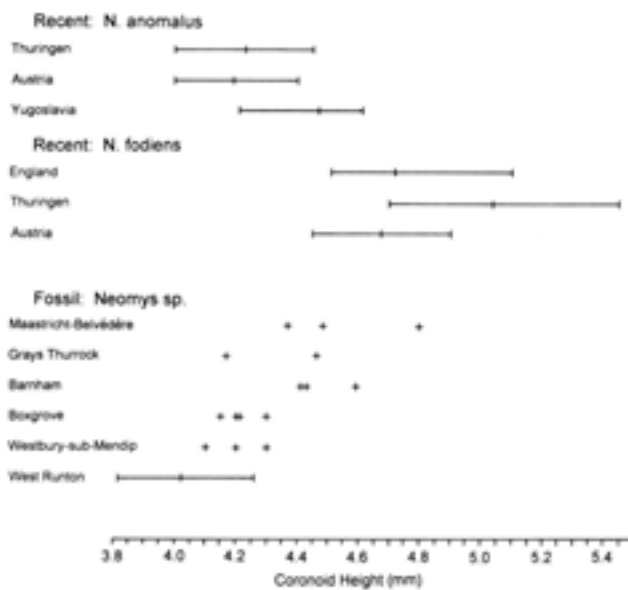


Fig 117 *Neomys* spp: Coronoid height in fossil and Recent specimens. The fossil samples are arranged in a temporal series from the early Middle Pleistocene to late Middle Pleistocene; the observed range and mean are indicated for samples of more than four specimens

Hinton based his description of *N. browni* and *N. newtoni* on a small number of specimens, and it is now apparent from an examination of the much larger sample of *Neomys* from West Runton, as well as comparisons with Recent *Neomys*, that the characters used to distinguish the two fossil forms are variable in Recent *Neomys* and do not provide adequate taxonomic characters. This is supported by a morphometric and multivariate analysis of Recent and fossil *Neomys* (Parfitt and Rosas personal communication) which failed to find

any features which separate Middle Pleistocene *Neomys* from Recent *N. fodians*. Although early Middle Pleistocene *Neomys* is small in comparison with Recent *N. fodians*, there is evidence for an increase in size and robusticity of the *Neomys* during the Middle Pleistocene (Fig 117). The relationship of the early Middle Pleistocene form to the living species is uncertain, and until further material is available to clarify this relationship, the Boxgrove material is identified as *Neomys* sp.

The present day distribution of water shrews covers most of Europe, with the exception of the extreme north of Scandinavia and parts of the Mediterranean region. The water shrew is a semi-aquatic species which shows a preference for still or slow flowing bodies of water.

Genus *Sorex*

Sorex minutus Linnaeus 1766

Pygmy shrew

Unit 4c: Q2 GTP 3 BS87-251 No 25 right mandible frag

Unit GC: Q2 GTP 3 BS87-175 No 65 left mandible with M₁-M₂

The mandibles and dental remains of this species (Fig 118a-c) are characterised by their small size in comparison with other shrews from Boxgrove. Although the Boxgrove sample is sparse, the specimens conform closely in size and are indistinguishable in morphology from the pygmy shrew, *Sorex minutus*. Measurements of the mandibles are given in Table 40.

The pygmy shrew first appears in the Early Pliocene (Rzebik-Kowalska 1991) and is present as a rare element in many Pleistocene small mammal assemblages. Measurements of the mandible show a slight increase in the size of *S. minutus* during the Late Pliocene and Early Pleistocene (Fig 119), while Middle Pleistocene and Recent populations show a remarkable uniformity in size (von Kolfshoten 1985).

Table 40 Dimensions of Boxgrove *Sorex minutus* mandibles compared with British and European fossil material and a Recent sample from Poland

	height of coronoid process (mm)
Boxgrove	2.9, 3.0
Westbury (Bishop 1982)	2.8 (est), 3.1 (est)
Petersbuch (Koenigswald 1970)	2.8–3.2 (n=11)
West Runton (Harrison and Clayden 1993 ^a and NHM collection ^b)	3.07 ^b , 3.07 ^a , 3.14 ^a
Kozi Grzbiet (Rzebik-Kowalska 1991)	2.98–3.09 (n=3)
Osztramos 3/2 (Reumer 1984)	3.01–3.61 (n=23)
Tegelen (Reumer 1984)	3.14–3.43 (n=7)
Csarnóta 2 (Reumer 1984)	2.96–3.38 (n=9)
Osztramos 7 (Reumer 1984)	2.81, 2.94
Poland, Recent (Rzebik-Kowalska 1991)	3.01–3.61 (n=23)

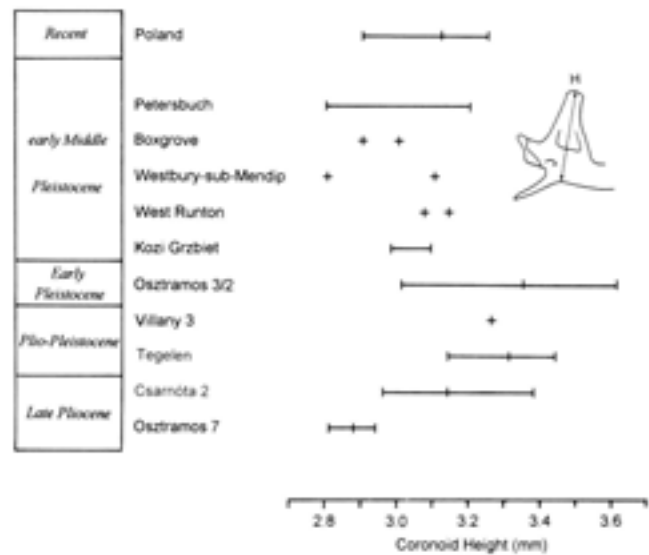


Fig 119 *Sorex minutus*: coronoid height in fossil and Recent specimens

Table 41 Measurements (mm) of *Sorex runtonensis* mandibles from Boxgrove

	n	min	\bar{x}	max
Height of coronoid process	30	3.82	4.01	4.20
Height of condyle	17	1.52	1.74	1.90
Length of upper condylar facet	12	0.70	0.82	0.95
Length of lower condylar facet	18	1.00	1.06	1.15

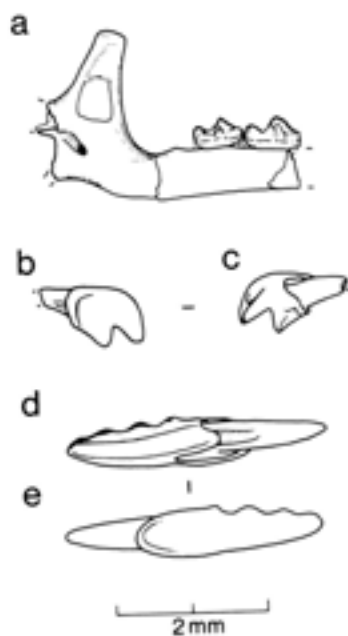


Fig 118 *Sorex minutus*: a) left mandible with M_1 and M_2 (Q2 GTP 3 BS86-175 Unit GC No 65), lingual view; (b–c) right upper incisor (Q2 GTP 3 BS86-55 Unit 5a), b) buccal view, c) medial view; (d–e) left lower incisor (image reversed) (Q2 GTP 3 BS87-252 Unit 6'3'Fe), d) symphyseal view, e) buccal view

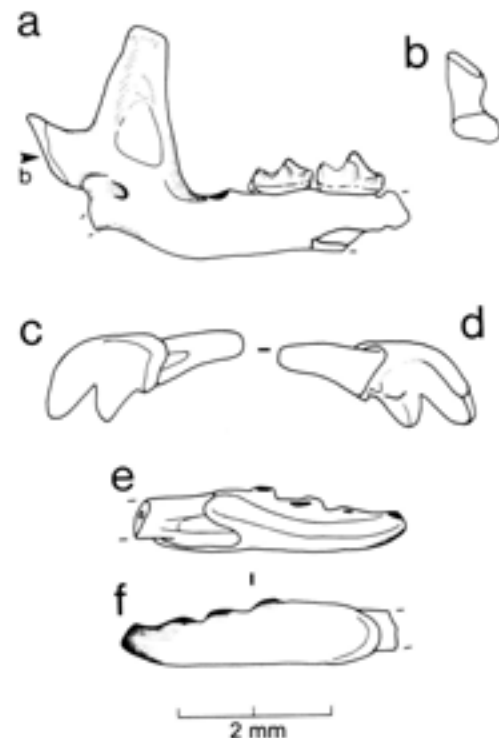
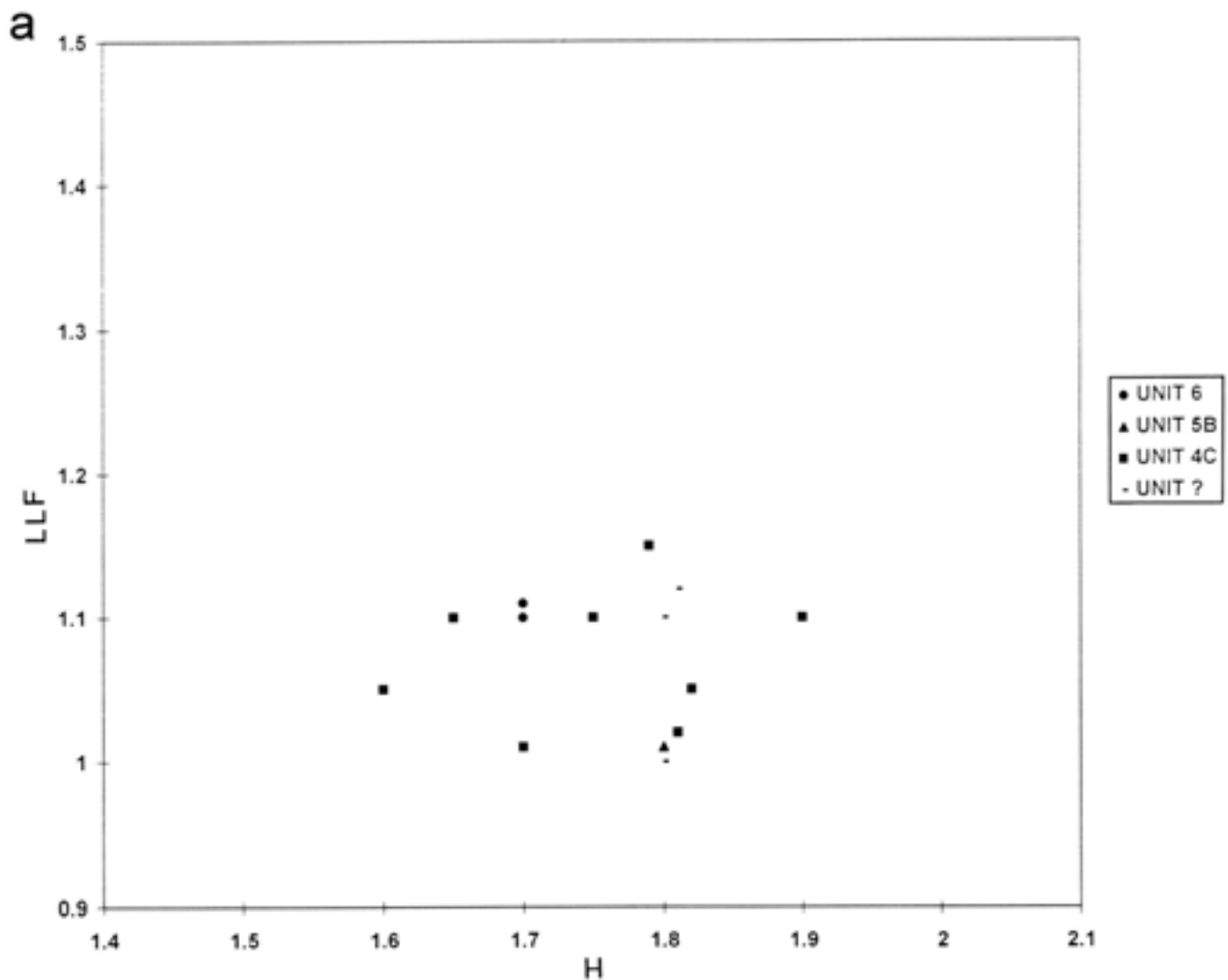


Fig 120 *Sorex runtonensis*: a) left mandible with M_1 and M_2 (Q2 GTP 15 BS86-16 Unit 4c No 14), lingual view, b) caudal view of condyle; (c–d) left upper incisor (Q2 GTP 3 BS87-251 Unit 4c), c) buccal view, d) medial view; right lower incisor (image reversed) (Q2 GTP 3 BS87-322 Unit 6'3), e) symphyseal view, f) buccal view



Today, the pygmy shrew is widely distributed in Eurasia, inhabiting a broad range of habitats which provide adequate vegetation cover.

Sorex runtonensis Hinton 1911
Extinct shrew

- Unit 4c: Q1/B BS87-172 No 3 right mandible frag, BS88-894 No 11 mandible frag; Q2/B BS87-100 left mandible frag; Q2 GTP 3 BS87-181 No 2 right mandible frag with M_2 , BS87-251 No 27 left mandible frag with M_2 , BS87-156 No 30 left mandible frag with M_2 , BS88-539 No 5 left mandible frag, BS86-8 No 9 mandible frag, BS87-270 No 28 left mandible frag, BS86-36 Nos 40, 41 two right mandible frags, BS87-24 Nos 33, 34 two left mandible frags; Q2 GTP 15 BS86-16 No 14 left mandible frag with M_1 - M_2 ; Q2 GTP 17 BS87-96 No 12 mandible frag, BS87-98 No 16 right mandible frag, BS86-52 right mandible frag, BS86-27 No 32 left mandible frag, BS87-97 Nos 38, 39 two left mandible frags
- Unit 5a: Q2 GTP 3 BS86-35 Nos 43, 44 two left mandible frags
- Unit 6'3: Q2 GTP 3 BS87-156 No 29 right mandible frag with M_2 , Q2 GTP 3 BS87-322 No 53 left mandible frag; Q2 GTP 17 BS87-97 No 37 right mandible frag with M_1 - M_2
- Unit LGC: Q2/B BS87-116 Nos 68, 69 two right mandible frags, Nos 70, 71 two left mandible frags
- Unit 5b: Q2 TP 4 BS90-1165 No 60 left mandible frag, No 61 right mandible frag; Q2 SEP 2 BS86-38 No 62 right mandible frag, No 63 left mandible frag
- Unit 6: Q1/B BS88-931 No 50 right mandible frag, BS87-120 No 58 right mandible frag; Q2 SEP 2 BS86-42 No 49 left mandible frag

Table 42 Comparisons of coronoid height measurements in Pleistocene *Sorex runtonensis*, *Sorex* sp from Barnham (Hoxnian) and Recent *Sorex araneus*

	height of coronoid process (mm)			
	n	min	\bar{x}	max
<i>Sorex runtonensis</i>				
Boxgrove	30	3.82	4.01	4.2
Westbury (Bishop 1981)	-	3.80	-	4.4
West Runton	-	3.5	-	4.3
<i>Sorex</i> sp				
Barnham	8	3.95	4.07	4.23
<i>Sorex araneus</i>				
Recent	-	4.2	-	4.9

The extinct shrew *Sorex runtonensis* is the most abundant species of soricid in each of the fossiliferous deposits at Boxgrove. The mandible of *S. runtonensis* differs from other medium-sized species of *Sorex* in having a narrow anteriorly inclined coronoid process. Mandibles and incisors are shown in Figure 120a-f and measurements of the mandible are given in Tables 41 and 42.

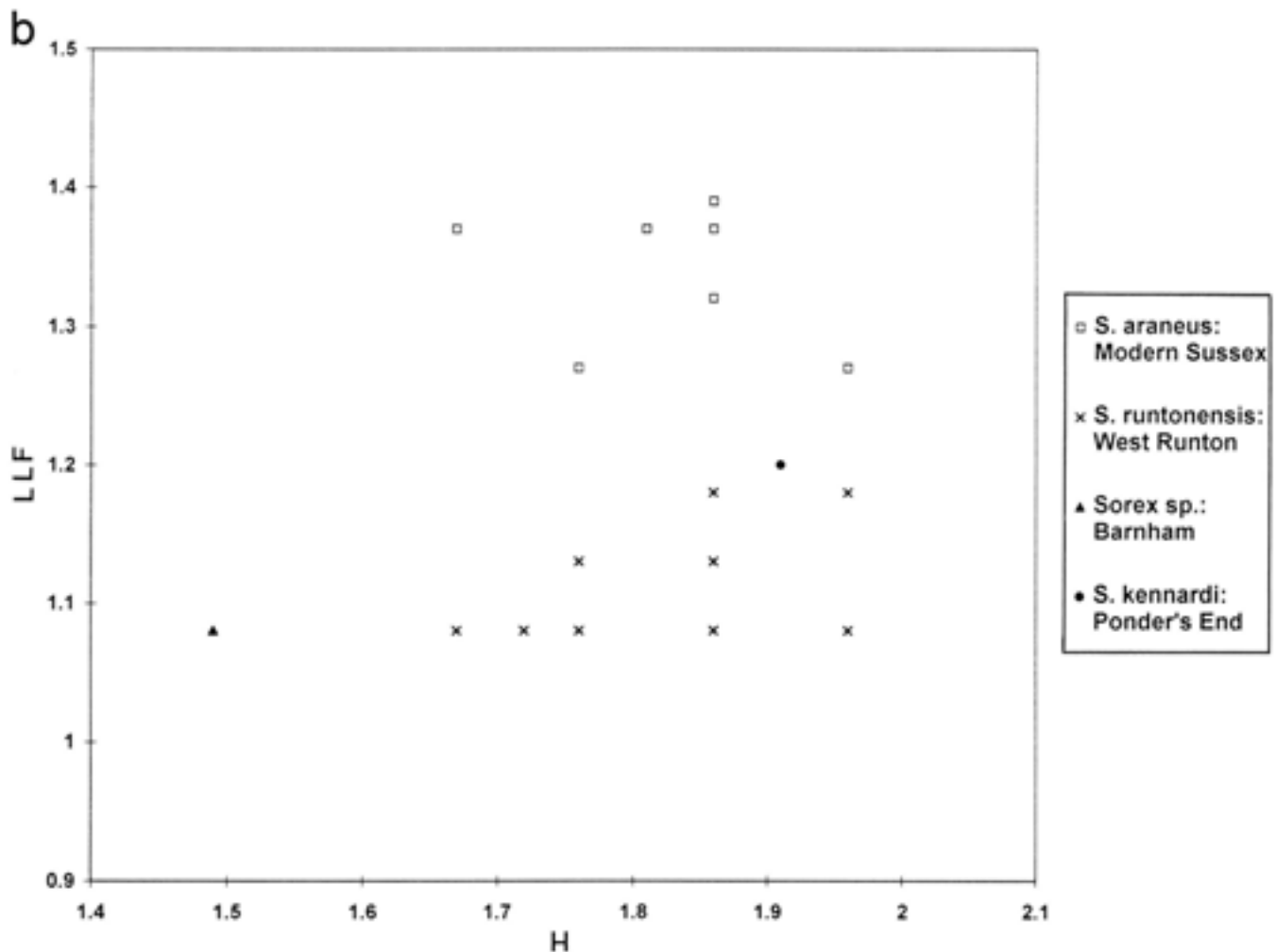


Fig 121a–b (left and above) *Sorex spp.*: length of the lower facet of condyle plotted against condyle height for fossil and Recent specimens. *S. runtonensis* (West Runton, Cromerian sensu stricto, and Boxgrove); *Sorex sp.* (Barnham, early Middle Pleistocene, Hoxnian); *Sorex kennardi* (Ponder's End, Late Pleistocene); *Sorex araneus* (Recent, Sussex)

The Boxgrove mandibles compare closely in size and morphology with *S. runtonensis* from West Runton. *Sorex runtonensis* is common in faunas of Cromerian sensu lato age but is not recorded after the Anglian/Elsterian glaciation (Roberts and Parfitt Chapter 5.9). The sparse remains of a medium-sized *Sorex* from British Hoxnian localities (Barnham and Beeches Pit, Suffolk), although of a similar size to *S. runtonensis* (Table 42) differ in the morphology of the articular condyle (Fig 121a–b).

Sorex (Drepanosorex) savini Hinton 1911
Extinct shrew

Unit 4c: Q2/B BS87-100 No 17 right mandible frag; Q2 GTP 3 BS87-260 No 19 right mandible with M_1 – M_3 , BS86-70 No 20 right mandible frag with M_2 – M_3 , BS87-181 No 1 right mandible frag, BS86-36 No 4 left mandible frag, BS87-263 No 8 right mandible frag, BS86-70 No 21 left mandible frag, BS87-251 No 26 left mandible frag; Q2 GTP 17 BS86-75 No 10 right mandible frag, BS87-97 Nos 35, 36 two left mandible frags
 Unit 5a: Q1/B BS89-1021 No 46 left mandible frag
 Unit 5b: Q2 TP4 BS90-1165 No 59 right mandible frag; Q2 SEP 2 No 64 right mandible frag
 Unit 6: Q1/B BS88-931 No 51 right mandible frag, BS88-931 No 52 left mandible frag, BS87-120 No 57 right mandible frag; Q2 SEP 2 BS86-42 No 48 right mandible with M_1

Sorex (Drepanosorex) savini (Fig 122a–f) is a large shrew with a distinctive ascending ramus and an anterior dentition which shows extreme exo-daenodonty. The mandibles from Boxgrove show a strong resemblance to the type collection of this species described by Hinton (1911) from the Upper Freshwater Beds at West Runton. The mandible (Fig 122a–b) is characterised by a comparatively robust condyle, a large coronoid process with a well developed external temporal fossa, and the tip of the coronoid process is large and boss-like with a distinct coronoid spicule. Measurements of the Boxgrove mandibles are given in Table 43 and comparisons with Middle Pleistocene *S. (Drepanosorex) spp.* are given in Table 44.

The *Sorex (Drepanosorex)* lineage appears to have its origin in the Plio-Pleistocene of Europe. *Sorex (D.) praearaneus*, the oldest and the most primitive member of the subgenus, is first recorded in the Villanyian at such sites as Villany and Tegelen. This species is considered by Reumer (1984; 1985) to be close to the origin of *Drepanosorex* from an ancestral *Sorex* stock. Reumer (1984; 1985) has revised the taxonomy of the *S. (Drepanosorex)* group and described a sequence of forms from the primitive *S. (D.)*

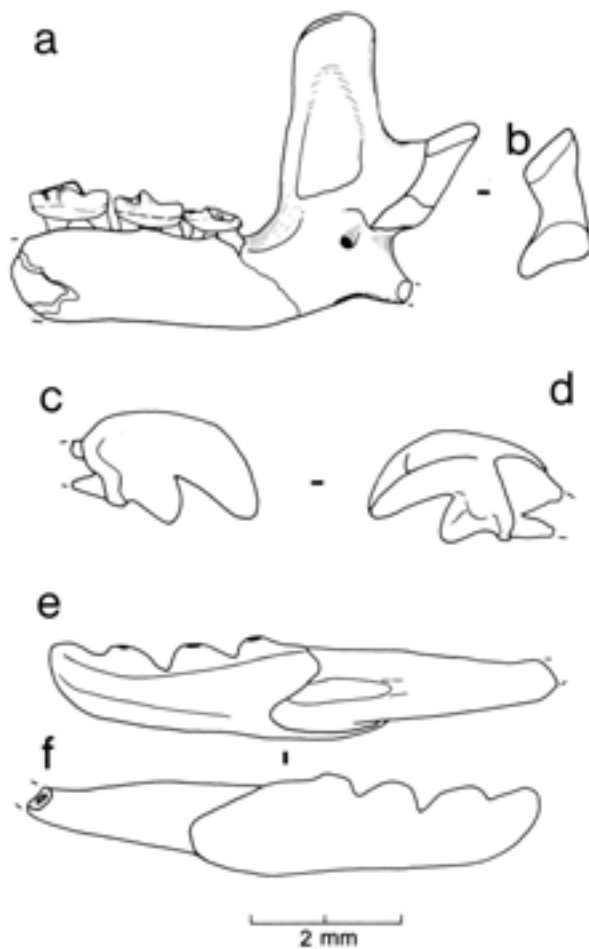


Fig 122 *Sorex (D.) savini*: (a–b) right mandible with M_{1-3} (Q2 GTP 3 BS87-260 Unit 4c No 19), a) lingual view, b) caudal view of condyle; (c–d) left upper incisor (Q2 GTP 3 BS86-36 Unit 4c), c) buccal view, d) medial view; (e–f) left lower incisor (image reversed) (Q2 GTP 3 BS86-36 Unit 4c), e) symphyseal view, f) buccal view

praeareaneus (late Villanyian and Biharian) to *S. (D.) margaritodon* (early Biharian) and thence to *S. (D.) savini* and *S. (D.) austriacus* in the Cromerian *sensu lato*. Morphological trends in the evolution of the lineage during the Early and Middle Pleistocene include an increase in size, enlargement of the mandibular condyle and the development of a more exoedaeodont (bulbous) anterior dentition. These dental and mandibular modifications reach their most extreme form in *S. (D.) savini* and *S. (D.) austriacus* which are recorded from the end of the 'Cromerian Complex'. Although generally considered to be distinct species, *S. (D.) savini* and *S. (D.) austriacus* are morphologically indistinguishable, the only difference being the larger size of *S. (D.) austriacus*.

A further species of *S. (Drepanosorex)* from the late Biharian is the enigmatic species, *S. (D.) postsavini* Horáček and Lozeck (1988), which was originally described by von Koenigswald (1970) as *Sorex* cf *S. margaritodon*, from the Middle Pleistocene site of Petersbuch. This species has a less specialised dentition and is somewhat smaller than the contemporary *S. (D.) savini/austriacus* group. The origin and relationship of this species is

Table 43 Mandible measurements (mm) of *Sorex (Drepanosorex) savini* from Boxgrove

	n	min	\bar{x}	max	SD
Height of coronoid process	15	5.32	5.66	6	0.21
Height of condyle	13	2.5	2.87	3.15	0.17
Length of upper condylar facet	12	1	1.26	1.45	0.12
Length of lower condylar facet	14	1.25	1.53	1.7	0.11

Table 44 Comparative measurements (mm) of the coronoid process height in early Middle Pleistocene *Sorex (Drepanosorex) spp*

	height of coronoid process (mm)
Boxgrove	5.32–6 (n=15)
<i>S. (D.) savini</i> , Westbury (Bishop 1982)	5.4–5.7
<i>S. (D.) postsavini</i> (<i>S. cf S. margaritodon</i> cf von Koenigswald 1970, Petersbuch)	4.4–5.5
<i>S. (D.) austriacus</i> , Hundsheim (Rabeder 1972)	5.7–6.4
<i>S. (D.) savini</i> , West Runton (Jánossy 1969)	5.3–5.9 (n=24)
<i>S. (D.) savini</i> , Kozi Grzbiet (Rzebik-Kowalska 1991)	5.68

problematic, although Horáček and Lozeck (1988) have suggested that it evolved from *S. (D.) savini* during the 'Cromerian Complex'. An alternative phylogenetic scheme is proposed by Rzebik-Kowalska (1991) who advocated that the two lineages diverged as early as the Pliocene, giving rise to a lineage of large forms with specialised dentition and a small and relatively conservative lineage *S. (D.) praeareaneus*–*S. (D.) postsavini*.

Whereas the more specialised forms become extinct during the Anglian/Elsterian, the fate of *S. (D.) postsavini* is less certain, although it may have survived until the late Pleistocene (Rzebik-Kowalska 1991). According to Horáček and Rzebik-Kowalska, there are morphological similarities between *S. (D.) postsavini* and the living dusky shrew (*Sorex isodon*) and they suggest that *S. (D.) postsavini* may be the ancestor of this species. What is certain is that the specialised forms of *Sorex (Drepanosorex)* which were widespread in faunas of the Cromerian *sensu lato* in western Europe are not recorded from post Anglian/Elsterian contexts. The presence of *Sorex (D.) savini* at Boxgrove is therefore of biostratigraphic importance (Roberts and Parfitt Chapter 5.9).

Family Talpidae

Genus *Talpa*

Talpa europaea Linnaeus 1758

European mole

Material summarised in Table 94

The highly distinctive bones and teeth of the mole are common in the main fossiliferous deposits at Boxgrove. Humeri measurements given in Fig 123a–c

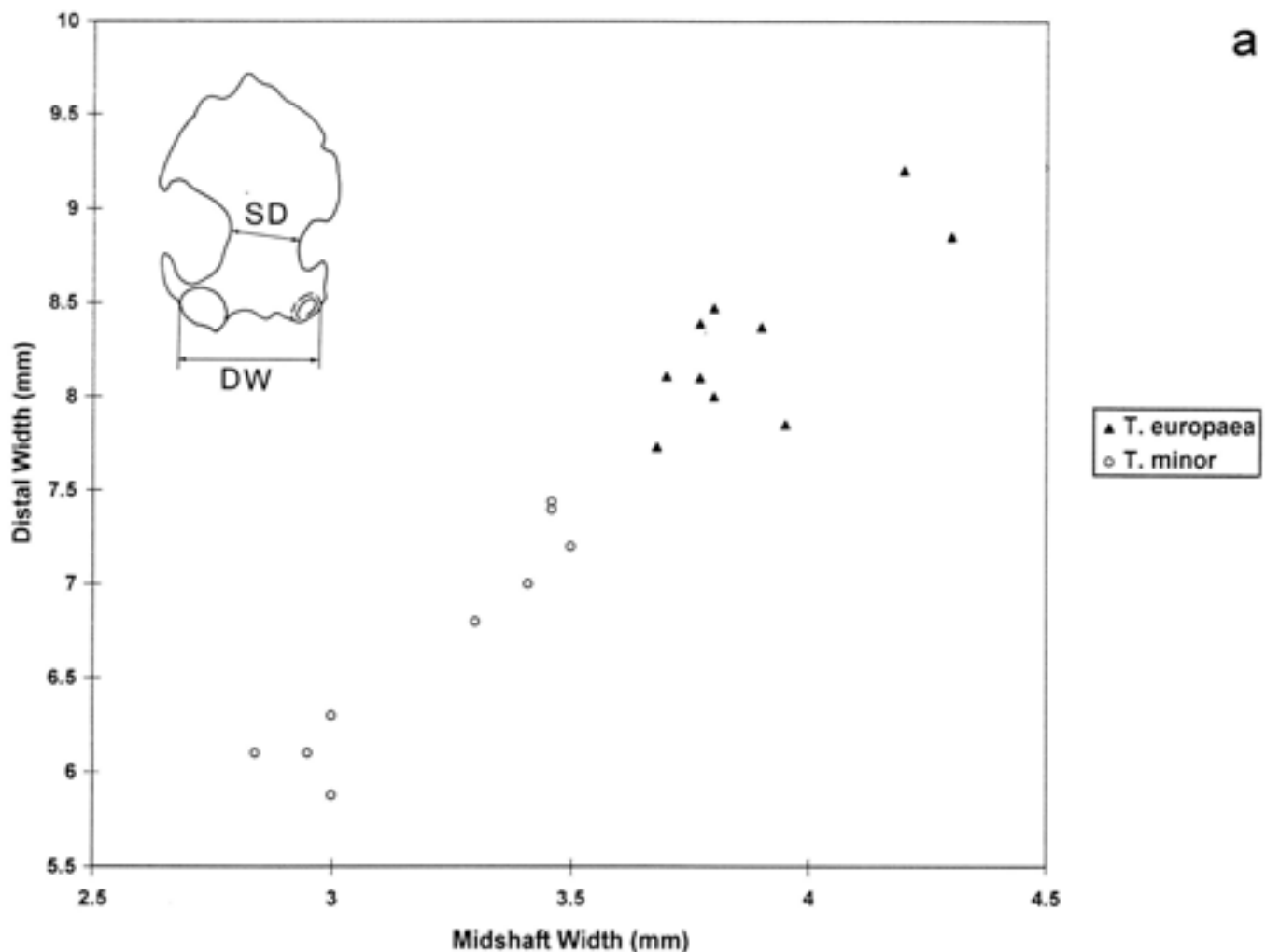


Fig 123a *Talpa* spp: distal epiphysis width (DW) in relation to shaft width (SD) of humeri from Boxgrove Unit 5a

Table 45 *Talpa* spp. Measurements (mm) of Pleistocene and Recent mole humeri

	<i>n</i>	<i>distal width</i>	<i>n</i>	<i>diaphysis width</i>
<i>T. europaea</i> , Boxgrove	29	7.30–8.28–9.20	38	3.59–3.87–4.30
<i>T. minor</i> , Boxgrove	29	5.88–6.73–7.85	40	2.73–3.18–3.52
<i>T. europaea</i> , Ostend	7	7.8–8.11–8.76	8	3.91–4.14–4.60
<i>T. europaea</i> , Petersbuch (von Koenigswald 1970)	–	7.4–9.4	–	3.3–3.4
<i>T. europaea</i> (= <i>T. magna</i>), Kleine Scheuer (Late Pleistocene)	–	8.4–10.8	–	3.9–5.3
<i>T. europaea</i> , Igtham Fissure (Late Devensian/Holocene)	37	7.89–8.48–9.45	37	3.69–3.94–4.31
<i>T. europaea</i> , Recent, Germany	14	7.8–9.2	14	3.8–4.6
<i>T. europaea</i> , Recent, Spain	16	8.1–9.9	16	4.3–4.7

and Table 45 show the presence of two mole species, the smaller extinct mole *T. minor* and the larger European mole *T. europaea*. The material from Unit 5a plotted in Fig 123a shows four clusters of measurements; the two clusters of smaller size represent males and females of *T. minor* and the two clusters of larger size represent males and females of *T. europaea*. This size variation within the two species is consistent with the range of sexual dimorphism observed in the skeleton between males and females in Recent mole populations (Neithammer and Krapp 1990). Based on the

comparative measurements given in Table 45, it can be seen that the humeri of *T. europaea* from Boxgrove are within the range of measurements of living *T. europaea* and of those from the early Middle Pleistocene site of Petersbuch.

Moles are widely distributed in Europe with the exception of northern Scandinavia. They occur in a range of habitats, in particular deciduous woodland and open grassland, and they favour dry fertile soils with an abundant burrowing invertebrate fauna. The northern range of their distribution is probably limited

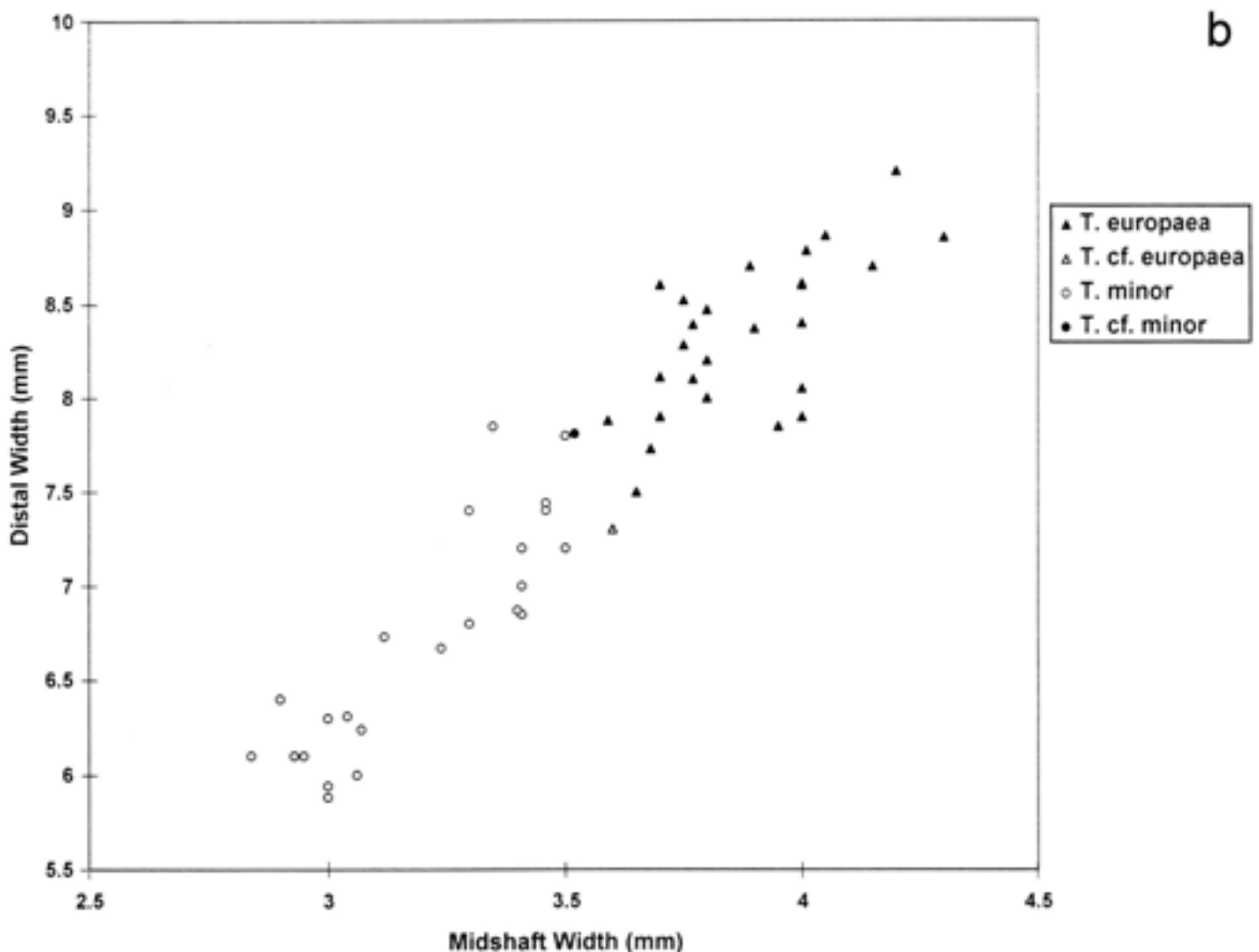


Fig 123b *Talpa* spp: distal epiphysis width (DW) in relation to shaft width (SD) of humeri from Boxgrove combined sample

Table 46 Comparative measurements (mm) of Recent and fossil *Plecotus* spp

	length	width	crown height
<i>P. auritus</i> (Recent, British Isles)			
upper canine (n=9)	0.89–0.97–1.07	0.80–0.84–0.89	–
M ² (n=9)	1.20–1.26–1.33	1.69–1.83–1.87	–
lower canine (n=9)	0.72–0.80–0.87	0.79–0.81–0.87	1.08–1.29–1.56
P ₂ (n=9)	0.44–0.51–0.58	0.54–0.57–0.61	–
<i>P. austriacus</i> (Recent, British Isles)			
upper canine (n=6)	1.16–1.22–1.27	0.98–1.02–1.07	–
M ² (n=6)	1.42–1.49–1.53	1.93–1.98–2.09	–
lower canine (n=5)	0.89–0.94–0.99	0.93–0.98–1.01	1.42–1.49–1.6
P ₂ (n=6)	0.56–0.61–0.63	0.62–0.64–0.67	–
<i>P. auritus</i> (Boxgrove)			
upper canine (BS88-955)	(1.07)	(0.89)	–
lower canine (BS86-18)	(0.88)	(0.87)	(1.43)
lower canine (BS86-62)	–	(0.81)	–
M ² (BS86-25)	(1.41)	(1.96)	–
P ₂ (BS86-25)	(0.79)	(0.63)	–
<i>P. auritus</i> (= <i>P. abeli</i>) (Late Pleistocene, Mixnitz)			
upper canine	(0.81, 0.82, 0.84)	(0.57, 0.64, 0.62)	–
M ² (n=23)	1.28–1.39–1.44	1.75–1.88–1.98	–
lower canine (n=10)	0.90–0.97–1.03	0.80–0.83–0.92	–
<i>P. auritus</i> (Hundsheim)			
M ²	1.33, 1.39, 1.35	1.92–1.86–1.95	–

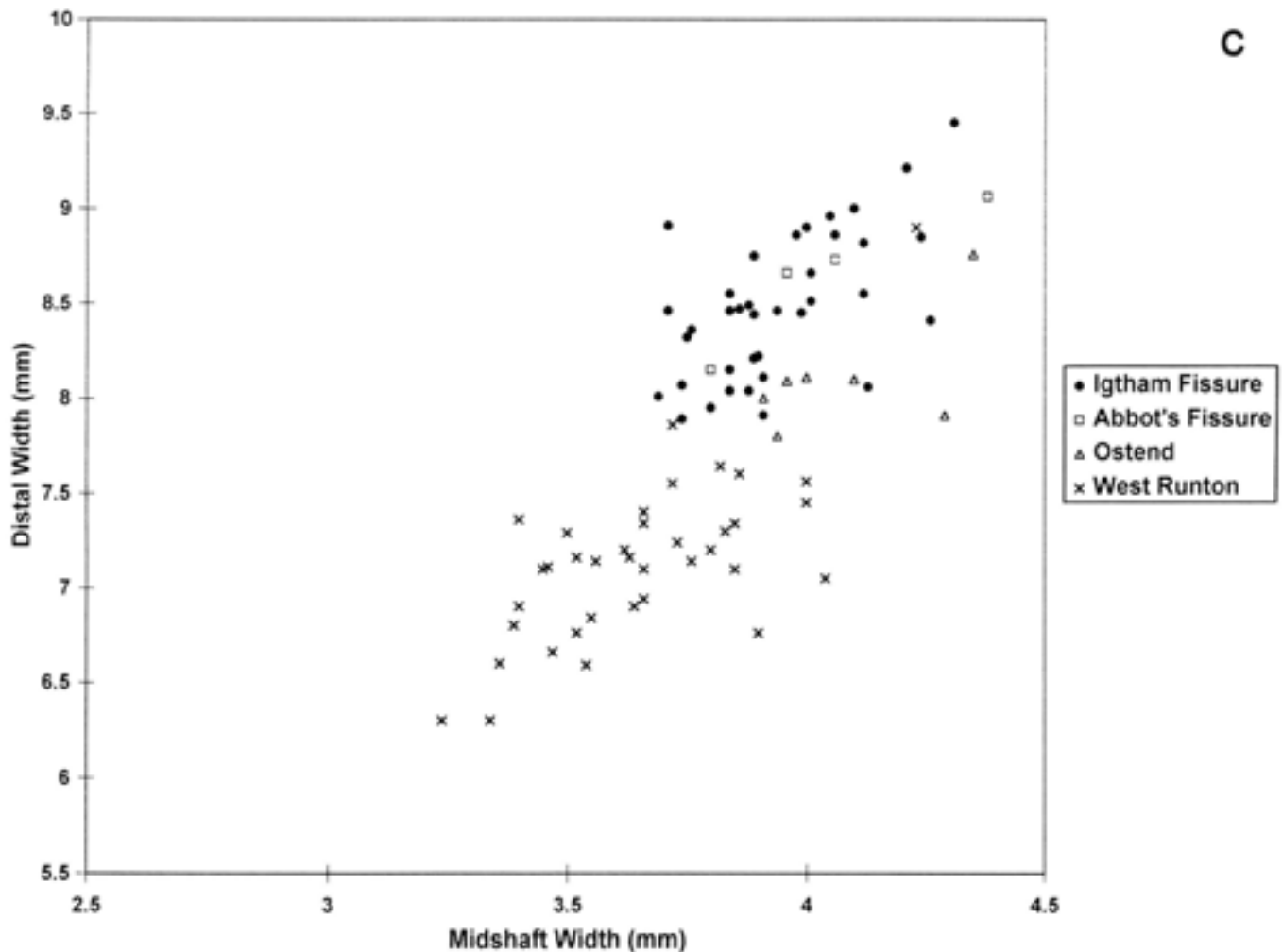


Fig 123c *Talpa* spp: distal epiphysis width (DW) in relation to shaft width (SD) of *homeri* from *T. europaea*: Igtham Fissure and Abbot's Fissure (Late Devensian/Holocene), Ostend (early Middle Pleistocene); *T. europaea* and *T. minor*: West Runton (Cromerian sensu stricto)

by temperature and the scarcity of earthworms in permanently or seasonally frozen soils.

Talpa minor (Freudentberg 1914)
Extinct mole

Material summarised in Table 94

In addition to the material from Boxgrove, *T. minor* is known from three other pre-Anglian sites, West Runton, Sugworth and the Calcareous Member of Westbury-sub-Mendip (Bishop 1982), as well as from Swanscombe, Barnham, and Beeches Pit which are thought to be Hoxnian in age. According to Kurtén (1968), it is not recorded in north-western Europe after the Hoxnian/Holstenian Interglacial.

Order Chiroptera
Family Vespertilionidae
Genus *Plecotus*
Plecotus auritus Linnaeus 1758
Common long-eared bat

Unit 4c: Q1/B BS 88-955 right upper canine; Q2 GTP 3 BS 87-251 right M³, left P₂
Unit 5a: Q2 GTP 17 BS 86-18 right lower canine, left lower canine, left P₁ fragment; Q2 GTP 17 BS86-62 left lower canine

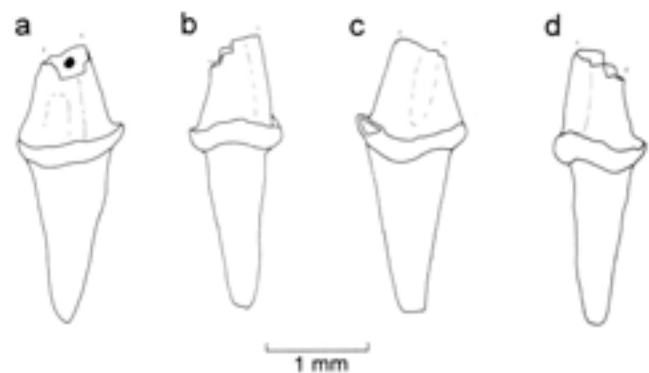


Fig 124 *Plecotus auritus*: right upper canine (Q1/B BS88-955 Unit 4c), a) lingual view, b) mesial view, c) buccal view, d) distal view

The upper canine has pronounced labial and lingual furrows and the cross-section below the cingulum is triangular (Fig 124a-d). This tooth is identical to the upper canine of *P. auritus*. The lower canines (Figs 125a-d, 126a-d), P₄, P₂ (Fig 127a-d) and M² (Fig 128) are indistinguishable from those of *P. austriacus* and *P. auritus*.

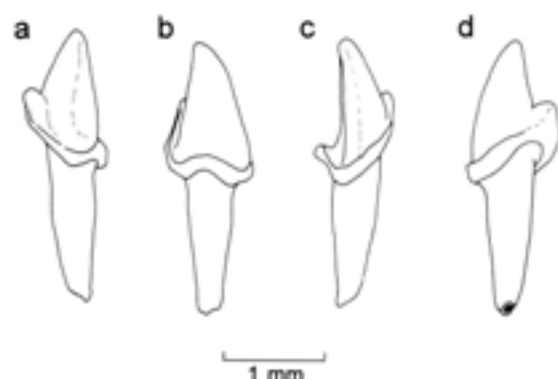


Fig 125 *Plecotus auritus*: right lower canine (Q2 GTP 17 BS86-18 Unit 5a), a) lingual view, b) distal view, c) buccal view, d) mesial view

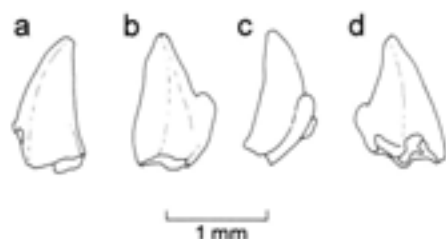


Fig 126 *Plecotus auritus*: left lower canine fragment (Q2 GTP 17 BS86-62 Unit 5a), a) buccal view, b) distal view, c) lingual view, d) mesial view

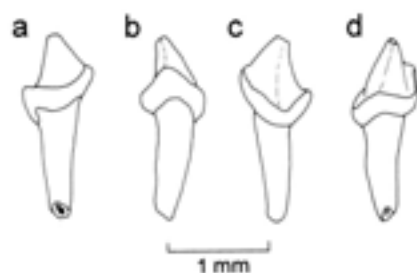


Fig 127 *Plecotus auritus*: left P₂ (Q2 GTP 3 BS87-251 Unit 4c), a) lingual view, b) distal view, c) buccal view, d) mesial view



Fig 128 *Plecotus auritus*: right M₂ (Q2 GTP 3 BS87-251 Unit 4c), occlusal view

The upper canine can be attributed to *P. auritus* on the basis of its distinctive crown morphology (Stebbing 1967). The remaining teeth, although identical to *Plecotus* spp, are not sufficiently diagnostic to refer to species. Measurements of the Boxgrove specimens given in Table 46 are larger than the mean values of *P. auritus*, and in some cases exceed the range of variation observed in the Recent sample. The measurements are consistent with the larger size of this species during the Pleistocene and indicate that a single species is represented by this material.

In Europe, the long-eared bats are represented by two closely related species: *P. auritus* and *P. austriacus*. Fossil long-eared bats are known from many Pleistocene localities and according to Sevilla (1988) this material can be referred to *P. auritus*. *P. austriacus* is not recorded in the European Pleistocene and the species probably spread into Europe during the Holocene.

As with the other bats recorded at Boxgrove, the common long-eared bat is a woodland species which favours deciduous and to a lesser extent mixed woodland.

Genus *Myotis*

Myotis mystacinus (Kuhl 1817)

Whiskered bat

Unit 4c: Q2 GTP 3 BS 87-273 right upper canine; Q1 GTP 16 BS86-24 right upper canine, left upper canine, molar fragments

A small species of *Myotis*, either *M. mystacinus* or *M. brandti* is represented by three upper canines (Figs 129a-d, 130a-d) and a number of molar fragments. The sibling species *M. brandti* (Brandt's bat) and *M. mystacinus* (whiskered bat) are difficult to distinguish using external morphology and were only recognised as separate species in 1970 (Hanák 1970; 1971). The dentition of these two forms is distinctive; in particular, the relationship in size between the P₂ and P₃, the position of the P₃, the morphology of the lower canine (Gauckler and Kraus 1970) and the morphology of the P⁴ (Rylsar 1976) allow separation of living and fossil material. Unfortunately, these diagnostic elements are not represented in the Boxgrove sample. However, comparisons with recent reference material shows that the Boxgrove specimens are similar to *M. mystacinus* in their morphology and dimensions (Table 47).

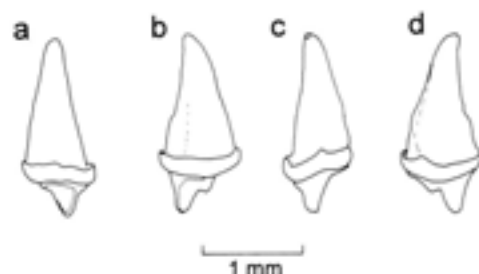


Fig 129 *Myotis mystacinus*: left upper canine (Q1 GTP 16 BS86-24 Unit 4c), a) mesial view, b) buccal view, c) distal view, d) lingual view

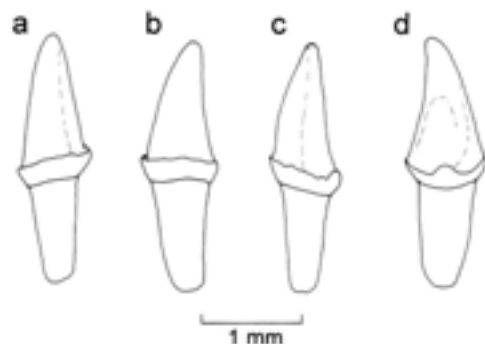


Fig 130 *Myotis mystacinus*: right upper canine (Q2 GTP 3 BS87-273 Unit 4c), a) mesial view, b) buccal view, c) distal view, d) lingual view

The fossil history of these two forms (*M. brandti* and *M. mystacinus*) is poorly known. According to Rylsar (1976) *M. mystacinus* is not present in Europe before the Holocene, whereas *M. brandti* is recorded from a number of Pleistocene localities.

Both *M. mystacinus* and *M. brandti* are widely distributed across most of Europe although *M. brandti* is not found in southern and western Europe at the present day. *M. brandti* is characteristic of broadleaved woodlands and is often found roosting with *M. mystacinus*. Although *M. mystacinus* is also found in woodland it favours more open habitats than *M. brandti*. The whiskered bat feeds in practically any biotope, eating a wide range of small insects.

Myotis bechsteini (Kuhl 1817)
Bechstein's bat

Unit 4c: Q1/B BS87-247 left upper incisor; Q2 GTP 3 BS83-36 left lower canine, right upper incisor

Myotis bechsteini is represented by three isolated teeth from Unit 4c (Fig 131a-d, 132a-d). A minimum of two individuals are represented by a left upper incisor

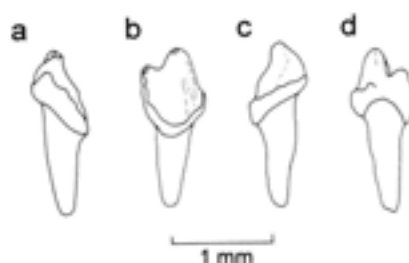


Fig 131 *Myotis bechsteini*: left upper incisor (Q2 GTP 3 BS86-36 Unit 4c), a) lingual view, b) distal view, c) buccal view, d) mesial view

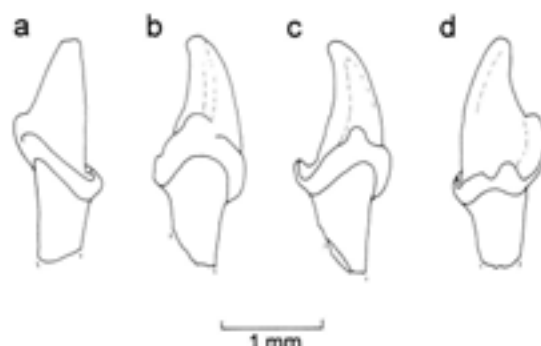


Fig 132 *Myotis bechsteini*: left lower canine (Q1/B BS87-247 Unit 4c), a) buccal view, b) mesial view, c) lingual view, d) distal view

from GTP 16 and an associated left lower canine and right upper second incisor from GTP 3. The morphology of these specimens agree with Recent *M. bechsteini* to which the fossil material is assigned. The measurements given in Table 48, compared with those given by Topal (1963; 1964), show that the Boxgrove specimens fall within the combined size range of Recent *M. bechsteini* from the British Isles and continental Europe.

Table 47 Comparative measurements of the upper canines of *Myotis mystacinus* from Boxgrove and Recent specimens from England

	length min- \bar{x} -max	width min- \bar{x} -max	crown height min- \bar{x} -max
<i>M. mystacinus</i> (Recent, England) (n=6)	0.80-0.83-0.89	0.63-0.73-0.76	1.25-1.36-1.47
<i>M. mystacinus</i> (Boxgrove)			
BS87-273	0.8	0.69	1.33
BS86-24	0.81	0.70	1.26

Table 48 Comparative measurements of *M. bechsteini* from Boxgrove and Recent specimens from England

	length min- \bar{x} -max	width min- \bar{x} -max	crown height min- \bar{x} -max
<i>M. bechsteini</i> (Recent, England)			
Upper incisor (n=7)	0.62-0.67-0.74	0.53-0.56-0.61	/
Lower canine (n=7)	0.98-1.06-1.16	0.81-0.9-0.98	1.33-1.37-1.42
<i>M. bechsteini</i> (Boxgrove)			
Upper incisor (BS87-247)	0.73	0.62	/
Lower canine (BS86-36)	0.97	0.89	1.53

Bechstein's bat has been recorded from many Pleistocene sites in continental Europe dating from the Early Pleistocene until the Holocene (Ryslár 1976; Sevilla 1988).

The presence of *M. bechsteini* at Boxgrove is environmentally important as it is dependent on extensive areas of deciduous and mixed woodland at the present day. It is a solitary species which roosts in trees throughout the year and feeds almost exclusively on moths and beetles which it captures in flight or gleans from foliage.

Order carnivora
Family Canidae
Genus *Canis*

Canis lupus Linnaeus 1758
Wolf

Unit 4b: Q1/A F3445 skull with complete dentition

Unit 4c: Q1/B F6 left P¹, F25 right ulna frag, proximal, F9 right metacarpal V frag; Q1 TP4 F1* maxilla, crushed, with left I¹-P¹ right P¹-M¹=same individual (F1*-F15*), F11* right I¹, F12* left I¹, F10* right I¹, F13* left I¹, F15* right I¹, F5* right C¹, F6* right P¹, F14* left M¹ with maxilla frag, F7* left M¹, F3* right mandible with right I¹-M¹, ascending ramus missing, F2* left mandible with I¹-M¹, ascending ramus missing, F4* left I¹, F8* right I¹, F9* right I¹; Q2 GTP 13 F23 right I¹ frag, F3 left C¹, crushed, F2 right C¹ root missing, F7 right P¹, F1 left M¹, F6 right M¹, F19 left M¹, F8 right humerus, distal, F25 left radius shaft frag, F12 ulna frag shaft, F17 metapodial shaft frag (cf); Q2 GTP 17 F3 left I¹; F6 right I¹, F7 right C¹, F8 left C¹, F1 right P¹, F9 mandible with left C¹P¹-M¹ + attached right I¹, right with I¹C¹P¹-M¹, refits, F63 right M¹, F4 right M¹, refits (F4, F9, F10), F10 left M¹, refits, F399 left metacarpal V frag, F34 left calcaneus, F56 left metatarsal III shaft, F615 first phalanx; EQP Q2 TP6 right P¹

Unit 5a/4c: Q2 GTP 17 F41 right radius, distal and shaft

Unit 5a: Q1/B BS87-233 F314 metapodial shaft frag (cf); Q2 GTP3 F58 left I¹; Q2 GTP 13 F4 left I¹, BS86-3 F26 right I¹, BS86-3 F27 left P¹, F22 left P¹, F9 right ulna shaft; Q2 GTP 17 BS86-81 F1039 right C¹, BS86-81 F1040 left C¹ crown, BS86-83 F1041 left P¹, BS86-83 F1042 right P¹, F50 right P¹, F73 left M¹, BS86-83 F1044 right I¹, BS86-83 F1043 right I¹, F501 right C¹, F65 left C¹, BS86-81 F1048 right scapula frag, glenoid and neck, F499 left humerus shaft frag, F135 right radius shaft, F53 left ulna, proximal, BS86-83 F1050 right ulna, distal, F159 left ulna shaft frag, BS86-81 F1059 pisiform, F52 trapezoid, BS86-83 F1051 left accessory carpal, BS86-81 F1055 left carpal IV, BS86-81 F1057 right metacarpal III shaft, BS86-81 F1058 sesamoid (cf), F66 left patella, BS86-80 F1054 patella, BS86-80 F1053 right calcaneus, proximal, F70 left astragalus, BS86-81 F1056 left tarsal II, F1063 right metatarsal II, proximal and shaft frags, F39 right metatarsal II, proximal and shaft, BS86-80 F1061 metatarsal IV frag, F40 first phalanx (cf), F97 first phalanx, BS86-83 F1052 second phalanx frag (cf)

Unit 5b: Q2 GTP 17 F586 left P¹, F317 left radius, proximal and shaft, F101 right navicular frag, F588 right metatarsal II, F68 left metacarpal III, proximal and shaft, F587 first phalanx

Unit 5c: Q2 GTP 17 F318 metapodial shaft (cf)

Unit 6/5a: Q2 GTP 17 F83 left I¹

Unit 8 (Upper Chalk Pellet Beds): Q2 GTP3 F74 left humerus frags, proximal and part of distal

Unit 6: Q1/B F134 right ulna frag (trochlear notch), left accessory carpal, right and left radial, right acetabulum frag, left patella, two metapodial frags (distal), 10 sesamoids, 4 first phalanx frags, second phalanx, F301 BS87-120 left I¹; Q2 GTP 4 F1* maxilla with right I¹C¹P¹-M¹, left I¹C¹P¹-M¹=same individual (F1*-F5*), F4* right I¹, F5* left I¹, F3* left I¹, F2* left M¹ frag

Misc: EQP Q1 TP1 (gully fill 11) left I¹

The wolf, *Canis lupus*, is the most abundant of the large carnivores in the Boxgrove assemblage. The material includes a complete cranium from Unit 4b

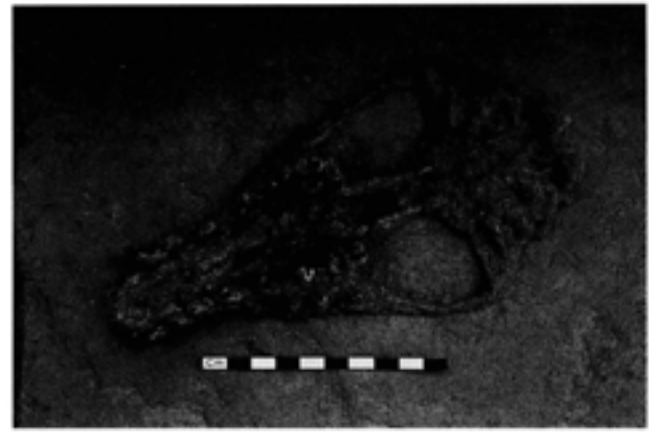


Fig 133 *Canis lupus*: skull (Q1/A F3445 Unit 4b); scale unit 10mm



Fig 134 *Canis lupus*: left mandible (Q2 TP4 F2 Unit 4c)

(Fig 133), two maxillae, and a number of mandibles (Fig 134), as well as a relatively large number of isolated teeth and postcrania. Measurements are given in Table 49 and the length of the lower carnassials from Boxgrove and other British Pleistocene localities is given in Table 50.

The taxonomy of the European wolf has been discussed by Kurtén and Poulanos (1977) who suggest that *C. lupus* probably derived from one of the small Villafranchian wolf-like canids, either *C. etruscus* Major or *C. arnensis* Del Campana. The Middle and Late Pleistocene history of the European wolf lineage is characterised by a gradual but significant size increase from the relatively small early Middle Pleistocene wolf to those of the last glaciation, which represent animals of a size larger than the living north European wolf. Comparisons with other Pleistocene samples show that the Boxgrove specimens are of a similar size to those from other European early Middle Pleistocene sites such as Mosbach and smaller than those from the Holstenian site of Lunel-Viel (Bonifay 1971). Whether the small Middle Pleistocene wolf should be referred to a separate taxon, *C. l. mosbachensis* or *C. mosbachensis*, as suggested by some authors, is still unresolved.

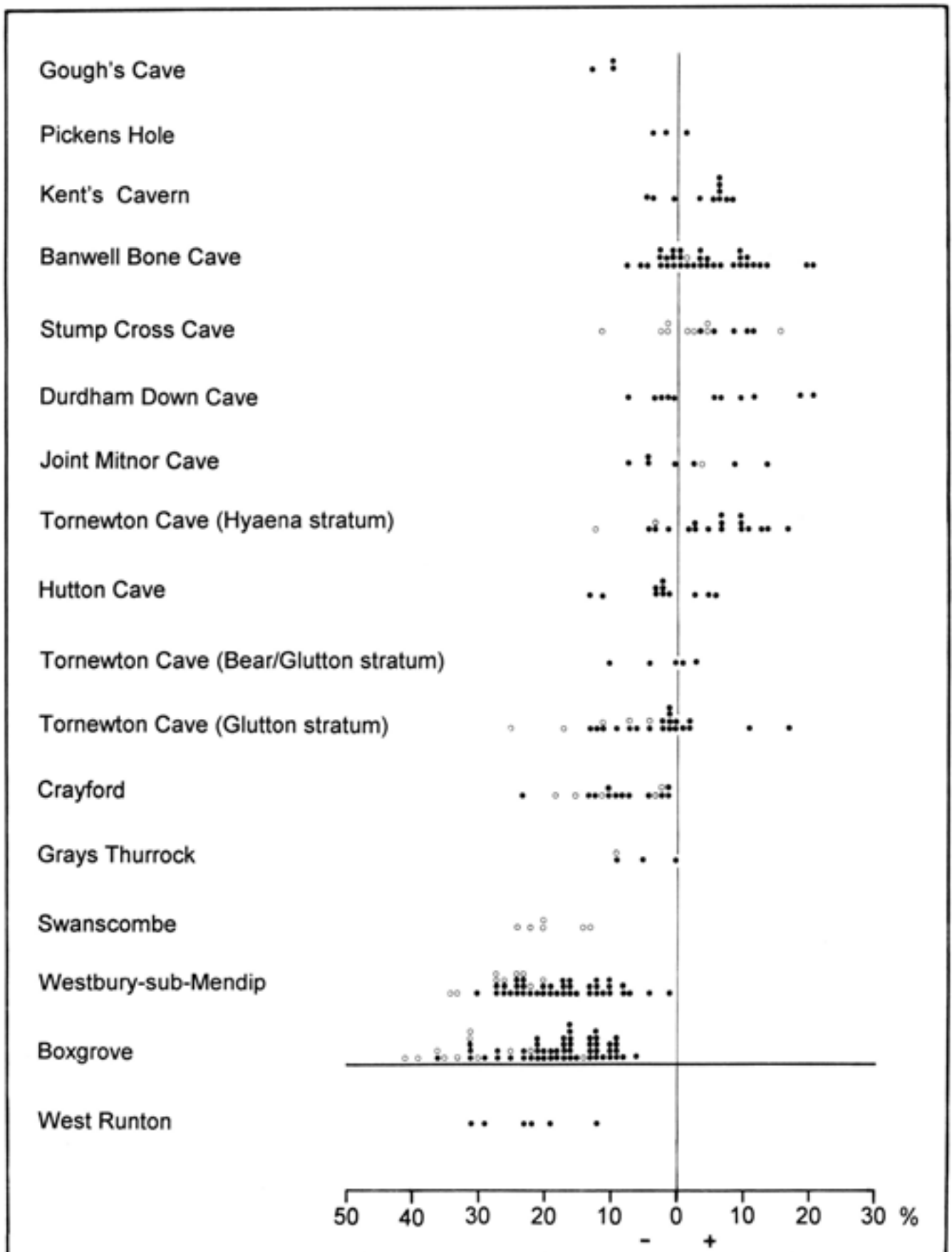


Fig 135 *Canis lupus*: measurement comparisons of British Pleistocene with Recent European wolf. The fossil specimens are plotted as a percentage deviation from the mean of the Recent sample (vertical line), and the sites are arranged in an approximate temporal sequence (circles = postcrania; dots = teeth)

Table 50 Comparative measurements (mm) of the lower carnassial in British Pleistocene and Recent *Canis lupus*

	<i>n</i>	<i>min</i>	\bar{x}	<i>max</i>
Recent				
Europe	12	25.4	28.3	31.8
Devensian				
Goughs Cave	1		(25.7)	
Pickens Hole	1		(27.6)	
Kents Cavern (Cave Earth)	4	27.6	29.2	30.4
Banwell Cave	7	28.2	29.8	31.4
Stump Cross Cave	1		(31.5)	
Durdham Down	1		(31.2)	
Last Interglacial				
Tornewton Cave (Hyaena Stratum)	8	27.3	29.7	32.0
'Saalian Complex'				
Hutton Cave	1		(28)	
Tornewton Cave (Bear/Glutton Stratum)	1		(29.2)	
Tornewton Cave (Glutton Stratum)	5	24.5	27.2	28.1
Crayford	2		(25.4, 25.5)	
Grays	1		(25.9)	
Pre-Anglian				
Westbury	4	21.2	23.1	24.2
Boxgrove	3	23.3	22.6	23.7

However, as there are no significant morphological differences between the early Middle Pleistocene and Recent European wolf, the designation of the Middle Pleistocene form to a separate taxon on the basis of size is probably not warranted.

The question of the timing and nature of the size increase in the British Pleistocene wolf lineage was investigated by comparing the postcranial and dental dimensions from a number of localities by means of a percentage diagram (Fig 135). This method compares each measurement of the fossil sample with a standard set of measurements, in this case a sample of Recent European wolf in the collections of the Natural History Museum (London). The percentage diagram has an advantage in that it allows comparisons to be made between localities when the sample size is too small to compare individual bone measurements. In Figure 135, the samples from the available British Pleistocene localities are arranged in a temporal series spanning the Cromerian to Devensian Lateglacial Interstadial. The percentage diagram shows that there was a gradual size increase in the wolf lineage between the Cromerian and the last interglacial, followed by a period of stasis during the last interglacial and the Devensian. In this series, the Boxgrove sample agrees in size with West Runton, Westbury, and the limited sample of postcrania from Swanscombe which, *contra* Bishop (1981) indicate an animal of similar size to the pre-Anglian group.

Family Ursidae
Genus *Ursus*
Ursus deningeri Reichenau 1906
Extinct cave bear

- Unit 4: Q1/B F340 right mandible frag, horizontal ramus with M_2 alveolus, F341 right M_2 , early wear, juvenile
Unit 4c: Q1/B F163 right prob I, F5 right C, F122* left ectoconiform, F124 left cuboid, F119* left navicular, * = same individual (F119*, F120*, F121*, F122*, F124*), F125 left metatarsal V, F121 left metatarsal IV, F120 left metatarsal III; Q1 TP220-80 F1 left humerus, proximal and posterior missing, F2 right fibula shaft; Q2/B F50* right mandible with C_1 , P_1 - M_2 , early wear, juvenile/subadult, F90* left M_2 , crushed, F47* right I_1 , * = same individual (F47*, F48*, F49*, F50*, F90*), F48* left I_1 , F49* right I; Q2 GTP 3 F1 left zygomatic process of temporal, refits (F1, F41), F41 left zygomatic process of malar, refits, BS87-124 F78 right P_2 , F71 left mandible frag with M_2 , M_3 , mid-wear, adult
Gully Fill (Deformed Unit 4): Q1/A F3501 right calcaneus, proximal missing
Unit 4c/5a: Q1/B F43 right ulna shaft frag, crushed
Unit 5a: Q1/A F3360 left astragalus; Q1/B F87 left humerus, proximal missing, crushed, F267 left patella (cf), F144 left metatarsal II, distal frag, F98 left I, F7 left I
Unit 6: Q1/A F3500 right M_2 , early-mid wear, young adult, F1 right I_2 ; Q1/B BS87-120 F302 right I
Unit 6-8: Q1 TP220-80 F3 humerus shaft frag
Unit 8: Q2 GTP 25 F11 C, frag, F14 right humerus frag, proximal, crushed

The bear (*Ursus deningeri*) is the second most abundant large carnivore at Boxgrove. The material consists mainly of postcrania (Figs 137, 138), although a small number of isolated teeth and a complete mandible (Fig 136) were also recovered. Measurements are given in Table 51 and biometrical comparisons are shown in Figures 139-41.

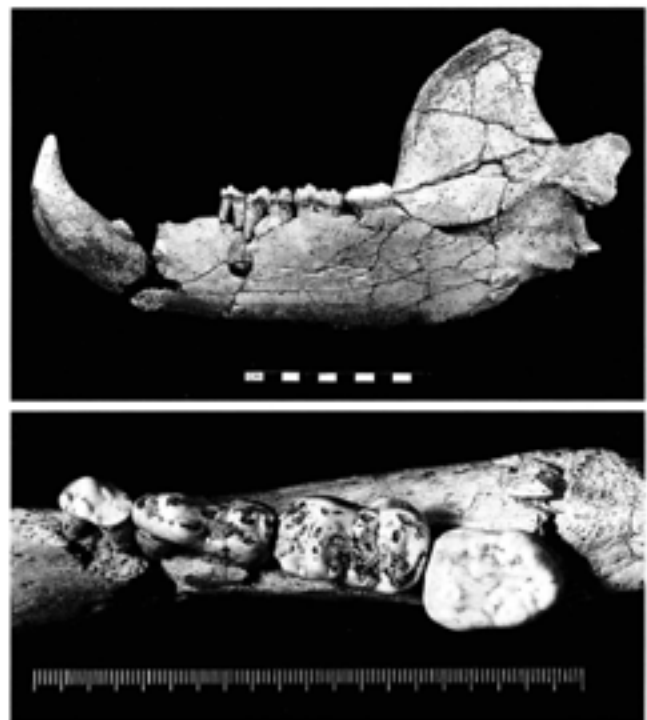


Fig 136 *Ursus deningeri*: right mandible (Q2/B F50 Unit 4c), a) lingual view; scale unit 10mm, b) occlusal view; scale unit 1mm

Table 51 *Ursus deningeri*: measurements (mm) of postcrania and teeth

length (est) = estimated due to interstitial wear

q	area	unit	fauna no	bone element	GL	GB	Bp	SD	BD	BD artic
1	1/B	5a	F87	humerus	-	-	-	-	133.5(est)	81.7
1	TP220-80	4c	F1	humerus	-	-	-	-	-	73.3
1	1/A	5a	F3360	astragalus	49.6	-	-	-	-	-
1	1/A	G	F3501	calcaneus	-	54(est)	-	-	-	-
1	1/B	4c	F120	metatarsal III	80.2	-	17.1	14.1	22.2	-
1	1/B	4c	F121	metatarsal IV	88.7	-	-	15.6	24.7	-
1	1/B	4c	F125	metatarsal V	89	-	-	14.8	24.3	-

upper dentition				C'		M'	
q	area	unit	fauna no	L	W	L	W
1	1/B	4c	F5	18.2	13.7	-	-
2	2/B	4c	F90	-	-	25.3(est)	25.3

lower dentition				C ₁		P ₁		M ₁		M ₂			M ₃		
q	area	unit	fauna no	L	W	L	W	L	W	L	W	W	W	L	W
												anterior	post		
2	2/B	4c	F50	33.3	20	13.7	8.9	27.8(est)	12.8	33.2(est)	17.8	16.2	17.8	25.7	18.5
2	GTP 3	4c	F71	-	-	-	-	-	-	31.0(est)	18.5	16.7	18.5	26.9	18.5
1	1/A	6	F3500	-	-	-	-	-	-	33.2(est)	19.2	18.4	19.2	-	-
1	1/B	4	F341	-	-	-	-	-	-	31.7	18.7	17.9	18.7	-	-

Fig 137 *Ursus deningeri*: left humerus (Q1 TP220-80 Unit 4c); scale unit 10mm

The taxonomy of the European cave bears has been reviewed by Bishop (1982) and Kurtén and Poulianos (1977). Although most authors recognise a number of species from the Early and Middle Pleistocene, they probably represent stages in a progressively evolving lineage which is characterised by gradual changes in dental morphology and body size. Early Middle Pleistocene cave bears are usually referred to the species *Ursus deningeri*. Two subspecies are recognised: *U. d. savini* from the Cromerian *sensu stricto* and *U. d. deningeri*, which occurs between the Cromerian *sensu stricto* and the Hoxnian. These two subspecies are similar in dental morphology and can only be separated when large collections are available. *Ursus deningeri* is somewhat more primitive and smaller than *U. spelaeus* which is first recorded from the Hoxnian at Swanscombe. The dental and skeletal features which distinguish *U. deningeri* from *U. spelaeus* and *U. arctos*

Fig 138 *Ursus deningeri*: rearticulated tarsals and metatarsals (Q1/B Unit 4c), F122 L ectocuneiform, F124 L cuboid, F119 L navicular, F125 L metatarsal V, F121 L metatarsal IV, F120 L metatarsal III; scale unit 10mm

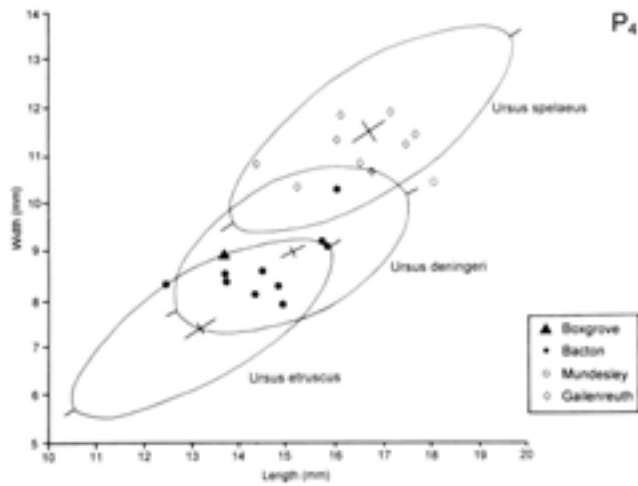


Fig 139 *Ursus spp.*: bivariate plot of length against width of P_4 (after Kurtén and Poulianos 1977)

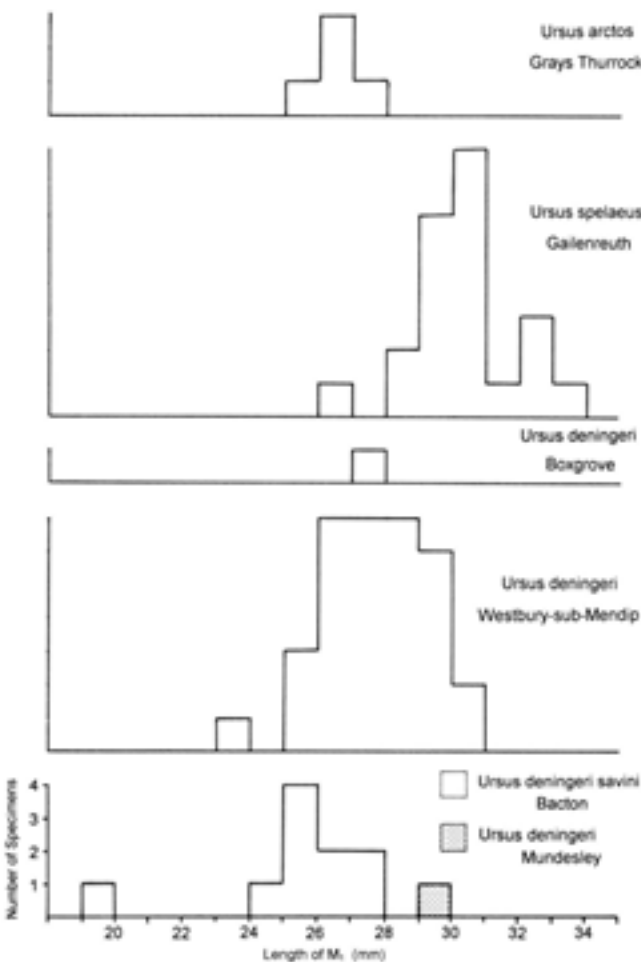


Fig 140 *Ursus spp.*: histograms of length of M_1

have been described in detail by Bishop (1982) for the large collection of *U. deningeri* from Westbury. The relatively small sample of cave bear from Boxgrove resembles *U. deningeri* from Westbury and Petralona (Kurtén and Poulianos 1977) in both morphology and dimensions (Figs 139, 140, 141), and is therefore referred to *U. deningeri*.

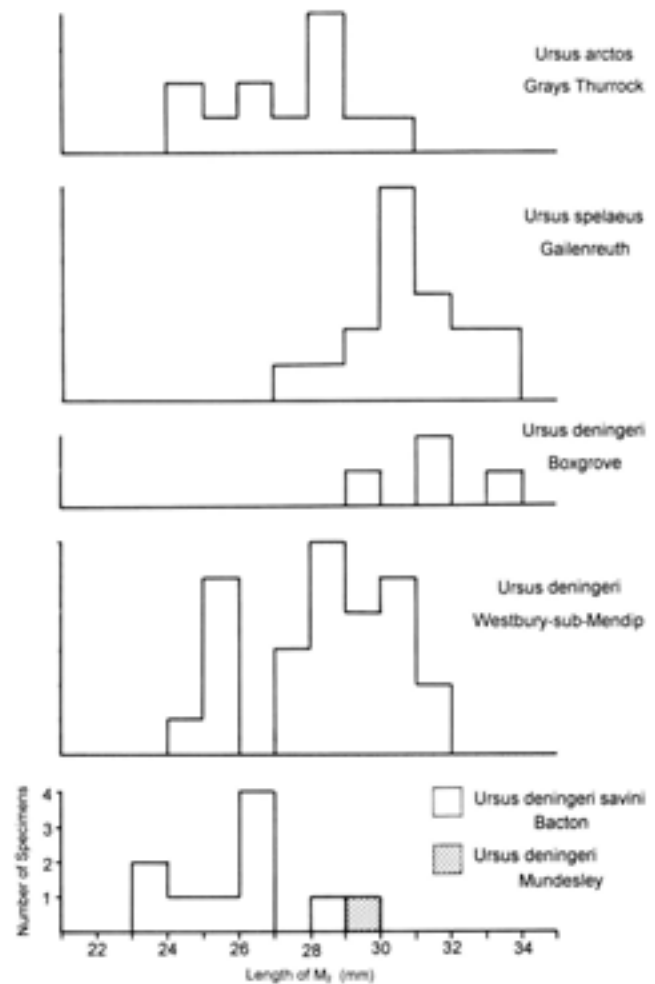


Fig 141 *Ursus spp.*: histograms of length of M_2

Although there are too few elements to provide information on the size of the bears from Boxgrove, the teeth are all large and could represent male animals. Comparisons of the size of the Boxgrove teeth are illustrated in Figures 140-1.

Family Mustelidae

Genus *Mustela*

Mustela erminea Linnaeus 1758

Stoat

Unit 4b: Q1 GTP 22 BS88-701 right P_2

Unit 4c: Q1/B BS88-955 left P^1 , P^4 , M^1 ; BS87-290 right M_1 frag (cf); Q2 GTP 3 BS87-124 right P^1 frag, right M^1 , BS87-136 right P^1 frag, mandible with P_2 - M_2 , acetabulum frag, BS86-36 left C_1 ; Q2 GTP 17 BS87-263 left P^1 , left P_2 , BS86-70 left P^1 , left I_2 , left P_2 , left P_3 frag, left P_4 , left mandible frag with M_1 , right I_1 , right C_1 , right P_2 , right P_3 , right P_4 , right M_2 , right mandible frag with M_1 , scapula frag, tibia frag, astragalus

Unit 5a: Q1/B BS87-134 right M_1 frag, BS87-133 left P^1 , left C_1 , left P_2 , left M_1 frag; Q2 GTP 17 BS86-74 right P^1 , M_1 frag, C frag, BS86-68 left C_1 , left M_1 , P frag, BS86-76 right C^1

Unit 5b: Q2 TP4 BS90-1165 left P^1 , left C^1 frag, left P^2 , left P^3 frag, left M^1 frag, left C_1 , left P_2 , left P_3 , left M_1 , left M_2 , left humerus frag

Unit 5c: Q2 GTP 17 BS90-1130 right P_1

Fossil *M. erminea* and *M. nivalis* do not differ in morphology from the Recent species which, although similar, can be separated on the basis of size (Fig 143).

Table 52 *Mustela erminea*: measurements (mm) of teeth

upper dentition				C^1		P^c		P^s		P^a			M^1				
q	area	unit	fauna no	L	W	L	W	L	W	L	L pc	W ant	W post	L bucc A	L bucc B	L lingual	W
2	TP 4	5b	BS90-1165	-	-	1.34	0.77	-	-	3.93	-	-	1.19	1.09	1.39	1.31	3.38(est)
2	GTP 17	5a	BS86-74	-	-	-	-	-	-	0.81	2.31	1.49	-	-	-	-	
1	GTP 17	5a	BS86-76	1.78	1.42	-	-	-	-	-	-	-	-	-	-	-	
1	1/B	5a	BS87-133	-	-	-	-	1.88	0.9	-	-	-	-	-	-	-	
2	GTP 17	4c	BS86-70	-	-	-	-	-	-	3.75	-	-	1.21	-	-	-	
2	GTP 17	4c	BS87-263	-	-	-	-	-	-	-	-	-	1.29	-	-	-	
2	GTP 3	4c	BS87-124	-	-	-	-	-	-	-	-	-	-	1.13	1.39	1.49	2.05
1	1/B	4c	BS88-955	-	-	-	-	2.31	0.96	3.96	-	1.17	-	1.09	1.29	1.62	3.29
lower dentition				C_1		P_1		P_2		P_3		M_1				M_2	
q	area	unit	fauna no	L	W	L	W	L	W	L	W	L	L tr	W tr	W tal	L	W
2	GTP 17	5c	BS90-1130	-	-	-	-	1.62	0.91	-	-	-	-	-	-	-	-
2	TP4	5b	BS90-1165	-	1.58	1.25	0.79	1.77	0.99	2.15	1.16	4.26	3.18	1.43	1.22	1.07	1.02
2	GTP 17	5a	BS86-68	2.16	1.64	-	-	-	-	-	-	-	-	1.27	-	-	
1	1/B	5a	BS87-133	-	-	1.42	0.73	-	-	-	-	-	-	1.15	1.01	-	
1	1/B	5a	BS87-134	-	-	-	-	-	-	-	-	-	-	-	0.92	-	
2	GTP 17	4c	BS86-70	-	1.41	1.16	0.73	1.65	0.87	2.15	1.05	4.09	3.14	1.45	1.2	0.82	0.71
2	GTP 17	4c	BS87-263	-	-	-	-	1.62	0.86	-	-	-	-	-	-	-	
2	GTP 3	4c	BS87-136	-	-	-	-	1.62	1.01	2.18	1.02	4.21	3.14	1.55	1.19	1.04	0.96
1	1/B	4c	BS87-290	-	-	-	-	-	-	-	-	-	-	0.89	-	-	
1	GTP 22	4b	BS88-701	-	-	1.12	0.73	-	-	-	-	-	-	-	-	-	

Fig 142 *Mustela erminea*: right mandible (Q2 GTP 3 BS87-136 Unit 4c) with P_1 - M_2 , buccal view; scale unit 1mm

M. erminea is the most abundant of the small carnivores, represented mainly by isolated teeth. A mandible is illustrated in Figure 142, and measurements are given in Table 52. It can be seen from the plot of M_1 length (Fig 143) that the Boxgrove *M. erminea* is small in comparison with the Recent sample from Europe, and comparable in size to *M. erminea* from Westbury and from the early Middle Pleistocene of Europe which has been referred to *M. palerminica*.

Given the pronounced differences in body size in Recent *M. erminea*, and the cyclical changes in body size associated with Pleistocene climatic fluctuations, a specific designation for the Middle Pleistocene form is not warranted and the Boxgrove material is referred to the living species.

Mustela lutreola (Linnaeus 1761)

European mink

Unit 4b: Q1/B BS87-288 left M_1 , prob female; Q1 GTP 30* B* left I_1 , C_1 , right mandible with P_1 - M_1

Unit 4c: Q1/B BS88-958 right C_1 , prob female; Q1 GTP 8 F6* left mandible with I_1 , C_1 - M_2 , F3* right mandible with I_2 , I_3 , C_1 - M_2 , * = same individual, prob male (F3*, F6*); Q1 GTP 30* A* right C_1 , left mandible frags, left P_3 , left P_4 , left M_1 , left M_2 , right I_3 , * = same individual, prob male (A*, B*)

Unit 5a: Q1 GTP 14 BS86-12 right M_1 , M_2 , prob male; Q1/B BS87-233 right P_1 , right M_1 frag, left P_2 , left P_3 , left P_4 , left M_1 , left M_2 , I frags, all prob same individual male, BS87-129* left mandible frags, C_1 , P_3 , P_4 , M_1 ; BS87-126* right mandible frags, I_1 , C_1 , P_2 , P_3 , P_4 , M_1 , M_2 * = prob same individual female (BS87-126, BS87-129); Q2 GTP 20 BS86-72 right P^2 (cf)

The dentition and mandible is of the typical *Mustela* pattern. The enamel surface of the canines are distinctly rugose, a feature which appears to be a characteristic of *M. lutreola*. Other differences in dental morphology allow distinction from the medium-sized mustelids, *M. putorius* and *M. eversmanni*. Eight individuals are represented by isolated teeth, associated dental remains and two well-preserved mandibles (Fig 144). The measurements of the dentition are given in Table 53 and the length of the lower first molars are

Table 53 *Mustela lutreola*: measurements (mm) of teeth

upper and lower dentition				C_1		P_2		P_3		P_4		M_1				M_2		C'	
q	area	unit	sample no	L	W	L	W	L	W	L	W	L	L	W	W	L	W	L	W
													tr	tr	tal				
1	GTP 14	5a	BS86-12	-	-	-	-	-	-	-	-	7.27	5.19	-	2.43	2.05	1.88	-	-
1	1/B	5a	BS87-126	-	2.24	2.15	1.45	2.74	1.55	3.17	1.73	6.37	4.8	2.31	2.05	1.66	1.53	-	-
1	1/B	5a	BS87-129	-	2.28	-	-	2.71	1.58	3.07	1.68	6.37	4.7	2.28	2.08	-	-	-	-
1	1/B	5a	BS87-233	-	-	2.45	1.56	3.48	-	4.12	2.33	7.35	5.39	-	2.11	-	-	-	-
1	1/B	4c	BS88-958	-	2.11	-	-	-	-	-	-	-	-	-	-	-	-	-	-
1	GTP 8	4c	-	-	2.95	2.55	1.47	3.14	1.85	3.93	2.31	7.35	5.39	2.81	2.28	2.06	1.82	-	-
1	GTP 30	4c/4b	-	-	-	-	-	3.14	1.96	3.82	-	7.32	5.29	2.61	2.36	1.85	-	3.16	2.28
																(est)			
1	1/B	4b	BS87-288	-	-	-	-	-	-	-	-	6.09	4.51	2.24	1.88	-	-	-	-

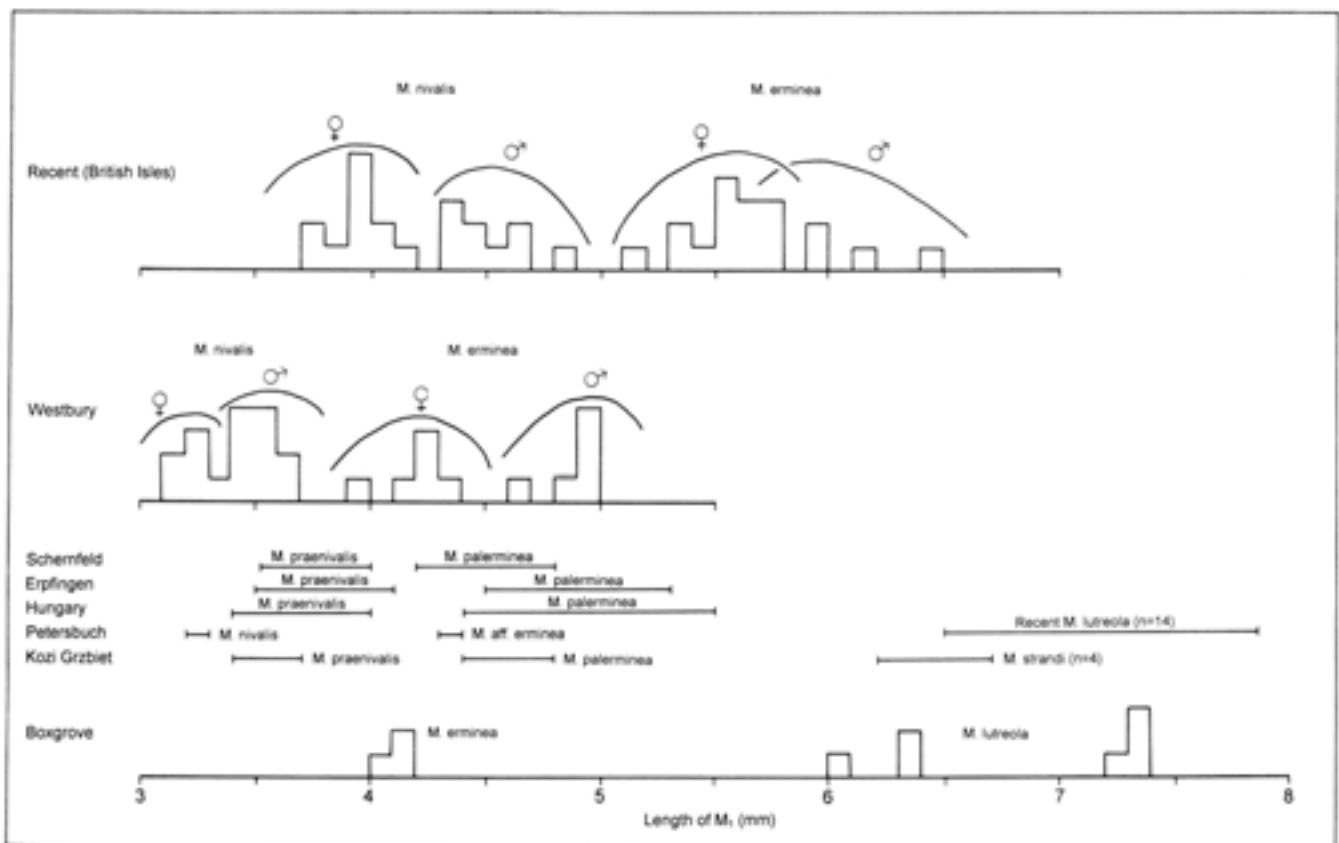


Fig 143 *Mustela* spp: histograms and ranges of M_1 length of early Middle Pleistocene and Recent small mustelids. Westbury-sub-Mendip (Bishop 1982), Schernfeld (Dehm 1962), Erpfingen (Heller 1958), Hungary (Kormos 1934), Petersbuch (Koenigswald 1970)

plotted in Figure 143. The M_1 measurements show that the Boxgrove material is slightly smaller than the Recent sample of European *M. lutreola*.

The presence of the European mink in the Boxgrove fauna is of considerable interest as it represents the earliest fossil record of this species. The only other Pleistocene record of European mink is from last glaciation deposits at the Grotte de l'observatoire, Monaco. Kurtén (1968) considers the American mink (*M. vison*) to be the closest living relative of the European mink, which he suggests evolved in North America and

reached Europe during the last glaciation. However, despite a superficial resemblance to the American mink, the European mink is genetically distinct and is probably more closely related to the Siberian weasel, *M. sibirica* (Volobuev *et al* 1974). The fossil record of the medium sized species of *Mustela* is poorly known; however, it is possible that the early Middle Pleistocene *M. strandi* is conspecific with the European mink.

In relation to the palaeoenvironment, the presence of European mink is of interest as it is a semiaquatic species inhabiting marshes and the fringes of ponds

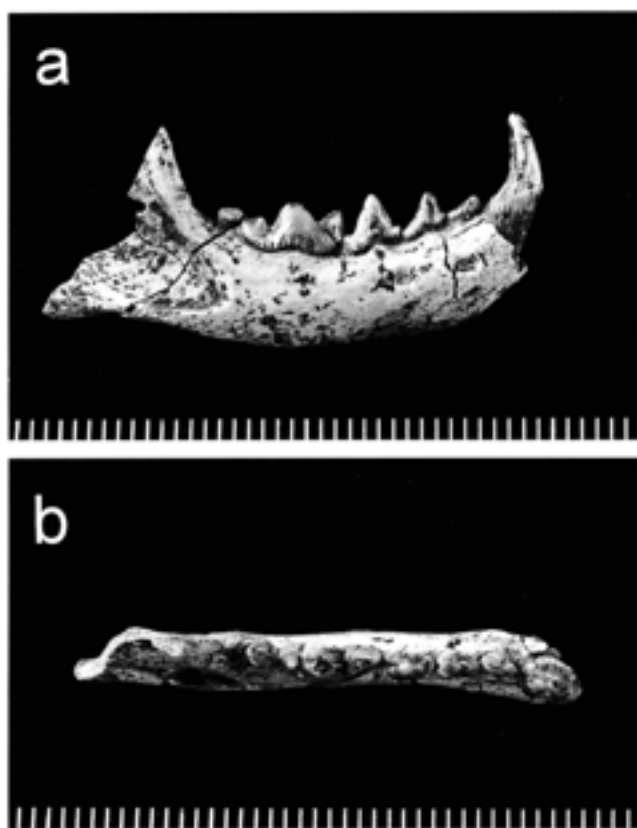


Fig 144a-b *Mustela lutreola*: left mandible with I_1 , C_1 - M_2 (Q1 GTP 8 Unit 4c): a) buccal view, b) occlusal view; scale unit 1mm

and rivers with densely overgrown banks. A wide range of prey species are taken, although amphibious and aquatic vertebrates such as fish, waterfowl, amphibians, reptiles, and small mammals, form the largest proportion of its diet.

Mustela nivalis Linnaeus 1766
Weasel

Unit 5a: Q2 GTP 17 BS86-84 right C_1 , right P_3 , C frag prob same individual

Unit 6: Q2 GTP 3 BS87-118 left M_1 frag

Measurements:

Length upper canine	1.20mm
Width upper canine	0.96mm
Length P_3	1.78mm
Width P_3	0.73mm
Length M_1 (buccal B)	0.94mm

The weasel (*Mustela nivalis*) is represented by four specimens comprising two individuals. In comparison with Recent *M. nivalis* from the British Isles, the Boxgrove specimens are small. As with *M. erminea*, the weasel shows a considerable size variation across its range, and the size of the Boxgrove specimens can be matched with those from Scandinavia. For this reason and the lack of morphological differences between Recent *M. nivalis* and the Boxgrove specimens, this material is referred to the living species *M. nivalis*.

Mustela sp
Mustelid

Unit 4c: Q2 GTP 3 BS87-149 right C_1 frag, BS87-251 P frag, BS88-461 left distal tibia frag, right calcaneus, phalanx, BS88-504 right metacarpal IV

Gully fill: Q1/A F1203 left M_1 frag

Unit 5a: Q1/B BS88-502 C frag

Genus *Meles*
Meles sp
Badger

Unit 4c: Q1/A F3165* right temporal frag *same individual (F3165*, F414*, F227*, F369*, F206*), F1740 left M_1 , F268 left scapula frag, F266 left humerus, F271 right humerus frag, F267 radius frag, F265 left ulna, F1825 femur frag, right femur frag, F270 right tibia frag, F1337 right astragalus

Gully fill: Q1/A F3441 right C_1 , F227* left mandible with M_1 , F369* right mandible frag, F414* left C_1 , F3024 right C_1 , F227A* left P_2 frag, F206* right M_2

Unit 4c/5a: Q1/A F1743 left C_1 , F1827 right P_2 frag

The badger is represented by the dispersed remains of a single individual from Quarry 1 Area A. The postcrania were recovered from the surface of Unit 4c and its contact with the overlying deposits, whereas the majority of the teeth and the mandible fragments were recovered from an area of disturbed stratigraphy (gully fill) which crosses the excavated area (Austin and Roberts Chapter 6.2, Figs 226-9). There can be little doubt that the two sets of bones represent a single individual as the articular process of the right mandible (F369) from the disturbance refits to the temporal fragment (F3165) recovered from the surface of Unit 4c.

The postcranial skeleton is represented by a scapula, right and left humeri, a radius and ulna, two femur fragments, a tibia fragment and an astragalus. With the exception of the astragalus these bones are badly crushed and distorted. The cranial skeleton is represented by a temporal bone fragment, six isolated teeth, part of the right mandible, and a relatively complete left mandible with M_1 (Fig 145). Measurements of the Boxgrove specimens and comparisons are given in Tables 54-6.

The badger is a widespread Eurasian species, but it is poorly represented in Pleistocene faunal assemblages. Fossil material from the Early and Middle

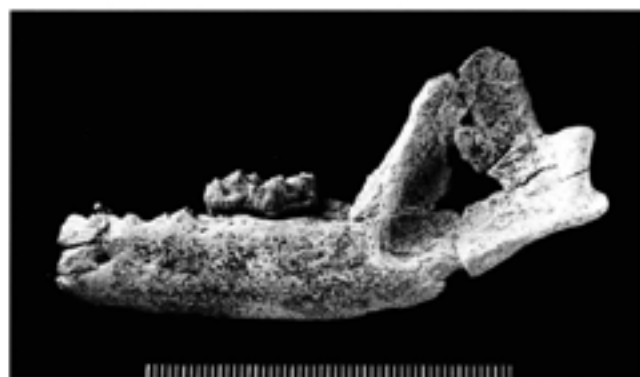


Fig 145 *Meles* sp: left mandible with M_1 (Q1/A F227 Unit 4c), buccal view; scale unit 1mm

Table 54 *Meles* sp. Measurements (mm) of mandible and astragalus from Boxgrove

mandible (F227)	
length of mandible (measured from condyle process to arboreal border of canine alveolus)	71.3
length of toothrow (P ₂ -M ₂) measured along alveoli	40.0
length of molar row (measured along alveoli)	22.8
ramus depth between P ₁ and M ₁ (measured on lingual side)	13.6
mandible (F369)	
ramus depth behind M ₁ (measured on lingual side)	16.1
astragalus (F1337)	
greatest length	20.3

Pleistocene of Europe is sparse and there is some uncertainty regarding the evolution and variation of *Meles* during the Pleistocene. The probable ancestor of the living badger is *Meles thoralis* described by Viret (1950) from loess deposits of Villafranchian age at St Vallier, France. This form is characterised by a number of primitive dental features which distinguish it from Recent *M. meles*. The dentition of *M. meles* is adapted to an omnivorous diet and is characterised by a reduced premolar dentition, hypertrophy of the upper first molar and a lower carnassial with an expanded talonid. In *M. thoralis*, the premolar dentition is well developed; in particular, the upper carnassial is elongated and longer than the M¹ measured along the external face. The lower carnassial of *M. thoralis* from

St Vallier is distinguished from Recent badgers by a relatively well developed trigonid and reduced talonid. The morphology of the upper M¹ of *M. thoralis* is also distinctive (Viret 1950). Identification of the Boxgrove specimens is hampered by the lack of the characteristic upper carnassial; however, the presence of the well-preserved upper and lower first molar and the mandibular ramus allow comparisons to be made with both *M. thoralis* and *M. meles*.

According to Viret (1950) the mandibular ramus of *M. thoralis* is more slender than Recent *M. meles*. Although the mandibular ramus of the Boxgrove mandible is slender, this is related to the age of the individual, and the height of the Boxgrove mandibular ramus is not unusual in comparison with those of Recent badger at a similar stage of development.

The relative length of the premolar tooth row in comparison to the total toothrow length is another feature used by Viret (1950) to distinguish *M. thoralis* from Recent badger. The lower premolar toothrow of *M. thoralis* is more developed than in Recent badgers, although Viret's data show some overlap between the two groups. A comparison of the relationship of the premolar length to toothrow length between *M. thoralis* with the Boxgrove specimen is hampered by the juvenile age of the Boxgrove specimen. As growth of the mandible continues after the permanent dentition has erupted, the length of the premolar row was compared with Recent specimens of similar ontogenetic age. Based on the data given in Table 54, the premolar length of the Boxgrove mandible is very close to the mean of the Recent *M. meles*, which is 17.3mm.

Table 55 Comparative measurements (mm) of dentition in Recent and fossil *Meles* spp

	<i>Boxgrove</i>	<i>M. thoralis</i> St Vallier ^{1,4}	<i>M. t. spelaeus</i> Lunel Viel ²	<i>M. meles</i> W Europe (Recent) ³
M₁				
length	15.8	15.5-15.9-16.3 (n=3)	15.8, 16.7	15-16.2-17.5 (n=23)
width	7.2			7.3-7.8-8.2 (n=23)
length trigonid ⁵	8.5	9.5-9.7-9.9 (n=4)	9.2.9.5	8.3-9-9.8 (n=23)
M₂				
length	5.4		5.2, 4.8	3.6-5.2-6.7 (n=30)
width	5.5		6.1, 5.7	4.1-5.8-6.5 (n=30)
crown shape index ⁶	101.9		117.3, 118.8	97-112-125 (n=30)
M¹				
length	13.6	13.5, 14.5, 15	12.8	11.2-13-14.8 (n=20)
width	11.8	12.9, 12.3, 12	12	10.2-11.3-12.6 (n=20)
crown shape index ⁶	86.5	80, 84.8, 95.6	93.8	78.4-87-93.9 (n=20)
angle*	133	134	134, 136	138-150-179 (n=20)
upper canine				
length	6.8			
width	5.1			
lower canine				
length	7.7		7.2, 8.8	
width	5.3			

¹ Data from Viret (1950)² Data from Bonifay (1971)³ Parfitt (unpublished)

* = Angle between paracone/metacone and metastyle

⁴ Kurtén and Poulanos (1977)⁵ Trigonid length measured internally⁶ Crown shape index = BL/MD x 100

Table 56 *Meles* spp. Comparative measurements (mm) of lower carnassial in Recent and fossil samples

	Length M_1	Length M_1 trigonid	Length of M_1 trigonid as a % of total length of M_1
<i>Meles</i> sp (Boxgrove)	15.8	8.5	53.8
<i>M. thoralis</i> (St Vallier n=4)	15.5–15.9–16.3	9.5–9.7–9.9	60.1–60.9–61.5
<i>M. t. spelaeus</i> (Lunel Viel)	15.8, 16.7	9.2, 9.5	56.9, 58.2
<i>M. meles</i> (Petralona)	16.3, 17	8.9, 9.4	54.6, 55.3
<i>M. meles</i> (England, Recent n=23)	15–16.2–17.5	8.3–9–9.8	51.8–55.6–59.6
<i>M. meles</i> (France, Recent n=5)	15.3–16.1–17.1	8.3–8.6–8.8	50.9–53.6–55

In the upper dentition, *M. thoralis* is characterised by a distinctive M^1 (Viret 1950; Bonifay 1971). The occlusal outline of the M^1 in the Recent badger is approximately a trapezoidal rectangle in comparison to *M. thoralis* which is less expanded mesio-distally, giving the tooth a square occlusal outline. In *M. thoralis* the cusps on the external border (paracone and metacone) are large and elevated and the paracone is slightly smaller than the metacone. In comparison, these cusps are less well developed and the paracone is larger than the metacone in Recent *M. meles*. The postero-buccal face of the M^1 is concave in *M. thoralis* in contrast to the straight or slightly convex border seen in *M. meles*. The concavity of the border in *M. thoralis* is due to the more internal position of a small external tubercle (metastyle). Biometric data for the M^1 of fossil and Recent *Meles* are given in Table 55.

The crown shape index ($BL/MD \times 100$) of the Recent sample shows a wide range of variation which, with the exception of a single molar from St Vallier, encompasses the values of the fossil specimens. Viret's description of the shape of the M^1 of *M. thoralis* is not supported by these data. In the Boxgrove M^1 (Fig 146), the postero-buccal border of the tooth is concave and the metastyle is more internally placed than in Recent *M. meles*. This is a particularly distinctive feature of *M. thoralis* from St Vallier (Viret 1950) and Lunel-Viel (Bonifay 1971). The position of the metastyle cusp in relation to the external border of the tooth was measured as the angle of the metastyle from

a line through the tips of the paracone and metacone. This angle is more acute in *M. thoralis* from St Vallier and Lunel-Viel than in the Recent sample and supports the distinction between these two forms on the basis of cusp morphology given by Viret (1950). The metastyle-paracone/metacone angle in the Boxgrove M^1 is similar to that of *M. thoralis* and outside the range of Recent *M. meles*.

According to Viret (1950) the lower carnassial of *M. thoralis* is characterised by a relatively well developed trigonid. However, this feature shows a wide range of variation in Recent *Meles* and the trigonid length of the M_1 in *M. thoralis* falls within the range of variation found in the Recent sample. Consequently this feature is of limited taxonomic value when small samples are available.

This foregoing discussion shows that the Boxgrove specimens resemble *M. thoralis* in some features and Recent *M. meles* in others. The Boxgrove form may represent a transitional form and is referred to *Meles* sp.

Family Hyaenidae

Genus *Crocota*

Crocota crocota Erxleben 1777

Spotted hyaena

Unit 4c: Q2 GTP 3 F12 fourth cervical vertebra frag, centrum missing

The spotted hyaena is represented by a fourth cervical vertebra (Fig 147) which closely resembles Recent and fossil *Crocota* in size and morphology. The dorsal surface has a distinct depression on either side of the

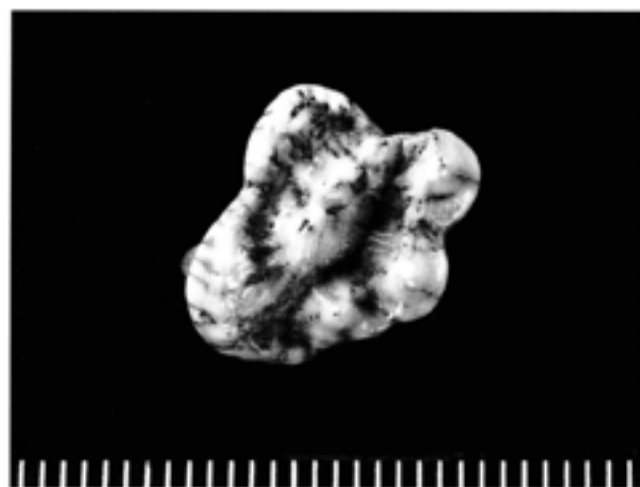


Fig 146 *Meles* sp: left M^1 (Q1/A F1740 Unit 4c), occlusal view; scale unit 1mm

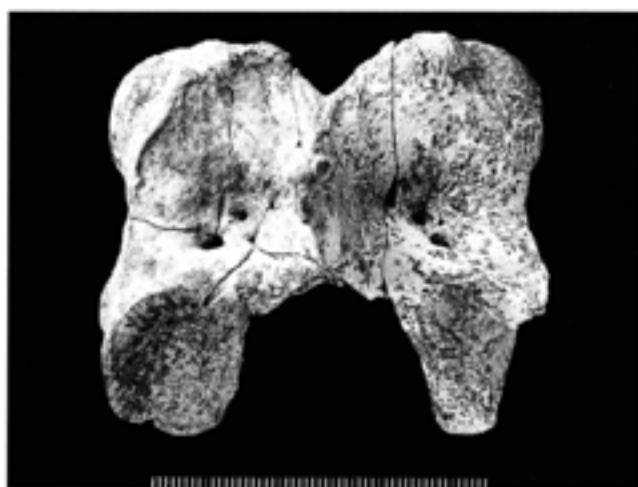


Fig 147 *Crocota crocota*: fourth cervical vertebra fragment (Q2 GTP 3 F12 Unit 4c), caudal view; scale unit 1mm

Table 57 Measurements of fourth cervical vertebra (mm) from Pleistocene and Recent *Crocota crocuta*

GLPa, greatest length between articular processes; BPacr, greatest breadth across cranial articular processes; BPacd, greatest breadth across caudal articular processes. For the comparative sample, the minimum, maximum, and mean values are given

	n	GLPa	BPacr	BPacd
Boxgrove	1	60.8	65.6 (est)	
Ipswichian				65.4
Kirkdale Cave	1	56	64	
Tornewton Cave	1	59.7	64.7	64.3
Recent <i>Crocota crocuta</i>	6	54–59.4–66.5	57.9–60.3–62	54.5–58.2–61

spinous process which is perforated by a number of small foraminae. The spinous process is pointed and slightly inclined posteriorly. In lateral view, the cranial articular process has a hooked appearance which appears to be characteristic of *Crocota*.

Measurements of the Boxgrove specimen are compared with data from Recent and Upper Pleistocene *Crocota crocuta* in Table 57. The length of the fossil vertebra fall within the range of variation observed in Recent east African *C. crocuta*, although the fossil specimens are broader (Fig 148).

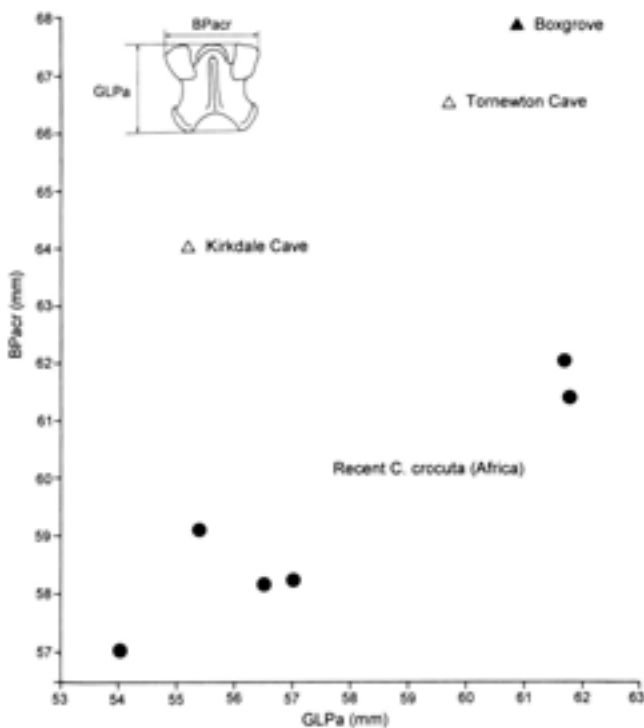


Fig 148 *Crocota crocuta*: bivariate plot of greatest length against greatest breadth across the cranial articular process of the fourth cervical vertebra of Recent and fossil spotted hyaena

Family Felidae
Genus *Felis*
Felis cf silvestris Schreber 1775
Wild cat

Unit 4b: Q1/B F438 right ulna, proximal frag, olecranon missing (cf Unit 4c: EQP Q2 TP13 F114* left metacarpal III, proximal *=same individual [F114*, F119*, F125*])

Unit 5a: EQP Q2 TP13 F119* right astragalus; EQP Q2 TP14 F125* right tarsal II, right tarsal III, left metatarsal II (proximal), right metatarsal III, three metapodial shaft frags, phalanx II

The remains of wild cat from Boxgrove consist of the associated bones of a hindlimb and a fragment of the proximal end of an ulna which are morphologically identical to those of Recent *Felis silvestris*. Of these specimens, only two are complete enough to provide measurements, which are plotted, together with a sample of Recent Scottish *F. silvestris*, in Figures 149 and 150. As these graphs show, bones of Recent *F. silvestris* exhibit a marked sexual dimorphism in size. Compared to this sample, the Boxgrove specimens fall within the size range of Recent male *F. silvestris*.

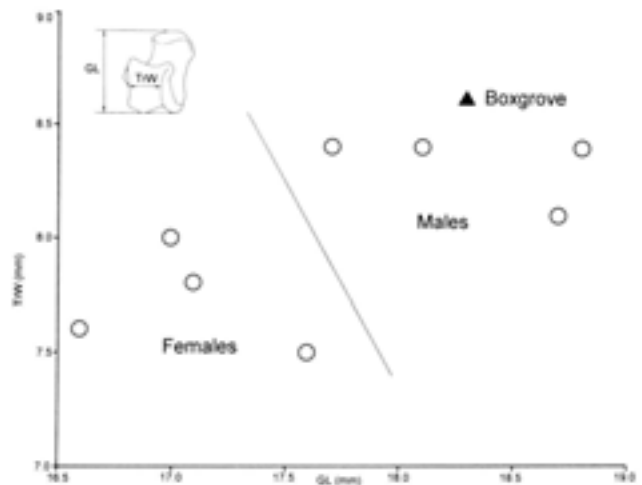


Fig 149 *Felis silvestris*: bivariate plot of astragalus greatest length against trochlea width for Recent Scottish male and female wild cat compared with *F. cf silvestris* from Boxgrove

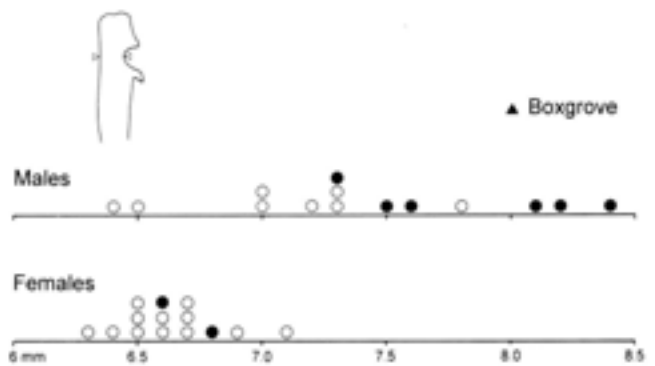


Fig 150 *Felis silvestris*: histograms of the minimum antero-posterior height of the ulnar semilunar notch for Scottish male and female wild cat (open circles=distal ulna unfused, closed circles=distal ulna fused) compared with *F. cf silvestris*

Although wild cats occur during the Cromerian, Hoxnian, and Flandrian interglacials in Britain, their remains are never abundant, and this is particularly so with postcranial material. The Pleistocene history of the European wild cats has been reviewed by Kurtén (1965) and Kurtén and Poulanos (1977), who refer the Early Pleistocene wild cat to a separate species, *Felis lunensis*. This species is linked by morphologically intermediate forms to the living species which is first recorded in the Holsteinian locality of Heppenloch (Kurtén 1965). *Felis lunensis* and *F. silvestris* differ in dental morphology; however, the postcrania are of little use in distinguishing between these two forms. Due to the fragmentary nature of the Boxgrove sample, and the lack of dental remains, we refer the Boxgrove sample to *Felis cf silvestris*.

Wild cats are closely associated with deciduous woodland, particularly clearings and the edges of large forests. They feed mainly on rodents, lagomorphs and, more occasionally, on birds and amphibians which are ambushed in open woodland and grassland.

Genus *Panthera*
***cf Panthera leo* (Linnaeus 1758)**
Lion

Unit 4d: Q1/B F276 right metatarsal II shaft frag (cf)

Lion is represented by a partial second metatarsal comprising the proximal end of the shaft. Although the specimen is incomplete, corroded, and lacks the proximal and distal articular ends, it is clearly felid in morphology and compares closely with Recent and Pleistocene *Panthera leo*.

In Table 58, the midshaft dimensions of the Boxgrove metatarsal are compared with those of Recent African lion and Pleistocene material in the Natural History Museum collections. The dimensions of the Boxgrove specimen are substantially larger than the Recent sample, although specimens from Westbury, Swanscombe, and Gailenreuth Cave (Late Pleistocene) are of an equally large size.

Table 58 *Panthera leo*. Comparative measurements of midshaft diameters (mm) in fossil and Recent lion

		<i>antero-posterior</i> <i>diameter</i>	<i>medio-lateral</i> <i>diameter</i>
Boxgrove		20.1 (est)	17.7 (est)
Westbury	M.47622	20.5	19.7
	M.47574	19.8	18.4
Swanscombe	M.16502	19.4	18.8
Ilford		17.8	15.3
Gailenreuth Cave	M.278	17.4	16.6
	M.198	21.4	16.7
	M.378	18.8	15.9
Recent Africa (Male)		14.9	16.4
Recent Africa (Female)		12.5, 12.7, 13.0, 13.4	11.9, 12.1, 13.0, 13.4

The lion is first recorded in Europe from the end of the Villafranchian (Vallonnet, France), whilst the earliest British records are from Westbury-sub-Mendip (Calcareous Member) and Boxgrove. Although early Middle Pleistocene records of lion are sparse, the available material represents a lion of considerable size; nevertheless there appear to be no significant differences in skeletal morphology from the living species.

Carnivora gen et sp indeterminate

Unit 4c: Q1/A F3206 tooth frag, ?canine, large carnivore, F3166, F3167 fibula frags, *canis* size; Q2 GTP 17 F603 right C¹ frag, large carnivore, BS86-52 F1046 tooth frag, small carnivore
Unit 5a: Q2 GTP 13 F14 fibula shaft frag; Q2 GTP 17 BS86-83 F1045 MP frag, small carnivore
Unstratified: Q2 SEP 2 F19 fibula shaft frag

Order Proboscidea
Family Elephantidae
Elephantid sp
Elephant

Unit 4b: Q1/B F317 bone frag (cf)
Unit 4c: Q1/B cheek tooth frag (from bulk sample)
Unstratified: Q1 bone frag (cf Elephantid)

Proboscidea
Elephantidae, gen et sp indet, elephant

A fragment of cheek tooth enamel (Q1/B Unit 4c) and two unstratified fragments of cortical bone are the only proboscidian bones recovered from Boxgrove.

Order Perissodactyla
Family Equidae
Genus *Equus*
***Equus ferus* Boddaert 1785**
Horse

Unit 4: Q1/B F447 right humerus shaft frag
Unit 4b: Q1/A F3386 right humerus shaft frag; Q2 SEP 2 F18 tibia shaft frag
Unit 4b: Q2 GTP 17 All bones from this context represent one individual female: F377a left petrosal frag, F616 petrous temporal frag, F249 right temporal frag, F957 left temporal frag, F312 left temporal frag, F364 right sphenoid frag, F210 right pterygoid/sphenoid frag, F465b stylohyoid frag, F954, F755 maxilla frags, F187 right maxilla and premaxilla frag with C¹, F605 maxilla and palatine frag, F455 left premaxilla frag, F266, F291, F425, F645, F652, F654, F743, F771, F938, F946, F971, F989, F990, F992, F993, F1003, F1006, F1007, F1008, F1011, F1014, F1020 all cheek tooth frags, F648 left P₂, F545 left P₂ with root and mandible frag, F981, F328, F1019 left P₁, F691, F943 left M₁, F186 right M₁, F650 left M₁ frag with associated mandible, F176, F182, F184, F409, F419, F458, F461a, F461b, F565, F567, F632, F656, F855, F964 mandible frags, F518, F544, F600, F744, F818 left mandible frags, F183 left mandible frag, refits {F183, F314}, F243 mandible frag, refits {F243, F256}, F256 mandible frag, refits {F256, F243}, F258 mandible frag, refits {F258, F306b}, F283a mandible frag, refits {F283a, F285, F426, F307b, F306b, F283b mandible frag, ?refits, F285 mandible frag, refits {F285, F283a, F426}, F306a mandible frag, refits {F306a, F241, F290, F305}, F306b mandible frag, refits {F306b, F258, F283a}, F307a mandible frag, refits {F307a, F314}, F307b mandible frag, refits {F307b, F283a}, F314 mandible frag, refits {F314, F307a, F183}, F386 mandible frag, refits {F386, F396}, F396 mandible frag, refits {F396, F452, F386}, F426a mandible frag, refits {F426, F283a, F285}, F452 mandible frag, refits {F452, F396}; F239,

Table 59 *Equus ferus*: measurements (mm) of teeth

* Note: measurements taken at (A) occlusal surface and (B) mid-height of crown

lower dentition

q	area	unit	tooth	crown height	maximum length		preflexid length		length of double knot		postflexid length		maximum width	
					A	B	A	B	A	B	A	B	A	B
2	GTP 17	4b	P ₂	74.5	37.8		11.1	-	15.9	-	19.5	-	17.3	-
2	GTP 17	4b	P ₃	-	33.5	34.1	11.5	12	18.4	20.9	16.8	16.7	17.2	19.2
2	GTP 17	4b	M ₁	-	33.6	30.4	10.8	10.6	17	16	12.9	10.1	15	17.3
2	GTP 17	4b	M ₂	>91	34.5	31	10.6	8.4	15.5	15.5	14.2	9.3	14.9	16
2	GTP 17	4b	M ₃	-	-	37.3	-	10.3	-	16	-	10.5	-	14.5
2	GTP 25	-	M _{1,2}	-	32.6	30.5	9.2	8.2	14.3	15.2	11.9	-	12.9	15.5

F240, F710 left M₃, F290, F306a, F241, F459, F305 left M₃, F242 axis frag, F173, F366 atlas frags, F658 2nd cervical vertebra frag, F260 5th cervical vertebra frag, F247 7th cervical vertebra, F356 thoracic vertebra frag, F304a 13th/14th thoracic vertebra frag, F127 5th/6th lumbar vertebra frag, F178, F659 lumbar vertebra frags, F417, F487, F832 transverse processes of lumbar vertebra, F456 rib tubercle frag, F204 right scapula neck frag, F277 right scapula blade frag, F296, F262, F301, F553 right humerus shaft frags, F571 humerus distal frag, F569 right humerus distal frag, F174, F413, F436, F405, F1000, F273, F439, F402, F442, F821a, F175, F441, F688, F438 left radius shaft frags, F662 radius shaft; F362 right pubis frag, F300 right pubic symphysis frag, F734 left ischium frag, F470, F275 right ischium frags, F209 right ischial crest, F222, F208, F276, F278 right ilium frags, F254, F437, F944 right acetabulum frags, F196 left acetabulum frag, F295, F360, F465a, F766 right femur shaft frags, F391, F463, F488, F837 left femur shaft frags

Unit 4c: Q2 GTP 17 F138 atlas, crushed, F26 terminal phalanx

Unit 8: Q1 TP4 F1(1984) atlas frag

Unstratified: Q2 GTP 25 left M_{1,2}, roots missing, early wear, juvenile/subadult

Equus ferus is represented by a partial skeleton which includes the lower dentition (reconstructed from associated teeth) from GTP 17 Unit 4b ('horse butchery site'), illustrated in Figure 152. In addition, a lower first or second molar (Fig 151a-b) was recovered from a unstratified context in Quarry 2. This specimen probably derives from the chalk gravel sequence overlying the marine deposits in GTP 25. Measurements of the teeth are given in Table 59. Postcranial material is on the whole fragmentary; measurements of the few relatively complete specimens are listed below.

Atlas (Q1 TP4 F1)

Greatest length from cranial to caudal articulation (GLF) 80.3mm

Third phalanx (Q2 GTP 17 F26)

Greatest length (GL) 62.6mm

Greatest breadth (GB) 80.8mm

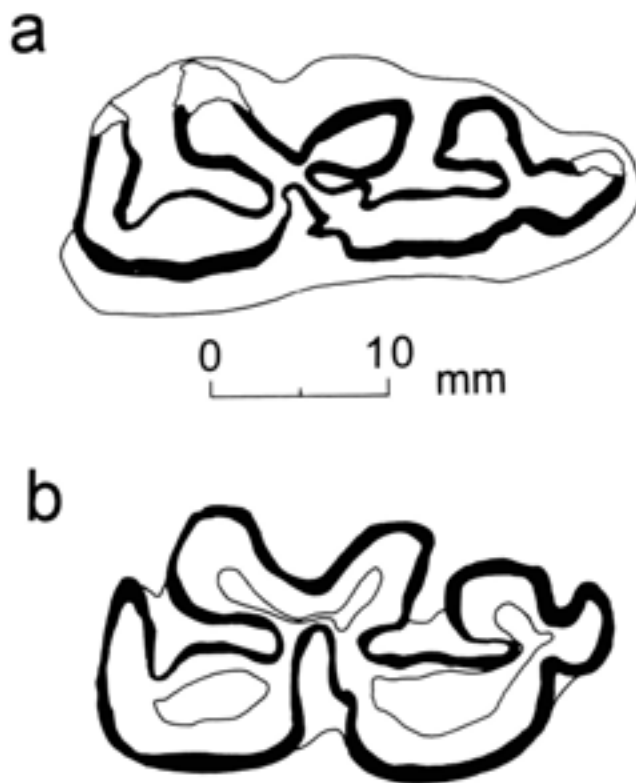
Breadth of articular facet (BF) 54.1mm

Length of articular facet (LF) 30.7mm

Length of dorsal surface (Ld) 62.2mm

Height (HP) 45mm

Characters used in the identification of equid teeth are discussed by Hopwood (1934). In the Boxgrove teeth (Figs 151a-b, 152), the lingual folds of the lower premolars and molars are distinctly U-shaped in contrast

Fig 151 *Equus ferus*: left M_{1,2} (Q2 GTP 25), a) occlusal view, b) mid-crown break

to the V-shaped fold in zebrine horses. In the lower premolars, the buccal fold is relatively deep, whereas in zebrine horses the fold is shallow. The characters of the Boxgrove equid teeth are clearly caballine, and the measurements illustrated in Figure 153 show that the Boxgrove specimens represent a horse of very large size.

Apart from the scarce remains of *E. hydruntinus* from Swanscombe and Oreston, Devon (Owen personal communication), and *E. altidens* from the Cromerian of Sugworth and West Runton, the British Middle and Late Pleistocene horses are all referable to *E. ferus*, a species which is first recorded in Eurasia in the Galerian (0.9myr) fauna of Lakhuti 2 in Tadzhikistan (Azzaroli 1989; 1991). The early Middle

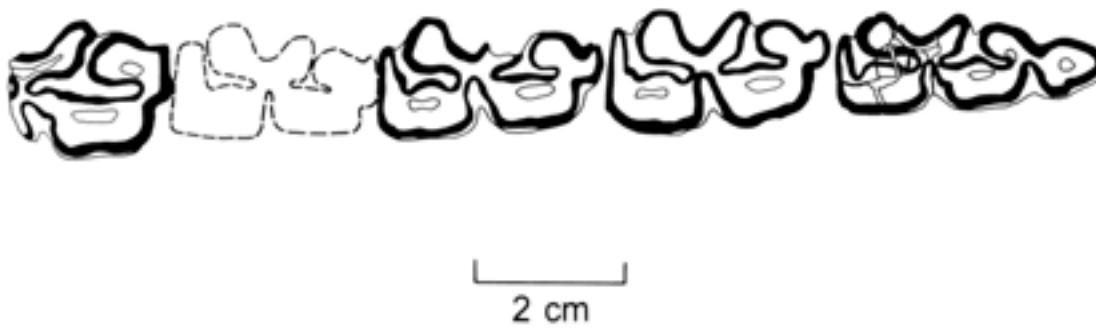


Fig 152 *Equus ferus*: associated P_2 fragment and M_{1-3} (Q2 GTP 17 Unit 4b)

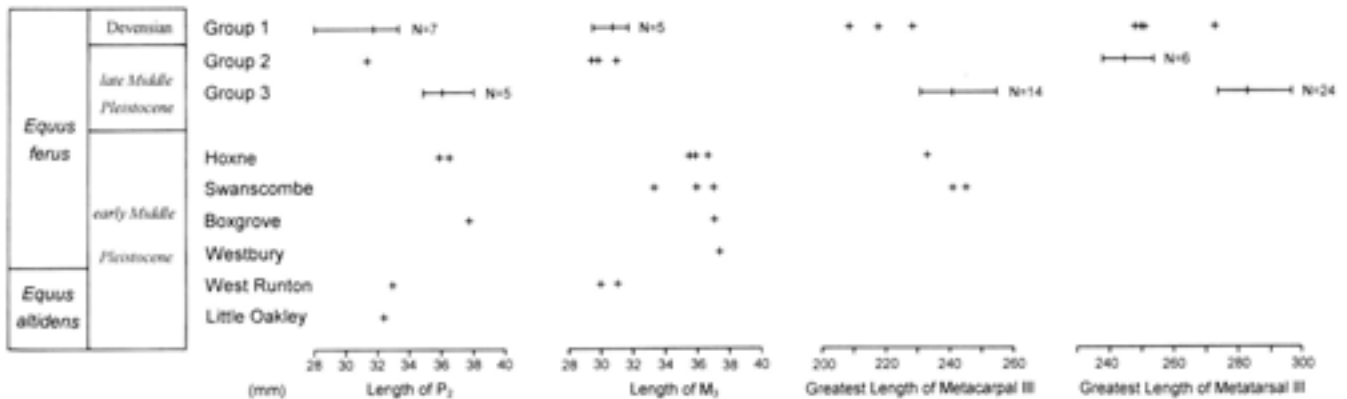


Fig 153 *Equus* spp: measurement comparisons of early Middle Pleistocene *E. altidens* with early Middle to Late Pleistocene *E. ferus* (Group 3: Ilford, Crayford, Brundon, Erith, Stoke Tunnel; Group 2: Brighton, Marsworth; Group 1: Gough's Cave, Brixham Cave, Ponder's End, Banwell Bone Cave)

Pleistocene caballine horses are of large size and often referred to a separate species, *E. mosbachensis* or to the subspecies *E. f. mosbachensis*. The small 'caballine' horse from Little Oakley, originally identified as *E. ferus* by Lister *et al* (1990), is probably the extinct small equid *E. altidens*. This species is also found in the Upper Freshwater Bed of West Runton (Azzaroli 1989), along with fragmentary remains of a larger equid.

According to Bishop (1982), the large early Middle Pleistocene *E. ferus* was replaced by a smaller caballine horse during the Hoxnian. The presence of a large caballine horse in the mammal assemblage would therefore indicate a pre-Hoxnian age. Evidence for size change in the British Pleistocene *E. ferus* is at present poorly known; however, Egginton (in Singer *et al* 1993) has shown that Hoxnian *E. ferus* from both Swanscombe and Hoxne is of a similar size to specimens attributed to early Middle Pleistocene *E. f. mosbachensis*. There is therefore some ambiguity regarding the timing of the size reduction in the British Pleistocene sequence and consequently the utility of *E. f. mosbachensis* as a biostratigraphic indicator is in question.

In Figure 153, measurements of the metapodials and lower M_3 and P_2 are plotted for a series of British localities spanning the early Middle to Late Pleistocene. In this graph, the small number of early Middle Pleistocene sites are shown separately together with a combined sample broadly dating to the 'Saalian Complex', and a second combined group of Last

Glaciation age (Tables 4, 8). The material from Black Rock, Brighton, and Marsworth (Lower Channel) are plotted as an intermediate group, between the 'Saalian' and Devensian samples, as the dimensions of this sample are significantly smaller than the other pre-Ipswichian post-Hoxnian sites and of a similar size to those of Devensian age. The sites grouped in the 'Saalian Complex' include Brundon, Crayford, Erith, Ilford, and Stoke Tunnel, which have been assigned to Oxygen Isotope Stage 7 by Bridgland (1994). The broad contemporaneity of these sites is supported by the faunal similarities which exist within this group. Although the lower channel deposits at Marsworth may also date to this time period, there is evidence that the dates are based on an earlier tufa incorporated into deposits of later age; therefore, the faunal remains could conceivably post-date the stage 7 sites listed above. The evidence for the Brighton sample post-dating the Group 3 sample is more convincing as the majority of the specimens from this locality were recovered from cold stage deposits which immediately overlie the raised beach deposits. Keen (1994) has suggested a revised chronology for the Black Rock sequence, and he assigns the lower chalk rubble to OIS 6.

Although the relative ordering of the sites and their absolute age are still the subject of considerable debate, it can be seen that horses of relatively large size were present in Britain throughout the Middle Pleistocene, and that a significant size reduction

probably occurred during the end of the 'Saalian Complex' represented by the cold stage deposits at Black Rock, Brighton, and the lower channel at Marsworth.

The horse is well represented in British Middle and Late Pleistocene faunas and is present in both cold and temperate episodes with the exception of the last interglacial. It is a grazing species and its presence during interglacial episodes is usually connected with open environments such as river floodplains and open woodland.

Family Rhinocerotidae
Genus *Stephanorhinus*
Stephanorhinus hundsheimensis
Extinct rhinoceros

Unit 4: Q1/B F439 left maxillary cheek tooth frag, F342 right M³, F410 right mandibular condyle frag, F352 cheek tooth frag, F446 cheek tooth root frag, F412 right ulna, olecranon and distal missing

Unit 4b: Q1/A F3446 phalanx III; Q2 GTP 17 (4b surface) F319 right scapula frag, F112 left scapula

Unit 4c: Q1/A F3090 left metacarpal IV, distal unfused; Q1/B F271 cervical vertebra, F38 right scapula; Q2 SEP 2 F11 left P³, ESR dated (F11* ectoloph refits to F10*), F10 left P³, early-mid wear, young adult, F13 tooth frags (enamel and root frags), F12 root frag; Q2 GTP 17 F64 right humerus, lateral condyle and lateral tuberosity missing, F12 left pelvis, crushed, F11 right pelvis and sacrum, crushed

Unit 4d: Q1/B F293 right patella, slightly crushed

Unit 5a: EQP Q2 TP4 B3 right calcaneus*, proximal and medial process missing, right astragalus*, complete (*=same individual)

Unit 8: Q1/B F300 right deciduous P³, late wear

Misc: EQP Q1 TP1 right lower cheek tooth frag; EQP Q1 TP1 B right P³ + mandible frag, mid-wear, adult; EQP Q1 TP1 C left M₃, mid-wear, adult, F24 cervical vertebra

Stephanorhinus hundsheimensis is relatively common in the Boxgrove assemblage, where it is represented by some complete postcranial remains and a small number of teeth. Following Fortelius *et al* (1993) and Groves (1983), the European Plio-Pleistocene rhinoceroses are assigned to *Stephanorhinus Kretzoi* (1942). Measurements are given in Table 60, and some of the more complete specimens are illustrated in Figures 154-9.



Fig 154 *Stephanorhinus hundsheimensis*: left P⁴ (Q2 SEP 2 F10 Unit 4c), a) occlusal view, b) buccal view; scale unit 1mm

Table 60 Measurements of *Stephanorhinus hundsheimensis* (* measured according to Fortelius *et al* 1993; other measurements follow von den Dreisch 1976)

element	measurements (mm)
dP ² (Q1/B Unit 8 F300)	LdP ² * 36.1 (est) wdP ² * 35.8 Ht dP ² * 17.8
P ⁴ (SEP 2 Unit 4c F10)	LP ⁴ * 39.9 WP ⁴ * 55.9 Ht P ⁴ * 44.8
P ₃ (Q1 TP1)	LP ³ * 37.5 WP ³ * 27.8 Ht P ³ * 20.6
M ₃ (Q1 TP1)	WM ³ 27.9 (est) Ht M ³ 20.3
cervical vertebra: (Q1/B Unit 4c F271)	BP acr 96.9 (est) GLPa 77.2 (est)
scapula (Q1/B Unit 4c F38)	SLC 121 (est)
scapula (Q2 GTP 17 Unit 4b F112)	SLC 113.8 LG 84 GLP 134 (est)
humerus (Q2 GTP 17 Unit 4c F64)	GLC 376 SD 66 DTCH * 89.4 DS * 62.8 HT ant * 47.7 HT post * 38.2 DT trochlea trough * 50.8
ulna (Q1/B Unit 4 F412)	DPA 113.5 BPC 81 DAP dia 46.9 BSU * 39.8 HSIU * 160
patella (Q1/B Unit 4d F293)	GB 99.9 (est) GL 102 (est) L art facE * 80.2
phalanx III (Q1/A Unit 4b F3446)	BFp 44
calcaneus (Q1 TP4 Unit 5a)	DT min post* 41.6 DAP bec 69
astragalus (Q1 TP 4 Unit 5a)	DL * 48.7 (est) H 77 B * 91 BD * 80.8 BPa * 75.4 DD * 45.6 (est) LL * 79.4 ML * 73.1 LmT * 58.0 DmT * 46.1 LIT * 61.4 Htt * 44.9 (est)



Fig 155 *Stephanorhinus hundsheimensis*: mandible fragment with right P_3 (EQP Q1 TP1 B)



Fig 156 *Stephanorhinus hundsheimensis*: left M_2 (EQP Q1 TP1 C)



Fig 157 *Stephanorhinus hundsheimensis*: right humerus (Q2 GTP 17 F64 Unit 4c); scale unit 10mm

Three species of *Stephanorhinus* occur in the European early Middle Pleistocene: *Stephanorhinus hundsheimensis*, *S. kirchbergensis*, and *S. hemitoechus*. *S. hundsheimensis* occurs widely in European faunas of early Middle Pleistocene age, and is probably a distinct species from the lower Pliocene to early Pleistocene *S. etruscus* to which it was formerly assigned. *S. hundsheimensis* did not persist through the Anglian/Elsterian Glaciation, while *S. hemitoechus* and *S. kirchbergensis* are recorded for the first time during the early Middle Pleistocene at Mosbach and persist through the Late and late Middle Pleistocene respectively. In Britain, only *S. hundsheimensis* is recorded from the early Middle Pleistocene ('Cromerian Complex') deposits of the 'Cromer Forest-bed Formation' (eg West Runton), Sugworth, and Westbury-sub-Mendip.

The distinguishing features of *S. hundsheimensis* have been described in detail by Fortelius *et al* (1993), who provide descriptions of the dentition and postcrania of this species. Although *S. hundsheimensis* is skeletally



Fig 158 *Stephanorhinus hundsheimensis*: right ulna (Q1/B F412 Unit 4); scale unit 10mm



Fig 159 *Stephanorhinus hundsheimensis*: right astragalus (EQP Q2 TP4 B3 Unit 5a); scale unit 10mm

similar to *S. etruscus*, it differs from this species in its larger size and in certain morphological features of the appendicular skeleton. The upper fourth premolar (Fig 154) from Boxgrove is characterised by a well developed lingual cingulum, a relatively brachydont crown and the high position of the lingual valley above the cingulum. These dental features characterise rhinos of the *S. etruscus/hundsheimensis* group. The morphology and dimensions of the postcranial remains closely match those of *S. hundsheimensis* described by Fortelius *et al* (1993).

S. hundsheimensis was a relatively lightly built cursorial species with a dentition and head posture which suggest a browsing diet in grassland or open woodland. This is consistent with the known fossil records of this species in the British Pleistocene, which are confined to interglacial assemblages with evidence for a mixed vegetation of grasses and open deciduous woodland.

S. hundsheimensis is an important biostratigraphic indicator species since it is generally thought to have become extinct during the Anglian/Elsterian glaciation (Roberts and Parfitt Chapter 5.9). The records of *S. hundsheimensis* from Boxgrove and Westbury, which date to the end of the 'Cromerian Complex', may represent the latest known records of this rhinoceros.

Order Artiodactyla

Family Cervidae

Genus *Cervus*

Cervus elaphus Linnaeus 1758

Red deer

Unit 3: Q2 GTP 13 F24 right tibia shaft frag

Unit 4: Q1/B F367 left P² frag, buccal missing, early wear, juvenile/subadult, F456 left M^{1,2}, prob M², very worn, old adult, F373 right M¹, early wear, subadult

Unit 4b: Q1/A F3502 left P², early wear, subadult; EQP Q1 TP10 F57 left deciduous P₁ frag, unworn, juvenile (cf); Q2 GTP 17 F515* (4b surface) left antler base attached to frontal frag (cf), F343 right mandible frag, ascending ramus (cf), F333 right mandible with P₂-M₁, early wear, subadult

Unit 4c: Q1/A F3418* right M¹, mid-wear, adult refits, F3194* right M¹, mid-wear, adult *same individual (F3194*, F3418*), F46 left scapula, F71, F1731, F2188 right radius shaft frags refitting group; Q1/B F51 right frontal, F97* right P¹, buccal frag *same individual (F93*-F97*), F95* right P¹, unworn, F96* right M¹, early wear, F94* right M¹, early wear, F93* right M¹, early wear, F63 right deciduous P₁, F45 right M_{1,2}, prob M₁; Q2/B F93 right radius, proximal, F10 right metacarpal shaft frag (cf); Q2/C F62*, F63, F67, F69 left maxilla frags; F51* left P¹, buccal frag; F43* left M¹, F68* left M¹, F33* left M¹, *same individual, mid-wear, adult (F33*, F43*, F51*, F62*, F63*, F67*-F69*), F70 left radius, proximal frag (cf), F34 phalanx II, proximal (cf), F35 phalanx II, distal (cf); Q2 GTP 3 F2 right deciduous P₁, mid-late wear, juvenile; Q2 GTP 17 F637* right antler base attached to frontal frag (cf) *same individual (F515, F637), F507 right C (cf), F313 left M^{1,2}, prob M², unworn, subadult, F513 left M¹, slight wear, subadult; F508 right I₁ (cf), F506 right I₁ (cf); Q2 GTP 20 F22 left pubis frag (cf), F20 pelvis, crushed (cf), F8* femur, proximal epiphysis *same individual (F8*, F11*, F13*, F14*, F19 (I, II), F18*(5a)), F11* right femur, crushed, F19(II)* right cuneiform, F14* right naviculo-cuboid, F13* right astragalus, F19(D)* right metatarsal, crushed, distal missing; Q2 GTP 25 F8 left humerus shaft, juvenile; F9 left radius, distal missing, and ulna shaft, juvenile; EQP Q2 TP5 right metatarsal, distal

missing; Q2 SEP 2 F3* left unciform, F6* left scaphoid, F4* left magno-trapezoid, F5* left lunate, F2* left metacarpal, distal and posterior missing * = same individual {F2*-F6*}, F17* left lateral malleolus, F16* left calcaneus * = same individual {F16*-F17*}

Unit GC: Q2 GTP 3 BS87-236 F87 right M¹², prob M¹, early wear, young adult, F88 right deciduous P₁, posterior frag, mid-late wear, juvenile

Gully fill: Q1/A F199 left M₁₂, prob M¹, mid-late wear, adult

Unit 4d: Q1/B F295 skull frags: occipital condyle, basi-sphenoid, petrosal, F287 right metatarsal, proximal and shaft frag; Q2 GTP 17 F333 right mandible with P-M₁, early wear, subadult

Unit 5a: Q1/B F15 right petrosal, F16 right M₁ frag, very worn, old adult; Q2 GTP 3 F23 right deciduous P₁, unworn, juvenile; Q2 GTP 20 F18* right tibia, crushed, F12 femur, proximal epiphysis; Q2 GTP 25 F2 left scapula frag, glenoid and neck; EQP Q2 TP4 right calcaneus, right navicular and mid cuneiform (all postcranials = same individual), left decid P₁ (early wear), left decid P₄ (early wear), left M₁₂, prob M₁ (unworn), (all teeth = same individual juvenile), F88 left decid P₂ (unworn) + mandible frags, F83 right tibia, crushed; right femur shaft, crushed; Q2 SEP 3 F1* left mandible, crushed, with M₂-M₁, * = same individual, early wear, young adult {F1*-F2*}, F2* right mandible with P₂-M₁

Unit 5b/6: EQP Q2 TP4 right femur, distal epiphysis

Unit 6: Q2 GTP 10 F1 left mandible with M₁-frag M₁, mid-late wear, adult

Unit 7: Q2 GTP 25 F10 right antler base attached to frontal

The red deer (*Cervus elaphus*) is the most common cervid at Boxgrove with a stratigraphic range spanning the marine sands of the Slindon Sand Member through to the Brickearth Beds of the Eartham Upper Gravel Member. Dental remains are well preserved, although postcranial material, with a few exceptions (Fig 160), is fragmentary. Measurements of the Boxgrove red deer are given in Table 61 and metrical comparisons with other Pleistocene and Recent red deer are given in Table 62. Based on the small sample of M₃s from the site, the Boxgrove red deer seem to have been of small body size, comparable to those of the Hoxnian interglacial.

The red deer first appears in the early Middle Pleistocene Cromerian Interglacial (West Runton) and persists until the present day. The late Cromerian/early Anglian red deer from Mosbach and Mauer have a characteristic antler morphology with a simple two-pointed antler top (*C. e. acoronatus*). This form differs from the Hoxnian and Recent red deer which have a complex antler top, a form which is first recorded from the Hoxnian channel deposits at Clacton (Lister 1986). The transition between the two antler morphologies presumably took place at some stage during the Anglian/Elsterian glaciation. Unfortunately, antler material is sparse at Boxgrove and no antler tops are present in the sample.

The red deer is an extremely adaptable species and it occurred throughout Europe in the early Holocene. The red deer now inhabits a wide range of habitats from treeless moorland, mountains, grassy plains, and open woodland, feeding on shrubs, tree shoots in woodland, and grasses, sedges, and rushes in open habitats. Although the red deer is often regarded as an interglacial woodland species, it is also found in cold stage faunas in open conditions.

Table 62 Comparison of M₃ length of *Cervus elaphus* from Swanscombe, Hoxne, Star Carr (from Lister 1993b), and Boxgrove

site	n	length M ₃		
		min	\bar{x}	max
Star Carr	30	31.6	34.55	39.0
Hoxne	3		(28.5, 30.2, 30.7)	
Clacton	1		(28.6)	
Swanscombe	3		(27.8, 27.9, 28.3)	
Boxgrove	3		(29.3, 30.1, 31.4)	



Fig 160 *Cervus elaphus*: rearticulated lower hind limb bones (Q2 TP4 and TP6): right calcaneus, navicular, mid-cuneiform, and metatarsal; scale unit 10mm

Table 63 *Dama dama*: measurements (mm) of teeth

upper dentition												
q	area	unit	fauna no	<i>P¹</i>			<i>M¹</i>			<i>M²</i>		
				L	W	Ht	L	W	Ht	L	W	Ht
1	1/B	4c	F8	9.9	-	11	-	-	-	-	-	-
1	1/B	4c	F12	-	-	-	17.1	-	19.2	-	-	-
1	1/B	4c	F4	-	-	-	-	-	-	16.6(est)	20.8	13.3

lower dentition																		
q	area	unit	fauna no	<i>P₃</i>			<i>P₄</i>			<i>M₁</i>			<i>M₂</i>			<i>M₃</i>		
				L	W	Ht	L	W	Ht	L	W	Ht	L	W	Ht	L	W	Ht
1	1/B	5a	F264	11.5	8.1	11.1	12.9	7.8	12.9	15.7	10.8	12.4	18.1	12.7	16.8	23.8	11.5	15.5
1	1/A	G	F296	-	-	-	-	-	-	-	-	-	17.2	13.1	16.1	-	-	-

Genus *Dama*
Dama dama (Linnaeus 1758)
 Fallow deer

Unit 4c: Q1/B F8 left *P¹*, lingual missing, mid-wear, adult, F12 left *M¹*, mid-late wear, adult, F4 left *M¹*, mid-late wear, adult, F13 right *M¹*, mid-late wear, adult
 Gully fill: Q1/A F216, F296 left *M_{1,2}*, prob *M₂*, mid-wear, adult, refitting frags
 Unit 4d: Q1/B F461 right metatarsal
 Unit 5a: Q1/B BS87-170 F303 upper molar frag, mid-late wear, adult (cf), F264 right mandible frag with *P₃*-*M₃*, mid-wear, adult refits (F264, F263), F263 right *M₃* frag refits; EQP Q2 TP13 F117 right magnum, unciform, unfused distal metapodial epiphysis

The fallow deer (*Dama dama*) is represented by 11 specimens from Units 4c, 4d and 5a. Measurements of the Boxgrove fallow deer are given in Table 63, and comparisons with other Pleistocene assemblages are given in Table 64. The more complete dental remains are illustrated in Figures 161-4.

The Pleistocene record of the fallow deer in the British Isles is confined to the wooded interglacial periods, where it is recorded for the first time in the Upper Freshwater Bed of West Runton (Cromerian Interglacial). The Middle Pleistocene fallow deer from Clacton was formerly referred to *D. clactoniana* based on the larger body size and the presence of antlers with a narrow palmation and an additional third anterior tine. This form is now regarded as a subspecies, *D. d. clactoniana*. In addition to changes in antler form and body size during the early Middle to Late Pleistocene, the morphology of the teeth also underwent significant changes in occlusal pattern. The morphology of the Boxgrove teeth appears to be distinct from both the Cromerian fallow deer from West Runton and from those of Hoxnian age from Swanscombe. The dental remains from Boxgrove show a combination of features found in the Cromerian and Hoxnian sample, while

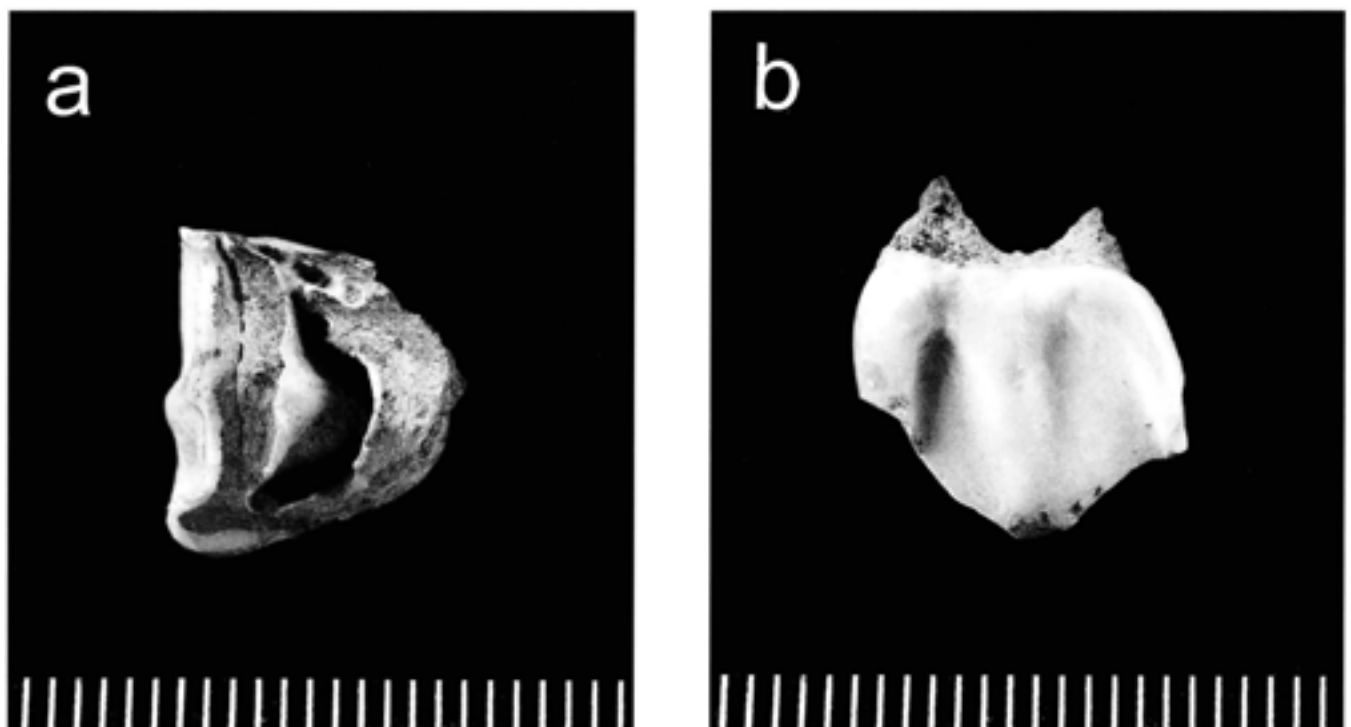


Fig 161 *Dama dama*: left *P¹* (Q1/B F8 Unit 4c), a) occlusal view, b) buccal view; scale unit 1mm

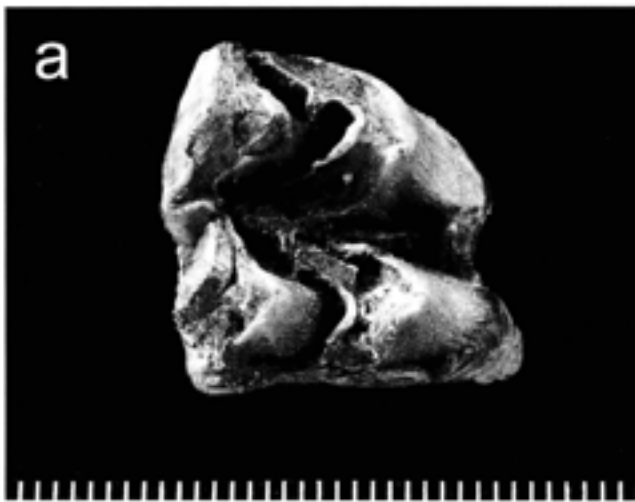


Fig 162a–b *Dama dama*: left M^1 (Q1/B F12 Unit 4c), a) occlusal view, b) buccal view; scale unit 1mm

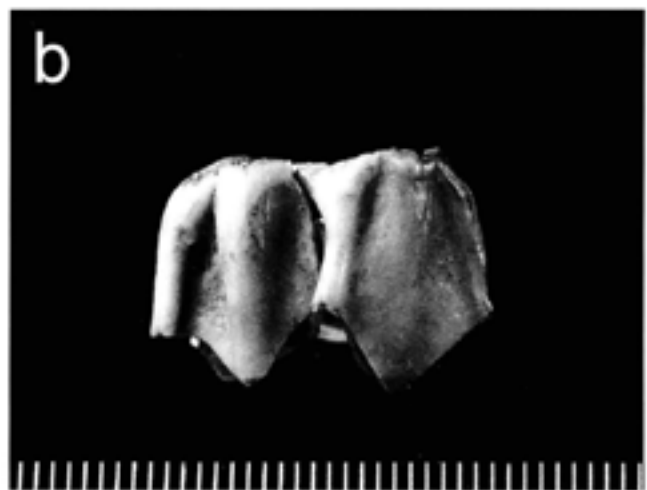
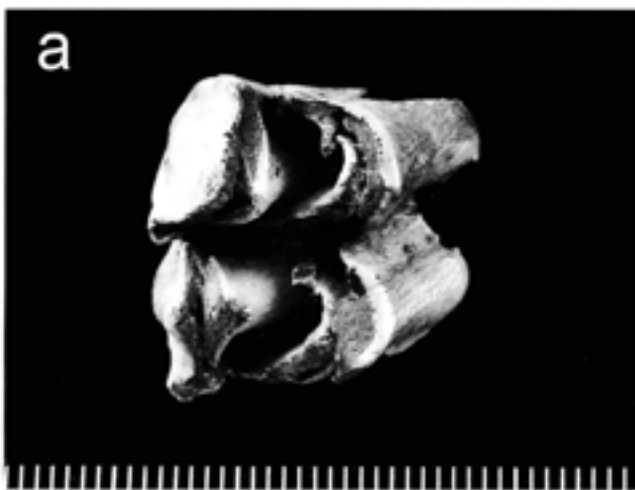


Fig 163a–b *Dama dama*: left M^2 (Q1/B F4 Unit 4c), a) occlusal view, b) buccal view; scale unit 1mm

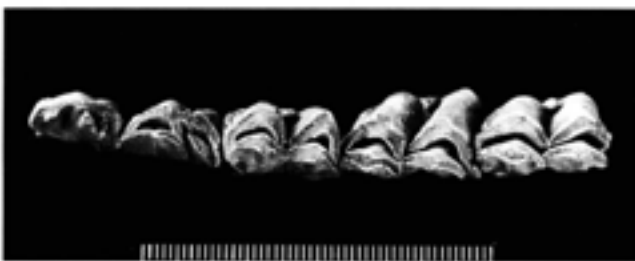


Fig 164 *Dama dama*: right mandible with P_3 – M_3 (Q1/B F264 Unit 5a), occlusal view (note broken third lobe of M_3 has not been reattached); scale unit 1mm

Table 64 Comparison of M_3 length (mm) in Recent and fossil *Dama dama*

	n	length M_3		
		min	\bar{x}	max
Recent (England)	11	20.7	21.6	22.5
Hoe Grange (Ipswichian)	10	23.6	24.3	25.0
Joint Mitnor Cave (Ipswichian)	4	23.2	24.0	25.0
Swanscombe (Hoxnian)	10	24.8	25.9	27.0
Westbury ('Cromerian Complex')	1		23	
Boxgrove	1		23.8(est)	
West Runton (Cromerian)	4	25.9	26.3	26.7

other features appear to represent transitional morphologies. This pattern is in accordance with the intermediate age of the Boxgrove sample.

In Table 64 the length of the lower third molar is given for 'Cromerian', Hoxnian, and Recent fallow deer. The largest fallow deer occur in the Cromerian *sensu stricto* and the Hoxnian (eg Swanscombe), while the Ipswichian fallow deer was intermediate in size between the small living fallow deer and the extremely large form of the Hoxnian. In comparison, the Westbury and Boxgrove teeth are seen to be relatively small, falling within the range of Recent fallow deer from southern England.

The record of fallow deer from Units 4c, 4d, and 5a is of particular palaeoenvironmental interest as the distribution of this species is limited to regions with a temperate or oceanic climate. The fallow deer is intolerant of cold climates and its present day range extends no further north than southern Sweden. The reproductive biology of the fallow deer, notably the relatively late rut which leaves males in poor condition during the winter and the birth of the fawns in late summer, appear to be important factors limiting the distribution of the fallow deer in northern latitudes. The habitat

preferences of the fallow deer are also specific, and the species is mostly found in open deciduous or mixed woodland with a well developed shrub layer. Fallow deer are mainly a grazing species feeding in forest clearings and woodland margins. The British Pleistocene record of the fallow deer is entirely restricted to woodland interglacial episodes, which corresponds with the ecological requirements of this species.

Genus *Capreolus*

Capreolus capreolus (Linnaeus 1758)

Roe deer

- Unit 4: Q1/B F372 left humerus shaft frag (cf), F368 left radius shaft frag, F400 right tibia, unfused distal epiphysis, F404 right calcaneus, proximal unfused, juvenile, F402 right metatarsal, proximal and shaft, juvenile, F363 metatarsal shaft frag (cf)
- Unit 4b: Q1 GTP 22 F20 metatarsal shaft frag (cf); Q2 GTP 17 F660 left mandible frag with M₁ and M₂ roots, F1064 metatarsal shaft frag, ?juvenile
- Unit 4c: Q1/B F29 right lower molar frag; Q1 GTP 15 F1 two first year antlers, shed; Q1 GTP 30 F7* (Sq A) left radius, distal and shaft, F5* (Sq B) left scapoid * = same individual {F5*-F7*}, F6* (Sq B) left cuneiform, F14 (Sq A) metatarsal shaft frag, F18 (Sq A) metatarsal shaft frag, F17 (Sq A) first phalanx and vestigial phalanx; EQP Q1 TP6 F91a left decid P₁, M₁^{1/2}, early wear, juvenile, F91b phalanx I, proximal and distal frags; Q2/B F13 left mandible with P₁-M₂, mid-wear, adult refits {F13, F20}, F20 left M₁, mid-wear, refits, F17 right femur, proximal epiphysis; Q2/C F2 right deciduous P₁ frag, late wear, juvenile; Q2 GTP 3 F21 antler frag, shed refits {F21, F22}, F22 antler frag, BS87-242 F79 right decid P₁, early wear, juvenile, BS87-263 F81 right M₁^{1/2} frag, early, subadult, BS87-251 F85 molar frag (cf), BS86-36 F80 right P₁, mid-wear, adult, F67 right I₂, P₁-M₁, mid-late wear, adult, F19 right mandible with P₁-M₂, late wear, adult, F72 left mandible frag with P₁-M₂, mid-wear, adult, F68 right radius shaft frag, F18 right calcaneus frag, F66 left metatarsal, proximal and shaft frags, F63 right P₁, M₁^{1/2}, prob M₁, and mandible frags; Q2 GTP 13 F5 left mandible frag with M₁-M₂ (damaged), mid-wear, adult; Q2 GTP 17 F38 antler burr frag, F46 right scapula, glenoid and neck, F535 metatarsal shaft frag, ?juvenile, F638 metapodial shaft frag; EQP Q2 TP2 F26 metatarsal shaft frag, juvenile, F28 metatarsal shaft frag, juvenile; EQP Q2 TP3 left P₁, early-mid wear, young adult, F68 molar frag; EQP Q2 TP6 right metatarsal proximal frag, F93 right mandible frag with decid P₁, decid P_{1,4} (early wear, juvenile), prob M₁ frags; Q2 SEP 2 F15 right antler, missing base
- Unit GC: Q2 GTP 3 F101 upper molar frag, BS88-468 F98 left I₂ (cf), BS88-466 F97 right I₂, root missing, BS88-468 F99 left I₁, root missing
- Unit 4 (undifferentiated): EQP Q2 TP3 right calcaneus, F55 left femur shaft frag (cf)
- Unit 5a: Q1/B BS87-126 F304 right M₁^{1/2} frag, buccal wall, early wear, subadult, F2 right M₁, mid-wear, adult, F28 left P₁, buccal wall; Q2 GTP 3 BS88-469 F95 right I₁ frag, root missing; Q2 GTP 17 F534 metatarsal shaft frag, ?juvenile; EQP Q2 TP2 right humerus shaft frag (cf); EQP Q2 TP7 left M₁, partially decalcified; Q2 SEP 2 F1 right P₁-P₄, early-mid wear, young adult
- Unit LGC: Q2/B F10 left mandible, ascending ramus frag (cf), F1 right mandible with decid P₂ (early wear), decid P₃ (mid-wear), decid P₄ (mid-wear), M₁ (very little worn), M₂ (unworn), juvenile
- Misc: EQP Q1 TP14 No 71 left M_{1,2}, prob. M₂, mid-wear, adult, F65 metacarpal shaft frag, F58 metapodial shaft frag
- Unstratified: Q2 SEP 2 F23 metatarsal shaft frag

The roe deer (*Capreolus capreolus*) is abundant in the Boxgrove fauna, although it is more restricted in its stratigraphic range than the red deer. It is well represented in the upper part of the Slindon Silt Member and the base of the Eartham Lower Gravel Member.

The occurrence of this species in the temperate part of the sequence is in accordance with its present ecological requirements.

The roe deer is poorly represented in British Pleistocene localities, where it is recorded from each of the major temperate episodes. According to Lister (1993), the earliest record of the roe deer is from the late Early Pleistocene of Untermassfeld (Germany). The early Middle Pleistocene roe deer from Sussenborn (Germany) has been referred to a separate species, *C. sussenbornensis*, because of its large size and more elliptical antler section than in living roe deer. Lister (1993) has questioned this specific designation, and this is clearly justified given the size range and morphological differences seen in Recent roe populations, such as those between the European and Siberian roe deer *C. c. pygargus*.

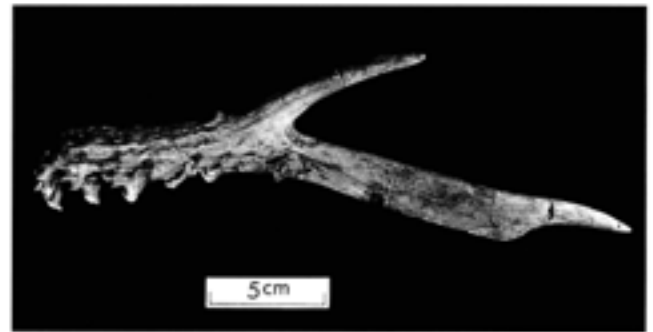


Fig 165 *Capreolus capreolus*: right antler (Q2 SEP 2 F15 Unit 4c)

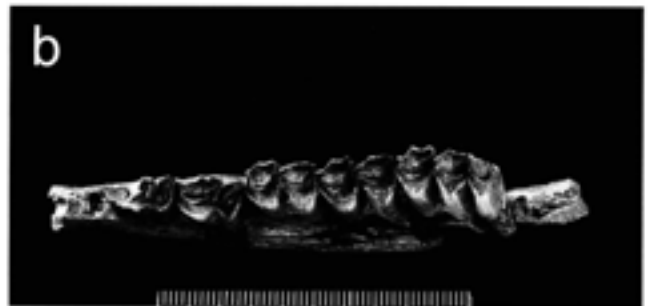


Fig 166 *Capreolus capreolus*: left mandible with P₁-M₂ (Q2 GTP 3 F72 Unit 4c), a) buccal view, b) occlusal view; scale unit 1mm

Table 65 *Capreolus capreolus*: measurements (mm) of postcrania and teeth

q	area	sex	specimen no.	bone element	GLP	Bp	S/LC	DC	BD	RFJ	DD	LG	BG
2	GTP 17	4c	F46	scapula	-	33.3	-	21.5	-	-	-	-	25.8
1	GTP 30	4c	F7	radius	-	-	-	-	-	30.8	29.8	-	-
2	2B	4c	F17	femur	-	-	-	-	23.7	-	-	-	-
1	1B	4	F400	tibia [unfused epiphysis]	-	-	-	-	-	30.4	-	23.5	-
1	1B	4	F340	metatarsal [juvenile]	-	-	21.4	-	-	(est)	-	(est)	-

upper dentition														
q	area	sex	specimen no.	L	W	Ht	P ^c	L	W	Ht	P ^c	L	W	Ht
1	TP6	4c	F91a	-	-	6.4	-	-	-	-	-	-	-	-
2	SEP 2	5a	F1	-	-	-	-	-	-	-	-	-	-	-
1	B	4c	F2	-	-	-	11.3	9.7	9.4	8.6	12.2	9.3	9.1	11.4
				-	-	-	-	-	-	-	-	-	11.7	14
				-	-	-	-	-	-	-	-	-	-	9.9

lower dentition														
q	area	sex	specimen no.	L	W	Ht	L	W	Ht	P ₃	L	W	Ht	M ₁
2	2B	LGC	F1	6.6	3.9	4.2	10.7	5.5	5.3	-	-	-	-	-
2	BQP/TP6	4c	F93	6.7	4	4.7	9.6	5.5	4.5	14.6	7.8	5.9	-	-
2	GTP 3	4c	F72	-	-	-	-	-	-	-	-	-	-	-
2	GTP 3	4c	F67	-	-	-	-	-	-	9.8	6.8	5.7	10.9	7.8
2	2B	4c	F13	-	-	-	-	-	-	9.9	6.8	5.8	10.6	8.3
2	GTP 3	4c	F19	-	-	-	-	-	-	9.4	7.7	6.4	11.5	8.1
2	GTP 3	4c	F19	-	-	-	-	-	-	10.2	7.7	5.6	11.3	9.3
2	GTP 17	5a	F63	-	-	-	-	-	-	10.3	8	6.7	11.6	8.9
2	BQP/TP3	4c	-	-	-	-	-	-	-	9.8	7.3	6.3	-	-
2	GTP 13	4c	F5	-	-	-	-	-	-	-	-	-	11.1	9.1
2	2B	4c	F1	-	-	-	-	-	-	-	-	-	11.7	8.8
2	BQP/TP4	-	No 71	-	-	-	-	-	-	-	-	-	(est)	(est)
				-	-	-	-	-	-	-	-	-	12.3	8.7
				-	-	-	-	-	-	-	-	-	6.7	6.7

q	area	sex	specimen no.	L	W	Ht	L	W	Ht	M ₁	L	W	Ht	M ₁	L	W	Ht	M ₁	post lobe	
2	2B	LGC	F1	6.6	3.9	4.2	10.7	5.5	5.3	-	-	-	-	-	-	-	-	-	-	
2	BQP/TP6	4c	F93	6.7	4	4.7	9.6	5.5	4.5	14.2	6.9	5.9	-	-	-	-	-	-	-	
2	GTP 3	4c	F72	-	-	-	-	-	-	-	-	-	-	-	-	-	-	-	-	
2	GTP 3	4c	F67	-	-	-	-	-	-	9.8	6.8	5.7	10.9	7.8	7.3	5.1	6.7	17	12.4	8.2
2	2B	4c	F13	-	-	-	-	-	-	9.9	6.8	5.8	10.6	8.3	7.1	5	6.7	17.4	12	8.5
2	GTP 3	4c	F19	-	-	-	-	-	-	9.4	7.7	6.4	11.5	8.1	8	7.6	8.9	17.2	12.4	9.1
2	GTP 3	4c	F19	-	-	-	-	-	-	10.2	7.7	5.6	11.3	9.3	3.4	5	5	16.3	12.2	9.3
2	GTP 17	5a	F63	-	-	-	-	-	-	10.3	8	6.7	11.6	8.9	6.4	-	-	-	-	-
2	BQP/TP3	4c	-	-	-	-	-	-	-	9.8	7.3	6.3	-	-	-	-	-	-	-	-
2	GTP 13	4c	F5	-	-	-	-	-	-	-	-	-	-	-	12	9.3	8.7	17.9	11.8	-
2	2B	4c	F1	-	-	-	-	-	-	-	-	-	-	-	11.9	9.2	9.9	-	-	-
2	BQP/TP4	-	No 71	-	-	-	-	-	-	-	-	-	-	-	(est)	(est)	-	-	-	-
				-	-	-	-	-	-	-	-	-	-	-	12.3	8.7	6.7	-	-	-



Fig 167 *Capreolus capreolus*: comparison of Boxgrove scapula fragment (Q2 GTP 17 F46 Unit 4c) with that of a Recent roe deer from West Sussex; scale unit 1mm



Fig 168 *Capreolus capreolus*: comparison of Boxgrove calcaneus (Q2 GTP 3 F18 Unit 4c) with that of a Recent roe deer from West Sussex; scale unit 1mm

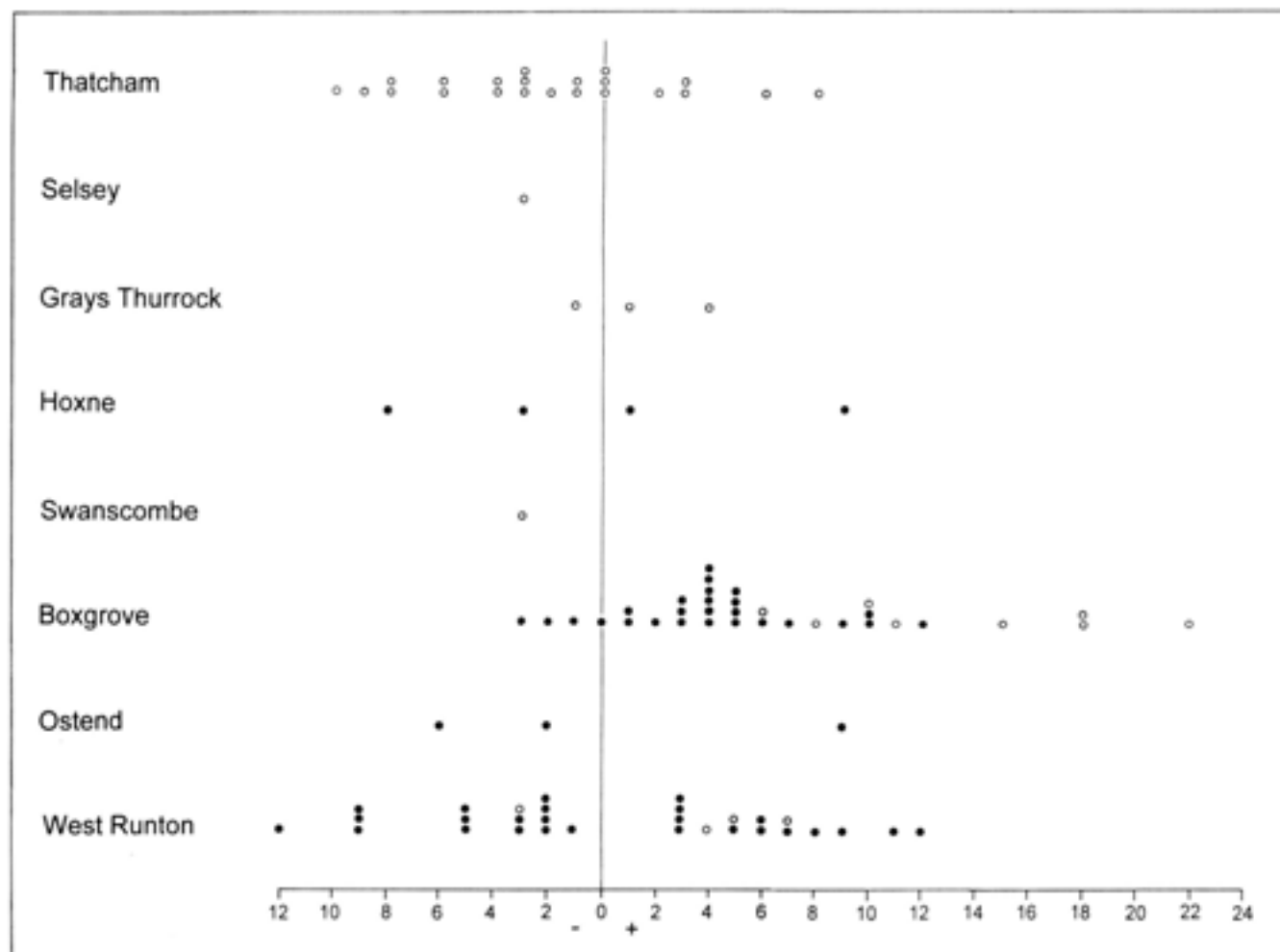


Fig 169 *Capreolus capreolus*: measurement comparisons of British Pleistocene and early Holocene with Star Carr roe deer (early Holocene). The fossil specimens are plotted as a percentage deviation from the Star Carr sample (vertical line), and the sites are arranged in a temporal sequence: early Middle Pleistocene: West Runton (Cromerian sensu stricto); Ostend, Boxgrove; Middle Pleistocene: Swanscombe, Hoxne; late Middle Pleistocene: Grays Thurrock, Selsey; early Holocene: Thatcham (circles=postcrania, dots=teeth)

Measurements of the Boxgrove roe deer sample are given in Table 65 and some of the more complete elements are illustrated in Figures 165–8. Size comparisons between the Boxgrove sample and those from other British localities is problematic due to the small size of the samples from many of the sites. In Figure 169 the dimensions of roe deer from the Middle Pleistocene of West Runton, Ostend, Swanscombe, and the later Middle Pleistocene sites of Grays and Selsey are compared with a Holocene sample from Star Carr by means of a percentage diagram. The large size of the Boxgrove roe deer in comparison with the other samples is immediately apparent from this diagram, while those of the other localities cluster around the mean of the standard sample. In addition to these size differences, the Boxgrove roe deer is also distinguished by morphological peculiarities which are rare or absent in the dentition of Recent European roe deer. In the Boxgrove P_3 , the metaconid is inflated and unlike those of Recent roe deer, which have a narrow metaconid. The posterior lobe of the Boxgrove M_3 is enlarged compared to the Recent European samples which have a reduced third lobe. In the upper premolars from Boxgrove, the lingual wall has a pronounced furrow dividing the protocone from the hypocone, whilst in the Recent sample this furrow is absent or indistinct. These features are also found in the other large sample of early Middle Pleistocene roe deer from West Runton. Unfortunately, the sample of roe deer from Hoxne lacks these teeth and it is therefore not possible to determine whether the dental peculiarities of the Boxgrove sample are present in Hoxnian roe deer.

The present day distribution of the roe deer covers most of Europe with the exception of the far north. It is found in deciduous, mixed and coniferous woodlands with open ground, and occasionally in open terrain if shelter is available. The British Pleistocene record of the roe deer is restricted to woodland interglacial episodes although it is rarely a common component of these assemblages.

Genus Megaloceros
Megaloceros cf verticornis
Extinct giant deer

Unit 4b: Q1/A F3353* left P^2 *same individual, mid-late wear, adult (F3325*, F3353*, F3355*, F3356*, F3357*, and Unit G F303), F3357* left P^3 , F3325* right M^1 , F3361 left M^1 , mid-late wear, adult, F3355* right M^2 , F3356* right M^3 + maxilla frags
Gully fill: Q1/A F303* left M^3 , mid-late wear, adult
Unit 5a: Q1/A F389 left M^3 , prob M^3 , frag, mid-late wear, adult

Remains of a megalocerine deer are represented by a partial upper dentition from Unit 4b and a fragment of an M^{c2} from Unit 5a. These teeth, found in association in Quarry 1/A, are illustrated in Figures 170a–b, 171a–b, and measurements are given in Table 66. Size comparisons with early Middle Pleistocene and Late Pleistocene *Megaloceros* spp are illustrated in Figures 172 and 173.

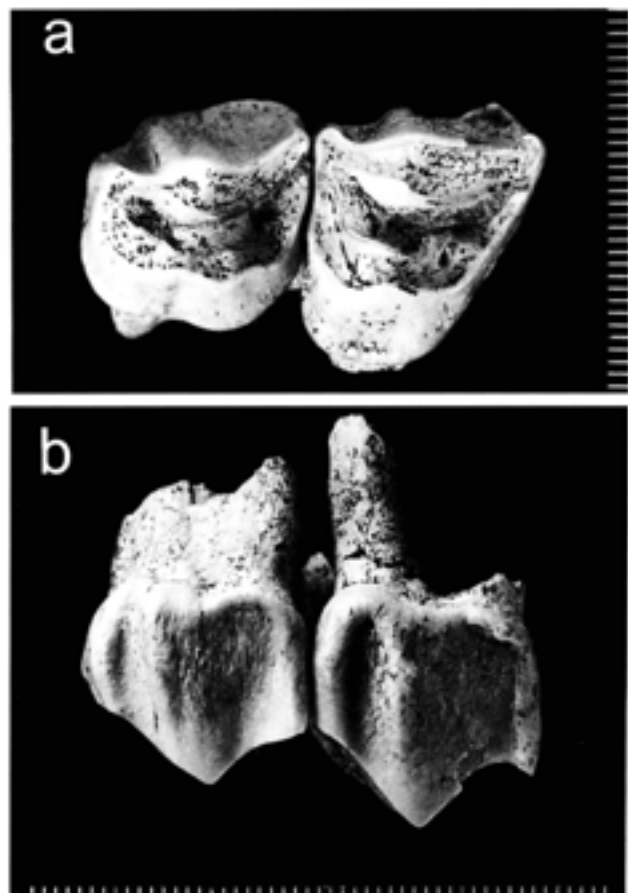


Fig 170 *Megaloceros cf verticornis*: left P^2 and P^3 (Q1/A F3353 and F3357 Unit 4b), a) occlusal view, b) buccal view

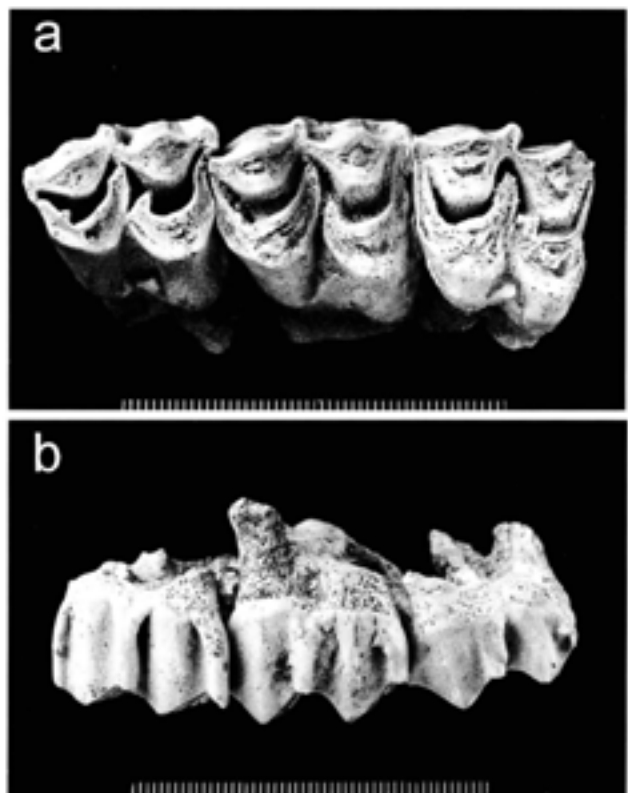


Fig 171 *Megaloceros cf verticornis*: right M^1 – M^3 (Q1/A F3325, F3355, F3356), a) occlusal view, b) buccal view; scale unit 1mm for Figs 170–1

Table 66 *Megaloceros cf verticornis*: measurements (mm) of teeth

upper dentition				P^2			P^3			M^1			M^2			M^3		
q	area	unit	fauna no	L	W	Ht	L	W	Ht	L	W	Ht	L	W	Ht	L	W	Ht
1	1/A	4b	F3353	16	19.1	16.7	—	—	—	—	—	—	—	—	—	—	—	—
1	1/A	4b	F3357	—	—	—	16.4	21	19.4	—	—	—	—	—	—	—	—	—
1	1/A	4b	F3361	—	—	—	—	—	—	23.4	24.2	10.8	—	—	—	—	—	—
1	1/A	4b	F3355	—	—	—	—	—	—	—	—	—	24.4	27.8	15.7	—	—	—
1	1/A	4b	F303	—	—	—	—	—	—	—	—	—	—	—	—	23.2	25.7	14.3
1	1/A	5a	F389	—	—	—	—	—	—	—	—	—	24.9	—	14.2	—	—	—

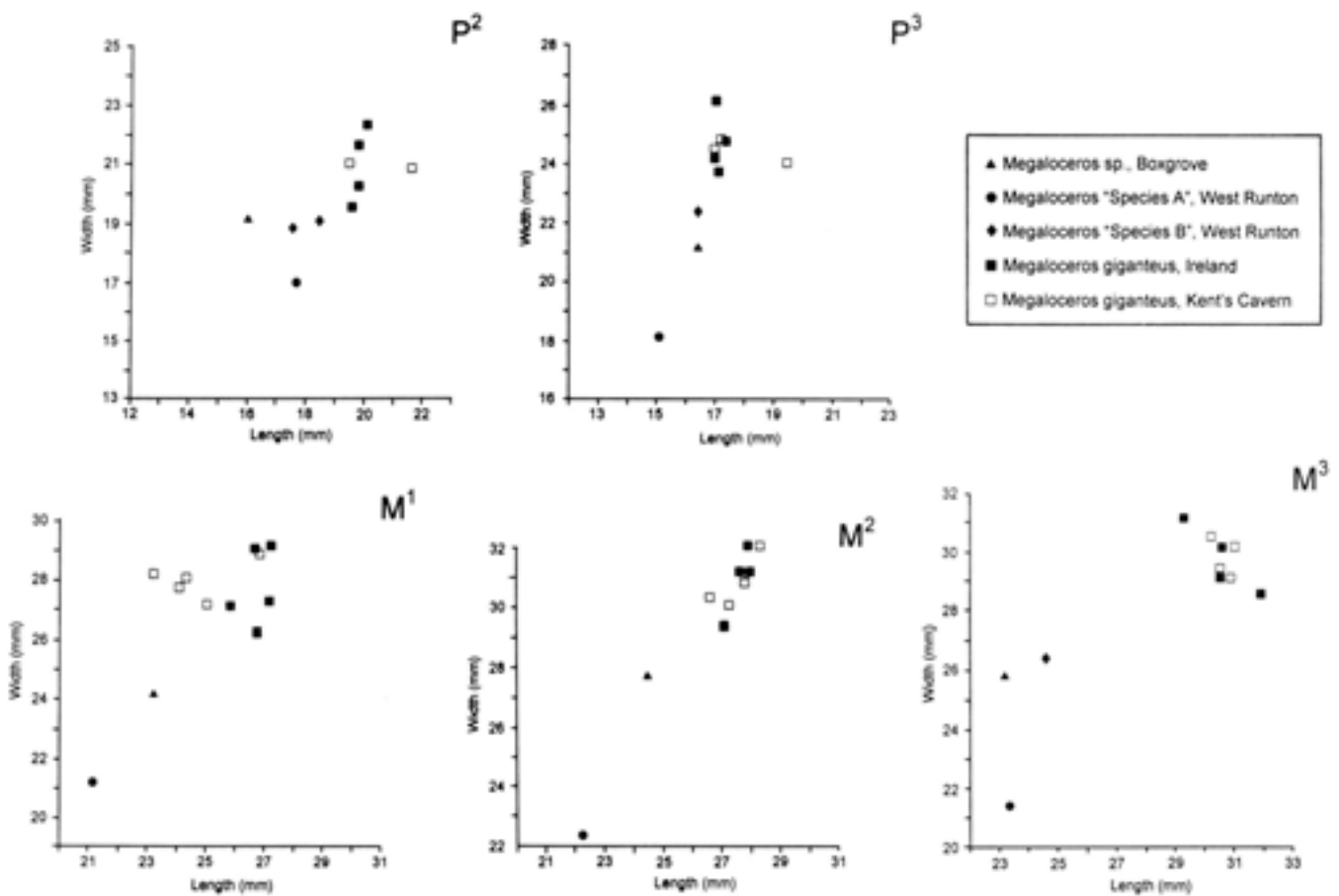


Fig 172 *Megaloceros* spp: length-width scatterplots of upper premolars and molars of giant deer from Boxgrove, West Runton (*Megaloceros* sp 'A' and 'B', Cromerian *sensu lato*), Kent's Cavern (*M. giganteus*, Devensian), and Ireland (*M. giganteus*, Devensian Lateglacial)

The Pleistocene history of the megalocerine deer has been reviewed by Lister (1993; 1994), who recognises three species from the British Cromerian *sensu lato*: *Megaloceros verticornis* (Dawkins), *M. dawkinsi* (Newton), and *M. savini* (Dawkins). Both *M. verticornis* and *M. savini* are recorded from the Upper Freshwater Bed of West Runton. The sample of antler remains from this site is rather small and the absence of *M. dawkinsi* from the locality may well be a sampling artefact or the result of a taphonomic factor (Lister 1993). The three Cromer Forest-Bed species are not recorded in post Anglian/Elsterian contexts, but are replaced by *Megaloceros giganteus* which is recorded for the first time in the Homersfield Gravels (Norfolk) of probable late Anglian age, and from the Hoxnian/Holsteinian of

Steinheim and Swanscombe (Lister 1993; 1994). This species is well represented in both warm and cold stage faunas of the Middle and Late Pleistocene and persists until the end of the last glaciation.

Based on the collection of megalocerine teeth from West Runton in the Natural History Museum (London), it can be shown that two distinct morphological groups are represented. In the following comparisons and discussion these are referred to *Megaloceros* sp A and B. *Megaloceros* sp A is represented by a maxilla fragment with P^2 - M^3 . In this specimen, the cones of the upper molars are poorly developed and buccal faces of the metacone and paracone are only slightly raised. The basal cingulum is well developed and the profile of the crown-root junction at the

base of the cones is rounded. *Megaloceros* sp B is the more common form and is represented by a number of isolated upper teeth and an associated P²⁻⁴ which are readily distinguishable from *Megaloceros* sp A in morphology and dental proportions. In this group, the cones of the upper molars are well developed and the teeth are broad in contrast to the relatively narrow teeth of *Megaloceros* sp A (Fig 172).

Dimensions of *Megaloceros* sp from Boxgrove have been compared with those of other megalocerine deer by means of Simpson's (1941) ratio diagram (Fig 173). The comparisons made in this diagram are between Irish Devensian Lateglacial *M. giganteus* (standard for comparison), *Megaloceros* sp A and B from West Runton, and the associated teeth from Boxgrove. The comparisons given in Figure 173 indicate that the giant deer from Boxgrove and West Runton are smaller than Lateglacial *M. giganteus*. In addition, the British early Middle Pleistocene giant deer differ from *M. giganteus* in dental proportions. The Boxgrove dentition differs markedly from those of *Megaloceros* sp A, in which the teeth are relatively narrow in comparison to their length (Fig 173). In contrast, the size and dental proportions of *Megaloceros* sp B from West Runton are almost identical to those of the Boxgrove sample.

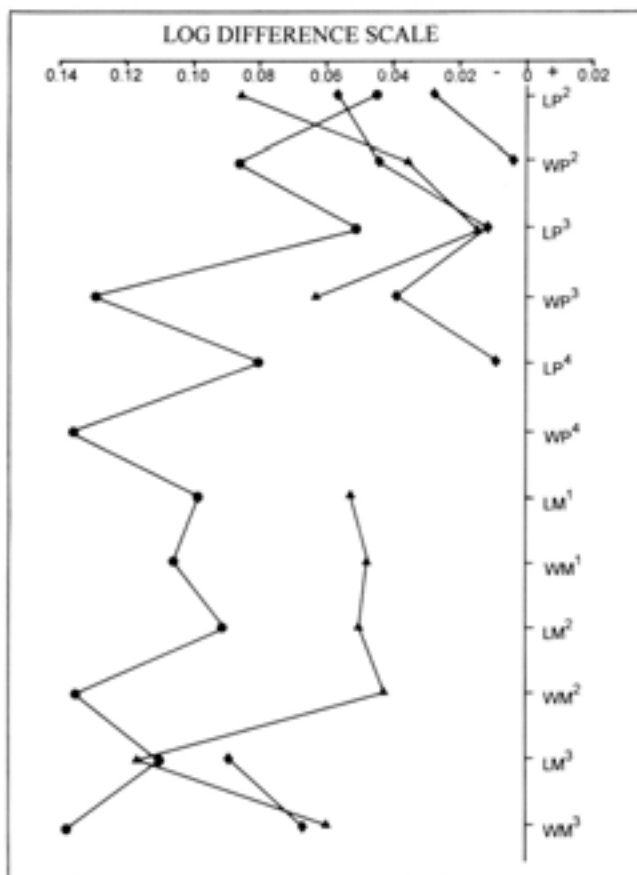


Fig 173 *Megaloceros* spp: log ratio diagram showing the relative proportions in the upper dentition of giant deer. The standard (vertical line) is Lateglacial *M. giganteus* from Ireland (for key see Fig 172)

The taxonomy of the early Middle Pleistocene giant deer is based almost exclusively on antler form. Given that two or more megalocerine deer are commonly represented in the Cromer Forest-bed sites, it is impossible to refer isolated teeth from these sites to species with certainty. However, based on the relative abundance and size of the West Runton giant deer teeth, *Megaloceros* sp A is tentatively referred to *M. savini*, and *Megaloceros* sp B is referred to *M. verticornis*. The Boxgrove giant deer is clearly distinct from *M. giganteus*, and, on the basis of its similarity to *Megaloceros* sp B of West Runton, it is tentatively referred to *M. verticornis*.

Cervidae gen et sp indeterminate Cervid

- Unit 4: Q1/B F348 antler frag (M/L= medium/large sized cervid); F421 antler frag (L=large sized cervid), F442 antler frag (L), F428 right temporal condyle frag (L), F432 right basi-sphenoid frag (L), F381 radius shaft frag (S/M), F351 radius shaft frag (M/L), F347 metacarpal shaft frag (M/L), F389 metatarsal shaft frag (L), F350 phalanx II, distal (L)
- Unit 4b: Q1/A F3255, F3320, F3335 (refits to F3494), F3494, F3443, F3456, F3459, F3464, F3466, F3469, F3476, F3419, F3420, F3412 antler frags (L), F3331 left humerus shaft frag (L), F3317 left tibia shaft frag (L/M), F3350 left tibia shaft frag (L/M), F3321 left tibia shaft frag (L), F3430 left tibia shaft frag (L), F3433 right tibia shaft frag (L) refits {F3433, F3397}, F3397 right tibia shaft frag (L), F3402 left femur shaft frag (L), F3232 1st tarsal (L), F3465 metatarsal shaft frag (L); Q1/B F256 petrosal frag (cf) (M/L), F259 left radius, distal frag (M/L); F328 left patella (L), F392 sacrum frag (L), F255 vestigial phalanx I (M/L); Q1 GTP 8 F21 right humerus shaft frag (L), F22 left tibia shaft frag (L), F9 right femur shaft frag (L) refits {F9, F20}, F20 right femur shaft frag (L) refits, F7 metapodial shaft frag (L); Q1 GTP 30 F28 tibia shaft frag (L); EQP Q1 TP5 F78 phalanx I frag (L); EQP Q1 TP7 No 51 rib, proximal (L); Q2 GTP17 F585 metatarsal shaft frag (M/L)
- Unit 4c: Q1/A F1885 right I₂, ?deciduous (M/L), F2206 right I₂ (L), F2161 molar frag, unworn, juvenile (M/L), F2780 molar frag, unworn, juvenile (L), F1615 molar frag (L), F3191 sacrum frag (M/L), F2197, F2709 metapodial shaft frags (M/L); Q1/B F52* right frontal frag (L) * = poss same individual {F52*, F54*}, F54* left frontal frag (L), F309 P/M frag (S/M); F131 molar frags, early-mid wear, adult (M/L), F32 thoracic vertebra spine frag (L), F127, F128, F153 left humerus shaft frags (S) refitting group, F74 ?metacarpal shaft frag (M/L), F72 ?metacarpal shaft frag (?M), F207, F225, F233 metapodial shaft frags (M/L) refitting group; Q2 GTP 8 F1 metapodial shaft frag (L); Q1 GTP 15 F2 metatarsal shaft frag (L); Q1 GTP 16 F2 antler frag (M/L), F1 right femur shaft frag (S/M); Q2/B antler frag (M/L), F69 molar frags (M/L), F16 left lateral malleolus (L), F65 vestigial phalanx I (L), F60 left tibia, distal frag (L); Q2/C F5 right radius shaft frag (M/L); Q2 GTP 3 F75 antler tine tip, F55 antler frag (M/L), BS87-136 F82 molar frag, F83 P frag, BS87-156 F92 molar frags, unworn, juvenile (L), F48 molar frag (L); BS88-461 F86 molar frag, F31 upper molar frag, unworn, juvenile (S/M), F29 upper molar frag, unworn, juvenile (M/L), BS87-148 F94 lower M frags, unworn, juvenile (L), F7 mandible, ascending ramus frag (M/L), F3 mandible frag, ?juvenile (S/M), BS87-148 F93 mandible frags (L), F8 humerus, distal epiphysis frag (L), F44 humerus shaft frag (S), F100 left humerus shaft frag, F76, F77 left tibia shaft frags (M/L) refitting group, F69 right femur shaft (L), F20 metatarsal shaft frag (L), F5 metapodial shaft frag (L); Q2 GTP 13 F28 cervical vertebra frag (L); Q2 GTP 17 F308 antler frag, F1077 tooth frag (?cervid), F1074 tooth frag, F1084 molar frags, F15 left scapula, glenoid and neck (L), F320 right radius shaft frag (M/L), F154, F157 tibia, distal epiphysis frags, unfused (L) refitting group, F167 metapodial shaft frag, F1070 metapodial shaft frag; EQP Q2 TP2 F53 metapodial shaft frag (L); EQP Q2 TP6 F94 left mandible, diastema frag, ?juvenile (M); Q2 SEP 2 F27 left femur shaft frag

- Unit GC: Q2 GTP 3 BS88-466 F96 I, frag (L), F84 P, frag, unworn, juvenile (L)
- Gully fill: Q1/A F3429, F3505, F3507a, F3510, F3512, F3513, F3514, F3515 antler frags (L), F331 maxilla frag (L), F364 molar frag, unworn, juvenile (L), F3510 right humerus, distal epiphysis frag (M/L), F3507b right tibia shaft frag, F3515a metapodial shaft frag (M/L)
- Unit 4c/5a: Q1/B F86 frontal-parietal frag (L)
- Unit 4d: Q1/B F284 molar frag (M), F279 left mandible, ascending ramus frag ?juvenile (M/L)
- Unit 5a: Q1/B BS87-132 F305 P/M frag (M/L), BS87-131 F306 P/M frag (M/L), BS87-233 F307 P/M frag (M/L), BS87-139 F308 molar frag (M/L), BS87-131 F311 metapodial, proximal frag (M); EQP Q1 TP6 F47 right unciform (L); EQP Q1 TP7 F52 antler base frag (M/L); Q2/C F42 left femur shaft frag (L); Q2 GTP 3 F90, F91 M frags (L), F24, F25 upper molar frag, unworn, juvenile (M/L), F56 metapodial shaft frag (M/L); Q2 GTP 17 F526 metacarpal shaft frag (M/L), F527, F528 metatarsal shaft frags (L) refitting group, F1071 metapodial shaft frag; EQP Q2 TP5 F89 right humerus, distal, crushed (M); EQP Q2 TP13 F116 antler frags (M/L)
- Unit 5b: Q2 GTP 17 F330 antler tine frag (M/L), F237 metapodial shaft frag (L)
- Unit 5c: Q2 GTP 17 F152 metatarsal, proximal frag (M), F530 metatarsal shaft frag (L), F329 metapodial shaft frag (L)
- Unit 5a/6: Q2 GTP 3 BS88-460 F89 M frags (L)
- Unit 1129 (Table 9b): Q2 GTP 25 F4 left metatarsal shaft frag (L)
- Unit 6: Q1/A F67 metatarsal, distal condyles frag (L), F215 metapodial shaft frags (L)
- Misc: Q1 GTP 22 F1 molar frag, unworn, juvenile (M/L), F16 lower molar frag, unworn, juvenile (M/L); EQP Q1 TP1 Gully Unit 1 No F metacarpal shaft frag (M) refits [No F, No G]; Gully Unit II No G metacarpal shaft frag refits; EQP Q1 TP14 No 74 cervical vertebra frag (L); Q2 GTP 17 F355 right mandible, diastema frag (L), F783 rib (S/M)
- Unstratified: Q2 SEP 2 F31 right humerus shaft frag (M/L), F29 ulna, distal frag (S/M), F14 metapodial shaft frag (L), F28 metapodial shaft frag (L)

Family Bovidae
Genus *Bison*
Bison sp
Bison

- Unit 4c: Q2/C F3 left femur shaft frag (cf); Q2 1984 No 50 right metacarpal, proximal frag (lateral missing); Q2 GTP 3 F70 right cuneiform; Q2 GTP 17 F22* left humerus, proximal missing * = same individual {F22*, F28*, F137*}, F28* left radius (crushed) and ulna, F137* left metacarpal
- Unit 8 Chalk Pellet Beds: Q2 GTP 25 F16* 3rd cervical vertebra, F15* 6th cervical vertebra, F17* thoracic spine frag, F18* rib, proximal frag (cf)
- Unit 6: Q1/A F5 phalanx II
- Misc: EQP Q1 TP1 F22 left M¹/₂

Bison is uncommon in the Boxgrove assemblage being represented by 12 specimens. Measurements are given in Table 67 and the associated forelimb bones from GTP 17 (Unit 4c) are illustrated in Figures 175 and 176. The occlusal view of an upper first or second molar is shown in Figure 174.

The distinction between *Bos* and *Bison* is difficult in fossil assemblages in the absence of skulls and horn cores. However, differences in postcranial morphology described by Sala (1987) and Gee (1993) may allow more complete elements to be referred to *Bos* or *Bison*.

The morphology of the complete radioulna, humerus and the two metacarpals from Boxgrove is consistent with *bison*. However, some of the features

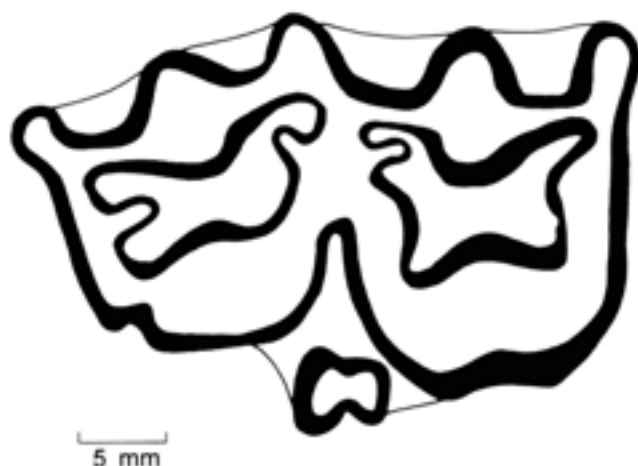


Fig 174 *Bison* sp: left M¹ or M² (EQP Q1 TP1 F22)



Fig 175a-b *Bison* sp: left metacarpal (Q2 GTP 17 F137 Unit 4c), a) anterior view, b) proximal articular surface; scale unit 10mm

described by Gee (1993) as characteristic of *bison* are less well developed than in Late Pleistocene *Bison priscus* from Isleworth. This feature of the postcrania of early Middle Pleistocene *bison* has been described by Sala (1987) who notes the primitive aspect of the postcranial skeleton of *Bison schoetensacki* from Isernia (Italy).

Bison of Early and early Middle Pleistocene age have been referred to *B. schoetensacki* Freudenburg, a relatively small species with short dorso-ventrally flattened horn cores. This species is common in the early

Table 67 *Bison* sp: measurements (mm) of postcrania

q	area	unit	fauna no	bone element	GL	Bp	SD	BD	BFd	BT	DD	DPA	SDO	BPC
2	GTP 17	4c	F22	humerus	—	—	55(est)	116	—	94.8	—	—	—	—
2	GTP 17	4c	F28	radius	384	—	64.6(est)	102	98.5	—	—	—	—	—
2	GTP 17	4c	F28	ulna	—	—	—	—	—	—	—	102	81.5	63
2	GTP 17	4c	F137	metacarpal	261	79.9	46.9	79.4	—	—	32.9	—	—	—
1	1/A	6	F5	phalanx 2	49.2(est)	30.1	—	21.4	—	—	—	—	—	—



Fig 176 *Bison* sp: rearticulated forelimb bones (Q2 GTP 17 Unit 4c): F22 left humerus, F28 radius and ulna, F137 metacarpal; scale bar = 0.1m

Middle Pleistocene, being represented in the Cromer Forest Bed Formation at Trimingham and West Runton. In the later part of the early Middle Pleistocene, the long-horned *Bison priscus* replaces *B. schoetensacki*, and is the characteristic species of the late Middle and Late Pleistocene. The bison material from the Siliceous Member (Lower Pleistocene) at Westbury-sub-Mendip has been referred to *B. schoetensacki* by Bishop (1982). This form is replaced in the Calcareous Member of probable late 'Cromerian' age by *B. priscus*. In Table 68, measurements of the Boxgrove bison are compared with *B. priscus* from the Calcareous Member from Westbury. It is evident from

Table 68 Comparisons of postcranial measurements (mm) in British early Middle Pleistocene *Bison*

	greatest length	shaft diameter
radius		
Boxgrove (Q2 GTP 17 Unit 4c F28)	384	64.6(est)
Westbury (M 33144)	382	64.7
metacarpal		
		proximal breadth
Boxgrove Q2 GTP 17 Unit 4c F137)	261	79.9
Westbury M 33758a	254	90.5
M 33758b	267	96
M 33758c	266	—
M 33146	256	97
M 33148	232	95

these measurements that the Boxgrove bison is of a similar size to that of the Westbury Calcareous Member sample.

Subfamily Caprinae
Caprinae gen et sp indeterminate
Ovicaprid

Unit 6: Q1/A F366 right navicular-cuboid frag

A fragment of a navicular-cuboid (Q1/A Unit 6) comprising the proximal articular surface was identified as a small caprid. The size, relative proportions of the articular facets, and the shape of the anterior margin are similar to *Capra* spp/*Ovis* spp ('goat/sheep'), *Rupicapra rupicapra* (Chamois), and *Saiga tartarica* (saiga antelope) with which the Boxgrove specimen was compared. Unfortunately, the navicular-cuboid lacks both the posterior part of the proximal end and the distal articular facets which would allow a more precise identification. Caprids are uncommon in the European early Middle Pleistocene. British records include the caproid (*Capra* or *Ovis* sp), identified by Bishop (1981) from the Calcareous Member of Westbury-sub-Mendip which is of a similar age to the deposits at Boxgrove. In addition, saiga antelope (*Saiga tartarica*) is present in the British Devensian Lateglacial (Currant 1987). Where these species occur outside their present-day range, they are generally associated with dry continental climates and open grassland vegetation. This is in accordance with the inferred environmental conditions during the deposition of Unit 6 at Boxgrove (Chapter 2).

Large Artiodactyl

Unit 3: Q1/B F457 tibia shaft frag
 Unit 4: Q1/B F354 cervical vertebra frag, F420 pelvis frag
 Unit 4b: Q1/B F338 right mandible symphysis frag
 Unit 4d: Q1/B cervical vertebra frag
 Misc: EQP Q1 TP1 tibia shaft frag

Small Artiodactyl

Unit 5a: Q2 SEP 2 F7 ulna, distal frag

Order Rodentia
 Family Sciuridae
 Genus *Sciurus*
Sciurus sp
 Squirrel

Unit 4c: Q1/A F1932 right lower incisor frag
 Unit 4d: Q1/B F459 left femur, proximal and shaft frag
 Unit 5a: Q2 GTP 17 BS86-25 deciduous P₄
 Unit GC: Q2 GTP 3 BS87-308 left M₃

A lower incisor fragment, M₃, dP₄ and the proximal end of a femur represent the only remains of *Sciurus* identified from Boxgrove. Measurements of these specimens are given in Tables 69–71 with comparative measurements for a sample of Recent *Sciurus vulgaris*.

M₃

The morphology of the M₃ is typical of *Sciurus* with a wide talonid basin surrounded by marginal cusps (Fig 177). The tooth differs from Recent *S. vulgaris* in occlusal outline. In *S. vulgaris*, the occlusal outline of

the M₃ is nearly rectangular and the lingual border between the entoconid and metaconid is more or less parallel to the buccal face of the tooth. In contrast the Boxgrove molar has a distinctly trapezoidal outline and an obliquely oriented lingual border which is a result of the mesial placement of the entoconid.

Measurements of Recent *S. vulgaris* are given in Table 69 and plotted in Figure 178 along with Pleistocene material from Meisenheim I (van Kolfschoten in prep), St Esteve-Janson (Chaline 1972), Marjan (Chaline 1972) and Beeches Pit (Parfitt in prep). From these measurements it is apparent that the Boxgrove specimen is similar in size and proportions to *Sciurus* sp from Meisenheim I and Marjan. These teeth are small and relatively narrow in comparison with extant *S. vulgaris*.

Femur

Measurements of the proximal femur are given in Table 70. The depth of the caput femoralis is within the range of measurements of Recent *S. vulgaris* while the breadth is smaller than any of the Recent specimens. This dimension is similar to those given by Jánossy (1962) for *Sciurus whitei hungaricus* from Tarko (Table 70).

Lower incisor

The lower incisor is relatively narrow, but falls within the range of the comparative sample (Table 71).

Table 69 Comparative measurements (mm) of *Sciurus* sp M₃

M ₃	n	length			n	width		
		min	\bar{x}	max		min	\bar{x}	max
<i>Sciurus</i> sp (Boxgrove)	1		(2.74)			(2.25)		
<i>S. vulgaris</i> (Recent, British)	8	2.72	2.84	3.06	2.36	2.54	2.74	
<i>S. vulgaris</i> (Recent, Norway)	5	2.61	2.80	3.08	2.36	2.49	2.72	
<i>S. vulgaris</i> (Recent, Madrid)	5	3.06	3.38	3.6	2.36	2.54	2.86	

Table 70 Comparative femur measurements (mm) of *Sciurus* sp

femur	n	Bp (greatest breadth of proximal end)			n	DC (greatest depth of caput femoralis)		
		min	\bar{x}	max		min	\bar{x}	max
<i>Sciurus</i> sp (Boxgrove)	1		(8.3)			(4.6)		
<i>S. whitei</i> (Tarko)	2		(8.0, 8.3)			–		
<i>S. vulgaris</i> (Recent, British)	10	9.1	9.51	10.3	4.54	4.72	4.72	

Table 71 Comparative lower incisor measurements (mm) of *Sciurus* sp

lower incisor	n	bucco-lingual width			n	mesio-distal length		
		min	\bar{x}	max		min	\bar{x}	max
<i>Sciurus</i> sp (Boxgrove)	1		(3.4)		1		(1.25)	
<i>S. vulgaris</i> (Recent, British)	12	2.82	3.06	3.30	12	1.25	1.36	1.5
<i>S. vulgaris</i> (Recent, Norway)	5	2.85	3.25	3.45	5	1.2	1.26	1.35
<i>S. vulgaris</i> (Recent, Madrid)	6	3.6	3.74	3.9	5	1.45	1.57	1.65

dP₄

The deciduous lower fourth premolar fragment consists of the posterior part of the tooth. The morphology of this specimen does not differ from Recent *S. vulgaris*.

Discussion

The Pleistocene history of *Sciurus* is unclear due to the small size of the sample and the lack of associated dental remains. The early Middle Pleistocene *S. whitei*, described by Hinton (1914) on the basis of a single P⁴ recovered from the 'Monkey Gravel' overlying the West Runton freshwater beds, is distinguished from the P⁴ of Recent *S. vulgaris* by its small size and differences in cusp morphology. The stratigraphic range of this species is unknown; however, squirrel material from the early Middle Pleistocene locality of Tarko appears to be similar to *S. whitei*. Jánossy (1962) described the Tarko specimens as a new sub-species, *S. whitei hungaricus* and concluded that the Tarko material represented an intermediate population between *S. whitei* and *S. vulgaris*.

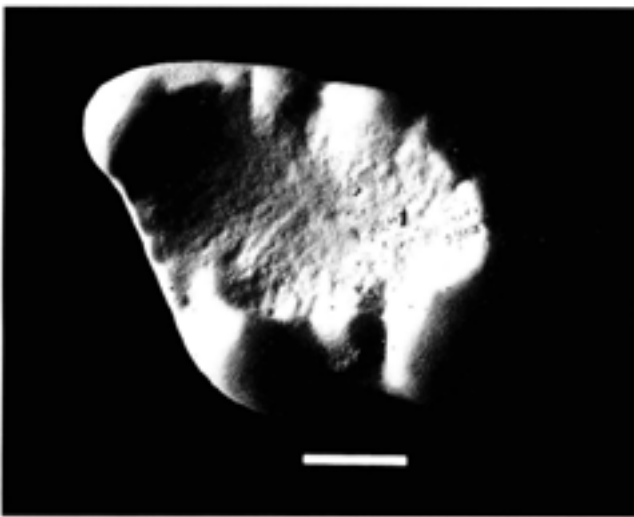


Fig 177 *Sciurus* sp: left M₃ (Q2 GTP 3 BS 87-308), occlusal view (scale bar = 500µm)

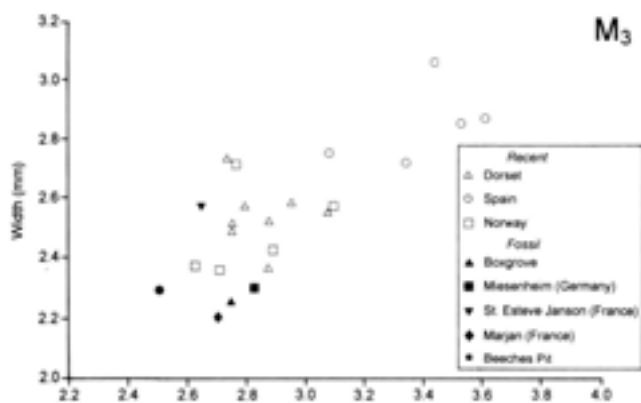


Fig 178 *Sciurus* spp: bivariate plot of M₃ length against width in Pleistocene and Recent squirrel species

The M₃s from Boxgrove and Meisenheim ('Cromerian Complex'), St Esteve-Janson (Mindel Interstadial), and Beeches Pit (Hoxnian) all fall within the lower end of Recent *Sciurus vulgaris* size variation. In addition, the Boxgrove, Meisenheim, and Marjan M₃s are relatively narrow and the Boxgrove M₃ has a distinctive occlusal morphology which distinguishes it from the Meisenheim specimen which more closely resembles Recent *S. vulgaris*. The specific designation of this material will remain uncertain until more material becomes available to assess the degree of variation within Middle Pleistocene *Sciurus*.

Family Arvicolidae

Genus *Myopus**Myopus schisticolor* (Lilljeborg 1844)

Wood lemming

Unit 4c: Q2 GTP 3 BS87-263 right M₁, BS88-474 right M₁, BS88-504 left M₁ frag, BS87-243 left M₁, BS87-149 right M₁, BS86-36 left M₁, left M₁ frag; Q2 GTP 13 BS86-8 left M₁ frag, left M₁ frag; Q2 GTP 17 BS87-114 left M₁, left M₁, BS86-76 left M₁ frag, right M₁ frag, right M₁ frag

Unit 5a: Q1/A F 14 left M₁, left M₂ frag; Q1/B BS88-497 left M₁, BS88-495 right M₁ frag, left M₁, left M₂, BS90-1323 left M₁, three left M₁, left M₂, BS88-492 right M₁, BS87-168 left M₁, BS87-133 left M₂; Q2/B BS86-99 right M₁; Q2 GTP 3 BS87-122 left M₁, BS86-35 left M₁, left M₂ frag, BS88-464 left M₂; Q2 GTP 17 right M₁, BS86-25 right M₁ frag, BS86-84 right M₂ frag, BS86-80 right M₁, left M₁, BS86-81 right M₁ frag, right M₁ frag, BS86-83 molar frags

Unit 6'20: Q2 GTP 20 BS86-54 right M₁, left M₁ frag

Unit LGC: Q2/B BS87-116 two left M₁, right M₁, right M₁, left M₁, left M₁ frag, right M₁ frag, left M₂ frag, right M₂, right M₂

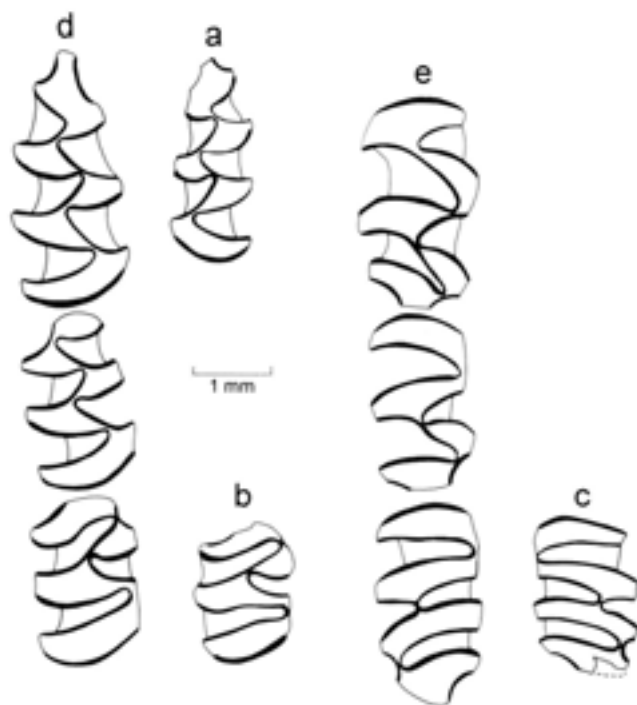


Fig 179 *Myopus schisticolor* and *Lemmus lemmus*: *Myopus schisticolor* a) left M₁ (Q2 GTP 3 BS86-36 Unit 4c), b) right M₂ (Q2 GTP 17 Unit 5a), c) left M₁ (Q2 GTP 17 BS87-114 Unit 4c); *Lemmus lemmus* d) right M₁₋₃ (Q1/A BS90-1136 Unit 6), e) right M₁₋₃ (Q1/A BS90-1136 Unit 6)

The M_1 consists of a narrow pointed anterior loop, three closed triangles and a posterior loop (Fig 179a). Enamel is equally thick on both the concave and the convex sides of the salient angles, but lacking from the tips of the triangles (Fig 179a-c). This dental pattern is characteristic of the Norway lemming *Lemmus lemmus* and the wood lemming *Myopus schisticolor*. The molars of these two lemmings are difficult to separate, but they differ in the smaller size of the teeth of *M. schisticolor* and as Chaline *et al* (1988; 1989) have shown, it is possible to distinguish isolated teeth by multivariate methods. Following Chaline *et al* (1988; 1989) a discriminant analysis was undertaken on the Boxgrove lemming molars. In Figure 180, the discriminant function values are plotted against tooth size, calculated as a percentage of molar length in a Recent population of *Lemmus lemmus*. This graph shows the presence of two groups which, although overlapping to some extent, indicate the presence of both *Lemmus* and

Table 72 Stratigraphic occurrence of *Lemmus* and *Myopus* at Boxgrove

	<i>Myopus schisticolor</i>	<i>Lemmus lemmus</i>
Unit 8	-	+
Unit 6	-	+
Unit 5b	-	+
6'20	+	-
LGC	+	-
Unit 5a	+	-
Unit 4c	+	-

Myopus at Boxgrove. Table 72 shows the stratigraphic distribution of the two species within the sequence.

The record of the wood lemming from Boxgrove represents the first occurrence of this species from Britain. The Pleistocene record of this species is poorly known although it has recently been recorded from a

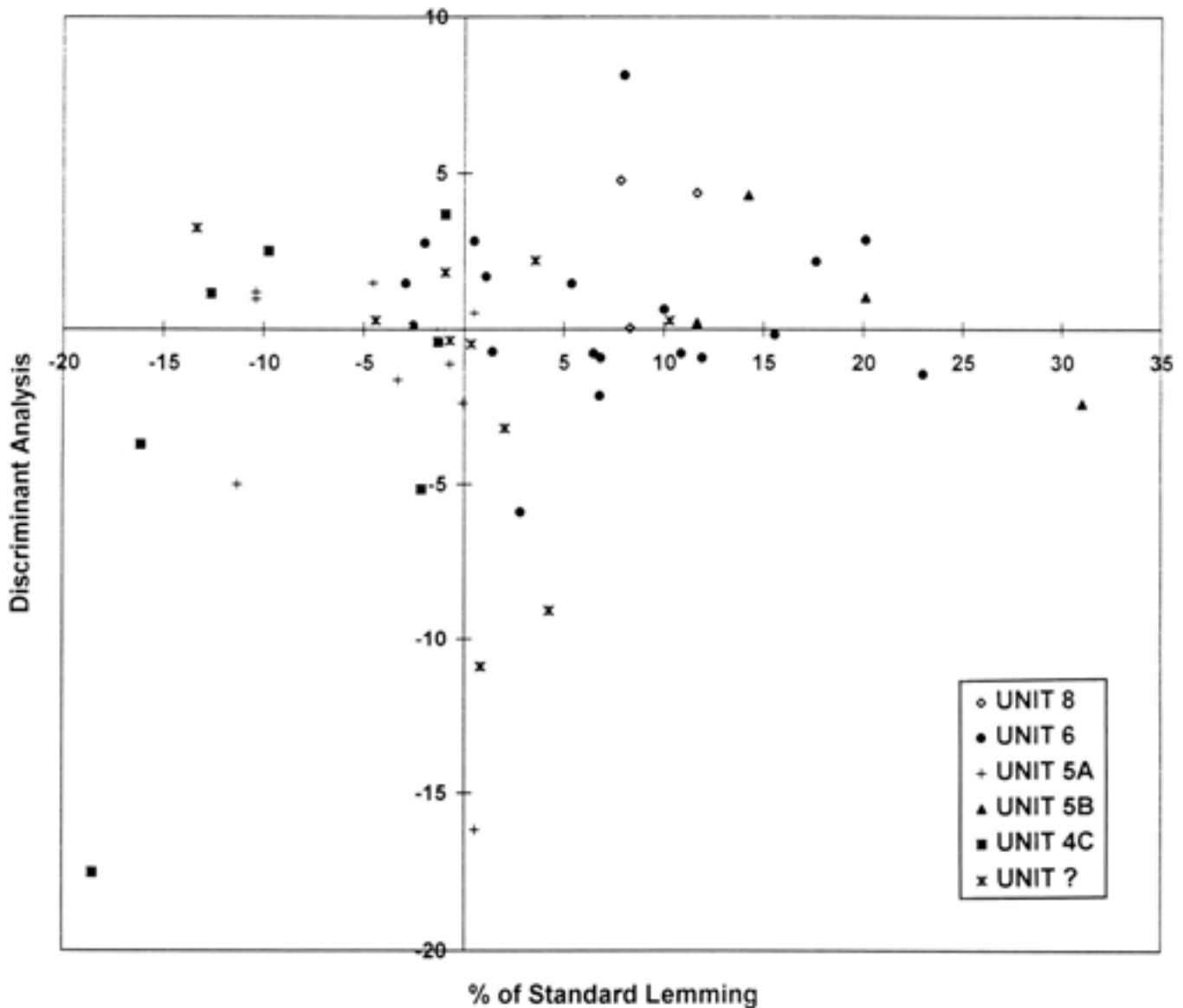


Fig 180 Myopus schisticolor and Lemmus lemmus: discriminant function (Chaline et al 1988) plotted against molar length as a percentage of Recent Lemmus lemmus

number of European Middle and Late Pleistocene localities (Chaline *et al* 1989). The wood lemming is currently found in the sub-arctic zone and coniferous forests of northern Europe and in the northern part of the mixed forest zone of Scandinavia. Its occurrence in Units 4c, 5a, and in the mainly calcareous silty clays (Table 9b) may indicate a degree of climatic continentality during the end of the interglacial period represented by these deposits.

Genus *Lemmus*
Lemmus lemmus (Linnaeus 1758)
Norway lemming

Unit 5b: Q2 BS90-1165 maxilla frag with right M^2 , left M^2 frag, right M^3 frag, mandible with right M_1 frag, right M_1 , left M_1 , right M_2 , left M_2 , left M_3 , right M_3 frag, BS86-38 left M^3 frag
Unit 6: Q1/A F1127 skull, crushed, with incisors, left M^1 - M^2 , right M^1 , F481 skull frag with right M^1 , right M^2 , left M^1 , left M^2 , F433 skull frag with I, right M^1 , right M^2 frag, left M^1 frag, right M^2 , right M^3 frag, left M^3 frag, right mandible with M_1 - M_2 , left mandible frag, F1125 right and left mandible with M_1 - M_2 , F501 right mandible with M_1 , left mandible with M_1 - M_2 , F462 right mandible frag with M_1 - M_2 , left mandible with M_1 - M_2 , F678 right M^1 , F1313 molar frags, F637 M^1 - M^2 , crushed, F484 left M^1 , left M^2 , F452 left and right mandibles with M_1 - M_2 , F644 left M_1 , right M_2 , left M_2 , right M_1 , BS90-1136 left and right M^1 - M^2 , left and right M_1 - M_2 , BS87-120 left M^1 , left M^2 , right M_1 frag
Unit 8 Chalk Pellet Beds: Q2 SEP 2 BS86-41 left M^1 , right M_1 , right M_2 , right M_3 frag

This species is found in Units 5b, 6, and Unit 8. Illustrations of the teeth are given in Figures 179d-e and 181a-j. The Norway lemming is an indicator of dry

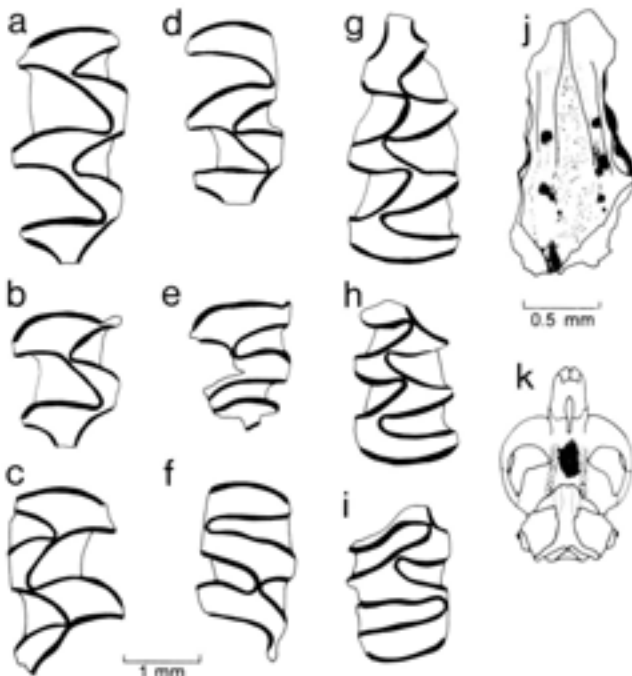


Fig 181 *Lemmus lemmus*: a) right M^1 , b) right M^1 fragment, c) left M^1 fragment, d) right M^2 , e) right M^2 fragment, f) left M^2 fragment (Q1/A F433 Unit 6); g) left M_3 , h) left M_3 , i) right M_3 (Q1/A F1125 Unit 6); j) maxilla fragment (Q1/A F433 Unit 6). The position of the maxilla fragment is indicated on the outline of a lemming skull (k)

continental conditions and it occurs today in the tundra and alpine zone in Scandinavia. The occurrence of this species in the Eartham Upper Gravel Member is consistent with other environmental and sedimentary information which indicates cold open grassland conditions.

Lemmus or *Myopus* spp
Lemming

Unit 5c: Q2 GTP 17 BS90-1130 molar frags

Genus *Clethrionomys*
Clethrionomys glareolus (Schreber 1780)
Bank vole

Material summarised in Table 94

The adult molars are rooted with rounded salient angles, thick enamel and crown cementum in the re-entrant angles (Fig 182a-g). In younger individuals, the teeth have relatively thin enamel and lack crown cementum and roots. In the M_1 , the four posterior triangles are narrowly confluent and the T5 is broadly connected to the simple oval shaped AC2 (Fig 182a-d). The morphology of these specimens is characteristic of the bank vole *C. glareolus*. The M_1 is smaller than Recent *C. glareolus* from Poland (Table 73).

In Europe, the bank vole is a common and widely distributed species which lives in deciduous and mixed woodland or densely overgrown scrub. It is essentially

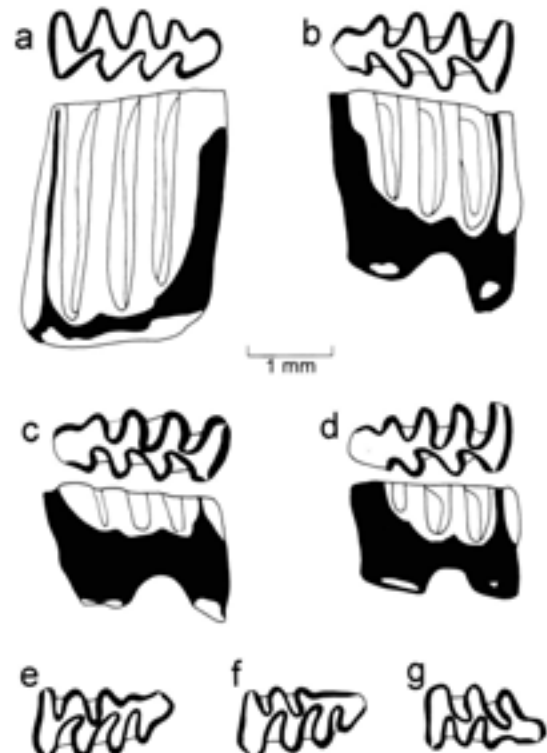


Fig 182 *Clethrionomys glareolus*: a) right M_1 (Q1/B BS86-197 Unit 4c), b) left M_1 (Q1/B BS88-95 Unit 4c), c) left M_1 (Q2 GTP 3 BS87-270 Unit 4c), d) left M_1 (Q2 GTP 3 BS87-156 Unit 4c), e-f) left M^2 (Q2 GTP 3 BS87-251 Unit 4c), g) right M^2 (Q2 GTP 3 BS87-149 Unit 4c)

Table 73 Comparative measurements (mm) of *M*₁ of *Clethrionomys glareolus* from Boxgrove and Poland (Recent)

	n	min	length <i>M</i> ₁	
			\bar{x}	max
Poland (Recent)	25	2.07	2.29	2.55
Boxgrove	130	1.65	2.05	2.31

a temperate woodland species with a Palaearctic distribution covering the whole of Europe with the exception of the Mediterranean coast, Iberian peninsula, and extreme northern Scandinavia. *Clethrionomys glareolus* or related forms are first recorded in the Early Pleistocene and it is well represented in temperate woodland small mammal assemblages from the Cromerian onwards in the British Isles. Although its Pleistocene occurrence in Britain is mainly confined to temperate interglacial episodes, it is also known from Bed 15/8 at Westbury-sub-Mendip in association with *Lemmus* and *Dicrostonyx*, and at Boxgrove in Unit 6 with *Lemmus lemmus*. This is perhaps a reflection of the bank voles' wide climatic tolerance, and, given the presence of dense vegetation, it is able to survive in cold continental climates.

Clethrionomys rufocanus (Sundevall 1846)
Grey-sided vole

Material summarised in Table 94

A second species of *Clethrionomys*, much larger than *C. glareolus*, is represented by associated molars from Q1/A Unit 6 (Fig 183). In addition to the larger size of the teeth, the *M*₁ differs from *C. glareolus* in having five closed triangles (Table 74); this morphology is characteristic of the grey-sided vole *C. rufocanus*. The length of the *M*₁ is 2.43mm.

This is the first record of this characteristic boreal vole from the British Isles. Currently the grey-sided vole occurs throughout Scandinavia and extends eastwards across the arctic and subarctic regions of northern Eurasia. Characteristic habitats of the grey-sided

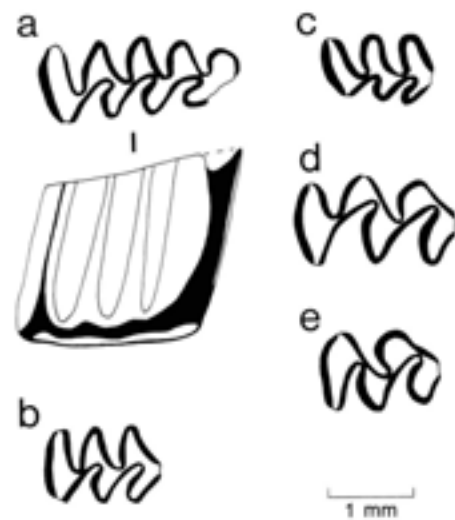


Fig 183 *Clethrionomys rufocanus*: a) right *M*₁, b) right *M*₂, c) right *M*₃, d) right *M*₁', e) right *M*₁'' (Q1/A BS86-85 Unit 6)

vole include rocky or mountainous areas, birch forests and, more occasionally, coniferous woodlands. The presence of this species in Unit 6 indicates a cold climate, which is supported by other environmental evidence from this unit.

Genus *Plionys*
Plionys episcopalis Mehely 1914
Extinct vole

Material summarised in Table 94

The molars of *Plionys* are rooted, lack crown cementum, and have differentially thickened enamel (Fig 184a-f). The *M*₁ has four closed triangles and a fifth triangle confluent with a simple anterior loop (Fig 184a). The morphology of these teeth closely match those of the extinct vole *Plionys episcopalis*. The *M*₁s from Boxgrove (Table 75) are of a similar size to the small sample from Sugworth and West Runton, while the single molar from Westbury is larger than the Boxgrove specimens (Bishop 1981).

Table 74 Dental characters of the European red backed voles (*Clethrionomys* spp)

	<i>C. glareolus</i> England (NHM)	<i>C. rutilus</i> Finland (NHM)	<i>C. rufocanus</i> Norway (NHM)
length <i>M</i>₁			
n	39	21	-
mean	2.33	2.11	2.84
range	2.03-2.54	1.83-2.21	2.48-3.07
<i>M</i> ₁	T4-5 and 5-6 confluent	T4-5 closed, 5-6 confluent	T4-5 and 5-6 closed
<i>M</i> ₂	T1-2 broadly confluent	T1-2 closed	T1-2 closure variable
<i>M</i> ₃	Buccal re-entrant angles shallow	Buccal re-entrant angles deep	Buccal re-entrant angles deep
<i>M</i> ₃ morphology	variable	complex	simple
Relative size <i>M</i> ₃ and <i>M</i> ₁	<i>M</i> ₃ smaller than <i>M</i> ₁	<i>M</i> ₃ generally larger than <i>M</i> ₁	<i>M</i> ₃ smaller than <i>M</i> ₁



Fig 184 *Pliomys episcopalpis*: a) right M_1 (Q2 GTP 3 BS87-183 Unit 4c), b) left M_2 (Q2 GTP 3 BS87-273 Unit 4c); c) right M_3 (Q1/B BS88-894 Unit 4c); d) left M^1 (Q2 GTP 3 BS88-463); e) right M^2 (Q2 GTP 17 BS87-114 Unit 4c); f) left M^1 (Q2 GTP 3 BS87-273 Unit 4c)

Table 75 Comparative measurements (mm) of M_1 in *Pliomys episcopalpis*

	n	min	length M_1	
			\bar{x}	max
Boxgrove	12	2.18	2.32	2.41
Westbury	1		2.65	
West Runton	3	2.16	2.24	2.48
Sugworth	2		(2.35, 2.35)	

Fossil remains of *P. episcopalpis* are not abundant in the British Pleistocene and this is only the third record of this species from Britain. The previous records are from the Cromerian Upper Freshwater Bed at West Runton, the early Middle Pleistocene channel deposits at Sugworth and the cave deposits at Westbury-sub-Mendip. This species is an important biostratigraphic indicator as it last occurs in Interglacial deposits immediately pre-dating the Anglian/Elsterian glaciation (Roberts and Parfitt Chapter 5.9).

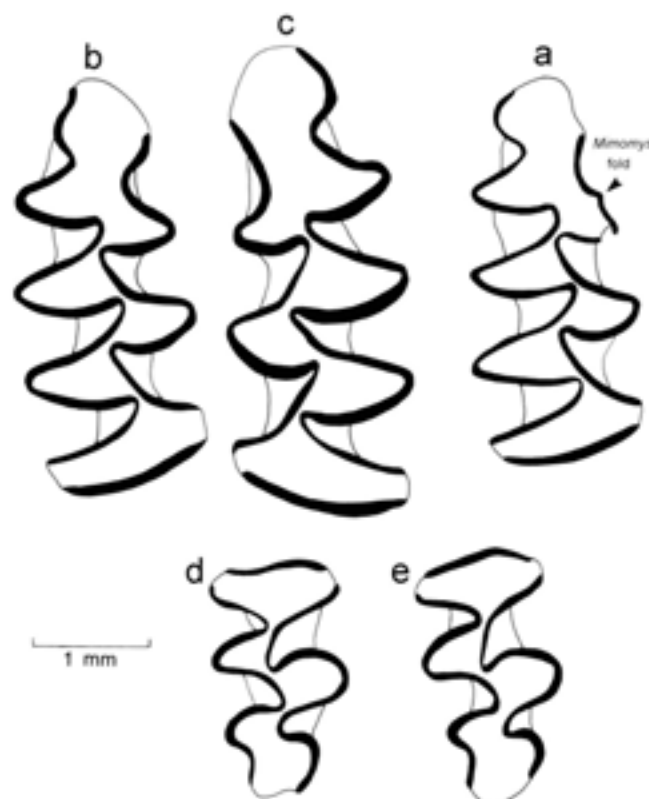


Fig 185 *Arvicola terrestris cantiana*: a) right M_1 (Q1 GTP30 Unit 4b, Unit 4b No 48) with 'Mimomys fold', b) right M_1 (Q2 GTP 17 BS87-98 Unit 4c No. 59), c) left M_1 (Q2/B Sample 68 No 19), d-e) right M^2 (Q2 GTP 17 BS87-98 Unit 4c)

Genus *Arvicola*
Arvicola terrestris cantiana
Water vole

Material summarised in Table 94

The M_1 has a posterior loop, three closed triangles and a trefoil-shaped anterior loop (Fig 185a-c). These features, the large size of the teeth and the lack of roots indicates that they belong to the genus *Arvicola*. The enamel is thicker on the convex sides of the triangles which is characteristic of *Mimomys* and Middle Pleistocene *Arvicola* in north-western Europe.

The taxonomy of *Arvicola* has been reviewed by Koenigswald and Kolfshoten (1996), who have demonstrated its evolutionary lineage from *M. savini* during the 'Cromerian Complex'. In the Cromerian *sensu stricto* of West Runton, the molars of adult individuals have rooted teeth, whereas the descendant form (*Arvicola*) has continuously growing molars. This transition represents a stage in the evolution of the water vole lineage which is characterised by a gradual increase in crown height and the acquisition of continuously growing teeth during the 'Cromerian Complex'. The earliest well-dated record of *Arvicola* is from marine deposits underlying the Elsterian till at Nordbergum (Netherlands) which is the type site of the Cromerian IV Interglacial. The occurrence of this

conspecific with living European pine vole *M. (T.) subterraneus* (= *Pitymys subterraneus*). Although the modern *M. (T.) subterraneus* is slightly larger than the early Middle Pleistocene form (Table 76), it closely resembles the Boxgrove material in occlusal pattern. The Boxgrove pine vole is therefore referred to *M. (T.) cf. subterraneus*.

The European pine vole is a common component of a number of British Middle Pleistocene small mammal assemblages, with a stratigraphic range which encompasses the 'Cromerian Complex' and Hoxnian Interglacial.

Today, the European pine voles are a southern European subgenus of which the most widespread species, *M. (T.) subterraneus*, ranges no further than 53°N. They inhabit a wide range of habitats, but are most numerous in open woodland and grassland.

Microtus agrestis (Linnaeus 1761)
Field vole

Material summarised in Table 94

The M_1 has a typical 'arvalid' morphology with five closed triangles and a well developed T6 and T7. This morphology is characteristic of the living field vole (*M. agrestis*) and the common vole (*M. arvalis*). The differentiation of these two species in fossil assemblages is problematic since their morphological features and dimensions overlap to a large degree. Nevertheless, the wide variation in the size of the M_1 s from Boxgrove *M. arvalis/agrestis* group suggests the presence of both species in the assemblage. These two forms may be distinguished on the basis of the morphology of the M^2 . In *M. agrestis*, the M^2 has an additional posterolingual salient angle ('*agrestis* loop') which is not found in *M. arvalis*. In the Boxgrove assemblage, M^2 s with an extra salient angle indicate the presence of this species.

In a metrical analysis of the M_1 in Recent *M. arvalis* and *M. agrestis*, Nadachowski (1984) showed that the two species can be separated on the basis of M_1 length

Table 77 Comparison of M_1 length (mm) of *Microtus agrestis* from Boxgrove and from Poland (Recent)

	n	min	length M_1	
			\bar{x}	max
Poland (Recent)	30	2.50	2.94	3.30
Boxgrove	24	2.30	2.70	2.95

Table 78 Comparison of M_1 length (mm) of *Microtus arvalis* from Boxgrove and from Poland (Recent)

	n	min	length M_1	
			\bar{x}	max
Poland (Recent)	30	2.48	2.67	2.84
Boxgrove	24	1.99	2.40	2.71

and the degree of symmetry of the T4 and T5 (LT4/LT5 index). In Figure 187, the length of the Boxgrove M_1 s are plotted against the LT4/LT5 index and this diagram shows the presence of two groups. The larger, 'asymmetrical', teeth represent *M. agrestis*, while the smaller, 'symmetrical', teeth are *M. arvalis*. As can be seen from Table 77, the M_1 lengths of *M. agrestis* from Boxgrove are smaller than those of Recent *M. agrestis*.

The field vole is a grassland species which favours damp ground with tall ungrazed grass cover. It is widely distributed in western, central, and eastern Europe at the present day.

Microtus arvalis (Pallas 1778)
Common vole

Material summarised in Table 94

Distinguishing characters are given in the description of *M. agrestis*. The Boxgrove common vole is smaller than that of the Recent Polish sample given in Table 78.

The typical habitat of the common vole is short grazed grassland. It avoids wet grassland and is rare in areas with tall grasses particularly when the field vole is present.

Microtus gregalis (Pallas 1779) (*gregaloides* morphotype)
Narrow-skulled vole

Material summarised in Table 94

The M_1 consists of a posterior loop, five triangles and a simple crescent shaped anterior loop (Fig 188). In the majority of the M_1 s, the T4-5 is closed (Fig 188b). A second, less common, morphotype has a broad confluence between the T4 and T5 (Fig 188a), reminiscent of the dental pattern found in European pine voles (subgenus *Terricola*). These '*Pitymys*-like' forms were originally described as the fossil species *P. gregaloides*, by Hinton (1923) on material from the Cromerian Upper Freshwater Bed at West Runton. Currant (in Roberts 1986) suggests it is probable that this form is the ancestral morphotype of the living narrow-skulled



Fig 188 *Microtus gregalis*: (*gregaloides* morphotype), a) left M_1 , b) right M_1 (*gregalis* morphotype) (Q1/A Unit 6)

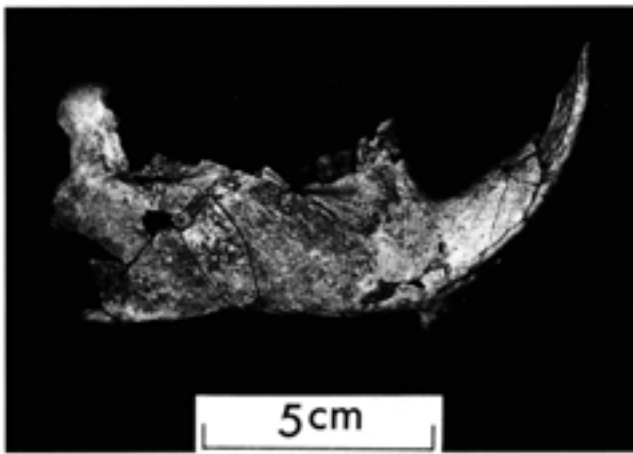


Fig 190 *Castor fiber*: right mandible (Q1 GTP 14 F1 Unit 6), buccal view

Unit 6: Q1/A F155, F387 skull frags, F186 occipital condyle, F15, F35, F386 left upper I frags, F145 left P₄, F3 right M₁, F141 left M₁, F361 right M₁, F401 right radius; Q1 GTP 14 F1 right mandible with I, P₄-M₂; Q1 TP220-80 F4 right femur shaft frag
Misc: EQP Q1 TP1 right lower I frag; EQP Q1 TP14 tibia shaft frag, proximal unfused

European beaver is represented by a total of 32 bones which include parts of a disarticulated and fragmentary skeleton from Q1/A and a number of mandibles with nearly complete dentitions (Figs 190-2). Stratigraphically these finds are restricted to Units 5a and 6, and significantly beaver appears to be absent in the main faunal horizon (Unit 4c).

The teeth are high crowned with the enamel folded into three re-entrant folds on one side and one fold on the other (Figs 191-2). Morphologically these specimens do not differ from Recent *Castor fiber*. Biometric data for the Boxgrove specimens are given in Table 81.

Mayhew (1975) has shown that the dental pattern and size of the occlusal surface vary as a result of wear and growth. In earlier taxonomic work on fossil beavers the extent of age-related variation was not taken into account and this has resulted in the somewhat confused taxonomy of the Plio-Pleistocene beavers. Mayhew's work on a Recent aged series of specimens has shown that the dimensions of the incisors and cheek teeth vary with ontogenetic age. For the incisors the dimensions of the tooth increase until about five years of age when adult size is attained. The cheek teeth also vary in dimensions along the height of the crown and, to provide comparable data with those of Mayhew, the cheek teeth were measured towards the base of the crown. In addition a second set of measurements were taken at the occlusal surface of the cheek teeth (Table 81).

Using the criteria outlined by Lason and van Nostrand (1968), the ontogenetic age of the Boxgrove material was assessed using the degree of closure of the basal opening and the height of the cheek teeth. In the associated mandibles from GTP 17 (F 1085/1086), the cheek teeth with the exception of the P₄ were still retained in the mandible and the basal openings of these teeth were not visible. The basal opening of the P₄ is constricted and indicates an approximate age of

Table 81 Measurements of upper and lower dentitions (mm) of *Castor fiber* from Boxgrove; (a) occlusal measurements (b) measurements taken above crown base following Mayhew (1975)

lower dentition													
	I				P ₄		M ₁		M ₂		M ₃		
	B-L	M-D	L	W	L	W	L	W	L	W	L	W	
EQP Q1 TP1	10.5	9.6											
GTP 14	(a) 9.1	8.4	11.5	11.2	8.8	8.7	8.2	8.35	-	-	-	-	
	(b) -	-	11	8.6	9.0	8.8	8.7	8.4	-	-	-	-	
GTP 17													
F 1086	(a) 8.2	6.9	9.1	8.8	7.9	8.24	-	-	-	-	-	-	
	(b) -	9.9	9.1	-	-	9.4	-	-	-	-	-	-	
F 1085	(a) 8.3	7.2	9.1	8.8	8.0	8.1	7.2	-	-	-	-	-	
	(b) -	-	-	-	-	-	-	-	-	-	-	-	
Q1/A													
left	(a) 8.4	8.0	9.4	7.3	8.2	8.1	-	-	-	-	-	-	
	(b) -	-	8.4	7.0	-	-	-	-	-	-	-	-	
right	(a) -	8.0	9.6	7.4	8.1	7.9	7.6	-	-	7.0	7.2	-	
	(b) -	-	-	-	-	-	-	-	-	7.0	6.0	-	
upper dentition													
	I				P ₄		M ₁		M ₂		M ₃		
	B-L	M-D	L	W	L	W	L	W	L	W	L	W	
Q1/A													
left	(a) -	7.6	9	7.4	7.5	8.0	6.7	7.4	-	-	-	-	
	(b) -	-	6.9	7.5	5.6 (est)	8.3	5.5	7.3	-	-	-	-	
right	(a) -	-	-	-	7.2	7.9	6.7	7.5	6.3	7.2	-	-	
	(b) -	-	-	-	5.6	5.2	-	-	6.0	6.3	-	-	

Table 79 Comparative measurements (mm) of M_1 in *Microtus gregalis* and *M. gregalis* ('*gregaloides*' morphotype)

	n	min	length M_1	
			\bar{x}	max
Poland (<i>M. gregalis</i> Recent)	20	2.52	2.68	2.92
Boxgrove	8	2.18	2.35	2.57
Westbury	-	2.30	-	2.80
West Runton	-	2.10	-	2.60

vole, *M. gregalis*. This is supported by the presence of 'Pitymys' type M_1 s in Recent populations of the narrow-skulled vole described by Nadachowski (1984), and the occurrence of intermediate morphologies in early Middle Pleistocene sites such as Westbury and Boxgrove. Measurements of the Boxgrove specimens given in Table 79 illustrate the small size of early Middle Pleistocene *M. gregalis* in comparison with Recent populations of *M. gregalis*.

Today the narrow-skulled vole is an open country species with a disjunct Recent distribution in the tundra zone of the northern palaeartic and a steppe population in central and eastern Asia. The British Pleistocene record of *M. gregalis* and its ancestral early Middle Pleistocene form provide clear evidence for a change in the environmental preferences of this species during the Pleistocene. In the Late Pleistocene, *M. gregalis* is restricted to cold stages in an open environment. In contrast to the present day ecology of the species, during the early Middle Pleistocene it is found in association with regional deciduous woodland in a temperate environment at West Runton, and it also occurs in the peak interglacial horizons at Westbury (Andrews 1990). However, at the latter site, it dominates the microtine fauna of the cold stage deposits, and is absent or less common in the peak interglacial faunas. In the Boxgrove sequence, *M. gregalis* has a restricted stratigraphic range and it is apparently absent from the rich small mammal assemblages of Units 4c and 4b. The species appears for the first time in the Organic Bed (Unit 5a) and becomes common in Unit 6. The record of *M. gregalis* at Boxgrove suggests that it was absent during the end of the interglacial period represented by the lagoonal and palaeosol horizons, and that its appearance is associated with a cooling climate during the deposition of the Organic Bed.

Microtus oeconomus (Pallas 1776)
Northern vole

Material summarised in Table 94

The M_1 is composed of a posterior loop, four closed triangles and a T5 broadly confluent with the anterior field (Fig 189). This morphology is typical of the Recent northern vole, *M. oeconomus*. Measurements of the M_1 of the Boxgrove northern vole are given in

Table 80 Comparative measurements (mm) of M_1 in *Microtus oeconomus*

	n	min	length M_1	
			\bar{x}	max
Poland (Recent)	-	2.74	2.98	3.37
Boxgrove	8	2.29	2.48	2.67
Westbury	-	2.25	2.48	2.70
West Runton	-	2.20	2.35	2.50



Fig 189 *Microtus oeconomus*: a) right M_1 (Q1 GTP 30 Unit 4c), b) left M_1 (Q1/A)

Table 80. The M_1 is smaller than those of a Recent sample from Poland, but similar in size to those from other early Middle Pleistocene localities such as Westbury-sub-Mendip and West Runton.

The northern vole is at present widely distributed in the boreal zone of northern Eurasia, where it inhabits river banks, marshes and open grassland. Relict populations are also found in The Netherlands, Poland, and Scandinavia where they are able to survive in favourable microhabitats in the absence of competition from other species of *Microtus*. Although the northern vole is common in the Middle and Late Pleistocene cold stage faunas of the British Isles, it is also present as a minor component of a number of interglacial small mammal assemblages. At Boxgrove, the northern vole is rare in the interglacial deposits of Unit 4c, but more common in the cold stage deposits of Unit 6.

Family Castoridae
Genus *Castor*
Castor fiber Linnaeus 1758
Beaver

Unit 4c/5a (unit undetermined): EQP Q1 TP6 F50 left tibia shaft frag

Unit 5a: Q1/A F396 skull, crushed, with right M^2 and M^3 , F394, F132, F129, F422, F138, F146, F157 skull frags, F395 right upper I frag, F352 left M^3 , F395 right mandible, crushed, ascending ramus missing, with I, P₁-M₂, F400 left mandible, ascending ramus missing, with I, P₁-M₂, F1765 right lower I frag, F418 right ulna frag, F363 left ulna; Q2 GTP 17 F1085 right mandible with I, P₁-M₂, F1086 left mandible with I, P₁-M₁, BS86-58 F1047 lower I frag

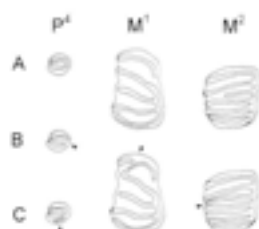
Table 82 Comparison of morphotypes in P^4 , M^1 , and M^2 of *Muscardinus avellanarius* from Boxgrove and four Recent populations. Note M^1 morphotypes A and B are calculated separately from C

P^4 morphotype	A		B		C		total n
	n	%	n	%	n	%	
Boxgrove	3	30	7	70	10	100	10
England	10	100	0	0	0	0	10
Switzerland	3	75	1	25	0	0	4
Hungary/Romania	6	100	0	0	0	0	6
France	9	75	2	25	7	58	12

M^1 morphotype	A		B		C		total n
	n	%	n	%	n	%	
Boxgrove	23	92	2	8	0	0	25
England	10	100	0	0	0	0	10
Switzerland	6	100	0	0	0	0	6
Hungary/Romania	9	100	0	0	0	0	9
France	11	100	0	0	5	45	11

M^2 morphotype	A		B		total n
	n	%	n	%	
Boxgrove	12	92	1	8	13
England	1	10	9	90	10
Switzerland	2	33	4	67	6
Hungary/Romania	0	0	9	100	9
France	4	36	7	64	11

Key to morphotypes



The teeth are low crowned with transverse enamel ridges forming a 'rasp-like' occlusal surface. The size and morphology of these teeth closely resemble Recent *M. avellanarius*, although there are slight differences in the pattern of the enamel ridges. Figure 193a-h illustrates a representative sample of *M. avellanarius* teeth; variation in the morphology of P^4 - M^2 is shown in Table 82. Measurements of the Boxgrove specimens and Recent specimens in the Natural History Museum (London) collections are given in Tables 83-4 and Figure 194. Comparisons of dental proportions for Recent and fossil samples are shown in a log ratio diagram (Fig 195).

Upper dentition

P^4

The occlusal surface of the P^4 in Recent *M. avellanarius* consists of two transverse ridges which are connected at the lingual border to form a crescent shaped cusp. In the Recent sample this morphology was recorded in

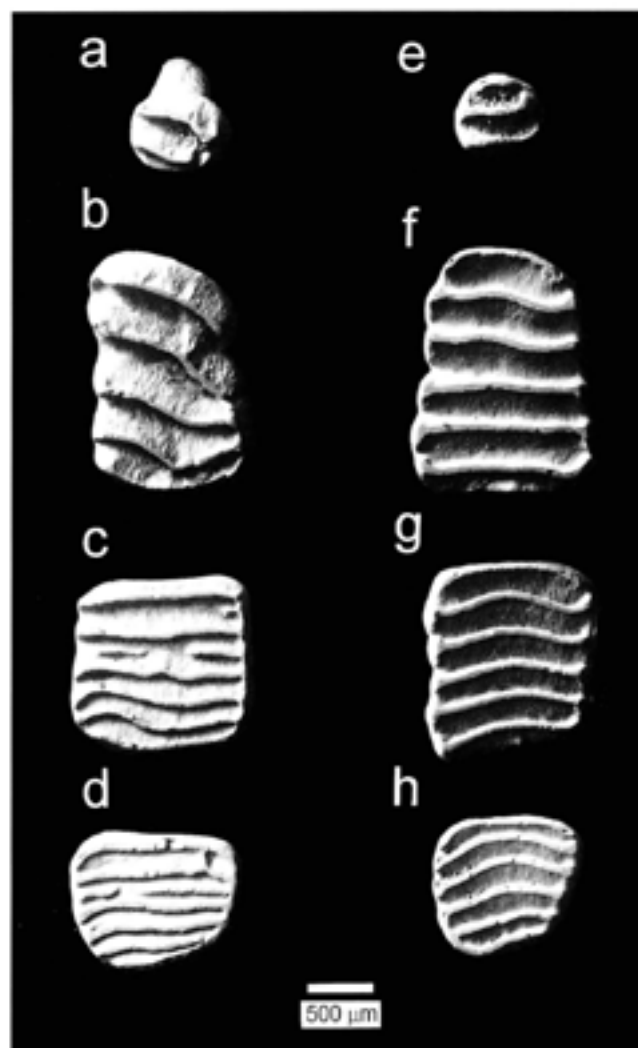


Fig 193 *Muscardinus avellanarius*: a) right P^4 , b) right M^1 , c) right M^2 , d) right M^1 , e) right P^4 , f) right M^1 , g) right M^2 , h) right M^1

90% of the P^4 s. In contrast, the Boxgrove specimens usually have two transverse ridges which lack a lingual connection (Fig 193a). Only three (30%) of these teeth resemble the Recent P^4 pattern in this feature. A second variant of the premolar is the presence of a short posterior ridge which is parallel to the two main ridges. This ridge is present in all of the Boxgrove specimens. In the Recent samples, the occurrence of this cusp is variable. It was not observed in the British, Swiss or south-eastern European sample although an additional cusp is present in 58% of the French sample.

M^1

The majority of the M^1 s do not differ from the Recent comparative sample (Table 82). However, two specimens have an unusual pattern not found in the Recent sample. In these teeth, the postero-buccal part of the anterior ridge is connected to the lingual end of the second ridge leaving a segment of the anterior ridge at the lingual border of the molar.

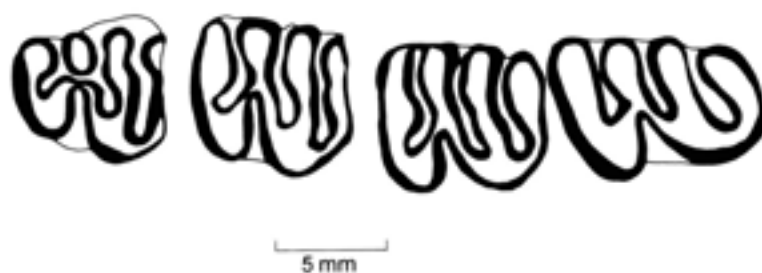


Fig 191 Castor fiber: right P_1 - M_1 (Q1/A Unit 5a), occlusal view

two years at the time of death. The mandible from GTP 14 has worn cheek teeth with closed basal openings indicating that the individual was at least five years old at the time of death. In addition, the metaflexid of the M_1 and M_2 is isolated within the crown as a fossetid. The isolation of flexids occurs in old animals due to extreme wear of the teeth. The age of the Q1/A individual was difficult to assess from the state of the basal openings as the mandibular teeth are retained in the mandible and all of the detached upper cheek teeth are damaged at the crown base. However, a comparison of the crown height of the P_1 with those in the other mandibles showed that this tooth was slightly more worn than GTP 17 but less worn than those from GTP 14. This indicates that the individual was sub-adult at the time of death.

Biometric comparisons of the Boxgrove specimens are hampered by the small size of the sample. Where comparisons can be made, however, the size of the Boxgrove sample is similar to that of Holocene material from the Cambridgeshire fens (Mayhew 1975).

Beaver remains are known from a number of British Pleistocene localities and these records are confined to wooded temperate episodes. Palaeoecologically the beaver is important as it is an aquatic species closely associated with lakes and rivers in wooded country. Beavers prefer broad river valleys and lakes with slow flowing or still water bordered by stands of deciduous trees and a rich aquatic vegetation. They are closely associated with woodland and in autumn and winter, the bark and twigs of deciduous trees such as aspen, willow and poplar form the main component of their diet. A varied range of aquatic plants and bankside herbs and grasses form the bulk of the diet in summer.



Fig 192 Castor fiber: right P_1 - M_2 (Q1/A GTP 14 F1 Unit 6), occlusal view

The presence of the beaver in Unit 5a is in accordance with the palaeoenvironmental reconstruction of the deposit. The lithology and microsedimentary structure of this horizon indicates deposition in temporary streams or small ponds in a fen-carr environment. At odds with the palaeoenvironmental picture is the presence of beaver in the basal brickearth sequence (Unit 6), which accumulated in a grassland landscape during a period of deteriorating climate. This may indicate a more complex sequence of climatic and vegetational change during the deposition of the Brickearth Beds or, alternatively, it may indicate the existence of a mosaic of habitats with areas of localised woodland.

Castor or *Trogotherium* (Linnaeus 1758)

Unit 4d: Q1/B F460 left radius, proximal and shaft

Family Gliridae

Genus *Muscardinus*

Muscardinus avellanarius (Linnaeus 1758)

Hazel Dormouse

Unit 4c: Q1/B BS88-955 left P_1 ; Q2 GTP 3 left M_1 , BS88-463 right M_1 , M_2 , BS88-490 left M_1 , M_2 , BS87-263 left M_1 frag, right M_1 ; BS87-251 left M_1 , BS87-156 right M_1 , right M_1 , left M_1 , right M_1 , left M_1 frag, BS86-36 right M_1 , left M_1 , left M_1 frag, right M_1 , left M_1 , left P_1 , right M_1 , right M_2 , BS86-36 right M_1 , left M_1 , two left M_2 , BS87-124 right M_1 , BS87-124 left M_2 , BS87-260 left M_2 , BS87-186 right M_2 , BS88-461 right M_1 , M_2 , BS87-136 right M_1 , M_2 , BS87-270 right M_1 frag, M_2 , BS87-251 left P_1 , right P_1 , left M_1 , P_1 , left M_2 , right M_2 ; Q2 GTP 13 BS86-8 left M_1 frag; Q2 GTP 15 BS86-16 left M_1 ; Q2 GTP 16 BS86-24 left M_2 ; Q2 GTP 17 BS86-20 left M_1 frag, BS86-56 right P_1 , right M_1 , right M_1 frag, right M_2 , left M_2 , BS86-26 right P_1 , M_1 , BS86-26 right P_1 , M_1 , BS86-30 left M_1 , BS87-96 left M_1 , BS87-96 left two M_1 , BS86-30 two P_1 , left M_1 , two left M_2 , left M_2 , three P_1 , two right M_2 , left M_2 , right M_2 , left M_2

Unit GC: Q2 GTP 3 BS87-175 left M_1 , BS87-175 left and right M_1 frag, left M_2 , right M_2 , BS87-236 P_1 , right M_2 , right M_2 , left M_2 , right M_1 , BS87-308 left M_1 , BS87-178 left M_1 , BS87-189 left M_1

Unit GB4: Q2 GTP 3 BS87-123 right M_1 , left M_2 , left M_2

Unit 4c/5a: Q2 GTP 17 BS86-19 molar frag

Unit 4d: Q1B BS88-471 M_1 frag

Unit LS>5a (Table 9b): Q2 GTP 20 BS86-73 right M_1

Unit 5a: Q2 GTP 3 BS86-35 left M_1 , right M_1 ; Q2/B BS90-1323 right M_1 , left M_2 ; Q2 GTP 13 BS86-3 left M_1 ; Q2 GTP 17 BS86-51 right M_1 , right P_1 , left M_1 , left M_2 , BS86-28 right M_1 , left M_1 , left M_1 , BS86-84 P_1 , right M_1 , right M_1 frag, left M_1 , P_1 , BS86-25 right M_1

The hazel dormouse is one of the less common rodents from Boxgrove, represented by 107 isolated teeth. The majority of remains were recovered from the palaeosol (Unit 4c) and the overlying fen-carr deposit (Unit 5a).

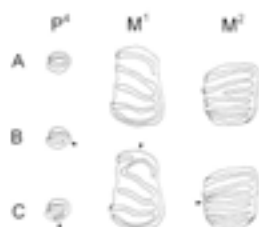
Table 82 Comparison of morphotypes in P⁴, M¹, and M² of *Muscardinus avellanarius* from Boxgrove and four Recent populations. Note M¹ morphotypes A and B are calculated separately from C

<i>P⁴</i> morphotype	A		B		C		total n
	n	%	n	%	n	%	
Boxgrove	3	30	7	70	10	100	10
England	10	100	0	0	0	0	10
Switzerland	3	75	1	25	0	0	4
Hungary/Romania	6	100	0	0	0	0	6
France	9	75	2	25	7	58	12

<i>M¹</i> morphotype	A		B		C		total n
	n	%	n	%	n	%	
Boxgrove	23	92	2	8	0	0	25
England	10	100	0	0	0	0	10
Switzerland	6	100	0	0	0	0	6
Hungary/Romania	9	100	0	0	0	0	9
France	11	100	0	0	5	45	11

<i>M²</i> morphotype	A		B		total n
	n	%	n	%	
Boxgrove	12	92	1	8	13
England	1	10	9	90	10
Switzerland	2	33	4	67	6
Hungary/Romania	0	0	9	100	9
France	4	36	7	64	11

Key to morphotypes



The teeth are low crowned with transverse enamel ridges forming a 'rasp-like' occlusal surface. The size and morphology of these teeth closely resemble Recent *M. avellanarius*, although there are slight differences in the pattern of the enamel ridges. Figure 193a–h illustrates a representative sample of *M. avellanarius* teeth; variation in the morphology of P⁴–M² is shown in Table 82. Measurements of the Boxgrove specimens and Recent specimens in the Natural History Museum (London) collections are given in Tables 83–4 and Figure 194. Comparisons of dental proportions for Recent and fossil samples are shown in a log ratio diagram (Fig 195).

Upper dentition

P⁴

The occlusal surface of the P⁴ in Recent *M. avellanarius* consists of two transverse ridges which are connected at the lingual border to form a crescent shaped cusp. In the Recent sample this morphology was recorded in

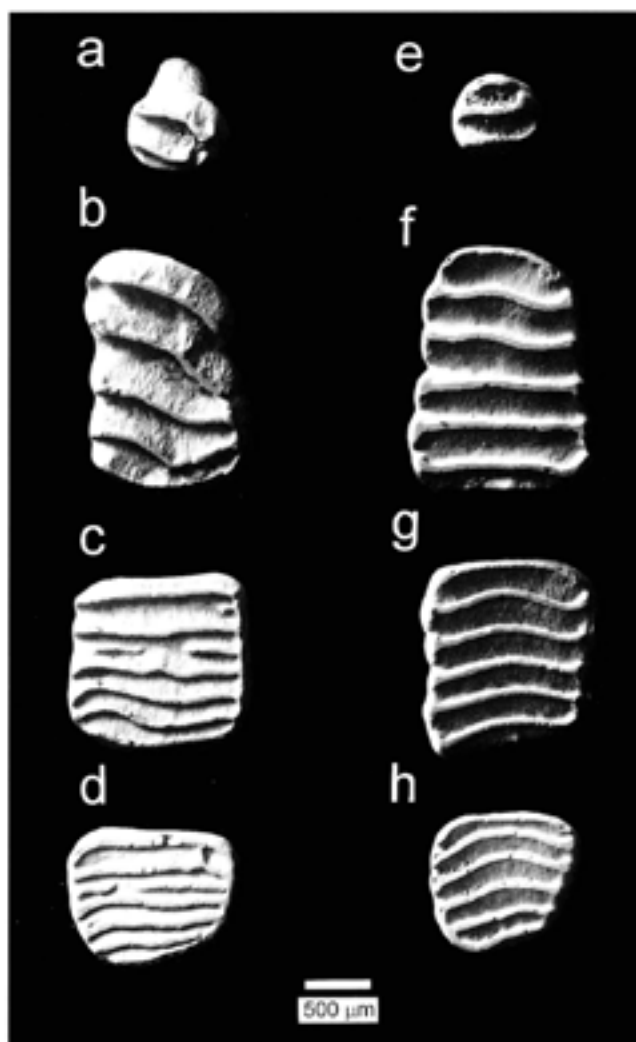


Fig 193 *Muscardinus avellanarius*: a) right P⁴, b) right M¹, c) right M², d) right M¹, e) right P⁴, f) right M¹, g) right M², h) right M¹

90% of the P⁴s. In contrast, the Boxgrove specimens usually have two transverse ridges which lack a lingual connection (Fig 193a). Only three (30%) of these teeth resemble the Recent P⁴ pattern in this feature. A second variant of the premolar is the presence of a short posterior ridge which is parallel to the two main ridges. This ridge is present in all of the Boxgrove specimens. In the Recent samples, the occurrence of this cusp is variable. It was not observed in the British, Swiss or south-eastern European sample although an additional cusp is present in 58% of the French sample.

M¹

The majority of the M¹s do not differ from the Recent comparative sample (Table 82). However, two specimens have an unusual pattern not found in the Recent sample. In these teeth, the postero-buccal part of the anterior ridge is connected to the lingual end of the second ridge leaving a segment of the anterior ridge at the lingual border of the molar.

Table 83 Measurements of lower cheek teeth (mm) of *Muscardinus avellanarius* from Boxgrove and Recent comparative specimens

P_2	n	length			n	width		
		min	\bar{x}	max		min	\bar{x}	max
Boxgrove (4c)	5	0.6	0.62	0.65	5	0.65	0.69	0.7
Boxgrove (5a)	2		(0.62,		2		(0.73,	
			0.64)				0.75)	
England	9	0.44	0.52	0.6	9	0.67	0.73	0.8
France	8	0.49	0.58	0.62	8	0.73	0.8	
Switzerland	6	0.58	0.61	0.62	4	0.73	0.76	0.8
M_1	n	length			n	width		
		min	\bar{x}	max		min	\bar{x}	max
Boxgrove (4c)	14	1.62	1.69	1.77	15	1.2	1.29	1.33
Boxgrove (5a)	3		(1.61,		3		(1.25,	
			1.72, 1.72)				1.29, 1.38)	
England	10	1.51	1.61	1.73	10	1.13	1.23	1.29
France	8	1.51	1.64	1.77	8	1.16	1.22	1.28
Switzerland	6	1.53	1.6	1.64	6	1.16	1.22	1.28
M_2	n	length			n	width		
		min	\bar{x}	max		min	\bar{x}	max
Boxgrove (4c)	14	1.33	1.4	1.45	14	1.2	1.3	1.36
Boxgrove (5a)	1		(1.32)		1		(1.39)	
England	10	1.29	1.36	1.47	10	1.14	1.28	1.14
France	8	1.24	1.31	1.33	8	1.16	1.23	1.33
Switzerland	6	1.29	1.33	1.42	6	1.24	1.26	1.29
M_3	n	length			n	width		
		min	\bar{x}	max		min	\bar{x}	max
Boxgrove (4c)	7	1.0	1.07	1.11	7	1.09	1.14	1.17
Boxgrove (5a)	1		(1.32)		1		(1.18)	
England	10	1.02	1.10	1.2	9	1.07	1.12	1.18
France	8	1.07	1.09	1.24	8	1.07	1.09	1.16
Switzerland	4	1.07	1.09	1.11	4		1.16	

M^2

In the M^2 of Recent *M. avellanarius*, the enamel ridges are complete and reach the lingual side of the molar in the majority of cases. A small proportion of the molars have a short third ridge which does not reach the lingual border. This morphotype is uncommon, occurring in less than 30% of the Recent specimens (Table 82). In comparison, the Boxgrove M^2 s are clearly distinguished from Recent *M. avellanarius* by a high proportion of teeth (92%) with a short third ridge (Table 82).

M^3

The ridge pattern of the M^3 is variable and the Boxgrove sample is too small for a detailed comparison.

Lower dentition

The morphology of the lower dentition does not differ markedly from Recent *M. avellanarius*. Minor differences were noted in the shape of the P_4 and the size of the M_1 and M_2 .

Table 84 Measurements of upper cheek teeth (mm) of *Muscardinus avellanarius* from Boxgrove and Recent comparative material

P^1	n	length			n	width		
		min	\bar{x}	max		min	\bar{x}	max
Boxgrove (4c)	9	0.52	0.57	0.62	9	0.61	0.69	0.73
Boxgrove (5a)	1		(0.6)		1		(0.78)	
England	10	0.49	0.58	0.62	10	0.71	0.76	0.8
France	8	0.49	0.62	0.74	8	0.71	0.8	0.89
Switzerland	4	0.58	0.62	0.64	4	0.8	0.81	0.83
M^1	n	length			n	width		
		min	\bar{x}	max		min	\bar{x}	max
Boxgrove (4c)	12	1.69	1.82	1.96	14	1.16	1.27	1.33
Boxgrove (5a)	5	1.71	1.79	1.86	6	1.2	1.27	1.33
England	10	1.69	1.77	1.87	10	1.23	1.29	1.38
France	8	1.73	1.86	1.97	8	1.2	1.27	1.34
Switzerland	6	1.82	1.87	1.98	6	1.25	1.38	1.32
Romania	5	1.74	1.78	1.87	5	1.19	1.28	1.33
M^2	n	length			n	width		
		min	\bar{x}	max		min	\bar{x}	max
Boxgrove (4c)	9	1.2	1.29	1.34	9	1.24	1.34	1.42
Boxgrove (5a)	2		(1.24,		2		(1.33,	
			1.24)				1.33)	
England	10	1.24	1.33	1.47	10	1.29	1.35	1.45
France	8	1.24	1.27	1.33	8	1.33	1.35	1.47
Switzerland	6	1.24	1.30	1.36	6	1.38	1.40	1.47
Romania	5	1.38	1.44	1.51	5	1.33	1.4	1.42
M^3	n	length			n	width		
		min	\bar{x}	max		min	\bar{x}	max
Boxgrove (4c)	6	0.98	1.03	1.07	6	1.16	1.25	1.29
England	9	0.95	0.99	1.07	10	1.16	1.24	1.33
France	8	0.88	0.98	1.08	7	1.16	1.21	1.27
Switzerland	8	1.0	1.01	1.11	7	1.17	1.26	1.33
Romania	4	1.03	1.05	1.09	4	1.24	1.31	1.33

P_4

The P_4 has a rounded occlusal outline in the Boxgrove sample (mean length-width ratio 0.9) whereas the Recent P_4 s are more oval (mean length-width ratio 1.31)

M_1 and M_2

The M_1 is slightly larger than the Recent sample and the M_2 is longer. However, the measurements show a broad overlap between the two groups (Fig 194a-b).

Discussion

Although the hazel dormouse is a relatively uncommon rodent in the Boxgrove assemblage, its presence is significant as it is rare in other Pleistocene faunal assemblages. The absence of *M. avellanarius* in some assemblages may be due to the small size of the molars; however, it is also poorly represented where collecting methods have recovered other small rodent and insectivore teeth. The hazel dormouse, in common with other arboreal rodents, is rarely captured by owls and

other birds of prey. This may account for the under-representation of the dormouse in some small mammal accumulations. The main predators of this species are mammals such as small mustelids, fox and badgers which are capable of hunting in dense undergrowth favoured by this species. The hazel dormouse is found in the mink scat accumulations in Q1/B. Additionally, digestion on a relatively high proportion of the dispersed teeth suggests a predator was involved in the accumulation of these elements.

M. avellanarius is an important palaeoenvironmental indicator as it requires thick vegetation to provide cover, food and support for nests as well as providing arboreal runways between bushes. It feeds on a range of fruits and seeds from trees and bushes supplemented by insects and other animal matter.

The range of habitats in which *M. avellanarius* is found includes deciduous woodland, swampy forest, dense shrub and reed beds. An important characteristic

of these habitats is the presence of a dense floor of shrub or other overgrown vegetation. In deciduous woodland, the hazel dormouse is usually found in woodland clearings and along the margins of woods where shrubs and brambles can develop.

Genus *Eliomys*

Eliomys quercinus (Linnaeus 1766)

Garden dormouse

Unit 5a: Q2/B BS90-1323 left dP⁴

Unit LGC: Q2/B BS87-116 right M², left M₁

The garden dormouse is represented by a single deciduous upper fourth premolar from Unit 5a, and an M² and M₁ from Q2/B (Unit LGC). The occlusal outline of the dP⁴ (Fig 197) is triangular with five transverse enamel ridges. The anteroloph is short and separated from the posteroloph by the paraflexid. The protoloph runs diagonally from the paracone to a relatively large

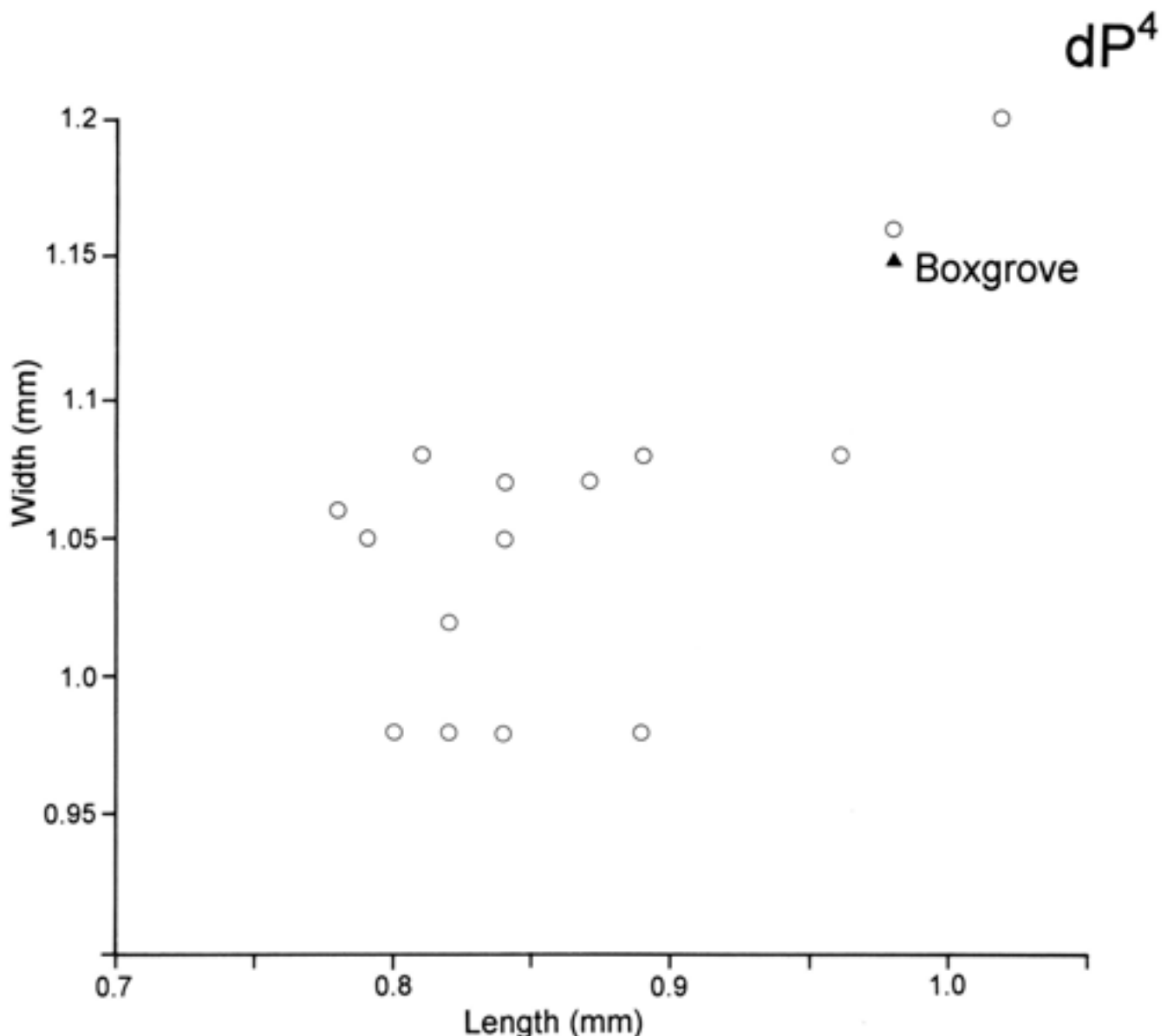


Fig 196 *Eliomys quercinus*: bivariate plot of length against width of deciduous P⁴ in Recent and fossil garden dormouse

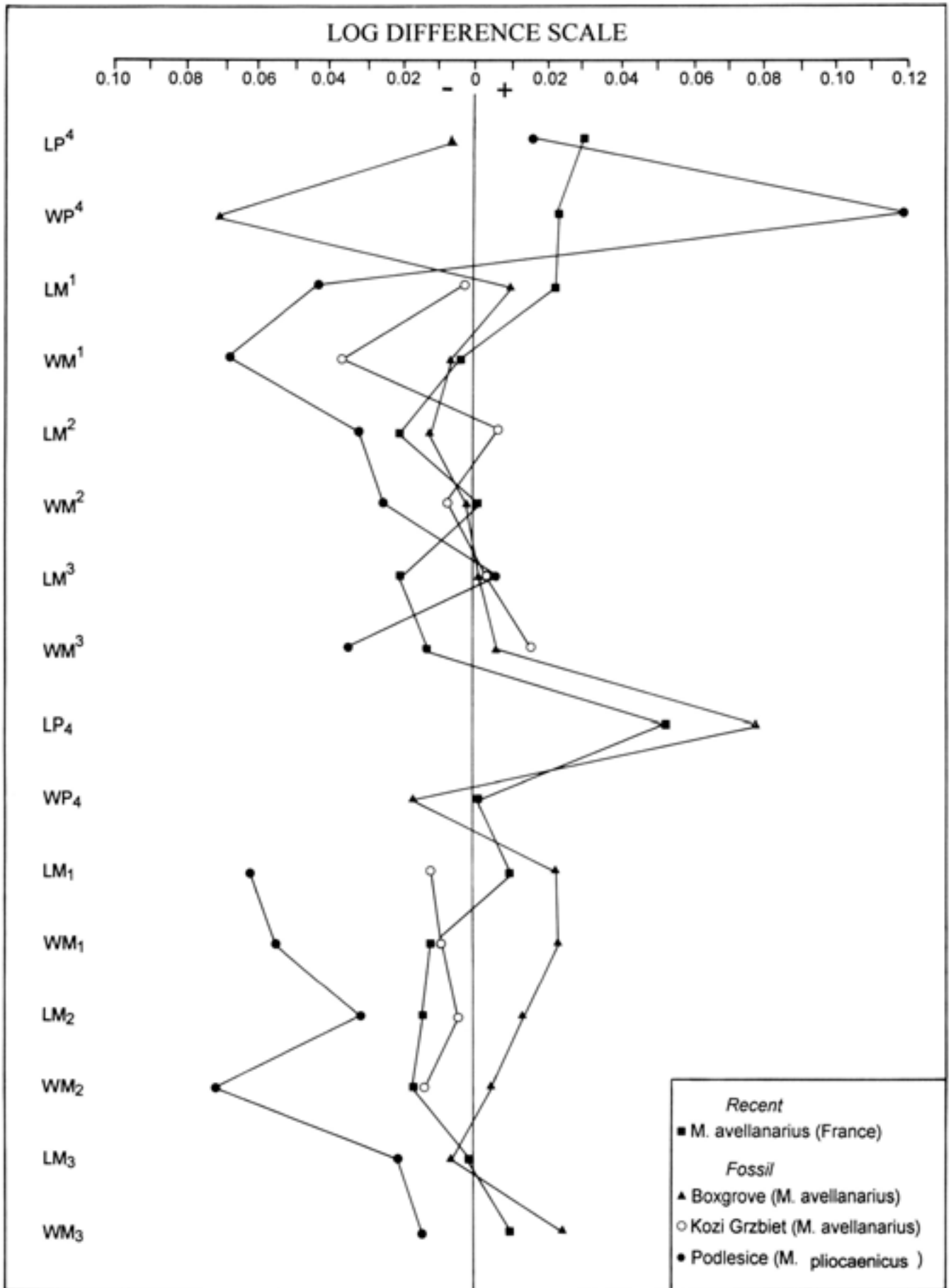


Fig 195 *Muscardinus avellanarius*: log ratio diagram for tooth dimensions of Recent and fossil hazel dormouse. The standard for comparison (vertical line) is Recent *M. avellanarius* from England

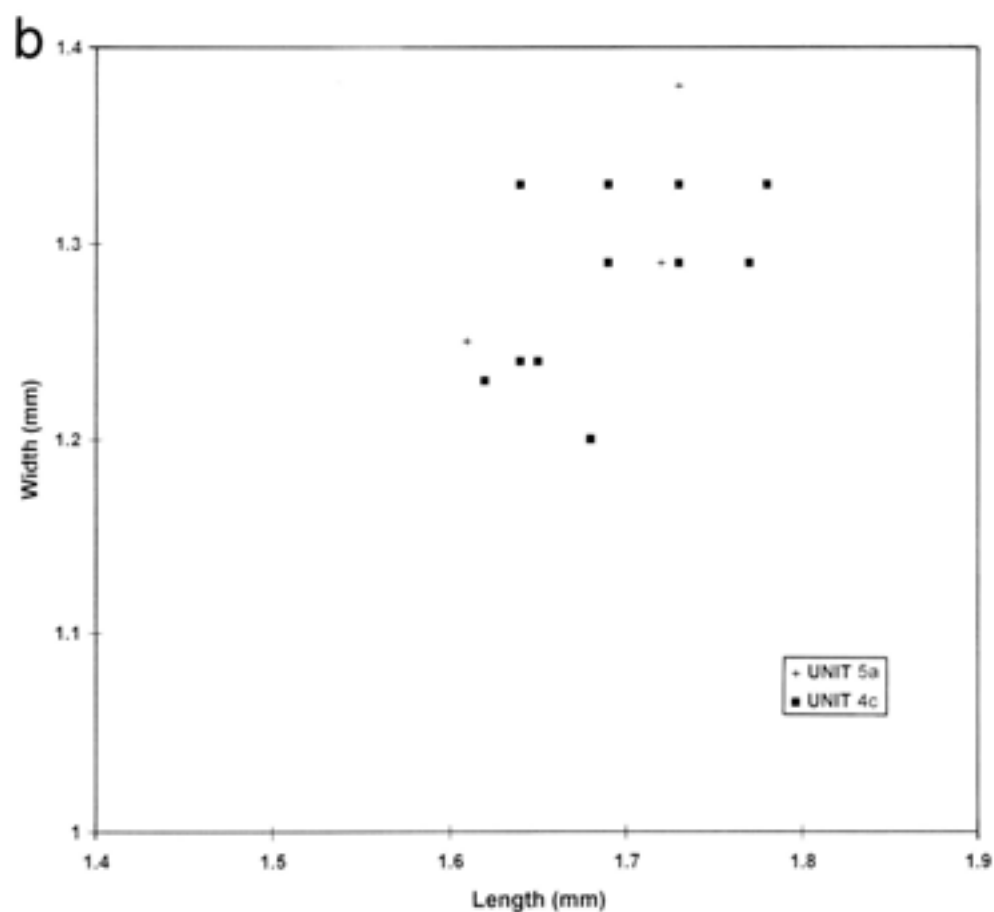
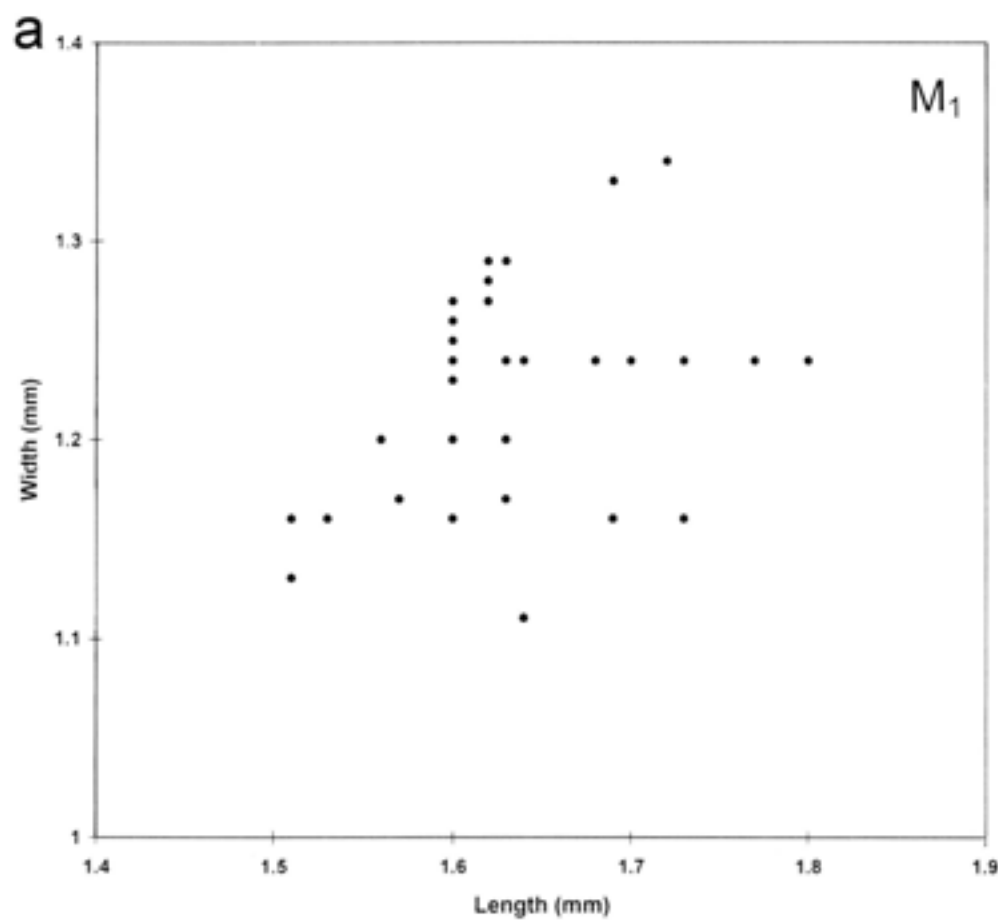


Fig 194 *Muscardinus avellanarius*: bivariate plot of length against width of M_1 in a) Recent and b) Boxgrove hazel dormouse

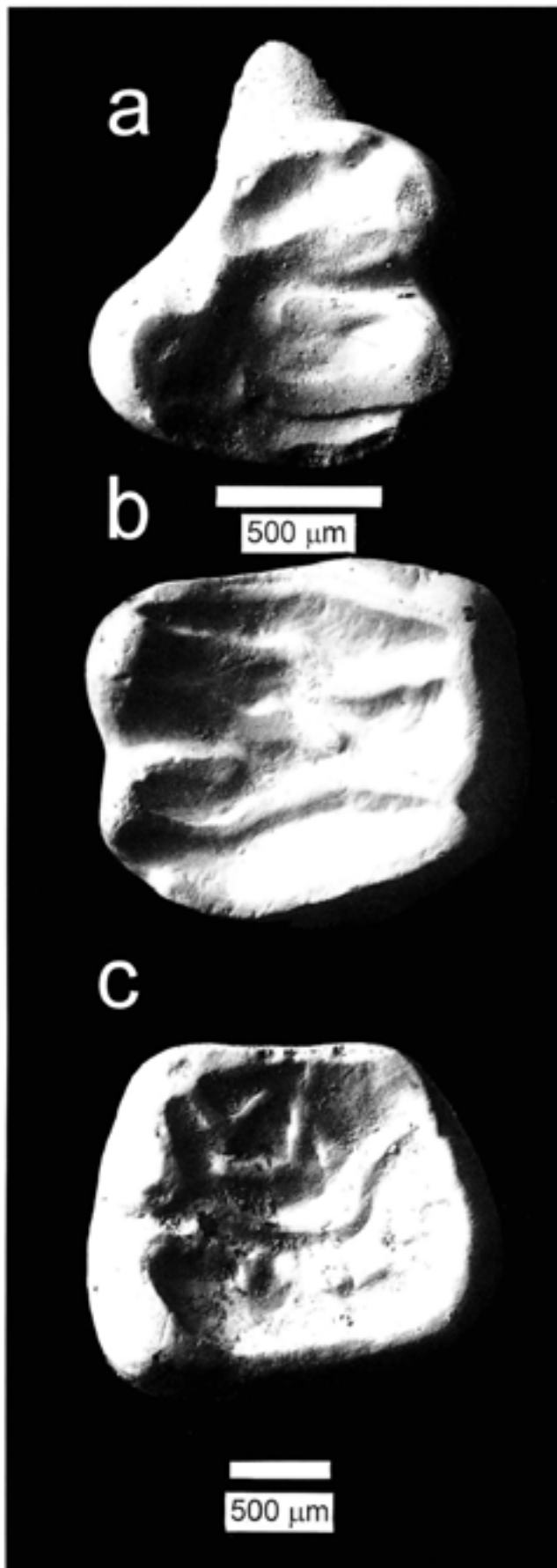


Fig 197 *Eliomys quercinus*: a) left deciduous P^4 (Q2/B BS90-1323 Unit 5a), b) right M^2 , c) left M^1 (Q2/B BS87-116 LGC), occlusal view

Table 85 *Eliomys quercinus*: measurements (mm) of dP^4 in Recent comparative specimens from Spain and France compared with Boxgrove

dP^4	n	length			width		
		min	\bar{x}	max	min	\bar{x}	max
Boxgrove	1		(0.98)			(1.15)	
France	8	0.79	0.85	0.96	0.98	1.04	1.08
Spain	4	0.87	0.91	1.07	1.05	1.10	1.20

postero-lingual cusp. The metaconule is short and does not reach the postero-lingual cusp. A low posteroloph runs along the posterior margin of the tooth. There is a well developed posterior centroloph situated between the metaloph and protoloph.

The morphology of the dP^4 is comparable to that of Recent *E. quercinus*. Although the tooth is larger than Recent comparative material from France and northern Spain (Table 85), it is within the size range of Recent specimens from the southern part of the Iberian peninsula and Italy (Fig 196).

The present day range of the garden dormouse extends across much of southern and central Europe. In north-western Europe it has a more southerly distribution than in the eastern part of its range. The garden dormouse primarily inhabits coniferous and mixed woodland with a well-developed shrub layer. Garden dormice are less arboreal than other European dormice and they show a distinct preference for areas with rocky ground cover (Horáček 1986). The degraded cliff and associated scree slopes would have provided such a habitat at Boxgrove.

The Pleistocene record of the garden dormouse is sparse and it is only known from two other Pleistocene localities in the British Isles. At Westbury-sub-Mendip, the garden dormouse is present in small numbers in the Calcareous Member, associated with a temperate woodland fauna (Andrews 1991), and at Beeches Pit (Suffolk) a single molar was recovered from deposits associated with a Hoxnian tufa.

Family Zapodidae

Genus *Sicista*

Sicista cf. betulina Pallas 1779

Birch mouse

Unit 4c: Q2 GTP 13 BS86-5 right M^1 , left M^2 , right M^2 , left M^3 ; Q2 GTP 17 BS86-26 left P^4 , right M^1

Unit 5a: Q1/B BS87-126 left M^1 , BS87-287 right M^1 frag, M^2 ; Q2 GTP 3 BS88-461 right M^1 , BS87-251 left M^2 , BS86-36 right M^2 , M^3 , M^3 ; Q2 GTP 17 BS86-81 right M^1 , BS86-57 right P^4 , right M^1 , right M^2 , left M^2 , right M^2 , BS86-56 right P^4 , left M^2 , left M^1 , right M^2 , right M^1 , BS86-84 right M^1 , right M^1 , left M^1 , right M^2 , right M^2 frag, BS86-25 left M^2 , M^1 , BS86-51 left M^1 , BS86-74 right M^1 , BS86-52 left M^1 frag, right M^2

Unit 6'20: Q2 GTP 20 BS86-54 right M^2

Unit 5c: Q2 GTP 17 BS90-1130 right M^1

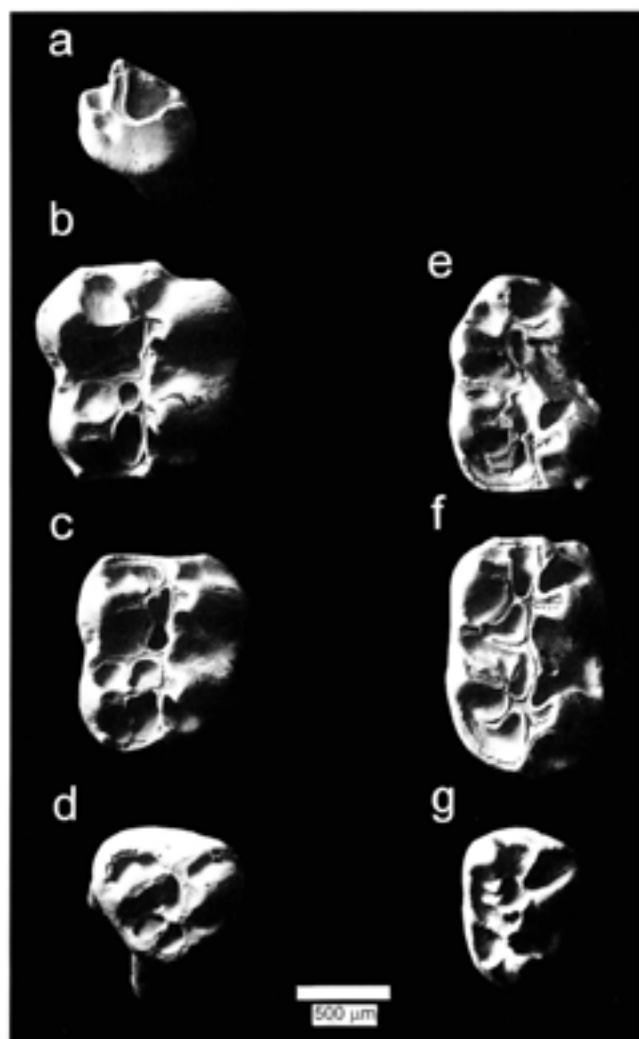


Fig 198 *Sicista cf. S. betulina*: a) right P^4 , b) right M^1 , c) right M^2 , d) right M^3 , e) right M^1 , f) right M^2 , g) right M^3

Description

The birch mouse is represented by 41 isolated teeth which were mainly recovered from Unit 5a (31 specimens) and Unit 4c (6 specimens). In addition single teeth were recovered from Units 5c and 6'20

The teeth are brachydont and display the typical *sicista* morphology with two parallel mesiodistal rows of cusps joined by enamel ridges. The occlusal structure of the teeth is complicated by additional crests and ridges. In the upper molars these are often fused to form closed fossettes during wear. Examples of the *sicista* teeth are shown in Figure 198a-g. Measurements of the teeth are shown in Figure 199.

Discussion

The birch mice (Sicistinae) are primarily an Asiatic family, with two species which extend into central and western Europe. The southern birch mouse (*S. subtilis*) is a species of the central Asian steppes, with a continuous distribution from Lake Baikal in the east

to Romania. Scattered populations occur in favourable habitats as far as west as eastern Austria (Fig 200). The smaller northern birch mouse (*S. betulina*) occurs across much of northern Asia, westwards into southern Finland and along the eastern Baltic coast. Towards the limit of its range, the distribution is patchy with isolated populations distributed across a wide zone from Romania in the south-east to Czechoslovakia, Germany, Denmark, and Norway (Fig 200). The northern birch mouse is primarily a forest species which favours woodland with dense undergrowth. It is also found in waterlogged situations such as peat bogs and occasionally inhabits overgrown grassland. The northern birch mouse is semi-arboreal and has a powerful hindlimb grip and a flexible tail which enable it to climb through dense undergrowth. The southern birch mouse prefers more open terrain and characteristic habitats include rough grassland, scrub, woodland margins and wooded steppe. The present day distribution of the northern and southern birch mice is shown in Figure 200.

Kowalski (1979), Kowalski and Nadachowski (1982), and Mayhew (1978) have shown that the teeth of Recent *S. subtilis* can be distinguished from those of *S. betulina* on size and on the presence and complexity of the accessory enamel ridges. In *S. subtilis*, the teeth are larger than *S. betulina* and lack additional crests and ridges. In *S. betulina* the dental surface is complicated, with supplementary crests and ridges. According to Mayhew (1978), the M^1 of *S. subtilis* is longer and wider than M^2 , whereas in *S. betulina*, the M^1 is shorter and wider than M^2 . The relationship between the length and width of these teeth is shown in the log ratio diagram (Fig 201).

Absolute size is not a reliable character for differentiating between the fossil forms as there is considerable overlap and variation in molar dimensions of the fossil species (Kowalski and Nadachowski 1982). For example, Late Pleistocene *S. betulina* is significantly larger than Recent populations and dental measurements of this species overlap with those of Recent *S. subtilis*. Last glaciation *S. subtilis* is also larger than contemporary populations.

Sicista has been found at a number of Late Pleistocene sites in Europe. During the Late Pleistocene, *S. subtilis* had a widespread distribution and fossil remains of this species have been found in Germany, northern Italy, south-western Austria, France, and in Bulgaria and Romania in south-eastern Europe. The relict distribution of the northern birch mouse at its western limits suggests a previously more widespread distribution. This is supported by the presence of fossil *S. betulina* from Late Pleistocene localities outside its present day range.

The two lineages of *Sicista* appear to be distinct from at least the Early Pleistocene. The earliest record of *S. subtilis* is from the Greek island of Chios (Storch 1975). The probable ancestor of *S. betulina* is *S. praeloriger* which occurs in the Early and Middle

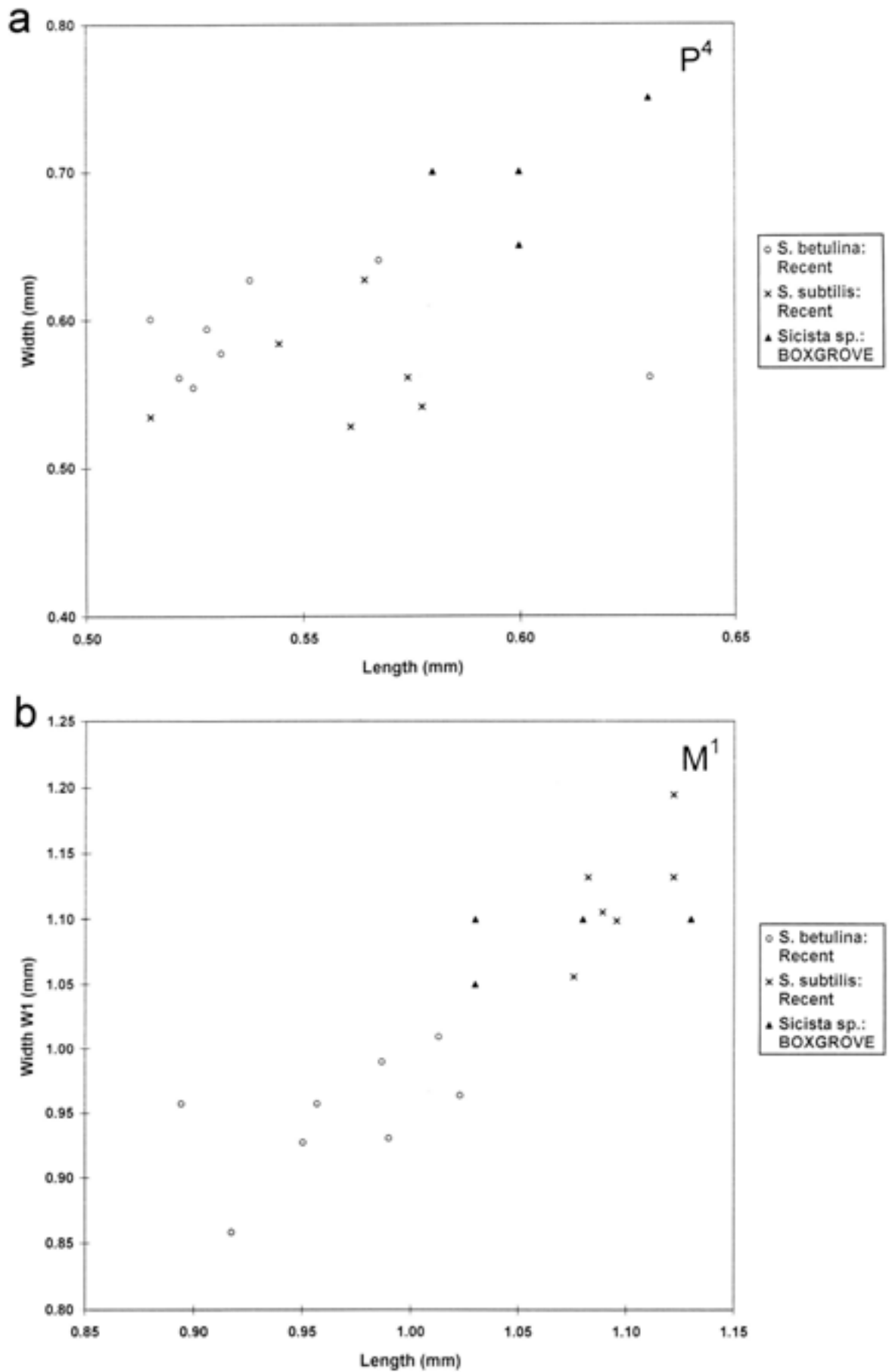
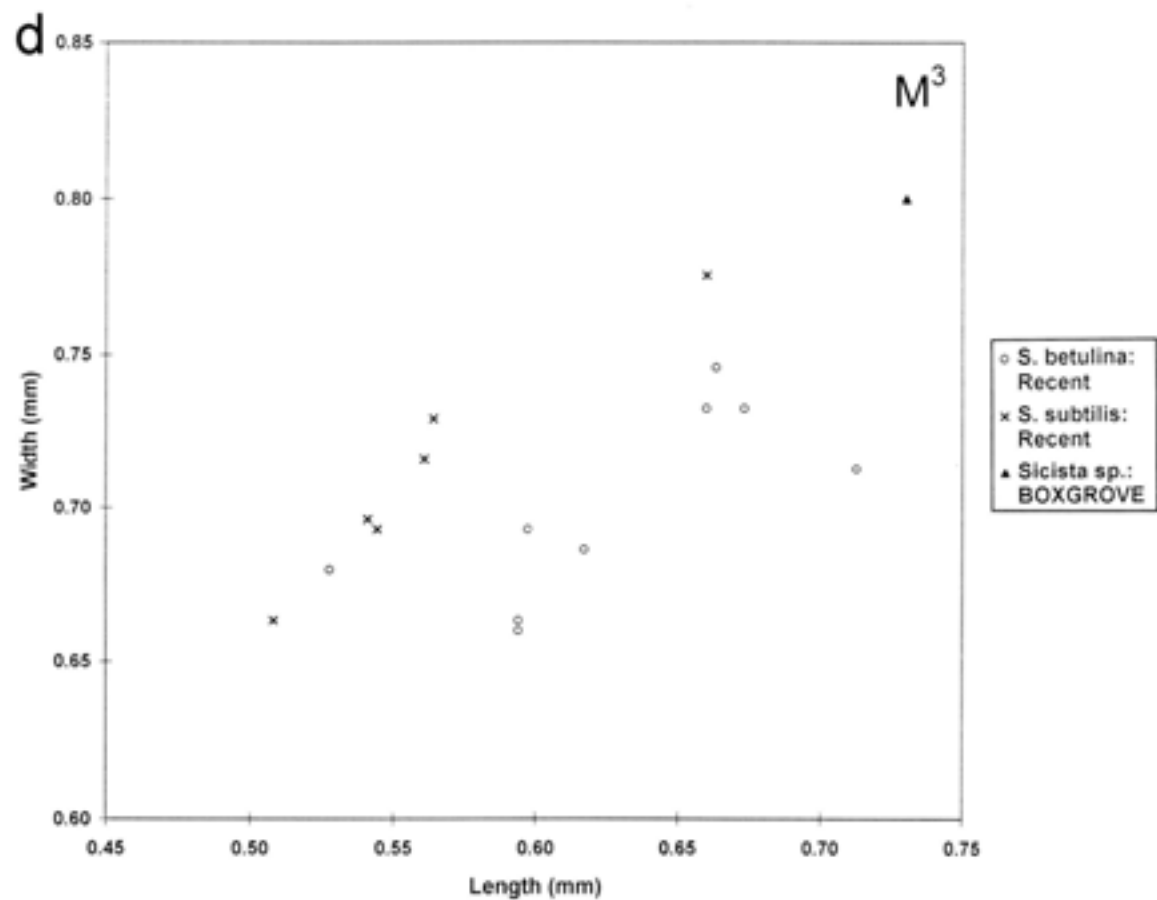
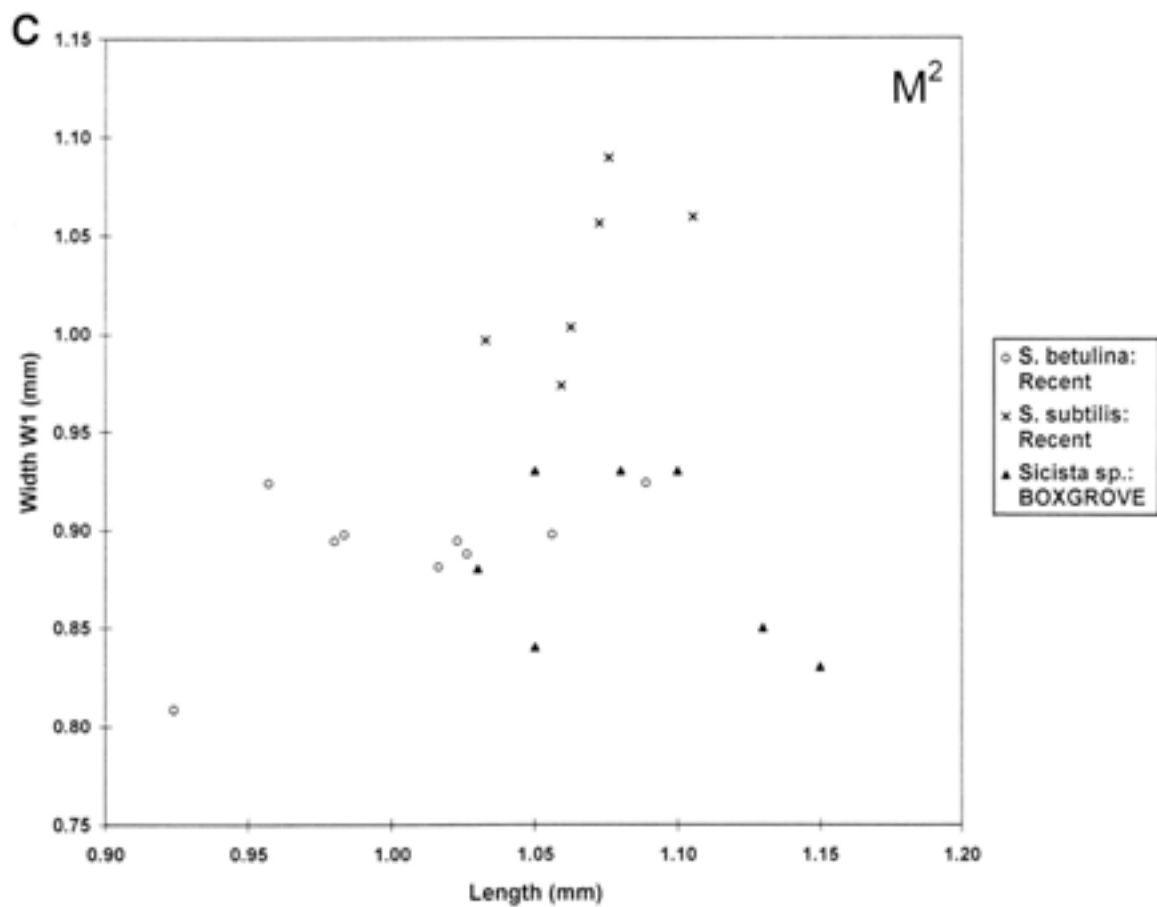


Fig 199 *Sicista* spp: bivariate plots of length against width in Recent and fossil birch mouse, a) P^4 , b) M^1 , c) M^2 , d) M^3 , e) M_1 , f) M_2 , g) M_3



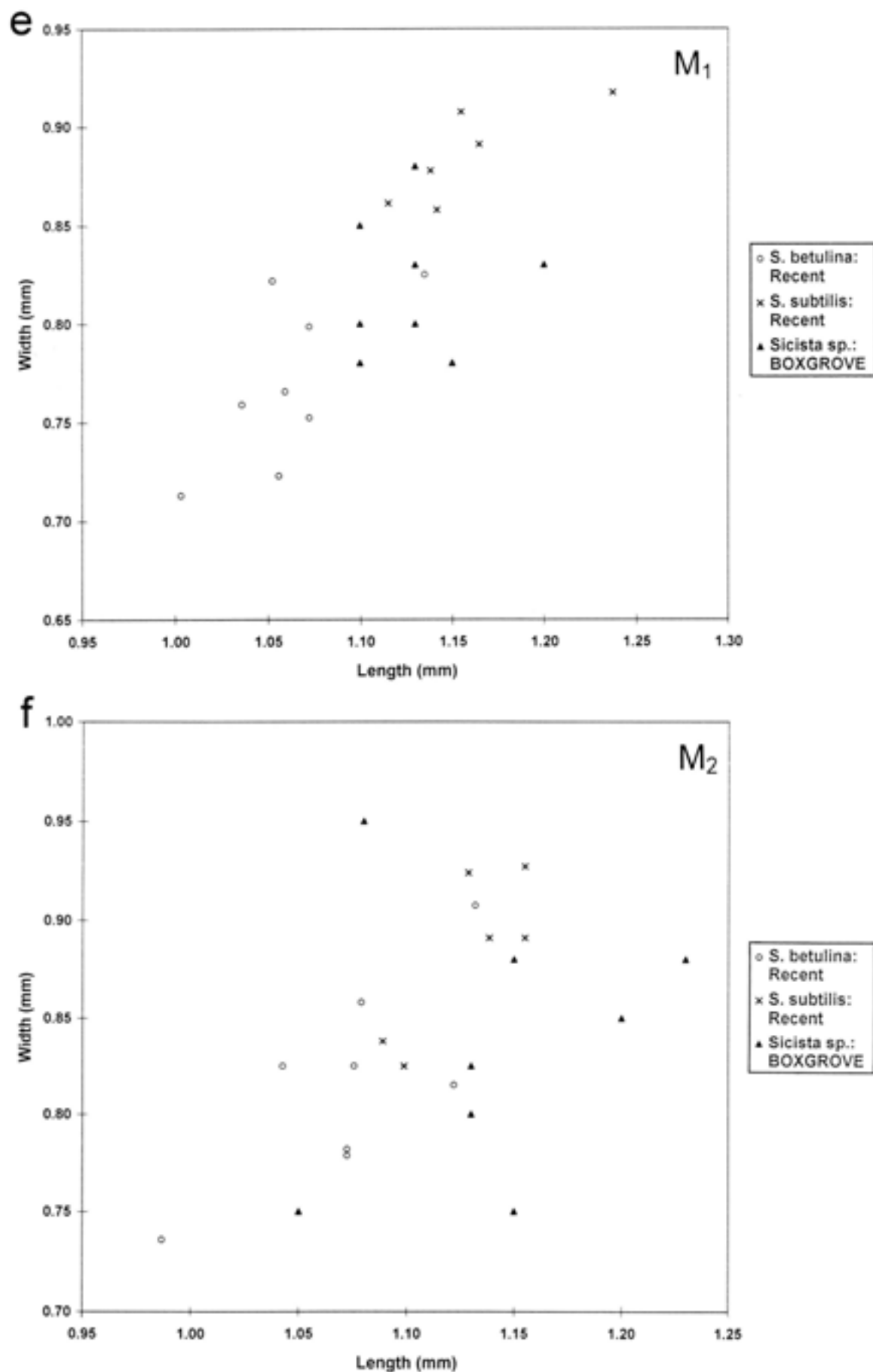


Fig 199 (continued) *Sicista* spp: bivariate plots of length against width in Recent and fossil birch mouse, a) M^0 , b) M^1 , c) M^2 , d) M^3 , e) M_1 , f) M_2 , g) M_3

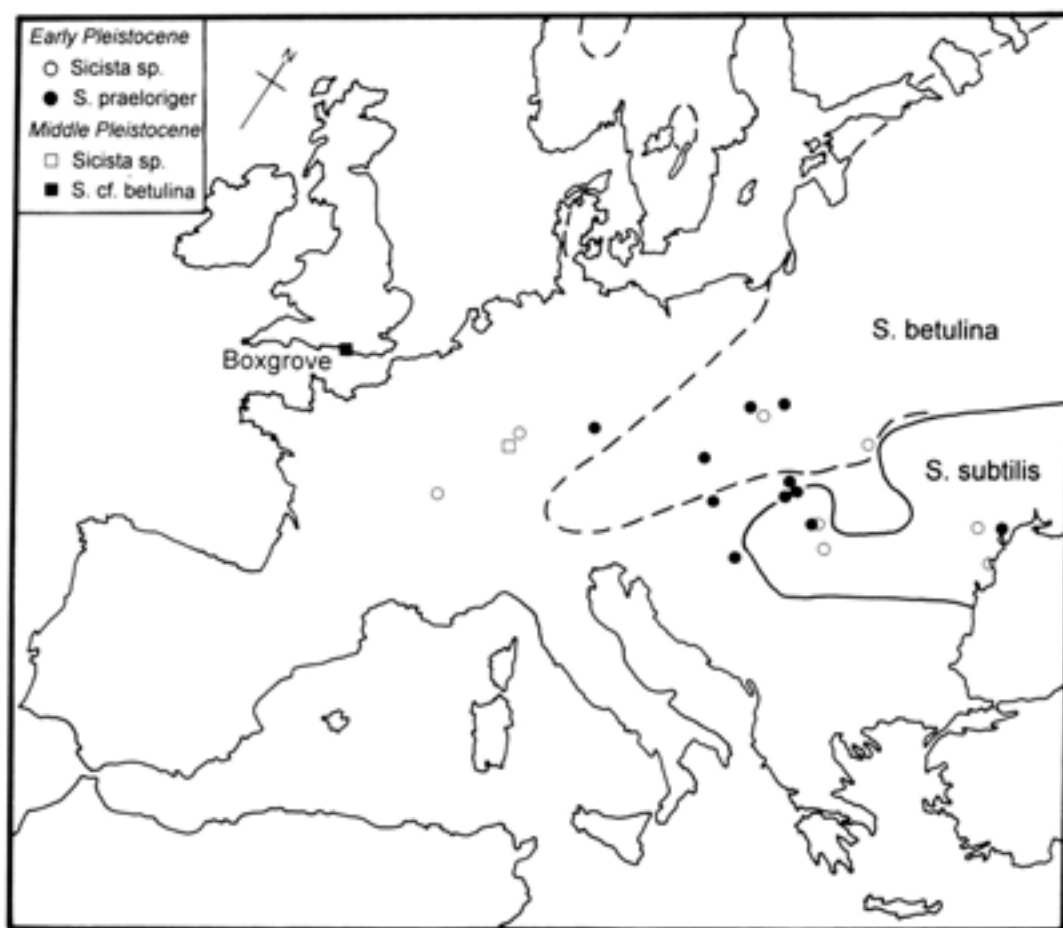
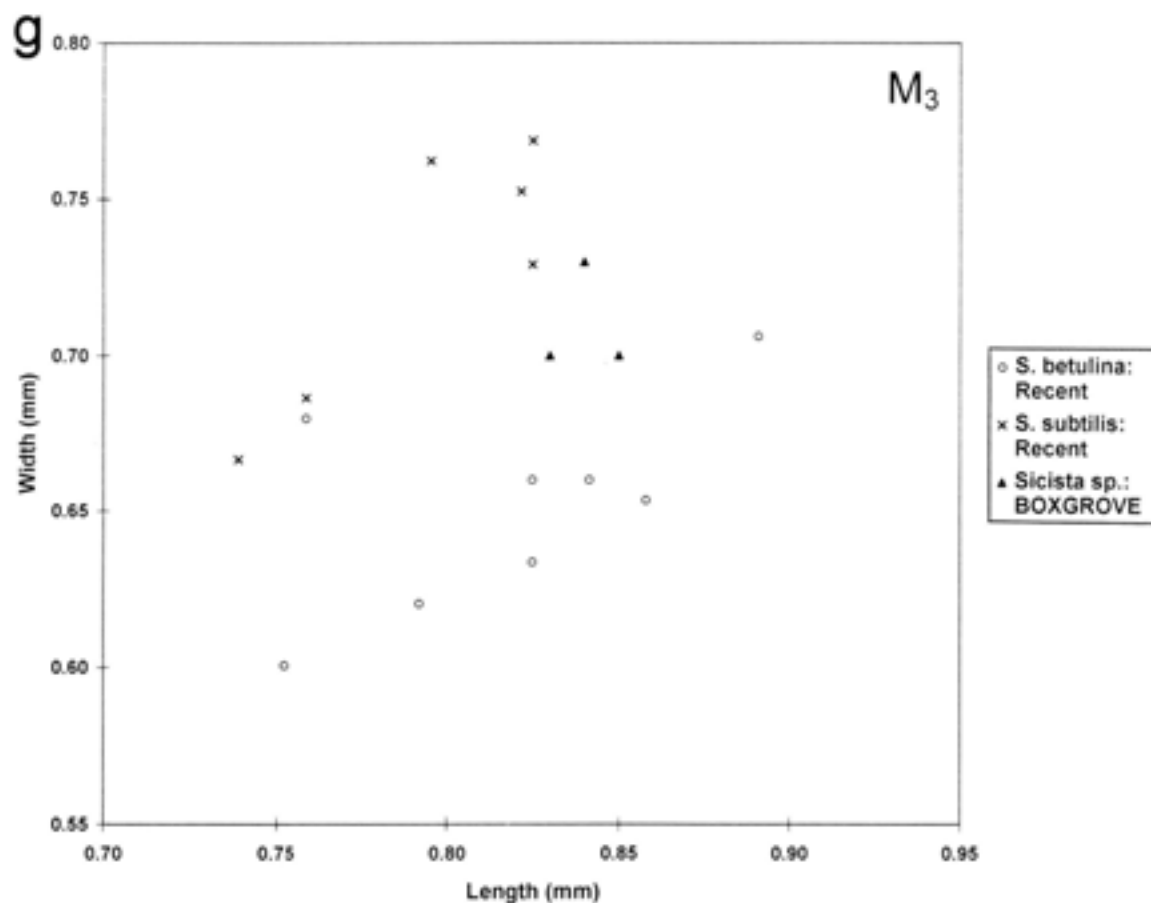


Fig 200 *Sicista* spp: distribution of living northern birch mouse (*S. betulina*) and southern birch mouse (*S. subtilis*) compared with the Pleistocene distribution of *Sicista* spp

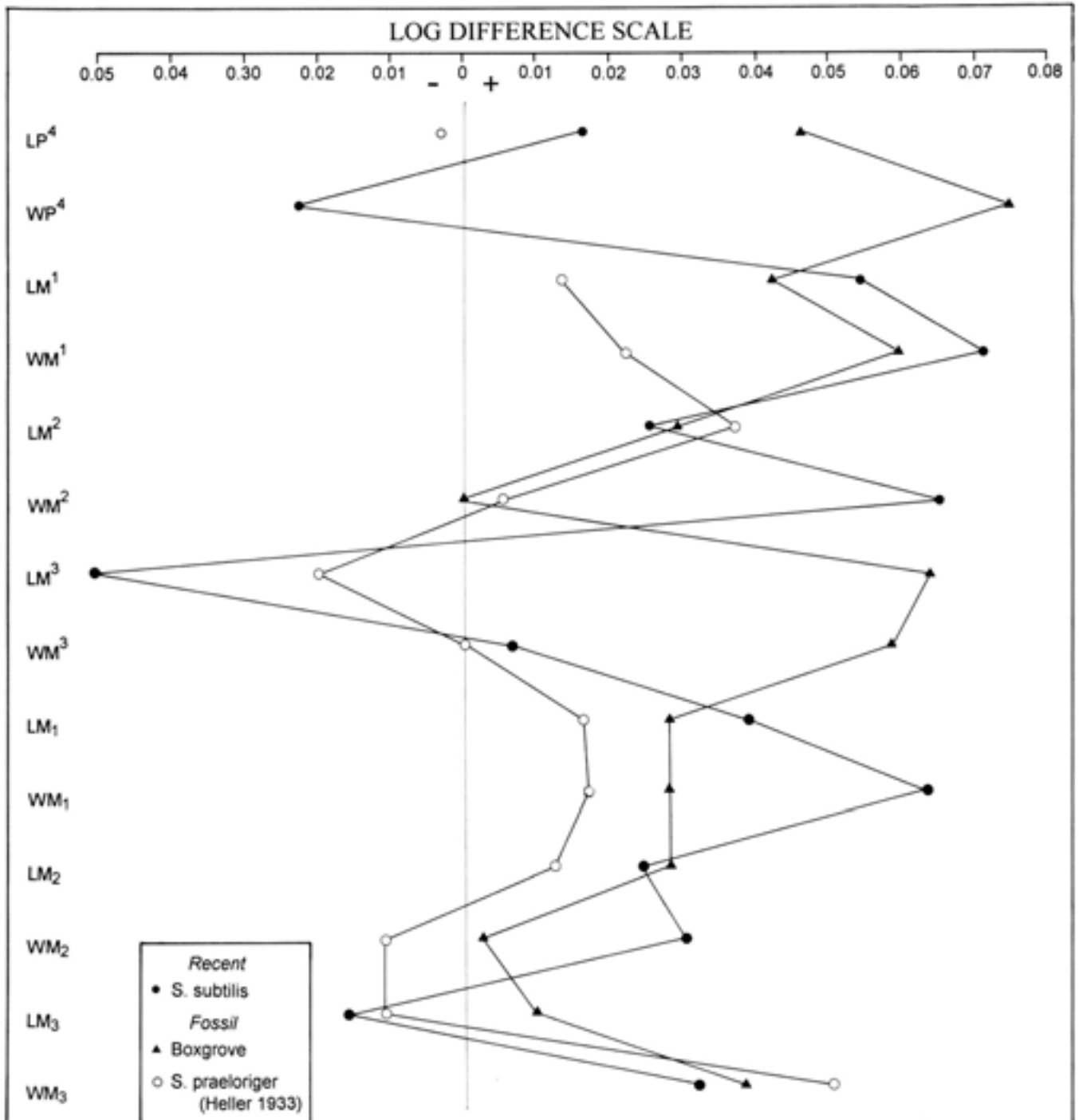


Fig 201 *Sicista* spp: ratio diagram for measurements of Recent and fossil birch mouse on log difference scale

Pleistocene of central Europe. *S. praeloriger* was described from Puspokfurdo, Hungary, and resembles *S. betulina* in the complexity of accessory crests on the molars. *S. praeloriger* differs from *S. betulina* in mandibular morphology and dental proportions, and in addition the occlusal surface is more complex than western populations of the northern birch mouse. The origin of *S. betulina* is at present unknown due to the poor fossil record of this species during the later part of the Middle Pleistocene.

The Boxgrove sample is of considerable interest as it is the most westerly record of *Sicista* known from the Middle Pleistocene. The material is also important as a relatively large sample was recovered. The uniform size and morphology of the Boxgrove sample indicate that the sample is homogeneous and represents a single species. Tooth dimensions plotted in Figures 199 and 201 fall within the known range of variation as *S. praeloriger* from Poland (Kowalski 1979). The M₁ is larger than Recent *S. betulina* and overlaps slightly with

Table 86 Measurements (mm) of *Sicista cf betulina* cheek teeth from Boxgrove (L=length, W=width)

		n	min	\bar{x}	max
P ⁴	L	4	0.58	0.60	0.63
	W	4	0.65	0.70	0.75
M ¹	L	5	1.03	1.07	1.13
	W	5	1.05	1.09	1.1
M ²	L	8	1.03	1.08	1.15
	W	8	0.83	0.89	0.93
M ³	L	1		(0.73)	
	W	1		(0.80)	
M ₁	L	8	1.1	1.13	1.20
	W	8	0.78	0.82	0.88
M ₂	L	9	1.05	1.14	1.23
	W	9	0.75	0.83	0.95
M ₃	L	3		(0.83, 0.84, 0.85)	
	W	3		(0.7, 0.7, 0.73)	

S. subtilis. The M¹ measurements fall within the range of *S. subtilis* and the length of M² is also similar to *S. subtilis*; however, the teeth are narrow and fall within the range of *S. betulina* for this dimension. In Figures 199 and 201 the length and width of M¹ and M² of *S. subtilis* and *S. betulina* and the Boxgrove material are shown. The diagram shows that the relative size of M¹ and M² are similar to Recent *S. betulina*. Although the occlusal morphology of the Boxgrove molars are complicated by interconnecting ridges, a similar degree of complexity is also found in Recent *S. betulina*. Comparisons of the figured specimens of *S. praeloriger* (Kowalski 1979) suggest a similar degree of complexity to living *S. betulina*; however, until larger samples of this species are described and figured, this cannot be stated with certainty. The Boxgrove birch mouse

Table 87 Measurements (mm) of *Apodemus maastrichtiensis* molars from Boxgrove

	n	min	\bar{x}	max
LM ¹	4	1.62	1.71	1.82
WM ¹	4	1.01	1.06	1.11
LM ²	3	–	1.11, 1.16, 1.18	
WM ²	3	–	0.97, 1.03, 1.08	
LM ₁	4	1.56	1.61	1.66
WM ₁	4	0.89	0.91	0.93
LM ²	1	–	(0.98)	–
WM ²	1	–	(0.98)	–

(Table 86) therefore has features which are similar to *S. praeloriger*, but it differs from this species in certain dental measurements and possibly in the degree of complexity of the occlusal surface. The Boxgrove specimens are referred to *S. cf betulina* on the basis of their morphology which is more similar to Recent *S. betulina* than Early Pleistocene *S. praeloriger*.

Family Muridae

Genus *Apodemus**Apodemus maastrichtiensis* Van Kolfschoten 1985

Extinct mouse

Unit 3: Q2 GTP 13 BS88-985 left M²Unit 4b: Q2 GTP 22 BS88-673 M₂Unit 4c: Q2 GTP 3 BS88-490 right M¹, BS87-124 right M₁; Q2 GTP 17 BS86-20 left M₁, M¹, M²Unit 5a: Q2 GTP 17 BS86-28 right M¹, left M₂, BS86-81 right M₁Unit 5a/6: Q2 GTP 17 BS86-17 right M²Unit 6/20: Q2 GTP 20 BS86-54 right M¹, left M₁

Apodemus molars from Boxgrove fall into two size categories (Fig 202) which differ in dental morphology (Fig 203). The smaller specimens are similar in size

Table 88 Dental characters of *Apodemus maastrichtiensis* and European *Apodemus* spp

	<i>Apodemus maastrichtiensis</i> extinct mouse (van Kolfschoten 1985)	<i>A. sylvaticus</i> wood mouse (NHM)	<i>A. flavicollis</i> yellow-necked mouse (NHM)	<i>A. mystacinus</i> rock mouse (Niethammer and Krapp 1978)	<i>A. microps</i> pygmy field mouse (NHM)	<i>A. agrarius</i> striped field mouse (NHM)
M ₁ mean range n	1.50 1.37–1.60 11	1.71 1.61–1.79 17	1.82 1.70–1.90 18	2.37 2.30–2.45 27	1.06 0.96–1.14 14	– 1.47 1
M ¹	t9 smaller than t6 t9 and t7 reduced	t9 and t6 equal size t9 and t7 well developed			t9 smaller than t6 t9 reduced t7 well developed	
M ²	t3 incipient or absent t9 and t7 small	t3 large t9 and t7 large			t3 absent t9 reduced t7 well developed	
M ₁₋₂	sides of cusps vertical angle of chevrons large	sides of cusps sloping angle of chevrons small				
M ₂	no additional cuspid labial to hypoconid					additional cuspid present

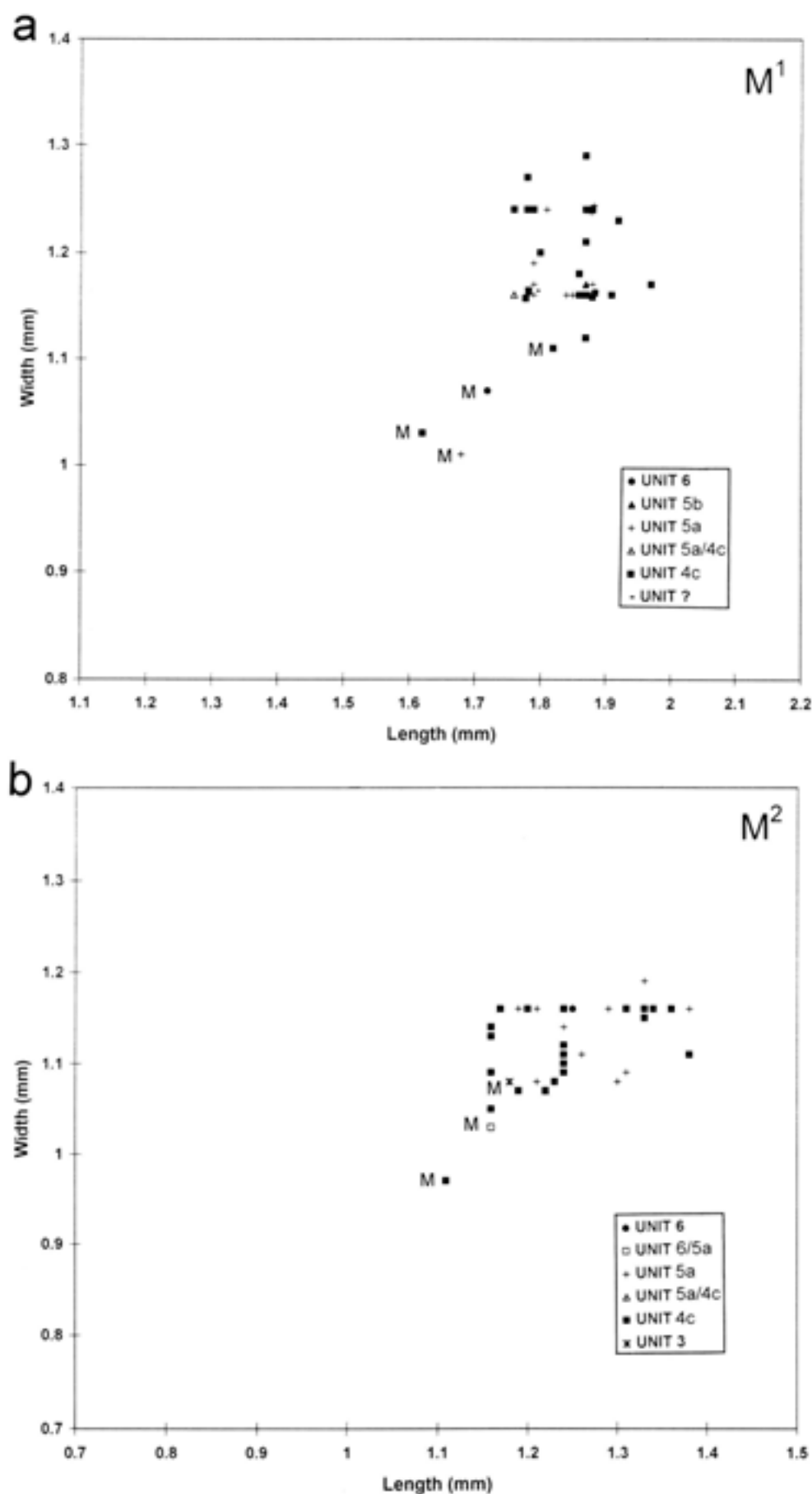


Fig 202a–d *Apodemus* spp: bivariate plot of length against width of *Apodemus sylvaticus* and *A. maastrichtiensis* (marked *M*) molars from Boxgrove, a) M^1 , b) M^2 , c) M_1 , d) M_2

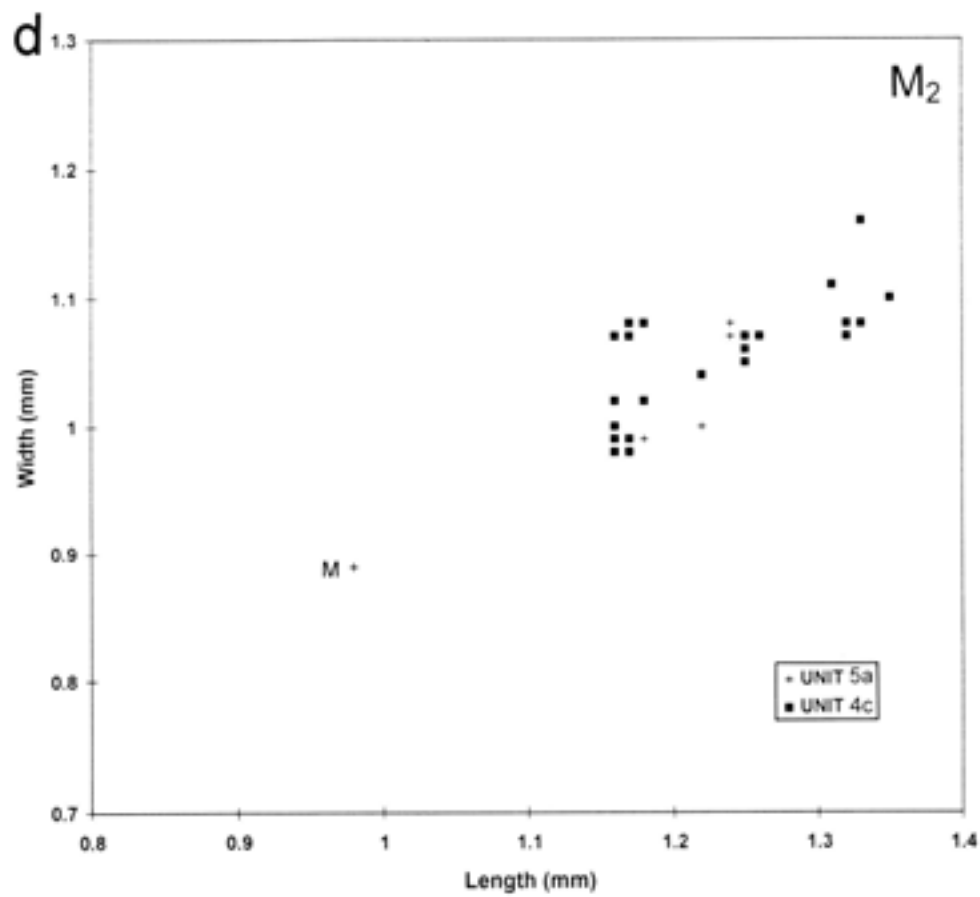
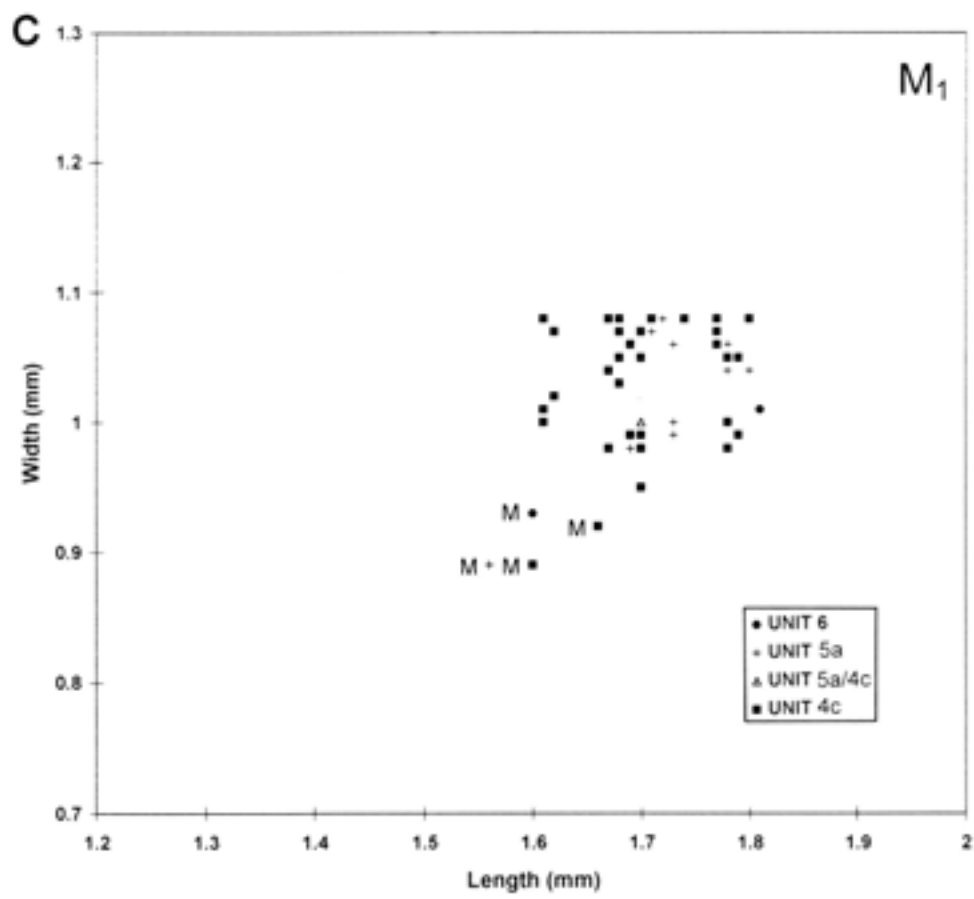


Table 89 Occurrence of British Pleistocene *Apodemus*: a summary of species and localities

	<i>Apodemus</i> sp	<i>A. maastrichtiensis</i>	<i>A. sylvaticus</i>	<i>A. flavicollis</i>
Cromerian complex				
Sugworth	-	-	+	-
Little Oakley	+	-	+	-
Boxgrove	-	+	+	-
West Runton	-	-	+	-
Westbury-sub-Mendip	-	+	+	-
Hoxnian				
Barnham	-	+	+	-
Beeches Pit	-	+	+	-
Hoxne	-	-	+	-
Grays Thurrock	-	-	+	?
Pre-Ipswichian-Post-Hoxnian				
West Wittering	-	+	-	-
Selsey West St	-	-	+	-
Stutton	-	-	+	-
Bacon Hole	-	-	+	-
Ipswichian				
Kirkdale Cave	-	-	+	-
Swanton Morley	-	-	+	-
Holocene	-	-	+	+

and morphology to the extinct mouse *A. maastrichtiensis* first described by van Kolfschoten (1985) from late Middle Pleistocene deposits at Maastricht-Belvédère. Cheek teeth of *Apodemus maastrichtiensis* are relatively scarce in the Boxgrove assemblage. Molars are illustrated in Figure 203 (b, d, f, h), and measurements are given in Table 87. *A. maastrichtiensis* may be distinguished from the larger *A. sylvaticus* on the basis of size and morphological differences of the first and second molars, as listed in Table 88.

A. maastrichtiensis is recorded from a number of sites in continental Europe including Maastricht-Belvédère (Maastricht-Belvédère 3 and 4), Fransche Kamp II and Miesenheim (van Kolfschoten 1990). These sites range in age from the end of the 'Cromerian Complex' to the Saalian. A re-examination of British Pleistocene *Apodemus* (Table 89 and Parfitt in prep) has shown that this species is present in a number of early Middle and Middle Pleistocene localities (Westbury, Boxgrove, Barnham and Beeches Pit) and in pre-Ipswichian/post-Hoxnian channel deposits at West Wittering (West Sussex). The range of this species, based on the British and the continental records, extends from the 'Cromerian Complex' until the Saalian, and it is not recorded from deposits of last interglacial age. Although well-dated assemblages of *Apodemus* from late Middle Pleistocene contexts are scarce, the absence of *A. maastrichtiensis* from the last interglacial contexts suggests that it probably become extinct during the 'Saalian Complex'.

The Boxgrove *A. maastrichtiensis* molars also resemble those of the poorly known Early Pleistocene species '*Parapodemus coronensis*'. However, as noted by van Kolfschoten (1991), this species has a more developed t9, which is poorly developed in the upper molars from Boxgrove. Nevertheless, the close morphological and metrical resemblance of these two species suggests they may be related.

Apodemus sylvaticus (Linnaeus 1758)
Wood mouse

Unit 4b: Q2 GTP 22 BS88-673 M₂

Unit 4c: Q1/A BS87-87 M₂; Q1/B BS87-197 right M₁, right M₂ (cf), BS87-247 2 right M₁, left M₂; Q1 GTP 16 BS86-24 right M₁, right M₂, right M₃, right M₄, right M₅ (cf); Q2 GTP 3 BS87-183 left M₁, right M₁, BS88-463 left M₂, BS87-124 right M₁ (cf), left M₂, BS87-156 right M₂ (cf), BS86-186 right M₂, left M₂, BS87-327 right M₂, left M₂, BS87-149 right M₁, left M₂, right M₂, right M₃ (cf), BS88-463 right M₁, left M₁, right M₂, right M₃ (cf), BS87-119 right M₁, left M₁, M₂ (cf), BS87-124 left M₂, two right M₂ (cf), M₃ (cf), BS86-36 left M₁, right M₂, left M₃ (cf), two left M₂, right M₂, two left M₂, right M₂, two right M₃ (cf), BS88-461 left M₁, right M₁ (cf), left M₂, two right M₂, right M₃ (cf), BS88-490 left M₁, right M₂, BS87-270 left M₂, two right and three left M₂, M₃ (cf), BS87-156 left M₁ frag, M₂, left M₃ (cf), right M₂, BS87-251 three right M₁, left M₁, left M₂, two left M₂, two right M₂, left M₂, right M₂, two right M₃ (cf), left M₃ (cf), BS87-273 three left M₁, M₁ frag, BS87-263 two right M₁, left M₂, two left M₂, two right M₂, right M₃ (cf), BS87-136 two left M₁, two right M₂, left M₂, right M₂ (cf), BS87-136 two left M₁, two right M₂, left M₂, right M₂; Q2 GTP 13 BS86-8 left M₂, left M₃ (cf), left M₃, right M₃, BS86-2 left M₁, right M₂, left M₂; Q2 GTP 15 BS86-16 maxilla frag, two right M₁, left M₁, two right M₂, left M₂, two left M₂ (cf), two right M₂, right M₂, left M₂, two left M₂ (cf); Q2 GTP 17 BS86-29 left M₁, BS86-70 left M₁, right M₁, BS87-70 left M₂, BS86-26 right M₂, right M₃ (cf), left M₃ (cf), left M₃, right M₃, two left M₂, right M₂, right M₃ (cf), two M₃ (cf), BS86-30 right M₁, left M₁, left M₂, left M₂, right M₂, BS87-114 left M₁ (cf), left M₂, right M₂, BS86-20 left M₁ frag, left M₁, left M₂, BS86-69 two right M₁, right M₂; Q2 GTP 20 BS86-53 right M₂

Unit GC: Q2 GTP 3 BS87-178 left M₂, BS87-236 left M₂, right M₂ (cf), BS87-192 right M₁, left M₁, right M₁, BS87-175 right M₁, right M₂, left M₂, two left M₂, right M₂, M₃ (cf)

Unit GB4: Q2 GTP 3 BS87-123 two left M₁, left M₂ (cf), right M₂

Unit 4c/5a: Q2 GTP 17 BS86-19 left M₁, right M₂, left M₂

Unit 5a: Q1/B BS88-502 right M₁, left M₁, left M₂, left M₂; Q2/B BS90-1323 three left M₁, left M₂ (cf), right M₂, left M₂; Q2 GTP 3 BS86-35 M₁ frag, right M₁ frag, left M₁ frag, two right M₁, right M₂; Q2 GTP 17 BS86-68 right M₁ (cf), left M₂, BS86-18 right M₁, left M₂, two left M₂, BS86-67 right M₁, right M₂, BS86-76 right M₁, BS86-55 right M₂, BS86-3 left M₂, BS86-84 left M₂, M₃ (cf), BS86-60 left M₂ frag, BS86-25 left M₁ frag, four left M₁, two left M₂, three right M₂, left M₃ (cf), left M₃, right M₂, left M₃ (cf), right M₃ (cf), left M₃ (cf), BS86-28 two left M₁, two left M₂, right M₂, right M₃, left M₃, left M₂

Unit 620: Q2 GTP 20 BS86-54 right M₂, right M₃, M₃ (cf)

Unit 5b: Q2 SEP 2 BS86-38 left M₁

Unit 637e: Q2 GTP 3 BS87-252 right M₂

Apodemus sylvaticus, the woodmouse (Figs 202, 203a, c, e, g), is more common than *A. maastrichtiensis* in the Boxgrove sample. Measurements of the teeth are given in Table 90. The Boxgrove material does not differ in morphology or dimensions from modern British *A. sylvaticus*.

The woodmouse is found across most of Europe with the exception of northern Scandinavia. It inhabits a wide range of environments with dense ground cover.

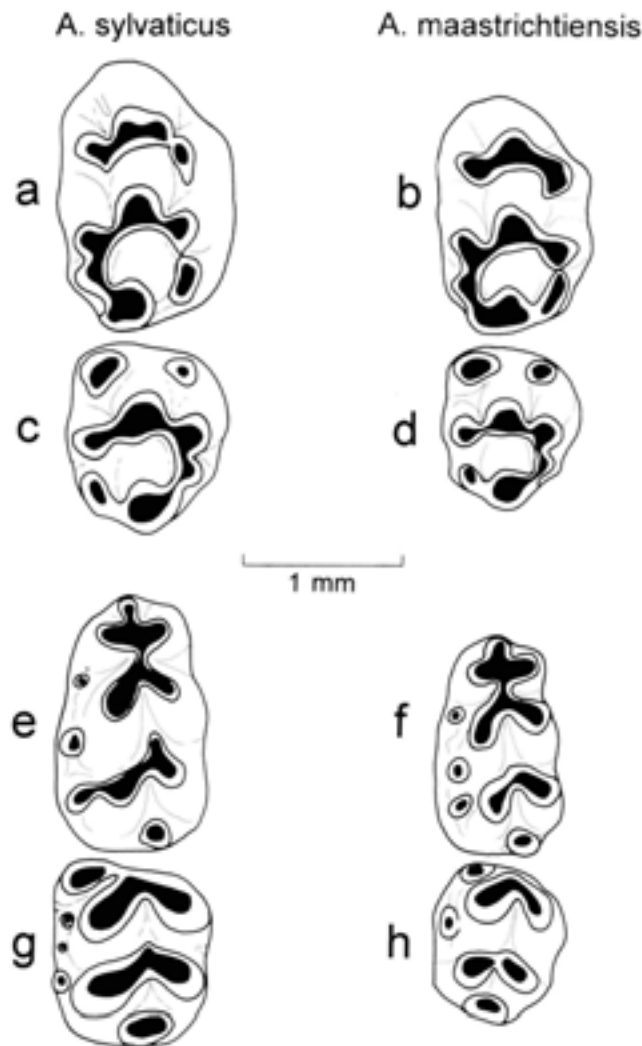


Fig 203 *Apodemus* spp: *A. sylvaticus*, a) right M^1 , c) left M^2 , e) left M^3 , g) left M^3 ; *A. maastrichtiensis*, b) right M^1 , d) left M^2 , f) left M^3 , h) left M^3

Table 90 Measurements (mm) of *Apodemus sylvaticus* (M^1 , M^2 , M^3 , M^3) and *Apodemus* spp (M^1 , M^1) from Boxgrove

	<i>n</i>	<i>min</i>	\bar{x}	<i>max</i>
LM ¹	36	1.76	1.84	1.97
WM ¹	36	1.12	1.19	1.29
LM ²	37	1.16	1.25	1.38
WM ²	37	1.05	1.13	1.19
LM ³	14	0.75	0.87	0.96
WM ³	14	0.80	0.87	0.93
LM ₁	45	1.61	1.72	1.81
WM ₁	45	0.95	1.03	1.08
LM ₂	32	1.16	1.22	1.35
WM ₂	31	0.98	1.05	1.16
LM ₃	23	0.88	0.97	1.05
WM ₃	23	0.74	0.85	0.95

Order Lagomorpha
Family Leporidae
Genus *Lepus*
Lepus timidus Linnaeus 1758
Mountain hare

Unit 4b: Q1/A BS87-92 right P^3
Unit 4c: Q2 GTP 17 left $M^{1/2}$ or P^1 , left lower I frag, right M^2 , two lower M frags (juvenile)
Unit 5a: Q2 GTP 3 BS86-35 right lower I frags
Q2 GTP 17 right P^3 , lower cheek tooth frags, BS86-51 left Mef,
Unit 5a/6: Q1/A F255 right Mef, right M^1

At least six individuals are represented by isolated teeth and three groups of associated dental remains. A number of the teeth are heavily digested as a result of ingestion by a mammalian predator.

Lower incisors

The two lower incisors taper towards the occlusal surface and are clearly from young individuals. Both incisors have a square cross-section (Fig 204) which is typical of *Lepus timidus*. *Oryctolagus* and *L. europaeus* have incisors with rectangular cross-sections and this is reflected in the low value for the incisor index (Table 91). The incisor index for the Boxgrove specimens (87 and 107%) are within the range of variation observed in Recent *L. timidus* (Koby 1959). The bucco-lingual width and mesio-distal length of Recent *L. timidus*, *L. europaeus* and *Oryctolagus* are plotted in Figure 205 along with fossil *O. cuniculus* from Swanscombe and *L. timidus* from Boxgrove.

P^3

The P^3 (length: 3.39mm, width 2.7mm) has a square occlusal outline with an angular entoconid, a large hypoconid and a moderately developed anterior lobe (Fig 206). The hypoflexid is straight, smooth and reaches the lingual border. In comparison, the P^3 of *Oryctolagus* has a characteristic occlusal profile with a rounded entoconid. The anterior lobe is large in *Oryctolagus* and the lingual anteroconid is also well developed. The presence of a centroflexid of the P^3 hypoflexid distinguishes the P^3 of *O. cuniculus* from *L. timidus* and *L. europaeus*. The Boxgrove specimen is similar to *L. timidus* and differs from *L. europaeus* which has a small anteroconid and a projecting hypoconid.



Fig 204 *Lepus timidus*: right lower incisor (Q2 GTP 3 BS86-35 Unit 5a), cross-section

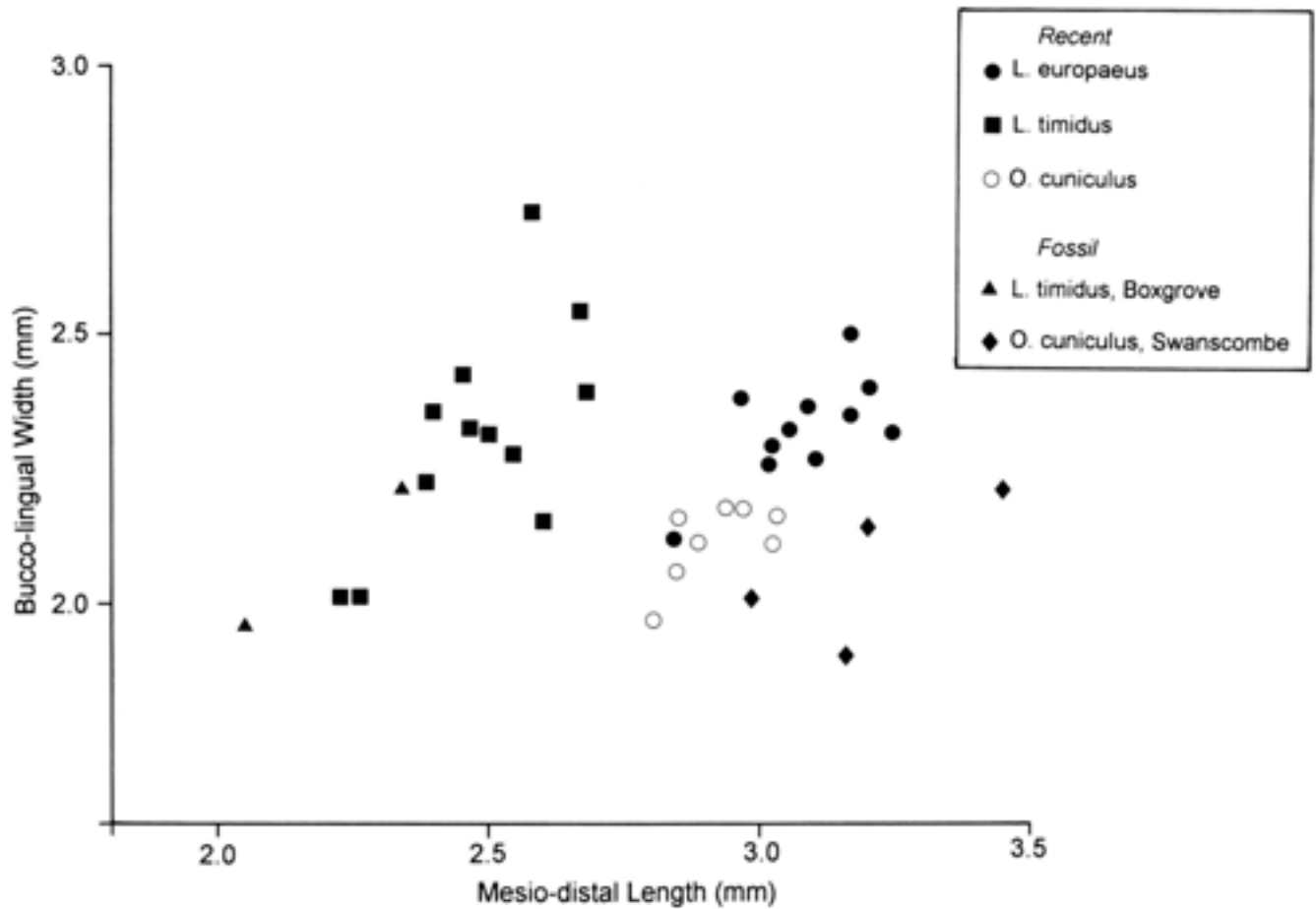


Fig 205 *Lepus* spp and *Oryctolagus cuniculus*: bivariate plot of bucco-lingual width against mesio-distal length of lower incisor in Recent *Lepus timidus*, *L. europaeus*, *Oryctolagus cuniculus*, and fossil *L. timidus* from Boxgrove and *O. cuniculus* from Swanscombe

Table 91 Comparative measurements (mm) of the lower incisor in Recent *Oryctolagus cuniculus*, *Lepus europaeus*, and Recent and fossil *Lepus timidus*. The incisor index (Koby 1960) is the bucco-lingual diameter as a percentage of the mesio-distal diameter. For the Recent samples, the observed range and the mean of each measurement are given, *n* is sample size

	<i>n</i>	mesio-distal diameter			bucco-lingual diameter			incisor index		
		min	\bar{x}	max	min	\bar{x}	max	min	\bar{x}	max
Recent										
<i>O. cuniculus</i>	8	1.96	2.1	2.18	2.8	2.9	3.03	70	73	76
<i>L. europaeus</i>	12	2.12	2.3	2.5	2.84	3.1	3.24	69	75	81
<i>L. timidus</i>	12	2.01	2.3	2.73	2.23	2.5	2.67	83	94	106
Boxgrove										
<i>L. timidus</i>	2	(1.95, 2.20)			(2.35, 2.05)			(83, 107)		

Table 92 Measurements (mm) of upper incisors in Recent and fossil *Oryctolagus* and *Lepus* spp. Details as in Table 91

	<i>n</i>	mesio-distal diameter			bucco-lingual diameter			incisor index		
		min	\bar{x}	max	min	\bar{x}	max	min	\bar{x}	max
<i>Oryctolagus</i> sp (Boxgrove)	1		(1.85)			(2.6)			(71)	
<i>O. cuniculus</i> (Swanscombe)	3		(1.89, 2.0, 2.08)			(2.6, 2.75, 2.75)			(69, 77, 76)	
<i>O. cuniculus</i> (Recent)	11	1.55	2	2.35	2.5	2.8	3.34	59	72	81
<i>Lepus europaeus</i> (Recent)	3		(2.1, 2.15, 2.23)			(3.06, 3.3, 3.35)			(64, 67, 70)	
<i>L. timidus</i>	1		(2.2)			(2.4)			(92)	

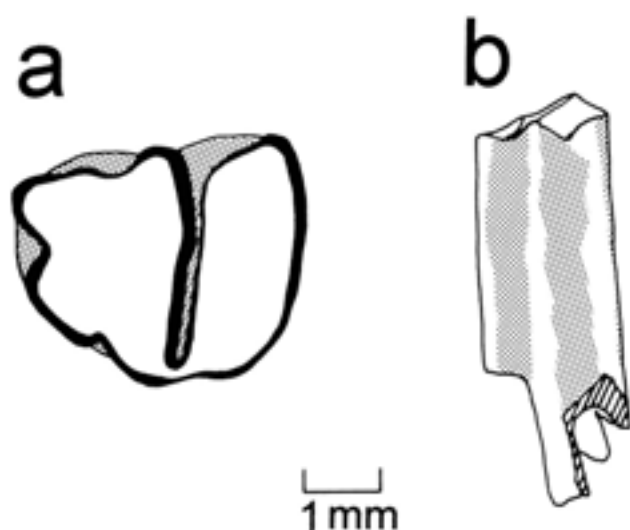


Fig 206 *Lepus timidus*: right P_3 (Q2 GTP 17 Unit 5a), a) occlusal view, b) buccal view



Fig 207 *Lepus timidus*: right P_3 fragment (Q1/A BS87-92 Unit 4b), occlusal view



Fig 208 *Lepus timidus*: right M^2 (Q1/A F255 Unit 5a/6), occlusal view



Fig 209 *Oryctolagus* cf *O. cuniculus*: right upper incisor (Q2 SEP 2 Unit 5a), cross-section

An unusual feature of the Boxgrove P_3 is the presence of a cementum filled paraflexid. According to Palacios and López-Martínez (1980), this feature is not found in *L. capensis*, *L. timidus* or *L. castrovajoi*, but it is present in 32% of a sample of *L. grantensis* from Spain. However, the occurrence of a cementum filled paraflexid appears to be highly variable in Recent populations of *Lepus* and was recorded in 8% of *L. timidus* from Scotland and 13% of *L. europaeus* from southern England.

P^3 and M^2

In the upper P^3 and M^2 (Figs 207, 208) of *L. timidus*, the hypoflexid is straight and the enamel walls are smooth or only slightly crenulated. Although there is some variability in this characteristic, the hypoflexid walls are crenulated in *L. europaeus* and highly folded in *O. cuniculus*. The P^3 of *L. europaeus* also has a small flexid at the entrance of the hypoflexid which is absent in *O. cuniculus*, *L. timidus* and the Boxgrove specimen. In these characters the Boxgrove P^3 resembles *L. timidus*.

Genus *Oryctolagus*

Oryctolagus cf *O. cuniculus* (Linnaeus 1758)

Rabbit

Unit 5a: Q2 SEP 2 right upper I

The rabbit is represented by an upper first incisor from Unit 5a (Currant in Roberts 1986) which is indistinguishable from that of Recent *Oryctolagus cuniculus* (Fig 209). The tooth is rectangular in cross-section (B-L width: 1.85mm, M-D length: 2.6mm) with two anterior lobes which are separated by a shallow mesial groove. The rounded medial lobe and a shallow mesial groove are both characteristic of *Oryctolagus*. In *Lepus timidus* and *L. europaeus*, the medial lobe is often asymmetric with the highest part situated towards the medial border of the tooth. The mesial groove in *L. timidus* is deep and frequently filled with cementum. In addition to these morphological characters, the cross-sectional dimensions of the upper incisors can be used to separate *Oryctolagus* from *Lepus* (Donard 1981; Koby 1960). In Table 92, the length and width of the upper incisors of Recent and fossil *Oryctolagus* and Recent *L. timidus* and *L. europaeus* are given. The measurements show a clear separation in cross-section dimensions between the three lagomorph species. The Boxgrove specimen falls within the range of Recent *O. cuniculus*.

According to Donard (1981) the earliest remains of *Oryctolagus cuniculus* are from Montoussé I and II dated to the Mindel glaciation. Later occurrences are sparse and mainly confined to the Iberian peninsula. In Britain, *O. cuniculus* has been identified from the Lower Loam at Swanscombe (Mayhew 1975) and from Hoxnian deposits at East Farm Barnham. The occurrence of the rabbit in the British Pleistocene may be of stratigraphic significance as it is not recorded from post-Hoxnian faunas (Corbet 1986).

Lagomorpha gen et sp indeterminate

Unit 4c: Q1/A *F1607*, *F2001*, *F2163* cheek tooth frags; Q1/B BS 87-206 upper cheek tooth frag; Q2 GTP 3 BS87-124 upper cheek tooth frags, BS86-36 lower I frags; EQP Q2 TP2 *F42* upper cheek tooth frag

Unit 5a: Q1/A *F390* right P₁ or M₁; Q2 GTP 17 BS86-76 *F1049* lower cheek tooth frag; BS86-82 *F1062* patella

Unit 5a/6: Q2 GTP 17 *F84* upper cheek tooth; BS86-28 cheek tooth frags

4.3 Summary: taphonomy and palaeoecology

Introduction

This chapter discusses the mammalian evidence for changing environments and climate and briefly describes the taphonomy of the Boxgrove faunas. The sedimentary sequence at Boxgrove represents a complex succession of environmental and climatic change which covers at least part of an interglacial cycle and the start of the ensuing Anglian cold stage. This episode appears to be more complex than the initial interpretations suggested (Roberts Chapters 2.1, 2.7; Tables 9a, 9b), and the excavation and sampling of the cliff collapse and colluvial deposits adjacent to the buried cliff has provided evidence for succession of climatic and environmental change which was not observed in the attenuated stratigraphic sequence described previously (Woodcock 1981; Roberts 1986).

Though the abundance of fossil vertebrates varies through the sedimentary sequence, the upper part of the Slindon Silt Member and the Earham Lower Gravel Member (Tables 8, 9a) have provided a diverse and abundant vertebrate fauna (Table 93) which allows a detailed interpretation of the palaeoecology to be undertaken. In contrast, calcareous units bracketing these members have produced limited faunal assemblages which have enabled the palaeoecology of these units to be interpreted with varying degrees of resolution.

Methods

In the following section a detailed analysis of the palaeoecology of the Boxgrove succession is presented, based primarily on the taxonomic habitat index scores for the small mammal faunas. The rationale and methods used in this analysis have been discussed in detail by Evans *et al* (1981), and by Andrews (1990) in his analysis of the Westbury small mammal faunas. In this method, individual species are defined in terms of their ecological preferences based on the range of habitats in which they occur at the present day. The index scores for individual species are derived from the proportion of each habitat type in which the species is known to occur. These index values are then combined for all the species in the assemblage and a cumulative index is then calculated by dividing the combined score by the number of species. The taxonomic habitat indices for

the Boxgrove assemblages, derived from the small mammal faunal lists, are plotted as histograms in Figure 210. In Figure 211 the scores are shown in a simplified form for the main fossiliferous units to show trends in taxonomic habitat index through the sequence.

The taxonomic habitat spectra of the Boxgrove units can be compared with similar diagrams constructed for modern small mammal faunas from a number of European habitats shown in Figure 212. In this diagram, the differences in the taxonomic habitat spectra between the major habitat types are readily apparent. Boreal forest faunas of north-western Russia and across central and northern Scandinavia show the highest proportion of boreal forest elements, with relatively high proportions of deciduous woodland and tundra elements. The fauna of the mixed deciduous/coniferous forest zone (southern Sweden) is similar to the deciduous forest fauna with a dominance of deciduous woodland elements, although boreal and, to a lesser extent, tundra elements are also well represented. The deciduous forest faunas of western and central Europe show the highest proportion of deciduous forest elements and a relatively high representation of Mediterranean and boreal elements. The deciduous forest fauna differs markedly from those of Mediterranean Europe, which have a nearly equal representation of Mediterranean and deciduous woodland elements with a negligible representation of boreal and tundra elements. The steppe and forest steppe zones of Eastern Europe are characterised by high proportions of deciduous forest and steppe elements: boreal and Mediterranean elements form a minor component of these faunas. Although direct comparison can be made between Recent temperate woodland faunas and those of the Pleistocene interglacial periods, the species composition of the British Pleistocene cold stages show markedly different patterns from those of the modern tundra and boreal habitats in having a combination of steppe and tundra elements. These steppe-tundra habitats appear to have no modern analogues and this illustrates that caution should be observed in making direct comparisons of fossil assemblages with modern habitat types.

The relative proportions of vertebrates in the stratigraphic succession can also provide palaeoecological information, although the interpretation of abundance must take into account the taphonomy of the faunal assemblage. Andrews (1990) has shown that modern assemblages derived from predators often bear little relationship to the living community from which they were derived. Furthermore, this problem is compounded in the analysis of fossil bone assemblages as the predator or other taphonomic agents can only be inferred. In the case of the Boxgrove vertebrate remains, the taphonomic analysis of the faunal assemblages shows that they are predominantly attritional assemblages derived from a mixture of predator, natural deaths and hominid accumulation. The fossil

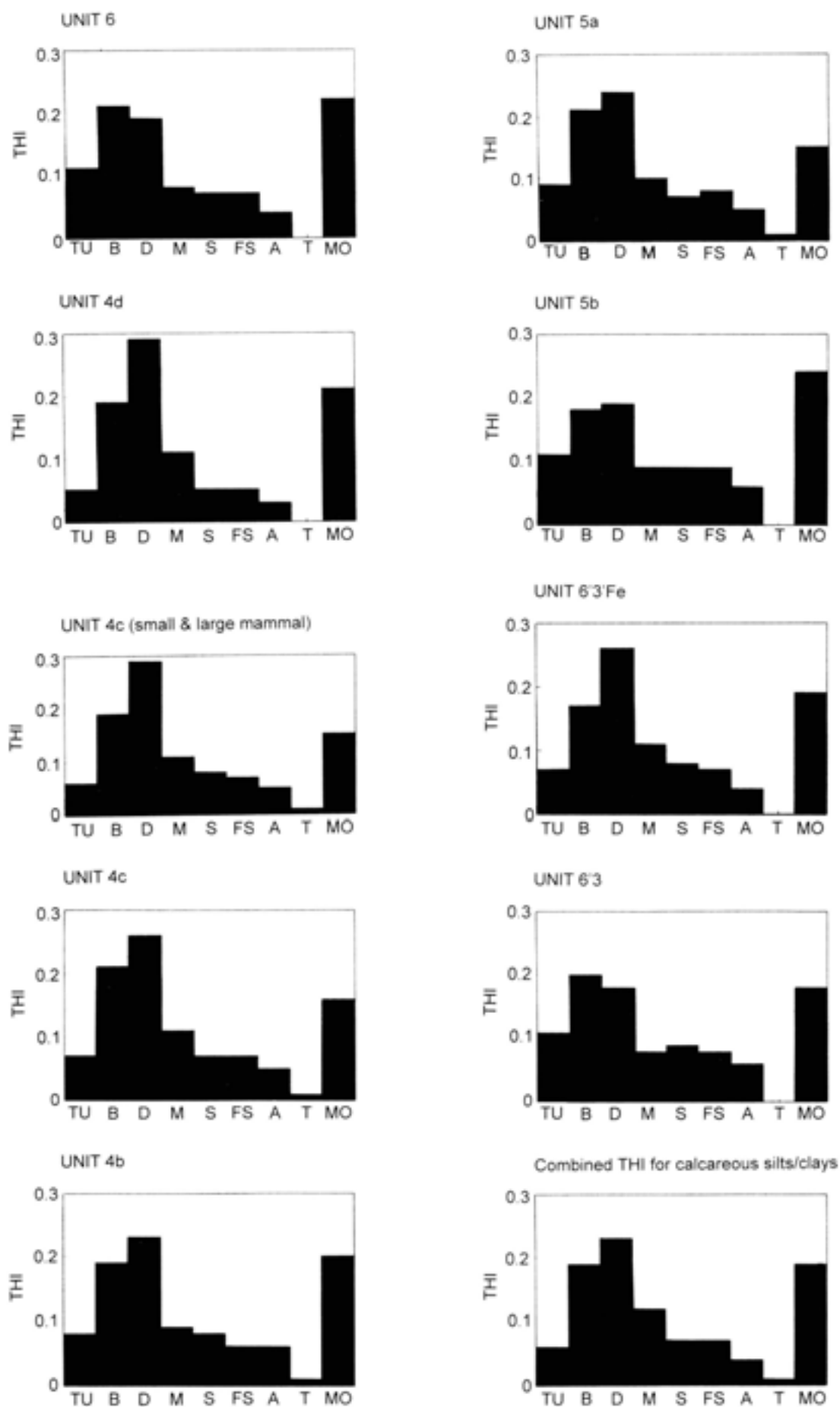


Fig 210 Taxonomic Habitat Index distributions of faunas from Boxgrove arranged in stratigraphic order with the oldest assemblage (Unit 4b) at bottom left and the youngest assemblage (Unit 6) at top right. The habitat types are: Tundra (Tu), Boreal Forest (B), Deciduous Forest (D), Mediterranean (M), Steppe (S), Forest Steppe (FS), Arid (A), Tropical (T), and Montane (Mo) habitats

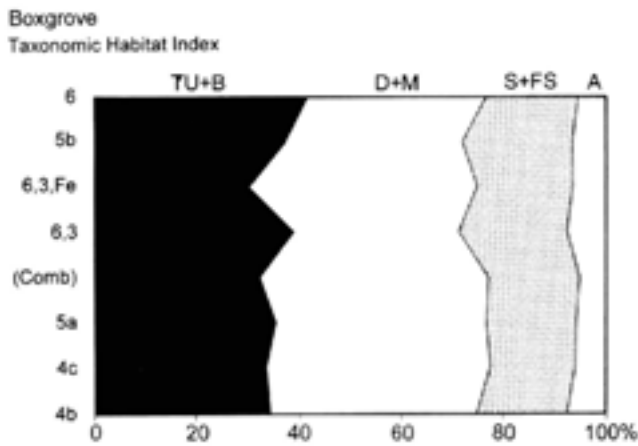


Fig 211 Summary of the Taxonomic Habitat Index for the main fossiliferous deposits at Boxgrove plotted as a cumulative percentage frequency graph. Tundra/Boreal, Deciduous/Mediterranean, and Forest and Forest/Steppe types have been combined in this diagram

assemblages should therefore reflect more accurately the relative abundances of species in the living community than those derived from a selective predator. That the relative proportions of small mammals and other vertebrate classes reflect closely the environmental and climatic changes is shown by a comparison of changes in the proportions of the taxa with the palaeoenvironmental interpretation derived from the taxonomic habitat index and information provided by other environmental remains. The relative proportions of vertebrate taxa indicate a similar pattern of environmental and climatic change to that shown by these methods. The quantitative comparison of the Boxgrove small mammal faunas is based on frequency distributions derived from percentages of the number of elements identified to taxa (NISP) and on minimum numbers of individuals (MNI). The basic data for the NISP and MNI counts are given in Table 94 and plotted as frequency diagrams in Figure 213. For other vertebrate groups, fragment count data for the successive levels are shown graphically in Figures 214 and 215, and the raw data are presented in Table 95a.

The interpretation of the taphonomic history of the faunas is based on analysis of data recorded in the field, i.e. bone orientation and distribution, and on a detailed analysis of bone modification undertaken during the identification of the faunal remains. A summary of the main conclusions concerning the taphonomy of the assemblages is given in Table 95b.

Slindon Formation

Slindon Sand Member. Unit 3: Marine sands

The faunal assemblage from the marine sands consists primarily of marine fish (Parfitt and Irving, Chapter 3.4). Remains of other vertebrates are uncommon and the mammalian fauna, consisting of only three species,

is too poorly known to provide useful palaeoclimatic or environmental information. The scarcity of terrestrial vertebrate remains is perhaps not surprising given the nearshore marine depositional environment of these deposits. Little can be said regarding the taphonomy of the mammalian remains, although the small number of large mammal bones from the upper part of Slindon Sands are generally rolled and abraded bone 'pebbles'. This type of alteration is consistent with a prolonged period of transport and exposure in a marine environment. A fragment of red deer tibia from Marine Cycle 3 is well preserved and shows evidence for human alteration in the form of cutmarks and marrow fracture impact damage. This evidence, as well as the occasional artefact from the marine sands, suggests sporadic human utilisation of the foreshore during low tides.

Slindon Silt Member. Units 4a and 4b: Lagoonal/Intertidal Beds

These units are composed of finely laminated calcareous silts and clays which were deposited under gentle sedimentary conditions in an enclosed lagoon. Evidence for mud cracking and ripening in localised horizons within this unit indicate periods of emergence, and possible colonisation of the mudflats by vegetation and mammals (Macphail Chapter 2.6). Vertebrate remains are uncommon within this unit, and the majority of the large mammal bones are found in concentrations associated with flint knapping debris. Cutmarks and marrow fracture of the limb bones indicate that these concentrations represent localised episodes of tool manufacture and butchery in otherwise sterile deposits. The lack of weathering on the bones and the discrete nature of the large mammal bone and artefact clusters suggest that the periods of emergence were short lived. This is confirmed both by the analysis of bone and artefact refits, and by the preferred long axis orientation of the bone fragments, which suggest rapid burial under gentle sedimentary conditions. The presence of rootlet corrosion on a significant proportion of the large mammal bones may be evidence for vegetation cover; however, this is inconclusive as the rootlet corrosion features may equally represent rooting from higher stratigraphic levels.

Terrestrial small vertebrates and the sparse small mammal remains are dispersed throughout the deposits with no evidence for clustering. Evidence for predator modification of the bones is slight and the degree of digestive corrosion of the bones and teeth indicates that an avian predator was involved in the accumulation of the small mammal bones. The bone element representation of the small mammal bones shows evidence for winnowing by tidal action, showing that the bones were either washed into the lagoon from a terrestrial environment, or deposited on the mudflats by a predator and subsequently dispersed by tidal currents.

In Figure 214, the proportions of the major small vertebrate groups are shown for the lowermost part of the lagoonal sequence (4a) compared with the

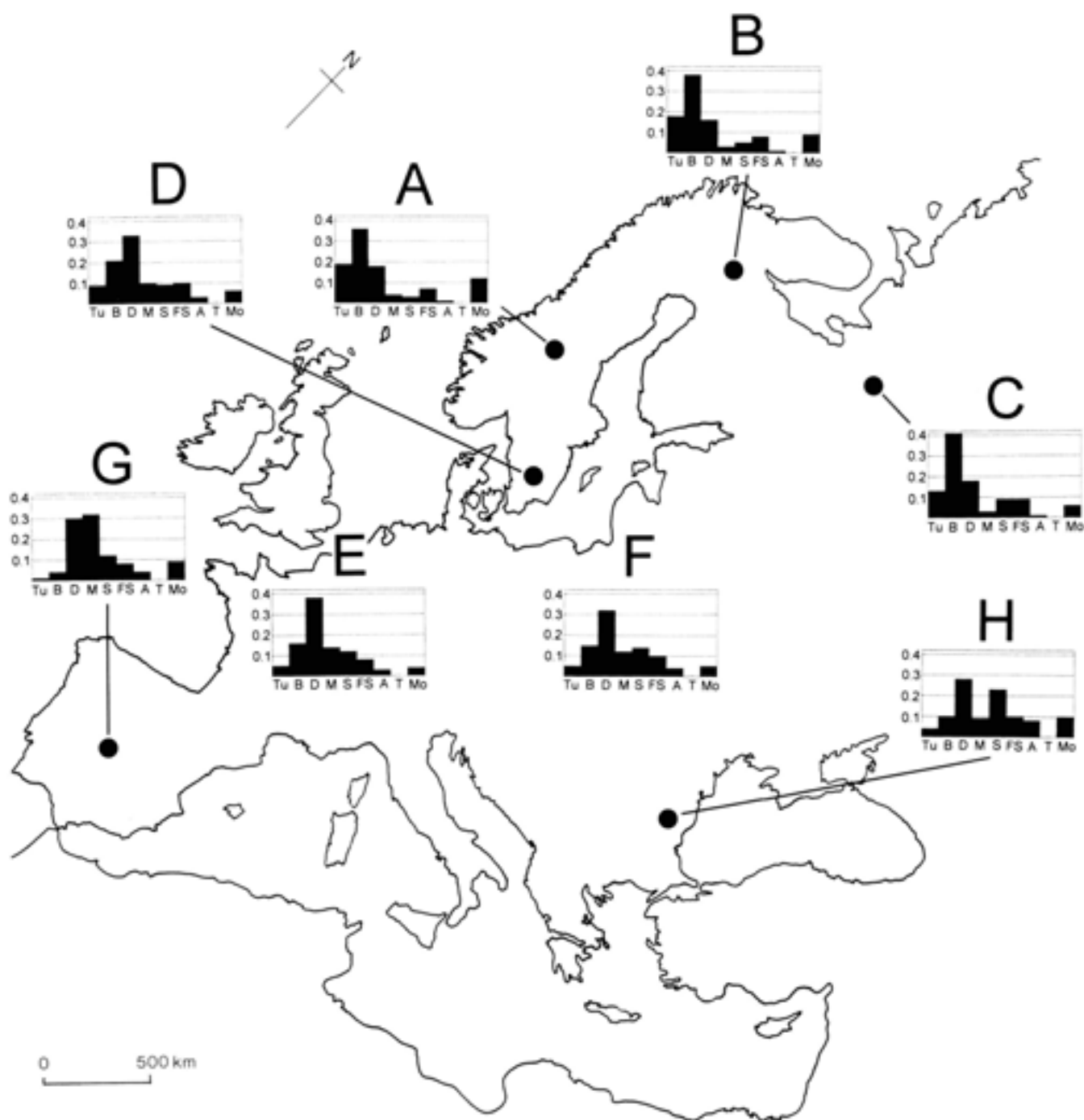


Fig 212 Taxonomic Habitat Index spectra for Recent European habitats. A–C) Boreal Forest Zone, D) Mixed Deciduous/Coniferous Forest, E–F) Deciduous Woodland, G) Mediterranean, and H) Forest/Steppe

uppermost part of the Unit (4b). This diagram shows that the proportion of terrestrial elements increases through the sequence, the lowermost part being dominated by fish bones, whilst the uppermost part is dominated by small mammals. Sixteen species of small mammals are known from Unit 4b (Table 93). Voles are the dominant group of small mammals, of which the most common species are the water vole (*Arvicola terrestris cantiana*) and the pine vole (*Microtus (Terricola) cf. subterraneus*). The majority of the small mammal species from the lagoonal beds are predominantly found in open grassland, although the woodmouse

(*Apodemus sylvaticus*) and certain of the large mammals (roe deer (*Capreolus capreolus*) and wild cat (*Felis silvestris*)) indicate woodland or dense vegetation close to the depositional site.

The taxonomic habitat index distribution of this part of the sequence indicates deciduous or mixed woodland conditions in a temperate climate. However, the fauna does not represent a period of peak interglacial conditions, as the taxonomic habitat index shows a higher proportion of boreal and tundra elements than faunas of the central and western European deciduous forest belt at the present day (Fig 212).

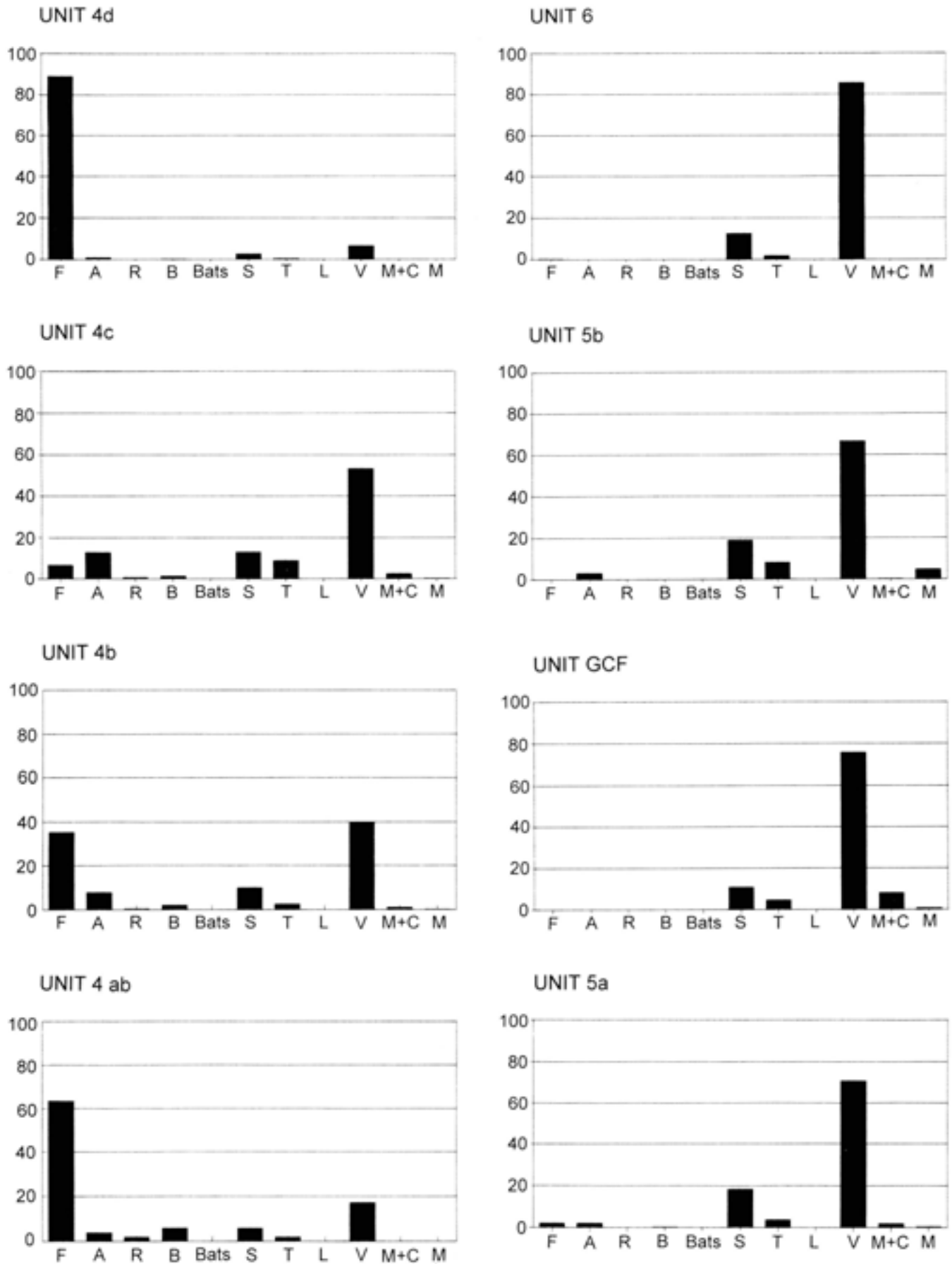


Fig 214 Percentage frequency histograms of major vertebrate groups in the Boxgrove sequence. The groups are fish (F), amphibians (A), reptiles (R), birds (B), bats, shrews (S), moles (T), lagomorphs (L), voles (V), murids and cricetids (M+C), and mustelids (M). The histograms are arranged in stratigraphic order with the oldest (Unit 4a/b) at bottom left and the youngest (Unit 6) at top right

Unit 4c: Slindon Soil Bed

This horizon has produced the richest and most diverse vertebrate fauna of all the Boxgrove units (Table 93 and Fig 214). Large mammals are abundant and dispersed across the site with no obvious indications of concentration. The taphonomic history of the large mammal remains is complex, with evidence for carnivore gnawing, sub-aerial weathering and post-depositional soil corrosion. Evidence for human modification of the bones is also present, although concentrated clusters of modified bones such as those found in the underlying unit are not apparent. The taphonomic analysis of the large mammal bones indicates that the fauna represents an attritional assemblage which accumulated on a landsurface and was buried within an active soil horizon. The scarcity of refitting bone fragments along with evidence for carnivore gnawing and trampling damage to the bones indicates that carcasses were dispersed by a range of natural agencies. Weathering observed on a small number of bones indicates exposure on the surface for a number of years prior to burial. The large mammal fauna from the Soil Bed therefore represents a palimpsest of both natural and human agents of accumulation and the fauna probably provides an accurate representation of the mammals living in the vicinity of the site.

Small mammal remains are also abundant in this horizon and, as with the large mammal bones, they are on the whole dispersed across the site, although dense clusters of small vertebrate bones have been recorded from the margin of the pond feature in Q1/B. Characteristic modification of the bones from these concentrations, including heavy digestive corrosion of the teeth, rounding of the broken bone fragments, and tooth puncture marks, indicate that the Q1/B accumulations resulted from a mammalian predator. The range of prey species, which includes fish, amphibians, reptiles, and birds, as well as a diverse range of small mammals, including semi-aquatic and arboreal rodents, strongly suggest European mink (*Mustela lutreola*) as the likely agent of accumulation. This species is a generalist predator which feeds on a wide range of small vertebrates, and therefore provides an accurate reflection of the range and abundance of the small vertebrates in the community. The dispersed remains from this unit are more difficult to interpret in terms of their taphonomic history, due to the mixing of bones derived from a number of sources.

The small mammal assemblage from the Slindon Soil Bed indicates an increase in vegetational diversity compared with the underlying Slindon Silts. The range of mammals shows that the vegetation in the vicinity of the site consisted of a mosaic of different types, including grazed grassland, scrub and woodland. The overwhelming dominant species, comprising not less than 34% of the rodents, is the pine vole (*Microtus (Terricola) cf. subterraneus*), which inhabits grassland

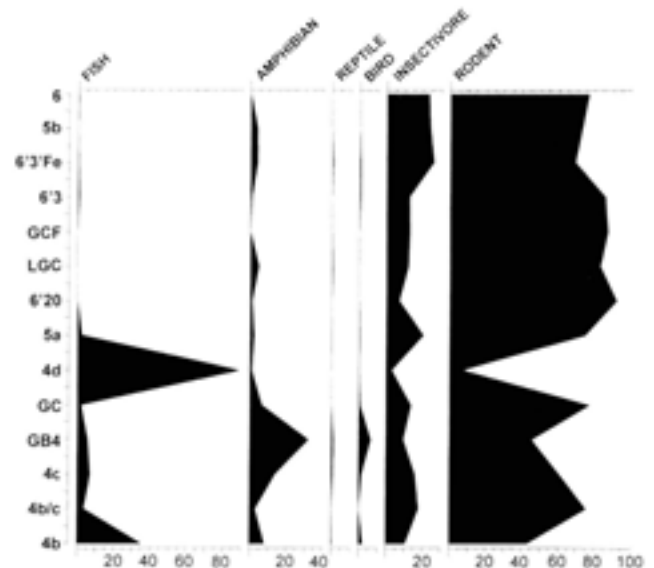


Fig 215 Histograms showing the relative abundance of fish, amphibians, reptiles, birds, insectivores, and rodents. The relative abundance of the faunal groups is calculated from the number of identifiable bone fragments listed in Table 95a



Fig 216 Area of sympatry for the Unit 4c small mammals and herpetofauna. The stippled zone shows the region where all 9 of the amphibian and reptile species are found at the present day, and the hatched zone shows where 17 out of 18 of the living small mammal species from Unit 4c occur together

and open forests today. The field and common voles (*M. agrestis* and *M. arvalis*) also indicate grassland cover and both species form a significant proportion of the small mammal assemblage. Also common is the water vole (*Arvicola t. cantiana*), a species which is closely associated with water-bodies and grasslands at the present day. Both the bank vole (*Clethrionomys glareolus*) and the wood mouse (*Apodemus sylvaticus*)

are well represented in the fauna. The co-occurrence of these two forms in British Pleistocene fossil assemblages is generally taken to be an indication of temperate woodland conditions (Currant 1989).

Woodland species are also common in the Unit 4c fauna. These include several arboreal species such as the squirrel (*Sciurus* sp), the semi-arboreal birch mouse (*Sicista* cf *S. betulina*) and hazel dormouse (*Muscardinus avellanarius*), the badger (*Meles* sp), roe deer (*Capreolus capreolus*), and fallow deer (*Dama dama*). The whiskered bat (*Myotis mystacinus*) and Bechstein's bat (*Myotis bechsteini*) are also woodland species which have a present day distribution which is closely associated with deciduous and mixed woodland habitats.

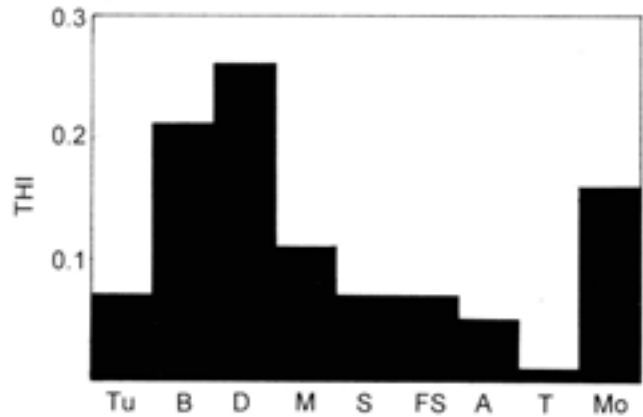
The association of a range of woodland species with those indicating open grassland conditions may appear to be contradictory; however, the majority of the woodland species venture into grassland or scrub to feed and this may account for their presence in an otherwise open grassland environment. Analysis of the soil micromorphology of Unit 4c (Macphail Chapter 2.6) provides evidence that the plain to the south of the cliff-line was open grassland and that trees and scrub did not colonise the area. The abundant grazing herbivore fauna living on the plain may provide an explanation for the lack of colonisation by woody vegetation.

Aquatic habitats are implied by the presence of semi-aquatic species such as the water shrew (*Neomys* sp), northern vole (*Microtus oeconomus*), and especially the European mink (*Mustela lutreola*). The freshwater ponding at Quarry 1/B (Unit 4d) may have provided a suitable habitat for these species.

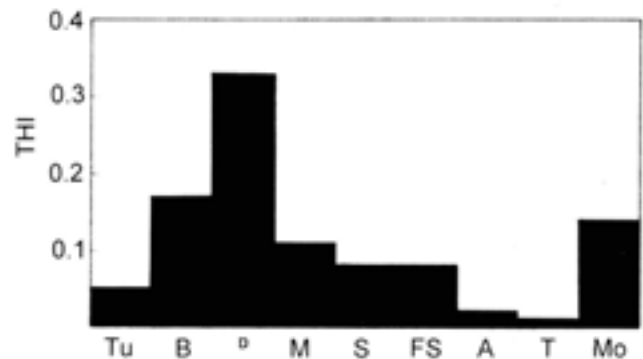
The analysis of the taxonomic habitat index for this unit (Fig 210), shows that the greatest contribution to the fauna is made by temperate deciduous elements; boreal species are also well represented and the contribution made by tundra elements is negligible. In Figure 210, the taxonomic index for the combined large and small mammal fauna is given. This shows a similar pattern to that derived from the small mammal fauna, although deciduous woodland elements are proportionately better represented in the combined sample. It can also be seen that the taxonomic habitat index for this unit is similar to that of Unit 4b, and indicates a deciduous or mixed woodland environment in a temperate climate.

The majority of the mammal species present in Unit 4c are currently found within a broad region of the deciduous and mixed forest zones of western Europe, and this strongly suggests that this type of vegetation existed in the vicinity of the site during the deposition of the Slindon Soil Bed. Comparing this fauna with the Recent habitats shown in Figure 212, it can be seen that the taxonomic habitat index for Unit 4c fauna bears the strongest similarities to that of the mixed coniferous/deciduous zone of southern Sweden. Indications of a cooler, perhaps more continental, climate than the present day are also provided by an analysis of the modern day distributions of the small

Boxgrove (Unit 4c)



Barnham



Beeches Pit

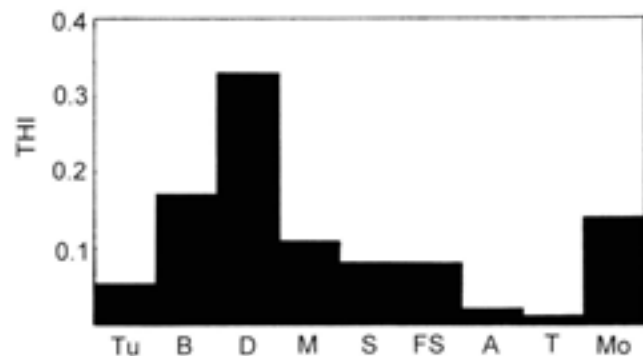


Fig 217 Taxonomic Habitat Index spectra of two British peak interglacial small mammal assemblages compared with the Taxonomic Habitat spectrum of Unit 4c from Boxgrove

mammals found in Unit 4c. In Figure 216, the area of maximum sympatry of the living small mammals from Unit 4c is found in the western Ukraine and eastern Poland. It is notable that this area is also included in

the zone of sympatry for all the amphibians and reptiles found in the Slindon Soil Bed. Although the environmental and climatic factors controlling the distributions of small mammals are still poorly known, the combined taxonomic habitat index and sympatry analysis suggest that the climate during the deposition of Unit 4c was possibly cooler and more continental than the present day. This conclusion is further supported by a comparison of the taxonomic habitat index for Unit 4c with those of British interglacial sites with evidence for peak interglacial conditions and temperatures warmer than the present day (Fig 217). The taxonomic habitat index distribution for Barnham and Beeches Pit (Fig 217) both conform to the pattern found in western European temperate broad-leaved woodland faunas, and differ from that of Unit 4c in having a much lower proportion of boreal and tundra elements.

Unit 4d: Spring deposits

The faunal assemblage from this horizon is dominated by fish remains (Figs 214, 215) which make up over 80% of the vertebrate assemblage. The fish remains, which consist almost exclusively of the three spined-stickleback, are interpreted as a natural death assemblage (Parfitt and Irving Chapter 3.4) which accumulated in a calcium carbonate-rich pool at the base of the cliff. The presence of fish in this deposit suggests that either permanent or intermittent connections existed between the pond and other bodies of water, and this is supported by the gully feature in Q1/A which may represent a temporary drainage channel connected to the pond. The long-axis orientation of large mammal bones from this deposit show a clear north-south preferred orientation which indicates flowing water, although associated bones from a disarticulated carcass suggest that this was slow moving. Water birds are common and well preserved in this unit (Harrison and Stewart Chapter 3.6), supporting the interpretation of this deposit as a pond.

Eleven species of small mammal are recorded from this unit (Table 93), and the large mammal fauna, although represented by a small number of bones only, is diverse and includes fallow deer (*Dama dama*), an indeterminate cervid, extinct rhinoceros (*Stephanorhinus hundsheimensis*), lion (*Panthera leo*), and the sole remains of hominid so far recovered from the site. This unit also produced the remains of beaver (*Castor* or *Trogotherium*). The small mammal fauna is relatively sparse and dominated by remains of the water-vole (*Arvicola t. cantiana*). The occurrence of this species with the beaver adds further support to the sedimentological interpretation of this deposit.

The analysis of the taxonomic habitat index distribution of the 4d small mammal fauna (Fig 210) shows that it is identical to that of the penecontemporaneous deposits of Unit 4c.

Unit 5a: Organic Bed

The taxonomic habitat index distribution for this unit is very similar to that from Unit 4c, although the proportions of boreal and tundra elements are slightly higher (Fig 210). This may indicate some cooling in climate, although the fauna is still temperate in character. The Organic Bed has produced the first record of the narrow-skulled vole (*Microtus gregalis*) in the stratigraphic succession, and this species is generally associated with open conditions and cool climates during the latter part of the early Middle Pleistocene. The presence of fallow deer (*Dama dama*), roe deer (*Capreolus capreolus*), common long-eared bat (*Plecotus auritus*), and woodland rodents such as the beaver (*Castor fiber*), the bank vole (*Clethrionomys glareolus*), hazel dormouse (*Muscardinus avellanarius*), and the garden dormouse (*Eliomys quercinus*) all indicate woodland or dense scrub vegetation during the deposition of the Organic Bed. The rodent fauna is dominated by the water vole (*Arvicola t. cantiana*), with lesser numbers of common and field voles (*Microtus arvalis* and *M. agrestis*) and the highest representation of bank vole (*Clethrionomys glareolus*) in the sequence.

The sedimentology and micromorphology of this unit (Macphail Chapter 2.6) suggest deposition in a fen-carr environment with braided seasonal streams. Evidence for flowing water is indicated by a strong preferred orientation in the long axis of the bones from this unit. The main axis of orientation is east-west implying water flow in this direction. Large mammal bones are scarce in the Organic Bed, whereas small mammals are common although dispersed throughout the unit. Evidence for human modification of the bones consists of a single cutmarked bone, which was recovered from the interface of this unit with the underlying palaeosol unit, and therefore probably derives from Unit 4c. The lack of artefacts from this horizon and the absence of definitely stratified humanly modified bones implies that the area was not occupied by hominids during this phase.

The Eartham Formation

Eartham Lower Gravel Member, Units 7-8: Angular Chalk Beds, calcareous silty clays, and Lower Chalk Pellet Beds

The sediments of the Eartham Lower Gravel Member (Tables 9a, 9b), exposed in the northern part of Quarry 2, is composed of a massive sequence of chalky gravels and calcareous silty clays which thin rapidly from the cliff. This sequence of deposits has a temperate climatic history, as indicated by the palaeoenvironmental interpretation of the mammal faunas (Table 9b). The stratigraphic succession is briefly described in the following section, with a discussion of the main palaeoecological conclusions derived from an analysis of the taxonomic habitat index.

Table 95a Summary of the number of identifiable fragments and concentration (NISP/kg) for the major vertebrate groups from the Boxgrove sequence, as calculated from the samples taken from each unit. Units are arranged in approximate stratigraphic order with the oldest at the top of the table

unit	sample	quarry	locality	Kg	fish		amphibian		reptile		bird		invertebrate		rodent		small mammal		total NISP
					NISP	NISP/Kg	NISP	NISP/Kg	NISP	NISP/Kg	NISP	NISP/Kg	NISP	NISP/Kg	NISP	NISP/Kg	NISP	NISP/Kg	
3		2		125.50	1	<0.01	-	-	-	-	1	<0.01	-	-	1	<0.01	1	<0.01	3
4		2	GTP00	131.00	8	0.06	-	-	-	-	-	-	-	-	1	<0.01	1	<0.01	9
4a/4b		2		238.00	33	0.15	2	<0.01	1	<0.01	3	0.01	3	0.01	9	0.04	12	0.06	51
4b(2L)		2		69.00	-	-	-	-	-	-	-	-	2	0.03	-	-	2	0.03	2
4b		1		1132.50	65	0.06	47	0.04	2	<0.01	9	<0.01	69	0.06	213	0.19	282	0.25	405
4b		2		1367.50	184	0.13	10	0.01	1	<0.01	6	<0.01	6	<0.01	91	0.07	97	0.07	298
4b total		1+2		2500.00	249	0.10	57	0.02	3	<0.01	15	<0.01	75	0.03	304	0.12	379	0.15	703
4	87-239	2	GTP20	52.00	-	-	-	-	-	-	-	-	1	0.02	24	0.46	25	0.48	25
4b/4c		1		147.00	7	0.05	6	0.04	-	-	-	-	36	0.24	152	1.05	188	1.28	201
4c		1		1038.00	34	0.03	38	0.04	-	-	6	<0.01	108	0.10	608	0.59	716	0.69	794
4c		2		4382.75	497	0.11	992	0.23	62	0.01	106	0.02	1074	0.25	3914	0.89	4908	1.14	6645
4c total		1+2		5420.75	531	0.10	1030	0.19	62	0.01	112	0.02	1182	0.22	4532	0.83	5704	1.05	7439
GB4	87-123	2	GTP5	34.00	12	0.35	69	2.03	2	0.06	14	0.41	20	0.59	97	2.85	117	3.44	214
GC	87-175	2	GTP5	25.00	3	0.12	10	0.40	-	-	1	0.04	21	0.84	119	4.76	140	5.60	154
LS	86-15	1	GTP15	2.00	-	-	1	0.50	-	-	-	-	-	-	1	0.50	1	0.50	2
4d		1		407.50	1665	2.61	11	0.03	-	-	2	<0.01	35	0.09	82	0.20	117	0.29	1195
5a		1		194.25	61	0.31	8	0.04	-	-	4	0.02	326	1.68	882	4.54	1208	6.22	1281
5a		2		1061.00	23	0.02	72	0.07	5	<0.01	8	<0.01	441	0.42	1936	1.82	2377	2.24	2485
5a total		1+2		1255.25	84	0.07	80	0.06	5	<0.01	12	<0.01	767	0.61	2818	2.24	3585	2.86	3766
LS>5a	86-73	2	GTP20	6.00	2	0.33	1	0.17	-	-	1	0.17	-	-	23	3.83	23	3.83	27
6	86-54	2	GTP20	99.00	-	-	3	0.03	-	-	-	-	22	0.22	295	2.98	317	3.20	329
	90-1129	2	GTP25	5.00	1	0.20	-	-	-	-	-	-	2	0.40	14	2.80	16	3.20	17
LCG	87-116	2	Q2/B	466.25	-	-	12	0.03	1	<0.01	-	-	32	0.07	221	0.47	253	0.54	266
GCF	86-71	2	GTP20	44.00	-	-	-	-	-	-	-	-	18	0.41	124	2.82	142	3.23	142
6		2	GTP5	472.50	2	<0.01	2	<0.01	-	-	2	<0.01	40	0.08	278	0.59	318	0.67	324
6fe		2	GTP5	115.50	1	<0.01	15	0.11	2	0.02	2	0.02	92	0.80	245	2.12	337	2.92	355
SG	87-117	2	GTP5	33.00	-	-	-	-	-	-	-	-	-	-	4	0.12	4	0.12	4
5b		2		562.00	-	-	14	0.02	-	-	-	-	96	0.17	293	0.52	389	0.69	403
6		1		579.00	1	<0.01	-	-	-	-	-	-	36	0.14	252	0.47	328	0.61	329
8		2	SEP 2	106.00	-	-	-	-	-	-	-	-	-	-	4	0.04	4	0.04	4
5c*	90-1130	2	GTP17	8.00	-	-	3	0.38	-	-	-	-	6	0.75	51	6.38	57	7.13	60
BCG*	86-50	2	GTP20	32.00	-	-	-	-	-	-	-	-	-	-	-	-	-	-	-
MB*		1	GTP21	186.00	-	-	-	-	-	-	-	-	-	-	-	-	-	-	-
faunal group totals				13061.25	2000		1314		76		165		2526		9934		12460		16015

* Stratigraphic position of unit uncertain

Table 95b Summary of the taphonomy of the Boxgrove mammal faunas

* SM = small mammal, LM = large mammal

unit	sediment and depositional environment	mammal size category(*)	faunal quantity	distribution	bone articulation/association	spatial arrangement		weathering	post-depositional modification
						bone orientation	hominid alteration		
8	colluvial and cryoclastic chalk gravel	SM	scarce	dispersed	-	-	-	-	-
		LM	scarce	dispersed	-	-	-	occasional	-
6	water-lain clayey silt	SM	scarce	concentrated and dispersed	-	-	-	-	-
		LM	scarce	dispersed	isolated/dispersed	-	none	rare	rootlet corrosion
5a	fen/alder carr peat	SM	abundant	dispersed	-	-	-	-	-
		LM	scarce	dispersed	associated and dispersed	preferred (E-W)	rare	rare	soil corrosion
4c	palaeosol	SM	abundant	dispersed and concentrated	-	-	-	-	-
		LM	abundant	dispersed	associated and dispersed	random	common	rare	soil corrosion and rootlet marks
4b	lagoonal/intertidal clayey silt	SM	scarce	dispersed	-	-	-	-	-
		LM	scarce	concentrated	disarticulated but associated	preferred (N-S)	abundant	rare	rootlet marks

The lowermost subunit in this sequence is a relatively thin pale silty clay with abundant molluscs, which extends from the base of the cliff to beyond the southernmost extent of area Q2/B (Fig 4). This unit was assigned a number of informal unit designations (6'20, LGC, GCF, 1129) for each of the excavation areas in which it was exposed. The sedimentological and faunal similarities between the deposits in the different exposures, as well as the stratigraphic position of the subunits, indicate that they represent the same deposit. In the analysis of the taxonomic habitat index, the faunas of this unit from the separate excavation areas have been combined to increase the sample size and the number of taxa. This deposit is relatively rich in small mammal remains (Tables 93 and 95a); large mammals are rare and the only species recovered is the roe deer (*Capreolus capreolus*). The taxonomic habitat distribution for the basal brickearth is similar to that of Unit 5a and it is probable that the climatic and vegetational conditions were similar. The most common small mammal species are the common/field vole, water vole, and pine vole. Bank voles and woodmice are also relatively common. This unit has also produced one of the few records of the garden dormouse from the site, as well as the hazel dormouse and birch mouse, which indicate woodland or dense scrub vegetation.

The deposits overlying the basal shelly brickearth consist of a stratified series of angular chalky gravels representing cliff falls, interspersed with layers of rounded chalk pellet gravels (the Lower Chalky Pellet

Gravels) which indicate episodes of colluviation. This unit has produced a sparse large mammal fauna of red deer, bison and possibly horse. Artefactual material is common in this unit and a small number of indeterminate large mammal bone fragments exhibit evidence of human modification. Despite extensive sampling of these deposits, no identifiable small mammal remains have been recovered.

Eartham Upper Gravel Member, Calcareous silty clay

The chalky gravels thin rapidly away from the cliff and in GTP 3 the sediments of the Eartham Lower Gravel Member are replaced by a thin silty clay brickearth resting on Unit 5a. This unit (6'3) (Tables 9a, 9b), is distinguished from the basal silty clays immediately to the south of the cliff by its sedimentological characteristics and also by the rarity of molluscs contained in this horizon. The taxonomic habitat index distribution for this unit (Fig 210) strongly indicates cold conditions. The small mammal fauna is dominated by boreal forest elements with a slightly lower representation of deciduous woodland elements and a relatively high proportion of tundra elements. It may be significant that the boreal northern vole (*Microtus oeconomus*) is relatively common, although woodland species such as the bank vole and wood mouse are also present in some numbers.

Immediately overlying this layer is a thin iron-stained clay (6'3Fe) which is similar in its field characteristics to the Organic Bed (Unit 5a). The small

mammal fauna from this level suggests a return to warmer, more wooded, conditions (Fig 210), and the taxonomic habitat index distribution, which is similar to that from the Slindon Soil Bed, is dominated by deciduous woodland elements and indicates a deciduous woodland or mixed forest habitat and a temperate climate. The small mammal fauna is dominated by the water vole, pine vole, field/common vole and bank vole, and the semi-arboreal hazel dormouse is also found in this horizon. Species indicating cold or boreal habitat such as the northern vole and the narrow-skulled vole are absent.

Unit 5b: Calcareous Marl

This unit exists as discrete patches of often shell-rich clays underlying Unit 6 in parts of Quarry 2. Molluscan and sedimentological evidence suggests these deposits formed in small pools in a predominantly open environment. A limited small mammal fauna consisting of twelve species has been recovered from this unit, the only large mammal being the wolf (*Canis lupus*). The Norway lemming (*Lemmus lemmus*) is recorded for the first time in the Boxgrove sequence in this unit, and the taxonomic habitat index distribution indicates a return to cold and open conditions (Fig 210).

Unit 6: Brickearth Beds

Large mammals are rare in Unit 6, although the presence of a caprine is noteworthy as this group is only found in cold stages in north-western Europe during the Middle and Late Pleistocene. Although the mammal fauna indicates predominantly open grassland conditions, the European beaver suggests the presence of some woodland cover, perhaps restricted to the margins of water bodies. Areas of dense scrub or woodland are also indicated by the bank vole which occurs in low numbers in the Brickearth Beds. Of particular interest

is the presence of the grey-sided vole (*Clethrionomys rufocanus*), which is a good indicator of a boreal environment, since it occurs today in the coniferous and tundra zone of Scandinavia and north-western Russia. The Norway lemming (*Lemmus lemmus*) is also present in Unit 6, and boreal/tundra/steppe species such as the narrow-skulled vole (*Microtus gregalis*) and northern vole form an important part of the microtine rodent fauna. Soricids and mice are uncommon, which probably reflects the cold climate and open grassland conditions during the deposition of this unit.

The taxonomic habitat index distribution for this part of the sequence indicates cold conditions and continues the cooling trend observed at the base of the Brickearth Beds in the calcareous marl (Unit 5b). Figure 210 shows that the taxonomic habitat index distribution is dominated by boreal/tundra elements with a relatively low contribution from deciduous woodland species.

Summary

The mammalian faunas from Boxgrove provide important information on climate and environment during the deposition of the sequence. The stratigraphic succession of faunas from the upper part of the Slindon Silt and the Eartham Gravel Members provide evidence for a sequence of climatic fluctuations (Fig 211), rather than a simple cooling trend marking the end of an interglacial period.

Significant faunal changes can be detected through the sequence which provide evidence for temperate woodland conditions during the deposition of the Slindon Silt Member and Eartham Lower Gravel Member, followed by a significant climatic cooling within the basal part of the Eartham Upper Gravel Member. This phase of cold open conditions is followed by a return to fully temperate conditions in Unit 6'3'Fe, and thence to cold and subsequently periglacial conditions during the deposition of the Brickearth Beds of the Eartham Upper Gravel Member.

5 Methods of age estimation

5.1 Introduction

Dating the sediments at Boxgrove and their associated archaeology has involved undertaking many different methods of age estimation. Some of the methods used produce relative chronologies which are then cross-correlated with other sequences, whilst other, radiometric, methods provide dates in terms of years before present.

Some of the methods are obviously, in their present state, inapplicable to sediments of this age; for example Uranium-series dating was attempted by A M Rae, but the age of the site was beyond the limit of the method (see also Parks and Rendell Chapter 5.3). The ongoing Boxgrove Projects continue to employ the amino acid geochronology technique, on both molluscs and foraminifera, and new research is being undertaken on dating methods using stable isotopes.

The age of the Boxgrove sediments and their associated archaeological, palaeontological, and palaeo-environmental components, along with the temporal relationship of Boxgrove to other Middle Pleistocene sites is also discussed in detail by Roberts in Chapters 1.2, 2.1 and 6.1. An overview of age estimation techniques relevant to this period is provided by Aitken (1995).

5.2 Uranium series dating

A M Rae

Four bones from Boxgrove were analysed (Table 96), three from Unit 4c and one from Unit 4b. Samples were taken from the bone surface and across the total bone.

Unfortunately, the results were not very favourable but two main conclusions can be drawn from the data.

Samples that were taken from the bone surfaces show significantly lower uranium contents than those from the total cross-sections. Previous research (Rae and Ivanovich 1986) indicates that this implies post-depositional leaching of uranium, and hence undatable samples.

All the $^{230}\text{Th}/^{234}\text{U}$ activity ratios are greater than one, the theoretical maximum achieved by samples unaffected by post-depositional alteration. Hence, this confirms the impression of leaching given by the uranium concentrations. Two of the total samples, Q1/A Unit 4c and Q1/A Unit 4b, give total bone $^{230}\text{Th}/^{234}\text{U}$ activity ratios with errors that overlap one. If it is assumed that these represent unaltered ratios, this means age estimates of greater than 350kyr bp, which correlates to either a stage 11 (Gard Chapter 5.8, Bowen and Sykes Chapter 5.6) or stage 13 (Roberts and Parfitt Chapter 5.9). Additionally, a test for collagen was undertaken on the bone from Q1/A Unit 4c. Most of the samples are very 'chalky' and soft textured, but this bone exhibited a core in a different state of preservation from the others by nature of its colour, dark brown, and its greater hardness. Comparison between the outer layer and the core showed that the former contained no collagen (although there may be free amino acids present), whereas the latter showed evidence of trace collagen. It might therefore be possible to undertake amino acid analyses of this and other bones in a similar state of preservation.

Table 96 Activity ratios from Boxgrove bone samples

<i>samples</i>	<i>[U] ppm</i>	$^{234}\text{Th}/^{234}\text{U}$	<i>activity ratios</i> $^{230}\text{Th}/^{234}\text{U}$	$^{230}\text{Th}/^{232}\text{Th}$
Q1/A Unit 4c				
bone surface	12.986 ±1.739	1.010 ±0.152	1.293 ±0.195	6.084 ±0.736
total bone	18.442 ±0.729	1.358 ±0.027	1.046 ±0.072	396
Q2 SEP 1/4c				
bone surface	6.828 ±0.618	1.301 ±0.124	1.244 ±0.132	2.7 ±0.252
total bone	14.861 ±0.879	1.438 ±0.055	1.436 ±0.105	19.868 ±1.844
Q2 GTP 17/4c				
bone surface	4.881 ±0.738	1.283 ±0.126	2.544 ±0.236	4.315
total bone	10.582 ±0.738	1.337 ±0.037	1.388 ±0.103	199
Q1/A Unit 4b				
bone surface	6.514 ±0.367	1.309 ±0.086	1.509 ±0.096	4.186
total bone	18.309 ±0.455	1.367 ±0.025	1.063 ±0.034	56

[U] ppm is uranium concentration of the samples, based on the ^{238}U value. Age is calculated from the activity ratios

5.3 Luminescence dating of brickearth

D A Parks and H M Rendell

Thermoluminescence (TL) techniques were originally developed in the 1960s for dating pottery and burnt stone (Aitken 1985). Following the pioneering work of Wintle and Huntley (1979; 1980), the use of TL techniques was extended to the dating of sediments from a wide variety of depositional environments. The key factor is the 'zeroing event'. In pottery, TL signal levels are reduced to zero during the firing of the material. In the case of sediments, signals are reduced to a measurable 'residual' TL level by exposure to light. Therefore, in the TL dating of sediments, the event being dated is the last exposure of the sediment grains to light.

The discovery by Huntley *et al* (1985) that luminescence signals could be stimulated by light in addition to heat, has resulted in the development of optically stimulated luminescence (OSL) techniques. The particular advantages of the OSL methods are that the signals are effectively zeroed by light exposure, and the rate of signal reduction is such that only short light exposures are required to achieve zeroing. In this study infra-red stimulated luminescence (IRSL) is used to date silt beds from within Q1 Unit 11 (Table 9a, Fig 33) (Roberts Chapter 2.1, Macphail Chapter 2.6).

In the case of both luminescence methods, two values are required in order to obtain an age estimate; first, the radiation dose absorbed since last exposure to light of the sediment grains and second, the annual radiation dose. The annual radiation dose is produced from within the sediment itself, by the decay of naturally occurring radionuclides from uranium and thorium decay series, and from ⁴⁰K. The annual radiation dose also includes an external dose from cosmic rays. At Boxgrove, dosimetry measurements were made on site using a portable gamma spectrometer. The radiation dose absorbed since burial of the sediment grains (the Equivalent Dose) is a function of the natural TL or OSL signal and the sensitivity to dose. The age equation is simply:

$$\text{TL age} = \frac{\text{Equivalent Dose}}{\text{Annual Radiation Dose}}$$

TL analysis was undertaken on the Brickearth Beds (Unit 6) samples from sections GTP 9, GTP 11, GTP 13 and GTP 5 during 1987–8 (Parks and Rendell 1992). Additional OSL measurements were made on samples from Q1 Unit 11 in 1993. Blocks of brickearth were cut from clean sections, wrapped in aluminium foil and sealed in plastic bags. All subsequent sample preparation and analysis was carried out in subdued red light in the laboratory.

Sample preparation and analysis

Material was prepared for luminescence measurements by acid pretreatment, to remove any carbonates, and then by separation of the 2–10 micron size fraction by sedimentation. Aliquots of this size fraction, in acetone suspension, were pipetted on to clean 10mm diameter aluminium discs and allowed to evaporate to dryness at room temperature.

Generally 30–40 discs were prepared per sample. For TL measurements, sample discs were heated in an argon atmosphere at a rate of 300°C min⁻¹ and were monitored through Schott UG11 and Chance-Pilkington HA3 filters using an EMI 9635Q photomultiplier tube. OSL measurements were made while holding the sample discs at 50°C and using infra-red stimulation at 880nm and emissions were measured via a Hoya U-340 filter on an automated Riso TL/OSL reader. Laboratory radiation doses were given using ²⁴¹Am alpha and ⁹⁰Sr/⁹⁰Y beta sources.

The programme of laboratory measurements designed to assess the value of the Equivalent Dose (ED) essentially involves two main approaches (see Aitken 1985) and both the Additive Dose and the Regeneration methods were used for the Boxgrove samples. Problems can arise with the Additive Dose approach once the growth of luminescence signal with dose becomes non-linear, as saturation is approached. Extrapolation of the laboratory growth curve may give an ED which is too large and which therefore overestimates the age of the material. The Regeneration technique involves the simulation of the sample history in the laboratory, by exposing some discs to light and then adding laboratory radiation doses until the level of the natural TL signal is matched exactly. The Regeneration method is based on the assumption that the sample's sensitivity to dose (ie TL/unit radiation dose) is not altered by laboratory light exposure. Such an assumption may be false (see Rendell and Townsend 1988), and there is now considerable evidence that use of the Regeneration technique results in the underestimation of the age of samples (Berger 1988).

The results for TL and OSL dating of samples from Boxgrove are summarised in Table 97. Most of the age estimates are for the Regeneration method and should therefore be regarded as minimum age estimates. It was possible to determine Additive Dose ED estimates for the IRSL signals from the Q1 Unit 11 samples. In the case of samples from section GTP 13, the scatter on the TL Additive Dose measurements was sufficiently small for an estimate of ED to be made with some confidence.

Discussion of results

The age estimates obtained by the Regeneration method are probably best regarded as minimum age estimates. The TL results from section GTP 11 give an age estimate of 229kyr, which is distinctly older than

Table 97 Luminescence age estimates for Boxgrove silt samples. The first four samples are from the Brickearth Beds (Table 9a)

sample	annual dose	TL ED estimates		TL age estimates	
		additive	regenerative	additive	regenerative
Q1 GTP 9	1.97±0.15	–	344.5±35.0	–	175.3±19.5
Q2 GTP 11	1.94±0.16	–	444.0±45.0	–	229.4±27.7
Q2 GTP 13	1.98±0.17	348.5±35.0	365.0±30.0	175.8±19.3	184.3±20.2
Q2 GTP 5	1.95±0.16	–	347.5±29.0	–	177.9±19.9

sample	annual dose	IRSL ED estimates		IRSL age estimates	
		additive	regenerative	additive	regenerative
Q1 Unit 11 U Silt Bed	2.08±0.20	398.0±46.2	316.4±21.9	191.3±22.2	152.1±10.5
Q1 Unit 11 M Silt Bed	2.08±0.20	665.35±195.1	–	319.9±93.8	–

for the other sections sampled for TL. The mean value for the 11 sub-samples from sections GTP 9, GTP 13, and GTP 5 is 180.7±17.8kyr which indicates a surprising level of consistency. The IRSL Additive dose result from the Upper Silt Bed in Q1 Unit 11 of 191.3±22.2kyr is also consistent with the TL data. The IRSL result for the Middle Silt Bed from the same section appears to indicate a much greater antiquity for this sample, but it should be noted that the errors are extremely large (ie +93.8kyr), and with the OSL values approaching saturation, the age may be overestimated. The reasonably good level of agreement between the results for the different sections for both methods may simply be a function of the fact that, for this material, we are approaching the limits of this dating technique. Nevertheless, the luminescence dates do provide a series of minimum age estimates for the brickearths.

5.4 Optically stimulated luminescence

E J Rhodes

Four OSL samples were collected from the Slindon Sands and Slindon Silts in Quarry 2, at areas GTP 10, GTP 13, and GTP 17 and from the Brickearth Bed, near Q2/A (Fig 4). The lower sample positions, from the Slindon Sands in GTP 13, had very low natural environmental radiation levels, which suggested that the OSL signals from these samples might not be in saturation. The shallow marine depositional environment is considered suitable from the angle of providing the grains with sufficient daylight exposure prior to burial, and preliminary results of analysis are presented here.

The 125–180µm quartz grains were separated from the lower two sand samples (lab refs 290 and 291) using standard luminescence dating techniques and preliminary OSL dating runs were made for these samples. The relative antiquity of the site, expected from independent chronological information (biostratigraphy) (Roberts and Parfitt Chapter 5.9), suggests that the most likely limitation to successful luminescence dating would be luminescence signal saturation. However, the signals were observed to be not saturated,

though were associated with rather a high degree of scatter, leading to increased uncertainties in the age estimates. For the lowest sample, the preliminary date measured 356±178kyr. On close examination, the nature of the scatter observed between the different aliquots of this sample during the construction of the growth curve from which this preliminary age estimate was derived, did not appear to be randomly scattered around a single saturating exponential growth function.

In order to increase the precision of the OSL measurements a new procedure, which is still in the development stage, was employed. This consisted of grinding the separated 125–180µm quartz grains of approximately 1–10µm onto aluminium discs using acetone. This was performed in order to even out the distribution of sample between aliquots and to attempt to reduce scatter due to variations in OSL characteristics between individual grains. The sample discs were then used in the usual manner to construct a growth curve. This procedure was successful in reducing the degree of scatter, and as a result of this increased precision it was possible to detect a strong deviation from a single saturating exponential function in the form of growth, as had been tentatively observed for the uncrushed sample. Applying a single saturating exponential function to these data provides an age estimate of 630±125kyr. However, the complex form of growth indicates that this is not an appropriate step.

The observation that significant signal growth is observed with added laboratory dose, means that there is the potential for deriving age estimates but, as noted earlier, a complex form of growth curve for sample 290 was observed, rendering that dataset unsuitable for deriving an age estimate. Recently, several samples from other sites have been measured using a similar procedure, which involves a step known as natural normalisation. Close examination of these data, and of the original Boxgrove data, leads to the conclusion that the observed complex growth behaviour for sample 290 is a function of this natural normalisation procedure, and is not a fundamental characteristic of the quartz. This is demonstrated by plotting the growth curve from the unnormalised data for sample 290. This growth curve appears to follow the expected single saturating

Table 98 Dose rate data and equivalent dose (from un-normalised total integral equal weights data, sample 290) used to calculate age estimate

external attenuation factor			results		
	Alpha	Beta	Age [a]	559,850	±326,588
U	0.001±0.001	0.829±0.19	Σ Dose rate	[μGy/a]	475±13
Th	0.004±0.004	0.751±0.24		Internal	External
K		0.934±0.012	α	0±0	0±0
			β	0±0	294±9
			γ+cos		181±6

exponential form of OSL signal growth. From the data treated in the above manner, it is now possible to derive, tentatively, an age estimate for this sample. The very preliminary date derived in this manner is 560 ± 330 kyr. The figures used to obtain this age estimate are contained in Table 98. This age estimate is associated with a very large degree of uncertainty at present. However, no deviation from saturating exponential growth behaviour is observed and this uncertainty is derived purely from the low precision at each dose point. This scatter is characteristic of unnormalised data, and this statistical effect may be overcome simply by repeated measurement.

With further laboratory luminescence measurement, and the application of several independent techniques to assess the sample dose rate (thick source alpha counting, INAA, Ge high resolution gamma spectroscopy, flame photometry etc), quartz and possibly feldspar OSL measurements may be derived for the Slindon Sands at Boxgrove.

5.5 Electron spin resonance: coupled ESR-U series dating

R Grün

Two tooth samples (519 rhinoceros and 520 deer) were provided by M B Roberts from the palaeosol Unit 4c. Both samples were investigated by electron spin resonance ESR following a routine procedure as outlined by Grün *et al* (1987) and Grün (1989a; 1989b). The samples were irradiated with the γ -source of the Department of Physical Chemistry in Köln. The external γ -dose rate was measured in the field with a portable, calibrated gamma-spectrometer; the external beta-radiation was determined by beta-counting. Uranium-concentrations were measured by delayed neutron activation analysis.

In order to overcome the uncertainty in ESR-age calculation which is introduced by the history of U-uptake, dentine from sample 519 was measured by U-series analysis (samples 2228 and 2229, A Mangini, Heidelberg). Due to the small sample size and the low U-concentration it was not possible to obtain reliable U-series results on the enamel (see Table 99, sample KU 930; R Hausmann, Köln). The lowest U-series values (2229) were then used for modelling the

U-accumulation after Grün *et al* (1988). This was done to achieve the highest possible age-values. Since sample 520 was too small for U-series dating, the values from sample 519 were also used to calculate the open system data for sample 520.

The analytical data of U-series analysis are given in Table 99 and of ESR in Tables 100–101. The external gamma dose rate was measured with a portable gamma-spectrometer and the external beta dose rate by beta counting. The U-concentrations were measured by neutron activation analysis. The ADs were calculated with the computer program FITT (Grün and MacDonald 1989) and the ages were calculated following Grün *et al* (1988).

Discussion of results

From the U-series data it appears valid to use the dentine values for the open system calculations (the mean isotopic ratios of the enamel are close to the dentine values). The lower value was used in order to calculate the maximum ages. However, when the ratios from sample 2228 were used for open system calculations, the mean values are only about 10% smaller (the errors are also about 10% smaller). All values suggest that the uranium was accumulated shortly after deposition of the tooth.

Table 99 U-series analyses of sample 519

lab no	component	$^{234}\text{U}/^{238}\text{U}$	$^{230}\text{Th}/^{238}\text{U}$	$^{230}\text{Th}/^{232}\text{Th}$	age kyr
2228	dentine	1.28±0.03	0.858±0.001	>1000	186 +14/-12
2229	dentine	1.28±0.03	0.80±0.001	>1000	160 +10/-8
KU929	enamel	1.052±0.196	0.968±0.17	>100	>169

Table 100 ESR analysis of samples 519 and 520

lab no	AD [Gy]	U enamel [ppm]	U dentine [ppm]	thickness [μm]	ext β [μGy/a]	ext γ [μGy/a]
519a	453.2±139.7	0.4	33.0	1300	252	888
519b	448.9±69.7	0.2	37.4	1300	252	888
519c	441.1±57.5	0.3	25.3	1500	222	888
519d	420.8±52.2	0.3	36.7	1600	208	888
519e	392.0±77.7	0.3	32.8	1600	208	888
520a	365.0±191.1	0.4	18.4	700	312	693
520b	369.2±39.6	0.3	18.4	850	362	693

Table 101 ESR age estimates of samples 519 and 520

lab no	EU	LU	NU	ρ	US-ESR
519a (1)	220,000	288,000	397,000	0.68	247,000 +93,000 -89,000
519a (2)	-	-	-	0.88	229,000 +88,000 -44,000
519b	217,000	284,000	393,000	0.70	241,000 46,000 -45,000
519c	248,000	310,000	397,000	0.58	281,000 +43,000 -41,000
519d	217,000	281,000	384,000	0.71	240,000 +36,000 -36,000
519e	210,000	269,000	358,000	0.74	231,000 +55,000 -54,000
520a	195,000	241,000	363,000	0.72	237,000+151,000 -79,000
520b	192,000	236,000	350,000	0.73	205,000 +27,000 -27,000

The mean age-data all lie around the beginning of stage 7 (190–244kyr; Martinson *et al* 1987). If an average U-series value (instead of the lowest) was used for modelling, all mean data would fall within this stage (see calculation for 519a[2]). The large age-uncertainties which are based on the uncertainties in AD-determination do not exclude a possible age of stage 9 (303–339kyr) (the laboratory uncertainties of the other values will contribute another 1–2% to the total error; however, this is too time-consuming to compute). An age in the range of stage 13 or older (524–478kyr), as based on the faunal evidence, seems rather unlikely.

The major source of radioactivity is the sediment matrix. Even without any internal dose rate contribution (ie no U in the sample), the samples would not fall into this age range (see NU-values in Table 101). Since the sediment is nearly saturated with water and the U-concentration in the sediment is relatively high, one would expect to find high U-concentrations in the dentine (several 100ppm) in the case of an old tooth and at least a few ppm in the enamel of the deer sample (520). However, this is not the case. As can be seen in Table 100, the U-concentration in the enamel is exceptionally low, even in the thin deer sample (enamel c 750 μ m). Additionally, the U-concentration in the dentine is also comparatively low. This strongly supports a relatively young age for the teeth.

It could be argued that the radioactive elements were incorporated into the sediment at a late stage. However, the minimum age for this must be at least 160kyr, since the uranium would migrate first into the sediment and then into the tooth, which gives in turn a closed system value of 160kyr. If the system is open, then 160kyr would only represent a minimum value, ie a possible U-migration would have happened before that date. Therefore, a late incorporation of uranium into the sediment cannot be an explanation for the young ESR dates.

5.6 Amino acid geochronology

D Q Bowen and G A Sykes

The use of data from the diagenesis of proteins and their component amino acids for dating is well documented (see reviews by Williams and Smith 1977; Wehmiller 1982; Sykes 1988; 1991). Racemization or epimerization of amino acids has proved to be the most reliable age indicator; in this study the epimerization of L-isoleucine to D-alloisoleucine has been used as the basis for amino acid geochronology. Three major comparable studies of D-alloisoleucine/L-isoleucine (D/L) ratios from Britain (Bowen *et al* 1985; 1989; Bowen and Sykes 1988) and north Europe (Miller and Mangerud 1985) have been published for marine interglacial sites. Three studies of D/L ratios from British non-marine sites have been reported (Hughes 1987; Bowen 1992; Bowen *et al* 1989).

Analytical procedure

Samples for amino acid analysis were prepared by Method B of Miller *et al* (1982). D/L ratios from samples prepared by this method cannot be compared to D/L ratios from other preparation procedures. The extent to which the different preparation methods have been used by the Amino Acid laboratories at INSTAAR, Colorado, Aberystwyth, and London, are given in Sykes (1991). Amino acids were separated by High Performance Liquid Chromatography (HPLC) on a cation exchange resin and detected by the fluorescence of their Ortho-Phthaldialdehyde (OPA) derivatives. Peaks, heights, and areas corresponding to individual amino acids were measured by the IMI Chromatograph or Nelson Analytical 900 series integrators.

Interpretation

All of the data in this study are from slow epimerizers (*Nucella* sp and *Littorina* sp, Miller and Mangerud 1985; Bowen *et al* 1985; *Trichia hispida*, Hughes 1987; Bowen *et al* 1989) and, for the sake of comparison with other sites, *Macoma* sp, *Mya* sp and *Arctica islandica* (Miller and Mangerud 1985), which are moderate racemizers. The epimerization rate of *Neptunia contraria* is unknown (Tables 102–4).

The D/L ratios from the Boxgrove marine units correlate with those from the nearby raised beach at Waterbeach (*Nucella* sp 0.284 \pm 0.004 [3], *Macoma balthica* 0.386 [since there was only one sample of *M. balthica*, no standard deviation can be quoted]). Within a European context the D/L ratios from Boxgrove correlate with those from Vognsbøl Sand, Denmark (*Littorina littorea* 0.247 \pm 0.038 [6] *Arctica islandica* 0.375 \pm 0.041 [4] and *Mya truncata* 0.435 \pm 0.023 [5]; Miller and Mangerud 1985) and are ascribed to High-sea-level event 2 of Bowen and Sykes (1988), as is Hummelsbuttel, West Germany (*Macoma balthica* 0.382 \pm 0.016 [5]) (Miller and Mangerud 1985).

Table 102 Amino acid D/L ratios on nucellids from Boxgrove and Waterbeach. H = total D/L ratio, F = free D/L ratios

lab no	site/area	species	mean	SD	n	free/total D/L ratio
Aber 659	Waterbeach	<i>Nucella</i> sp	0.284	0.005	3	H
Lond 8	Q2 SEP 1 Unit 4b	<i>Nucella lapillus</i>	0.282	0.015	5	H
Lond 501	Q2 GTP 13 Unit 3 (chalk raft)	<i>Nucella lapillus</i>	0.309	0.027	4	H
			0.438	0.046	4	F
Lond 502	Q2 GTP 13 (basal beach)	<i>Nucella lapillus</i>	0.319	0.020	9	H
			0.479	0.050	9	F
Aber 1153	Q2 GTP 17 Unit 4b	<i>Nucella lapillus</i>	0.286	–	1	H
			0.421	–	1	F
Aber 1154	Q2 SEP 1 Unit 4b	<i>Nucella lapillus</i>	0.292	–	1	H
			0.369	–	1	F
Aber 1155	Q2 GTP 13 (basal beach)	<i>Nucella lapillus</i>	0.298	–	1	H
			0.449	–	1	F
Aber 1157	Q2 GTP 17 Unit 4b	<i>Nucella lapillus</i>	0.337	0.014	3	H
			0.378	0.103	3	F
Aber 1159	Q2 GTP 13 (basal beach)	<i>Nucella lapillus</i>	0.290	0.011	4	H
			0.460	0.017	4	F
Aber 1161	Q2 GTP 25 Unit 3	<i>Nucella lapillus</i>	0.291	–	1	H
			0.425	–	1	F
Aber 1162	Q1/A Unit 4b	<i>Nucella lapillus</i>	0.305	0.012	2	H
			0.460	0.006	2	F

Table 103 Amino acid D/L ratios on Littorinids from Boxgrove and Waterbeach. H = total D/L ratio, F = free D/L ratios

lab no	site/area	species	mean	SD	n	free/total D/L ratio
Aber 1156	Q2 SEP 1 Unit 4b	<i>Littorina littorea</i>	0.373	0.112	3	H
Aber 1158	Q2 GTP 13 Unit 3	<i>Littorina littorea</i>	0.267	0.021	3	H
			0.372	0.015	3	F
Lond 346	Q2 GTP 13 (chalk raft)	<i>Littorina saxatilis</i>	0.256	0.009	4	H
Lond 503	Q2 GTP13 (chalk raft)	<i>Littorina saxatilis</i>	0.282	0.029	5	H
			0.380	0.050	5	F
Lond 346	Q2 SEP 1 Unit 4b	<i>Littorina</i> sp indet	0.476	0.230	9	H
			0.349	0.017	5	F

Table 104 Amino acid D/L ratios on miscellaneous species from Boxgrove and Waterbeach, including the terrestrial mollusc *Trichia hispida*. H = total D/L ratio

lab no	site/area	species	mean	SD	n	free/total D/L ratio
Aber 389	Waterbeach	<i>Macoma balthica</i>	0.386	–	1	H
Lond 180	Unit 4 Slindon Silts	<i>Neptunea contraria</i>	0.315	0.023	3	H
Lond 49	Q2 GTP 25 Unit 5b	<i>Trichia hispida</i>	0.237	0.016	3	H

Correlation of High-sea-level event 2 with an Oxygen Isotope Stage is difficult; at present the best estimate is stage 11, based on ESR dates of 371kyr bp, for Hummelsbittel (Sarnthein *et al* 1986, ie Model 1 of Bowen and Sykes 1989), though stage 13 can not be ruled out (Model 2).

T. hispida D/L ratios (Table 104) from the terrestrial sequence are more problematic as they correlate with Woodston (0.236 ± 0.027 [4]) and Bushley Green basal beds (0.235 ± 0.01 [2]) in the correlation of Bowen *et al* (1989), which are ascribed to Oxygen Isotope Stage 9. These apparently young ratios could be due to either

a geochemical anomaly or, as they are from late in the interglacial sequence at Boxgrove and may only have been subjected to interglacial temperatures for a short period before climatic deterioration, a temperature anomaly.

At the present time the majority of the amino acid data suggests a correlation of Boxgrove with Oxygen Isotope Stage 11.

5.7 Palaeomagnetic measurements

A David and P Linford

Introduction

The tendency of sediment particles to become oriented in approximately the direction of the ambient magnetic field during deposition — depositional remanent magnetisation (DRM) — is a well known phenomenon (Tarling 1983). Together with the stronger thermoremanent magnetisation (TRM) recorded in many igneous rocks, measurements of DRM can play an effective role in geological dating and correlation. In particular, reversals in magnetic polarity may provide global stratigraphic markers. Partial reversals, or magnetic 'excursions', along with smaller amplitude secular variations, are of value at a local scale over the last million years. A detailed knowledge of the palaeomagnetic secular variation record, calibrated with radiocarbon and other chronologies, allows the direct dating of some archaeological features and deposits since *c* 10,000 bp (Clark *et al* 1988; Aitken 1990).

In Britain, studies of sediment remanent magnetisation have been most successfully applied to Holocene lake sediments (Turner and Thompson 1981; 1982) and occasionally also to cave sediments (eg Gale *et al* 1984; Noël 1986). Pleistocene sediments which are suitable for sampling are rare however, and magnetostratigraphy has so far made little effective contribution to the British stratigraphic record for this period (Shotton 1986; but see Gale 1986). Only at Hoxne, Suffolk, has any previous palaeomagnetic study been attempted for sediments of direct relevance to a Lower Palaeolithic occupation site (Thompson *et al* 1974).

The excavations at Boxgrove have now provided a second opportunity, albeit with limited expectations, for a magnetostratigraphic study linked to horizons of known hominid activity. The Slindon Sands and Silts (Units 3 and 4), as water-laid deposits immediately underlying the principal archaeological levels, were both considered possible candidates for retention of a contemporary DRM. The low energy deposition of the Slindon Silts, in particular, may have been favourable for depositional alignment. However, the higher energy deposition of the Slindon Sands and the evidence for bioturbation, mineral translocation, and structural distortion throughout both deposits, suggested that any surviving directional information was likely to be minimal.

The objectives for this study were therefore to establish whether the Boxgrove sediments retained a measurable DRM and, if so, whether this demonstrated any distinctive signature relatable to other 'known' magnetic events, or of value to future local or regional stratigraphic correlation.

Sampling and method

A representative sequence of deposits exposed at GTP 13 in Quarry 2 was chosen for sampling. The sequence included approximately 1.3m of Slindon Silts and Sands (see Fig 46) and the exact sampling site was selected at a part of the section where disturbance to these deposits appeared to be at a minimum.

Three samples were extracted from each of 16 horizontal spits spaced at 50mm intervals down the section. Each sample was carefully excavated as a free-standing pillar of sediment which was then encapsulated with Plaster of Paris within a 50mm x 50mm plastic cylinder. The sample container was levelled and the direction of present-day magnetic north marked on it with a compass whilst the sediment within was still *in situ*. The sampling process began at the top of the sequence, in the Brickearth Beds (Unit 6), and worked downwards in successive levels towards the base of the Slindon Sands (Unit 3). Care was taken to avoid sampling material which would obviously have given spurious data, eg Unit 5a and the top of Unit 4c, both of which apparently coincide with a period of sub-aerial exposure and bioturbation (Collcutt Chapter 2.3; Catt Chapter 2.5; MacPhail Chapter 2.6). A thin sandy layer at the junction of the Slindon Silts and Sands (Collcutt and MacPhail *ibid*) was also purposely not sampled.

Table 105 Mean NRM values of declination, inclination, and intensity calculated from the three samples taken from each level, including the alpha-95 precision statistics

<i>sample</i>	<i>depth (m)</i>	<i>declination°</i>	<i>inclination°</i>	<i>intensity (mA/m)</i>	<i>α95°</i>
Box01a-c	0.5-0.10	26.8	60.1	38.5	8.5
Box02a-c	0.15-0.20	38.9	59.7	19.3	7.9
Box03a-c	0.25-0.30	-18.7	21.3	3.2	>90
Box04a-c	0.35-0.40	-43.2	65.4	4.5	88.9
Box05a-c	0.45-0.50	56.0	57.8	5.3	39.5
Box06a-c	0.55-0.60	19.7	60.8	4.1	50.6
Box07a-c	0.65-0.70	64.9	78.3	3.8	>90
Box08a-c	0.75-0.80	-20.7	63.2	5.4	18.9
Box09a-c	0.85-0.90	-64.5	43.5	3.9	51.2
Box10a-c	0.95-1.00	-2.3	71.1	11.8	7.8
Box11a-c	1.05-1.10	7.5	59.5	13.9	26.0
Box12a-c	1.15-1.20	34.2	66.2	10.3	31.5
Box13a-c	1.25-1.30	-24.6	57.1	9.3	26.9
Box14a-c	1.35-1.40	40.3	55.5	8.5	74.7
Box15a-c	1.45-1.50	27.5	58.5	10.6	9.0
Box16a-c	1.55-1.60	12.5	64.5	8.3	30.5

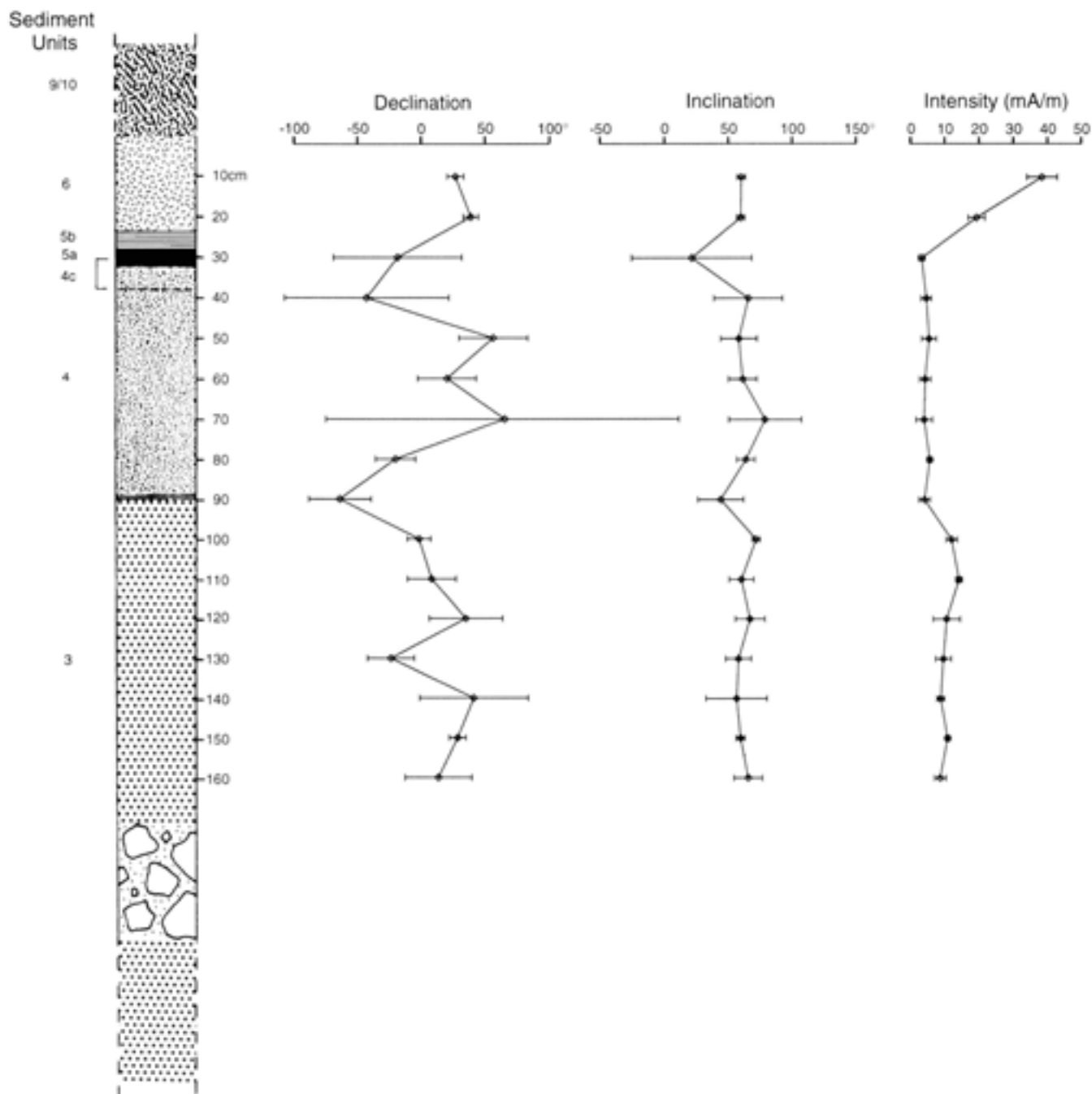


Fig 218 NRM values of declination, inclination, and intensity at each depth, plotted in relation to the stratigraphy at the sampling site

The natural remanent magnetisation (NRM) of all samples was measured using a Molspin fluxgate magnetometer (Molyneux 1971). The remanence stability of pilot samples from the Brickearth Beds, Slindon Silts and Slindon Sands was examined by alternating field (AF) demagnetisation up to 50 millitesla (mT) peak field. The NRM values are tabulated in Table 105 and the data are illustrated graphically in Figures 218 and 219. The measurements from each set of three samples have been averaged to minimise the effects of spurious errors within individual samples.

Results

Values for both inclination and declination are consistent with normal geomagnetic polarity throughout the sequence. However, both directions display erratic fluctuations — declination being particularly wayward, covering a total range of 130°; inclination is less variable. The alpha-95 statistic listed in Table 105 is an indication of the precision of the determination of direction based on the average of each set of three inclinations and declinations. The values confirm

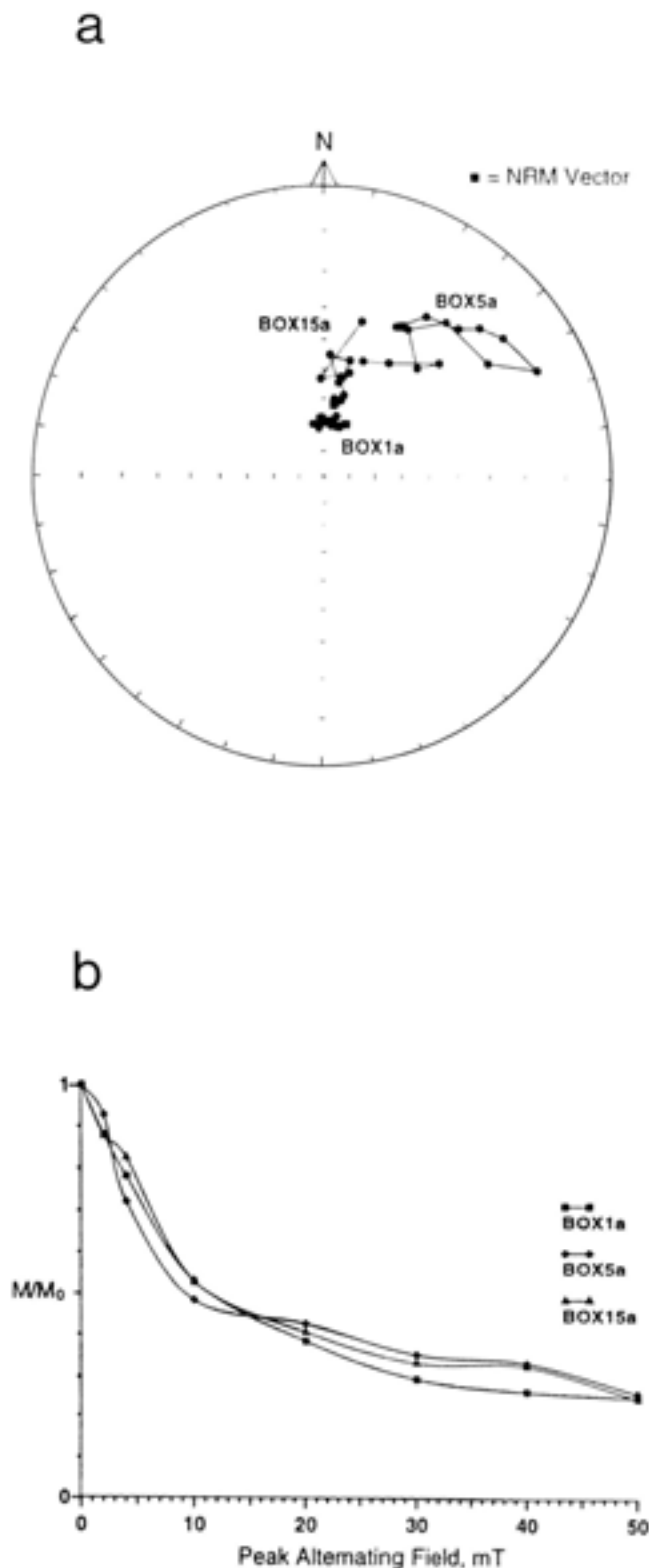


Fig 219 Changes in direction and intensity of remanent magnetism in samples BOX1a, BOX5a, and BOX15a, during increasing, stepwise demagnetisation with alternating magnetic fields: a) variation of direction, depicted on an equal angle stereogram, b) variation of intensity, M , as a fraction of the NRM intensity, M_0

substantial imprecision at each level (although it must be noted that the alpha-95 statistic is only fully reliable when calculated from an average of seven or more samples).

Magnetic intensity values are very low, near the limit of resolution of the magnetometer, and this may partly account for the data scatter. Changes in remanence intensity clearly reflect the stratigraphy; values are highest in the Brickearth Beds, dropping off substantially throughout the very calcareous Slindon Silts, before increasing again in the more ferruginous sands below.

On demagnetisation, the magnetic intensity of the pilot samples is shown to decline rapidly (Fig 219b) suggesting that the bulk of the remanent magnetisation is recorded in low coercivity domains. It is thus likely that the remanence is unstable and perhaps this is a reason for the inconsistency of directions between each demagnetisation step (Fig 219a, particularly sample BOX5a).

Conclusions

The erratic remanence directions throughout these deposits are a reflection both of their very weak magnetisation and the fact that the sediments, whilst generally horizontal, have undergone considerable post-depositional changes (Chapter 2). Potential sources of error in the DRM of sediments are complex (Tarling 1983), and several can be identified here. The Slindon Silts, although a low energy accumulation, have only a very slight magnetic mineral content and also preserve some evidence of bioturbation, for instance by mollusca. Both the Silts and Sands show localised depositional distortions, and the more rapidly deposited Sands contain bedding structures which will also have introduced errors. The Sands may also have been rooted at one time and are mottled by iron-staining suggestive of diagenetic alteration.

It is clear from these results that, although further work on magnetic characterisation is possible, magnetostratigraphy is unlikely to make a significant contribution to either the dating or stratigraphic correlation of deposits at this site.¹ These sediments do not retain a sufficient or reliable remanent magnetisation, and it can only be stated that magnetic polarity at the time of their deposition was normal with an overall easterly bias as in Recent times (Clark *et al* 1988). It can only be concluded therefore that the deposition must have taken place within the Brunhes magnetic chron which is dated on other evidence from 0–780,000 years ago.

¹ More detailed and sensitive magnetic measurements were made at Boxgrove by a team from the Geomagnetism Laboratory of the University of Liverpool in 1995. The results obtained confirm those reported here (Heslop and Shaw 1996; Heslop personal communication).

5.8 Calcareous nannoplanktons

G Gard

Introduction

The aim of this report is to describe the calcareous nannofossils (coccoliths) that are present in the sediments at the quarry, and attempt to use them for dating the strata.

Materials and methods

Approximately 2cc of sediments were collected by M B Roberts from GTP 13 and GTP 35 (Figs 4, 39a-b, 44, 45a, 220) for studies of calcareous nannofossils (coccoliths) (Table 106). At GTP 13 the base of the sampling column (Fig 220a; Table 106) began in the fine-grained sediments (Fig 44), approximately 0.5m above the wave-cut platform. Geological descriptions of the sections can be found in Colcutt (Chapter 2.3).

Table 106 Samples collected for studies of calcareous nannofossils; heights (m) above the wave-cut platform

<i>quarry 2 GTP 13</i>	<i>quarry 2 GTP 35</i>
*0-0.20	0-0.05
0.20-0.40	0.05-0.10
0.40-0.60	0.10-0.15
0.60-0.80	0.15-0.20
0.80-1.00	0.20-0.25
1.00-1.20	0.25-0.30
1.20-1.40	0.30-0.35
1.60-1.70	0.35-0.40
1.70-1.80	0.40-0.45
1.80-1.90	0.45-0.50
1.90-2.00	0.50-0.55
2.00-2.20	0.55-0.60
2.20-2.40	0.60-0.65
2.40-2.45	0.65-0.70
2.45-2.50	0.70-0.75
2.50-2.55	0.75-0.80
2.95-3.05	0.80-0.85
3.05-3.15	0.85-0.90
3.15-3.25	0.90-0.95
3.25-3.35	0.95-1.00
3.35-3.45	1.00-1.05
3.45-3.55	1.05-1.10
3.55-3.65	1.15-1.20
3.65-3.75	1.20-1.25
3.75-3.85	1.25-1.30
3.85-3.95	1.30-1.35
3.95-4.05	1.35-1.40
4.05-4.15	1.40-1.45
4.15-4.25	1.45-1.50
4.25-4.40	1.50-1.55

* Column begins 0.5m above wave-cut platform

GTP 35 continues up to 2.50m

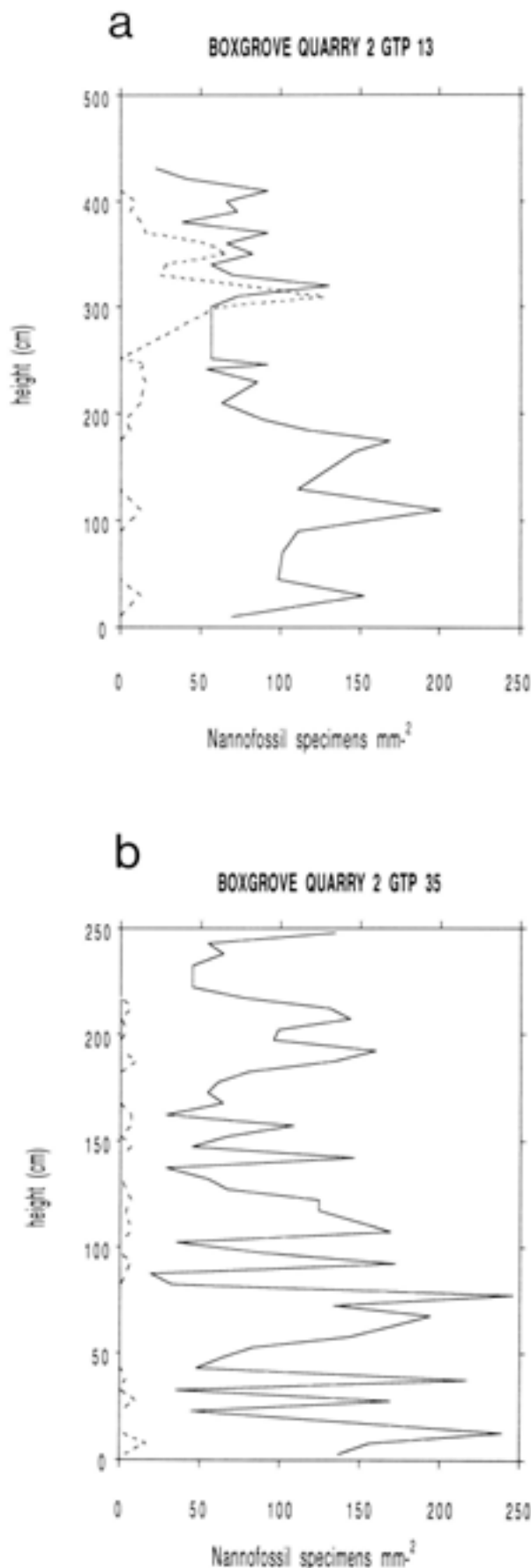


Fig 220 Abundance of calcareous nannofossils in a) GTP 13 and b) GTP 35. Solid line: reworked specimens, stippled line: Quaternary specimens

Table 107 Reworked Cretaceous and Tertiary nannofossils

reworked nannofossils		reworked nannofossils	
<i>Rhagodiscus achlyostaurion</i>	(Hill) Doeven	<i>Quadrum gartneri</i>	Prins & Perch-Nielsen
<i>Bukryolithus ambiguus</i>	Black	<i>Lithastrinus grillii</i>	Stradner
<i>Helicolithus anceps</i>	(Gorka) Noel	<i>Discorhabdus ignotus</i>	(Gorka) Perch-Nielsen
<i>Cretarhabdus angustiforatus</i>	(Black) Bukry	<i>Corollithion kennedyi</i>	Crux
<i>Rhagodiscus angustus</i>	(Stradner) Reinhardt	<i>Reinhardtites levis</i>	Prins & Sissingh
<i>Reinhardtites anthophorus</i>	(Deflandre) Perch-Nielsen	<i>Kamptnerius magnificus</i>	Deflandre
<i>Watznaueria barnsae</i>	(Black) Perch-Nielsen	<i>Lucianorhabdus maleformis</i>	Reinhardt
<i>Braarudosphaera bigelowii</i>	(Gran & Braarud) Deflandre	<i>Zeugrhabdotus noeliae</i>	Rood, Hay & Barnard
<i>Watznaueria biporta</i>	Bukry	<i>Gartnerageo obliquum</i>	(Stradner) Thierstein
<i>Watznaueria britannica</i>	(Stradner) Reinhardt	<i>Calculites obscurus</i>	(Deflandre) Prins & Sissingh
<i>Orastrum campanensis</i>	(Cepek) Wind & Wise	<i>Ahmuellerella octoradiata</i>	(Gorka) Reinhardt
<i>Lithraphidites carniolensis</i>	Deflandre	<i>Lithastrinus orbiculatus</i>	(Forchheimer) Crux
<i>Lucianorhabdus cayeuxii</i>	Deflandre	<i>Tranolithus orionatus</i>	(Reinhardt) Perch-Nielsen
<i>Microstaurus chiastius</i>	(Worsley) Grun	<i>Calculites ovalis</i>	(Stradner) Prins & Sissingh
<i>Glaukolithus compactus</i>	(Bukry) Perch-Nielsen	<i>Broinsonia parca constricta</i>	Hattner <i>et al</i>
<i>Grantarhabdus coronadventis</i>	(Reinhardt) Grun	<i>Broinsonia parca parca</i>	(Stradner) Bukry
<i>Cretarhabdus crenulatus</i>	Bramlette & Martini	<i>Manivitella pennatoidea</i>	(Deflandre) Thierstein
<i>Prediscosphaera cretacea</i>	(Arkhangelsky) Gartner	<i>Lithastrinus planus</i>	(Stover) Crux
<i>Staurolithites crux</i>	(Deflandre) Caratini	<i>Rhagodiscus plebeius</i>	Perch-Nielsen
<i>Cylindralithus sp</i>		<i>Lucianorhabdus quadrifidus</i>	Forchheimer
<i>Arkhangelskiella cymbiformis</i>	Vekshina	<i>Ahmuellerella regularis</i>	(Gorka) Verbeek
<i>Microhabdulus decoratus</i>	Deflandre	<i>Broinsonia signata</i>	(Noel) Noel
<i>Gribrosphaera ehrenbergii</i>	Arkhangelsky	<i>Zeugrhabdotus sisyphus</i>	(Gartner) Crux
<i>Biscutum ellipticum</i>	(Gorka) Grun	<i>Zeugrhabdotus spiralis</i>	Bramlette & Martini
<i>Zeugrhabdotus embergeri</i>	(Noel) Perch-Nielsen	<i>Rhagodiscus splendens</i>	(Deflandre) Veerbeek
<i>Broinsonia enormis</i>	(Shumenko) Manivit	<i>Micula staurophora</i>	(Gardet) Stradner
<i>Eiffelithus eximius</i>	(Stover) Perch-Nielsen	<i>Helicolithus trabeculatus</i>	(Gorka) Verbeek
<i>Lithastrinus floralis</i>	Stradner	<i>Nannoconus truttii</i>	Brönniman
<i>Tranolithus gabalus</i>	Stover	<i>Eiffelithus turriseiffelii</i>	(Deflandre) Reinhardt
<i>Chiasmolithus bidens</i>	(Bramlette & Sullivan) Hay & Mohler	<i>Chiasmolithus solitus</i>	(Bramlette & Sullivan) Locker

Smear slides were prepared from the untreated sediments and studied in a light microscope using magnification of $\times 1250$. The abundance of nannofossils was estimated by counting the numbers of specimens observed in ten fields of view in the light microscope. The abundance is expressed as the numbers of specimens per square mm (Backman and Shackleton 1983).

Results

Calcareous nannofossils were found in all samples from GTP 13 (Fig 220a). The assemblage is dominated by reworked Cretaceous specimens but small amounts of Quaternary nannofossils were found in most samples. One exception was the sample collected from the 3.05–3.15m level (Fig 44) which contains slightly more Quaternary specimens than reworked specimens (Fig 220a). This sample is from finely bedded sands and clay deposited during the early part of Marine Cycle 3 (Collcutt Chapter 2.3). In GTP 35 (Fig 220b), the reworked specimens are always significantly more common than the Quaternary specimens.

The Quaternary assemblage is extremely monotonous, consisting almost entirely of variants of the genus *Gephyrocapsa* Kamptner. Rare specimens of *Coccolithus pelagicus* (Wallich) Schiller, *Calcidiscus leptoporus*

(Murray and Blackman) Loeblich and Tappan, small *Dictyococites* sp and rims of *Syracosphaera* are also observed.

Table 107 lists the reworked taxa found. These are derived from the surrounding Cretaceous and early Tertiary deposits. The reworking indicates sediment sources which include Albian or older strata, Cenomanian, Turonian to Maastrichtian and Palaeocene to Eocene (Roberts Chapter 2.1) (Fig 15; Tables 6, 7). The most precise ages are indicated by *Watznaueria britannica* – Albian or older, *Corollithion kennedyi* – Cenomanian, *Micula staurophora* – Coniacian to Maastrichtian, *Eiffelithus eximius* – Turonian to Campanian, *Orastrum campanensis* – Campanian, *Reinhardtites levis* – late Campanian to Maastrichtian and *Chiasmolithus bidens/C. solitus* – Palaeocene to Eocene.

Age significance of the calcareous nannofossils

Pseudoemiliana lacunosa (Kamptner) Gartner which became extinct in mid Oxygen Isotope Stage 12 (about 460kyr bp) (Thierstein *et al* 1977) was not observed. The absence of this species may be because the sediments are younger than Isotope Stage 12, but this is

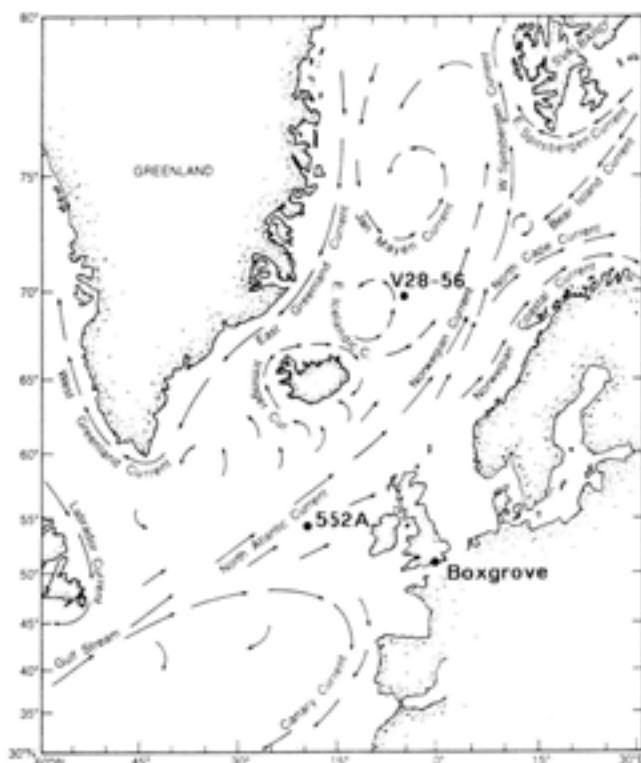


Fig 221 Location of DSDP Hole 552A, V28-56, Boxgrove and present day surface current patterns (from Eldholm et al 1987)

not conclusive evidence since this species is very rare as it nears extinction (Backman and Shackleton 1983), and the sediments do not contain abundant coccoliths. *Emiliana huxleyi* (Lohmann) Hay and Mohler, which first appears in Oxygen Isotope Stage 8 about 260kyr bp, and which becomes the dominant taxon in Stage 4 and younger sediments (Gard 1986), was not observed. Again, this is not conclusive evidence since *E. huxleyi* is very difficult to identify and not very abundant in its early range. Still, with the cautions discussed above, the calcareous nannofossils present in the Boxgrove sediments suggest that they were deposited some time between OIS 12 and 8.

A higher resolution chronology in the Pleistocene can be obtained through analyses of abundance variations in morphogroups of the nannofossil genus *Gephyrocapsa* as described by Gard (1988). In the northern North Atlantic DSDP Hole 552A (56°N, 23°W, water depth 2311m) (Fig 221), the abundance variations of *Gephyrocapsa* morphogroups are correlated to the oxygen isotope stratigraphy (Fig 222). Only those samples from Boxgrove GTP 13 levels 295 through 365 contain enough *Gephyrocapsa* specimens to make statistical abundance counts meaningful (Fig 220a). The results show that morphogroup 1 is the most common, but that groups 2 and 3 also reach significant abundances (Fig 223). A correlation with DSDP Hole 552A is not straightforward but suggests that the Boxgrove samples may have been deposited during Isotope Stage 11. A better correlation is

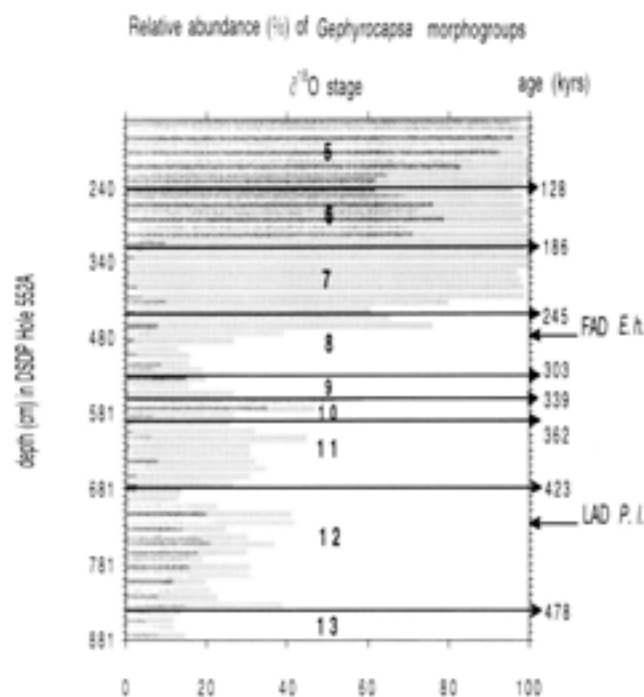


Fig 222 Relative abundance of *Gephyrocapsa* morphogroups in DSDP Hole 552A in Oxygen Isotope Stages 5 to 13: darkest shading, group 1; intermediate shading, group 2; palest shading, group 3. Oxygen isotope stratigraphy from Shackleton and Hall (1984). Ages of isotope boundaries from the SPECMAP time scale (Imbrie et al 1984)

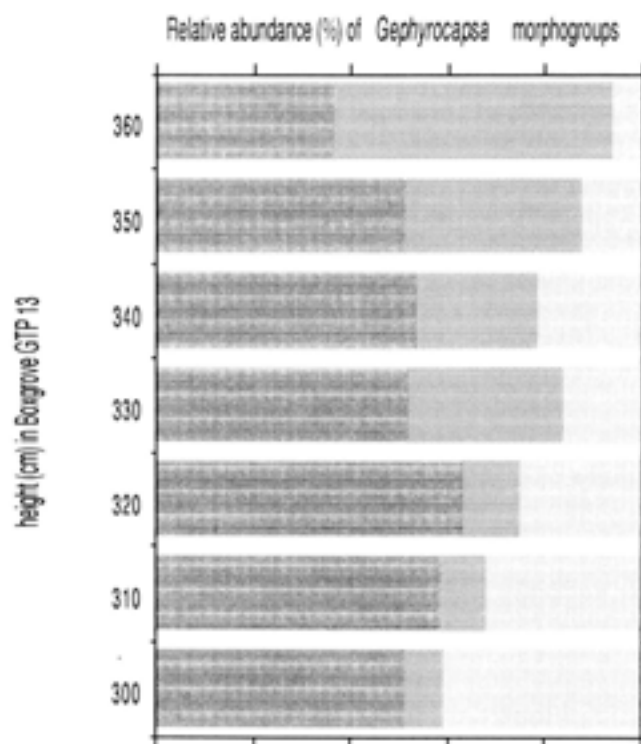


Fig 223 Relative abundance of *Gephyrocapsa* morphogroups in Boxgrove GTP 13, from 2.95m through to 3.65m in height (Fig 220a): darkest shading, group 1; intermediate shading, group 2; palest shading, group 3

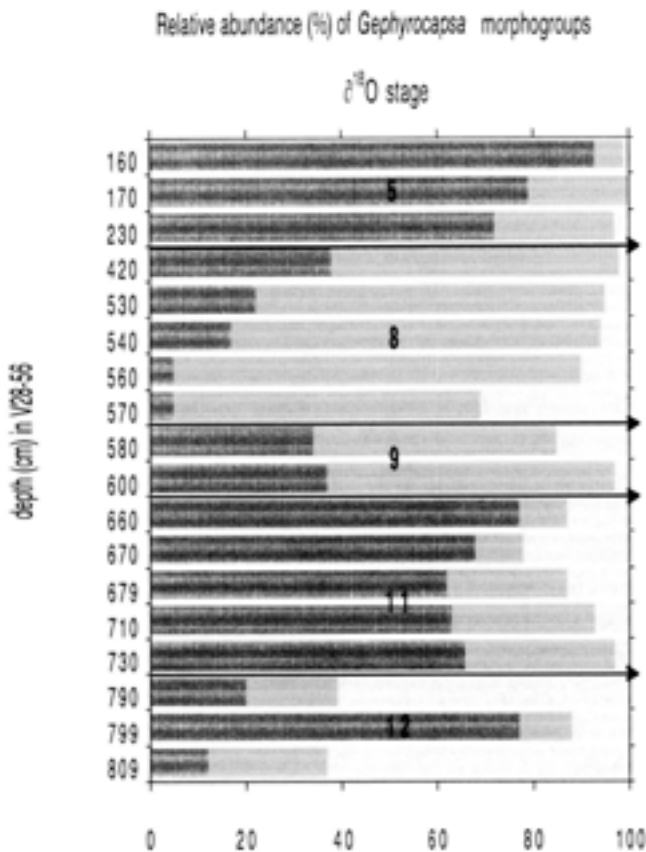


Fig 224 Relative abundance of *Gephyrocapsa* morphogroups in V28-56: darkest shading, group 1; intermediate shading, group 2; palest shading, group 3 (Oxygen isotope stratigraphy from Kellogg *et al* 1978)

achieved if the Boxgrove coccoliths are compared with those deposited in core V28-56 from the Norwegian Sea (68°N, 29°W, 1855m water depth) (Figs 221, 224). This core is also dated by oxygen isotope stratigraphy (Kellogg *et al* 1978) and strongly suggests that the Boxgrove coccoliths were deposited during Isotope Stage 11. This excellent correlation to Oxygen Isotope Stage 11 is also achieved with ODP Hole 643A and all other studied cores from the Norwegian Sea (Gard and Backman 1990). Unfortunately, from the northern North Atlantic, only DSDP 552A has been studied for relative abundance of *Gephyrocapsa* morphogroups in OIS 8 through 13. Hole 552A is located in the centre of the North Atlantic Current which only marginally reaches southern Britain, and conditions at Boxgrove may more closely resemble those in the northerly Norwegian Sea.

It is very unlikely that the Quaternary coccoliths in the Boxgrove sediments were deposited during stages 12 or 10, since coccoliths were very rare in the northern North Atlantic during glacial stages (McIntyre *et al* 1972; Gard 1988). Also, during glacial stages sea-levels are lower and marine sediments would not be deposited in an environment that now is non-marine. It is also unlikely that the observed coccoliths were deposited during interglacial stage 13, since the *Gephyrocapsa* specimens during this time period in

both the northern North Atlantic and the Norwegian Sea were characterised by very heavy specimens belonging to morphogroup 3 (Gard and Backman 1990), which is the group that is most difficult to destroy. In addition, the absence of *Pseudoemiliania lacunosa* infers that the sediments are younger than stage 13.

5.9 Biostratigraphy and summary

M B Roberts and S A Parfitt

Introduction

The dating of the Boxgrove site remains problematic, in that the variety of methods utilised have given varying results. The chronometric techniques of T/L, ESR, and Uranium series have produced the following age estimates:

Thermoluminescence	175.3–319.9kyr bp
Electron spin resonance	205–281kyr bp
Uranium series	>350kyr bp

If these dates are correlated with Specmap ages for the deep ocean isotopic stages (Imbrie *et al* 1984) they range from stage 6 to stage 11.

The Boxgrove Project has therefore pursued various techniques of relative dating in an attempt to resolve this problem. D/L ratios, produced using the amino acid racemization/epimerization method, have been correlated with Oxygen Isotope Stages: aminostratigraphy (Bowen and Sykes Chapter 5.6). Similar correlative processes have been applied to the coccolith floras (Gard Chapter 5.8) and the mammal faunas (Roberts and Parfitt, this chapter).

However these correlations have led to conflicting results:

Aminostratigraphy (on	
nucellids and littorinids)	Stage 11, 423–362kyr bp
Calcareous nannoplanktons	Stage 11
Mammalian biostratigraphy	Stage 13, 524–478kyr bp

The Boxgrove sediments were deposited during a major temperate stage (Slindon Formation and Eartham Lower Gravel Member), and an ensuing cold stage (Eartham Upper Gravel Member). Analysis of the lines of evidence presented in this publication suggests that the Slindon Formation dates either from a temperate stage between 524–478kyr bp or 423–362kyr bp (Specmap time scale Imbrie *et al* 1984); these cycles correspond to Oxygen Isotope Stages 13 and 11 respectively.

The amino acid data (Bowen *et al* 1989; Bowen 1991; Bowen and Sykes 1994) and the composition of the calcareous nannoplankton flora indicate correlation with OIS 11, the younger stage, whereas the mammalian biostratigraphy (Stuart 1988; 1990; Lister *et al* 1990;

Currant 1989; van Kolfschoten and Turner 1996; van Kolfschoten in Gibbard *et al* 1991; von Koenigswald and van Kolfschoten 1996; Roberts *et al* 1994; Roberts *et al* 1995) suggests a pre OIS 11 age. The lithological evidence combined with the other lines of biological investigation are inconclusive and suggest an uncontroversial Middle Pleistocene age. The use of archaeological typology as a method of dating or as a corollary to other dating techniques is rejected (Roberts 1992; Roberts 1994; Roberts *et al* 1995; Ashton *et al* 1992). The chronometric age estimates discussed earlier in this chapter range over a period of two hundred thousand years and are regarded as being inappropriate for the resolution of the age of the Boxgrove sediments.

The cold stage between stages 13 and 11 is known in Britain as the Anglian Glaciation; the use of the terms glacial and interglacial are sometimes avoided following the reasoning of West (1988) and Gibbard and Turner (1990), and the cyclical climatic episodes that characterise the Pleistocene are described as being temperate and cold. During the Anglian Stage extensive ice sheets covered most of the British Isles (Bowen *et al* 1986; Shotton 1986; Allen *et al* 1991); these ice sheets reached furthest south during this period, with the eastern end of the terminal moraine running through North London and laterally eastwards across Essex (Whiteman and Rose 1992; Whiteman 1992). Shackleton (1987) suggests correlation of the Anglian with OIS 12 on the basis of oxygen isotope data from the deep sea record, as does Bridgland (1994), following his work on the Thames sequence. Establishing the position of this cold episode in the Pleistocene sequence is important for resolving many of the problems currently encountered in Middle Pleistocene geological, archaeological, and biostratigraphical research.

The conventional British subdivision of Quaternary time (Mitchell *et al* 1973, see also Bowen 1978) places the Cromerian Interglacial *sensu stricto* (Tables 3, 5), as represented at the type site of West Runton, immediately prior to the Anglian cold stage, which is then followed by the Hoxnian warm stage. These correlations were based on palynological (West and McBurney 1955; West 1956; 1980a; 1980b) and lithological evidence. However, at the time of writing this succession is no longer thought to be valid. At West Runton there is now believed to be a major unconformity between the temperate deposits and the overlying diamicts and outwash deposits. This hypothesis is based on the presence of the water vole, *Mimomys savini*, at the type site whereas at Ostend, further south along the coast (Stuart and West 1976), the deposits underlying the same tills contain the evolutionary successor to *Mimomys savini*, *Arvicola terrestris cantiana*. The change from *Mimomys* to *Arvicola* was originally explained as occurring late in the Cromerian stage *sensu stricto* during pollen zone IV. However, it is now accepted by most workers (Stuart personal communication; 1988; Lister *et al* 1990) that the transition would have required more time than that afforded by

one pollen zone. Recent re-investigation of the Ostend fauna also produced samples for pollen analysis from the tooth of *Palaeoloxodon antiquus* (Preece personal communication). This pollen spectra contained the species Type X (Turner 1970; West 1963) which is unknown from Cromerian *sensu stricto* deposits, and was previously thought to be exclusively from the Hoxnian.

The surface of the Anglian till in East Anglia contains temperate deposits preserved in depressions in the till surface. These temperate deposits are described as belonging to the Hoxnian stage, again on a lithostratigraphic and palynological basis. The best known of these sites are at Marks Tey (Turner 1970) and Hoxne (West 1956; Mullenders 1993; Singer *et al* 1993). Recently Bowen *et al* (1989; 1991; Bowen 1992) have stated that the aminostratigraphy correlates Hoxne with stage 9 and accordingly there must be a hiatus between the Hoxne deposits and the underlying tills, although this proposal, which necessitates special pleading to produce solution of the chalk underlying the till rather than infilling of kettle holes, has not received widespread acceptance. The correlation of Hoxne with stage 9, is not supported by evidence from the mammalian fauna. Sites such as Swanscombe, Barnham, and Hoxne have very different faunas to those of OIS 9 such as Purfleet and Grays. Palynologically the sites at Marks Tey, Clacton, and Hoxne are similar, but the age grouping of sites on the basis of similar pollen profiles is now also thought to be untenable because similar evidence is produced in successive temperate stages; this is known as *homotaxis*. An example of the above problems in reverse can be seen at Walton-on-the-Naze (Boatman *et al* 1973) where deposits were assigned to the Hoxnian as a result of palynological studies, but lithologically and altitudinally must pre-date this stage and are probably part of the Colchester Formation of the Kesgrave Group (Bridgland personal communication; Whiteman and Rose 1992). The solution to the problems of the post-Anglian Lowestoft Till succession in East Anglia may be resolved by current investigations at Clacton (Bridgland in press), Beeches Pit (Preece *et al* 1991), Barnham (Ashton *et al* 1994a), and Elveden (Ashton in prep). A study of the *Arvicola* fauna from Beeches Pit (Parfitt in prep) shows a significant difference in the molar morphology between this assemblage and Boxgrove. Similar evidence comes from Ingress Vale, Swanscombe, another post-Anglian, temperate stage site. Barnham, Beeches Pit, and Swanscombe have also produced amino acid ratios that suggest a correlation with stage 11 (Ashton personal communication), and the mammalian taxonomy is consistent with this. As well as a more advanced form of *Arvicola*, these sites contain none of the other species which are characteristic of a pre-Anglian mammalian fauna (Table 108).

The mammalian fauna from Boxgrove points strongly to an age earlier than the Hoxnian interglacial since it is quite different from assemblages of this age

from Swanscombe, Clacton, Beeches Pit, and Barnham. A broadly Cromerian age is suggested by the presence of the shrews *Sorex runtonensis*, *Sorex (Drepanosorex) savini*, the rodents *Pliomys episcopalis*, the cave bear *Ursus deningeri*, rhinoceros *Stephanorhinus hundsheimensis*, and the giant deer *Megaloceros dawkinsi* and *Megaloceros cf verticornis*, all of which became extinct during the Anglian/Elsterian stage. An assemblage with a corresponding fauna has been found in the Calcareous Member at Westbury-sub-Mendip, Somerset (Bishop 1982). Bishop recorded a mammalian fauna of Cromerian aspect which, significantly, included the water vole *Arvicola terrestris cantiana*. Bishop's interpretation of the Westbury Calcareous Member fauna was that it represented a separate and later interglacial than the Cromerian *sensu stricto* from the Upper Freshwater Bed at West Runton. Further work on the Westbury mammalian fauna has shown that the Calcareous Member consists of a complex sequence of climatic fluctuations, including two major temperate episodes. Andrews (1990) has argued that the climatic sequence as represented by the Calcareous Member fauna rules out correlation with the end of the Cromerian Interglacial *sensu stricto* as suggested by Stuart (1982). In addition to the complexity of the climatic events, the depth of the deposits and evidence for stratigraphic hiatuses within the Westbury sequence indicate deposition over a considerable period of time. The mammalian fauna from Ostend, Norfolk, corresponds closely to the fauna from both Boxgrove and Westbury (Calcareous Member). The importance of this locality lies in the stratigraphic position of the fossiliferous deposits below diamictons deposited during the Anglian glaciation (see above).

Mammalian faunas immediately post-dating the Anglian are represented at the sites of Swanscombe, Hoxne, Clacton, Barnham, and Beeches Pit. The recently collected faunas from Beeches Pit and Barnham are particularly significant as they have produced a diverse and abundant small vertebrate fauna.

Table 108 shows the biostratigraphically important mammals identified to date from Boxgrove. The information synthesised below concerns the stratigraphic range of the taxa, and is principally derived from

publications on the British mammalian sequence by Bishop (1982), Curren (1989), Lister (1993), Stuart (1982), and Sutcliffe and Kowalski (1976), and on the continental European sequence by van Kolfschoten (1990) and von Koenigswald (1973). Whilst last and first occurrences of these taxa serve to bracket the age of the sequence at Boxgrove, other long-ranging species such as the wolf (*Canis lupus*), horse (*Equus ferus*), fallow deer (*Dama dama*) and roe deer (*Capreolus capreolus*) show significant morphological and/or size differences which appear to be of stratigraphic importance (see Parfitt Chapter 4.2).

Insectivores

Sorex runtonensis

Sorex runtonensis is a medium-sized shrew which was first described from the type Cromerian deposits at West Runton by Hinton (1911). The medium-sized shrew from Boxgrove closely resembles those from the type locality and differs morphologically from similar sized shrews from the Hoxnian localities of Barnham and Beeches Pit (Suffolk). It is generally accepted that *Sorex runtonensis* became extinct during the end of the 'Cromerian Complex' or during the Anglian/Elsterian cold stage.

Sorex (Drepanosorex) savini

Members of the subgenus *Sorex (Drepanosorex)* have a time range from the Late Villafranchian (Early Pleistocene) to the Anglian/Elsterian. This highly characteristic soricid has not been identified from contexts of Hoxnian/Holsteinian age, despite extensive sieving of sediment from a large number of localities. The latest occurrence of *Sorex (Drepanosorex) savini*, was originally described from West Runton, but its range has subsequently been extended into the previously unidentified interglacial immediately pre-dating the Anglian (Table 5). This shrew has been found at Westbury-sub-Mendip and Boxgrove.

Talpa minor

The extinct mole *Talpa minor* occurs from the Early Pleistocene, Tegelen Formation (Gibbard *et al* 1991) to the early Middle Pleistocene. In north-western Europe it is last recorded in the Hoxnian at sites such as Swanscombe, Barnham and Beeches Pit. Despite extensive sieving at these and other British Hoxnian localities, the living north European mole (*Talpa europaea*) has not been recovered. The mole fauna from Boxgrove consists of two species, *Talpa minor* and *Talpa europaea*, which are also present at Westbury-sub-Mendip and West Runton. However the assemblage from Westbury and Boxgrove differ from West Runton in the smaller size of *Talpa minor*. The difference in the size of *T. minor* between sites of an early Cromerian aspect and those dating to the end of the 'Cromerian Complex' is a consistent feature of the mole remains from a number of European sites.

Table 108 Biostratigraphically significant mammalian taxa from Boxgrove

small mammals	large mammals
Insectivora	Carnivora
<i>Sorex runtonensis</i>	<i>Crocota crocuta</i>
<i>Sorex savini</i>	<i>Ursus deningeri</i>
Rodentia	Perissodactyla
<i>Pliomys episcopalis</i>	<i>Stephanorhinus hundsheimensis</i>
<i>Arvicola terrestris cantiana</i>	Artiodactyla
<i>Microtus gregalis</i>	<i>Megaloceros dawkinsi</i>
(<i>gregaloides</i> morphotype)	and <i>cf verticornis</i>

Rodents

Pliomys episcopalus

The vole, *Pliomys episcopalus*, is biostratigraphically important as it is extinct by the Anglian/Elsterian glaciation. It first occurs in the Early Biharian, and is recorded from a number of British faunas of Cromerian aspect such as West Runton and Westbury-sub-Mendip and is relatively common in the Slindon Formation at Boxgrove.

Arvicola terrestris cantiana

The water vole lineage is perhaps the most important and well known in terms of the biostratigraphic dating of European Pleistocene faunal assemblages (von Koenigswald 1973; von Koenigswald and van Kolfschoten 1996; van Kolfschoten 1990). This lineage is characterised by an increase in crown height of the molar teeth during the Early and Middle Pleistocene which culminated in forms with continuously growing molars during the early Middle Pleistocene. There has been considerable debate on the mode and rate of this evolutionary change, which has had important implications on the age and number of temperate episodes represented in the European early Middle Pleistocene sequence. For northern Europe the date of the evolutionary transition between water voles with rooted molars (*Mimomys savini*) and the earliest representatives of the genus *Arvicola*, with continuously growing cheek teeth, has been determined for a number of localities in Germany and The Netherlands. At Kärlich Gb (Germany) a fauna with *Arvicola terrestris cantiana* has been collected from hornblende-bearing deposits pre-dating the Dutch Cromerian Interglacial IV. Van Kolfschoten therefore suggests that the earliest occurrence of *Arvicola* might correlate with Cromerian Interglacial III (van Kolfschoten and Turner 1996). At Nordbergum (The Netherlands), *Arvicola* is known from marine deposits of the Urk Formation which are stratigraphically below deposits assigned to the Elsterian. The implications of these finds is that the transition between *Mimomys* and *Arvicola* occurred by at least the Dutch Cromerian III. If this is correct then this places West Runton, the type site of the Cromerian, in an earlier Cromerian stage, therefore implying a substantial hiatus may exist between the Cromerian *sensu stricto* and sites dating to the end of the 'Cromerian Complex'. This conclusion may be supported by the significant differences which exist between common elements of the mammal assemblage present at West Runton and those from Boxgrove and Westbury-sub-Mendip.

Microtus agrestis

Fossil remains indicate that this species first occurs in pre-Anglian/Elsterian faunas such as Westbury and Miesenheim 1 (Turner 1989; in press), while it is absent from earlier, Cromerian *sensu stricto*, faunas such as West Runton. It is probable that this species first appears in north-western European mammal faunas

during the end of the 'Cromerian Complex', although it is present with *Mimomys savini* at the Biharian site of Kozi Grzbiet (Poland).

Carnivores

Canis lupus

The taxonomy of the Early and Middle Pleistocene *Canis* is somewhat confused, with some authors preferring to distinguish the earliest European forms as separate species from the living Holarctic species. Morphologically, these forms are indistinguishable from the living wolf, although they are small in comparison with those living in northern Eurasia at the present day. Bishop (1982) has suggested that the small Westbury specimens, which he refers to *Canis lupus mosbachensis*, are significantly smaller than those from the succeeding Hoxnian stage. However an examination of the only available British Hoxnian sample (from Swanscombe) shows that it is identical in size to that from Boxgrove and Westbury-sub-Mendip. The increase in the size of the wolf appears to have occurred in the period post-dating the Hoxnian interglacial. Apart from indicating a broadly early Middle Pleistocene date, the presence of a small wolf at Boxgrove is therefore of little biostratigraphic significance.

Ursus deningeri

The cave bear, *Ursus deningeri*, occurs in abundance at Westbury-sub-Mendip, and is also present in the Cromer Forest Bed localities of West Runton and Bacton. It is replaced by *Ursus spelaeus* by the beginning of the Hoxnian Interglacial, where it is known from the Lower Loam at Swanscombe. Boxgrove has produced a small assemblage of cave bear bones which are morphologically and metrically similar to *Ursus deningeri* from Westbury-sub-Mendip. The presence of this species at Boxgrove suggests a pre-Anglian age for the deposits.

Crocota crocuta

The earliest European occurrence of the spotted hyaena dates to the end of the Villafranchian and it occurs above the Brunhes/Matuyama boundary in TD 3 deposits from Atapuerca (Spain). Early records from the British Pleistocene include those from Palling, which probably dates to the 'Cromerian Complex' and from the type Cromerian of West Runton. As well as the single specimen from Boxgrove, the spotted hyaena is also recorded from the upper part of the Calcareous Member at Westbury-sub-Mendip. Although *Crocota crocuta* is common in Last Interglacial and Devensian deposits in the British Isles, it is uncommon in post-Hoxnian, pre-Last Interglacial localities. Significantly, it is absent from the extensive large mammal assemblages from Hoxnian localities such as Clacton, Swanscombe and Hoxne. The absence of the spotted hyaena in the British Hoxnian stage is another factor which separates Hoxnian assemblages from that of Boxgrove.

Perissodactyls

Stephanorhinus hundsheimensis

The taxonomy of the European rhinoceroses of the genus *Stephanorhinus* has recently been revised and clarified by Fortelius *et al* (1993). The early Middle Pleistocene rhinoceros *Stephanorhinus hundsheimensis* is now recognised as a separate species from *Stephanorhinus etruscus* which occurs in the Late Pliocene and Early Pleistocene. Several localities in Italy, Germany and the Netherlands, dating from the latest part of the Early Pleistocene, have produced a small, possibly transitional, form that suggests that *Stephanorhinus hundsheimensis* might be a descendant of *Stephanorhinus etruscus*. The *Stephanorhinus etruscus*/*Stephanorhinus hundsheimensis* group is recorded from a number of Cromer Forest-bed localities, including the Pastonian and earlier deposits at East Runton, 'Cromerian' deposits at Trimmingham, Mundesley, and from the type Cromerian Upper Freshwater Bed of West Runton. The samples from most of these localities are sparse and it is difficult to identify this material to species, although Fortelius *et al* (1993) have identified *Stephanorhinus hundsheimensis* from both Trimmingham and Mundesley. Both Boxgrove and Westbury-sub-Mendip have produced *Stephanorhinus hundsheimensis*, from contexts which date to the end of the 'Cromerian Complex'. The presence of *Stephanorhinus hundsheimensis* at Boxgrove is biostratigraphically important as this species is unknown from any fauna post-dating the Anglian/Elsterian cold stage.

Artiodactyls

Megaloceros dawkinsi and *Megaloceros cf verticornis*

A rare but highly significant record from Boxgrove is provided by the presence of two species of giant deer (*Megaloceros dawkinsi* and *Megaloceros cf verticornis*). These are biostratigraphically important records as both species are unknown after the Anglian/Elsterian glaciation. The pre-Anglian giant deer fauna, represented

mainly from sites of the Cromer Forest-bed Formation, consists of three species: *Megaloceros verticornis*, *M. savini*, and *M. dawkinsi*; none of these species are present in the Hoxnian or later stages. The earliest British interglacial records of *M. giganteus* are from Swanscombe. (*M. dawkinsi* is included in this section on biostratigraphy but is not included in the taxonomic descriptions by Parfitt in Chapter 4.2, as remains of this species were not found until work during 1995.)

Summary

The stratigraphic implications of the biostratigraphically important mammalian species strongly indicate a pre-Anglian, post-Cromerian *sensu stricto*, date for Boxgrove.

The evidence presented here shows that the mammalian faunas that immediately pre- and post-date the Anglian cold stage exhibit very different taxonomic composition. The molluscan faunas (Preece *et al* 1991), herpetofaunas (Ashton *et al* 1994a; Holman Chapter 3.5, personal communication), and oxygen isotope record (Shackleton 1987) suggest that the post-Anglian temperate stage was also significantly warmer than the last temperate stage of the 'Cromerian Complex'. Reconciling these data with the correlation of the Boxgrove temperate sediments to OIS 11, as suggested by aminostratigraphy (Bowen and Sykes Chapter 5.6) and the composition of the nannofossil geophyrocapsid flora (Gard Chapter 5.8), is therefore a problem.

The aminostratigraphic correlation of Boxgrove to OIS 11 requires that the other sites correlated with this stage, such as Barnham, Swanscombe, and Clacton, would have to move to the next temperate stage, OIS 9. The alternatives to this suggestion are that either species evolution and faunal turnover is encompassed within a single, perhaps more climatically complex stage, or that a refugia existed in Sussex for the Boxgrove fauna. Neither hypothesis is considered valid.

6 Archaeology

6.1 Introduction

M B Roberts

Palaeolithic archaeological fieldwork and research has, in the past, suffered in comparison with archaeology from later periods of human history, such that it is often perceived as the haphazard collection of artefacts, which tend to be almost exclusively stone tools and the debitage from their manufacture. This statement holds true for most of the history of Palaeolithic research with a few notable exceptions.

The reasons behind this perception are essentially twofold. The first reason is the nature of the Palaeolithic record, especially the context of the finds. Most Palaeolithic archaeology, whether in a derived context (thus immediately complicating interpretative work) or in a primary context, is often located in large bodies of sediment that bear little relevance to present day geomorphological features such as relief and drainage. For example, in a fluvial system archaeology may be located in gravel aggradations that are tens of metres thick. These in turn form part of a multi-terrace complex that relates to hundreds of thousands of years of geological time. The river may have migrated through several courses and may subsequently have been covered with glaciogenic or periglacial mass movement deposits. Extreme as this example may seem, parts of it hold true for nearly every Middle Pleistocene site in Britain. Given such a post-depositional history, it is not surprising that a large percentage of Palaeolithic material was and is recovered/discovered by methods that require deep excavation of geological strata. The most productive of these methods in the history of Palaeolithic archaeology has been mineral extraction by quarrying.

Secondly, the research emphasis in the past has been very much dominated by the lithic remains. This results from the stratigraphical complexity outlined earlier, the poor preservation of other items of the material culture, a lack of landsurfaces preserving *in situ* archaeology, and the dominance of the culture history approach to European Palaeolithic archaeology (Binford 1983; Flannery 1967; Gamble 1986; 1993).

It was in Britain at the end of the eighteenth century that artefacts such as handaxes were first recognised as being of great antiquity (Frere 1800). There followed in the succeeding century an increase in finds from both Britain and France, and accordingly a transfer of information from scholars on both sides of the channel. (Prestwich 1861; 1864; Evans 1860; 1861; 1872; Boucher de Perthes 1859). The work of these and other early researchers such as de Mortillet (1866), Lartet and Christy (1875), and most importantly Breuil (1932; 1939; 1945), led to the typostratigraphic subdivisions of flint tools for the Palaeolithic period.

A multidisciplinary tradition, most commonly between geologists and archaeologists, did exist but did not result in the multi-authored papers that are today becoming the norm. Some early researchers in the Palaeolithic certainly appreciated the value of a sound geological context as this quote from Dewey (1919) admirably illustrates: 'Without the aid of geology no precise chronology among cultural stages could be traced; with its aid, time relationships can be determined and the several types of flint implements, instead of being mere *objects de vertu*, acquire a new value as zone fossils.' Although recognising the advantages of a geological framework, it is precisely the concept of zone fossils based on artefact morphology that has generated many of the problems currently confronting Palaeolithic researchers in Europe (Roberts *et al* 1995), with regard to the ordering of the Pleistocene archaeological succession. However, it is essential to undertake typological/attribute analyses of stone tools. The information yielded is valuable in reconstructing adaptation and technological development but the results must only be used under the tightest control as time/age indicators.

Throughout the twentieth century, multidisciplinary work into Palaeolithic sites became widespread (see references in Chapter 1.4) although what was done with the archaeological material after excavation, most especially in Europe, did not fundamentally change from the initial nineteenth century approach. Archaeologists were still studying the record of the presence of Palaeolithic peoples in isolation from their interaction with each other and the environments they occupied and exploited (Gamble 1986).

Until the beginning of the 1980s mainstream academic, archaeological, thought held that Britain was first 'colonised' at the end of the country's most extensive glaciation in terms of ice cover, the Anglian cold stage (Mitchell *et al* 1973). There then followed a marked increase in population density and geographical distribution in the ensuing temperate event, the Hoxnian Stage (Table 5) (Mitchell *et al* 1973; West 1956; Turner 1970). This scheme of events was justified on the evidence available to archaeologists at the time, who were working within the stratigraphical boundaries proposed by colleagues in the geological and biological sciences. Palaeolithic stone artefacts had been found in the diamicts and outwash gravels associated with the Anglian ice advance and in fluvial deposits contemporaneous with this cold stage (Wymer 1985; 1988; Bridgland 1994). The sediments of the Hoxnian Stage in many cases directly overlie the Anglian Till (Perrin *et al* 1979): at Marks Tey, Hoxne,

Barnham, and Beeches Pit (Ashton *et al* 1994a; Preece *et al* 1991; Wymer 1985). Also, it could be inferred that sites immediately post-dated the Anglian, as in the case of the Swanscombe sediments, which were deposited by the Thames after it had been pushed south into its present valley by the Anglian ice advance (Gibbard 1985; Bridgland 1994; Bridgland *et al* 1985).

The 1973 lithostratigraphic subdivision of the Middle and Upper Pleistocene was supported by palynological work carried out mainly in East Anglia and within the Kesgrave and post-diversion courses of the Thames (West 1956; 1957; 1980a; 1980b; Turner 1970; 1975; Stuart and West 1976; Ventriss 1986; Gibbard and Peglar 1989; 1990). The palynological work showed that the Hoxnian warm stage was followed by another cold stage, which the stratigraphic table showed to correlate with a glacial event called the Wolstonian Stage. This ordering process carried on up to the present Flandrian period. Thus, not surprisingly, the biostratigraphical correlation based on palynology matched exactly the 1973 lithostratigraphic table of the Geological Society of London (Table 3).

Utilising this rigid framework meant that all the British Palaeolithic material belongs either to the time represented by Anglian/Hoxnian/Wolstonian events or to the time represented by the last glacial complex, the Devensian, as no human remains or cultural material have been found from the Ipswichian (Tables 4, 5) in Britain (Gamble 1986; Wymer 1988; Roebroeks *et al* 1992).

The publication by Shackleton and Opdyke (1973) of the oxygen isotope curve from the deep oceans showed, however, that the number of warm and cold stages post the Matuyama/Brunhes boundary was far greater than the Geological Society scheme (described above) could accommodate. The pertinent question asked was, could the events recorded in the oceans by the oxygen isotope curve be applied to continental stratigraphy? The publication of the Loess stratigraphy in Central Europe by Kukla (1975; 1977) suggested that correlation was possible. In Britain, palaeontologists Sutcliffe and Kowalski (1976) suggested that mammalian biostratigraphy in the Thames Valley showed that events were more complicated than the palynologists and the ongoing lithostratigraphic subdivision of the post-Anglian Thames sequence allowed for. There was also at this time the first challenge to the view that man first entered Britain in the Anglian cold stage. At High Lodge in Suffolk work on the sedimentary sequence, revealed by G de G Sieveking's excavation in the 1960s, and undertaken by C Turner and E Francis showed that the temperate deposits containing the archaeology pre-dated the underlying diamicton (Turner 1973) and was thus pre-Anglian in age. This work was recently vindicated by the publication of the High Lodge monograph (Ashton *et al* 1992). At Westbury-sub-Mendip (Andrews 1990; Bishop 1975; 1982) cave deposits were shown to contain flint artefacts in association with a pre-Anglian/Hoxnian fauna.

Interestingly, this fauna also differed from the Cromerian *sensu stricto* fauna that was believed to pre-date the Anglian stage directly (Stuart 1974; 1975; 1981; Stuart and West 1976). Bishop believed this fauna was the equivalent of a similar group found throughout northern and central Europe (von Koenigswald 1973) that pre-dated the Elsterian glaciation (Tables 4, 5). Thus evidence was beginning to come together to show that continental lithological sequences, including Britain, were likely to mirror the complex climatic record observed in the oceans.

Although, as mentioned previously, an appreciation of a greater number of stages and variability within the stages has freed Palaeolithic archaeologists from the strict confines of earlier beliefs, the problem of correlation between the isotope curve and the terrestrial stratigraphy, in even the broadest sense, remains today. There are, however, two fixed correlation points that are generally accepted by researchers: the Matuyama/Brunhes magnetic reversal at *c* 780kyr bp and OIS 5e, which represents the last interglacial stage prior to the Flandrian (Shackleton 1977) (Roberts Chapter 1.2). More recently (Shackleton 1987) it has been accepted as most likely that the Anglian cold stage correlates with OIS 12 (Šibrava *et al* 1986; Bowen 1991). The correlation of the Anglian with OIS 12 is supported by recent research by Bridgland (1988; 1994) in the Lower Thames Valley, which shows a correlation between terrace formation events (lithostratigraphy) and the expected climatostratigraphy inferred from the oceanic record which shows four major temperate episodes post-dating the Anglian diversion of the Thames.

Fixing the Anglian Glaciation within the Quaternary timescale is of immense importance (Roberts and Parfitt Chapter 5.9, Roberts Chapter 6.8), as there are notable differences in the pre- and post-Anglian mammalian faunas (Bishop 1982; Currant 1989; Roberts *et al* 1995; Roberts 1996; Stuart 1982) which are of biostratigraphical importance. These changes are also mirrored in the faunas of the same age in central and northern Europe (von Koenigswald 1973; 1992; von Koenigswald and van Kolfschoten 1996; Kahlke 1975; Cordy 1982; van Kolfschoten 1985; 1990; van Kolfschoten and Turner 1996).

Accordingly, it is the composition of the fossil mammal assemblages that is the main tool used in separating pre- and post-OIS 12 sites in Britain; this work is undertaken in conjunction with a thorough analysis of the site lithostratigraphy and the geology of the surrounding area. Studies of preserved pollen, ostracods, foraminifera, and herpetofaunas are of less use in a biostratigraphical context because of homotaxis in successive warm and cold events and thus only broad subdivisions, which equate, interestingly, to the initial 1973 stratigraphic sequence, are visible.

This last point is very important because it shows that there are large blocks of time where changes between successive temperature stages are not readily

visible; for example it is difficult to differentiate between stages 15 and 13 of the Cromerian complex and stages 11 and 9 after the Anglian glaciation. The very short cold stage lasting *c* 25kyr between 11 and 9 probably accounts for the similarity in the floras of these two temperate stages as well as the difficulty in separating them using amino acid racemization (M R Bates personal communication). The period between the Hoxnian (OIS 11) and the Ipswichian (OIS 5e) is not very well understood in Britain (Gibbard and Turner 1988; Lewis 1993; Rose 1987; 1988) but is now being viewed as the equivalent in time to the continental Saalian Complex (Roebroeks and van Kolfschoten 1995a, 299, 301).

In Britain both pre-Anglian and post-Anglian Pleistocene deposits are best represented as a continuum in fluvial deposits, such as the Kesgrave Group (Bridgland 1988; 1994; Bridgland and Lewis 1991; Bridgland *et al* 1995b; Whiteman 1992; Whiteman and Rose 1992), which represents the ancestral pre-diversion course of the lower Thames and the sediments of the present Thames Valley (Gibbard 1985; Bridgland 1988; 1994). Other long fluvial sequences are also being recognised and worked on from the Midlands/Bytham River (Lewis 1992; Maddy and Lewis 1991; Maddy *et al* 1994; Rose 1989; 1992; 1994), River Avon (Bridgland *et al* 1989; Whitehead 1989) and Solent Valleys (Allen and Gibbard 1993). Another source of continuous deposition of Middle to Late Pleistocene sediments is to be found on the coastal plain of East Hampshire and West Sussex (Bates *et al* 1997; ApSimon *et al* 1977; Shephard-Thorn *et al* 1982; Roberts 1990; 1996; Chapter 2.1). Both the fluvial and marine events of the Middle Pleistocene contain archaeological material that may now be more satisfactorily interpreted (Table 5) using the expanded chronology (Bowen and Sykes 1988). Sites that fall outside the long running sequences often, as a result of the mode of deposition of their sediments, contain better preserved biological material; for example Sugworth (Shotton *et al* 1980), Beeches Pit (Preece *et al* 1991), and Westbury-sub-Mendip (Bishop 1982; Andrews 1990). These may then be used to enhance the knowledge of the palaeoenvironmental conditions pertaining at various times during the Pleistocene and, where direct comparison with the long running sequences is available, enrich the database of stages where the bulk of the information is of a lithostratigraphic nature.

The traditional archaeological sequence in the British Lower Palaeolithic begins with the Clactonian (Paterson 1937) (but see Ashton *et al* 1994b; McNabb and Ashton 1992), followed by the Acheulean, which is characterised towards the end of its duration by increased numbers of flake tools and specialised flake production from prepared cores, namely the Levallois technique. This is superseded by the rare (in Britain) Mousterian industries of the Middle Palaeolithic. The subdivision of the Palaeolithic into Lower, Middle, and

Upper stages is a somewhat *ad hoc* arrangement, developed very early in the history of Palaeolithic archaeology. These stages do not reflect a logical subdivision of archaeological time, the duration of the Lower Palaeolithic being four to five times greater than the two following stages. Neither do they reflect accurately manufacturing techniques used by different species of the genus *Homo*, as there is a demonstrable overlap between all three ages and specific hominid types. Accordingly, this author believes that it is better to describe the industries in relation to the geological sub-series within which they occur, namely Middle and Upper Pleistocene and, further, by naming the chronostratigraphic stage from which the assemblages occur. These are fixed points in time which are synchronic across large distances, the definition of stages and sub-stages are laid down by the stratigraphic code (Hedburg 1976), and utilisation of such a scheme would facilitate interdisciplinary communication. The degree of exactitude of description of assemblages and industries would reflect the accuracy of the dating of the sites and their associated archaeological material. Thus if sites are attributed to chronostratigraphic stages or chronozones within a stage, then it would be expected that a rigorous and agreed age estimation programme had been undertaken. Sites which cannot be dated, either directly or by tight correlation with the local lithostratigraphic model, should be assigned to within the chronostratigraphic sub-series until more evidence as to their age becomes available.

Following the points outlined above, a chronological assessment of the earliest archaeological material in Britain is now possible without resorting to typological or metrical attributes of stone tools, which caused so many problems for earlier researchers. These problems have been recently highlighted by the lessons of High Lodge (Ashton *et al* 1992; Coulson 1990) and the Clactonian debate (McNabb and Ashton 1992; Ashton *et al* 1994b).

In Britain, the oldest archaeological sites are dated to the warm stage that occurs immediately before the Anglian: stage 13 using the model preferred here (Roberts *et al* 1995). These sites include: Boxgrove (Bergman and Roberts 1988; Bergman *et al* 1990; Roberts 1986; 1990; 1992; 1994; Roberts *et al* 1994; 1997), Waverley Wood in Warwickshire (Shotton 1989; Shotton *et al* 1993; Wise 1993), High Lodge in Suffolk (Ashton *et al* 1992; Cook *et al* 1991; Rose 1992), Warren Hill (Wymer 1985; Wymer *et al* 1991), Westbury-sub-Mendip (Andrews 1990; Bishop 1975; 1982), and probably Kent's Cavern (Campbell and Sampson 1971; Roe 1981).

This volume and other recent monographs (Ashton *et al* 1992; Conway *et al* 1996; Singer *et al* 1993) have demonstrated that landscape and environmental reconstruction are currently feasible and attainable goals for those researching the Middle Pleistocene. The level of integrity of this information, combined with analyses of the material culture remains and other

traces of hominid activity, for example butchery, means that testable models of human behaviour may be postulated. Although this approach will not produce definitive statements of behaviour, it does demonstrate the potential variables, allowing hypotheses to be created, and these may then be supported or refuted from work on other sites and/or further analyses of the site archive. These issues are addressed briefly in Chapters 6.5, 6.6, and 6.8, and will be studied in more detail in the second Boxgrove monograph (Roberts *et al* in prep).

6.2 Archaeology of the excavated areas

L A Austin, C A Bergman, M B Roberts, and K H Wilhelmsen

Introduction and methodology

M B Roberts

The areas described here were excavated between 1983 and 1992 (Fig 4). Some of them are described in detail, such as the Quarry 1 main area excavations and Quarry 2 Area A. Others, such as Q2 GTP 17 and other test pits, will be covered in more detail in the second Boxgrove monograph, which will deal with the interpretation of hominid behaviour in much greater depth than is possible in the current volume. The main areas, Q2/C and Q2/D, have already been published as a separate report (Roberts *et al* 1997). Q2/B was abandoned at an early stage of excavation after its covering shelter was destroyed in the great storm of 1987.

The main areas were located either as the result of test pitting (Q1/A, Q1/B) or in response to quarrying activity (Q2 GTP 17), and sometimes involved a combination of the two (Q2/A, Q2/C, Q2/D). The areas cover a large part of the available conformable landscape in front of the cliff (Figs 4, 34, 35). They also

cover a significant part of the east-west sweep of available landsurface, especially when combined with data from boreholes and test pits (Fig 33).

The methods of excavation and recording were broadly similar in all the areas; precise methodologies are given in the relevant sections. Test pitting and sample sections had shown that *in situ* lithic material was largely restricted to the sediments of the Slindon Formation, although faunal remains were often present in the basal silts/brickearths of the Earham Formation but only where there was a calcareous gravel cover. Therefore as a general rule the areas were machine dug down to the surface of the brickearth prior to the outer limits of the trench being laid out. The brickearth was then removed throughout the area; where it was thick as at Q2/A it was removed by mattock down to the last 50mm before removal by trowel. In areas with only a thin cover, the unit was trowelled from the outset. Upon reaching the surface of Unit 5a, the surface was gridded into metre squares. If upon taking down the area the archaeology proved very rich, then the squares were reduced to 0.25m² (Q2 GTP 17) or even smaller divisions if required, as was the case with the Q1/A Unit 4b scatter (Austin and Roberts this chapter).

Archaeology and faunal remains uncovered during excavation were marked with coloured flags, which designated their category. The areas were dug in arbitrary spits, the thickness of which was determined by the density of finds; separate spits were assigned to different sedimentary units and sub-units. The spit system of excavation was used as a tool to control and facilitate the excavation, often in conjunction with the size of the site grid. The application of the spit system was useful for the excavation of archaeology in Unit 4c and the largely sterile silts between 4c and the main level of archaeology in Unit 4b. However, at this latter level the archaeology is often very dense, little disturbed, and often follows discontinuous clay microlaminations. Over-rigorous following of the spit system

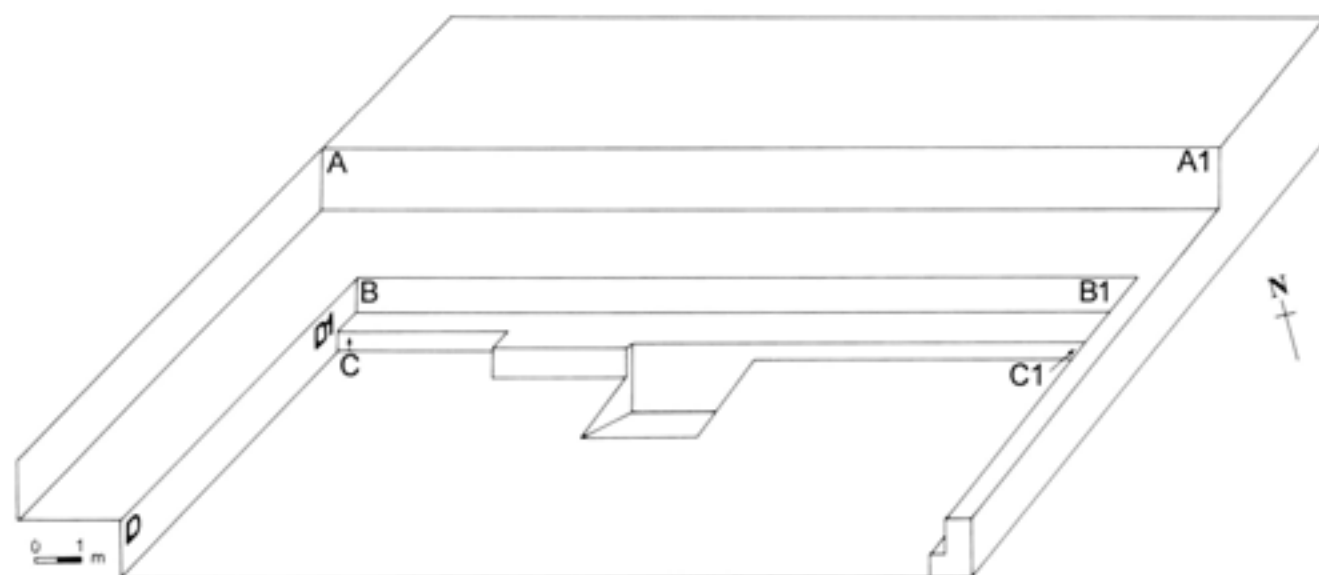


Fig 225 Three-dimensional plan of section locations of Quarry 1/A

without consideration of the micro-sedimentology would have resulted in truncation of the micro-topography and the archaeological horizon, especially where sparsely distributed lithics were not able to provide a guide to the correct level. Accordingly, the micro-stratigraphy of the sediments was closely followed to ensure controlled and precise excavation.

Faunal remains, lithics, and pebbles were recorded in three dimensions; the X and Y coordinates were generated by the site grid. The Z coordinate was obtained from site bench marks, brought into the site from the Ordnance Survey bench mark at Warehead Stud Farm (Fig 4). The dip, orientation, and morphological characteristics of pieces was also recorded to allow reconstruction of the relationships of artefacts to the excavated landsurface and to each other. These data were also used to study the taphonomy and integrity of the assemblages with respect to post-depositional movement of the archaeology by biological, sub-aerial and burial processes. Further recording involved the use of photography, both generally and as the main recording tool, as at GTP 17 (Roberts this chapter). Site distribution plans were drawn directly (Q1/B), drawn from photographs (Q1/A Unit 4b scatter), or generated from recording sheet data (Q1/A, Q1/B). Section plans were drawn at the conclusion of excavation with the involvement of the project sedimentologists.

After conservation work, cleaning and packing, the artefacts were taken to London for further analysis. The flintwork is kept at the British Museum, and the faunal remains and environmental samples are in the Palaeontology Department of the Natural History Museum.

Quarry 1 Area A

L A Austin and M B Roberts

Area A is located in the north-west corner of Quarry 1 (Figs 4, 7), approximately 100m south of the buried cliff-line (Figs 29, 33, 35). This area was identified

after sampling this part of the quarry by test pit during the winter of 1985. The sediments at Q1/A are calcareous (Figs 225, 226) with the exception of isolated solution hollows, the bases of which sometimes extend below the base of the gravels and into the Slindon Silts (Fig 226). The chalk solifluction gravels (Table 9a) overlie finer chalky pellet gravels, which are separated from the mineralised organic horizon (Unit 5a) by a calcareous brickearth that varies in thickness from 20mm to 0.2m. The calcareous nature of the capping over the Slindon Silts has resulted in good preservation of faunal remains in this area *contra* Q2/A (Bergman and Roberts, below). A small gully-like feature runs north-south (Fig 227) across the site, a section through which is shown in Figure 226. The feature was probably formed in two stages, firstly by a temporary source of freshwater running over the surface of the silts and secondly by deformation of the saturated sediment during emplacement of the overlying gravels. This feature closely resembles those found at the eastern end of Quarry 1/B (Fig 4), that were uncovered during the excavations of the trench which produced the hominid tibia (Roberts *et al* 1994). The sediment deformation has resulted in the mixing of the subunits of the Slindon Silts. However, the archaeology associated with Unit 4c has remained in the top 0.15m of the sediment, although its stratigraphic integrity has been lost. Apart from the deformation associated with the gully feature, the surface of the excavated area is generally flat with minor topographic variations (Fig 228) resulting from post-depositional warping after burial.

Methods

The overlying gravels were stripped off by machine down to the surface of the brickearth, which was then removed by trowelling in 1m² grids. Although no lithic material was found at this level, faunal remains were encountered and recorded from the site grid (Parfitt Chapter 4.2). An area of 15m x 6m was then gridded

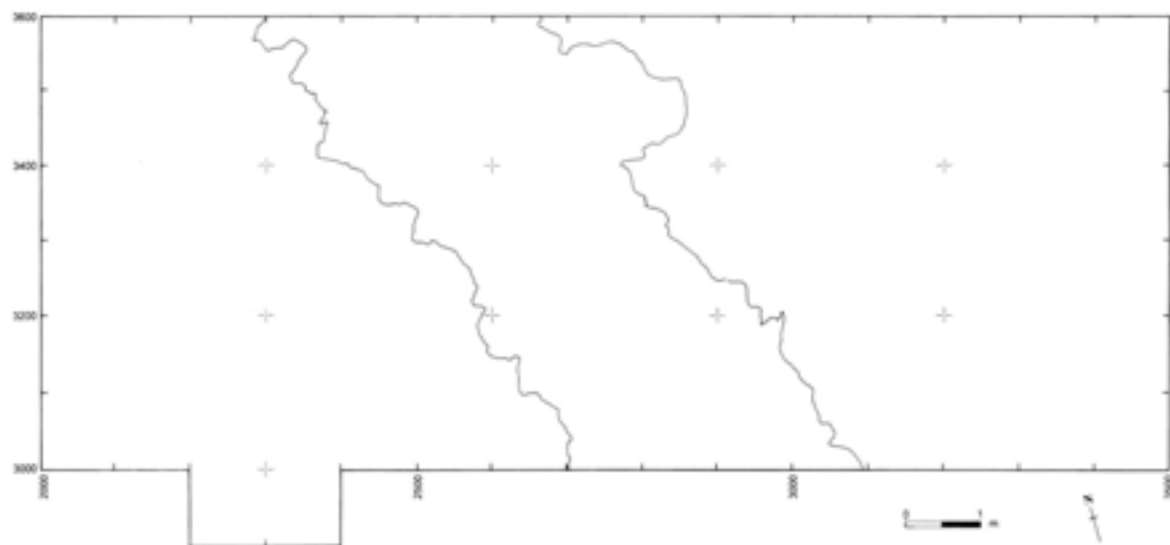


Fig 227 The excavation area of Quarry 1/A

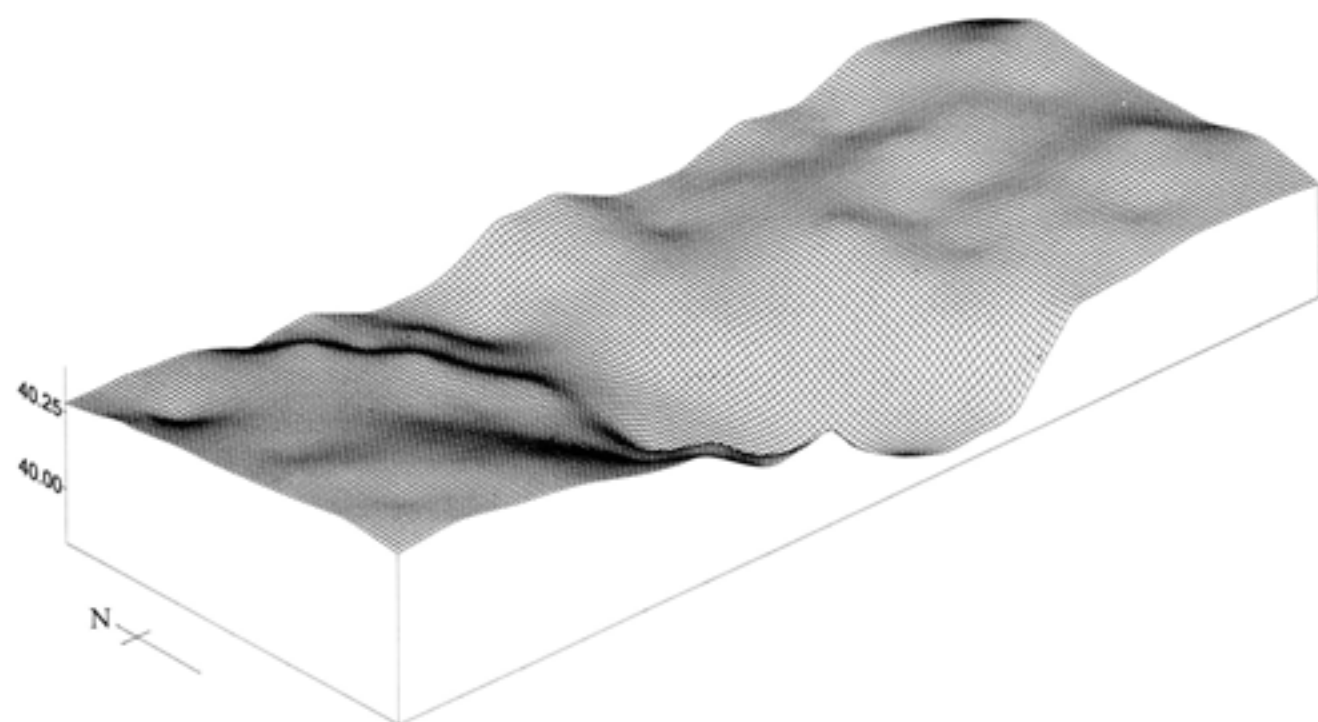


Fig 228 Isometric plot of the Quarry 1/A Unit 4c surface



Fig 229 Quarry 1/A in 1985: sediments removed down to the surface of Unit 5a, viewed from the east; 0.5 x 0.5m grid



Fig 230 Quarry 1/A: excavation of Unit 4c, viewed from the east; scale unit 0.5m

into 0.25m² on top of the mineralised organic horizon, Unit 5a (Fig 229). From this surface the area was excavated in a series of spits into Unit 4 (Table 9a, Fig 230). Excavation was completed two spits below the archaeological horizon in Unit 4b, where the silts became sterile. The spits were normally 20mm deep, although, as mentioned above, they were variable at unit boundaries and where the archaeology increased in density. X, Y, and Z coordinates were taken for all pieces over 20mm in maximum dimension; dip and orientation were also measured for every artefact in this size class. Pieces under 20mm were recorded by square and spit number. A total of 2200 lithics were recorded in this way (Fig 231). A very dense and completely undisturbed knapping scatter was found in Unit 4b which necessitated a different recording system, which will be explained later in this section.

Unit 4c

The flint assemblage

The majority of the assemblage consists of artefacts with a maximum dimension of less than 20mm (86%), with only 317 pieces having a maximum length of over 20mm. This is not surprising as experimental replication of handaxes (eg Newcomer 1971; Schick 1986)

have shown that over 70% of debitage from the production of handaxes, by flake count, is less than 20mm in length. Most of the flints (64%) show evidence of patination, although this is not uniform, varying from slight traces to heavy patination which is present on 3% of the assemblage. Staining, from iron salts, also varies throughout the assemblage with 35% having some degree of staining and 1% heavily stained. In general the flintwork is in a fresh condition with only 1% of the material showing signs of abrasion. This abrasion may result from these pieces having been reworked, and therefore subject to other processes of damage before incorporation into the sediments of Unit 4c. A total of 17 pieces (5%) have some limited edge damage of between 5% and 25% of the total edge. None of this edge damage can be identified as deliberate retouch. Possible causes of this damage includes spontaneous retouch, accidental damage, or the utilisation of these pieces by hominids (Keeley 1980).

The initial appearance of the assemblage was very similar to that from Q2/A, both in condition and in assemblage composition (see Bergman and Roberts this chapter). It comprised in the main waste flakes from the production of handaxes and five finished bifacial tools. No flake tools were identified, although a number of the flakes which exhibited some macroscopic edge damage appear to have been selected from other waste flakes and deliberately utilised.

Further analysis was undertaken using only pieces greater than 20mm in maximum length. This analysis included both complete and broken flakes.

The study aimed to answer a number of questions:

- were the artefacts *in situ*?
- what was being produced?
- was this an isolated episode or an accumulation over time?
- how did the events in Q1/A relate to other activities across the site?

The information used to answer these questions was generated by the analysis of the distribution of the assemblage, its composition, and the refitting of individual elements within the excavated area.

Distribution

The distribution of all flint artefacts >20mm in maximum length was plotted (Figs 231, 232). Unlike Q2/A Unit 4c, where distinct concentrations of debitage were obvious from the distribution of the artefacts (Bergman *et al* 1990, fig 5), no discrete knapping episodes were readily identifiable. The distribution of material at Q1/A was more evenly spread across the whole of the trench. The density of material varies between 0 and 19 pieces per metre square, with a slight accumulation in the south-western area of the trench. In Q2/A Unit 4c the density of material varied from 0 to over 50 flakes per square metre.

The initial interpretation of this distribution of the Q1/A Unit 4c flintwork was that it came from an area between main concentrations of *in situ* debitage (Roebroeks *et al* 1992b). The centre of the nearest concentration was thought to lie to the south-west of the excavated trench. However, there are other possible explanations for this spatial distribution pattern.

The factors which control the initial deposition of knapped flint are totally dependent on the knappers and users of the flint. If a radically different method of deposition were to be proposed, then different ways of initial production of debitage would have to be discussed. The experimental forms of flint and stone tool production which have become so familiar (Wenban-Smith Chapter 6.4) may not be the only possible ways of replicating archaeological material, but they have certainly been found to be valid in answering the majority of the questions which have been asked of such experimentation. One aspect of the production of recognisable patterning in the archaeological record is the need for the knapper to remain static during a knapping episode. There is no reason, particularly if a knapper is not seated, that he or she may not move around between hammer blows. This would mean that there would be no tightly constrained and identifiable knapping scatter visible in the archaeological record and only through refitting could the sequence of the movement of the knapper be discovered. Other activities which may not be habitual, or accidental, could

affect distribution, particularly if flakes which are not selected for use are also moved from their original point of deposition. Even if these types of activities are often repeated, the chance of them being recognised in the archaeological record is slim to say the least, and the sort of dispersed patterning which would result from such activity could easily be attributed to other, non-deliberate, mechanisms. Therefore these other mechanisms must be recognised and isolated first in order to discover if any information on such behavioural aspects can be identified from the archaeological record. These mechanisms are fluvial transportation, biological activity, and trampling (Macphail Chapter 2.6).

Refitting was undertaken in order to study spatial distribution, technology, and to identify any post-depositional movement of artefacts. It was hoped that the mechanisms which caused this movement might then be identified from the distribution of the conjoinable artefacts. The results of this analysis are discussed together with the technological information obtained from refitting the assemblage.

Assemblage composition

Of the 317 pieces over 20mm, 193 were broken (Table 109). Experimental work replicating biface manufacture was undertaken using local flint nodules (Bergman, in Roberts 1986; Wenban-Smith 1988; Chapter 6.4). These were obtained from the cliff collapse at GTP 25 (Fig 4) the probable source of the archaeological raw material. It was found that between 50% and 60% of the flakes broke during knapping due to flexion. A similar percentage of flexion breaks was assumed to be present in the archaeological material. However, at Q2/A breaks were found to be present in over 80% of flakes over 20mm (Table 128). Other factors such as sediment loading, surface warping caused by solution of the chalk bedrock and trampling may have contributed to the numbers of broken pieces within the assemblage. In order to distinguish between these it may be necessary to undertake experimental work to identify the characteristics of each type of break. It is considered most likely that the sediments at Q1/A were more stable post the deposition of the lithics, and this has led to a degree of breakage that is closer to the experimental figures.

Table 109 Number and percentage of individual fragments of flakes from Q1/A Unit 4c

<i>part of flake</i>	<i>number (n)</i>	<i>%</i>
proximal	81	41.97
mesial	31	16.06
distal	72	37.31
siret	9	4.66
total broken	193	60.88
complete flakes	124	39.12

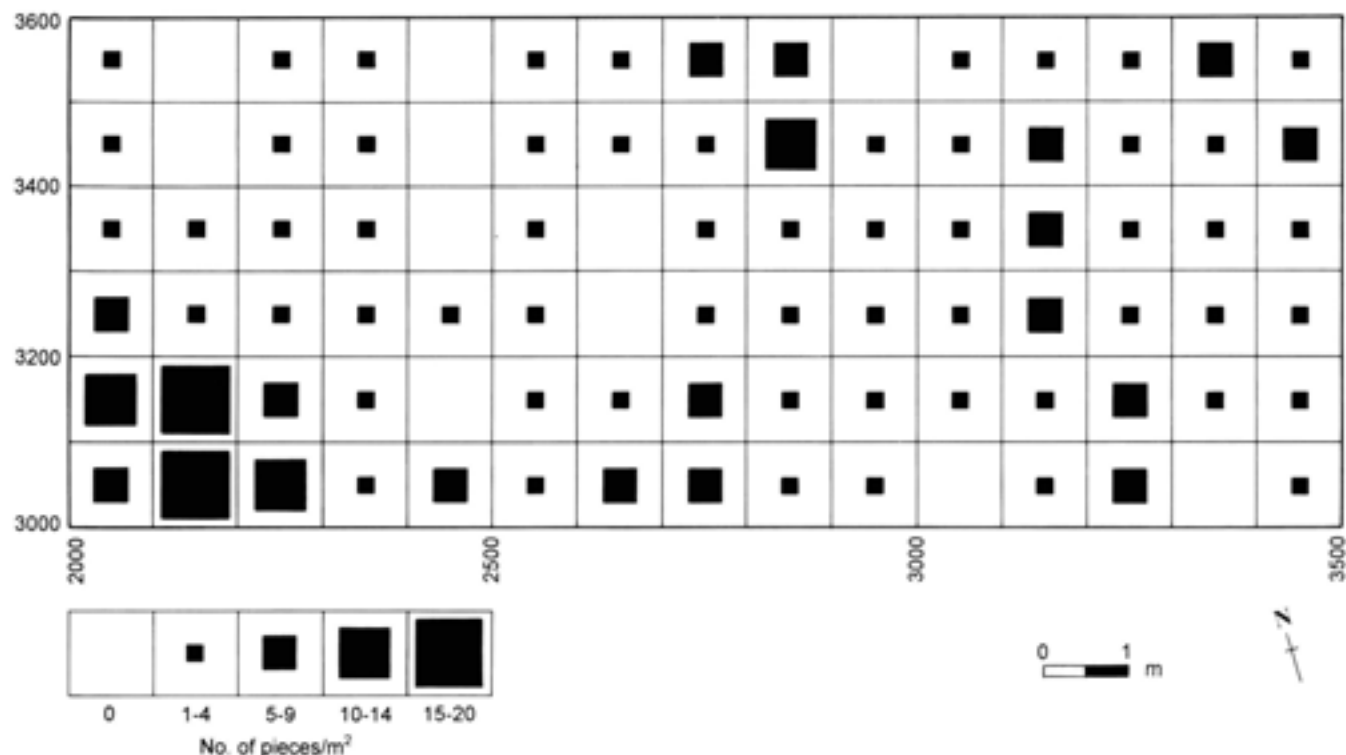


Fig 231 Frequency diagram of flintwork distribution in Unit 4c

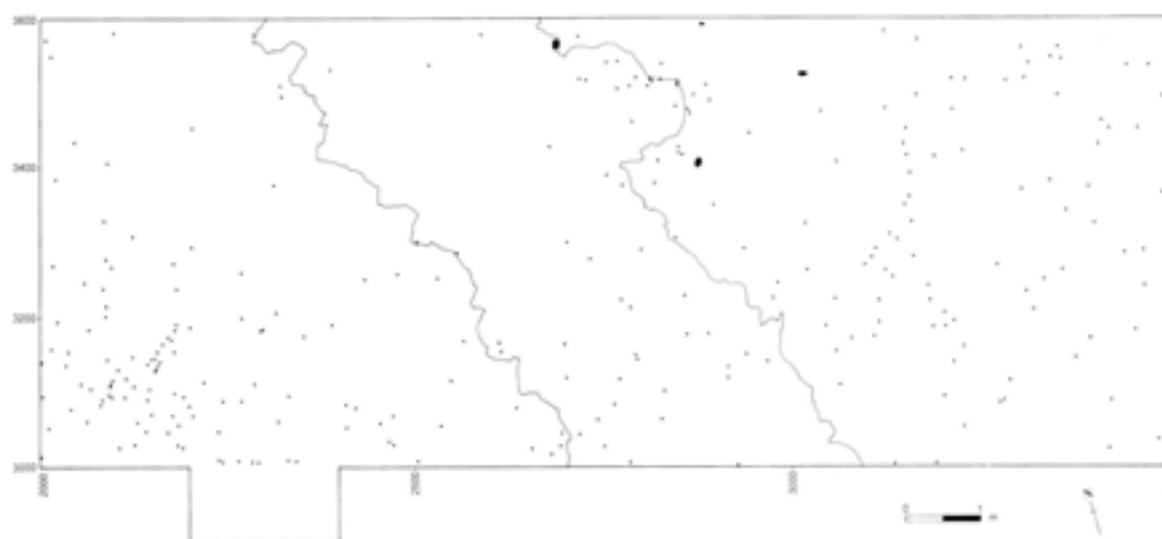


Fig 232 Plan of flintwork larger than 20mm in Unit 4c

A fuller analysis was undertaken of all complete flakes (Table 110). These were divided into three technological groups on the basis of morphology, and included the waste products from the three stages of handaxe manufacture as recognised by Newcomer (1971). These were roughing-out, thinning, and finishing flakes. A fourth category, that of flake production, was also considered but all possible examples proved to be indistinguishable from roughing-out flakes and the two groups were therefore combined. The flakes were measured and technological attributes noted; ie butt type, profile shape, dorsal scar pattern, and the proportion of the dorsal surface which was cortical.

The numbers and proportions of roughing-out flakes (14.5%), thinning flakes (29%), and finishing flakes (56.5%), are not what would be expected from a complete handaxe reduction sequence such as that found in experimental work (Newcomer 1971; Bradley and Sampson 1986).

This suggests that the complete reduction sequence from nodules to handaxes is not represented by the assemblage. If it is assumed that the assemblage is the result of handaxe manufacture, then some mechanism must be responsible for this bias. Either the complete reduction sequence was originally deposited within the excavated area or nearby and has been sorted by

Table 110 Technological attributes of complete flakes from Q1/A Unit 4c

category	roughing-out		thinning		finishing		total	
	n	%	n	%	n	%	n	%
butt type								
plain	4	22.22	10	27.27	22	31.43	36	29.03
cortical	1	5.56	3	8.33	2	2.86	6	4.84
dihedral	2	11.11	5	13.89	7	10.00	14	11.29
polyhedral	3	16.67	3	8.33	4	5.71	10	8.06
faceted	–	0	3	8.33	3	4.29	6	4.84
crushed/broken	5	27.78	9	25.00	32	45.71	46	37.10
indeterminate	3	16.67	3	8.33	–	0	6	4.84
cortex %								
0	2	11.11	19	52.78	57	81.43	78	62.90
1–25	7	38.89	13	36.11	8	11.43	28	22.58
26–50	3	16.67	3	8.33	4	5.71	10	8.06
51–75	3	16.67	1	2.78	1	1.43	5	4.03
76–100	3	16.67	–	0	–	0	3	2.42
profile								
straight	10	55.56	15	41.67	44	62.86	69	55.65
curved	5	27.78	14	38.89	23	32.86	42	33.87
indeterminate	3	16.67	7	19.44	3	4.29	13	10.48
dorsal scars								
unidirectional	6	33.33	12	33.33	49	70.00	67	54.03
bidirectional	4	22.22	12	33.33	15	21.43	31	25.00
multidirectional	4	22.22	11	30.56	6	8.57	21	16.94
indeterminate	4	22.22	1	2.78	–	0	5	4.03
flaking mode								
hard	2	11.11	6	16.67	–	0	8	6.45
soft	16	8.88	30	83.33	70	100	116	93.55
totals	18		36		70		124	

Table 111 Technological attributes of all pieces with edge damage/wear from Q1/A Unit 4c

Dorsal scars: M=multidirectional, B=bidirectional, U=unidirectional. Position of damage/wear: DT=distal, DTDL= distal dorsal, RHDL=right hand dorsal, LHDL=left hand dorsal, LHV=left hand ventral, C/B=crushed/broken

flint number	length mm	breadth mm	max dim	part of flake	flake type	profile	butt type	cortex	dorsal scars	position of damage/wear
7	14	21	21	mesial	indeterminate	indeterminate	indeterminate	–	–	LHV
18	66	53	53	complete	thinning	curved	indeterminate	0	M	DT+RHDL+LHV
509	57	95	97	complete	roughing-out	curved	dihedral	0	M	DTDL
560	28	18	28	complete	finishing	curved	dihedral	0	U	DT+LHDL
596	17	41	40	distal	indeterminate	indeterminate	C/B	–	–	DTDL
604	21	25	28	complete	thinning	straight	indeterminate	0	B	DTDL
754	45	42	45	complete	roughing-out	curved	polyhedral	<25%	B	Notch
803	72	38	75	complete	roughing-out	straight	faceted	>50%	B	DT+LHDL
1008	75	50	81	complete	thinning	curved	polyhedral	0	U	DTDL
1137	43	20	44	complete	thinning	straight	dihedral	0	U	RHDL+LHDL
1331	62	49	58	complete	thinning	curved	C/B	0	M	RHDL
1427	57	62	63	proximal	indeterminate	indeterminate	indeterminate	–	–	DTDL+LHDL
1595	44	24	45	complete	thinning	straight	C/B	0	B	LHDL
1834	45	36	46	proximal	indeterminate	indeterminate	indeterminate	–	–	DTDL
1855	48	30	48	complete	finishing	curved	C/B	0	B	DTDL
1947	40	32	43	complete	thinning	straight	C/B	5%	M	RHDL
2028	54	40	69	complete	thinning	curved	C/B	5%	M	DTDL
2170	47	39	52	mesial	indeterminate	indeterminate	indeterminate	–	–	RHDL

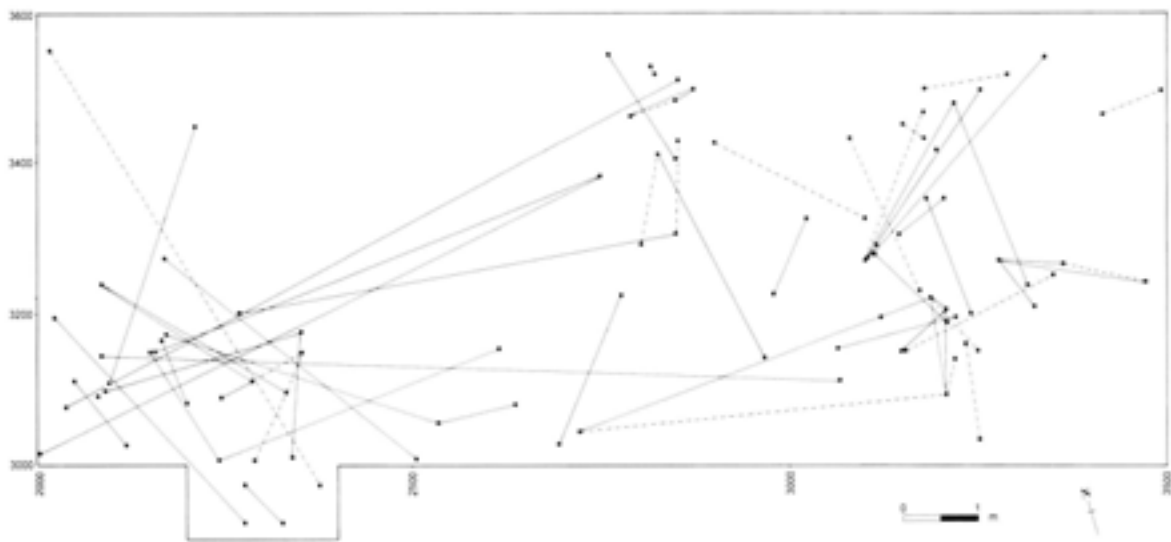


Fig 233 Refitting flintwork from Unit 4c: dashed lines = break refits; solid lines = ventral/dorsal refits

post-depositional processes, or the majority of the knapping episodes which took place in the vicinity of the excavated area were not of the complete reduction sequence but mainly from the finishing stage of hand-axe manufacture on part finished tools or tools that were modified and resharpened. In order to determine which scenario was the most likely it was necessary to identify any post-depositional processes which may have affected the distribution of artefacts in order to isolate any possible hominid cause of the recorded proportion of flake types. As part of this process, edge damage on flakes was studied in order to identify if they had been utilised or if any damage was the result of accidental abrasion, eg trampling. The results of this analysis are summarised in Table 111. It has been difficult to draw conclusions from studying the pieces and the data but the following observations may be made. The damage is not thought to result from the lithics being moved by geological or sub-aerial weathering processes, since the nature of the sedimentary regime precludes the transport of material of this size except by seaweed rafting (Bridgland Chapter 2.4). Additionally, no other wear associated with this type of movement, such as abrasion and dulling of flake scar ridges, has been identified. Unfortunately, due to the patination process, and in some cases sediment polish caused by slickensliding (ie the movement of one sediment over another under pressure (Whitten and Brooks 1983)), it has not been possible to study use wear traces on these pieces under the microscope.

Therefore it is impossible to differentiate between damage caused, for example, by the flake edge coming into contact with bone material and other natural mechanisms such as spontaneous retouch, pressure flaking against other flints or trampling. The flakes themselves are not particularly diagnostic and further work is required to solve this problem.

Handaxes

Five handaxes were excavated from Unit 4c in Q1/A (Fig 236a-e). Typologically, all five fall into Roe's broad ovate group (Roe 1968); additionally, the metrical analysis of Bordes (1961) and Wymer's descriptive categorisation (Wymer 1968) were also utilised (Table 112). The handaxes are all well made and typical of those found at Boxgrove, exhibiting slight asymmetry of shape and tranchet sharpening flakes at their tips. There is no evidence of macro damage on the remnant edges of the tranchet flakes nor elsewhere on the pieces, which fits well with their perceived use as butchery tools rather than for any heavy duty activity. No flake refits were made onto the handaxes and this fact, taken in conjunction with the assemblage composition (Table 110) suggests they were made outside the area of excavation. The small amount of butchered bone associated with the handaxes further complicates matters. There are no dense concentrations of butchered bone, such as those at GTP 17 (Parfitt and Roberts Chapter 6.5) or from

Table 112 Handaxes from Q1/A Unit 4c. Width=thickness

flint no	length mm	breadth mm	width mm	weight g	Roe's classification	Bordes' classification	Wymer's classification
54	144	83	34	419.10	ovate	IV cleaver	KHvi
1349	83	60	20	81.20	ovate	III cordate	Jvi
1739	104	71	30	227.80	ovate	IV ovate	Kvi
1906	132	74	28	244.5	ovate	III elongated cordate	JKvi
2128	107	69	26	179.70	ovate	IV cordate	JKvi

the 1995–6 excavations at Q1/B (Roberts *et al* in prep). It must however be considered that the handaxes could have been deposited on the surface over tens of years and are therefore chronologically discrete. The bioturbation of Unit 4c (Macphail Chapter 2.6, Wilhelmsen below), combined with its shallow profile, means that depositionally determined stratigraphic separation of the archaeology is not feasible.

Refitting

Refitting can be used to study at least two aspects of hominid behaviour, namely the technology of the production of flint artefacts and the use of space, as well as an aid in identifying post-depositional processes affecting the distribution of an assemblage.

Initial work looked for break conjoins before ventral/dorsal refits were attempted (Table 113). The pieces were arranged so that they could all be viewed at the same time, and laid out to show the relative positions of the flints as they had been distributed in the ground. Raw material type, inclusions, and the morphology of the piece were used as indicators of possible fits. Of the three types of refits described by Czesla (1990) (breaks, production sequences, and tool modifications), only break refits and production sequence (ventral/dorsal) refits were found (Table 114).

Table 113 Refitted broken flakes from Q1/A Unit 4c

number of refitted pieces	number of groups
2	13
3	3
4	1
total	39 individual pieces

Table 114 Ventral/dorsal refits from Q1/A Unit 4c

number of flakes in each group	number of groups
2	17
3	10
4	1
total	68 individual flakes

Table 115 Distance between the refits of the different handaxe reduction groups from Q1/A Unit 4c

refitting groups	number of groups	% of groups	average distance between refits(m)
roughing-out	18	64.29	2.82
thinning	3	10.71	1.34
finishing	4	14.29	1.36
indeterminate	3	10.71	3.60
totals	28	100	

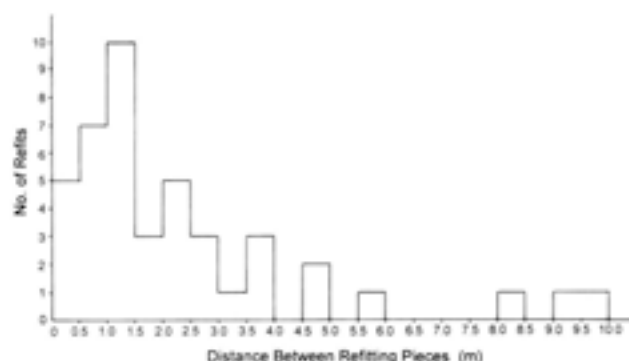


Fig 234 Graph showing distance in metres between refitting pieces

A success rate of 20% was achieved for refitting broken flakes. This compared favourably with that for refitting broken flakes from Q2/A, which was 17%. When both break refits and ventral/dorsal refits were counted, 31.2% of the 317 pieces were refitted. Although not particularly high, this figure compares very favourably with results produced by other refitters and would certainly suggest that the material had not moved any great distance from the point or points of original manufacture (Fig 233).

When the separate groups of refits are examined none comprise a great number of pieces. The largest number of individual flakes in a group is only four. Certainly no complete reduction sequences can be represented within these small groups.

The distribution of the refits was then examined. The distances between refitting pieces was found to be far greater than had been found in other excavated areas of the Unit 4c sediments (Fig 234). The distances between conjoining pieces ranged from 0.2m to 9.1m (Table 115). This certainly suggests that some form of movement of pieces has occurred after the initial deposition of the flint. Experimental work on knapping scatters (Newcomer and Sieveking 1980; Schick 1986) has demonstrated that even knapping from a standing position produces scatters which have a restricted distribution which can be identified if discovered *in situ* in an archaeological context, since the vast majority of debitage falls within an area of 4m².

None of the pieces refitted to any of the handaxes, and there were no distinct removal sequences identified which could be associated with the production of any of the handaxes recovered from the trench. The quantity of debitage recovered is too small to account for the complete production of five handaxes. As there is no recognisable link between the tools and the debitage it must be assumed that the tools were not manufactured where they were found. Equally, the tools which were the result of the debitage found within the excavated area have either been transported away from their original place of manufacture or, alternatively, the point of manufacture was outside the trench. Since there is no evidence to suggest that any of the handaxes recovered from Unit 4c were made or sharpened within

the excavated area, these tools must therefore have been transported, either deliberately or accidentally, away from where they were manufactured to where they were found. If movement had been accidental, similar movement of other pieces of debitage from the tools' manufacture would be expected. This, however, is not the case and deliberate movement must therefore be assumed. Whether this movement was as a result of the use of the tools or purely through discard has not been ascertained.

Mechanisms of the movement

Possible mechanisms which may have caused the flint to be moved from the original point of manufacture include fluvial transportation, biological activity, trampling (by hominids as well as other animals), and deliberate transportation by the knappers/users of the flint.

Fluvial transportation

Experimental work (Schick 1986) has shown that although in general terms 'smaller particles move first and further', a sudden flow surge may affect a large range of materials nearly simultaneously (Wilhelmsen below). However, a more slowly rising or waning flow would bring about size sorting of the material. Directional flow of water across a site can also be identified by scatter stretching in the direction of water flow. Where only a small part of a scatter is excavated, this directional movement may be identified by a consistent linear trend between groups of conjoining flakes.

In order to identify any possible specific directional movement, a rose diagram was constructed using the orientations of the lines between individual refits (Fig 235). If fluvial transportation had occurred it was not in one direction. If water flow was responsible for the movement of artefacts it must have taken place in several directions, none of which are now distinguishable.



Fig 235 Rose diagram showing orientation of refits

As fluvial transportation cannot be recognised in either the archaeological or the sedimentological records it must be discounted as a major factor in causing the distribution of artefacts.

Biological activity (bioturbation)

Extensive invertebrate and mammal activity (see Macphail Chapter 2.6) is known to have reworked human artefacts throughout Unit 4c. Although most of this movement is recognisable in the vertical distribution of the artefacts, some element of horizontal movement will also have occurred. However, it is extremely unlikely if not improbable that distances of several metres between refitting artefacts could be explained by such biological activity. Biological activity is, therefore, a factor contributing to the post-depositional horizontal movement of artefacts, but it cannot account for the more extensive movement found within Q1/A.

Trampling

Various studies have investigated the processes affecting the vertical and horizontal distributions of artefact scatters (Barton 1992). Trampling has been suggested as an important factor in the vertical arrangement of finds (Villa 1982), while experiments have also shown that scuffing, kicking, and trampling can move artefacts significant horizontal distances from their original points of deposition. Barton (1992) has demonstrated that movement is not only dependent on the degree of trampling but also, and perhaps primarily, on the nature of the ground surface. A soft, moist, substrate will ensure the relative stability of debitage knapped onto it, while dry, hard, substrate will less readily allow the artefacts to become anchored into the sediment. Vegetational cover will also affect the chances of pieces being caught and becoming buried.

The degree of trampling can also be related to the extent and degree of edge damage of artefacts. If burial is not rapid, for example if the sediment is hard and dry, the artefacts will remain exposed on the surface for longer with increased chance of disturbance, resulting in further horizontal spread and a greater possibility of edge damage. If trampling is a major element in the post-depositional horizontal movement of flint artefacts, then high levels of edge damage might be expected on pieces which had moved furthest, although this is not the case at Q1/A.

Conclusion

The artefacts from Unit 4c are not strictly *in situ*. It is certain that they have been subjected to a number of post-depositional processes which have altered the vertical and horizontal distribution. However, there is no equivocal evidence for the extensive 'natural' movement of pieces over several metres once they had been deposited on the ground surface. The distribution of

Table 116 Handaxes from Q1/A Unit 4b. Width=thickness

flint number	length mm	breadth mm	width mm	weight g	Roe's classification	Bordes' classification	Wymer's classification
2286	85	57	28	105.3	ovate	III amygdaloid	Jvi
3096	123	78	29	255.8	ovate	IV ovate	JKvi
3097	102	77	28	217.2	ovate	IV ovate	K

the artefacts is therefore likely to be the result of hominid activity with only slight post-depositional disturbance, though the spatial patterning can be viewed as a result of hominid behaviour.

The production of bifacially flaked handaxes can account for all of the debitage recorded from the excavated area. The production of these artefacts though does not include the complete reduction sequence but is the result of thinning and, predominantly, the finishing stage of handaxe manufacture.

There is nothing to indicate that all of the debitage in the assemblage is from a single piece of raw material. Neither is there any evidence to suggest that all of the material was knapped in a single episode. It is known from the investigation of the sediments that a stable land surface was present for many years (Macphail Chapter 2.6). The assemblage could have accumulated as a result of repeated knapping episodes over this time rather than as the result of a single short-term period of occupation by a group of hominids.

It is possible that the varying distances between groups of conjoined artefacts are not only dependent on aspects of hominid behaviour but also on the length of time that the debitage was exposed on that stable land surface. The effects of post-depositional processes, such as trampling, on the degree of spread of any initially concentrated knapping scatters, although slight, are likely to increase with the length of time that the debitage is exposed. Therefore scatters which have been exposed for varying lengths of time may result in varying degrees of spread in their debitage.

Unit 4b

During the excavation of the Unit 4c sediments in Q1/A, a test pit, Q1 GTP 8, originally dug as a drainage sump, was investigated a few metres to the south of the main area (Fig 4). During the course of excavation *in situ* flint artefacts and faunal remains were identified from within the Unit 4b sediments. The material from the pit included the limb bones of *Cervus elaphus* which had been split open with a large beach cobble on a flint anvil, and a few flint flakes. The most significant find was a bone percussor made on one of the limb bone fragments (Parfitt and Roberts Chapter 6.5). Prior to this excavation, none of the test pits in either quarry had revealed similar material within Unit 4b; it was therefore apparent that, unlike the artefacts in Unit 4c, the distribution of this lower level material was restricted. It was not part of a general spread of knapped flint across a stable landsurface but

likely to be confined and defined by the modes and environments of deposition of the Slindon Silts (Chapter 2). Accordingly, it was decided, in the light of these finds, to take the excavation in the main area Q1/A down to the second level in Unit 4b.

The level of archaeology within Unit 4b was recovered from a depth of between 0.3m and 0.5m below the interface of Units 4c and 5a. The flint artefacts from this level are in a fresher condition than those from the soil horizon, with no trace of patination, staining or abrasion. In Q1/A further *in situ* flint artefacts were discovered. Although not completely sterile, the sediment between the two archaeological levels contained very few flints. A small number of these intermediate flints have been refitted to material from Unit 4c, by Austin, which indicates that some, if not all, are contemporary with the material from this level. These pieces appear to have been subject to a greater amount of vertical movement, probably as a result of bioturbation. No similar vertical movement was apparent in the material from the main level in Unit 4b. Where it was possible to trace the laminae within the sediment, the positions of the artefacts appeared to conform to the undulating surface of a particular lamina. Across the excavated area of Unit 4b in Q1/A a general background, low density, scatter of lithic debris was recovered, which included three handaxes (Fig 236f-h, Table 116). The handaxes are typical of the Boxgrove assemblages and, as with the younger material from Unit 4c, appear to have been brought into the area rather than manufactured there; indeed there is even less debitage at this level. No flakes could be refitted to the handaxes. Associated with the Unit 4b archaeology are fragmentary remains of a giant deer, *Megaloceros* sp, the teeth of which exhibit cut marks.

The scatter

A small and extremely dense knapping scatter was discovered amongst a more general spread of apparently *in situ* artefacts, at the southern edge of Q1/A between coordinates 2260/3030 and 2330/3030 (Figs 227, 237). Even the smallest flint chips and dust were present both between and surrounding the flakes (Fig 238). As the scatter was excavated the positions of the flints were recorded using vertical photography. Prints of the photographs were made to scale and used to record the position of each flake over 5mm. A total of 1715 pieces were recorded in this way and thousands of chips between 1mm and 5mm were bagged by 0.1m squares.

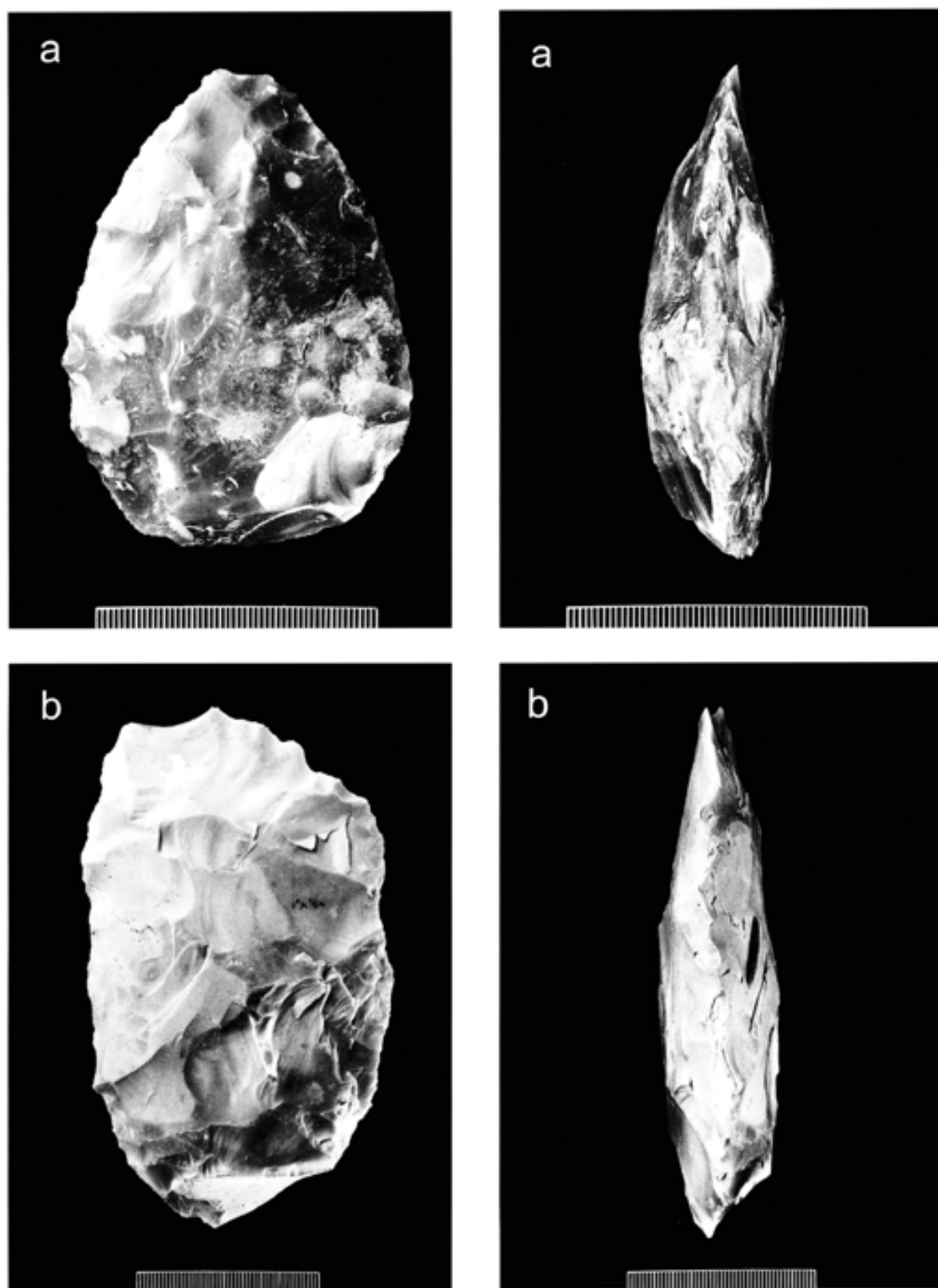


Fig 236a–h Handaxes from Units 4c and 4b at Q1/A; scale unit 1mm

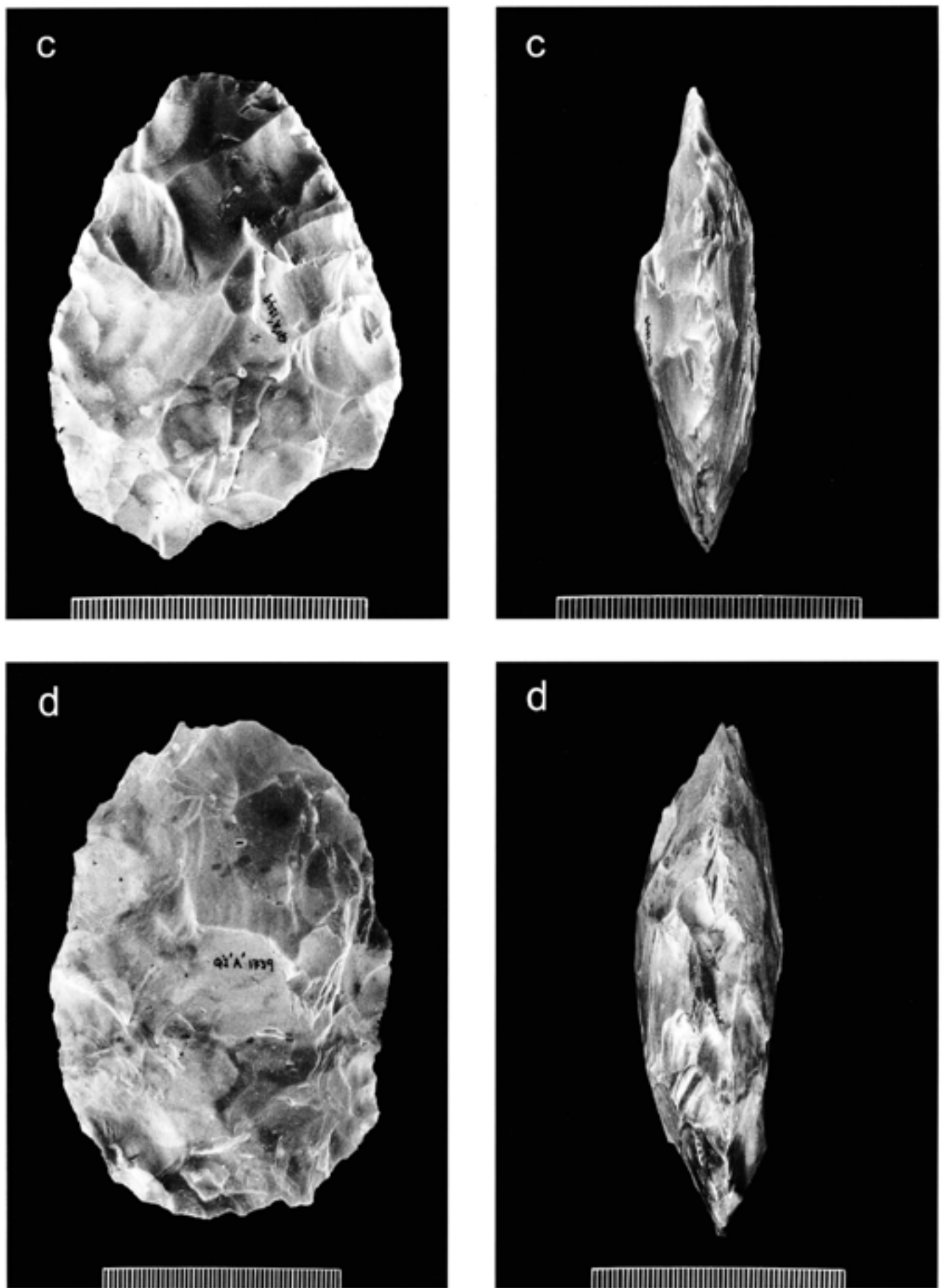
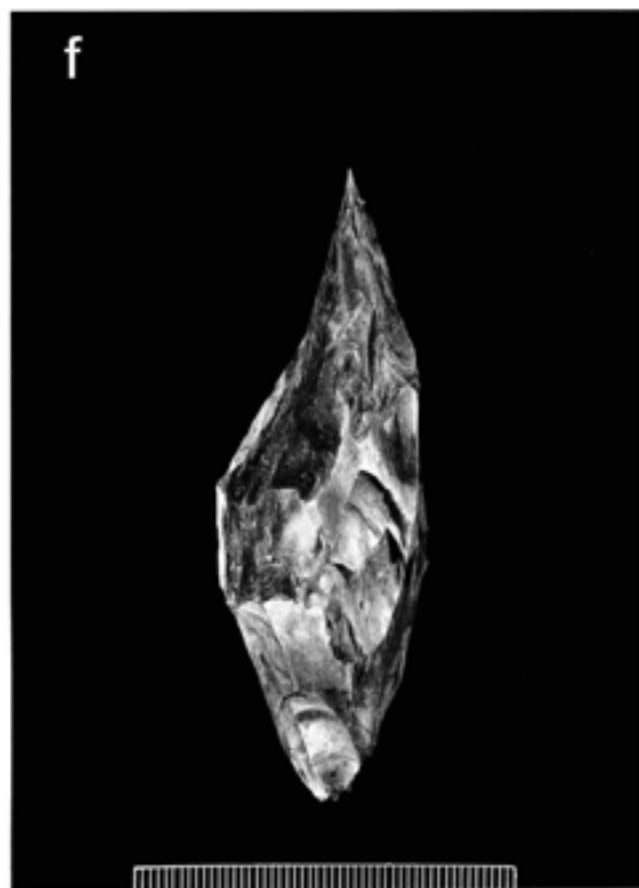
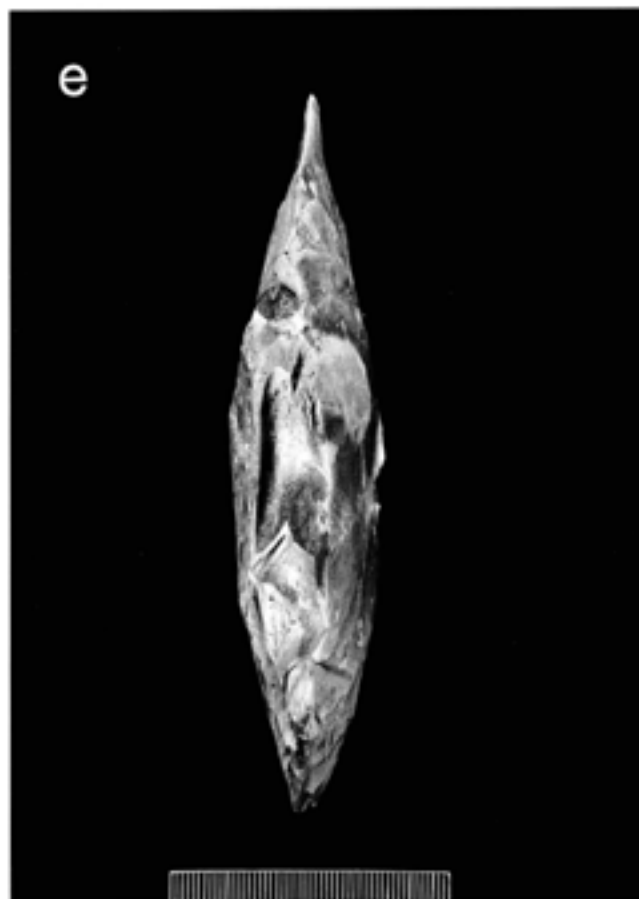


Fig 236a–h Handaxes from Units 4c and 4b at Q1/A; scale unit 1mm



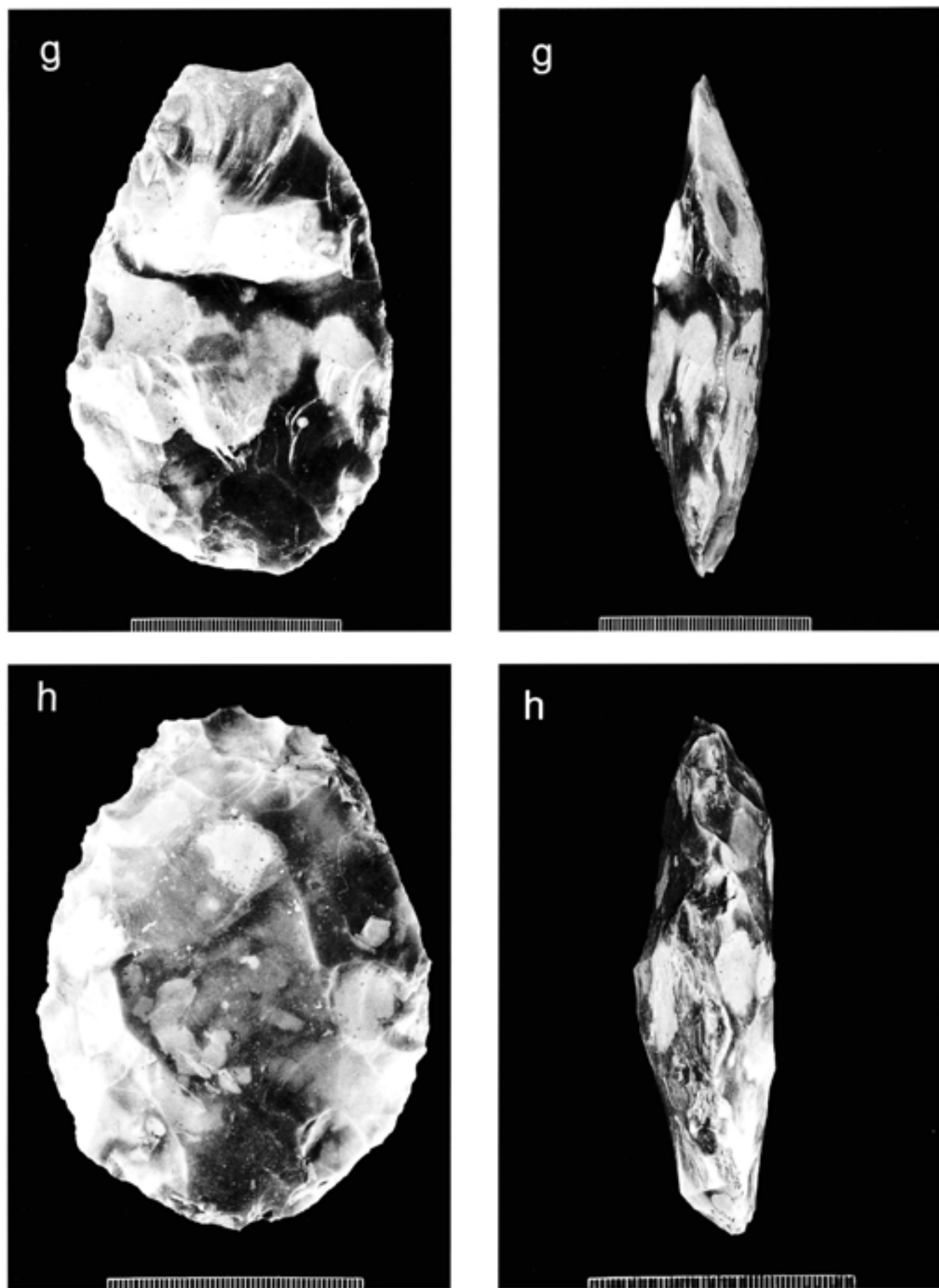


Fig 236a-h Handaxes from Units 4c and 4b at Q1/A; scale unit 1mm

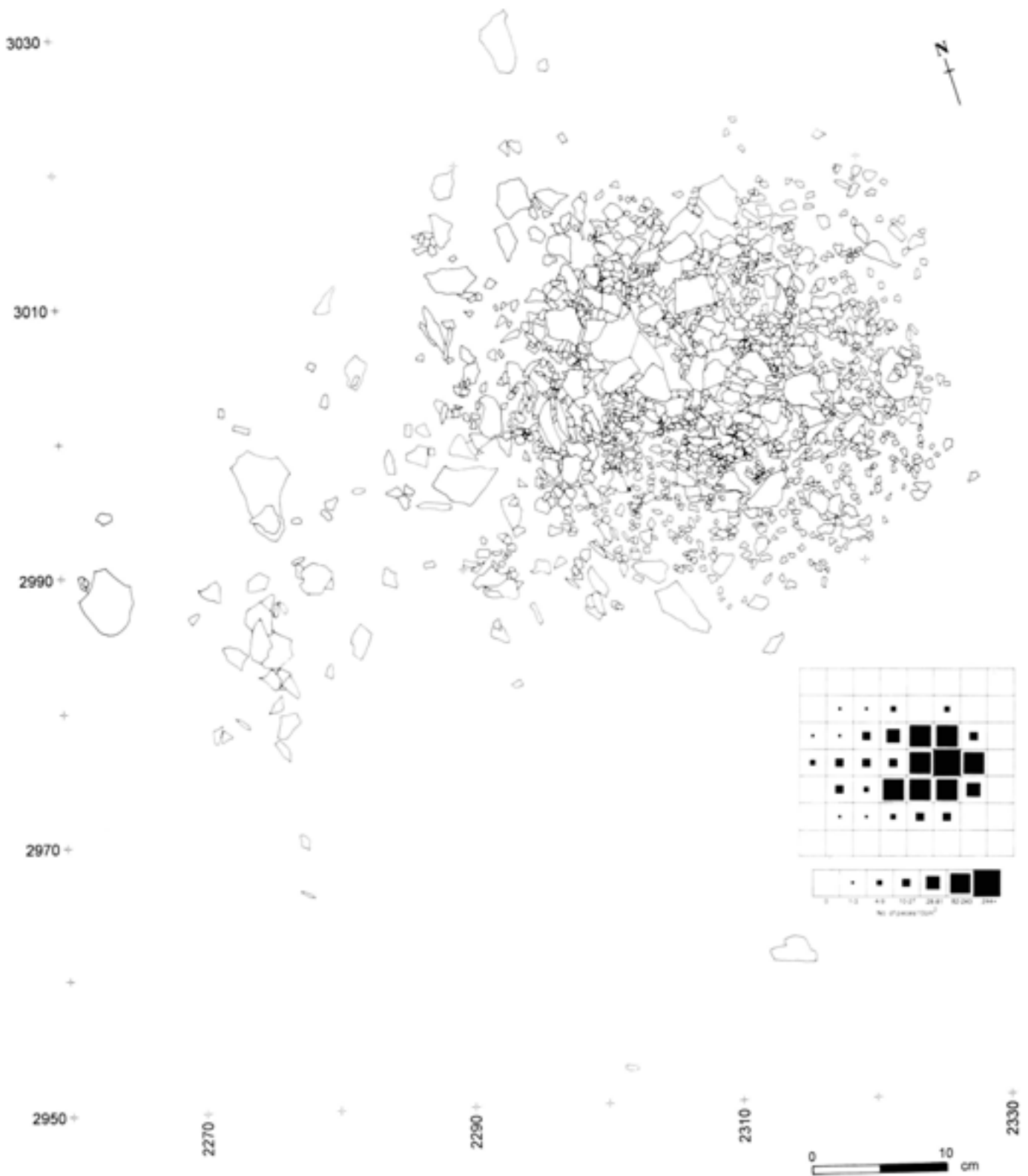


Fig 237 Scatter in Unit 4b prior to excavation; inset shows flint density (location of scatter is shown on Fig 238 (inset))

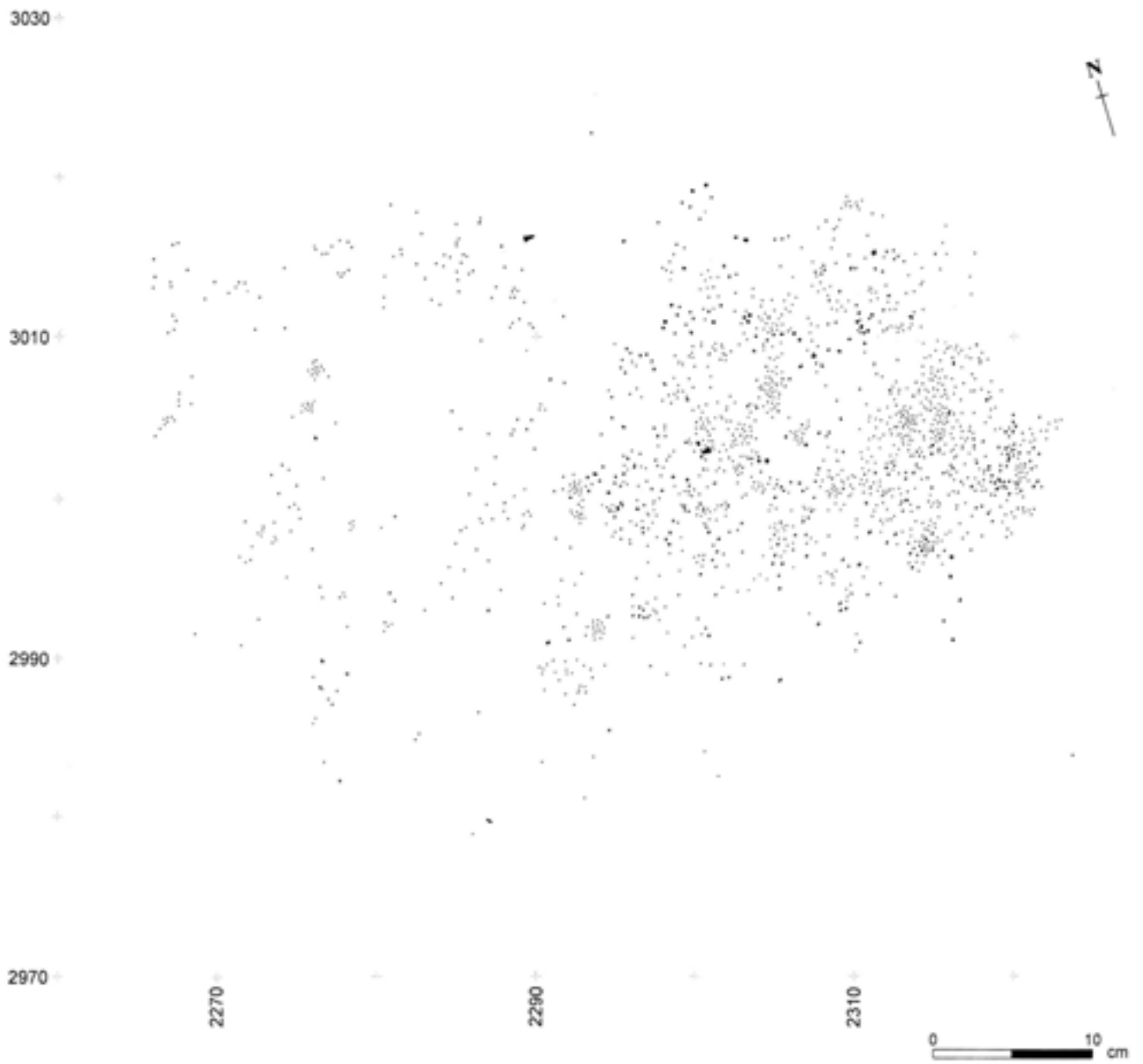
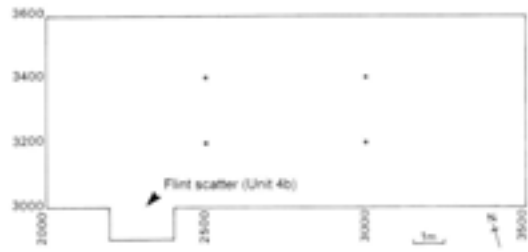


Fig 238 Spall distribution of scatter in Unit 4b; inset shows location of scatter within Q1/A



Fig 239 Unit 4b scatter after first cleaning; scale unit 50mm

Distribution

The density of the artefacts compared with that of Unit 4c was remarkable. The bulk of the scatter was restricted to a quarter of a square metre (Figs 237, 239), whereas in Quarry 2 the scatters identified in Unit 4c covered an area of over 2 square metres.

After cleaning, the scatter was found to have a very clear and definite shape (Figs 239, 240). The edges to the north and west were clear and discrete while that to the south was slightly blurred by the distribution of the smaller pieces, the density of which decreased with distance from the centre of the scatter. This distribution has a remarkable similarity to an experimental scatter produced by Newcomer and Sieveking (1971). In this example the knapper had been sitting on the ground knapping between his legs, which had resulted in the same highly defined and compact distribution of debitage (Fig 240).

In the archaeological scatter a small group of flakes were situated some centimetres to the west of the main mass (Fig 237). They had apparently been deliberately placed to one side during knapping. These flakes included the largest flake from the scatter and were later found to refit into the main refitting sequence. The knapper's intention may therefore have been to sort through them, after completing the task in hand, to pick out any flakes which might have been suitable for further use.

The concentration of debitage is at its greatest towards the west side of the triangle and along this edge a number of flints were standing vertically in the sediment (Fig 239). Due to the remarkable preservation of the original position of the debitage in the silts, study of the distribution of the flakes suggested not only the exact position on the ground where the knapper was seated during the flaking episode but also on which leg the knapper had held the original core/handaxe. From this it is therefore possible to suggest that the knapper had been holding the hammer in his or her left hand.

Debitage

The size and number of flakes from the scatter indicate that it is not the result of the complete reduction of a nodule to a biface/handaxe. Only 7% of the flakes over 5mm are greater than 20mm in length and only 12 of those are flakes greater than 40mm. Because so few flakes are above 20mm, all flakes and flint fragments over 15mm were looked at for refitting which resulted in a total of 257 pieces.

A higher proportion of the flakes were broken than in the Q1/A Unit 4c material (77%) (Tables 109, 117). This is still not as high as that of the Q2/A Unit 4c material (80%) (see Table 128).

Table 117 Number and percentage of individual fragments of flakes from the Unit 4b scatter

part of flake	number (n)	%
proximal	69	34.85
mesial	61	30.80
distal	65	32.83
siret	3	1.52
total broken	198	77.04
complete flakes	59	22.96

Table 118 Technological attributes of complete flakes from Q1/A Unit 4b scatter

category	thinning		finishing		total	
	n	%	n	%	n	%
butt type						
plain	8	50.00	7	16.28	15	25.42
cortical	1	6.25	–	0	1	1.69
dihedral	1	6.25	4	9.30	5	8.47
polyhedral	–	0	2	4.65	2	3.39
faceted	–	0	8	18.60	8	13.56
crushed/broken	5	31.25	20	46.5	25	42.37
indeterminate	1	6.25	2	4.65	3	5.08
cortex %						
0	12	75.00	42	97.67	54	91.53
1–25	1	6.25	–	0	1	1.69
26–50	2	12.5	1	2.33	3	5.08
51–75	1	6.25	–	0	1	1.69
76–100	–	0	–	0	–	0
profile						
straight	9	56.25	23	53.49	32	54.24
curved	6	37.50	17	39.53	23	38.98
indeterminate	1	6.25	3	6.98	4	6.78
dorsal scars						
unidirectional	10	62.5	37	86.05	47	79.66
bidirectional	4	25.00	5	11.63	9	15.25
multidirectional	2	12.50	1	2.33	3	5.08
indeterminate	–	0	–	0	–	0
flaking mode						
hard	–	0	–	0	–	0
soft	16	100	43	100	59	100
totals	16		43		59	

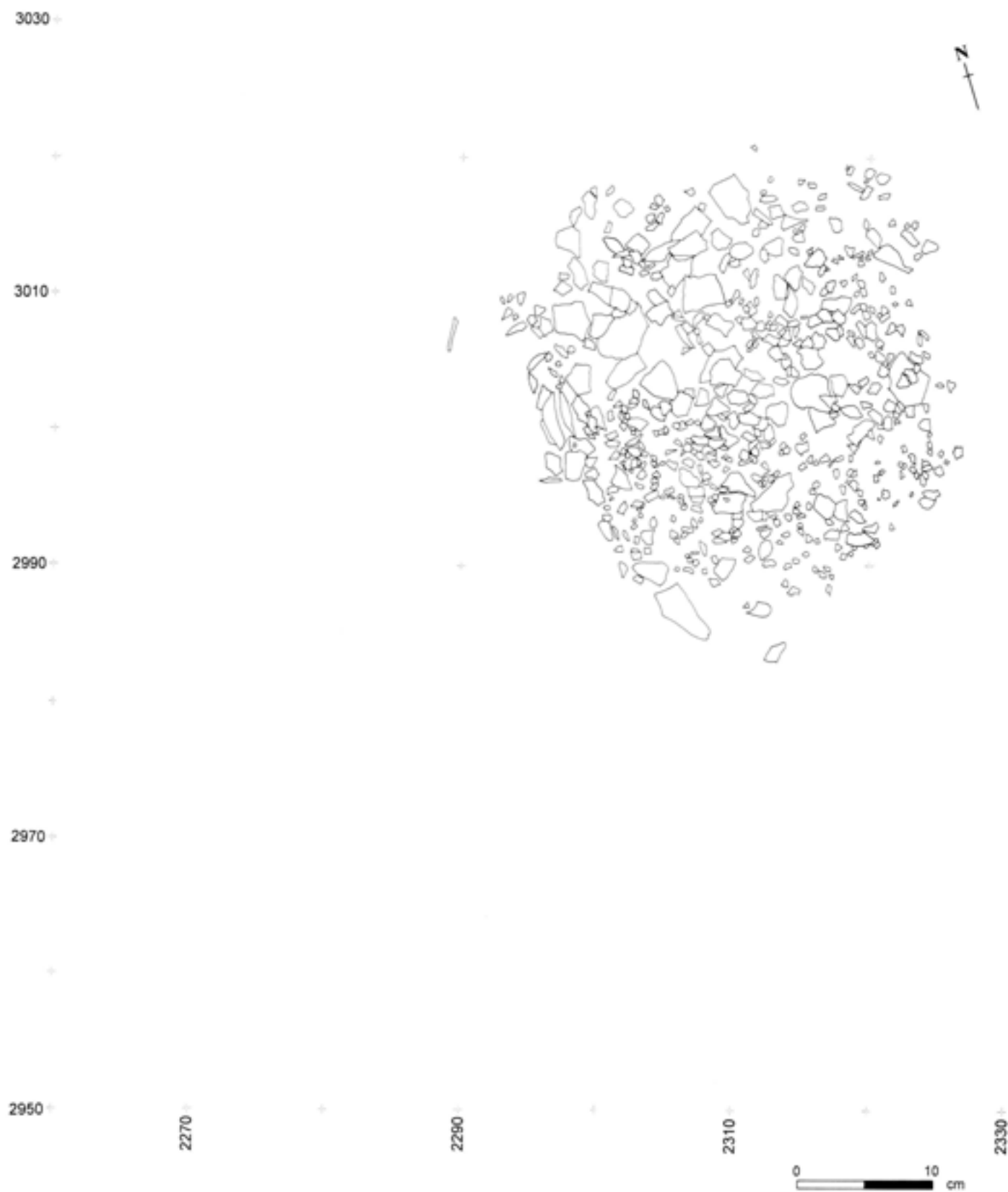
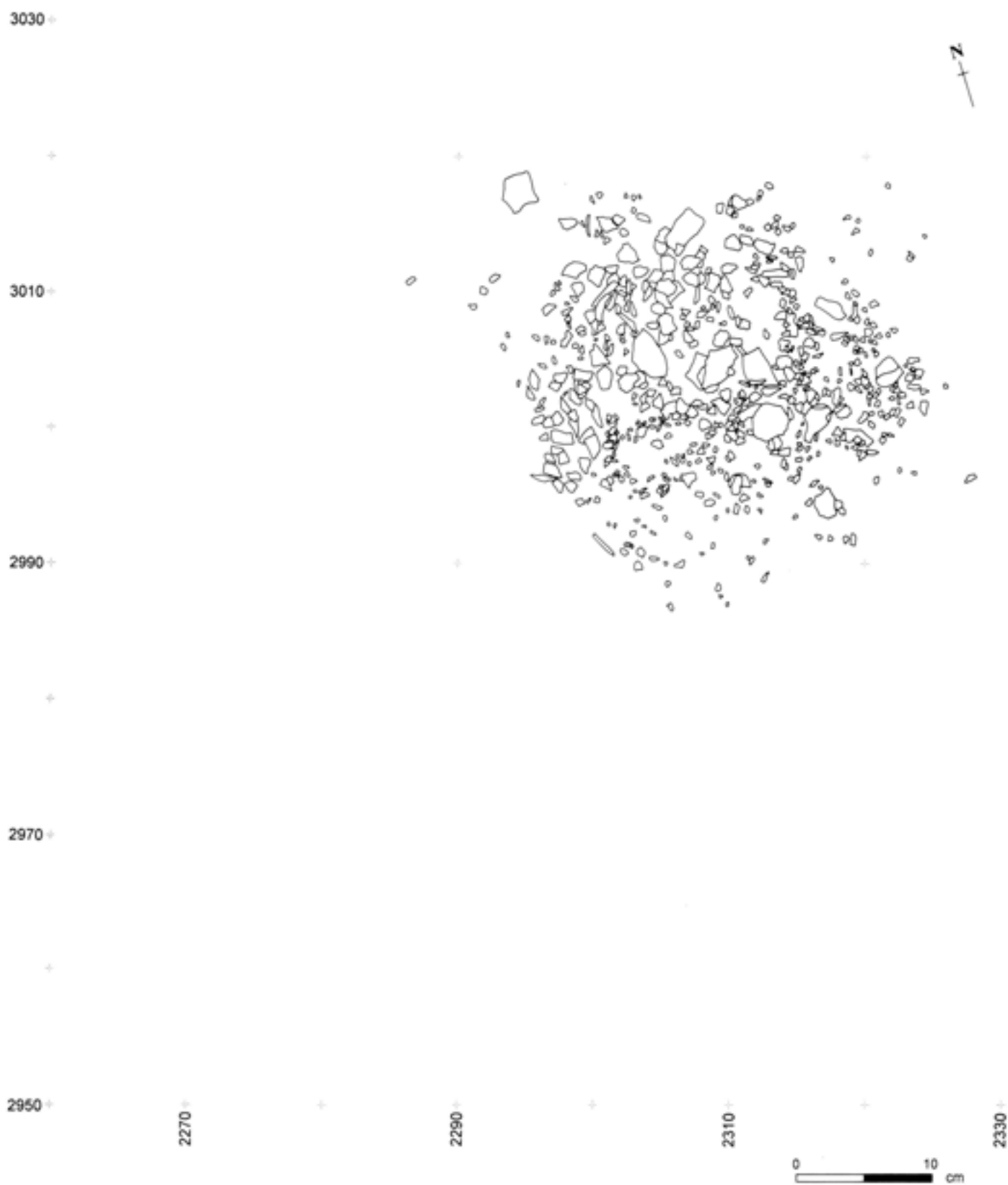


Fig 240a-e Sequential excavation of the Unit 4b scatter



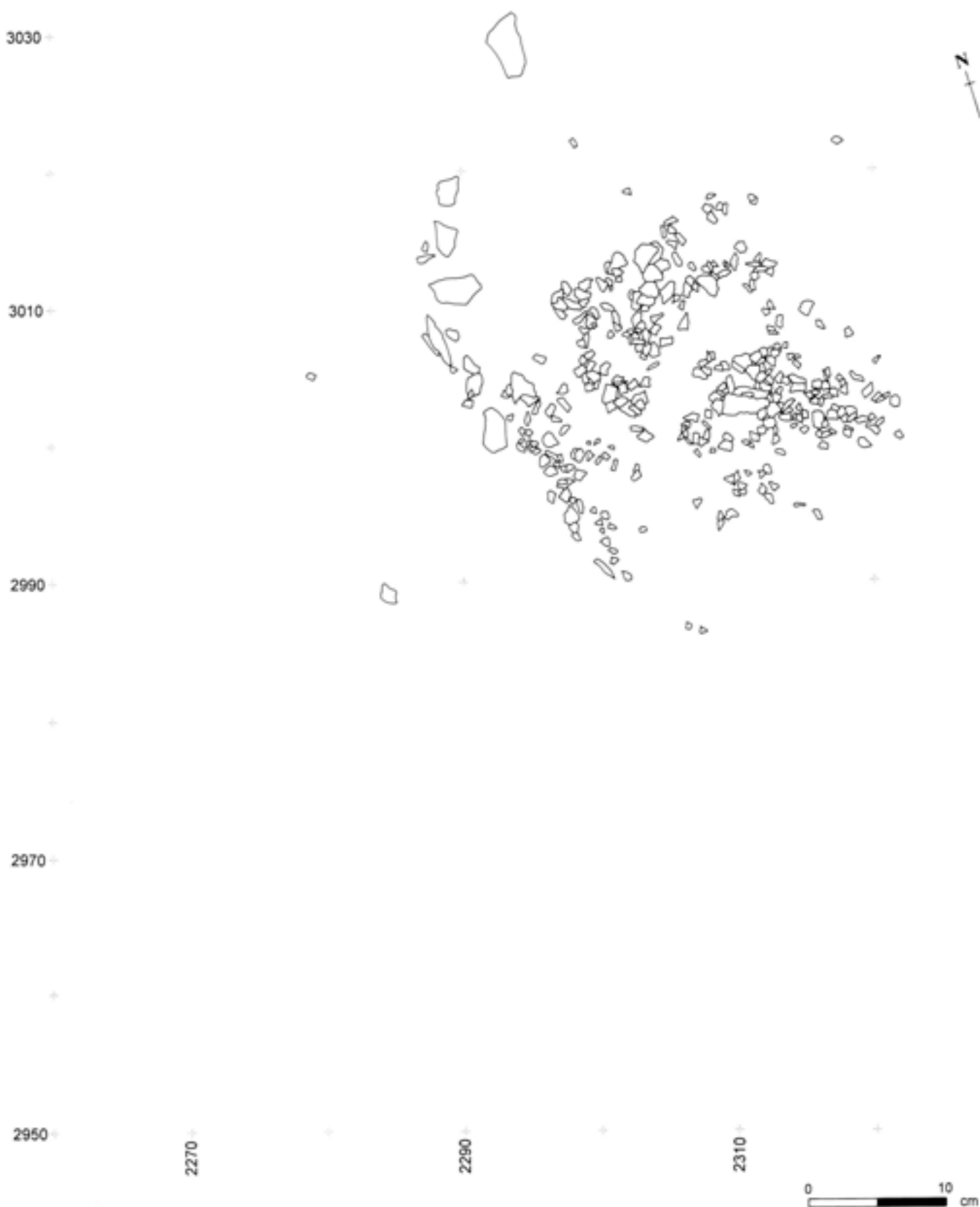


Fig 240a-e Sequential excavation of the Unit 4b scatter



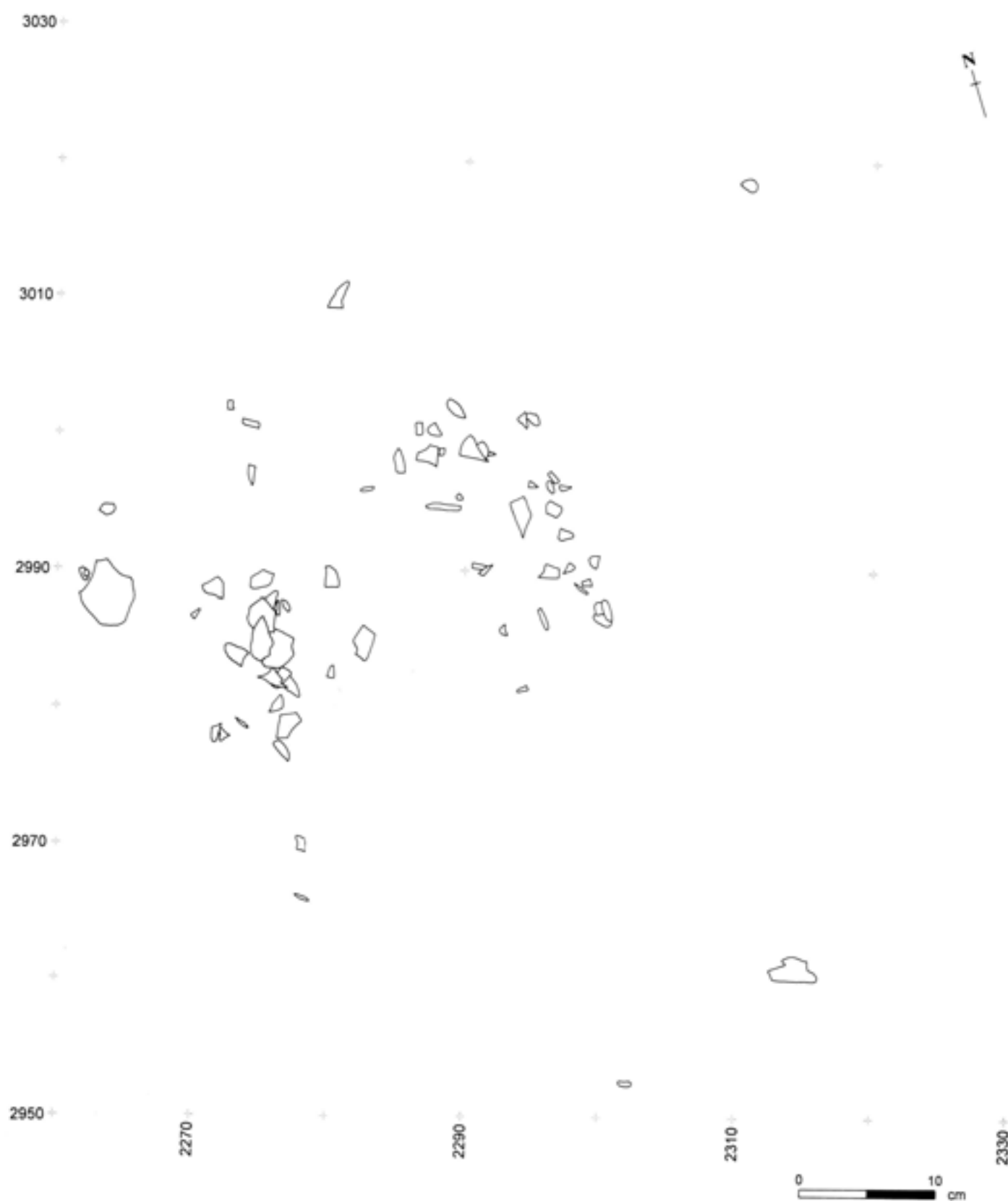


Fig 240a-e Sequential excavation of the Unit 4b scatter

Flexion breaks are the likely cause of a large proportion of the broken flake fragments. A small number of the flakes, however, appear to have been broken after knapping. The fragments of these flakes lie adjacent to each other, the broken edges either in contact or closely associated. This pattern of breakage could be accounted for either by trampling once the flake has been deposited on the original ground surface or sediment loading once the artefact had become incorporated into the sediment.

On a morphological basis the complete flakes were divided into technological groups, in a similar way to those from Unit 4c (Table 118). Only finishing flakes and thinning flakes could be identified from the three stages of biface manufacture, and no products of flaking from cores were evident. None of the flakes showed evidence of the use of a hard hammer, all being of typical soft hammer production or marginal flaking mode (Bradley and Sampson 1986). Butts, profiles, dorsal scars, and cortex were noted and are recorded in Table 118.

Refitting

Of the 198 flake fragments, 96 (48%) were refitted to one or more other pieces forming a total of 36 flakes (Table 119). The total number of complete flakes was thereby increased to a total of 95. Ventral/dorsal refits were found for 132 (51%) of the individual flakes (Fig 241), including many of the flakes made up of separate fragments (Table 120). Two sequences of over 20 flakes were found (Fig 242).

Because the distribution of the scatter was tightly confined, the possibility that it had not been knapped *in situ* was investigated. It was possible that

Table 119 Refitted breaks from Unit 4b scatter

number of pieces	number of flakes
2	20
3	10
4	5
5	—
6	1
total	96 individual pieces

Table 120 Ventral/dorsal refits from Unit 4b scatter

number of flakes in each group	number of groups
2	9
3	3
4	12
5	1
6	—
7	1
21	1
24	1
total	132 individual flakes

the distribution was the result of the debitage being dumped, in a similar way to that identified at the site of Pincevent (Karlin and Newcomer 1982). The presence of very small chips and flint dust within the scatter indicates that if the material had been dumped, it must have been knapped into a container of some description for all of the debitage to be transported.

The position of the flints on the ground and their position within refitting sequences were therefore compared (Figs 240, 241). As flakes were removed from the core/biface, the expected result would be that the later removals would obscure the earlier ones. Four pieces from one refitting group overlapped and for all of these the earlier removals were found below the later removals. Only two flakes were found to overly others in the same refitting sequence and one of these was not in the expected order. Part of the later flake to be detached had ended up beneath the previous one. On balance the combined evidence, including distribution and the presence of small chips, indicate a complete, unmoved, *in situ* knapping scatter.

From the morphological analysis of the debitage, it was apparent that the scatter was not the result of the complete reduction of a nodule to a handaxe as the amount of material was too small and there were no large cortical roughing-out flakes and only a small number of typical thinning flakes.

One of the two large refitting groups is a sequence of soft hammer removals, including 21 flakes and 31 individual pieces, from a break surface across a previously bifacially worked piece (Fig 242). The sequence resulted in the thinning of the break to form a cutting edge. The break occurred after the initial working of the piece and was not an original feature. Flake scars on both surfaces of the piece would have had points of percussion on the missing part. A number of the flakes have cortex on their dorsal surfaces.

The second large refitting sequence is made up of 24 flakes and 37 individual pieces. It is a predominantly unifaceally flaked sequence associated with a break surface. No connecting refits have been found between the two groups but it is likely that the break surface is one and the same.

The group comprises a series of soft hammer flakes removed in order to thin down a specific section of a previously worked piece. Two of the larger removals are missing from the scatter. Their complete absence suggest that they were deliberately removed. The final removal is the largest flake from the scatter and it is morphologically and typologically a thinning flake. This flake was discovered in a separate group a short distance from the main scatter and appeared to have been deliberately placed there. This suggests that the debitage may have been sorted through in order to pick out flakes which could be utilised either immediately or at a later date. It should be noted that terms such as 'thinning flake', without refitting the actual sequences, can only be broad indications of the position of a flake within a reduction sequence.

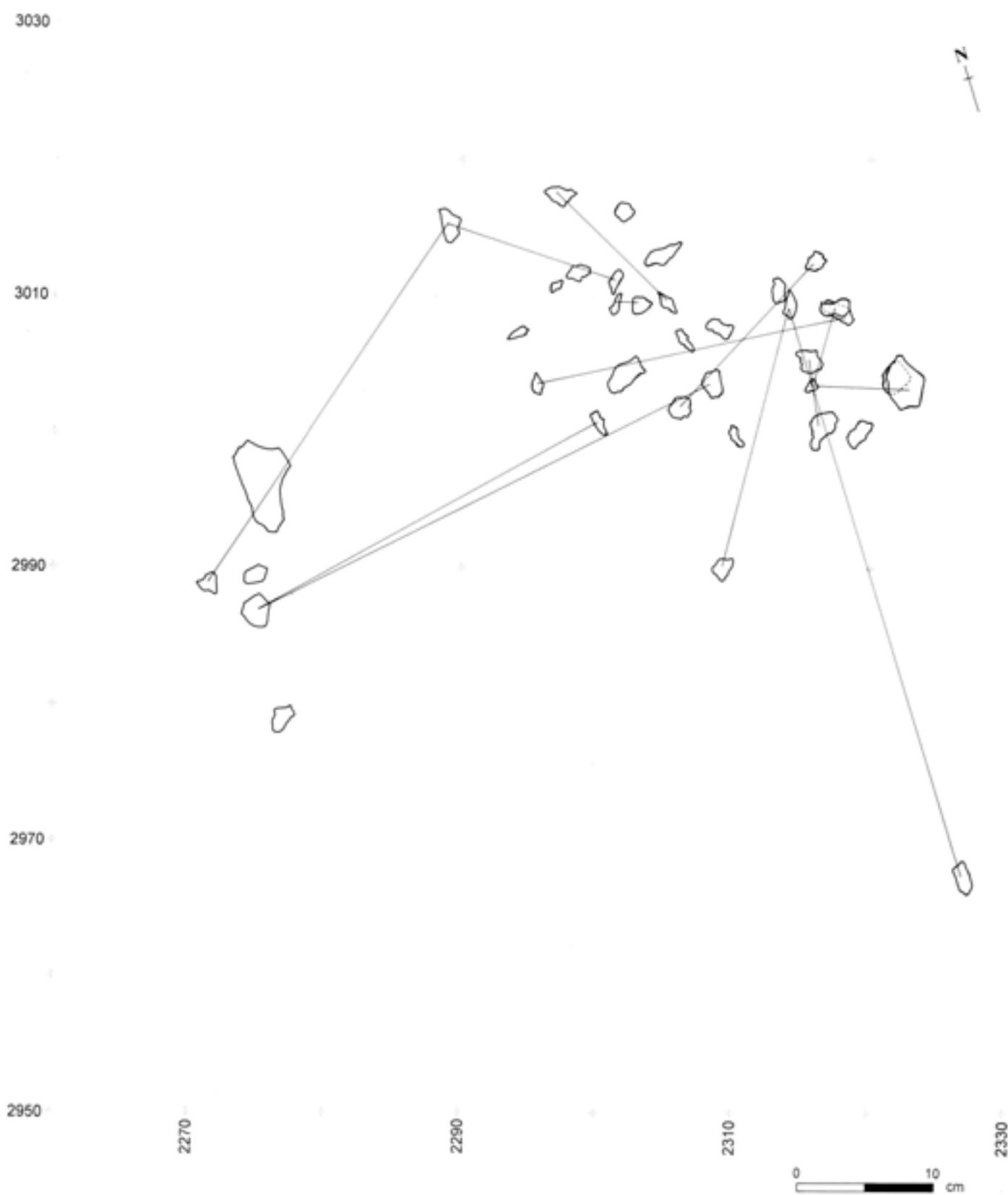
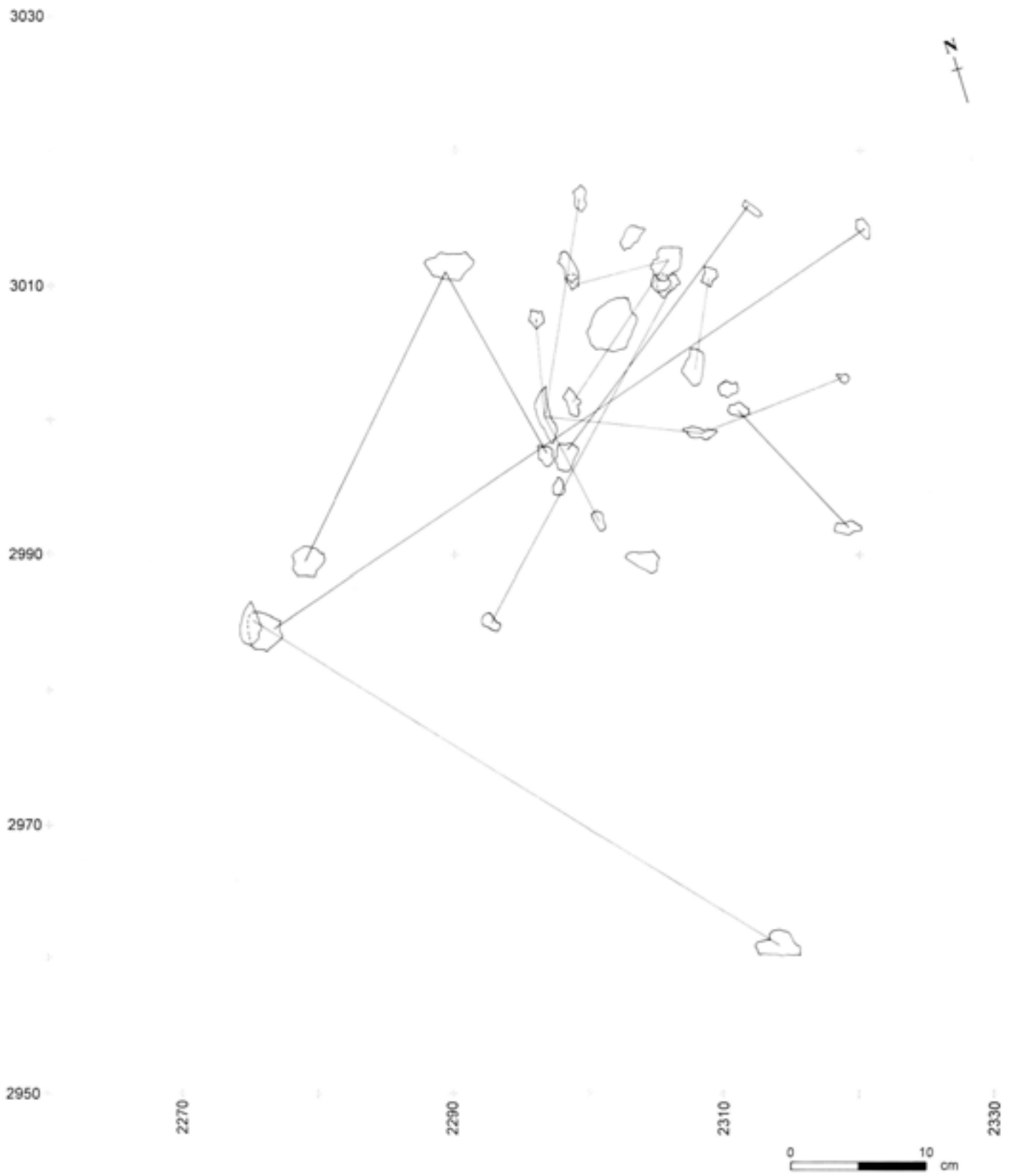


Fig 241a-c Main refitting groups from Unit 4b scatter



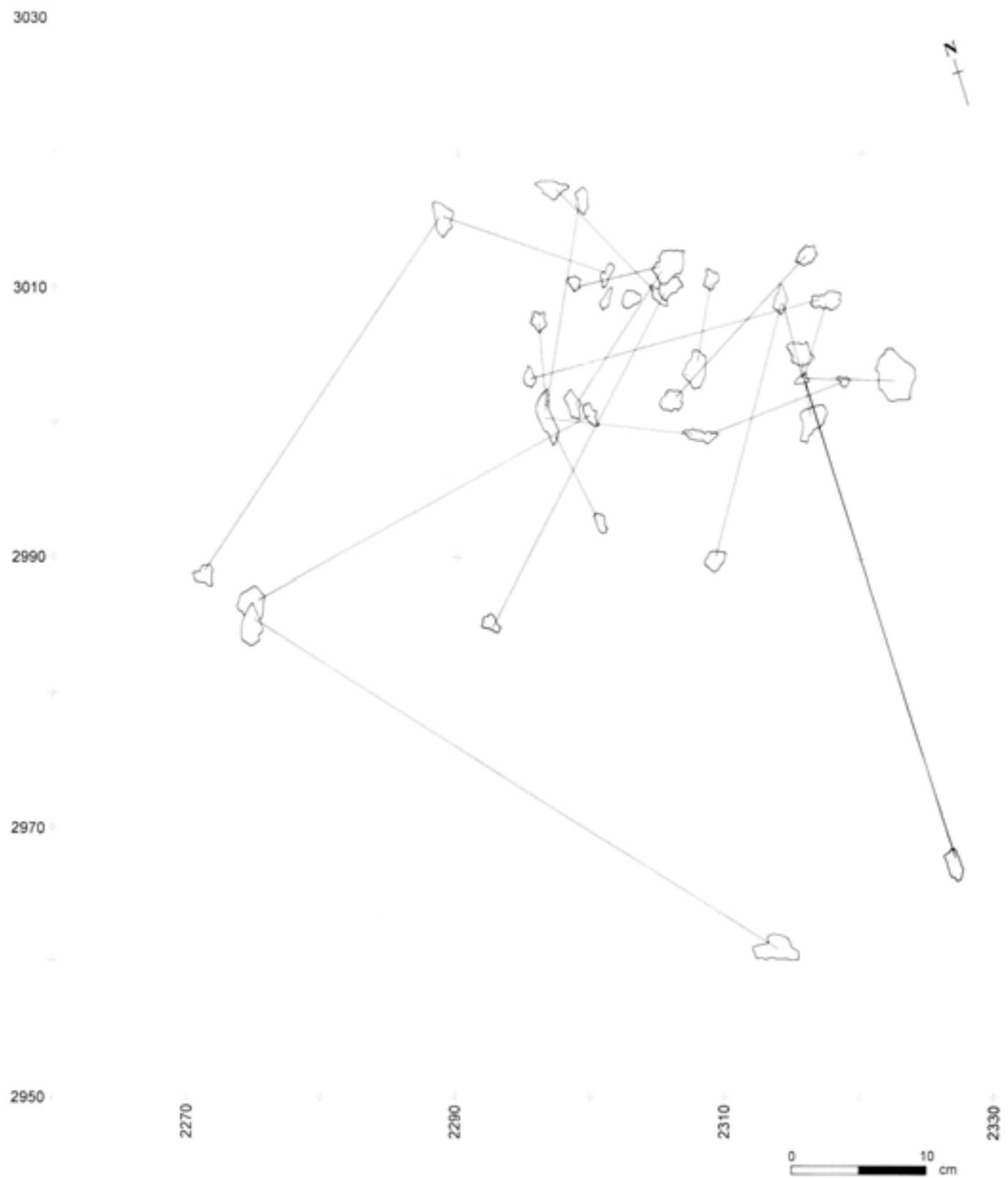


Fig 241a-c Main refitting groups from Unit 4b scatter



Fig 242 Refitting group B from Unit 4b scatter. This refitted group comprises 21 individual flakes

The scatter is the result of the final thinning and finishing of a bifacially worked handaxe. The initial stages of reduction are not present. The break surface, having occurred on an already partially worked piece, is likely to be the result of end-shock. This phenomenon has been noted in a number of unfinished handaxes at Boxgrove and also at other sites such as Caddington (Sampson 1978), where end-shock was a persistent problem. Ten out of twenty-five handaxes suffered from end-shock and most of these cases were associated with the thinning stage of manufacture.

Quarry 1 Area B

L A Austin and M B Roberts

Introduction

Between Q1/A and the line of the relict chalk cliff a second area excavation was undertaken in Quarry 1 (Fig 4). The purpose of this excavation was to uncover a large area of the palaeosurface of Unit 4c (Fig 35). The information obtained could then be used to get a better idea of the activities which took place on this surface, and provide a basic understanding of the use of available space by the tool makers and users who occupied the area between the cliff base and the sea.

In keeping with this objective, the strategy of excavation was adapted to enable the work to be undertaken at a faster rate than at Q1/A and Q2/A. All pieces over 20mm were recorded two dimensionally, with the height of each piece ascribed to the 20mm spit by which the sediment was excavated. The area was excavated stratigraphically, with the spits subdividing the geological Units 4c and 4d. Pieces smaller than 20mm were bagged by spit and metre square.

Q1/B is located approximately 60m south of the relict cliff-line (Figs 4, 29). At its extreme western edge the geological succession was similar to that found in Q1/A and GTP 26 (Figs 4, 35), and thus part of the normal conformable sequence found in the quarry complex. However, in addition to the normal calcium carbonate-rich nature of deposits encountered this close to the cliff, a new highly calcareous silt was discovered. This sediment, Unit 4d (Table 9a), interdigitated with and partially replaced Unit 4c throughout

the area investigated at Q1/B. Field evidence procured during excavation strongly suggested a source for the unit further to the north and east in Q1/B, as the unit thickened in this direction. Another feature associated with Unit 4d is the deformation of the underlying sediments of Unit 4, the Slindon Silts. This deformation was similar to that encountered at the Q1/A gully feature (Austin and Roberts above). The soft sediment deformation was caused by differential pore water expulsion rates from silt beds and silty clay laminae, to meet a pressure front created by the emplacement of the overlying colluvial chalky gravels. Common features of this are upward cresting flame structures, festoons and downward injection of overlying chalky gravel. In some places the deformation has almost totally removed the primary bedding structures. The concept of a wet area as attested to by the deformation of the Slindon Silts, is supported by the work of Macphail (Chapter 2.6), who has shown that Unit 4d is likely to be a spring deposit deriving from the chalk cliff; this hypothesis is further supported by study of the fish (Irving and Parfitt Chapter 3.4) and fauna from Unit 4d (Parfitt Chapters 4.2 and 4.3).

The archaeology recovered from Q1/B during this period of excavation came only from Unit 4c and its time equivalent unit, depositionally, Unit 4d. Further work on the spring deposits and the underlying Slindon Silts and Sands was undertaken between 1994 and 1996; this period of work revealed the Boxgrove hominid remains and will be published in a separate monograph.

A total area of 120m² was opened in four trenches; each area measured 5m by 6m. These trenches were numbered 1 to 4 from east to west. The majority of the artefacts were recovered from Trenches 1 and 2; Trenches 3 and 4 were only partly excavated and Trench 5 was not opened until 1993 (Fig 243).

Distribution

Flint material was recovered from all four of the trenches within Area B; however the distribution of pieces between the trenches was not even (Figs 244–7). Within each trench specific concentrations of material were evident and the more generalised spread of material recognised in Q1/A Unit 4c was not present. Trenches 1 and 2 contained the vast majority of the flint; Trench 1 had 176 pieces >20mm and Trench 2 had 480 pieces >20mm. Trenches 3 and 4 combined had 50 pieces >20mm. The density of flint per metre square varied in Trench 1 from 1 to 17 pieces, while in Trench 2 the range was from 0 to 77. Clustering of flint in particular areas of the trenches is therefore evident and can be seen in the plans of the flint distribution at Q1/B (Figs 244–7).

As stated, this distribution, with its areas of marked concentrations of artefacts, differs greatly from that seen in the distribution of the artefacts in Q1/A (see above). The general spread or 'background scatter' of

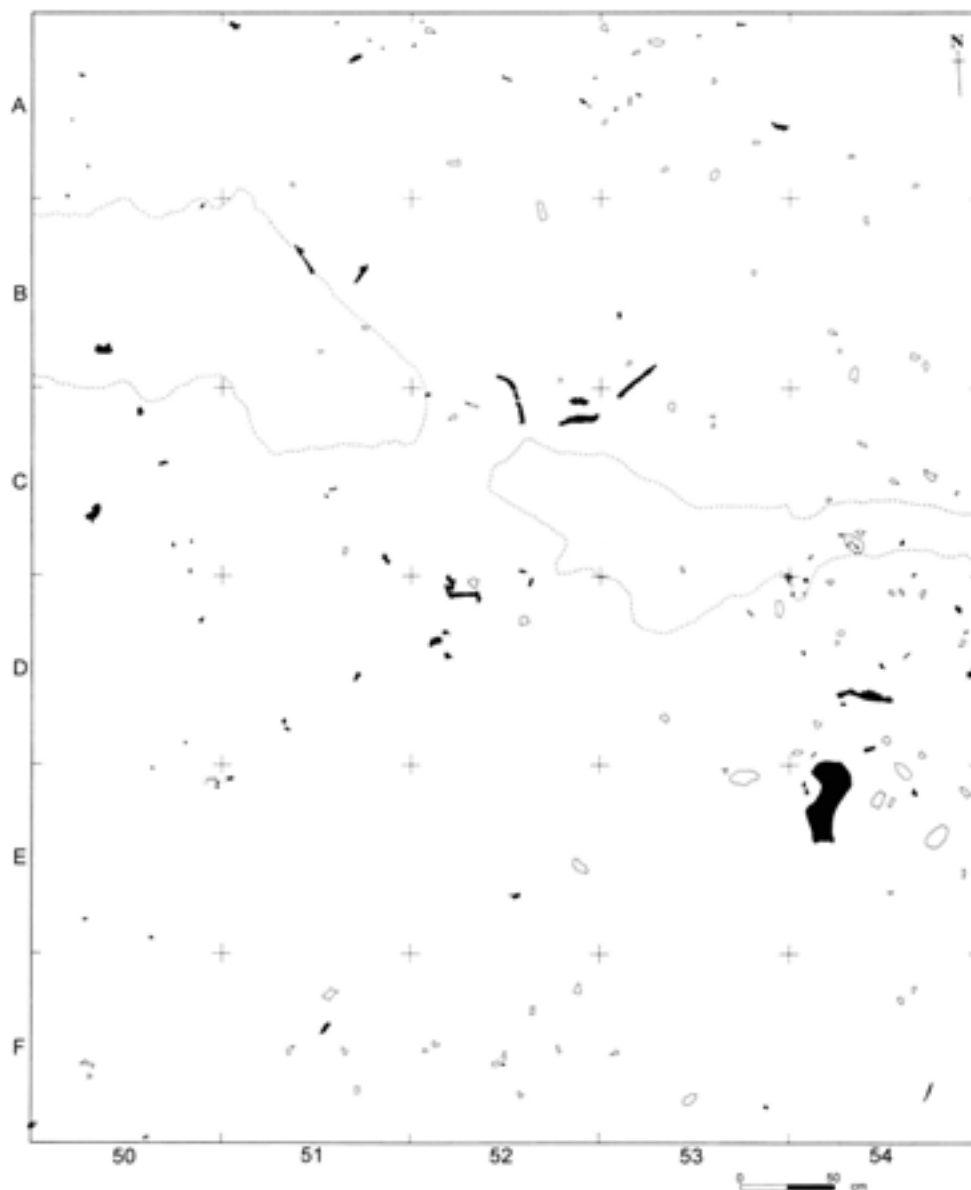


Fig 244 Flint and fauna distributions at Q1/B Trench 1, fauna infilled and stippled

Q1/A is not evident, and where artefacts do occur they tend to form smaller/tighter clusters. There are a number of possible reasons for the differences in the distribution of artefacts between Q1/A and Q1/B. They may represent areas where two entirely different activities occurred, or where different aspects of different (or similar) activities were revealed by the location of the excavated trenches. Alternatively, the different scatter patterns may reflect different post-depositional modification processes affecting the two locations.

The debitage from areas Q1/A and Q1/B is the waste from handaxe production. There is very little difference in the proportions of flake types recovered from the two areas (Table 121). This indicated that, as far as tool production goes, the same activity was taking place in both areas, and in much the same way. Therefore tool production itself cannot be responsible for any differences in distribution.

As already discussed, whether the knapper sits or stands can alter the concentrations of debitage left behind after handaxe production considerably (Newcomer and Sieveking 1976). To match like with like, however, it is necessary to identify that the same part of the reduction sequence is being compared, and that in both cases the original position of the knapper is known. In Q1/A Unit 4c it was not possible to do this.

Since both areas are so close (Fig 4), the macro-scale post-depositional processes which have affected them are unlikely to be different. Simple explanations such as fluvial activity affecting Q1/A and not Q1/B are unlikely, since the proportions of debitage present in both are broadly similar (Table 122). It is only within the local microenvironment that there may be totally different processes occurring. It is, therefore, the varying extent to which similar processes have affected the two assemblages which will have caused the differences in distribution.

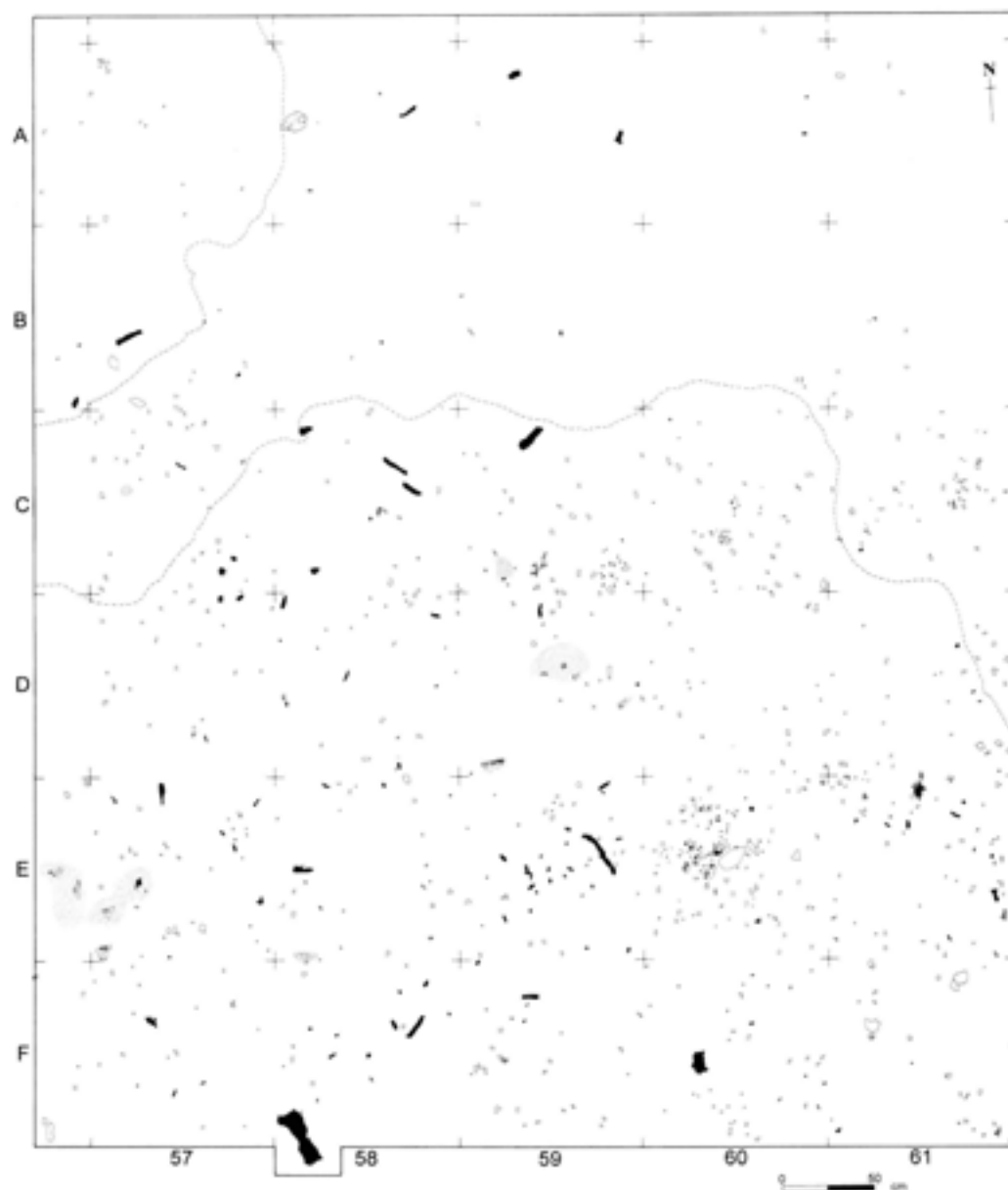


Fig 245 Flint and fauna distributions at Q1/B Trench 2

The rate at which flints were incorporated into the sediment will have affected the length of time that the assemblage was exposed on the surface, and therefore the time that processes such as surface water flow and trampling will have had to take effect. If the debitage in Q1/B was buried relatively quickly then the original scatter density could have remained largely unchanged. Conversely, if the debitage in Q1/A was incorporated into the sediment less rapidly, more time would be available for the scatter to become increasingly more dispersed. How the ground surface conditions affect artefact distribution has already been discussed earlier in this chapter (Barton 1992). Therefore, in the absence of other data, it is the state of the ground surface on which the debitage fell, and consequently the length of time that the debitage was exposed, that is tentatively considered to explain the initial differences in the scatter patterns noted between Q1/A and Q1/B.

This conclusion is supported by the evidence for a wetter, flooded, surface at Q1/B, where the soil horizon of Unit 4c could only form at the western edge of the area. Thus, it is likely that artefacts at Q1/B were buried more quickly and were in contact with a more plastic substratum, *contra* Q1/A. Additionally, the preservation of mink scats (Macphail Chapter 2.6, Parfitt Chapter 4) in Q1/B attests to rapid burial of the land surface.

The assemblage

The raw material from which these artefacts have been produced comprise fresh, unrolled nodules from the chalk. This is evident from the condition of the cortex. The flint is a mid-grey colour with frequent lighter grey inclusions and occasional flaws. Separate nodules vary slightly but are not always easily distinguishable.

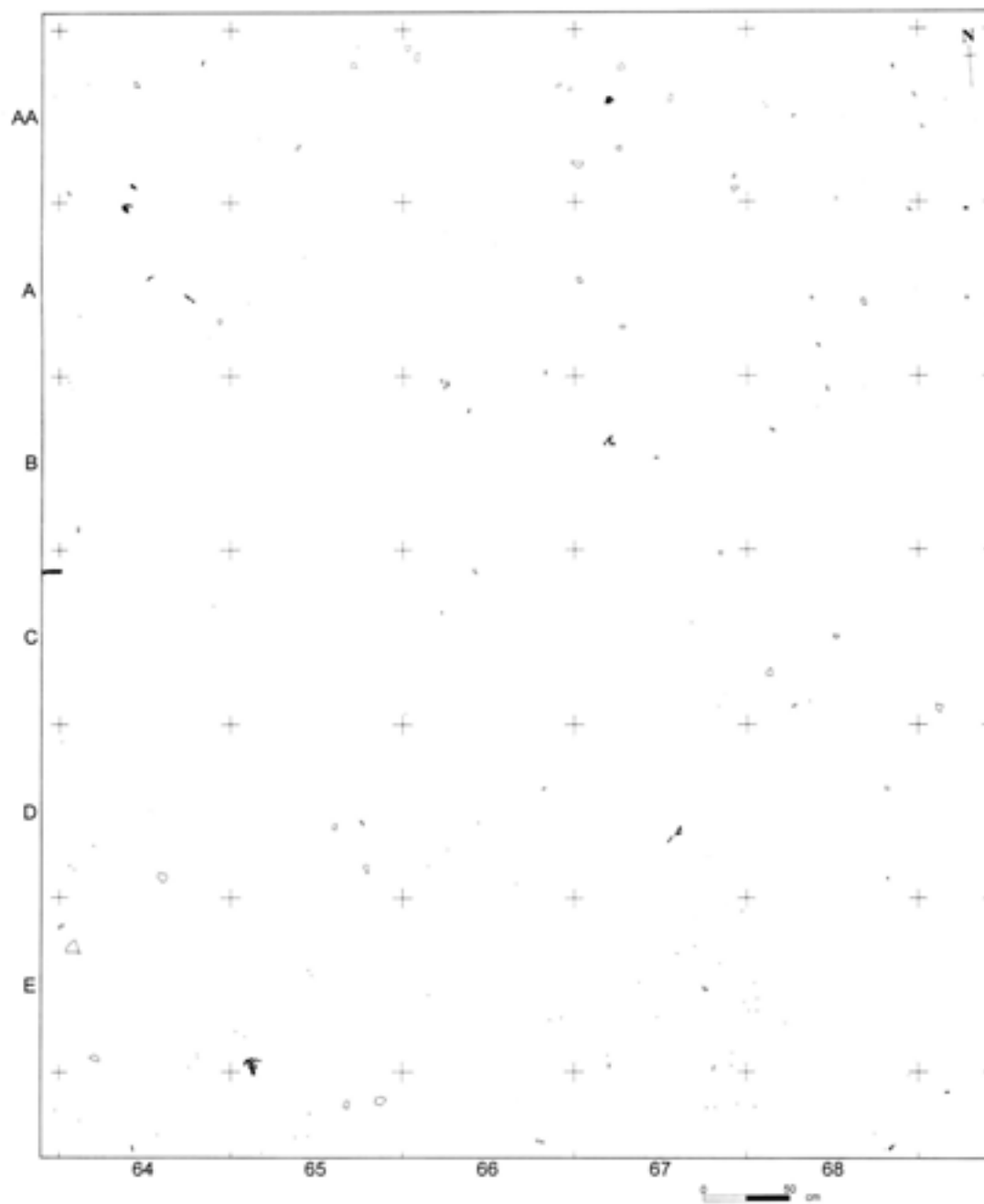


Fig 246 Flint and fauna distributions at Q1/B Trench 3

The number of flint artefacts over 20mm totals 706 from the four trenches. This comprises flakes, tools, and rare cores and hammerstones (Table 122, Fig 248).

The majority of the assemblage is in a fresh condition with only 5.7% showing signs of edge damage. Most flints (80%) are patinated to varying degrees, the vast majority having only very slight patination. 31% of the assemblage is stained with iron salts.

Natural abrasion is evident on 1% (six pieces) of the assemblage. These rolled pieces appear to be unrelated to the rest of the assemblage due to their condition and are therefore believed to be reworked by natural processes from earlier deposits within the

Quarry 1 sequence, possibly from the beach to the north. Of these six rolled pieces, two are heavily stained with the rest being either patinated or stained.

The remaining edge damage is considered to be the result of 'spontaneous retouch' (Newcomer 1975), or accidental damage, or use wear (Keeley 1980). In the majority of cases the damage is no more than occasional small notches (<20mm) or breaks along feathered lateral, or distal, edges of flakes. This abrasion is considered to be natural in origin, most probably a combination of accidental damage and trampling. A few pieces are interpreted as showing evidence of intentional use wear. These pieces are discussed below.

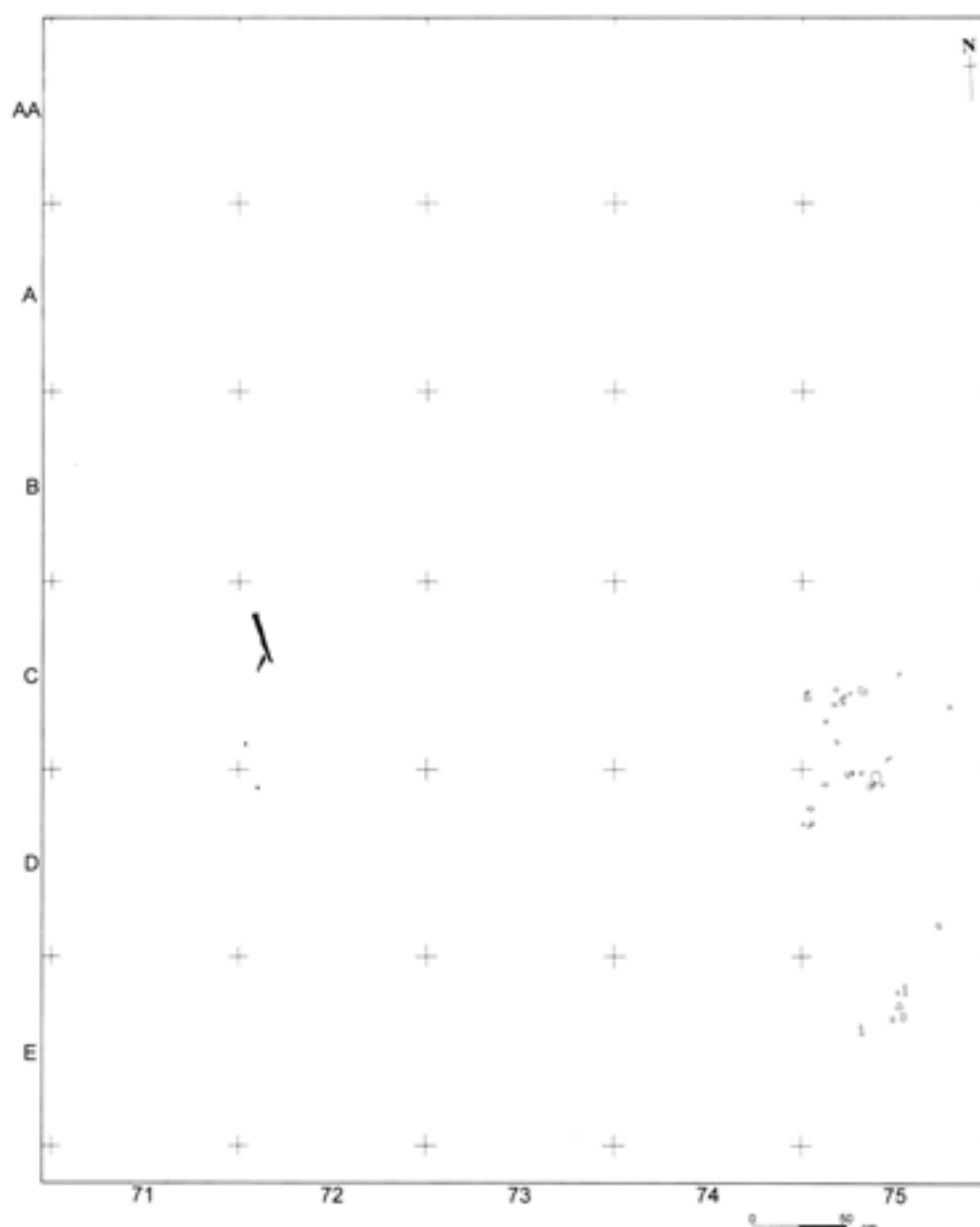


Fig 247 Flint and fauna distributions at Q1/B Trench 4

Tools

Eight handaxes were recovered; five from Trench 1 and three from Trench 2 (Table 123). A brief description of each handaxe follows (Fig 249):

- 1 (Fig 249e) A thick, heavy ovate handaxe. Two tranchet removals from opposite faces of the piece have been used to sharpen the same edge. The rest of the edge is regular and carefully finished except for a short length on the opposite edge to the tranchet sharpening where cortex has been retained. It is quite heavily iron-stained with moderate patination.
- 2 (Fig 249h) Irregular, thick and heavy, this handaxe has no tranchet sharpening. None of the edges have been particularly carefully finished and it is possible that it was abandoned before final finishing. There is cortex in the centre of one face and along a short part of the edge. On one face there is moderate iron staining while on the other the staining is heavy with the whole piece being moderately patinated.
- 78 (Fig 249a) This is a very fine and well finished handaxe. There are the remains of a scar, possibly resulting from a tranchet sharpening blow across the tip, but this has been masked by subsequent retouch, damage or use wear. A small amount of cortex remains on one face and on a short length of the edge. It is not stained and only slightly patinated around the remaining cortex.
- 95 (Fig 249g) Irregular and thick, this handaxe was abandoned before it was finished. It is the only tool from Q1 to which flakes have been refitted. There is cortex in the centre of one face and along a short length of the edge on the opposite face

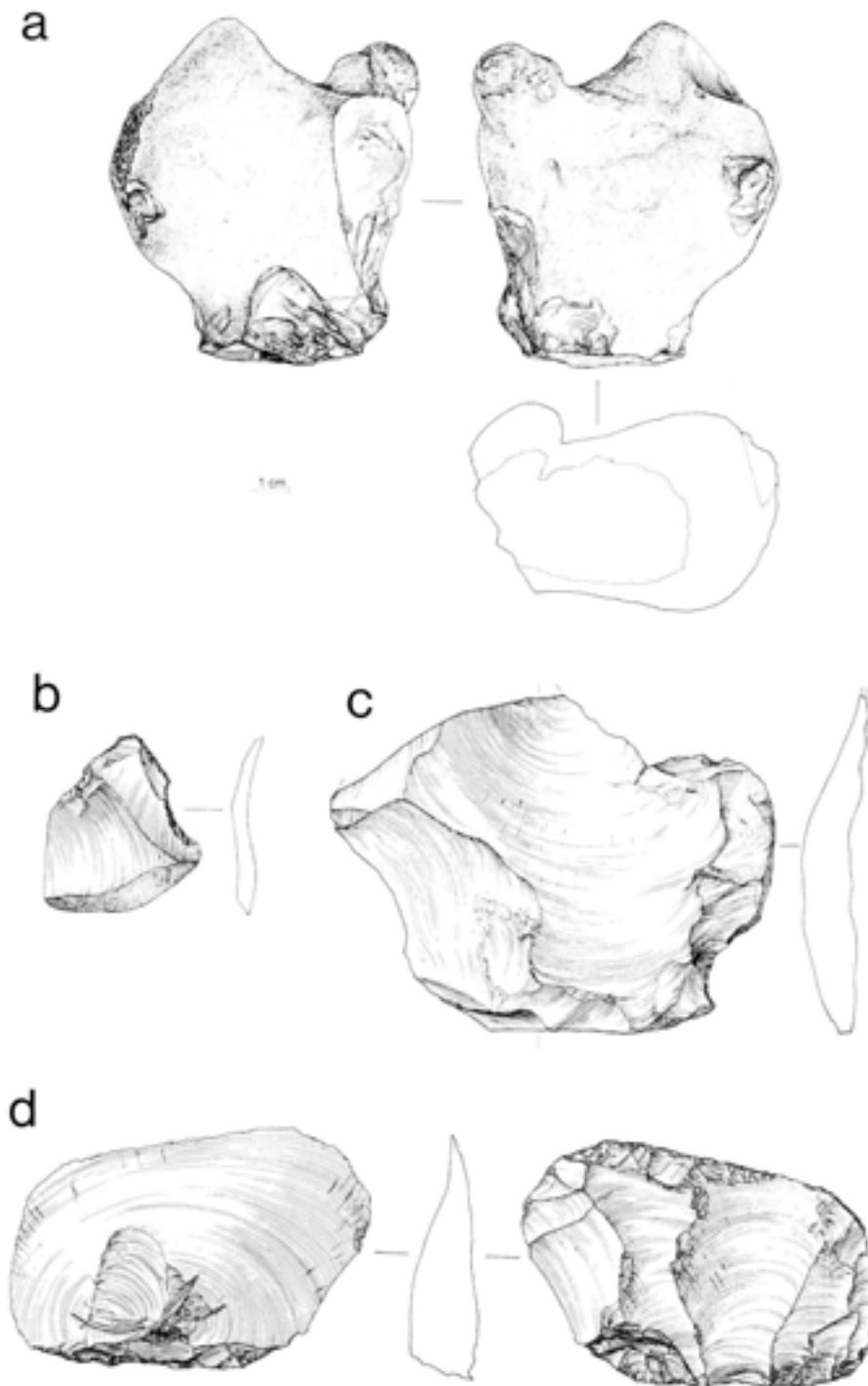


Fig 248 Hammerstone and flake tools from Unit 4c, a) hammerstone (Q1/B) b) retouched piece (Q1/B), c) flake/notched piece (Q1/B), d) transverse scraper Q1 GTP 27

towards the butt end. The handaxe was roughed out and partially thinned elsewhere before being transported into the excavated area. At least three flakes were subsequently removed from the piece before it was abandoned. A large crystalline inclusion was visible in the handaxe when these final removals occurred, two of which were attempted from the opposite face. The first of these hit a flaw in the flint and a lump was broken out of the working edge of the handaxe. A second removal adjacent to this failed to even up this damage.

The third removal was at the butt end of the piece and could have been made before or after the other two. It appears that once the working edge of the tool had been broken the knapper did not consider it worthwhile attempting to rethin and shape the handaxe tip in order to obtain a new working edge and the piece was therefore abandoned.

96 (Fig 249c) A regular and finely finished handaxe. The tip has been sharpened using a tranchet blow. The possible remains of an earlier tranchet removal survive on the opposite face. It has been

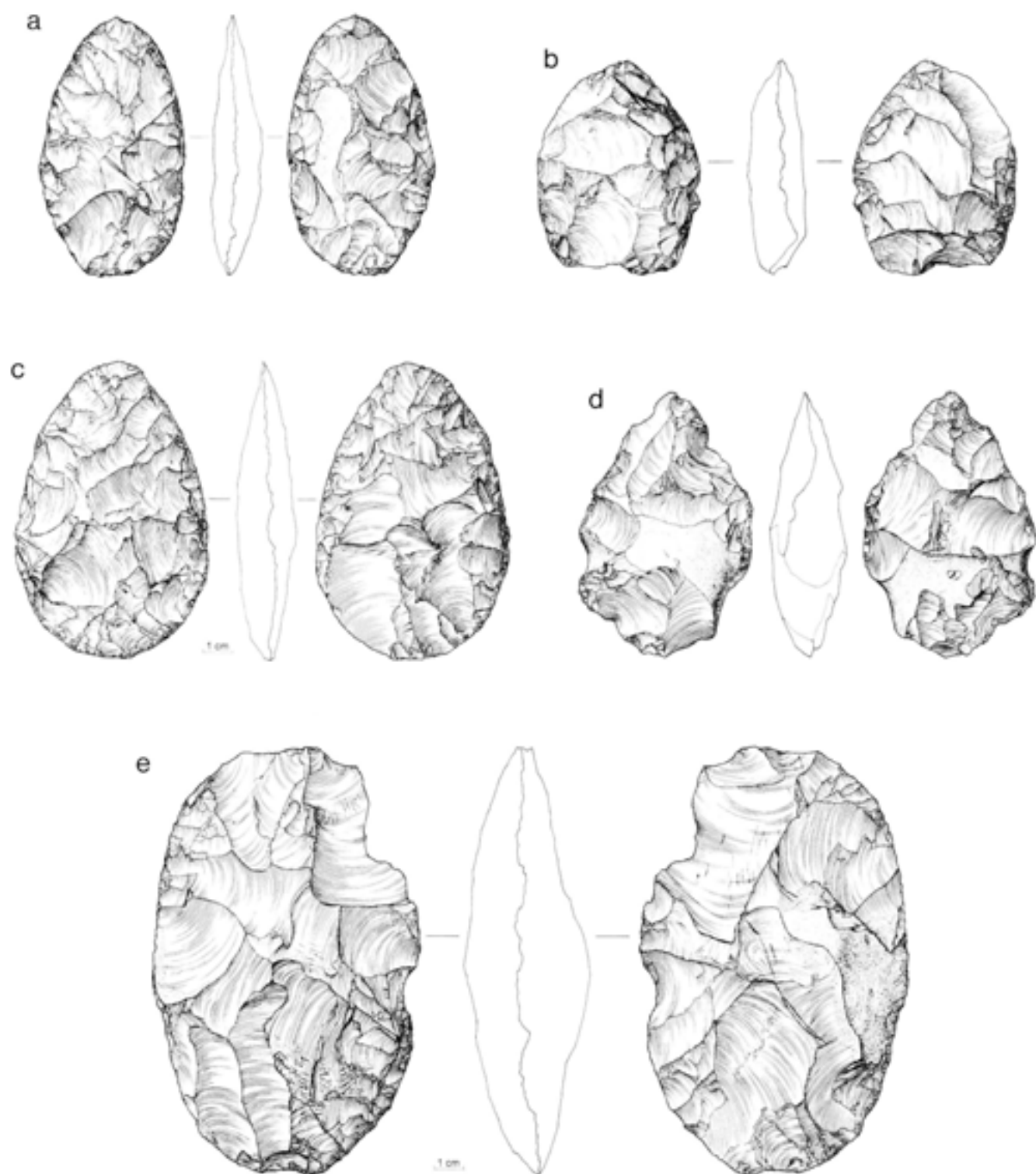


Fig 249a-h (above and facing) Handaxes from Unit 4c at Q1/B

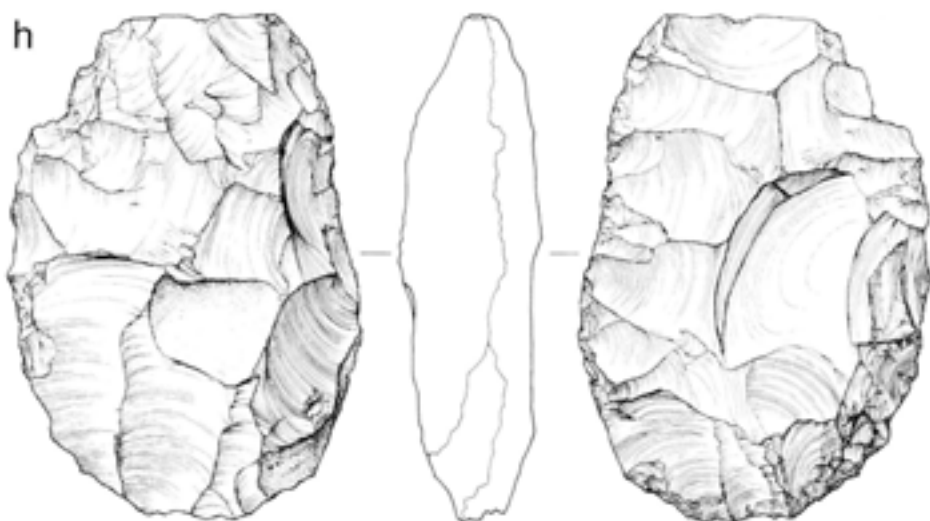
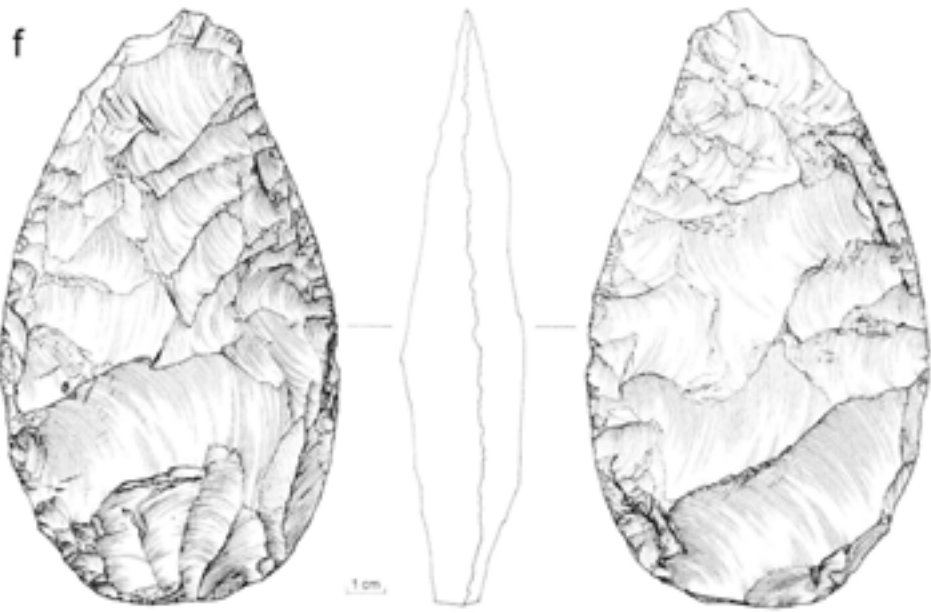


Table 123 Handaxes from Q1/B, Unit 4c. Width=thickness

<i>flint no</i>	<i>length mm</i>	<i>breadth mm</i>	<i>width mm</i>	<i>weight g</i>	<i>Roc's classification</i>	<i>Bordes' classification</i>	<i>Wymer's classification</i>
1	145	91	43	503.1	ovate	IV ovate	Kvi
2	136	94	38	524.4	ovate	IV ovate	Hv
78	90	50	17	71.2	ovate	V limande	Jvi
95	154	91	40	459.7	ovate	IV ovate	Kvi
96	101	66	20	129.4	ovate	IV ovate	Kvi
205	159	92	32	456.9	ovate	V limande	Kivvi
315	90	60	27	125.9	ovate	IV ovate	Kiii
754	73	55	20	85.7	ovate	IV ovate	Gvi

carefully finished around its entire edge and has no remaining cortex. It has no staining and is moderately patinated.

- 205 (Fig 249f) This is a large and well finished handaxe with a continuous cutting edge around its entire circumference except for a short length of flat edge at the butt end, which is thicker and heavier than the more refined tip. The tip is finished by a large tranchet removal and is slightly asymmetrical with a basil point (ie it has a straight edge at the tip of the handaxe).
- 315 (Fig 249d) A small irregular handaxe with an uneven edge. It has cortex on both faces and parts of the edges on both sides. It has been produced from a small nodule and is more pointed than the other handaxes from this area.
- 754 (Fig 249b) The handaxe is small with a completely finished edge which is irregular along the butt edge. Sub-triangular in shape, it is unlike the rest of the Q1/B handaxes.

These eight handaxes cover a great range of size, shape and form (Table 123). Four are finely finished in a standardised shape (ovate) with classic tranchet sharpening of the tip of each. Of the other four, two may have been abandoned before final finishing, explaining their irregularity and thickness. Neither have tranchet sharpening blows. The remaining two are small, both less than 100mm long with unusual forms. With all of them except 315, the initial intention appears to have been to produce a finely finished ovate handaxe. This was successful in only four out of the seven attempts. In the case of 754, the preferred shape was not produced. This may have been related to the raw material or the skill of the knapper. Nonetheless, a useable tool was produced.

The complete removal of cortex from the faces and edges of the handaxes appears not to be important to the knapper(s). Once a regular and even shape had been achieved, with a tip and an even cutting edge, further removal of cortex was not considered necessary.

Apart from the final three removals from 95, none of the debitage from Q1/B appears to relate to the handaxes found in the area. The debitage is therefore from the production of tools which are no longer with- in the excavated area.

It is shown elsewhere in this chapter that the debitage from Q1/B is, for the most part, from the later stages of handaxe manufacture. This indicates that the manufacture of these tools was not wholly confined to a single location, and furthermore that their manufacture was not entirely restricted to a single episode of flaking. Although one or two roughing-out flakes do occur, they are not sufficiently numerous to identify Q1/B as an area where roughing-out activity occurred to the same extent as thinning and finishing. Where the initial roughing-out took place has not yet been identified, although numbers of rough-outs have been found close to the base of the cliff.

Refitting

Since the distance between each of the four trenches in the Q1/B area was only 2m, it was considered likely that refits would occur between trenches. Five individual flakes were identified that refitted between Trenches 1 and 2; one a group of three flakes considered to have been part of the roughing-out of a handaxe, and one group of flakes from the thinning and finishing of a handaxe. No other conjoins were identified between individual trenches.

As in Q1/A, only the first and second categories of refits described by Cziesla (1990) have been identified in Q1/B. The first category of refits, breaks, will be considered first, and the data for this will be presented in the form of the combined evidence for all four trenches (Table 124).

The break refit data for Q1/B as a whole indicates that 24% of all broken pieces were refitted compared with only 20% from Q1/A. This adds support to the

Table 124 Refitted broken flakes from Q1/B Unit 4c

<i>number of refitted pieces</i>	<i>number of groups</i>
2	33
3	10
4	1
5	1
total	105 individual pieces

Table 125 Ventral/dorsal refits from Q1/B Unit 4c

<i>number of flakes in each group</i>	<i>number of groups</i>
2	19
3	4
4	3
5	2
6	3
7	1
10	1
13	1
total	120 individual flakes

contention that the flintwork in Q1/B was less disturbed than that from Q1/A. This is further emphasised by the evidence from Trench 2 where, within the first category of Czesla (1990), 29.5% of the broken flakes (88 out of 281) were successfully refitted. This is a higher percentage of break refits than for any other area of Unit 4c.

The data for ventral/dorsal refits, the second category identified by Czesla, are presented in Table 125. This combines the data for the four trenches in Q1/B.

The majority of the refits from Q1/B fall into this second category of refit. The main refitting groups are described below, but the technological data that these ventral/dorsal refits preserve can be briefly summarised here. The full spectrum of activity corresponding with handaxe manufacture is present in Q1/B; limited roughing out, thinning, and final trimming and shaping. Refitting group A from Trench 1 represents an episode of thinning and finishing from a handaxe which was roughed out elsewhere and brought to the vicinity of Trench 1 for finishing (Fig 250). Similarly, the handaxe represented in Trench 1 group B was also roughed out outside the excavated area and brought to this locale, where thinning activity was centred around ameliorating two break surfaces. Groups A and B from Trench 2 represent contemporary episodes of decortication and thinning on the same handaxe which had not been roughed out within the excavated area. The single handaxe represented by refitting groups D and E from Trench 2 was similarly roughed out beyond the excavated area (Fig 251). This handaxe was also finished off with three refitting tranchet type flakes. Unfortunately the handaxe from which these pieces came was not located within the excavated area. The tranchet flakes in group E are considered to be part of the same handaxe as refitting group D on the basis of proximity of location and of distinctive raw material.

Although roughing-out activity is not preserved within the major refitting groups, and the vast majority of roughing out was conducted elsewhere, this activity certainly did occur within Q1/B. This is demonstrated by the roughing-out flakes refitted between Trenches 1 and 2 as mentioned above.

One other aspect is demonstrated by the ventral/dorsal refits (Table 125). In the section on distribution it was stated that the clustered distribution of the flintwork

in Q1/B was perhaps due to the material being dropped onto a soft, wet, ground surface, and then being quickly incorporated into the sediment thereby preserving the original clustering of the material. This hypothesis was suggested as a possible explanation for the differing distributions of flintwork in Q1/A and Q1/B. As the refitting of the Q1/B material progressed it was noted that the average distances between refitting pieces varied among the different refitting groups. One group of refitted pieces, more dispersed than the others, presented a slightly more patinated appearance and lacked the fresh lustreless quality of the remainder of the material. The area of the distribution of this group of refits also covers that of the most tightly clustered refitting groups. Tentatively, this is interpreted as evidence for different episodes of individual handaxe working (group C representing one episode of activity and groups D and E a second) having been carried out at different times. However, it is not possible to assert that the more patinated/dispersed material is earlier than the less patinated material. It is possible that rapid burial of the latter material could have been succeeded by a second episode of handaxe working which left material exposed on the ground surface for a longer period of time before it was incorporated into the sediments. Therefore, although later, this material would become more patinated and more dispersed. At present all that can be demonstrated is that the refitting groups represent at least two different individual episodes of handaxe-working, whose exact relationship as yet cannot be determined.

Descriptions of refitting groups

Trench 1

Group A

This group, which includes a handaxe, has been described previously, along with the tool (see handaxe 95, Fig 249g).

Group B – six flakes

This sequence of six flakes represents an attempt to thin down two break surfaces on opposite lateral edges of the same handaxe. The first two flakes in the sequence were removed from one edge of the handaxe. A third flake was removed as part of this sequence from the same edge, but was not recovered. It is likely that it was incorporated into the sediments outside the excavated area. After the missing flake, a sequence of four flakes were removed on the same face as the previous removals but from the opposite edge of the handaxe.

The rest of the ventral/dorsal refits from Trench 1 consist of only two or three pieces. They are, however, interesting in that they are from different stages of handaxe manufacture: three groups of roughing-out flakes, one of thinning flakes and three of finishing flakes.

Within the vicinity of Trench 1, and therefore within the Q1/B area as a whole, it can be seen that all aspects of handaxe manufacture, from the initial stages to final shaping and trimming, are represented by the debitage and the refitting. The main emphasis of knapping in Q1/B, however, is thinning.

None of the refits occur over distances of more than 3m, with the majority being much less. However, small isolated groups of refitting pieces indicate that the rest of the reduction sequences are not present within the excavated area. It is likely that the small groups of refitting pieces are outliers from the edges of dispersed scatters, the centres of which lie outside the excavated area. These dispersed scatters must have been subject to more horizontal movement than the larger refitting groups from Q1/B.

Trench 2 (Fig 250)

Group A – 13 flakes

This refitting sequence includes 13 flakes made up from 23 individual fragments. It is part of the thinning of an already partly reduced nodule, the earlier stages of which, for reasons already discussed, are believed to have occurred outside the excavated area. The initial flakes from the refitting sequence were knapped in order to remove the remaining cortex adjacent to the edge on this part of the piece. The next series of flakes were removed in order to reduce the thickness of this same edge, but were located further down and at right-angles to the decortication sequence.

This refitting group therefore represents a nest of flakes which, from the combined ventral surfaces of the conjoined pieces, show the negative of a larger part of one surface of the finished tool itself.

Group B – 6 flakes

From the colour and inclusions of the flint it appears likely that this group is from the reduction of the same tool as group A and is possibly from the opposite face of the piece, although no point of contact for the two groups was found. The initial detachment in the sequence removed some of the remaining cortex and continued across the surface to reduce the thickness of the piece near the opposite edge. All the subsequent removals were from that opposite edge.

Group C – 10 flakes

As with group A, the conjoins represent a reduction sequence which took place after the initial roughing out of the piece had occurred elsewhere. A series of large thinning flakes were removed in order to reduce a thick square edge as well as the remaining cortex. The first two removals left flake scars which were subsequently used as platforms for three removals on the opposite face. The sequence of refits as a whole preserves the traces of a single flake, which had already

been detached from this opposite face. This indicates that the knapper was at this point working on thinning both faces from the same edge, and had also thinned the thick square edge in the same way.

Group D – 6 flakes

A thinning sequence which reduced a thick cortical edge. The flint colour and inclusions suggests that this group may be part of the same piece as those flakes in group E.

Group E – 7 flakes

Included in this group of refits are three tranchet type flakes which have each removed a length of the bifacially worked edge of the handaxe. It is apparently a sharpening sequence, although at the same time the tool is also being thinned down and partly re-shaped. The technique of removing a tranchet flake does not need to be restricted to the final finishing removal in the production of a handaxe, but can be profitably employed throughout the late stages of handaxe manufacture. The resulting flakes, which are backed by earlier finishing flakes on one edge, may then have been used as knives, although no evidence for such utilisation has been proven.

Cores

There are no classic cores for flake production within the assemblage from Q1/B. However, four small nodules were recovered, each with one or two removals. Although they show no systematic removal of flakes they do nonetheless exhibit evidence of modification. All four are vaguely sausage-shaped and range from 55mm to 124mm long, 34mm to 57mm wide and from 14mm to 37mm thick.

Hammerstones

Three small nodules with evidence of battering were recovered from the excavation and these are interpreted as hammerstones; one such nodule is illustrated in Figure 248. The first, 96mm by 55mm, weighs 464.9g. The majority of the nodule is cortical, with a few small, probably incidental, flake removals adjacent to the area of battering. The battered area is a gently rounded cortical surface which has numerous incipient percussion cones. These are the result of the nodule having been used as a hammer.

The second nodule measures 125mm by 101mm by 65mm and weighs 666.9g. The central portion of one surface of the nodule shows evidence of battering. A number of quite forceful blows have caused numerous incipient cones and removed two flakes. It may have been used as a hammerstone for flaking, or it may have been used to smash or crush another medium.

The third is a long thin nodule, one end of which shows evidence of battering. There are two removals from the battered end, accompanied by severe cracking. The piece measures 85mm by 47mm by 33mm and weighs 111.3g.

Only a very small percentage (3%) of the flakes from Q1/B may have been detached using a hard hammer and none of these flakes is very diagnostic of hard hammer percussion. Research by Bradley and Sampson (1986) has suggested that characteristics of flakes ascribed to hard hammer and soft hammer flaking should be rejected. They maintain that it is the position and angle of the impact relative to the edge that determines the attributes of the flakes. This hypothesis is comprehensively rejected by Wenban-Smith (Chapter 6.4), and thus it would appear that the soft hammers responsible for the Q1/A and Q1/B flaking were removed from the area after use.

Debitage

The debitage consists of 691 flakes and flake fragments over 20mm long, of which 253 are complete (Table 126). The high proportion of broken flake fragments, 63.4%, is very similar to that from Q1/A.

The complete flakes were studied in further detail. A threefold division was made (as for Q1/A), dividing the complete flakes on the basis of morphology into

Table 126 Number and percentage of individual fragments of flakes from Q1/B Unit 4c

<i>part of flake</i>	<i>number (n)</i>	<i>%</i>
proximal	161	36.76
mesial	114	26.03
distal	133	30.37
other	30	6.84
total broken	438	63.39
complete flakes	253	36.61

technological groups consisting of the waste products from the three stages of biface manufacture (as recognised by Newcomer 1971). These were roughing out, thinning, and finishing flakes (Table 127). The knapping of cores for flakes was considered as a fourth category but proved to be indistinguishable from roughing-out flakes.

The following technological aspects of these complete flakes were noted: butt types, proportions of dorsal cortex, profile shape, dorsal scar pattern, and if produced by hard or soft hammer (Table 127).

The technological attributes of the unbroken waste flakes reinforce their threefold division into roughing-out, thinning and finishing flakes. The butt types of flakes from roughing-out activities reflect the position

Table 127 Technological attributes of complete flakes from Q1/B Unit 4c

<i>category</i>	<i>roughing out</i>		<i>thinning</i>		<i>finishing</i>		<i>total</i>	
	<i>n</i>	<i>%</i>	<i>n</i>	<i>%</i>	<i>n</i>	<i>%</i>	<i>n</i>	<i>%</i>
butt type								
plain	9	33.33	24	27.27	17	12.32	50	19.76
cortical	8	29.64	5	5.68	3	2.17	16	6.33
dihedral	3	11.11	11	12.5	19	13.77	33	13.04
polyhedral	3	11.11	9	10.23	13	9.42	25	9.88
faceted	–	0	4	4.55	9	6.52	13	5.14
crushed/broken	3	11.11	33	37.50	76	55.07	112	44.27
indeterminate	1	3.70	2	2.27	1	0.73	4	1.58
cortex %								
0	–	0	33	37.50	115	83.33	148	58.50
1–25	6	22.22	33	37.50	19	13.77	58	22.92
26–50	5	18.52	12	13.63	3	2.17	20	7.91
51–75	9	33.33	9	10.23	1	0.73	19	7.51
76–100	7	25.93	1	1.14	–	0	8	3.16
profile								
straight	18	66.67	36	40.91	91	65.94	145	57.31
curved	4	14.81	43	48.86	38	27.54	85	33.60
indeterminate	5	18.52	9	10.23	9	6.52	23	9.09
dorsal scars								
unidirectional	16	59.26	40	45.46	112	81.16	168	66.39
bidirectional	7	25.93	21	23.86	11	7.97	39	15.42
multidirectional	1	3.7	25	28.41	13	9.42	39	5.42
no scars	3	11.11	2	2.27	2	1.45	7	2.77
flaking mode								
hard	1	3.70	6	6.82	–	0	7	2.77
soft	26	96.30	82	93.18	138	100	246	97.23
totals	27		88		138		253	

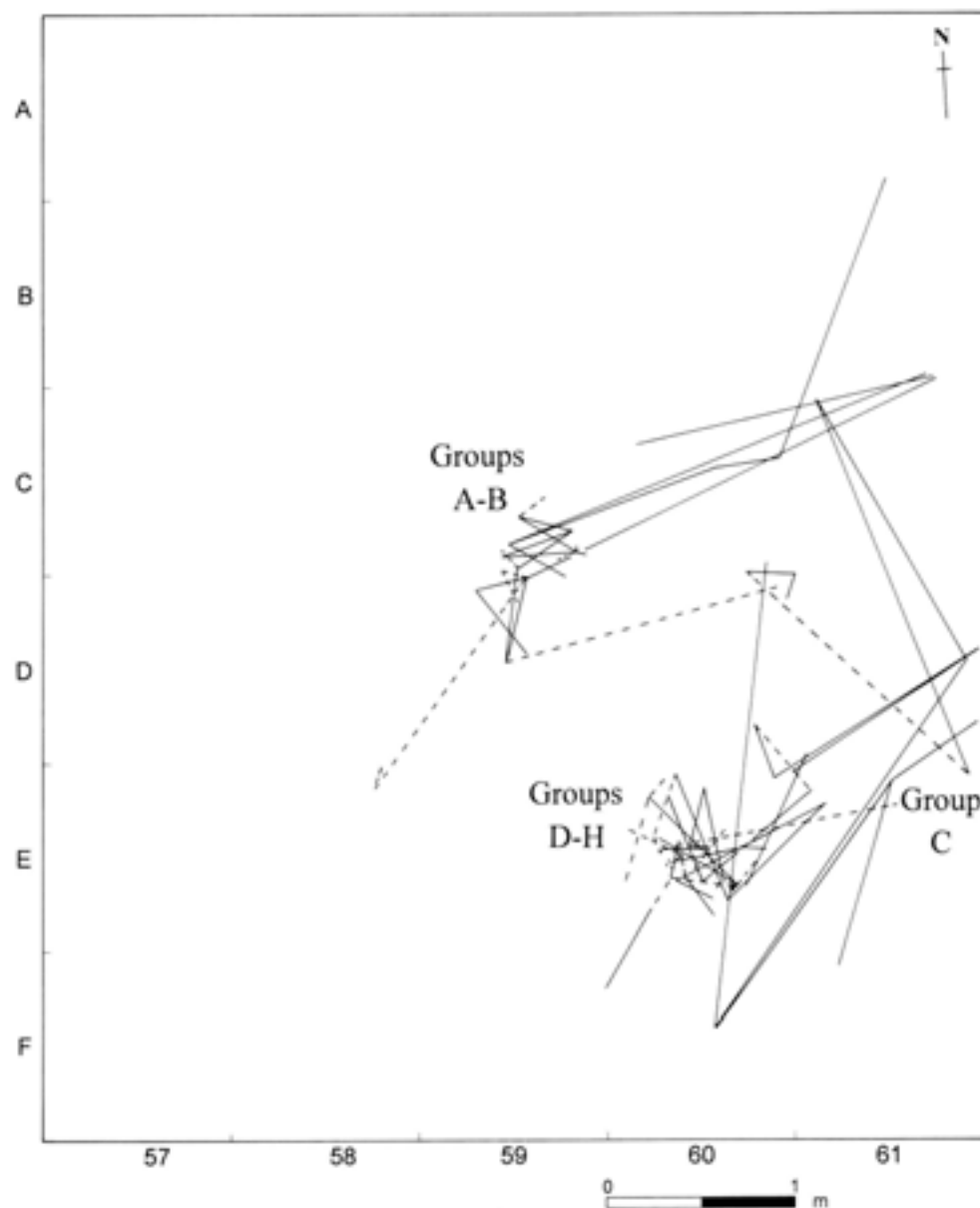


Fig 250 Refitting groups A-H from Trench 2, Unit 4c at Q1/B

of these flakes in the reduction sequence. For the most part they are undistinguished flakes with plain butts, 63% of which are either plain or cortical. A non-marginal flaking mode (Bradley and Sampson 1986) is also reflected in the low proportion of crushed or broken butts. Towards the finishing stage of the handaxe manufacture the proportion of flakes removed using marginal flaking increases, as can be seen in the increased proportion of crushed and broken butts on thinning flakes. At the same time, the proportion of cortical and plain butts decreases as the edge of the handaxe is increasingly more finely worked.

The proportion of cortex on the dorsal surface of a flake is associated with the position of the flake in the reduction sequence. Over half of all roughing-out flakes had cortex covering more than half their dorsal surface. The proportion of flakes with cortex decreased through

thinning flakes to finishing flakes where the vast majority (83.3%) had no cortex at all. The profiles of roughing out flakes are predominantly straight, while those of thinning flakes are predominantly curved. Finishing flakes, which tend not to travel so far across the face of the handaxe have a more even mix of straight and curved profiles.

Dorsal scar patterns are more likely to be bidirectional or multidirectional on thinning flakes than on either of the other categories. This is because the flakes remove more of the already knapped surface of the handaxe than finishing flakes.

As stated above, some of the roughing-out and thinning flakes have a number of features which have been associated with hard hammer percussion. These are the product of non-marginal flaking, resulting in a large butt (Bradley and Sampson 1986; Bergman and Roberts 1988). However, the ventral features of these flakes

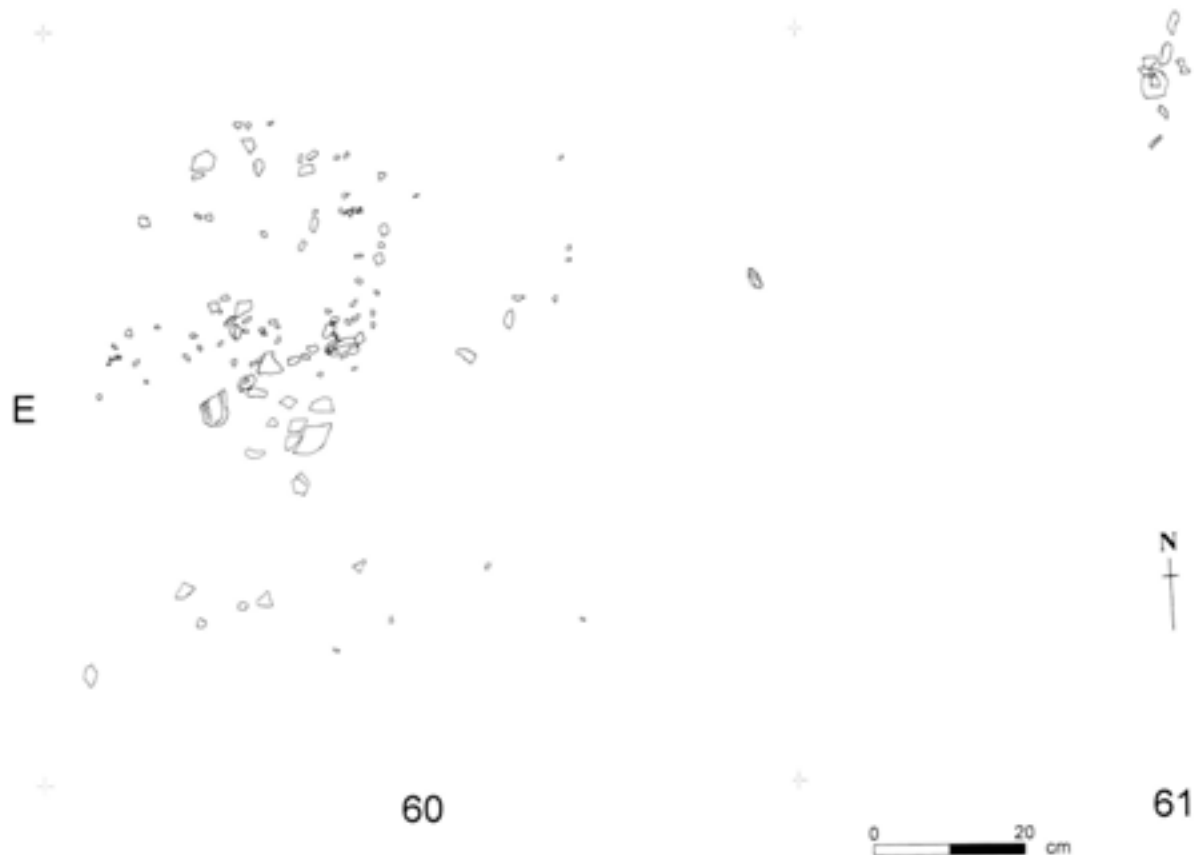


Fig 251 Plan of flints comprising refitting groups D-H from Unit 4c at Q1/B

suggests that a soft hammer was used to detach them. Seven of the flakes have pronounced bulbs although this feature alone may not necessarily be the result of the use of a hard hammer (Wenban-Smith Chapter 6.4).

The waste flakes within the excavated assemblage are debitage from the production of handaxes. However, they do not represent the complete reduction sequence from nodule to handaxe. Experimental work by Bradley and Sampson (1986) reproducing handaxes from the site of Caddington produced roughing-out, thinning and finishing flakes in the following proportions: 40%, 50% and 10% respectively. Similar work reproducing handaxes by Newcomer (1971) produced proportions of 26% roughing out, 38% thinning and 36% finishing. Compared with these figures, the proportions of the complete flakes in Q1/B (Table 127) show a distinct lack of flakes from the initial stages of handaxe manufacture. This bias towards finishing flakes is also evident in the assemblage from Q1/A Unit 4c. Complete nodules were not being transported to this area of the landsurface for the production of handaxes. Only pieces which had already been partially reduced were transported into this area.

Discussion

From the distribution of the artefacts, clusters of flint debitage were recognisable, particularly in Trench 2. Analysis of the assemblage composition identified the

flintwork as debitage from, predominantly, the later stages of handaxe manufacture. Two distinct groups were identifiable from Trench 2, one centred on grid square E60 and one on C59 (Figs 250-1). These were distinguishable not only by their distributions but also from the colour, pattern of inclusions, and the patination of the raw material. Refitting found no link between these two groups.

The cluster of flint artefacts centred on grid square E60 (Fig 251) (which include refitting groups D and E) are all made from similar raw material and all lie within an area of 1m². It is probable that these pieces are part of the final thinning and finishing of one handaxe which was roughed out outside the excavated area. Transportation of flint can be seen to have taken place at various stages of handaxe manufacture.

Overlapping with groups D and E is the distribution of another refitting group, group C (Fig 250). The length between refits is much greater in group C than in D and E; the group C flints also display a slight patination and lustre. This material has not been affected by post-depositional processes in the same way as the tightly clustered group.

The concentration of material, centred on C59, is more dispersed (Fig 250). There are two main refitting groups from this debitage (Trench 2 groups A and B) which appear to represent the final thinning and finishing stage of a single biface.

It is therefore evident that at least three knapping events took place within Trench 2, two of which are distinguished from each other by the combination of raw material type, refitting and distribution, while the other is distinguishable by refitting and condition (patination). The less dispersed material must have become more quickly incorporated into the sediment than the more dispersed material. Flintwork exposed on the ground surface was susceptible to various post-depositional processes (as described in the discussion of Q1/A), and the degree to which these processes affected the distribution of the pieces was dependent on the length of time they were exposed. It is therefore probable that, in addition to variations in dispersal caused by knapping stance, the distribution of the artefacts is dependent on the length of time they were exposed on the ground surface before incorporation into the sediment.

A comparatively long exposure on the ground surface resulting in a dispersed distribution does not necessarily indicate that this material pre-dates the material which has a more concentrated distribution. It is the rate of incorporation into the sediment which is the vital factor. Fast incorporation will have resulted in little movement, with slow incorporation resulting in greater movement.

The local environmental conditions of an area may have varied over time to the extent that the rate of incorporation of debitage into the sediment in that area could also have varied. Conditions which enabled the rapid incorporation of debitage into the sediment (eg soft and wet) may have been followed by those which resulted in the extended exposure of material on the ground surface (eg hard and dry).

Without stratigraphic evidence of overlying debitage from separate groups, it is not possible to say which were earlier and which later knapping events. The only thing that can be asserted is that all three of these events did not take place at the same time. It is possible that the refitted groups of material from the rest of Q1/B and Q1/A Unit 4c do not represent a single, short term occupation of the area, but are a series of knapping events spread out over time representing the repeated return of flint knappers to that particular location.

Quarry 2 Area A

C A Bergman and M B Roberts

Quarry 2 main area A was located at the very southern edge of the conformable sequence (Fig 4) (Roberts 1986; Bergman and Roberts 1988; Bergman *et al* 1990). Five metres to the south of the excavation the Slindon Silts and overlying Brickearth Beds have been eroded away (Figs 22, 24a–b, 34), and the sediments of the Earham Upper Gravel Member unconformably cut into and overlie the Slindon Sands (Roberts Chapter 2.1). The position of the main excavation trench was based on geological test pitting carried out by M B Roberts in 1982–3, and the proximity of the



Fig 252 Q2/A excavation in 1983, Brickearth Beds removed down to the surface of Unit 5a; scale unit 0.5m



Fig 253 Q2/A, looking east; scale unit 0.5m

working face of sand extraction, which was moving northwards into Quarry 2 (Fig 13). Excavation of the area commenced in 1983 (Fig 252) and continued until 1987 (Figs 253–4), culminating in the microartefact project (Wilhelmsen this section).

The geology at this area is comparatively simple (Chapter 2), as many of the gravel and silt units associated with the higher relief at the cliff line do not extend this far south (Tables 9a, 9b; Fig 22). Unfortunately the archaeologically rich sediments of the Slindon Silts are completely decalcified in this area, due to both an original paucity of calcareous material in the overlying sediments and secondary decalcification by ground water movement (Catt Chapter 2.5; Macphail Chapter 2.6). These factors are the consequence of the location of the site, which is over 200m from the cliff-line (Fig 29). There is considerable surface relief of up to 0.8m over the excavated area. This is largely the result of post-depositional solution of the chalk, the surface of which is 5m below the surface of the Slindon Silts, which has resulted in microfaulting in the silts, Unit 5a, and the overlying brickearth (Fig 255). Other causal factors in the surface relief include the depositional regime of the Slindon Silts this far offshore (Collcutt Chapter 2.3), and general flexuring of the sediments as a result of pressure loading during burial.



Fig 254 Flintwork scatter in Q2/A east extension; 0.25m² grid

The site was excavated in 1m² and 0.25m² (Fig 254) following the methodology described in the introduction. The location of all flakes and spalls was recorded in three dimensions, and there was no size cut off point for recording additional information about flake attributes and orientation. Artefact distribution plans were generated from the data on the record sheets. No faunal remains survived in the sediments at Q2/A. The excavated spits followed as nearly as possible the contours of the surface of the silts; thus there was considerable, post-depositionally induced, vertical separation of material from the same spit over the area (Fig 255).

The presence of artefacts throughout the 100–150mm thickness of Unit 4c and also in the overlying mineralised organic horizon of Unit 5a suggests movement of the lithics as a result of bioturbation and soil formation processes. Wilhelmsen (this chapter) has calculated that the material he examined was probably knapped onto a surface 60mm into Unit 4c. The exact temporal relationships between various knapping episodes in Unit 4c is unlikely to be ascertained by either conventional excavation or statistical analyses. It is likely that material was deposited onto the surface of the silts as the sea regressed and that this depositional process continued when the open grassland soil developed.



Fig 255 Flint scatter affected by faulting in Q2/A; scale unit 10mm



Fig 256 Refitted broken flakes from Q2/A; scale unit 10mm

Refitting of flintwork is arguably the most useful tool in establishing the relationship between knapping events, with the proviso that our understanding of site formation processes at this level recognises horizontal displacement by kicking and scuffing and also the possibility of scatters being knapped on top of each other through time.

The raw material used by the Acheulean knappers for tool manufacture was obtained from the chalk cliffs between 200–300m away from Area A. Two types of flint exist in the chalk at Boxgrove: tabular and nodular flint. The nodular flint, however, was almost exclusively used for tool manufacture because the tabular flint has coarse bands running through it which make flaking difficult. On the whole the flint from Boxgrove works well, although it is prone to internal fractures and contains inclusions. The flint nodules would have been collected as they eroded out of the chalk and dropped to the base of the cliff, or from the screes that developed in front of the cliff.

The majority of flakes from Area A in Quarry 2 are broken as can be seen in Table 128 (Fig 256). Much of this breakage is probably due to the nature of the local flint which often has internal flaws. An additional cause of breakage is undoubtedly related to the fact that the thin flakes removed during the later stages of handaxe manufacture are curved and prone to snap as they are detached. The horizontal distribution of refitted breaks (Fig 257) shows that individual fragments of the same flake may be spread out over several metres. This means that these breaks occurred before the deposit formed and are not the result of sediment loading. It has been suggested that the dispersal of broken pieces indicates that the artefact scatters have been subjected to some minor disturbance and the flakes are not in the position they originally fell as they were knapped (Roberts 1986; Bergman and Roberts 1988; Bergman *et al* 1990; Austin and Roberts above).

An examination of the flakes shows that most of them derive from handaxe manufacture. There are also a small number of pieces which have been refitted to

Table 128 Number and percentage of individual flake fragments and complete flakes from Q2/A Unit 4c

part of flake	number (n)	%
proximal	320	31.28
mesial	349	34.12
distal	354	34.60
total broken	1023	82.77
complete flakes	213	17.23

two blocks which may be cores or simply discarded nodules that proved unsuitable for handaxe manufacture. For the purposes of analysing the products and methods of handaxe reduction at Boxgrove, the complete flakes (Table 129) were divided into three groups based on the following categories defined by Newcomer (1971): roughing-out, thinning/shaping, and finishing. Each of these stages in the manufacture of a handaxe is part of a continuum which begins with the selection of the raw material and continues through the reduction sequence. The continuous process interlinking each of the stages makes it difficult to assign all of the flakes, with certainty, to discrete categories which contain only the products of a single stage. Bearing this problem in mind, it was still felt useful to separate the flakes into broad groups to reflect the different kinds of debitage which result from handaxe reduction. Once this was done it would then be possible to make general statements about handaxe manufacture at the site.

Roughing-out flakes

These flakes are the primary removals from a flint nodule and therefore have varying degrees of cortex on the dorsal surface. In addition, they tend to be relatively large and have plain or cortical butts which are thick, reflecting the fact that they are detached by a non-marginal blow. Not surprisingly, roughing-out flakes represent the most numerous category of complete flakes (Table 129). This is largely due to the fact that these pieces are relatively thick and tend not to have profiles with a pronounced curve; the presence of both of these features make a flake less prone to snap as it is detached.

Table 129 Categories of complete flakes from Q2/A Unit 4c by number and percent

flake category	number (n)	%
roughing-out	111	52.11
thinning flakes	59	27.70
finishing flakes	43	20.19
total flakes	213	100

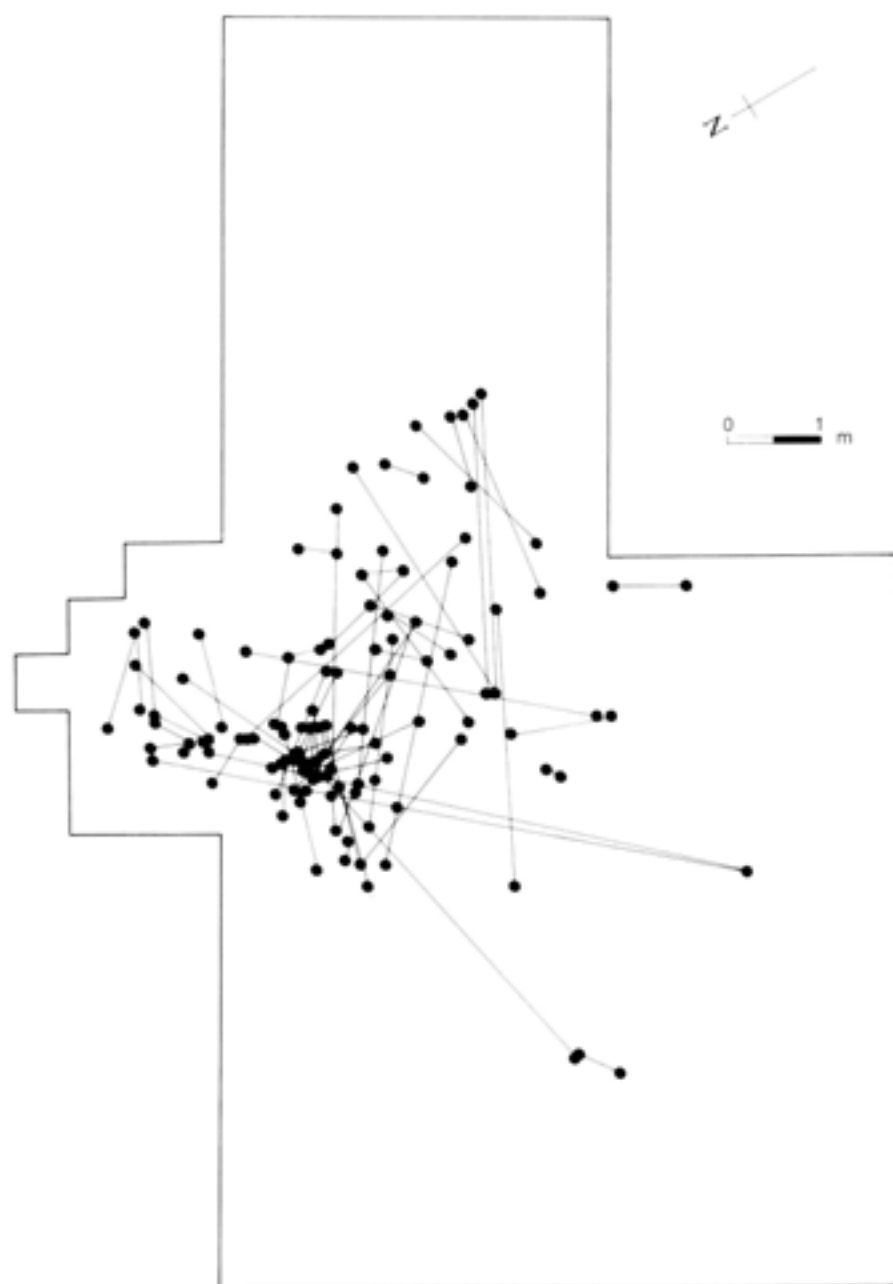


Fig 257 Horizontal distribution of refitted broken flakes from Q2/A

Thinning/shaping flakes

Flakes from this stage are produced as the handaxe rough-out is reduced in thickness as well as being given a plan shape; in the case of Boxgrove the plan shape is almost always an ovate or elongated ovate (Tables 112, 116, 123). Most of the cortex has been removed from the block by this stage, but some flakes still have small cortical areas on the dorsal surface. The flakes are relatively thin and have small butts. The reduction in the overall dimension of the butts is caused by the fact that these flakes are more often detached by a marginal blow which removes a smaller part of the handaxe's edge. There is an increase in the overall percentage of flakes with faceted butts which reflects careful attention to platform preparation prior to the delivery of the blow.

Also important among this category of flakes are the number of pieces with crushed or broken butts; crushed butts are more common among flakes detached with a marginal blow aimed close to the handaxe edge (Bradley and Sampson 1986). Thinning/shaping flakes are quite invasive and often have removal scars from the opposite edge of the handaxe. In profile, they show a marked curvature due to the lenticular cross-section of the handaxe.

Finishing flakes

The finishing stage is largely devoted to the careful flaking of the handaxe's edges. These flakes are shorter than those in the previous stage (Newcomer 1971; Bradley and Sampson 1978; 1986) and are usually

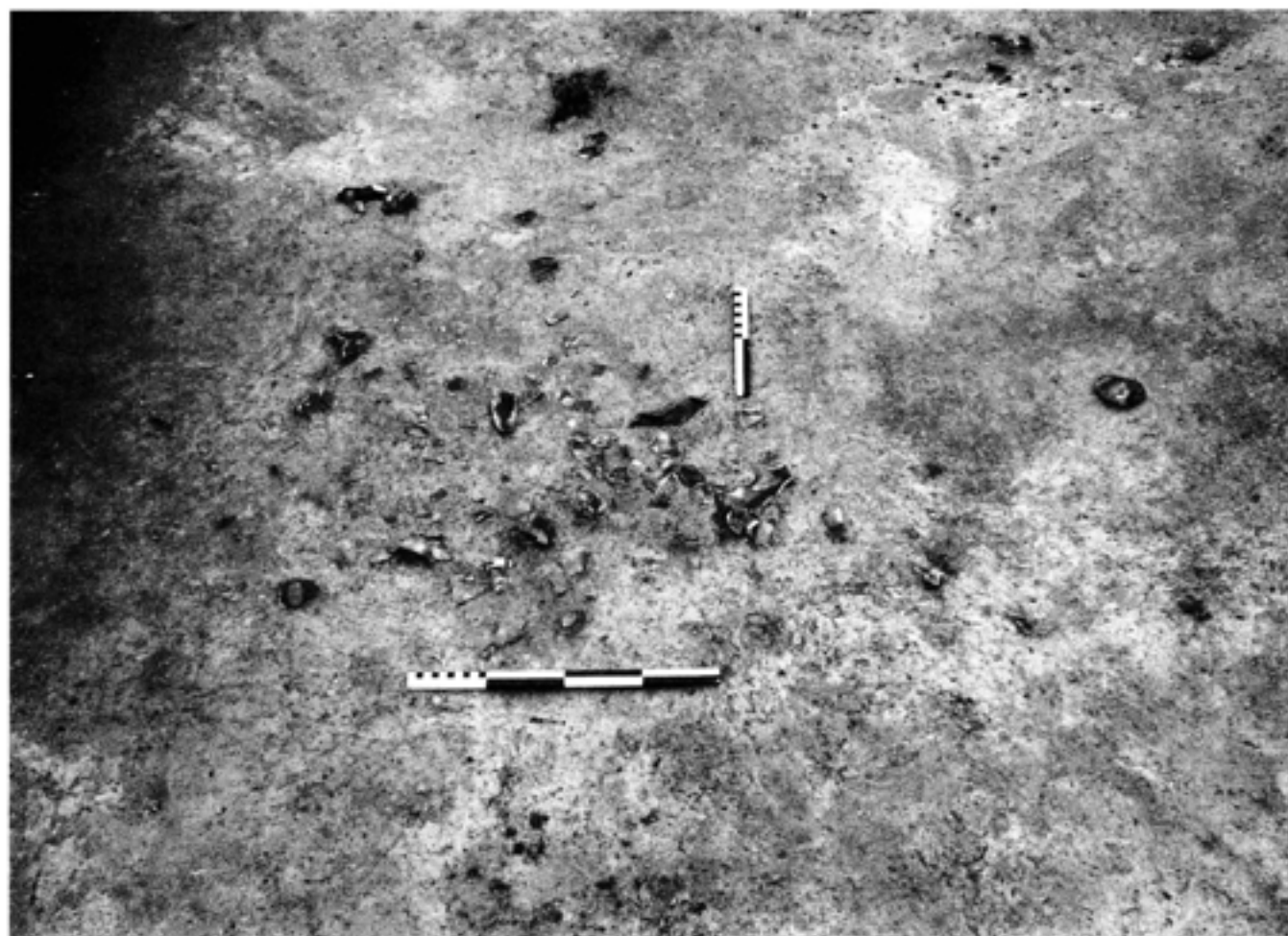


Fig 258 Main refitting scatter in Q2/A: note the handaxe on the right of the picture; scale units 10mm and 0.1m

wholly non-cortical. With regard to the butt types, they display a similar distribution to the thinning/shaping stage, although there is an increase in pieces with crushed or broken butts. The dorsal scar pattern shows a higher percentage of unidirectional scars when compared with the thinning/shaping flakes. As the purpose of the finishing stage in handaxe reduction seems to be largely devoted to preparing the edges, the flakes detached tend not to be so invasive and do not travel to the central axis of the tool. A final stage of finishing practised at Boxgrove is the careful preparation of one or both sides of the tip of the handaxe for the removal of tranchet flakes.

As can be seen there is an overall reduction in artefact size, particularly in thickness, as flaking proceeds; this is mirrored by a sharp decrease in pieces with cortex on the dorsal surface. The shift from a non-marginal to a marginal flaking mode between the roughing-out and thinning/shaping stages is clearly seen in the reduction of butt thickness and the increase in flakes with crushed butts. When the handaxe becomes more lenticular in cross-section, a greater number of pieces with curved profiles are produced. As the tool is thinned and shaped there is an increase in bidirectional and multidirectional dorsal scars; this reflects the

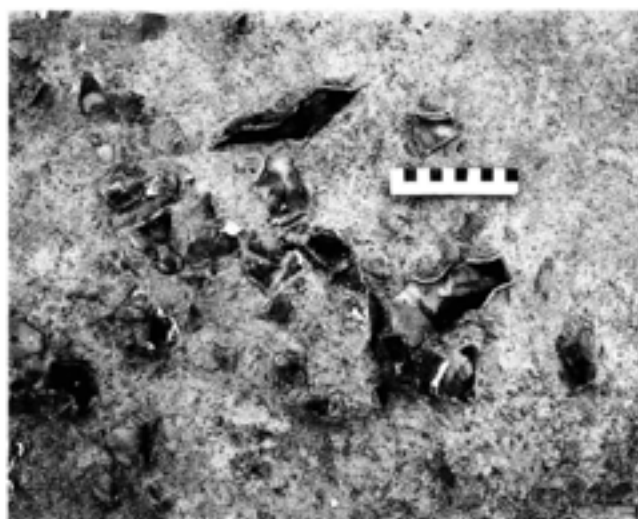


Fig 259 Detail of scatter from Fig 258; scale unit 10mm

invasive nature of the flakes detached during this stage, which often meet the removals coming from the opposite edge. This pattern, however, changes to unidirectional by the finishing stage where more attention is paid to preparing the edge and, hence, the removals are shorter and do not travel to the handaxe's centre.

A visual examination of the ventral surfaces of the flakes indicates that soft hammers were used for all stages of handaxe reduction at Q2/A (Ohnuma and Bergman 1982; Roberts 1986; Wenban Smith 1989). The impression given is that no rigid reduction scheme, of roughing-out with a hard hammer and finishing with a soft hammer, existed. However, Wenban-Smith (Chapter 6.4) has shown that cortical flint hammers will also produce characteristics of soft hammer flaking and that more detailed analysis of the flakes is required to discriminate between these two groups of processes. Experimental work by the authors has shown that nodule preparation is much easier to undertake using a cortical flint hammer. Although only refitting of the flakes

from each individual handaxe at Boxgrove will reveal exactly the flaking strategy employed in the reduction sequence, all of the above accords with the experimental work of the authors as well as that published by Newcomer (1971) and Bradley and Sampson (1978).

Refitting and spatial analysis

The spatial distribution of the lithics and the pattern of refits at Q2/A indicates a complex series of activities (Figs 257–60). As stated earlier, raw material for tool manufacture was obtained at the chalk cliff, probably among the debris at the base. Near the cliff a large number of handaxe rough-outs have been recovered,

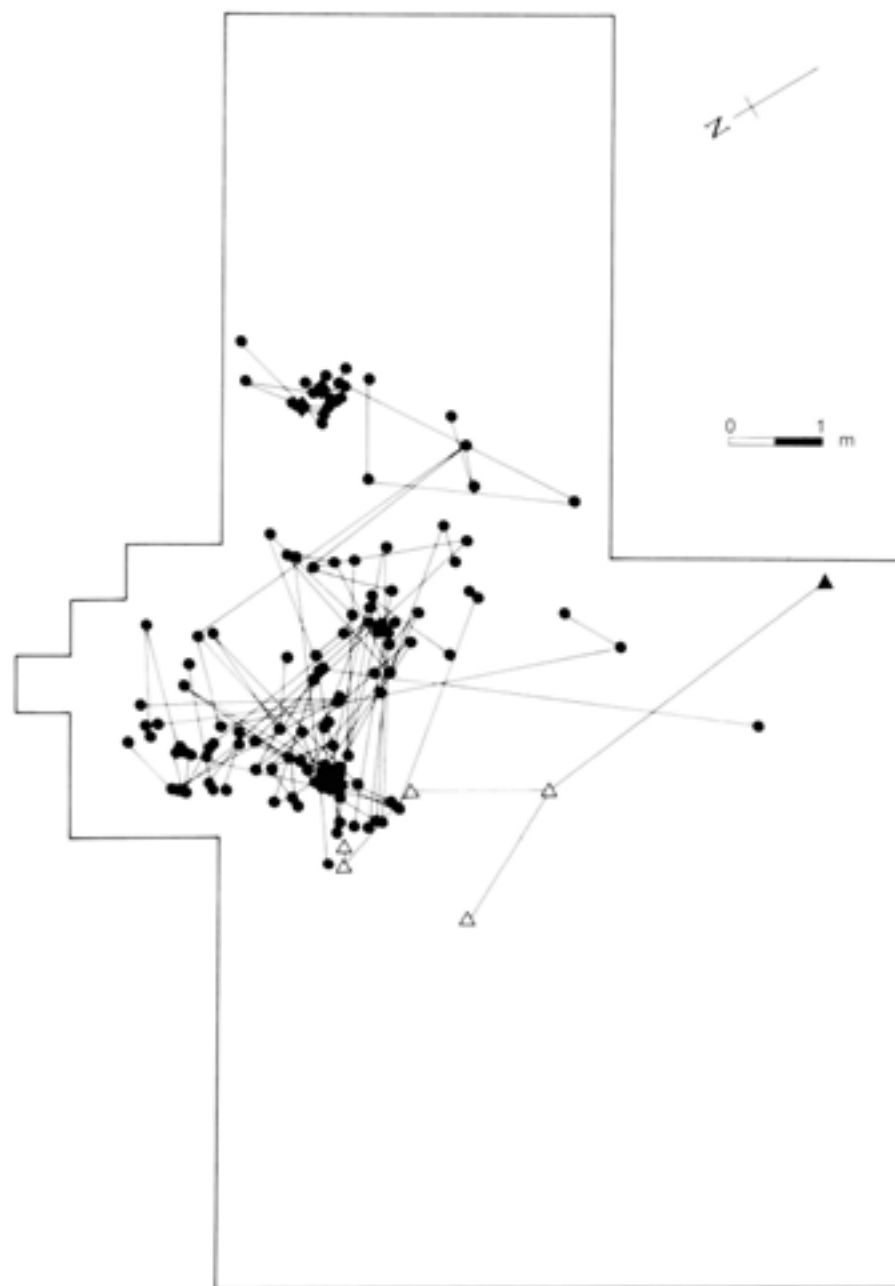


Fig 260 Horizontal distribution of flakes refitted by ventral/dorsal contact from Q2/A; the black triangle represents handaxe 9070, the open triangles are refitting tranchet flakes (Figs 262–3)



Fig 261 Refitted nodule from Q2/A; scale unit 10mm

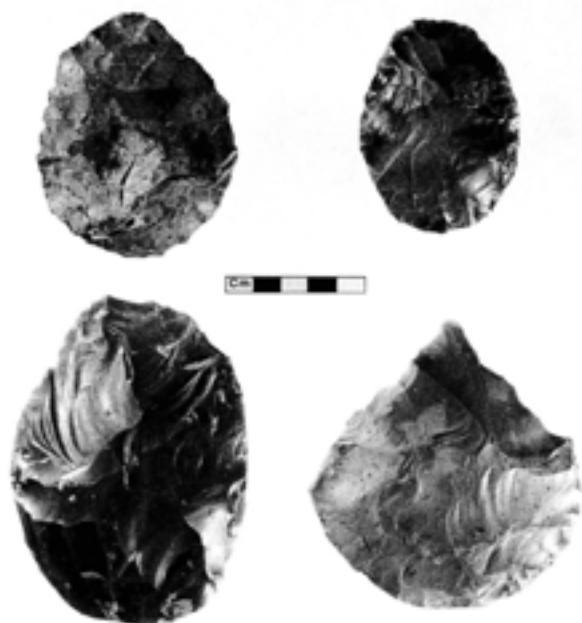


Fig 262 Variability in handaxe shape from Q2/A; handaxe 9070 can be seen at bottom left; scale unit 10mm

abandoned in an early stage of reduction (Roberts 1986); these pieces often display flaws in the raw material or faults in the flaking strategy. The fact that flaking took place so close to the source of raw material probably indicates an attempt to assess the quality of the flint to avoid carrying flawed material elsewhere.

Area A is some 200–300m from the cliff and it is certain the Acheulean knappers were bringing flint there in several different forms. First it is clear that nodules were being carried over from the cliff. One nodule,

which has been almost entirely refitted, is made on a small piece weighing almost 1kg (Fig 261). Fifteen flakes were detached from this block before it was abandoned; most of the flakes detached are cortical and none of them have good cutting edges. These flakes were detached by a hard hammer (Wenban-Smith Chapter 6.4). Another group of 35 refitted flakes represent the outer surface of a large, relatively heavy, nodule. The flakes in the group are among the largest found in Area A with some over 130mm long. It is unclear what became of this block but the 35 refitted flakes may ultimately be related to another large group of flakes associated with a major break surface inside a nodule. It is also possible that only the initial stage of reduction of the nodule took place in Q2/A and final flaking took place elsewhere.

As well as the two groups of artefacts above, complete handaxes or those which needed little additional modification were brought to Area A. The handaxes are typically thin with straight edges and three examples have tranchet blows at their tips (Fig 262). There have been no flake tools such as side-scrapers recovered from the excavated area.

It has only proved possible to refit flakes to one handaxe, which has three tranchet flakes refitted to its tip (Fig 263). These were the last removals from this tool before it was abandoned. The knapper was only marginally successful in removing the first two flakes, while the third attempt ended when the tip snapped off. Aside from the handaxes, it would also appear that a few large flakes with good cutting edges were carried to Area A. These flakes are in distinctive flint types, often with large fossil inclusions, and can not be refitted to any other artefacts.

Artefacts also seem to have been carried away to locations outside the excavated area as stated earlier, the handaxe is missing from the main nest of refitted flakes. Aside from this there are several examples of large tranchet flakes which are too big for the relatively small handaxes recovered in Area A. The handaxes from which these flakes were detached were presumably removed from the area or, as suggested by Austin and Roberts (above), tranchet flakes were also removed earlier in the reduction sequence. Alternatively, the recovered handaxes may be the product of a resharpening process, with the large tranchet flakes corresponding to an earlier period of use of the same handaxe.

Returning for a moment to the analysis of the individual flakes it will be remembered that pieces from each stage of handaxe reduction have been identified in the collection from Area A. The current evidence from the refitting shows that these probably come from a number of different blocks. So far it has not proved possible to refit, even to a moderate extent, an entire reduction sequence (Tables 130, 131). The refits are formed of clusters of flakes representing different stages of reduction, probably coming from different nodules.



Fig 263 Refitted tranchet flakes on handaxe 9070 from Q2/A; scale unit 10mm

Table 130 Refitted broken flakes from Q2/A Unit 4c

<i>number of refitted pieces</i>	<i>number of groups</i>
2	27
3	8
4	1
total	82 individual pieces

Fig 131 Ventral/dorsal refits from Q2/A Unit 4c

<i>number of flakes in each group</i>	<i>number of groups</i>
2	19
3	7
4	6
5	2
10	3
total	123 individual flakes

Interpretation

The refitting of flakes from Area A is beginning to indicate that a much more complex set of activities than previously believed has taken place in this part of the site. As the amount of refitted pieces has increased, it is becoming possible to map the movement of artefacts around the excavated area. From the refitted groups, at least two discrete concentrations of knapping debris surrounded by more diffuse zones have been identified (Figs 256, 260). The first is a large concentration referred to as scatter 1 (Figs 258, 259). In this pile of debris there seems to be material from several different blocks representing different stages of reduction. About a metre away from this, to the west, is the tightly clustered group of flakes with their two cores (Figs 260, 261). Scatter 1 covers an area of roughly 3m² and is clearly too large to be in a primary context. The present understanding of the environment local to Q2/A is that it consisted of a relatively unvegetated mudflat, prior to regression and the beginning of the grassland phase. This is certainly the case if Wilhelmsen is correct (see below) and the flints were knapped on a surface 60mm into Unit 4c. However, it should be noted that the hypothesis pertaining to a lack of vegetation during the mudflat phase is based upon an absence of bioturbation in the underlying Unit 4b. Macphail (Chapter 2.6) has pointed out that the structure of Unit 4c has been lost and the unit compressed post its deposition. Accordingly, there may have been a greater amount of vegetation present than is preserved in the sedimentary record. The proposed lack of closed ground-level vegetation means that the artefacts would have been directly subjected to a variety of natural effects, especially during dry periods, leaving plenty of scope for some minor disturbance.

The refitting shows that flint reached the excavated part of Area A in several forms. The fact that nodules, partially completed rough-outs and finished handaxes were brought into the area whilst finished tools were carried away argues for a certain amount of planning and forethought in these early people. This pattern of behaviour has also been described at other early sites, most notably at Maastricht-Belvédère. At Maastricht the pattern is very similar to that discussed above, with movement around the site of raw materials in a variety of stages of reduction (Roebroeks 1988).

In summary, the work outlined above indicates that at Boxgrove the Acheulean knappers engaged in varied activities, at least in relation to artefact movement. Due to the absence of faunal remains in the area, because of decalcification over a long period of time, it is difficult to link these activities to specific tasks; the artefacts are stained and have not proved suitable for microwear analysis. In order to ascertain in a broad sense the kinds of tasks these people engaged in, it is necessary to examine evidence from other parts of the site.

Quarry 2 Area A: microartefact project

K H Wilhelmsen

Introduction

In 1986 a 1 x 1m test pit was excavated in Area A of Quarry 2, utilising detailed sediment sampling techniques, to determine the potential for microscopic artefact analysis. This preliminary analysis suggested the presence of large quantities of microscopic lithic artefacts though no faunal remains were preserved. On the basis of these results, a project was designed to recover microscopic artefacts and was carried out in Quarry 2 during the 1987 field season. This section presents the research goals of the Microartefact Project (Q2/A MAP) as well as the field and laboratory techniques utilised. An analysis of the spatial distribution and abundance of microscopic artefacts indicates the spatial context of the lithic assemblage is relatively unaltered from its primary depositional context. Thus, there is good reason for employing site-functional analyses, at least of the assemblage related to the soil horizon of the Slindon Silts (Unit 4c), that may identify areas utilised for specific activities such as tool manufacture, tool rejuvenation, and butchery.

Background and research goals

The Microartefact Project was undertaken to collect data on the abundance and spatial distribution of lithic artefacts down to the size of 0.5mm. The research utilised spatial-analytic techniques to understand the depositional and post-depositional history of lithic artefacts in Area A of Quarry 2 (Q2/A). An analysis of the vertical distribution of lithic artefacts in the surface of the Slindon Silts (Unit 4c, Slindon Soil Bed) was undertaken to determine the extent of disturbance that might be expected to result from trampling, differential settling, or deflation. An analysis of the horizontal distribution was undertaken to determine whether natural processes such as tidal fluctuation, sheet wash, or aeolian transport have altered the pattern of cultural deposition and, if so, to what extent. *K*-means cluster analysis and the Pearson product-moment correlation coefficient (*r*) were used to examine the spatial patterning of lithic artefacts in relationship to Units 4c and 5a. Finally, the distributions were assessed on the basis of sedimentological principles and by comparison with ethnographic and contemporary field data. Field observations and documentation of sedimentary structures are also discussed below.

Sedimentologists have long appreciated the fact that the grain-size distribution (texture) and composition of a sediment is indicative of its source, transport medium, environment of deposition, and post-depositional alterations (Reineck and Singh 1980). Reconstructing these stages in the 'life history' of a sediment is based on the analysis of relatively small sediment samples using rigorous sampling techniques.

These techniques have been developed so that the proportions (ie percentages) of various material types and particle sizes of both the sample and the deposit are statistically equivalent. In this way, inferences about the entire deposit, such as composition, grain-size distribution, skewness, and kurtosis can be reliably based on parameters of the sample.

Like sedimentologists, archaeologists are also interested in understanding the life history of sediments (Rapp and Gifford 1985; Stein and Farrand 1985). Sediments include both non-cultural and cultural particles which often come from diverse sources; they can be transported by one or more agencies, they may be lost or intentionally discarded, and they may be differentially preserved, moved, curated, etc. To facilitate an understanding of these processes, archaeologists now collect sediment samples from archaeological deposits on a routine basis. The sediment samples are usually sent to a contract laboratory that performs standard physical and chemical analyses, while the archaeologist retains the artefactual materials for analysis. When it comes to making assumptions about material types or artefact types, however, the assumptions are often based on spurious numbers. For example, the relative frequency of artefact types cannot be compared across excavation units unless the type frequencies are corrected by the total volume of sediment (including artefacts) removed from the units. Volumetric data however, are not often recorded. At other times, archaeologists may only collect the cultural component of a sediment, which is separated by the use of sieves or visually identified and removed for analysis. The size of a sieve, however, limits the minimum size of particles recovered, and visual identification biases recovery toward more obtrusive shapes and colours. As a consequence, collection and/or identification techniques may alter the formal and quantitative characteristics of an archaeological assemblage, making it difficult or impossible to understand formation processes fully. Small, often microscopic, particles often hold the clues necessary for environmental reconstruction, artefact movement, and differential preservation.

Fieldwork procedures

The following section outlines the procedures used in the field for describing the surface characteristics of the Organic Bed (Unit 5a) including surface contour, micro-faulting, and desiccation cracks. Procedures for distinguishing, collecting, and sampling artefacts in the field are also discussed.

Surface features of the excavation area

The area excavated and sampled for microartefacts measured 3.5 x 4.0m and adjoined the eastern end of Area A in Quarry 2. To begin, the Brickearth Beds (Unit 6) were carefully removed by trowel to expose the surface of the Organic Bed (Unit 5a) (Table 9a).

Elevations for 1476 points were recorded at 100mm intervals across the surface prior to excavation. The elevations were used to generate a large-scale topographic map with contour intervals of 20mm (Fig 264). Depth of macroartefacts below the Organic Bed, into Unit 4c, was determined by superimposing the piece-plotted artefacts on the topographic map and subtracting artefact height from the value of the nearest contour interval. Height was always calculated relative to sea level. The large-scale topographic map and a two-dimensional posting (Figs 264 and 265) were generated on an IBM compatible computer using SURFER trend surface mapping software (Golden Software Inc).

After surveying the surface of Unit 5a, a plan was constructed to indicate the distribution of surface micro-faulting (Fig 266). These faults are believed to have been caused by structural collapse within the Slindon Sand (Unit 3) as a result of post-depositional solution of the underlying chalk bedrock (Roberts 1986; Bergman and Roberts above). High-angle (normal) micro-faulting is accompanied by secondary dome-and-basin morphology affecting Unit 5a, and the Slindon Silts (Unit 4) upon which it is formed. Basins occur with frequencies ranging from 3 to 5m and amplitudes of up to 0.8m. Dislocation along semi-lunar micro-faults ranges from 5 to 80mm. In addition, there are other indications that artefacts have been subjected to geological processes post-dating cultural deposition and associated with deformation of Unit 5a (Bergman and Roberts above). Lithic flakes up to 100mm in length were often found snapped into two or more pieces, sometimes with no measurable dissociation, whereas in other instances they were found metres apart (Bergman *et al* 1990). This was probably a result of the aforementioned faulting, in association with the enormous pressures exerted on such flakes by the weight of overlying deposits, together with the effects of scuffing and trampling of the scatters by large mammals. Other lithic flakes are found vertically oriented within the adjacent slip faces of micro-faults and within desiccation cracks. While desiccation cracks were physically absent during excavation they were well defined by ferruginous staining in a weak polygonal pattern. Although these processes have not moved lithic artefacts significantly, they explain why the Organic Bed/Unit 5a is so irregular, and why artefact depth must be related firstly to this surface and, secondly, to a general datum such as sea level.

Lithic-artefact size classes

Lithic-artefact size classes were established using the phi scale (Krumbein and Sloss 1963) which is the standard classification system used in geology and sedimentology for expressing particle size. The phi scale conveys particle size as a negative logarithm of diameter in base 2, ie:

$$(\phi) = -\log_2(d)$$

where ϕ = phi size

d = particle diameter in mm

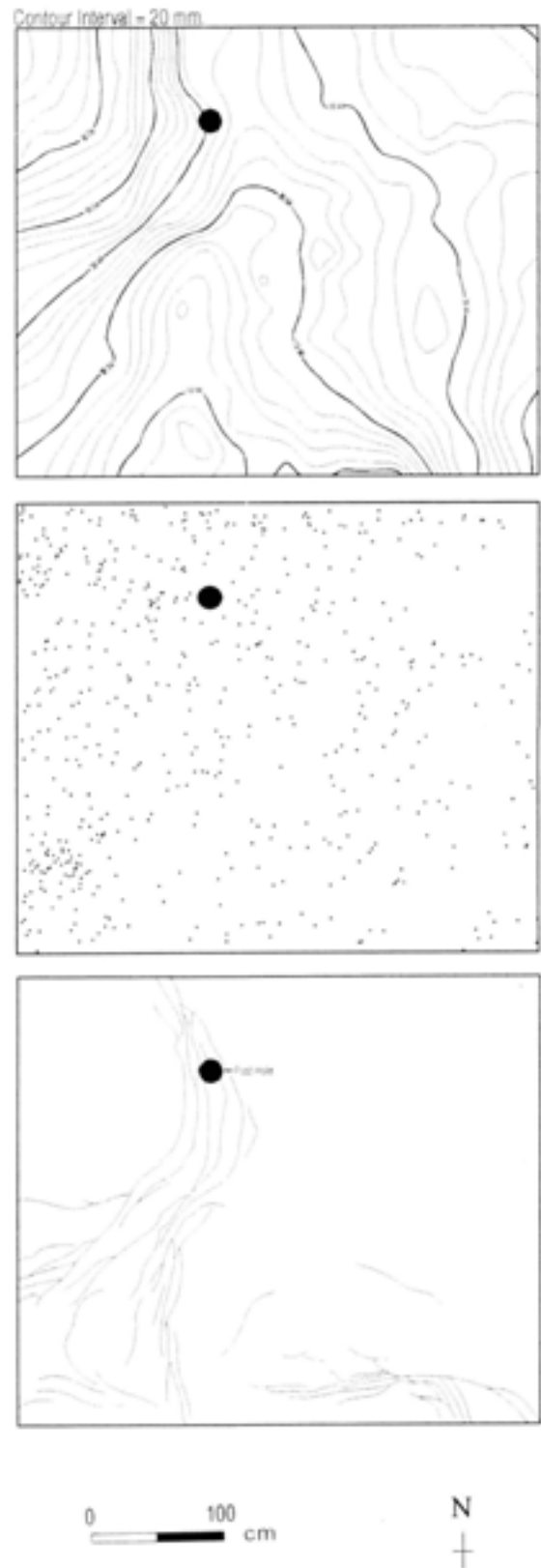


Fig 264 Surface topography of the Organic Bed, Unit 5a. The post-hole visible in Figs 264–6 is modern

Fig 265 Distribution of macroartefacts

Fig 266 Distribution of microfaulting across the Organic Bed (Unit 5a) and underlying deposits

The ϕ scale is particularly useful in the case of distributions based on weight because it normalises non-random data making it possible to use statistical techniques for analysis based on the normal distribution (Shackley 1975).

The two lithic artefact classes discussed below are macroartefacts and microartefacts. Macroartefacts are defined as any artefact that is -2.5ϕ (6.0mm) or greater along the b (intermediate) axis. Microartefacts are defined as any artefact smaller than -2.5ϕ (6.0mm) and larger than 1.0ϕ (0.5mm) also along the b axis. In recent literature, investigators typically define microartefacts, also referred to as micro-debitage, as any artefact less than -1.0ϕ (2.0mm) (Clark 1984; Dunnell and Stein 1989; Fladmark 1982; Hull 1984; Madsen 1992; Nicholson 1983; Stein 1987; Stein and Teltser 1989). In the context of this study, however, the arbitrary size division between macroartefacts and microartefacts is related to collection and sampling techniques rather than size. This is addressed in further detail in the following sections.

Macroartefact collection procedures

The nature of the archaeological deposit at Boxgrove simplifies the recognition of macroartefacts. The Organic Bed formed upon the surface of a soil horizon (Macphail Chapter 2.6) composed of approximately 50% clean rounded quartz grains, 39% ferruginous concretions, and 11% other minerals including lithic artefacts and, to a lesser extent, preserved bone (Wilhelmsen 1986). In pedological terms the deposit is a silty-clay loam with a texture of approximately 10% sand, 60% silt and 30% clay (Macphail and McConnell in Roberts 1986; Wilhelmsen 1986). The mean-grain size of the sediment is 7.15ϕ or 0.0078mm in diameter whereas the lower boundary of macroartefacts is -2.5ϕ or 6.0mm. Because of this vast size differential the probability of recognising and collecting even the smallest macroartefact is quite high. Consequently, all macroartefacts from the excavation area have been collected rather than sampled.

To collect macroartefacts they must be distinguished from microartefacts during the course of excavation. When an artefact was encountered, the b axis was measured using a plastic template with a square hole measuring -2.5ϕ (6.0mm) from side to side. If the artefact did not pass through the template it was considered a macroartefact and collected along with provenance and orientation data. Macroartefacts were then taken to the laboratory where they were further sorted into size classes at half- ϕ intervals and measured to determine mean-artefact diameter.

Microartefact sampling procedures

In contrast to macroartefacts, it was impractical to collect all microartefacts with their own size and provenance data. As such, representative samples were taken

from 56 squares, each measuring 0.5 x 0.5m. Spatial patterning was assessed on the basis of excavation unit frequencies for the 56 squares. Collection of microartefact samples in the field can best be described in terms of a single 0.5 x 0.5m excavation unit.

As excavation of a unit proceeded, the sediment, including microartefacts, was placed in an 8-litre bucket and filled to a line indicating approximately 10kg in weight. Sediment weight was recorded and the sediment was repeatedly poured through a Jones Sample Splitter (or 'riffle box') until a representative sub-sample of approximately 2kg was obtained. This procedure was repeated and all 2kg sub-samples were added to a single airtight bag until excavation of the unit was complete. At that time, the combined sub-samples were thoroughly mixed and poured through the sample splitter until two sub-samples were obtained, one weighing approximately 1.8kg and the other weighing approximately 100g. To avoid transporting the 1.8kg sub-sample back to the laboratory it was dispersed in a solution of water and sodium bicarbonate and sieved through a 1.0ϕ (0.5mm) geological sieve. All microartefacts collected in the 1.0ϕ sieve were then passed through additional sieves nested in half- ϕ intervals. The number of microartefacts in each ϕ -size class was then multiplied by a splitting factor to estimate their frequencies for the entire volume of sediment removed from the excavation unit. For example, a splitting factor of 26.67 was derived when the total unit weight (including sediment and artefacts) equalled 48kg, and the sub-sample weight equalled 1.8g. This was determined by dividing the total unit weight by the sub-sample weight. If there were six microartefacts measuring 1.5ϕ , this was multiplied by the splitting factor of 26.67 to yield a unit total of 160 microartefacts in that ϕ -size class.

All 100g sub-samples were then transported to the laboratory where they were used for textural analysis of the sand, silt and clay fractions. This procedure is described in further detail in the following section.

Analytical procedures

The following section describes laboratory techniques and procedures used to analyse the artefacts and archaeological sediment from Boxgrove. These techniques include textural analysis for the purpose of assessing grain-size distributions, and axial analysis for determining the mean diameter of macroartefacts.

Textural analysis

The grain-size distribution for each quarter-metre excavation unit was determined by sorting each 100g sub-sample into size classes using the sieve and pipette techniques described by Folk (1980). This combined the use of standard geological sieves for sorting the sand-size fraction, and a settling-tube technique for sorting silt- and clay-size fractions. The settling-tube

technique is based on Stoke's Law which governs the frictional resistance of a fluid to a particle falling through it (Shackley 1975). In general, Stoke's Law defines the settling velocity of a particle as a function of time, gravitational acceleration, particle size, shape and density, and the density of the fluid through which it settles. By reference to this law, it is possible to calculate the grain-size distribution of silt and clay fractions in a sediment when dispersed in a fluid medium.

A 100g sub-sample was oven dried at 95°C for 24 hours and then reduced to a sub-sample of approximately 30g using the Jones Sample Splitter. The sub-sample was then placed in a flask containing a dispersing agent of 1% sodium hexametaphosphate (NaPO_3)₆ to prevent flocculation (the aggregation of silt and clay particles). If no flocculation occurred within 24 hours of agitation, the sample was sieved through a 4.0 ϕ (0.0625mm) wet-sieve. The sand fraction was caught on the sieve, oven dried at 95°C for 24 hours, and passed through nested sieves of 0.5 ϕ intervals.

The silt and clay fractions passing through the dry and wet sieves were placed in a graduated cylinder containing 1 litre of dispersing agent. After agitating the cylinder, 20ml aliquots were removed by pipette at specific time and depth intervals, placed in tared beakers, and oven dried at 95°C. Weights of all ϕ size fractions were then entered into a computer programme that generates descriptive statistics such as grain-size distribution, mean-grain size, standard deviation, skewness, and kurtosis (after Folk 1980).

Axial analysis of macroartefacts

Although artefact- ϕ classes are used to examine the horizontal patterning of macroartefacts, these classes are too agglomerative and therefore insensitive for the analysis of vertical patterning. This is particularly true when the total vertical distribution is only 200 to 300mm. Consequently, a mean measure of diameter was calculated for each macroartefact so that vertical patterning could be assessed on the basis of individual artefacts rather than artefact-size classes. Mean diameter was calculated by adding the three prime axes of a macroartefact and dividing the sum by three.

Results of the analysis

Vertical distribution of macroartefacts

The Pearson product-moment correlation coefficient (r) was used to assess the significance of non-random macroartefact distribution in the vertical dimension. In particular, it was used to test for correlation between depth below Unit 5a, and macroartefact frequency, weight, and mean diameter.

Figure 267a shows the relationship between macroartefact frequency and depth below Unit 5a in Unit 4c, the soil horizon. The frequency distribution indicates that, as expected, only 1.25% ($n = 7$) of lithic

macroartefacts come from the surface of Unit 5a. Furthermore, it indicates that macroartefacts are almost normally distributed about a mode of 60mm below the surface, though the distribution is slightly skewed toward greater depth. An r -value of 0.438 corroborates that there is no significant relationship between frequency and depth ($p > 0.01$).

While macroartefact depth is almost normally distributed, the distribution of ϕ -size classes is skewed toward the negative ϕ sizes, ie larger artefacts (Figure 267b). The skewness results from an absence of microartefact data which truncates the distribution at -2.5ϕ (6mm), the boundary between macroartefacts and microartefacts. In this case the truncation of the distribution does not inhibit the use of correlation coefficients in the analysis. As long as the Pearson's correlation coefficient r is used strictly as a descriptor for the strength of association between variable pairs, there are no restrictions on sample kind or sample distribution (Thomas 1986). Normal distributions are

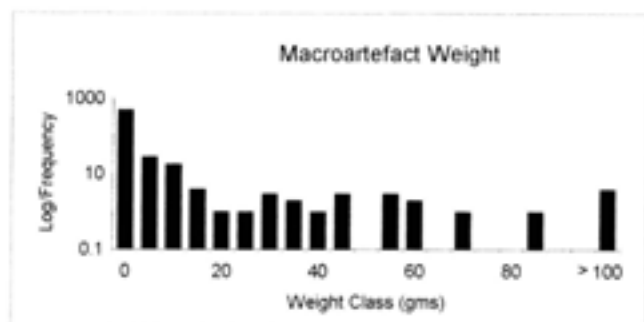
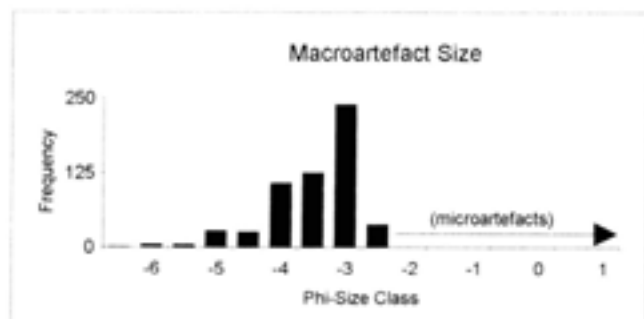
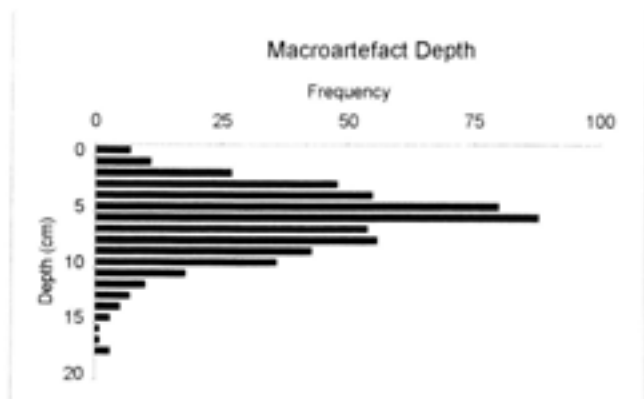


Fig 267a-c Plots of macroartefact frequency, depth, size, and weight ($n=573$)

only necessary when population parameters are inferred on the basis of Pearson's r . Correlation of macroartefact depth below Unit 5a with ϕ -size (at 0.5 ϕ intervals) indicates that there is no significant relationship or trend ($r = -0.1823$, $p = >0.01$).

Figure 267c shows the frequency of macroartefacts plotted against weight using class intervals of 5g. The shape of the distribution has been altered using \log_{10} transformation because of the relatively high frequency of macroartefacts between 5 and 10g. Correlation of artefact weight and depth shows no significant relationship between these variables ($r = 0.138$, $p = >0.01$).

In review, correlation analysis using Pearson's product-moment correlation coefficient (r) has demonstrated that no significant vertical sorting is evident when macroartefact frequency, size, and weight are examined.

Horizontal distribution of macroartefacts

K-means non-hierarchical cluster analysis was used to assess macroartefact patterning in the horizontal dimension. In particular, it was used to examine the horizontal distribution of macroartefacts assigned to size classes based on half- ϕ intervals. In so doing, the

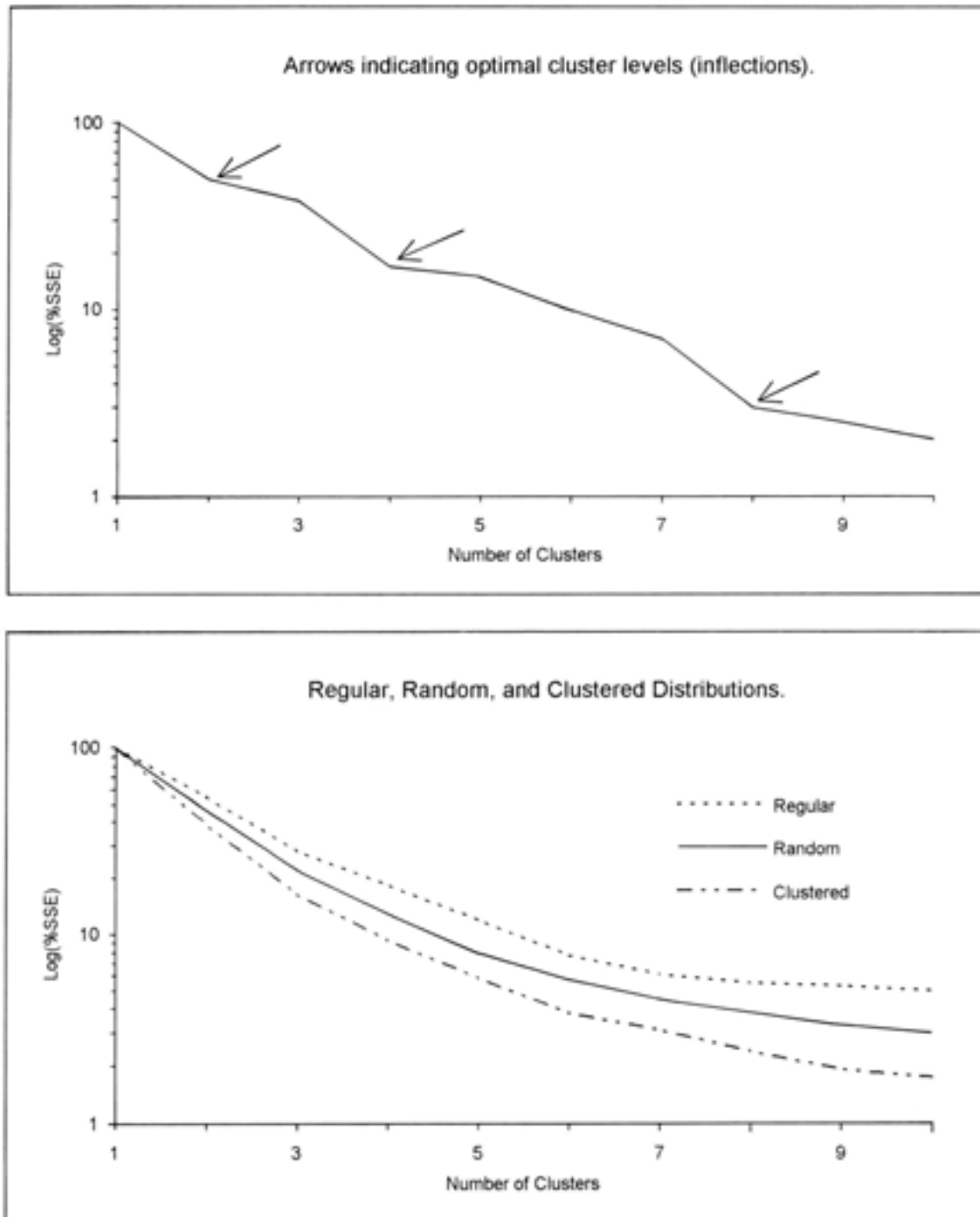


Fig 268 Log (% SSE) plots indicating characteristics of a hypothetical distribution

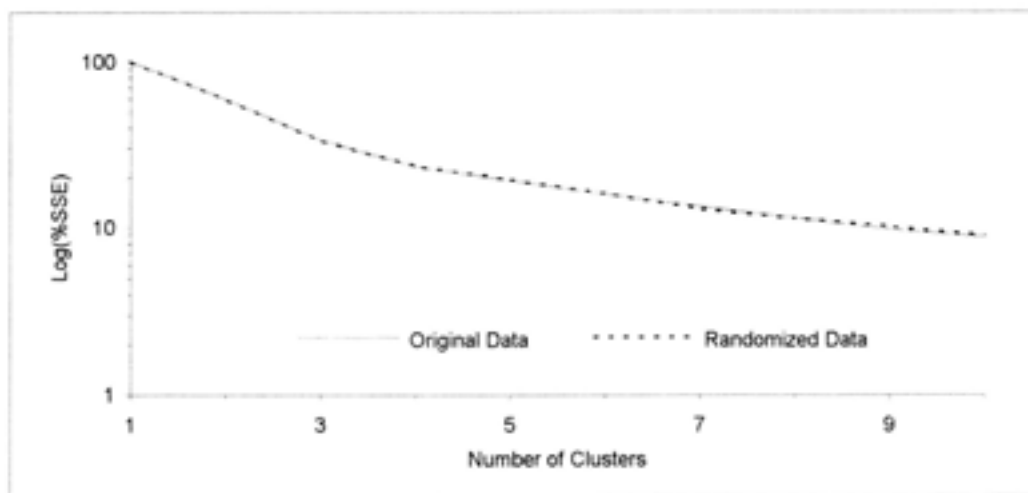


Fig 269 Log (% SSE) plot of macroartefacts (n=573)

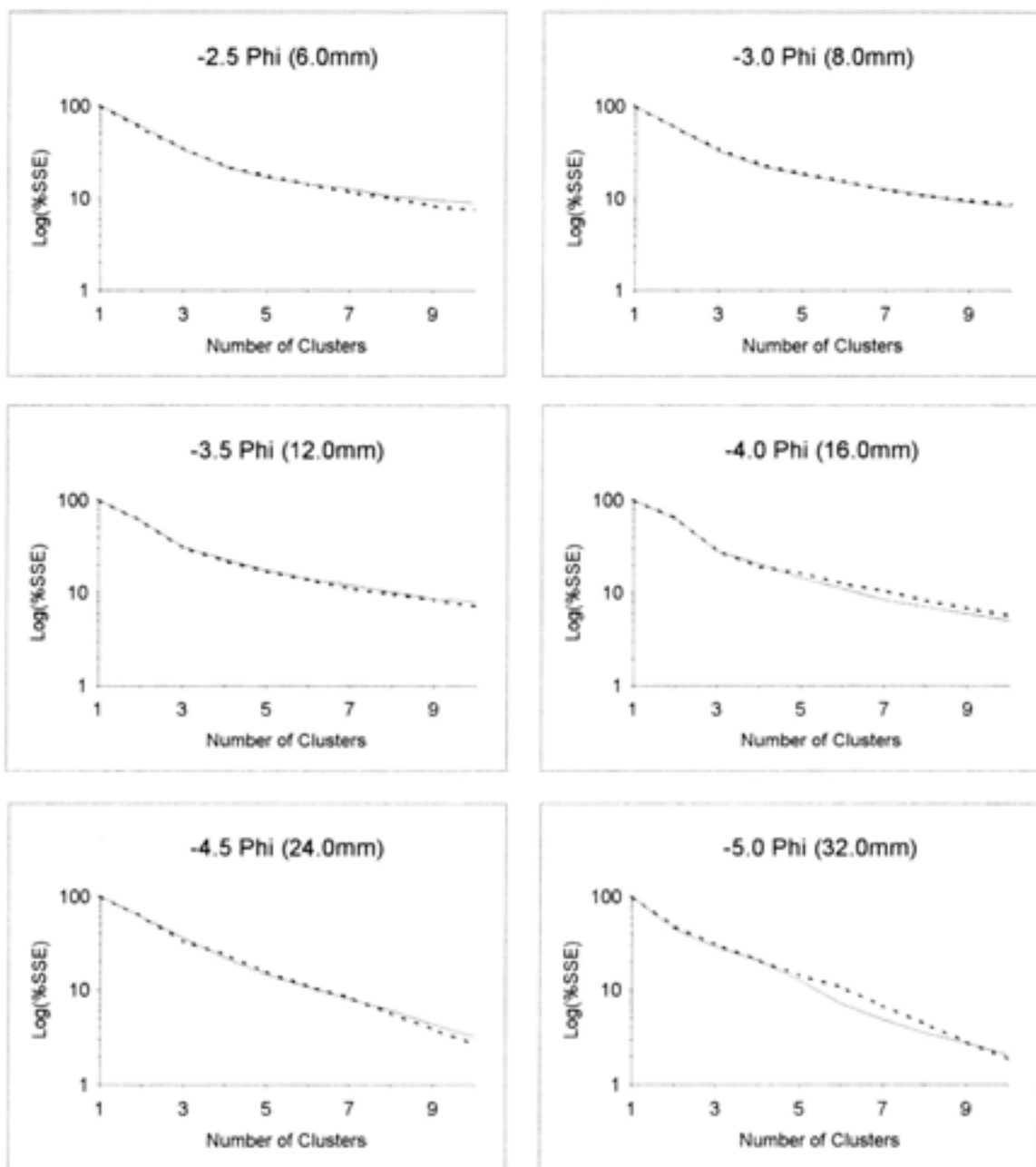


Fig 270 Log (% SSE) plots of individual macroartefact classes (solid lines are original data and dashed lines are randomised data)

tendency for spatially discrete artefact clustering could be examined and compared with the horizontal distribution of microartefacts and the Unit 5a surface.

The *k*-means algorithm is both divisive and iterative in that it initially defines a point distribution as a single cluster and then successively subdivides this cluster until a user-specified number of clusters is reached, hence the name *k*-means (Kintigh and Ammerman 1982). The programmes first locate the cluster centroid based on the mean X and Y coordinates of all points. The farthest point from the centroid is located and used as a seed for a new cluster. All points are then grouped with the seed or the centroid, whichever is nearest, and two new centroids are located based on the mean X and Y coordinates of the points in each group. This process continues until a stable solution is obtained in which the two clusters with the smallest SSE values are obtained. The SSE is the summed squared error statistic which reflects the sum of the squared distances between all points in the distribution and their nearest centroid. Hence, the two final clusters at the two-cluster solution level are those which are more clustered than any other two cluster combination. This step is carried out repeatedly until the user-specified number of solution levels is reached.

The clusters with the smallest SSE values for any given cluster level were determined by plotting the \log_{10} transformed SSE percentages ($\text{Log}(\%SSE)$) against the cluster levels. The plot in Figure 268a shows that $\text{Log}(\%SSE)$ could be expected to decrease naturally as more and more clusters were formed, since the distances between data points and centroids decreased with increasing numbers of clusters. However, when a substantial improvement in the 'tightness' of clustering occurred from one cluster solution to the next, an inflection, or drop, in the $\text{Log}(\%SSE)$ values was also apparent. These inflections were used to identify the optimal cluster solutions for a given distribution. Optimal cluster solutions were then selected for interpretation based on the assumption that the more tightly associated clusters were indicative of specific formation processes.

In addition to indicating the optimal cluster solution level, these same plots may indicate whether a distribution of points was random, regular or clustered. Figure 268b shows the $\text{Log}(\%SSE)$ values plotted against cluster levels for a random, regular and clustered distribution of points. The most important feature of this plot is the location of the regular and clustered curves with respect to the curve for randomised data. $\text{Log}(\%SSE)$ curves for regular distributions will always fall above a curve that is generated from the same data in which X and Y values are randomised. Curves for clustered distributions of points will always fall below the curve generated from the randomised data. Therefore, the degree and direction of a line's deviation from a curve derived from randomised data is indicative of a dataset's tendency toward randomness, regularity, or clusteredness.

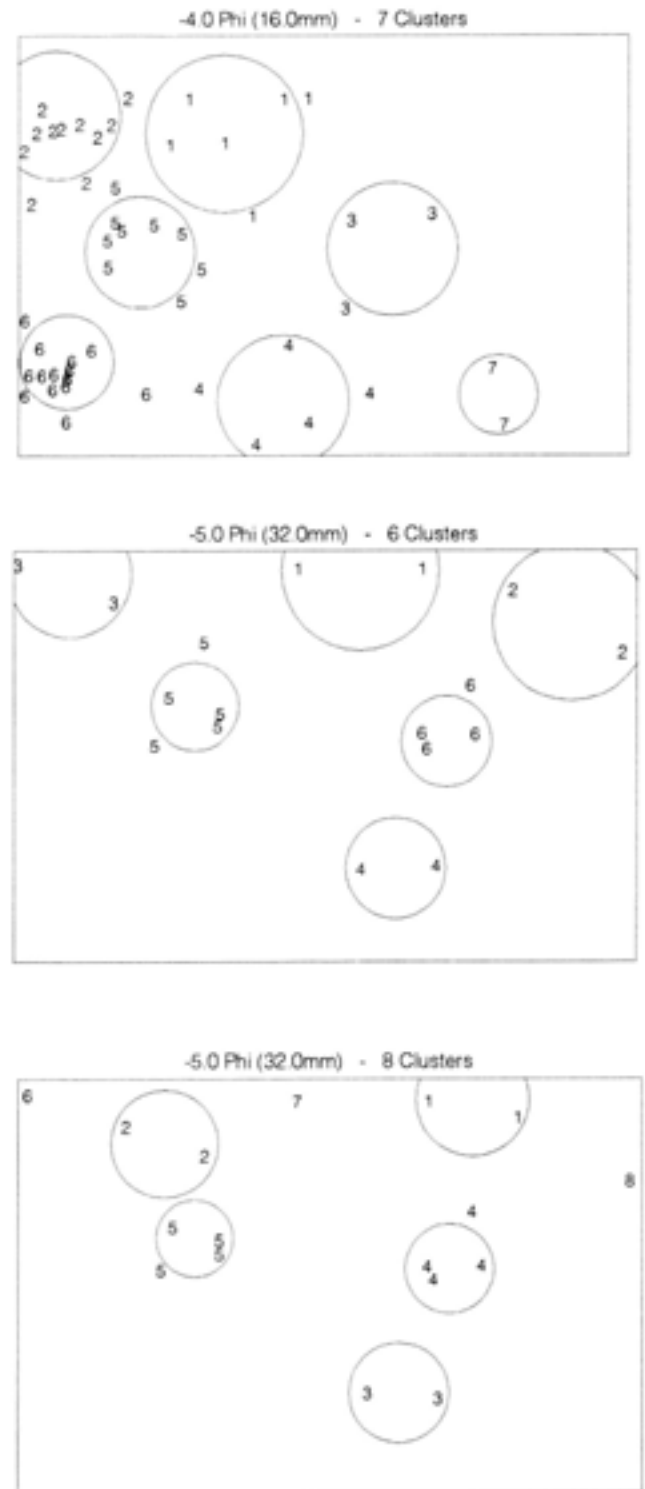


Fig 271 Plots of optimal cluster solutions

Figure 269 shows the $\text{Log}(\%SSE)$ curve for all macroartefact size classes, plotted with a curve produced from the randomised data. The curves are almost identical, indicating that the distribution of points is random when all macroartefacts are included in the cluster analysis.

Figure 270 shows $\text{Log}(\%SSE)$ curves for six different size classes of macroartefacts, along with curves generated from randomised data. The plots

indicate that only the -4.0 , and -5.0 ϕ -size classes have a tendency to be clustered, and only at certain cluster levels. The curve for the -4.0 ϕ class exhibits an inflection at the 7 cluster level while the -5.0 ϕ class exhibits inflections at the 6 and 8 cluster levels. Figure 271 presents graphs of these cluster

levels with circles drawn around the significant clusters. When the location of these clusters is compared with the contour map of the Unit 5a surface (Fig 264) it is apparent that there is no significant relationship between clustering and surface contour.

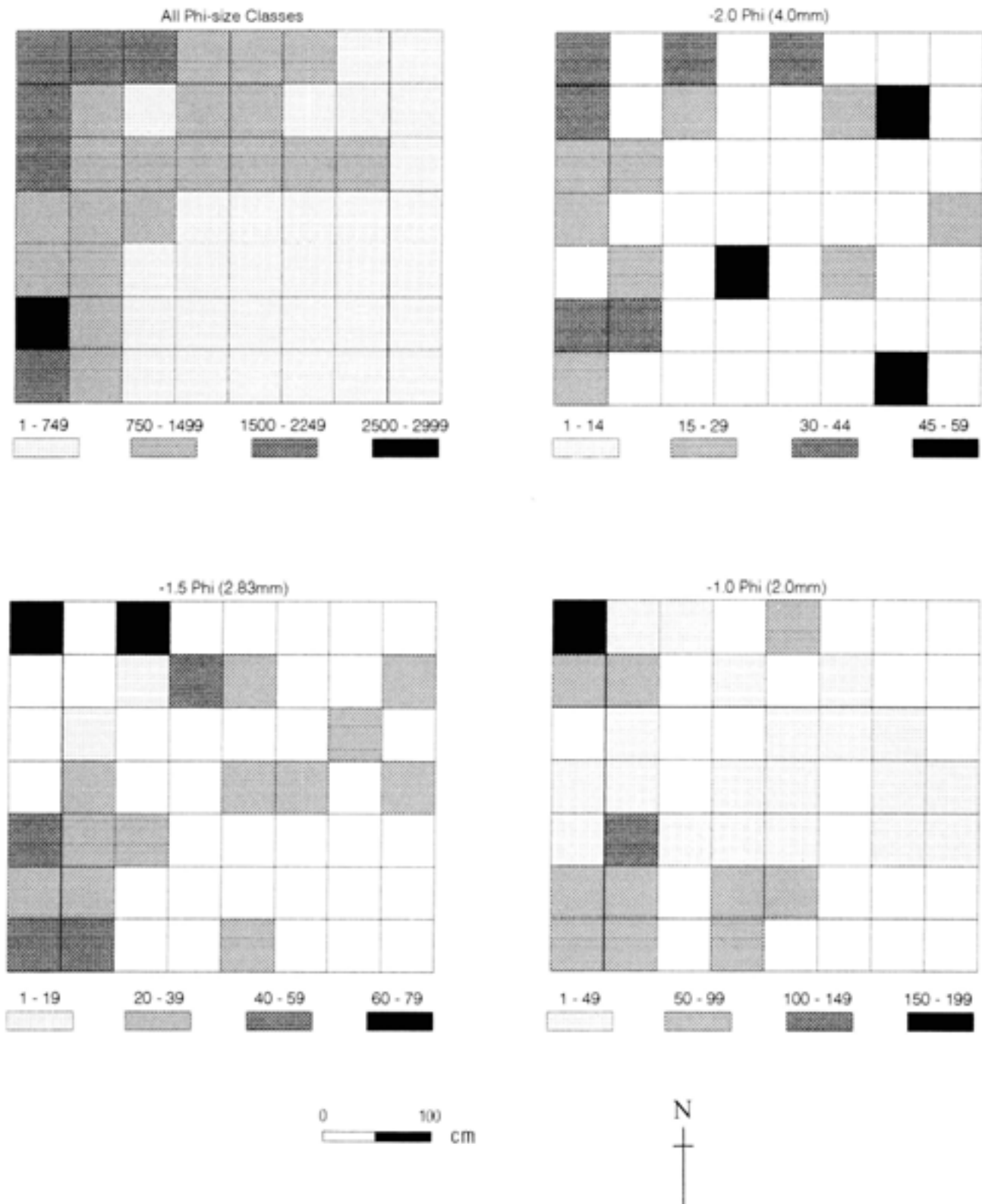


Fig 272 Density of macroartefacts in 0.5 x 0.5m excavation units

Horizontal distribution of microartefacts

Spatial patterning of microartefacts was assessed on the basis of artefact frequencies for the 56 excavation unit squares. Figure 272 shows that when individual size classes were aggregated, microartefacts occurred in all of the collection units. In addition, high densities were exhibited in the westernmost excavation units, while even higher densities were indicated in the north-western and south-western corners of the excavation.

Figures 272 and 273 also show the total frequency of microartefacts in each collection unit, broken down into individual size classes (note different class intervals). Several trends are indicated by these figures. The most notable trend is that the number of collection units containing microartefacts increases as the size classes decrease. The smaller microartefacts, such as the 0.5 and 1.0 ϕ classes (0.71 and 0.5mm respectively), are more evenly dispersed across the 56 collection units than larger size classes. The tendency for higher

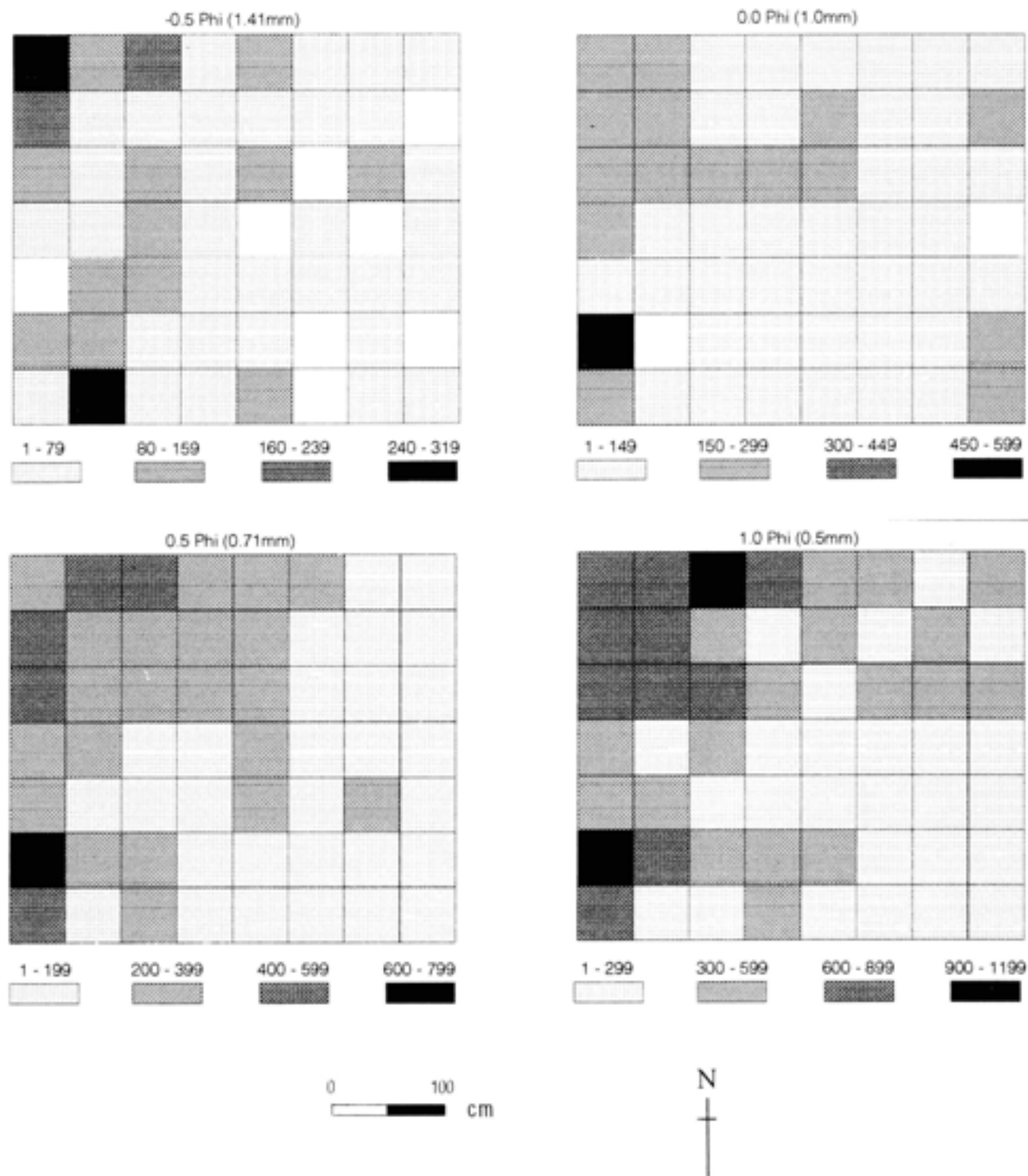


Fig 273 Density of microartefacts in 0.5 x 0.5m excavation units

densities in the north-western and south-western collection units is common among most of the size classes but is most apparent in the 1.0 ϕ (0.5mm) class.

Interpretation of results

Vertical distribution of macroartefacts

The histogram in Figure 267a shows that lithic macroartefact frequency is almost normally distributed with respect to depth below Unit 5a. A leptokurtic mode appears at 60mm and the distribution is slightly skewed toward greater depth. The shape and unimodality of this distribution indicates that the lithic artefacts were the result of a single depositional event within the soil horizon Unit 4c, rather than two or more temporally separate events.

The mode at 60mm most likely represents the surface on which the artefacts were deposited, suggesting that some upward and downward movement of artefacts has taken place. If this movement was substantial (ie statistically significant), we would expect a correlation coefficient indicating an inverse relationship between artefact depth and weight, but this is not the case. There is no significant vertical patterning that would suggest kinetic-sieve sorting induced by physical or biologicalurbation (Bourgeois personal communication), although it is known that earthworms and small mammals were active in the soil horizon of Unit 4c (Macphail Chapter 2.6; Parfitt Chapter 4.3). Furthermore, the range of the distribution is as little as 195mm arranged somewhat symmetrically about the mean. This evidence seems to suggest that there has been minimal vertical dissociation of macroartefacts since their deposition.

Figure 274 shows the composite vertical distribution of lithic macroartefacts from Unit 4c and faunal material from Unit 5a. Data for the faunal material come from around GTP 20, which is closer to the relict cliff line. As a result of the chalk gravel cover in this area, faunal preservation is good to excellent and many bones were recovered. Data for lithic artefacts, however, come from Q2/A, to the south (Fig 4). This far from the cliff, preservation of faunal material is very poor due to lower pH values. Only one poorly preserved bone was found in this area, making it necessary to compare lithic and faunal material from the two different areas. Unfortunately, it was not possible to obtain a sample of the fauna from Unit 4c, the soil horizon, for this analysis but work by Parfitt (Chapter 4.3) indicates that this unit has its own faunal assemblage that is temporally separate and taxonomically more diverse than that from the overlying Unit 5a. This separation is further emphasised by the fact that bones recovered from Unit 5a have a highly leptokurtic vertical distribution and exhibit a very narrow range (Fig 274). The mode of the distribution is at 0.0mm in depth, corresponding to the Organic Bed surface. The two distributions are clearly distinct and

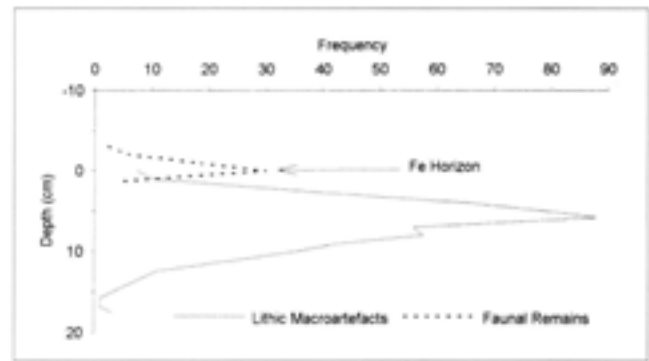


Fig 274 Composite distribution of lithic macroartefacts and faunal remains

slightly overlapping. This indicates that the Unit 4c lithic and Unit 5a faunal materials were deposited sequentially.

Horizontal distribution of macroartefacts

A *k*-means cluster analysis of the horizontal distribution of macroartefacts indicated that, regardless of the size class, there were very few clustered artefacts. Weakly developed clusters at -4.0 and -5.0 ϕ (Fig 271) did occur, but these bear no significant relationship to the topography of the Unit 5a surface (Fig 264). That this should be the case is understandable. Deformation of the fine-grained marine/lagoonal sediment (Unit 4c) took place after deposition of the overlying brickearth and solifluction gravels. This is indicated by the irregular surface contour of Unit 4 and the pattern of micro-faulting. Consequently, there is no reason to expect small macroartefacts to cluster within surface depressions. The artefacts were already deposited and held in place within the surrounding sediment matrix when deformation of the Unit 5a surface and underlying sediments took place. The horizontal distribution of macroartefacts, then, is related more strongly to cultural processes than to natural geological processes.

Horizontal distribution of microartefacts

The horizontal distribution of microartefacts as expressed by excavation unit frequencies supports the notion that minimal disturbance has taken place (Figs 272 and 273). The smaller size classes are distributed across the entire excavation surface. This seems to suggest that aeolian or alluvial processes were not of sufficient energy to disturb or selectively remove even the smallest microartefacts. The trend towards higher densities in the north-western and south-western excavation units is common in most classes of microartefact-size. While the *K*-means analysis did not indicate significant clusters of macroartefacts in these areas, visual examination suggests that macroartefact frequency increases outside the excavation boundary in these areas (Fig 265). Such a correspondence between macro- and microartefacts again suggests that artefact patterning is related more to cultural processes than to natural geological processes.

Conclusion

This research has employed spatial analysis to understand the depositional history of artefacts within certain archaeological deposits at the Boxgrove site and hence the integrity of the artefact assemblages. An analysis of the horizontal distribution of lithic artefacts was conducted to determine whether natural processes have significantly altered the pattern of cultural deposition. Perhaps most revealing is that microartefacts are nearly ubiquitous, especially the smaller size classes. These sizes are the most sensitive indicators of surface processes such as wind winnowing and sheet wash. No significant evidence of such processes is exhibited, however, indicating that the artefacts were effectively held in place by overlying sediment before they could be affected. Macroartefacts show no sign of being clustered horizontally. However, a visual examination of macroartefact locations suggests that their frequency increases outside this excavation boundary to the south-west and north-west, into the main area excavation of Q2/A (Bergman *et al* 1990). The vertical distribution of macroartefacts is more problematic, since the movement of the lithics through the soil must, in the absence of post-depositional and geological processes, be related to bioturbation by roots growing through the soil, earthworms and burrowing small mammals (Parfitt Chapter 4). However, as pointed out in the interpretation of results, these activities were occurring at a low frequency.

This study has shown that the lithic assemblage at Boxgrove is unique because it has escaped the dramatic effects of repeated glaciations that have disturbed or destroyed most other archaeological sites of similar age in Britain. Future spatial analysis of lithic artefacts from the quarry may be useful for distinguishing areas of raw material abundance, organised or opportunistic manufacturing, and functional specialisation.

Quarry 2 GTP 17

M B Roberts

GTP 17 is located at the north-western end of Quarry 2 (Figs 4, 275, 276), some 40m south of the buried cliff-line (Figs 22, 29, 33, 34). It is at the northern edge of the area known as Sand Extraction Area 2 (SEP 2) between the type section at GTP 13 and the beach section GTP 25. Accordingly, excavation and analysis have been facilitated by tight sedimentological control. The geology at the site is highly calcareous, given the proximity to the cliff; some localised decalcification resulted from solution hollows in the overlying gravels (Fig 277). These fan gravels are largely calcareous but show signs of general calcium carbonate depletion by percolating ground water. Between the fan gravels and Unit 5a (Table 9a) are bands of silts with varying calcium carbonate content (Units 5b, 6) and a restricted organic horizon (Unit 5c) (Macphail Chapter 2.6).

Excavation began here in 1989, in response to quarrying for marine sand. The area to the south of the excavation trench was stripped to the top of the silts by a box-scraper (Fig 275), while to the west a drag line removed the gravels to just above the silts. This part of the site is represented on Figure 275 by the unexcavated area. Large scale excavation continued until 1991 and all fieldwork was complete by the end of 1992. The results of this work are given here in brief, because of the importance of this area to the overall interpretation of the site. A full account of research at GTP 17 will appear in the second Boxgrove monograph (Roberts *et al* in prep).

The surface of the silts, Unit 4c, was partly disturbed by quarrying. However an area of 234m² was rapidly excavated within a 2m grid system. Two hand-axes (Fig 278), a broken handaxe and 500 flakes over 20mm were recovered, either by direct excavation or collection when the surface was disturbed. The flint-work was in fresh condition but quite heavily patinated.

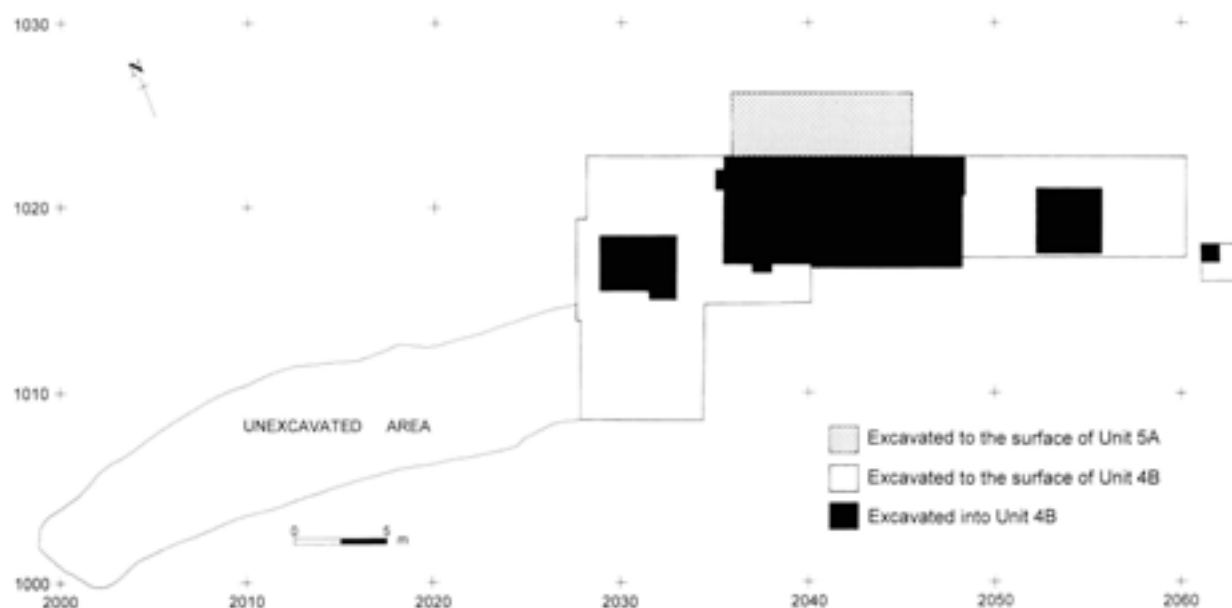


Fig 275 Plan of excavated areas at Quarry 2 GTP 17



Fig 276 GTP 17, looking east; scale unit 0.5m



Fig 277 Excavated trench in Q2 GTP 17; note the areas of darker sediment due to the effect of solution on the sediments; scale unit 0.1m

The fauna was composed of deer, rhino, and bison and included butchered material (Parfitt and Roberts Chapter 6.5, Figs 322, 323).

In 1989 a test pit was dug through the excavated Unit 4c into the silts (Unit 4b), which revealed an archaeological horizon similar to that from Q1/A (Austin and Roberts this chapter). The test pit was expanded to a 4 x 4.5m area and the grid size was reduced from 4m² to 0.25m²; this grid was then suspended above the site. As in Q1/A, flints were occasionally found in the sediment between Unit 4c and the archaeological horizon in Unit 4b but it has not been possible to refit them to material from either horizon. Upon reaching the main archaeological horizon, c 0.4m below the 4b/4c interface, a spit system was introduced to facilitate excavation. In all, four spits were used to complete the excavation, through a layer that varied in thickness between 40mm and 70mm. Recording at GTP 17 was by direct overhead photography, which produced photographs to scale that were then inked in as the artefacts were numbered (>1800 pieces over

20mm) and lifted. Detailed plans were then made from these photographs to cover the whole area (Figs 279, 280). Contour maps were made at the end of spit 1 and two spits below the lowest occurrence of archaeological material. This meant the heights of the assemblages were tightly constrained relative to the local microtopography. While the main focus of the excavation is shown in Figure 275, two smaller areas were dug to the east and west to trace the extent of the archaeological horizon. These trenches revealed a barren area to the east and a reduction in material to the west of the western pit. Looking at the overall densities of material, it is considered that the scatter probably runs north-east/south-west through the middle of GTP 17.

At GTP 17 Unit 4b there is evidence of a single episode of horse butchery (Parfitt and Roberts Chapter 6.5). The carcass was complete when either killed or secured via confrontational scavenging by hunters (O'Connell and Hawkes 1988; O'Connell *et al* 1988). Large flint nodules were then brought to the carcass from the cliff, and knapped around it (Figs 281, 282). Analysis being undertaken at the time of publication suggests that six or seven nodules were brought to the site, although the distribution diagram (Fig 279) indicates that there was more material outside the excavation trench. The reduction of these blocks appears on preliminary analysis to have occurred in two phases. Firstly there were the main reduction episodes which dressed the raw nodules, then part of the thinning and shaping process also took place. The virtually completed handaxe then appears to have been finished at another location, not far away, generally between 1 and 2m, but definitely separate from the original activity.

The reduction scatters remain *in situ* and refitting of the first group (Figs 283, 284) has had a success rate of over 60%, which is higher than at any of the other main areas (Austin and Roberts, Bergman and Roberts above). The primary reduction sequence and initial thinning and shaping sequence (Fig 283) has been refitted into a single, almost round, nodule that exhibits over 70% cortex on its outer surface. The void in the middle of the nodule conforms to the shape of an ovate handaxe rough-out. The large size of the raw material is surprising, given the amount of reduction required to produce the rough-out. However, this level of reduction does provide many large primary flakes with extensive cutting edges. The difference between nodule reduction and handaxe finishing can be seen in Figures 285 and 286. The scatters of lithic and faunal debris were so dense that recording (Fig 287) and excavation (Fig 288) became very difficult, which was the main reason that the photographic method of recording was employed.

The spreads of knapping debris and the comprehensive butchery of the horse suggest that a group of people took part in this activity over a period of several hours. This implies control over the kill and the ability to protect it from other predators, without the use of fire for which there is no evidence at this location.

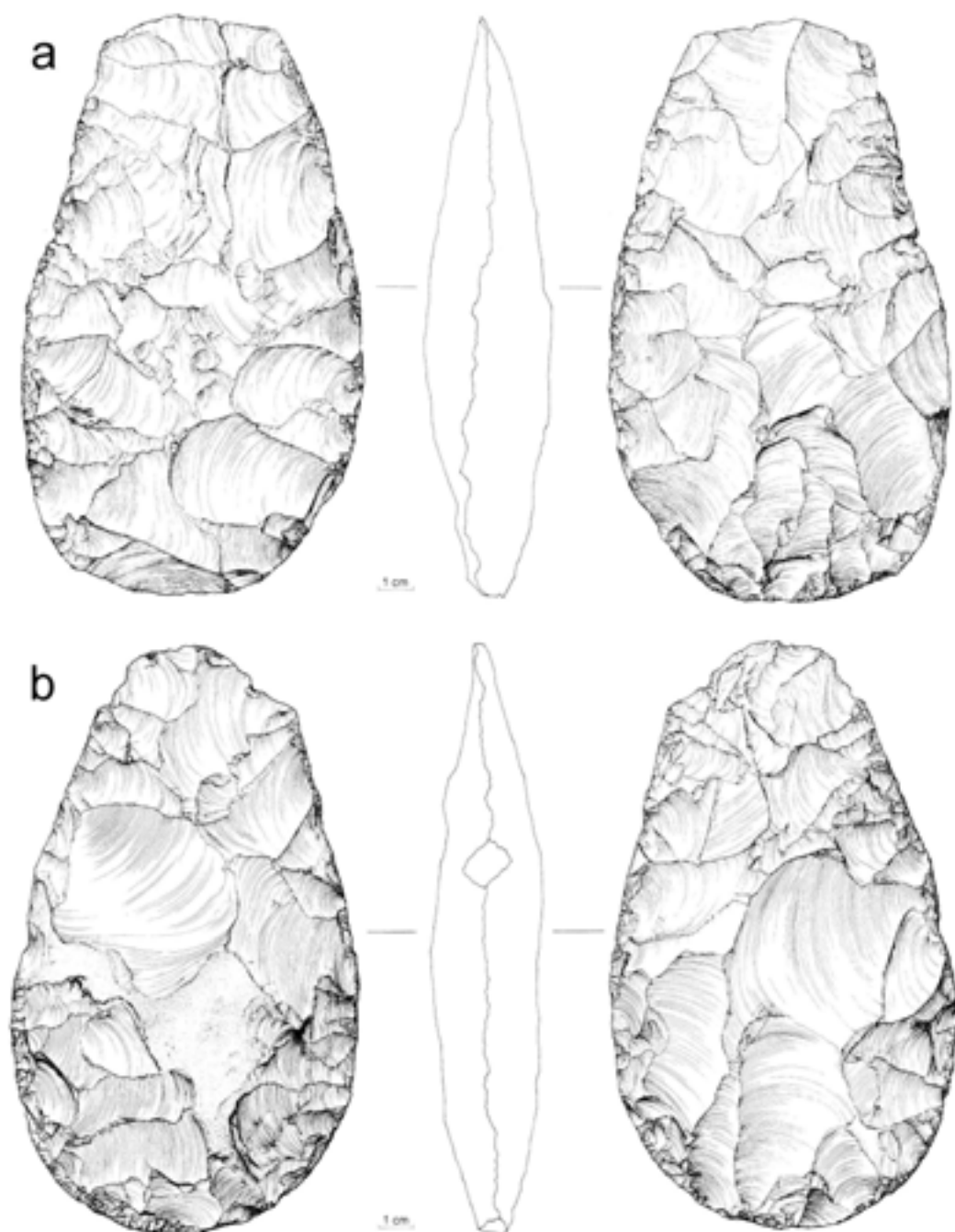


Fig 278a–b Handaxes from Unit 4c at GTP 17

It has been suggested (C Gamble personal communication) that the complex of knapping scatters at GTP 17 might have been the result of discrete episodes of lithic reduction by an individual, rather than a group. This hypothesis is, however, rejected on the following grounds.

The horse butchery site half a million years ago would have been on an exposed mudflat some 40m from the cliff-line. There were no topographic features which would have made this an attractive place to stop and knap flint. Similarly, there is no evidence for freshwater, shade, or any other determinant which marks this spot out as being more clement than any other on this landsurface. Archaeologically, the assemblage

composition points towards an area of butchery rather than any other activity, and there is no suggestion of more intensive and repeated use of the area.

The horse remains represent the only butchered fauna in this area at this level; therefore there would have been no reason to continue bringing large blocks of flint into the locale, to reduce, after the horse was butchered. There would be little point one person repeatedly bringing nodules back to the carcass, as adequate raw material for butchery would already be present from the flakes and tools of the initial reduction sequence.

The horse carcass would have quickly been eaten and disaggregated by carnivores, such as lions, hyaenas, and wolves. If an individual was scavenging the carcass



Fig 281 Flintwork scatter from horse butchery from GTP 17; note the large primary flakes; scale unit 50mm

Fig 282 Detail of Fig 281; scale unit 10mm

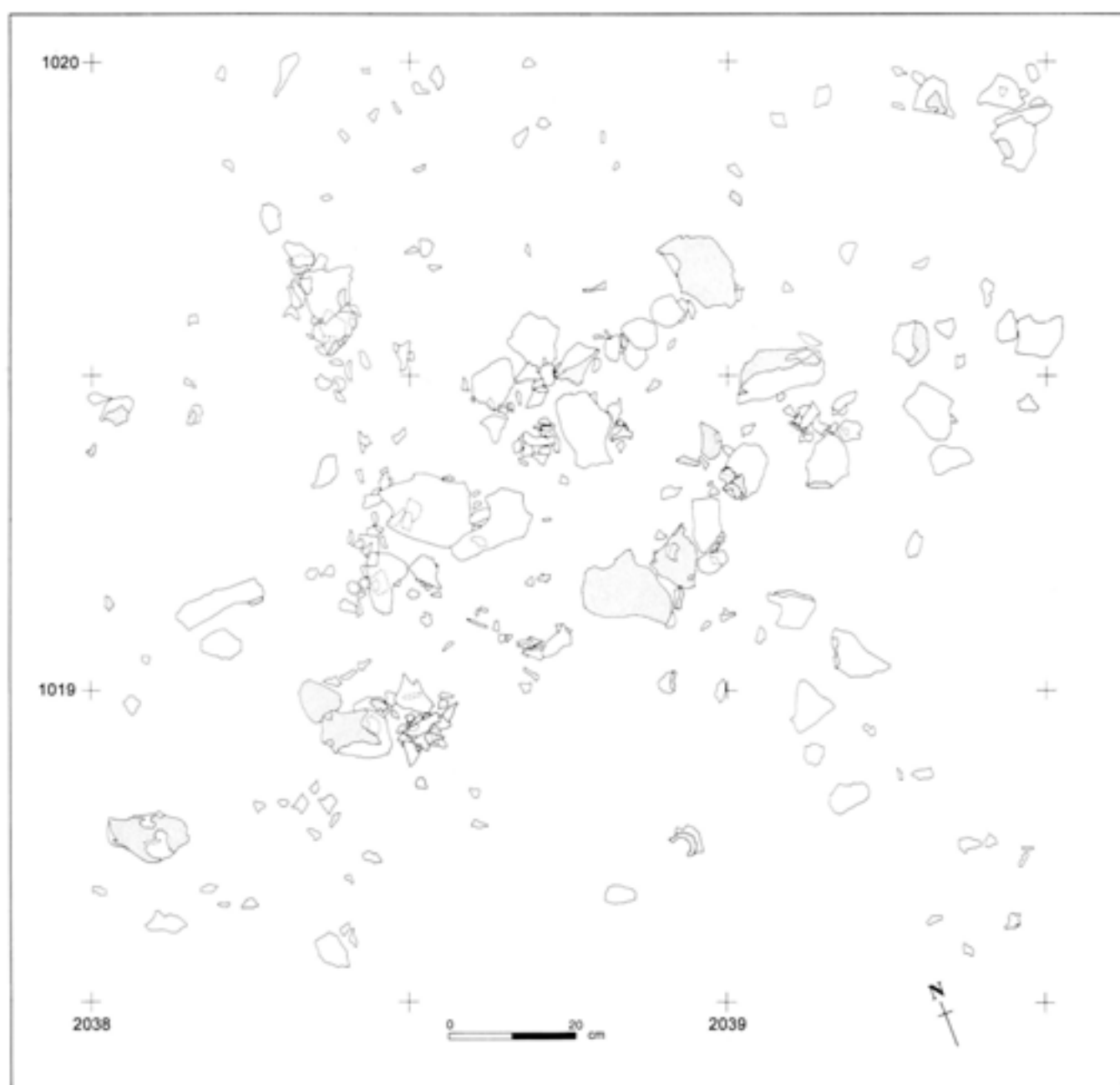


Fig 283 Artefact plan of scatter in Fig 281

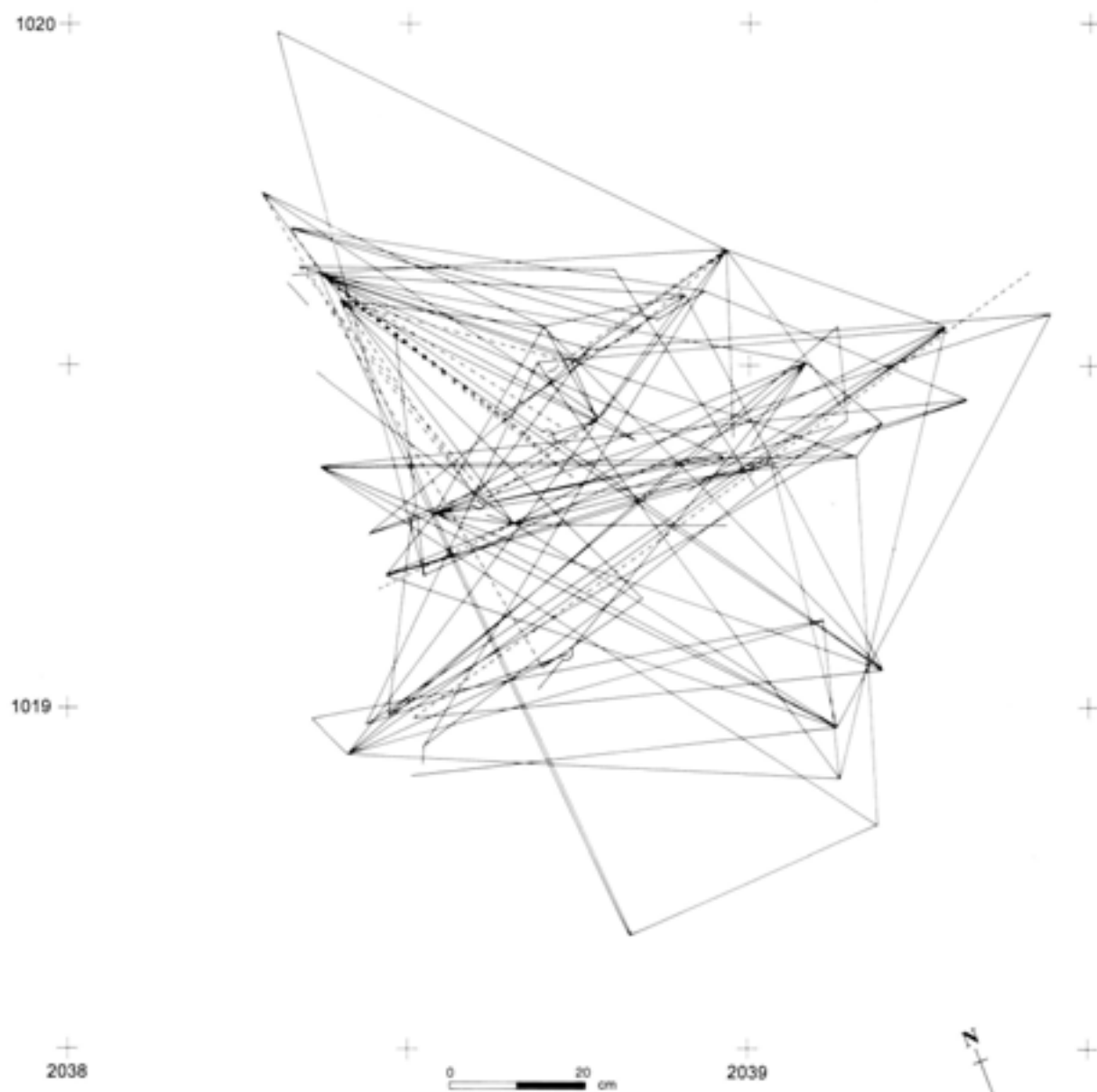


Fig 284 Ventral/dorsal and break refits from scatter in Fig 281

over an extended period of time, there would be a higher incidence of gnawing marks on the faunal elements analysed (Parfitt and Roberts Chapter 6.5), and cut marks would overlie gnawing marks, a feature never observed in the Boxgrove fauna. It is also doubtful whether the nutritional return from the carcass, after carnivore processing, would have warranted the labour of repeated knapping events and return trips to the site of the kill.

Empirical and analytical observation of the evidence from GTP 17 points to the horse having been complete when reached by the hominids; the evidence

suggests this was probably because they had just killed it. Forty metres from the cliff, some of the group would have had to go to the screens at the foot of the cliff to obtain raw material, whilst others of the group would have kept a watch for predators. The carcass was then skinned, disarticulated, and butchered (Parfitt and Roberts Chapter 6.5). Finally, all the major marrow bearing bones were smashed and the marrow extracted.

The large numbers of nodules (>6) brought to the kill probably give an indication of the minimum group size. The refitting of the scatters (Figs 283, 284), and the sedimentological context confirm that they are *in situ*,



Fig 285 Dense distribution of primary knapping debris at the horse butchery site; scale unit 50mm



Fig 286 Handaxe reduction scatter from the horse butchery site; compare with Fig 285; scale unit 50mm



Fig 287 Recording the archaeology at GTP 17



Fig 288 Excavation at GTP 17



Fig 289 Part of the horse scapula exhibiting semicircular wound, probably from a projectile impact; scale unit 50mm

therefore the separation of tasks between nodule dressing and handaxe reduction is a real phenomenon. At present, however, the reasons behind the division remain unknown. The *in situ* spread of lithic material also suggests that the dismembered carcass elements were butchered by individuals at different locations across the site (Fig 279), although the final position of the smashed bone fragments is likely to have undergone alteration by carnivores picking over the remains of the butchery episode (Fig 280). It is difficult to conceive why an individual would move about the area in the manner illustrated by the lithics, and produce tools that were used for major muscle block butchery. An individual returning to the depleted carcass would have been better equipped with a sharp flake and a hammerstone and anvil.

Nine main knapping episodes were uncovered in the excavated area and it is logical to assume that this number would rise with further excavation. This site provides the first good evidence for social interaction and other behavioural patterns among Middle

Pleistocene hominids at Boxgrove. If the puncture mark in the horse scapula (Fig 289) is confirmed by forthcoming analytical work as a projectile wound (Bernard Knight personal communication), then we shall have another line of evidence, in addition to the total primacy of cut marks and access to complete carcasses, that points towards the hunting of large mammals as opposed to confrontational scavenging.

6.3 Flintwork from other contexts

M B Roberts

At Boxgrove, the term residual flintwork is used to describe material from contexts where there has been post-depositional movement of the sedimentary body containing the archaeology. Bioturbation in the form of small mammal burrowing, rooting, or horizontal displacement by the scuffing action of large mammals is not considered sufficient at this site to move the assemblages from *in situ* to residual status. Residual flintwork has been found in Units 2, 3, 7, 8, 9, 10, and 11 (Table 9a). However, some units contain both *in situ* and residual material, such as the Slindon Sands and Chalk Pellet Beds.

With the exception of the material from the marine Slindon Sands (Unit 3) (Fig 290) and the main phase of cliff collapse (Unit 7), all the other units of the Earham formation were known to contain archaeology prior to the inception of this project, due mainly to the labours of Woodcock (1981), who sampled the gravel horizons in the 1970s. The present research under the direction of the author has confirmed many of Woodcock's observations, but for researchers wishing to compare the two reports certain differences in sedimentary nomenclature need to be clarified. The unit described by Woodcock (*ibid*, 106) as the Slindon Sand is now called the Slindon Silt (formally defined here, see also Roberts 1996). The buried channels are now referred to as the Path/Fan Gravels, Unit 9. The Lower Chalky Coombe rock is now divided into three major units: the Angular Chalk Bed (Unit 7), the Chalk Pellet Bed (Unit 8) and the Calcareous Head Gravel (Unit 10) (Table 9a). The Middle Brickearth of Woodcock is described here as the Upper Silt Bed (Figs 22, 33, 34, 79). At present, however, this is the only unit of the Silt Beds in which archaeological material has been found.



Fig 290 Handaxe thinning flake in basal sediments of Marine Cycle 3 at GTP 13; scale unit 50mm



Fig 291 Cleaned section through the beach deposits and overlying Chalk Pellet Beds at GTP 25. The section revealed a flint scatter 2m above the top of the beach; location of scatter is shown on Fig 42a; scale unit 0.5m

The excavations at Boxgrove presented here have concentrated on the *in situ* archaeology from Unit 4 in Quarries 1 and 2, which was under the threat of destruction from quarrying. Accordingly, most of the material from other units has been recovered as the result of geological investigation and/or palaeoenvironmental sampling of the relevant units. Two controlled excavations were carried out in younger units, the first by Woodcock (1981, 134) in the Upper Silt Bed (Eartham Upper Gravel Member) and the second by the author on scatters of material in the Upper Chalk Pellet Beds of Unit 8, revealed in the beach cutting GTP 25 (Figs 291–4); these latter scatters were *in situ* (Macphail Chapter 2.4). The results of these excavations and general study of the residual flintwork contain significant implications for the hominid exploitation of the region and are discussed below.



Fig 292 Relationship of the flint scatter to the chalky gravels; scale unit 50mm



Fig 293 Vertical view of the refitting flint scatter; scale unit 50mm

The archaeological material from units other than Unit 4 consists almost entirely of lithic material; fauna is sometimes found in the calcareous gravels but none of it is attributable to human collection or butchery, although one butchered bone has been recovered from the body



Fig 294 Detail of Fig 293; note the sharpness of the flakes; scale unit 50mm

of the Slindon Sands. The lithic material shows no major variation in style or assemblage composition from the oldest, in the raised beach of the marine phase, to that in the Upper Silt Bed. The production of handaxes appears to be the main consideration for the hominid flint knappers throughout the temperate and into the ensuing cold stage. When comparing material from these varying units, especially when looking at the handaxe form, the following points need to be borne in mind.

- The environmental conditions prevailing at the time of unit/assemblage deposition.
- The availability of flint generally, and specifically the size and type of nodules available.
- The degree to which the final shape of the handaxe, after geological processes have acted upon it as a sedimentary constituent, reflects the original finished shape.
- The bias in the collection towards large, readily observable, pieces like handaxes and primary reduction flakes, compared with smaller elements of the debitage.

Taking these points into consideration, a number of general points may be made. Variation in handaxe shape becomes greater if all bifacially worked pieces

are considered (Fig 295a). However, when completed pieces only are compared there is little or no variation from the bottom to the top of the units (see below for discussion on handaxes from the Upper Silt Bed). Much debate has taken place on the subject of handaxe rough-outs (Bordes 1961; 1968; 1984; Woodcock 1981). The term implies that these are part of a staged production process in that a nodule is reduced to a certain state and then set aside for further use (Roberts Chapter 2.2, GTP 17). Analysis of all the Boxgrove assemblages suggests that this hypothesis is difficult to test. Most of the artefacts described as rough-outs appear to have been discarded without use, often because of flaws in the nodule, although experienced modern knappers will often consider that they could have been reduced further to produce a serviceable handaxe (Bergman and Wenban-Smith personal communication). Thus distinguishing what has been put aside for further use and what has been discarded is a particularly difficult task. It is worth considering that amongst the finished handaxes recovered from Boxgrove there are very few which can be considered failures (<2%); it is therefore likely that there was a fairly rigorous selection of nodules and an equally firm discard policy. Additional confusion is caused by the fact that many so called rough-outs were used as tools and there was no requirement to finish them further. Many of these pieces exhibit characteristics such as tranchet blows and secondary working of small areas of edge.

There is one type of handaxe/rough-out from the gravel units that needs further examination, particularly as it has not yet been discovered in an *in situ* context. This is the long, rectangularly shaped artefact, where length is always two times breadth in complete pieces (Fig 295a). As the preferred finished shape of Boxgrove handaxes is ovate or elongated ovate, then it can be seen that it is almost technologically impossible to reduce most of the Boxgrove rough-outs of this type to the preferred shape. These bifacially worked pieces occur in units containing a wide variety of nodule shapes and thus a raw material constraint upon shape can be disregarded, with the exception of Unit 11 (White 1995). If they were tools then a heavy duty activity may be inferred, since the sinuous edges produced by the final flake removals and the thickness of the pieces preclude a skinning or meat cutting role. Experimental butchery and study of butchered faunal remains at Boxgrove has revealed that disarticulation is achieved far more easily by anatomical knowledge and a sharp instrument (Parfitt and Roberts Chapter 6.5), be it a handaxe or a flake, than by a bludgeoning approach. Post-depositional abrasion on the residual pieces means that it is difficult to speculate how much of the edge damage could be due to use as opposed to sedimentary processes. Again, experimentation and exploration of potential uses are the only methods available to investigate how these artefacts may have been employed. The author agrees with Ashton *et al* (1992) and McNabb (1992) that it is extremely unlikely

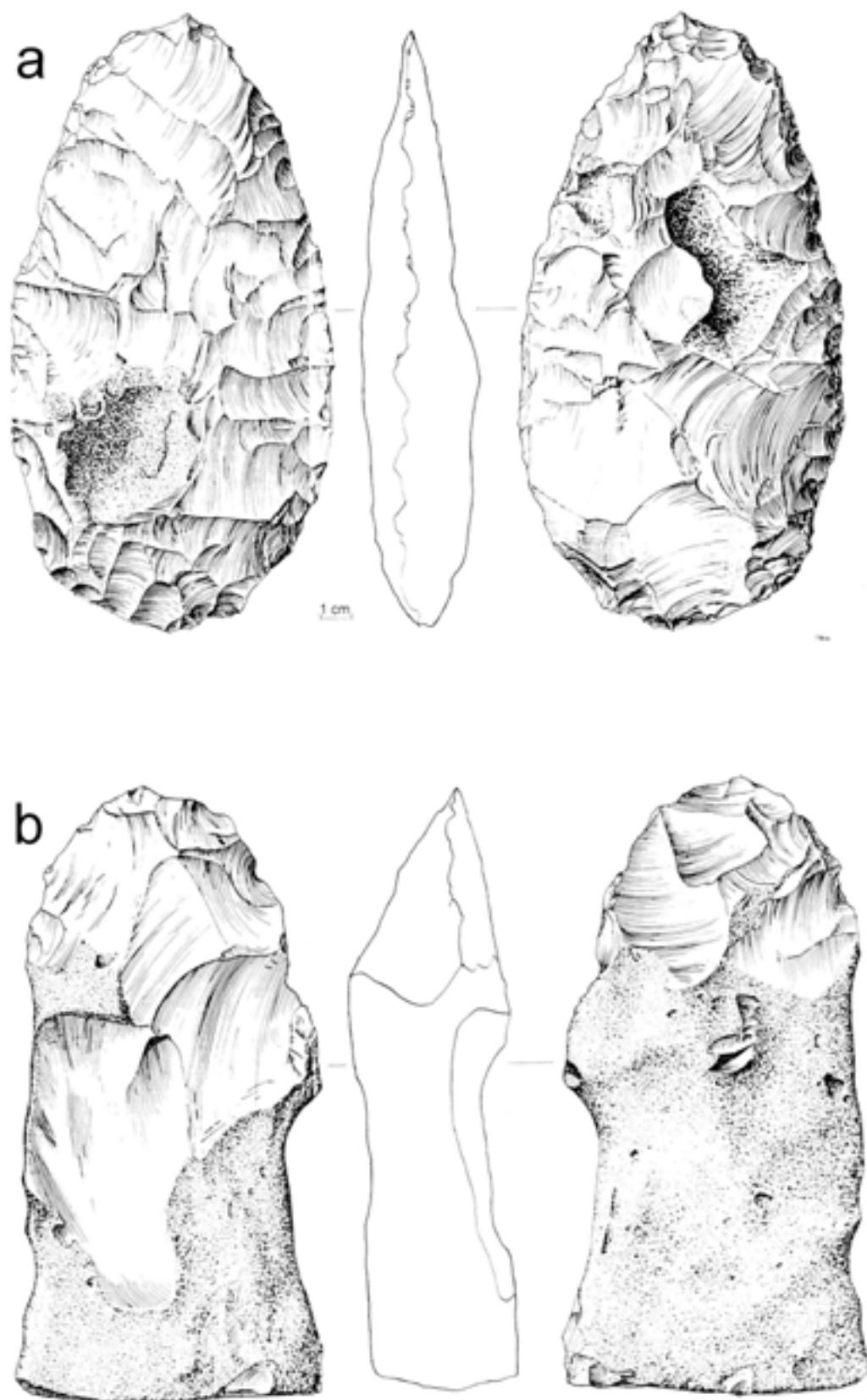


Fig 295a–b a) 'Rough-out' from the gravels of the Earham Formation, b) Handaxe from the head gravel deposits of the Earham Formation (see Fig 298)

that tools such as these were ever used as choppers due to their basic inefficiency for the tasks of chopping wood or bone, and the fact that these tasks are better undertaken by other tools such as flakes and large beach cobbles respectively. Other tasks, such as the processing of roots, opening nuts and cracking bones for marrow, are all more successfully achieved using nodules or beach pebbles and an anvil, techniques which were in use at Boxgrove, as demonstrated at Q1/A and GTP 17 (Parfitt and Roberts Chapter 6.5). The one remaining task for which these are effective tools is digging, although it should be noted that none of the finished forms displays any evidence for this activity (J C Mitchell personal communication). However, palaeoenvironmental reconstruction of the landscape pertaining to the times when material was being worked suggests that once slope/cliff stability was established then soil cover would have built up very quickly, even on very steep slopes, a fact that can be ascertained readily from an examination of the chalk slopes around the Dover area today. Micromorphological evidence (Macphail Chapter 2.6), points to the build up of calcareous soil horizons which can only have occurred in the region of the cliff and scree slopes, as the Tertiary regolith covered the upper dip slope and Downland surface. Therefore at certain times it may have been necessary to dig nodules from the chalk sources at the base of the slope. This model does not entail an organised mining of raw material but perhaps an opportunistic prospecting of an area, just subsurface, which provided the best raw material. As mentioned above, there is no definite evidence for this behaviour but it can be inferred that at certain times the raw material would be buried and that a best fit model based on this particular handaxe morphology suggests the likelihood of such an activity. Thus it may be stated that the evidence from Boxgrove suggests that using the term rough-out solely to suggest a blank for handaxes can be misleading, and in this context at least should be used with caution. Pieces that typologically fall into the catch-all category of rough-outs may actually be either usable tools or discarded pieces.

The range of lithic material from largely residual contexts varies. In the beach gravels of Unit 2, occasional rolled handaxes and flakes are found (Fig 42a). These lithics are the oldest at Boxgrove but, as stated earlier, they are typologically similar to all the later material. The material exhibits all the characteristics of flint artefacts from an active rudaceous sedimentary context: chatter marks across the surfaces, smoothing and dulling of features such as *arrêtes* and percussion rings. The presence of flintwork in this context suggests that it was knapped directly on the beach, on blocks obtained from marine erosion of the chalk cliff. Lithics from Unit 3, the Slindon Sands, have been found in the Boxgrove type section GTP 13. The oldest piece, a handaxe finishing flake, was found in the sediments of Marine Cycle 2 (Collcutt Chapter 2.3) (Fig 56), and handaxe thinning flakes have been found

on the surface of the cliff collapse (Chalk raft) material at the base of Marine Cycle 3 (Figs 44, 45a, 46, 290). These lithics are unrolled and in very sharp condition, so it is therefore likely that they were dropped on surfaces revealed at low tide and were incorporated quickly into the sediment body. This hypothesis was further strengthened by the discovery of a fragment of butchered cervid tibia shaft, in the sands just above the aforementioned chalk raft of collapse material (Parfitt and Roberts Chapter 6.5; Figs 333–4). The preservation of this bone confirms that it was dropped or worked at this location rather than reworked from an inshore surface or deposits.

After the Slindon Sands, residual flintwork is encountered again in the sediments of the Eartham Formation. These units contain enormous amounts of flintwork, with a known extent from Boxgrove in the west to Slindon in the east (Figs 1a, 9, 10) (Woodcock 1981; Roberts Chapter 1.3). The material in the gravel members is very similar throughout the constituent units, the major change being the degree of rolling which increases with transport and thus distance away from the chalk cliff. All the calcareous units and the fan gravels contain thin, finished, ovates as well as heavy bifacial pieces (see above). All the ranges of debitage are also present, as well as cores which display the characteristic Lower Palaeolithic forms, namely unidirectional, migrating platform and alternating platform technique (McNabb 1992). The cores are often developed on nodules which began life as handaxe reduction sequences and failed either through end shock or the realisation that they would not reduce sufficiently to produce a usable tool. Throughout the residual assemblage, analysis of the cores has shown that there is not a single example producing flakes that could not also have been produced as a by-product of the complete reduction of a nodule to produce a handaxe. The calcareous units above the beach have also produced an endscraper. Although this is only a single piece, its occurrence in GTP 25 in conjunction with finished and usable handaxes suggests that activities other than just flint procurement and knapping occurred at the cliff edge and upon the various surfaces that developed on the calcareous gravels through time. Study of the knapping patterns from the *in situ* area excavations (Austin and Roberts, Bergman and Roberts Chapter 6.2) shows that raw material was taken to these areas for knapping in the form of complete or almost complete nodules, often involving a walk of over two hundred and fifty metres carrying the raw material. If the theory of factory sites (Woodcock 1981) was tenable then such an activity would be unnecessary. The evidence from both the *in situ* and residual contexts points towards the opportunistic procurement of flint and knapping of the nodules where they were to be used.

No hammerstones or other types of percussors have been recovered from units other than the Slindon Silts, although this is again likely to be a product of collection bias. The flakes from the gravels exhibit evidence

of hard and soft hammer flaking (Bergman in Roberts 1986; Bergman and Roberts 1988; Bergman *et al* 1990) and a range of platform types. Statistical comparison between the *in situ* and residual flakes is considered to be invalid given the difference in collection techniques, although this could be done for the *in situ* scatter found within Unit 8, see below (Figs 291–4).

The age of the lithics from other units relative to the *in situ* material of Unit 4 involves solving the complex problem of estimating rates of deposition of geological units. It may be stated that the lithics from the Slindon Gravel and Sand Members were deposited during the interglacial stage and pre-date the lithics from Unit 4. However, there can be no doubt that some material from the early stage of deposition of the Angular Chalk Bed (cliff collapse) is penecontemporaneous with the archaeology from the levels in Unit 4 (Table 9a). The most interesting fact about the material from the units of the Eartham Gravel Upper Member is that some of the lithics were deposited by hominids into the sediments during the cold stage that followed the temperate episode (Roberts Chapter 6.8). Other material in these units has been swept up and mobilised from surfaces extant during the interglacial. The calcareous gravel over the most southerly part of the raised beach (Fig 42a) post-dates the deposition of the brickearth and represents a mass movement deposit deriving from the scree slope and cliff collapse to the north. At a level two metres above the raised beach, a refitting scatter of flakes has been excavated and recorded (Figs 292–4). There is no doubt that this scatter is contemporaneous with the surface upon which it rests and on which a restricted soil has developed (Macphail Chapter 2.6). This is interpreted as representing a hiatus in chalk gravel deposition and minor climatic amelioration (earthworm activity), equivalent to Unit 6'3'Fe (Table 9b). The flakes represent the reduction of a large nodule and contain primary cortex removals and some removals into the centre of the piece. Unfortunately, the core and the later removals were lost during the cutting of GTP 25 so it is not known whether this reduction sequence represents core reduction for flakes or the preparation of a nodule for handaxe production. The scatter does however confirm a human presence in the landscape after the climatic optimum. The survival of hominids well into the Anglian Cold Stage is further confirmed by the occurrence of handaxes and flint scatters in the Upper Silt Bed and Head Gravels of Unit 11 (Roberts 1992) (Table 9a, Figs 295b–298). Three flakes were recovered from the Upper Silt Bed during sampling; this unit has been correlated as the sedimentological equivalent of Woodcock's Middle Brickearth, which yielded seven handaxes and over fifty other artefacts including two cores. These handaxes, which Woodcock says are dissimilar to his other material from the gravels, compare closely in technology with the Boxgrove *in situ* industry. Five out of the seven, 70%, have tranchet flake removals from the tip



Fig 296 The head gravel deposits containing refitting flintwork in the western edge of Quarry 2; the location of the scatter is marked by the bottom of the 2m scale

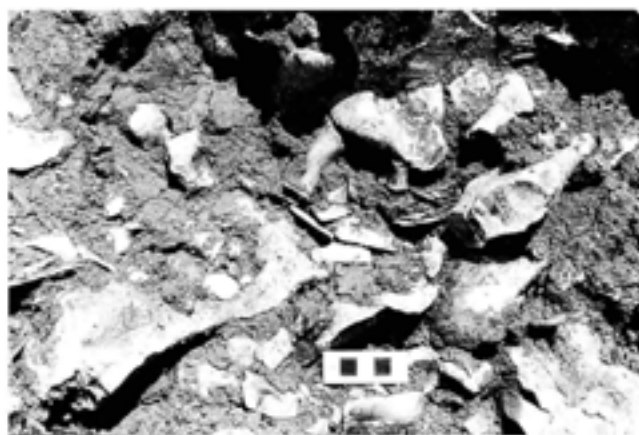


Fig 297 Refitting flintwork from the mass movement head gravels; scale unit 10mm



Fig 298 Handaxe from the mass movement head gravels, found 0.4m away from the refitting scatter; scale unit 10mm

(Woodcock 1981, 139), although they are longer and more pointed in form. This material is in very sharp condition although it is uncertain whether it was incorporated in the unit from further up-slope and thus moved southwards as part of the unit. The lack of coarse material in the Brickearth would mean that, during a mud flow, the artefacts would not be damaged except by contact with each other. Whichever of these scenarios is correct, landscape reconstruction shows that the artefacts must have been incorporated into the unit a considerable time after the end of the climatic optimum. Handaxes and flakes have also been found in the gravels of Unit 11 (Fig 296). At first it appeared that this was normal residual material but upon closer inspection the flakes were found to occur at a discrete level in the gravel and to refit (Fig 297). The handaxes found in association with this level, one of which is shown in Figures 295b and 298, were longer and less ovate than other handaxes from the underlying units, confirming the observations made by Woodcock (1981). Current thinking suggests that this change in shape was the result of changes in raw material supply after the chalk cliff was buried by the mass movement of non-calcareous head gravel deposits.

The lithic material from units other than Unit 4 at Boxgrove has proved to be an important component in understanding the continuity of hominid technology at this period in time. When studied in conjunction with sedimentological and environmental data, these lithics also make an important contribution to understanding human behaviour in terms of the ability to exploit and survive in very different climatic and environmental regimes.

6.4 Knapping technology

F F Wenban-Smith

Introduction

Boxgrove's rich archaeological resource of essentially undisturbed knapping debitage preserved in its original position in the landscape, has enabled us to address many questions concerning the spatial organisation of human behaviour in relation to flint knapping. The aims of this chapter are to consider: 1) which of the materials available to the Palaeolithic people of Boxgrove could potentially have been used as percussors for the manufacture of handaxes and 2) what materials were they actually using. The answers to these questions can help determine to what extent Palaeolithic knapping at Boxgrove depended upon the exploitation of immediately available local resources, how the locations of knapping activity were related to the likely sources of the necessary percussor and flint nodule, and so finally the degree of forward-planning which went into knapping activity. Therefore, in order to identify which materials could have been used as percussors, and to learn to distinguish between them

by studying the debitage attributes, a programme of knapping experiments was carried out. In these experiments a variety of potential percussors were used for the manufacture of handaxes from local Boxgrove flint, and numerous flake attributes were recorded to investigate the extent to which any particular attribute might relate to a percussor. The knapping and attribute recording were carried out by John McNabb and the author.

As a result of this experimental work it was possible, using discriminant multi-variate statistical analysis (Canonical Variates), to establish: a) that debitage from soft, organic percussors (antler or bone), soft-stone percussors (cortical flint), and hard percussors (rolled flint or quartzite) could be consistently distinguished from each other, and b) that hard, soft, and cortical flint percussors were used by the Palaeolithic knappers at Boxgrove. Subsequent examination of the faunal remains and worked flint recovered from the archaeological levels confirmed the presence of bone, cortical flint, and rolled flint pebble percussors.

Artefactual remains are found at many different levels within the Boxgrove sequence but are richest within the inter-tidal zone of regressional/lagoonal sediments (Unit 4b), and on the surface of these sediments (Unit 4c). Units 4b and 4c are preserved in a band approximately 250m wide to the south of a chalk cliff, now truncated by erosion and buried by later solifluction deposits, which would have been a prominent feature of the Palaeolithic landscape. Along the base of the buried cliff runs the well-known Goodwood-Slindon Raised Beach (Fowler 1932; Roberts 1986; Shephard-Thorn *et al* 1982). The chalk cliff would have provided a plentiful supply of flint, which could have been grubbed directly from the chalk, or gathered from the base of the cliff where it had eroded out. The beach would have provided numerous well-rolled flint pebbles suitable for knapping.

The artefactual remains comprise numerous ovate handaxes in association with many thousands of flint flakes of all sizes, lying in clusters indicative of minimal disturbance, and in mint condition (Wymer in Singer *et al* 1973). Refitting studies (Austin 1994; Austin and Roberts Chapter 6.2; Bergman and Roberts 1988; Bergman *et al* 1990; Bergman and Roberts Chapter 6.2) and experimental knapping (Wenban-Smith 1985) suggest that the artefacts in Unit 4b remained almost completely undisturbed since they were knapped, whereas those in Unit 4c have been subject to greater disturbance, some having been moved up to several metres in one direction or another.

Experimental percussors

Experimental knapping has been a part of lithic study since the nineteenth century when it played a major role in demonstrating the hominid origin of flint handaxes and debitage (Johnson 1978). Since then there has been a great deal of interest in the manufacturing aspects of

lithic studies, with a cumulative quantity of experimental work throughout the twentieth century devoted to establishing, among other issues, how lithic artefacts from all periods were made, and what percussors (or 'hammers') were suitable. The earliest experimental knappers identified hand-held rounded quartzite or flint pebbles as suitable percussors for the manufacture of Palaeolithic artefacts (eg Evans 1872, 20, 33) and subsequent experimenters have continued to find quartzite an ideal stone percussor (or 'hard-hammer') being dense, tough and durable (eg Newcomer 1971). Coutier (1929) provides the first recorded instance of experimenting with softer organic materials (bone and acacia wood) as percussors for the manufacture of handaxes, and came to the conclusion that thin and sharp handaxes could not be made without the use of a soft percussor (or 'soft-hammer') such as wood. Bordes (1947) also emphasised the usefulness of wooden or long-bone soft-hammers for the thinning and finishing of handaxes. More recently, the sawn-off beams of shed antlers have become the preferred soft-hammer of experimental knappers. Crabtree (1967) is the first published reference to the use of antler as a soft-hammer for direct percussion flaking, although he does not specifically refer to its use for bifacial thinning. Bordes is shown using an antler soft-hammer for bifacial thinning in photos which date to the mid-late 1960s (Howell 1968, 118–19). Newcomer (1971) used three different-sized red deer antler soft-hammers in his experiments making handaxes, as well as two quartzite hammerstones as hard-hammers.

Crabtree (1967) also recognised that 'soft' stones can be used in a similar way, and have the same qualities as organic soft-hammers. Ohnuma and Bergman (1982) used a soft-stone (sandstone) pebble as a percussor in a set of experiments designed to investigate the identification of percussors, and found it worked well, with the flakes produced being hard to distinguish from those produced by an organic soft-hammer. Subsequently, Bergman conducted experiments at Boxgrove in 1985 in which he succeeded in making typical Boxgrove handaxes using a piece of cortical flint as a percussor. As well as the experimental work which has led to the identification of possible prehistoric percussors, such tools have also been identified from archaeological contexts. For instance, Evans (1872, 31) interpreted battered quartzite pebbles found in abandoned Neolithic flint mines at Grimes Graves as having been used in the manufacture of flint axes, Spurrell (1880) interpreted two rounded pieces of flint retaining most of their cortex as having been used as hammers at the Middle Palaeolithic site of Crayford, and Bordes (1974) identified a reindeer antler soft-hammer from Solutrean levels at Laugerie-Haute in France. McNabb (personal communication) reports flint pebbles possibly used as hammerstones amongst collections from the British Lower Palaeolithic sites of Swanscombe (Wymer 1968, 332–54), Little Thurrock (Wymer 1957), and Caddington (Smith 1894; 1916).

Additionally, Chase (1990) has identified fragments of long-bone with marks suggesting use as a retouching percussor for flint scrapers at the site of La Quina, in France.

Following the work of Coutier and Bordes, handaxe manufacture has generally been conceived as being divided into two main stages. The first stage or 'roughing-out' involves the removal of large flakes from a nodule whilst giving it a generally bifacial shape and removing any gross protrusions from its surfaces. For roughing-out, hard-hammers of most types of stone, including flint itself provided a well-rolled pebble is used, have proved effective in experimental work, with quartzite being preferred. While it is possible to use a large soft-hammer for roughing out, modern knappers have found this highly impractical (eg Bordes 1947; Crabtree 1970). Therefore the experimental programme did not attempt to use soft-hammers for roughing-out handaxes. The second stage, or 'thinning and shaping', involves the removal of flakes from both surfaces whilst refining the thinness and symmetry of the handaxe. Some workers (eg Newcomer 1971) identify a third 'finishing' stage in which the thinned handaxe is further refined and sharpened. In these knapping experiments a bi-partite sequence of reduction was followed, with roughing-out and thinning/finishing stages being recognised. However, it should be acknowledged that a strict separation between a roughing-out stage and a thinning/finishing stage may exist only in the minds of modern experimental knappers (Wenban-Smith 1988). For the thinning/finishing of handaxes, it has been considered since the work of Coutier (1929) that organic soft-hammers are essential to produce sharp and thin handaxes such as are found throughout the north-west European Lower/Middle Palaeolithic. Suitable soft-hammers might have been made of hardwoods such as acacia, oak or boxwood, or animal parts such as bone or deer antler. However, Bradley and Sampson (1986) have suggested that, contrary to the assertions of previous workers such as Bordes and Coutier, it was possible to thin and finish a handaxe with a quartzite pebble, striking on the carefully prepared margins of the handaxe. This work, together with that of Ohnuma and Bergman (1982) with a sandstone hammer, and of Bergman at Boxgrove with a cortical flint hammer, suggests that stone (and especially softer types) can be useful for knapping tasks generally conceived as requiring an organic soft-hammer. Therefore the experimental programme included the use of rolled flint pebbles and cortical flint for the thinning/finishing of handaxes. The only hard-hammers available in the immediate area of Boxgrove were rolled flint pebbles from the beach at the base of the chalk cliff (see Chapters 2.4, 6.2, and 6.3). As this was the likely source of raw material, this would have been convenient for the Palaeolithic knappers. In the experimental programme both rolled flint pebbles from the Boxgrove raised-beach and also quartzite pebbles from the Dorset coast (about 80km away) were used as hard-hammers.

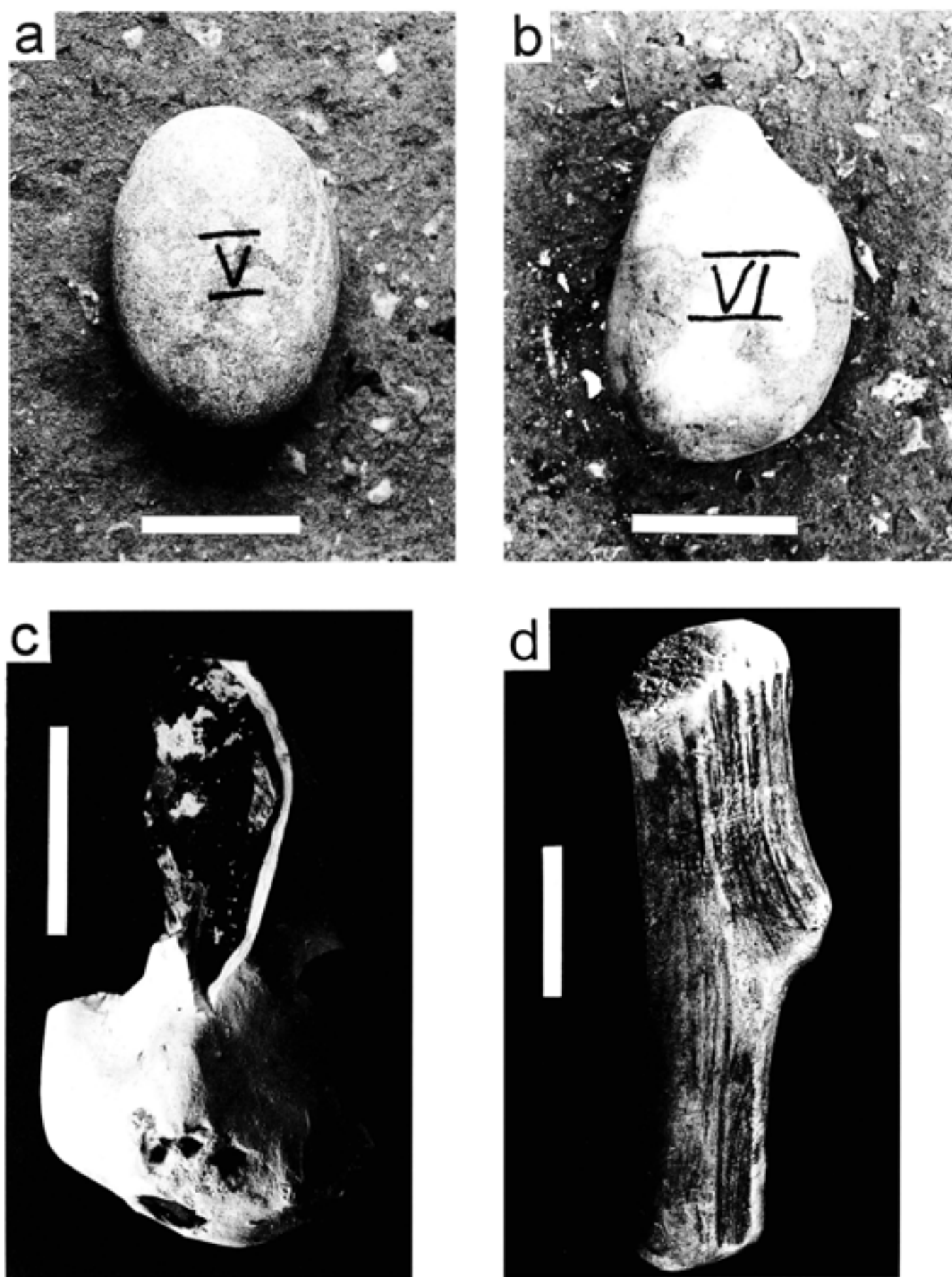


Fig 299 Different percussors used in the knapping experiments: a) quartzite pebble, b) rolled flint pebble, c) cortical flint, d) trimmed antler, and e) bone (facing page)



There were at least three organic types of soft-hammer potentially available to the Palaeolithic people at Boxgrove: wood, bone, and antler. Past experience of the author and McNabb using wooden hammers had not produced good results for thinning and finishing handaxes. This observation is supported by Crabtree (1970, 150) who experimented extensively with wooden percussors and reported: 'the wooden billet is practically worthless for [among other things] making handaxes and large uniface or biface implements'. Antler is well-established as the preferred soft-hammer for thinning and finishing of experimental handaxes (eg Newcomer 1971; Harding *et al* 1987) despite a lack of archaeological evidence to support this prior to the Solutrean in France (Bordes 1974). Faunal remains from Boxgrove show that there were suitable deer in the local area to provide shed antler, which however would have required modification before it could have been used as a soft-hammer. Deer species identified at Boxgrove include red deer, fallow deer, and giant deer. The knappers in this experimental programme used Père David and red deer antler percussors. (MBR adds that bone and antler hammers were recovered from the 1995 and 1996 excavations at Boxgrove.) Bone is less popular among modern knappers as a soft-hammer than is antler, and even wood, for the thinning and finishing of handaxes, despite evidence for its use as a Lower/Middle Palaeolithic percussor at the site of La

Quina (Chase 1990). It is more awkward to obtain (in Britain), requiring access to a suitable part of the skeleton of a large animal which has either been heated or been exposed for sufficient time and under the right conditions to dry the bone a certain amount, but not so much that it loses all its toughness. The skeletal parts of a large deer or bovid most suitable for use as a hammer would be one end of a long bone or the metapodial. Several mammals from Boxgrove would have been of an appropriate size for their skeletal remains to furnish soft-hammers. These include horse, rhinoceros, bison, and the above-mentioned deer. The knappers used a bovid metapodial in the experimental programme, prepared by drying under cover but in the open-air for a few weeks. In view of the increasing recognition of the possibilities of both soft and hard stone as a percussor for what has generally been regarded as soft-hammer work, inorganic percussors were also used to thin and finish handaxes. Two rounded pieces of flint which retained most of their cortex, recovered from the collapsed and buried chalk cliff at Boxgrove, were utilised. These are described below as 'cortical flint hammers'. Finally, abraded rolled flint beach pebbles were also used to thin and finish handaxes. These would have been convenient for the Palaeolithic knappers as a thinning/finishing percussor as they could have been retained from their use for roughing-out. Examples of the range of percussors used in the knapping experiments are shown in Figure 299.

Flake attributes for distinguishing percussor

A certain amount of work has already been done concerning the use of flake-attributes to identify percussor (Fig 300). Bordes (1947; 1948) discussed the distinction of hard-hammer and (organic) soft-hammer flakes, and considered that flakes detached by hard-hammer generally have large striking platforms, clear points and cones of percussion, pronounced bulbs, and clear conchoidal ripples. In contrast flakes detached by soft-hammer generally have narrow striking platforms, lips, diffuse bulbs, and no points or cones of percussion. Knowles (1953) also identified salient bulbs and a clear cone of percussion as being characteristic attributes of hard-hammer struck flakes. Crabtree (1970) identified a lip as being a characteristic feature of flakes struck with a wooden soft-hammer, although he did not refer to characteristics of flakes struck with other types of soft-hammer such as antler or bone. Within the context of these general assertions concerning the distinction of flakes struck by hard and soft hammers, Ohnuma and Bergman (1982) conducted a series of experiments in which they attempted to identify the hardness of the percussor for sets of flakes for which the percussor was known. They concluded that hard-hammer struck flakes were characterised by a clear point and cone of percussion, pronounced conchoidal fracture marks on the bulb, and an unlippled striking

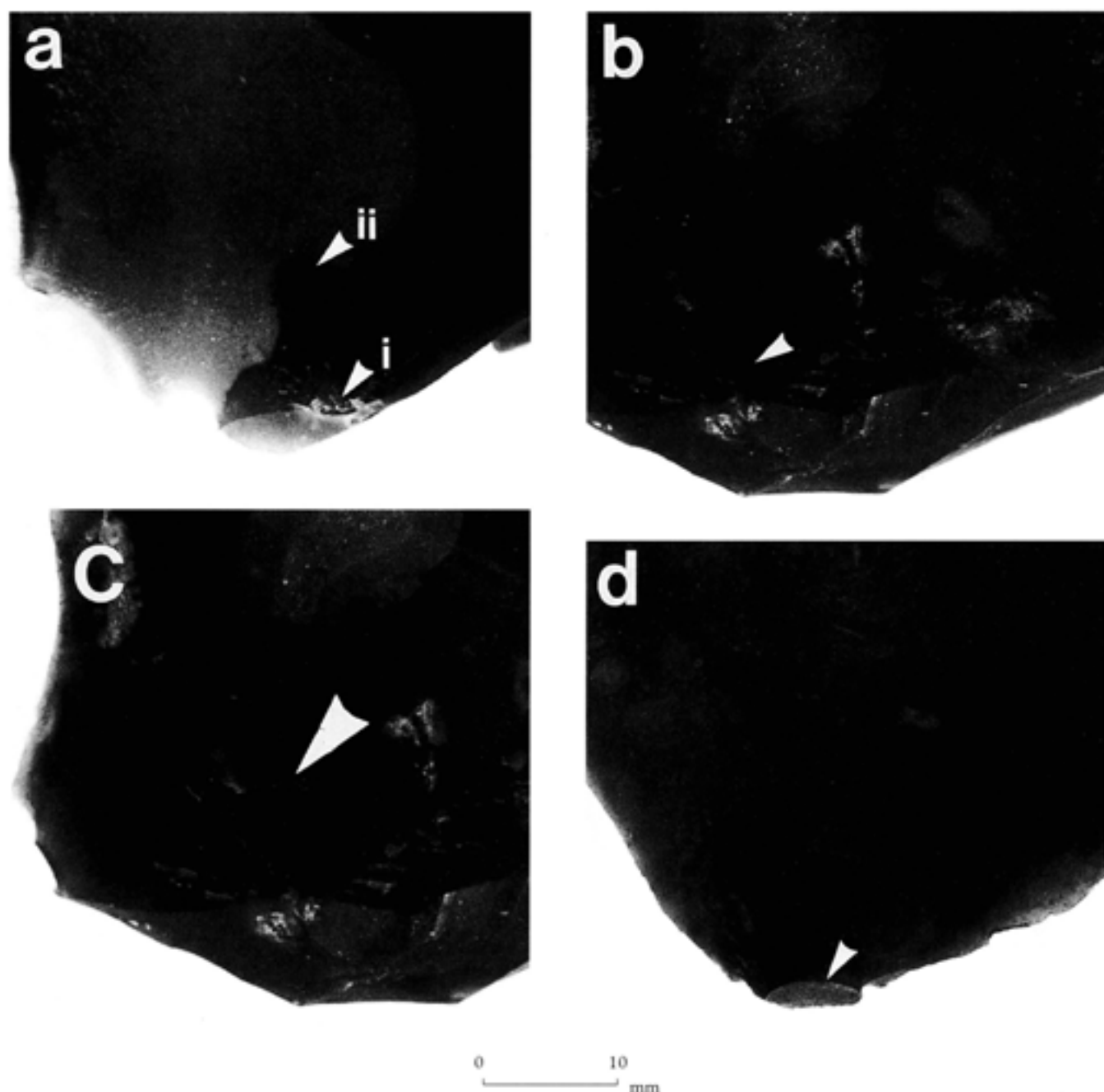


Fig 300 Flake attributes potentially significant in identifying percussor: a) point of percussion (i) and bulb (ii), b) cone of percussion, c) bulbar scar, and d) lip

platform with a pronounced bulb. In contrast, soft-hammer struck flakes were characterised by a lipped striking platform with a diffuse bulb, and a vague point and cone of percussion with a diffuse bulb. Therefore, by the mid-1980s the following five flake characteristics were widely accepted as distinguishing hard and soft percussors: 1) point of percussion (clear or vague), 2) cone of percussion (clear or vague), 3) lip on striking platform (present or absent), 4) bulb (pronounced or diffuse), and 5) conchoidal fracture marks on bulb (pronounced or indistinct).

However, Crabtree (1967) and Ohnuma and Bergman (1982) recognised that a soft stone can be used in the same way as an organic soft-hammer, and

Ohnuma and Bergman were unable to distinguish between soft-stone and antler percussors in their experiments. Furthermore, Bradley and Sampson (1986) concluded on the basis of their experimental knapping work that previous distinctions between hard and soft percussor flake characteristics were in fact reflecting not the percussor itself, but the way in which it was used (notwithstanding the fact that Ohnuma and Bergman's experiments in fact used both soft and hard hammers in identical ways to produce flakes). This is evidently the case for the characteristic of striking platform size referred to by Bordes which in fact is directly related to where a knapper chooses to direct the point of impact (Bordes 1947; 1948). However, Bradley and

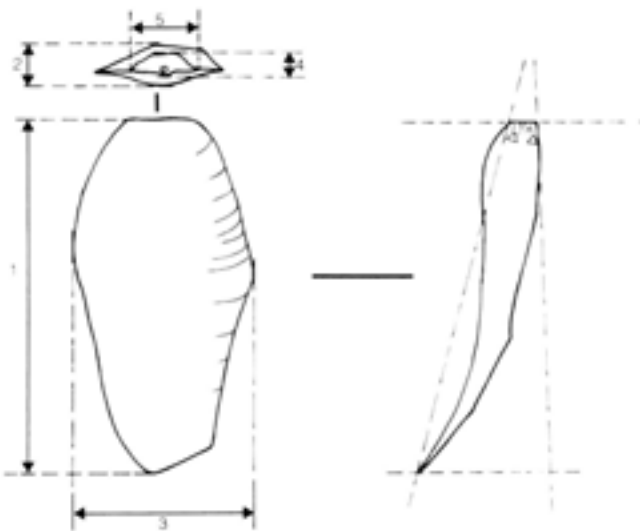


Fig 301 Diagram of flake showing measured attributes: 1) flake length, 2) flake thickness, 3) flake width, 4) striking platform length, 5) striking platform width, 6) external angle, and 7) internal angle

Sampson went further in claiming that all flake characteristics previously associated with hard-hammer percussion are a reflection of a 'non-marginal mode' of knapping where the point of impact is directed away from the margin of the core (or handaxe) being worked. Similarly, they claimed that all flake characteristics previously associated with soft-hammer percussion are in fact a product of a 'marginal mode' of knapping, where the margin of the core (or handaxe) being worked is strengthened and abraded prior to being directly struck in order to remove a flake. The results of the Boxgrove experimental knapping programme have enabled both the problem raised by Ohnuma and Bergman and also the claims of Bradley and Sampson to be investigated. The use of cortical flint, rolled flint pebbles, and organic soft-hammers to thin handaxes enabled the question of what flake characteristics might distinguish soft-stone from antler and hard-stone percussors to be investigated. The use of rolled flint pebbles both to rough-out (in a non-marginal mode) and also to thin (in a marginal mode) handaxes enabled a clear assessment to be made of which flake characteristics were most dependent upon knapping mode, and which were genuinely dependent upon the type of percussor used. Of the five flake-attributes mentioned above as being potentially significant for the identification of percussor, three were used in the experimental programme: 1) lip, 2) point of percussion, and 3) cone of percussion. It was felt by the experimenters that the pronounced bulb of percussion was directly contingent upon the development of the cone and so there was no point in recording both. With regard to the clarity of the conchoidal ripples on the bulb, the practical difficulties of deciding which part of the bulb to examine, and distinguishing objectively

Table 132 Attributes recorded for experimentally produced flakes

attribute	type of data recorded
platform	categorical – cortex/plain/inclusion
flake length	quantitative – mm
flake width	quantitative – mm
flake thickness	quantitative – mm
platform length	quantitative – mm
platform width	quantitative – mm
external angle	quantitative – degrees
internal angle	quantitative – degrees
lip	categorical – present/absent
bulbar scar	categorical – present/absent
cone	categorical – developed/diffused
point	categorical – present/absent

Table 133 Groups of flakes produced by different percussors

knapping group/unit	total tools produced	percussor	reduction task
1–10	10	beach pebble (F)	roughing out
11–20	10	quartzite pebble (Q)	roughing out
21–25	5	beach pebble (F')	thinning/finishing
26–31	6	cortical flint (C)	thinning/finishing
32–36	5	antler (A)	thinning/finishing
37–40	4	bone (B)	thinning/finishing

between clear and indistinct ripples led to the exclusion of this attribute. The following data were also recorded for individual flakes: internal flaking angle, external flaking angle, length, width, thickness, striking platform length, striking platform width, bulbar scar (present or absent), and platform-type (cortex, plain or inclusion). All of the flake attributes recorded are shown in the photographs in Figure 300, or in diagrammatic form in Figure 301, and are summarised in Table 132.

Experimental methodology

Twenty nodules of flint were collected from the area of the buried chalk cliff at Boxgrove. These were not selected at random but were chosen with the intention of converting them into ovate handaxes similar to those found in the archaeological horizons. Ten handaxe rough-outs were produced using quartzite hard-hammers and ten rough-outs were produced using rolled flint pebbles. The flakes from the sequence of reduction associated with each rough-out were collected and kept together as a unit which it was known related to a single roughing-out sequence, all knapped with the same percussor. The twenty rough-outs were then thinned/finished with a variety of percussors; five of them with an abraded rolled flint pebble, five of them with an antler soft-hammer, three of them with a cortical flint hammer, and four of them with a bone soft-hammer. The flakes

from each of the thinning/finishing reduction sequences were also collected and kept together as separate units. Table 133 summarises the different units of flakes produced in the experiments.

Each of the experimental units was studied separately. It was felt that by examining a group of flakes all known to have been struck off by the same percussor it would be possible to develop an appreciation not just of what attributes definitively implied a particular percussor, but also of the likelihood of a particular percussor causing certain attributes. It was thought that such an approach would be more sensitive in distinguishing percussors such as soft-stone and antler, which other approaches based on the study of individual flakes had failed to differentiate. This unit-based approach is also particularly applicable to archaeological situations such as Boxgrove where debitage is preserved in minimally disturbed clusters which likely relate to separate sequences of reduction, and which in several cases have already been proven by refitting studies to be single knapping episodes. The 12 attributes listed in Table 132 were recorded for each flake over 20mm maximum dimension. Therefore, 40 separate bodies of data were created, each representing the flakes from the different experimental reduction units.

Discrimination of percussors

The first step of the analysis was to use the absolute measurements taken on the flakes to produce two statistics which it was felt would be more useful in identifying flakes struck by the more elastic bone and antler hammers. It was noted during the experiments that the flakes produced by these hammers tended to be more elongated and thinner than comparable flakes produced by inorganic hammers. Therefore two statistics were created, and calculated for each flake: 1) (surface area)/(thickness), and 2) (length)/(platform length), referred to as SA and PL respectively.

One issue which had to be considered was the influence upon percussion features of the type of striking platform for each flake. The flint at Boxgrove is not very fine-grained and is full of coarse inclusions. The flakes of each reduction unit were grouped according to whether their striking platform was cortical, plain, or on an inclusion, and the arithmetic mean of each attribute was calculated for each platform type group. For the attributes scored on a presence/absence basis, this mean represents the proportion of flakes in a group with the attribute, with an average value of '0' equivalent to 'none' and an average value of '1' equivalent to 'all'. It was found that flakes struck on cortical platforms did not have many percussion features as the cortex deadened the blow, so these flakes were excluded from further analysis, along with those for which the striking platform had been crushed and destroyed. It was found that, within reduction units, striking on an inclusion did not significantly alter the attribute-means.

Therefore, this distinction was not continued, and each reduction unit was characterised by a single set of attribute means.

A preliminary examination of the complete set of attribute-means made it clear that many of the attributes recorded bore no relation to the type of percussor. From initial inspection, five flake-attributes were seen to be potentially significant in distinguishing percussor. These were: SA, PL, lip, cone, and point. In order to explore the potential of these attributes for distinguishing percussor, Canonical Variates Analysis (CVA) was applied to the data. CVA, also referred to as discriminant analysis (Alvey *et al* 1983, chapter 8.6), is a multivariate technique which can be applied to a set of data which contains known groupings. It does not matter if the variable scores in the input data have different orders of magnitude as the version of CVA used (from the IASTATS package, created at the London Institute of Archaeology) automatically standardises the input data. CVA 'visualises' the data in multi-dimensional space and derives axes (or canonical variate components) which try to illustrate the known groupings as spherical constellations separated as widely as possible.

The output of the version of CVA used in this work includes a summary of the new variates, raw variate loadings, standardised variate loadings and a set of X and Y coordinates for plotting the first two CVA components in two dimensions. The summary of the new variates gives the proportions of the data's variability which are reflected in each of the new CVA components. The raw variate loadings are multiplying factors which can be used to transform the input data onto new axes which best illustrate the known clusters within the data. The standardised variate loadings give the relative contributions of each of the input data variables (in this case of each flake-attribute) to the new axes. The X and Y coordinates are the automatically calculated product of the raw variate loadings and the input data, enabling a straightforward visual representation in two dimensions of the extent to which the known clusters can be separated.

CVA was initially applied to a set of experimental data which contained the attribute means of SA, PL, lip, cone, and point for 37 reduction units made by five different types of percussor (Wenban-Smith 1989). The results of this preliminary analysis (CVA 1) suggested a) that cone was not significant in distinguishing percussor, and b) that the percussor of an assemblage of flakes could be identified as one of soft organic, soft-stone and hard-stone by weighting the significance of SA, PL, lip, and point appropriately. However, it was not possible to separate bone and antler hammers from each other, nor was it possible to separate quartzite from flint hammers. The lack of significance of cone in CVA 1 led to the exclusion of this flake-attribute from the subsequent analyses discussed here.

One problem with CVA 1 was the low number of soft-stone reduction units. Therefore three extra experiments have since been carried out in which handaxes

Table 134 Flake attribute means for all of the experimental reduction groups. *Control units; (1) etc correspond to numbers on Figure 303

knapping group/unit	percussor	sa	pl	lip	point	number of flakes
1	F	182.2	4.94	0.35	0.44	23
2	F	225.5	7.18	0.06	0.94	31
3	F	198.8	6.49	0	1.0	5
4	F	244.7	9.04	0	1.00	28
5	F	156.7	5.77	0.44	0.56	16
6	F	280	6.51	0.08	0.88	35
7	F	201.4	4.97	0	1.0	26
8	F	202.4	5.19	0.1	0.9	15
9	F	261.1	12.2	0	0.88	18
10	F	222	5.29	0.07	0.54	19
11	Q	220.7	5.14	0.23	0.92	14
12	Q	229.6	6.6	0.33	0.67	32
13	Q	281.6	5.05	0.36	0.8	16
14	Q	230.9	5.41	0.17	0.67	7
15	Q	226.7	7.07	0	1.0	10
16	Q	226.9	5.52	0.06	0.78	26
17	Q	227.5	5	0.04	0.92	27
18*	Q (1)	221.9	7.7	0.25	0.5	18
19	Q	198.4	8.96	0.11	0.96	35
20	Q	191.2	7.27	0.13	0.93	18
21	F	179.3	8.52	0.19	0.75	19
22*	F (2)	216.7	9.74	0.6	0.6	20
23	F	149.4	9.35	0.58	0.75	20
24	F	140.5	7.7	0.25	0.5	24
25	F	129.8	10.7	0.18	0.59	18
26	C	201.2	8.22	0.65	0.43	68
27	C	262.5	10.6	0.5	0.5	11
28	C	223.5	13.3	0.3	0.52	24
29*	C (5)	233	26	0.06	0.82	17
30	C	235	23	0.1	0.57	21
31	C	293	26	0	0.63	16
32*	A (3)	308.8	31.3	0.65	0	21
33	A	359.9	30.7	0.93	0	21
34	A	269.4	12	0.88	0	39
35	A	289.3	17	0.9	0	13
36	A	298.4	15.3	1.0	0	16
37	B	227.9	11.4	0.8	0	19
38*	B (4)	148.4	9.07	0.7	0	29
39	B	235.5	19.5	0.83	0	29
40	B	186.5	11.4	0.88	0	43
41*	Q (6)	185.4	11.4	0.09	0.73	33
42*	A (7)	225.3	13	0.58	0.13	24

were thinned/finished with cortical flint hammers, and the flakes from each of these experiments are included in the analyses discussed in this report. A second problem was that no control experiments or blind-tests were carried out to prove that the attribute-weightings identified by CVA 1 were valid for independent assemblages of flakes. Therefore, of the 40 experimental reduction units available for study, one made by each of the five different percussors under investigation was excluded from the CVA analyses discussed below. These reduction units were subsequently used as controls to demonstrate the efficacy of the attribute

Table 135 Results of canonical variates analysis 2

new CVA components				
component	variance	as % of total	cumulative	
1	10.689	76.64	76.64	
2	1.267	9.09	85.72	
3	1.109	7.95	93.67	
4	0.882	6.33	100.00	
raw variate loadings				
attributes	comp 1	comp 2	comp 3	comp 4
SA	-0.0151	0.0233	0.0002	0.0127
PL	-0.1049	-0.0743	0.1823	-0.1207
lip	-3.5308	3.0382	-1.5638	-6.2144
point	4.0589	-3.6765	1.11	-6.2149
standardised variate loadings				
attributes	comp 1	comp 2	comp 3	comp 4
SA	-0.572	0.881	0.0074	0.480
PL	-0.459	-0.325	0.7982	-0.529
lip	-0.598	0.515	-0.265	-1.053
point	0.614	0.556	0.1679	-0.941

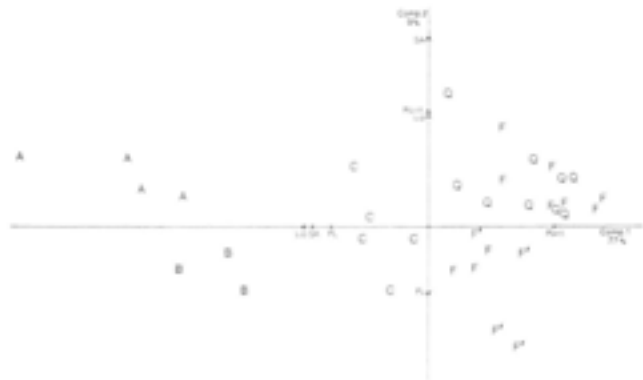


Fig 302 Plot of positions of experimental units along first two components of CVA 2 A = antler; B = bone; C = cortical flint, Q = quartzite; F = flint roughing-out; F* = flint thinning/finishing

weightings produced by the CVA analyses in identifying percussors. The selection of the control units was based upon the number of flakes they contained. For each percussor type, the reduction unit with the median number of flakes was selected as a control. This procedure by-passed the temptation to select controls which it was felt were 'typical' and so would probably produce conveniently neat test results. As it was, this strategy happened to select the most atypical reduction units as controls, making the controls a severe test of the validity of the discriminatory criteria. In addition to the controls selected from the experimental reduction units, Bergman made two extra reduction units with his own percussors for blind testing.

As CVA 1 had shown that cone was not a significant flake attribute, a second CVA was carried out (CVA 2) which included 35 reduction units (ie all apart from the controls), and which made use of only the four flake attributes SA, PL, lip, and point. The attribute mean values and sample sizes for the experimental and

Table 136 Results of canonical variates analysis 3

new CVA components			
component	variance	as % of total	cumulative
1	9.4	75.54	75.54
2	1.16	9.34	84.88
3+	0.94	7.56	92.44
raw variate loadings			
attributes	comp 1	comp 2	comp 3
SA	-0.0103	0.0053	0.0173
PL	-0.0953	-0.1984	0.0032
lip	-2.9204	2.3016	-3.2445
point	4.5043	-0.1619	-4.2377
standardised variate loadings			
attributes	comp 1	comp 2	comp 3
SA	-0.448	0.232	-0.752
PL	-0.420	-0.873	-0.014
lip	-0.483	0.387	-0.537
point	0.678	-0.024	-0.638

control units are given in Table 134. CVA 2 attempted to separate all the five percussor types used in the experiments, and the results are shown in Table 135 and in Figure 302. The standardised contributions of each flake-attribute to the first two new CVA components are shown along the two axes.

Figure 302 shows that the first new component of CVA 2 has been able to separate the percussors into three main groups (Tables 133, 134): soft-organic (A and B), soft-stone (C), and hard-stone (Q, F, and F'), regardless of the fact that four of the reduction units created by a rolled flint pebble hammer relate to the thinning/finishing of a handaxe and not its roughing-out. The soft organic hammers are well-separated from the other two groups. However, the separation between the soft-stone and the hard-stone hammers is less marked, although still reasonably distinct. The standardised weightings show that all four flake-attributes contribute significantly to distinguishing the different percussors. The most significant flake-attribute is the presence or absence of a point. A higher proportion of points in an assemblage indicates a harder percussor. The second most significant flake attribute is the presence or absence of a lip. Higher proportions of lips in an assemblage indicate a softer percussor. Almost as significant as lips are higher average values of SA and PL, both of which also indicate softer percussors.

When the second new component is looked at, there is a slight separation between the bone and antler percussors. However, despite a tendency for units struck by flint percussors to have lower second component values, there is still considerable overlap between units struck by flint percussors and those struck by quartzite ones. Two of the thinning/finishing units struck by flint percussors have particularly low second component values. This reflects a high PL value in conjunction with a low SA value. The high PL value relates to the marginal mode of knapping required for thinning/finishing handaxes. However, other attributes,

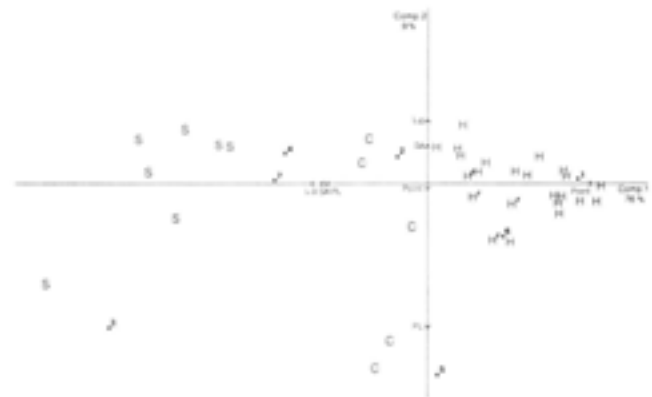


Fig 303 Plot of positions of experimental units and controls along first two components of CVA 3: S = soft organic; C = soft stone; H = hard stone roughing out; H' = hard stone finishing. The numbers refer to the control units used (Table 134)

such as the proportion of points and lips and the average SA value for these units, are comparable with those recorded for the roughing-out units.

Two conclusions were reached from CVA 2. Firstly, it is possible to distinguish assemblages of flakes made by organic soft percussors (antler and bone), soft-stone percussors (cortical flint), and hard percussors (rolled flint and quartzite) from each other. However, it is not possible to distinguish between assemblages of flakes made by bone and antler, nor between assemblages made by rolled flint and quartzite. Secondly, it is clear that the flake-attributes recorded here (particularly point and lip) are mainly affected by percussor-type and not by mode of flaking, contrary to the suggestion by Bradley and Sampson (1986).

Therefore a final analysis was carried out (CVA 3) which used the same input data as CVA 2, but which only attempted to separate three groups of percussors: antler and bone (S), cortical flint (C), and rolled flint and quartzite (H). The results of CVA 3 are shown in Table 136 and Fig 303.

The flake attribute means for the control units were transformed into the first two new CVA 3 components using the raw variate loadings. Figure 303 shows the positions of the control units along these two axes in relation to the positions of the input units. The control units are represented by numbers which correspond to the numbers in the second column of Table 134. The standardised contributions of each flake-attribute to the first two new CVA components are shown along the two axes. Figure 303 shows a similar distribution of the experimental input units as in Figure 302, with three well-differentiated groups of percussor: soft-organic hammers (S), soft-stone cortical flint hammers (C), and hard-stone hammers (H and H'). Superimposed upon this pattern of distribution are the experimental control units.

Controls 1 and 6 are correctly identified from Figure 303 as having been made by hard-stone hammers. Control 5 is correctly identified as having been

made by a soft-stone cortical flint hammer. Control 3 is correctly identified as having been made by a soft-organic hammer. Controls 4 and 7 lie in between the area of Figure 303 dominated by soft-organic hammers and the area of the figure dominated by soft-stone cortical flint hammers. However, they are closer to the soft-organic cluster, and this is their correct attribution. In the case of control 4, the position has been influenced by abnormally low values of SA and PL for a soft-organic hammer assemblage. If control 4 had been included in the input data for CVA 3, then SA and PL would have been weighted down and lip weighted up as soft-organic indicators, making the analysis more robust. In the case of control 7, the antler used by Bergman was that of a North American moose. This material is particularly dense and hence lower proportions of lips and higher proportions of points than is usual for soft-organic hammers were produced, leading to a slightly ambiguous result. However, mammals with such dense antler were probably not available to the Palaeolithic people of Boxgrove, and so this result need not influence the use of CVA 3 to identify the percussor of archaeological assemblages from Boxgrove. The location of controls 4 and 7 on Figure 303 suggests that the boundary between soft-organic hammers and soft-stone hammers can be regarded (for CVA 3) as lying closer to the soft-stone cluster than to the soft-organic cluster. Finally, control 2 lies in between the hard-stone hammer and the soft-stone cortical hammer areas of Figure 303, although closer to the soft-stone cluster. However, control 2 was in fact made by a flint hammer, representing the thinning/finishing of a handaxe. In mitigation, it was clear from the outset when this unit was selected as a control that the abnormally high proportion of lips in this unit would create problems in correctly identifying its percussor as a hard-stone hammer, despite the equally high proportion of points. If this unit had been included in CVA 3 then the weighting given to points would have finished even higher, again making the analysis more robust. The proportion of lips was probably also influenced by the marginal mode of flaking used for this unit. However, the control was still almost identified as being made by a hard-stone hammer, and there was no question of attribution to a soft-organic hammer. The position of control 2 on Figure 303 suggests that there is a zone of ambiguity between the soft-stone cortical cluster and the hard-stone cluster in which the mode of flaking may influence the attribution of percussor, and in which soft-stone and hard-stone percussors cannot be reliably distinguished.

The results of the discriminant analysis of the experimental flake assemblages show that using the raw variate loadings produced by CVA 3 it is possible to identify unknown percussors and to distinguish soft-organic, soft-stone and hard-stone percussors by recording the proportions of points and lips in a flake-assemblage, and by recording the average values of the

statistics SA and PL. While the characteristics of individual flakes can be misleading for the identification of percussor, the analysis of the frequency of certain flake-attributes in assemblages of flakes can reliably identify the percussor. The flake-attributes point and lip were found to be most significant, with a combination of higher proportions of points and lower proportions of lips indicating harder hammers, and lower proportions of points and higher proportions of lips indicating softer hammers. It was also found that the soft-organic hammers tended to produce high values of the statistics SA and PL, representing the thinness and elongation of a flake. This suggests that the toughness and elasticity of bone and antler provides improved knapping properties for tasks such as the thinning/finishing of a handaxe which require controlled invasive flaking. Having shown that CVA 3 can be used to identify unknown experimental reduction units, it was used to investigate six flake-assemblages from the archaeological levels at Boxgrove.

Archaeological application

The archaeological samples were selected from discrete clusters of artefacts, believed to exhibit a high chance of representing single knapping episodes. In several cases this supposition was confirmed by refitting. Furthermore, samples were chosen to cover different areas and archaeological levels of the Boxgrove site. Details of the six archaeological assemblages studied are given below and their location is shown on Figure 4.

Sample 1: Quarry 2, Area A, Unit 4c, Scatter 1. This sample was assessed as having been produced by a soft-organic hammer in the preliminary report of the knapping experiments (Wenban-Smith 1989). The flakes comprising this sample did not refit with each other, although many flakes within Scatter 1 did (Bergman and Roberts Chapter 6.2). The sample included flakes from all stages of handaxe manufacture.

Sample 2: Quarry 2, Area A, Unit 4c, Scatter 1. This sample was from the same scatter as sample 1, but in contrast constituted a sequence of refitting flakes. This sequence related to the thinning stage of handaxe manufacture.

Sample 3: Quarry 2, GTP 17, Unit 4b, Scatter 2044/1020.5. This sample was from one of two small and tightly grouped clusters of handaxe thinning debitage close to each other in GTP 17.

Sample 4: Quarry 2, GTP 17, Unit 4b, Scatter 2044.5/1021. This sample was from the second of the two small and tightly grouped clusters of handaxe thinning debitage close to each other in GTP 17. In the absence to date of a refitting study, it is not clear whether these clusters represent one or two reduction episodes.

Table 137 Flake attribute means for archaeological samples

sample	sa	pl	lip	point	number of flakes
1 Q2/A	237.6	18.1	0.67	0.09	27
2 Q2/A	329.6	19.9	0.8	0	10
3 Q2 GTP 17	276.0	21.9	0.68	0.05	19
4 Q2 GTP 17	272.5	19.2	0.74	0	19
5 Q2 GTP 17	228.8	14.8	0.22	0.33	27
6 Q1/A	303.6	26.6	0.8	0.05	20

Sample 5: Quarry 2, GTP 17, Unit 4b, Scatter 2043.5/1022. This sample was from a cluster of debitage representing the early roughing-out stages of handaxe manufacture. It is not known whether this cluster represents the same reduction sequence as one or both of the clusters from which samples 3 and 4 were taken.

Sample 6: Quarry 1, Area A, Unit 4b, Scatter 1. This sample was taken from a tightly spaced cluster of debitage representing the thinning/finishing of a handaxe (Fig 239, Austin and Roberts Chapter 6.2). The tight spacing of the cluster and the large number of refits found within it indicate that the cluster represents the undisturbed debitage from a single knapping episode.

The flake assemblages in each of the archaeological samples were analysed in the same way as the experimental reduction units. The values of the attribute means and the sizes of the archaeological samples are shown in Table 137.

The flake attribute means for the archaeological samples were transformed into the first two new CVA 3 components using the raw variate loadings. Figure 304 shows the positions of the archaeological samples along the first two CVA 3 axes in relation to the positions of the experimental reduction units. It is clear from Figure 304 that samples 1, 2, 3, 4 and 6 all reflect soft-organic percussors, and that sample 5 reflects a cortical flint percussor. Finally, there is a refitting sequence of flakes (Fig 261) from Quarry 2, Area A, Unit 4c (Bergman *et al* 1990; Bergman and Roberts Chapter 6.2) which, although not included as a sample in this analysis, exhibits a high proportion of clear points of percussion, a lack of lips, and low PL ratios, indicating that they were knapped by a hard-stone percussor.

Discussion

The results of the analysis of the archaeological samples clearly indicate that soft-organic percussors were commonly being used by the Palaeolithic people at Boxgrove to thin/finish handaxes. They were also using (on at least one occasion) a cortical flint percussor to carry out the early roughing-out of a handaxe. If it could be shown by refitting that the debitage clusters

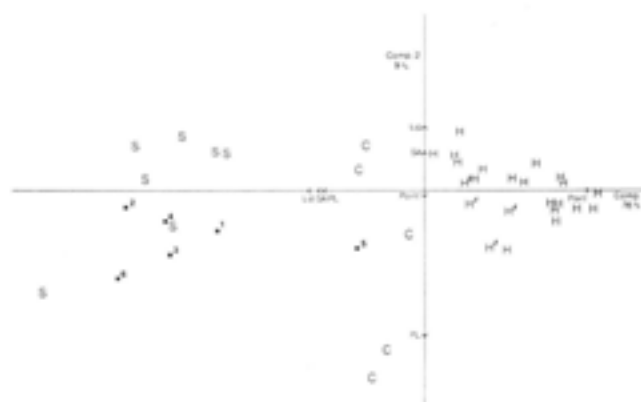


Fig 304 Plot of positions of experimental units and archaeological samples along first two components of CVA 3: S = soft organic; C = soft stone; H = hard stone roughing out; H' = hard stone finishing. The numbered asterisks refer to the archaeological samples (Table 137)

from which sample 5 (GTP 17, Unit 4b, roughing-out) and one or both of samples 3 and 4 (GTP 17, Unit 4b, thinning/finishing) were taken represent the manufacture of a single handaxe, this would imply a conceptual distinction by the Palaeolithic people at Boxgrove between roughing-out and thinning/finishing stages requiring different equipment for their execution. This is obviously a subject for future research.

It is not possible using the analytical technique applied here to distinguish between antler and bone percussors. It is clear that the Palaeolithic people at Boxgrove were using one or the other or both, assuming there is no other viable substance omitted from the experimental programme which produces similar flake attributes. A shed antler would require exhausting work cutting off the basal part before it could be used as a percussor. Several skeletal parts of various large mammals could be used as percussors without further modification, and the ends of long-bones which had been broken in two by animal or hominid scavengers would also make suitable percussors. If soft-organic percussion was habitual in the manufacture of handaxes (as is suggested by this analysis of the debitage samples and the quality of most of the Boxgrove handaxes) and as suitable percussors must have been scarce, then it would have been necessary for Palaeolithic people either to retain soft-organic percussors about their persons or in caches, or to memorise a mental map of potential sources of percussors in their territorial range (Roberts *et al* in prep).

Cortical flint hammers would have been easily available all along the cliff-line for the people at Boxgrove. The cliff-line is approximately 40m from GTP 17 (Fig 29) where the flake assemblage made by a cortical flint hammer is located. The cliff would also have been the most likely source of the raw material. Therefore both flint nodule and cortical flint hammer were first collected and then transported at least 40m to GTP 17 from the nearby cliff, where the latter was

used to knap the former. This movement of resources around the landscape before their exploitation seems planned, although the transported distance is small in this case. This analysis is focussed upon the identification of percussor by investigation of debitage; however, several actual percussors have also been found in the main archaeological levels. Firstly, two fragments of bone showing marks reflecting use as a flint-knapping percussor have been found in Q1/A, Unit 4b (Parfitt and Roberts Chapter 6.5, Fig 307). Secondly, nodules of cortical flint were found in Q2 GTP 17, Unit 4b and in Unit 4c of both Q1/A and Q1/B (Fig 248a); the fracture damage indicates that they were used as a percussors. The former is possibly the actual percussor used to knap the assemblage of flakes studied as sample 5.

Conclusion

This programme of experimental knapping has shown that certain flake attributes are determined by percussor independently of the mode of knapping or the knapping task being undertaken, contrary to the assertions of Bradley and Sampson (1986). The flake-attributes which have been shown to be significant are: a clear point of percussion, a lip on the ventral side of the striking platform, the ratio of surface area to thickness, and the ratio of length to striking platform length. The first two of these attributes were also indicated by Ohnuma and Bergman (1982) as being significant when applied to individual flakes. However, it has been shown in this knapping programme, as well as in the work of Ohnuma and Bergman, that individual flakes can have misleading or ambiguous combinations of flake attributes. The multivariate analysis of assemblages of flakes has enabled this problem to be overcome, and it has proved possible to distinguish soft-organic percussors (antler and bone), soft-stone percussors (cortical flint) and hard-stone percussors (quartzite and rolled flint pebbles) from each other by examining the proportions of the flake attributes mentioned above. Attributes which were not found to be useful in identifying percussor included cone, bulbar prominence, bulbar scar, and conchoidal ripples.

It has been shown by both analysis of the archaeological debitage and also by actual finds of percussors that at least four of the materials proposed as potential percussors were in fact used by the Palaeolithic people of Boxgrove. These were soft-organic percussors (bone and antler), a soft-stone percussor (cortical flint), and a hard-stone percussor (rolled flint beach pebble). All these materials would have been available within the local area, but the locations at which they were used indicates that they were transported within the area covered by the archaeological investigations at Boxgrove. The overall picture derived from an investigation of the knapping technology practised at Boxgrove is one of an adaptable hominid, using a variety of available materials for knapping, able to distinguish the different knapping properties of these

materials and select an appropriate percussor for particular knapping tasks, able to remember the locations of useful resources or carry equipment in anticipation of its use, and able to plan ahead to the extent of conceiving a task, collecting the appropriate resources, and finally executing the task. Additionally, there is now evidence of making tools to make tools, such as the breaking of a bone and the removal of the periosteum from the bone surface (Fig 307), and the preparation of shed antlers from *Megaloceros dawkinsi* and *Cervus elaphus* (Roberts 1996 and personal communication).

6.5 Human modification of faunal remains

S A Parfitt and M B Roberts

Introduction

The analysis and interpretation of butchery marks has made an important contribution to the understanding of hominid behaviour and carcass processing activities. In this section we describe the evidence for human modification of the large mammal bones from Boxgrove and discuss the behavioural inferences that this information provides. In comparison with other British Lower Palaeolithic sites, Boxgrove has produced a significant sample of humanly modified bones. In addition, the unusual sedimentary conditions during the deposition of the lagoonal intertidal silts (Unit 4b) have preserved episodes of activity representing the processing of individual carcasses which are associated with flint tools and debitage.

Until recently, it has generally been assumed that the bones associated with archaeological remains were a direct result of human activity. However, concentrations of bones can be formed by a number of natural processes, such as fluvial action, natural deaths, and carnivore activity, that can concentrate and alter bones in ways that could be mistaken for human activity (Binford 1983). Consequently, before questions about human behaviour can be realistically answered, the bones must be shown to be there as a direct result of human activity rather than fortuitously associated or the result of some other bone accumulating agent. Attempts have been made therefore to identify the agent or agents responsible for the accumulation of, or alteration to, assemblages of bones. This has been partially achieved by analyses of well documented modern bone accumulations from a variety of ethnoarchaeological situations (Gifford and Behrensmeier 1977; Binford 1978; 1981; Gifford 1980; Yellen 1977; Crader 1983; Bunn 1983), carnivore den and kill sites (Hill 1980; Sutcliffe 1970; Haynes 1981; 1982; 1983a; 1983b; Binford 1981; Brain 1983; Hill 1975), and through experimental butchery and fracturing of bones (Stanford *et al* 1981; Sadek-Kooros 1972; Olsen 1984). In these examples, the factors that lead to the



Fig 305 Scanning electron micrograph of a cut mark on a fragment of red deer skull from Q1/B (magnification $\times 75$)

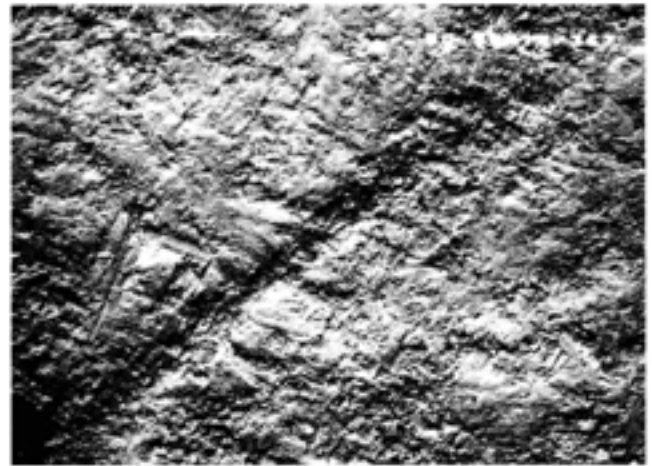


Fig 306 Sediment scratches on vertebra fragment from Q2 GTP 17; note the u-shaped cross-section, irregular morphology, and orientation of the marks in comparison with the cut marks illustrated in Fig 305 (magnification $\times 75$)

Table 138 Summary of hominid modification of large mammal bones

<i>species</i>	<i>anatomy</i>	<i>inferred butchery process</i>
<i>Ursus deningeri</i>	skull (zygomatic)	skinning
<i>Cervus elaphus</i>	skull (frontal)	skinning, removal of mandible
	skull (antler base)	skinning
	skull (maxilla)	?
	upper premolars/molars	?skinning/filleting of facial region
	radius	dismemberment, filleting, marrow bone breakage
	tibia	filleting, marrow bone breakage
	metacarpal	marrow bone breakage
<i>Megaloceros</i> sp	upper premolars/molars	?skinning/filleting of facial region
indeterminate cervid	skull (frontal)	skinning
	rib	dismemberment
	humerus	dismemberment, filleting, bone breakage
	femur	filleting
	tibia	filleting
	first tarsal	disarticulation
	metatarsal	?
	metapodial	marrow bone breakage
	first phalanx	dismemberment
<i>Equus ferus</i>	skull	?
	mandible	disarticulation, filleting, marrow bone breakage
	atlas	disarticulation
	axis	disarticulation
	cervical vertebrae	filleting
	thoracic vertebrae	filleting
	lumbar vertebrae	filleting
	scapula	disarticulation, filleting
	humerus	disarticulation, filleting, marrow bone breakage
	radius	filleting
	pelvis	disarticulation, filleting
	femur	disarticulation, filleting, marrow bone breakage
<i>Stephanorhinus hundsheimensis</i>	mandible (M ₁)	?
	mandible (condyle)	disarticulation
	scapula	disarticulation, filleting
	pelvis	disarticulation, filleting
	calcaneus	disarticulation
<i>Bison</i> sp	femur	filleting
large artiodactyl	pelvis	breakage

Table 139 List of percussion-marked bone fragments

<i>species</i>	<i>anatomy</i>	<i>number</i>	<i>unit</i>	<i>impact type</i>
<i>Cervus elaphus</i>	right radius prox frag	Q1/A F93	4c	impact notch
<i>Cervus elaphus</i>	right tibia shaft frag	Q2 GTP 13	3	impact notch
cf <i>Cervus elaphus</i>	right metacarpal shaft frag	Q2/B F10	4c	bipolar impact notches.
Cervidae indet	metapodial shaft frag	Q1 GTP 8 F7	4b	impact notch
Cervidae indet	right humerus shaft frag	Q1 GTP 8 F21	4b	percussor and impact notch
<i>Equus ferus</i>	right humerus shaft frag	Q1/B F447	4b	bipolar impact notch
<i>Equus ferus</i>	right femur prox shaft frag	Q2 GTP 17 F360	4b	impact notch
<i>Equus ferus</i>	mandible frag	Q2 GTP 17 F567	4b	?impact notch
<i>Equus ferus</i>	tibia shaft frag	Q2 SEP 2 F18	4b	?impact notch
large artiodactyl	pelvis frag	Q1/B F420	4(b)	?depressed margin
indet large mammal	indet bone frag	Q2 GTP 17 F294	4b	impact notch (flake)
indet large mammal	indet bone frag	Q2 GTP 17 F401	4b	impact notch (flake)
indet large mammal	indet bone frag	Q2 GTP 17 F448	4b	impact notch (flake)
indet large mammal	indet bone frag	Q2 GTP 17 F738	4b	?impact notch (flake)
indet large mammal	indet bone frag	Q2 GTP 17 F750	4b	impact notch (flake)
indet large mammal	indet bone frag	Q2 GTP 17 F851	4b	?impact notch (flake)
indet large mammal	indet bone frag	Q2 GTP 17 F853	4b	impact notch (flake)
indet large mammal	indet bone frag	Q2 GTP 17 F869	4b	?impact notch (flake)
indet large mammal	indet bone frag	Q2 GTP 17 F920	4b	?impact notch (flake)
indet large mammal	indet bone frag	Q1 GTP 8 F25	4b	?impact notch (flake)
indet large mammal	long bone shaft frag	Q1/A F3138	4b	impact notch
indet large mammal	long bone shaft frag	Q1/A F3496	4b	percussor and impact notch
indet large mammal	indet bone frag	Q1/B F323	4b	?impact notch
indet large mammal	indet bone frag	Q1/B F325	4b	?impact notch
indet large mammal	indet bone frag	Q2/B	8	percussor and impact notch

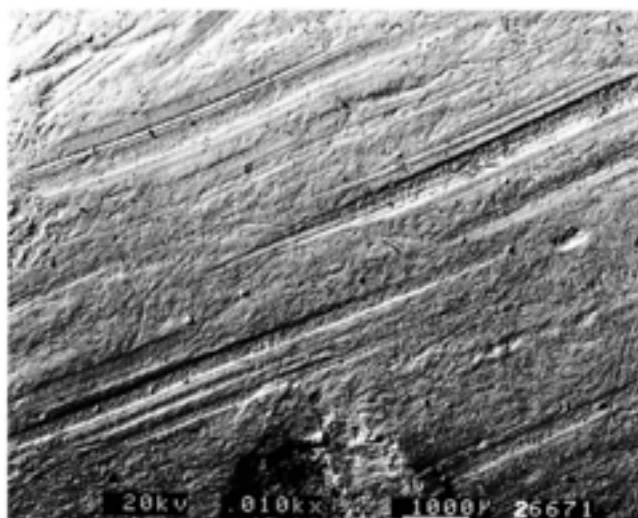


Fig 307 Scrape marks, probably produced during periosteum removal, on the shaft of a horse humerus from Q1/B

accumulation, alteration, and destruction of the bones have been directly observed and provide a basis for the interpretation of the taphonomic processes which affected the assemblage.

Methods

The large mammal bone assemblage was systematically examined for bone surface alterations with an emphasis on identifying hominid modification of the bones. Initially, all the large mammal bone fragments were

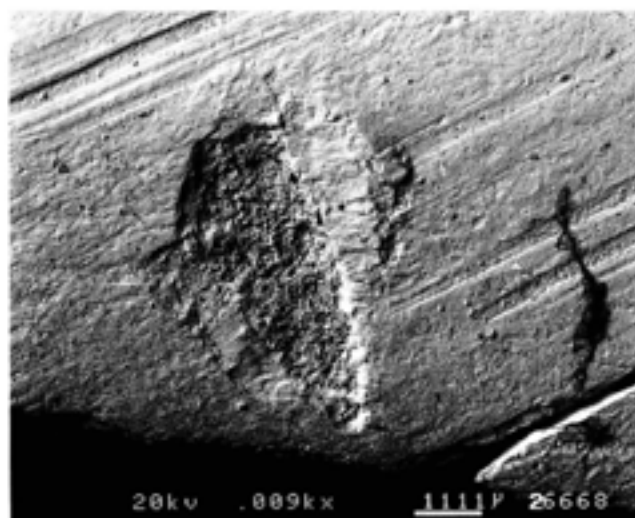


Fig 308 Impact damage produced during marrow bone breakage on the shaft of horse humerus from Q1/B

examined under a variable magnification binocular microscope, illuminated with an oblique light source. In addition to cut marks and impact damage, other surface alterations such as sedimentary abrasion, carnivore gnawing and weathering were also recorded. The relationship between the various types of alterations was examined to infer the sequence of taphonomic events which the bones had undergone. The majority of the linear grooves recorded on the surface of the bones were then examined using a scanning electron microscope (SEM) to distinguish sediment abrasion



Fig 309 Opposing impact scars, produced during marrow bone breakage

from cut marks and to record the microtopography of the marks. High resolution casts of a representative sample of the marks were made using a dental impression rubber. These were then sectioned using a scalpel and mounted on stubs to examine the cross-sectional morphology of the marks.

Hominid modification of the bones consisted of cut marks, chop and scrapemarks and percussion damage made with a hammerstone to extract the bone marrow (Tables 138 and 139). The types of alteration are described in the following sections.

Cut marks

Cut marks made during cutting with a flint tool are the most common type of hominid alteration observed in the Boxgrove assemblage. Cut marks are not always readily distinguishable from other types of damage produced by natural agencies such as carnivore gnawing, weathering and sediment abrasion. Bunn (1983) has suggested that macroscopic inspection can be used to identify cut marks; however, there is considerable overlap in width and cross-sectional morphology between carnivore gnaw marks and cut

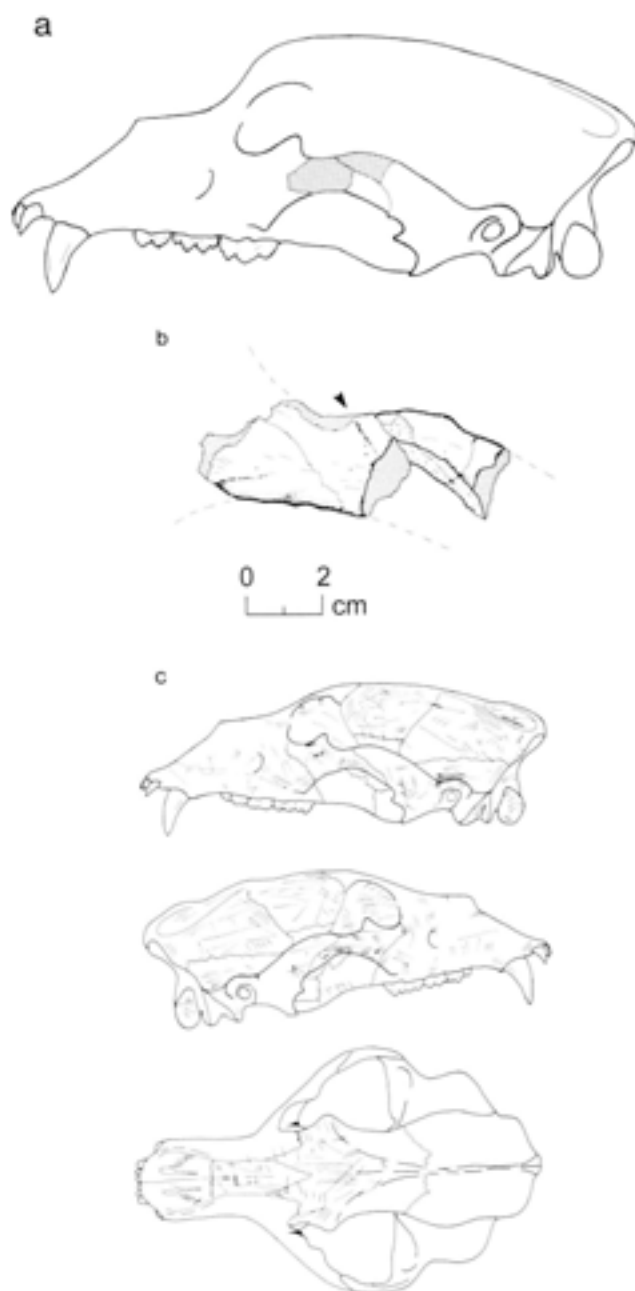


Fig 310a-c Cut marks on the zygomatic arch of bear: a) location of skull fragments, b) detailed drawing of fragments showing location of cut marks, c) cut marks on modern comparative brown bear skull showing location of marks made during filleting and defleshing

marks (Shipman 1983), and visual inspection alone cannot be used to identify cut marks in all cases. The work of Shipman and others (Shipman 1981; Shipman and Rose 1983a; Potts 1982) has shown that microscopic examination of linear marks on bones using the scanning electron microscope provides a more reliable means of distinguishing cut marks from naturally produced linear grooves. When observed under the scanning electron microscope, cut marks are characterised by multiple linear microstriations oriented longitudinally within the groove (Fig 305).



Fig 311 Outline of horse skeleton showing the anatomical location of bone fragments recovered from Q2 GTP 17 Unit 4b (estimated height at shoulder = 1.5–1.7m)

Table 140 Distribution of humanly modified large mammal bones from the main faunal horizons at Boxgrove. The percentage of humanly modified bones (no M) is given as a percentage of the total number of identifiable bones (NISP) from each unit

Species	Unit 4b			Unit 4c			Unit 5a		
	NISP	no M	%	NISP	no M	%	NISP	no M	%
<i>Canis lupus</i>	1	0	0	43	0	0	40	0	0
<i>Ursus deningeri</i>	2	0	0	18	1	6	6	0	0
<i>Meles sp</i>	0	0	0	10	0	0	0	0	0
<i>Crocota crocuta</i>	0	0	0	1	0	0	0	0	0
<i>Equus ferus</i>	150	69	46	2	0	0	0	0	0
<i>S. hundsheimensis</i>	9	2	22	7	2	29	2	1	50
<i>Cervus elaphus</i>	8	3	38	53	13	25	17	0	0
<i>Dama dama</i>	0	0	0	4	0	0	6	0	0
<i>Capreolus capreolus</i>	9	0	0	39	0	0	8	0	0
<i>Megaloceros sp</i>	6	4	67	0	0	0	1	0	0
Cervidae indet	48	13	27	65	1	2	19	0	0
large artiodactyl	3	1	33	0	0	0	0	0	0
<i>Bison sp</i>	0	0	0	6	0	0	1	0	0

However, as Andrews and Cook (1985) have described, 'cut mark-like' grooves can be produced in natural situations where bones are trampled on a stony substrate or incorporated in rubbly debris flows. Nevertheless, these marks can be identified by a detailed analysis of the sedimentary context, location and orientation of the marks as well as the considerable variation in mark morphology produced by sedimentary abrasion. Sediment abrasion and trampling marks are uncommon in the Boxgrove faunal assemblage (Fig 306), due to the fine-grained nature of the main faunal horizons.

The frequency and location of cut marks can provide information on the type of butchery undertaken and the sequence of carcass processing activities. As Binford's (1978; 1981) observations of Nunamiut butchery have shown, the location, orientation and morphology of cut marks can be used to distinguish between skinning, dismemberment and filleting processes (Table 138). Dismemberment and filleting marks are usually located on or near bone articulations where tendons, ligaments or muscle attachments are cut to separate the articulations between bones or to remove muscle blocks. In the situations that Binford examined, cuts are rarely observed on the midshaft region of limb bones, except for skinning marks encircling metapodials

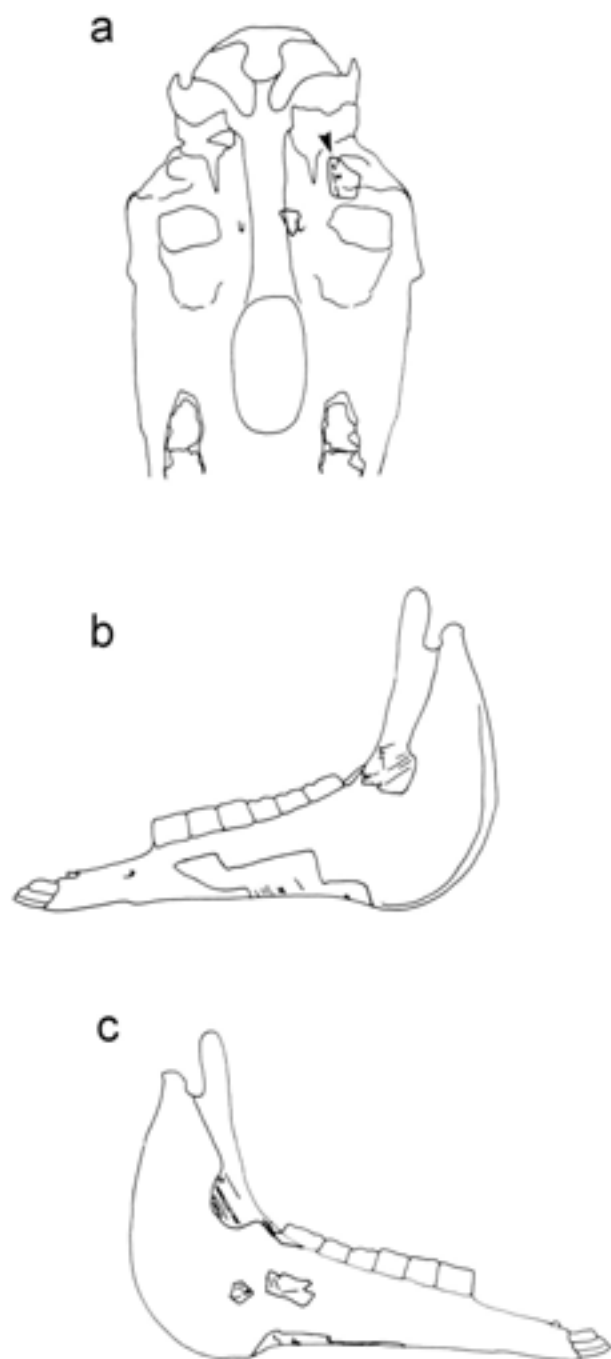


Fig 312a-c Location of cut marks on a) skull and b-c) mandible of horse from Q2 GTP 17 (estimated greatest breadth of skull = 240mm; estimated length of mandible from condyle to arboreal border of condyle process-infradentale = 530mm)

and other lower limb bones (Binford 1981; Guilday *et al* 1962; Wilson 1982). Skinning marks are also commonly located on the skull where the skin is in close proximity to the underlying bone.

The morphological characteristics of cut marks may also provide information on the type of tool used. Experimental work producing cut marks with replicas

of Boxgrove artefacts has shown that the morphology of the cutting edge determines the microscopic characteristics of the cut mark. Bifacially worked edges generally produce broad cuts with a series of parallel or sinuous grooves, whereas straight unworked flake edges and tranchet edges produce single, relatively narrow, grooves.

Scrape and chopmarks

Scrapemarks, produced by a flint edge held at an oblique angle and scraped across the bone surface, were observed on a small number of bone fragments from Boxgrove (Fig 307). Scraping the surface of a bone with a flint tool produces a characteristic surface modification that consists of a relatively broad area of fine superficial microstriations. These marks, which are often oriented along the long axis of limb bones, are generally sinuous in plan with 'chattermarks' oriented at right angles to the linear striations (Fig 307). 'Chattermarks' are produced when the flint edge meets resistance as it crosses the bone surface causing the flint to 'jump', producing ripples which are aligned transversely to the direction of the scrape. In contrast to cut marks produced during skinning, dismemberment, and filleting, scrapemarks are often located on the shafts of limb bones. Binford (1981) has recorded the scraping of limb bones to remove the periosteal sheath prior to marrow fracturing. Scrapemarks are also found along areas of muscle attachment, and in these instances are probably produced during filleting of muscle blocks.

Chopmarks consist of broad, often deep, 'hackmarks' with straight planar edges. They are generally short in comparison to cut marks. Under the SEM, fine microstriations are visible running along the edges of the mark and orientated at right-angles to the chopmark.

Impact damage

The breakage of bones to extract bone marrow produces a characteristic damage pattern (Table 139). When a limb bone is broken with a hammerstone or against a stationary anvil to extract bone marrow, a circular hole or 'impact notch' is produced by the removal of a bone flake at the point of impact (Fig 308). A similar type of damage is produced when thin-walled or cancellous areas of bone are struck in the same way. In this case, the impact notch tends to be less regular with a zone of small crushed bone flakes extending into the medullary cavity of the bone. The first impact type is referred to as an 'impact notch', the second as a 'depressed margin' (Binford 1981). A third type of impact damage was observed on a small number of limb bone shaft fragments from Boxgrove. In these examples, two impact zones are present on opposing sides of the diaphysis (Fig 309). This type of

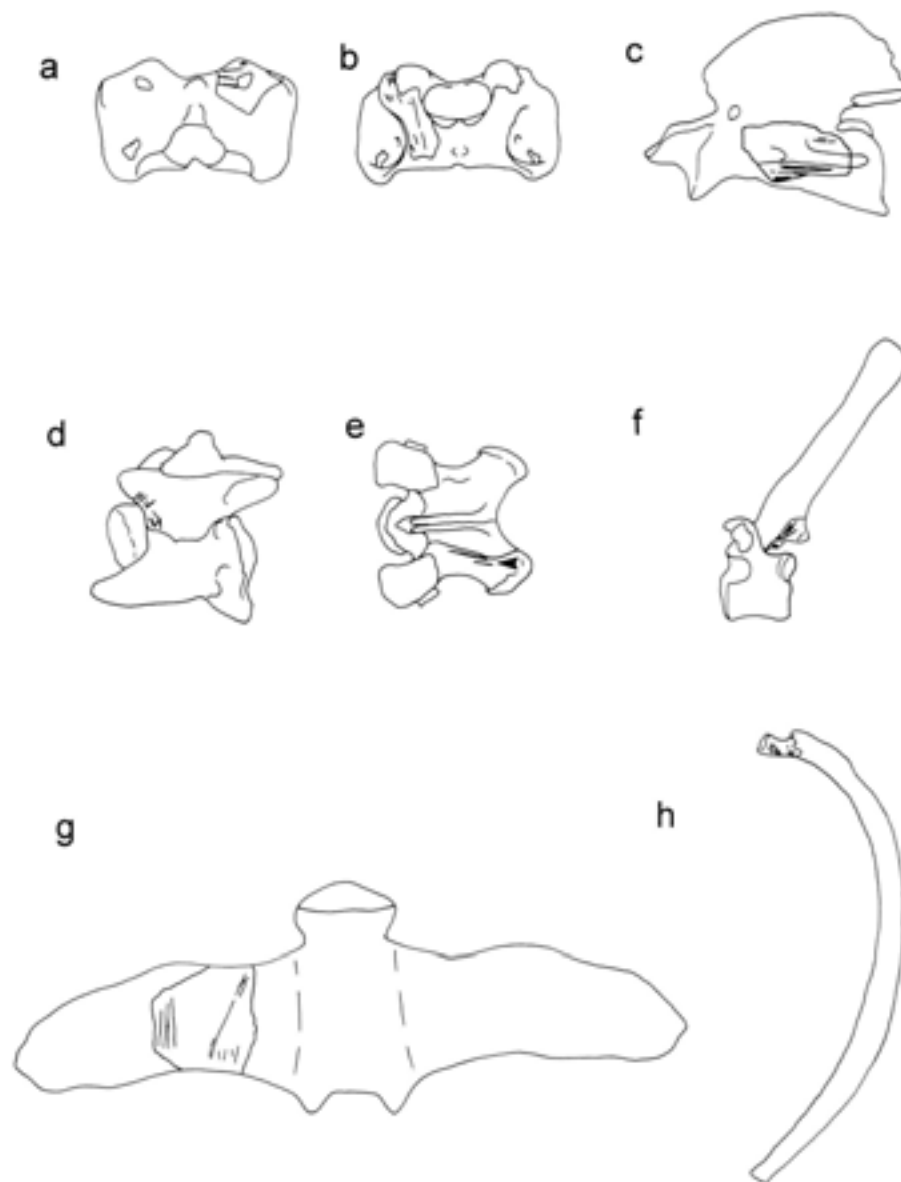


Fig 313a-h Location of cut marks on horse vertebrae and rib from Q2 GTP 17 (estimated dimensions of bones: a-b) greatest breadth = 175mm, c) greatest length $LCDe$ = 170mm, d-e) greatest length $GLPa$ = 150mm, f) greatest height = 260mm, g) greatest breadth $Bptr$ = 280mm, h) greatest length = 460mm)

percussion damage is produced when a bone is placed on an anvil and struck with a hammerstone. The frequency of bipolar impact notches in the Boxgrove assemblage is probably an underestimate of the actual number of anvil-broken bones as their recognition requires the presence of at least half of the original bone circumference. The majority of the impact notches observed in the Boxgrove assemblage were located on relatively small bone splinters, which preserved less than half of the original bone circumference. Anvil breakage was recognised following the refitting of limb bone shaft fragments and on one relatively complete humerus shaft fragment (Table 139).

The identification of marrow bone impact damage was relatively straightforward in the majority of cases,

but a small number of impact-type marks in the assemblage could not be positively identified as impact damage (Table 139). Damage similar to marrow bone impact marks can be produced when large carnivores crush, break or gnaw bones. Flake scars or lunate fracture scars produced by carnivore gnawing may resemble impact scars and are often impossible to distinguish from impact damage produced by hominids during marrow extraction. Lunate fracture scars produced by carnivore gnawing are usually associated with surface scoring and pitting which are indicative of carnivore gnawing. In addition, Blumenschine and Selvaggio (1988) have recorded microscopic damage produced by the hammerstone at the point of impact which appears to be characteristic of marrow bone breakage.

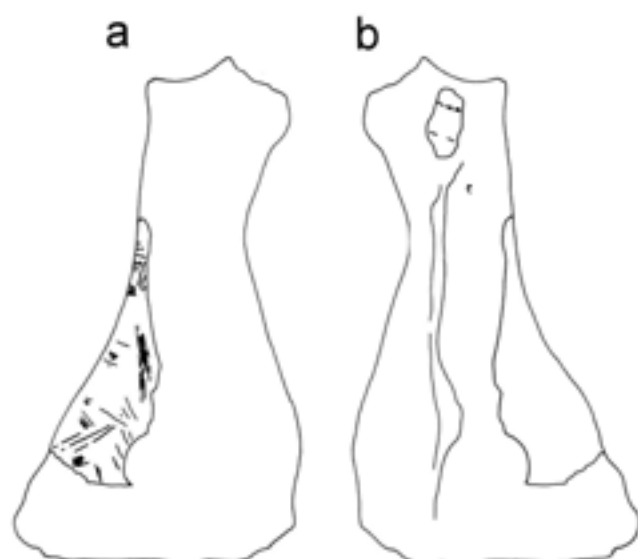


Fig 314a-b Position of cut marks on horse scapula from Q2 GTP 17: a) lateral view, b) medial views (estimated height along spine = 450mm)

In the following section the evidence for hominid alteration of the faunal remains is summarised and the processing activities represented by the cut marks and impact damage are listed for each of the large mammal taxa for which hominid alterations were recorded (Table 138). This is followed by a discussion of the behavioural implications of the butchery evidence.

Bear (*Ursus deningeri*)

The sole bear specimen with evidence for hominid modification consists of a fragment of the zygomatic process of the malar, from Unit 4c, GTP 3 (Tables 138, 140). This fragment (F41) refits along the suture to a small piece of the zygomatic process of the temporal bone (F1) recovered approximately 0.5m away and within the same stratigraphic horizon. The anatomical location of these pieces is shown in Figure 310a, and the location of the cut marks is illustrated in Figure 310b. Examination of these pieces under a binocular light microscope showed a complex sequence of alterations on the medial surface. This damage consists of areas of pitting and dendritic grooves which show clear features characteristic of rootlet corrosion. Areas of shallow, sub-parallel grooves and micro-striations resemble sediment abrasion (Andrews and Cook 1985), which probably occurred following breakage of the skull and as a result of the fragments being trampled prior to burial.

The lateral face of F41 exhibits three parallel incisions which show features characteristic of cut marks. The longest incision has a cross-section consisting of three sub-parallel grooves which coalesce towards one end to produce a single, relatively deeply incised, groove with a V-shaped cross-section. Observation of the marks under the scanning electron microscope showed fine parallel micro-striations within the main incisions. In addition to the characteristic morphology

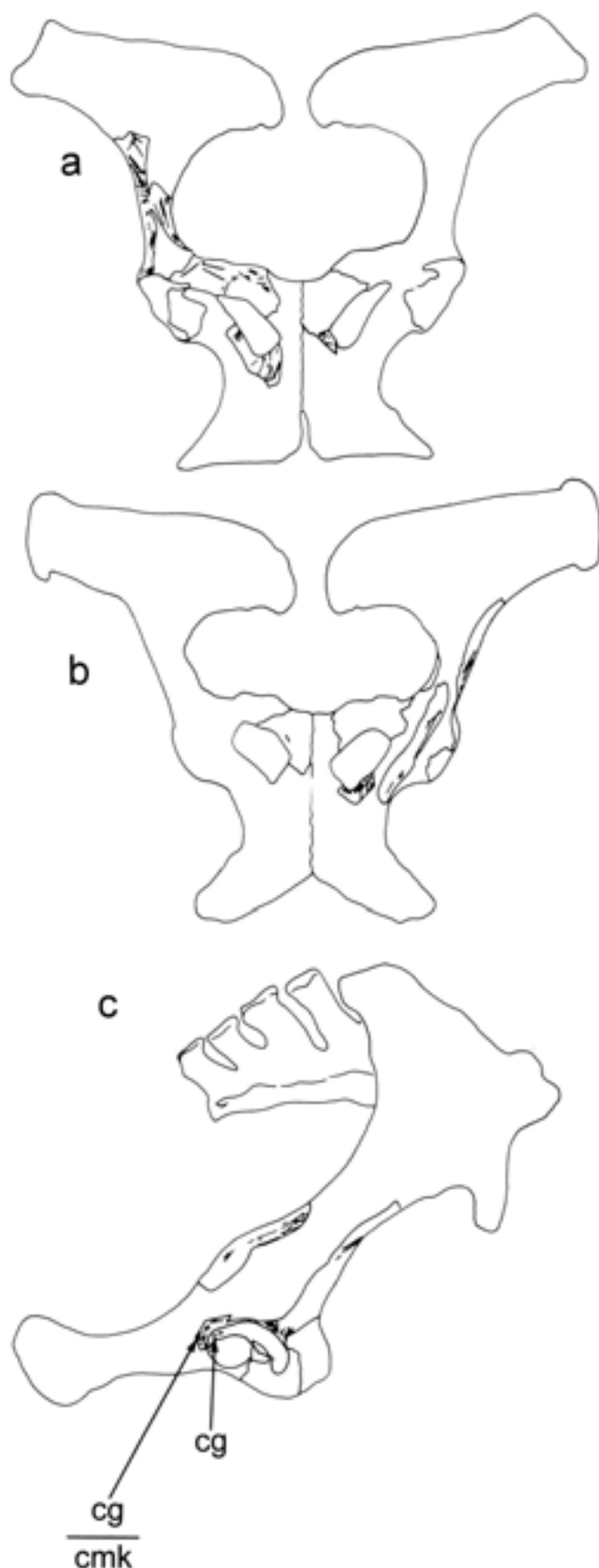


Fig 315a-c Cut marks on the pelvis of horse from Q2 GTP 17. The location of carnivore gnawing (Cg) and position of cut marks truncated by carnivore tooth impressions is indicated (cg/cm k) (estimated greatest length = 500mm)



a b c

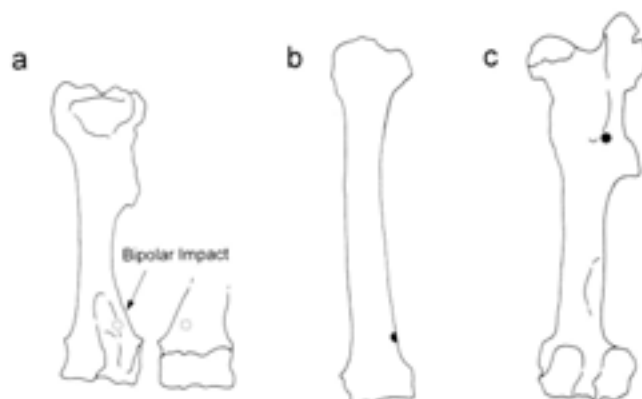


Fig 317 Location of marrow bone impact damage on horse limb bones from Q2 GTP 17: a) humerus, b) radius, and c) femur

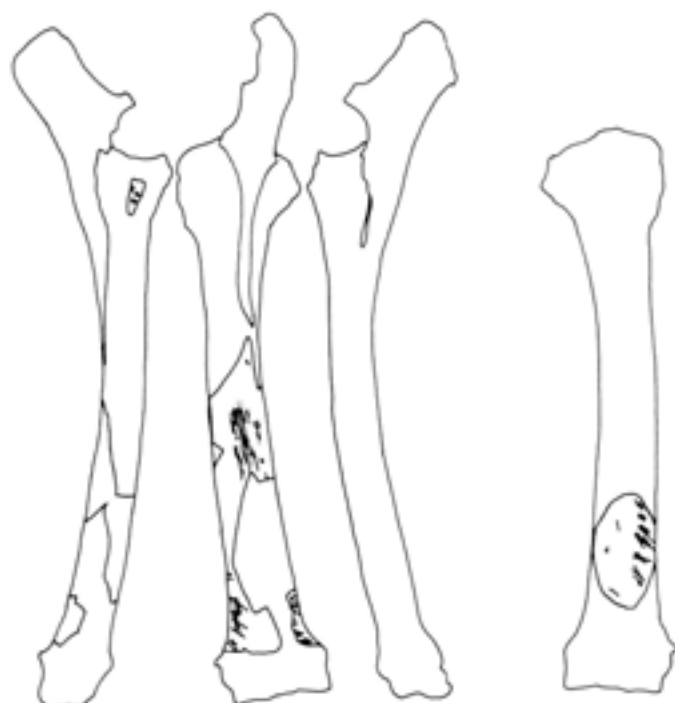


Fig 316a-g Location of cut marks on horse humerus (a-c) and radius (d-g) from Q2 GTP 17

of the marks, the anatomical position of the incisions is also consistent with an interpretation of tool inflicted cut marks. The morphology and location of the marks are suggestive of skinning and perhaps defleshing of the skull (Binford 1981; Guilday *et al* 1962). This interpretation of the marks is supported by observations on a number of recently prepared bear skulls (Fig 310c) in the comparative collections of the Natural History Museum (London) which displayed skinning marks with an identical placement and orientation to those observed on the Boxgrove specimen.



Fig 318a-b Cut marks on horse femur from Q2 GTP 17 (estimated greatest length = 510mm)

Horse (*Equus ferus*)

The modified horse bones are described in two groups; those from the horse butchery site GTP 17 (Roberts Chapter 6.2), and a small number of pieces from other excavation areas (Tables 138-40). Excavations at GTP 17, Unit 4b, produced the single largest assemblage of butchered bones from Boxgrove. Identification of this material was hampered by the extremely fragmentary nature of the sample. However, a concerted attempt to find refits between bone fragments allowed a larger number of otherwise indeterminate fragments to be identified. In total, 245 out of 2400 of the fragments were identified to taxa and/or body part, and the majority of the bones represent a large horse (*Equus ferus*). Other vertebrates recovered from this level include a large cervid, roe deer, fish, and small mammals, none of which show evidence for human modification and

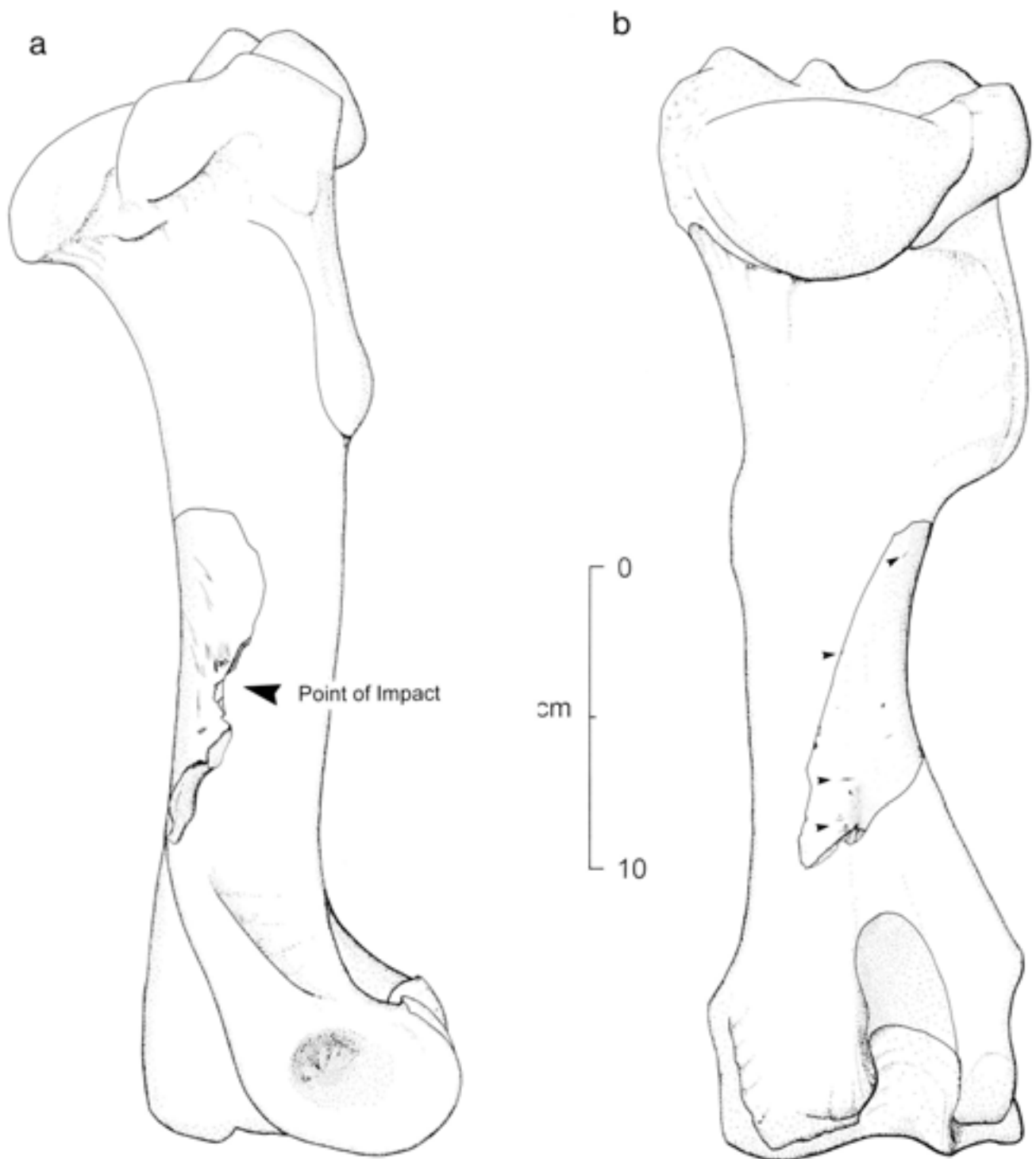
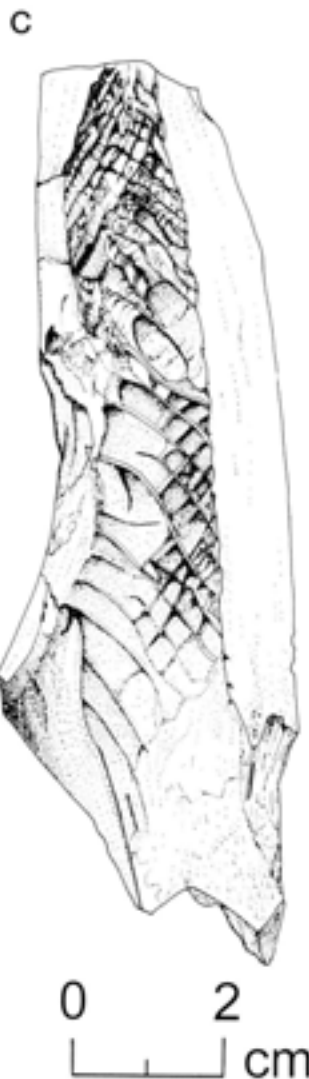


Fig 319a-c (above and facing) Horse humerus from Q1/B showing the location of filleting, disarticulation, and impact scars

probably represent a natural background accumulation of faunal remains. The horse bones were found in the same horizon and within a restricted vertical range. The taphonomic and sedimentological context of the material, together with the lack of duplication of elements and refits between bone fragments across the site, suggest that the material belongs to a single adult female dispersed over an area of at least 150m² (Figs 279, 280).

Evidence for exploitation of the carcass is provided from information on the presence of bone elements, butchery traces and breakage patterns. As can be seen from Figure 311, the identifiable horse bones represent a small fraction of the original skeleton, although bones are present from all parts of the axial skeleton as well as the limbs, with the notable exception of the distal limb elements. Evidence for butchery of the carcass is provided by the distribution of cut and scrape marks



and the fragmentation pattern inferred from the refitting pieces and the location of impact notches (Tables 138–40). The presence of cut marks on most of the larger bone fragments and impact marks on the limb bones and the mandible indicate intensive butchery of the carcass, which included skinning, disarticulation, filleting, and bone marrow extraction. Figures 312 to 318 illustrate the distribution of cut marks and impact notches on individual bones and these traces are briefly described in the following section.

One fragment of skull preserves cut marks (Fig 312a); this is a portion of the squamous temporal bone comprising the temporal condyle and glenoid cavity which form the articular area for the mandibular condyle. The cut marks on this piece are probably related to the detachment of the mandible from the skull. Marks on the buccal and lingual faces of the ascending and horizontal ramus of the mandible (Fig 312b) are from filleting of the mandibular muscles or the disarticulation of the mandible. An impact notch is present on a fragment of the horizontal ramus below the second molar (Fig 312b). This damage is the result of direct percussion to fracture the mandible to extract fatty tissue contained within the mandibular canal. Filleting marks are present on most of the vertebral

fragments (Fig 313a–h); these marks are oriented longitudinally on the body of the cervical and thoracic vertebrae and on the transverse process of the lumbar vertebrae. Transverse cut marks on the axis vertebra (Fig 313a–b) are from the disarticulation of the vertebral column from the skull. Two fragments of scapula consist of part of the neck of the scapula and a fragment of the blade (Fig 314a–b). Two sets of marks on the scapula reflect disarticulation of the humerus/scapula joint (marks on the neck), and broad scrapes and cuts on the blade indicating filleting. Filleting marks are also found across broad areas of the pelvis, mainly concentrated on the ilium but also on the pubis and around the obturator foramen (Fig 315a–c). Marks are also present encircling the acetabulum, which were produced during the separation of the femur from the pelvis. Relatively large portions of both the humerus and radius were reconstructed from fragments of diaphysis (Fig 316a–g) and both bones are heavily marked. Cuts on the humerus located close to the distal end are from the dismemberment of the humerus from the radius and ulna and oblique marks on the midshaft portion are from filleting of muscles attached to the shaft. Two opposing impact notches are present on the lateral condyloid crest (Fig 317a), which indicate that the humerus was placed on an anvil and struck with a hammerstone to fracture the bone. Marrow bone breakage of the radius is indicated by an impact notch located on the medial face of the bone just above the distal articulation (Fig 317b). Filleting marks are numerous on this bone and consist of broad scrape marks on the midshaft and parallel oblique cuts on the distal portion of the shaft (Fig 316d–g). An impact mark (Fig 317c) and cut marks on the femur (Fig 318a–b) are located on the shaft and third trochanter; these marks are from filleting of the large muscle blocks which are attached to this bone. In addition to the cut marks, a single impact notch on the posterior face, medial to the third trochanter, provides further evidence for marrow bone breakage.

Similar marks to those described from GTP 17 can be seen on a fragment of horse femur from area Q1/B, also from Unit 4b (Slindon Silts). Filleting marks on this specimen are orientated parallel to the bone's long axis (Fig 319a), whilst disarticulation marks are perpendicular to the long axis (Fig 319b). The location and orientation of these marks is consistent with cut marks recorded from ethnographic contexts and butchery experiments. Two impact marks with the scars running into the medullary cavity of the bone are also evident (Fig 319c). These impacts are consistent with the use of an anvil and hammerstone to break the bone. Figure 319c demonstrates that the bones must have been hit with a stone that had a large total surface area at its impact point. A large beach cobble, such as the one found in Q1 GTP 8, was probably used for this purpose, as the impact scars are 'clean' and bear none of the splintering effects observed when the worked edge of a tool such as a handaxe or cleaver is used to break bone.

Rhinoceros (*Stephanorhinus hundsheimensis*)

A total of six (23%) of the rhinoceros bones show evidence for human alteration (Tables 138, 140). These include a left lower third molar, part of a right mandibular condyle, an almost complete scapula, a crushed pelvis with associated sacrum, and a calcaneus.

The left lower molar illustrated in Figure 320 has short cuts on the distal and buccal face of the crown, parallel to the crown-root junction. These cut marks were probably made during the severing of the masticatory muscles to detach the jaw from the skull. Disarticulation of the jaw is evidenced by cut marks on a medial fragment of the mandibular condyle illustrated in Figure 321. A well preserved scapula from Unit 4c (GTP 17) has cuts located towards the distal portion of the supraspinous fossa (Fig 322a). These cuts were probably made during filleting of meat from the scapula blade. A second group of marks close to the neck of the scapula and on the distal end between the glenoid cavity and the tuber scapulae (Fig 322b) are attributed to dismemberment of the scapula from the humerus. Extensive areas of cut and scrape marks are present on the pelvis and sacrum from Unit 4c (GTP 17) (Table 138). This fragment consists of the greater part of the pelvis, lacking only the crest of the ilium and areas of the ischium and pubis. The pelvis and associated sacrum were badly crushed and distorted, with some areas of surficial bone missing, particularly around the acetabulum. Figure 323a illustrates the regions of bone



Fig 320 Rhinoceros left lower third molar with cut marks on enamel



Fig 321 Rhinoceros mandible fragment from Q1/B showing location of fragment and position of disarticulation marks on the condyle

present, while the location of cut marks is shown in Figure 323b-f. These marks were produced during the filleting of the large muscle blocks which attach to the pelvis and occur in similar locations to those described by Binford (1981).

A particularly important piece of bone is a calcaneus (Fig 324a-c) which shows evidence for both carnivore and hominid alteration. The calcaneus is virtually complete although it is missing the medial process, and the proximal end shows clear evidence for carnivore gnawing consisting of deep, broad, furrows and tooth impressions. The size of the tooth marks imply a relatively powerful carnivore was responsible. Comparisons with hyaena-gnawed bones show a close match to the type of gnawing damage, which suggests that hyaena was responsible for the damage. Cut marks are located on the plantar border, and on both the medial and lateral faces. These cuts are located close to areas of muscle tendon attachment and are attributable to disarticulation and filleting of the hindlimb. Of particular interest is the information that this piece provides on the relative timing of carnivore and human



Fig 322a-b Rhinoceros scapula showing the location of filleting and disarticulation cut marks; a) lateral view, b) distal view

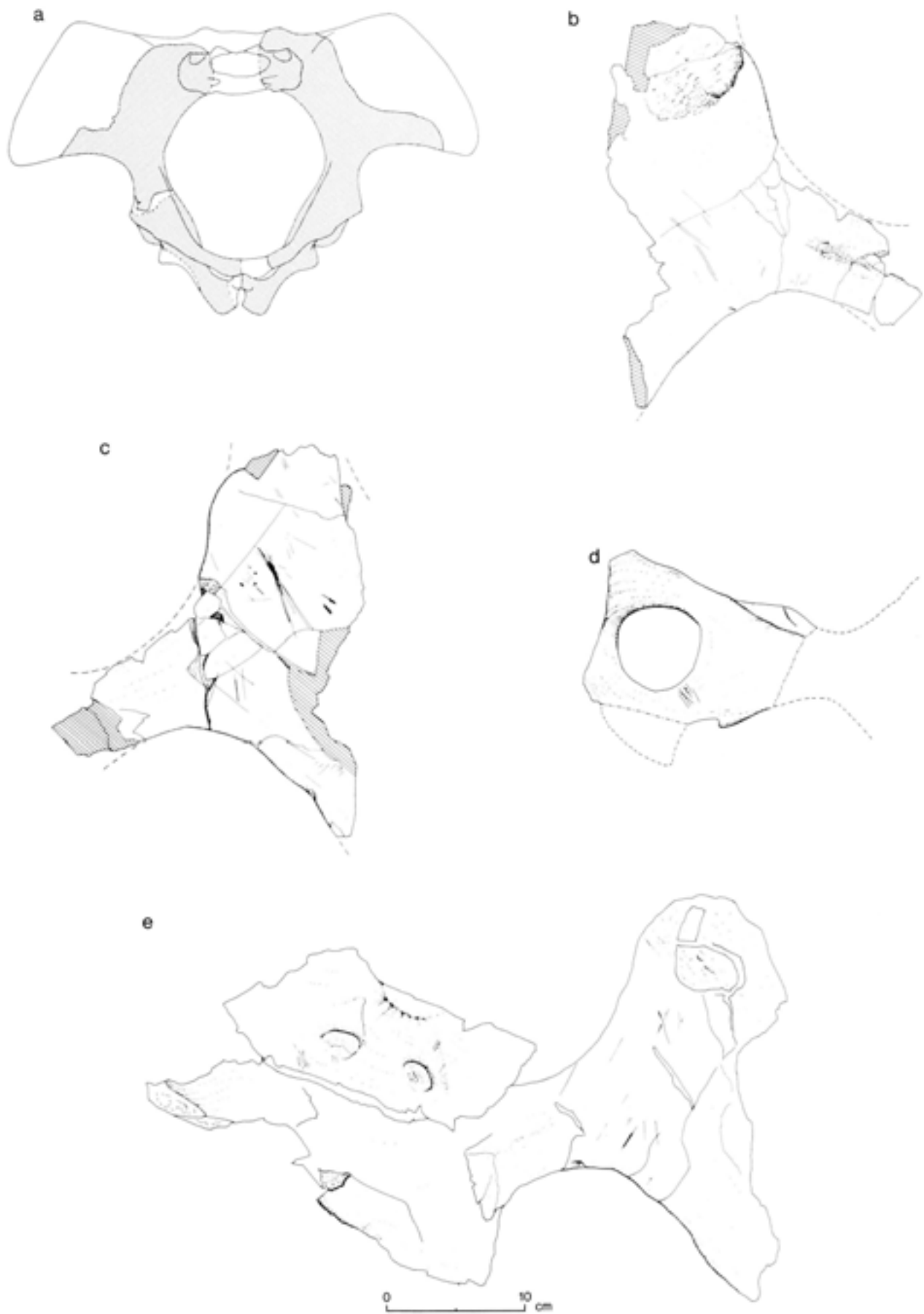


Fig 323a–e (323f overleaf) Rhinoceros pelvis showing the portions of the pelvis present and the location of disarticulation and filleting marks



Fig 323f Rhinoceros pelvis showing the portions of the pelvis present and the location of disarticulation and filleting marks

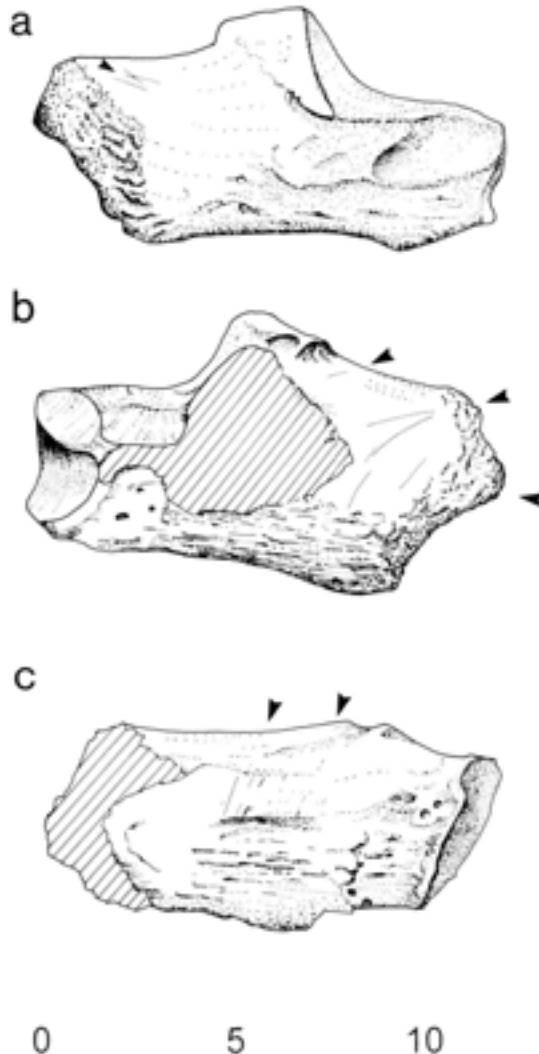


Fig 324 Rhinoceros right calcaneus showing the location of disarticulation cut marks and carnivore, possibly hyaena, gnawing which occurred after the butchery of the animal



Fig 325 Scanning electron micrograph showing the truncation of a cut mark a) by carnivore gnawing b) on the rhinoceros calcaneus illustrated in Fig 324

access to the carcass. The superimposition of carnivore gnawing and cut marks on the medial face is one of the few examples in the Boxgrove assemblage where it is possible to infer such a sequence of events. The region of overlap is illustrated in the scanning electron micrograph (Fig 325) which shows clearly the truncation of the cut mark by a carnivore tooth impression and groove, and illustrates carnivore involvement subsequent to dismemberment of the carcass by hominids.

Red deer (*Cervus elaphus*) and indeterminate large cervids

Sixteen red deer bones exhibit evidence for hominid modification (Tables 138–40). These include parts of the skull, teeth, and elements of the appendicular skeleton. Also included in this discussion are modified bones which were identified as those of large cervids. Although these remains were either too incomplete or insufficiently diagnostic to refer to species, the size of the majority of these pieces compared closely with those of red deer. The giant deer (*Megaloceros* sp) and fallow deer (*Dama dama*) are present in small numbers in the Boxgrove assemblage and it is possible that some of the more fragmentary pieces may be from these species. One notable feature is the lack of evidence for human utilisation of the roe deer (*Capreolus capreolus*). Sample size does not appear to be an explanation for the lack of modification of these bones as the roe deer is the most numerous cervid species at the site.

Activities represented by the butchered bones include skinning, dismemberment, filleting and marrow bone breakage. Although the material is on the whole scarce and fragmentary, there are nevertheless some skeletal elements represented by more than one butchered bone. This provides the opportunity to observe repeated patterns of butchery marks on localised anatomical regions.

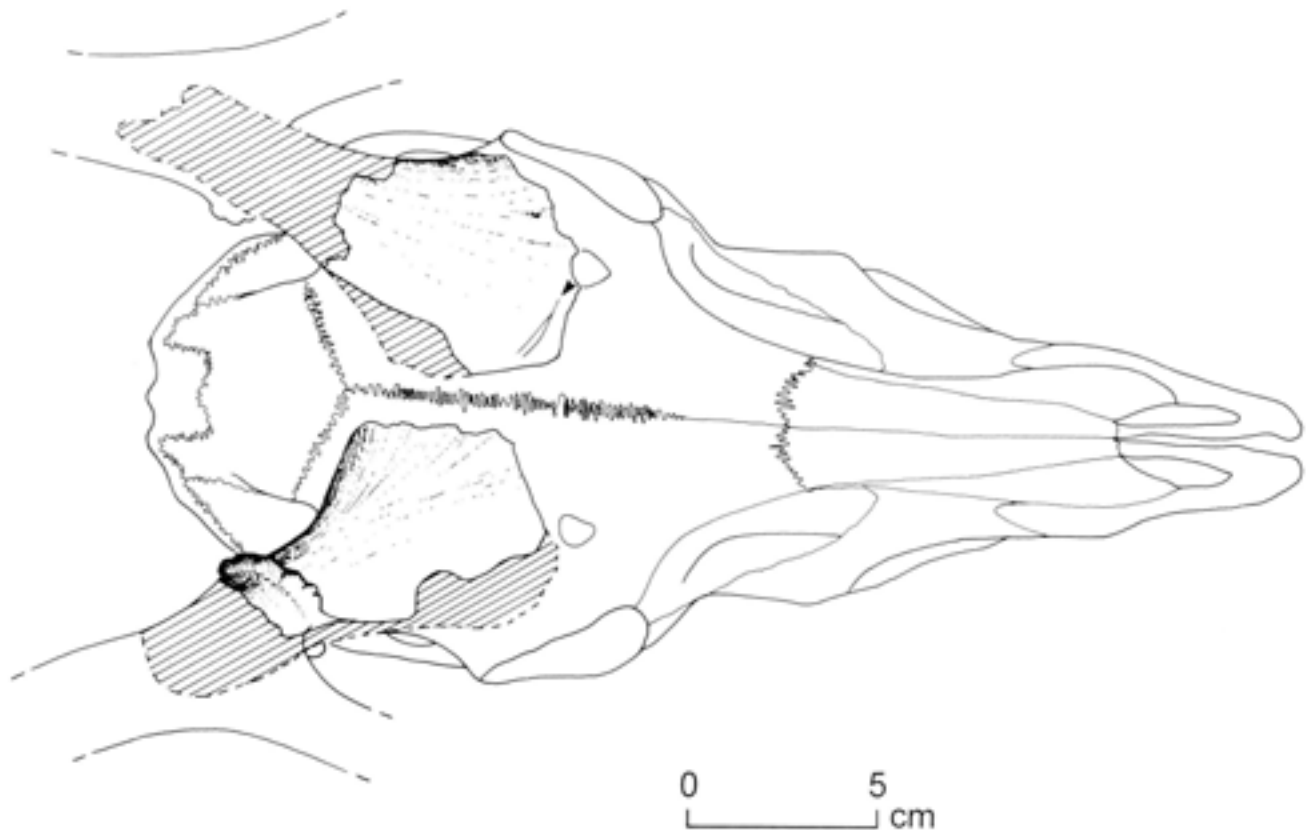


Fig 326 Skull fragments of red deer from GTP 17 showing the location of the pieces and cut marks close to the base of the antler produced during skinning

Two red deer skull fragments have cut marks on the frontal bone. Those on the male skull from GTP 17 consist of two cuts close to the base of the antler (Fig 326). The surface of this specimen and the associated right antler base are poorly preserved, and consequently it is uncertain whether similar marks were present around the base of the right antler. These marks are likely to be from skinning. Cuts encircling the antler base have been described previously by Binford (1981).

The second skull fragment is that of a female and consists of part of the right temporal (Fig 327a). Associated with this piece were other cervid skull fragments which are probably derived from the same skull. Cut marks located in the orbit (Fig 327b) most probably reflect removal of the eye or soft tissue lining the orbital cavity, whereas cuts on the temporal part of the frontal are filleting marks and derive from the removal of the temporal muscle. The location and orientations of both sets of marks are matched by cut marks on recent comparative skulls illustrated in Figure 327c. These skulls have been deliberately skinned and defleshed for their use as anatomical specimens.

Additional evidence for the skinning and defleshing of the skull is provided by an upper second premolar illustrated in Figure 328. Marks on the buccal surface of this specimen are derived from the skinning and/or filleting of the facial region of the skull (see description of giant deer teeth).

A cervid rib fragment (Fig 329) has two cut marks located just below the tubercle which correspond with similar cuts described by Binford (1981) as resulting from the removal of meat.

A portion of the proximal end of a red deer radius (Fig 330) has multiple, closely spaced, cuts on the lateral face directly below the proximal articulation. These are attributable to disarticulation of the humerus from the radioulna. The anterior face of the radius has a large impact notch resulting from marrow bone breakage. In contrast to the fractured horse limb bones described previously, this piece has had a single impact which shows that the bone was broken by direct percussion rather than by placing the bone on an anvil and striking it with a hammerstone.

The femur (Fig 331a-c) and tibia (Figs 332a-e, 333a-b) are represented by midshaft fragments, and both sets of bones exhibit scrape and cut marks along the length of the diaphysis resulting from filleting. A fragment of tibia shaft from Unit 3 (GTP 13) has evidence for marrow bone breakage in the form of a prominent percussion point and a large flake removed from the medial face and flaking of the medullary cavity. This piece also has flint fragments preserved in the cut marks on the bone surface which are visible under the SEM (Fig 334).

Cervid metapodial fragments are well represented, although only two pieces have definite evidence for human alteration. Part of the midshaft of a red deer

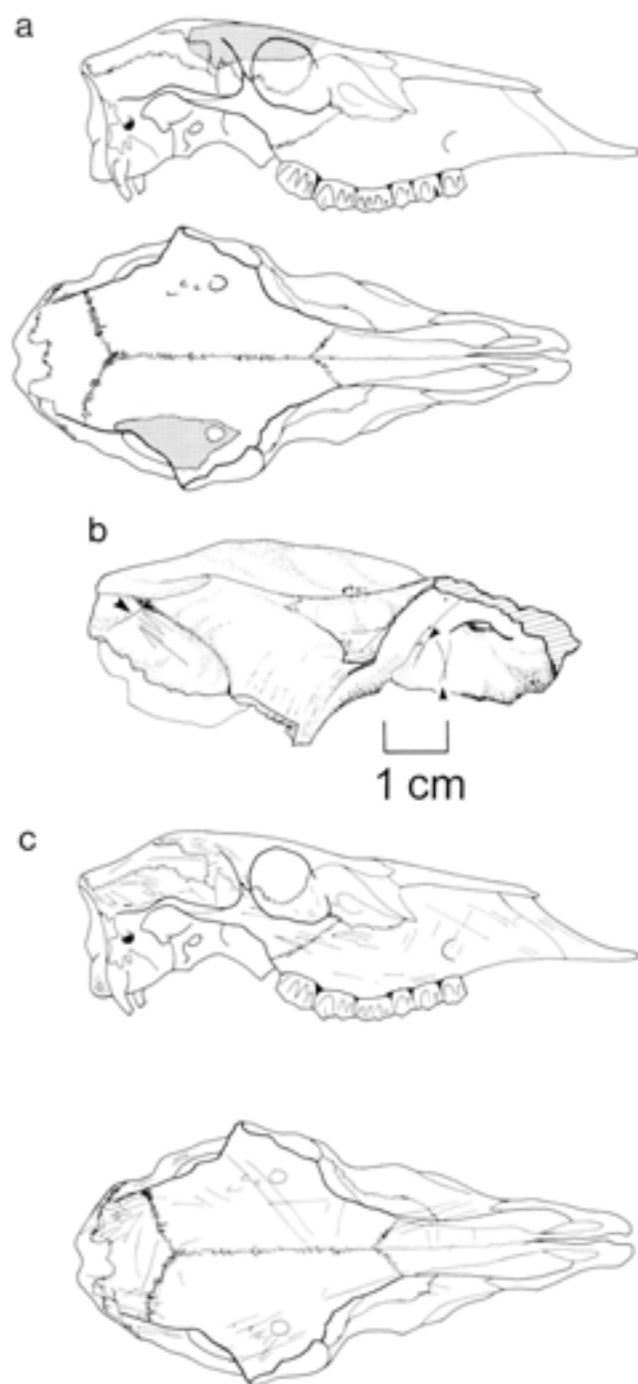


Fig 327a–c Skull fragments of a female red deer with cut marks; a) location of the piece, b) location of filleting and disarticulation marks, c) location of skinning, defleshing, and disarticulation marks on modern museum skulls (composite drawing produced from a sample of skulls examined in the Natural History Museum, London)

metacarpal (Fig 335a–b) has two opposing impact notches located on the anterior and posterior faces, and a splinter of metatarsal shaft has a single impact located on the anterior face near the middle of the diaphysis (Fig 336a–c). Phalanges are poorly represented; one first phalanx of a red deer-sized cervid has transverse cuts close to the distal end which are probably from skinning (Fig 337).



Fig 328 Red deer left upper second molar with cut marks on buccal face

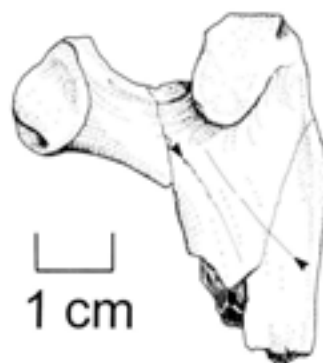


Fig 329 Cervid rib fragment (proximal end) showing location of cut marks

Giant deer (*Megaloceros cf verticornis*)

Remains of the giant deer consist of a number of upper teeth from Unit 4b (Q1/A), some of which are illustrated in Figure 338. Cut marks were observed on the buccal face of the left upper second and third molars and on the lingual face of the left second upper premolar and third upper molar. These marks are located on projecting areas of the crown such as the buccal cones and styles and are oriented parallel to the enamel/root junction. These marks are attributed to the severing of the masticatory muscles and/or cutting of the skin of the muzzle to facilitate the removal of the mandible. Marks on the lingual face of the teeth are less easy to interpret, although similar marks have been recorded on red deer molars from Q2/C (Roberts *et al* 1997). Associated with the Q2/C teeth are refitting and associated fragments of maxilla which display longitudinal cuts that are interpreted as evidence for the removal of soft tissue overlying the hard palate. It is possible that marks on the buccal face of the giant deer teeth were produced during a similar process.

Discussion

The large mammal bones from Boxgrove are concentrated in three stratigraphic horizons; the Slindon Silts (Unit 4b), the soil horizon at the surface of the Slindon Silts (Unit 4c), and the overlying Organic Bed (Unit 5a) (Table 140). These remains are associated with lithic material, with the possible exception of Unit 5a,

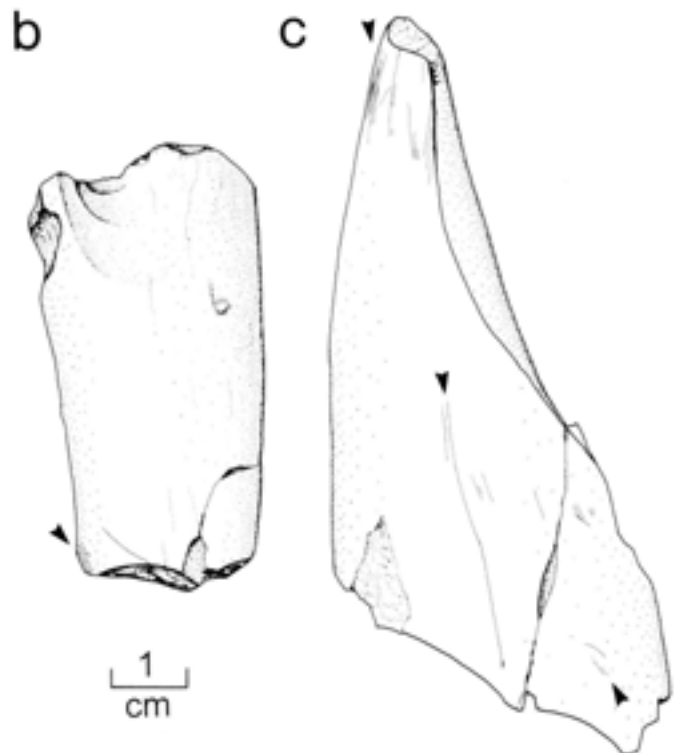
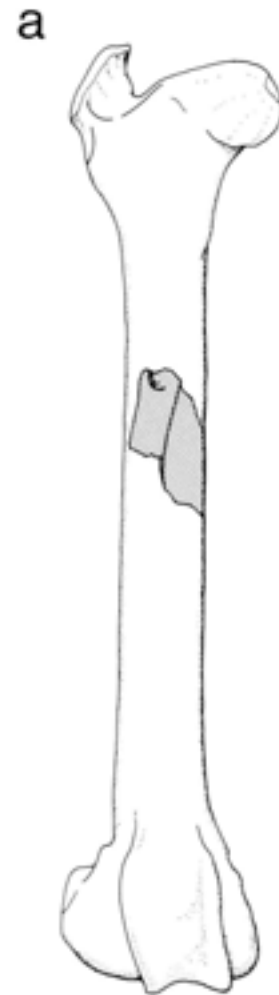


Fig 330 Red deer proximal radius fragment showing disarticulation cuts and impact mark located just below the proximal articular surface

which has produced a limited number of artefacts which are probably reworked from the underlying palaeosol (Wilhelmsen Chapter 6.2). The taphonomic history of the large mammal faunal remains is complex, and they represent attritional assemblages that accumulated on a series of landsurfaces. Micromorphological evidence (Macphail Chapter 2.6) indicates that the soil horizon (Unit 4c) was exposed for a comparatively short period of time. This is supported by evidence of weathering on a number of the large mammal bones. Humanly modified bones from this horizon are dispersed across the site with no obvious indication for concentrations which may represent butchery or carcass processing locations. In addition, the percentage of butchered bones from this horizon is low in comparison with the underlying lagoonal deposits. The nature of the large mammal accumulations suggest

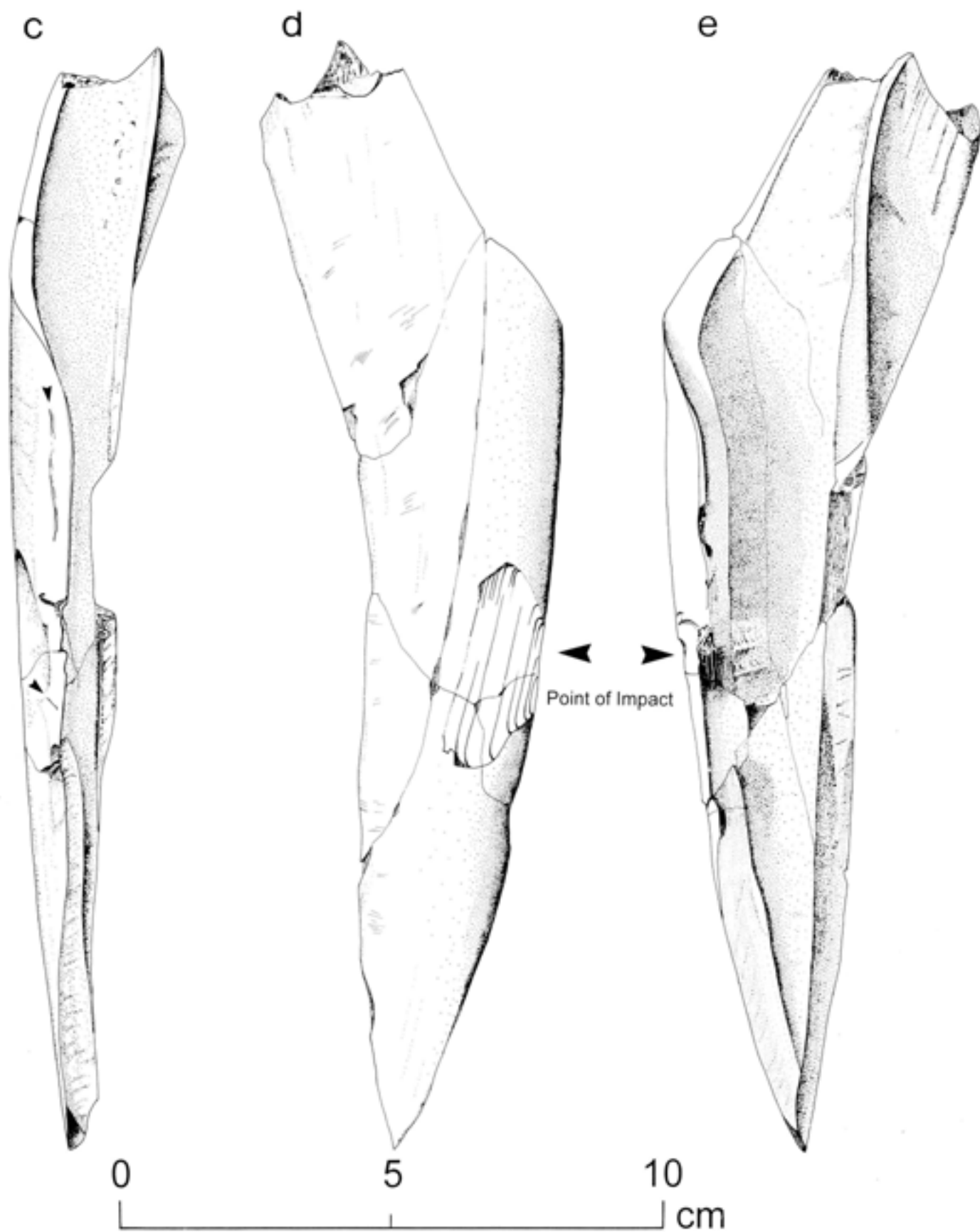
Fig 331a-c Red deer femur showing a) anatomical location of the conjoining fragments from Q1 GTP 8 and b-c) position of scrape and cut marks



Fig 332a-e (above and facing) Red deer tibia shaft fragment; a) and b) location of fragment, c-e) cut marks produced during filleting and marrow bone impact mark

that the majority of the bones in Unit 4c represent natural deaths, with limited hominid involvement in the accumulation of the bone assemblage. Taphonomic analysis of recent butchery sites (Gifford and Behrens-meyer 1977; Binford *et al* 1988) on modern day land-surfaces have shown that bones are rapidly dispersed by large carnivores and trampling. In these situations it is highly unlikely that butchery sites will survive exposure in an environment where the rate of sedimentary deposition is low.

In contrast with the soil horizon, large mammal bones from the Slindon Silts (Unit 4b) are found in discrete concentrations in association with large quantities of flint debitage. These concentrations of faunal and artefactual remains occur within deposits that are otherwise archaeologically sterile. Evidence for hominid modification of the bones from the concentrations is abundant and includes cut marks, marrow fractured bone, and bone flakes from marrow bone processing. Refitting of the bone and flint assemblages



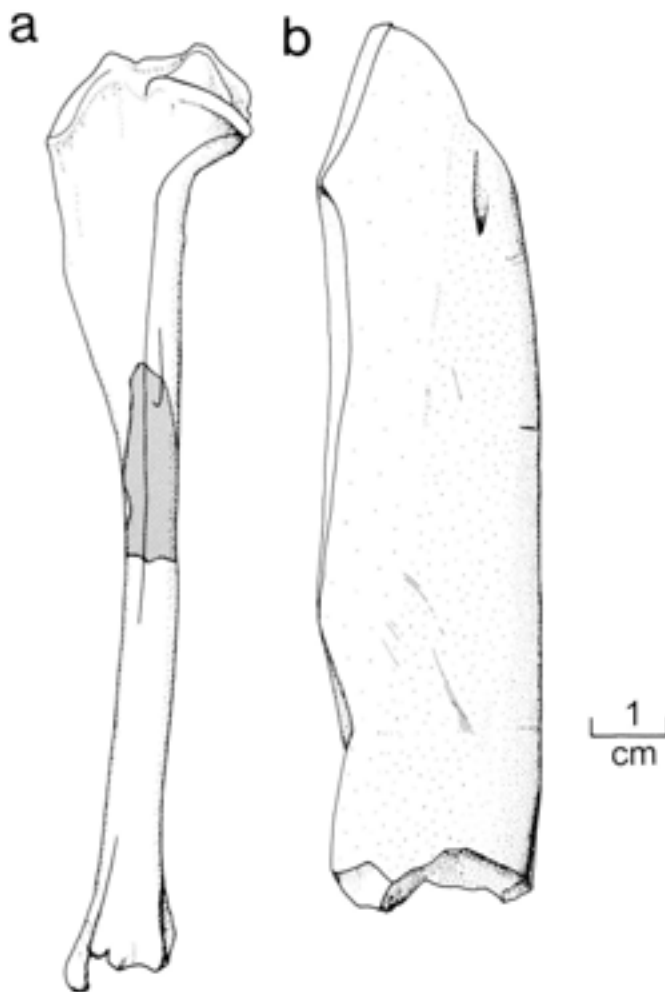


Fig 333a–b Cervid tibia showing location of the fragment (a) and position of cut marks

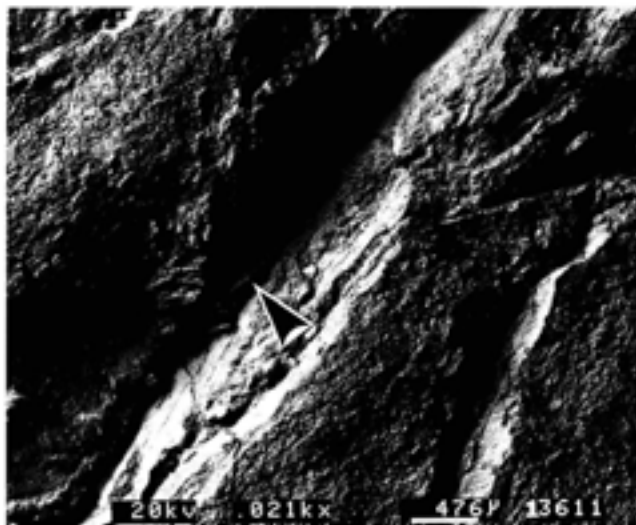


Fig 334 Scanning electron micrograph of flint chip (arrowed) embedded within a cut mark

shows that these concentrations have undergone minimal disturbance prior to burial. Large-scale excavation of three of these bone and flint concentrations has been undertaken in Q1/A, GTP 8 and in Q2 GTP 17 ('horse butchery site'). The faunal and artefactual remains from Unit 4b in GTP 17 are confined to a thin layer of deposits that can be traced above a clay lamination extending across most of the excavated area. Identification of the faunal remains was hampered by the small size of the majority of the bone fragments; nevertheless, the identifiable component of the assemblage can be shown to represent the remains of a single large horse (*Equus ferus*). The discrete nature of the fauna and flintwork from this area indicates that the remains represent a single episode of flint knapping associated with the processing of a horse carcass.

A similar concentration was excavated in Q1 GTP 8, just to the south of main area Q1/A. Although the extent of the excavated deposits in this area was limited, the fauna and artefacts were located within a discrete horizon. The lithic material consisted of flakes, a shattered anvil block, and two beach-pebble hammerstones, associated with the bones of a medium-sized cervid, possibly red deer (*Cervus elaphus*). Cut marks, indicating filleting and dismemberment, were recorded on a number of the bones, as well as marrow bone breakage evidenced by impact notches on two bone fragments.

The preservation of single episode flint knapping and butchery sites in the lagoonal deposits is a result of the depositional environment under which this horizon was deposited. The silt and clay laminations probably represent deposition during high tides in an extensive lagoon and the micromorphological evidence indicates that deposition was rapid. The preservation of such single episode activity sites is extremely uncommon in the Pleistocene archaeological record and provides an important source of information on Palaeolithic carcass processing and behaviour.

The evidence for hominid modification of the large mammal bones from Boxgrove is summarised in Table 138. The cut marks provide evidence for skinning, dismemberment and filleting and percussion marks indicate marrow bone breakage. The occurrence of cut marks produced during skinning and filleting indicate that the carcasses were relatively complete prior to butchery. This is supported by the faunal assemblage from GTP 17 which represents the remains of a complete horse carcass. The distribution and sequence of carnivore damage on the cut-marked bones indicates priority of access for the hominids. A total of five hominid-modified bones provide evidence of carnivore gnawing damage. Significantly, in three of these pieces the carnivore gnaw marks overlie the cut marks; on the other two bones there was no overlap between cut marks and the carnivore damage. The evidence provided by the cut marks and the presence of carnivore gnawing overlying cut marks is evidence for very early access to the carcass by hominids,

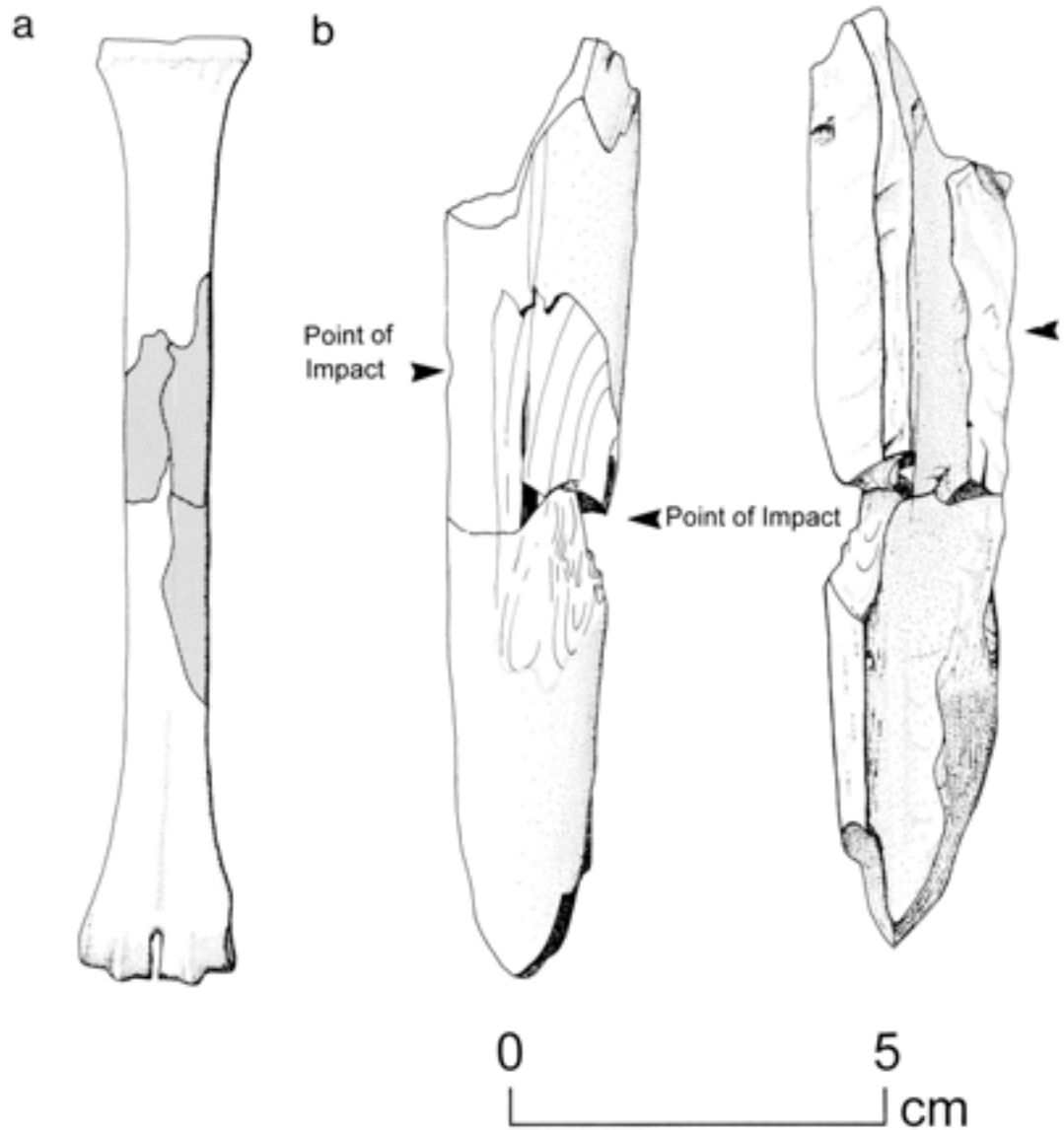


Fig 335a–b Red deer metacarpal showing the location of the fragment (a) and position of opposing impact damage (b)

although the evidence available to date, with the possible exception of a puncture wound in the scapula from GTP 17 (Fig 289), does not allow us to distinguish definitively between hunting or confrontational scavenging as the main method of carcass procurement. The circumstantial evidence, however, favours the former method.

6.6 The Middle Pleistocene hominid record

C B Stringer

Europe has held a central place in discussions of Pleistocene human evolution since the Neander Valley discovery of 1856 consisting of a Late Pleistocene archaic human skeleton (Stringer and Gamble 1993). The discovery of the Mauer mandible in 1907, coupled with the subsequent and spurious Piltdown material, ensured that Europe remained a focus of interest

for those investigating the origins of both Neanderthal and modern humans. The gradual demise of Piltdown was counterbalanced by a plethora of discoveries of important new material such as those from Ehringsdorf, Steinheim, Swanscombe, and Montmaurin, and Europe has continued to produce important material, right up to the remarkable collection of disassociated skeletons from Atapuerca, Spain. Palaeoanthropologists no longer expect Europe to provide evidence of very early hominids, and claims for archaeological evidence of an Early Pleistocene colonisation of Europe are still treated with scepticism by many workers (see eg Roebroeks and van Kolfschoten 1994). However, the discovery of a human mandible associated with Villafranchian mammals at Dmanisi, Georgia, and hominid fossils at Gran Dolina, Atapuerca, suggests that Europe may yet prove to have had at least sporadic human occupation in the earlier Pleistocene (Gabunia and Vekua 1995; Carbonell *et al* 1995).

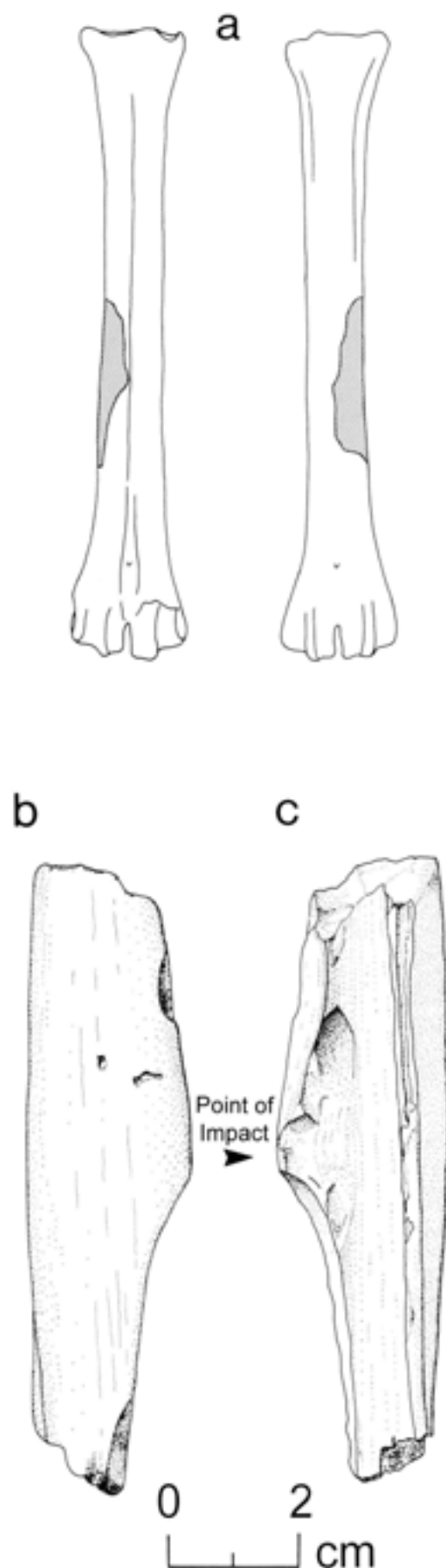


Fig 336a-c Red deer metatarsals; a) location of fragments, b) and c) impact damage and cut marks

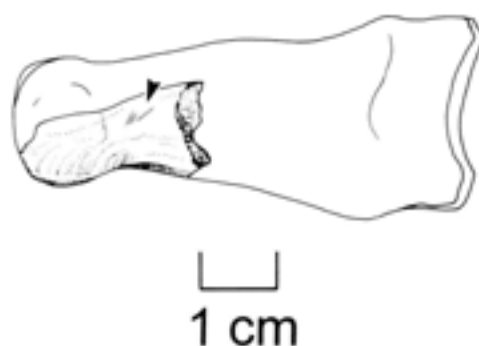


Fig 337 Red deer sized cervid first phalanx showing location of cut marks

Even today, Europe undoubtedly has the best record of Middle Pleistocene hominids (Table 141), although significant finds continue to be made in Africa, mainland Asia, and Indonesia. European specimens include rather incomplete material such as the fossils from Mauer, Vértesszöllös, and Bilzingsleben, which are classified as *Homo erectus* by some workers, and from their preserved parts it is difficult to resolve their taxonomic status (Stringer *et al* 1984).

The Dmanisi mandible, which does appear to represent an Early Pleistocene *Homo erectus*, lies outside the borders of Europe, and so apart from the Atapuerca Gran Dolina material and some fragmentary and disputed finds, the Mauer jaw is probably the oldest European fossil hominid yet discovered. This mandible was discovered during quarrying at a sandpit at Mauer, near Heidelberg, Germany, in 1907. The associated fossil mammals suggest a Middle Pleistocene and post-Cromerian *sensu stricto* age, perhaps about 500kyr. The mandible has a thick corpus and a very broad ascending ramus. There is no chin development, but the teeth are quite small, leading to the suggestion that this could represent a female individual, despite its robusticity. Although there is no retromolar space development, characteristic of Neanderthal jaws, the specimen is long, indicating that the associated face was probably quite projecting. It was originally classified as the type of a new species, *Homo heidelbergensis*: some workers accept this designation as valid, while others regard the jaw as representing a European form of *Homo erectus*. However, both assignments are subject to further discussion as a result of new material from Atapuerca (see below). Boxgrove, correlated with the Mauer site by biostratigraphy, provides us with the first definite postcranial evidence of these earliest known Europeans (Stringer and Trinkaus Chapter 6.7).

The travertine site of Vértesszöllös, near Budapest in Hungary, produced two hominid specimens in 1964 and 1965. The site is generally dated to an interstadial within the 'Mindel' glaciation of continental Europe or to an undesignated post-Cromerian interglacial. Uranium Series dates originally suggested an age of greater than 300kyr. However, recent dating by the

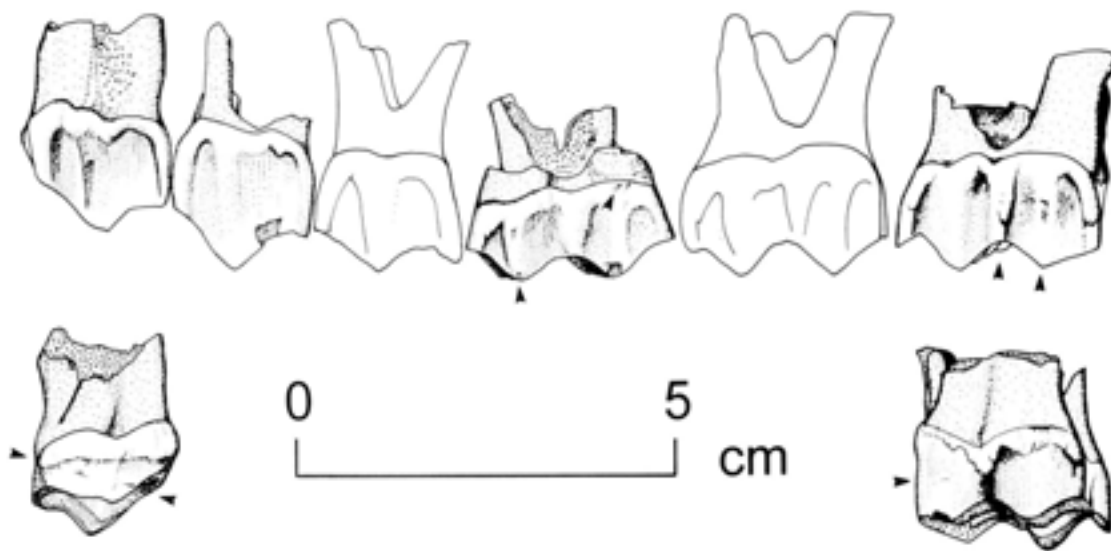


Fig 338 Giant deer teeth with cut marks on buccal and lingual part of the crown

Table 141 European Middle and Late Pleistocene hominid sites and lineages

Age (kyr)	Site	Lineage
30	Cro-Magnon Mladeč	<i>Homo sapiens</i>
50	Late Neanderthals	<i>Homo neanderthalensis</i>
120	Saccopastore Biache	
220	Ehringsdorf Pontnewydd Atapuerca SH site	
300	Steinheim Reilingen Swanscombe Arago	
400	Bilzingsleben Vértesszöllös Petralona Boxgrove	<i>Homo heidelbergensis</i>
500	Mauer Ceprano	
600		
700		
800		
900	Atapuerca Gran Dolina	

same method suggest an age of only about 200kyr for the hominid levels, in conflict with the biostratigraphy (Schwarcz and Latham 1984). The hominid specimens comprise some teeth of a child and an adult occipital bone. The latter specimen has been the subject of much dispute regarding its affinities. It is quite thick and fairly angulated, with a centrally developed occipital torus, but it is also large and relatively rounded in

its occipital portion. Endocranial size was probably more than 1300ml, leading some to suggest that it represents *Homo heidelbergensis* or 'archaic *Homo sapiens*'. Others emphasise its supposed antiquity, thickness and shape, and classify it as *Homo erectus*.

The large sample of fossil human material from the Arago Cave has also been classified as *Homo erectus* by some workers, mainly on the basis of primitive characteristics such as a projecting face, strong brow ridge, and small endocranial size, as well as the claimed high antiquity of the specimens (*c* 400kyr) (Stringer *et al* 1984). The cave, near Tautavel in the French Pyrenees, has been under excavation since 1964. The Arago specimens include a face, facial fragments, mandibles, a hip bone, teeth, and limb bone fragments. As an alternative to classification as *Homo erectus* it has been suggested that the Arago material represents *Homo heidelbergensis* or 'archaic *Homo sapiens*', or even that it derives from a population related to the ancestry of the Neanderthals: characters of the Arago 21 face and the Arago 2 mandible have been cited in support of this view.

An appropriate taxonomic assignment for the Bilzingsleben cranial fragments has also been much debated. The open travertine site of Bilzingsleben in eastern Germany had long been known to palaeontologists but it is only since 1973 that its importance has been realised through large-scale, productive, excavations. Abundant faunal and archaeological remains have been found in hominid occupation levels which apparently include extensive butchery debris and possibly even remains of hut structures. The faunal and palaeobotanical remains indicate a warm interglacial stage, and various lines of evidence, including U-S dating, suggest correlation with Oxygen Isotope Stages 9 or 11 (Mania *et al* 1994). The frontal and occipital fragments are certainly the most *Homo erectus*-like of all the European cranial specimens in the strong brow ridge and occipital torus development, and in the proportions

and angulation of the back of the skull. However, the occipital region is less robust than that of any of the Zhoukoudian *Homo erectus* adults and is similar in proportions to that of the African Elandsfontein cranium, which is usually referred to *Homo heidelbergensis*, *Homo rhodesiensis*, or 'archaic *Homo sapiens*' (Stringer 1989). New cranial fragments, including a large frontal fragment and temporal bone, will certainly help in more definitely reconstructing and assigning this material. A new Middle Pleistocene calvaria from Ceprano, Italy, shows a number of resemblances to the Bilzingsleben material, and will also be important in resolving taxonomic issues surrounding it (Ascenzi *et al* 1996).

Where more complete Middle Pleistocene material is known from Europe, it is apparent that referral to *Homo erectus* is not the most appropriate option. One specimen is a particularly fine example of such a fossil, and it is unfortunate that dispute about its antiquity has clouded its significance. It was found in 1960 deep within a cave near the village of Petralona in north-eastern Greece (Stringer 1983). Although it has been claimed that a whole skeleton was originally present, this seems unlikely. Because the original location was not excavated carefully at the time of discovery, many uncertainties about the associations and age of the skull can never now be resolved. Absolute age estimates by U-series, TL, and ESR suggests that the cranium could be as young as 200kyr or older than 350kyr. Study of mammalian fauna supports the more ancient age estimates, but claims for an antiquity of more than 700kyr are extremely unlikely. The cranium does show some *erectus*-like characters in its uniformly thick brow ridge, its broad upper face, palate and base, its centrally strong occipital torus, and thickened brain case. Endocranial size is about 1220ml while the endocranial cast of the brain cavity is rather less flattened than in typical *erectus* specimens. There are also advanced (derived) characters which are shared with later Pleistocene (especially Neanderthal) crania. These include a lesser degree of total facial prognathism, but increased midfacial projection, a double curvature of the brow ridge, prominent nasal bones, an occipital torus which is lower in position and reduced laterally, and extensive pneumatization, including an enormous frontal sinus.

The Steinheim skull was found in a quarry near Stuttgart, Germany, in 1933 together with fauna suggesting a Holsteinian age (Stringer *et al* 1984). It is nearly complete but badly distorted. Endocranial size is less than 1200ml and the cranial walls are thin, but the brow ridges are strongly developed. The back of the vault is evenly curved, and in its present state of preservation the position of maximum breadth is quite high. The damaged face is relatively small, broad, and flat, with a large nasal opening and cheek bones with an apparent canine fossa. It is an enigmatic specimen, small brained and relatively large browed, yet in other respects it shows advanced characteristics in the thin vault and occipital shape. In certain respects the back

of the skull resembles that of Swanscombe and the Neanderthals, yet the shape and proportion of the face seem rather primitive. The combination of a somewhat Neanderthal-like occiput and apparently primitive face is exactly the opposite of the situation in the Petralona skull.

The back part of a human skull associated with Acheulean artefacts, and a fauna with Hoxnian affinities derive from a gravel pit at Swanscombe, Kent (Stringer *et al* 1984). The occipital bone was discovered in the Middle Gravels in 1935, followed by the left parietal in 1936 and the less well preserved right parietal in 1955. The bones are thick by Neanderthal or modern European standards, but the occipital is rounded in profile with a torus which is only slightly developed, as are the muscle markings, leading to the suggestion that the skull belonged to a female individual. The brain size of the Swanscombe woman was probably about 1300ml and the overall cranial shape lacks the angularity of more archaic hominids. However, the parietal is relatively flat and short, while the base of the occipital is broad. Two features in particular suggest Neanderthal affinities. These are the slight, double arched occipital torus surmounted by a central depression (a suprainiac fossa), and the suggestion at the occipital margins of a developed juxtamastoid eminence. However, such Neanderthal-like characters are surprising if an immediate post-Anglian (OIS 11) dating can be confirmed for the Middle Gravels at Swanscombe (Bridgland 1994; Roberts *et al* 1995). The back half of a calvaria bearing many resemblances to the Swanscombe fossil was found in a quarry at Reilingen in Germany in 1978. Despite such resemblances, the dating of the fossil cannot yet be confirmed as Middle Pleistocene, because of uncertain faunal associations (Dean *et al* 1994).

The Ehringsdorf hominids were recovered during both commercial and controlled excavations between 1908 and 1925 from interglacial travertine deposits near Weimar in Germany (Stringer *et al* 1984). The most significant specimens are an adult cranial vault, an adult lower jaw, a child's lower jaw, and parts of a child's skeleton. Found in association with artefacts of Middle Palaeolithic affinities, from U-series and ESR dating techniques the material appears to date from OIS 7 (Blackwell and Schwarcz 1986). Also apparently deriving from this interglacial are a collection of 20 fragmentary hominid fossils from Pontnewydd Cave in Wales, associated with handaxes, discovered since 1980. The teeth are small, but some show clear taurodontism, similar to that found in some Neanderthals (Green 1984).

As we have seen, a number of Middle Pleistocene fossil hominids are difficult to assign because of incomplete or conflicting data. This is especially true of mandibular specimens such as the ones from Mauer and Montmaurin. The latter site (a fissure filling) produced a nearly complete lower jaw in 1949, which probably dates from the late Middle Pleistocene.

Some of the less complete specimens do appear to show either *erectus* or Neanderthal characteristics but it seems premature to classify them while the informative samples of hominids from Altamura and Atapuerca await detailed publication. A remarkable find, which appears to be of Middle Pleistocene antiquity, is the recent discovery of a virtually complete human skeleton deep in a cave system at Altamura, in southern Italy. Originally found by cavers, the fossil skeleton is well preserved, but encrusted by speleothem, and includes a cranium with evident affinities to other Middle Pleistocene specimens (it is described briefly in Delfino and Vacca 1994).

The complex of separate fissure fillings and caves at Atapuerca in Spain has produced stratified sequences of Middle Pleistocene fauna and artefacts, as well as a number of hominid fossils from stratified and unstratified contexts. Most of the hominids are from the 'Sima de los Huesos', deep within a cave system, although significant and more ancient finds were made in the 'Gran Dolina' site during 1994–5. These are associated with *Mimomys savini* and a claimed Lower Pleistocene stratigraphy and could therefore antedate the Mauer mandible (Carbonell *et al* 1995). From U-series dates, an age of about 300kyr was suggested for the 'Sima' fossils, but this is currently under revision. The material represents over 1300 jumbled cranial and postcranial bones, teeth, and fragments from at least 32 individuals, including crania from at least 6 adults and children. The best preserved cranial specimens display features found in the rest of the Middle Pleistocene sample, including facial resemblances to both the Petralona and Steinheim crania. The temporal and occipital bones show few *erectus*-like features, and foreshadow those of Neanderthals in the presence of an incipient suprainiac fossa. Temporal morphology looks more 'modern' in the relatively large mastoid process and small juxtamastoid eminence (as appears to be the case for fossils like Reilingen and Ehringsdorf), but one younger individual does display a closer resemblance to the Neanderthal morphology. However, the clearest sign of Neanderthal affinities is the well developed midfacial prognathism of the small cranium 5 (Arsuaga *et al* 1993). The extensive postcranial sample shows archaic and Neanderthal features, but overall body size does not appear to be large, and the teeth are certainly small overall, while showing some Neanderthal features in occasional taurodontism and relative anterior/posterior proportions (Bermúdez de Castro 1993).

Discussion

Discoveries made in the last five years ensure that Europe retains its position as the region with the best documented record of Middle Pleistocene hominids. Particularly important, the recovery of substantial new postcranial remains will allow a much more balanced assessment of human evolution in the region.

The Boxgrove tibia (Roberts *et al* 1994) provides a glimpse of the physique of the earliest known inhabitants of Europe, and suggests that both height and size were large, although it is not yet known whether body proportions were closer to those of warm-adapted Plio-Pleistocene African hominids assigned to *Homo erectus* or '*Homo ergaster*' than to Late Pleistocene Neanderthals. However, on the slender (perhaps an inappropriate word!) evidence available so far, limb bone biomechanical strength (and body weight?) may have been at its peak in these early Middle Pleistocene populations. Probably much later in time, the abundant Atapuerca fossils will permit an examination of the transition to an early Neanderthal morphology. If, as some evidence now suggests, hominids were adapting to colder environments well before OIS 6, changes in body proportions should be documented in the postcranial evidence long before such changes were evident in the late Neanderthals.

The taxonomy of the Middle Pleistocene hominids of Europe has not yet been clarified by the plethora of new discoveries, as they have not been described and interpreted in detail. Nevertheless, it is evident that in the later Middle Pleistocene, Europe is recording the early stages of Neanderthal evolution. How far back that evolution can be traced depends on how certain fossils are dated and interpreted. Initial indications that the Atapuerca 'Sima' sample was stratified below a speleothem dated by Uranium series to about 300kyr has proved mistaken, and further dating work is in progress. Whether this material will eventually prove to be no older than the stage 7 age fossils from Ehringsdorf and Pontnewydd, which it resembles, remains to be seen. These do provide clear and early evidence of specific Neanderthal features in the dentitions, and in the occipital region of Ehringsdorf 9. However, the dating and classification of the Swanscombe hominid remains a problem, for its Neanderthal-like occipital morphology would be exceptional as far back as a stage 11 age interglacial (*c* 400kyr), and would imply at least approximate contemporaneity with the decidedly more archaic Bilzingsleben fragments. Either Middle Pleistocene European human evolution was more complicated than is generally believed, with extreme polymorphism or even contemporaneity of distinct grades or even species, or Neanderthal-like specimens such as Swanscombe and Atapuerca cranium 5 derive from later in the Middle Pleistocene than has been indicated by recent dating work. If the latter possibility proves correct, then it would still be possible to argue for an *in situ* evolution or replacement event switching from a pre-Neanderthal stage to a clear early Neanderthal one. The earlier Middle Pleistocene hominids, combining *erectus* plesiomorphies with synapomorphies found in *Homo sapiens* and *Homo neanderthalensis* could then be confirmed as *Homo heidelbergensis*, with a primitive form of *neanderthalensis* succeeding this species in the late Middle Pleistocene.

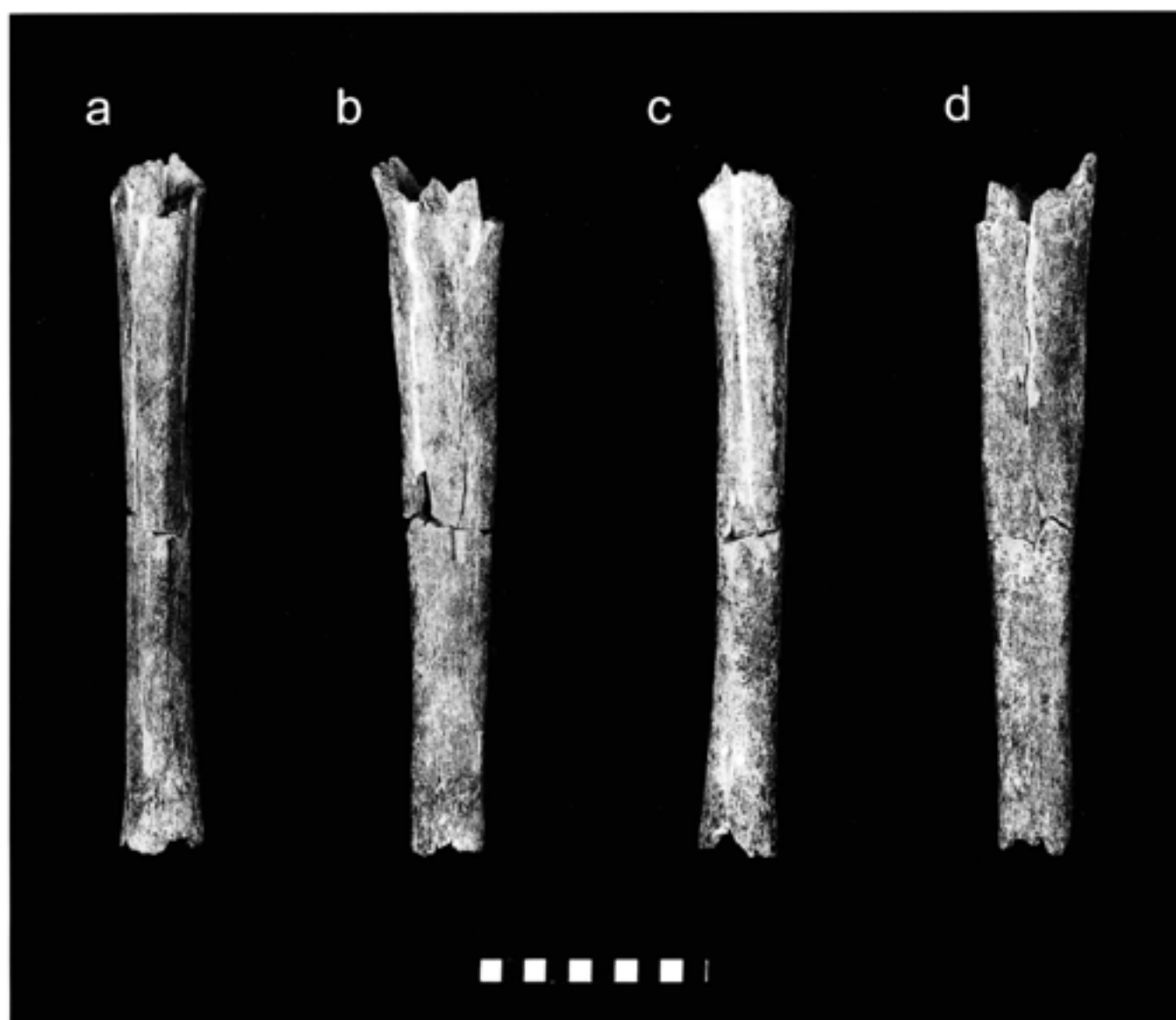


Fig 339 The hominid tibia from Q1/B, showing a) anterior, b) medial, c) posterior, d) lateral; scale unit 10mm, e) mid-shaft cross-section; scale unit 1mm

6.7 The human tibia from Boxgrove

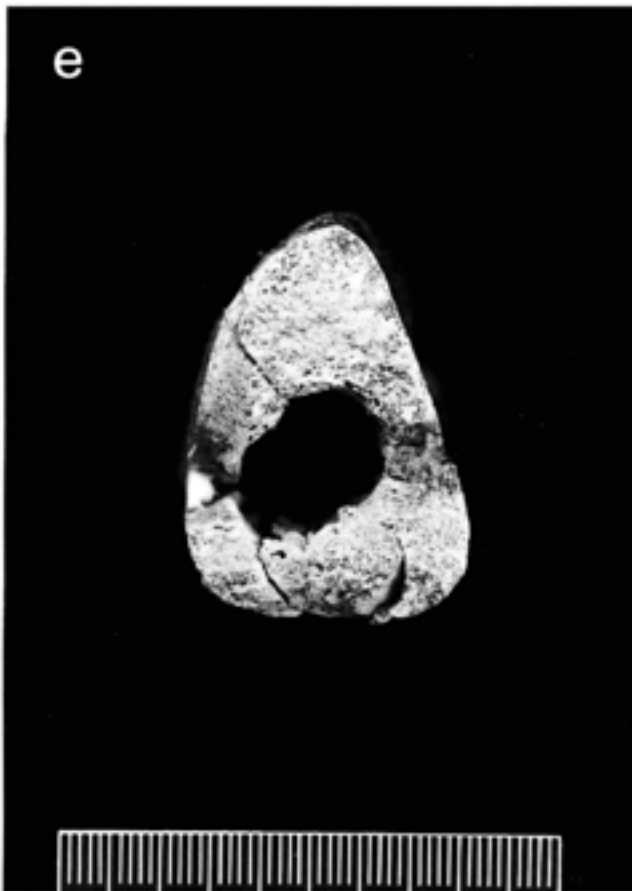
C B Stringer and E Trinkaus

Introduction

The preservation and morphology of the Boxgrove human tibia is briefly described, and comparative measurements are provided for fossil and recent human samples. The large transverse and circumferential dimensions of the diaphysis place the Boxgrove tibia near or beyond the limit of the ranges of the comparative samples (Table 142). Disagreement about the taxonomy of Middle Pleistocene hominids and lack of comparable fossil material makes a specific assignment for the Boxgrove tibia problematic, and the two authors of this paper themselves take different views on hominid taxonomy, and the validity of species such as

H. heidelbergensis and *H. neanderthalensis*. The tibia can only definitely be assigned to *Homo* sp with possible affinities to either *H. heidelbergensis* (Schoetensack 1908), *H. erectus* (Dubois 1892), *H. neanderthalensis*, (King 1864), or *H. sapiens* (Linnaeus 1758).

The discovery of the Boxgrove human tibia in December 1993 is described elsewhere (Roberts *et al* 1994), as is the nature of the existing Middle Pleistocene fossil record in Europe (Stringer Chapter 6.6). As the latter review indicates, there are a number of problems which prevent a satisfactory integration of the existing fossil material of the European early hominid record. One is the continuing uncertainty about the timing of the earliest human colonisation of Europe and the concomitant debate about which hominid specie(s) was actually first present there, a debate which seemingly cannot be resolved at present from the disparate nature of the relevant fossils and their morphology. The type specimen of *H. heidelbergensis*



(Schoetensack 1908) is a mandible, without associated calvarial or postcranial material, and the most complete cranium which is often allocated to that species, from Petralona, lacks a mandible and associated postcrania. The best preserved and most appropriate tibial comparisons for Boxgrove are the uncertainly dated Sambungmachan and Ngandong specimens from Indonesia (*Homo erectus?*), the Broken Hill tibia from Zambia (probably associated with the E.686 cranium, but both only of assumed Middle Pleistocene age), and the unpublished Altamura and Atapuerca 'Simade los Huesos' tibiae of presumed later Middle Pleistocene age, and possible early Neanderthal affinities. Only an indirect link between the Boxgrove tibia and cranial or mandibular specimens attributed to *H. heidelbergensis* can thus be made, based on common high levels of skeletal robusticity and assumed or actual chronology (the latter a poor substitute for shared morphological characters). Thus no definitive taxonomic allocation beyond *Homo sp* can yet be made for the tibia, but the taxonomic usage employed here will follow the multiple species attribution preferred by CBS.

Preservation and morphology

Before reassembly, the left tibia consisted of four major proximal portions, and two distal. The proximal and distal segments were separated by a clean transverse

break, close to the midshaft. The first fragment of the proximal half contains the anterior crest with the anterior half of the lateral surface and the anterior third of the medial surface, and the second fragment is from the mid-medial section. The third fragment is from the posterior-medial corner, with the nutrient foramen and the soleal line, and the fourth fragment is lateral to the postero-lateral piece, containing the flexor line and buttress, and the interosseus line. Two smaller proximal pieces were also preserved, including a medio-anterior flake at the distal break, which is being used for a histomorphometric analysis of bone turnover patterns and an estimate of age at death. The distal half consisted of two pieces, medial and lateral, with a clean break down the mid-posterior surface, and a clean break medial of the anterior crest at midshaft going to full anterior at the distal break.

The fragments were assembled in the Natural History Museum Palaeontology Laboratory, by L. Cornish, into complete proximal and distal segments (Fig 339a–e). The proximal pieces were aligned to continue distal contours across the midshaft break. This resulted in small gaps of 1–2mm between pieces of the shaft at the proximal end, and some cracks (posterior and postero-medial) were filled with plaster to stabilise the reconstruction. The distal pieces had clean joins for reassembly. Where present, the external surface is in excellent condition. The internal surface is well preserved in the distal half. However, in the proximal half, a fair amount of bone is absent endosteally along breaks, resulting in open wedge-shaped gaps along the proximal endosteal surface. Nevertheless, enough of the endosteal contour is present to fill in satisfactorily across the gaps.

On the anterior surface of the proximal half (Fig 339a), the distal end of the tibial tuberosity is present. On the posterior surface (Fig 339c), there is a full and broad soleal line and a prominent flexor crest, which crosses a plaster-filled break to meet the soleal line. On the postero-medial surface (Fig 339b), there is a large and clear nutrient foramen and the proximal part is thinning and starting to flare posteriorly for the epiphysis, with increasing trabeculae. The distal half has its angles all clearly present, but there is little in the way of proximo-distal landmarks. There is a hint of the beginning of the medial flare for the proximal end of the medial malleolus, the anterior crest has flattened to a rounded profile and the lateral-posterior crest is starting to curve back to the mid-lateral surface, almost to the rugosity of the attachment for the distal tibio-fibular ligament.

The anterior crest is very straight with only a suggestion of a lateral concavity (Fig 339a). It is rounded medio-laterally and continues distally with only a hint of an anterior angle until it flattens out completely near the minimum circumference. Anterior of the Interosseus Crest, the antero-lateral surface is convex anteriorly, and passes onto a rounded anterior crest (Fig 339d). It is mostly flat on the lateral side and is

Table 142 Boxgrove and comparative tibia dimensions. Boxgrove midshaft measurements taken immediately below the transverse break. Comparative data from Endo and Kimura (1970), Day and Leakey (1974), Trinkaus (1983), Baba *et al* (1990), Arsuaga *et al* (1991), Hartwig-Scherer (1993), Nelson (1995), and this study

<i>hominid</i>	<i>site/specimen</i>	<i>midshaft circumference</i>	<i>midshaft antero-posterior diameter</i>	<i>midshaft medio-lateral diameter</i>	<i>distal minimum circumference</i>
<i>H. erectus</i>	KNM-ER803	80	28.6	20	71
	Zhoukoudian	78	27	21	–
	Ngandong	82–102 (n=2)	29.7–38 (2)	22.1–27.2 (2)	82 (1)
	Sambungmachan	86	32	21.2	76
<i>H. cf heidelbergensis</i>	Broken Hill E.691	91.5	34	24	80
	Boxgrove	105	39.5	30	96.5
<i>H. cf neanderthalensis</i>	Atapuerca	76–80 (n=2)	27.6–29.3 (2)	20–22.5 (2)	67–84 (2)
<i>H. neanderthalensis</i>	Neanderthal	75–98 (n=12)	27–38.4 (13)	20–25.8 (13)	70–87 (4)
<i>H. sapiens</i>	Upper Palaeolithic	74–100 (n=6)	27–39 (6)	17–24 (6)	62–89 (7)
	Spanish medieval	69.5–101.3 (n=23)	19.5–34.3 (100)	17–30 (100)	53–83 (99)

slightly depressed near the interosseus line. However, this may well be the product of a postmortem break, and alignment problems during reassembly. The area remains smooth and flat distally, until it becomes rounder antero-laterally for the distal epiphysis.

There is essentially no change in bone surface morphology for the interosseus line, once allowance for reconstruction is made. Proximally it is noticeable at the level of the distal tuberosity. It meets the postero-lateral corner at the midshaft, and then becomes imperceptible distally (Fig 339d). The soleal line is broad and roughened, extending from the proximal capsule to the medial side (Fig 339c). It remains similar in breadth across most of its middle section, and forms a raised, rugose area, producing only a slight change in the bone contour across the posterior diaphysis. It is unclear how much of a flexor line (between the *M tibialis posterior* and *M flexor digitorum longus* origins) exists because of damage, but the flexor crest (or buttress) is very prominent (Fig 339c), and it is positioned more to the lateral side of the diaphysis. When the bone surface resumes distal of the midshaft break, there is no trace of the flexor line/crest. The posterior shaft is dominated proximally by the soleal line and the flexor crest, and the nutrient foramen is located on the postero-medial corner of the proximal shaft, medial to the soleal line (Fig 339c). The whole of the medial surface is gently convex proximally to the anterior crest, and maintains this as it goes distally.

Comparative data

Measurements of the Boxgrove diaphysis and other fossil and recent samples are provided in Table 142, and indicate the large cross-sectional and circumferential size of the fossil. The large midshaft circumference was used to estimate a body weight of more than 80kg, using Hartwig-Scherer's modern human data (Roberts *et al* 1994) but work is in progress to provide a more

precise estimate, using computed tomography (C-T) generated cross-sectional data. A conservative estimate of articular length of more than 355mm was also provided in Roberts *et al* (1994), and work in progress (by ET) provides a best estimate of about 375mm for this, and 400mm for maximum length, providing (male) stature estimates of *c* 1.77–1.82m (5'10"–6'0"). The Boxgrove estimate is exceeded only among known archaic hominids by African examples (KNM-WT 15000, Broken Hill E-691 and Berg Aukas), although the Amud 1 Near Eastern Neanderthal at *c* 1.79m overlaps the lower estimate for Boxgrove. These estimates therefore place Boxgrove within the range of male African archaic hominids and at the upper end of the known Neanderthal range.

Concluding remarks

The Boxgrove fossil tibia is a relatively well-preserved fragment of most of the left diaphysis. Its large dimensions clearly reflect the very strong build and large body size of this early European individual. However, a clearer understanding of the behavioural basis for this robust physique will only emerge from a wider study of Boxgrove and other postcranial material, and we are as yet unable to provide a definitive taxonomic designation for this important fossil.

6.8 Concluding remarks and discussion

M B Roberts

Just over half a million years ago the first hominid colonisers entered the land mass known as the British Isles. At this time Britain was a peninsula of continental Europe rather than an island; linked to north-east France by the Cretaceous chalk of the Weald-Artois anticline, the sea now known as the English Channel

was closed at its eastern end. The area of this landbridge is unknown but its presence is confirmed by the sedimentological analyses of Collcutt (Chapter 2.3) and by recent multidisciplinary work on 'Island Britain' (Preece 1995). The initial breaching of this landbridge is thought to have occurred during the Anglian Glaciation (Table 5), as the result of meltwater from the North Sea ice sheet combining with the main drainage confluence of the Rhine, Meuse and Baltic Rivers (Gibbard 1988; 1995). At Boxgrove these cold stage events are approximately time equivalent with the deposition of the gravel suites of the Earham Upper Gravel Member (Table 8).

The place of origin of the early colonisers, whether directly from Africa or a pre-existing foothold in Europe, is unknown but it appears that the occupation of northern and western Europe (Roebroeks and van Kolfschoten 1995b) took place very quickly during the interglacial period beginning 524kyr bp (Imbrie *et al* 1984). Sites (Fig 1b) appear in France at Abbeville (Tuffreau 1992), in Germany at Kärlich and Miesenheim (van Kolfschoten and Turner 1996), in Italy at Isernia (Peretto 1994), and in Spain at Atapuerca (Aguirre 1991; Aguirre *et al* 1987; 1990; Carbonell *et al* 1995a): the oldest layers with evidence for human occupation at this site, may date back into the Early Pleistocene (Carbonell *et al* 1995b). There may have been earlier, sporadic, occupation of the Mediterranean coast, especially in southern Spain (Gibert *et al* 1995), although this remains to be conclusively proven. It is a possibility that colonisation may have also come from eastern and/or central Europe, especially in the light of recent estimates for the age of Dmanisi in the Caucasus (Gabunia and Vekua 1995) and Korolevo in the Ukraine (Gladiline and Sitlivi 1991). A demographic expansion from this direction may have been fed from Asia and the far east, as there is now evidence of occupation in these areas back to 2myr bp (Swisher *et al* 1994; Wood and Turner 1995). In support of an additional colonisation from the east is the fact that early assemblages in eastern and central Europe do not contain handaxes (Mania 1995; Svoboda 1987; Valoch 1995), unlike early sites in western Europe. The handaxe is a tool form that does not appear outside Africa until around 500kyr bp.

It has been argued that as the lithic assemblages of the earliest occupants of northern France and the United Kingdom are dominated by handaxes, then the source area for the European hominids was from the Levant and Africa, where handaxes were in use from *c.* 1.5myr bp, more so as handaxes appear later in the archaeological record of Asia and central and eastern Europe. Whilst this hypothesis is persuasive, it must be remembered that handaxe manufacture is very much determined by raw material sources (White 1995) and caution must be exercised in using tool types as source fossils. Another potential solution to the question of European hominid origins may come from the study of the hominid fossils themselves. Stringer (Chapter 6.6) sees the European

Middle Pleistocene hominid *Homo heidelbergensis* as having African origins, and the species is thought to have evolved from the African lineage of *Homo erectus*. Unfortunately, the paucity of hominid remains in Europe from this crucial early period means that the exact relationship between such spatially diverse groups is a long way from being resolved.

On the current evidence, it would appear that hominids moved into Europe from Africa in large numbers around half a million years ago (Fig 1b). The reasons for this movement into Europe are largely speculative. It has been suggested that the climate and hence the palaeoenvironments of central and north-west Europe were potentially hostile to hominids from the Levant and eastern and north Africa, although there is no corresponding response visible, for example, as changes in material culture, unless the proposed dates for the earliest sites are accepted. There is, however, a gradual morphological change in the hominids which culminates in the classic Neanderthal anatomy, seen in Europe during the Late Pleistocene. Schick and Toth (1993) have argued that one reason for the lack of Acheulean material in the earliest European sites, and especially those around the Mediterranean and southern Europe, may be due to the poor communicative capabilities and geographical knowledge of these early communities. The changes encountered in climatic and environmental regimes, together with fragile network communications, led to a state where the Acheulean level of technological competence was isolated and eventually lost. This hypothesis, although valid, is considered dubious. At the sites of Isernia, Orce, and Atapuerca suitable raw material was present for the production of handaxes; at the latter site these tools occur higher up the sequence in younger deposits. With the exception of plant resources, it is difficult to envisage major differences between the palaeoenvironments at early European sites and potential source area for colonisation such as the Levant. Although the climate in Europe fluctuates, it is possible, by avoiding extreme environments like mountain ranges and dense Taiga forest, to subsist within relatively stable environmental niches for twelve months in most parts of western Europe. It should also be noted that prey animals suffer less seasonal stress in temperate latitudes and maintain relatively consistent levels of body fat throughout the year (R North personal communication). Extremes of climate, notwithstanding major glacial-interglacial cycles, are rarer in the temperate zone and accordingly catastrophic events affecting plant and animal resources are minimal. When the main colonising thrust begins at around 500kyr bp, the hominids reach Britain and Germany at the latest before the mid point of the interglacial, i.e. within 15kyr, suggesting fairly rapid movement across the continent. In both France and Britain the earliest assemblages contain handaxes.

Another hypothesis for the late colonisation of Europe has been proposed by Turner (1992). In brief, it revolves around the composition of the European

carnivore guilds. Prior to 500kyr bp there was a more diverse carnivore fauna in Europe, especially in terms of complete carcass processors like the large hyaenas. After 500kyr, probably during the stage 12 glacial period, after many extinctions (ibid), the European faunas became more African in their general trophic structure. This development it is argued, made more carcasses available for hominid exploitation. This model may, however, simply be reversed; the decline of the large carnivores could be directly related to the colonisation of Europe by hominids, who reduced the available carcasses by being in direct competition with other carnivores. The evidence from Boxgrove (Parfitt and Roberts Chapter 6.5) supports the latter hypothesis. Butchery at the site indicates that hominids had first access to prey animals, with cut marks under any, rare, gnawing marks and complete carcasses being secured. Where individual body parts, for example heads, are examined, again human primacy is shown by the fact that the eyes and other soft perishables were present. The Boxgrove butchered faunal remains suggest that prey animals were hunted rather than scavenged; although scavenging is not dismissed as a food procurement strategy. Thus, it is considered that throughout the Early and Middle Pleistocene there were no obstacles to hominids entering and thriving in Europe, the paucity of early sites and the late colonisation of Europe are more likely the result of the fact that there was no pressure for large scale population movement from Africa and the Levant until 500kyr bp. The colonist expansion out of Africa was therefore probably the result of internal factors, either climatic or demographic or a combination of both.

Upon arrival in Britain hominids dispersed widely (Roberts *et al* 1995, fig 1). Pre-Anglian sites are found in the west at Westbury-sub-Mendip in Somerset and Kent's Cavern in Devon. In south-east England the only site definitely associated with this period is Boxgrove, although Red Barns at Portsdown is another possibility (ApSimon *et al* 1977; Gamble and ApSimon 1986). The most northerly site is at Waverley Wood in Leicestershire, with other sites located in East Anglia at High Lodge, Warren Hill and, further to the south, at Wivenhoe (Roberts *et al* 1995). It is possible that other sites exist or existed outside this area but glacial activity removed many early Middle Pleistocene sediments to the north and west. The handaxes from Waverley Wood are a possible indicator of activity outside the area delimited by the above mentioned sites. If the raw material for these tools was not collected from diamicts from an earlier glaciation, then they must have come from a source up to 200km from the site. The English sites from this period contain both handaxe and flake tool assemblages. Both variability within handaxe morphology and absence of handaxes are interpreted as being determined by raw material availability at sites such as Kent's Cavern and Westbury. At High Lodge, the flake and scraper industry is thought to be a specialised area of tool making or

plant processing rather than the manifestation of a separate cultural group. Handaxes that date from the same period are found both near the site and at Warren Hill, so the possibility of the assemblages being distinct responses to groups living in open and closed (wooded) parts of the landscape (Mithen 1994) is negated.

It is most likely that the hominids at Boxgrove would have travelled along the coastal plains or littoral zones to reach the Boxgrove area. The coastline, from east to west, would have been virtually continuously backed by chalk cliffs, from the landbridge to the mouth of the Solent River. Access to the interior would have been through the numerous river valleys flowing into the Channel. It is considered likely that these same valleys and the developing coastal plain, provided movement corridors for the large herds of game that were present at the time. Evidence for the occupation of the Boxgrove area is first seen during the fully marine phase, in the beach gravels of Marine Cycle 1, and in the sands of Marine Cycle 2 (Colcutt Chapter 2.3, Roberts Chapter 6.3), when the sea was coming directly into the coast (ie not obstructed by offshore landforms or other features). It should be noted that the archaeology in this part of the Slindon Formation represents only the earliest recorded finds; occupation may have occurred earlier in the interglacial but the sediments that potentially contained artefacts were reworked by the prograding coastline of the marine transgression. In the subsequent major temperate stage, OIS 11, evidence for hominid presence is found at the transition between the cold and temperate stages at Swanscombe and Clacton. These assemblages may be interpreted in two ways; either hominids survived in the locality throughout the Anglian cold stage or they recolonised old niches very quickly, upon climatic amelioration of biotopes close to refugia areas. As the Boxgrove interglacial/Cromerian IV saw the first occupation of this part of Europe it remains, at present, largely conjectural exactly when in the interglacial colonisation began. Given the evidence from OIS 11, later in the Middle Pleistocene, it is considered most likely to have taken place at the beginning, perhaps within the first five thousand years, of the interglacial, although concrete evidence for this timing is still required. Evidence for occupation at Boxgrove during the marine phase is limited to occasional flint flakes, handaxes, and butchered red deer limb bones from GTP 13. As the archaeology in the sands has not been rolled, it was most likely discarded by people walking across the flats at low tide. Although the lithics are similar to those in the higher units, the immediate palaeoenvironment would have been very different. Most noticeably the intertidal zone would have been diurnally flooded and vegetation cover, apart from seaweed, minimal. The cliffs were almost certainly used as a source of raw material; rolled lithics are found in the beach levels at Boxgrove (Roberts Chapter 6.3) and at Slindon (Calkin 1934) and freshwater run-off from the Downs and via springs, ie Q1/B, would have attracted

game and provided drinking water. Gradually, the open shore face gave way to a gentler depositional regime of lagoonal mudflats and it is within these units that the first landsurface containing *in situ* archaeology is found. The vast expanse of mud flats in front of the cliff, supported a limited vegetation cover but probably saw a greater density of mammal activity. In Quarry 1 there were large numbers of wildfowl associated with shallow freshwater and euryhaline lakes that were present at this time. Butchered bones (Parfitt and Roberts Chapter 6.5) and flint scatters at Q1/A, Q1/B, and GTP 17 attest to the activity of hominids at this level. The sites mentioned above indicate periodic drying out of a landsurface within the silts of very short duration, probably less than a year. The mudflats of the Slindon Silts subsequently developed into a large grassy plain as the sea regressed and marine influence on the sedimentary regime was lost. A soil developed on the surface of the silts, which remained open for between 20 and 100 years. Excavation has shown that this surface was extensively used by hominids, and indeed over 90% of all the test pits and areas opened at Boxgrove have had some archaeology, normally in the form of lithics, at this level.

The grassland and the forest cover of the Downland block, supported a varied fauna (Table 26), many larger elements of which were eaten by the hominids. At both the silt and soil levels, large carcasses were fully processed, from skinning down to marrow extraction. Unfortunately, it appears that other facets of hominid behaviour are unlikely to be found on these surfaces in front of the cliff. All the evidence suggests that in these environments the primary aim of hominids was meat procurement. Evidence for other food gathering activities, such as collection of molluscs and vegetable matter is absent. Also absent are areas for further working of skins and other organic material. The technology for these activities certainly existed in the form of various scrapers, but the recovery densities at Boxgrove are so low that it is most likely that they were used elsewhere. The lack of any campsites, sleeping areas or activity areas apart from butchery sites suggests that the hominids probably lived away from the coastal plain and up in the Downland forest, although the possibility must be entertained that the range of these hominids was greater than presently envisaged, and that their 'home bases' were further away from the site, perhaps in the valley of the River Arun. The indications of human activity found at Boxgrove, such as hunting, task sharing, food sharing, curation, and using tools to make tools, indicate cooperative and complex behaviour. The evidence suggests that Middle Pleistocene hominids had the capability to exploit a wide range of environments; a point evinced at Boxgrove, where in a confined geographical area there existed a mosaic of different landscapes, environments and ecosystems, all of which contain evidence of hominid activity. Further evidence of the adaptability of these Middle Pleistocene hominids is to be found in the cold stage sediments of the Eartham Formation. Lithics are

found in cold climate gravels, near to the cliff, in the chalk pellet gravels (Macphail Chapter 2.6), and in the gravels and fine deposits of the mass movement deposits. Some of these assemblages are interpreted as being contemporary with the deposition of these units (Roberts Chapter 6.3) and thus demonstrate the presence of hominids well into the cold stage.

The reconstruction of palaeolandscapes, palaeoenvironments and climatic variation through the geological sequence at Boxgrove, thus providing a secure context for the archaeology, was the primary aim of the first stage of work at Boxgrove and is presented here. Although there are problems applying chronometric dating techniques, and that there exists a clear split in the relative dating between mammalian biostratigraphy and aminostratigraphy and coccolith assemblage zones, there is on the whole a high level of agreement between disciplines engaged in the various aspects of reconstruction work at Boxgrove. The unresolved discrepancies; such as the presence of interglacial woodland mollusc species in the basal deposits of the Eartham Upper Gravel Member, the relationship of freshwater deposits at Q1/B to the standard sequence and the commencement, nature and duration of the change from warm to cold stage, will be addressed during the next period of research work.

At this stage of the project's research we can piece together at least some of the activities of the Boxgrove hominids. From these insights it is clear that we are looking at a species that had already achieved primacy among the Middle Pleistocene fauna group. Elements of planning depth, cooperation, and technology, often assumed to be restricted to modern humans, are already within the behavioural repertoire of these hominids. Combining these elements with their large physique (Stringer Chapter 6.6, Stringer and Trinkhaus Chapter 6.7), the Boxgrove hominids would have cut formidable figures in the landscape.

Subsequent to the fieldwork and research described in this monograph, further fieldwork was undertaken at Boxgrove between 1989 and 1991 to sample a large area of the Unit 4c landsurface; the analysis of data generated by this project has been recently published (Roberts *et al* 1997). During late 1991 and 1992 a test pitting programme was undertaken in advance of further mineral extraction at the eastern edge of Quarry 1 and the western margin of Quarry 2. The results of this work, the Eartham Quarry Project, are being written up at the time of going to press. In 1993 geological work in Q1/B (Fig 4) resulted in the discovery of a hominid tibia and a new complex of freshwater and marine sediments containing dense lithic and faunal material. This discovery led to a further sixteen months of fieldwork in 1995 and 1996. The writing up of this fieldwork has been combined with that from the Eartham Quarry Project and is ongoing at the time of publication. It is envisaged that analysis and writing up of this work for the second Boxgrove monograph will be completed in the summer of 2000 (Roberts *et al* in prep).

The aims of the analysis and research involved in the production of the second monograph are to move away from the framework building and descriptive background approach of this monograph, as these goals have been largely achieved, towards a more detailed analysis of the activities of the Boxgrove hominids and their relationships with the changing palaeogeography and palaeoenvironments of the region. This approach will involve establishing the technical and environmental parameters for hominids operating during the Middle Pleistocene, together with determining the social organisation and behavioural repertoire of the Boxgrove hominids. To achieve these aims the Project will need to understand fully the site formation processes that have produced the unique sedimentary sequences and archaeological remains at area Q1/B and the western (Q1) test pits of the Earham Quarry Project and assess their relationship with the standard stratigraphy published here. The conclusion of the next phase of work will entail placing

the site at Boxgrove in a wider palaeogeographical, environmental and chronological context. From this base it will be possible to examine and apply the Boxgrove data in the wider context of research into the archaeology and hominid populations of the Middle Pleistocene.

The long term future of the site at Boxgrove is currently (1997/98) under review but already the northern end of Quarry 2, containing the type sections of GTP 25 and GTP 13, and the archaeological area, GTP 17, has been declared a site of special scientific interest (SSSI). All parts of the quarry complex containing the conformable sequence are no longer under threat from mineral extraction: the excavated areas have been backfilled and are awaiting further landscaping and low level restoration. The restoration schemes were drawn up by the author (MBR) and the quarry company ARC to ensure that the remaining intact landsurfaces are left undisturbed and safely buried for future generations of scientists and students to study.

Appendices

Appendix 1 Charcoal

C R Cartwright

The paucity of charcoal and other charred plant remains at Boxgrove limits the potential for evaluation of the vegetational and climatic history of the site. Only seven tiny charcoal fragments could be identified (out of eight). These fragments were recovered by excavation.

Area	Unit	Species	
Q2/B	4c	<i>Betula</i> sp (birch)	2 fragments
Q1/A	4b	<i>Pinus</i> sp (pine)	5 fragments

Interpretation is further complicated by the fact that the sandy soils of Boxgrove may be a determining local factor which influenced dominant vegetation whilst regional or national climatic trends may have had secondary influence. As the full vegetational spectrum is not available at Boxgrove for evaluation, the presence of birch and pine cannot necessarily be assumed to represent dominance of either of the taxa in the two contexts cited. Pine is common on well drained sandy soils (Stace 1991). In Scottish Highland *Pinus sylvestris*-*Hylocomium splendens* woodland communities today, birch is noted as the most common companion (Rodwell 1991). Although this example may serve for examination of possible associations of vegetation within communities currently being studied, birch and pine can also be traced as components of a variety of mixed deciduous woodlands of the south-east, including those with a maritime facies. Furthermore, the presence of birch and pine within climatically distinguishable phases associated with the development of flint industries of Britain needs to be recognised. There is no doubt that more charcoal from Boxgrove would greatly assist in palaeoecological reconstruction.

Appendix 2 Dinoflagellate cyst analysis

R Harland

Introduction

This analysis was undertaken to assist in the palaeoenvironmental reconstruction of the site at Boxgrove, and conditions of deposition of the associated sediments.

Table 143. Samples for dinoflagellate analysis from GTP 13

sample no	collect no	lithology	depth (mm)	result
RH63	427	Slindon Silt	200-300	-
RH64	428	Slindon Sand	900-1000	-
RH65	429	Slindon Sand	2200-2300	-
RH66	430	Slindon Sand	3000-3400	-
RH67	431	Slindon Sand	4100-4200	-

Five sediment samples were submitted for analysis to check for the occurrence of dinoflagellate cysts. The samples were taken from the Slindon Silts and the Slindon Sands at Q2/GTP 13 (Fig 4, Table 143), and were processed in the palynological laboratories at the Natural History Museum prior to analysis.

Results

Unfortunately, all the dinoflagellate cysts observed were broken, derived and probably reworked from the chalk. In particular, samples RH65 and RH66 appeared to have rather higher numbers of reworked cysts than the other samples. All the samples, however, did contain reworked dinoflagellate cysts. Cysts that were observed included some marginate and chorate species, including those that could probably be included in the genera *Arcoligera*, *Cyclonephelium*, *Ellipsodinium*, *Spiniferites*, and *Systematophora*.

In addition, many samples contained bisaccate gymnospermous pollen, especially those from higher in the sequence. Also noted were some angiosperm pollen, tracheids, and dark organic material. Many of the samples contained undigested mineral matter.

The results confirm the notion that the sediments of the Slindon Formation are largely derived from the Cretaceous Chalk. It is, however, unfortunate that indigenous dinoflagellate cysts are not present and therefore cannot be used to assist in palaeoenvironmental or climatic analysis of the sediment, let alone in age determination. It is suspected that the environment was perhaps too marginal marine in its position, and possibly slightly too coarse in its clastics to yield a reasonable indigenous dinoflagellate cyst assemblage.

Appendix 3 The Slindon Formation

M B Roberts

Description of the Slindon Formation: littoral, intertidal and near-shore marine sediments of proposed late Cromerian Complex age from the Upper Coastal Plain of West Sussex

Named and defined by: Roberts, M B, this volume. Roberts, M B and Parfitt, S A, 1999 *A Middle Pleistocene hominid site at Eartham Quarry, Boxgrove, West Sussex*. London: English Heritage Monograph Series No 17.

See also: Roberts, M B, Stringer, C B, and Parfitt, S A, 1994 A hominid tibia from Middle Pleistocene sediments at Boxgrove, UK, *Nature* **369**, 311–13

Roberts, M B, Parfitt, S A, Pope, M I, and Wenban Smith, F F, 1997 Boxgrove, West Sussex: Rescue excavations of a Lower Palaeolithic landsurface (Boxgrove Project B 1989–1991). *Proceedings of the Prehistoric Society*, **63**, 303–58

Shephard-Thorn, E R, Berry, F G, and Wyatt, R J, 1982 *Geological notes and local details for 1:10000 sheets SU80NW, NE, SW and SE, SU90 NW, NE, SW and SE, TQ00NW, SW*. West Sussex Coastal Plain between Chichester and Littlehampton. Keyworth: Institute of Geological Sciences

Named from: The village of Slindon in West Sussex, 8km east-north-east of Chichester.

Holostratotype locality: ARC Eartham Quarry in the parish of Boxgrove, West Sussex, 5km east-north-east of Chichester. Between grid references SU 917 086 and SU 925 086. Latitude 50° 52' N.

Definition: The Slindon Formation is composed of littoral, intertidal, and near-shore marine sediments; a thin layer (<0.2m) of terrestrial sediments comprising a palaeosol and organic bed are present at and on the surface of the Slindon Silt Member. Three members are recognised: the Slindon Gravel Member, which is composed of flint and, to a lesser degree, chalk cobbles, and chalk blocks, the Slindon Sand Member, which forms the largest part of the formation, and the Slindon Silt Member, which marks marine regression and the onset of terrestrial sedimentation on the exposed marine landsurface.

Holostratotype section: Geological Test Pit (GTP) 13 in Quarry 2 at ARC Eartham Quarry, SU 925 0862. GTP 13 is 15m wide (east-west) and contains all the members of the Slindon Formation. The section is located c 60m south of the cliff line. The Slindon Formation is overlain at this section by the sediments of the Eartham Upper Gravel Member. Parastratotype sections: GTP 25 in Quarry 2 SU 9245 068 contains the full range of littoral deposits from the junction with the cliff to 20m to the south. GTP 26 in Quarry 1 SU 9164 0867 shows another section through the Slindon Formation c 50m south of the buried cliff line. GTP 13 and 25 are part of the geological SSSI in Quarry 2.

Boundaries: Base – The Slindon Formation rests upon the Upper Cretaceous Chalk of the Campanian Stage. Top – The upper surface of the Slindon Formation is overlain by sediments of the Eartham Formation. Near to the buried cliff line (GTP 25) these are sediments of the Eartham Lower Gravel Member, further away from the cliff the upper beds of the Slindon Formation are overlain by sediments of the Eartham Upper Gravel Member (GTP 13).

Additional information: A detailed description of the sediments of the Slindon Formation is given by Colcutt, Chapter 2.3. Colcutt has divided the Slindon Sand Member into informal intra-unit subdivisions based upon rises and falls in sea level; these are described as Marine Cycles 1–3. The Slindon Silt Member has been subdivided into two units, 4 and 5a. Unit 4 is split into three subunits 4a, 4b, and 4c.

Regional extent: Sediments of the Slindon Formation have been mapped and sampled between the Valdoe Quarry, Goodwood SU 876 085 and, West Stubbs Copse Pit, Slindon SU 978 078. In the area of the holostratotype site they extend up to 1km south of the buried cliff line; however, the complete/conformable sequence extends only 250m south of the cliff. It is considered likely that the sediments of this Formation extend westwards to the eastern flank of the Portsdown Anticline and eastwards, at least as far as the River Arun.

Geological age: The three members of the Slindon Formation were laid down during a single temperate stage or interglacial towards the end of early Middle Pleistocene. Mammalian biostratigraphy, based upon the taxonomic composition of the Boxgrove fauna, together with correlation between other European sites suggests that the sediments were laid down at the end of the Cromerian Complex, most likely in Stage Cromerian IV. No lithological evidence in the form of superposition of strata exists to support this biostratigraphical age estimate.

A formal definition of the Eartham Formation will be given in the next Boxgrove Monograph (Roberts *et al* in prep), after analysis of the gravel suites in Quarry 1 by S G Lewis.

Bibliography

- Adams, A E, MacKenzie, W S, and Guilford, C, 1984 *Atlas of sedimentary rocks under the microscope*, New York
- Agassiz, L, 1840a *Etudes sur les glaciers*, Neuchâtel
- , 1840b On glaciers, and the evidence of their having once existed in Scotland, Ireland and England, *Proc Geol Soc London*, **3**, 327–32
- Aguirre, E, 1991 Les premiers peuplements humains de la Péninsule Ibérique, in *Les premiers Européens* (eds E Bonifay and B Vandermeersch), Paris
- Aguirre, E, and Hoyos, M, 1992 Climate record in cave deposits: the Atapuerca TD case, in *Start of a glacial* (eds G J Kukla and E Went), NATO ASI Series, Vol 13, 127–36, Berlin
- Aguirre, E, Arsuaga, J-L, Bermúdez de Castro, J M, Carbonell, E, Ceballos, M, Díez, J C, Enamorado, J, Fernández-Jalvo, Y, Gil, E, Martín-Nájera, A, Martínez, I, Rosas, A, Sánchez, A, Sánchez, B, Sesé, C, and Soto, E, 1987 Occupations humaines au Pléistocène Moyen dans la Sierra d'Atapuerca (Ibeas, Burgos, Espagne), *L'Anthropologie*, **91**, 29–44
- Aguirre, E, Arsuaga, J-L, Bermúdez de Castro, J M, Carbonell, E, Ceballos, M, Díez, J C, Enamorado, J, Fernández-Jalvo, Y, Gil, E, Gracia, A, Martín-Nájera, A, Martínez, I, Morales, J, Ortega, A I, Rosas, A, Sánchez, A, Sánchez, B, Sesé, C, Soto, E, and Torres, T J, 1990 The Atapuerca sites and the Ibeas hominids, *Hum Evol*, **5**, 55–73
- Aitken, M J, 1985 *Thermoluminescence dating*, London
- , 1990 *Science-based dating in archaeology*, London
- , 1995 Chronometric techniques for the Middle Pleistocene, in *The earliest occupation of Europe* (eds W Roebroeks and T van Kolfschoten), 269–77, Leiden
- Allen, L G, and Gibbard, P L, 1993 Pleistocene evolution of the Solent River of southern England, *Quat Sci Rev*, **12**, 503–28
- Allen, P, 1960 Strand-line pebbles in the mid-Hastings Beds and the geology of the London Uplands, general features: Jurassic pebbles, *Proc Geol Assoc*, **71**, 156–68
- , 1961 Strand-line pebbles in the mid-Hastings Beds and the geology of the London Uplands: Carboniferous pebbles, *Proc Geol Assoc*, **72**, 271–85
- Allen, P, Cheshire, D A, and Whiteman, C A, 1991 Glacial deposits in southern East Anglia, in *Glacial deposits in Great Britain and Ireland* (eds J Ehlers, P L Gibbard, and J Rose), 455–69, Rotterdam
- Alvey, N G *et al*, 1983 Genstat, a general statistical programme. Harpenden, Rothamsted Experimental Station
- Andrews, C W, 1920 Remains of the great auk and ptarmigan in the Channel Islands, *Ann Mag Nat Hist*, **6**(2), 166
- Andrews, H, 1930 On some fossil mammals of western Suffolk, *Trans Suffolk Nat Soc*, **1**, 195–9
- Andrews, P, 1990 *Owls, caves and fossils*, London
- Andrews, P, and Cook, J, 1985 Natural modifications to bones in a temperate setting, *Man*, **20**, 675–91
- Andrews, P, Cook, J, Carrant, A, and Stringer, C, in press. *The Pleistocene cave at Westbury-sub-Mendip, Somerset*, London
- Anon, 1968 High Lodge Palaeolithic industry, *Nature*, **220**, 1065–6
- , 1984 *Sand and gravel mobility in relation to offshore dredging. A radioactive tracer study in the Shipwash Channel of the Suffolk coast*, Hydraulics Research Report No EX1176
- ApSimon, A M, Gamble, C S, and Shackley, M L, 1977 Pleistocene raised beaches on Ports Down, Hampshire, *Proc Hampshire Fld Club Archaeol Soc*, **33**, 17–32
- Arnold-Bemrose, H H, and Newton, E T, 1905 On an ossiferous cavern of Pleistocene age at Hoc Grange Quarry, Longcliffe, near Brassington (Derbyshire), *Q J Geol Soc Lond*, **61**, 43–63
- Arnold, E N, and Burton, J A, 1978 *A field guide to the reptiles and amphibians of Britain and Europe*, London
- Arzuaga, J-L, Carretero, J M, Martínez, I, and Gracia, A, 1991 Cranial remains and long bones from Atapuerca/Ibeas (Spain), *J Hum Evol*, **20**, 191–230
- Arzuaga, J-L, Martínez, I, Gracia, A, Carretero, J-M, and Carbonell, E, 1993 Three new human skulls from the Sima de los Huesos Middle Pleistocene site in Sierra de Atapuerca, Spain, *Nature*, **362**, 534–7
- Ascenzi, A, Biddittu, I, Cassoli, P F, Segre, A G, and Segre-Naldini, E, 1996 A calvarium of late *Homo erectus* from Ceprano, Italy, *J Hum Evol*, **31**(5), 409–23
- Ashton, N M, 1992 The High Lodge flint industries, in Ashton *et al* 1992a, 124–63
- Ashton, N M, and David, A (eds), 1994 *Stories in stone*, London
- Ashton, N M, and Lewis, S G, in prep Excavations at Elveden 1997, *Proc Suffolk Inst Archaeol and Hist*
- Ashton, N M, and McNabb, J, 1992 The interpretation and context of the High Lodge industries, in Ashton *et al* 1992a, 164–8
- Ashton, N M, and McNabb, J, 1994 Bifaces in perspective, in Ashton and David 1994, 182–91
- Ashton, N M, Dean, P, and McNabb, J, 1991 Flaked flakes: what, where, when and why? *Lithics*, **12**, 1–11
- Ashton, N M, Cook, J, Lewis, S G, and Rose, J (eds), 1992a *High Lodge: excavations by G de G Sieveking 1962–68 and J Cook 1988*, London
- Ashton, N M, McNabb, J, and Parfitt, S A, 1992b Choppers and the Clactonian: a reinvestigation, *Proc Prehist Soc*, **58**, 21–8
- Ashton, N M, Bowen, D Q, Holman, J A, Hunt, C O, Irving, B G, Kemp, R A, Lewis, S G, McNabb, J, Parfitt, S A, and Seddon, M B, 1994a Excavation at the Lower Palaeolithic site at East Farm Barnham, Suffolk: 1989–1992, *J Geol Soc*, **151**, 599–605
- Ashton, N, McNabb, J, Irving, B, Lewis, S, and Parfitt, S, 1994b Contemporaneity of Clactonian and Acheulian flint industries at Barnham, Suffolk, *Antiquity*, **68** (260), 585–9
- Aspinall, A, and Walker, A R, 1975 The earth resistivity instrument and its application to shallow earth surveys, *Underground Services*, **3**, 12–15
- Athersuch, J, Horne, D J, and Whittaker, J E, 1989 Marine and brackish water ostracods, in *Synopsis of the British Fauna* (new ser), **43** (eds D M Kermack and R S K Barnes) (for Linn Soc, London, and the Estuarine and Brackish-water Sciences Assoc), London
- Austin, L, 1994 The life and death of a Boxgrove biface, in Ashton and David 1994, 119–26
- Avery, B W, 1980 *Soil classification for England and Wales*, Soil Survey Technical Monograph, **14**, Harpenden
- , 1990 *Soils of the British Isles*, Wallingford
- Avery, B W, and Bascomb, C L (eds), 1974 *Soil survey laboratory methods*, Soil Survey Technical Monograph, **6**, Harpenden

- Avery, B W, Stephen, I, Brown, G, and Yaalon, D H, 1959 The origin and development of Brown Earths on Clay-with-Flints and Coombe Deposits, *J Soil Sci*, **10**, 177-95
- Avery, B W, Bullock, P, Catt, J A, Rayner, J H, and Weir, A H, 1982 Composition and origin of some brickearths on the Chiltern Hills, England, *Catena*, **9**, 153-74
- Azzaroli, A, 1989 The genus *Equus* in Europe, in *European Neogene mammal chronology* (eds E H Lindsay, V Fahlbusch, and P Mein), 339-56, New York
- , 1991 Ascent and decline of the monodactyl equids: a case of prehistoric overkill, *Annls Zool Fenn*, **28**(3-4), 151-163
- Baales, M, 1992 Accumulation of bones of *Lagopus* in Late Pleistocene sediments. Are they caused by man or animals? *Cranium*, **9**(1), 17-22
- Baba, H, Aziz, F, and Watanabe, N, 1990 Morphology of the fossil hominid tibia from Sambungmacan, Java, *Bull Natn Sci Mus, Tokyo, Series D* **16**, 9-18
- Babel, U, 1975 Micromorphology of soil organic matter, in *Soil Components, Volume 1: organic components* (ed J E Geiseking), 369-473, New York
- Bacher, A, 1967 Vergleichend morphologische Untersuchungen an Einzelknochen des postkranialen Skeletts in Mitteleuropa vorkommender Schwäne und Gänse. München: Dissertation. Institut für Paläoanatomie
- Backman, J, and Shackleton, N J, 1983 Quantitative biochronology of Pliocene and Early Pleistocene calcareous nannofossils from the Atlantic, Indian and Pacific oceans, *Mar Micropaleont*, **8**, 141-70
- Bal, L, 1982 *Zoological ripening of soils*, Wageningen
- Barker, R D, 1981 The offset method of electrical resistivity sounding and its use with a multicore cable, *Geophysical Prospecting*, **29**, 67-79
- Barker, R D, and Harker, D, 1984 The location of the Stour buried tunnel-valley using geophysical techniques, *Quart J Engng Geol*, **17**, 103-15
- Barker, R D, and Worthington, P F, 1972 Location of disused mineshafts by geophysical methods, *Civil Engineering and Public Works Review*, **67**(788), 275-6
- Barton, R N E, 1992 *Hengistbury Head, Dorset, Volume 2: the Late Upper Palaeolithic and Early Mesolithic sites*, Oxford University Committee for Archaeology, Monograph **34**, Oxford
- Bascomb, C L, 1961 A calcimeter for routine use on soil samples, *Chemistry in Industry*, 1826-7
- Bassinot, F C, Labeyrie, L C, Vincent, E, Quidelleur, X, Shackleton, N J, and Lancelot, Y, 1994 The astronomical theory of climate and the age of the Brunhes-Matuyama reversal, *Earth Planet Sci Lett*, **126**, 91-108
- Bate, D M A, 1916 *Aves*, in *The site, fauna and industry of La Cotte de St Brelade, Jersey* (R R Marett), *Archaeologia*, **67**, 75-118
- , 1928 The animal remains, in *Excavations of a Mousterian rock-shelter at Devil's Tower, Gibraltar* (D A E Garrod, L M D Buxton, G Elliot-Smith, and D M A Bate), *J Roy Anthropol Inst Gr Brit Ire*, **58**, 33-115
- Bates, M R, 1986 Molluscan analysis, in Roberts 1986, 231-2
- Bates, M R, and Roberts, M B, 1986 Geology and geomorphology, in Roberts 1986, 216-22
- Bates, M R, Parfitt, S A, and Roberts, M B, 1997 The chronology, palaeoecology and archaeological significance of the marine Quaternary record of the West Sussex Coastal Plain, Southern England, UK, *Quat Sci Reviews*, **16**(10), 1227-52
- Bates, M R, Gibbard, P L, Macphail, R I, Owen, F J, Parfitt, S A, Preece, R C, Roberts, M B, Robinson, J E, and Wilkinson, K N, in press Late Middle Pleistocene deposits at Norton Farm on the West Sussex coastal plain, southern England, *J Quat Sci*
- Beckman, G G, and Smith, K J, 1974 Micromorphological changes in surface soils following wetting, drying and trampling, in *Soil microscopy* (ed G K Rutherford), 832-45, Ontario
- Bell, M, Fowler, P J, and Hillson, S W, 1996 *The experimental earthworks project 1960-1992*, CBA Res Rep, **100**, York
- Bengston, S-A, 1984 Breeding ecology and extinction of the great Auk (*Pinguinus impennis*): anecdotal evidence and conjectures, *The Auk* **101**(1), 1-12
- Bennett, M R, Doyle, P, Mather, A E, and Woodfin, J L, 1994 Testing the climatic significance of dropstones: an example from southeast Spain, *Geol Mag*, **131**, 845-8
- Berger, G W, 1988 Dating Quaternary events by luminescence, in *Dating Quaternary sediments* (ed D J Easterbrook), Geological Society of America Special Paper, **227**, 13-50
- Bergman, C A, 1986 Refitting of the flint assemblages, in Roberts 1986, 235-6
- Bergman, C A, and Roberts, M B, 1988 Flaking technology at the Acheulean site of Boxgrove, West Sussex (England), *Revue archéologique de Picardie*, **1-2** (numéro spécial), 105-13
- Bergman, C A, Roberts, M B, Colcutt, S N, and Barlow, P, 1990 Refitting and spatial analysis of artefacts from Quarry 2 at the Middle Pleistocene Acheulean site of Boxgrove, West Sussex, England, in *The big puzzle* (eds E Ciesla, S Eickhoff, N Arts, and D Winter), 265-82, Bonn
- Bermúdez de Castro, J M, 1993 The Atapuerca dental remains. New evidence (1987-1991 excavations) and interpretations, *J Hum Evol*, **24**, 339-71
- Biberson, P J, 1977 Le Villafranchien du nord de l'Afrique, *G Geol, Series iia*, **41**, 225-41
- Bickart, K J, 1984 A field experiment in avian taphonomy, *J Paleont*, **4**(4), 525-35
- Binford, L R, 1978 *Nunamiut ethnoarchaeology*, New York
- , 1981 *Bones: ancient men and modern myths*, New York
- , 1983 *In pursuit of the past: decoding the archaeological record*, London
- , 1989 *Debating archaeology*, San Diego
- Binford, L R, Mills, M G L, and Stone, N M, 1988 Hyena scavenging behavior and its implications for the interpretation of faunal assemblages from FLK 22 (Zinj Floor) at Olduvai Gorge, *J Anthropol Res*, **7**, 99-135
- Bishop, M J, 1975 Earliest record of man's presence in Britain, *Nature*, **253**, 95-7
- , 1976 Notes on the mammalian remains from Amey's Earham Pit, Boxgrove, unpubl report, 3pp
- , 1982 The mammal fauna of the early Middle Pleistocene cavern infill site of Westbury-sub-Mendip, Somerset, *Spec Pap Palaeont Assoc*, **28**, 1-108
- Björdal, H, 1988 Metrical and mechanical properties of some skeletal elements from the house sparrow, *Passer domesticus*, a contribution to the understanding of zooarchaeological problems, *Ossa*, **13**, 49-59
- Blackwell, B, and Schwarcz, H, 1986 U-series analyses of the lower travertine at Ehringsdorf, DDR, *Quat Res*, **25**, 215-22

- Blanc, G A, 1928 Sulla presenza di *Alca impennis* Linn nella formazione pleistocenica superiore di Grotta Romanelli in Terra Otranto, *Archivio Archivio Per l'Anthropologia e l'Ethnologia*, **58**, 155-86
- Blumenschine, R J, 1986 *Early hominid scavenging opportunities*, BAR Int Ser, **283**, Oxford
- Blumenschine, R J, and Selvaggio, M M, 1988 Percussion marks on bone surfaces as a new diagnostic of hominid behaviour, *Nature*, **333**, 763-5
- Boatman, A R C, Bryant, R H, Markham, R A D, Turner, C, and White, P C S, 1973 Walton on the Naze, in *Quaternary Research Association field meeting guide*, Clacton (eds J Rose and C Turner), 21-9, London
- Bochenski, Z M, Tomek, T, Boev, Z, and Mitev, I, 1993 Patterns of bird bone fragmentation in pellets of tawny owl (*Strix aluco*) and the eagle owl (*Bubo bubo*) and their taphonomic implications, *Acta Zool Cracov*, **36**(2), 313-28
- Bogaard van den, C, Bogaard van den, P, and Schminke, H-U, 1989 Quartärgeologisch-tephrostratigraphische Neuaufnahme und Interpretation des Pleistozänprofils Kärlich, *Eiszeitalter und Gegenwart*, **39**, 62-86
- Böhme, G, 1977 Zur Bestimmung quartärer Anuren Europas an Hand von Skelettelementen, *Wiss Z Humboldt-Universität Berlin, Mathematik-Naturwissenschaft*, **26**, 283-300
- Bonifay, M F, 1971 Carnivores quaternaires du sud-est de la France, *Mém Mus Natn Hist Nat Paris*, NSC **21**, 43-377
- Bonifay, E, and Vandermeersch, B (eds), 1991 *Les Premiers Européens*, Paris
- Bonneau, M, and Souchier, B, 1982 *Constituents and properties of soils*, London
- Bordes, F, 1947 Etude comparative des différentes techniques de taille du silex et des roches dures, *L'Anthropologie*, **51**, 1-29
- , 1948 Les couches moustériennes du gisement du Moustier (Dordogne): typologie et techniques de taille, *Bull Soc Préhist Fr*, **45**, 113-25
- , 1961 *Typologie du Paléolithique ancien et moyen*, Mémoire 1-2, l'Institut de Préhistoire de Université de Bordeaux
- , 1968 *Le Paléolithique dans le monde*, Série: L'Univers des connaissances, Paris
- , 1974 Percuteur en bois de renne du Solutrén supérieur de Laugerie-Haute Ouest, in *Premier colloque internationale sur l'industrie de l'os dans la préhistoire* (ed H Camps-Fabrer), 97-100, University of Provence
- , 1984 *Leçons sur le Paléolithique. Tome II Le Paléolithique en Europe*, Cahiers du Quaternaire 7, Paris
- Bordes, F, and Thibault, C, 1977 Thoughts on the initial adaptation of hominids to European glacial climates, *Quat Res*, **8**, 115-27
- Bosinski, G, Brunnacker, K, Lanser, K P, Stephan, S, Urban, B, and Würges, K, 1980 Altpaläolithische Fünde von Kärlich, Kreis Mayen-Koblenz (Neuwieder Becken), *Archäologisches Korrespondenzblatt*, **10**, 295-314
- Boucher de Perthes, M, 1859 Antiquités antédiluviennes. Réponse à MM les antiquaires et géologues présents aux assises archéologiques de Laon, *Bulletin de la Société Antiquaires de Picardie*, **2**, Amiens
- Bouma, J, Fox, C A, and Miedema, R, 1990 Micromorphology of hydromorphic soils: application for soil genesis and land evaluation, in *Soil micromorphology: a basic and applied science* (ed L Douglas), *Developments in Soil Science*, **19**, 257-78, Amsterdam
- Bowen, D Q, 1978 *Quaternary geology: a stratigraphic framework for multidisciplinary work*, Oxford
- , 1989 The last interglacial-glacial cycle in the British Isles, *Quat Int*, **34**, 41-7
- , 1991 Amino acid geochronology, in *Central East Anglia and the Fen Basin: field guide* (eds S G Lewis, C A Whiteman, and D R Bridgland), 21-4, London
- , 1992 Aminostratigraphy of non-marine Pleistocene mollusca in southern Britain, *Sver Geol Unders Afh*, **81**, 65-7
- Bowen, D Q, and Sykes, G A, 1988 Correlation of marine events and glaciations on the north-east Atlantic margin, *Phil Trans R Soc London*, **B318**, 619-35
- Bowen, D Q, and Sykes, G A, 1994 How old is 'Boxgrove man'? *Nature*, **371**, 751
- Bowen, D Q, Sykes, G A, Reeves, A, Miller, G H, Andrews, G T, Brew, J S, and Hare, P E, 1985 Amino acid geochronology of raised beaches in southwest Britain, *Quat Sci Rev*, **4**, 279-318
- Bowen, D Q, Rose, J, McCabe, A M, and Sutherland, D G, 1986 Correlation of Quaternary glaciations in England, Scotland and Wales, in *Quaternary glaciations in the Northern Hemisphere* (eds V Šibrava, D Q Bowen, and G M Richmond), Report of the International Geological Correlation Programme Project 24, *Quat Sci Rev*, **5**, 293-8
- Bowen, D Q, Hughes, S, Sykes, G A, and Miller, G H, 1989 Land-sea correlations in the Pleistocene based on isoleucine epimerization in non-marine molluscs, *Nature*, **340**, 49-51
- Bradley, B, and Sampson, C G, 1978 Artifacts from the Cottages Site, in *Paleoecology and archaeology of an Acheulian site at Caddington, England* (ed C G Sampson), 83-137, Dallas
- Bradley, B, and Sampson, C G, 1986 Analysis by replication of two Acheulian artefact assemblages from Caddington, England, in *Stone Age prehistory: studies in memory of Charles McBurney* (eds G N Bailey and P Callow), 29-46, Cambridge
- Brady, G S, Crosskey, H W, and Robertson, D, 1874 *A monograph of the post-Tertiary Entomostraca of Scotland (including species from England and Ireland)*, London
- Brain, C K, 1983 *The hunters or the hunted? An introduction to African cave taphonomy*, Chicago
- Bramwell, D, 1978 The fossil birds of Derbyshire, in *Birds of Derbyshire* (R A Frost), 160-3, Buxton
- , 1984 The birds of Britain: when did they arrive? in *In the shadow of extinction: a Quaternary archaeology and palaeoecology of the lake, fissures and smaller caves at Crestwell Crags SSSI* (eds R D S Jenkinson and D D Gilbertson), 89-99, Sheffield
- Breuil, H, 1932 Les industries à éclats du Paléolithique Ancien, *Préhistoire Paris*, **1**, 125-90
- , 1939 The Pleistocene succession in the Thames Valley, *Proc Prehist Soc*, **5**, 33-8
- , 1945 The discovery of the antiquity of man, *J R Anthropol Inst*, **75**, 21-31
- Bridgland, D R, 1983 *The Quaternary fluvial deposits of north Kent and eastern Essex*, unpubl PhD thesis, City of London Polytechnic
- , 1986a The rudaceous components of the East Essex Gravels; their characteristics and provenance, *Quaternary Studies*, **2**, 34-44
- , 1986b *Clast lithological analysis. Technical Guide 3*, Cambridge
- , 1988 The Pleistocene fluvial stratigraphy and palaeogeography of Essex, *Proc Geol Assoc*, **99**, 291-314

- , 1990a The recognition and distinction of flint and chert in the analysis of clasts from Pleistocene gravel in south-east England, *Cahiers du Quaternaire No 17 — Le Silex de sa genèse à l'outil. Actes du Vème Colloque international sur le silex, 1990*, 119–30
- , 1990b Lithological composition and morphology of the gravel clasts, in *The Pleistocene sea-level and neotectonic history of the eastern Solent, southern England* (R C Preece, J D Scourse, S D Houghton, K L Knudsen, and D N Penny), *Phil Trans R Soc London*, **B328**, 440–1
- , 1994 *Quaternary of the Thames*, London
- , 1996 Quaternary river terrace deposits as a framework for the Lower Palaeolithic record, in *The English Palaeolithic reviewed* (eds C G Gamble and A Lawson), 23–39, Salisbury
- Bridgland, D R, and Harding, P, 1993 Middle Pleistocene Thames terrace deposits at Globe Pit, Little Thurrock, and their contained Clactonian industry, *Proc Geol Assoc*, **104**, 263–83
- Bridgland, D R, and Lewis, S G, 1991 Introduction to the Pleistocene geology and drainage of the Lark Valley, in *Central East Anglia and the Fen Basin: field guide* (eds S G Lewis, C A Whiteman, and D R Bridgland), 37–44, London
- Bridgland, D R, and D'Olier, B, 1995 The Pleistocene evolution of the Thames and Rhine drainage systems in the southern North Sea basin, in Preece 1995, 27–46
- Bridgland, D R, Gibbard, P L, Harding, P, Kemp, R A, and Southgate, G, 1985 New information and results from recent excavations at Barnfield Pit, Swanscombe, *Quaternary News*, **46**, 25–39
- Bridgland, D R, Allen, P, Currant, A P, Gibbard, P L, Lister, A M, Preece, R C, Robinson, J E, Stuart A J, and Sutcliffe, A J, 1988 Report of the Geologists' Association field meeting in north-east Essex, May 22nd–24th, 1987, *Proc Geol Assoc*, **99**, 315–33
- Bridgland, D R, Keen, D H, and Maddy, D, 1989 The Avon Terraces: Crophorne, Ailstone and Eckington, in *West Midlands: field guide* (ed D H Keen), 51–67, Cambridge
- Bridgland, D R, Gibbard, P L, and Preece, R C, 1990 The geology and significance of the interglacial sediments at Little Oakley, Essex, *Phil Trans R Soc London*, **B328**, 307–39
- Bridgland, D R, Davey, N D W, and Keen, D H, 1991 Northam Pit, Eye, near Peterborough, in *Central East Anglia and the Fen Basin: field guide* (eds S G Lewis, C A Whiteman, and D R Bridgland), 173–83, Cambridge
- Bridgland, D R, Keen, D H, Green, C P, Bowen, D Q, and Sykes, G A, 1995a Last Interglacial deposits at Folkestone, Kent, *Proc Geol Assoc*, **106**, 183–93
- Bridgland, D R, Lewis, S G, and Wymer, J J, 1995b Middle Pleistocene stratigraphy and archaeology around Mildenhall and Icklingham, Suffolk: report on the Geologists' Association Field Meeting, 27th June, 1992, *Proc Geol Assoc*, **106**, 57–69
- Bridgland, D R, Field, M H, Holmes, J A, McNabb, J, Preece, R C, Selby, I, Wymer, J J, Boreham, S, Irving, B G, Parfitt, S A, and Stuart, A J, in press Middle Pleistocene Interglacial Thames-Medway deposits at Clacton-on-Sea, England; reconsideration of the biostratigraphical and environmental context of the type Clactonian Palaeolithic industry, *Quat Sci Rev*
- Bristow, C R, Mortimore, R N, and Wood, C J, in press Lithostratigraphy for mapping the Chalk of southern England, *Proc Geol Assoc*
- British Geological Survey, 1996 *Chichester and Bognor. England and Wales Sheet 317/332. Solid and Drift Geology. 1:50,000*, Nottingham
- Bromley, R G, 1990 *Trace fossils: biology and taphonomy*, London
- Brown, J, 1837 Observations upon the boulders of trap rocks etc, which occur in the diluvium of Essex, *Ann Mag Nat Hist, Series 2*, **1**, 145–50
- , 1840 Notice of a fluvio-marine deposit containing mammalian-remains occurring in the parish of Little Clacton on the Essex coast, *Ann Mag Nat Hist, Series 2*, **4**, 197–201
- Browne, S, 1983 Investigations into the evidence for post-cranial variation in *Bos primigenius* (Bojanus) in England and the problem of differentiation from *Bison priscus* (Bojanus), *Inst Archaeol Bull*, **20**, 1–42
- Brunnacker, K, Boenigk, W, Koči, A, and Tillmans, W, 1976 Die Matuyama/Brunhes-Grenze am Rhein und an der Donau, *Neues Jb Geol Paläont Abh*, **151**, 358–78
- Bullock, P, and Loveland, P J, 1982 Mineralogical analyses, in *Soil survey laboratory methods* (eds B W Avery and C L Bascomb), 57–69, Soil Survey Technical Monograph, **6**, Harpenden
- Bullock, P, and Murphy, C P, 1979 Evolution of a palaeo-argillic brown earth (Paleudalf) from Oxfordshire, England, *Geoderma*, **22**, 225–52
- Bullock, P, Fedoroff, N, Jongerius, A, Stoops, G, and Tursina, T, 1985 *Handbook for soil thin section description*, Wolverhampton.
- Bunn, H T, 1981 Archaeological evidence for meat-eating by Plio-Pleistocene hominids from Koobi-Fora and Olduvai Gorge, Tanzania, *Nature*, **299**, 574–7
- , 1983 Comparative analysis of modern bone assemblages from a San hunter-gatherer camp on the Kalahari Desert, Botswana, and a spotted hyaena den near Nairobi, Kenya, in *Animals and archaeology 1, hunters and their prey* (eds J Clutton-Brock and C Grigson), BAR Int Ser, **163**, 143–8, Oxford
- Calkin, J B, 1934 Implements from the Higher Raised Beaches of Sussex. *Proc Prehist Soc E Anglia*, **7**, 333–47
- Callow, P, and Cornford, J M (eds), 1986 *La Cotte de St Brelade 1961–1978: excavations by C B M McBurney*, Norwich
- Campbell, J B, and Sampson, C G, 1971 A new analysis of Kent's Cavern, Devonshire, England, *University of Oregon Anthropological Papers*, **3**
- Carbonell, E, and Rodriguez, X P, 1994 Early Middle Pleistocene deposits and artefacts in the Gran Dolina site (TD4) of the 'Sierra de Atapuerca' (Burgos, Spain), *J Hum Evol*, **26**, 291–311
- Carbonell, E, Bermúdez de Castro, J M, Arsuaga, J I, Diez, J C, Rosas, A, Cuenca-Bescós, G, Sala, R, Mosquera, M, and Rodriguez, X P, 1995a Lower Pleistocene hominids and artefacts from Atapuerca-TD6 (Spain), *Science*, **269**, 826–30
- Carbonell, E, Mosquera, M, Rodriguez, X P, and Sala, R, 1995b The first human settlement of Europe, *J Anthropol Res*, **51**, 107–14
- Carreck, J N, and Adams, S J, 1969 Field extraction and laboratory preparation of fossilised bones and teeth using expanded polyurethane, *Proc Geol Assoc*, **80**, 81–9
- Carroll, R, 1988 *Vertebrate paleontology and evolution*, New York
- Catt, J A, 1986 *Soils and Quaternary geology in Britain. Monographs on Soil and Resources Survey*, **11**, Oxford

- Catt, J A (ed), 1990 Paleopedology manual, *Quat Int*, **6**, 1-95
- Catt, J A, and Hagen, R E, 1978 Geological background, in *Paleoecology and archeology of an Acheulian site at Caddington, England* (ed C G Sampson), 17-28, Dallas
- Catt, J A, and Hodgson, J M, 1976 Soils and geomorphology of the chalk in south-east England, *Earth Surface Processes*, **1**, 181-93
- Chaline, J, 1972 *Les Rougeurs du Pléistocène moyen et supérieur de France (Systématique, biostratigraphie, paléoclimatologie)*. Cahiers de Paléontologie, Paris
- Chaline, J, Brunet-Lecomte, P, Kaikusalo, A, Martin, F, and Brochet, G, 1988 Discrimination de la morphologie dentaire de *Lemmus lemmus* et *Myopus schisticolor* (Arvicolidae, Rodentia) par l'analyse multivariée, *Mammalia*, **52**(2), 259-73
- Chaline, J, Brunet-Lecomte, P, Martin, F, 1989 Les lemmings fossiles du genre *Lemmus* (Arvicolidae, Rodentia) dans le Pléistocène de France, *Geobios*, **22**(5), 613-23
- Champion, D E, Lanphere, M A, and Kuntz, M A, 1988 Evidence for a new geomagnetic reversal from lava flows in Idaho: discussion of short polarity reversals in the Brunhes and late Matuyama polarity chrons, *J Geophys Res*, **93**, 11,667-80
- Chapman, F, 1900 The Raised Beach and Rubble Drift between Hove and Portslade-by-Sea, Sussex, *Proc Geol Assoc*, **16**, 259-70
- Chase, P G, 1990 Tool-making tools and Middle Paleolithic behaviour, *Curr Anthropol*, **31**(4), 443-7
- Clark, A J, Turling, D H, and Noël, M, 1988 Developments in archaeomagnetic dating in Britain, *J Archaeol Sci*, **15**, 645-67
- Clark, J E, 1984 *Another look at small debitage and microdebitage*, unpubl mss
- Codrington, T, 1870 On the superficial deposits of the south of Hampshire at the Isle of Wight, *Quart J Geol Soc Lond*, **26**, 528-50
- Conway, B W, and Waechter, J d'A, 1977 Lower Thames and Medway valleys — Barnfield Pit, Swanscombe, England, in *South East England and the Thames Valley*. (eds E R Shephard-Thorn and J J Wymer), 38-44, Norwich
- Conway, B W, McNabb, J, and Ashton, N M, 1996 *Excavations at Barnfield Pit, Swanscombe, 1968-72*, London
- Cook, J, Ashton, N M, Coope, G R, Hunt, C O, Lewis, S G, and Rose, J, 1991 High Lodge, Mildenhall, Suffolk (TL 739754), in *Central East Anglia and the Fen Basin: field guide* (eds S G Lewis, C A Whiteman, and D R Bridgland), 21-4, London
- Cooke, A S, and Scorgie, H R A, 1983 The status of the commoner amphibians and reptiles in Britain, *Focus on Nature Conservation No 3*, Huntingdon
- Coope, G R, 1993 Coleoptera, in Shotton *et al* 1993, 304-15
- Corbet, G B, 1986 Relationships and origin of the European lagomorphs, *Mammal Rev*, **16**(3/4), 105-10
- Cordy, J M, 1982 Biozonation du Quaternaire post-Villafranchien continental d'Europe occidentale à partir des grands mammifères, *Annls Soc Géol Belg*, **105**, 303-14
- Coulson, S D, 1990 *Middle Palaeolithic industries of Great Britain, Studies in modern archaeology*, Vol 4, Bonn
- Courty, M A, Goldberg, P, and Macphail, R I, 1989 *Soils, micromorphology and archaeology*, Cambridge
- Courty, M A, Marlin C, Dever, L, Tremblay, P, and Vachier, P, 1994 The properties, genesis and environmental significance of calcitic pendants from the High Arctic (Spitsbergen), *Geoderma*, **61**, 71-102
- Coutard, J P, and Mûcher, H J, 1985 Deformation of laminated silt loam due to repeated freezing and thawing cycles, *Earth Surface Processes and Landforms*, **10**, 309-19
- Coutier, L, 1929 Expériences de taille pour rechercher les anciennes techniques paléolithiques, *Bull Soc Préhist Fr*, **26**, 172-4
- Coxon, P, 1979 Pleistocene environmental history in Central East Anglia, unpubl PhD thesis, Univ Cambridge
- Crabtree, D E, 1967 Notes on experiments in flintknapping: 4 — tools used for making flaked stone artefacts, *Tébita*, **10**(1), 60-73
- , 1970 Flaking stone with wooden implements, *Science*, **169**, 146-53
- Crader, D C, 1983 Recent single-carcass bone scatters and the problem of 'butchery' sites in the archaeological record, in *Animals and archaeology 1, hunters and their prey* (eds J Clutton-Brock and C Grigson), BAR Int Ser, **163**, Oxford, 107-42
- Cramp, S, 1985 *Handbook of the birds of Europe, the Middle East and North Africa: the birds of the western Palaearctic, Vol 4: terns to woodpeckers*, Oxford
- Cramp, S, and Perrins, C, 1994 *Handbook of the birds of Europe, the Middle East and North Africa: the birds of the western Palaearctic, Vol 8: crows to finches*, Oxford
- Cramp, S, and Simmons, K E L, 1977 *Handbook of the birds of Europe, the Middle East and North Africa: the birds of the western Palaearctic, Vol 1: ostrich to ducks*, Oxford
- Cramp, S, and Simmons, K E L, 1980 *Handbook of the birds of Europe, the Middle East and North Africa: the birds of the western Palaearctic, Vol 2: hawks to bustards*, Oxford
- Cramp, S, and Simmons, K E L, 1983 *Handbook of the birds of Europe, the Middle East and North Africa: the birds of the western Palaearctic, Vol 3: waders to gulls*, Oxford
- Crowther, J, Macphail, R I, and Cruise, G M, 1996 Short-term, post-burial change in a humic rendzina. Overton Down Experimental Earthwork, Wiltshire, *Geoarchaeology*, **11**(2), 95-117
- Currant, A P, 1986 Interim report on the small mammal remains, in Roberts 1986, 229-31
- , 1987 Late Pleistocene Saiga Antelope *Saiga tartarica* on Mendip, *Proc Univ Bristol Spelaeol Soc*, **18**(1), 74-80
- , 1989 The Quaternary origins of the the modern British mammal fauna, *Biol J Linn Soc*, **38**, 23-30
- Curwen, E, 1925 Palaeolith from raised beach in Sussex, *Antiqs J*, **5**, 72-3
- , 1946 A hand-axe from the Chichester Gravels, *Proc Prehist Soc*, **12**, 172-3
- Cziesla, E, 1990 On refitting of stone artefacts, in *The big puzzle* (eds E Cziesla, S Eickhoff, N Arts, and D Winter), 9-44, Bonn
- Dalrymple, J B, 1957 The Pleistocene Deposits of Penfold's Pit, Slindon, Sussex, and their chronology, *Proc Geol Assoc*, **68**, 294-303
- Day, M H, and Leakey, R E F, 1974 New evidence of the genus *Homo* from East Rudolf, Kenya (III), *Am J Phys Anthropol*, **41**, 367-80
- Dean, D, Hublin, J-J, Ziegler, R, and Holloway, R, 1994 The Middle Pleistocene pre-neandertal partial skull from Reilingen (Germany), *Am J Phys Anthropol*, Supplement **18**, 77
- Dehm, R, 1962 Altpleistozäne Säuger von Schernfeld bei Eichstätt in Bayern, *Mitt bayer staatslg Paläont hist Geol*, **2**, 17-61

- Delfino, V P, and Vacca, E, 1994 Report of an archaic human skeleton discovered at Altamura (Bari), in the 'Lamalunga' district, *Hum Evol*, **9**, 1-9
- Dewey, H, 1919 Palaeolithic flint implements from high level terraces of Thames Valley, *Geol Mag*, **6**(2), 49-57
- Dines, H G, Hollingsworth, S E, Edwards, W, Buchan, S, and Welch, F B A, 1940 The mapping of Head Deposits, *Geol Mag*, **77**, 198-226
- Dines, H G, Holmes, S C A, and Robb, J A, 1954 Geology of the country around Chatham, *Mem Geol Surv UK*
- Dixon, F, 1850 *The geography and fossils of the Tertiary and Cretaceous formations of Sussex*, London
- Dobney, K, and Rielly, K, 1988 A method for recording archaeological animal bones: the use of diagnostic zones, *Circaea*, **5**(2), 79-96
- Donaldson, A C, Martin, R H, and Kanes, W H, 1970 Holocene Guadalupe delta of Texas Gulf Coast, in *Deltaic sedimentation: modern and ancient* (ed R P Morgan), Society, Economic Palaeontologists and Mineralogists, Special Publication, **15**, 107-16
- Donard, E, 1981 *Oryctolagus cuniculus* dans quelques gisements Quaternaires Française, *Quaternaria*, **23**, 145-57
- von den Driesch, A, 1976 *A guide to the measurement of animal bones from archaeological sites*, Peabody Museum Bulletin **1**, Harvard
- Dubois, E, 1892 Bivoegsel tot de Javasche Conrart, *Verslag van het Minjntwezen*, Batavia, 3rd quarter, 10-14
- Duchaufour, P, 1982 *Pedology*, London.
- Dunnell, R C, 1978 Style and function: a fundamental dichotomy, *Am Antiq*, **43**, 192-202
- Dunnell, R C, and Stein, J, K, 1989 Theoretical issues in the interpretation of micro-artifacts, *Geoarchaeology*, **4**, 31-42
- Eastham, A, 1967 The avifauna of Gorham's Cave, Gibraltar, *Bull Inst Archaeol*, **7**, 37-42
- Eldholm, O, Thiede, J, and Taylor, E, 1987 Evolution of the Norwegian continental margin: background and objectives, *Proc Int Repts (Pt A)*, *ODP*, **104**, 5-25
- Elsden, J V, 1887 Superficial geology of the southern portion of the Wealden area, *Quart J Geol Soc Lond*, **43**, 642-5
- Endo, B, and Kimura, T, 1970 Postcranial skeleton of the Amud man, in *The Amud man and his cave site* (eds H Suzuki and F Takai), 231-406, Tokyo
- Ericson, P G P, 1987 Interpretation of archaeological bird remains: a taphonomic approach, *J Archaeol Sci*, **14**, 65-75
- Estes, R, 1981 Gymnophiona, Caudata, in *Handbuch der Paläoherpelologie*, Teil 2, Stuttgart
- Evans, E M N, van Couvering, J H, and Andrews, P, 1981 Palaeoecology of Miocene sites in western Kenya, *J Hum Evol*, **10**, 91-106
- Evans, J, 1860 On the occurrence of flint implements in undisturbed beds of gravel, sand and clay, *Archaeologia*, **38**, 280-307
- , 1861 Account of some further discoveries of flint implements in the Drift on the continent and in England, *Archaeologia*, **39**, 57-84
- , 1872 *The ancient stone implements, weapons and ornaments of Great Britain*, London
- Evernden, J F, Curtis, G H, and Kistler, R, 1957 Potassium argon dating of Pleistocene volcanics, *Quaternaria*, **4**, 1-5
- Fedoroff, N, and Goldberg, P, 1982 Comparative micromorphology of two Late Pleistocene paleosols (in the Paris Basin), *Catena*, **9**, 227-51
- Fedoroff, N, De Kimpe, C R, Page, F, and Bourbeau, G, 1981 Essai d'interprétation des transferts sous forme figurée dans les podzols du Québec méridional à partir de l'étude micromorphologique des profils, *Geoderma*, **26**, 25-45
- Fedoroff, N, Courty, M A, and Thompson, M L, 1990 Micromorphological evidence of palaeoenvironmental change in Pleistocene and Holocene paleosols, in *Soil micromorphology: a basic and applied science* (ed L A Douglas), 653-65, Amsterdam
- Fisher, P F, and Bridgland, D R, 1986 Analysis of pebble morphology, in *Clast lithological analysis: technical guide 3* (ed D R Bridgland), Cambridge
- Fladmark, K R, 1982 Microdebitage analysis: initial considerations, *J Archaeol Sci*, **9**, 205-20
- Flannery, K V, 1967 Culture history versus cultural process: a debate in American archaeology, *Scient Am*, **217**, 119-22
- Folk, R L, 1959 Practical petrographic classification of limestones, *Bull Am Ass Petrol Geol*, **43**, 1-38
- , 1980 *Petrology of sedimentary rocks*, Austin Texas
- Fortelius, M, Mazza, P, and Sala, B, 1993 *Stephanorhinus* (Mammalia: Rhinocerotidae) of the western European Pleistocene, with a revision of *S etruscus* (Falconer, 1868), *Palaeontogr Ital*, **80**, 63-155
- Fowler, J, 1929 Palaeoliths found at Slindon, *Sussex Archaeol Collect*, **70**, 197-200
- , 1931 Palaeolith from West Sussex, *Sussex Archaeol Collect*, **72**, 158-9
- , 1932 The 'One Hundred Foot' Raised Beach between Arundel and Chichester, *Sussex, Quart J Geol Soc*, **88**, 84-99
- Frazer, D, 1983 *Reptiles and amphibians in Britain*, London
- Frechen, J, and Lippolt, H J, 1965 Kalium-Argon-Daten zum Alter des Laacher Vulkanismus, der Rheinterrassen und die Eiszeiten, *Eiszeitalter Gegenwart*, **16**, 5-30
- Freethy, R, 1987 *Auks, an ornithologist's guide*, Poole
- Frere, J, 1800 Account of flint weapons discovered at Hoxne in Suffolk, *Archaeologia*, **13**, 204-5
- Frost, D R (ed), 1985 *Amphibian species of the world: a taxonomic and geographical reference*, Lawrence, Kansas
- Gabunia, L, and Vekua, A, 1995 A Plio-Pleistocene hominid from Dmanisi, East Georgia, Caucasus, *Nature*, **373**, 509-12
- Gale, S J, 1986 Quaternary magnetostratigraphy in Britain, *Quaternary News*, **48**, 29-33
- Gale, S J, Hunt, C O, and Southgate, G A, 1984 Kirkhead Cave: biostratigraphy and magnetostratigraphy, *Archaeometry*, **26**, 192-8
- Gamble, C S, 1986 *The Palaeolithic settlement of Europe*, Cambridge
- , 1993 *Timewalkers: the prehistory of global colonization*, Stroud
- Gamble, C S, and ApSimon, A M, 1986 Red Barns — Portchester, in *The Palaeolithic of Britain and its nearest neighbours: recent trends* (ed S N Colclutt), 8-12, Sheffield
- Gard, G, 1986 Calcareous nannofossil biostratigraphy of late Quaternary Arctic sediments, *Boreas*, **15**, 217-29
- , 1988 Late Quaternary calcareous nannofossil biozonation, chronology and palaeo-oceanography in areas north of the Faeroe-Iceland Ridge, *Quart Sci Rev*, **7**, 65-78
- Gard, G, and Backman, J, 1990 Synthesis of Arctic and Sub-Arctic coccolith biochronology and history of North Atlantic drift water influx during the last 500,000 years, in

- Geological history of the polar oceans: Arctic versus Antarctic* (eds U Bleil and J Thiede), 417–36, Dordrecht
- Gardiner, V, and Dackombe, R V, 1983 *Geomorphological field manual*, London
- Garraway-Rice, R, 1905 Some Palaeolithic implements from the terrace gravels of the River Arun and the western Rother, *Proc Soc Antiq*, **20**, 197–207
- , 1911 Report to the local Secretary for Sussex, the Palaeolithic period, *Proc Soc Antiq*, **23**, 371–3
- , 1920 Note on a Palaeolith from West Chiltington, near Pulborough, Sussex, *Proc Soc Antiq*, **32**, 79–82
- Gaukler, A, and Kraus, M, 1970 Kennzeichen und Verbreitung von *Myotis brandtii* (Eversmann 1845), *Z Säugetierk*, **35**, 113–24
- Gé, T, Courty, M A, Matthews, W, and Watez, J, 1993 Sedimentary formation processes of occupation surfaces, in *Formation processes in archaeological context* (eds P Goldberg, D T Nash, and M D Petraglia), Monographs in World Archaeology 17, 149–63, Madison
- Gee, H E, 1993 The distinction between postcranial bones of *Bos primigenius* Bojanus, 1827 and *Bison priscus* Bojanus, 1827 from the British Pleistocene and the taxonomic status of *Bos* and *Bison*, *J Quat Sci*, **8**, 79–92
- Geyer, G de, Vandenbergh, R E, Verdonck, L, and Stoops, G, 1985 Mineralogy of Holocene bog-iron ore in northern Belgium, *Neues Jb Miner Abh* (Stuttgart), **153**(1), 1–17
- Gibbard, P L, 1985 *The Pleistocene history of the Middle Thames Valley*, Cambridge
- , 1988 The history of the great northwest European rivers during the past three million years, *Phil Trans R Soc London*, **B318**, 559–602
- , 1995 The formation of the Strait of Dover, in *Preece 1995*, 15–26
- Gibbard, P L, and Peglar, S M, 1989 Palynology of the fossiliferous deposits at Witham on the Hill, Lincolnshire, in *The Pleistocene of the West Midlands: field guide* (ed D H Keen), 131–3, Cambridge
- Gibbard, P L, and Peglar, S M, 1990 Palynology of the interglacial deposits at Little Oakley, Essex, and their correlation, *Phil Trans R Soc London*, **B328**, 341–57
- Gibbard, P L, and Turner, C, 1988 In defence of the Wolstonian Stage, *Quaternary News*, **54**, 9–14
- Gibbard, P L, and Turner, C, 1990 Cold stage type sections: some thoughts on a difficult problem, *Quaternaire*, **1**, 33–40
- Gibbard, P L, West, R G, Zagwijn, W H, Balson, P S, Burger, A W, Funnell, B M, Jeffery, D H, de Jong, J, van Kolfschoten, T, Lister, A M, Meijer, T, Norton, P E P, Preece, R C, Rose, J, Stuart, A J, Whiteman, C A, and Zalasiewicz, J A 1991 Early and early Middle Pleistocene correlations in the southern North Sea basin, *Quat Sci Rev*, **10**, 23–52
- Gibert, L, Gibert, J, Albadalejo, S, and Maestro, E, 1995 Geología del Plio-Pleistoceno de la Región de Orce, *Congreso Internacional de Paleontología Humana — Los homínidos y su entorno en el Pleistoceno inferior y medio europeo. Once de Septiembre de 1995, 3a circular*, 110–14
- Gifford, D, 1980 Ethnoarchaeological contributions to the taphonomy of human sites, in *Fossils in the making* (eds A K Behrensmeier and A Hill), 93–106, Chicago
- Gifford, D, and Behrensmeier, A K, 1977 Observed formation and burial of a recent human occupation site in Kenya, *Quat Res*, **8**, 245–66
- Gladiline, V, and Sitlivy, V, 1991 Les premières industries en sub-Carpathie, in *Les Premiers Européens* (eds E Bonifay and B Vandermeersch), 217–31, Paris
- Godwin-Austin, R A C, 1857 On the newer Tertiary deposits of the Sussex Coast. *Q J Geol Soc Lond*, **13**, 40–72
- Goldberg, P, and Macphail, R I, 1990 Micromorphological evidence of Middle Pleistocene landscape and climatic changes from southern England: Westbury-sub-Mendip, Somerset and Boxgrove, W Sussex, in *Soil micromorphology: a basic and applied science* (ed L A Douglas), 441–7, Amsterdam
- Green, C P, and McGregor, D F M, 1978 Pleistocene gravel trains of the River Thames. *Proc Geol Assoc*, **89**, 143–56
- Green, C P, and McGregor, D F M, 1983 Lithology of the Thames gravels, in *Diversion of the Thames: field guide* (ed J Rose), 24–8, Cambridge
- Green, C P, and McGregor, D F M, 1990 Pleistocene gravels from the north Norfolk coast, *Proc Geol Assoc*, **101**, 197–202
- Green, H S, 1984 *Pontnewydd Cave: a Lower Palaeolithic hominid site in Wales: the first report*, Cardiff
- Green, J F N, 1943 The age of the Raised Beaches of south Britain, *Proc Geol Assoc*, **54**, 129–40
- Greenland Ice-core Project (GRIP) Members, 1993 Climate instability during the last interglacial period recorded in the GRIP ice core, *Nature*, **364**, 203–7
- Griffiths, D H, and King, R F, 1985 *Applied geophysics for geologists and engineers*, 2nd Edition, Oxford
- Grinsell, L V, 1929 The Lower and Middle Palaeolithic periods in Sussex, *Sussex Archaeological Collections*, **70**, 172–82
- Groves, C P, 1983 Phylogeny of the living species of rhinoceros, *Zool Syst Evolvforsch*, **21**, 293–313
- Grün, R, 1989a *Die ESR-Altersbestimmungsmethode*, Berlin
- Grün, R, 1989b Electron spin resonance (ESR) dating, *Quat Int*, **1**, 65–109
- Grün, R, and MacDonald, P D M, 1989 Non-linear fitting of TL/ESR dose response curves, *Applied Radiation and Isotopes*, **40**, 1077–80
- Grün, R, Schwarcz, H P, and Zymela, S, 1987 ESR dating of tooth enamel, *Can J Earth Sci*, **24**, 1022–37
- Grün, R, Schwarcz, H P, and Chadam, J M, 1988 ESR dating of tooth enamel: coupled correction for U-update and U-series disequilibrium, *Nuclear Tracks*, **14**, 237–41
- Guilday, J E, Parmalee, P W, and Tanner, D P, 1962 Aboriginal butchering techniques at the Eschelman site (36 La 12), Lancaster County, Pennsylvania, *Penn Archaeol*, **32**, 59–83
- Guilloré, P, 1985 *Méthode de Fabrication Mécanique et en Série des Lames Minces*, Paris
- Hanák, V, 1970 Notes on distribution and systematics of *Myotis mystacinus* Kuhl 1919, *Bijdr Dierk* **40**, 40–4
- , 1971 *Myotis brandtii* (Eversmann 1845) (Vespertilionidae, Chiroptera) in der Tschechoslowakei, *Vest Cs Spol Zool*, **25**, 175–85
- Hallock, L A, Holman, J A, and Warren, M R, 1990 Herpetofauna of the Ipswichian Interglacial Bed (Late Pleistocene) of the Itteringham Gravel Pit, Norfolk, *J Herpet*, **24**, 33–9
- Harding, P, Gibbard, P L, Lewin, J, Macklin, M G, and Moss, E H, 1987 The transport and abrasion of flint handaxes in a gravel-bed river, in *The human uses of flint and chert: proceedings of the fourth international flint symposium held at Brighton Polytechnic 10–15 April 1983* (eds G de G Sieveking and M H Newcomer), 115–26, Cambridge
- Harris, J M, and Jefferson, G T, 1985 *Rancho La Brea: treasure of the tar pits*, Los Angeles

- Harrison, C J O, 1980a Pleistocene bird remains from Tornewton Cave and Brixham Windmill Hill Cave in south Devon, *Bull Br Mus Nat Hist (Geology)*, **33**(2), 91-100
- , 1980b A re-examination of British Devensian and earlier Holocene bird bones in the British Museum (Natural History), *J Archaeol Sci*, **7**, 53-68
- , 1982 *An atlas of the birds of the western Palaearctic*, London
- , 1985 The Pleistocene birds of south-eastern England, *Bull Geol Soc Norfolk*, **35**, 53-69
- , 1986 Bird remains from Gough's Cave Cheddar, Somerset, *Proc Univ Bristol Spelaol Soc*, **17**(3), 305-10
- , 1987 Pleistocene and prehistoric birds of south-western Britain, *Proc Univ Bristol Spelaol Soc*, **18**(1), 81-104
- Harrison, C J O, and Walker, C A, 1977 A re-examination of the fossil birds from the Upper Pleistocene in the London Basin, *London Nat*, **56**, 6-8
- Harrison, D L, and Clayden, J C, 1993 New records of *Beremendia fissidens* (Petenyi 1864) and *Sorex minutus* Linnaeus 1766 (Insectivora: Soricidae) from the British Lower and Middle Pleistocene, *Cranium*, **10**(1), 97-9
- Hartwig-Scherer, S, 1993 Body weight prediction in early fossil hominids: towards a taxon-independent approach, *Am J Phys Anthropol*, **92**, 17-36
- Hatch, F H, and Rastall, R H, 1965 *Petrology of sedimentary rocks*, London
- Hawkes, L, 1943 The erratics of the Cambridge Greensand, *Q J Geol Soc Lon*, **99**, 93-104
- , 1951 The erratics of the English Chalk, *Proc Geol Assoc*, **62**, 257-68
- Haynes, G, 1981 Bone modifications and skeletal disturbances by natural agencies: studies in North America, unpubl PhD thesis, Catholic University of America
- , 1982 Utilisation and skeletal disturbances of North American prey carcasses, *Arctic*, **35**, 266-81
- , 1983a A guide for differentiating mammalian carnivore taxa responsible for gnaw damage to herbivore limb bones, *Paleobiology*, **9**, 164-72
- , 1983b Frequencies of spiral and green-bone fractures on ungulate limb bones in modern surface bone assemblages, *Am Antiq*, **48**, 102-14
- Haynes, J R, 1973 Cardigan Bay Recent foraminifera (Cruises of the R V *Antur*, 1962-1964), *Bull Br Mus Nat Hist (Zool Suppl)*, **4**, 1-245
- Hays, J D, Imbrie, J, and Shackleton, N J, 1976 Variations in the earth's orbit: pacemaker of the ice ages, *Science*, **194**, 1121-32
- Hazzledine-Warren, S, 1897 Note on a section of the Pleistocene Rubble Drift near Portslade, Sussex, *Geol Mag*, **4**(4), 302-4
- Hedberg, H D, 1976 *International stratigraphic guide*, New York
- Heller, F, 1958 Eine neue altquartäre Wirbeltierfauna von Erpfingen (Schwäbische Alb), *Neues Jb Geol Paläont Abh*, **107**, 1-102
- Heron-Allen, E, 1912 Archaeological discoveries in Selsey in 1912, *Sussex Archaeol Collect*, **50**, 315-17
- Heslop, D, and Shaw, J, 1996 *A palaeomagnetic study of an archaeological section in Boxgrove, West Sussex*, unpubl report, University of Liverpool
- Hey, R W, 1965 Highly quartzose Pebble Gravels in the London Basin, *Proc Geol Assoc*, **76**, 403-20
- , 1967 The Westleton Beds reconsidered, *Proc Geol Assoc*, **78**, 427-45
- , 1976 Provenance of far-travelled pebbles in the pre-Anglian Pleistocene of East Anglia, *Proc Geol Assoc*, **87**, 69-81
- , 1980 Equivalents of the Westland Green Gravels in Essex and East Anglia, *Proc Geol Assoc*, **91**, 279-90
- , 1986 A re-examination of the Northern Drift of Oxfordshire, *Proc Geol Assoc*, **97**, 291-301
- Hill, A, 1975 Taphonomy of contemporary and late Cenozoic East African vertebrates, unpubl PhD thesis, University of London
- , 1980 A modern hyaena den in Amboseli National Park, Kenya, *Proceedings, 8th pan-African Congress of Prehistory and Quaternary Studies, Nairobi*, 137-8
- Hinton, M A C, 1911 The British Fossil Shrews, *Geol Mag*, **8**, 529-39
- , 1914 On some remains of rodents from the Red Crag of Suffolk and from the Norfolk Forest Bed, *Ann Mag Nat Hist, Series 8*, **13**, 186-95
- , 1923 Diagnosis of species of *Pitymys* and *Microtus* occurring in the Upper Freshwater Bed of West Runton, Norfolk, *Ann Mag Nat Hist, Series 9*, **12**, 541-2
- , 1926 *Monograph of the Voles and Lemmings (Microtinae), living and extinct. Vol. 1*, London
- Hodgson, J M, 1964 The low-level Pleistocene marine sands and gravels of the West Sussex coastal plain, *Proc Geol Assoc*, **75**, 547-61
- , 1967 *Soils of the West Sussex coastal plain*, Soil Survey of Great Britain, Bulletin **3**, Harpenden
- , 1976 *Soil Survey Field Handbook*, Soil Survey Technical Monograph, **5**, Harpenden
- Hodgson, J M, Catt, J A, and Weir, A H, 1967 The origin and development of the Clay-with-Flints and associated soil horizons on the South Downs, *J Soil Sci*, **18**, 85-102
- Hodgson, J M, Rayner, J M, and Catt, J A, 1974 The geomorphological significance of Clay-with-Flints on the South Downs, *Trans Inst Br Geog*, **61**, 119-29
- Hollin, J T, 1977 Thames interglacial sites, Ipswichian sea levels and Antarctic ice surges, *Boreas*, **6**, 33-52
- Holman, J A, 1989 Identification of *Bufo calamita* and *Bufo bufo* on the basis of skeletal elements, *Br Herp Soc Bull*, **29**, 54-55
- , 1991 North American Pleistocene herpetofaunal stability and its impact on the interpretation of modern faunas: an overview, in *Beamers, Bobwhites and Blue Points: tributes to the career of Paul W Parmalee* (eds B R Purdue, W E Klippel, and B W Styles), 227-35, Springfield
- , 1993 British Quaternary herpetofaunas: a history of adaptations to Pleistocene disruptions, *Herpet J*, **3**(1), 1-7
- Holman, J A, and Stuart, A J, 1991 Amphibians from the Whitemoor Channel early Flandrian site near Bosley, East Cheshire; with remarks on the fossil distribution of *Bufo calamita* in Britain, *Herpet J*, **1**, 568-73
- Holman, J A, Stuart, A J, and Clayden, J D, 1990 A Middle Pleistocene herpetofauna from Cudmore Grove, Essex and its paleogeographic and paleoclimatic implications, *J Vertebr Paleontol*, **10**(1), 86-94
- Holyoak, D T, and Preece, R C, 1986 A reassessment of some British Pleistocene land snails, *J Conch Lond*, **32**, 199-200
- Hopwood, A T, 1934 The former distribution of caballine and zebline horses in Europe and Asia, *Proc Zool Soc London*, **4**, 897-912
- Horáček, I, 1986 Fossil records and chronological status of dormice in Czechoslovakia. Part 1 *Glis glis*, *Eliomys quercinus*, *Folia Mus Rerum Nat Bohemiae Occident Zoologica*, **24**, 45-59

- Horáček, I, and Lozeck, V, 1988 Paleozoology and the Mid-European Quaternary past: scope of the approach and selected results. *Rozprawy CSAV, r. MPV*, **98**(4), 106pp
- Horn, P, Hölzl, S, and Storzer, D, 1994 Habitat determination on a fossil stag's mandible from the site of *Homo erectus heidelbergensis* at Mauer by use of $^{87}\text{Sr}/^{86}\text{Sr}$. *Naturwissenschaften*, **81**, 360-2
- Horne, D J, and Whittaker, J E, 1983 On *Baffinicythere howei* Hazel, *Stereo-Atlas Ostracod Shells*, **10**, 53-62
- Horne, D J, Lord, A R, Robinson, J E, and Whittaker, J E, 1990 Ostracods as climatic indicators in interglacial deposits, or, on some new and little-known British Quaternary Ostracoda, *Cour Forsch Inst Senckenberg*, **123**, 129-40
- Howell, F C, 1968 *Early man*, New York
- Hubbard, R N L B, 1982 The environmental evidence from Swanscombe and its implications for Palaeolithic archaeology, in *Archaeology in Kent to AD 1500* (ed P E Leach), CBA Res Rep, **48**, 3-7, London
- Hufthammer, A K, 1982 Geirfuglens utbredelse og morfologiske variasjon i Skandinavia, unpubl thesis, Universitet I Bergen
- Hughes, S A, 1987 The aminostratigraphy of British Quaternary non-marine deposits, unpubl PhD thesis, University of Wales
- Hull, K L, 1984 *Microdebitage analysis applied to spatial patterning*. Paper presented at the 49th Annual Meeting of the Society for American Archaeology, Portland, Oregon
- Huntley, D J, Godfrey-Smith, D I, and Thewalt, M L W, 1985 Optical dating of sediments, *Nature* **313**, 105-7
- Imbrie, J, Hayes, J D, Martinson, D G, McIntyre, A, Micks, A C, Morley, J J, Pisias, N G, Prell, W L, and Shackleton, N J, 1984 The orbital theory of Pleistocene climate: support from a revised chronology of the marine O^{18} record, in *Milankovitch and climate* (eds A Berger, J Imbrie, J D Haynes, G Kukla, and B Saltzman), Part 1, 269-306, Dordrecht
- Imbrie, J, Berger, A, Boyle, A, Clemens, S C, Dutty, A, Howard, W R, Kukla, G, Kutzbach, J, Martinson, D G, McIntyre, A, Mix, A C, Molino, B, Morley, J J, Petersen, L C, Pisias, N G, Prell, W L, Rayme, M E, Shackleton, N J, Toggweiler, J R, 1993 On the structure and origin of the major glaciation cycles; 2, the 100,000 year cycle, *Paleoceanography*, **8**(6), 698-735
- Isaac, G L, 1977 *Ologesalie: archaeological studies of a Middle Pleistocene lake basin in Kenya*, Chicago
- Jammot, D, 1973 Les Insectivores (*Mammalia*) du gisement Pléistocène Moyen des Abîmes de La Fage (Corrèze), *Nouv Arch Mus Hist Nat Lyon, fasc* **13**, 29-46
- Jánossy, D, 1962 Vorläufige Mitteilung über die Mittelpleistozäne Vertebratenfauna der Tarkö-Felsniche (NO-Ungarn, Bükkgebirge), *Annls Hist-Nat Mus Natn Hung* **54**, 155-76
- , 1969 Stratigraphische Auswertung der europäischen mittelpleistozänen Wirbeltierfauna. Teil 2. *Ber Dt Ges Geol Wiss. Geologie und Paläontologie. Ser A*, **14**(5), 573-643
- Jeffrey, R W, 1957 Slindon hand-axe, *Sussex Notes and Queries*, **14**, 242
- , 1960 Fresh facts relating to the Raised Beach at Slindon, Sussex, *The Archaeological News Letter*, **6**, 258-9
- Johnson, L L, 1978 A history of flint-knapping experimentation, 1838-1976, *Curr Anthropol*, **19**(2), 337-73
- Johnson, R G, 1982 Brunhes-Matuyama magnetic reversal dated at 790,000yr BP by marine-astronomical correlations, *Quat Res*, **17**, 135-47
- Jong, J de, 1988 Climatic variability during the past three million years, as indicated by vegetational evolution in north-west Europe and with emphasis on data from The Netherlands, *Phil Trans R Soc Lond* **B318**, 603-17
- Kahlke, H D, 1975 The macro-faunas of continental Europe during the Middle Pleistocene: stratigraphic sequence and problems of intercorrelation, in *After the Australopithecines* (eds K W Butzer and G L Isaac), 309-74, The Hague
- Kalembasa, S J, and Jenkinson, D S, 1973 A comparative study of titrimetric and gravimetric methods for the determination of organic carbon in soil, *J Food Agric Sci*, **18**, 85-102
- Karlin, C, and Newcomer, M H, 1982 Interpreting flake scatters: an example from Pincevent, in *Tailler! pourquoi faire: préhistoire et technologie lithique II: recent progress in microwear studies* (ed D Cahen), Tervuren, *Studia Praehistorica Belgica* **2**, 159-65
- Kearey, P, and Brooks, M, 1984 *An introduction to geophysical exploration*, Oxford
- Keeley, L H, 1977 An experimental study of microwear traces on selected British Palaeolithic implements, unpubl PhD thesis, University of Oxford
- , 1980 *Experimental determination of stone tool uses: a microwear analysis*, Chicago
- Keen, D H, 1995 Raised beaches and sea-levels in the English Channel in the Middle and Late Pleistocene: problems of interpretation and implications for the isolation of the British Isles, in Preece 1995, 63-74
- Keen, D H, Robinson, J E, West, R G, Lowry, F, Bridgland, D R, and Davey, N D W, 1990 The fauna and flora of the March Gravels at Northam Pit, Eye, Cambridgeshire, England, *Geol Mag*, **127**, 453-65
- Kellaway, G A, Redding, J K, Shephard-Thorn, E R, and Destombes, J P, 1975 The Quaternary history of the English Channel, *Phil Trans R Soc Lond*, **A279**, 189-218
- Kellogg, T B, Duplessy, J C, and Shackleton, N J, 1978 Planctonic foraminiferal and oxygen isotope stratigraphy and paleoclimatology of Norwegian deep-sea cores, *Boreas*, **7**, 61-73
- Kemp, R A, 1985a The decalcified Lower Loam at Swanscombe, Kent: a buried Quaternary soil, *Proc Geol Assoc*, **96**, 343-54
- , 1985b The Valley Farm Soil in southern East Anglia, in *Soils and Quaternary landscape evolution* (ed J Boardman), 179-196, Chichester
- , 1986 Pre-Flandrian Quaternary soils and pedogenic processes in Britain, in *Paleosols: their recognition and interpretation* (ed V P Wright), 242-62, Oxford
- Kenworthy, J W, 1898 Meeting at Braintree and 181st ordinary meeting, *Essex Nat*, **10**, 404-6
- Kerney, M P, 1956 An interglacial tufa near Hitchin, Hertfordshire. *Proc Geol Assoc*, **70**, 322-37
- , 1976 Mollusca from an interglacial tufa in East Anglia, with the description of *Lyrodiscus Pilsbry* (Gastropoda: Zonitidae), *J Conch Lond*, **29**, 47-50
- Kerney, M P, Brown, E H, and Chandler, T H, 1964 The late glacial and post glacial history of the chalk escarpment near Brook, Kent, *Phil Trans R Soc Lond*, **B248**, 135-204
- Kerr, P F, 1959 *Optical mineralogy*, New York
- King, W, 1864 The reputed fossil man of the Neanderthal, *Q J Sci*, **1**, 88-97

- King, W B R, and Oakley, K P, 1936 The Pleistocene succession in the lower part of the Thames valley, *Proc Prehist Soc*, **2**, 52–76
- Kintigh, K, and Ammerman, A, 1982 Heuristic approaches to spatial analysis in archaeology, *Am Antiq*, **47**(1), 31–63
- Knowles, F H S, 1953 *Stone-worker's progress*, Occasional paper on technology, **6**, Pitt Rivers Museum.
- Koby, F E, 1959 Contribution au diagnostic osteologique différentiel de *Lepus timidus* Linné, et *L. europaeus* Pallas, *Vérh Naturf Ges Basel*, **70**(1), 19–44
- Koby, F E, 1960 Contribution à la connaissance des Lièvres fossiles, principalement de ceux de la dernière glaciation, *Vérh Naturf Ges Basel*, **71**(1), 149–73
- Koči, A, and Šibrava, V, 1976 The Brunhes-Matuyama boundary at Central European localities, in *Glaciations in the Northern Hemisphere*, Project 73/1/24, IGCP-UNESCO, 135–60, Prague
- Koči, A, Schirmer, W, and Brunnacker, K, 1973 Paläomagnetische Daten aus dem mittleren Pleistozän des Rhein-Main-Raumes, *Neues Jb Geol Paläont*, 545–54, Stuttgart
- Koenigswald, W von, 1970 Mittelpleistozäne Kleinsäugerfauna aus der Spaltenfüllung Petersbuch bei Eichstätt, *Mitt Bayer St Paläont Hist Geol*, **10**, 407–32
- , 1973 Veränderungen in der Kleinsäugerfauna von Mitteleuropa zwischen Cromer und Eem (Pleistozän), *Eiszeitalter Gegenwart*, **23/24**, 159–67
- , 1992 Zur Ökologie und Biostratigraphie der beiden pleistozänen Faunen von Mauer bei Heidelberg, in *Schichten von Mauer – 85 Jahre Homo erectus heidelbergensis* (eds K W Beinauer and G A Wagner), 101–10, Mannheim
- Koenigswald, W von, and Kolfschoten, T van, 1996 The *Miomys-Arvicola* boundary and the enamel thickness quotient (SDQ) of *Arvicola* as stratigraphic markers in the Middle Pleistocene, in *The early Middle Pleistocene in Europe* (ed C Turner), 211–26, Rotterdam
- Kolfschoten, T van, 1985 The Middle Pleistocene (Saalian) and Late Pleistocene (Weichselian) mammal faunas from Maastricht-Belvédère, (Southern Limburg, The Netherlands), *Meded Rijks Geol Dienst*, **39**(1), 45–74
- , 1990 The evolution of the mammal fauna in the Netherlands and the Middle Rhine area (western Germany) during the Late Middle Pleistocene, *Meded Rijks Geol Dienst*, **43**(3), 1–69
- , 1991 The Saalian mammal fossils from Wageningen-Fransche Kamp, *Meded Rijks Geol Dienst*, **46**, 37–54
- Kolfschoten, T van, and Roebroeks, W, 1985 *Maastricht-Belvédère: stratigraphy, palaeoenvironment and archaeology of the Middle and Late Pleistocene deposits*, *Analecta Praehistorica Leidensia*, **18**, Leiden
- Kolfschoten, T van, and Turner, E, 1996 Early Middle Pleistocene mammalian faunas from Kärlich and Miesenheim I and their biostratigraphical implications, in *The early Middle Pleistocene in Europe* (ed C Turner), 227–54, Rotterdam
- Kooistra, M J, 1978 *Soil development in Recent marine sediments of the intertidal zone in the Oosterschelde – The Netherlands: a soil micromorphological approach*, Soil Survey Papers, **14**, Wageningen
- Kormos, T, 1934 Neue und Wenig bekannte Musteliden aus dem ungarischen Oberpliozän, *Folia Zool hydrobiol*, **5**, 129–58
- Kowalski, K, 1979 Fossil Zapodidae (Rodentia, Mammalia) from the Pliocene and Quaternary of Poland, *Acta Zool Cracov*, **23**(9), 199–212
- Kowalski, K, and Nadachowski, A, 1982 Rodentia, in *Excavation in the Bacho Kiro Cave (Bulgaria) Final report* (ed J K Kozłowski) 45–51, Warszawa
- Krumbein, W C, and Sloss, L L, 1963 *Stratigraphy and sedimentation*, San Francisco
- Kukla, G J, 1975 Loess stratigraphy of Central Europe, in *After the Australopithecines: stratigraphy, ecology and culture change in the Middle Pleistocene* (eds K W Butzer and G L Isaac), 99–188, The Hague
- , 1977 Pleistocene land-sea correlations, I: Europe, *Earth Sci Rev*, **13**, 307–74
- Kurtén, B, 1965 On the evolution of the European wild cat *Felis sylvestris* Schreber, *Acta Zool Fenn*, **111**, 1–26
- , 1968 *Pleistocene mammals of Europe*, London
- Kurtén, B, and Poulanos, N A, 1977 New stratigraphic and faunal material from Petralona Cave with special reference to the Carnivora, *Anthropos*, **4**, 47–130
- Landuydt, C J, 1990 Micromorphology of iron minerals from bog ores of the Belgian Campine area, in *Soil micromorphology: a basic and applied science* (ed L A Douglas), 289–94, Amsterdam
- Lartet, E, and Christy, H, 1865–1875 *Reliquae Aquitanicae, being contributions to the archaeology and palaeontology of Périgord and the adjoining provinces of southern France*, London
- Lason, J S, and van Nostrand, F C, 1968 An evaluation of beaver ageing techniques, *J Wildl Mgmt*, **32**, 99–103
- Leakey, M D, 1971 *Olduvai Gorge: excavations in Beds I and II 1960–1963*, Cambridge
- Lecointre, G, 1952 Recherches sur le Neogène et la Quaternaires marins de les côtes Atlantique du Maroc. Tome I: Stratigraphie. Tome II: Paleontologie. *Protectorat de la République Française au Maroc, direction de la production industrielle et des mines, division des mines et de la géologie, service géologique, Notes et Memoires*, **99**(I), 1–198, (II), 1–173
- Lewis, J, Wiltshire, P, and Macphail, R, 1992 A Late Devensian/Early Flandrian site at Three Ways Wharf, Uxbridge: environmental implications, in *Alluvial Archaeology in Britain* (eds S Needham and M G Macklin), Oxbow Monograph, **27**, 235–48, Oxford
- Lewis, S G, 1992 High Lodge — stratigraphy and depositional environments, in Ashton *et al* 1992a, 51–85
- , 1993 The status of the Wolstonian glaciation in the English Midlands and East Anglia, unpubl PhD thesis, University of London
- Lindholm, R, 1987 *A practical approach to sedimentology*, London
- Linnaeus, C, 1758 *Systema Naturae*, 10th edn, Stockholm
- Lister, A M, 1986 New results on deer from Swanscombe, and the stratigraphic significance of deer in the Middle and Upper Pleistocene of Europe, *J Archaeol Sci*, **13**, 319–38
- , 1989 Mammalian faunas and the Wolstonian debate, in *The Pleistocene of the West Midlands: field guide* (ed D H Keen), 5–12, Cambridge
- , 1993a The stratigraphic significance of deer species in the Cromer Forest-bed formation, *J Quat Sci*, **8**(2), 95–208
- , 1993b Cervidae and a method for comparing body size in small samples of fossil species, in Singer *et al* 1993, 174–90
- , 1994 The evolution of the giant deer, *Megaloceros giganteus* (Blumenbach), *Zool J Linn Soc*, **112**, 65–100

- Lister, A M, McGlade, J M, and Stuart A J, 1990 The early Middle Pleistocene vertebrate fauna from Little Oakley, Essex, *Phil Trans R Soc Lond*, **B238**, 359–85
- Livingston, S D, 1989 The taphonomic interpretation of avian skeletal part frequencies, *J Archaeol Sci*, **16**, 537–47
- Loveday, J, 1962 Plateau deposits of the southern Chiltern Hills, *Proc Geol Assoc*, **73**, 83–102
- Lovell, J H, and Nancarrow, P H A, 1983 The sand and gravel resources of the country around Chichester and north of Bognor Regis, Sussex. Description of 1:25000 resource sheet SU 80 and 90, *Miner Assess Rep Inst Geol Sci*, **138**
- Lumley, H de, 1969 A Palaeolithic camp at Nice, *Scient Am*, **220**, 42–50
- Lyell, C, 1841 *Elements of geology*, London, 2nd Edition
- Macdonald, D W, and Barrett, P, 1993 *Mammals of Britain and Europe*, London
- Macphail, R I, 1986a *Soil report on brickearth deposits associated with a palaeolith (hand axe) on the Taplow Terrace at Sipsons Lane, Middlesex*, Ancient Monuments Laboratory Report **4942**
- , 1986b Palaeosols in archaeology, in *Palaeosols: their recognition and interpretation* (ed V P Wright), 263–90, Oxford
- , 1988 *Soil report on the Upper Palaeolithic and Early Mesolithic sites and late glacial and Flandrian soil formation at Hengistbury Head, Dorset*, Ancient Monuments Laboratory Report **79/88**
- , 1990 *Soil report on the Hullbridge Project: the sites of Purfleet, the Stumble and others on the Blackwater River*, Ancient Monuments Laboratory Report **39/90**
- , 1991 *Soil report on Three Ways Wharf, Oxford Rd, Uxbridge, Middx*, Ancient Monuments Laboratory Report **120/91**
- , 1992a Late Devensian and Holocene soil formation, in *Hengistbury Head, Dorset, Volume 2: the Late Upper Palaeolithic and Early Mesolithic sites* (ed R N E Barton), Oxford University Committee for Archaeology Monograph, **34**, 44–51, Oxford
- , 1992b Soil micromorphological evidence of ancient soil erosion, in *Past and present soil erosion* (eds M Bell and J Boardman), Oxbow Monograph, **22**, 197–218, Oxford
- , 1994 Soil micromorphology investigations in archaeology, with special reference to drowned coastal sites in Essex, in *SEESOIL 10* (eds H F Cook and D T Favis-Mortlock), 13–28, Wye
- Macphail, R I, and Goldberg, P, 1995 Recent advances in micromorphological interpretations of soils and sediments from archaeological sites, in *Archaeological sediments and soils: analysis interpretation and management* (eds A J Barham and R I Macphail), 1–24e, London
- Macphail, R I, and McConnell, A, 1986 Preliminary report on the sediments, in Roberts 1986, 224–7
- Macphail, R I, and Scaife, R G, 1987 The geographical and environmental background, in *The archaeology of Surrey to 1540* (eds J Bird and D G Bird), 31–51, Guildford
- Maddy, D, and Lewis, S G, 1991 The Pleistocene deposits at Snitterfield, Warwickshire, *Proc Geol Assoc*, **102**(4), 289–300
- Maddy, D, Keen, D H, Bridgland, D R, and Green, C P, 1991 A revised model for the Pleistocene development of the River Avon, Warwickshire, *J Geol Soc*, **148**, 473–84
- Maddy, D, Coope, G R, Gibbard, P L, Green, C P, and Lewis, S G, 1994 Reappraisal of Middle Pleistocene fluvial deposits near Brandon, Warwickshire and their significance for the Wolston glacial sequence, *J Geol Soc*, **151**, 221–33
- Madsen, M E, 1992 Lithic manufacturing at British Camp: evidence from size distributions and micro-artifacts, in *Deciphering a shell midden* (ed J K Stein), 193–210, New York
- MAFF (Ministry of Agriculture, Fisheries and Food), 1981 *Atlas of the seas around the British Isles*, London
- Mangerud, J, Sonstegaard, E, and Sejrup, H-P, 1979 The correlation of the Eemian (interglacial) Stage and the deep-sea oxygen isotope stratigraphy, *Nature*, **277**, 189–92
- Mania, D, 1995 The earliest occupation of Europe: the Elbe-Saale Region (Germany), in *The earliest occupation of Europe* (eds W Roebroeks and T van Kolfschoten), Leiden
- Mania, D, and Weber, T, 1986 Bilzingsleben III, *Veröff Landesmus Vorgeschich Halle*, Band **39**
- Mania, D, Toepfer, V, and Vlcek, E, 1980 Bilzingsleben I, *Veröff Landesmus Vorgeschich Halle*, Band **32**
- Mania, D, Mania, U, and Vlcek, E, 1994 Latest finds of skull remains of *Homo erectus* from Bilzingsleben (Thuringia), *Naturwissenschaften*, **81**, 123–7
- Mantell, G A, 1822 *The fossils of the South Downs, or the illustrations of the geology of Sussex*, London
- , 1833 *The geology of the south-east of England*, London
- Marlin, C, Dever, L, Vachier, P, and Courty, M A, 1993 Variations chimiques et isotopiques de l'eau du sol lors de la reprise en gel d'une couche active sur pergélisol continu (Presqu'île de Brøgger, Svalbard), *Can J Earth Sci*, **30**, 806–13
- Martin, E C, 1938 The Littlehampton and Ports Down Chalk Inliers and their relation to the Raised Beaches of West Sussex, *Proc Geol Assoc*, **49**, 198–212
- Martin, P J, 1856 On some geological features of the country between the South Downs and the Sussex Coast, *Q J Geol Soc Lond*, **12**, 134–7
- Martinson, D G, Pisias, N G, Hays, J D, Imbrie, J, Moore, T C, and Shackleton, N J, 1987 Age dating and the orbital theory of the ice ages: development of a 0–300,000 year chronostratigraphy, *Quat Res*, **27**, 1–29
- Matz, G, and Weber, D, 1983 *Amphibien und Reptilien*, München.
- Mayhew, D F, 1975 The Quaternary history of some British Pleistocene rodents and lagomorphs, unpubl PhD thesis, University of Cambridge
- , 1978 Late Pleistocene small mammals from Arnissa (Macedonia, Greece), *Proc K Ned Akad Wet*, **B81**(3), 302–21
- McIntyre, A, Ruddiman, W F, and Jantzen, R, 1972 Southward penetrations of the North Atlantic polar front: faunal and floral evidence of large scale surface water mass movements after the last 225,000 years, *Deep-Sea Research*, **19**, 61–77
- McNabb, J, 1992 The Clactonian: British Lower Palaeolithic technology in biface and non-biface assemblages, unpubl PhD thesis, University of London
- McNabb, J, and Ashton, N M, 1992 The cutting edge, bifaces in the Clactonian, *Lithics*, **13**, 4–10
- Meijer, T, 1993 Stratigraphical notes on *Macoma* (Bivalvia) in the southern part of the North Sea Basin and some remarks on the arrival of Pacific species, *Scr Geol*, Special Issue **2**, 297–312
- Meijer, T, and Preece, R C, 1996 Malacological evidence relating to the stratigraphical position of the Cromerian, in *The early Middle Pleistocene in Europe* (ed C Turner), Rotterdam

- Melville, R V, and Freshney, E C, 1982 *British regional geology: the Hampshire Basin and adjoining areas*, London
- Merkel, R H, 1972 The use of resistivity techniques to delineate acid mine drainage in groundwater, *Groundwater*, **10**, 38-42
- Milankovitch, M, 1941 Kanon der Erdbeststrahlung und seine Anwendung auf das Eiszeitenproblem, *Edition spéciale de la Académie Royale Serbe*, **133**
- Miller, G H, and Mangerud, J, 1985 Aminostratigraphy of European marine interglacial deposits, *Quat Sci Rev*, **4**, 215-78
- Miller, G H, Hollin, J T, and Andrews, J, 1979 Aminostratigraphy of UK Pleistocene deposits, *Nature*, **281**, 539-43
- Miller, G H, Brigham, J K, and Clark, P, 1982 Alteration of the total alle/le ratio by different methods of sample preparation, in *Amino acid geochronology laboratory report of current activities* (ed G H Miller), 9-20, University of Colorado
- Milsom, J, 1989 *Field geophysics*, Geological Society of London Handbook, Chichester
- Mitchell, G F, Penny, L F, Shotton, F W, and West, R G, 1973 *A correlation of Quaternary deposits in the British Isles*, Geological Society of London Special Report, **4**, London
- Mithen, S, 1994 Technology and society during the Middle Pleistocene, *Cambridge Archaeol J*, **4**(1), 3-33
- Moir, J Reid, 1938 Four flint implements, *Antiq J*, **18**, 258-61
- Molyneux, L, 1971 A complete result magnetometer for measuring the remanent magnetisation of rocks, *Geophys J R Astr Soc*, **24**, 429-33
- Mortillet de, G, 1866 *Matériaux pour l'histoire de l'homme*, Paris
- Mortimore, R N, 1986 Stratigraphy of the Upper Cretaceous White Chalk of Sussex. *Proc Geol Assoc*, **97**, 97-139
- Mourer-Chauviré, C, 1983, Les oiseaux dans les habitats paléolithiques: gibier des hommes aux proies des rapaces? in *Animals in archaeology, tome II: shell middens, fishes and birds* (eds C Grigson and J Clutton-Brock), BAR Int Ser **183**, 111-234, Oxford
- Mourer-Chauviré, C, and Antunes, M T, 1991 Presence du grand pingouin, *Pinguinis impennis* (Aves, Charadriiformes) dans le Pleistocene du Portugal, *Geobios*, **24**, fasc 2, 201-5
- Mücher, H J, and De Ploey, J, 1977 Experimental and micromorphological investigation of erosion and redeposition of loess by water, *Earth Surface Processes*, **2**, 117-24
- Mücher, H J, and Vreeken, W J, 1981 (Re)deposition of loess in Southern Limbourg, The Netherlands, 2: micromorphology of the Lower Silt Loam Complex and comparison with deposits produced under laboratory conditions, *Earth Surface Processes and Landforms*, **6**, 355-63
- Mücher, H J, De Ploey, J, and Savat, J, 1981 Response of loess materials to simulated translocation by water: micromorphological observations, *Earth Surface Processes and Landforms*, **6**, 331-6
- Mullenders, W W, 1993 New palynological studies at Hoxne, in Singer *et al* 1993, 150-5
- Murchison, R, 1851 On the distribution of the Flint Drift of the south-east of England, on the flanks of the Weald, and over the surface of the South and North Downs, *Q J Geol Soc Lond*, **7**, 257-62; 349-98
- Murphy, C P, 1986 *Thin section preparation of soils and sediments*, Berkhamsted
- Murray, J W, 1979 British nearshore foraminiferids, in *Synopsis of the British Fauna (new ser)*, **16** (eds D M Kermack and R S K Barnes) (for Linn Soc, London and the Estuarine and Brackish-water Sciences Assoc), London
- , 1991 *Ecology and palaeoecology of benthic foraminifera*, Harlow
- Murray, P, 1984 Extinction down under: a bestiary of extinct Australian Late Pleistocene monotremes and marsupials, in *Quaternary extinctions: a prehistoric revolution* (eds P S Martin and R G Klein), 600-28, Tucson
- Nadachowski, A, 1984a Morphometric variability of dentition of the Late Pleistocene voles (*Arvicolidae*, *Rodentia*) from Bacho Kiro Cave (Bulgaria), *Acta Zool Cracov*, **27**(9), 149-76
- Nadachowski, A, 1984b Taxonomic value of anteroconid measurements of M₁ in Common and Field Voles, *Acta Theriologica*, **29**(10), 123-7
- Neithammer, J, and Krapp, F, 1988 *Handbuch der Säugetiere Europas, Band 1: Nagetiere 1*, Wiesbaden
- , 1990 *Handbuch der Säugetiere Europas. Band 3/1: Insectenfresser, Primaten*, Wiesbaden
- Nelson, A J, 1995 Cortical bone thickness in the primate and hominid postcranium, taxonomy and allometry, unpubl doctoral dissertation, Department of Anthropology, UCLA
- Nelson, C M, and Pain, T, 1986 Linnaeus' *Neptunea* (Mollusca: Gastropoda), *Zool J Linn Soc*, **88**, 291-305
- Newcomer, M H, 1971 Some quantitative experiments in hand-axe manufacture, *World Archaeology*, **3**, 85-94
- , 1975 Spontaneous retouch, *Staringia*, **3**, 62-4
- Newcomer, M H, and Sieveking, G de G, 1980 Experimental flake scatter-patterns: a new interpretive technique, *J Field Archaeol*, **7**, 345-52
- Newton E T, 1882 *The Vertebrata of the Forest Bed Series of Norfolk and Suffolk*, Memoirs of the Geological Survey, UK
- , 1923 List of avian species identified from Aveline's Hole, Burrington, *Proc Univ Bristol Spelaeol Soc* **1**, 119-21
- Nicholson, B A, 1983 A comparative evaluation of four sampling techniques and of the reliability of microdebitage as a cultural indicator in regional surveys, *Plains Anthropol*, **28**, 273-81
- Noël, M, 1986 The palaeomagnetism and magnetic fabric of sediments from Peak Cavern, *Geophys J R Astr Soc*, **84**, 445-54
- , 1992 Multicore resistivity tomography for imaging archaeology, in *Geoprospecting in the archaeological landscape* (ed P Spoerri), Oxbow Monograph, **18**, 89-99, Oxford
- Oakley, K P, and Curwen, E C, 1937 The relation of the Coombe Rock to the 135ft Raised Beach at Slindon, Sussex, *Proc Geol Assoc*, **48**, 317-23
- Oakley, K P, and Leakey, M, 1937 Report on excavations at Jaywick Sands, Essex (1934), with some observations on the Clactonian Industry, and on the fauna and geological significance of the Clacton Channel, *Proc Prehist Soc*, **3**, 217-60
- O'Connell, J F, and Hawkes, K, 1988 Hadza hunting, butchering and bone transport, and their archaeological implications, *J Anthropol Res*, **44**, 113-61
- O'Connell, J F, Hawkes, K, and Blurton-Jones, N, 1988 Hadza scavenging: implications for Plio/Pleistocene hominid subsistence, *Curr Anthropol*, **29**, 356-63

- Ohnuma, K, and Bergman, C A, 1982 Experimental studies in the determination of flaking mode, *Bull Inst Archaeol, Univ London*, **19**, 161-70
- Oliver, J S, and Graham, R W, 1994 A catastrophic kill of ice-trapped coots: time averaged versus scavenger-specific disarticulation patterns, *Paleobiology*, **20**(2), 229-44
- Olsen, S, 1984 Analytical approaches to the manufacture and use of bone artefacts in prehistory, unpubl PhD thesis, University of London
- Olson, S L, 1977 A great auk, *Pinguinis*, from the Pliocene of North Carolina (Aves: Alcidae), *Proc Biol Soc Wash*, **90**(3), 690-7
- , 1985 The fossil record of birds, in *Avian biology* Vol 7 (eds D S Farner and K C Parks), 79-238, New York
- Osbourne-White, H J, 1924 Geology of the country near Brighton and Worthing, *Mem Geol Surv UK*, 70-92
- Palacios, F, and López Martínez, L, 1980 Morfología dentaria de las liebres europeas (Lagomorpha, Leporidae), Doñana, *Acta Vertebrata*, **7**(1), 61-81
- Palmer, L S, 1922 The Ice Age and man in Hampshire, *Man*, **22**(7), 106-110
- Palmer, L S, and Cooke, J H, 1923 The Pleistocene deposits of the Portsmouth district and their relation to man, *Proc Geol Assoc*, **34**, 253-82
- Palmer, L S, and Cooke, J H, 1930 The Raised Beaches near Portsmouth, *S East Nat Canterbury*, **35**, 66-75
- Palmer, S, 1975 A Palaeolithic site at North Road, Purfleet, Essex, *Trans Essex Archaeol Soc*, **7**, 1-13
- Parfitt, S A, 1986 The Boxgrove bone recording system, unpubl manuscript, 38pp
- Parks, D A, and Rendell, H M, 1992 Thermoluminescence dating and geochemistry of loessic deposits in south-east England, *J Quat Sci*, **7**, 99-107
- Paterson, T T, 1937 Studies in the Palaeolithic succession in England, 1: the Barnham sequence, *Proc Prehist Soc*, **3**, 87-135
- Payne, S, 1975 Partial recovery and sample bias, in *Archaeozoological studies* (ed A T Clason), 7-17, Amsterdam
- Penck, A, and Bruckner, E, 1909 *Die Alpen im Eiszeitalter*, Leipzig
- Peretto, C, 1994 *Le Industrie Litiche del Giacimento Paleolitico di Isernia la Pinetta*. Isernia: Istituto Regionale per gli studi storici del Molise 'V. Cuoco'
- Perrin, R M S, Rose, J, and Davies, H, 1979 Lithology of the Chalky Boulder Clay, *Nature*, **245**, 101-4
- Potts, R B, 1982 Lower Pleistocene site formation and hominid activities at Olduvai Gorge, Tanzania, unpubl PhD thesis, Harvard University
- Powers, M C, 1953 A new roundness scale for sedimentary particles, *J Sedim Petrol*, **23**, 117-19
- Preece, R C, 1992 Episodes of erosion and stability since the late-glacial: the evidence from the dry valleys in Kent, in *Past and present soil erosion* (eds M Bell and J Boardman), Oxbow Monograph, **22**, 175-84, Oxford
- Preece, R C (ed), 1995 *Island Britain: a Quaternary perspective*, Geological Society Special Publication, **96**, London
- Preece, R C, and Scourse, J D, 1987 Pleistocene sea-level history in the Bembridge area of the Isle of Wight, in *Wessex and the Isle of Wight: field guide* (ed K E Barber), 136-49, London
- Preece, R C, Scourse, J D, Houghton, S D, Knudsen, K L, and Penney, D N, 1990 The Pleistocene sea-level and neotectonic history of the eastern Solent, southern England. *Phil Trans R Soc Lond*, **B328**, 425-77
- Preece, R C, Lewis, S G, Wymer, J J, Bridgland, D R, and Parfitt, S A, 1991 Beeches Pit, West Stow, Suffolk, in *Central East Anglia and the Fen Basin: field guide* (eds S G Lewis, C A Whiteman, and D R Bridgland), 94-104, London
- Prestwich, J, 1859 On the westward extension of the old Raised Beach of Brighton; and on the extent of the seabed of the same period, *Q J Geol Soc Lond*, **15**, 215-21
- , 1860 On the occurrence of flint-implements, associated with the remains of animals of extinct species in beds of a late geological period, in France at Amiens and Abbéville, and in England at Hoxne, *Phil Trans R Soc Lond*, **150**(2), 277-317
- , 1861 Notes on some further discoveries of flint implements in beds of Post-Pliocene Gravel and Clay; with a few suggestions for search elsewhere, *Q J Geol Soc Lond*, **17**, 362-8
- , 1864 Theoretical considerations on the conditions under which the (drift) deposits containing the remains of extinct mammalia and flint implements were accumulated and on their geological age; and also on the loess of the valleys of the south of England, and of the Somme and the Seine, *Phil Trans R Soc Lond*, **154**, 247-309
- , 1872 On the presence of Raised Beach on Portsdown Hill, near Portsmouth. *Q J Geol Soc Lond*, **28**, 38-41
- , 1890 On the relation of the Westleton Beds, or pebbly sands of Suffolk, to those of Norfolk, and on their extension inland; with some observations on the period of the final elevation and denudation of the Weald and of the Thames valley, *Q J Geol Soc Lond*, **46**, 84-181
- , 1892 The Raised Beaches and 'Head' or Rubble Drift of the south of England; their relation to the Valley Drifts and to the glacial period; and on Late Post-Glacial submergence, *Q J Geol Soc Lond*, **48**, 263-343
- Pryor, W A, 1971 Grain shape, in *Procedures in sedimentary petrology* (ed R E Carver), 131-50, New York
- Pyddoke, E, 1950 An Acheulian implement from Slindon, *University of London, Institute of Archaeology, 6th Annual Report*, 30-3
- Rae, A M, and Ivanovich, M, 1986 Successful application of uranium series dating of fossil bone, *Appl Geochem*, **1**, 419-26
- Rabeder, G, 1972 Die Insectivoren und Chiropteren (Mammalia) aus dem Altpleistozän von Hundsheim (Niederösterreich), *Annalen Naturh Mus Wien*, **76**, 375-474
- Rage, J-C, 1974 Les batraciens des gisements Quaternaires Européens détermination ostéologique, *Extrait du Bulletin Mensuel de la Société Linnéenne de Lyon*, **43**, 276-89
- , 1984 Serpentes, in *Handbuch der Paläoherpetologie*, Teil 11, Stuttgart
- Raines, M G, and Chadfield, B C, 1991 Geophysical survey across a buried valley at Langley near Stevenage, Hertfordshire, *Project note of the Regional Geophysics Group, British Geological Survey*, No PN/91/3
- Rapp, G Jr, and Gifford, J A, 1985 *Troy: the archaeological geology*, New Jersey
- Reid, C, 1887 On the origin of dry valleys and of Coombe Rock, *Q J Geol Soc Lond*, **43**, 364-73
- , 1892 The Pleistocene deposits of the Sussex Coast and their equivalents in other districts, *Q J Geol Soc Lond*, **48**, 344-61

- , 1903 The geology of the country near Chichester, *Mem Geol Surv UK*
- Reid, D G, 1996 *Systematics and evolution of Littorina*, London
- Reineck, H-E, and Singh, I B, 1980 *Depositional sedimentary environments*, Berlin
- Rendell, H M, and Townsend, P D, 1988 Thermoluminescence dating of a 10m loess profile in Pakistan, *Quat Sci Rev*, 7, 251–55
- Reumer, J W F, 1984 Ruscinian and Early Pleistocene Soricidae (Insectivora, Mammalia) from Tegelen (The Netherlands) and Hungary, *Scr Geol*, Leiden, 73, 1–173
- , 1985 The generic status and species of *Drepanosorex* reconsidered (Insectivora, Mammalia), *Revue de paléobiologie*, 4, 53–8
- Rich, P V, 1980 Preliminary report on the fossil avian remains from the late Tertiary sediments at Langebaanweg (Cape Province), South Africa, *S Afr J Sci*, 76, 166–70
- Richmond, G M, 1996 The INQUA-approved provisional Lower-Middle Pleistocene boundary, in Turner (ed) 1996, 319–28
- Rightmire, G P, 1990 *The evolution of Homo erectus*, Cambridge
- Rixon, A E, 1976 *Fossil animal remains: their preservation and conservation*, London
- Roberts, M B, 1986 Excavation of a Lower Palaeolithic site at Amey's Eartham Pit, Boxgrove, West Sussex: a preliminary report, *Proc Prehist Soc*, 52, 215–45
- , 1990 Amey's Eartham Pit, Boxgrove, in *The Cromer Symposium, Norwich 1990: field excursion guide* (ed C Turner), 62–7, Cambridge
- , 1992 Boxgrove: the Lower Palaeolithic site in Amey's Eartham Pit (SU 924 085), in *The Archaeology of Chichester and District* (ed S Woodward), 21–4, Chichester
- , 1994 How old is Boxgrove man? Reply to Bowen and Sykes, *Nature* 371, 751
- , 1996 The age and significance of the Middle Pleistocene sediments at Boxgrove, West Sussex, UK and their associated archaeology, in *Neue Funde und Forschungen zur frühen Menschheitsgeschichte Eurasiens mit einem Ausblick auf Afrika* (eds K W Beinbauer, R Kraatz, and G A Wagner), 63–78, Sigmaringen
- Roberts, M B, Stringer, C B, and Parfitt, S A, 1994 A hominid tibia from Middle Pleistocene sediments at Boxgrove, UK, *Nature*, 369, 311–13
- Roberts, M B, Gamble, C S, and Bridgland, D R, 1995 The earliest occupation of Europe: the British Isles, in *The earliest occupation of Europe* (eds W Roebroeks and T van Kolfschoten), 165–91, Leiden
- Roberts, M B, Parfitt, S A, Pope, M I, and Wenban-Smith, F F, 1997 Boxgrove, West Sussex: rescue excavations of a Lower Palaeolithic landscape (Boxgrove Project B 1989–1991), *Proc Prehist Soc*, 63, 303–58
- Roberts, M B, Parfitt, S A, and Pope, M I, in prep *The archaeology of the Middle Pleistocene hominid site at Boxgrove, West Sussex, UK. Excavations 1990–1996*, English Heritage Monograph Series, London
- Robinson, A H W, 1964 The inshore waters, sediment supply and coastal changes of part of Lincolnshire, *East Midland Geographer*, 22, 307–21
- Rodwell, J S (ed), 1991 *British plant communities, volume 1: woodland and scrub*, Cambridge
- Roe, D A, 1968 *A gazetteer of British Lower and Middle Palaeolithic sites*, CBA Res Rep, 8, London
- , 1981 *The Lower and Middle Palaeolithic periods in Britain*, London
- Roebroeks, W, 1988 *From find scatters to early hominid behaviour: a study of Middle Palaeolithic riverside settlements at Maastricht-Belvédère (The Netherlands)*, *Analecta Praehistorica Leidensia*, 21, Leiden
- , 1994 Updating the earliest occupation of Europe, *Curr Anthropol*, 35(3), 301–5
- Roebroeks, W, and Kolfschoten, T van, 1994 The earliest occupation of Europe: a short chronology, *Antiquity*, 68, 489–503
- Roebroeks, W, and Kolfschoten, T van, 1995a A reappraisal of the evidence, in Roebroeks and van Kolfschoten 1995, 297–316
- Roebroeks, W and Kolfschoten, T van (eds), 1995b *The earliest occupation of Europe*. Leiden
- Roebroeks, W, Conard, N J, and Kolfschoten, T van, 1992a Dense forests, cold steppes, and the Palaeolithic settlement of northern Europe, *Curr Anthropol*, 33(5), 551–86
- Roebroeks, W, Loecker, D, Hennekens, P, and van Leperen, M, 1992b 'A veil of stones': on the interpretation of an early Middle Paleolithic low density scatter at Maastricht-Belvédère (The Netherlands), *Analecta Praehistorica Leidensia*, 25, 1–16
- Romans, J C C, and Robertson, L, 1974 Some aspects of the genesis of alpine and upland soils in the British Isles, in *Soil microscopy* (ed G K Rutherford), 498–510, Ontario
- Rose, J, 1987 Status of the Wolstonian glaciation in the British Quaternary, *Quaternary Newsletter*, 53, 1–9
- , 1988 Stratigraphic nomenclature for the British Middle Pleistocene: procedural dogma or stratigraphic common sense? *Quaternary Newsletter*, 54, 15–20
- , 1989 Tracing the Baginton-Lillington sands and gravels from the West Midlands to East Anglia, in *The Pleistocene of the West Midlands: field guide* (ed D H Keen), 102–10, Cambridge
- , 1992 High Lodge — regional context and geological background, in Ashton *et al* 1992a, 13–24
- , 1994 Major river systems of central and southern Britain during the Early and Middle Pleistocene, *Terra Nova*, 6, 435–43
- Rose, J, Allen, P, Kemp, R A, Whiteman, C A, and Owen, N, 1985 The early Anglian Barham soil of eastern England, *Soils and Quaternary landscape evolution* (ed J Boardman), 197–230, Chichester
- Rose, J, Davies, H, and Lewis, S G, 1992 Heavy mineral composition of the sands at High Lodge, in Ashton *et al* 1992a, 94–102
- Rousseau, D-D, 1987 Les associations malacologiques forestières des tufs 'Holsteiniens' de la France septentrionale: une application du concept de biome, *Bulletin de la Centre Géomorphologique*, 32, 9–18
- Rousseau, D-D, and Puisségur, J J, 1990 Phylogénèse et biogéographie de *Retinella* (*Lyrodiscus*) Pilsbry (Gastropoda: Zonitidae), *Geobios*, 23, 57–70
- Rousseau, D-D, Puisségur, J J, and Lécalle, F, 1992 West-European terrestrial mollusc assemblages of isotopic stage 11 (Middle Pleistocene): climatic implications, *Palaeogeogr, Palaeoclimat, Palaeoecol*, 92, 15–29
- Rouvilleis, A, 1974 Un foraminifère reconnu du plateau continental du Golfe de Gascogne: *Pseudoeponides falsobeccarii* n sp, *Cah Micropaléont*, 3, 3–10
- Ryslár, P, 1976 A craniometric comparison of Holocene populations of *Myotis mystacinus* (Kuhl 1817) and *M brandtii* (Eversmann 1845) (Chiroptera, Mammalia), *Bijdr Dierk*, 46(1), 71–9

- Rzebik-Kowalska, B, 1991 Pliocene and Pleistocene *Insectivora* (Mammalia) of Poland. 8. *Soricidae*: *Sorex* Linnaeus, 1758, *Neomys* Kaup, 1829, *Macroneomys* Fejfar, 1966, *Paenelimmococcyus* Baudelot, 1972, and *Soricidae* indeterminata, *Acta Zool Cracov*, **34**(2), 323-424
- Sadek-Kooros, H, 1972 Primitive bone fracturing: a method of research, *Am Antiq*, **37**(3), 369-82
- Sala, B, 1987 *Bison shoetensacki* Freud from Isernia la Pineta (early middle Pleistocene - Italy) and revision of the European species of *Bison*, *Palaeontogr Ital*, **74**, 113-70
- Sampson, C G (ed), 1978 *Paleoecology and archeology of an Acheulian site at Caddington, England*, Dallas
- Sanchiz, F B, 1977 La Familia Bufonidae (Amphibia, Anura) en el Terciario Europeo, *Trab Neogeno-Cuaternario*, **8**, 75-111
- Sarnthein, M, Stremme, H E, and Mangini, A, 1986 The Holsteinian interglacial: time stratigraphic position and correlation to stable isotope stratigraphy of deep sea sediments, *Quat Res*, **26**, 283-98
- Scaife, R G, 1986 The pollen, in Roberts 1986, 227-9
- Schachtschabel, P von, 1971 Methodenvergleich zur pH-Bestimmung von Böden, *Zeits PflErnähr, Düng Bödenk*, **130**, 37-43
- Schick, K D, 1986 *Stone Age sites in the making: experiments in the formation and transformation of archaeological occurrences*, BAR Int Ser, **319**, Oxford
- Schick, K D, and Toth, N, 1993 *Making silent stones speak*, London
- Schneiderhohn, P, 1954 Eine vergleichende Studie über Methoden zur quantitativen Bestimmung von Abrundung und Form an Sandkörnern, *Heideln Beitr Miner Petrogr*, **4**, 172-91
- Schoute, J F T H, 1987 Micromorphology of soil horizons developed during semi-terrestrial phases in transgressive and regressive sedimentary sequences in northern Netherlands, in *Soil micromorphology* (eds N Fedoroff, L M Bresson, and M A Courty), 661-7, AFES Plaisir
- Schoetensack, O, 1908 Der Unterkiefer des *Homo heidelbergensis* aus den Sanden von Mauer bei Heidelberg, *Ein Beitrag zur Paläontologie des Menschen*, Leipzig
- Schwarz, H P, and Latham, A G, 1984 Uranium-series age determination of travertines from the site of Vértesszöllös, Hungary, *J Archaeol Sci*, **11**, 327-36
- Serjeantson, D, 1988 Archaeological and ethnographic evidence for seabird exploitation in Scotland, *Archaeozoologia* **2**(1, 2), 209-24
- Sevilla, P, 1988 Estudio paleontológico de los Quirópteros del Cuaternario Español. *Paleont Evoluc*, **22**, 113-233
- Shackleton, N J, 1977 The oxygen isotope record of the Late Pleistocene, *Phil Trans R Soc Lond*, **B280**, 169-182
- , 1987 Oxygen isotopes, ice volume and sea level, *Quat Sci Rev*, **6**, 183-90
- Shackleton, N J, and Opdyke, N D, 1973 Oxygen isotope and palaeomagnetic stratigraphy of equatorial Pacific core V28-238: Oxygen isotope temperatures and ice volumes on a 105 and a 106 year scale, *Quat Res*, **3**, 39-55
- Shackleton, N J, and Hall, M A, 1984 Oxygen and carbon isotope stratigraphy of Deep Sea Drilling Project Hole 552A: Plio-Pleistocene glacial history, in *Initial reports. DSDP 81* (eds D G Roberts, D Schnitker et al), 599-609, Washington
- Shackleton, N J, Berger, A, and Peltier, W R, 1990 An alternative astronomical calibration of the Lower Pleistocene timescale based on ODP Site 677, *Trans R Soc Edinburgh: Earth Sciences*, **81**, 251-61
- Shackley, M L, 1975 *Archaeological sediments: a survey of analytical methods*, New York
- Shephard-Thorn, E R, and Kellaway, G A, 1977 Aney's Earham Pit, Boxgrove Common, in *South East England and the Thames Valley* (eds E R Shephard-Thorn and J J Wymer) INQUA Excursion Guide, 66-8, Norwich
- Shephard-Thorn, E R, and Kellaway, G A, 1978 Quaternary deposits at Earham, West Sussex, *Brighton Polytechnic Society Magazine*, **4**, 1-8
- Shephard-Thorn, E R, Berry, F G, and Wyatt, R J, 1982 *Geological notes and local details for 1:10000 sheets SU 80 NW, NE, SW and SE, SU 90 NW, NE, SW and SE, TQ 00 NW, SW West Sussex Coastal Plain between Chichester and Littlehampton*, Keyworth
- Shipman, P, 1981 Applications of scanning electron microscopy to taphonomic problems, in *The research potential of anthropological museum collections*, *Annals NY Acad Sci*, **376**, 357-86
- , 1983 Early hominid lifestyles: hunting and gathering or foraging and scavenging? in *Animals and archaeology: hunters and their prey* (eds J Clutton-Brock and C Grigson), BAR Int Ser **163**, 31-49, Oxford
- Shipman, P, and Rose, J, 1983a Early hominid hunting, butchering and carcass processing behaviours: approaches to the fossil record, *J Anthropol Archaeol*, **2**(1), 57-98
- Shipman, P, and Rose, J, 1983b Evidence of butchery and hominid activities at Torralba and Ambrona: an evaluation using microscopic techniques, *J Archaeol Sci*, **10**, 465-74
- Shotton, F W, 1953 The Pleistocene deposits of the area between Coventry, Rugby and Leamington and their bearing upon the topographic development of the Midlands, *Phil Trans R Soc Lond*, **B237**, 209-60
- , 1968 The Pleistocene succession around Brandon, *Phil Trans R Soc Lond*, **B254**, 387-400
- , 1986 Glaciations in the United Kingdom, in Šibrava et al 1986, 293-8
- , 1989 The exposures at Waverley Wood Farm (SP 3262 7135) north of Leamington Spa, in *The Pleistocene of the West Midlands: field guide* (ed D H Keen), Cambridge
- Shotton, F W, Goudie, A S, Briggs, D J, and Osmaston, H A, 1980 Cromerian interglacial deposits at Sugworth near Oxford, England, and their relation to the Plateau Drift of the Cotswolds and the terrace sequence of the Upper and Middle Thames, *Phil Trans R Soc Lond*, **B289**, 55-86
- Shotton, F W, Keen, D H, Coope, G R, Currant, A P, Gibbard, P L, Aalto, M, Peglar, S M, and Robinson, J E, 1993 The Middle Pleistocene deposits of Waverley Wood Pit, Warwickshire, England, *J Quat Sci*, **8**, 293-325
- Shrubsole, O A, 1898 On some high level gravels in Berkshire and Oxfordshire, *Q J Geol Soc Lond*, **54**, 585-600
- Šibrava, V, Bowen, D Q, and Richmond, G M (eds), 1986 Quaternary Glaciations in the Northern Hemisphere. Report of the International Geological Correlation Programme Project 24, *Quat Sci Rev*, **5**, 293-8
- Simpson, G G, 1941 Large Pleistocene felines of North America, *Am Mus Novit*, **1136**, 1-27
- Simpson, G G, and Roe, A, 1939 *Quantitative zoology*, New York
- Sinclair, J M, 1990 Flint pebbles of northern provenance in East Anglian Quaternary gravels, *Quaternary News*, **62**, 22-6
- , 1993 The origin and sedimentology of the Lower Pleistocene Westleton Beds, East Anglia, UK, unpubl MPhil thesis, London Guildhall University

- Singer, R, Wymer, J J, Gladfelter, B G, and Wolff, R G, 1973 Excavation of the Clactonian Industry at the Golf Course, Clacton-on-Sea, Essex, *Proc Prehist Soc*, **39**, 6-74
- Singer, R, Gladfelter, B G, and Wymer, J J, 1993 *The Lower Palaeolithic Site at Hoxne, England*, Chicago
- Smith, A J, 1985 A catastrophic origin for the palaeovalley system of the eastern English Channel, *Mar Geol*, **64**, 65-75
- Smith, M, 1964 *The British amphibians and reptiles*, London
- Smith, R A, 1915 Prehistoric problems in geology, *Proc Geol Assoc*, **26**, 3-4
- Smith, W G, 1894 *Man, the primeval savage*, London
- , 1916 Notes on the Palaeolithic floor near Caddington, *Archaeologia*, **67**, 49-74
- Soil Survey Staff, 1975 *Soil taxonomy: a basic system of soil classification for making and interpreting soil surveys*, SCS, USDA, Agricultural Handbook **436**
- Somerville, E M, 1996 Piltown reflections: a mirror for pre-history, *Sussex Archaeol Collect*, **134**, 7-19
- Spurrell, F C J, 1880 On implements and chips from the floor of a Palaeolithic workshop, *Archaeol J*, **37**, 294-9
- Stace, C, 1991 *New Flora of the British Isles*, Cambridge
- Stanford, D, Bonnicksen, R, and Morlan, R, 1981 The Ginsberg experiment: modern and prehistoric evidence of a bone flaking technology, *Science*, **212**, 438-9
- Stebbing, R E, 1967 Identification and distribution of bats of the genus *Plecotus* in England, *J Zool, Lond*, **150**, 291-310
- Stein, J K, 1987 Deposits for archaeologists, in *Advances in archaeological method and theory vol 11* (ed M B Schiffer), 337-95, New York
- Stein, J K, and Farrand, W A, 1985 *Archaeological sediments in context*, Orono
- Stein, J K, and Teltser, P, 1989 Size distributions of artifact classes: combining macro- and micro-fractions, *Geoarchaeology*, **4**(1), 1-30
- Stinton, F, 1985 British Quaternary fish otoliths, *Proc Geol Assoc*, **96**, 199-215
- Storch, G, 1975 Eine Mittelpleistozäne Nager-Fauna von der Insel Chios, Ägäis. *Senckenberg Biol*, **56**(4-6), 165-89
- Stringer, C B, 1983 Some further notes on the morphology and dating of the Petralona hominid, *J Hum Evol*, **12**, 731-42
- , 1985 Middle Pleistocene hominid variability and the origin of Late Pleistocene humans, in *Ancestors: the hard evidence* (ed E Delson), 289-95, New York
- , 1989 A neglected Middle Pleistocene comparison for the Bilzingsleben hominid material, *Ethnogr Archäol Z*, **30**, 492-6
- Stringer, C B, and Gamble, C S, 1993 *In search of the Neanderthals*, London
- Stringer, C B, Hublin, J J, and Vandermeersch, B, 1984 The origin of anatomically modern humans in Western Europe, in *The origin of modern humans: a world survey of the fossil evidence* (eds F H Smith and F Spencer), 51-135, New York
- Stuart, A J, 1974 Pleistocene history of the British vertebrate fauna, *Biol Rev*, **49**, 225-66
- , 1975 The vertebrate fauna of the type Cromerian, *Boreas*, **4**, 63-76
- , 1980 The vertebrate fauna from the interglacial deposits at Sugworth, near Oxford, *Phil Trans R Soc Lond*, **B289**, 87-97
- , 1981 A comparison of the Middle Pleistocene mammal faunas of Voigtstedt (Thuringia, German Democratic Republic) and West Runton (Norfolk, England), *Quartärpaläontologie*, **4**, 155-63
- , 1982 *Pleistocene vertebrates in the British Isles*, London and New York
- , 1988 Preglacial Pleistocene vertebrate faunas of East Anglia, in *Pliocene-Middle Pleistocene of East Anglia: field guide* (eds P L Gibbard and J A Zalasiewicz), Cambridge
- , 1992 The Pleistocene vertebrate faunas of West Runton, Norfolk, England, *Cranium*, **9**(2), 77-84
- Stuart, A J, and West, R G, 1976 Late Cromerian fauna and flora at Ostend, Norfolk, *Geol Mag*, **113**, 469-73
- Sutcliffe, A J, 1970 Spotted hyaena: crusher, gnawer, digester and collector of bones, *Nature*, **227**, 1110-13
- , 1975 A hazard in the interpretation of glacial/interglacial sequences, *Quaternary News*, **17**, 1-3
- Sutcliffe, A J, and Kowalski, K, 1976 Pleistocene rodents of the British Isles, *Bull Br Mus Nat Hist (Geology)*, **27**(2)
- Svoboda, J, 1987 Lithic industries of the Arago, Vértesszöllös, and Bilzingsleben hominids: comparison and evolutionary interpretation, *Curr Anthropol*, **28**(2), 219-27
- Swisher, C C, Curtis, G H, Jacob, T, Getty, A G, Suprijo, A, and Widiasmoro, 1994 Age of the earliest known hominids in Java, Indonesia, *Science*, **263**, 1118-21
- Sykes, G A, 1988 Amino acids on ice, *Chemistry in Britain*, **24**(3), 235-40
- , 1991 Amino acid dating, in *Quaternary dating methods: a user's guide* (eds P L Smart and P D Frances), Technical Guide **4**, QRA, Cambridge
- Szyndlar, Z, 1984 Fossil snakes from Poland, *Acta Zool Cracov*, **28**(1), 1-156
- Tarling, D H, 1983 *Palaeomagnetism*, London and New York
- Thieme, H, and Maier, R, 1995 *Archäologische Ausgrabungen im Braunkohlentagebau Schöningen, Landkreis Helmstedt, Hannover*
- Thieme, H, Mania, D, Urban, B, and van Kolfschoten, T, 1993 Schöningen (Nordharzvorland). Eine altpaläolithische Fundstelle aus dem mittleren Eisezeitalter. *Archäologisches Korrespondenzblatt*, **23**, 147-63
- Thierstein, H R, Geitzenauer, K R, Molfino, B, and Shackleton, N J, 1977 Global synchronicity of late Quaternary coccolith datum levels: validation by oxygen isotopes, *Geology*, **5**, 400-4
- Thomas, D H, 1986 *Refiguring anthropology*, New York
- Thompson, R, Aitken, M J, Gibbard, P L, and Wymer, J J, 1974 Palaeomagnetic study of Hoxnian lacustrine sediments, *Archaeometry*, **16**, 233-45
- Topal, G, 1963 The bats of the lower Pleistocene site from Mt Kövesvarad near Répáshuta, Hungary, *Annls Hist-nat Mus Natn Hung*, **55**, 143-54
- , 1964 The subfossil bats of the Vass Imre Cave, *Vertebr Hung*, **6**(1-2), 109-20
- Trinkaus, E, 1983 *The Shanidar Neanderthals*, New York
- Tucker, M E, 1982 *The field description of sedimentary rocks*, Geological Society of London, New York
- Tuffreau, A, 1992 L'Acheuléen en Europe occidentale d'après les données du bassin de la Somme, in *I primi abitanti della valle padana: Monte Poggiolo* (ed A Tuffreau), 41-9, Milan
- Tuffreau, A, and Sommé, J, 1988 *Le gisement Paléolithique Moyen de Biache-Saint-Vaast (Pas de Calais), Volume 1*, Mémoires de la Société Préhistorique Française, **21**
- Turner, A, 1992 Large carnivores and earliest European hominids: changing determinants of resource availability

- during the Lower and Middle Pleistocene, *J Hum Evol*, **22**, 109–26
- Turner, C, 1970 The Middle Pleistocene deposits at Marks Tey, Essex, *Phil Trans R Soc Lond*, **B257**, 373–440
- , 1973 High Lodge, Mildenhall, in *Quaternary Research Association field meeting guide, Clacton* (eds J Rose and C Turner), 101–5, London
- , 1975 The correlation and duration of Middle Pleistocene interglacial periods in north-west Europe, in *After the Australopithecines* (eds K W Butzer and G L Isaac), 259–308, The Hague
- (ed), 1996 *The early Middle Pleistocene in Europe*, Rotterdam
- Turner, C, and Kerney, M P, 1971 The age of the freshwater beds of the Clacton Channel, *J Geol Soc*, **127**, 87–93
- Turner, E, 1989 Miesenheim I: A Lower Palaeolithic site in the Middle Rhineland (Neuwied Basin), FRG, *Ethnogr Archäol Z*, **30**, 521–31
- , 1990 Middle and Late Pleistocene macrofaunas of the Neuwied Basin Region (Rhineland-Palatinate) of West Germany, *Jahrbuch des Römisch-Germanischen Zentralmuseums Mainz*, **37**, 135–396
- , 1991 Pleistocene stratigraphy and vertebrate faunas from the Neuwied Basin region of Western Germany, *Cranium*, **8**, 21–34
- , in press *Miesenheim I. Excavations at a Lower Palaeolithic Site in the Central Rhineland of Germany*, Mainz, RGZM
- Turner, G M, and Thompson, R, 1981 Lake sediment record of the geomagnetic secular variation in Britain during Holocene times, *Geophys J R Astr Soc*, **65**, 703–25
- Turner, G M, and Thompson, R, 1982 Detransformation of the British geomagnetic secular variation record for Holocene times, *Geophys J R Astr Soc*, **70**, 789–92
- Tylor, A, 1869 On Quaternary Gravels, *Q J Geol Soc Lond*, **25**, 79
- Valoch, K, 1991 Les premiers peuplements humains en Moravie (Tchécoslovaquie), in *Les Premiers Européens* (eds E Bonifay and B Vandermeersch), 189–94, Paris
- , 1995 The earliest occupation of Europe: eastern central and southeastern Europe, in *The earliest occupation of Europe* (eds W Roebroeks and T van Kolfschoten), 67–84, Leiden
- Vandenbergh, J, Múcher, H J, Roebroeks, W, and Gemke, D, 1985 Lithostratigraphy and palaeoenvironment of the Pleistocene deposits at Maastricht-Belvédère, southern Limburg, The Netherlands, *Meded Rijks Geol Dienst*, **39**(1), 7–18
- Van Vliet-Lanoë, B, 1982 Structures et microstructures associées à la formation de glace de ségrégation: leurs conséquences, *Proceedings of the Fourth Canadian Permafrost Conference*, 116–22, Ottawa
- , 1985 Frost effects in soils, in *Soils and Quaternary landscape evolution* (ed J Boardman), 117–58, Oxford
- Ventris, P A, 1986 The Nar Valley, in *The Nar Valley and North Norfolk: field guide* (eds R G West and C A Whiteman), 7–55, Coventry
- Villa, P, 1982 Conjoinable pieces and site formation processes, *Amer Antiq*, **47**, 276–90
- Viret, J, 1950 *Meles thoralis* n sp du loess Villafranchien de Saint-Vallier (Drôme), *Eclog Geol Helv*, **43**, 274–87
- Volobuev, V, and Ternovskii, D V, 1974 Comparative studies of the Karyotypes of the European and American minks (*Lutreola lutreola*, *L. vison*), *Zool Zh*, **53**(10), 1579–80
- Vreken, W J, and Múcher, H J, 1981 (Re)deposition of loess in southern Limbourg, The Netherlands, 1: field evidence for conditions of deposition of the Lower Silt Loam complex, *Earth Surface Processes and Landforms*, **6**, 337–54
- Waechter, J, d'A, Hubbard, R N L B, and Conway, B W, 1972 Swanscombe 1971, *Proc Roy Anthropol Inst Gr Brit Ir* (for 1971), 73–85
- Walder, P S, 1964 Mineralogy of the Eocene sediments in the Isle of Wight, *Proc Geol Assoc*, **75**, 291–314
- Ward, D J, 1981 A simple machine for bulk processing of clays and silts, *Terr Res*, **3**(3), 121–4
- , 1984 Collecting isolated microvertebrate fossils, *Zool J Linn Soc*, **82**, 245–59
- Warren, S H, 1955. The Clacton (Essex) channel deposits, *Q J Geol Soc Lond*, **155**, 283–307
- , 1957 On the early pebble gravels of the Thames basin from the Hertfordshire-Essex border to Clacton-on-Sea, *Geol Mag*, **94**, 40–6
- Wehmiller, J F, 1982 A review of Amino acid racemization studies in Quaternary molluscs: stratigraphic and chronologic applications in coastal and interglacial sites, Pacific and Atlantic Coasts, United States, United Kingdom, Baffin Island and Tropical islands, *Quat Sci Rev*, **1**, 83–120
- Weir, A H, and Catt, J A, 1965 The mineralogy of some Upper Chalk samples from the Arundel area, Sussex, *Clay Miner*, **6**, 97–110
- Weir, A H, and Catt, J A, 1969 The mineralogy of Palaeogene sediments in northeast Kent (Great Britain), *Sedim Geol*, **3**, 17–33
- Wells, A K, Gossling, F, Kirkaldy, J, and Oakley, K P, 1947 Studies of pebbles from the Lower Cretaceous rocks, *Proc Geol Assoc*, **58**, 194–258
- Wenban-Smith, F F, 1985 Analysis of experimentally produced flint debitage and on-site application of results, unpubl BA dissertation, Institute of Archaeology
- , 1988 Experimental replication of bifacial reduction sequences: are we doing it right? unpubl MA dissertation, Institute of Archaeology
- , 1989 The use of canonical variates for determination of biface manufacturing technology at Boxgrove Lower Palaeolithic site and the behavioural implications of this technology, *J Archaeol Sci*, **16**(1), 17–26
- Wessex Archaeology, 1994 The Sussex Raised Beaches and the Bristol Avon, *The Southern Rivers Palaeolithic Project: Report No 3, 1993–1994*, Salisbury
- West, R G, 1956 The Quaternary deposits at Hoxne, Suffolk, *Phil Trans R Soc Lond*, **B239**, 265–356
- , 1957 Interglacial deposits at Bobbitshole, Ipswich, *Phil Trans R Soc Lond*, **B241**, 1–31
- , 1963 Problems of the British Quaternary, *Proc Geol Assoc*, **74**, 147–86
- , 1980a *The pre-glacial Pleistocene of the Norfolk and Suffolk coasts*, Cambridge
- , 1980b Pleistocene forest history in East Anglia, *New Phytol*, **85**, 571–622
- , 1988 The record of the cold stages, *Phil Trans R Soc Lond*, **B318**, 505–22
- West, R G, and McBurney, C M B, 1955 The Quaternary deposits at Hoxne, and their archaeology, *Proc Prehist Soc*, **20**, 131–54
- West, R G, and Sparks, B W, 1960 Coastal interglacial deposits of the English Channel, *Phil Trans R Soc Lond*, **B243**, 95–133

- West, R G, Devoy, R J N, Funnell, B M, and Robinson, J E, 1984 Pleistocene deposits at Earningley, Bracklesham Bay, Sussex, *Phil Trans R Soc Lond*, **B306**, 137-57
- West, R G, Knudsen, K L, Preece, R C, and Robinson, J E, 1994 Palaeontology and taphonomy of late Quaternary fossil assemblages at Somersham, Cambridgeshire, England, and the problem of reworking, *J Quat Sci*, **9**, 357-66
- Whatley, R C, and Haynes, J R, 1986 Foraminifera and ostracoda, in Roberts 1986, 232-4
- Wheeler, A, 1969 *The fishes of the British Isles and North West Europe*, London
- , 1977 The origin and distribution of the freshwater fishes of the British Isles, *J Biogeogr*, **4**, 1-24
- White, G M, 1934 An Acheulian hand-axe from Chichester, *Proc Prehist Soc E Anglia*, **7**, 420-1
- White, M J, 1993 Lower Palaeolithic core and flake technology: a comparison of Hoxne and High Lodge, unpubl BA dissertation, University of London
- , 1995 Raw materials and biface variability in Southern Britain: a preliminary examination, *Lithics*, **15**, 1-20
- Whitehead, P F, 1989 Development and sequence of deposition of the Avon Valley Terraces, in *West Midlands: field guide* (ed D H Keen), Cambridge
- Whiteman, C A, 1992 The palaeogeography and correlation of pre-Anglian/Glaciation terraces of the river Thames in Essex and the London Basin, *Proc Geol Assoc*, **103**, 37-56
- Whiteman, C A, and Rose, J, 1992 Thames river sediments of the British Early and Middle Pleistocene, *Quat Sci Rev*, **11**, 363-75
- Whitten, D G A, and Brooks, J R V, 1983 *A Dictionary of Geology*, London
- Wilding, L P, and Drees, L R, 1990 Removal of carbonates from thin sections for microfabric interpretations, in *Soil micromorphology: a basic and applied science* (ed L A Douglas), 613-20, Amsterdam
- Wilhelmsen, K H, 1986 An investigation of archaeological sediment from Amey's Eartham Pit, England, unpublished mss, University of Washington, Seattle
- , 1989 *Spatial analysis and formation processes: problems with the current affair*, Paper presented at the 54th Annual Meeting of the Society for American Archaeology, Atlanta
- , 1992 Depositional and post-depositional processes at a Mid-Pleistocene archaeological deposit near Boxgrove, West Sussex, England, unpubl MA thesis, University of Washington, Seattle
- Wilkinson, I P, 1994 *Foraminifera from a suite of samples from the Chalk of the Chichester Sheet*, BGS Technical Report, WH94/8R, Keyworth
- Wilkinson, T J, and Murphy, P, 1986 Archaeological survey of an intertidal zone: the submerged landscape of the Essex coast, England, *J Field Archaeol*, **13**(2), 177-94
- Williams, K M, and Smith, G G, 1977 A critical evaluation of amino acid racemization to geochronology and geothermometry, *Orig Life*, **8**, 91-144
- Willoughby, P R, 1987 *Spheroids and battered stones in the African Early and Middle Stone Age*, BAR Int Ser **321**, Oxford
- Wilson, C M, 1982 Cutmarks and early hominid evidence for skinning, *Nature*, **298**, 303
- Wintle, A G, and Huntley, D J, 1997 Thermoluminescence dating of a deep sea sediment core, *Nature*, **279**, 710-12
- Wintle, A G, and Huntley, D J, 1980 Thermoluminescence dating of ocean sediments *Can J Earth Sci*, **17**, 348-60
- Wise, P, 1993 Waverley Wood Farm Pit, *Curr Archaeol*, **133**, 12-14
- Woelfle, E, 1967 Vergleichend morphologische Untersuchungen an Einzelknochen des postkranialen Skeletts in Mitteleuropa vorkommender Enten, Halbänse und Säger, Dissertation, Institut für Paläoanatomie, München
- Wood, B, 1992 Origin and evolution of the Genus *Homo*, *Nature*, **355**, 783-90
- Wood, B, and Turner, A, 1995 Out of Africa and into Asia, *Nature*, **378**, 239-40
- Wood, S V, 1882 Snow melt as a possible source of head gravel, *Q J Geol Soc Lond*, **38**, 721-34
- Woodborne, M W, Rogers, J, and Jarman, N, 1989 The geological significance of kelp-rafted rock along the west coast of South Africa, *Geo-marine Letters*, **9**, 109-18
- Woodcock, A, 1981 *The Lower and Middle Palaeolithic periods in Sussex*, BAR, **94**, Oxford
- Wymer, J J, 1957 A Clactonian flint industry at Little Thurrock, Grays, Essex, *Proc Geol Assoc*, **68**, 159-77
- , 1968 *Lower Palaeolithic archaeology in Britain, as represented by the Thames Valley*, London
- , 1974 Clactonian and Acheulian industries in Britain — their chronology and significance, *Proc Geol Assoc*, **85**, 391-421
- , 1983 The Lower Palaeolithic site at Hoxne, *Proc Suffolk Inst Archaeol Hist*, **35**, 169-89
- , 1985 *Palaeolithic sites of East Anglia*, Norwich
- , 1988 Palaeolithic archaeology and the British Quaternary sequence, *Quat Sci Rev*, **7**, 79-98
- Wymer, J J, Lewis, S G, and Bridgland, D R, 1991 Warren Hill, Mildenhall, Suffolk (TL 744743), in *Central East Anglia and the Fen Basin: field guide* (eds S G Lewis, C A Whiteman, and D R Bridgland), 50-8, London
- Yellen, J E, 1977 Cultural patterning in faunal remains: evidence from the 'Kung Bushmen', in *Experimental archaeology* (eds D Ingersoll, J E Yellen, and W MacDonald), 271-331, New York
- Young, B, and Lake, R D, 1988 *Geology of the country around Brighton and Worthing, memoir of the BGS: Sheets 318/333 (England and Wales)*, British Geological Survey, Keyworth, Nottingham
- Zagwijn, W H, 1985 An outline of the Quaternary Stratigraphy of the Netherlands. *Geologie Mijnb*, **62**, 17-24
- , 1992 The beginning of the Ice Age in Europe and its major subdivisions, *Quat Sci Rev*, **11**, 583-91
- Zagwijn, W H, Montfrans, van H M, and Zandstra, J G, 1971 Subdivision of the 'Cromerian' in the Netherlands: pollen analysis, palaeomagnetism and sedimentary petrology, *Geologie Mijnb*, **50**, 41-58
- Zeuner, F E, 1945 *The Pleistocene period*, London
- Zeuner, F E, 1958 *Dating the past*, London

Index

by INDEXING SPECIALISTS, 202
Church Road, HOVE, East Sussex BN2
3DJ

Note: Page numbers in bold indicate main entries; those in *italics* denote figures or tables.

- Acanthinula aculeata* 172
Acheulean stone tools 4, 13, 423
Agopinella 172
Aethichinus algerius 198–9, 200–2
Agassiz, L. 5
age of Boxgrove site
 amino acid geochronology 295–7, 296, 303
 calcareous nannoplanktons 300–3, 300, 301, 302
 electron spin resonance 294–5, 294, 295, 303
 horse as indicator 228
 luminescence dating 292–4, 293, 294, 303
 mammalian fauna indicators 197, 303–7
 molluscan fauna indicators 175
 Oxygen Isotope Stage correlation 296–7, 301–3, 303–4, 307, 424
 palaeomagnetic measurements 297–9, 297, 298, 299
 uranium series dating 291, 291, 294–5, 294, 295, 303
 vertebrate fauna indicators 157, 160
Aldingbourne event 29
Aldingbourne Formation 21, 27, 29
Aldingbourne Park Pit 29
 gravel analysis 101–2, 110
 Aldingbourne raised beach 13
 gravel analysis 101–2, 104, 109, 110
 non-flint clasts 109, 110
 alkali feldspar, fine sand mineralogy 113, 116
alkaline marl, Unit 4d 131–2, 139
Alpine orogenic event 9, 21
Altamura, Italy, hominid remains 419, 421
amino acid geochronology 295–7, 296, 307
Annonia batavus 164, 165, 168
Annonia falobecarii 164, 165, 168
amphibians 131, 181–4, 185–7
Anas sp 189, 194
Anas crecca (teal) 189
Anas penelope (widgeon) 189
Anas platyrhynchos (mallard) 188–9, 188, 196, 196
cf. Anas querquedula (garganey) 189
anatase 114
andalusite 114
Andrews, P 399
Anglian Glaciation
 dating of 309–12
 European landbridge breaching 423
 faunal assemblage 304, 309–10
 hominid activity 383–4, 425
 palaeogeography 31, 31, 150
 Units 10 & 11 deposition 154, 155, 423
Anguilla anguilla (eel) 176, 180
Anguis fragilis (slow worm) 184–5, 184, 186
Angular Chalk Bed *see* Unit 7
angularity/roundness analysis, gravels 102–9, 103, 104, 105, 106–7
Anisus leucostoma 172
Anser sp 188
Anser anser (greylag goose) 188
antlers, as percussors 385, 386, 387, 394
apatite 114, 115, 116
Apodemus maastrichtiensis (extinct mouse) 267–70, 267, 268–9
Apodemus sylvaticus (wood mouse) 268–9, 270–1, 271, 277, 280–1, 289
Apus apus (swift) 192, 194
aquatic species
 birds 131, 187–91, 194, 282
 plants 83
 small mammals 281
Arago Cave, France, hominid remains 417
‘archaic *Homo sapiens*’ 417, 418
Arctica islandica 295
Arenicolites 60, 63, 64, 65, 69, 75, 77, 80
arkosic sandstone, presence in beach deposits 110
artefacts *see* flint artefacts
artiodactyla 231–44, 307
Arun, River 1, 9, 12
Arvicola terrestris cantiana (water vole)
 biostratigraphy 304, 305, 306
 palaeontology 160, 249, 249–50, 277, 280, 282, 289
Atapuerca, Spain, hominid remains 415, 419, 421
Aurila spp 164
Aveley, Palaeogene gravels 105
avifauna *see* birds
Avisford Bridge 9
Avisford Dell 9
Avisford Dell Pit 15
axes *see* flint artefacts, handaxes
Aythya fuligula (tufted duck) 189–90
Azeca goodalli 173
badger *see* *Meles*
Baffincyttere howei 168–9, 168
Balamis crenata 174
bank vole *see* *Clethrionomys glareolus*
barnacles 71
Barnham, dating of deposits 304–5
bats 211–14
beach deposits
 see also raised beaches
 angularity/roundness of flint 102–9, 104, 105, 106–7
 GTP 25 49–52, 50, 51, 52, 53, 61–2, 61, 70, 83
 stratigraphic sequence 49–52
bear *see* *Ursus*
beaver *see* *Castor fiber*
Bechstein’s bat *see* *Myotis bechsteini*
Beeches Pit
 dating of deposits 304–5
 faunal comparison with Boxgrove 244, 245, 260
Bembridge deposits 15, 29
Bembridge raised beach
 exotic rocks 110
 gravel analysis 102, 105
Bergman, C A 385, 387, 388, 395
Betula (birch), charcoal 427
Bilzingsleben, Germany, hominid remains 417–18
Binford, L R 399–400, 409
Binstead Valley 14
biostratigraphy 303–10
biotite 114, 115, 116
bioturbation
 basal beds 47
 flint artefacts 321, 372, 378
 Unit 3
 Marine Cycle 1 55, 58, 59, 60
 Marine Cycle 2 63, 64, 65, 66, 67, 68, 69
 Marine Cycle 3 71, 73, 74, 75, 76, 77, 79
 Unit 4a 81, 82
 Unit 4b 84, 86
 Unit 4c 152
birch mouse *see* *Sicista*
bird pellets, Unit 4c 130
birds
 aquatic 131, 187–91, 194, 282
 recovery methods 193, 196
 remains 187–96
 skeletal element ratios 193–4, 194
Birling Gap 12
Bishop, M J 160
Bison sp 242–3, 242, 243
Bison priscus 242–3
Bison schoetensacki 242–3
bivalves
 see also mollusca
 immature (*Mytilidae*) 60, 64, 68, 72, 74, 75, 76, 79, 80
Black Rock, Brighton, age of deposits 228–9
black-headed gull *see* *Larus ridibundus*
Blackwater, River estuary 131
blue-fin tunny *see* *Thunnus thynnus*
Bognor Rock
 erratics 12, 100
 presence in beach deposits 109
Bombina variegata 182
bone marrow, extraction 397, 398, 400–1
bones
 carnivore gnawing 401, 402, 406, 408, 408, 414
 chopmarks 400
 collecting methods 161–3
 cut marks 276, 398, 398–400, 400, 401, 402, 403, 414
 filleting marks 405, 407
 hominid 420–2, 420–1, 422
 human modification of 395–415, 396, 397, 399
 impact damage 397, 398, 400–1
 as percussors 385, 387, 387, 394
 scrapemarks 397, 400

- thin section micromorphology 121, 122
Unit 4c 129
uranium series dating 291, 291
- Bordes, F 385, 387
- Boxgrove roundabout 29
- Boyn Hill Sea 14
- Bracklesham 9
- Bracklesham Group 21, 169
- Bradley, B 388–9
- Brandt's bat *see Myotis brandti*
- Brickearth Beds *see* Unit 6
- Brighton Raised Beach 8–9, 13
age of deposits 228–9
exotic rocks 110
- Broadwater 9
- brookite 114, 117
- Brooks' Field, gravel analysis 101–2, 104, 110
- Brown, J 100–1
- Bruckner, E 5, 6
- Brunhes magnetic chron 299
Matuyama/Brunhes magnetic boundary 6
- Bucephala clangula* (goldeneye) 190
- Bufo* sp 185, 186
- Bufo bufo* (common toad) 182, 182, 183, 185, 186
- Bufo calamita* (natterjack toad) 182, 182, 183, 186
- Bufo viridis* 182, 183
- bulk sample analysis 120, 162–3
- bulk sieving 162–3
- Bunn, H T 398
- Burton Park 9
- butchery
see also horse butchery site
evidence 127, 276, 382, 399–401
tools 380
- Caddington 339, 385
- calcareous clay fragment 127, 128
- Calcareous Head Gravel *see* Unit 10
- calcareous nannoplanktons 300–3, 300, 301, 302
- Calcidiscus leptoporus* 301
calcite pseudomorphs, Unit 8 146
- calcium carbonate, sediment content 112, 113, 120
- Calkin, B 13
- Callistocythere curryi* 165
- Candona* 164
- Canis lupus* (wolf) 214, 214–17, 215, 216, 217, 290, 306
- 'Cannonshot Gravel' 109
- Canonical Variates Analysis (CVA), knapping experiments 390–3, 394
- Capreolus capreolus* (roe deer) 236, 236–9, 237, 238, 277, 281, 282, 289, 408
- caprids 243
- carnivores
biostratigraphy 306
bone gnawing 401, 402, 406, 408, 408, 414
European record 424
palaeontology 214–26
- Carychium tridentatum* 172
- Castor fiber* (beaver) 134, 252–4, 253, 254, 282, 290
- cave bear *see Ursus deningeri*
- cementation, Slindon Sands 56–7
- cervidae 231–42
- Cervus elaphus* (red deer)
human modification of bones 276, 322, 396, 408–10, 409, 410, 411, 412–13, 414, 415, 416
palaeontology 231–3, 232, 233
- Chalk
foraminiferal analysis 21
Pleistocene cliff collapse 21, 26
presence in beach deposits 109
stratigraphy 21, 22, 23
chalk mud, GTP 25 145
- Chalk Pellet Beds *see* Unit 8
- Charadriidae 190
- charcoal fragments
analysis 427
Unit 11 123, 148
- chatter marks 102, 103, 109
- chiroptera 211–14
- chlorite 114, 115, 116
- cf Chondrites* 59
- chopmarks, bones 400
- Cibicides lobatulus* 164
- Clacton
dating of deposits 304–5
faunal comparison with Boxgrove 233, 233, 234
- Clacton Channel Deposits 101
- clast-lithological analysis, gravels 100–2, 102
- clay mineralogy 113
- Clay-with-flints 12, 13, 21, 155
mineralogy 116, 117
- Clethrionomys glareolus* (bank vole) 247, 247–8, 280–1, 282, 289, 290
- Clethrionomys rufocanus* (grey-sided vole) 248, 248, 290
- cliff collapse, Pleistocene 21, 26, 38, 49, 382
- cliff-line, location 26, 37–42, 39, 49, 394–5
- climate indicators
ostracods 164–5, 168–9
small mammals 281–2
- Clupeidae (herring family) 176, 178
- coarse silt mineralogy 114–16, 115
- coccoliths *see* nannofossils
- Coccolithus pelagicus* 301
- cod *see Gadus morhua*
- Codrington, T 12
- collecting methods, vertebrate remains 161–3
- collophane 114, 117
- colours, sediments 74, 75, 79, 80, 99, 150
- Colomella edentula* 173
- common long-eared bat *see Plecotus auritus*
- common vole *see Microtus arvalis*
- Conger conger* (Conger eel) 176, 178
- Cook, J 399
- Cooke, J H 13
- cortical flint hammers 387
- Coutier, L 385
- Crabtree, D E 385, 387, 388
- Crayford 385
- Cretaceous geology 21, 22, 23, 26
- Crocata crocata* (spotted hyaena) 224–5, 224, 225, 306, 406
- Cromerian Complex
Apodemus maastrichtensis (extinct mouse) 270
Arvicola (water voles) 249–50
dating of 6
faunal assemblage 160, 304–5, 306
rhinoceros 230, 231
shrew fauna 208
- cryogenic features
Unit 8 146
Unit 11 98, 136
- cubicinia 42
- Culver Chalk 21, 26
- Curwen, E C 14
- cut marks, bones 276, 398, 398–400, 400, 401, 402, 403, 414
- Cygnus cygnus* (whooper swan) 187–8
- Cypridius torosa* 164, 169
- Cytheropteron latissimum* 164
- Cytheropteron nodosum* 164
- Dalrymple, J B 15
- Dama clactoniana* 234
- Dama dama* (fallow deer) 234, 234–6, 235, 281, 282, 408
- debitage, flint artefacts 320, 322
- decalcification, Slindon Silts, Q2/A 354
- deer
antlers as percussors 385, 386, 387, 394
remains 231–42
- deformation structures
possible human activity 129, 140
Unit 4 81, 85, 140, 313
Unit 5a (Organic Bed) 363
Unit 6 94
- depositional environments 124–49, 125, 136–42, 424–5
- depositional remanent magnetisation (DRM) 297
- diatoms 157
- Dictyococcus* sp 301
- digging tools 382
- Diluvium 5, 9
- dinoflagellate cyst analysis 427, 427
- cf Diplocraterion* 59, 65, 67, 74, 80
- Diplocraterion jayo* 46, 59
- Dixon, F 9
- Dmanisi, Georgia, hominid remains 415, 416
- doggers 47
- domichnia 42
- dormice 254–60
- Downland block, vegetation 157
- drainage patterns 149–50
- drift deposits, theories of origin 9, 12, 15
- drop-stone erratics 111
- dry valleys 13, 14, 14
- ducks 188–90, 194, 194
- dunnock *see Prunella modularis*
- Earnley 30–1
coccolith comparison with Boxgrove 164, 169, 170
exotic rocks 110
- Eartham Formation
see also Units 5b–11
depositional environment 154
flint artefacts 382–4
geological summary 153–5
palaeoecology 282, 289–90

- sediment source 153
 sediments 27, 35–6, 35, 36
 sub-units 37
- Eartham Quarry complex
see also Quarry 1; Quarry 2
 aerial view 4
 Boxgrove Project methodology 15–19,
 18
 excavation areas 3, 17
 quarrying methods 15–16
- Eartham Quarry Project 425–6
- Eartham Upper Gravel Member 98–9, 153
 fauna 289–90
- earthworm excrements 123, 129
- eel *see Anguilla anguilla*
- Ehringsdorf, Germany, hominid remains
 418
- electron spin resonance, U-series analysis
 294–5, 294, 295
- elephant 226
- Elephant Bed 9
- Elomys quercinus* (garden dormouse) 259,
 259–60, 260, 282, 289
- Elphidium clavatum* 164
- Elphidium crispum* 164, 165, 168
- Elphidium excavatum* gr 164, 168
- Elphidium selseyense* 165
- Elphidium williamsoni* 169
- Elsden, J V 12
- Elveden, dating of deposits 304
- Emiliaia husleyi* 302
- Enchytraeids 129, 130, 135
- environmental indicators
Castor fiber (beaver) 254
 fish 178, 180–1
 foraminifera and ostracods 164–5,
 168–9, 169–70
 herpetofauna 186–7
 molluscs 172
Muscardinus atellanarius (hazel dor-
 mouse) 259
 vertebrates 157
- Eocene geology 21, 22
- epidote 114, 115, 116
- Equus ferus* (horse)
 butchery site 127, 227, 373–8, 377, 378,
 399
 GTP 17 227, 228, 399, 403–5
 human modification of bones 397, 400,
 401, 402, 403–5, 403, 404
 palaeontology 226–9, 227, 228
- Erinaceus* sp. (hedgehog) 197, 198–9, 199,
 200–2
- cf. Erithacus rubecula* (robin) 192, 194, 196
- erratics, Selsey 9, 12, 100
- estuarine sediments, Unit 4a 126–7, 140
- Europe
 colonisation by hominids 422–4
 Middle Pleistocene hominids 415–19
 taxonomic habitat index spectra 274,
 277
- European mink *see Mustela lutreola*
- Everyman's Pit
 marsh sediments 153
 unconformity 150
- excavation, methodology 312–13
- exotic clasts 100–1, 109–11
- experiments, flint knapping 384–95
- extinct species 160
- Eye, gravel analysis 108
- facies analysis 42
- fallow deer *see Dama dama*
- Fan Gravel Beds
 gravel analysis 101, 102, 104, 104, 105
 sediment sequence 36, 78, 90, 97
- faunal groups, relative abundance 280
- faunal list 283–5
- Fe-Mn bands *see iron-manganese bands*
- Felis silvestris* (wild cat) 178, 225, 225–6,
 277
- field vole *see Microtus agrestis*
- filleting marks, bones 405, 407
- fine sand mineralogy 113–14, 114
- fish remains 175–81, 176, 177, 179, 180
 accumulation by predators 178–80
 as environmental indicators 178,
 180–1
 seriation 180–1, 180
 Slindon Sand Member 177–8
 Slindon Silts 127, 128, 140, 178–80
 Unit 4d 282
- flagstone, presence in beach deposits 110
- flint, fine sand mineralogy 113, 116
- flint artefacts
 Canonical Variates Analysis (CVA)
 390–3, 394
 cortical flint hammers 387, 394–5
 debitage
 Q1/A 320, 322, 329, 335, 341–2
 Q1/B 341–2, 348, 351–3
 distribution
 Q1/A 316, 329
 Q1/B 339, 341–2, 341, 342, 343, 344
 early finds 2–4, 13, 15
 Eartham Formation 382–4
 end-shock 339
 finishing flakes 357–9, 393
 flake attributes 387–94, 388, 389, 391,
 392, 394, 395
 flake tools, Q1/B 343, 345
 GTP 17 372–8, 374, 374/5, 375, 376,
 377
 hammerstones, Q1/B 343, 345, 350–1
 handaxes
 first appearance in Europe 423
 GTP 17 373, 374
 head gravels 381, 383–4, 383
 manufacturing technique 385
 Q1/A 319–20, 319, 322, 322, 323–6,
 339
 Q1/B 344–8, 346–7, 348
 Q2/A 360, 360, 361
 hard hammer flakes 352–3, 387–9
 hard hammer percussors 385, 386, 395
 knapper's position 329, 341, 382
 knapping experiments 320, 384–95
 knapping technology 384–95
 microartefact project 362–72
 movement of artefacts 320–1, 361,
 371–2
 nodules 356, 360, 360, 373
 percussors 384–95, 386–7
 post-depositional processes 321–2, 354,
 355, 361, 363, 371–2
- Q1/A
 Unit 4b 86, 121, 322–39, 322, 325–6,
 327, 328, 329, 330–4, 335, 336–8,
 339
 Unit 4c 315–22, 316, 317, 318, 319,
 320
- Q1/B 339–54, 340, 345, 346–7, 348,
 349, 351, 352, 353
- Q2/A 354–61
 reduction sequence 317, 319, 335, 339,
 353
 refitting
 GTP 17 373
 Q1/A 320–1, 320, 321, 335–9, 335,
 336–8, 339
 Q1/B 348–50, 348, 349, 352
 Q2/A 356, 356, 357, 358, 359–61,
 359, 360, 361
- residual 378–84
- roughing-out flakes 356, 380, 381, 385,
 394
- scatter
 GTP 17 373–8, 375, 376, 393–4
 GTP 25 379, 379, 380
 Q1/A 322, 327, 328, 329, 329, 330–4,
 394
 Q2/A 355, 361, 393
 soft hammer flakes 335, 359, 387–9
 soft hammer percussors 385, 386–7,
 387, 394, 395
 source of raw material 356, 359–60,
 360, 384, 394–5, 424
 technological attributes
 Unit 4b 329
 Unit 4c 318, 351–3, 351
 thinning flakes 72, 335, 357, 393
 tranchet flakes 360, 361, 385
 trimming flake, GTP 25 81
 Unit 5c 122, 135
 Unit 8 123, 379, 379, 380
 Unit 11 383–4, 383
 uses for 380, 382
- flint buildings 2
- flint clasts
 angularity/roundness analysis 102–9,
 103, 104, 105, 106–7
 post-depositional damage 10eworked
 103
- flint pebbles as percussors 385, 389
- flounder *see Platichthys flesus*
- fluvial gravels 108–9
- fodichnia 42
- foraminifera 163–70, 165, 167, 168
 Chalk 21
 Unit 3 126
- Fowler, J 13
- fragipan formation, Unit 6 144
- freshwater fauna, Unit 5a 134, 138
- frogs *see Rana*
- fugichnia 42, 69
- Gadidae (cod family) 177, 178
- Gadus morhua* (cod) 177, 178
- Gailenreuth Cave, faunal comparison
 with Boxgrove 226
- Gallinula chloropus* (moorhen) 190
- garden dormouse *see Elomys quercinus*
- garganey *see Anas querquedula*
- garnet 114, 116, 117
- Garraway-Rice, R 13
- Gasterosteus aculeatus* (three-spined stickle-
 back) 176, 177, 178, 180, 181, 282
- gastroliths, pebble transport mechanism
 111
- geological map 24
- geological summary 149–55

- Geological Test Pits *see* GTP
- Gephyrocapsa* 301, 302–3, 302, 303
- glacial periods
- Anglian Glaciation 31, 31, 150, 154, 155, 309–12, 423
 - chronostratigraphy 5–8, 6, 7
- glaciation, lack of evidence at Boxgrove 99, 111, 150
- glaciofluvial deposits, flint rounding 109
- glaucinite 113, 116, 127
- glaucinitic marl, presence in beach deposits 109
- cf* 'Glossifungites' 74, 80
- Glossifungites* ichnofacies 46
- Godwin-Austin, R A C 9
- goldeneye *see* *Bucephala clangula*
- Goodwood-Slindon Raised Beach (40m beach) 27–8, 384
- grain size data 124
- granite, presence in beach deposits 110
- grass snake *see* *Natrix natrix*
- grassland stage (Unit 4c) 152, 152, 280–1
- gravel, non-flint material 109–11
- gravel extraction 2
- gravels
- analysis 100–11
 - angularity/roundness analysis 102–9, 103, 104, 105, 106–7
 - clast-lithological analysis 100–2, 102
 - grazing animals 152
- great auk *see* *Pinguinus impennis*
- Green, J F N 14
- Greensand chert, presence in beach deposits 109, 110
- Grey Interval, GTP 13 74, 79, 80
- grey partridge *see* *Pardix perdix*
- grey-sided vole *see* *Clethrionomys rufocanus*
- greylag goose *see* *Anser anser*
- greywackes, presence in beach deposits 110
- Grimes Graves 385
- Grinsell, L V 13
- GTP 3
- bulk sample analysis 120
 - Capreolus capreolus* (roe deer) 236, 238
 - Clethrionomys glareolus* (bank vole) 247
 - Crocuta crocuta* (spotted hyaena) 224
 - fish remains 176
 - Mustela erminea* (stoat) 220
 - Myopus schisticolor* (wood lemming) 245
 - Myotis bechsteini* (Bechstein's bat) 213
 - Myotis mystacinus* (whiskered bat) 213
 - Neomys* sp (water shrew) 203
 - Plecotus auritus* (common long-eared bat) 212
 - Pliomys episcopalis* (extinct vole) 249
 - Sciurus* sp (squirrel) 245
 - Sorex (Drepanosorex) savini* (extinct shrew) 208
 - Sorex minutus* (pygmy shrew) 205
 - Unit 4c, micromorphology 121
 - Unit 5a 132, 134
 - Unit 5b 134, 137–8
- GTP 5
- Brickearth Beds 93–4, 93
 - luminescence dating 292–3, 293
 - sediment sequence 75–6, 75, 76, 77, 78, 91
 - Unit 4a 82
 - Unit 4b 84
- Unit 4c 87, 89
- Unit 5a 89
- Unit 5b 92
- Unit 9 97
- GTP 8
- bone and flint concentration 414
 - flint artefacts 322
 - Mustela lutreola* (European mink) 222
- GTP 9, luminescence dating 292–3, 293
- GTP 10
- Brickearth Beds 93
 - fish remains 178, 179
 - sediment sequence 56/7, 57, 58
 - Slindon Silts 80
 - stratigraphy 133
 - Unit 3
 - Marine Cycle 1 56, 59–60, 61
 - Marine Cycle 2 64, 68, 69–70
 - Marine Cycle 3 72, 75
 - Unit 4a 82
 - Unit 4b 84, 127, 128–9
 - Unit 4c 87, 89, 121
 - Unit 5a 89, 132, 134
 - Unit 5b 92
 - Unit 6 136–7, 143, 144, 145
- GTP 11, luminescence dating 292–3, 293
- GTP 13
- bulk sample analysis 120
 - chalk debris 21, 56, 83
 - chemical composition of sediments 112–13, 113
 - dating
 - calcareous nannofossils 300–3, 300, 302
 - luminescence dating 292–3, 293
 - palaeomagnetic measurements 297–9, 297, 298, 299 - deformation structures 81
 - dinoflagellate cysts 427, 427
 - fish remains 176, 178
 - flint artefacts 378, 382
 - foraminifera 163–5, 165, 167, 168
 - Grey Interval 74, 79, 80
 - mineralogy 113
 - ostracods 59, 67, 74, 163–5, 165, 166, 168
 - particle size distribution 112, 113
 - sediment sequence 54, 54/5, 55, 56, 58
 - stratigraphy 133
 - trace fossils 45
 - type section 26
 - Unit 3
 - Marine Cycle 1 52–5, 58–9, 60–1, 62
 - Marine Cycle 2 62, 63–4, 66–8, 67, 69
 - Marine Cycle 3 71–2, 72, 73–5, 378
 - Unit 4a 81–2, 82, 127
 - Unit 4b 84, 127, 127
 - Unit 4c 87, 89
 - Unit 5a 89, 112, 132, 134
 - Unit 5b 90, 92, 112, 134, 135, 137–8
 - Unit 6 93, 136–7, 143, 144, 145
 - Unit 9 97
 - Yellow Interval 74, 75, 79
- GTP 14, *Castor fiber* (beaver) 253, 254
- GTP 15, *Sorex minutus* (pygmy shrew) 205
- GTP 16, *Myotis mystacinus* (whiskered bat) 212
- GTP 17
- Bison* sp 242, 243
 - Capreolus capreolus* (roe deer) 238
 - Castor fiber* (beaver) 253–4
 - Cervus elaphus* (red deer) 409, 409
 - Equus ferus* (horse) 227, 228, 399, 403–5
 - Erinaceus* sp (hedgehog) 198
 - excavation methodology 312–13, 372–3, 372, 373
 - faunal remains 373, 374/5, 414
 - fish remains 176
 - flint artefacts 372–8, 374, 374/5, 375, 376, 377
 - granite pebbles 110
 - horse butchery site 127, 227, 373–8, 377, 378, 399, 400, 401, 402, 403, 414
 - Lepus timidus* (mountain hare) 273
 - Myopus schisticolor* (wood lemming) 245
 - Plecotus auritus* (common long-eared bat) 212
 - Pliomys episcopalis* (extinct vole) 249
 - sedimentary sequence 372
 - Stephanorhinus hundsheimensis* (extinct rhinoceros) 230
 - Unit 4b 127, 128, 128
 - Unit 4c 129, 130, 131, 139
 - Unit 5c 93, 135, 137, 142
- GTP 20, Unit 5a 88–9
- GTP 25
- beach deposits 49–52, 50, 51, 52, 53, 61–2, 61, 70, 83
 - chalk mud 73, 92, 145
 - deformation features 92
 - Equus ferus* (horse) 227
 - flint, angularity 104
 - gravel, lithological analysis 101–2
 - sediment sequence 32, 33, 54/5, 73
 - Unit 3
 - Marine Cycle 1 57–8, 60
 - Marine Cycle 2 61–3, 64–6
 - Marine Cycle 3 70, 72–3
 - Unit 4a 81
 - Unit 4b 83–4
 - Unit 4c 87
 - Unit 5a 88, 132, 138
 - Unit 5b 92, 92
 - Unit 8 95–6, 146
- GTP 26
- sediment sequence 56/7
 - Unit 3
 - Marine Cycle 1 55–6, 60, 61
 - Marine Cycle 2 62, 68–9, 70
 - Marine Cycle 3 72, 76–7, 79
 - Unit 4a 82
 - Unit 4b 86
 - Unit 5b 92
 - Unit 8 96
- GTP 30
- arkosic sandstone 110
 - Microtus (Terricola) cf subterraneus* (pine vole) 250
- GTP 35
- calcareous nannofossils 300–3, 300
 - section 48
- gurnard *see* Triglididae
- habitats
- see also* environmental indicators
 - taxonomic habit indices 274, 275, 276, 277
- haematite 113

- Halnaker Hill 150
 Hampshire Basin, pre-Pleistocene deposits 21
 handaxes *see* flint artefacts
 Havant Thicket 116
 hazel dormouse *see* *Muscardinus arvensis*
 head deposits *see* drift deposits
 Head Gravels 97–9, 97, 98, 99, 116
see also Unit 11
 hedgehog *see* *Erinaceus*
Hemicythere villosa 164
Hemicytherina clathrata 164, 168–9
 herpetofauna 181–7, 186
 herring family *see* Clupeidae
Heterocythereis albomaculata 164
 Hey, R W 101
Hiatella arctica 174
 High Lodge, Suffolk 310, 311, 424
 High-sea-level event 2, correlation 295–6
 Hodgson, J M 15
 hominid record, Pleistocene 415–19, 417
 hominid remains
see also human activity
 tibia 420–2, 420–1, 422
 Unit 4d 282
Homo erectus 416–17
 '*Homo ergaster*' 419
Homo heidelbergensis 416–17, 419, 420–1
Homo sapiens, 'archaic' 417, 418
homotaxis 304
 hornblende 114, 115, 116
 Horne, D J 165
 horse *see* *Equus ferus*
 horse butchery site, GTP 17 127, 227,
 373–8, 377, 378, 400, 403–5
 Hoxne, age of deposits 304–5
 Hoxnian interglacial 157, 160, 304, 306,
 309–10
 human activity
see also flint artefacts; hominid remains
 animal bone modification 395–415, 396,
 397, 399
 behavioural patterns 378, 425
 colonisation of Europe 422–4
 earliest British sites 311
 evidence for 123, 149, 192–3
 horse butchery site 127, 227, 373–8,
 377, 378, 400
 hunting 378, 415, 424
 Unit 3 276
 Unit 4b 127, 128–9
 Unit 4c 130, 280
 Unit 8 146
 Unit 11 136
 'hummocks', Unit 4b 84, 85, 86
 hunting by hominids, evidence for 378,
 415, 424
 hyaena *see* *Crocuta crocuta*
- ichnofossils 42, 45–6
 Slindon Sands 45, 59, 60, 69–70, 74, 80
 Slindon Silts 81
 ichthyofauna *see* fish
 IJsselmer, Holland 130
 illite 116
 ilmenite 113
Ilyocypris 164
 impact damage, bones 397, 398, 400–1
 infra-red stimulated luminescence (IRSL)
 dating 292–3, 293
- Ingham Gravel 109
 insectivores
 biostratigraphy 305
 palaeontology 197–211
 interglacial
 hominid activity 425
 Hoxnian 157, 160, 304, 306, 309–10
 iron, sediment content 112–13, 113
 iron-manganese bands, Unit 5a 88–90,
 89, 90, 121, 132, 134, 138
 ironpan, Unit 4c 129, 131
 ironstone, presence in beach deposits
 109, 110
 Isle of Wight 15
 gravel analysis 102, 108, 108
 London Clay mineralogy 116
- J-tubes 45, 46, 55, 65
 Jeffrey, R W 15
 Jurassic chert, presence in beach deposits
 110
- kaolinite 116
 Kellaway, G A 15
 Kent's Cavern 311, 424
 Kesgrave Group 311
 kittiwake *see* *Rissa tridactyla*
 Knowles, F H S 387
 kyanite 114, 116, 117
- La Quina 385, 387
 Labridae (wrass family) 177, 178
Lacerta cf. Lacerta vivipara (common
 lizard) 185, 186
 lagomorpha 271–4
 Lagoonal/Intertidal Beds *see* Unit 4a; Unit
 4b
 'lam-scrum' 59
 Lancing 9
 large mammals
 Unit 4c 280
 Unit 4d 282
Larus ridibundus (black-headed gull) 178,
 190
 Laugerie-Haute 385
 Lavant, River 1
 lemmings 245–7
Lemmus lemmus (Norway lemming) 245,
 246, 246, 247, 247, 290
Leptocythere spp 169
Lepus europaeus 271, 272, 273
Lepus timidus (mountain hare) 271–3,
 271, 272, 273
 leucosene 113
 limonite 113
 lion *see* *Panthera leo*
 Little Thurrock 385
 Littlehampton Anticline 14, 21, 27, 31
Littorina littorea 174
Littorina saxatilis 174, 175
Littorina sp 295
 lizards *see* *Lacerta*
 location of Boxgrove *see*
 loess, mineralogy 117–18, 118
 London Clay 21, 116
 longshore drift 80, 111, 150
 Lower Chalk Pellet Gravels 37, 95–6, 145
 faunal remains 289
 Lower Head Gravel 98
 Lowestoft Till 304
- Luxocoencha rhomboidea* 164
 luminescence dating 292–3, 293
Lymnaea peregra 172
Lymnaea truncatula 172
- Maastricht-Belvédère, knapping behav-
 iour 361
Macoma balthica 295, 296
 ?*Macoma obliqua* 175
 macroartefacts, Q2/A 365–9, 365, 367,
 369, 371, 371
 magnetite 113
 mallard *see* *Anas platyrhynchos*
 mammalian fauna
see also large mammals; small mammals
 biostratigraphy 303–7, 310
 systematic palaeontology 197–74
 taphonomy 286–7, 289
 Unit 4b 277
 Unit 4c 139
 Unit 5c 135
Mammuthus trogontherii 12
 manganese
 sediment content 112–13, 113
 Unit 5a 88–9, 89, 90, 132, 134
 Mantell, G A 8–9
 maps
 cliff-line 39
 European Pleistocene sites 1
 geological 24
 raised beaches 10, 11
 March Gravel, angular/roundness analysis
 108
 Marine Cycles *see* Unit 3
 Marks Tey 304
 marl
 glauconitic 109
 Unit 4d 131–2, 139
 Unit 5b 134–5
 marsh sediments (Unit 5a) 152–3, 152
 Marshall's Pit 14
 Martin, E C 14
 Matuyama/Brunhes magnetic boundary 6,
 310
 Mauer, Germany, hominid remains 416
Megaloceros spp 240–1, 240, 241, 322,
 408
Megaloceros dawkinsi 240, 305, 307
Megaloceros giganteus 240, 307
Megaloceros savini 240, 307
Megaloceros cf. verticornis (extinct giant
 deer) 239, 239–41, 240, 305, 307,
 410, 417
 Meisenheim, faunal comparison with
 Boxgrove 244, 245
Moles sp (badger) 222, 222–4, 223, 224,
 281
Moles moles 223–4
Moles thoralis 223–4
 metamorphic rocks, presence in beach
 deposits 110
 methodology of Boxgrove Project 15–19
 micro-crinkling 84
 microartefact project 362–72
 macroartefact analysis 365–9, 365, 367,
 369, 371, 371
 microartefact analysis 370, 370, 371
 microfaulting, Q2/A 354, 355, 363, 363
 micromorphology, sediments 118–49,
 136–42

- micropans 131
Microtus agrestis (field vole) 250, 251, 251, 280, 282, 289, 306
Microtus arvalis (common vole) 250, 251, 251, 280, 282, 289
Microtus cf. arvalis (common vole) 160
Microtus gregalis (narrow-skulled vole) 251, 251-2, 252, 282, 290
Microtus oeconomicus (northern vole) 252, 252, 281, 289
Microtus (Terricola) cf. subterraneus (pine vole) 250, 250-1, 277, 280, 289
 microvertebrates 71, 162, 163, 179-80
 micritic soil, Unit 8 146
 Milankovitch Theory 9
Mimomys savini (water vole) 304, 306, 419
 mineralogy
 clay 113
 coarse silt 114-16, 115
 fine sand 113-14, 114
 mink see *Mustela lutreola*
 Mitchell, G F 6
Modiolus modiolus 174, 174
 moles see *Talpa*
 Mollusca
 marine 173, 173-5, 174
 non-marine 170, 170-3, 171, 172
 Unit 4c 129, 130
cf. Monocraterion 46
 Marine Cycle 1 57, 59, 60, 61
 Marine Cycle 2 63, 66, 67, 68, 69, 70
 Marine Cycle 3 72
 Montmaurin, hominid remains 418
 moorhen see *Gallinula chloropus*
 mountain hare see *Lepus timidus*
 mudflats see Unit 4b
Muraena helena 178
 Murchison, R 9
Muscardinus avellanarius (hazel dormouse) 254-9, 255, 256, 257, 258, 281, 282, 289
 muscovite 113, 116
 mussel beds 83, 174
Mustela erminea (stoat) 219-20, 220
Mustela lutreola (European mink)
 habitat 281
 palaeontology 220-2, 221, 222
 as predator 178-80, 280
 scat 120, 122, 130, 134, 259, 342
Mustela nivalis (weasel) 222
 Myidae 74
Myopus schisticolor (wood lemming) 245-6, 245, 246
Myotis bechsteini (Bechstein's bat) 213, 213-14, 281
Myotis brandti (Brandt's bat) 212-13
Myotis mystacinus (whiskered bat) 212, 212-13, 213, 281
 Mytilidae 60, 64, 68, 72, 74, 75, 76, 79, 80
Mytilus 81, 82, 84, 86
Mytilus edulis 174
 nanofossils
 Quaternary 300-3, 300, 302, 307
 reworked 26, 301, 301
 narrow-skulled vole see *Microtus gregalis*
Natrix natrix (grass snake) 185, 186
 natural remanent magnetisation (NRM) 297, 298-9, 298, 299
 Neanderthal remains 415, 418, 419
Noemys sp (water shrew) 203, 203-4, 204, 281
Neptunea angulata 175
Neptunea contraria 81, 84, 173, 173, 175, 295, 296
 Newcomer, M H 385
 newts see *Triturus*
 Ngandong, Indonesia, hominid remains 421
 nomenclature, comparison with
 Woodcock's work 378
Nonion depressulatus 164
 North Atlantic, oxygen isotope stratigraphy 302-3
 northern vole see *Microtus oeconomicus*
 Norton event 29
 Norton Farm beach, non-flint clasts 109, 110
 Norton Formation 15, 21, 27, 29-30
 Norway lemming see *Lemmus lemmus*
 Norwegian Sea, oxygen isotope stratigraphy 303
Nucella 295
Nucella lapillus 84, 173, 174, 175
 number of identifiable fragments (NISP)
 small mammals 286-7
 vertebrates 288
 Oakley, K P 14
 Ohnuma, K 385, 387, 388, 395
Ophiomorpha 46, 59
 optically stimulated luminescence (OSL)
 dating 292-4, 293, 294
 Organic Bed see Unit 5a
 organic carbon, sediment content 112, 113, 120
 orthoquartzite, presence in beach deposits 110
Oryctolagus cuniculus (rabbit) 271, 272, 273, 273
 Osbourne-White, H J 12, 13
 ostracods 164-9, 165, 166, 168
 as climate indicators 164-5, 168-9
 Eye gravel 108
 Slindon Sands 59, 67, 71, 72, 74, 80, 164-9
 Overton Down, Wiltshire 130
 Oxygen Isotope Stages (OIS)
 Boxgrove correlation 296-7, 301-3, 303-4, 307, 424
 nanofossils correlation 301-3
 Pleistocene stratigraphy 6, 7, 8, 310
 Palaeocene geology 21
 palaeodrainage 149-50
 palaeoecology 274-90
 Eartham Formation 282, 289-90
 Slindon Formation 276-82
 Palaeogene, reworked pebbles 103
 Palaeolithic
 archaeological research 309-12
 archaeological sequence 311
 context of finds 18-19
 Pleistocene correlation 309-12
 Sussex flint tools 13, 15
Palaeoloxodon antiquus 12, 304
 palaeomagnetic measurements 297-9, 297, 298, 299
 palaeosol see Unit 4c
 Palmer, L S 13
 palygorskite 131, 134, 145
 palynology
 see also pollen
 Pleistocene lithostratigraphy 310
Panthera leo (lion) 226, 226, 282
 papules
 Unit 6 143-4
 Unit 8 136, 145
 Unit 11 147
 Paradoxostomatidae 164
 particle size distribution 111-12, 113
 partridge see *Pendix pendix*
 pascichnia 42
 passerines 194, 194
 Path Gravels 97
 Pectinidae 74
 pedogenesis 94
Pelobates fuscus (common spadefoot) 182, 182, 185, 186
 Penck, A 5, 6
 Penfold's Pit 15
 Peppering 9
 percussors, flint artefacts 384-95
Pendix pendix (grey partridge) 190, 194, 196
 periglacial conditions, Unit 11 147-8
Perissodactyla 226-31, 307
 Petralona, Greece, hominid remains 418
 pH, sediment content 112, 113
Pholas 56
 phytoliths, Unit 5a 132
 piddock 174, 174
 Pincevent 335
 pine vole see *Microtus (Terricola) cf. subterraneus*
Pinguinus impennis (great auk) 178, 181, 191, 191, 194, 196
Pinus (pine), charcoal 427
Psidium moitessierianum 172
 Pit C, Unit 5a 133
 Pit Q
 Unit 4c 130
 Unit 5a 132, 133, 134
Ptyomyia 250-1, 251-2
 plants
 aquatic 83
 root fragments 126, 127, 129, 143
Planichthys flesus (flounder) 176, 177, 178, 180
Plecotus auritus (common long-eared bat) 210, 211, 211-12, 212, 282
 Pleistocene
 chronostratigraphy 5-8
 climatic forcing 5
 European sites 1
 geochronology 7, 8
 hominid record 415-19, 417
 Palaeolithic correlation 309-12
 Pleuronectidae ('flatfish') 178
Pliomys episcopalis (extinct vole) 160, 248-9, 249, 305, 306
 pollen
 see also palynology
 samples 157
 Unit 5a 132, 134
 Polychaeta 66, 74, 79
 pond deposits
 Unit 4d 131-2, 139, 282
 Unit 5b 134-5

- Pontnewydd Cave, Wales, hominid remains 418
- Portsdown Anticline 15, 21, 27
- Portsdown Hill 12
- Portslade, raised beach 9, 12
- pre-Pleistocene deposits 21–6
- predators
- bird-eating 193, 196
 - effect on bone assemblage 274, 276, 280
 - fish-eating 178–80
- Prestwich, J 9, 12
- Priory Bay gravel, gravel analysis 102, 108
- Prunella modularis* (dunnock) 192, 194, 196
- Pseudomilvina lacunosa* 301–2
- Pupilla muscorum* 172
- Pyddoke, E 15
- pygmy shrew *see* *Sorex minutus*
- Q1/A**
- Canis lupus* (wolf) 214
 - Castor fiber* (beaver) 253, 254, 254
 - Clethrionomys rufocanus* (grey-sided vole) 248
 - deformation feature 96, 313
 - excavation 312, 313–39, 313, 314, 315
 - fish remains 176
 - flint artefacts
 - distribution 316, 329
 - Unit 4b 322–39, 322, 325–6, 327, 328, 329, 330–4, 335, 336–8, 339
 - Unit 4c 315–22, 316, 317, 318, 319, 320
 - geology of sections 312/13
 - Lemmus lemmus* (Norway lemming) 245, 247
 - Lepus timidus* (mountain hare) 273
 - Marine Cycle 3 79
 - Megaloceros cf. verrucosus* (extinct giant deer) 239
 - Moles* sp (badger) 222, 224
 - Microtus gregalis* (narrow-skilled vole) 251
- Q1/B**
- Clethrionomys glareolus* (bank vole) 247
 - Dama dama* (fallow deer) 234, 235
 - fish remains 176
 - flint artefacts 339–54, 340, 345, 346–7, 348, 349, 351, 352, 353
 - distribution 339, 341–2, 341, 342, 343, 344
 - handaxes 344–8, 346–7, 348
 - horse butchery 404–5, 405
 - Myotis bechsteini* (Bechstein's bat) 213
 - Plecotus auritus* (common long-eared bat) 211
 - small mammals 280
 - Stephanorhinus hundsheimensis* (extinct rhinoceros) 231
 - Unit 4d 87, 131–2, 139, 180, 281, 339
 - Ursus deningeri* (extinct cave bear) 218
- Q2/A**
- flint artefacts 354–61
 - microartefact project 362–72
 - microfaulting 354, 355, 363, 363
 - pebble clusters 83
 - sediment sequence 76, 79
 - Unit 4a 82
 - Unit 4b 85–6
 - Unit 4c 87
 - Unit 5a 89, 89
 - Unit 6 94
- Q2/B**
- Elionomys quercinus* (garden dormouse) 260
 - Ursus deningeri* (extinct cave bear) 217
- Quarry 1 4–5, 4, 5**
- Area A *see* Q1/A
 - Area B *see* Q1/B
 - bird remains 194, 195, 196
 - chalky pellet gravels 95, 96
 - quarrying methods 16
 - section 45
 - sedimentary log 56/7
 - TP1, *Bison* sp 242
 - TP220–80, *Ursus deningeri* (extinct cave bear) 218
 - unconformity 150
- Quarry 2 4, 4**
- Area A *see* Q2/A
 - Area B *see* Q2/B
 - bird remains 194, 195, 196
 - section 28, 44
 - sedimentary log 47, 56/7
 - TP4
 - Canis lupus* (wolf) 214
 - Cervus elaphus* (red deer) 233
 - Stephanorhinus hundsheimensis* (extinct rhinoceros) 231
 - TP6, *Cervus elaphus* (red deer) 233
 - unconformity 149–50
- quartz**
- exotic presence in gravels 110
 - fine sand mineralogy 113, 116
- quartzite, used as percussor 385, 386**
- Quaternary**
- British stratigraphy 6, 6
 - geochronology 7
 - history of research 8–15
- rabbit *see* *Oryctolagus cuniculus***
- raindrop impact craters 84, 86**
- raised beaches 2, 2, 8–15, 10, 11**
- see also* beach deposits
 - archaeological discoveries 13, 15
 - Slindon Gravel 34
 - uplift rate 29
 - West Sussex Coastal Plain 27–34
- Raja clavata* (Thornback Ray) 175, 176, 178**
- Rana* sp 183, 184, 185**
- Rana arvalis* (moor frog) 182, 183–4, 185, 186**
- Rana temporaria* (common frog) 182, 184, 185, 186**
- Reading Beds 21, 116, 126**
- Red Barns 15, 424**
- red deer *see* *Cervus elaphus***
- Reid, C 12, 13, 100**
- Reilingen, Germany, hominid remains 418**
- repichnia 42**
- reptiles 184–7**
- research**
- Palaeolithic 309–12
 - Quaternary 8–15
- resistivity survey, buried cliff-line 37–42, 39, 40**
- reworked pebbles 103**
- rhinoceros *see* *Stephanorhinus hundsheimensis***
- Rhizocoelallium/Thalassinoides* 74, 80**
- rhythmites, Unit 6 94**
- Rissa tridactyla* (kittiwake) 178, 190–1**
- river estuaries, sediment transport 111**
- river terraces, Pleistocene correlation 5–6**
- Robertsonites tuberculatus* 164**
- robin *see* *Erithacus rubecula***
- rodents 244–71, 306**
- roe deer *see* *Capreolus capreolus***
- root remains 126, 127, 129**
- '*Rosalina parisiensis*' 165, 168**
- Rother, River 9, 12, 13**
- rutile 114, 116**
- Saalian Complex 6, 228–9, 270, 311**
- St Esteve-Janson, faunal comparison with Boxgrove 244, 245**
- St Vallier, France, *Moles* (badger) 223, 224**
- Salmo trutta* (brown/sea trout) 176, 177, 178**
- Salmonidae (salmon/trout) 177, 178, 180, 181**
- Sambungmachan, Indonesia, hominid remains 421**
- Sampson, C G 388–9**
- sand extraction pit *see* SEP**
- sandstone, presence in beach deposits 109**
- scat**
- bone fragments in 132, 139
 - mink 120, 122, 130, 134, 259, 342
- schistose metamorphic rocks, presence in beach deposits 110**
- Sciurus* sp (squirrel) 244, 244–5, 245, 281**
- Scolopacidae 190**
- scrapemarks, bones 397, 400**
- sea level changes 29, 153**
- Seaford Head 37**
- seaweed rafting 83, 86, 111, 175**
- sediment ripening, Unit 4c 130, 139**
- sediments**
- micromorphology 118–49
 - mineralogy 111–18
- Selsey**
- artefacts 13
 - erratics 9, 12, 100, 110
 - pre-Pleistocene deposits 21
 - raised beach 9, 30
 - roe deer 238, 239
- SEM/EDXRA analysis 120, 127, 127, 128**
- Semicytherura* sp nov 168, 168**
- SEP 2**
- Capreolus capreolus* (roe deer) 236
 - Stephanorhinus hundsheimensis* (extinct rhinoceros) 229
- SEP 3**
- sedimentary sequence 46–9, 47, 48
 - Marine Cycle 1 61
 - Marine Cycle 2 64, 69, 70
 - Marine Cycle 3 72, 79
 - trace fossils 45
- Shephard-Thorn, E R 160**
- Shipman, P 398**
- Shoreham 9**
- shrews *see* *Sorex***
- Sicista* spp 262–5**

- Sicista cf. betulina* (northern birch mouse) 260–7, 261, 265, 267, 281, 289
- Sicista praedoriger* 266, 267
- Sicista subtilis* (southern birch mouse) 261, 265
- Silbury Hill, Wiltshire 130
- sillimanite 114
- silt, mineralogy 117–18, 118
- Silt Beds (Unit 11) 97–9
- skeletal element ratios, birds 193–4, 194
- Skolithos* 59, 66, 72, 80
- slate, presence in beach deposits 110
- Slindon
- dry valley 13, 14, 14
 - raised beach 13
- Slindon Bottom 13, 14
- Slindon Formation 16, 27, 34–5
- basal beds 46–9
 - depositional environment 151, 152
 - description 428
 - extent 29
 - geological summary 150–3
 - origin theories 15
 - palaeoecology 276–82
 - stratigraphic sequence 46–93, 54, 56
 - sub-marine Cycle 1 48–9
- Slindon Gravel (raised beach) 34, 49–52, 50, 51, 52, 53
- fish remains 177
- Slindon Sand Member
- see also Unit 3
 - depositional environment 151
 - fish remains 177–8
 - foraminifera 164–9, 165, 168
 - ostracods 164–9, 166, 168
 - palaeoecology 276
 - palaeomagnetism 297–9, 297, 298, 299
 - source of deposits 116
 - stratigraphic sequence 46–80, 54, 56/7
 - Waterbeach 12
- Slindon Silt Member
- depositional environment 151
 - fish remains 178–80
 - foraminifera and ostracods 169
 - Lagoonal/Intertidal Beds see Unit 4a; Unit 4b
 - Organic Bed see Unit 5a
 - palaeoecology 276–82
 - palaeomagnetism 297–9, 297, 298, 299
 - sediment sequence 80–7
 - Slindon Soil Bed see Unit 4c
 - source of deposits 116–17
- Slindon Soil Bed see Unit 4c
- slow worm see *Anguis fragilis*
- slug plates 172, 172
- small mammals
- percentage frequency histograms 278
 - taphonomy 286–7
 - Unit 4c 280–2
 - Unit 4d 282
 - Unit 6 289
- smectite 116
- snakes 185
- soil, micromorphology 118–49, 136–42
- Solent River 150
- solid geology of area 21–6
- Sorex (Drepanosorex) savini* (extinct shrew) 160, 207–8, 208, 305
- Sorex minutus* (pygmy shrew) 204–6, 205
- Sorex rimonensis* (extinct shrew) 160, 205, 206–7, 206–7, 305
- soricidae 203–8
- spadefoot see *Pelobates fuscus*
- Spermodesia lamellata* 172
- sphene 114
- spotted hyaena see *Crocuta crocuta*
- spreites 46, 59, 74
- squirrel see *Sciurus*
- Star Carr, faunal comparison with Boxgrove 238, 239
- starling see *Sturnus vulgaris*
- staurolite 114, 116, 117
- Steinheim, Germany, hominid remains 418
- Stephanorhinus etruscus* 307
- Stephanorhinus hundsheimensis* (extinct rhinoceros)
- biostratigraphy 160, 305, 307
 - human modification of bones 406–8, 406, 407, 408
 - palaeontology 229, 229–31, 230, 231, 282
- Steyne Wood Clay, coccolith comparison with Boxgrove 164, 169, 170
- stickleback, three-spined see *Gasterosteus aculeatus*
- stoat see *Mustela erminea*
- Stone Point, exotic rocks 110
- stratigraphy
- faunal list 283–5
 - summary 125
- Strix aluco* (tawny owl) 191
- Sturnus vulgaris* (starling) 192, 194, 196
- Succinea oblonga* 172
- Sussenborn, Germany 236
- Sussex, history of Quaternary research 8–15
- Sussex Pad 9
- swan see *Cygnus cygnus*
- Swanscombe
- age of deposits 304–5
 - decalcification 131
 - faunal comparison with Boxgrove 218, 226, 228, 234–5, 238, 239, 305
 - flint hammerstones 385
 - hominid remains 418, 419
- swift see *Apus apus*
- sympatry analysis, Unit 4c 280, 281–2
- Synsacophaera* 301
- Talpa* (mole), Unit 4c 130
- Talpa europaea* (European mole) 208–11, 209–11, 305
- Talpa minor* (extinct mole) 211, 305
- talus cone, GTP 25 62, 70
- taphonomy
- Eartham Formation 282, 289–90
 - mammals 286–7, 289
 - Slindon Sand Member 276
 - Slindon Silt Member 276–82
- Tarko, faunal comparison with Boxgrove 244, 245
- tawny owl see *Strix aluco*
- taxonomic habit indices 274, 275, 276, 277, 277
- taxonomic habitat indices
- Unit 4c 281–2, 281
 - Unit 6 290
- teal see *Anas crecca*
- tectonic uplift, raised beaches 29
- teeth, dating 294–5, 294, 295
- Tertiary, regolith 21, 26, 27
- Thalassinoides* 74, 79, 80
- Thames Basin
- fluvial deposits 311
 - Palaeogene gravels 103
- thermoluminescence (TL) dating 292–3, 293
- Thornback Ray see *Raja clavata*
- Thynnus thynnus* (blue-fin tunny) 176, 177, 178
- tiering 46
- toads see *Bufo*
- tools see flint artefacts
- tourmaline 114, 116
- trace fossils see ichnofossils
- trampling, artefact distribution 321
- transport mechanisms
- exotic rocks 111
 - flint artefacts 321
- tremolite 115
- Trichia hispida* 295, 296
- Triglidae (gurnard family) 176, 177
- Triturus* sp 185
- Triturus helveticus* 182, 185, 186
- Triturus vulgaris* (smooth newt) 181–2, 182, 185, 186
- trout see *Salmo trutta*
- Truncatellina cylindrica* 173
- tufted duck see *Aythya fuligula*
- Tylor, A 12
- U-series analysis, electron spin resonance 294–5, 294, 295
- U-tubes 45, 60, 63, 69, 74, 75
- unconformity
- Quarry 1 150
 - Quarry 2 149–50
- Unit 2
- beach deposits, GTP 25 49–52
 - flint artefacts 52, 382
- Unit 3
- cementation 56–7
 - colour changes 99, 150
 - depositional environment 124–6
 - flint artefacts 378, 382
 - foraminifera 126
 - junction with Unit 4a 125–6, 141
 - Marine Cycle 1 49–61
 - deeper water conditions 57–60
 - main beach 49–52
 - regression 60–1
 - seaward exposures 52–7
 - transgression 49 - Marine Cycle 2
 - deeper water conditions 64–9
 - regression 69–70
 - seaward exposures 63–4
 - transgression 61–3, 63 - Marine Cycle 3
 - deeper water conditions 72–80
 - Grey Interval 74, 79, 80
 - micromorphology 125, 141
 - seaward exposures 71–2
 - transgression 70, 72
 - Yellow Interval 74, 75, 79 - micromorphology 141–2
 - Mollusca 173–4, 174
 - palaeoecology 276
 - particle size distribution 112, 113

- Unit 3b 125–6
- Unit 4
- chemical composition 112–13, 113
 - particle size distribution 112, 113
 - sediment sequence 80–7
- Unit 4a
- deformation structures 81
 - depositional environment 126–7, 424–5
 - fish remains 178
 - herpetofauna 185–6
 - junction with Unit 3 125–6, 141
 - micromorphology 126–7, 140
 - mussels 83
 - palaeoecology 276–7
 - sediment sequence 81–3
 - taphonomy 276–7
- Unit 4b
- deformation structures 85, 129
 - depositional environment 128–9, 425
 - fish remains 127, 128, 140, 178
 - flint artefacts, Q1/A 322–39, 322, 325–6, 327, 328, 329, 330–4, 335, 336–8, 339
 - herpetofauna 185–6
 - horse butchery site 127, 227, 37–8, 377, 378
 - human activity evidence 127, 128–9, 322
 - 'hummocks' 84, 85, 86
 - mammalian fauna 277
 - micromorphology 121, 127–8, 127, 128, 140
 - mineralogy 113, 117
 - Mollusca 173, 174–5, 174
 - non-flint material 109–10
 - palaeoecology 276–7
 - sediment sequence 83–6
 - taphonomy 276–7
 - weathering evidence 117–18
- Unit 4c (palaeosol)
- bird remains 194
 - depositional environment 129–31, 152, 152
 - electron spin resonance (ESR) dating 294–5, 294, 295
 - faunal remains 129, 160, 161, 280–2
 - fish remains 178–80, 181
 - flint artefacts
 - Q1/A 315–22, 316, 317, 318, 319, 320
 - Q1/B 339–54, 340, 345, 346–7, 348, 349, 351, 352, 353
 - Q2/A 354–60
 - herpetofauna 185
 - micromorphology 121, 129, 139
 - mineralogy 113
 - non-flint material 109–10
 - origin 117–18
 - palaeoecology 280–2
 - sediment sequence 34–5, 35, 36, 78, 86–7, 87, 91
 - taphonomy 280–2
 - taxonomic habitat index 281–2, 281
 - vegetation 280–1
- Unit 4d
- depositional environment 131–2, 339
 - fish remains 180, 282
 - micromorphology 121, 131, 139
 - sediment sequence 87
 - small mammal fauna 281, 282
- Unit 5a (Organic Bed)
- Castor fiber* (beaver) 253, 254, 282
 - deformation structures 363
 - depositional environment 132–4, 152
 - faunal distribution 371
 - fish remains 180
 - herpetofauna 185
 - iron-manganese bands 88–9, 89, 90, 121
 - microartefact project 362–72
 - microfaulting 89, 363, 363
 - micromorphology 121, 132, 138
 - Micromys gregalis* (narrow-skulled vole) 252
 - mud cracks 89, 89
 - palaeoecology 282
 - particle size distribution 112, 113
 - sediment sequence 35, 87, 88–90, 91
 - surface topography 363, 363
 - vertebrate fauna 160, 161, 282
- Unit 5b
- depositional environment 134–5
 - faunal remains 290
 - micromorphology 134, 137–8
 - mineralogy 113
 - particle size distribution 112, 113
 - sediment sequence 90–3, 90
- Unit 5c
- depositional environment 135, 142
 - flint artefacts 122
 - micromorphology 137
 - sediment sequence 93
- Unit 6 (Brickearth Beds)
- Castor fiber* (beaver) 253, 254, 290
 - Clethrionomys rufocanus* (grey-sided vole) 248, 248
 - dating, thermoluminescence (TL) 292–3, 293
 - deformation structures 94
 - depositional environment 143–5, 153, 155
 - faunal remains 290
 - herpetofauna 185
 - micromorphology 122, 136–7, 142–3
 - mineralogy 113–14, 117
 - palaeomagnetism 297–9, 297, 298, 299
 - rhythmites 94
 - sediment sequence 35, 36, 78, 87, 90, 91, 93–5, 93
 - sub-facies 94
 - taxonomic habitat index 290
 - vertebrate remains 160
- Unit 7 (Angular Chalk Beds) 35, 95, 153
- Unit 8 (Chalk Pellet Beds)
- depositional environment 146, 153
 - flint scatters 379, 379, 380
 - micromorphology 122, 123, 136, 145–6
 - mineralogy 113, 115
 - sediment sequence 37, 95–7
 - source of deposits 117
- Unit 9 (Fan Gravel Beds)
- depositional environment 153, 155
 - sediment sequence 97
- Unit 10 (Calcareous Head Gravel) 97–9, 97
- Unit 11 (Head Gravels and Silt Beds)
- dating, infra-red stimulated luminescence (IRSL) 292–3, 293
 - depositional environment 147–8
 - flint artefacts 383–4, 383
 - micromorphology 123, 136, 146–7
 - mineralogy 113, 115
 - particle size distribution 112, 113
 - samples 147
 - sediment sequence 97–9
 - source of deposits 116–17, 116, 117
- Untermassfeld, Germany 236
- Upper Chalk, source of Boxgrove deposits 116
- Upper Chalk Pellet Beds 37, 95–6, 145
- uranium series dating 291, 291, 294–5, 294, 295
- Urocythereis britannica* 164
- Ursus deningeri* (extinct cave bear)
- biostratigraphy 160, 305, 306
 - human modification of bones 398, 402–3
 - palaeontology 87, 178, 217, 217–19, 218, 219
- Uxbridge, Middlesex 131
- Valdœ Quarry 34
- Vallonia* spp 172
- vegetation
- evidence for 157
 - molluscs as indicators 172
 - small mammal indicators 280–1, 282
 - Unit 4c 280–1
- vein quartz, presence in beach deposits 110
- vertebrate fauna 33, 157–63, 158–9
- collecting methods 161–3
 - number of identifiable fragments (NISP) 288
 - percentage frequency histograms 279
 - stratigraphic provenance 160–1
- Vértesszöllös, Hungary, hominid remains 416–17
- vertical electrical sounding (VES) 37–8
- Vértigo pusilla* 172
- Vértigo substriata* 172
- Vitrinobrachium breve* 172–3, 172
- voles
- extinct 160
 - palaeontology 247–52
 - Unit 4c 130
 - Unit 5b 134
- vuggy structure, Unit 6 143
- Walton-on-the-Naze 304
- Warehead Stud Farm 4, 313
- Warren Hill 311, 424
- Warren, S H 101
- water shrew *see Neomys*
- water vole *see Arvicola terrestris cantiana*
- Waterbeach Pit 9, 12, 295, 296
- Waverley Wood 311, 424
- Weald, formation 9
- weasel *see Mustela nivalis*
- weathering, Unit 6 94–5
- Wells, A K 100
- West, R G 6
- West Runton
- dating of 304, 305
 - faunal comparison with Boxgrove 203–4, 207, 211, 228, 234, 238, 239, 240–1, 248, 249, 250, 252, 305–7

- West Stubbs Copse Pit 34
West Sussex Coastal Plain 27-34
Westbury-sub-Mendip
 age 311, 424
 faunal assemblage 310
 faunal comparison with Boxgrove 211, 219,
 226, 243, 248, 249, 252, 260, 305-7
Westhampnett 15
Westleton Beds, gravel analysis 105
whiskered bat *see Myotis mystacinus*
whooper swan *see Cygnus cygnus*
wigeon *see Anas penelope*
wild cat *see Felis silvestris*
Wivenhoe 424
wolf *see Canis lupus*
Wolstonian Stage 310
wood, used as percussor 385, 387
wood lemming *see Myopus schisticolor*
wood mouse *see Apodemus sylvaticus*
Wood, S V 12
Woodcock, A 15, 160, 378
woodland species, Unit 4c 281
wrasse *see Labridae*
Xenothberis 164
Yellow Interval, GTP 13 74, 75, 79
Zeuner, F E 6, 15
zircon 114, 116

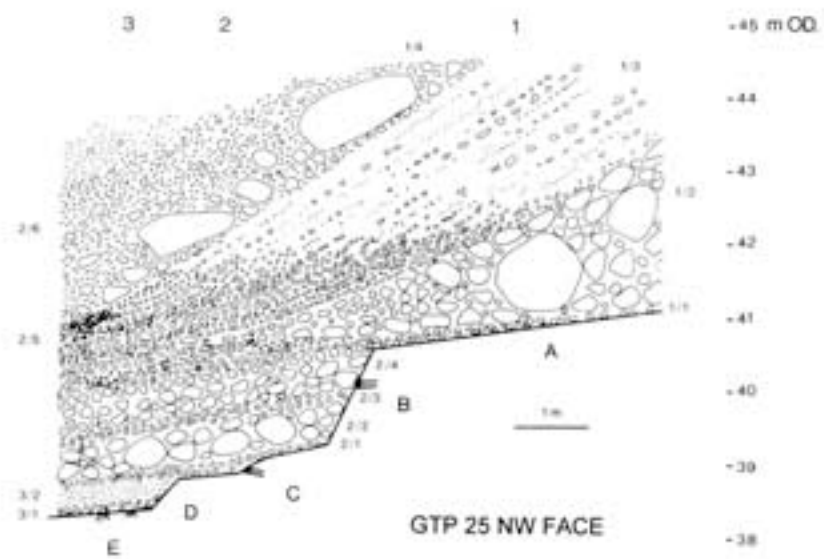


Fig 42b Detailed sedimentary log of combined section logs 1, 2, and 3 at GTP 25

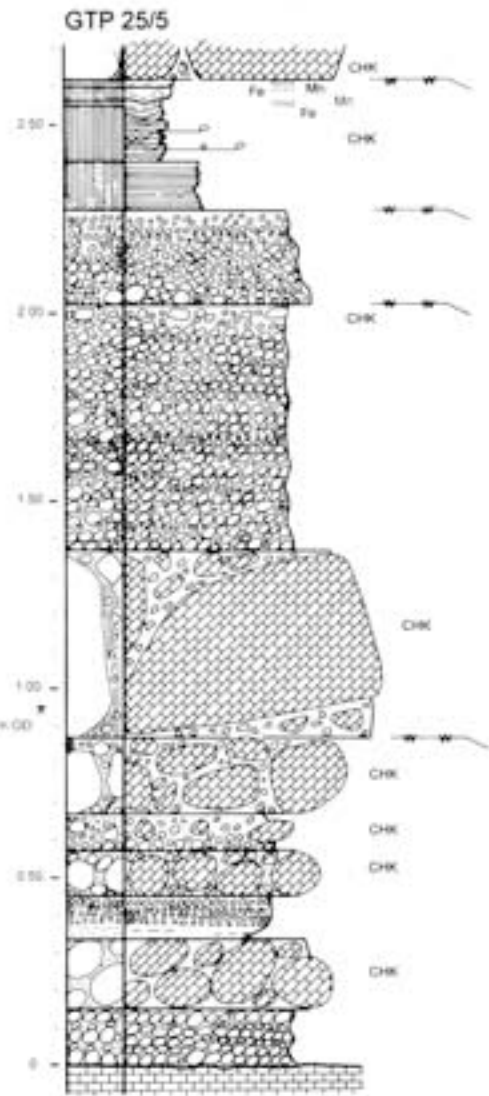


Fig 42c Detailed sedimentary log through the sediments at GTP 25/5

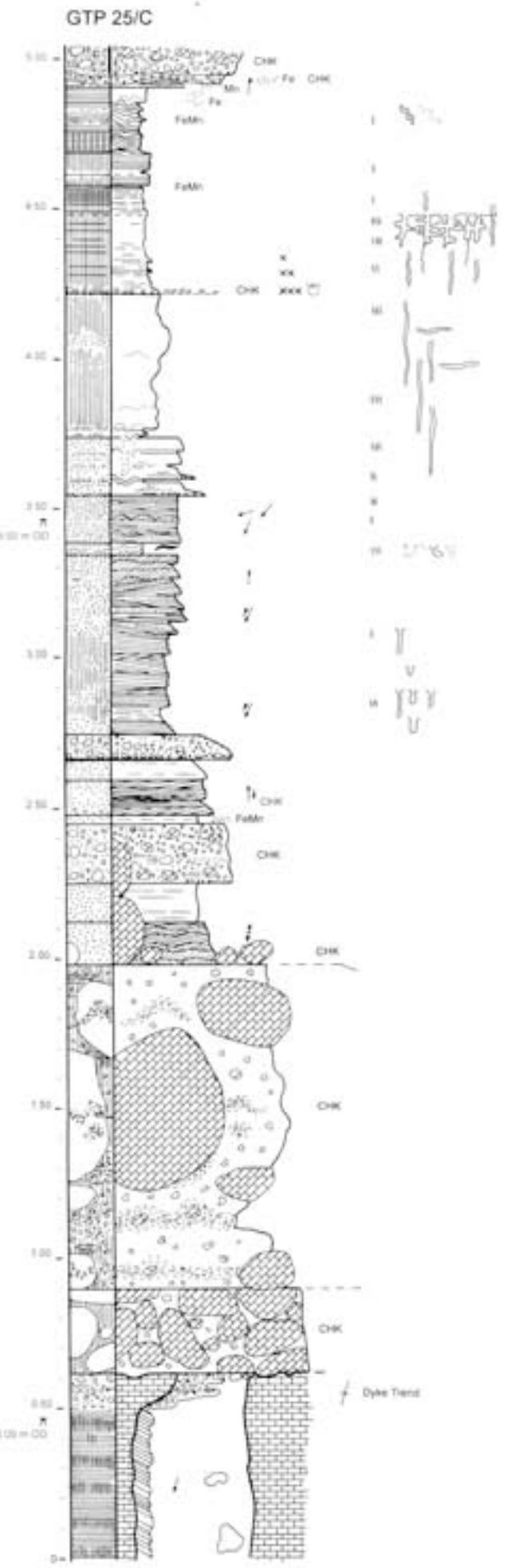


Fig 42f Detailed sedimentary log through the sediments at GTP 25 C

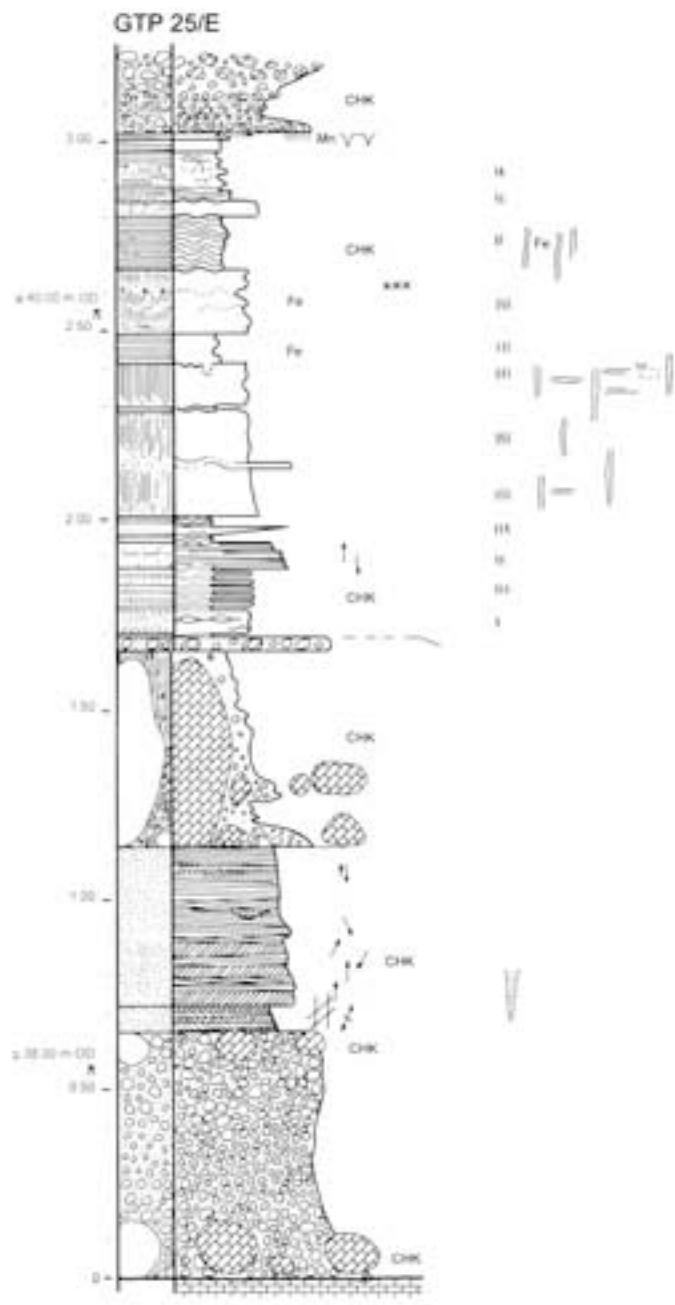


Fig 42d Detailed sedimentary log through the sediments at GTP 25 E

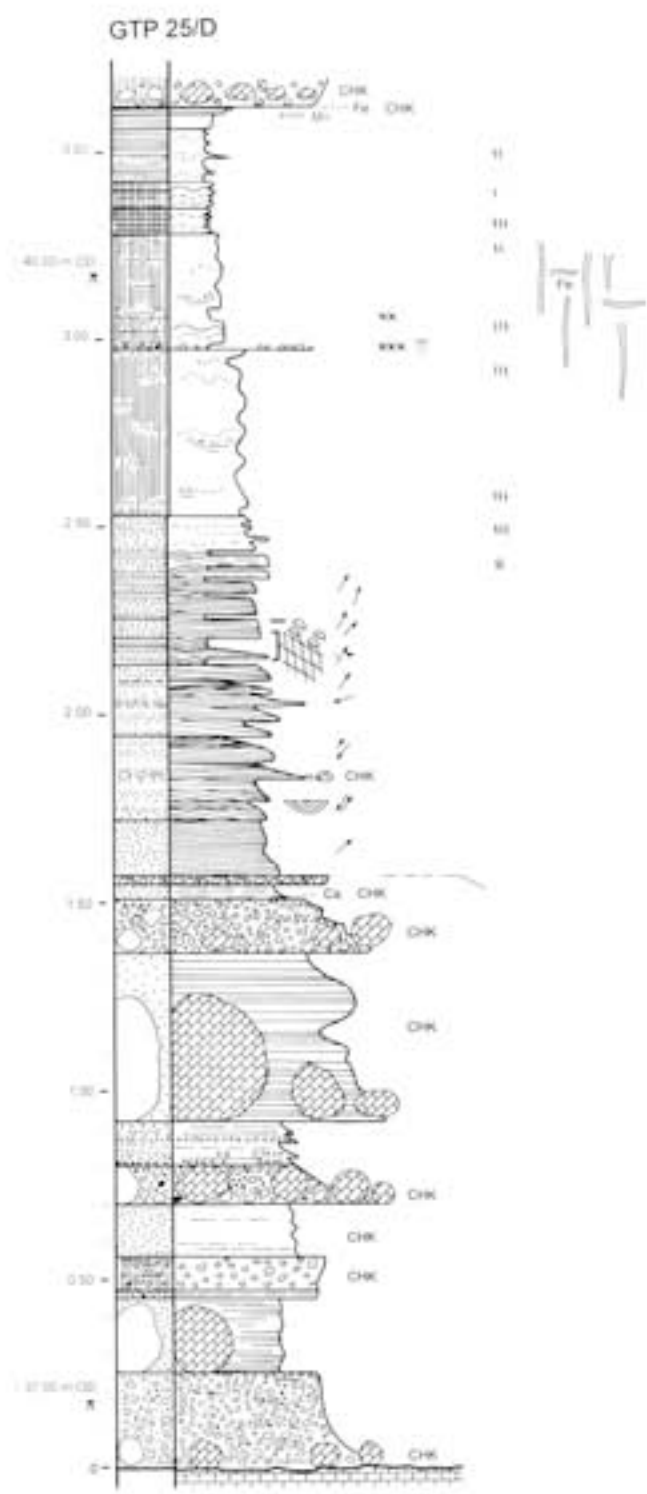


Fig 42e Detailed sedimentary log through the sediments at GTP 25 D

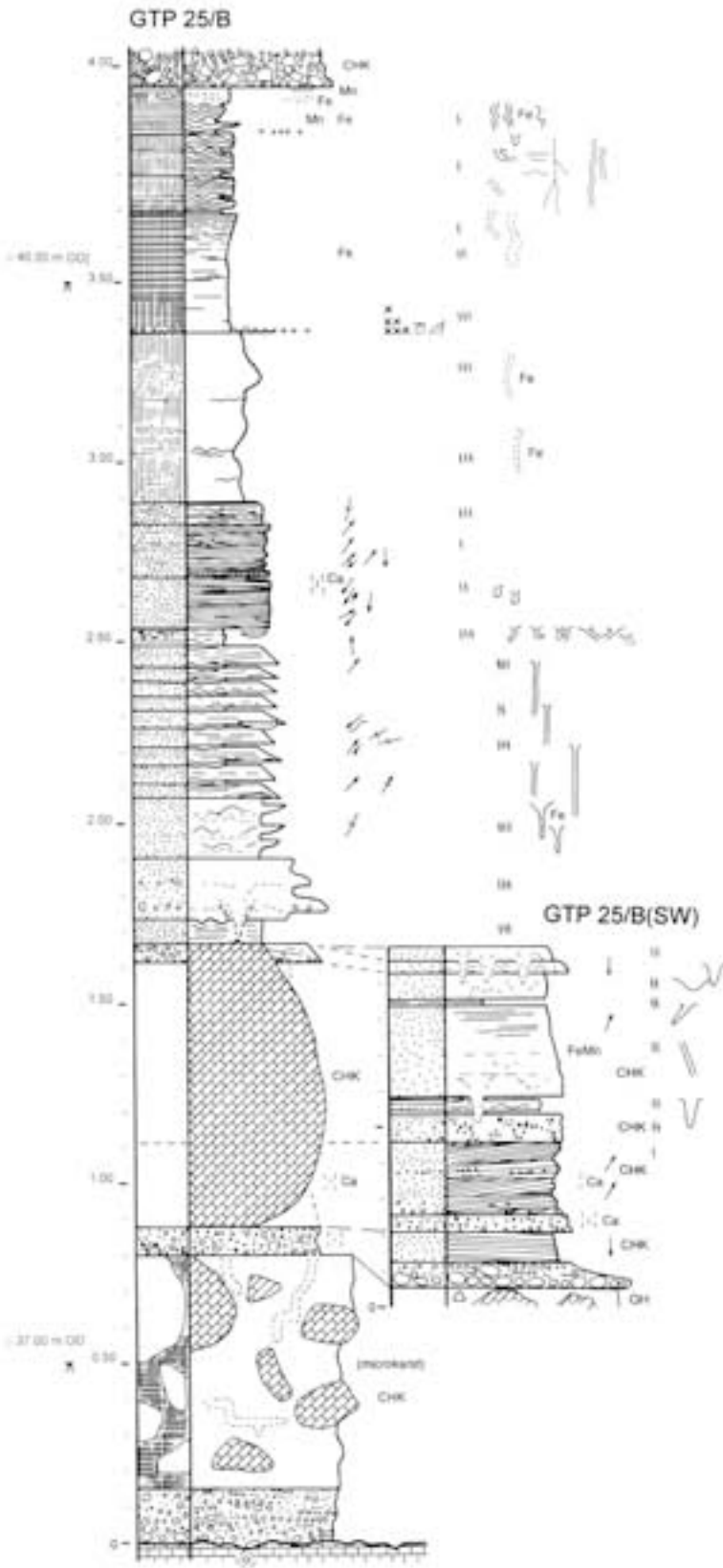


Fig 42g Detailed sedimentary log through the sediments at GTP 25 B
 Fig 42h (inset to the right of the main log) Detailed sedimentary log through the sediments at GTP 25 B SW

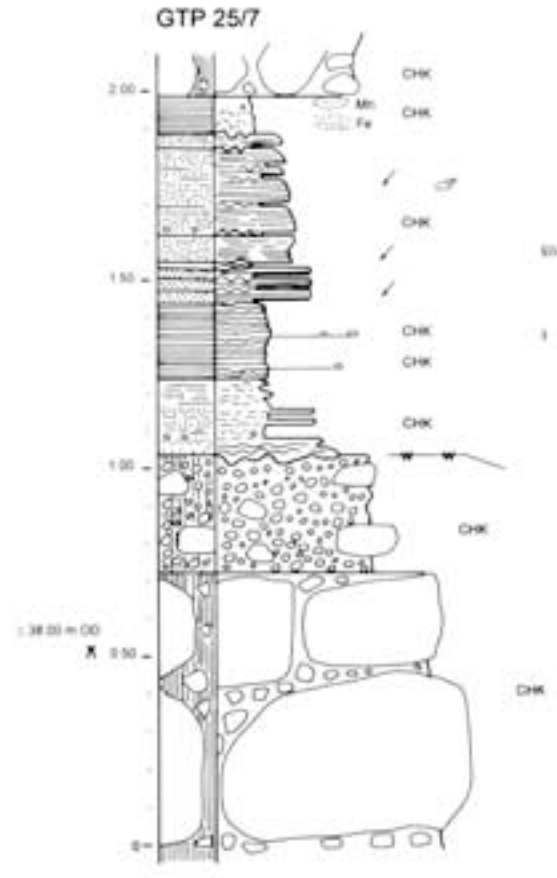


Fig 42j Detailed sedimentary log through the sediments at GTP 25 7

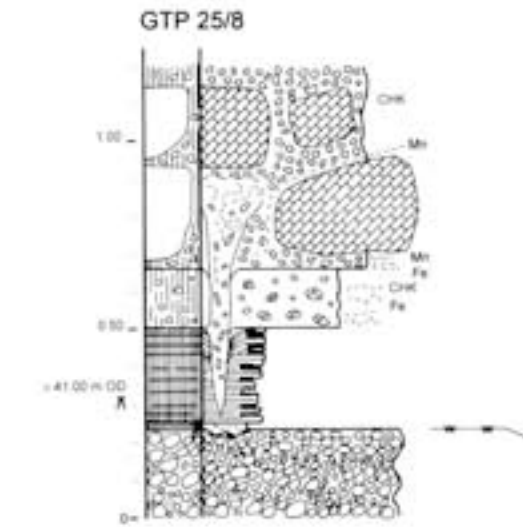


Fig 42k Detailed sedimentary log through the sediments at GTP 25 8

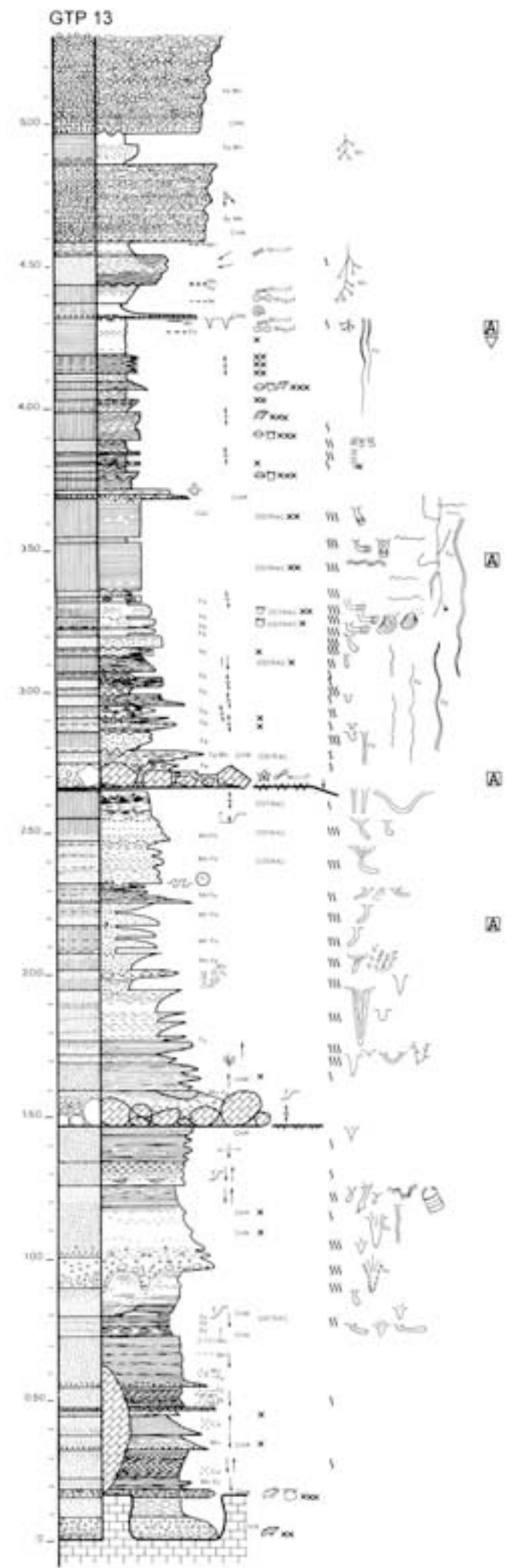


Fig 45a Detailed sedimentary log through the sediments at GTP 13 1

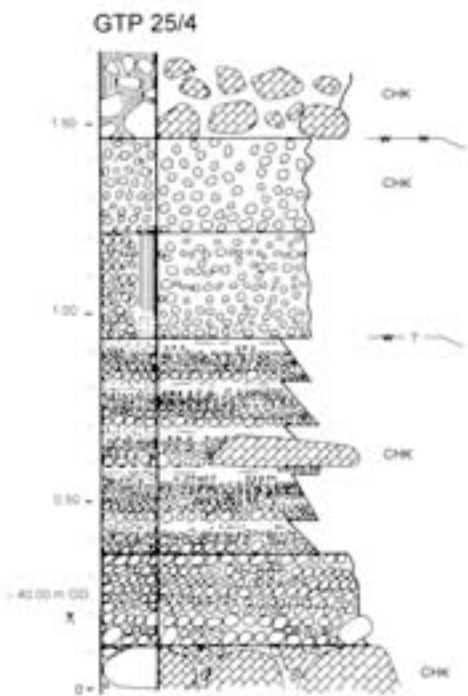


Fig 42i Detailed sedimentary log through the sediments at GTP 25 4

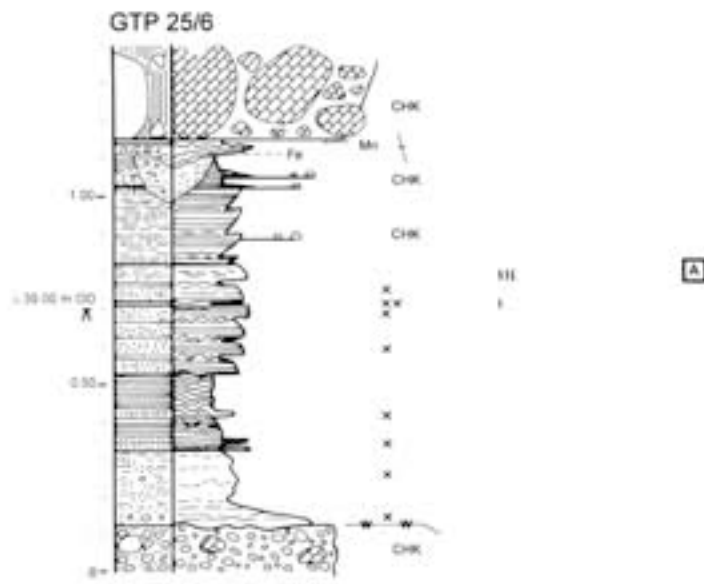


Fig 42l Detailed sedimentary log through the sediments at GTP 25 6

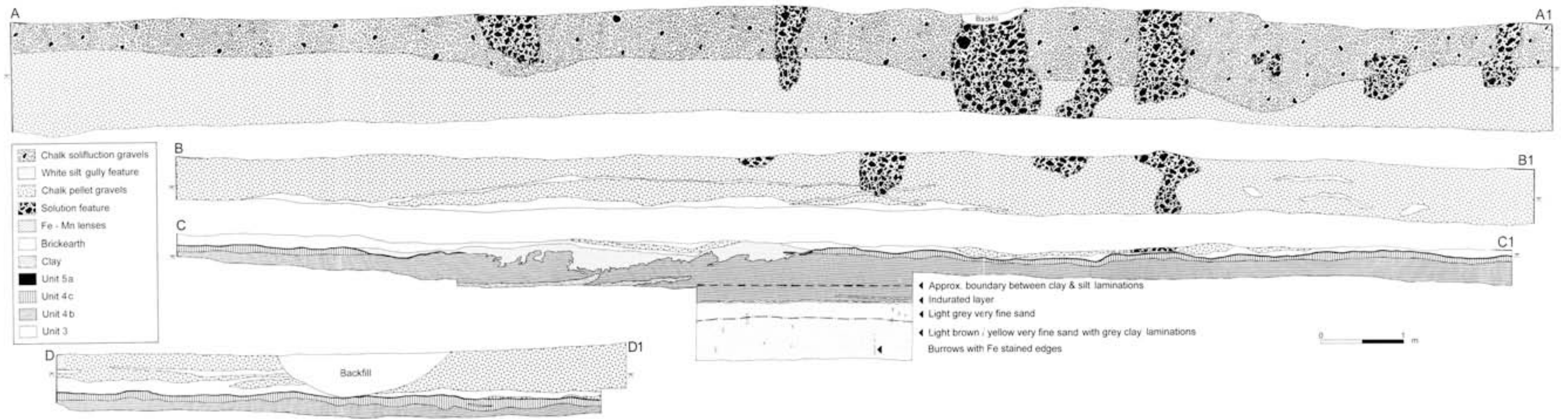


Fig 226 Geology of the sections of Quarry 1/A (positions of sections shown on Fig 225)

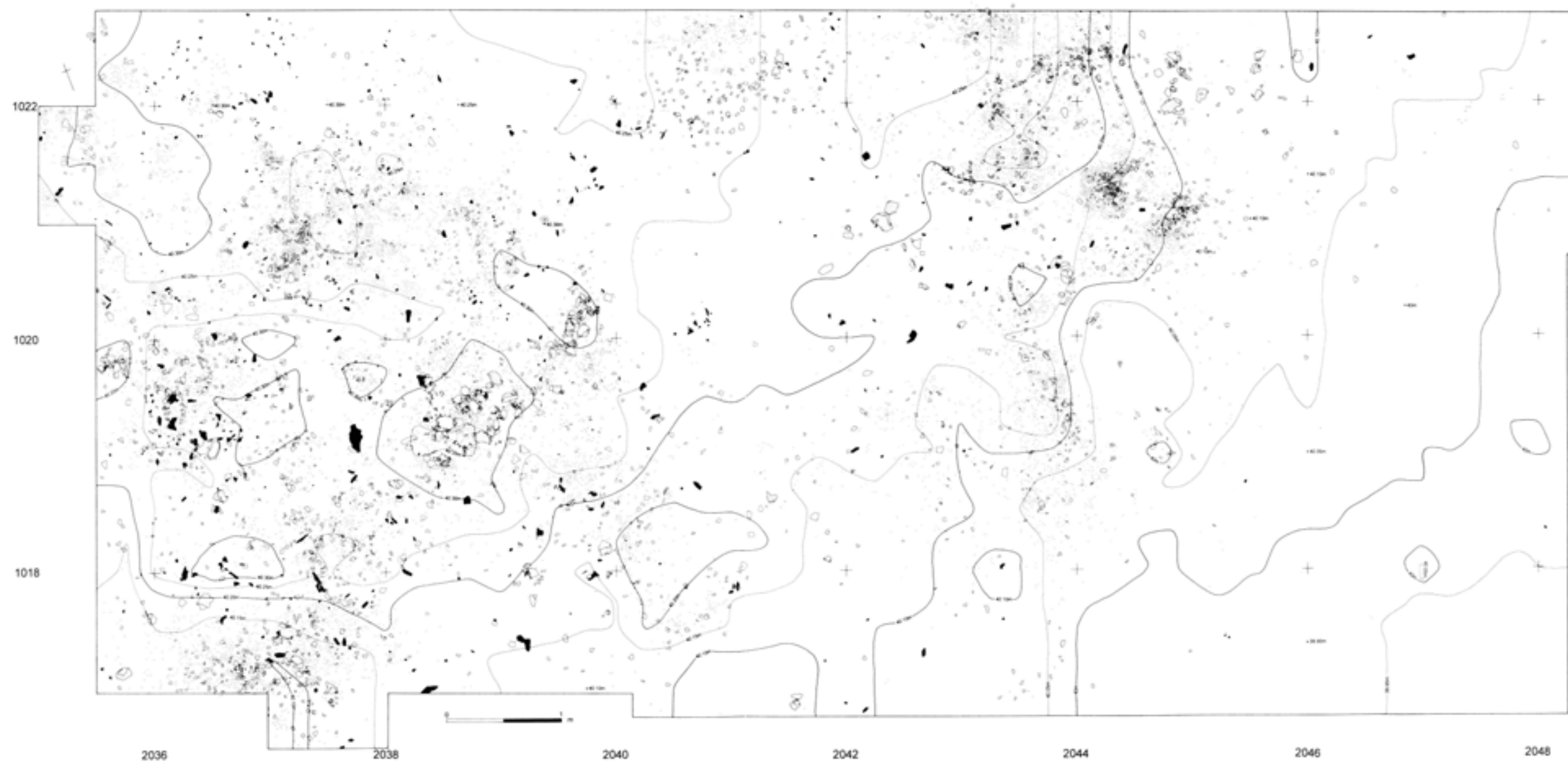


Fig 279 Plan of flintwork and faunal remains from Unit 4b at GTP 17; location of trench is shown on Fig 275

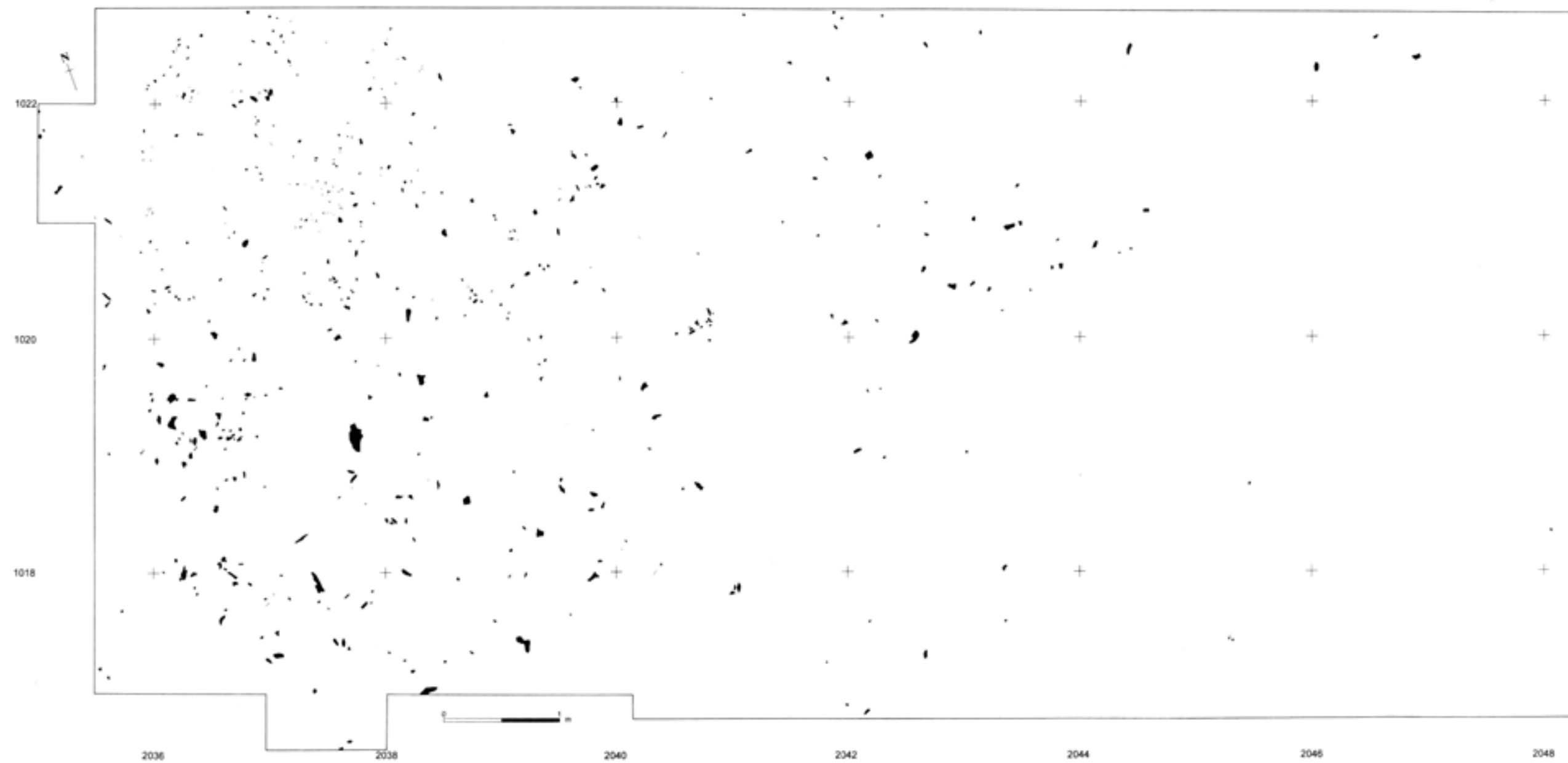


Fig 280 Plan of faunal remains from Unit 4b at GTP 17

Published by English Heritage, The Engine House, Fire Fly Avenue, Swindon SN2 2EH
www.english-heritage.org.uk
English Heritage is the Government's lead body for the historic environment.

© English Heritage 1999

Images (except as otherwise shown) © English Heritage or © Crown copyright. NMR

Ebook (PDF) published 2013

Ebook (PDF) ISBN 978 1 84802 179 2

Version 1.0

First published 1999 in paperback ISBN 1 85074 670 2

British Library Cataloguing in Publication data

A CIP catalogue record for this book is available from the British Library.

All rights reserved

No part of this publication may be reproduced or transmitted in any form or by any means, electronic or mechanical, including photocopying, recording, or any information storage or retrieval system, without permission in writing from the publisher.

Application for the reproduction of images should be made to English Heritage. Every effort has been made to trace the copyright holders and we apologise in advance for any unintentional omissions, which we would be pleased to correct in any subsequent edition of this book.

For more information about English Heritage images, contact Archives Research Services, The Engine House, Fire Fly Avenue, Swindon SN2 2EH; telephone (01793) 414600.

Edited and brought to publication by David M Jones, Tracey Croft and Andrew McLaren, Publishing, English Heritage.

Page layout by Val Kinsler, 100% Proof

Scanning and production of e-book (PDF) by H L Studios www.hlstudios.eu.com

Front cover

Micrograph of mink scat (in thin section) from Quarry 1 Area B Unit 4d, which shows both pale and reddish bone material and two vole teeth.